THE GEOLOGY OF KIMBERLITES FROM THE FORT A LA CORNE AREA, SASKATCHEWAN, CANADA

KEVIN LEAHY

SUBMITTED IN ACCORDANCE WITH THE REQUIREMENTS FOR THE DEGREE OF PhD

THE UNIVERSITY OF LEEDS, DEPARTMENT OF EARTH SCIENCES

JUNE 1996

The candidate confirms that the work submitted is his own and that appropriate credit has been made to the work of others.

Abstract

Kimberlites have been recently discovered beneath 100m of glacial sediment at Fort a la Corne, Saskatchewan, Canada. Crater and extra-crater facies have been intersected in borehole core, interstratified with coastal and marine sediments of Cretaceous age. Extra-crater kimberlite is very rare, and particularly well preserved at Fort a la Corne. It is encountered in five borehole intersections drilled by Rhonda Mining Corporation, sponsors of the Operation Fish Scale project, which included kimberlite research at the University of Leeds.

The regional setting and geological description of six kimberlite borehole intersections are presented. In addition, the broad geodynamic conditions and the stratigraphic context are described, and from these a model for kimberlite eruption is constructed. The kimberlites are then described at a range of scales from stratal thickness and disposition, to ultra-fine diagenetic mineral growth. A textural classification is then applied to the deposits. The volcanology of the Fort a la Cone kimberlites are then discussed: these are unusual in that the craters are preserved, and are broad and flat, rather than steep-sided tapering cones. A new term, *pateran crater*, and process of evolution is proposed for these and other kimberlites of similar morphology. The survival of these volcanic edifices in the sedimentary environment is also considered. The geochemistry of the kimberlites is presented, both bulk rock, and over 450 analyses of individual mineral grains by electron microprobe. These minerals are mostly garnet, ilmenite and pyroxene, of megacryst, kimberlite, crust, mantle peridotite and eclogite origin. The mineral chemistries are compared to those found in other kimberlites around the world, and the nature of the cratonic lithosphere is described. The P-T and compositional characteristics of the lithosphere are further refined from diamond and garnet trace element chemistry in collaborative works with Taylor and Griffin, described herein.

Economic aspects of the kimberlites are reviewed, and all the conclusions are presented in time order, from diamond growth in the Archean, crustal evolution in the Mid-Proterozoic, Early Cretaceous magma generation and eruption, to Late Cretaceous reworking and burial.

Table of Contents

List of Tables and Illustrations

List of Abbreviations

002, 003 etc to 017..... Boreholes OFS93-002 to OFS94-017
BRSZ..... Birch Rapids Shear Zone
CAVA..... coarse authigenic vermicular antigorite
c/ht..... carats per hundred tonnes
CI..... contamination indices
cpx..... clinopyroxene
CSIRO..... Centre for Scientific and Industrial Research Organisation
CT..... coarse tuff
DNAG.....decade of North American Geology
EDS..... electron dispersive spectra
EMHZ..... east median hinge zone
FALC.....Fort a la Corne
Ga..... giga-years (before present)
gcm^{-3}..... grams per cubic centimetre
GD..... Glennie Lake Domain
GSC..... Geological Survey of Canada
IR..... infra-red
JV..... joint venture
LOI.....loss on ignition
LT..... lapilli-tuff
Ma.....millions of years (before present)
MARID.....suite comprising mica, amphibole, rutile, ilmenite and diopside.
MLE.....Meadow Lake escarpment
Mt.....millions of tonnes
MT..... medium tuff
nT..... nano-tesla
OFS.....Operation Fish Scale
opx.....orthopyroxene
PDI..... peridotitic diamond inclusions
PK..... pyroclastic kimberlite (primary airfall)
PMP..... proton microprobe
RPK.....reworked pyroclastic kimberlite (epiclastic)
SEM.....scanning electron microscope

SF.....Stanley Fault
TC.....tuffaceous clastic
TF.....Tabbenor Fault
THO.....Trans Hudson Orogen
UEM.....Uranerz Exploration and Mining
UHP.....ultra-high pressure
WCSB.....Western Canadian sedimentary basin
XRD.....X-Ray diffraction
XRF.....X-Ray fluorescence

Definition of some terms used in this thesis

airfall	-	primary pyroclastic deposit or process of deposition (now an obsolete term, replace with tephra-fall).
archon	-	cratonic area comprising Archean-age rocks
chromite	-	any chromium-bearing spinel
craton	-	an area of crust and attached lithosphere that has not undergone any orogenic reworking, or major rifting, since at least the Middle Proterozoic (circa 1.7Ga).
eclogite	-	high temperature and pressure metamorphic rock from both the crust and the mantle, with a wide range of constituents. In this thesis mantle eclogites are regarded as subducted remnants of (oceanic) crust, comprising Fe-garnets, cpx (often omphacite) and kyanite. A diamond source rock.
enriched/fertile	-	a rock (in this context, a lithospheric peridotite), which contains the elements required to produce basaltic (or similar mafic) magma by partial melting. The antonyms used are depleted/infertile.
harzburgite	-	peridotite of mantle origin, comprising olivine and opx, with small amounts of cpx, Cr-rich spinel and garnets. Highly depleted, and a source rock of diamond.
lapilli	-	used either as a grain size term for pyroclastics >2mm (used in conjunction with the term tuff: lapilli-tuff). Or a pyroclastic grain of aggregated composition, either fluidal, rounded or autolithic. Magmatic and accretionary lapilli are not described in this thesis.

lherzolite	-	peridotite, typically of mantle origin, comprising mainly olivine, with opx, cpx and an aluminous phase (plagioclase and spinel in the upper lithosphere, garnet in the lower lithosphere). May have a range of fertility, but is more fertile than harzburgite. May be a source rock for diamond.
lithosphere	-	rigid, coherent and chemically distinct plate that overlies the mantle and is capped by the crust. Continental lithosphere ranges up to 220km depth, and the base is defined at the depth where depleted mantle peridotites are underlain by fertile, asthenospheric peridotites.
ilmenite	-	all iron and magnesian titanates of the ilmenite group
proton	-	cratonic area comprising Proterozoic-age rocks

INTRODUCTION

Geology of Kimberlites in the Fort a la Corne area,
Saskatchewan, Canada

Kimberlites are a rare igneous rock type of potassic-ultramafic affinity, mainly generated at, or near, the base of the continental lithosphere, and are usually found as volcanic diatremes at the surface. They characteristically occur in cratonic regions of the world where the lithosphere is thick (typically 200km), and are economically important as one of the primary sources of diamonds. Due to the age and location of kimberlite volcanism, the volcanic superstructures are prone to erosion. Most kimberlites are eroded to their conduit, or diatreme levels, which range from dykes to carrot-shaped bodies over a kilometre across. Some have crater sediments above the diatreme, but none have been reported with an intact volcanic superstructure. Fully preserved crater facies kimberlite and apron deposits have, however, recently been discovered in the Fort a la Corne area (FALC), Saskatchewan, Canada.

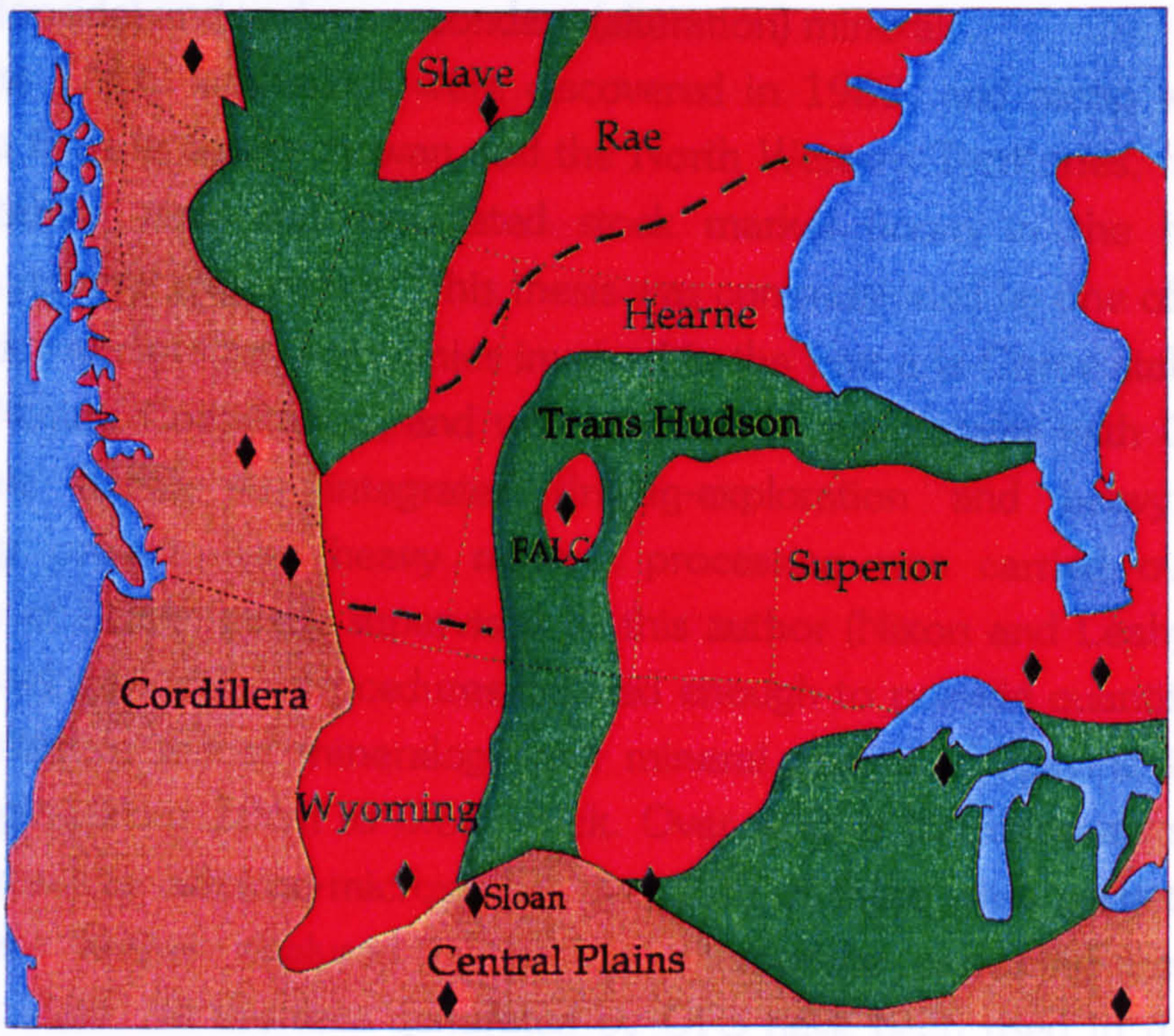

Figure i1. Sketch location map of Fort a la Corne (FALC) and other kimberlite localities (diamonds). Also showing the main tectonic regions of the North American Plate. Red ornament indicates Archean cratons, 'welded' by Proterozoic orogenic belts, shaded green. Note the Trans Hudson Orogen encases an Archean 'micro-craton' in Central Saskatchewan (the Glennie Domain).

The kimberlites were initially located by their magnetic signatures, and later intersected in boreholes at about 100m depth below Quaternary to Recent fluvio-glacial cover. They are interstratified with shallow marine sediments of the Westgate Formation in the Lower Colorado Group, which were deposited in the late Albian (circa 100Ma, at the end of the Early Cretaceous) in a shallow epicontinental sea that covered the western interior of North America during these times. Scott-Smith et al (1995), Kjarsgaard et al (1995) have reported

slightly older kimberlite occurrences the form of thin (<5m), carbonate-rich tuffs and reworked pyroclastics within the underlying continental sediment of the Mannville group (up to 110Ma). These are interpreted as precursors of kimberlite activity, too small to develop the craters observed in the later FALC kimberlites.

In the main FALC craters, kimberlite occurs as primary pyroclastic deposits, including crystal dominated tuffs and lapilli dominated tuffs, along with variable amounts of reworked pyroclastic sediment. The reworked deposits are the most common kimberlite facies in the extra-crater deposits. The FALC kimberlites are of typical Group I composition, with a typical altered kimberlite mineralogy comprising: multiple generations of olivine, now replaced by serpentine and carbonate, pyrope garnet, ilmenite, phlogopite, spinel, pyroxene (mostly diopside) and various secondary (alteration) minerals.

The FALC kimberlites were discovered in 1989, and along with other kimberlite finds in Saskatchewan and the North Western Territories, fuelled the largest staking rush and associated stock market boom in the history of Canadian mineral exploration. This thesis was commissioned by one of the most active junior exploration companies involved in the Fort a la Corne staking rush, Rhonda Mining Corporation, and was intended to run parallel with Operation Fish Scale (OFS); an integrated drilling-exploration and heavy mineral processing project. The heavy mineral processing was carried out at the University of Leeds, partly supervised by this author (Nixon and Leahy, 1995), and involved separation procedures detailed enough to provide quantitative and semi-quantitative modal mineralogy and mineral grades of specific kimberlite strata ranging from 20cm to 3.5m thick. Over 460 of the minerals separated were analysed by electron-microprobe, over 200 of these were garnets, half of which were further analysed by proton microprobe providing geothermo-barometric data. All the data generated by OFS have been used in this thesis, and acknowledgement is given to Peter Gummer of Rhonda Mining Corporation for initiating OFS and allowing use of the data in this thesis.

The overall aims of the thesis are to describe the unique occurrence of extra-crater facies kimberlite deposits in the sedimentary environment, and to study their constituent mantle minerals. From the observations and data gathered, unique processes of eruption, reworking and preservation are proposed, and aspects of kimberlite geochemistry, mantle constitution and geodynamic evolution of Central Saskatchewan are addressed. The economic viability of the FALC kimberlites is also discussed, but this is a complex issue and the conclusions reached should not be considered final .

Currently Rhonda Mining has sold its FALC kimberlite interests (including responsibility for this thesis) to Kensington Resources Ltd, who have themselves joined the main FALC joint venture, testing the large crater bodies as diamond ore reserves. They have provided much additional data on the main craters in subsequent press releases, which has been a useful source of information on topics that are usually propriety. Preliminary evaluation from the early stages of bulk sampling (approximately 1100t tested) suggests the crater facies kimberlites in Fort a la Corne are low to moderate grade diamond deposits; 3 carat/100 tonnes (c/ht) to 24c/ht, but with vast tonnages, up to 540 million tonnes in one crater (Kensington Resources press release, 1995). The tonnage is far in excess of most kimberlite pipes, and lies in a horizontal ore body, typically with the top at 100m depth and the base at about 250m to 350m depth. The extra-crater deposits may represent much higher grade diamond deposits (estimates of 3 to 9 fold the crater facies grade), but of a lower tonnage than crater facies kimberlite. Thus the kimberlites at FALC are unique from both an academic and an economic perspective, and continue to generate interest from both communities.

Because all of the exploration data generated in the FALC joint venture area is propriety, much of the detailed geology and associated data remains unpublished. Apart from this author (and co-authors: P.H. Nixon and W.R. Taylor), other workers in the area that have published information are Lenhert-Thiel et al (1992), Scott-Smith et al (1995) and Kjarsgaard et al (1995). Lenhert-Thiel et al are employees of Uranerz Exploration and Mining Corporation, who initially made the kimberlite discovery, and their publication is essentially an exploration methodology and preliminary description of the kimberlites. Scott-Smith was commissioned to report on the petrology and geology of the kimberlites by the FALC joint venture in the early 90's, and has presented a small number of lectures and papers on the subject. Kjarsgaard and his main co-author Leckie are employees of the Geological Survey of Canada, and were given the task of reporting on a crater facies kimberlite drilled by the GSC in the FALC cluster in 1993 ('Smeaton' borehole). Their preliminary report contains a detailed borehole log and other stratigraphic information, and further reports concerned with mantle xenolith geochemistry and isotopic dating are expected in late 1996. Other publications which are frequently cited in this thesis are listed at the end of this introduction.

This thesis has a extensive base of subjects, and attempts to cover a wide variety of material not considered by other workers on the FALC kimberlites. In the concluding Chapter a model for the evolution of the kimberlites is

constructed, extending from growth of some of the rare accessory minerals (diamond) in the Archean, through the main magmatic events, to post-eruptive processes in the earliest epochs of the Late Cretaceous.

Frequently cited publications:

1. Papers

- Bloch, J., Schröder-Adams, C., Leckie, D.A., McIntyre, D.J., Craig, J., Staniland, M. (1993). Revised stratigraphy of the lower Colorado Group (Albian to Turonian), Western Canada. Bulletin of Canadian Petroleum Geology Vol. 41, No.3. p.325-348.
- Gent, M.R. (1992). Diamonds and precious gems of the Phanerozoic basin, Saskatchewan: Preliminary Investigations. Saskatchewan Energy and Mines Open File Report 92-2.
- Kjarsgaard, B.A., Leckie, D.A., McIntyre, D.J., McNeil, D.H., Haggart, J.M., Stasiuk, L. and Bloch, J. (1995). Smeaton Kimberlite Drill Core, Fort a la Corne Field, Saskatchewan. Geological Survey of Canada Open File 3170, pp.57.
- Lehnert-Thiel, K., Loewer, R., Orr, R.G. and Robertshaw, P. (1992). Diamond-bearing kimberlites in Saskatchewan, Canada: The Fort a la Corne Case History. Exploration Mining Geology Vol.1 No.4 p.391-403.
- Lewry, J.F., Hajnal, Z., Green, A., Lucas, S.B., White, D., Stauffer, M.R., Ashton, K.E., Weber, W. and Clowes, R. (1994). Structure of a Paleoproterozoic continent-continent collision zone: a LITHOPROBE seismic reflection profile across the Trans-Hudson Orogen. Tectonophysics Vol.232, p.143-160.
- Lorenz, V. (1985). Maars and diatremes of phreatomagmatic origin. Transactions of the Geological Society of South Africa, Vol.88, p.459-470.
- Schmid, R. (1981). Descriptive nomenclature and classification of pyroclastic deposits and fragments: recommendations of the IUGS subcommission on the systematics of igneous rocks. Geology, Vol.9, p.41-43.

2. Books:

- Diamond Exploration: Into the 21st Century. Griffin, W.L. 1995. Journal of Geochemical Exploration Special Volume, Vol. 53, Nos. 1-3.
- Foreland Basins and Fold Belts. Macqueen, R.W. and Leckie, D.A. 1992. Association of American Petroleum Geologists, Memoir 55
- Kimberlites: mineralogy, geochemistry and petrology. Mitchell, R.H. 1986. Plenum Press, New York.
- Mantle Xenoliths. Nixon P.H. 1987. Wiley, Chichester.
- Proceedings of the 6th International Kimberlite Conference, Novosibirsk, Russia 1995. Extended Abstracts Volume.
- Volcanic Successions, Modern and Ancient. Cas, R.A.F. and Wright, J.V. 1988. Chapman and Hall, London.

CHAPTER 1 - REGIONAL BACKGROUND

Geology of Kimberlites in the Fort a la Corne area,
Saskatchewan, Canada.

1.1 Geographical and geological distribution of kimberlites in Central Saskatchewan

Saskatchewan is a province in western central Canada (Figure 1.1.1). The southern half comprises prairie farmland, generally flat, but with hilly topography in the south-west and pervasive river valley development due to Recent dissection of the prairie plateaux. The majority of Saskatchewan's two million population live in the south, which is heavily farmed, and exploited for natural gas, potash and salt. The northern half of Saskatchewan is mostly pine forest and lakeland, with thin soils and a harsher climate unsuited to farming. The population is very low outside of the mining towns and camps, with no permanent roads penetrating far north. This area is rich with gold, uranium, sulphides and other mineral wealth, which are currently being exploited as global metal prices allow.

The kimberlites covered in this study occur in a map area approximately 125km east-west by 100km north-south (Figure 1.1.2). This area lies on the borders between the southern farmlands and the northern forests in central Saskatchewan. The main local town is Prince Albert in the south-west of the area, with a great many farming communities in the southern half of the area. The Fort a la Corne (FALC) forest is a protected park, comprising mainly pine and birch on a thick, sandy soil of glacial-lake/deltaic origin. Small hillocks, sand dunes, lumber clearings and swamps are common in the forest, and the few access roads are of levelled sand. Within the FALC forest, drill hole positioning and access is by approval of the Forestry Commission. Access for drill equipment in areas around the FALC forest is excellent, the land being farmed, with numerous well maintained roads. Within the forest two main routes are maintained, north-south and east-west. These pass over, or very near to, many of the kimberlite bodies, and other access roads can be quickly developed.

The main cluster of kimberlite bodies occur within the boundary of the FALC forest (Figure 1.1.3), with outliers at Snowden, Wierdale and Smeaton. These occur on a gradient of low to normal regional magnetic susceptibility (0nT to -350nT residual total field), Figure 1.1.4. Similarly the regional gravity Bouguer anomaly is also on a gradient (-55mGal to -70mGal), Figure 1.1.5. The regional gravity-magnetic gradients are attributed to large-scale basement features, rather than an effect of the kimberlites, which have far smaller anomalies. These small-scale anomalies have been detailed by aeromagnetic and ground magnetic surveys, and help to define the kimberlite cluster. The cluster

Figure 1.1.1

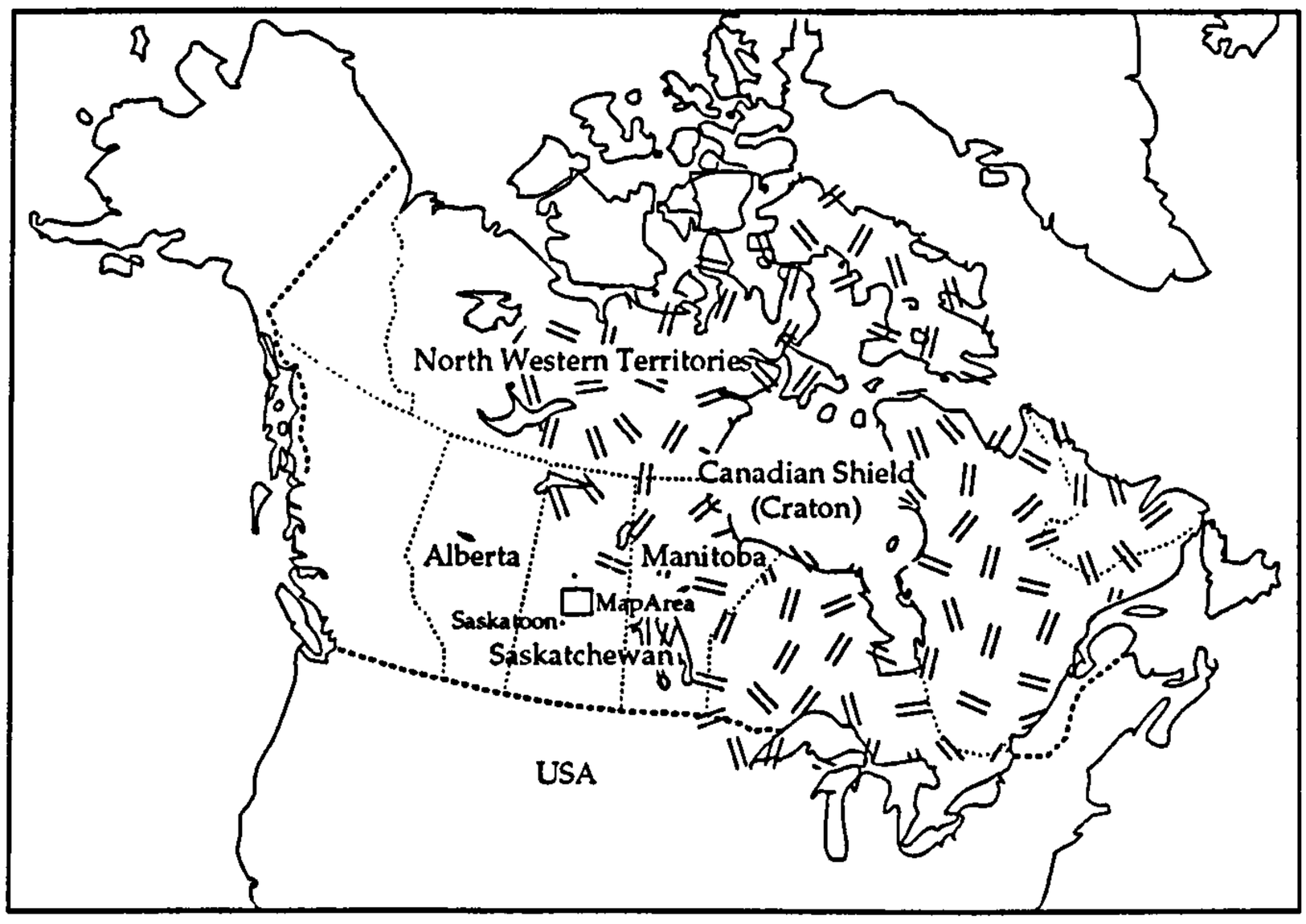

Map of North America, showing Canadian Provinces (dotted lines), approximate outcrop of the Canadian Shield (ornament is Archean and Proterozoic), the Map Area (see Fig. 1.1.2) and field office location (Saskatoon).

Figure 1.1.2.

The Map Area.
Showing areas of kimberlite occurrences (shaded area with dashed borders), towns of interest, major roads, trails through FALC forest (dotted) and borehole locations ⌖. Filled circles indicate boreholes from Simpson (1982).
Details of main kimberlite cluster shown in Fig 1.1.3. (boxed area).
For reference, Saskatoon lies about 125km SSW of Prince Albert.

Figure 1.1.3.

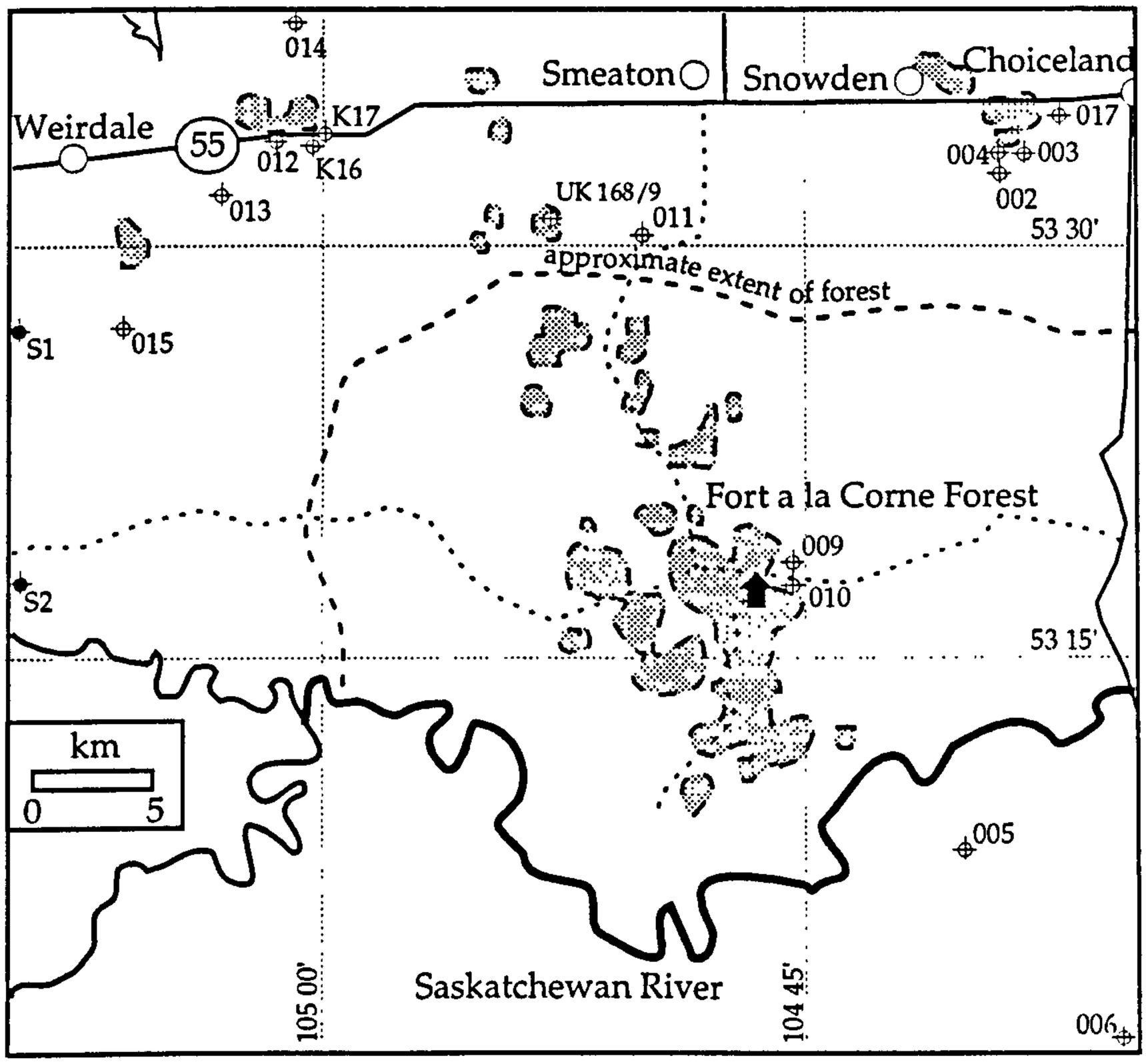

Detail of kimberlite cluster. Grey shaded areas, bordered with dashed lines are the kimberlite crater facies, as defined by magnetic anomalies. 41 anomalies of 71 verified as crater facies kimberlites by FALC joint venture drilling.
Boreholes indicated by ⌖, holes designated 0_ _ are Rhonda Operation Fish Scale (OFS) drilled in 1993 to 1994.
Boreholes 002, 003, 004, 009 and 010 intersected extra-crater kimberlitic deposits. 012 intersected crater facies kimberlite. S1 is Strong Pine No.1 in Simpson (1982), S2 is BA Halas 4-4 in Simpson (1982), K16 and K17 were drilled by Kensignton in 1994, UK 168/9 is the drill site for Geological Survey of Canada Smeaton drillhole, see Kjarsgaard et al (1995).
Hut symbol represents FALC JV drill camp. Land outside the approximate extent of the forest and south of the Saskatchewan River, is mostly farmland, with some Indian Reserve land.

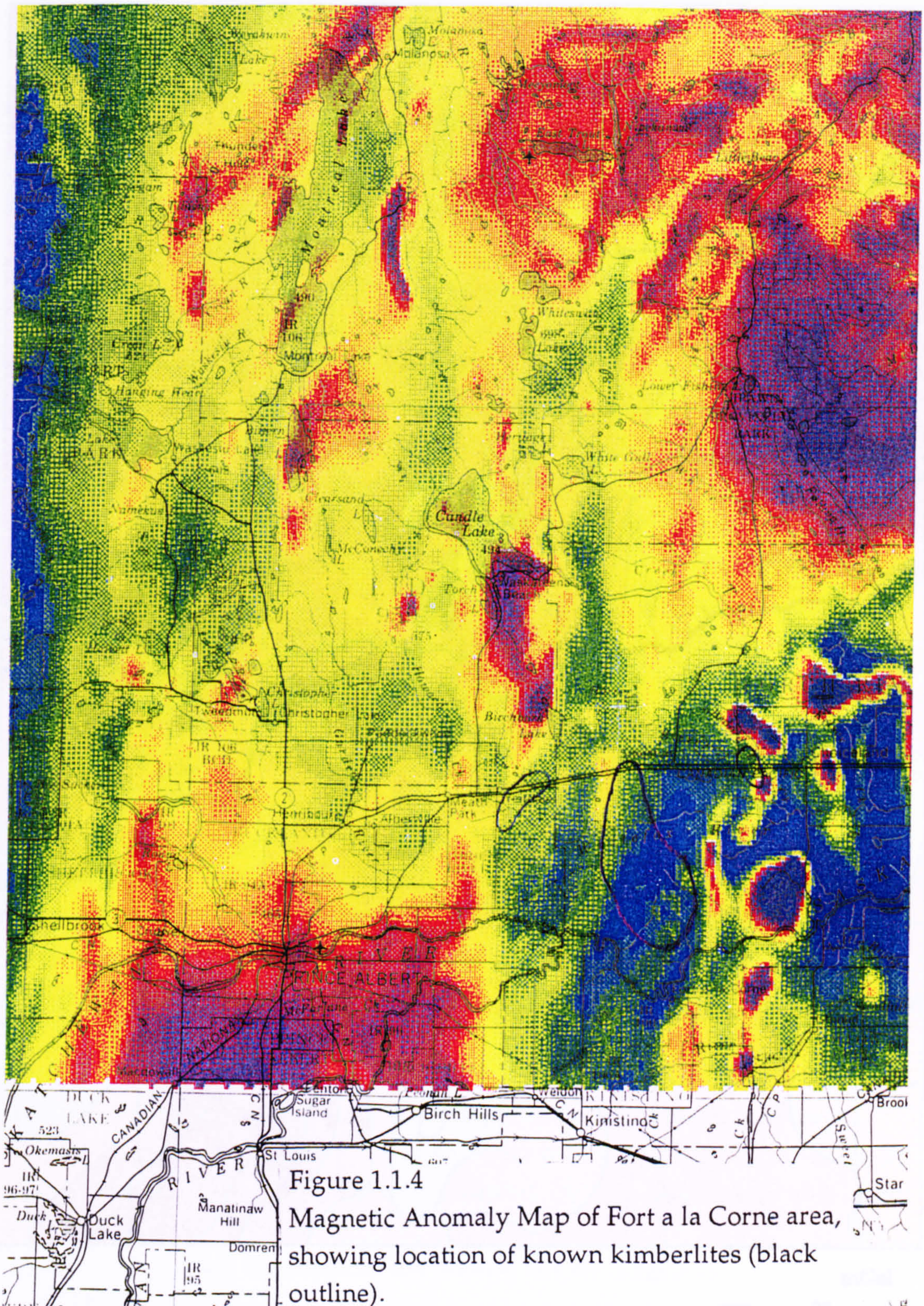

Figure 1.1.4
Magnetic Anomaly Map of Fort a la Corne area, showing location of known kimberlites (black outline).
From Geological Survey of Canada,
Map No. NN-13-M, Prince Albert.
Scale 1:1,000,000
dark blue to purple-red = -1000nT to +500nT

Note the strong linear and ovoid features to the east of the kimberlites, which are folded banded iron formations in the metamorphic basement (mid-Proterozoic, Gent, 1992).

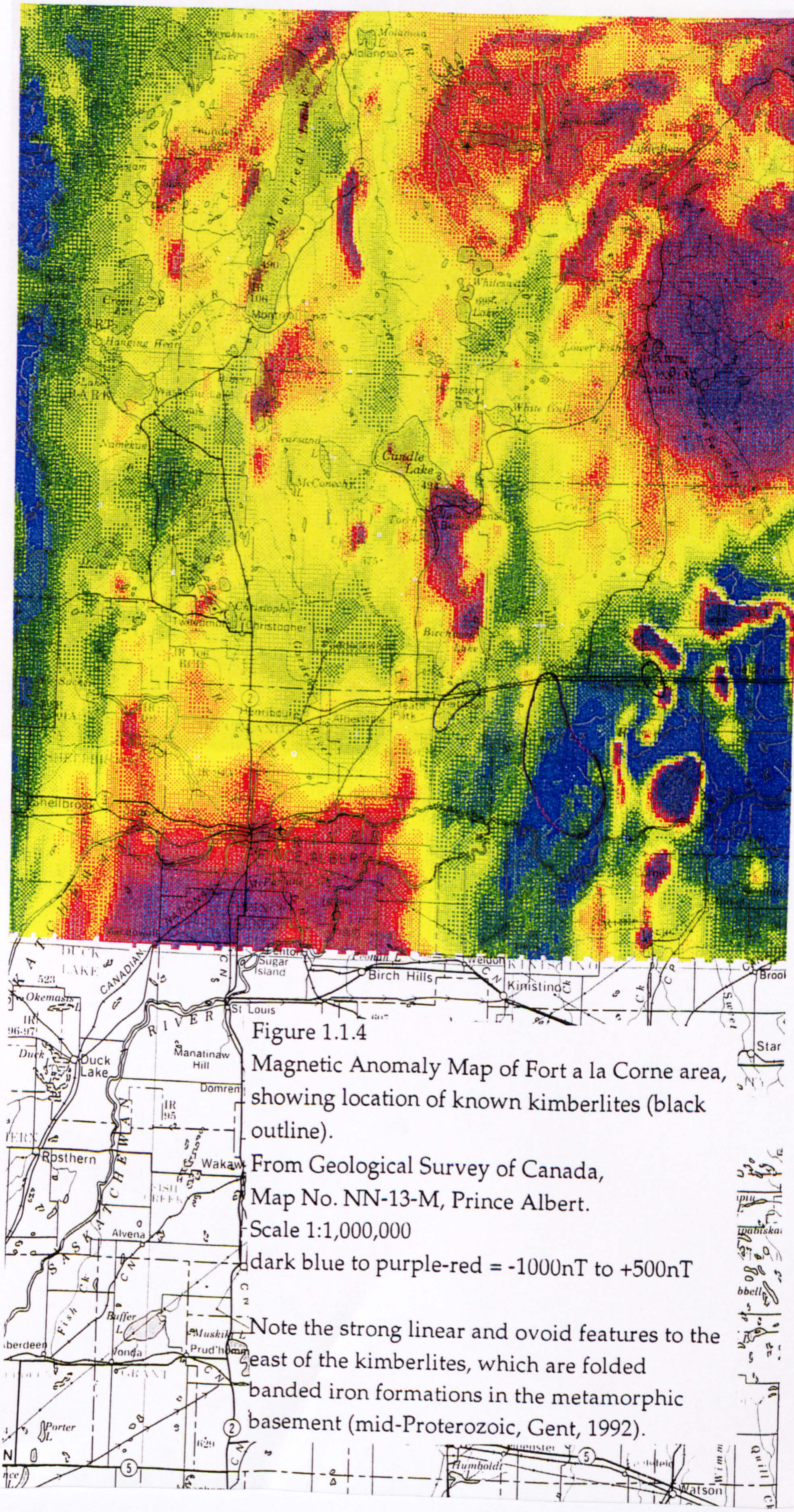

Figure 1.1.4

Magnetic Anomaly Map of Fort a la Corne area, showing location of known kimberlites (black outline).

From Geological Survey of Canada, Map No. NN-13-M, Prince Albert. Scale 1:1,000,000

dark blue to purple-red = -1000nT to +500nT

Note the strong linear and ovoid features to the east of the kimberlites, which are folded banded iron formations in the metamorphic basement (mid-Proterozoic, Gent, 1992).

Figure 1.1.5

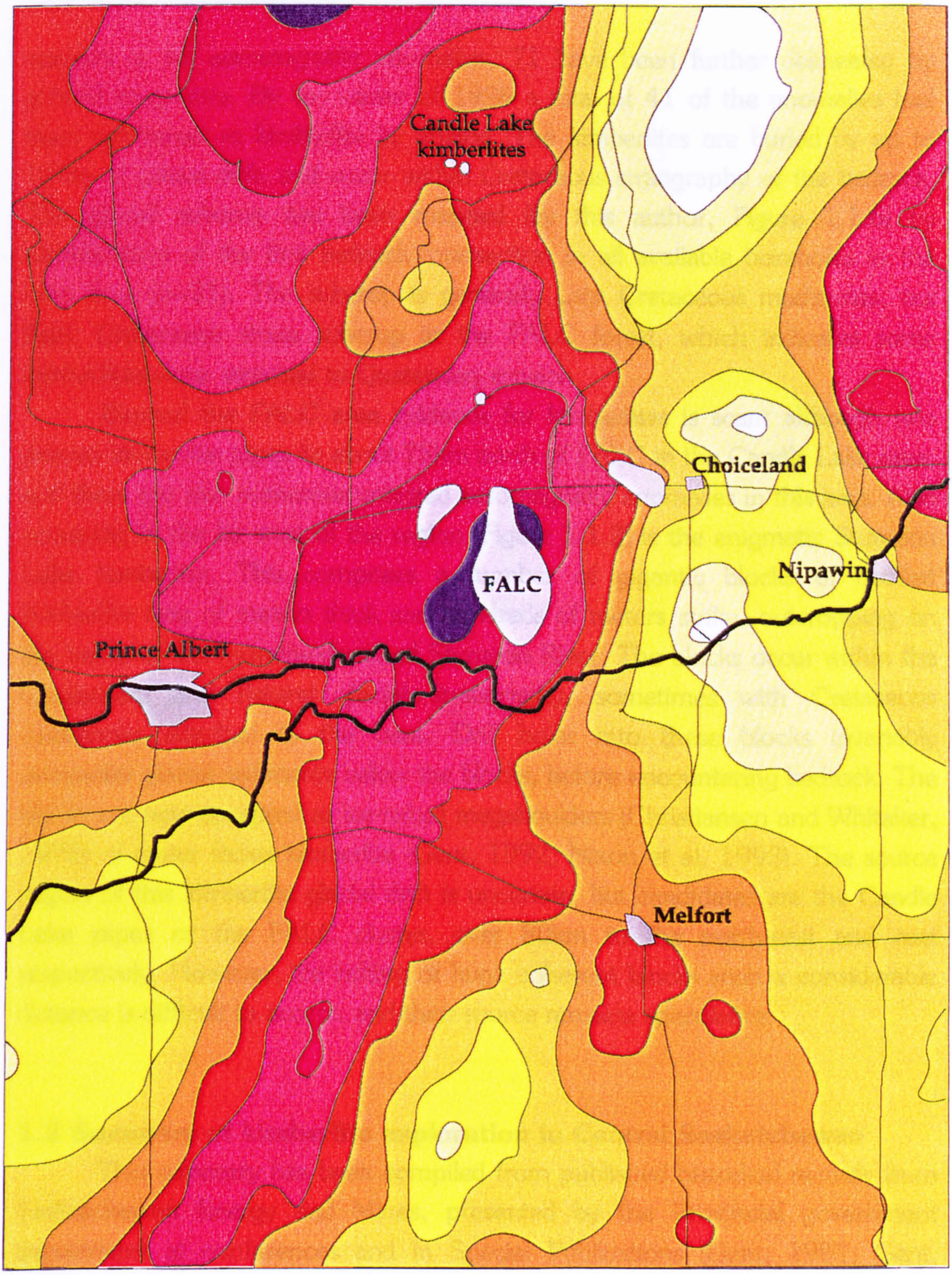

Gravity - Bouguer Anomaly Map of the Fort a la Corne area (FALC).
From Geological Survey of Canada,
Map No. NN-13-GR (BA), Prince Albert.
Scale 1:1,000,000.

Note the local gravity low in the area of the FALC kimberlites, which may be the result of the deep crustal root located to the east of Prince Albert (imaged by LITHOPROBE; Lewry et al, 1994).

consists of 88 aeromagnetic anomalies, 71 have been further delineated by ground magnetics. By the winter of 1996 a total of 41 of the anomalies had been confirmed as kimberlite by drilling. The kimberlites are buried by up to 120m of glacial drift, and occur within Cretaceous stratigraphy of the bedrock. The glacial subcrop has been mapped (by this author, Figure 1.1.6) by identification of the first bedrock intersection in all available boreholes in the map area (n=21). The subcrop is generally Late Cretaceous mudstones, but Early Cretaceous strata subcrop in the FALC forest, which indicates some kimberlites were exposed to Quaternary erosion.

Beyond the FALC area evidence for kimberlites is scant although two proven kimberlite pipes lie about 75km north of FALC in the Candle Lake area, and there are also numerous untested aeromagnetic anomalies in this area. Also occurring in the far west of the region (Figure 1.1.2) is the enigmatic Sturgeon Lake kimberlite. This comprises a number of gigantic blocks of bedded kimberlite tens of meters thick and hundreds of meters strike, outcropping on the banks of the moraine-dammed Sturgeon River. The blocks occur within the Quaternary and Recent glacial stratigraphy, sometimes with Cretaceous mudstones attached to the base. Drill holes into these blocks invariably encounter glacial sediments below the blocks, before encountering bedrock. The blocks are now accepted as ice-rafted megaboulders (Christiansen and Whitaker, 1976) of crater facies kimberlite (Gent, 1992; Nixon et al, 1993). The source region of this kimberlite glacial drift is uncertain, but candidates are the Candle Lake pipes or the FALC cluster, over 80km to the north-east and east respectively. However, ice rafting of huge coherent blocks such a considerable distance is difficult to accept, and their source remains speculative.

1.2 Summary of kimberlite exploration in Central Saskatchewan

This summary has been compiled from published historical records from Saskatchewan Energy and Mines, presented by the Provincial government department at conferences and in Special Publications (Gent, 1991; Gent, 1992), and Uranerz Exploration and Mining (UEM) publications (Lehnert-Thiel et al, 1992).

1948 Prospectors J.J. Johnson and S. Schiltroth recover five diamonds (one about 10mm) from "...kimberlite, a blue rock..." at an undisclosed locality. Claims diamond exploration rights for the whole central and

Figure 1.1.6

Sub-crop geology of bedrock (buried beneath 90-120m of Quaternary glacial and fluvial sediment) based on first bedrock intersection in the boreholes shown. Note that the deepest stratigraphic levels (stratigraphy shown in key below and Figure 1.3.2) are exposed in the FALC forest area and to the north-east (compare to kimberlite locations to in Figure 1.1.3). This apparent doming may be a result of differential compaction, basin tectonics, thermo-tectonic doming, or more likely, a glacial erosional feature (valley). This is discussed further in Section 1.4.

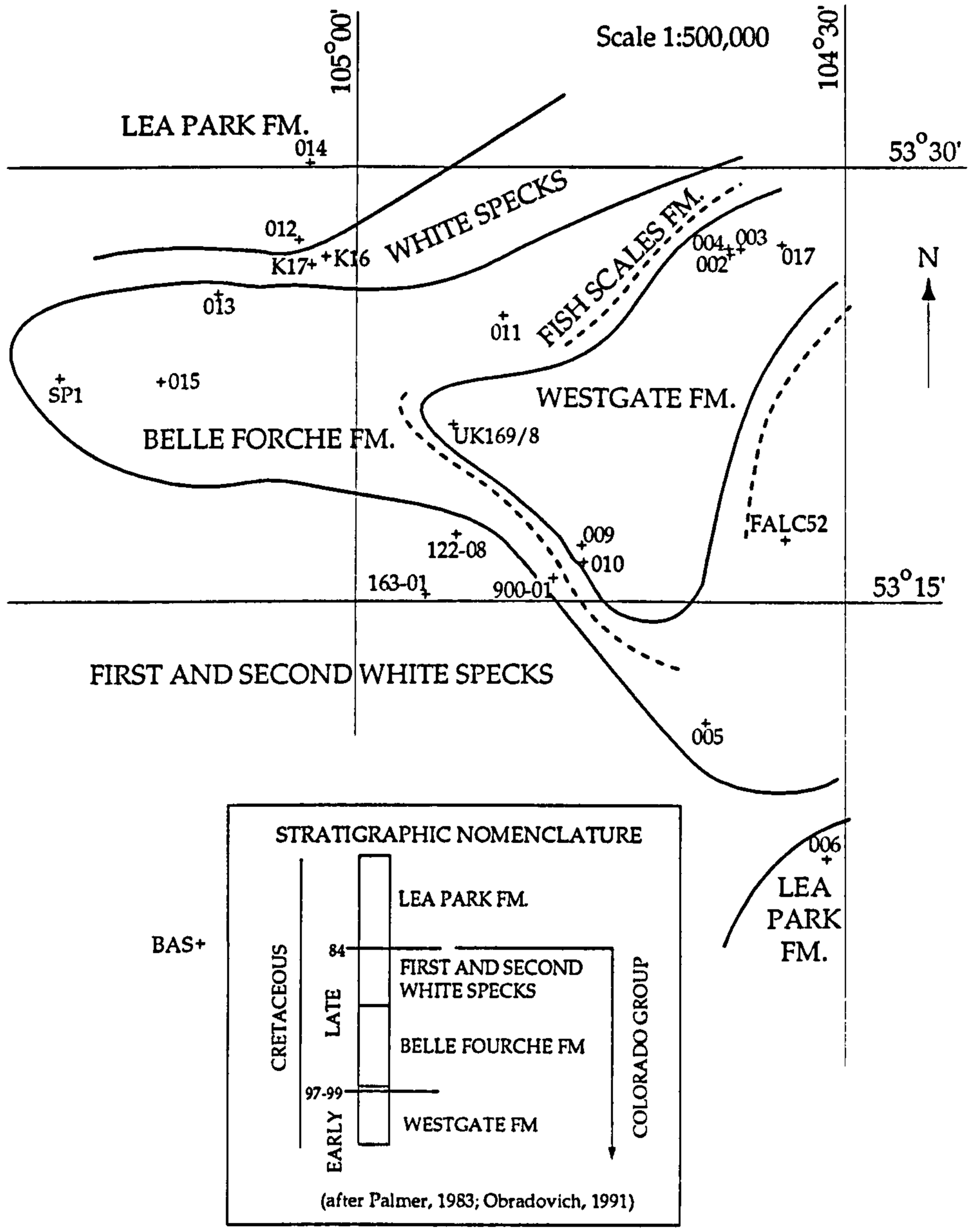

Borehole code key:
- all boreholes of the format 0xx (e.g. 006) are OFS 93-0xx (e.g. OFS 93-006) drilled by Rhonda Mining Corp. (and partners).
- K16 and K17 are FC-94-016/017 drilled by Kensington Resources Ltd.
- 122-08, 163-01 and 900-01 are FALC Joint Venture boreholes (data from Kensington Resources Ltd.)
- UK169/8 and FALC52 are boreholes reported in Kjarsgaard et al (1995), drilled by the GSC.
- SP1, BAH and BAS (Strong Pine No.1, BA Halas and BA Sarry) are boreholes described in Simpson (1982).

eastern portion of the map area (Figure 1.1.2). No further records of activity.

1961 First staking rush. M. Pellack reports two small diamonds (one about 6mm) in gravel soil sampled 6km west of Prince Albert. About five hundred claims filed, no further reports of diamond discoveries.

1963 Staking rush around Prince Albert ends. An undisclosed DeBeers affiliated group explore for diamonds and indicator minerals in southern Saskatchewan.

1987 Kimberlite positively identified at Sturgeon Lake by J. Letendre of Monopros, subsidiary of DeBeers. Outcrop exposed whilst extracting gravel for building purposes.

1988 Monopros test drill Sturgeon Lake block. Subsequent announcement triggers another staking rush in the land around Sturgeon Lake, participants include Claude Resources Ltd, Corona Resources, Cameco and UEM. UEM identify potential targets from government aeromagnetic maps 80km to the east at FALC, and immediately fly more detailed aeromagnetic coverage. Late in the year UEM/Cameco joint venture stake the majority of the FALC kimberlite cluster.

1989 Sturgeon Lake area still active, Corona drill diamond bearing kimberlite block 2km north of the Monopros block. Monopros complete evaluation and cease activity at Sturgeon Lake, staking rush switches to the areas around FALC with many participants. UEM/Cameco JV continue magnetic mapping, and early drilling confirms geophysical modelling of flat-lying kimberlite bodies.

1990/1 Staking rush continues in all areas of central Saskatchewan, many participants including Rhonda Mining Corp. and Aaron Oil. UEM/Cameco continue program, and release diamond results in 1991.

1992/3 Monopros join the UEM/Cameco JV, FALC exploration continues. Rhonda/Aaron and other joint venture partners drill apron deposits and outlying crater deposits around the FALC region. Geological Survey of

Canada drill test hole near Smeaton. WarEagle announce discovery of two kimberlite pipes 70km north of FALC. Staking rush ends.

1994 FALC exploration and sampling continues. Kensington Resources Ltd take over Rhonda's extensive diamond exploration claims and other responsibilities.

1995 Kensington join the UEM/Cameco/Monopros JV and continue FALC exploration and sampling. GSC release first Open File report on the FALC kimberlites, based on the results of the Smeaton borehole.

1996 FALC JV and continue exploration and sampling.

1.2.1 Field Sampling in Saskatchewan (K. Leahy)

1993 April to May - Visited Saskatchewan; Sturgeon Lake and Saskatoon. Logged and sampled seven boreholes, five kimberlitic. June 1st - officially began PhD. August - logged crater facies kimberlite core.

1994 April to May - Visited field office in Saskatoon. Researched local stratigraphy, aeromagnetic exploration and heavy mineral separation methods. November to December - Attended Saskatchewan Energy and Mines Open House, logged two stratigraphic boreholes.

1995 June to July - Field site geologist for UEM/Cameco/Monopros/ Kensington JV in the FALC central cluster.

1.2.2 Summary of exploration methods

Apart from the earliest discovery of kimberlite at Sturgeon Lake, accidentally uncovered in a gravel pit, all known kimberlites have been located by their magnetic anomalies. On the broadest scale, the magnetic anomalies of the FALC cluster were first mapped on the 1969 Geological Survey of Canada Aeromagnetic Map (Map 7743G). Map line spacing is 1200m (distance between east-west flight lines), flown at a mean altitude of 305m, and a contour interval of 10nT (Figure 1.2.1).

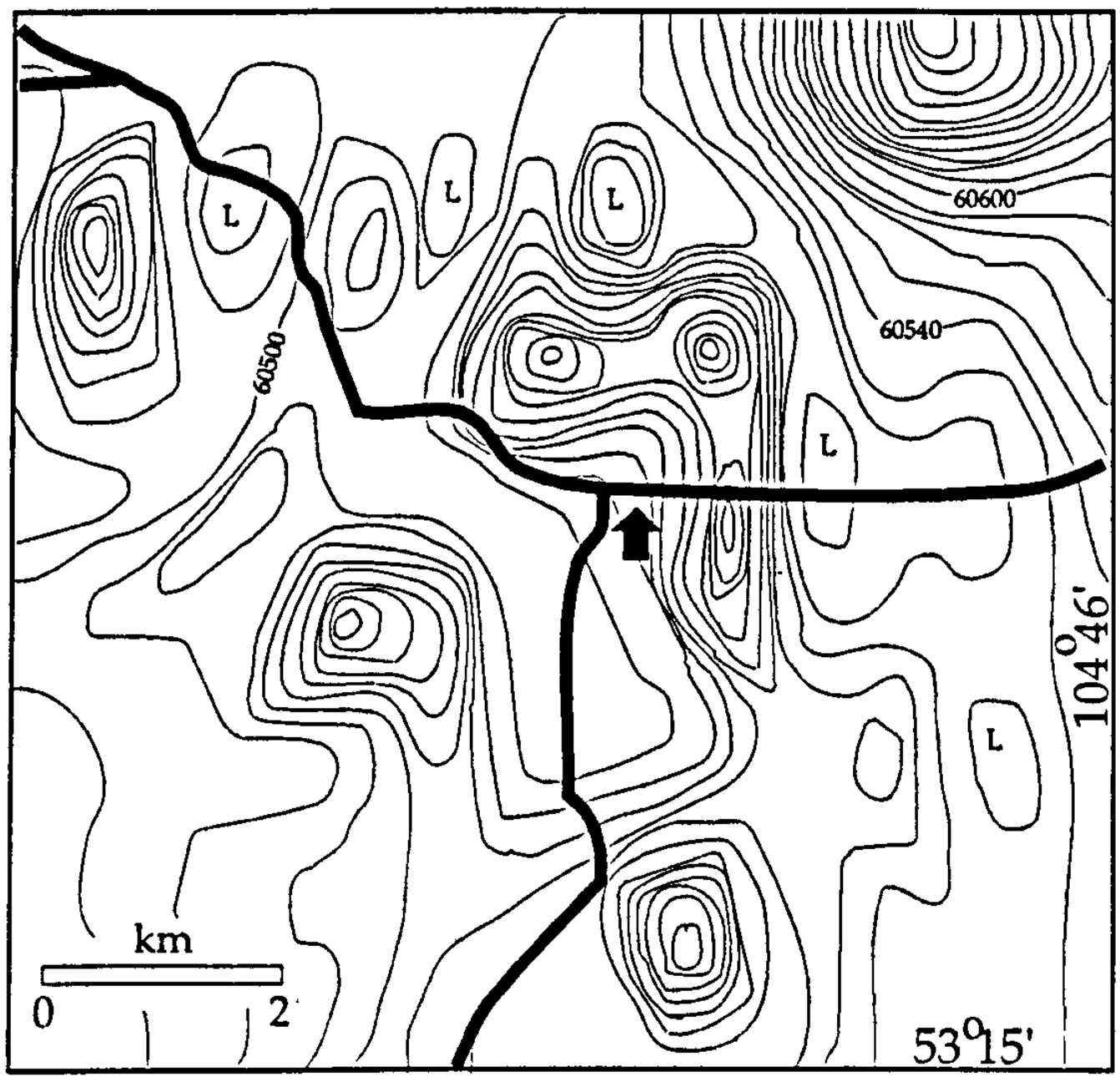

Figure 1.2.1.
Portion of aeromagnetic map by Geological Survey of Canada, 1969, Map 7743G. Showing the large positive anomalies in the centre of the FALC cluster. Roads and drill camp shown (refer to Fig.1.1.3.) E-W line spacing (distance betweenflight lines) is 1200m, and the contour interval is 10nT.
This diagram after Lehnert-Thiel et al, 1992.

The anomalies on this map are broad (2-3km), coalescing, and of an amplitude around 50nT, up to 140nT. They remained unnoticed until 1988 when exploration for kimberlite was widened from around the Sturgeon Lake area. Most exploration groups then flew more detailed aeromagnetic surveys over the areas of interest, using both fixed-wing and helicopter borne magnetometers. Typical survey specifications were a line spacing 200m or 300m and altitudes of 100m to 200m. These surveys produce far greater detail of the kimberlite cluster (Figure 1.2.2) and currently define the locations of the kimberlites (Figure 1.1.3).

Target selection from these more detailed magnetic maps relied on the eyes, experience and aims of the exploring parties. In the FALC area the kimberlites are clearly defined sub-circular broad 'bullseye' magnetic highs, 250m to 1300m in diameter, lacking large dipole negative anomalies; the signatures of the flat-lying crater facies. The extra-crater deposits of kimberlite often carry no magnetic anomaly, or only subtle signatures on the background gradients. To the north small kimberlite pipes (of carrot-shaped or cylindrical diatreme structure) were also located by magnetic means. These anomalies are much smaller than the broad crater facies, and have a strong dipole effect,

Figure 1.2.2.

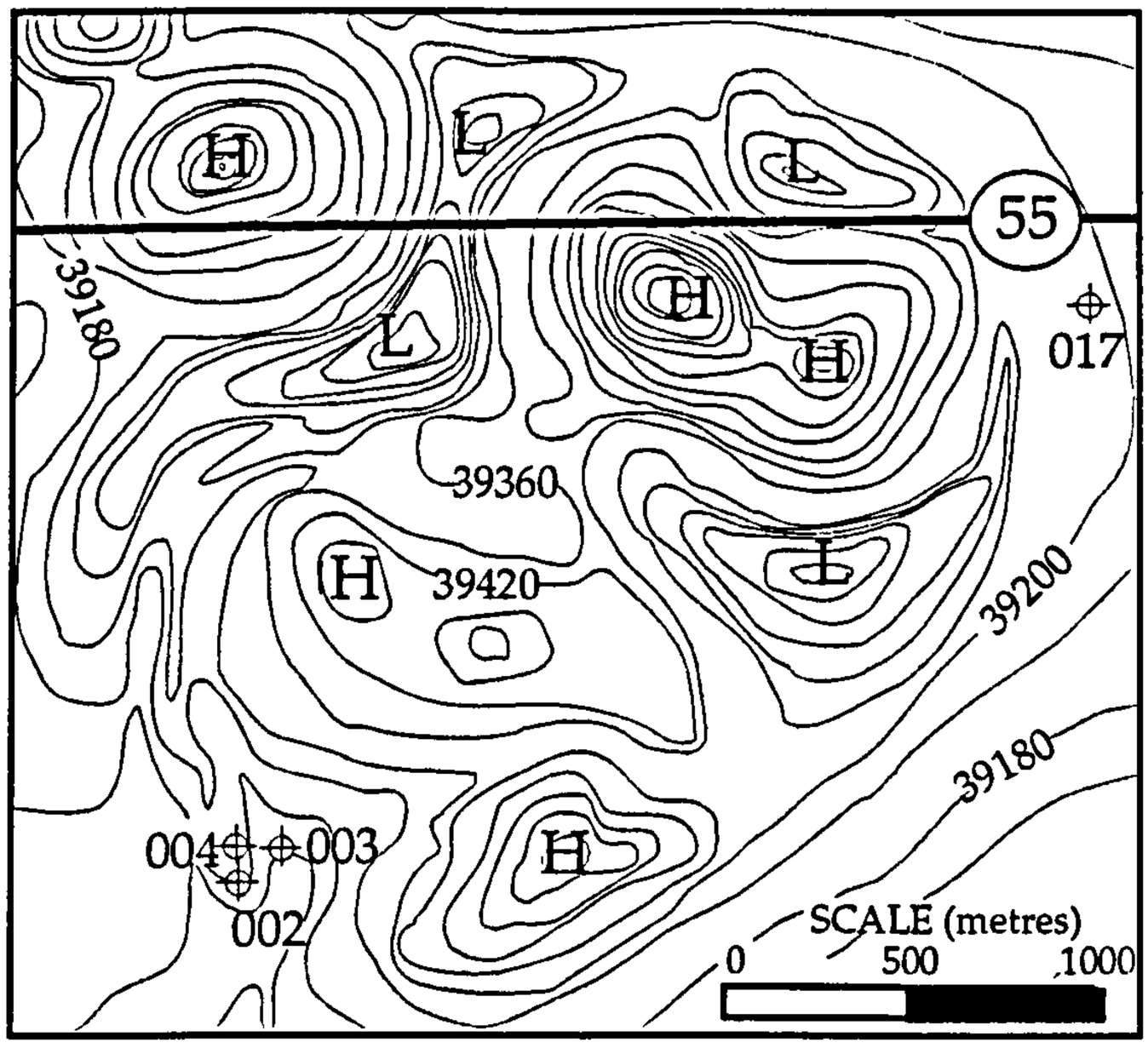

Detailed aeromagnetic map of the anomalies 4km east of Snowden, showing Highway 55 (latitude 55°35') and approximate borehole localities (see Fig 1.1.3). Contour interval is 80nT, flight line spacing was 100m.
Note complex magnetic contours of the broad crater structures, which also display some dipole effects (e.g. magnetic lows encircling north-eastern high).

Figure 1.2.3.

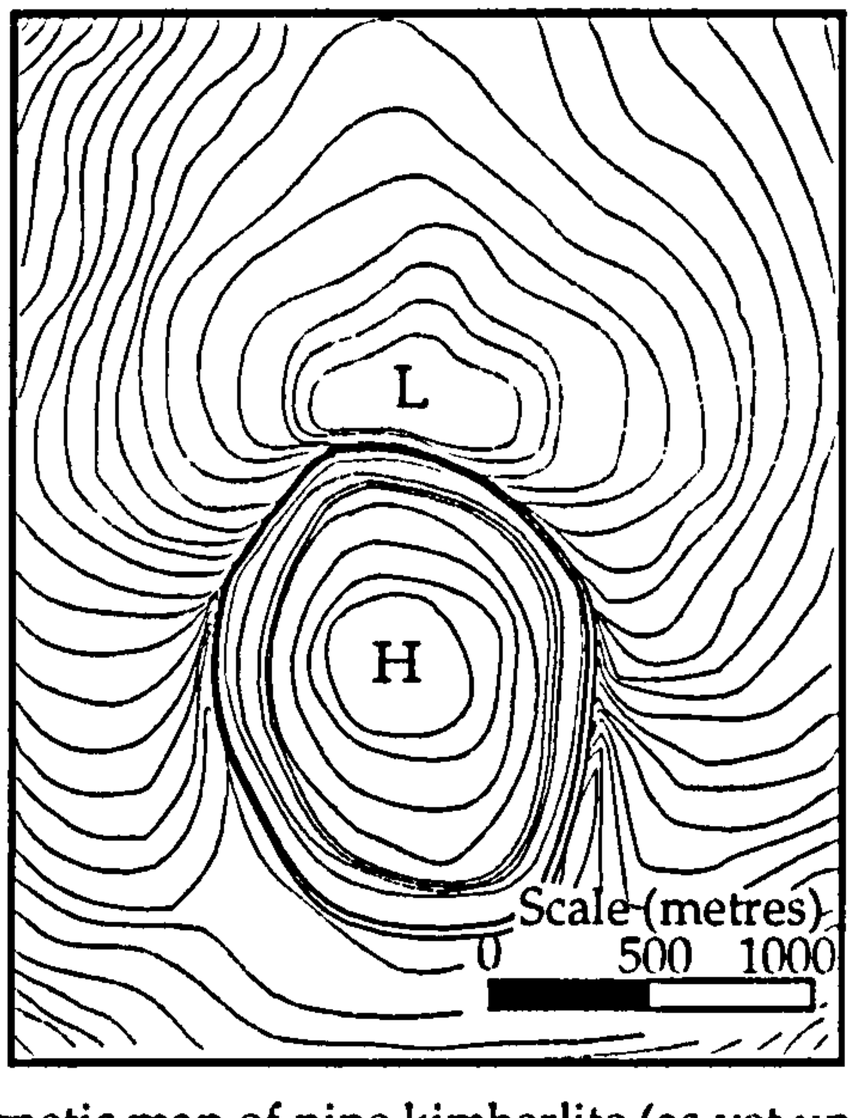

Aeromagnetic map of pipe kimberlite (as yet unproven by drilling). Contour spacing is 10nT, flight line spacing is 300m. This anomaly is located 25km north of Snowden (see Fig. 1.1.2.) Note the large diople effect, due to a vertical rather than horizontal magnetic body. Compare this single dipole low with the multiple, encircling lows of the horizontally disposed crater facies anomalies in the previous diagram.

giving an overall 'knotted wood' texture on the magnetic contour maps, Figure 1.2.3.

Whilst airborne surveys were carried out, many exploration groups simultaneously employed teams of ground magnetic surveyors to test individual anomalies. The scale of ground work ranged from hundreds of square metres to tens of square kilometres, depending on the extent of the anomaly. Lines were surveyed in and spaced from 25m to 250m depending on the detail required and the size of the budget. These give a tremendous amount of detail on individual anomalies, and allow assessment of terrain and any obvious anthropogenic sources of anomalies (e.g. steel grain silos, overhead cables and booster stations). The surveyed lines also provide a local geographic framework, and are used to position the drill hole sites exactly. Ground magnetic anomalies in FALC are typically 200 to 600nT (up to 1400nT) above the regional background, equating to 0.13% to 4% magnetite in buried kimberlite (Lehnert-Thiel et al, 1992).

More recently ground gravity surveys have been carried out in FALC, which have demonstrated that the kimberlites are some 0.18gcm^{-3} to 0.20gcm^{-3} denser than the surrounding Cretaceous sediments. The kimberlites produce positive Bouguer anomalies, typically of the order of 0.3milligals to 0.6milligals. These have been used to model thickness of the crater facies anomalies, which correspond fairly well with borehole data.

The only conclusive exploration method, of course, is to drill through the overburden and intersect kimberlite. In and around the FALC cluster at least one hundred test boreholes have been drilled, mostly by the FALC joint venture group over five years of exploration. Nearly all of these have intersected kimberlite, success due, no doubt, to the clarity of the magnetic anomalies, and the policy of drilling only within those anomalies. Forty-five of the seventy anomalies have been drilled and confirmed as kimberlite to date. Away from the obvious kimberlite craters at least seven drill holes have intersected extra-crater kimberlite, with a wide range in the degree of reworking and sedimentary admixture.

Exploration continues in the FALC cluster, with drilling on untested targets and bulk sampling for diamond content appraisal in the crater facies intersected. Beyond the crater facies at FALC and the pipes in the north, exploration has slowed and the staking rush ended. However interest remains in the extra-crater kimberlite facies and the sedimentary upgrading of diamond concentration in these rocks.

1.3 Phanerozoic cover of Central Saskatchewan

An understanding of the sedimentary cover in central Saskatchewan is vital to understand the surface environment that the kimberlites erupted in to and the processes that subsequently acted upon them. Details of the stratigraphy also provide additional information about the basin tectonic events, and therefore geodynamic conditions.

After the final cratonisation event of the North American craton (a stable area of continental crust that has not undergone orogenic reworking for at least 1Ga), at about 1.8Ga, there followed a prolonged period of erosion, peneplanation and non-deposition. This lasted to Cambrian times when a long-lived marine inundation occurred, depositing thick sequences of shelf carbonates over the western edge of the craton, as the on-craton part of a passive margin miogeocline sedimentary wedge (see reviews in Macqueen and Leckie, 1992). This general environment continued undisturbed into the latest Devonian, accumulating about 400m of sediment over 190Ma (note, this thesis uses the DNAG timescale, Palmer, 1983). Another period of non-deposition, with some erosion, lasted from Carboniferous to lower Cretaceous times. In the earliest Jurassic, changing plate motions in the proto-Pacific, thousands of kilometres to the west, caused the western passive margin of the North American craton to become subductive, accreting an allochthonous terrane over the shelf and margin deposits of the craton edge. The geodynamics of the subsequent Laramide orogeny, and its possible role in kimberlite volcanism, are discussed further in section 1.4.

Foreland basin filling in central Saskatchewan began in the Aptian (about 110Ma), with the Mannville group fluvial and nearshore sediments sourced from the east. Shallow marine sedimentation initiated in the late Albian (at around 102Ma to 105Ma, Figure 1.3.2), and was probably due to the global eustatic sea level rise (this global transgression is the highest long term sea level recorded (Leckie and Smith, 1992). Kimberlite volcanism occurred from about 102Ma to around 99Ma, and was subaerial with associated shallowing and input of kimberlite into the basin (see Chapter 4). Following the end of kimberlite volcanism the region rapidly subsided, the water depth augmented by peak transgression in the Turonian (at about 92Ma; see eustatic sea level curves in Haq, 1988). The water depth may have reached up to 300m during the mudstone deposition that followed to the end of the Cretaceous (Leckie et al, 1992). Further evidence of non-deposition and erosion, probably related to foreland basin tectonics (see section 1.4) are common in the mudstone sequence

(Simpson, 1982). The foreland basin sequence has been subsequently tilted, dipping by about 6° to the south, Figure 1.3.1.

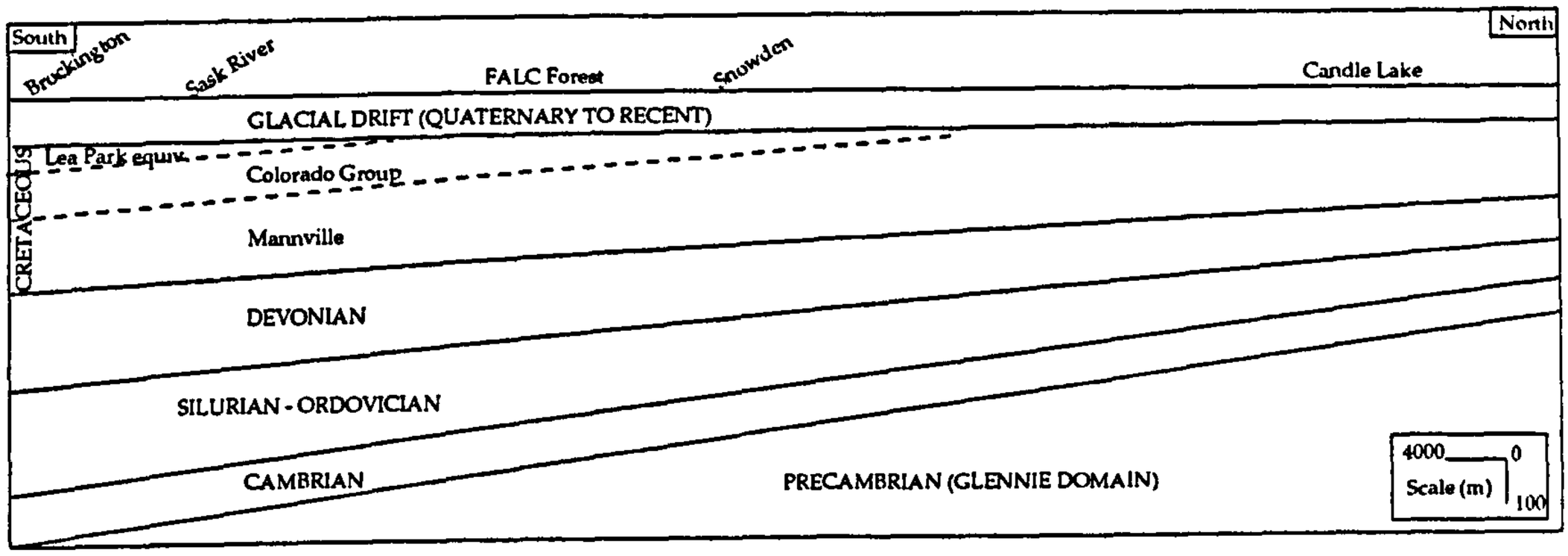

Figure 1.3.1.
Schematic stratigraphy to basement in the central Map Area (see Fig.1.1.2.). Thicknesses represent general trends, and do not account for local variation. Depth to basement in the north is about 480m, in the south about 940m. Vertical exaggeration on this diagram is x40.

To the north and east the Phanerozoic strata are eroded, most recently by glaciation, such that the Precambrian basement ('shield') is exposed about 100km north of FALC. In the map area (Figure 1.1.2) the sub-drift outcrop is of Upper and Middle Cretaceous strata in the southern and central areas, and Lower Cretaceous strata in the north, near Candle Lake, up to the shield exposure. The Devonian has only scattered outcrop at the shield boundary.

The depth to the crystalline basement in the map area (Figure 1.1.2) ranges from 480m in the north to 940m in the south, with a fairly constant slope. At the site of oil exploration borehole FALC52 (Kjarsgaard et al, 1995), on the eastern edge of the kimberlite cluster, depth to basement is 729m. Quaternary and Recent cover, mostly of glacial origin, is highly variable across the whole region, ranging from 60m to 120m, generally thicker in the south, typically 90m to 110m in FALC cluster. The thicknesses described below are derived from public access structural contour maps (Gent, 1992), and from the FALC52 borehole (Kjarsgaard et al, 1995). Regional thickness extrapolations can regarded as approximate, due to local variations in thickness, the error margin is at least ±10%.

1.3.1 Paleozoic

The Cambrian to Lower Ordovician sequence mostly comprises continental deposits. Typically there is a basal conglomerate containing clasts of the crystalline basement, overlain by shales interbedded with sands and arkoses

of the Cambrian Deadwood Formation, 90m to 185m thick. The strata from the Lower Ordovician to Upper Silurian consists of buff-brown dolomites of the Winnipeg Formation, Bighorn Group and Interlake Formation. The Upper Silurian Interlake Formation thins out and is absent in the north of the map area. Overall thickness is about 135m, thinner in the north of the map area.

These continental deposits are overlain by Devonian deposits of the Ashern, Winnipegosis and Dawson Bay Formations; a thick sequence of reef (corals and algal mats dominate) and shelf (precipitate) pale brown to red dolomites (Gent, 1992). These occur with sporadic red mudstone and bentonite horizons. Within this sequence are often thick evaporite deposits of potash, halite and minor clay beds and red bed clastics ('Prairie Evaporite Sequence'). These beds occur well to the south of the map area, showing mobilisation and recrystallisation features. It is unclear if evaporites exist in the map area in patches (and not yet intersected in boreholes), or once existed but have been removed (by dissolution or mobilisation), or were never deposited. The Upper Devonian consists of about 50m of pale grey limestones and dolomites of the Souris River Formation. Overall the Devonian sequence is 220m thick in the south, thinning to about 50m in the north. The top of the Souris River Formation represents a long hiatus in the sedimentary sequence, often with well developed paleosols, as the overlying deposits are of Lower Cretaceous age.

1.3.2 Mesozoic

During the Cretaceous, the foreland basin over central North America was flooded by a shallow epicontinental ocean up to 1500km wide east to west. To the south the ocean linked with the warm, saline, low oxygen waters of the Gulf of Mexico, and linked to the north with the cool, oxygenated waters of the Arctic Ocean (Hay et al, 1993). Mixing of these water masses had a profound influence on circulation and biological activity in the basin, and therefore on the sediments deposited. To the west was the newly developing Rockies Cordillera of the Laramide orogenic belt, tectonically and volcanically highly active (Fermor and Moffat, 1992). To the east lay the flat continental shield, partially covered with Paleozoic platform sediments. Between the shorelines lay the Western Canadian Sedimentary Basin (WCSB). The western half of the basin was a rapidly subsiding foredeep in response to the development of the Cordillera. The active orogenic belt also provided a substantial sediment supply for the WCSB, rapid uplift of terranes providing copious siliciclastics and volcanic activity providing basin wide bentonitic deposits and a steady airfall of ultrafine particles into suspension. The eastern half of the basin was much shallower with

lower subsidence rate and more prone to migration of the shoreline. Sediment supply in this region was still dominantly from the west, but eastward-sourced coarser deposits (mostly of reworked sediments) are common. Fort a la Corne lies in the centre of the eastern region. Between the basinal domains is the peripheral bulge, termed East Meridian Hinge Zone (EMHZ, Leckie and Smith, 1992), a zone of crustal flexure and uplift in the foredeep. The effects of uplift on the EMHZ, associated tectonics further west and global sea-level fluctuations on the shallow ('back-bulge') basin are significant. These include: widely migrating shorelines, local unconformities, reworking, condensed or missing sequences and anomalous lowstand deposits (Leckie and Smith, 1992). These features are common in the FALC area. Due to confusion with the local stratigraphy, most kimberlite workers (Scott-Smith et al, 1995; Lehnert-Thiel et al, 1991) in FALC name the Lower Colorado deposits as the Ashville Formation. The Ashville Formation is defined from work on the Manitoba Escarpment 600km south-east, and is in fact geographically limited to southern and western Mantioba (McNeil and Caldwell, 1981). The Saskatchewan equivalent is actually the Big River Formation (Simpson, 1982). However, in a recent review of the stratigraphy of the Albian and Cenomanian (approximately 105Ma to 93Ma) WCSB, Bloch et al (1993) define a holistic four-fold stratigraphy useful across the whole basin and used herein, Figure 1.3.2. In the following detailed description of the Mannville and Colorado groups reference should be made to Figures 1.3.3 and 1.3.4 cross sections of the map area.

Mannville Group

Unconformably overlying the Devonian are the continental deposits of the Lower Cretaceous Mannville Group, sourced from the north and east. This Group comprises up to five Formations, however in the map area three have been identified, Cantaur and Pense (Kjarsgaard et al, 1995), and the Colony. In the map area the uppermost Mannville Group is thought to be either the marine Pense Formation underlain by the more fluvially-dominated Colony and Cantaur Formations, or the Pense is misidentified Spinney Hill or Joli Fou Formations. A detailed Mannville stratigraphy in the map area is not complete, and varies considerably from author to author. Like all of the Mesozoic strata these sediments are unlithified, sands are patchily cemented, and mudstones rarely have developed fissility.

The Mannville was deposited in the Early Cretaceous, and is composed of a variable succession of interbedded shales silts and sands, representing a range of continental fluvio-deltaic to nearshore marine depositional

Figure 1.3.2.

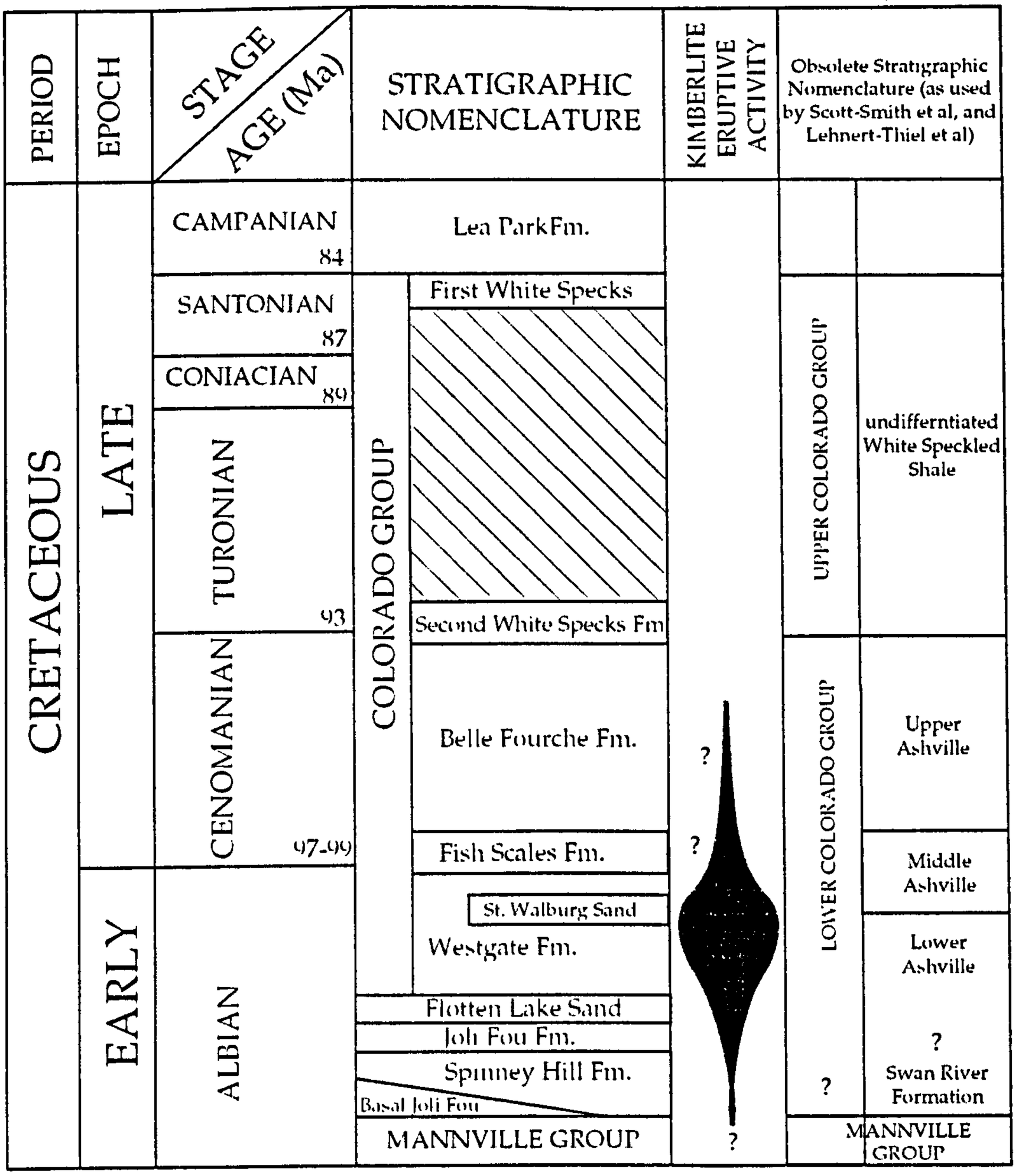

Stratigraphic nomenclature for the map area.
Adapted for this study from Bloch et al (1993), based on borehole core logged by the author and Brent Jellicoe (Kensington Resources Ltd). Dates (determined by radiometric means) from Obradovich (1991), DNAG timescale used (Palmer, 1983).
Stratigraphic notes accompanying text: i) Basal Joli Fou , immediately overlying the Mannville Group has been variously identified as the the Basal Colorado, Basal Spinney Hill or the Swan River member of the Mannville. Here it is interpreted as a western-derived distal deposit representing earliest Joli Fou strata. ii) In the absence of the Viking Fm. the base of the Colorado Group is underlain by the Flotten Lake Sand. This unit is often unrecognised. iii) Fish Scales Fm. is very poorly developed in the map area, and rarely recognised. Simpson (1982) suggests a constant thickness of 2m to 3m in the Map Area. iv) Diagonal ruling represents an erosional event at some point during Turonian to mid-Santonian times (about 93Ma to 86Ma). How prolonged this erosion and/or non-deposition event lasted is unknown.
Note peak kimberlite activity during the Westgate times (around 100Ma), derived from stratigraphic contacts (this author, see Chapter 2). Biostratigraphy and radiometric dating of zircon in kimberlite places Smeaton kimberlite at 99Ma (Kjarsgaard et al, 1995). Kimberlite age of 94Ma to 96Ma from phlogopite reported for central cluster crater (Lenhert-Thiel et al, 1992). Various undated thin kimberlite beds also reported in Spinney Hill and Mannville strata (this author; Nixon and Leahy, 1995; Kjarsgaard et al, 1995; Scott-Smith et al, 1995).

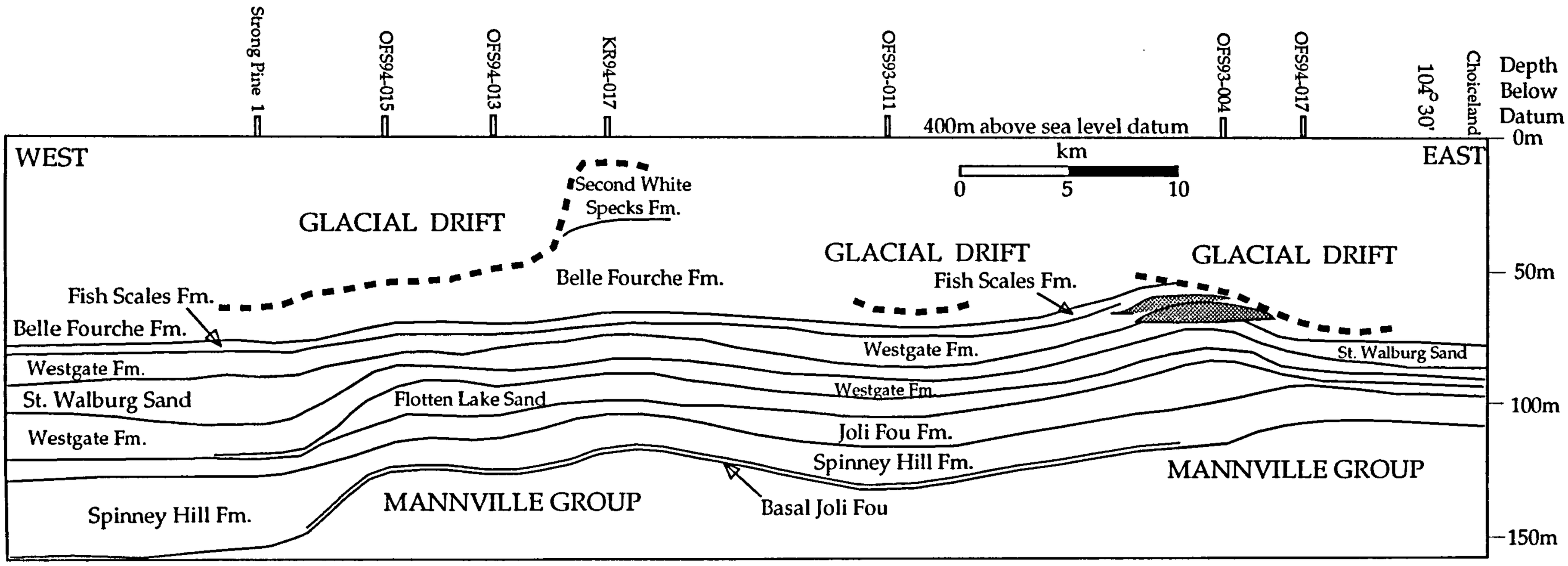

East-West cross section of Cretaceous Stratigraphy in the map area. Depths on right are nomalised to **Depth below 400m a.s.l. Datum.** Stratigraphic nomenclature is described in Fig.1.3.2. E-W section follows approximately latitude 53° 25' to 30' Refer to map Figs.1.1.2. and 1.1.3. for borehole and town locations. All boreholes, execpt Strong Pine 1 (from Simpson, 1982), have been logged by this author and Brent Jellicoe (Kensington Resources). Schematic shaded beds in OFS93-004 represent kimberlite strata. Note the apparent doming of the Mannville Group beneath areas where kimberlites are intersected.

Figure 1.3.3.

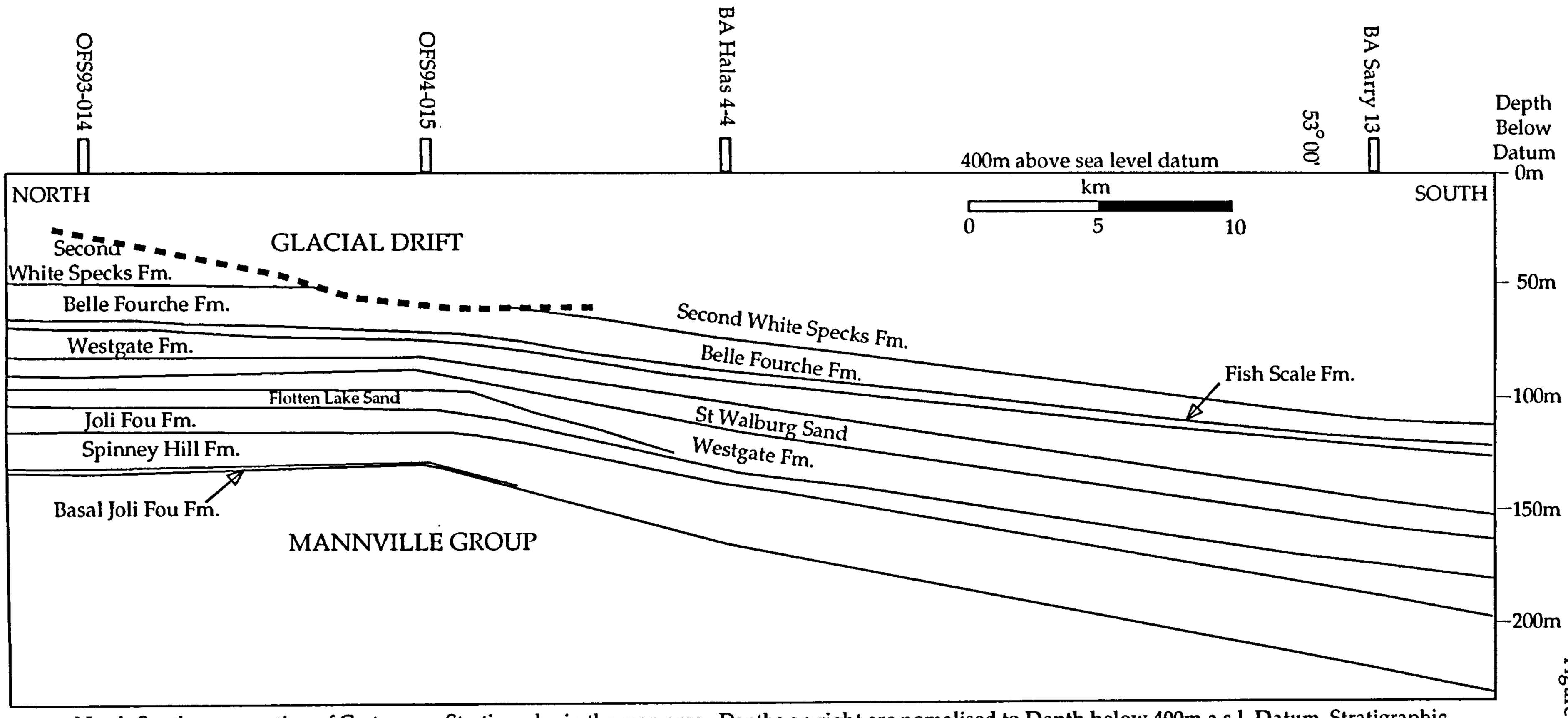

North-South cross section of Cretaceous Stratigraphy in the map area. Depths on right are nomalised to Depth below 400m a.s.l. Datum. Stratigraphic nomenclature is described in Fig.1.3.2. N-S section follows approximately longitude 105°05' to 15' Refer to map Figs.1.1.2. and 1.1.3. for borehole locations. Note that BA Sarry 13 lies 3km south of the southern edge of the Map Area, and this section is generally to the west of the kimberlite cluster Boreholes BA Sarry 13 and BA Halas 4-4 are from Simpson (1982), others have been logged by this author and B.C. Jellicoe (Kensington Resources Ltd).

Figure 1.3.4.

environments. The fluvio-deltaic facies consists of typical cross-stratified and fining-up channel sands. These are often very fine to medium sand grade, coloured white to buff and completely unlithified, with rare pyrite and carbonate cementation. Drilling through these sands is problematic because the sand fluidises in the drilling mud and jams the rods. However in the FALC region the uppermost sand of this type (the first encountered when drilling) is often tightly cemented with pyrite, a useful marker for the top of the Mannville. Other fluvio-deltaic lithotypes include coals (up to 1m thick), seatearths (paleosols with rootlets), lacustrine brown/grey shales, lagoonal black shales and interdistributary silts. These are intercalated with brackish to marine deposits or nearshore and estuarine facies. Typically these rocks are fine grained (silts and shales) with intense bioturbation and rare marine fossils. The nearshore lithofacies indicates that water depth during marine incursion remained shallow.

Kimberlites are reported in the Mannville strata (Scott-Smith et al, 1995; Kjarsgaard et al, 1995). These occur as thin (1m to 5m thick and laterally restricted), carbonate-rich, pale grey, crystal-rich olivine tuffs or reworked pyroclastic kimberlite. They are interpreted by Scott-Smith et al. as small, single-eruption, tuff cones, with no crater development, and precursors to the much larger kimberlites in the Colorado Group.

Spinney Hill Formation

Immediately overlying the top of the Mannville Group is the Spinney Hill Formation. This transgressive sand unit is derived from the east, probably with some reworking of the Mannville Group, and thins to the west (Simpson, 1982). In the map area it is typically 9m to 14m thick. The unit is composed of interbeds (up to 3m thick) of laminated silty shales, black to grey muds, argillaceous medium to gritty sands ('chaotic units') and fine to medium sand wisps, laminae and burrow-fill. Glauconite and bioturbation occur to varying degrees throughout, and organic debris (including fish bones, scales and shell fragments) is moderately common in the shale-dominated lithologies, see Plate 1.1 in Figure 1.3.5. These deposits are fully marine (indicated by the presence of glauconite), and represent fairly quiet shallow environment, the sandy component being introduced by tidal currents (Simpson, 1982). The Spinney Hill environment of the map area was less sand-dominated than the typical environment (producing 30m thick subarkoses and subgreywackes) described further south by Simpson.

The 'chaotic units' are useful markers, two or three separated by 2m of silts and shales are usually encountered near the base of the Spinney Hill in the

Figure 1.3.5

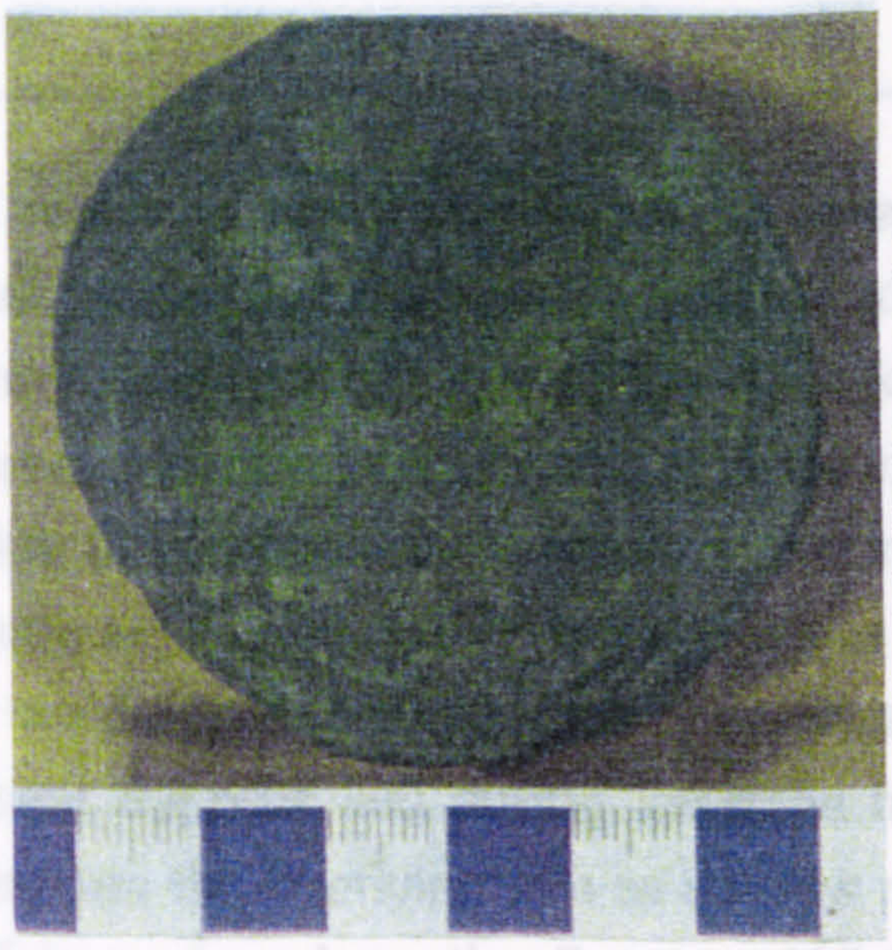

Plate 1.1
Bedding plane view of highly glauconitic laminae in very fine silts of the Spinney Hill Formation. (Scale bar is cms)

Plate 1.2
Bedding plane with concentration of fish debris (mostly scales in this example), from the upper Westgate Fm.

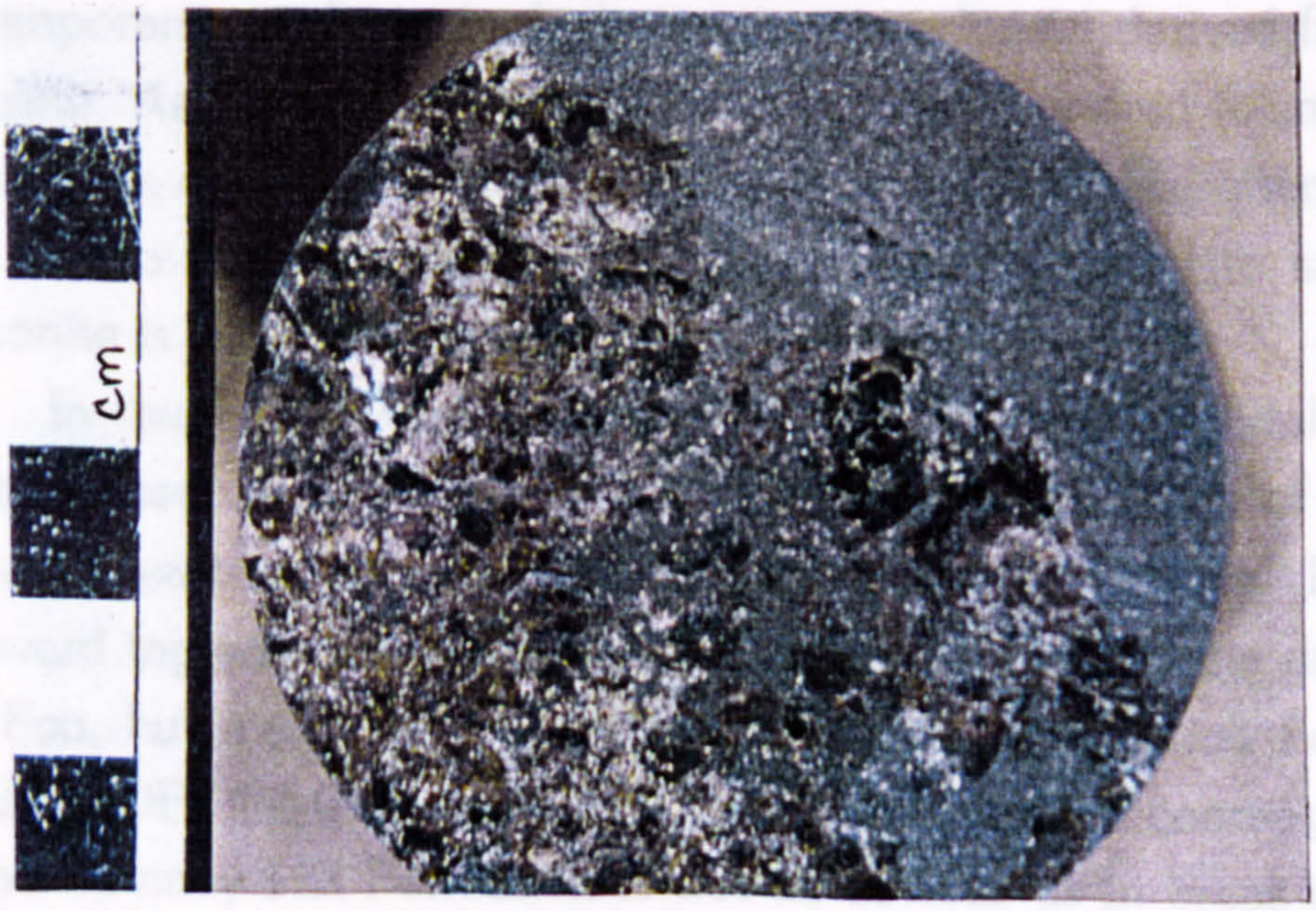

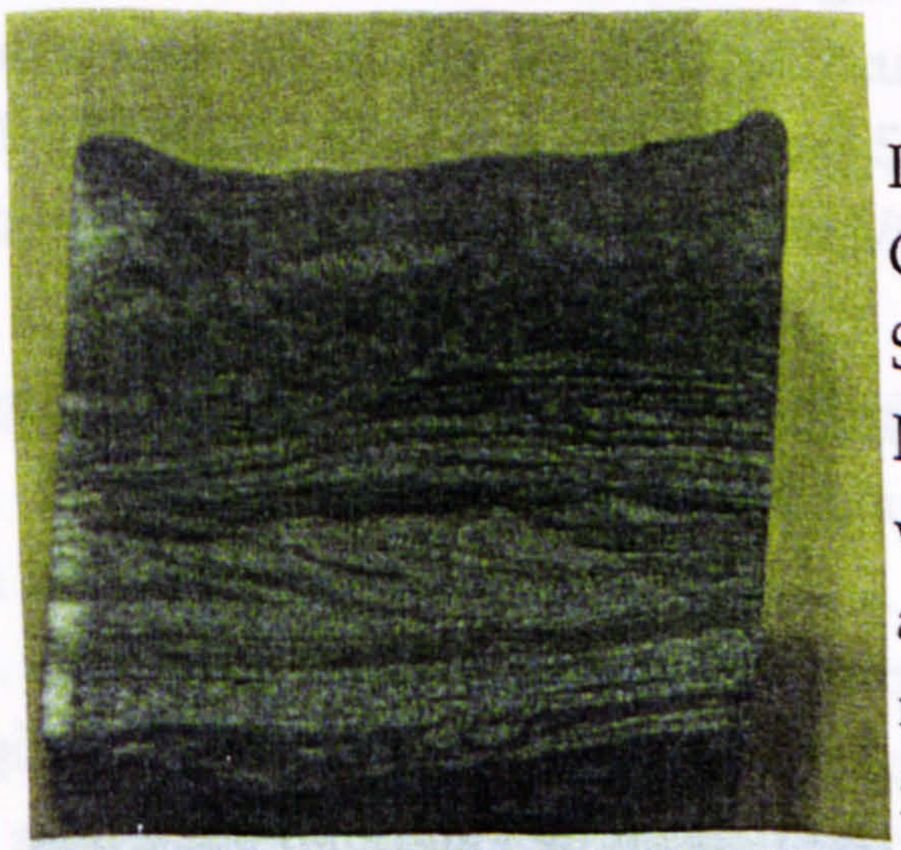

Plate 1.3
Core section of typical St Walburg Sand member of the Westgate Fm. Note the fine to medium sands with ripple cross-stratification and shaley partings. The dark material on the ripple forsets is fine glauconitic concentrations.

FALC region. They comprise poorly sorted 5cm to 30cm thick grits, often with scoured bases and a large amount of admixed silt and shale. The clasts are angular to sub-rounded quartz and lithic (chert, shales, sands) grains, with rarer pyroxene and opaque (probably ilmenite or spinel) grains. They are overlain by silts rich in glauconite, bioturbation and ripple cross-stratified fine sandy wisps and laminae. These may be interpreted as storm deposits, with the coarse, gritty clasts washed westwards from the shoreline. Alternatively the 'chaotic units' represent deposits laid during lowstand in a shoreline environment. This may also explain the overlying silts as shallow nearshore tidal deposits. This lowstand model is preferred, as the Spinney Hill is a transgressive sequence and basal lowstand deposits are expected in the initial shallow phases of flooding.

Joli Fou Formation

Whilst the Spinney Hill Formation represents coarse sediment supplied from the eastern shoreline of the Albian WCSB, the Joli Fou Formation is a contemporaneous deposit which represents sediment derived from the western shoreline. As the western shoreline was several hundred kilometres away, the deposits are of distal facies; very fine grained black shales, often calcareous with pale silty to fine sand laminae. Bioturbation is restricted to sandy layers, and glauconite is less common than in the Spinney Hill.

In the WCSB, deposition of the Joli Fou (from a distal western source) started penecontemporaneously and ended after deposition of the Spinney Hill (proximal eastern shoreline source). Typically the Spinney Hill comprises a westward tapering tongue of sandy material overlain by the dark shales of the Joli Fou, but may in places also be underlain by thin Joli Fou strata (e.g. in borehole OFS 94-015). However in the map area the coarse-grained character of the Spinney Hill Formation is not as obvious as in areas to the south (see Simpson, 1982). Therefore, although from different sources, the two formations are of similar lithology, difficult to discern, and can be considered mixed. The thickness of the Joli Fou and Spinney Hill are defined by the base of the Flotten Lake Sand (equivalent to the Viking Formation), described below.

Flotten Lake Sand - Viking Formation equivalent

In the WCSB the Joli Fou and equivalents are separated from overlying strata by the Viking Formation. This is a western-derived sand-dominated unit, often with cross-stratification, shaley partings, coal and wood fragments. It is thought to represent barrier island and tidal sand ridge deposits, to more distal shelf sand body deposits (Simpson, 1982). The Viking pinches out well to the

south and west of the map area, and no directly associated strata have been identified in borehole core. The Flotten Lake Sand, a minor sand body that thickens towards a proximal north-west high (Meadow Lake Escarpment, MLE), occupies the same stratigraphic position as the Viking Formation. The unit is represented by coarsening-up, grey, fine and medium sands, and sandy to silty muds, 7m to 9m thick in the map area. The unit has been interpreted as migrating shelf sand ridges and bars, prone to deposition in shallow marine conditions (shoaling). Thus thickening towards the MLE may be due to shallow water depth conditions in that region, rather than any sediment source derived from the 'escarpment'.

With the absence of the Viking Formation, and sporadic recognition of the Flotten Lake Sand, the shale dominated Joli Fou Formation is often not differentiated from the shale dominated Westgate Formation that overlies it. In borehole OFS 94-015 the upper boundary of the Joli Fou/Spinney Hill is against Flotten Lake Sand and has a combined thickness of about 24m. Further east into the north-centre of the FALC cluster OFS93-011 the combined thickness is about 28m. Extrapolation from cross-sections in Simpson (1982) allow the equivalent Viking strata to be placed at 660' in the Strong Pine No.1 borehole (section G-G', p.23). Here the top of the Mannville Group is at 770', therefore the combined thickness is about 30m to 35m. This borehole is located 6km south-west of the nearest kimberlite, 25km west of the main FALC cluster.

Colorado Group

In the field area from mid-Albian to the end of the Santonian stage (approximately 102Ma to 84Ma; Obradovich, 1991), fine-grained marine deposits hosting the kimberlites were deposited. This is the Colorado Group, representing a complex interplay of various marine formations, with sediment source regions both eastwards and westwards. In addition, active basin-wide tectonics and sea-level fluctuations have led to reworking of previous deposits, and disconformities are common throughout. Introduction of billions of tonnes of kimberlite into the area further complicates the stratigraphic record (see Figure 1.3.2).

Westgate Formation and the St.Walburg Sand

The Westgate Formation (previously called lower Big River, or mistakenly the lower and/or mid Ashville) is composed of finely interbedded shales, silts and fine sands. Shales are non-calcareous and organic poor, the silts occur as wisps or thin beds with scoured bases. Bioturbation is absent at the base,

becoming more common towards the top of the Formation (bounded by the base of the Fish Scales Formation). Glauconite is rare to absent, pyrite and siderite are rich in patches, fish and shell debris (mostly pelcypod) is moderately common, see Plate 1.2 in Figure 1.3.5. Some bentonite beds occur within the unit. The Westgate is derived from the western shoreline, and the deposits in the map area represent typical distal shelf muds.

Within the upper portion of the Westgate Formation is the St. Walburg Sand, this is derived from the same basin-high (MLE) as the Flotten Lake Sand, but is generally thicker, better developed and more extensive. Being fairly distal from its main depositional area, the St.Walburg in the map area is rather thin (5m to 20m) and fine grained. In boreholes K94-016 and K94-017 it comprises coarse silts interbedded with laminated shales which grade up to grey-green, glauconitic, coarsening-up, fine and medium sands with ripple cross-stratification and shaley partings, see Plate 1.3 in Figure 1.3.5. Like the Flotten Lake Sands these are interpreted as migrating shelf sand ridge and bar deposits. These strata are overlain by more typical fine grained marine deposits of the Upper Westgate which is bounded by the Fish Scales Formation. The depth to the Fish Scales Formation has been extrapolated, again from the Strong Pine No.1 borehole (Simpson, 1982, p.23), and suggests a total thickness for the Westgate Formation of about 30m to 40m.

The Westgate Formation represents the final deposits in the Albian stage, giving an absolute age of 97Ma to 99Ma (Obradovich, 1991). It is during this formation's depositional milieu that all the kimberlites thus far dated by stratigraphic means were erupted, particularly in the Lower Westgate.

Fish Scales Formation

In the map area the westward-sourced Fish Scales Formation is not easily recognised. The Formation consists of a basal thin gritty pebble conglomerate, overlain by 15m of organic-rich black shales and silts (lacking bioturbation), and a number of bentonite beds. Fish debris (scales, teeth and bones) is very common, often concentrated on individual bedding planes. Biostratigraphy indicates an earliest Cenomanian age (about 97Ma to 98Ma), and a lack of any foraminiferal assemblage (Bloch et al, 1993). The die-off of foraminifera, and the macrofossil features; abundant animal remains and lack of bioturbation, all suggest a period of basin water toxicity. This may be due to a water mixing event causing fatal environmental change to the established biota. Although undoubtedly a basin-wide event (Leckie et al, 1992), the Formation is very difficult to detect in the map area as the marker pebble conglomerate is missing,

and is otherwise similar to the underlying Westgate and overlying Belle Fourche Formations. An extrapolation of the Fish Scales in the Strong Pine No.1 borehole (Simpson, 1982, p.23) suggests that about 5m to 10m of shale strata exists, unrecognisable as the Fish Scale Formation in the map area.

Belle Fourche Formation

Grading upwards from the Fish Scales is the Belle Fourche Formation, a fine grained marine succession deposited slowly throughout the Cenomanian (about 93Ma to 97Ma). The Belle Fourche is equivalent to what has been previously named the middle to upper Ashville, or the upper Big River Formation. Biostratigraphy clearly illustrates deposition of the marine Belle Fourche in early, middle and late Cenomanian (Bloch et al, 1993), with no basin-wide evidence of a 3Ma depositional hiatus suggested by Scott-Smith et al (1995). More local depositional influences, however, cannot be ruled out. The Formation comprises slightly calcareous grey to black shales and more brownish fine silts, bioturbation and shell debris is common, but organic carbon is generally low. Fine sands are rare, and occur as wisps, burrow fill and laminae. A number of thin bentonites occur in the Formation. The depositional environments were quiet shallow marine conditions, with local reworking frequently resulting in disconformity. In the central and easterly regions of the map area this Formation subcrops beneath the Quaternary till (Figure 1.1.6). Where the succession is uneroded the Belle Fourche is 15m to 25m thick.

Second White Specks Formation

The Belle Fourche is overlain by a basin-wide marine deposit of the Second White Specks Formation deposited at the end of the Cenomanian (about 93Ma to 94Ma). The base of the Formation is commonly used as a horizontal datum across the WCSB. The Second White Specks consists of an organic-rich calcareous shale with an abundance of bioclastic material, mostly coccoliths, faecal pellets and rarer shell fragments. Bioturbation is not intense, and often absent. Bentonites are common, especially towards the base. This deposit represents a deep marine environment, a significant change from the previous Formation. This Formation and overlying strata contain no eruptive kimberlite, placing a constraint on the end of kimberlite activity at 93Ma.

In the FALC region the Second White Specks is partially eroded to about half its normal thickness and is disconformably overlain by the First White Specks, a similar deposit of end Santonian age (about 84Ma). The disconformity represents a period of 7Ma to 9Ma, during which erosion occurred. The First

White Specks represents the youngest sub-crop in the southern and western part of the map area (Figure 1.1.6), and is the youngest deposit to survive glacial erosion in the FALC area.

1.4 The cratonic basement and geodynamic evolution of Central Saskatchewan

As described in the sections above, the crystalline basement in the map area lies 480m to 960m below the surface, shallowing to the north. The nature of the basement can be extrapolated southwards from the shield outcrop, about 100km to the north, by large scale gravity and magnetic trends (Figures 1.1.3 and 1.1.4), and is fairly well constrained (Gent, 1992). The basement of Saskatchewan can be considered cratonic, comprising two Archean cratons, Hearne to the east and Superior to the west, 'welded' into a Proterozoic mobile belt, called the Trans-Hudson Orogen (THO), which curves through the Province (Figure 1.4.1). Most of central Saskatchewan is underlain by the THO, and in the map area by three domains; LaRonge in the west, Glennie in the centre and east and the Kisseynew Domain immediately to the east of the area (Figure 1.4.2).

The LaRonge domain subcrops the Phanerozoic west of Prince Albert, underlying the Sturgeon Lake area. It comprises mostly low grade mafic to felsic metavolcanics and subordinate metasediments. The Kisseynew Domain is composed mainly of high-grade metasedimentary migmatites (Lewry et al, 1994).

The central region, called the Glennie Domain (GD), comprises tectonically emplaced (aged 1.83Ga to 1.79Ga) arc volcanics and arc sediments bordered by shelf sediments of allochthonous origin (terranes). These Proterozoic rocks overlie an Archean core (Sm-Nd model age of 2.3Ga in borehole core 50km east of FALC, Collerson et al, 1989) composed of mylonitic and gneissic rocks, with scattered windows outcropping at surface along minor anticlinorial and thrust axes in the north (Figure 1.4.2).

Evidence from seismic reflection east-west profiling (LITHOPROBE at 55°N) confirms that the THO is a broadly anticlinal structure (Lewry et al, 1994). The entire THO is tectonised by transpressional structures, including thrusts and strike-slip faults, some of which extend into the lower crust. The deep structure of the GD consists of two lower crustal wedges, under both the eastern (Superior) and north-western boundaries (Hearne), i.e. GD underlies both cratons (Figure 1.4.3). The LITHOPROBE section includes a 48km crustal

Figure 1.4.1.

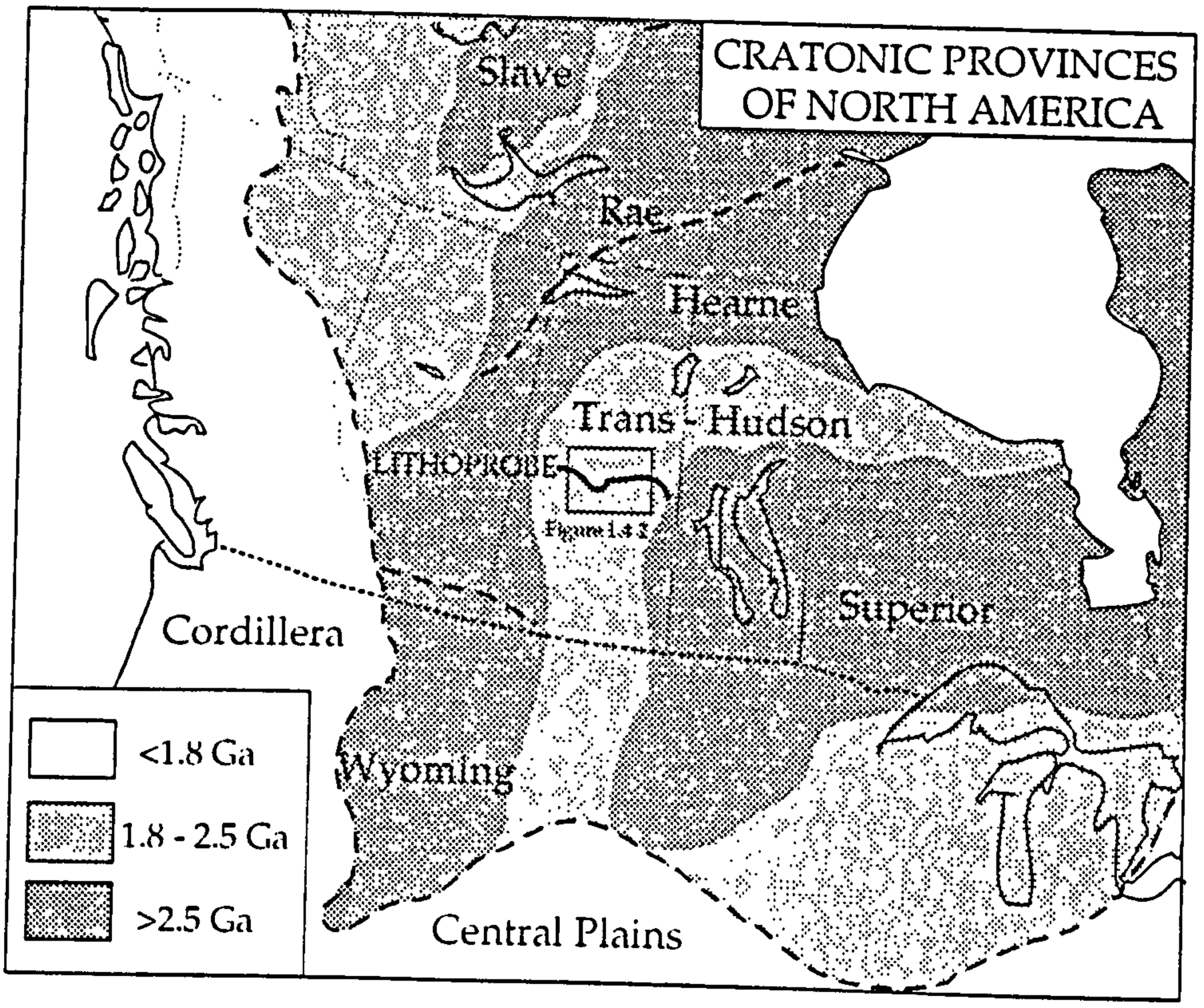

Map of Cratonic Provinces of North America and the approximate position of the LITHOPROBE seismic line (see Figure 1.4.3). Ages of regions are given in the lower left box, location of Figure 1.4.2 shown in central box.

Figure 1.4.2

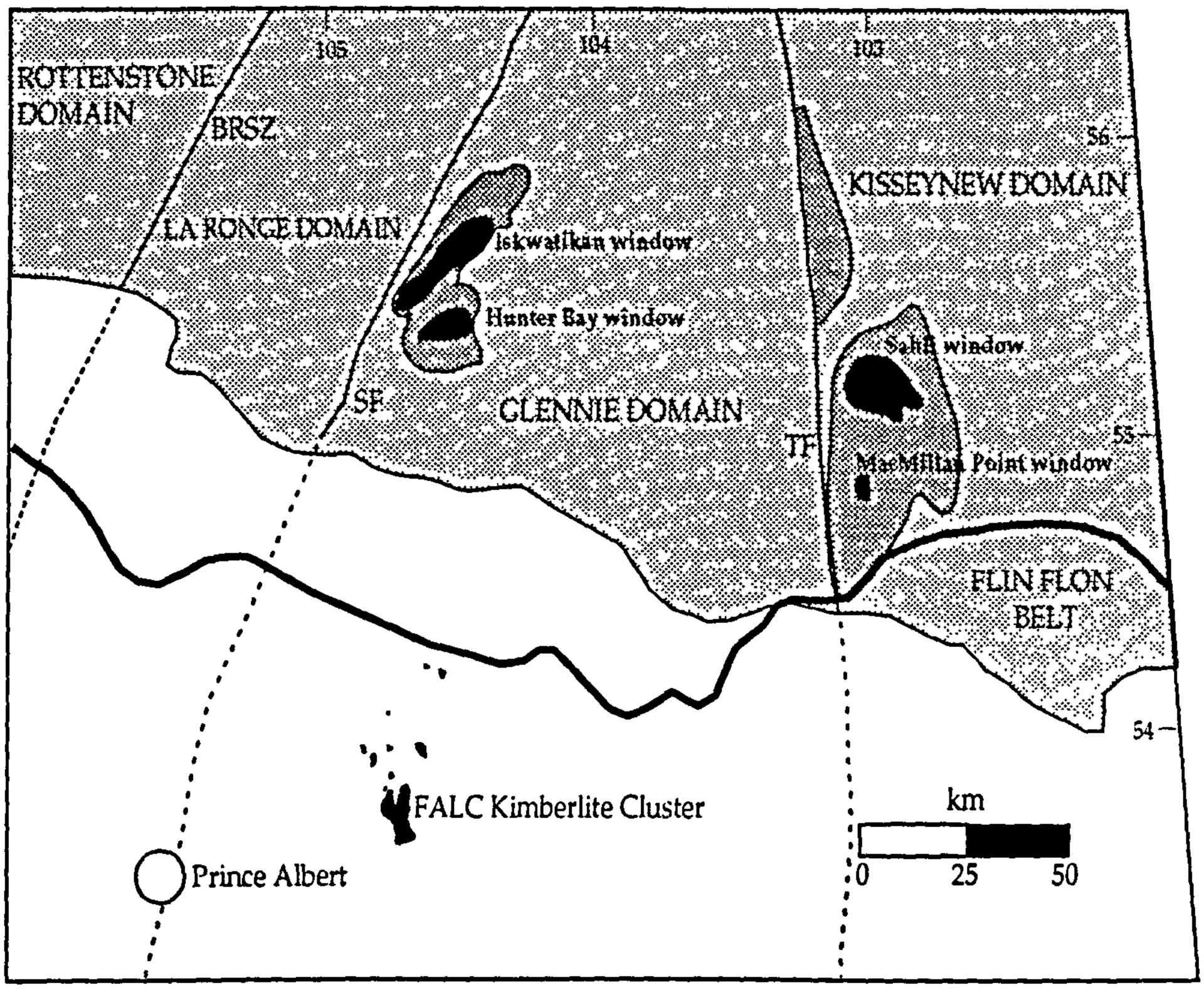

Domain map of the Trans Hudson Orogen. Shaded areas represent Precambrian Shield and south of this is the Phanerozoic cover sequence. Domain boundaries are extrapolated beneath the cover, supported by regional gravity and magnetic maps. Boundaries as follows: BRSZ = Birch Rapids Shear Zone, SF = Stanley Fault, TF = Tabbernor Fault. Black ornament in the shield represent Archean windows, the deepest structural levels that outcrop at surface. These are surrounded by Proterozoic ductile shear zones. Note the kimberlites occur in the western-central part of the Glennie Domain. The root zone lies immediately to the west of the cluster. The thick black line represents the seismic line of LITHOPROBE (see Fig.1.4.3). This diagram was adapted from Lewry et al (1994).

Figure 1.4.3

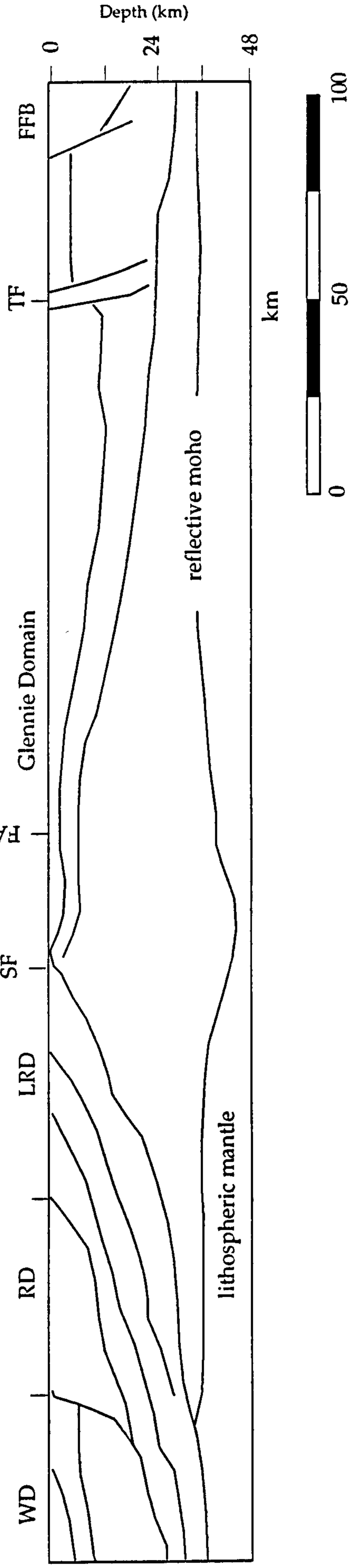

Interpretative geological cross-section of Line 9 LITHOPROBE (See Fig.1.4.2.). Central antiformal feature is the top of the Archean Glennie Domain, which lies between the Stanley Fault and the Tabbenor Fault, dipping beneath each bordering domain. Note the broad extent of the massif, and the root beneath the crest. Abbreviations as follows: FFB = Flin Flon Belt, TF = Tabbernor Fault, SF = Stanley Fault, LRD = La Ronge Domain, RD = Rottenstone Domain and WD = Wollaston Domain. FALC denotes northwards projected location of kimberlite cluster. Adapted from Lewry et al (1994).

root situated in the western half of the GD, a significant Moho topography of about 12km over 60km (½-wavelength). When correlated to the current topography the root zone occurs below Prince Albert. However, the root zone may not be present in a linear fashion along the entire north-south strike of the THO western boundary (Ellis et al, 1996).

By the end of cratonisation in this region of the North American plate, at about 1.7Ga, the crustal thickness was about 35km, with a root up to 48km thick. Under the GD the presence of Archean diamonds (see Chapter 6) indicates the lithosphere was of cratonic thickness (a minimum of about 150km).

Cratonisation in the mid-Proterozoic was followed by a prolonged period of erosion, and development of a passive margin about 1100km to the west. This margin developed a wedge of miogeoclinal shelf, slope, coastal and platform sediments from late Proterozoic times until the onset of the Laramide orogeny in the early Jurassic. In the central Saskatchewan area, platform sediments were deposited from the Cambrian onwards (see section 1.3).

The Laramide orogeny was initiated in the early Jurassic (about 200Ma) by thrust loading of the allochthonous terranes grouped as the Intermontane Superterrane (Stockmal et al, 1992). This loaded the plate margin and initiated lithospheric flexure and thrust-stacking of the miogeoclinal sediments wedge, but did not produce significant topography above sea-level (Stockmal and Beaumont, 1987). Foreland basin fill started in the foredeep around the mid-Jurassic (160Ma), and continued throughout the orogeny. Stratigraphic analysis of Jurassic to Tertiary strata in the foredeep, places a maximum distance of 400km to the peripheral bulge from the deformation front (Plint et al, 1993). This locates the bulge about 300km to 400km to the west of the FALC region, Figure 1.4.4). In central Saskatchewan broader scale lithospheric subsidence is not in evidence until the early Cretaceous (about 120Ma) with the Mannville deposits sourced from the eastern shield regions (Leckie and Smith, 1992).

Kimberlite volcanism at FALC, peaking at 100Ma, has a number of contemporary tectonic events in the WCSB and bordering Laramide orogeny, Figure 1.4.5. Eastward subduction was underway, about 1300km to the west, but subduction remnants would only directly influence the lower mantle under the FALC region if the subduction angle was lower than 30°, or if the cooler material travelled eastwards along some mantle thermocline (such as the base of the lithosphere, or over the upper/lower mantle boundary at 670km). Evidence from seismic tomography indicates that subduction angle was steep (about 60°), and that thermoclines are not currently active (Grand, 1994). Docking of the

Figure 1.4.4

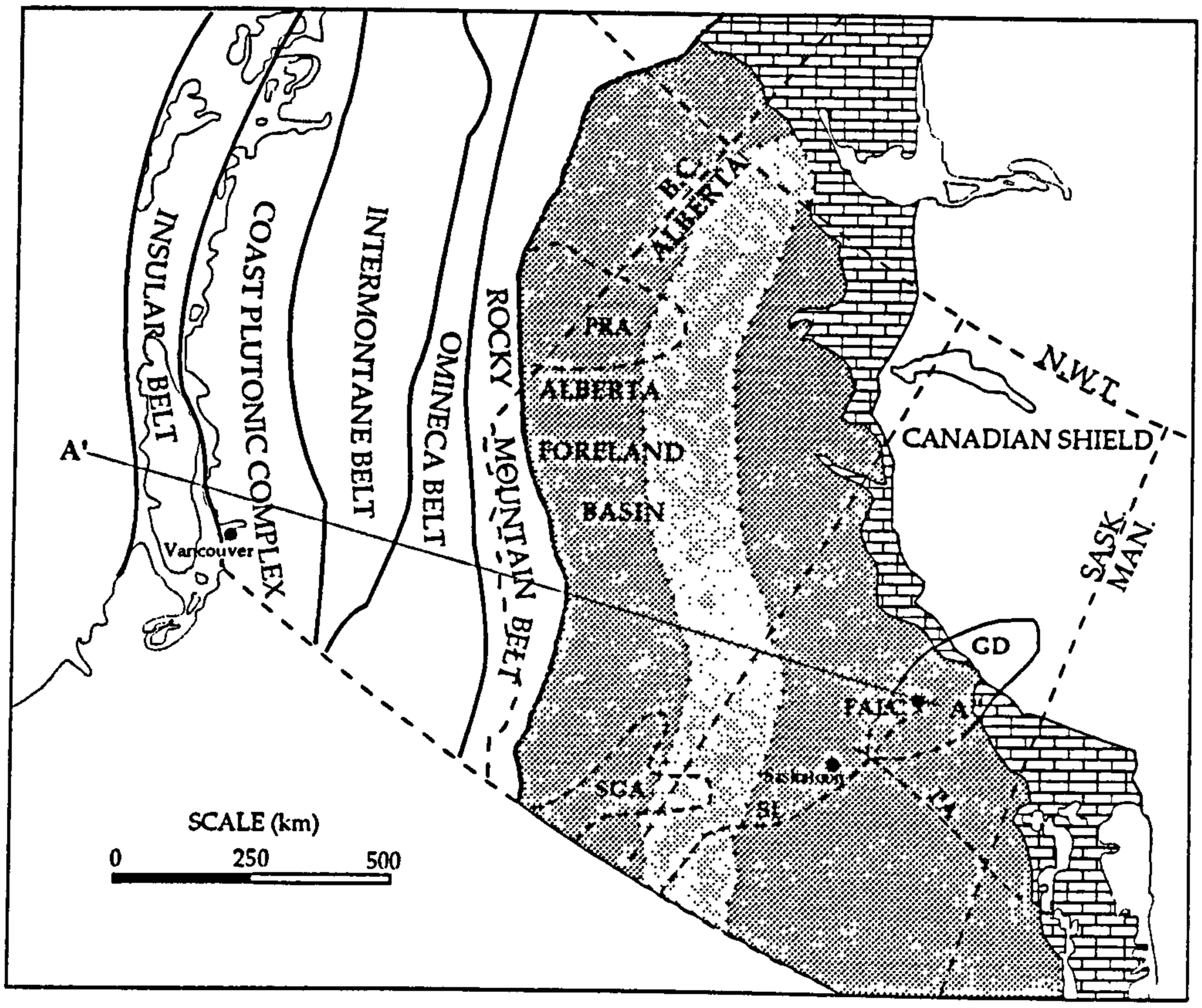

Tectonic subdivisions and features of the Western Canadian Sedimentary Basin and Candian Cordillera. From Stockmal et al (1992), basin tectonic features and outline of Glennie Domain from Gent (1992) and Lewry et al (1994). Brick ornament indicates Paleozoic miogeoclinal shelf deposits (mostly carbonates). Shaded area indicates foreland basin fill (Jurassic to Tertiary), paler dotted band illustrates approximate location of the peripheral bulge determined by stratigraphic analysis (Plint et al, 1993). Note the bulge occurs at least 250km west of the FALC kimberlites, too far to influence either magma generation or crustal location, see Fig. 1.4.5 (section A'-A" shown above). Abbreviations as follows: PRA = Peace River Arch, SGA = Sweetgrass Arch, SL = Shaunavon Linear, PA = Punnichy Arch, GD = Glennie Domain, FALC = Fort a la Corne kimberlite cluster.

Figure 1.4.5.

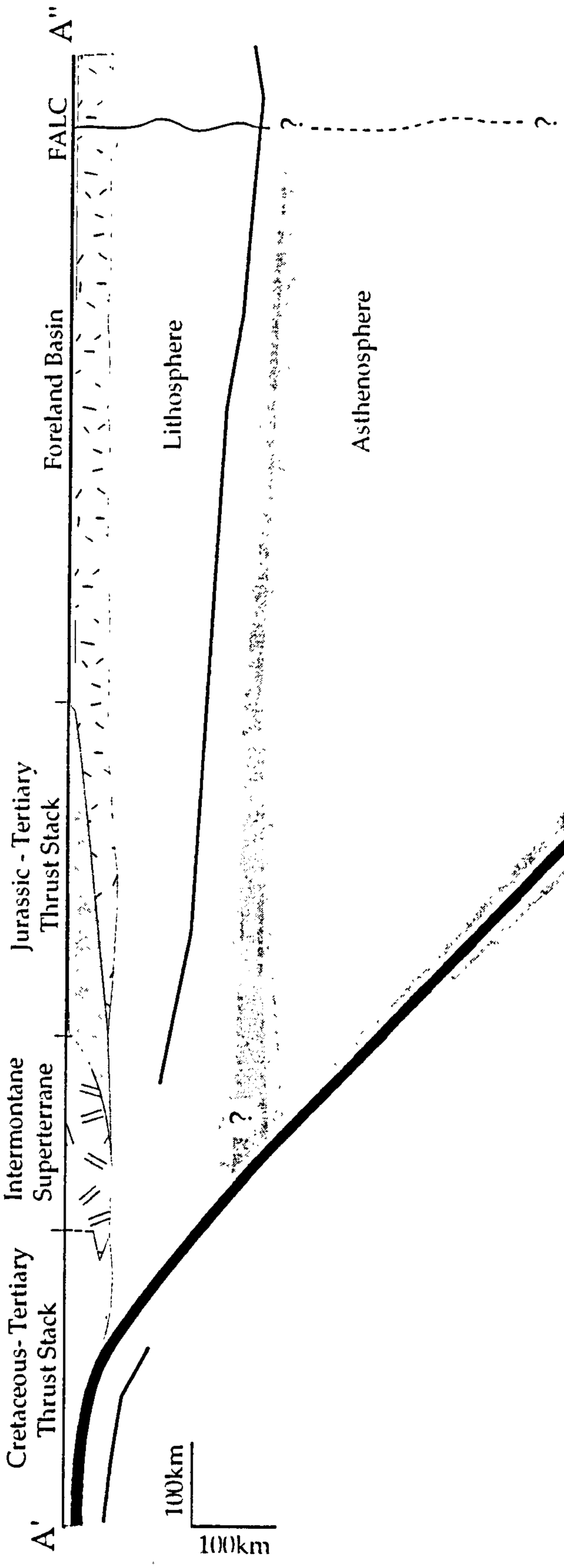

True scale simplified cross section of western Canada, including the Cordilleran thrust belts and the foreland basin. Proposed thermal triggers for FALC kimberlite magma generation illustrated: i) subduction influence along an asthenosphere thermocline, or base of the lithosphere. ii) indirect or non-subduction influence from plume at 670km discontinuity. Note thermal gradients are denoted schematically by shaded mantle areas, and are not present in the modern mantle (as indicated by seismic tomography; Grand, 1994). Lithospheric boundaries are conjectural. shown are realistic (from Stockmal et al, 1992 and Lewry et al, 1994), lithos

second superterrane (the Insular group) was completed at about 105Ma (Fermor and Moffat, 1992), resulting in further lithospheric flexure, thrust-stacking, peak calc-alkaline volcanism, regional metamorphism in the accreted terranes and initiation of subduction of the oceanic Farallon plate. The timing of tectono-volcanic peak is also contemporaneous with changes in the velocity of the North American plate (relative to reference hotspots). At about 100Ma the velocity was at a relative high of 5cm/a, compared to lows of 1.5cm/a at 125Ma and 75Ma (Armstrong, 1988).

Lateral stresses at the base of the lithosphere have been identified as a factor in triggering kimberlite volcanism by mobilising a kimberlitic proto-magma, generated by a fertilisation event that may have occurred somewhat earlier. For example, the Slave craton kimberlites (Tertiary) have been explained in terms of terrane collision in the later phases of the Laramide orogeny (Helmstaedt and Gurney, 1995).

Large scale tectonic features in the basin itself include the Sweetgrass, Punnichy and Peace River arches and the Shaunavon linear (Figure 1.4.4), broad anticlines that developed in response to the forces generated during oblique subduction (Gent, 1992). The FALC region is situated at the northern end of the Shaunavon linear, over the eastern slope of the Glennie Domain root zone. Effects of arching may be in evidence from the contour map of the depth to top Mannville Group, Figure 1.4.6. The apparent doming in areas overlain by kimberlites are so local that a thermal effect must be ruled out, and this probably also rules out regional arching effects. The top Mannville bulges may due to piles of kimberlites erupted during the Mannville depositional milieu as precursors to the main kimberlite activity, or the result of differential compaction of kimberlite relative to the surrounding muddy strata.

After the orogenic tectono-volcanic peak of 105Ma to 95Ma there is a period of quiescence lasting to the end of the Cretaceous. The combination of lithospheric flexure and subsidence, with a global sea-level highstand, floods most of the North American craton, depositing deep-shelf marine sediments over the whole foreland basin and beyond.

Other kimberlites and related rocks (e.g. lamproites and olivine melilitites) that occur on the North American craton cannot be directly related to the FALC cluster due to the great distances involved. Penecontemporaneous kimberlites and lamproites are located over 900km to the south (at the Colorado-Wyoming State-line) and 1500km to the north (Slave craton kimberlites), may have a similar orogeny-related genesis. This is also the currently favoured model for kimberlite generation world-wide (Helmstaedt and Gurney, 1995).

Figure 1.4.6

Depth to top Mannville Group contour map. Depth shown as metres below 400m a.s.l. datum. Note that domes locally occur at the top of the Mannville where kimberlites have been intersected (Figure 1.1.3). This may be due to: localised pre-eruptive thermo-tectonic doming; thicker Mannville where precursor kimberlites (of Mannville age) have been erupted; or due to later differential compaction of strata resulting in doming of areas overlain by the relatively competent kimberlite. The latter two models are preferred.

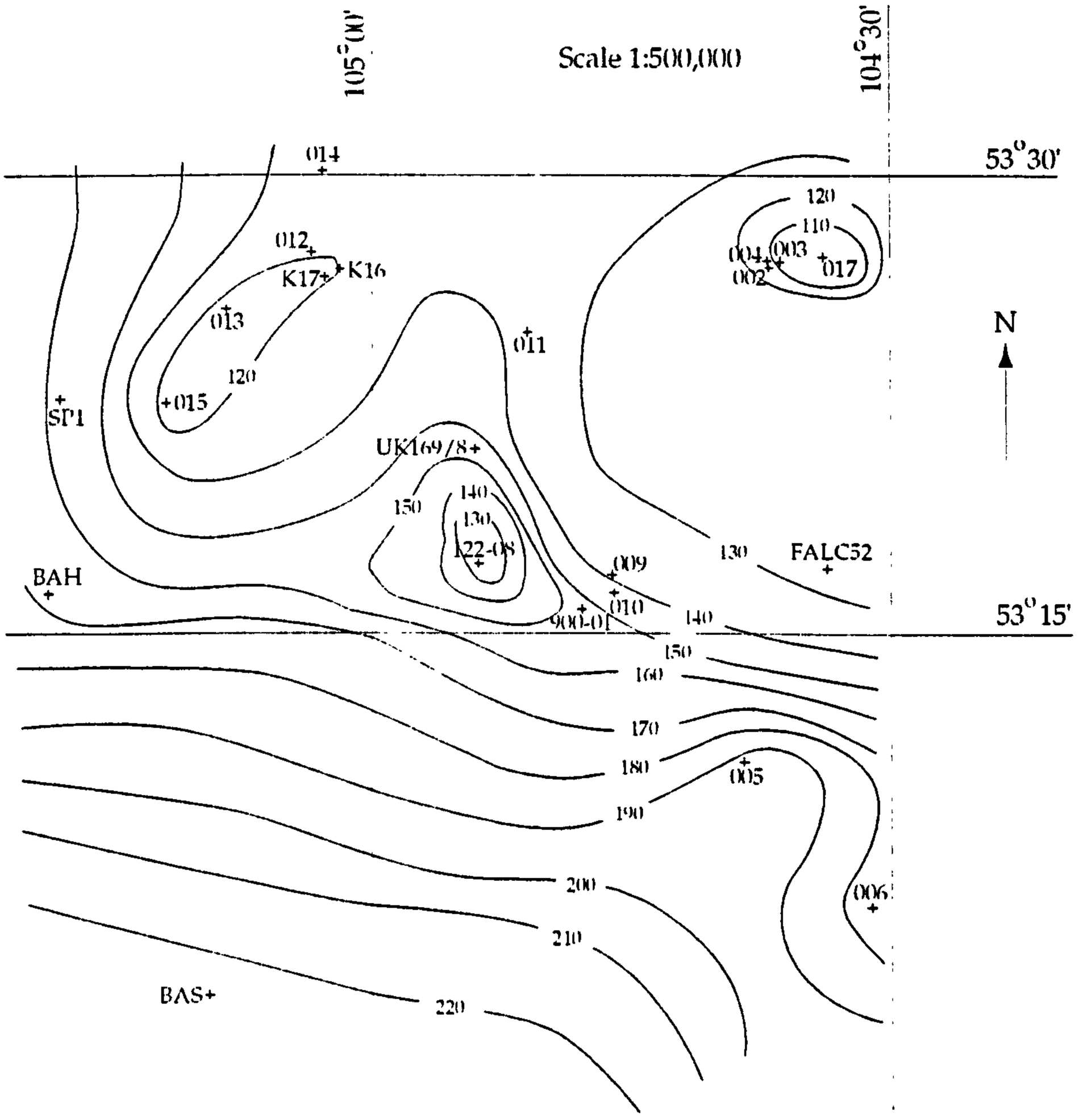

Borehole code key:
- all boreholes of the format 0xx (e.g. 006) are OFS 93-0xx (e.g. OFS 93-006) drilled by Rhonda Mining Corp. (and partners).
- K16 and K17 are FC-94-016/017 drilled by Kensington Resources Ltd.
- 122-08 and 900-01 are FALC Joint Venture boreholes (data released by Kensington Resources Ltd.)
- UK169/8 and FALC52 are boreholes reported in Kjarsgaard et al (1995), drilled by the GSC.
- SP1, BAH and BAS (Strong Pine No.1, BA Halas and BA Sarry) are boreholes described in Simpson (1982).

In summary the geodynamic evolution of the Laramide orogeny, largely controlled by plate motions, and their influence on the North American craton initiated kimberlite volcanism in FALC. Specific controlling elements are likely to be the lateral stresses generated at the base of the lithosphere when large terranes are accreted during orogeny. Subducted plate material may also play a role in inducing kimberlite magma formation. Crustal structures such as the root under the Glennie domain and the Shaunavon linear may have influenced the precise location of eruption. Crustal uplift and lithospheric flexure on peripheral bulge (or EMHZ) has been suggested as both a trigger and crustal control of the kimberlite volcanism (Nixon et al, 1993). This must be discounted, however, as recent stratigraphic analysis (Plint at al, 1993) indicates the bulge is located at least 300km to the west and south-west of FALC.

References cited in Chapter 1

- Armstrong, R.L. (1988). Mesozoic and early Cenozoic magmatic evolution of the Canadian Cordillera. In Clark, S.P., Burchfiel, B.C. and Suppe, J. (eds.) Processes in continental lithospheric deformation. Geological Society of America, Special Paper 218, p.55-92.
- Bloch, J., Schröder-Adams, C., Leckie, D.A., McIntyre, D.J., Craig, J., Staniland, M. (1993). Revised stratigraphy of the lower Colorado Group (Albian to Turonian), Western Canada. Bulletin of Canadian Petroleum Geology Vol. 41, No.3. p.325-348.
- Christiansen, E.A. and Whitaker, S.H. (1976). Glacial thrusting of drift and bedrock. In Leggert, R.F. (ed.), Glacial Till, Royal Society of Canada Special Publication No.12, p.121-130.
- Collerson, K.D., Lewery, J.F., Van Schmus, R.W. and Bickford, M.E. (1989). Sm-Nd isotopic constraints on the age of the buried basement in central and southern Saskatchewan. In Saskatchewan Energy and Mines, Misc. Report 89-4, p.168-171.
- Ellis, R.M., Hajnal, Z. and Bostock, M.G. (1996). Seismic studies on the Trans-Hudson Orogen of Western Canada. Tectonophysics (in press).
- Fermor, P.R. and Moffat, I.W. (1992). Tectonics and structure of the Western Canadian Foreland Basin. In Macqueen, R.W. and Leckie, D.A. (eds.) Foreland Basins and Fold Belts, AAPG Memoir 55, p.81-107.
- Gent, M.R. (1991). Diamond exploration in Saskatchewan. Proceedings of Canadian Institute of Minerals and Mines (Geology Division), 1st Annual Field Conference, Saskatoon.
- Gent, M.R. (1992). Diamonds and precious gems of the Phanerozoic basin, Saskatchewan: Preliminary Investigations. Saskatchewan Energy and Mines Open File Report 92-2.
- Grand, S.P. (1994). Mantle shear structure beneath the Americas and surrounding oceans. Journal of Geophysical Research, Vol.99, p.11591-11621.
- Hay, W.W., Eicher, D.L. and Diner, R. (1993). Physical oceanography and water masses in the Cretaceous Western Interior Seaway. In Caldwell, W.G.E and Kauffman, E.G. (eds.) Evolution of the Western Interior Basin, GAC Special Paper 39, p.297-318.
- Haq, B.U., Hardenbol, J. And Vail, P.R. (1988). Mesozoic and Cenozoic chronostratigraphy and cycles of sea-level change. In Wilgus et al (eds.) Sea level changes: an intergrated approach. SEPM Special Publication No.42, p.71-108.
- Helmstaedt, H.H. and Gurney, J.J. (1995). Kimberlites - why, where and when? A hierarchy of geotectonic controls. Proceedings of the 6th International Kimberlite Conference, Russia 1995, Extended Abstracts Volume.
- Kjarsgaard, B.A., Leckie, D.A., McIntyre, D.J., McNeil, D.H., Haggart, J.M., Stasiuk, L. and Bloch, J. (1995). Smeaton Kimberlite Drill Core, Fort a la Corne Field, Saskatchewan. Geological Survey of Canada Open File 3170, pp.57.

- Leckie, D.A. and Smith, D.G. (1992). Regional setting, evolution, and depositional cycles of the Western Canadian Foreland basin. In Macqueen, R.W. and Leckie, D.A. (eds.) Foreland Basins and Fold Belts, AAPG Memoir 55, p.9-47.
- Leckie, D.A., Singh, C., Bloch, J., Wilson, M. and Wall, J.H. (1992). An anoxic event at the Albian-Cenomanian boundary: the Fish Scale Marker bed, northern Alberta, Canada. Paleogeography, Paleoecology. Paleoclimatology, Vol.92, p.139-166.
- Lehnert-Thiel, K., Loewer, R., Orr, R.G. and Robertshaw, P. (1992). Diamond-bearing kimberlites in Saskatchewan, Canada: The Fort a la Corne Case History. Exploration Mining Geology Vol.1 No.4 p.391-403.
- Lewry, J.F., Hajnal, Z., Green, A., Lucas, S.B., White, D., Stauffer, M.R., Ashton, K.E., Weber, W. and Clowes, R. (1994). Structure of a Paleoproterozoic continent-continent collision zone: a LITHOPROBE seismic reflection profile across the Trans-Hudson Orogen. Tectonophysics Vol.232, p.143-160.
- Lucas, S.B., White, D., Hajnal, Z., Lewry, J.F., Green, A., Clowes, R., Zwanzig, H., Ashton, K., Schledewitz, D., Stauffer, M., Norman, A., Williams, P.F. and Spence, G. (1994). Three dimensional collisional structure of the Trans Hudson Orogen, Canada. Tectonophysics Vol.232, p.161-178.
- Macqueen, R.W. and Leckie, D.A. (1992). Foreland Basins and Fold Belts. Association of American Petroleum Geologists, Memoir 55
- McNeil, D.H. and Caldwell, W.G.E (1981). Cretaceous rocks and their foraminifera in the Manitoba Escarpment. GAC Special Paper 21, pp.439.
- Nixon, P.H., Gummer, P.K., Halabura, S., Leahy, K. and Finlay, S. (1993). Kimberlites of volcanic facies in the Sturgeon Lake area. Russian Geology and Geophysics, Vol.34, No.12, p.66-76.
- Obradovich, J.D. (1991). A revised Cenomanian-Turonian time scale based on studies from the Western Interior United States. Abstracts with Programs, GSA, 1991 Annual Meeting, San Diego, CA., p.A296.
- Palmer, A.R. (1983). The decade of North American geology, geologic timescale. Geology V.11, p.503-504.
- Plint, A.G., Hart, S.H. and Donaldson, W.S. (1993). Lithospheric flexure as a control on stratal geometry and facies distribution in Upper Cretaceous rocks of the Alberta foreland basin. Basin Research Vol. 5, p. 69-77.
- Scott-Smith, B.H., Orr, R.G., Robertshaw, P. and Avery, R.W. (1995). Geology of the Fort a la Corne Kimberlites. Proceedings of the 6th International Kimberlite Conference, Russia 1995, Extended Abstracts Volume.
- Simpson, F.R. (1982). Sedimentology, palaeoecology and economic geology of Lower Colorado (Cretaceous) strata of West-Central Saskatchewan. Saskatchewan Energy and Mines Report 150.

- Stockmal, G.S. and Beaumont, C. (1987). Geodynamic models of convergent margin tectonics: the southern Canadian Cordillera and the Swiss Alps. In Beaumont, C. and Tankard, A.J. (eds.) Sedimentary basins and basin forming mechanisms, Canadian Society of Petroleum Geologists, Memoir 12, and Atlantic Geoscience Society, Special Publication 5, p. 393-411.
- Stockmall, G.S., Cant, D.J. and Bell, J.S. (1992). Relationship of the Stratigraphy of the Western Canada Foreland Basin to Cordilleran Tectonics: Insights from Geodynamic models. In Macqueen, R.W. and Leckie, D.A. (eds.) Foreland Basins and Fold Belts, AAPG Memoir 55, p.9-47.

CHAPTER 2 - TEXTURAL CLASSIFICATION AND PETROGRAPHY OF FORT A LA CORNE KIMBERLITES

Abstract

This chapter describes six kimberlitic borehole intersections, focusing from large scale strata descriptions of macroscopic features, to hand sample and heavy mineral descriptions, followed by thin section description and point counting, and finally using electron microscopy to describe textures and chemistries on the micron scale. From these observations, grain-shape point-counting in particular, interpretations are made and a textural-genetic classification is devised (mainly adapted from existing pyroclastic nomenclature, based largely on Schmid (1981)). There are two main kimberlite genetic classifications, pyroclastic and reworked pyroclastic kimberlite (PK and RPK). Lithologies of PK type are fine to coarse tuffs and lapilli-tuffs. These may be either crystal or lapilli dominated, and lithics are common. Note that in the classification used in this thesis, the term 'lapilli-tuff' refers to a pyroclastic rock with a grain size >2mm, and the term 'lapilli' refers to the pyroclastic aggregated grain. Lithologies of the RPK are diverse, and include volcaniclastic silts to grits in massive, graded and laminated strata. Also in this group are marginal and shallow marine tuffaceous basin clastics (10% to 50% volcaniclastic material), mostly of silt and sand grade.

Three main kimberlite facies environments are recognised, crater, proximal (tuff ring) and distal. Each contain a different suite of lithologies, as defined by the classification presented in the final section:

Crater Facies: Typically the most common rock types are lapilli dominated lapilli-tuffs, and crystal dominated lapilli-tuffs. These may be interbedded and overlain by any of the reworked deposits, particularly the various pyroclastic sands and intraclast breccias (comprising large angular shale clasts, and typically kimberlitic matrix).

Proximal Facies: These commonly have a basal layer of coarse tuff of tephra-fall origin, overlain by massive or bedded pyroclastic sands, in turn overlain by graded pyroclastic sands. Intraclast breccias may occur, but are not well developed. Tuffaceous clastics may overlie the pyroclastic sands.

Distal Facies: The most common deposits are tuffaceous clastics, but thin (<2m) beds of massive pyroclastic sand may occur. Thin graded and bedded pyroclastic sands have not been observed, but may also be expected. No primary airfall deposits are likely to have been deposited (although very thin kimberlitic ultrafine ash beds are possible).

The recognition of particular lithologies in a borehole succession should, therefore, allow a general facies to be assigned for that locality.

Other data presented in this Chapter are the results of heavy mineral separations of the kimberlite intersected in the boreholes previously described. These give quantitative proportions of some minerals, and clearly show that heavy minerals, such as garnet and ilmenite, are of higher concentration in RPK relative to PK. The heavy mineral separation coupled with thin section and electron microscopy illustrates the altered nature of the kimberlites at FALC, with all the matrix and nearly all of the grains being replaced by serpentine, carbonate and magnetite. A model for the sequence of diagenesis is proposed, containing three phases of diagenetic alteration, including a pervasive serpentinisation event, and a recent authigenic growth. These events were preceded by magmatic alteration of phenocrysts and xenocrysts. Also point counting of olivine grains (now replaced) in thin section is demonstrated to discriminate between PK and RPK in extra-crater deposits, which is a useful aid to kimberlite exploration in the extra-crater environment.

2.1 Large-scale features of kimberlite strata.

Within this section six boreholes are used to illustrate the three main facies observed. These are:

i) Crater Facies kimberlite. Borehole OFS 93-012
ii) Proximal Extra-Crater kimberlite. Boreholes OFS 93-002, 003, 004, 009.
iii) Distal Extra-Crater kimberlite. Borehole OFS 93-010.

It is generally accepted that the assignment of a specific lithofacies to an ancient pyroclastic succession poses many difficulties (Cas and Wright, 1988), especially so in borehole core. The kimberlites at FALC have not undergone any metamorphism, other than low temperature diagenesis, nor experienced significant structural alteration since emplacement, and their geographical disposition and extent is well defined by high-quality aeromagnetic mapping (see Chapter 1). In addition a great deal of data have been collected from a wide range of pyroclastic environments in different boreholes, allowing a reasonable assessment of facies to be made.

The determination of facies is based not only on observed lithology, but also on geographic disposition relative to the magnetic anomalies, described in Chapter 1. For example, lithologies of crater facies kimberlite are found in borehole intersections located within the well defined circular magnetic anomalies; proximal facies rocks are intersected immediately on the edge of the anomalies, and more distal facies are on the order of kilometres from the

anomaly edge, Figure 2.1.1. Point counting has been applied to the proximal extra-crater kimberlite to aid differentiation of primary and reworked deposits.

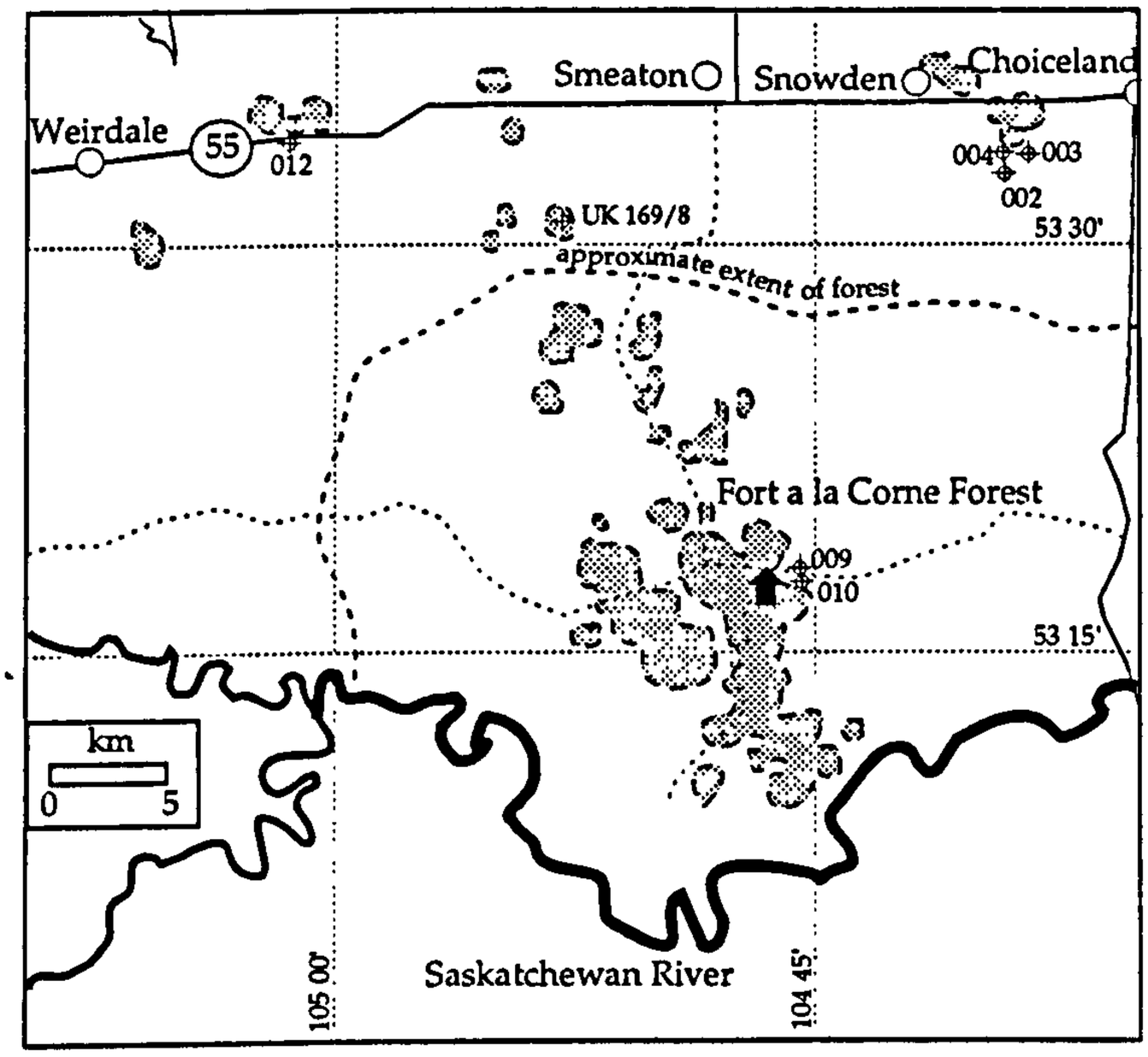

Figure 2.1.1.

Detail of kimberlite cluster. Grey shaded areas, bordered with dashed lines are the kimberlite crater facies, as defined by magnetic anomalies. Also shown are locations of boreholes referred to in this chapter. OFS 93-012 crater facies, OFS 93-002, 003 and 004 proximal facies, and OFS 93-009 and 010 distal facies. UK 169/8 represents the location of the GSC Smeaton borehole.
Hut symbol represents FALC JV drill camp. Land outside of the approximate extent of the forest, and south of the Saskatchewan River , is mostly farmland, with some Indian Reserve land.

2.1.1 Description and Interpretation.

Facies divisions are important because each contains a different suite of lithotypes, which are genetically distinct. Crater facies are mostly primary volcanic deposits overlain by crater lake reworked (known as epiclastic) kimberlite (Hawthorne, 1975), whilst proximal and distal deposits are mainly reworked kimberlite. Furthermore the concentration of heavy minerals (including diamond) is dependant upon the facies, with higher concentrations occurring with greater degrees of reworking. This is discussed in detail in Section 2.2.

All data, and their interpretation, presented in this chapter are from the authors own observation (unless otherwise referenced). Full descriptive logs are provided in Appendix II, and are a collaborative effort by the author and B.C. Jellicoe of Kensington Resources (formerly of Rhonda Mining Corp.) The following is a lithological **description** of the borehole, followed by an overall **interpretation** of the succession, based mainly on interpretation of volcanic

and sedimentary structures outlined in the literature (for example: Cas and Wright, 1988; Leeder, 1982).

Crater Facies Kimberlite

Description:

Borehole OFS 93-012 is located 8km east along Highway 55 from Weirdale (Figure 2.1.1), near the settlement of Shipman. This kimberlite locality is considered an outlier from the main kimberlite cluster in FALC forest, about 25km to the south-east. The borehole was drilled into a magnetic anomaly that also includes other sub-circular magnetic highs nearby. It is unclear whether this represents many small, coalescing craters, or a disrupted (faulted) single large crater.

The borehole intersection contains a 35m thick complex sequence of tuffs, sills and sediments, intersected at approximately 177.5m to 212.0m. Figure 2.1.2. gives the borehole lithology log. Faults are common in the kimberlite intersection, generally steep (0° to 45° from vertical), and typically filled with calcite, baryte and/or pyrite, the wall rocks often display well developed serpentine slickenside.

The base of the kimberlitic intersection is seated in dark grey glauconitic marine shales of the Spinney Hill Formation, which contain three intrusive horizons of kimberlitic carbonate-rich sills over 5m of shale intersection. These sills show some wall rock interaction; minor mineralization and flakes of shale near the upper and lower edges, as well as flow banding and some crystal/xenolith alignment. They comprise over 70% $CaCO_3$, the remainder mostly serpentine, often replacing the euhedral olivine crystals. Other primary kimberlite minerals include chromite, phlogopite, ilmenite and rare garnet. Authigenic minerals present are pyrite, calcite, baryte and fluorite. The upper and lower sills are only 30cm thick, the central one nearly 90cm. The upper sill unit is sharply faulted against the base of the tuffs (fault at 25° to vertical, at 206.5m) and the total thickness is unknown (Plate 2.1 in Figure 2.1.3).

The overlying basal tuffs consist of 5.5m of green, very coarse grained, crystal-lithic tuffs. Lapilli are fairly common, mostly fine (<2mm) rounded juvenile aggregates of microphenocrysts in a brown serpentinous matrix. Alignment of crystals in the lapilli is rare. Point counting of one thin section from 201.12m indicates crystals and lithics 57%, lapilli 16% and matrix (mostly serpentine) 27%. The unit contains many thin interbeds, irregularly distributed. These are often slightly graded and bedded with the crystal and lithic proportions and grain size varying between subunits. The texture is usually

Figure 2.1.2

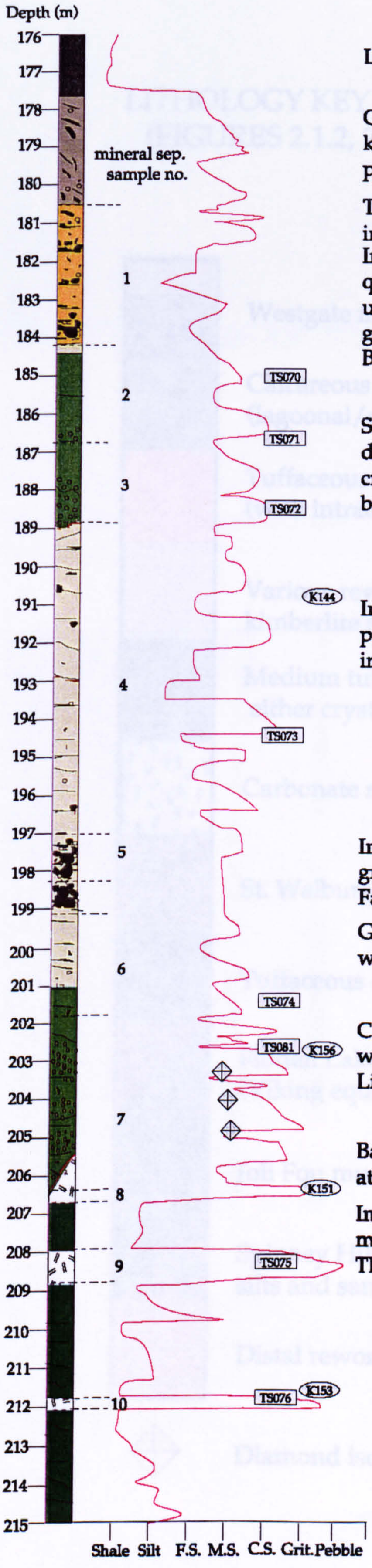

Lower Westgate dark grey mudstones

Calcareous sandy mudstone, with kimberlitic, xenolithic and shale pebble grade intraclasts.

Tuffaceous quartz sandstones with intraclastic shales as lags and floats.
Intraclastic breccia with tuffaceous quartz sandstone matrix. Clasts mostly up pebble grade, up to small boulder grade. Faults common.
Bedded pyroclastic sands

Slightly graded and slumped lapilli dominated lapilli-tuffs. Lithics and crustal xenoliths common. Pyrite and baryte veins common.

Interbedded massive and graded pyroclastic sands, with common shale intraclasts and plant fragments.

Intraclastic Breccia, clasts up to boulder grade (30cm). Matrix of pyroclastic sand. Faults common.

Graded and bedded pyroclastic sands, with shale intraclasts and plant fragments.

Coarse crystal dominated lapilli-tuff with sporadic thin bedding and grading. Lithics and crustal xenoliths common.

Base of crater facies kimberlite, inclined at 40°, mineralised with calcite.

Intruded Lower Spinney Hill Formation, marine mudstones and silts with glauconite. Three carbonate rich kimberlitic sills.

Borehole log of OFS93-012. Colours and ornament within the log are schematic, see key overleaf. 'Min sep sample no.' refers to heavy mineral sample intervals, see Fig. 2.2.3. Red line is a representative grain size log, N.B. this excludes the size of intraclast and xenolith components. Grey boxes indicate thin section sites codes. Grey ellipses indicate sites of XRF analysis.Grey diamonds indicate diamond size grade, and sample interval in which they were found. Log grain size terms are standard sedimentary nomenclature.

LITHOLOGY KEY FOR BOREHOLE LOGS (FIGURES 2.1.2, 2.1.5, 2.1.13 AND 2.2.4.)

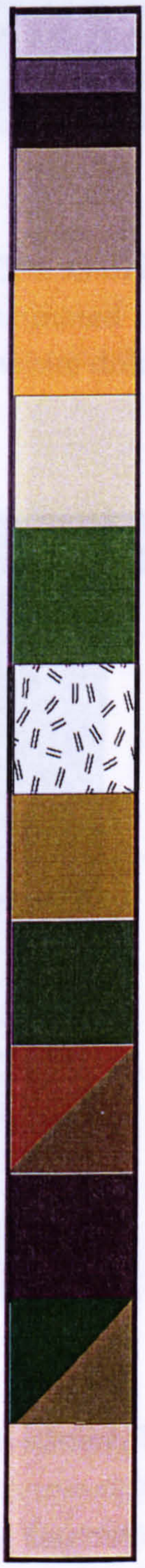

Westgate mudstones and silts

Calcareous sandy mudstone (lagoonal/crater fill)

Tuffaceous sandstone (with intraclsatic shale)

Various reworked pyroclastic kimberlite sands

Medium tuffs to lapilli-tuffs (maybe either crystal or lapilli dominated)

Carbonate rich kimberlite sills

St. Walburg Sand

Tuffaceous conglomerate

Flotten Lake Sand (Viking equivalent)

Joli Fou mudstones

Spinney Hill glauconitic muds silts and sands.

Distal reworked pyroclastic sand

Diamond isolated from this facies sample

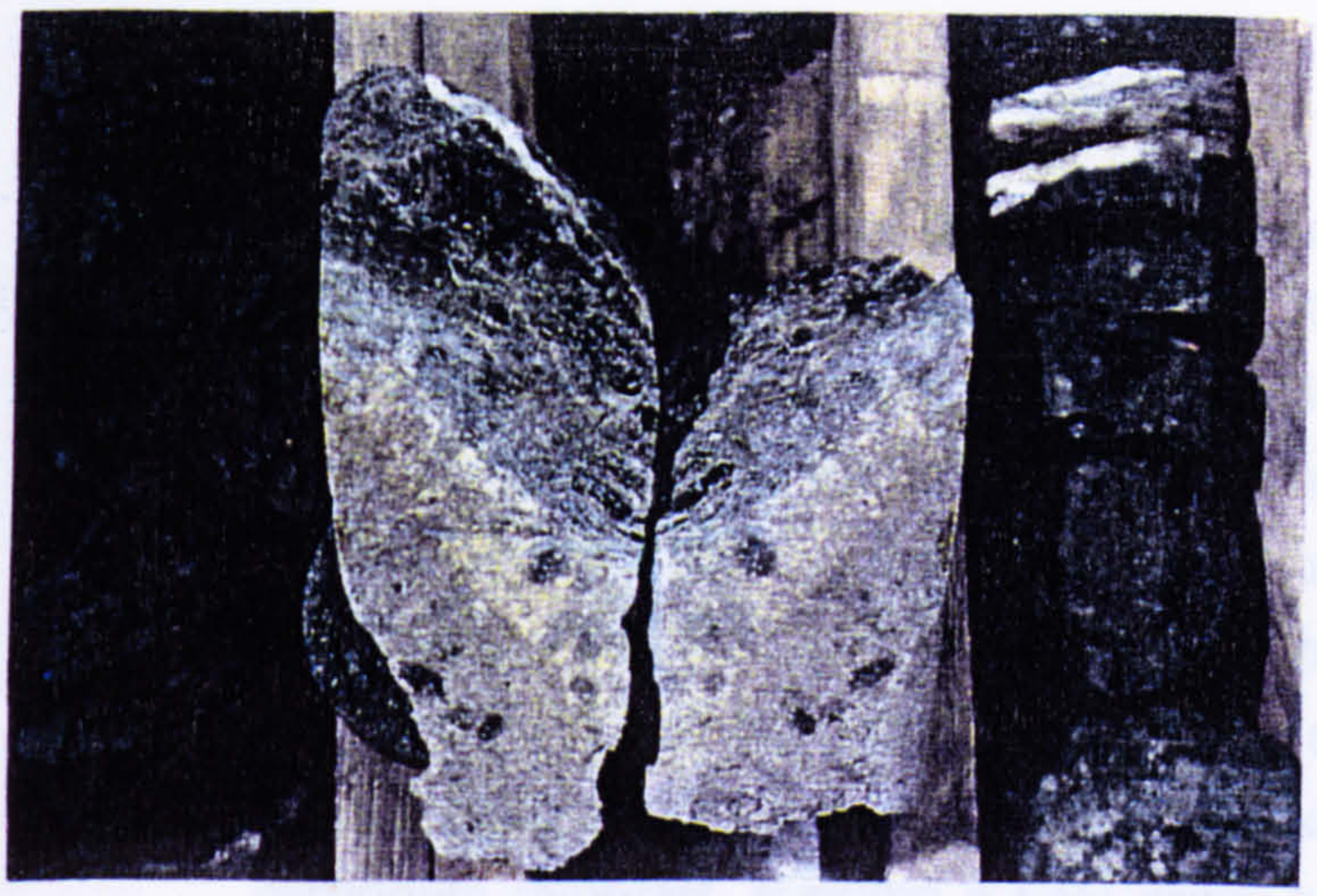

Figure 2.1.3.

Plate 2.1
Borehole OFS 93-012, 206.5m.
Inclined and mineralised base of crater facies. Contact faulted against pale-buff carbonate-rich kimberlite sill in Spinney Hill Fm.

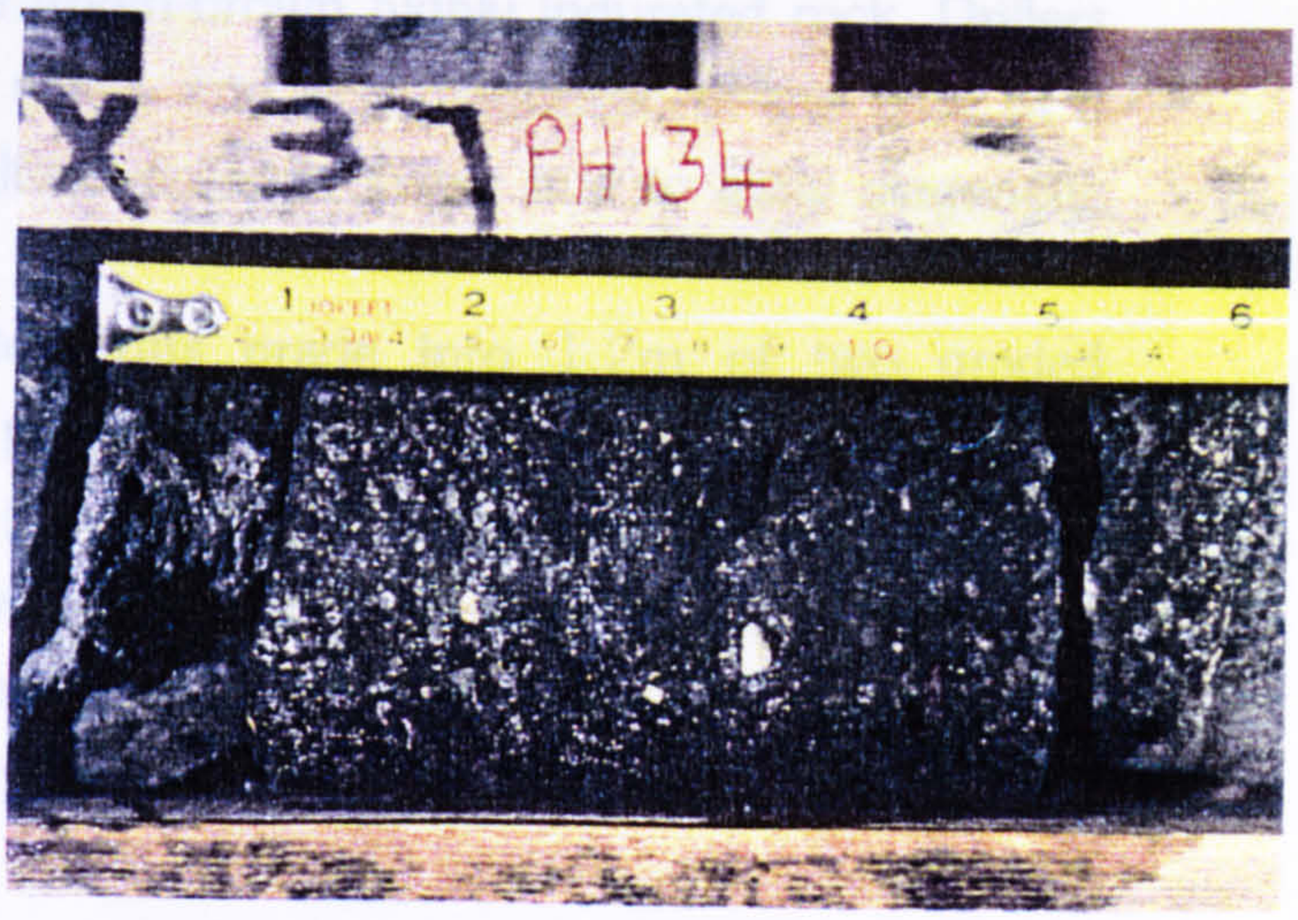

Plate 2.2
Borehole OFS 93-012, 201.6m.
Crystal dominated Lapilli Tuff. Note abundant white dolomite crustal xenoliths.

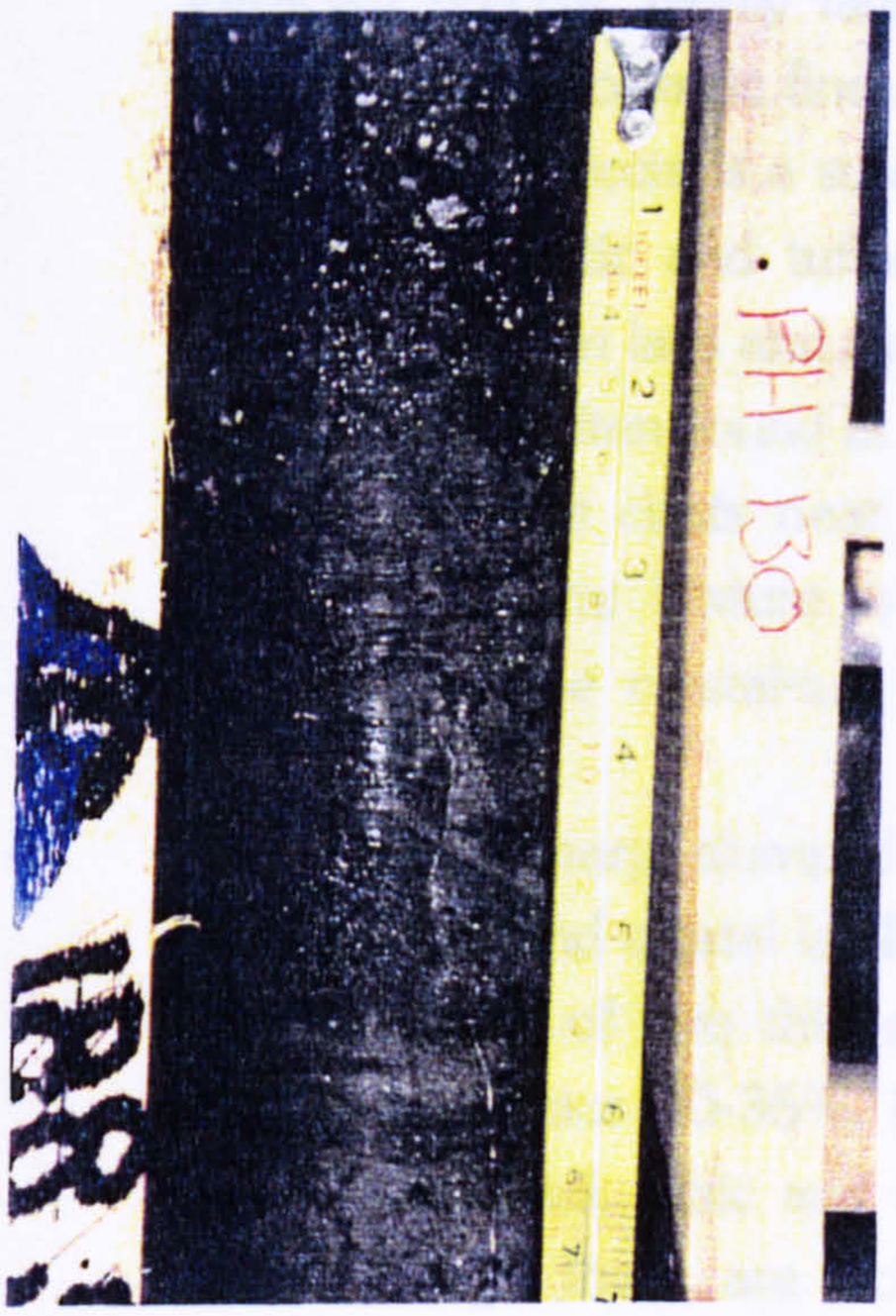

Plate 2.3
Borehole OFS 93-012, 188.5m.
Bedded pyroclastic silts to grits, overlain by lapilli dominated Lapilli Tuffs. Note disrupted bedding due to slumping.

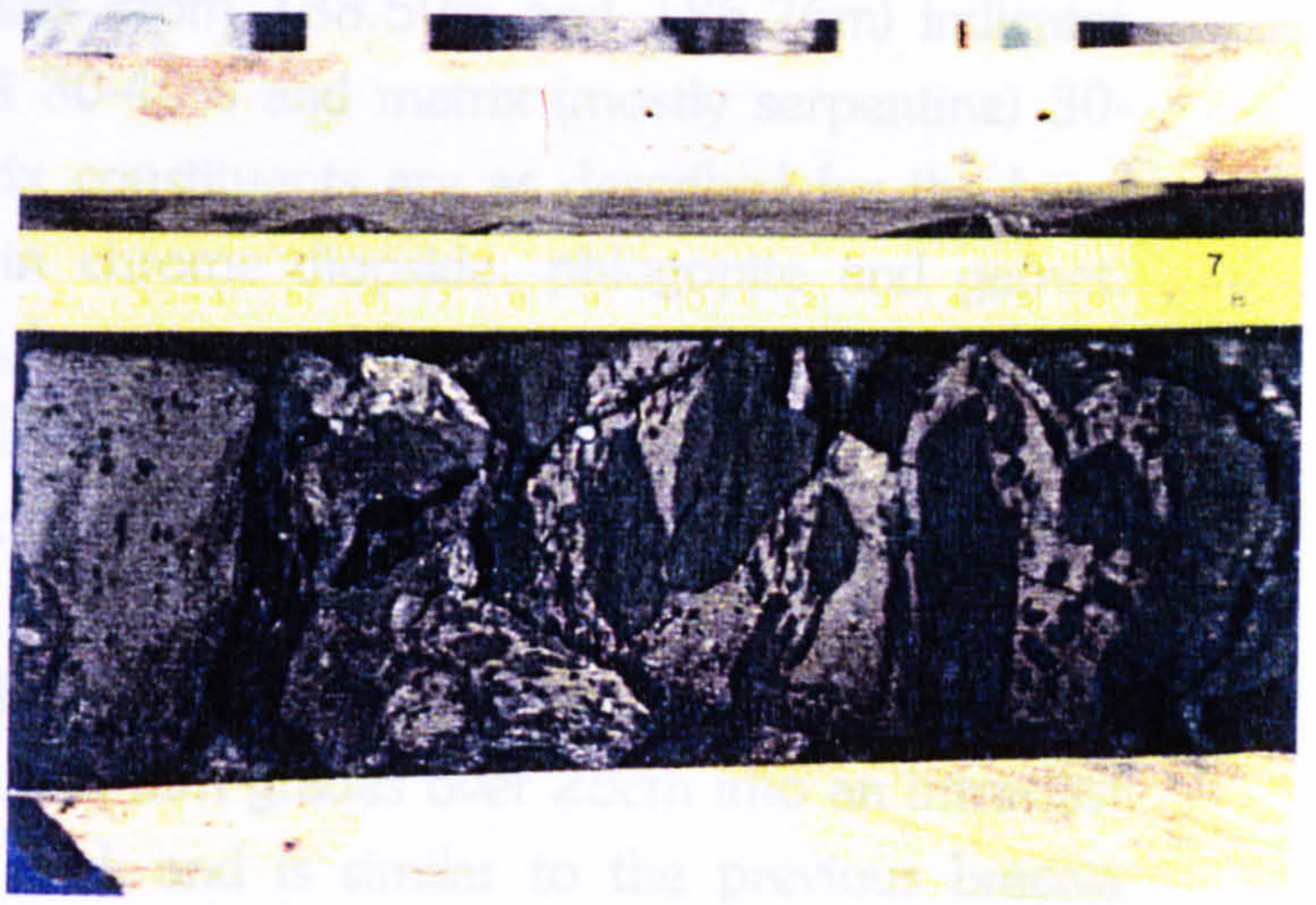

Plate 2.4
Borehole OFS 93-012, 181.2m.
Intraclastic breccia composed of >50% angular shale fragments in a brown tuffaceous quartz sand.

matrix supported and the dominant grains consist of psuedomorphic serpentine after euhedral olivine up to 3cm long. Olivine grain size is bimodal, with populations typically 0.2mm to 1mm and 3mm to 15mm. Chromite, chromium diopside, phlogopite, sphene and garnet also occur, along with fine (<2mm) rounded lapilli. Lithics occur up to 2cm, and include chert, dolomite, shale and rare gniess, Plate 2.2 in Figure 2.1.3. The matrix is composed mainly of brown-green amorphous serpentine, with patchy carbonate, and accessory pyrite and baryte, Plate 2.6 in Figure 2.1.4. The base of the tuffs is strongly altered by carbonate minerals, forming a pale green-brown highly indurated rock. Drillers in the FALC field term this 'hard shelf', and it is diagnostic of the base of a kimberlite succession. This basal alteration is probably due to early diagenetic mineralization (see Section 2.3).

The coarse crystal-dominated tuffs grade into 1.2m of two graded pyroclastic sand units, very rich in plant fragments (mainly branches and twigs, up to 5cm long and 1cm wide) in the top 10cm. These are capped by 2m of intraclast breccia, highly faulted, with shale fragments up to 30cm thick, and with a green pyroclastic fine sand matrix between clasts and along faults. Above the intraclast breccia is a succession 9.6m thick of 14 interbedded massive and graded pyroclastic and tuffaceous sands, with angular to well rounded shale intraclasts both in lags and as floating clasts. Lapilli are very rare to absent. Plant fragments are often found at the top of the units, and euhedral to sub-rounded crystal and lithic clasts near the base, of the same type as in the underlying coarse tuffs. The texture is granular and friable, in contrast to the tightly cemented coarse crystal-tuff below, Plates 2.3 and 2.8 in Figures 2.1.3 and 2.1.4.

With a sharp, slumped basal boundary (Plate 2.3 in Figure 2.1.3), coarse grained lapilli and crystal lapilli-tuffs, 4.7m thick, overlie the graded pyroclastics. Point counting of two thin sections (from 188.50m and 186.76m) indicates crystals and lithics 30-35%, lapilli 30-40% and matrix (mostly serpentine) 30-35%. The crystal, lithic and matrix constituents are as described for the basal tuffs, although these are richer in chrome diopside, phlogopite and garnet. Lapilli are the dominant clast type, however, and far coarser and highly fluidal in shape, with a pale brown matrix (Plate 2.5 in Figure 2.1.4). The unit is poorly bedded and slightly graded overall; the maximum grain size varying from 2cm at the base to 3mm at the top.

The top unit of the lapilli-dominated tuffs grades over 10cm into a tuffaceous coarse quartz sand which in turn grades over 25cm into an intraclast breccia. This breccia unit is 1m thick and is similar to the previous breccia

Figure 2.1.4.

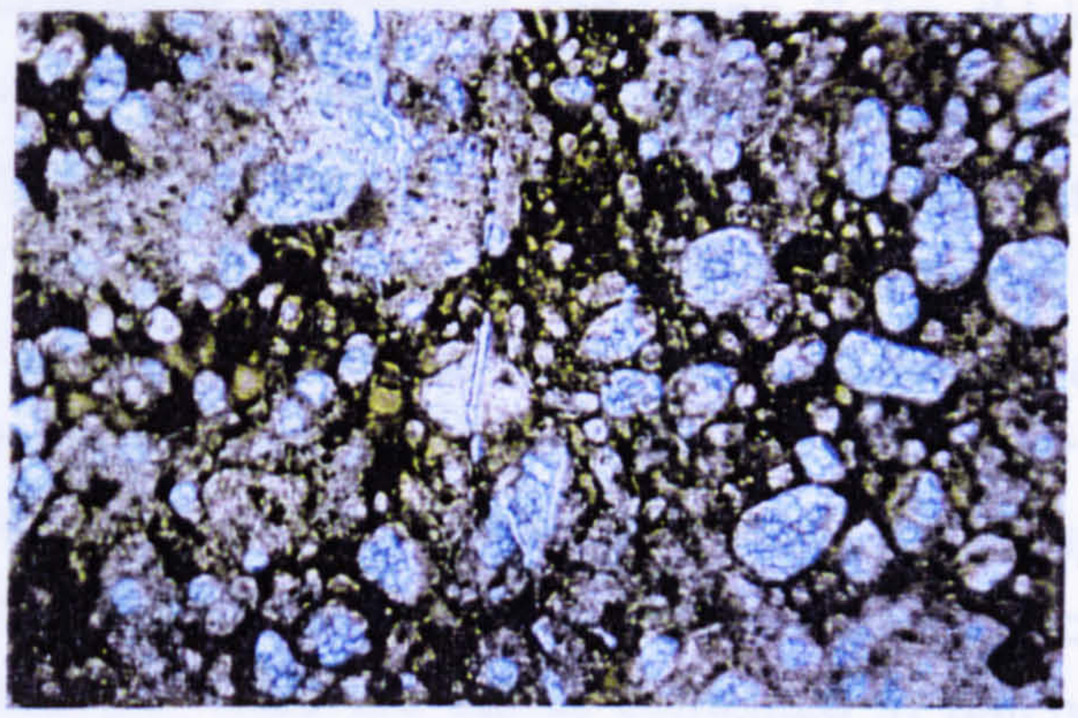

Plate 2.5
Borehole OFS 93-012, thin section at 184.7m, plain polarised light, magnification x 5.
Lapilli dominated Lapilli Tuff, note fluidal lapilli with paler brown matrix and amoeboid form. Matrix and grains mostly serpentine and calcite.

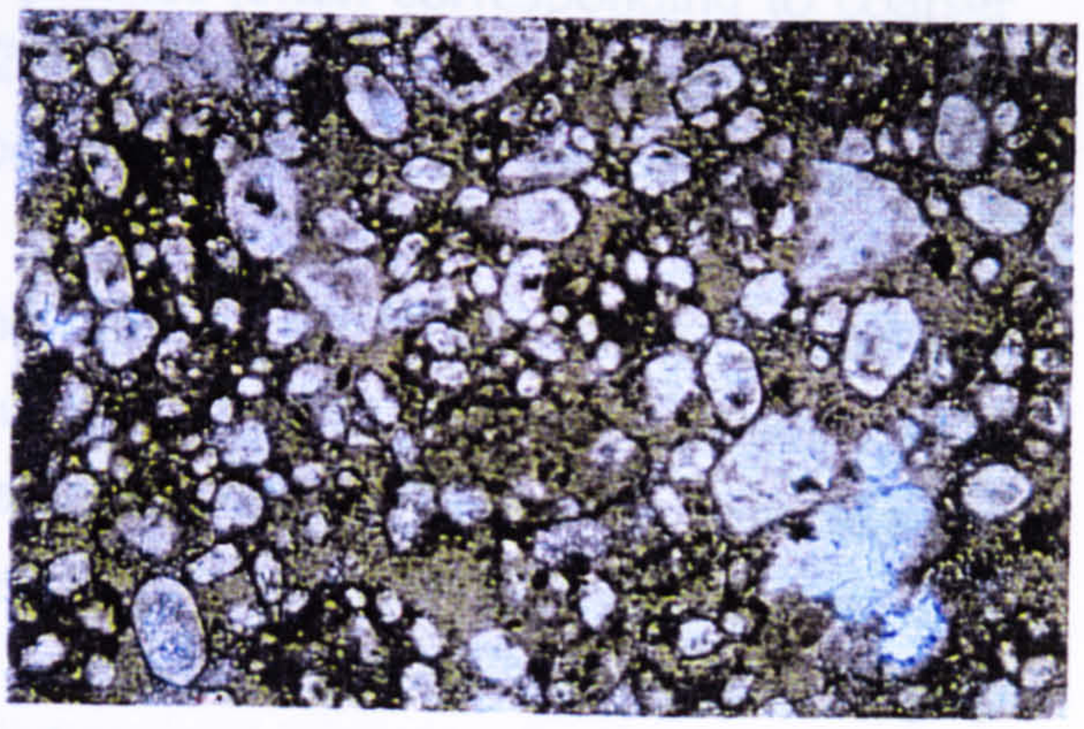

Plate 2.6
Borehole OFS 93-012, thin section at 204.2m, plain polarised light, magnification x 6.
Crystal dominated Lapilli Tuff. Note common large euhedral and fragmented crystals. Lapilli also common (centre, left and lower left), but of the rounded, non-fluidal type. Some may be autolithic. Matrix and grains mostly serpentine and calcite.

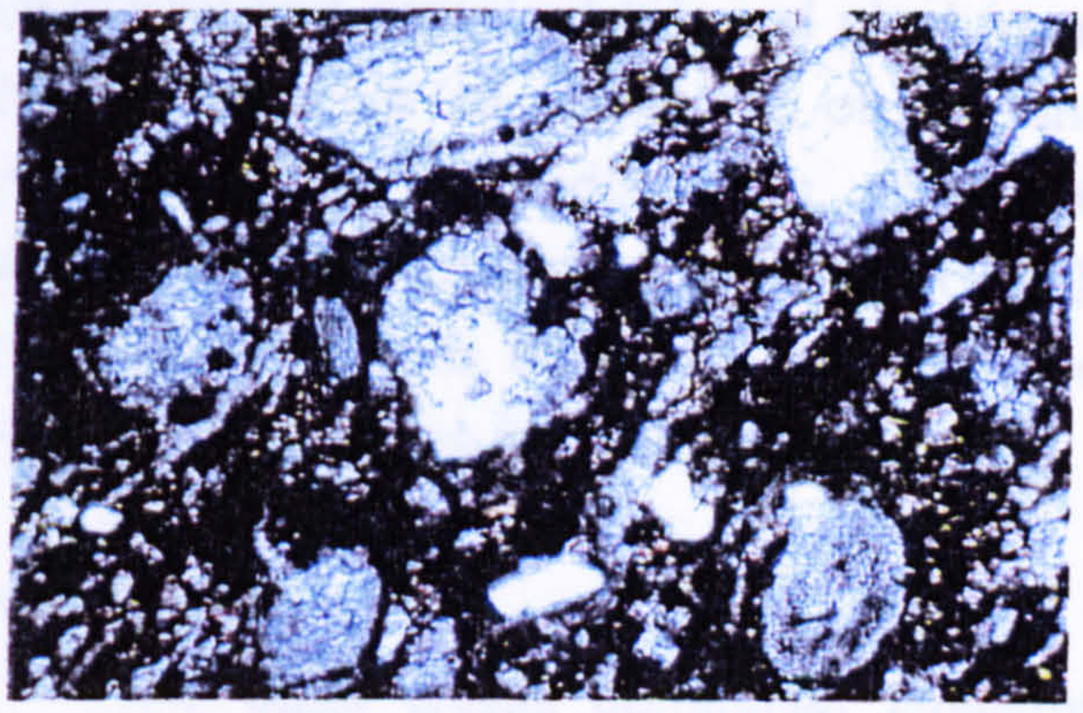

Plate 2.7
Borehole OFS 93-012, thin section at 179.9m, plain polarised light, magnification x 13.
Calcarous sandy mudstone of probable crater lake environment. Grains include quartz (top right) and calcite-after olivine (top centre). Matrix is mostly clays and organic matter (brown and black) finely intermixed with calcite and serpentine.

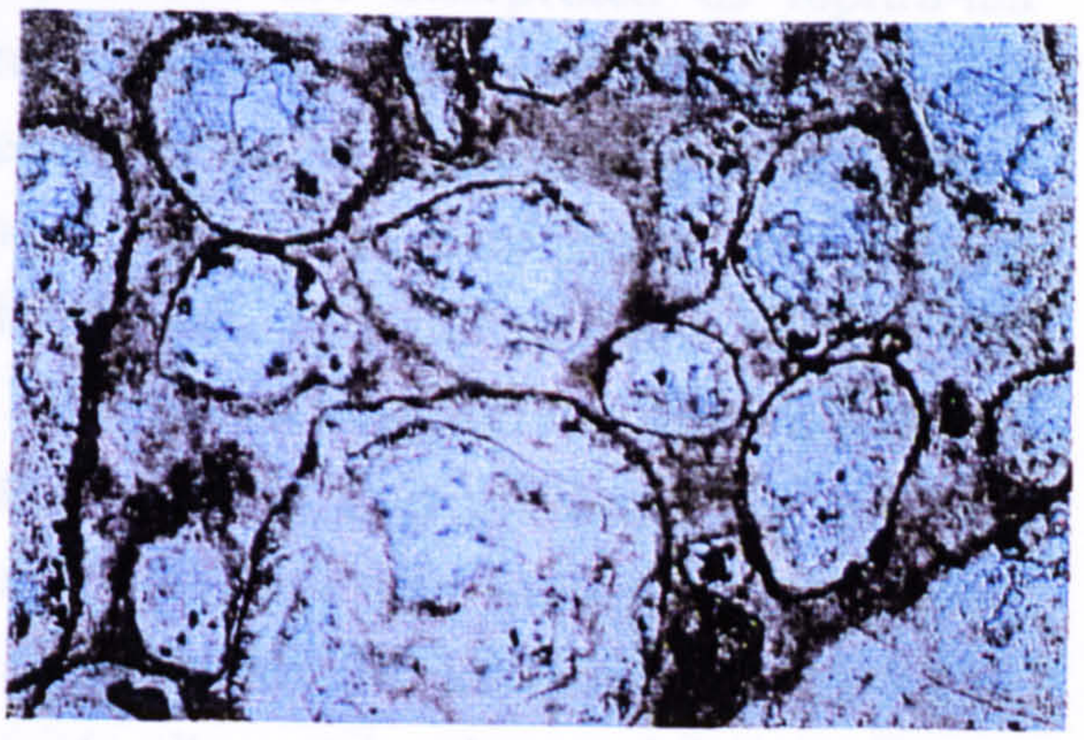

Plate 2.8
Borehole OFS 93-012, thin section at 192.5m, plain polarised light, magnification x 13.
Graded pyroclastic medium to coarse sand, composed of >90% volcaniclastic material. Note sub-rounded and rounded clasts, and clast-supported texture. Grains and matrix replaced mainly by serpentine, with a dusting of magnetite and calcite. Clear rhombs in the grains are dolomite crystals.

described above; the matrix is a brown tuffaceous fine sandstone, and the shale clasts range up to 30cm small boulders. Grading upwards from the breccia is an intraclastic tuffaceous sandstone 2.7m thick. The tuffaceous component (less than 25% of the total) includes phlogopite, garnet, rare chromite and diopside, and a pervasive pale green to brown serpentine-clay-carbonate matrix. Bedding is well defined, and the unit is divided into 5 subunits, all are rich (30% to 60%) in shale intraclasts up to pebble size, aligned along bedding planes, as either lags or floats. The shale intraclasts are angular or lath-shaped fragments and shards, forming a texture similar to sedimentary rip-up clasts (Leeder, 1982). The quartz grains dominate, varying between silt and coarse sand size, and are often well rounded. They are tightly cemented in patches (often corresponding to coarser strata) by pyrite and carbonate, Plate 2.4 in Figure 2.1.3. The top unit (30cm thick) is strongly cemented by carbonate and grades into the overlying tuffaceous marl.

The intraclastic tuffaceous sand grades with decreasing quartz and kimberlitic crystal content into a tuffaceous, intraclastic, calcareous sandy mud (marl), 2.75m thick, that caps the volcanic succession. Kimberlitic minerals are rare (phlogopite and a few spinels and garnets), but fine serpentine is a component of the matrix (Plate 2.7 in Figure 2.1.4). The unit is highly bioturbated and organic debris and plant fragments are common. Intraclasts are also common (up to about 5% of the unit), and of unusual composition, including typical Colorado shales, coals (probably from the Mannville) and rounded dolomite clasts (from the Devonian). The unit is sharply overlain by homogenous grey to black silty mudstones of the Westgate Formation, 12m below the base of the St. Walburg Sand.

Interpretation:

The basal crystal dominated lapilli-tuffs are interpreted as tephra-fall deposits produced by a single volcanic eruption. The overlying graded and bedded pyroclastic sand units are interpreted as local reworking of the basal coarse tuffs, within a crater environment. The absence of lapilli, well graded subunits, rounded crystals and shale intraclasts, and the granular texture are indicators of the reworked origin. The 13m thick succession would be deposited over a very short time interval after the eruption that produced the primary crystal-lithic dominated lapilli-tuffs. Slumping of the crater walls produced debris flows rich in crater wall fragments, accounting for the intraclast breccia beds. Other slumps of volcanic deposits into standing water (crater lake) produced volcaniclastic debris flows and density currents (turbidity flows) that deposits the

massive and graded pyroclastic sands observed. The concentration of plant fragments strongly suggests an emergent (sub-aerial) phase either before or after the first eruption.

The following lapilli dominated lapilli-tuff is interpreted as a primary tephra-fall deposit from a second phase of eruption, involving a different magma type or eruptive style (see Chapter 3) producing lapilli-dominated coarse tuffs, suggesting a more fluid (probably volatile-rich) magma.

In the overlying tuffaceous sands the immediate source of the quartz in the deposit is unclear; possibly like the shales it was eroded from the crater wall, or from inundation of the crater by fluvial or tidal sands (described in Chapter 4). The tuffaceous sand may be analogous to sandy tuffs described from the Ellendale lamproite, Australia (Scott-Smith, B.H., pers. comm. 1994). These have been demonstrated to be tephra-fall and debris flow deposits from crater excavation, during phreatomagmatic activity (Smith and Lorenz, 1988), and are discussed further in Chapter 3. This uppermost tuffaceous unit is interpreted as a lagoonal crater fill, with final erosion of the crater wall and the remainder of the crater edge pyroclastic deposits (including large, tough country rock xenoliths, such as dolomite). The volcanic edifice was finally fully submerged at earliest Westgate Formation times, and overlain by an unusually thick Westgate sequence, double the usual local thickness (see Chapter 1, Section 1.3 and further discussion in Chapter 4).

The stratigraphic constraint of late Flotten Lake Sand places the crater formation and fill period in the late Albian, probably around 102Ma, at about the same time as the nearby Smeaton kimberlite, and a central cluster kimberlite (Kjarsgaard et al, 1995). This is considerably earlier than the 94Ma reported for a central FALC cluster kimberlite (Lenhert-Theil et al, 1992). The base of the crater deposits are in early Spinney Hill strata, indicating a removal of the rest of the Spinney Hill Formation, the Joli Fou Formation and some of the Flotten Lake Sand (about 25m of rock) by the crater eruption.

In summary the crater facies is typified by dark olive green, lithic rich, coarse (to 3cm) crystal or lapilli dominated tephra-fall lapilli tuffs. They are finely bedded to massive, and often display slight normal grading, on both micro and macro scale. Typically they have inclined, mineralised bases (drillers term 'hard shelf'), and displace considerable stratigraphy, proving crater excavation. In the case of OFS 93-012 these primary coarse tuffs are interbedded with large amounts of reworked pyroclastic sands and intraclast breccias, probably derived from crater wall slumping. These reworked kimberlites may be prevalent in OFS

93-012 due the crater edge location (as defined by the magnetic anomaly), nearest to the supply of crater infill sediment.

Proximal Extra-Crater Facies Kimberlite

Description:

The three boreholes described below were drilled on the southern slopes of the magnetic highs that define the Snowden cluster of craters (Figure 1.2.2 in Chapter 1). The Snowden cluster consists of about five coalescing anomalies, about 30km north-east of the main FALC cluster, Figure 2.1.1. The boreholes were drilled at a spacing of 250m, in an L-shape, intersecting the same extra-crater deposits. In all the intersections a buff-brown, medium grained, quartz sandstone 55cm to 90cm thick was intersected, which represents the basal deposits of the St.Walburg Sand. Contact with the overlying kimberlites is horizontal, sharp and appears sedimentary (i.e. not faulted). Load and flame structures are present, comprising dark shaley material infiltrating the kimberlite. Refer throughout the following descriptions to borehole lithology logs, Figure 2.1.5.

Drill hole OFS 93-002:

The basal tuffs, 4m thick, are olive green, medium to coarse, indurated and with a slight overall coarsening towards the base. The lower 3m are highly veined parallel to bedding, which is near horizontal (Plate 2.9 in Figure 2.1.6). These veins are filled with calcite and serpentine and account for up to 30% of this unit. Beds are thick (1-2m), weakly defined and massive (Plate 2.10 in Figure 2.1.6). This unit is composed mostly of pseudomorphic serpentine after euhedral olivine, up to 1mm, and around 0.5% by weight of heavy minerals, including ilmenite, garnet and phlogopite. Lapilli and autoliths are extremely rare to common, fine (<2mm) and rounded. The texture is usually (but not exclusively) matrix supported. The matrix is mostly green-brown serpentine, dusted with magnetite and patchy carbonate, accounting for 30% to 45% of the rock (excluding veins)

Overlying the tuffs, with a sharp contact, are 7m of bedded, pale grey/green pyroclastic sands. They contain eight graded subunits, 0.2 to 1.0m thick, the other subunits are massive. Grit to pebble size angular intraclasts of shale are found sporadically. The basal lags of the graded units contain concentrations of minerals found in the underlying tuffs, including microdiamonds. Lapilli are absent, although fine grained, rare, angular to sub-angular autolithic fragments are found in the basal layers. Occasional carbonate

Figure 2.1.5

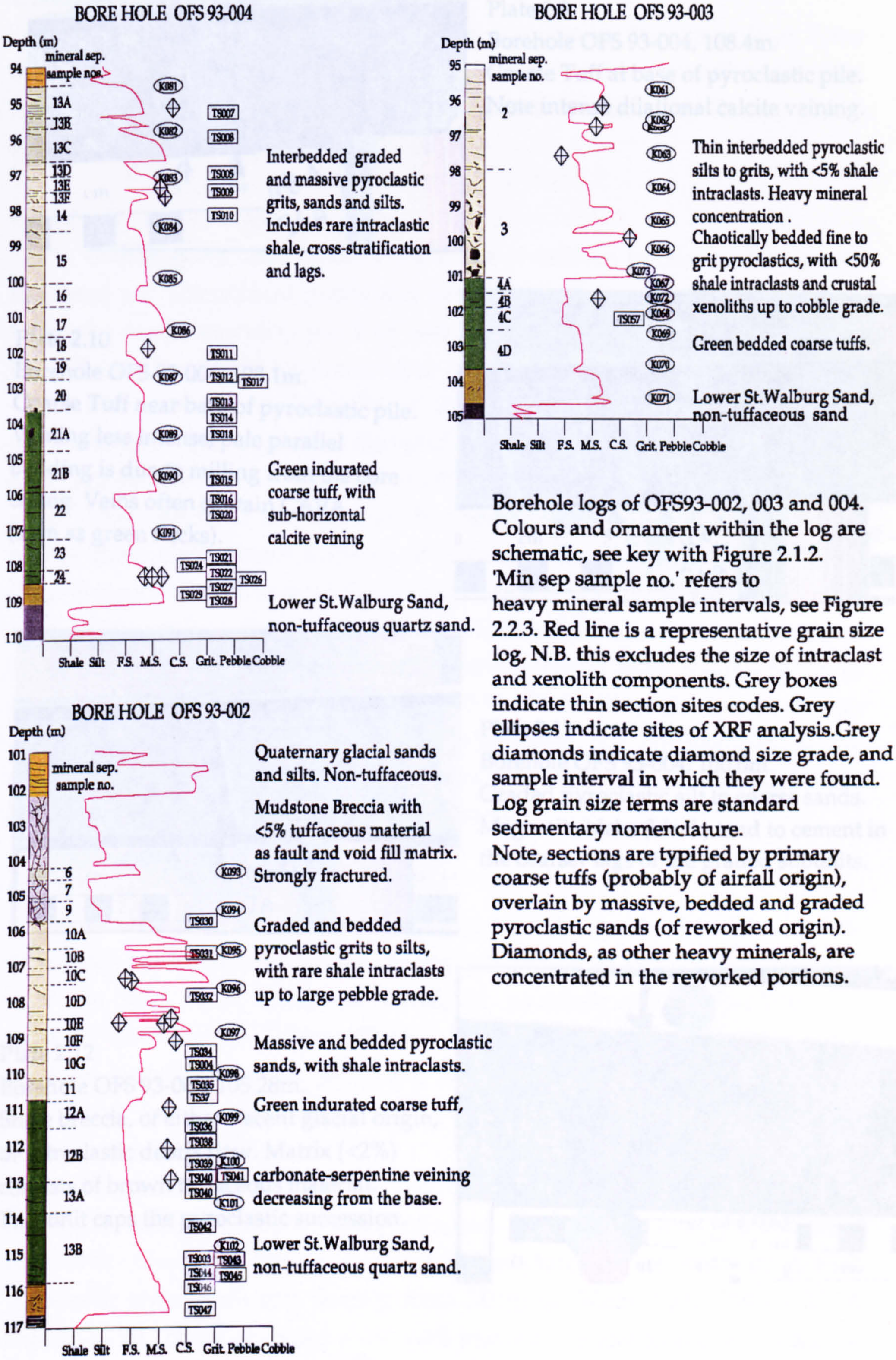

Borehole logs of OFS93-002, 003 and 004. Colours and ornament within the log are schematic, see key with Figure 2.1.2. 'Min sep sample no.' refers to heavy mineral sample intervals, see Figure 2.2.3. Red line is a representative grain size log, N.B. this excludes the size of intraclast and xenolith components. Grey boxes indicate thin section sites codes. Grey ellipses indicate sites of XRF analysis.Grey diamonds indicate diamond size grade, and sample interval in which they were found. Log grain size terms are standard sedimentary nomenclature.
Note, sections are typified by primary coarse tuffs (probably of airfall origin), overlain by massive, bedded and graded pyroclastic sands (of reworked origin). Diamonds, as other heavy minerals, are concentrated in the reworked portions.

Figure 2.1.6.

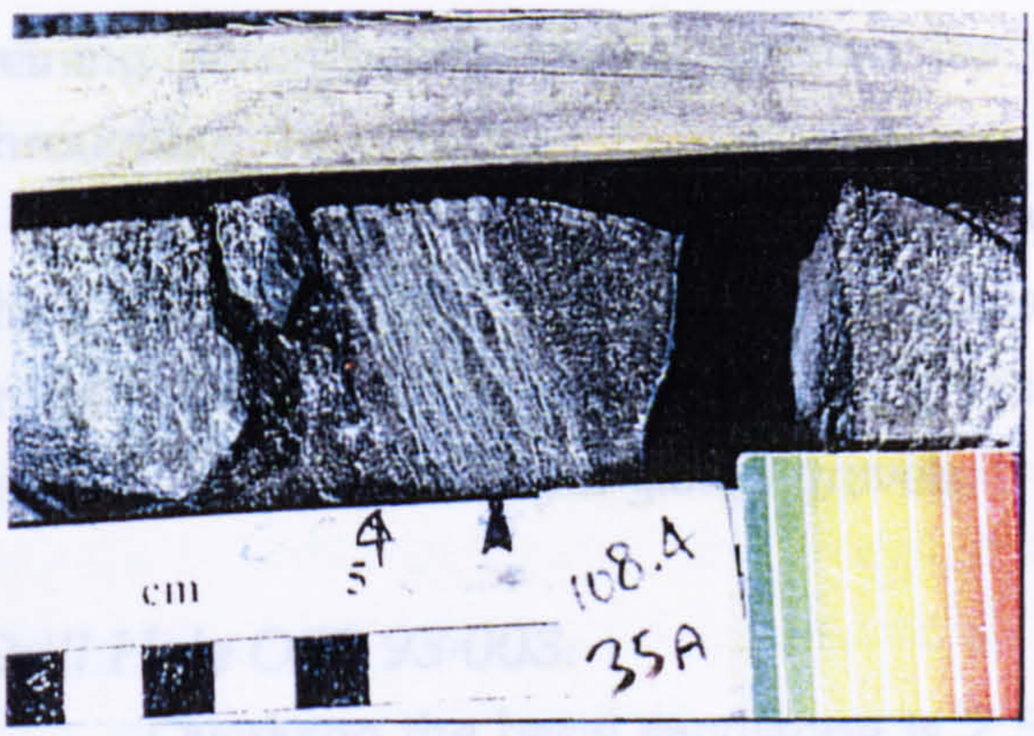

Plate 2.9
Borehole OFS 93-004, 108.4m.
Coarse Tuff at base of pyroclastic pile.
Note intense dilational calcite veining.

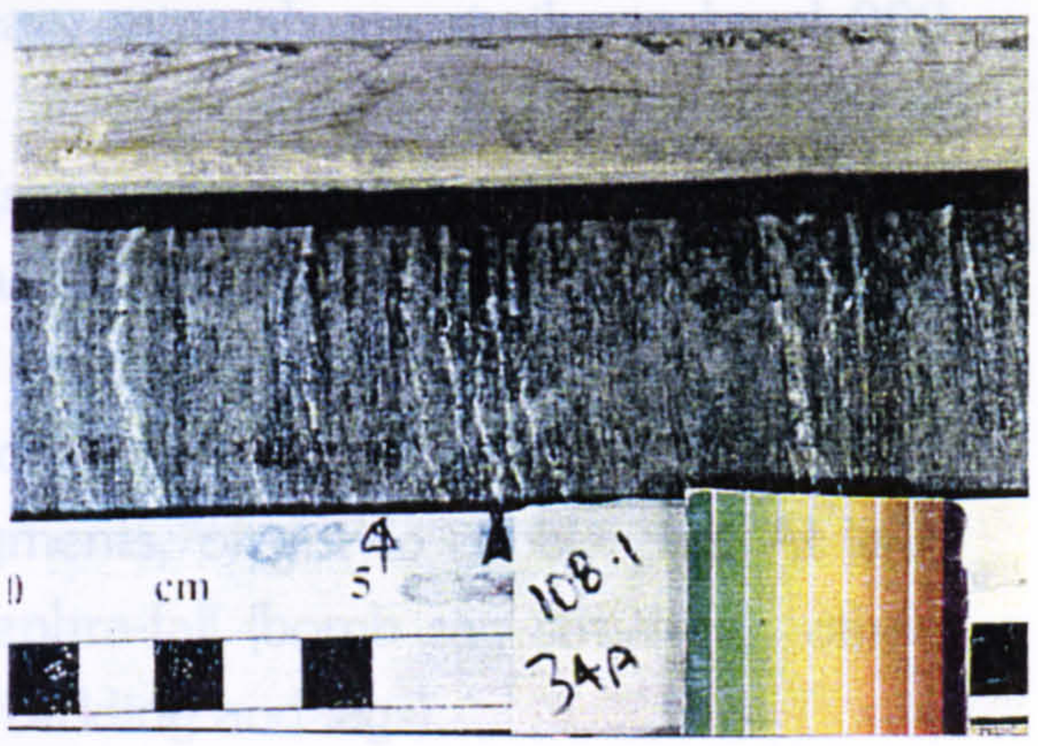

Plate 2.10
Borehole OFS 93-004, 108.1m.
Coarse Tuff near base of pyroclastic pile.
Veining less intense, pale parallel
banding is due to milling from the core
casing. Veins often contain CAVA
(seen as green flecks).

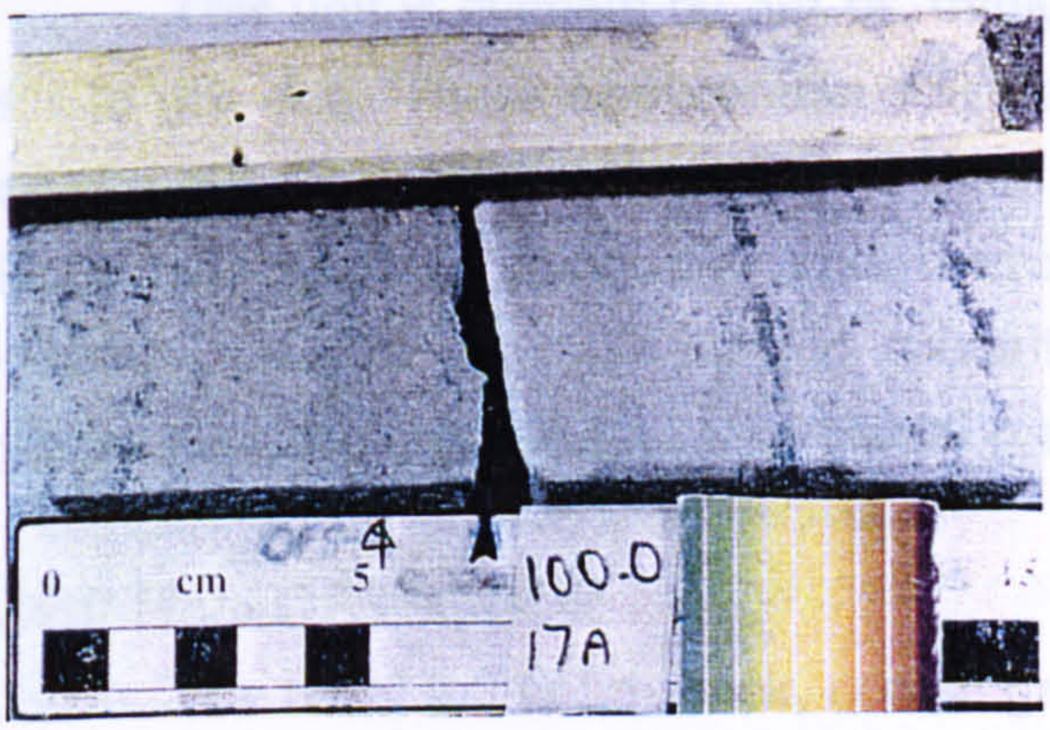

Plate 2.11
Borehole OFS 93-004, 100.0m.
Graded pyroclastic silt to coarse sands.
Magnetite blebs (black) tend to cement in
the coarser lags of the graded subunits.

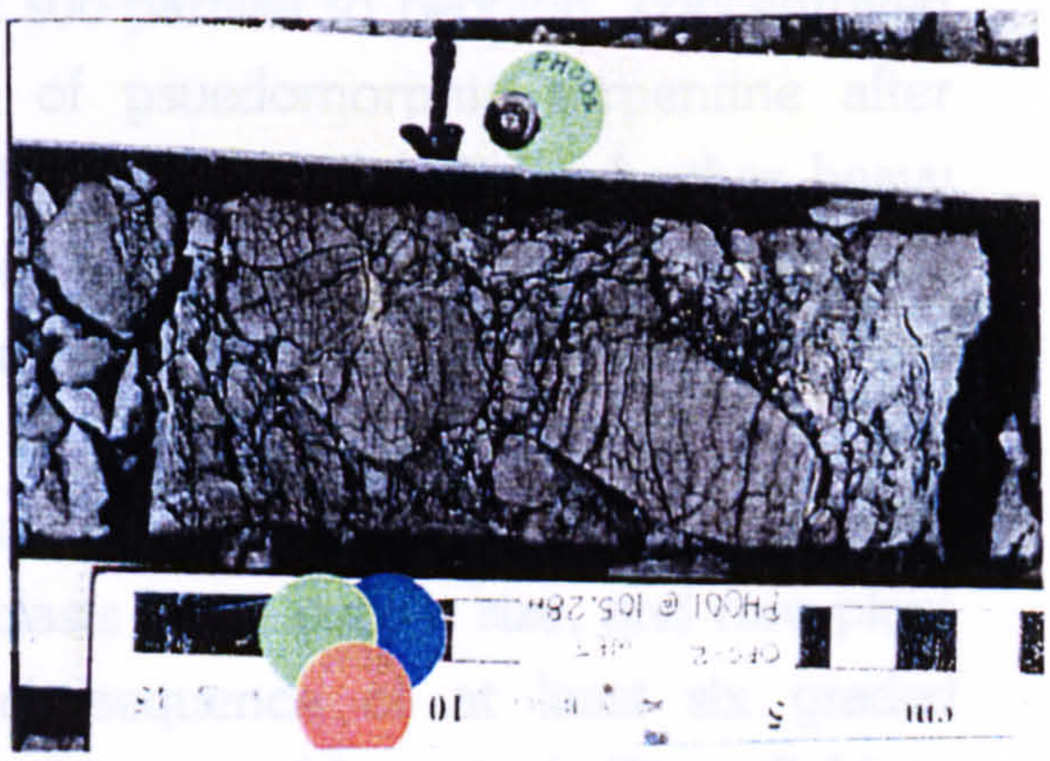

Plate 2.12
Borehole OFS 93-002, 105.28m.
Shale breccia, of either Recent glacial origin,
or intraclastic debris flow. Matrix (<2%)
consists of brown tuffaceous material.
This unit caps the pyroclastic succession.

veining accompanies blebby precipitates of magnetite that occur in patches throughout the unit.

The volcanic sequence is capped by a mudstone breccia at least 2.2m thick which contains 98% shale fragments, with a rare brown tuffaceous sand matrix (Plate 2.12 in Figure 2.1.6). This unit is truncated by Recent glacial erosion, and overlain by a glacial gravels.

Drill Hole OFS 93-003:

Overlying the basal sandstone is 2.5m of medium to coarse, dark green, indurated tuff. Constituent grains and heavy minerals are similar to basal 002 tuffs, plus much secondary pyrite as vein fill, amounting to 0.75% by weight of the tuff, based on heavy mineral analysis (see Section 2.2).

Above the basal tuffs are 3m of chaotically bedded, pale grey-green, fine to coarse tuffs. The bedding is disrupted by slumps, large intraclasts, syn- and post-depositional faulting and compaction sag structures. The tuff contains about 20% intraclastic angular shale fragments, of grit to cobble size. At least one of these clasts shows evidence of tephra-fall (bomb sag structure), others show evidence of surface deposition (interbedding and lags).

This unit is overlain by 3m of thinly interbedded pyroclastic sediments of silt to grit size. These also contain rounded intraclastic shale fragments, up to coarse grit size, which comprise less than 5% of the bulk rock. Heavy minerals (especially garnet, phlogopite and microdiamonds) are concentrated in the coarse lenses of the well bedded subunits. This unit is truncated by Recent glacial erosion, and overlain by a glacial gravels.

Drill Hole OFS 93-004:

The basal tuff is 5m thick, coarse grained, olive green and well indurated, with much calcite and serpentine veining sub-parallel to bedding, concentrated near the base. It is composed mostly of psuedomorphic serpentine after euhedral olivine up to 1.5mm (Plate 2.13 in Figure 2.1.8), and other heavy minerals, including ilmenite, garnet and phlogopite with rare chromite, diopside and zircon. Lapilli and autoliths are rare to fairly common (up to 1%), fine (<2mm) and rounded.

The tuffs are overlain by 2m of massive and graded, pale green pyroclastic sand with irregular coaly intraclasts up to cobble size, and rare plant fragments. Overlying this is a 7m thick sequence of at least six graded pyroclastic units, each unit ranging from 20cm to 90cm thick (Plate 2.11 in Figure 2.1.6). These are interbedded with massive medium to coarse pyroclastic

sands. Features of the graded units include; coarse sand and grit grade clasts in erosional lags, low angle cross-stratification in the silty upper layers, and heavy mineral concentration in the basal portions. Pebble size shale intraclasts occur sporadically. Grains in the graded subunits are the same as in the basal tuffs, but with more sub-rounded and rounded grains (see Point counting discussion below and Plate 2.14 in Figure 2.1.8). Lapilli are absent, although fine grained, rare, angular to sub-angular autolithic fragments are found in basal layers. This unit has patches of calcite and magnetite as the cement, which also occur with sulphides in veins throughout. Recent tills and associated clastics overlie the tuff and appear to truncate upper portions of the kimberlitic volcanic pile.

Interpretation:

The three sequences have similar lithofacies. Overlying the basal quartz sand is a crystal dominated tuff with rare lapilli and mostly euhedral grains (see Point Counting below). These are interpreted as tephra-fall (as in basal 002 and 004 intersections) and debris flow (as in central 003 intersection) deposits outside of the crater (crater edges are about 300m to the north and east), forming the lower slopes of a tuff ring. It is unclear whether the tephra-fall deposits also fell through a water column, or if the whole volcanic structure was sub-aerial. Immediately after eruption, slumping and erosion of the tuff ring, into probably a marine environment, produced the massive (debris flows) and graded (density current) deposits overlying the primary volcanics. In the 002 intersection, the unit is capped by a shale clast breccia, which may be derived from crater wall erosion producing a debris flow. Alternatively the breccia may be a recent phenomenon produced by the Recent glaciation (the apparent glacial erosional contact is only 2m above the base of the breccia). The latter model is preferred. Overlying deposits are not preserved in any of the intersections due to truncation by glacial erosion, Figure 2.1.7.

Figure 2.1.8.

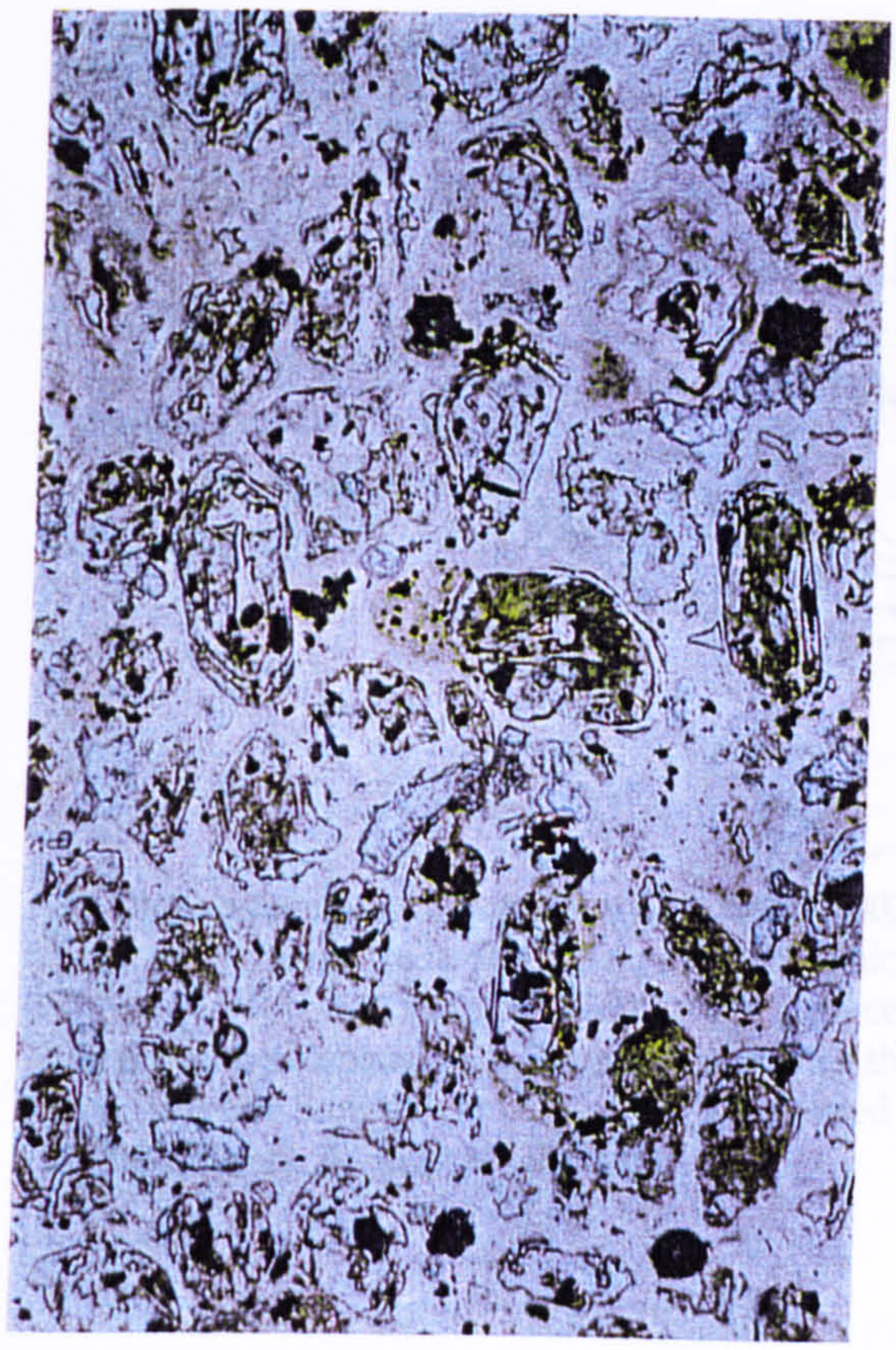

Plate 2.13
Borehole OFS 93-004, thin section at 107.7m, plane polarised light, magnification x 13. Primary pyroclastic - coarse tuff. Note the dominance of euhedral grains, and matrix supported texture. Grains are replaced by serpentine and calcite (higher relief), plus some magnetite.

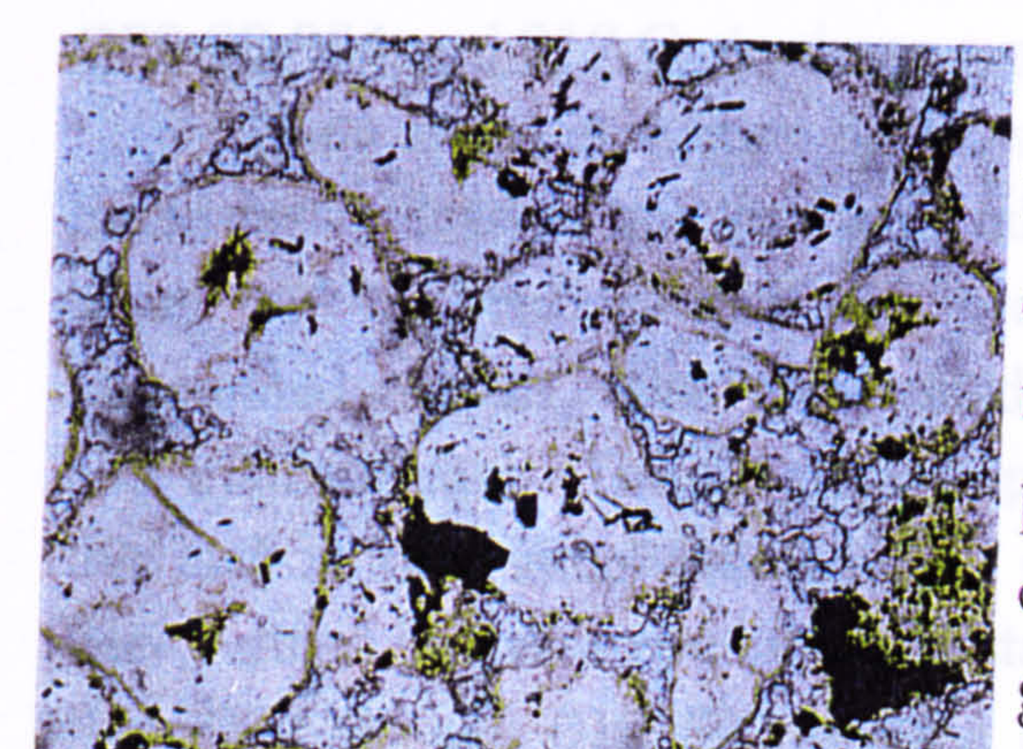

Plate 2.14
Borehole OFS 93-004, thin section at 97.7m, plane polarised light, magnification x 13. Reworked pyroclastic - graded pyroclastic coarse sand. Although euhedral grains are still present, many more subrounded and rounded grains occur. Grains are replaced by serpentine with a fine dusting of magnetite and calcite.

Figure 2..1.7.

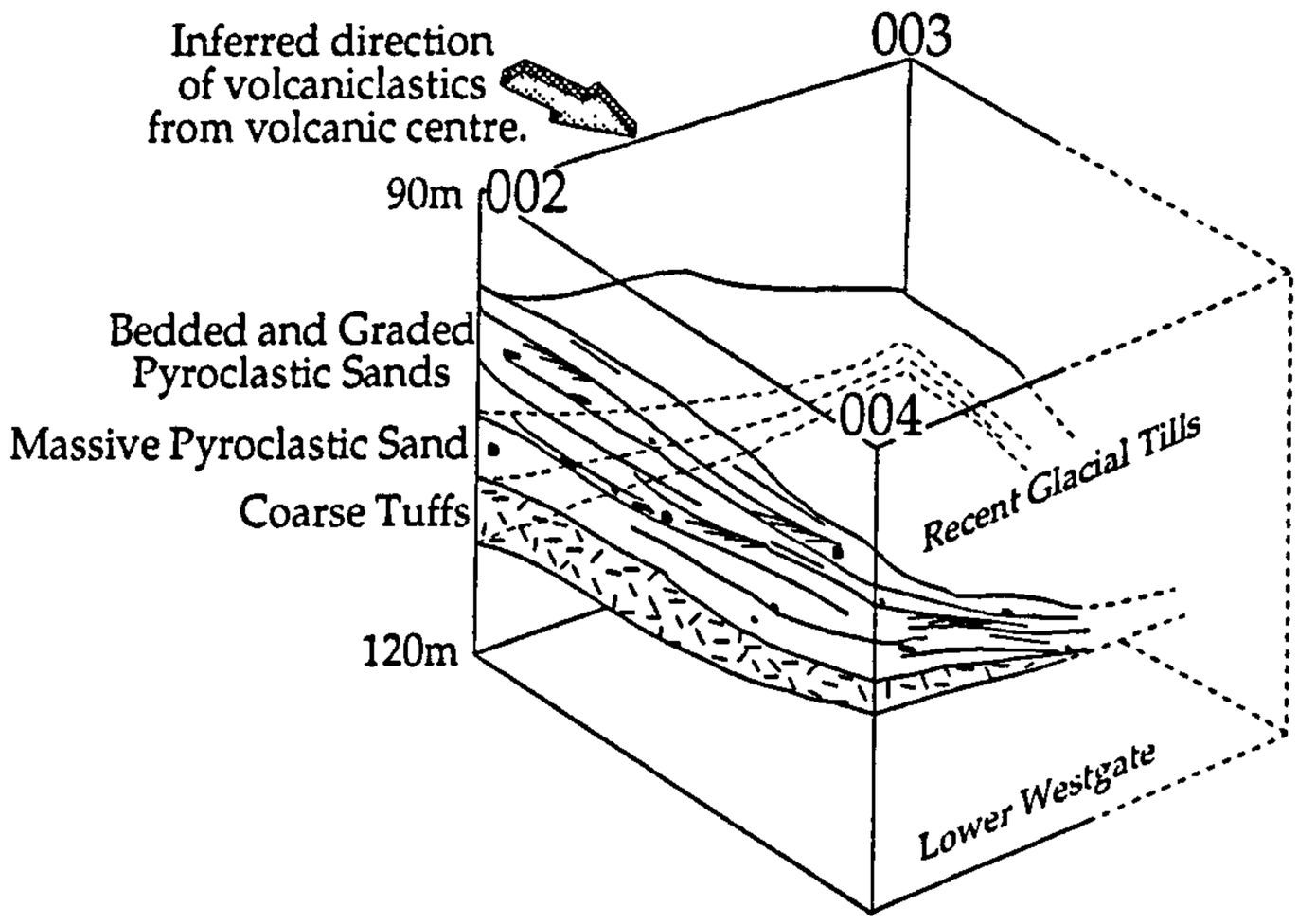

3D Block schematic of Boreholes OFS 93-002, 003 and 004. Inferred direction of pyroclastics from volcanic centre is derived from geographical disposition relative to nearest magnetic anomaly. Note that the upper kimberlite surface may be an erosional feature of Recent glacial times (i.e. a paleosurface). Diagram illustrates the consistent layering of Graded/Bedded Sands over Massive Sands over Coarse Tuffs observed in the three boreholes, and is representative of proximal facies kimberlite strata.

<u>OFS 93-004 and 012 Grain shape evaluation:</u>

Grain shape evaluation of thin sections of kimberlite strata can determine broad facies division into primary and reworked pyroclastic kimberlite. This is based on the notion that the proportion of rounded, subrounded and fragmented crystals, relative to euhedral crystals, will increase with reworking and transportation. The potential application of this notion was perceived by this author from visual estimation of olivine grain shapes in thin section, and later verified by point counting and statistical analysis. Thin sections from 004 (16), 002 (6) and 012 (6) were cut and described (see the Section 2.3 and Appendix III). From visual estimation it was clear that the proportion of euhedral crystals (mostly olivines) decreased up the intersections, relative to the proportion of sub-rounded and rounded grains, Figure 2.1.8. The terms use mixed igneous and sedimentary descriptions, but are the most appropriate for these rocks, Figure 2.1.9 below.

Figure 2.1.9

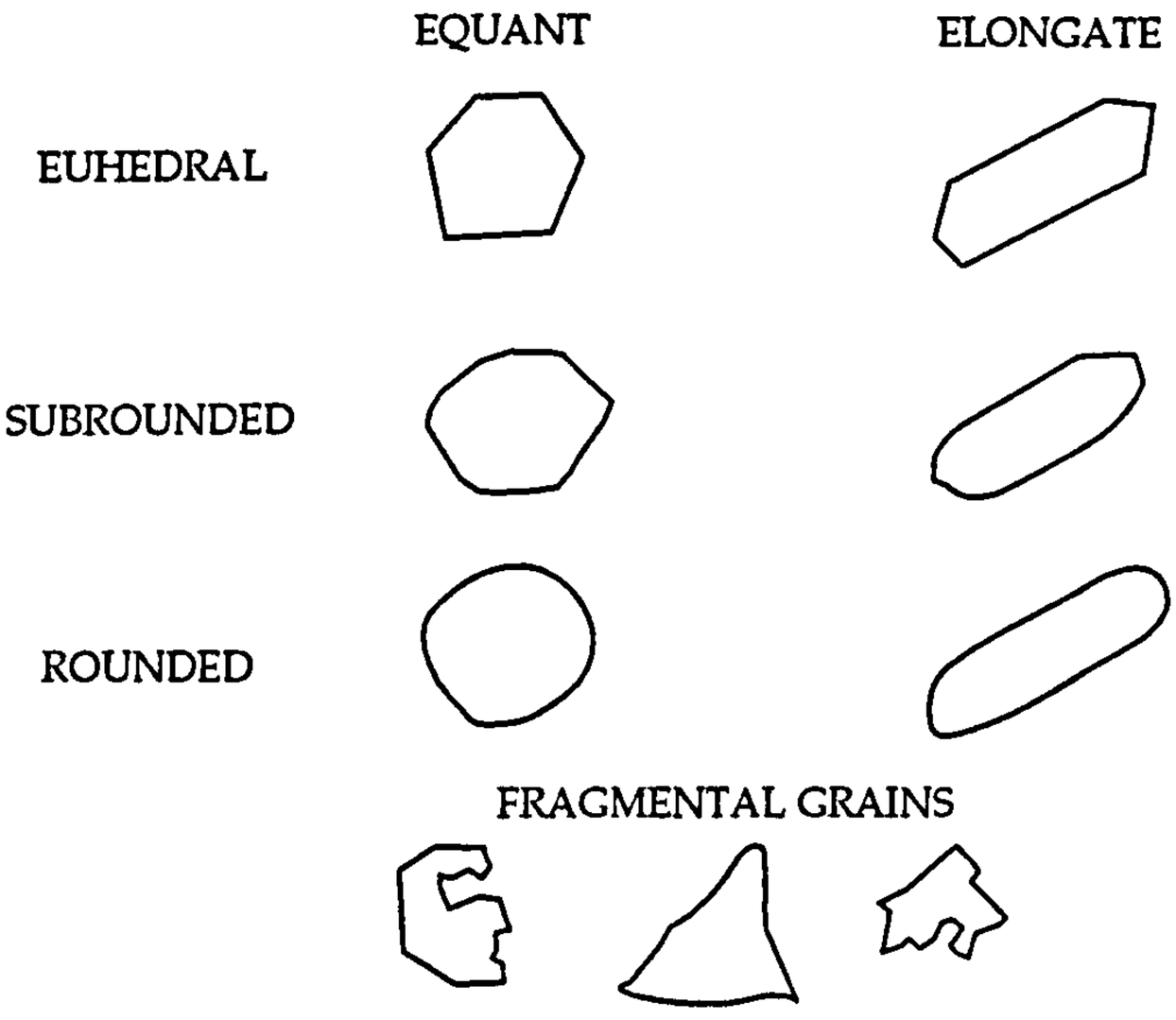

A visual estimation of grain shape proportions in a small, representative area on each slide was made, and recorded on the Petrology Sheets (Appendix III). The data were plotted on a Rounded-Subrounded-Euhedral ternary diagram, Figure 2.1.10 below.

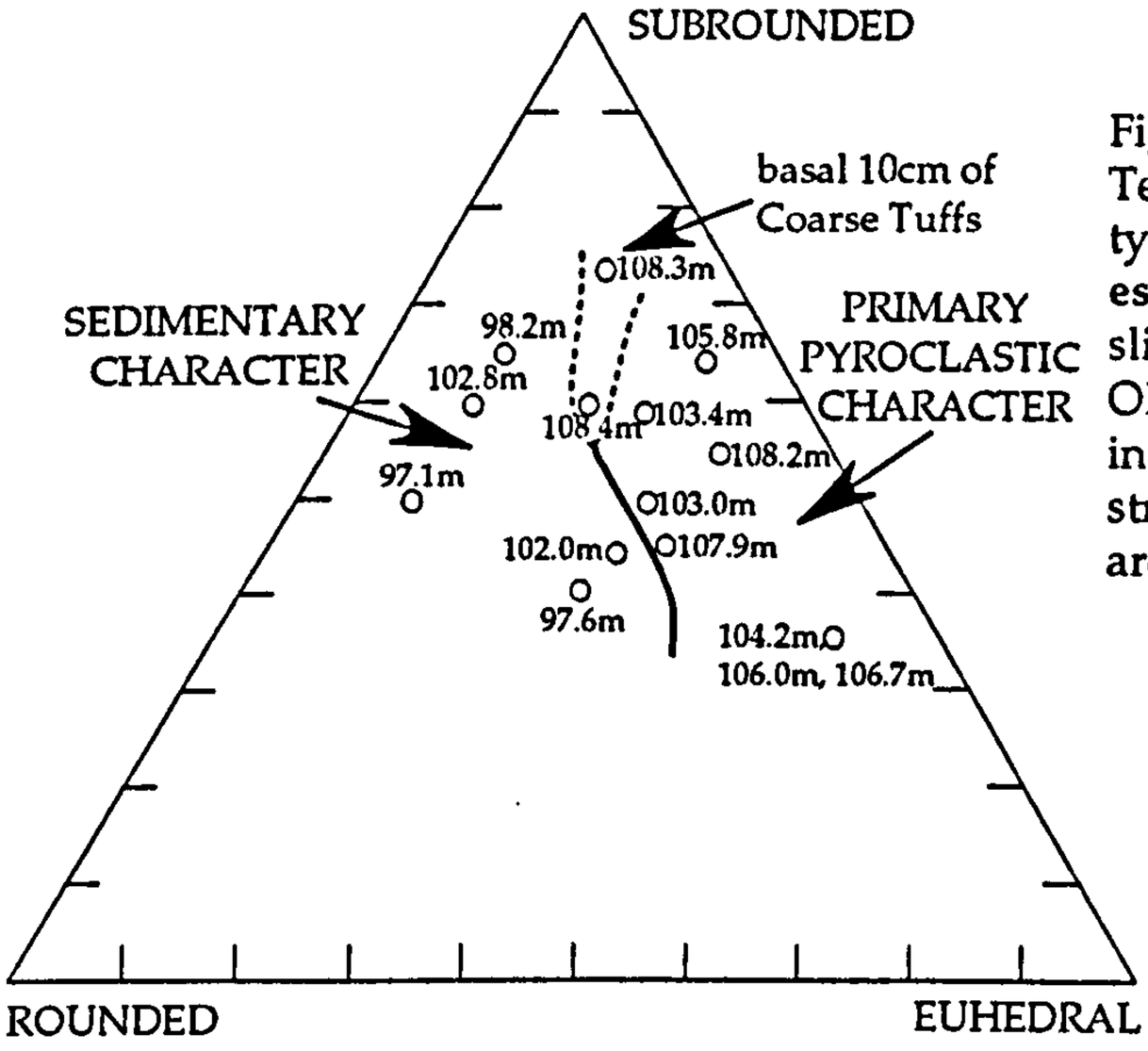

Figure 2.1.10.
Ternary point counting plot of grain types, as determined by visual estimation. Average of 40 grains per slide. All slides from Borehole OFS 93-004 Note two main fields, interpreted as primary and reworked strata. The transition appears to be at around 102.8m to 103.0m.

This striking difference in the degree of grain roundness suggested a powerful argument for primary versus reworked deposits. The primary deposits (including the demonstrable primary coarse tuffs in 012) always have more euhedral grains than rounded. The overlying strata appear to have at least equal amounts of rounded to euhedral grains.

The increase in the proportion of rounded grains must be due to sedimentary reworking, acting to abrade the crystals. In all but transitional cases the grain proportions matched the proposed lithofacies of either reworked or primary pyroclastics, determined from the core description.

To test this apparent petrological property of determining lithofacies from grain shape proportions, point counting was carried out on 15 slides from 004, and 3 from the lapilli-tuffs in 012.

Point counting was carried out using a Ziess electronic microscope counter attached to a standard petrological microscope. Microscope magnification was x10 for 004 slides, and x4 for 012 (much coarser grained) slides. A count of three hundred points has been determined as statistically meaningful for grain analysis of sedimentary rock thin sections (Friedman, 1958), and has been applied to pyroclastic rocks (Wright and Mutti, 1981). This study used 400 points, with an interval of 0.1mm in 004, and 0.9mm in 012 (typical grain size). The following separate point types were used: euhedral grains, subrounded grains, rounded grains, fragmented grain, mica, lapilli, CAVA crystal (coarse authigenic vermicular antigorite, see section 2.3), matrix - serpentine, matrix - carbonate, matrix - opaque (usually magnetite, some haemetite and pyrite) and vein fill (carbonate, magnetite, hematite and pyrite).

The results and data analysis of the point counting are tabulated in Appendix IV. The raw values of point type proportions were normalised to a pre-diagenetic state by redistributing proportionally to the other components the percentage of diagenetic material (vein fill and CAVA crystals). This was particularly important in the lowermost basal tuffs, where carbonate veins account for 55% of the rock, and CAVA crystals are common. From these data total amounts of grains and matrix were determined: Primary (including 012 tuffs) grains: 50 - 73%, matrix: 27 - 50%, and Reworked, grains: 62 - 80%, matrix: 20 - 38%. Note that reworked sections typically have a greater proportion of grains to matrix and are often more clast-supported, although there is significant overlap such that grain/matrix proportion and support is not diagnostic. Normalised grain type ternary diagrams have been calculated (as outlined above) for Rounded-Subrounded-Euhedral system and Rounded-(Subrounded + Fragmental)-Euhedral, Figure 2.1.11. Fragmental grains, apart from those with fragmentation preserved from the original volcanic eruption (about 3% to 10%, as determined from 012 tuffs), are products of transportation and grain breakage of brittle minerals (like olivine). Further transportation leads to grain abrasion, and rounding of fracture surfaces, producing rounded grains. Thus fragmental grains are grouped with sub-

Figure 2.1.11.

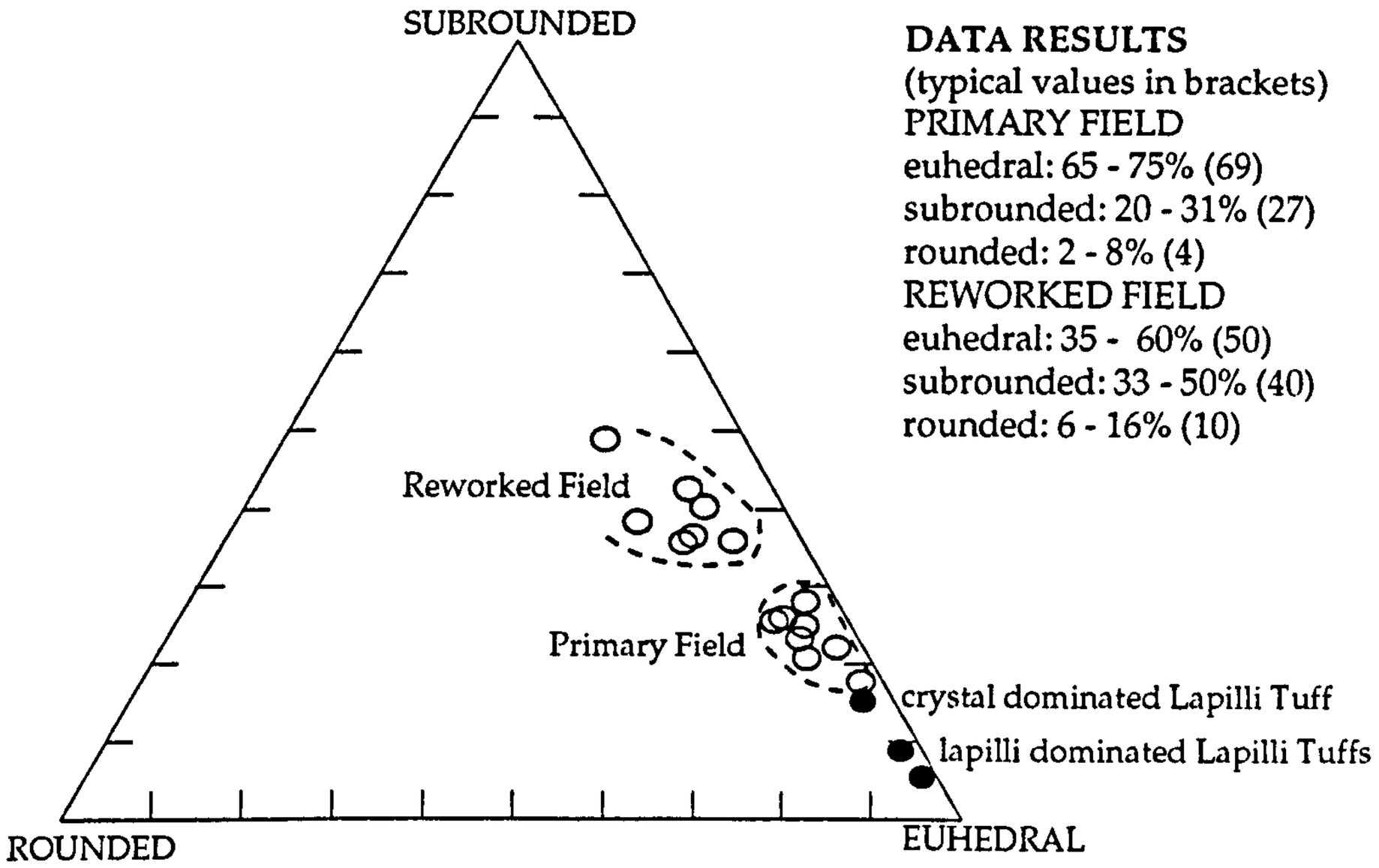

DATA RESULTS
(typical values in brackets)
PRIMARY FIELD
euhedral: 65 - 75% (69)
subrounded: 20 - 31% (27)
rounded: 2 - 8% (4)
REWORKED FIELD
euhedral: 35 - 60% (50)
subrounded: 33 - 50% (40)
rounded: 6 - 16% (10)

Ternary diagrams of grain types determined from point counting (see text for methodology). Open circles are data points collected from Borehole OFS 93-004, filled circles are from Borehole OFS 93-012. Note the distribution of OFS 93-004 points define two fields, all points in the reworked field contain the upper 6.3m, all points in the primary field contain the lower 5m. Transitional depth is between 103.4m and 104.2m in OFS 93-004. The OFS 93-012 data points provide a comparison to known primary pyroclastics (from crater fill). Note that the OFS 93-004 basal tuffs are crystal dominated and correlate well with the position of the OFS 93-012 crystal dominated tuffs. See Appendix V for raw data and data treatment.

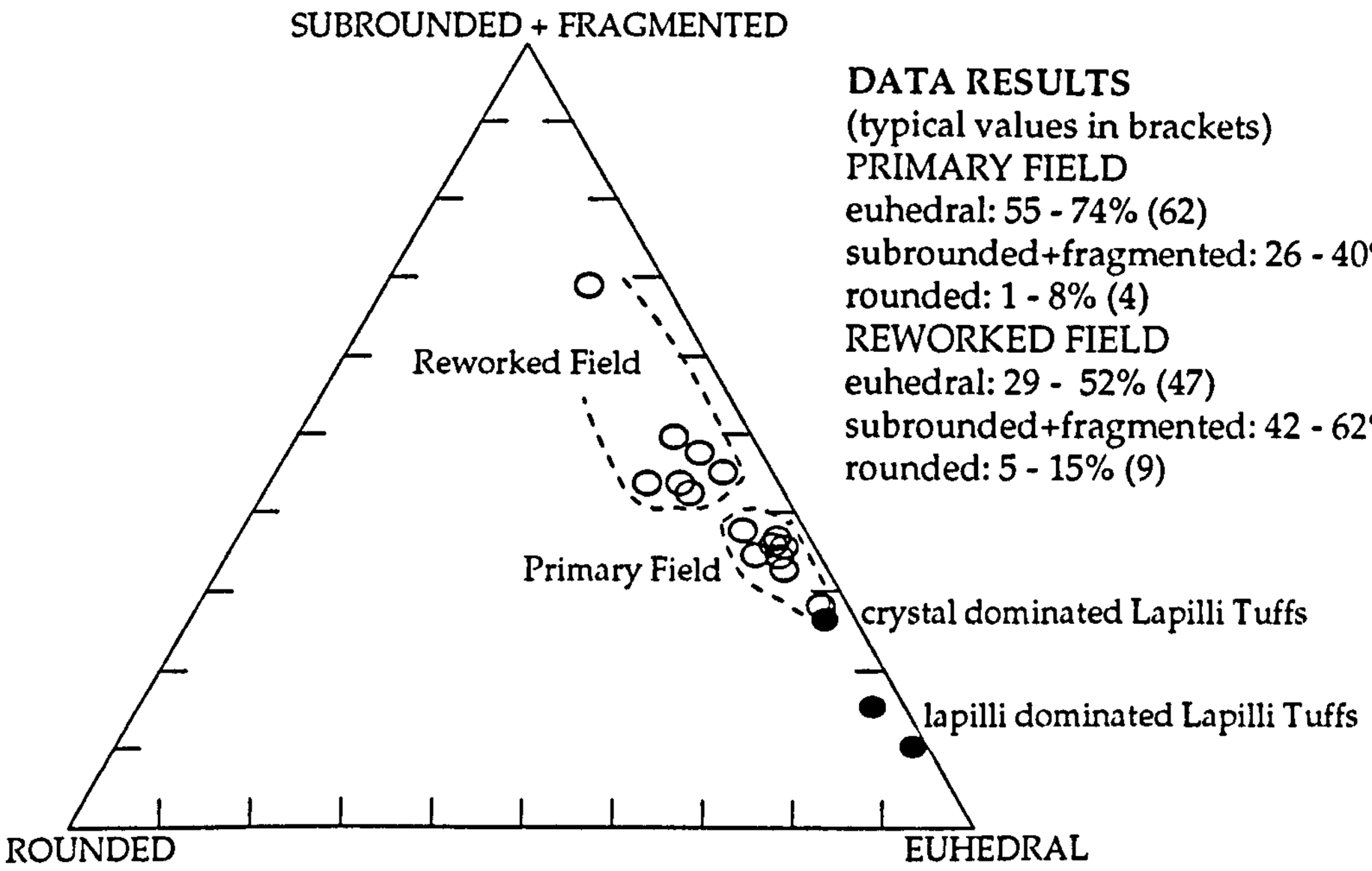

DATA RESULTS
(typical values in brackets)
PRIMARY FIELD
euhedral: 55 - 74% (62)
subrounded+fragmented: 26 - 40% (34)
rounded: 1 - 8% (4)
REWORKED FIELD
euhedral: 29 - 52% (47)
subrounded+fragmented: 42 - 62% (44)
rounded: 5 - 15% (9)

rounded grains, rather than rounded, for the purpose determining degree of reworking.

The difference in the grain type proportions in the ternary plots, Figure 2.1.11, is attributed to the different depositional modes of the primary (airfall tuff) and reworked (graded and massive) deposits. Although the differences in the proportions are not as marked as the visual estimation suggested, the point counting of grain shapes is a useful diagnostic tool, to supplement detailed hand sample description, when determining the primary versus reworked nature of pyroclastic kimberlite.

In summary point counting analysis has verified the primary nature of the basal 2.5m to 4.3m in 002, 003 and 004, interpreted as crystal dominated fine to coarse tuffs. Such a thickness of tephra-fall deposits can only accumulate in close proximity to a crater, i.e. adjacent to the tuff cone or crater rim (Cas and Wright, 1988), consistent with the borehole's geographical disposition to the crater, as defined by aeromagnetic anomalies. The primary deposits are then overlain by massive and graded pyroclastic kimberlite sands, derived from slumping from and erosion of the tuff ring (Figure 2.1.7).

Drill hole OFS 93-009:

Borehole OFS 93-009 was drilled on the eastern edge of the FALC cluster, within 50 metres of the edge of Anomaly 121, Figure 2.1.12. This provides another intersection of reworked proximal facies kimberlite, somewhat similar to the upper half of OFS 93-003 described above.

The base of the 6m kimberlitic intersection is a simple sedimentary contact of dark grey marine shales overlain by pale grey-brown pyroclastic sands with >50% intraclastic shale. This unit is 65cm thick, and contains mostly gritty (but up to cobble grade) sub-rounded to rounded shale intraclasts. Serpentine and/or carbonate after olivine is the dominant grain type, other rarer constituents include garnet, ilmenite, phlogopite, enstatite, chromite and diopside. Crustal xenolithic grains are common; tourmaline, pyroxene and amphiboles (the origins of these minerals are further discussed in Section 2.2).

Overlying the basal unit is a 1m thick sequence of about 7 grey-green coarse and fine interbedded pyroclastic sands, with some small-scale normal grading and many thin coarse-grained lenses. These have the same mineral constituents as described above. There follows another sequence 3m thick of both graded and bedded pyroclastic sands, with a basal lag of pebble size shale intraclasts. This is succeeded by a thin 30cm bed of intraclastic shale breccia,

very poorly sorted (due to shale pebbles), which has a small amount of coarse pyroclastic matrix, with rare, well sorted thin lenses, often with disrupted bedding (from slumps, and small syn- and post-sedimentary faults). The succession is capped by a 1m thick, pale green, medium grained, massive pyroclastic sand. This sand contains the constituent minerals described for the basal unit, but garnets are far more common. This unit is overlain with a sharp sedimentary contact by a dark-grey sandy mudstone of the central St. Walburg Sand.

Interpretation:

Borehole 009 contains a relatively thick intersection (6m) of reworked pyroclastic kimberlite derived from a debris flow, probably due to a tuff ring basinward slump. Together with the geographical disposition, the lithofacies is more likely to be proximal, rather than distal. The deposition occurs in mid-Westgate or earliest St.Walburg Sand times, around 100Ma, and may be the northern equivalent of the two youngest tuffaceous strata in 010. The OFS 93-009 kimberlitic intersection represents a proximal debris flow deposit, with the shale clasts probably ripped up locally, sourced at the adjacent crater wall. The three pulses of intraclast breccias overlain by pyroclastic sands and grits represent three successive subaqueous flow phases. The final deposit of well bedded and laminated pyroclastic sands represent wave reworking of the kimberlite deposits, overlain by coastal swamp and mud flat deposits.

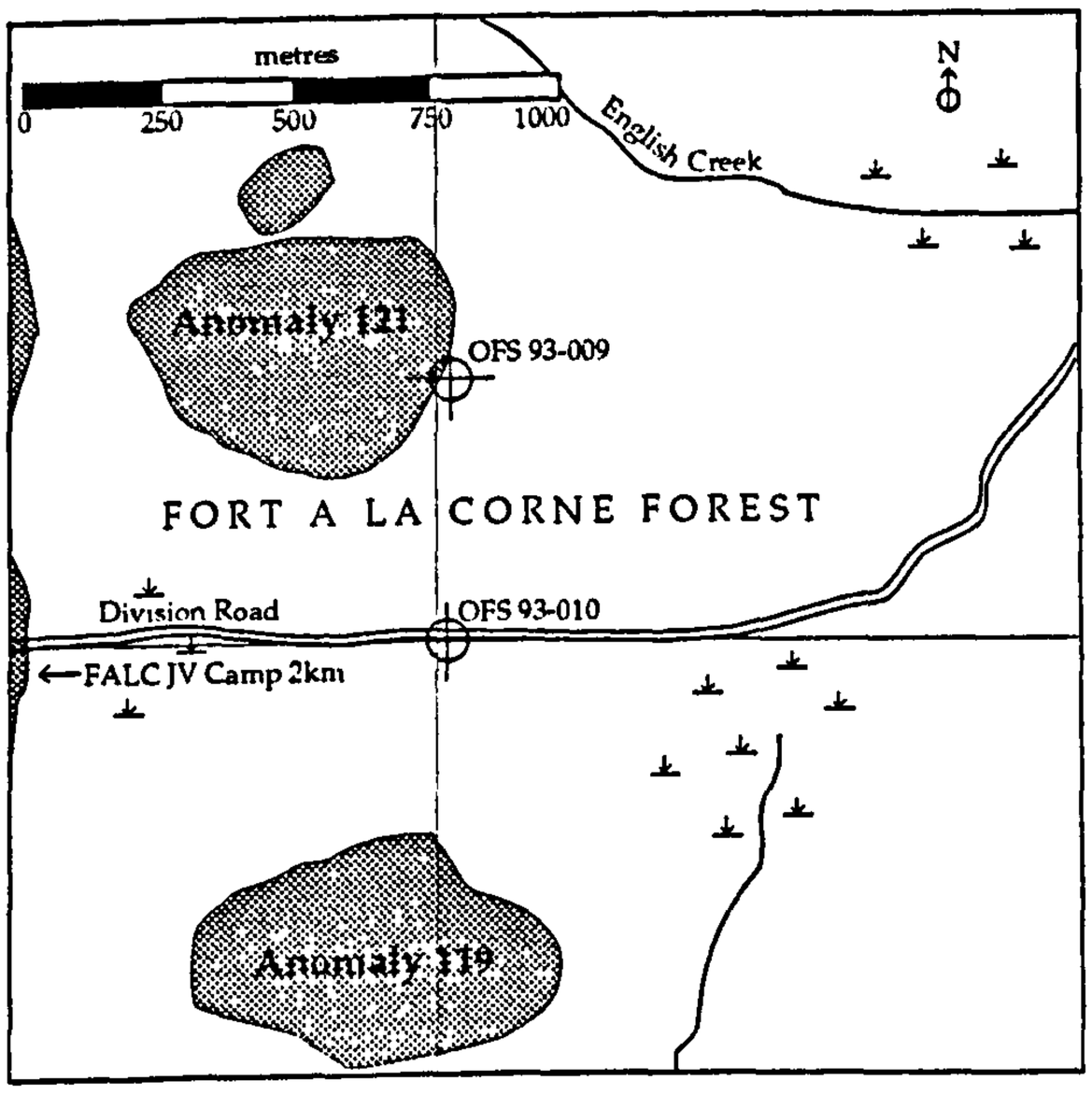

Figure 2.1.12.
Detailed sketch locality map of the eastern edge of the FALC main cluster, showing locations of of OFS 93-009 and 010. The main cluster to the west consists of largely coalecsing craters, see Fig. 2.1.1. Note the embayment into the edge of the cluster, where 010 is located. Both Anomaly 119 and 121 have been confirmed as kimberlite crater deposits by drilling.
For geographical position, refer features on this map to those on the larger scale map of the boreholes described, see Fig. 2.1.1.

Distal Extra-Crater Facies Kimberlite

Description:

Rocks of this facies typically range from thin beds (<2m) of pyroclastic to tuffaceous sands and silts, with between 10% to 90% pyroclastic material.

Borehole OFS 93-010 was drilled in the FALC forest, on the eastern boundary of the main cluster (Figure 2.1.12). It is located in an embayment between two craters to the north-west and south-west, and the kimberlite material intersected could be derived from either. Throughout the following description refer to the borehole litholog of OFS 93-010, Figure 2.1.13.

Drill Hole OFS93-010.

This sequence, over 50m thick, consists of four thin tuffaceous horizons isolated by stretches of normal Spinney Hill to St. Walburg Sand stratigraphy (see Chapter 1).

The basal deposit sharply overlies, with a load and flame base, the central Spinney Hill sands and muds. The unit is a 1.1m thick, pale cream-brown, massive pyroclastic sand. Constituent grains are medium grained, mostly carbonate and/or serpentine after olivine, with garnet, ilmenite and phlogopite common, and rare chromite and diopside. Well rounded fine to grit grade shale clasts (and rarer glauconite) are common (about 20% of all grains). Angular pebbles of intraclastic shale occur sporadically throughout. The matrix is mostly carbonate, with finely intermixed serpentine and clays. The upper boundary is sharp, with a small (0.3cm) vertical syn-sedimentary fault. 80cm below the base is a precursor 2.5cm thick, massive, medium grained pyroclastic sand. The precursor has a sharp erosional base, and a diffuse interbedded upper contact with the overlying black silts.

About 40m of normal stratigraphy overlie the basal deposits, comprising the upper Spinney Hill and Joli Fou Formations, overlain by the Flotten Lake Sand and the lower Westgate Formation. This marine sequence represents about 4Ma. The next kimberlitic strata consists of about 1.1m of a very poorly sorted, green-brown, matrix-supported tuffaceous conglomerate (Plate 2.15 in Figure 2.1.14). The base consists of a 20cm layer rich with rip-up clasts of the underlying shale, and displays slumped and disrupted bedding. Sub-rounded crustal xenoliths (dolomite, shale, quartzite and amphibolite) are common as clasts up to large pebble size. Grains include quartz, serpentine after olivine, very common garnets and ilmenite, and rarer phlogopite, chromium diopside and spinel. The unit grades into tuffaceous grey to brown-green silts, with two normally-graded subunits each about 20cm thick. These contain more

Figure 2.1.13

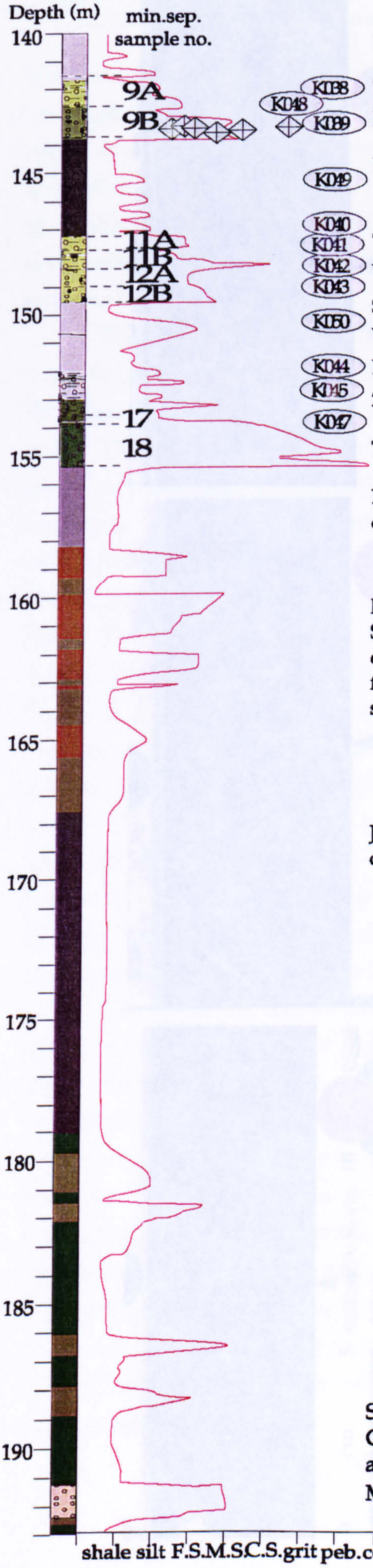

Upper Westgate Formation, dark grey mudstone.

K038 Tuffaceous silts, well laminated

K048

K039 Pyrite-cemented medium quartz sand, with diamonds

Black mudstones with rootlets and bioturbation.

K049

K040

K041 Tuffaceous laminated and cross-stratified silts to grits,

K042 with shale bomb at 148.5m.

K043

St. Walburg Sand equivalent, sandy mudstone
with rootlets and bioturbation.

K050

K044 Lower Westgate silts and mudstones.

K045 2 subunits of graded Tuffaceous Silt.

K047

Tuffaceous Conglomerate.

Lower Westgate
dark grey shales.

Flotten Lake Sand
Silty mudstones and
cross-stratified, fining-up
fine and medium grained
sandstones.

Joli Fou Formation
dark grey mudstones.

Borehole log of OFS93-010. Colours and ornament within the log are schematic, see key with Figure 2.1.2.
'Min sep sample no.' refers to heavy mineral sample intervals, see Fig. 2.2.3. Red line is a representative grain size log, N.B. this excludes the size of intraclast and xenolith components. Grey ellipses indicate sites of XRF analysis.Grey diamonds indicate diamond size grade, and sample interval in which they were found. Log grain size terms are standard sedimentary nomenclature. Note, normal section provides a representative stratigraphy, punctuated by tuffaceous strata. Borehole OFS 93-009 is not shown, as this represents a more proximal kimberlite facies, but is very similar in thickness and content to Borehole OFS 93-003, see Figure 2.1.5.

Spinney Hill Formation
Glauconitic sandy mudstones
and fine to medium sandstones.

Massive Pyroclastic Sand.

Figure 2.1.14.

Plate 2.17
Borehole OFS 93-010, 142.2m.
Non-tuffaceous (<10%) quartz medium sand, with shaley partings. Includes rare kimberlitic heavy minerals; garnet, perovskite and phlogopite. One macrodiamond (2.4mm) was separated from this subunit.

Plate 2.16
Borehole OFS 93-010, 148.7m.
Tuffaceous laminated silts and grits, with airfall shale bomb (of pyroclastic origin). Note well developed impact sag. Lower core fragment shows a gritty lens and hummocky cross-stratification. These units carry a large amount of kimberlitic trace elements (Nb >600ppm), probably due to silt grade perovskite in silty laminae.

Plate 2.15
Borehole OFS 93-010, 155.2m.
Tuffaceous conglomerate with kimberlite-derived xenolithic granules and pebbles (e.g. dolomite, kimberlite, amphibolite and chert.) Note 1cm rounded brown/red garnet in the lower core fragment. Matrix is clay and calcite rich.

terrigenous material than the conglomerate, mostly silt grade quartz and clays (although garnets, ilmenite and phlogopite still occur). The basal lag of the upper graded unit includes elongate (up to 4cm) rip-up clasts of pyroclastic kimberlite and shale. Overlying this silty subunit is 8cm of black shale, followed by a sharp sedimentary contact with 15cm of grey-green, coarse, massive pyroclastic sand. These are succeeded by 4.38m of Westgate Formation and lowermost St. Walburg Sand.

The central pulse of tuffaceous sedimentation, 2.69m thick, consists of much finer grained clastics - pale green-brown fine sands, silts and gritty lenses. The base is sharp, and overlain by 15cm tuffaceous laminated silts and fine sands. These are succeeded by 1.55m of green to grey interbedded tuffaceous silts, sands and grits. These consist mainly of quartz grains and clay matrix, but serpentine after olivine, ilmenite, garnets and phlogopite are common, with rarer chromium diopside and spinel. Within this there are numerous multi-directional cross-stratification structures and well sorted lenses of grit-grade clasts. The cross-stratified silt contains a volcanic ejectum: a rounded shale 'bomb' 24mm in diameter with a well preserved impact sag, Plate 2.16 in Figure 2.1.14. The upper part of the unit consists of strongly bioturbated mudstones, in which the bioturbation (*planolites* and *terebellina*) has introduced tuffaceous sand from below. Kimberlitic trace-elements (see XRF results, Chapter 5), specifically niobium (carried by perovskite and spinels) were found to be concentrated in the burrow-filling fine sands. The bioturbated tuffaceous muds are overlain by 3.85m of fine silts and shales, which are also strongly bioturbated (but do not have a tuffaceous filling), containing rootlets, pyrite and common plant debris.

The upper tuffaceous sediments consist of 1.2m of medium to coarse, pyrite cemented, grey-brown quartz sand with ripple cross-stratification and slump structures at the base (Plate 2.17 in Figure 2.1.14). This sandstone contained a 2.5mm diamond, chipped during heavy mineral separation. Other kimberlitic minerals are rare, and include; phlogopite, garnet, ilmenite, chromium spinel and diopside. The upper 40cm of the unit is composed of tuffaceous silts and fine sands, very similar to those in the central pulse. Kimberlitic components are rare, and include those listed above, plus perovskite. This unit has a sharp sedimentary boundary with the overlying dark shales 1.3m thick, rich in rootlets, plant and fish debris. In turn, these are overlain by dark grey homogeneous shales of more typical Westgate Formation marine sedimentation.

Interpretation:

The lowermost kimberlite unit in OFS 93-010 represents two separate high-density flow deposits, the 2.5cm thick precursor (at 193.2m) was of low volume, and/or high velocity (indicated by the very thin deposit). The main unit was a single-event deposit some considerable time after the precursor. Transportation distance was great, as evidenced by rounded shale clasts, and the incorporation of glauconite grains and clay matrix. Both deposits are likely to be density flows, restricted to a channel rather than a broad sheet.

The lower conglomeratic unit is of a similar origin to the basal kimberlitic deposits: high-density flow to debris flow, again probably of a channel rather than fan origin. The upper graded subunits represent probably two such events, the later being of much lower density, equivalent to a tuffaceous turbidite.

The central tuffaceous silt and sand deposits represent considerable shallowing relative to the earlier tuffaceous deposits. These tuffaceous deposits contain sedimentary features (hummocky and very low angle cross-stratification, upper phase plane beds) suggesting shoreface, possibly tidal flat environment. Certainly the water column must have been very shallow, if not absent, to allow a tephra-fall impact sag feature as well developed as has been observed. This allows a date equivalent to the basal St. Walburg Sand (about 100Ma) for nearby kimberlite extrusive activity, presumably from one of the two nearest craters (Figure 2.1.12). The tuffaceous tidal flat sands are overlain by mud flat then coastal swamp muddy deposits (as indicated by bioturbated muds and silts with rootlets and rich in plant and fish debris). These shoreline deposits indicate the kimberlitic volcanic source areas to the west were fully emergent.

The bedform and sedimentary structures in the overlying medium quartz sands are very similar to St. Walburg Sand medium sandstones, which have a well constrained paleoenvironment, shallow marine shoal deposits. This indicates a small-scale transgression over the tidal flat and coastal swamp deposits. The quartz sand incorporated only a small amount of kimberlitic material, probably derived from reworking of the distal deposits, rather than an influx of material from the kimberlite crater areas. The transgression recorded by the quartz sand must have been of low magnitude in time and space, as the 80cm sand grades into a tuffaceous silt of the same tidal flat and shoreface origin as the tuffaceous silts 6 metres below. Again the tidal flat deposits are overlain by coastal swamp muds, before a larger magnitude transgression returns the area to more typical shelf marine Westgate sedimentation.

In summary borehole 010 intersects four kimberlitic pulses in a wide range of sedimentary environments, offshore channel to coastal deposits. These had a long depositional history, sporadically from basal Spinney Hill to upper St.Walburg Sand times. This is equivalent to around 105Ma to 100Ma (see Chapter 1), a typical time in the kimberlite eruptive history, which appears to peak at about 100Ma (contrary to the 94Ma proposed by Lehnert-Thiel et al, 1992; Scott-Smith et al, 1995). It is significant that the area around the eastern side of the FALC main cluster experienced emergence and produced terrestrial and shoreline deposits during the St.Walburg Sand deposition. Elsewhere the St.Walburg lowstand event deposits shallow shelf sediment, still fully marine. This suggests a considerable topography (tens of meters above the usual shallow marine depths) in the FALC area at the time. See Chapter 4 for further discussion of kimberlite in the sedimentary environment, and paleogeographic reconstructions. See section 2.4 for the classification of kimberlites.

2.2 Composition of kimberlite from heavy mineral processing.

In parallel to the sponsorship by Rhonda Mining Corporation of this PhD, Leeds University Department of Earth Sciences was commissioned to carry out heavy mineral separation on the borehole cores described above. This was part of a project was called Operation Fish Scale (OFS), alluding to the Fish Scales Formation that immediately overlie the kimberlites (and which were initially thought to be linked). The aim of the heavy mineral separation was four-fold:

i) To extract all diamonds from the kimberlites
ii) To extract kimberlitic heavy minerals
iii) To prepare heavy minerals for microprobe analysis.
iv) To build a detailed database of heavy mineral distribution in the kimberlites.

From June 1993 to April 1994 OFS processed 72 samples of kimberlite, tuffaceous sediment and glacial till, amounting to a total weight of 320kg. At peak production (autumn 1993 to winter 1994) the project employed eight full-time and three part-time staff (including the author), and three consultants. Upon completion of the project, samples from the following boreholes had been processed: OFS 93-002, 003, 004, 009, 010 and 012. For separation methodology and procedures refer to Appendix V, a summary is shown on Figure 2.2.1, and illustrated in Figure 2.2.2.

Figure 2.2.1. Borehole core treatment and timing.

BOREHOLE CORE PROCESSING (for a notional 5kg sample)	Weight	Day
Receipt of sample, label, weigh and log. Take chips for thin-section microscope and SEM work.	5kg	1-2
50g sample for XRF geochemical analysis.		
Crush sample in jaw/roller crusher; screen to 3.5mm (later 2mm); reweigh.		-4
Acidify sample in 25% HCl to dissolve carbonates and fine clays, wash, settle, suspension and decant through 23micron sieve; dry and weigh.	3kg	-10
Screen fines (-100microns); weigh and store.	2kg	-11
Bromoform (S.G. 2.86) heavy mineral separation; wash all fractions in methanol; dry and weigh heavies; store light fraction.	100g	-16
Immersion in ultrasonic bath to assist liberation of magnetite; dry , weigh, magnetite separation.		-18
Screen heavies into >1000, >500, >250, >150, >100 and <100micron fractions, weigh each fraction.	.	
Frantz electromagnetic separation of each fraction into 4 further fractions: ilmenite/ chromite, garnet, pyroxene and the non-magnetic fraction containing diamond.		
All 20 fractions examined visually under binocular microscope to determine; i) diamond/diamond indicator minerals (picked for microprobe analysis), and ii) mineral percentages per fraction.		-21
Clerici Solution; all non-magnetic fractions bulk and separated at S.G. 3.5 for diamond. further hand picking under binocular microscope. Diamonds selected, confirmed later by laser Raman spectrometry.	1g	-24
Enter results into heavy mineral database (see Fig. 2.2.3.)		

Figure 2.2.2.

Plate 2.18
Bulk acidification stage. Each bucket contains a crushed sample interval. Drying lamps can be seen in the background.

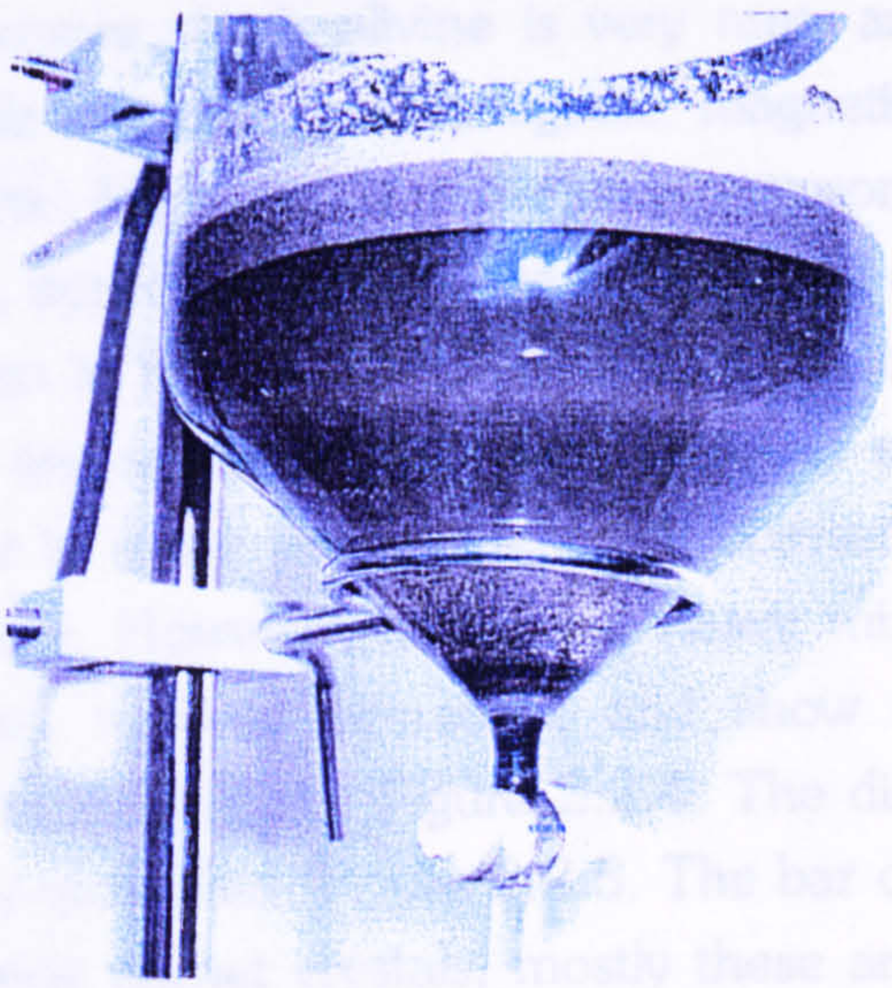

Plate 2.19
Five litre bromoform vessel. Note the pale grey 'lights' floating on the bromoform, and the black 'heavies' collecting in the funnel.

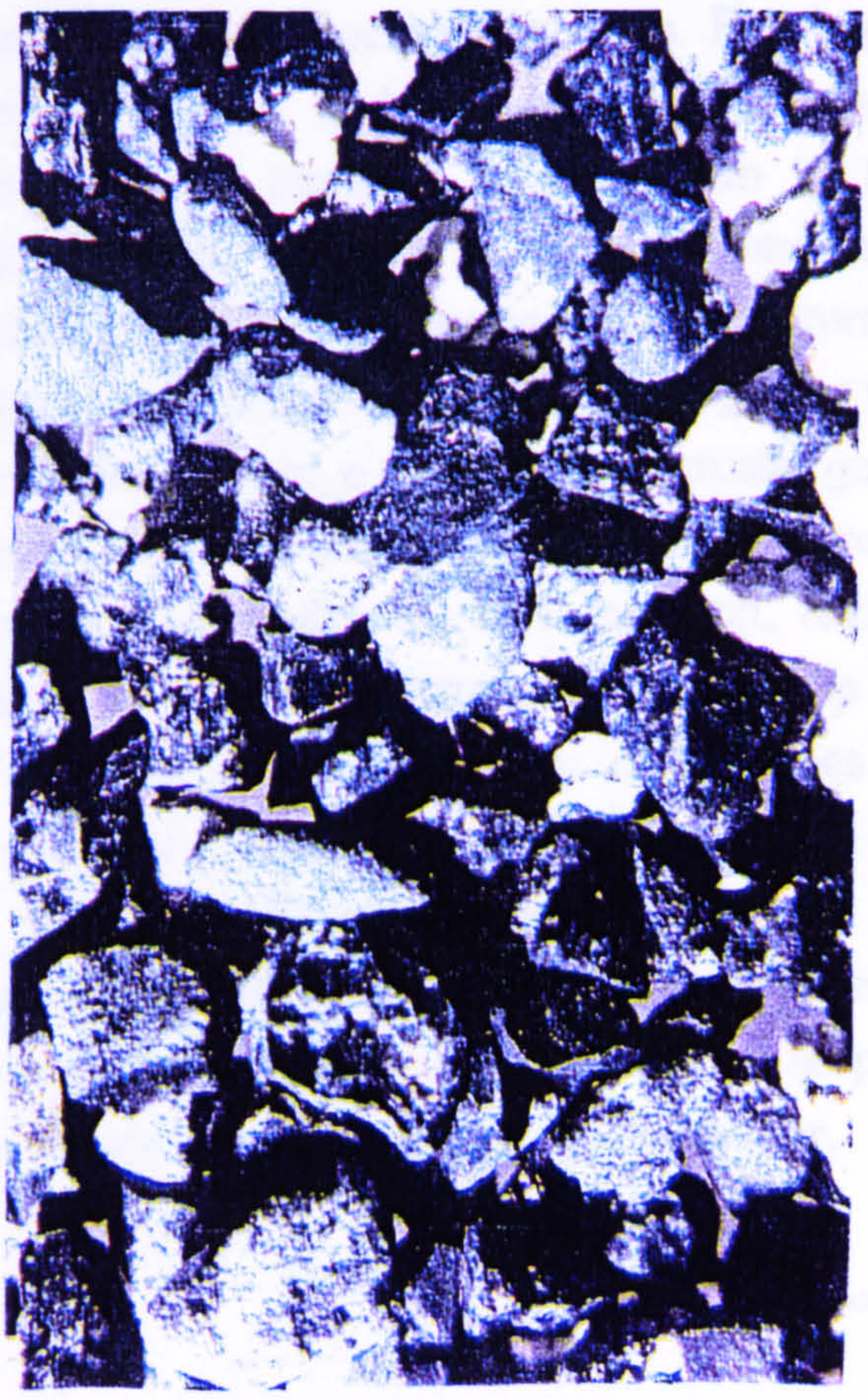

Plates 2.20 and 2.21
Heavy mineral fractions: ilmenite fraction (left) with chromite and white dusting of perovskite, and garnet fraction (right) with pyrite (brown and black) and a green chrome diopside (upper right). Field of view is 12mm in each.

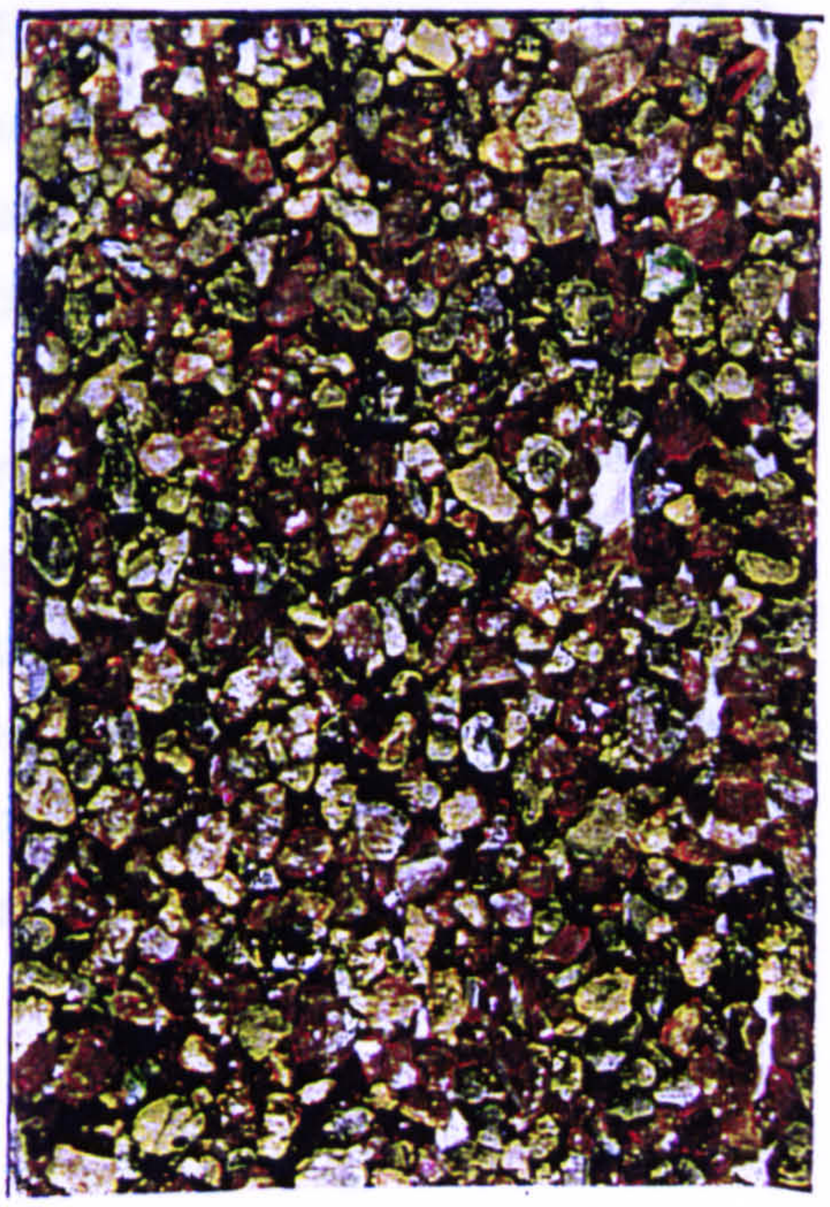

2.2.1 Separation Results

The heavy mineral database generated is presented in Appendix V (part 2), and the main points summarised on Figure 2.2.3. From the amount of the kimberlite lost to acid dissolution the data suggests that the kimberlite is mainly composed of secondary minerals, and therefore has been highly altered. For example much of the kimberlite strata, typically 30% to 70%, is composed of carbonate, serpentine and clays prone to dissolution in acid (or finer than the 23µm rinsing mesh). This amount apparently dissolved is often far greater than the total amount of matrix available in the rock (20% to 50%, see section 2.1). This lends further evidence of the pervasive alteration of the grains. Furthermore, fresh olivine is very rare, and a large proportion of the heavy minerals separated are authigenic: magnetite, pyrite (and other metal sulphides) or baryte. Magnetite is particularly common in the proximal facies, up to 6% by weight, pyrite is richest in the coarse distal clastics, up to 3%, and baryte is most common in the crater facies, up to 1.5% by weight. The magnetite, pyrite and baryte are secondary (post-eruptive) and are observed in the core as fault fill, cement in more porous (generally coarser) laminae, and replacing grains (less common). However, kimberlitic heavy minerals, such as ilmenite, garnet and diamond survived alteration, and show distinct concentration in the more reworked lithofacies, Figure 2.2.4. The distribution garnet types could also be broadly quantified, Figure 2.2.5. The bar charts illustrate the overall dominance of orange garnet crystals, mostly these analysed as pyrope almandines of the megacryst suite, and eclogitic garnets. Purple garnets of peridotitic paragenesis (chromium pyrope and low-calcium chromium pyrope) are also a common constituent, and increase in proportion in the reworked pyroclastic strata. Crustal garnets, of mid to lower crustal metamorphic paragenesis, occur sporadically throughout, due to the intermittent occurrence of gneissic xenoliths through the pyroclastic sections. Although the tuffaceous sands capping the 012 crater facies contain a great deal of crustal garnets, thus indicating the surface source of these sands. Other kimberlitic minerals such as phlogopite, zircon, perovskite and apatite are less common, and are usually concentrated in the reworked strata of the proximal facies. This is especially true for phlogopite which is trace to rare in primary (crater facies and basal proximal) deposits, but enriched in reworked strata, particularly in the top of turbiditic sequences.

Other kimberlitic minerals reflect the xenolith content of the original magma. Although purple pyrope garnets are fairly common, enstatite is very rare in all boreholes (probably prone to serpentinisation), chromium diopside being found more commonly. However, orange pyrope-almandines and

Figure 2.2.3

Sample no.	borehole depth (m)	Crushed weight (kg)	% of weight lost to HCl	Weight % S.G. >2.9 (heavies)	No. of DIAMONDS	ilmenite g/t	garnet g/t
Borehole Of S93-002							
6	104.42-104.67	1.041	50.8	0.6		3496	68
7	104.67-104.77	1.657	54.2	0.3		2522	145
9	105.17-105.84	2.250	51.7	0.7		5913	391
10A	105.81-106.54	2.952	62.2	0.5		3524	130
10B+D	106.54-107.02	7.573	37.0	5.6		5159	52
10C	107.02-107.56	1.731	45.7	2.2	2	2280	35
10E	108.50-108.81	3.525	39.2	3.0	3	8990	105
10F	108.81-109.35	5.172	42.8	1.7	1	7504	183
10G	109.35-110.16	3.077	57.5	0.9		7298	153
11	110.16-110.73	2.991	36.1	2.4		2387	85
12A	110.73-111.56	2.660	50.1	0.9		4147	105
12B	111.56-113.00	6.801	61.2	0.6	2	5382	199
13A	113.00-113.90	5.084	46.1	1.2		3052	62
13B	113.90-115.74	7.244	58.9	0.1		803	14
14A	115.74-116.30	2.995	80.7	0		0	0
14B	116.30-116.69	2.561	37.1	0.6		489	12
Borehole Of S93-003							
2	95.12-98.00	3.192	49.4	2.8	3	21521	394
3	98.00-101.10	14.077	56.6	1.0	1	9066	158
4A	101.10-101.38	0.628	62.6	1.1		6959	268
4B	101.38-101.88	4.524	48.6	0.8	1	6354	122
4C	101.88-102.50	1.625	73.5	0.6		4047	121
4D	102.50-103.88	2.868	72.5	0.6		3752	181
Borehole Of S93-004							
13A	94.41-94.57	4.660	28.1	0.8	1	4013	204
13B	94.57-95.64	1.581	28.0	7.0		4581	233
13C	95.64-96.71	6.545	24.1	9.3		6839	207
13D	96.71-97.06	2.190	32.0	1.4		6668	201
13F	97.06-97.48	1.818	27.5	6.5	1	5177	147
13F	97.48-97.70	1.624	36.5	3.5	1	4399	62
14	97.70-98.67	2.932	36.6	0.9		7224	64
15	98.67-100.03	3.873	30.8	6.9		10119	175
16	100.03-100.67	1.905	43.1	3.7		6861	183
17	100.67-101.50	3.246	46.3	1.4		5280	202
18	101.50-102.16	3.236	55.8	1.8	1	10021	139
19	102.16-102.86	1.989	42.6	0.9		6547	134
20	102.86-103.58	4.756	58.4	1.3		4410	107
21A	103.58-104.79	6.040	38.4	0.7		4529	48
21B	104.79-105.94	4.684	33.1	0.4		2096	64
22	105.94-107.19	4.561	35.2	0.5		3379	120
23	107.19-108.04	3.600	60.0	0.2		1217	36
24	108.04-108.42	2.909	63.1	0.2	3	1510	57
Borehole Of S93-009							
10	135.60-136.61	4.379	77.2	0.4		220	323
11A	136.61-136.91	1.842	74.8	3.1		61	49
11B	136.91-139.45	6.010	73.8	0.9		49	8
11C	139.45-139.95	3.478	74.5	0.9		49	20
12A	139.95-140.35	1.581	70.9	0.1		95	33
12B	140.35-140.50	0.527	73.5	0.1		44	68
12C	140.50-140.65	0.611	74.3	0.6		66	82
12D	140.65-141.00	1.613	57.7	0		171	81
12E	141.00-141.55	2.445	48.5	0.1		846	91
Borehole Of S93-010							
9A	141.65-142.29	2.969	68.0	3.0		615	4
9B	142.29-143.17	3.125	63.1	4.3	6 (1 macro)	59	24
11A	147.49-147.68	1.444	62.2	2.1		61	27
11B	147.68-148.40	2.131	33.1	1.0		1580	691
12A	148.40-149.00	2.211	67.6	0.1		106	86
12B	149.00-149.36	2.364	64.7	0.2		97	40
17	153.62-153.77	0.597	42.7	0.9		553	169
18	153.77-156.00	8.640	44.4	0.5		1347	1114
Borehole Of S93-012							
1	180.51-184.08	16.552	41.5	0.1		339	36
2	184.08-186.58	12.616	56.6	0.2		1075	9
3	186.58-188.80	12.864	59.2	0.6		4217	185
4	188.80-197.06	40.847	50.6	0.2		504	5
5	197.06-198.06	6.529	44.0	0.2		242	15
6	199.15-201.85	11.882	45.5	1.6		273	5
7	201.85-206.57	20.770	46.8	0.3	3	295	6
8	206.57-206.79	2.835	94.1	0.4		246	7
9	208.00-208.88	1.900	81.9	0.2		132	19
10	211.63-211.94	1.802	85.0	0.3		188	12

Figure 2.2.4

Heavy mineral concentrations in boreholes representative of the three main kimberlite facies; crater facies (OFS 93-012, see log in Figure 2.1.2), proximal facies (OFS 93-004, see log in Figure 2.1.5) and distal facies (OFS 93-010, see log in Figure 2.1.13).
Black bars indicate concentation of ilmenite per mineral separation unit, orange bars indicate concentration of garnets (all types). Diamonds indicate which unit they were separated from. Note the second pulse of lapilli tuffs in 012 contains a greater concentration of garnets, relative to the first. Also the concentrations in 010 compared to 004 clearly illustrate the potential for upgrading of heavy minerals with reworking.

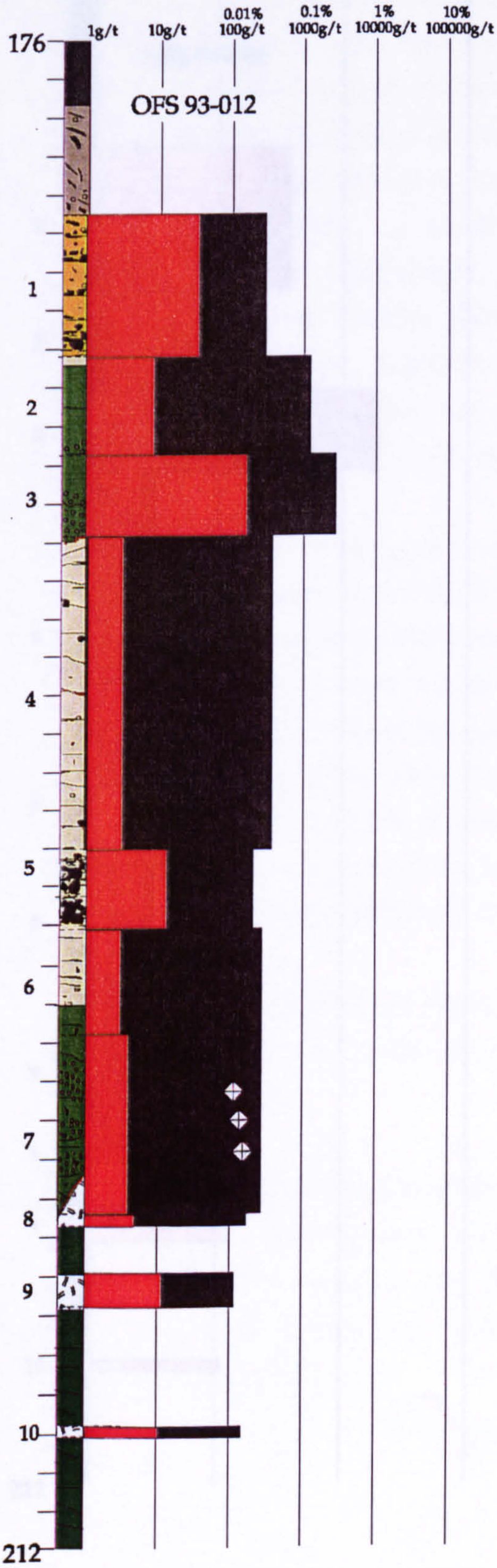

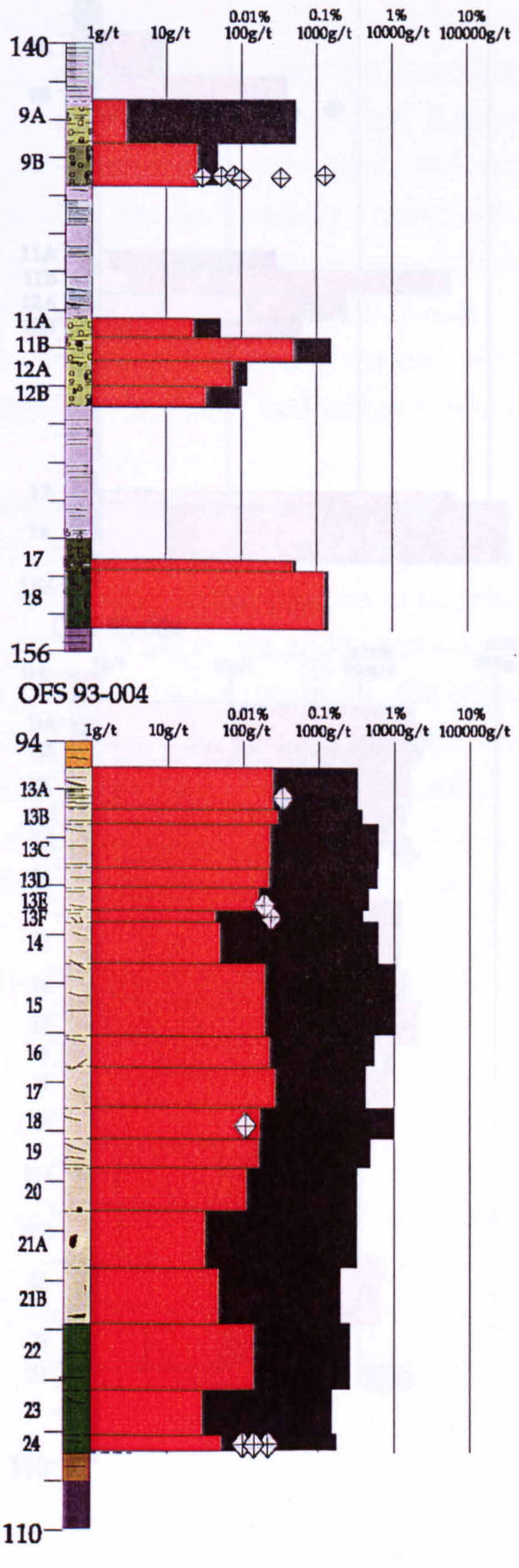

Figure 2.2.5

Heavy mineral concentrations in boreholes representative of the three main kimberlite facies; crater facies (OFS 93-012, see log in Figure 2.1.2), proximal facies (OFS 93-004, see log in Figure 2.1.5) and distal facies (OFS 93-010, see log in Figure 2.1.13).
Bars represent total garnet concentration per mineral separation unit. These bars are further divided in to three garnet colour classifications. Pale pink represents crustal garnets (including pale lilacs of gniessic origin), orange represents eclogitic and megacrystal garnets (and brown garnets) and purple represents peridotitic garnets (including greyish knorringite)

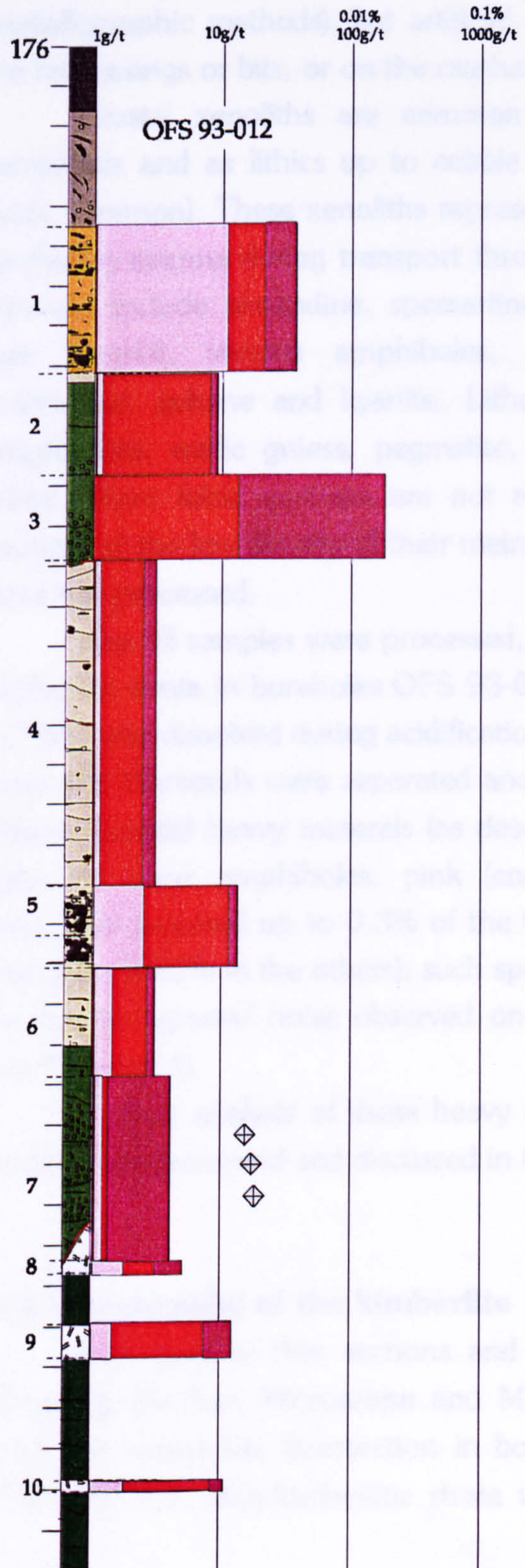

OFS 93-010 - upper 3 tuffaceous units.

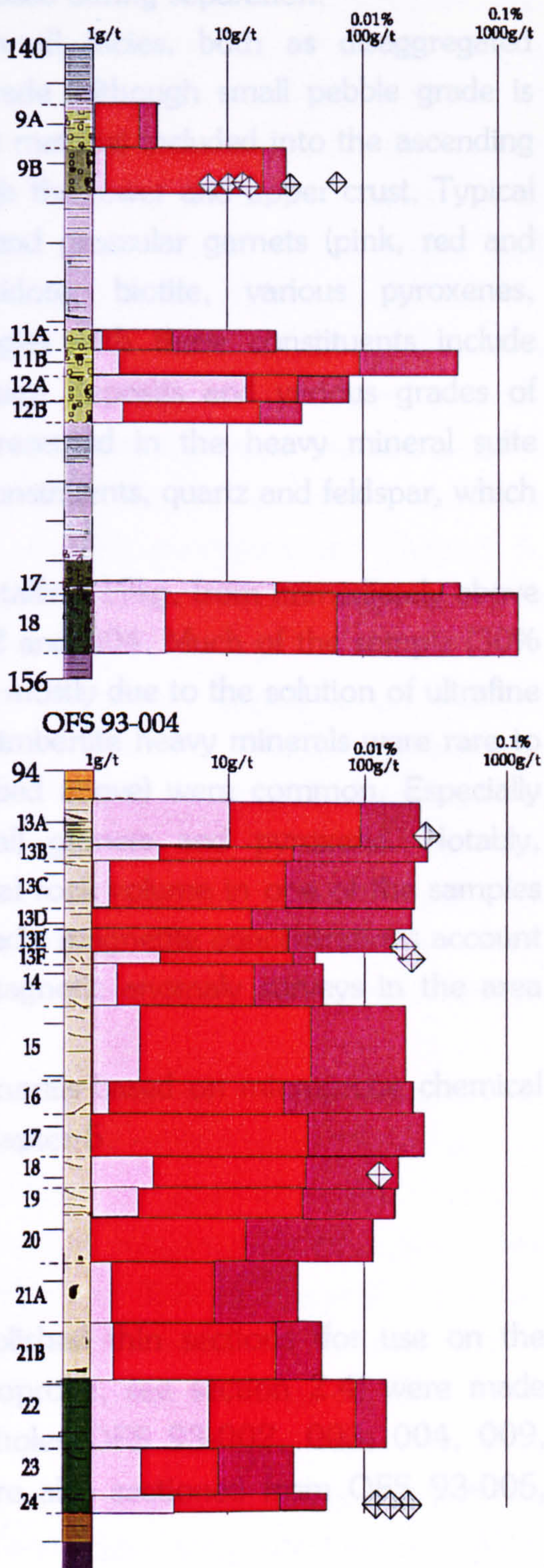

omphacite are more common than peridotitic minerals, and suggest a greater proportion of eclogitic xenoliths than peridotitic (see Chapter 5 for further discussion). Two grains of moissanite were separated from the 004 basal tuff, and suggest an ultradeep, highly reduced source for the diamond or xenolith that bore it (Leung, 1990). This grain has yet to be proven as natural (by crystallographic methods), but artificial silicon carbide was not used on any of the drill casings or bits, or on the crushers used during separation.

Crustal xenoliths are common in all facies, both as disaggregated xenocrysts and as lithics up to cobble grade (although small pebble grade is more common). These xenoliths represent material included into the ascending kimberlite magma during transport through the lower and upper crust. Typical minerals include almandine, spessartine and grossular garnets (pink, red and pale purple), various amphiboles, epidote, biotite, various pyroxenes, tourmaline, sphene and kyanite. Lithologies with these constituents include amphibolite, mafic gniess, pegmatite, skarn deposits and various grades of schist. More felsic gneisses are not represented in the heavy mineral suite because of the low density of their main constituents, quartz and feldspar, which were not processed.

Five till samples were processed, totalling 19kg, from immediately above kimberlite strata in boreholes OFS 93-002 and 004. Much of the sample (30% to 75%) was dissolved during acidification, mostly due to the solution of ultrafine clays. No diamonds were separated and kimberlite heavy minerals were rare to absent. Crustal heavy minerals (as described above) were common. Especially common were amphiboles, pink (crustal) garnets and pyroxene. Notably, magnetite occurred up to 0.3% of the total rock volume in one of the samples (less than 0.05% in the others); such sporadic magnetite concentrations account for the background noise observed on magnetic anomaly surveys in the area (see Chapter 1).

Further analysis of these heavy minerals based on microprobe chemical analysis are presented and discussed in Chapter 5.

2.3 Petrography of the kimberlite

Petrographic thin sections and polished thin sections (for use on the Scanning Electron Microscope and Microprobe, see section 2.4) were made from the kimberlitic intersection in boreholes OFS 93-002, 003, 004, 009, 010 and 012. Non-kimberlitic strata were also sectioned from OFS 93-005,

006, 007 and 008, and KR94-016 and 017, see Appendix VI for sample catalogue.

Thin section manufacture often required epoxy resin impregnation, as many of the samples were unlithified and friable, especially the reworked kimberlite and the terrigenous sediments. Because the samples were so soft, attaining a constant thickness (of 30μm) proved difficult, and some overthinned sections were produced. Polished thin sections were consistently overthick, and were difficult to use for optical identification of minerals. For example, a polished section of a Spinney Hill Formation 'chaotic unit' (Chapter 1) contained coarse angular clasts with second-order birefringence, initially thought to be pyroxene (some pyroxene had been noted in hand sample). Upon investigation under the microprobe, these were found to be quartz and orthoclase feldspar, the higher birefringence produced by the thicker section.

Features of the thin sections analysed are recorded on standard thin section petrography sheets, see Appendix III, and the results, in terms of facies delineation and point counting of grain and crystal shapes, are discussed in Section 2.1 above. In the crater facies, the determination of lapilli proportions and types is important for characterising volcanic processes (see Chapter 3). Two main types occur; fluidal and rounded, (Plates 2.24 and 2.25 in Figure 2.3.2) the fluidal lapilli are the main constituent of the lapilli-dominated tuffs, and range from 0.3cm to 2.0cm in size, amoeboid (larger) to sub-rounded (smaller) in shape. They often appear flattened and/or moulded, attesting to their fluidal nature. The rounded lapilli are a minor constituent (about 15%) in the crystal dominated tuffs, and are fine, 0.2cm to 0.8cm in size, and subrounded to rounded shape. No evidence of welding between lapilli was found, contrary to reports from other workers in the area (Scott-Smith et al, 1995), although only two slides of lapilli dominated tuffs were closely examined in this study.

The most obvious feature of kimberlitic thin sections is the diagenetic alteration throughout. Most of the grains were of olivine which, together with the matrix, have been replaced by green-brown and grey serpentine. Typically about 90% of the replacement is serpentine, the rest is mostly finely intermixed carbonate and a fine dusting of magnetite, Plates 2.22 in Figure 2.3.1. Grain edges are usually well defined, although in some areas the kimberlite is so altered as to obscure the original grain shapes and textures, Plates 2.23 in Figure 2.3.1. Other types of diagenetic alteration include: patches in which carbonate is the dominant matrix cement; magnetite replaces both cement and grains, and growth of coarse authigenic vermicular antigorite (termed CAVA,

Figure 2.3.1.

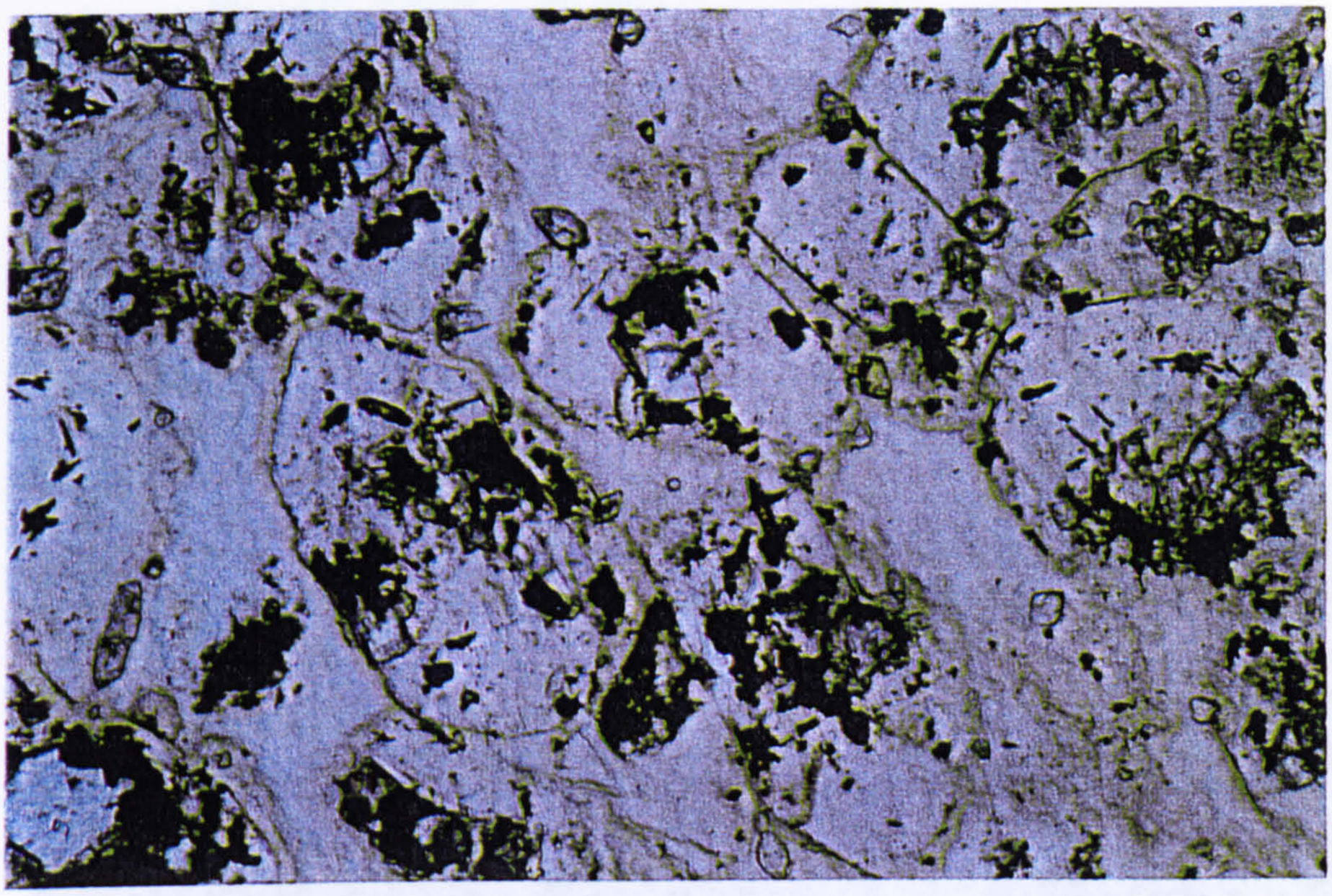

Plate 2.22
OFS 93-004, thin section at 103.3m, plane polarised light, magnification x 50. Good grain boundaries. Grains and matrix are mostly serpentine and magnetite, rare calcite (lower left).

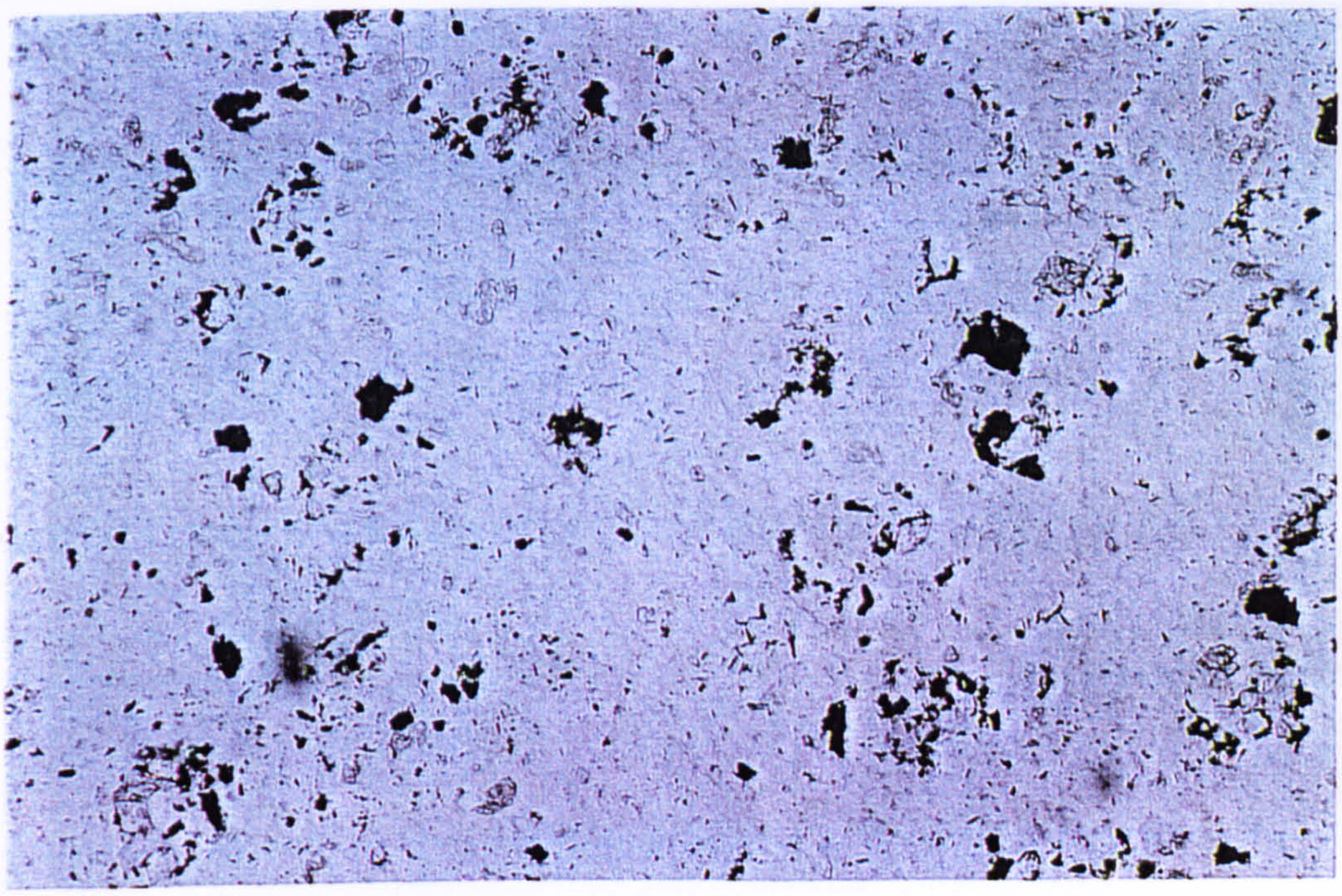

Plate 2.23
OFS 93-004, thin section at 105.8m, plane polarised light, magnification x 25. Total alteration texture - no grain boundaries discernible. Consists of serpentine, calcite (high relief) and magnetite (opaque).

Figure 2.3.2.

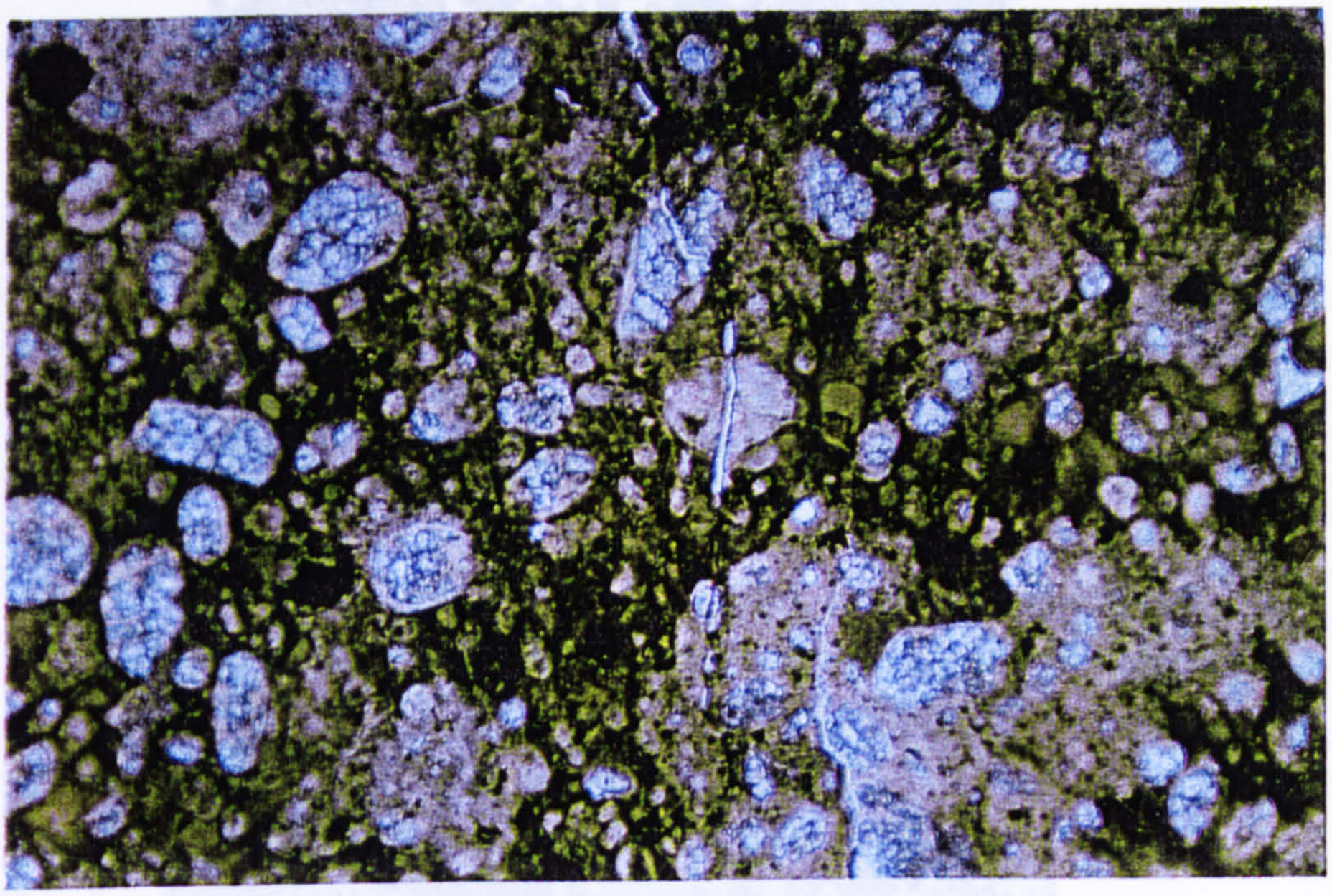

Plate 2.24
OFS 93-012, thin section at 184.8m, plane polarised light, magnification x 10. Fluidal lapilli in lapilli dominated Lapilli Tuff. Note finely curvilinear edges to the pale brown lapilli.

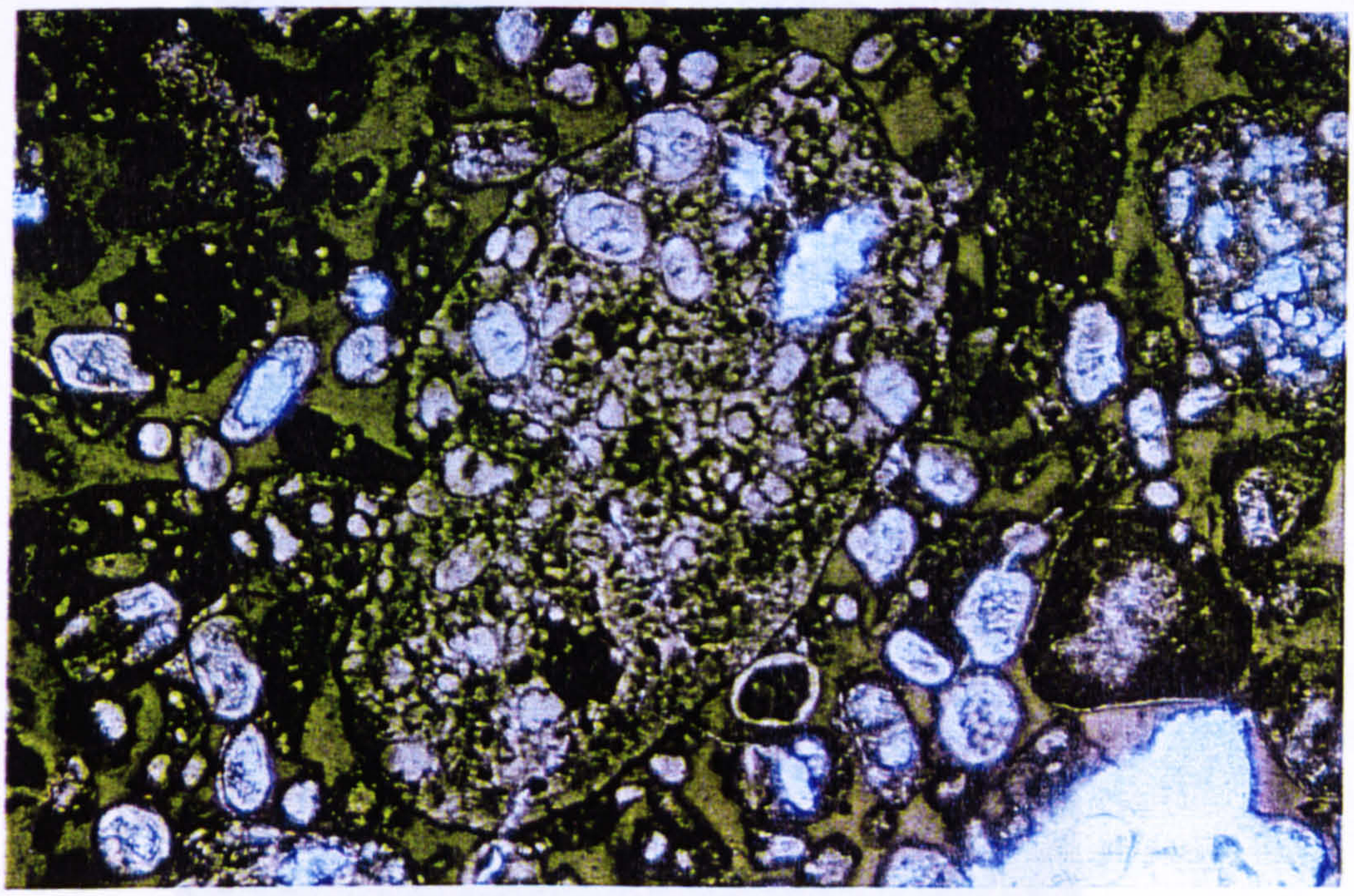

Plate 2.25
OFS 93-012, thin section at 204.4m, plane polarised light, magnification x 8. Rounded lapilli in crystal dominated Lapilli Tuff. Note that this example is unusually large (at 10mm long), most are 2mm to 4mm (see two lapilli on the left, touching the central lapilli).

Figure 2.3.3

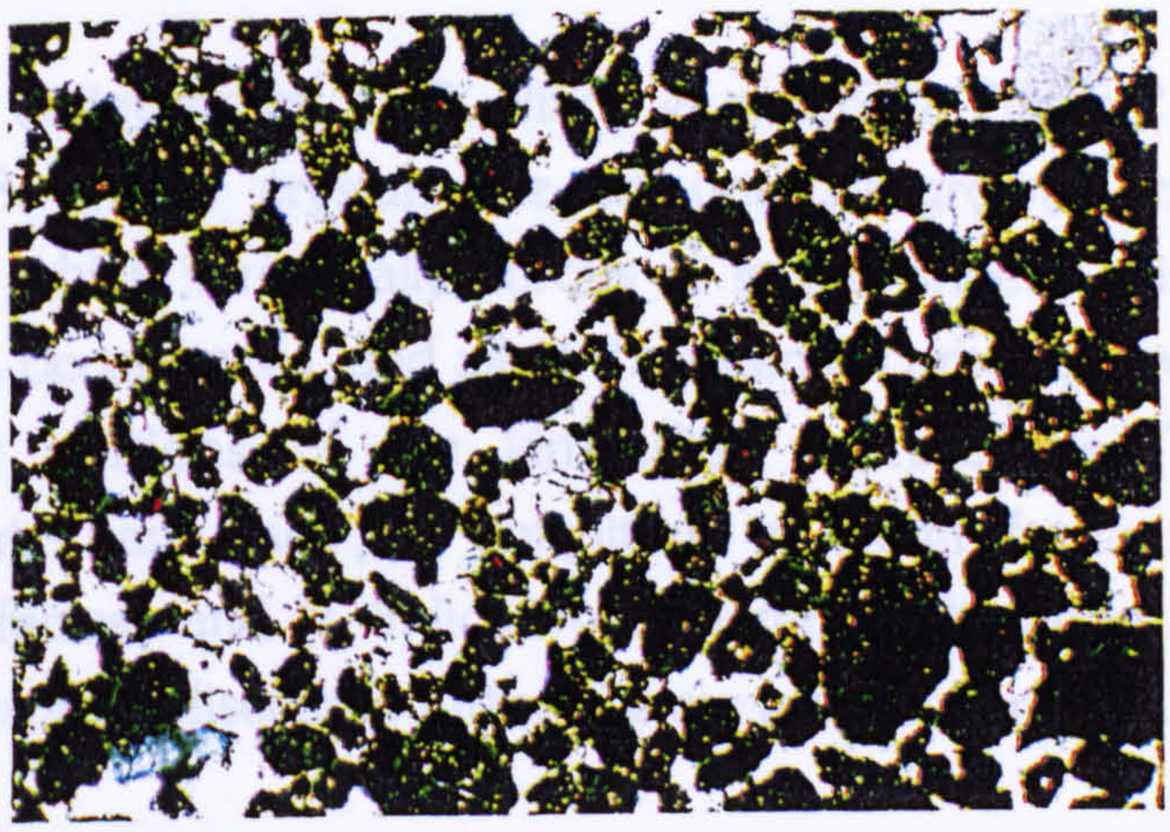

Plate 2.26
OFS 93-004, thin section at 101.2m, cross-polarised light, magnification x 10. Calcite matrix, with serpentine grains

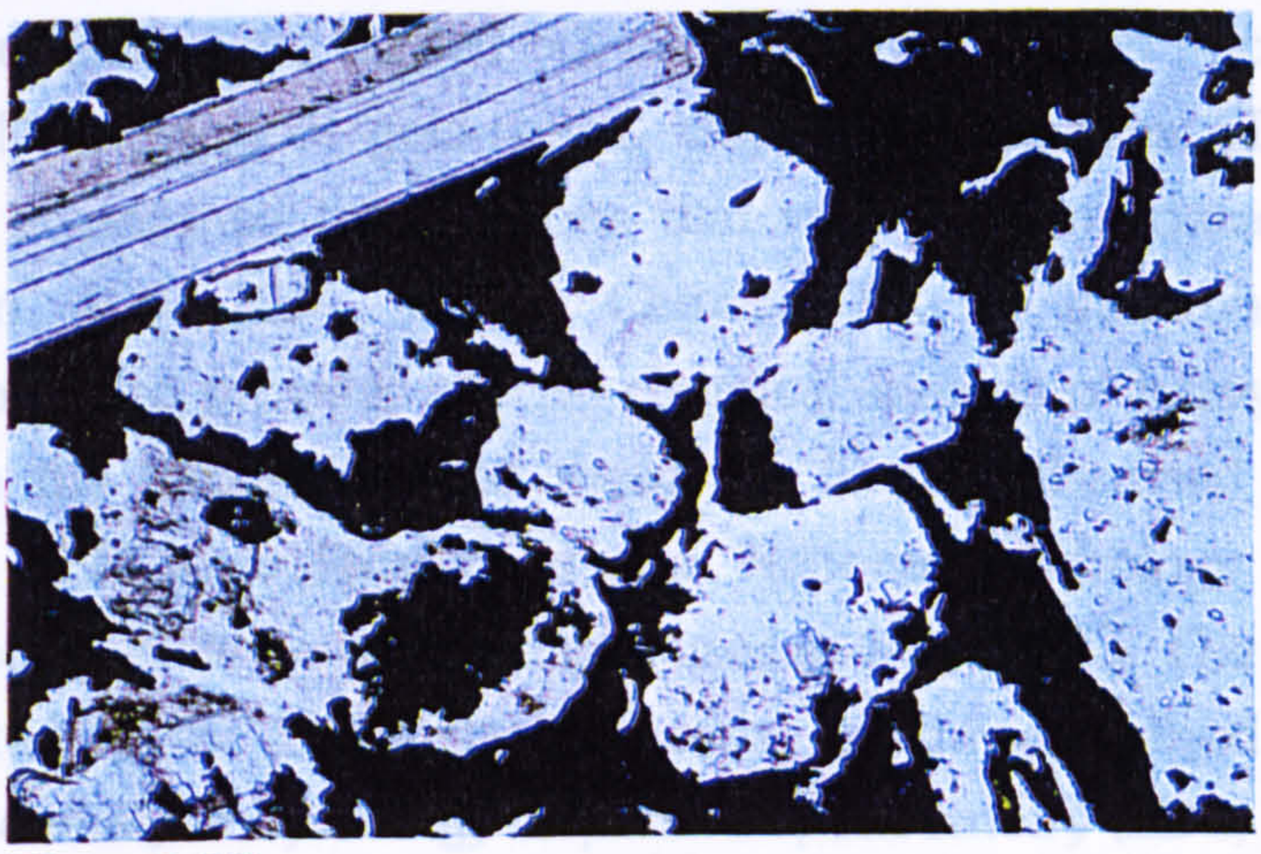

Plate 2.27
OFS 93-002, thin section at 112.4m, plane polarised light, magnification x 25. Magnetite matrix, with serpentine and carbonate grains. Note phlogopite in upper left.

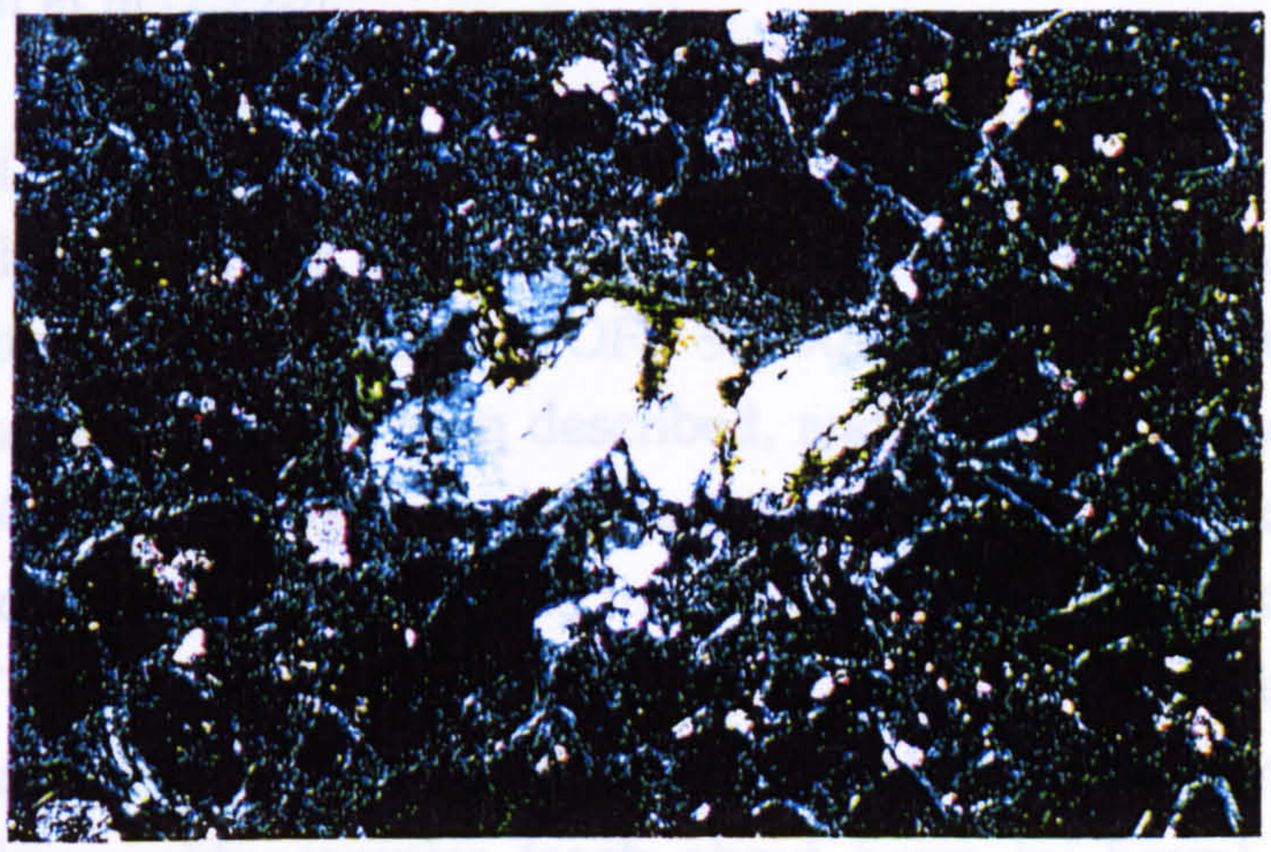

Plate 2.28
OFS 93-002, thin section at 114.2m, cross-polarised light, magnification x 12. CAVA helix, appears as a 'knot' of well cleaved serpentine in thin section.

verified as antigorite by XRD, Nixon et al 1993), Plates 2.26, 2.27 and 2.28 in Fig. 2.3.3. These crystals are an unusual growth shape for the mineral antigorite, which is normally fibrous or in fine sheets. It is notable that most of the CAVA occurrences, and all of the intense carbonate veining are restricted to the lower portions of the kimberlitic intersections. This basal carbonate enrichment ('hard shelf') is ubiquitous in crater facies, and common in the proximal facies, and is indicative of intense alteration. The development of CAVA crystals is discussed further below (see section 2.4).

2.4 Microtextural features of kimberlite

Two methods were used to characterise the microtextures of extra-crater kimberlite. Both were carried out on Scanning Electron Microscopes (SEM); the first a 3D imaging of gold-coated chips on a Cameca SEM, the second 2D imaging of polished thin sections that were carbon coated and imaged on a CamScan 400 SEM and a Cameca SX-50 electron microprobe. The microprobe also provided precise chemical analysis of heavy minerals and other grains in the kimberlite, and these are further discussed in Chapter 5. The Cameca SEM was located at the National Hydrology Research Institute, Saskatoon, Saskatchewan, and was used in May 1993. The two other machines are located at the University of Leeds. All three methods incorporated spot qualitative analysis by energy dispersive spectrometry (EDS) which aided mineral identification and provided a qualitative determination of the target's bulk chemistry. Full discussion of SEM and microprobe techniques and theory is contained within "Scanning Electron Microscopy & X-Ray Microanalysis" by Goldstein et al (1993).

2.4.1 3D Imaging

The aim of the 3D imaging was to determine the nature of the matrix of the proximal facies (boreholes OFS 93-002 and 004.) Previous to this analysis only hand samples had been described, and no other analysis (other than XRD on the CAVA crystals) or thin section work had been done. Hand sample descriptions did not identify the matrix, which was soft (less than hardness 2.5 on Moh's scale), cryptocrystalline, dull to pearly or ceramic-sucrosic lustre and texture, and variably intermixed with carbonate (from HCl treatment).

Eleven chip samples (each about 5mm by 5mm) were taken from a representative range of kimberlite facies and depths in 002 and 004. These were dried, gold coated and mounted on stubs that slotted into the stage of the

SEM. Over two sessions nine images were photographed, see Figures 2.4.1., 2.4.2. and 2.4.3. Numerous EDS spectra were collected of the typical minerals present; serpentine, phlogopite, magnetite/hematite, ilmenite and garnet (see Appendix VII). Note that spectral peaks of gold and copper (Au and Cu) are artificial, due to the conducting coat applied before analysis.

The main conclusions from the analysis is that the matrix is dominated by Mg, Fe serpentine, very similar in composition to the large CAVA crystals observed in hand sample. The matrix appears to have two main textures; a fine, porous mat of acicular and/or bladed antigorite (Plates 2.31 and 2.39 in Figures 2.4.1 and 2.4.3), and a solid, massive to slightly fibrous antigorite (Plate 2.34 in Figure 2.4.2). The acicular and bladed crystals are intergrown, and are typically 3μ to 5μ (ranging up to 12μ), long (and wide, if bladed) and 1μ to 2μ thick. Both types have variable amounts of interstitial carbonate (mostly calcite) and magnetite or hematite. Clays were not detected. Other matrix crystals include euhedral dolomite, pyrite and Ni-pyrite (rare). The texture of the matrix suggests an in situ growth of much of the serpentine, verifying the conclusions of the thin section petrography: the matrix is an alteration feature, retaining little of the original pyroclastic textures (such as fine ash particles and original porosity).

Grains of serpentinised olivine were not individually identified, probably because they are overgrown with serpentine (see section 2.3 above). Other grains showed varying degrees of corrosion (phlogopites and garnets), or remained unaltered by the diagenetic process (euhedral ilmenites). CAVA crystals are also euhedral, the crystal shape, when fully developed is a striated circular prism growing in a helical fashion (see Figure 2.4.4). This unusual growth structure may be due to the lattice buckle from the perfect basal plane, observed in antigorite (Kunze, 1956), further influenced by Fe^{2+} substitution in to the lattice. The CAVA is usually observed growing from massive serpentine patches (psuedomorphic serpentine-after-olivine grains), and cross-cut much of the matrix texture.

Figure 2.4.1.

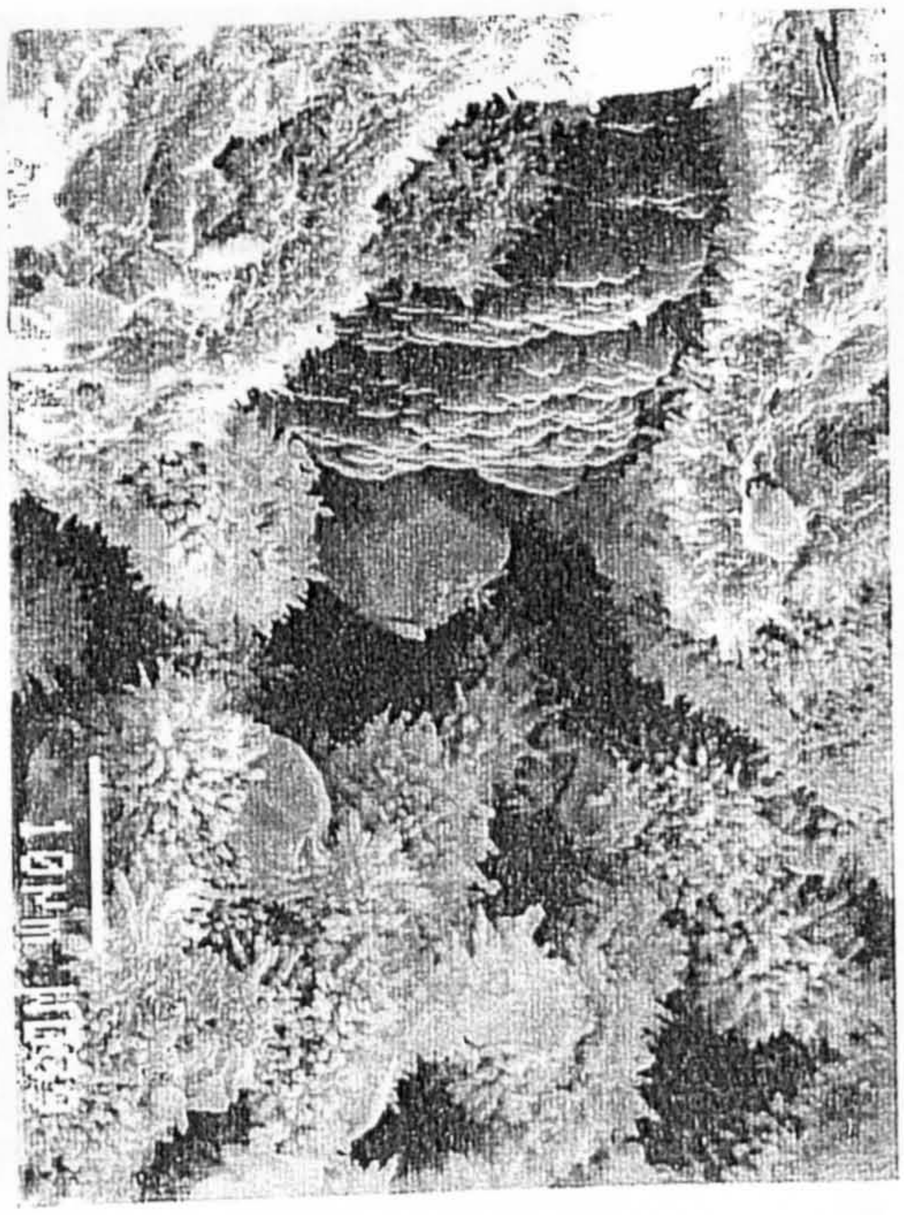

Plate 2.31 Acicular fine serpentine.

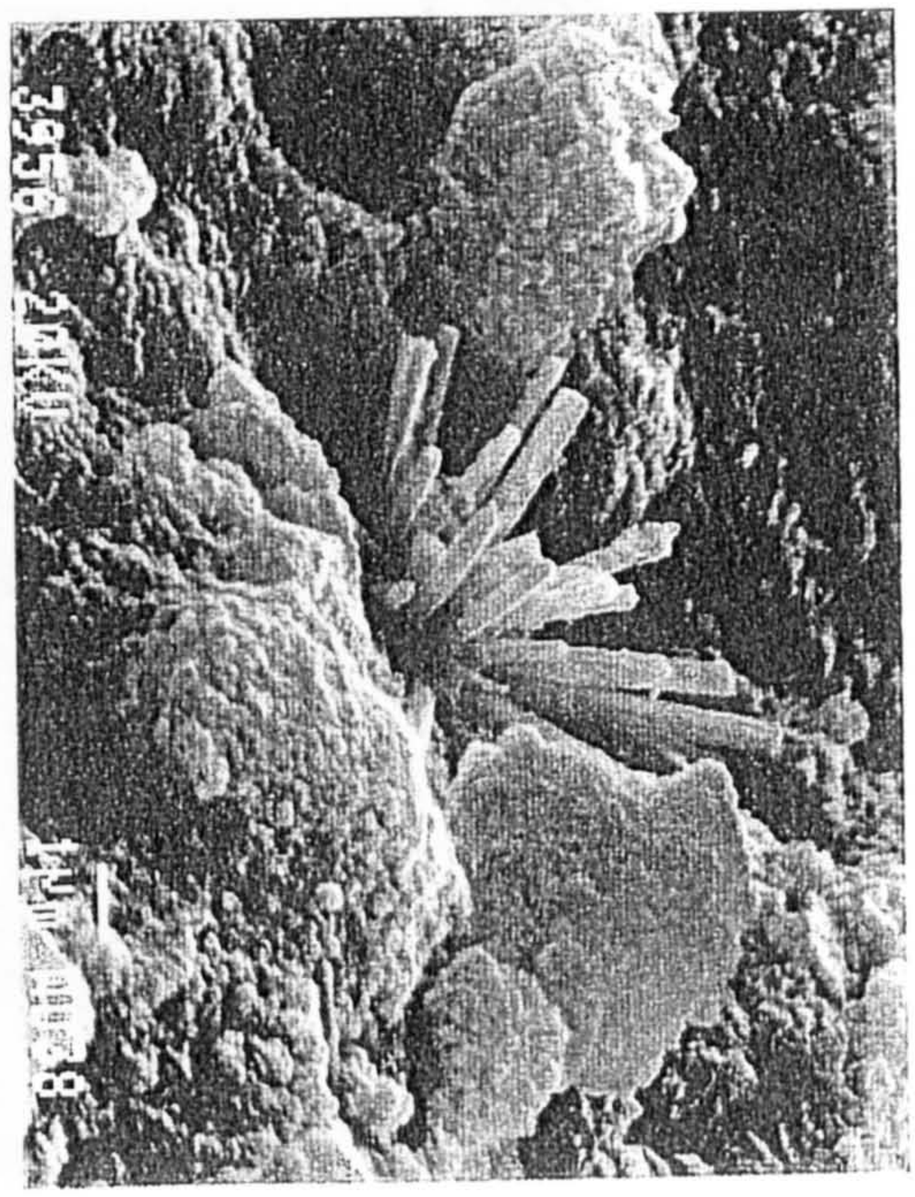

Plate 2.29 Fine authigenic Ni-pyrite.

Plate 2.32 CAVA, strongly cleaved.

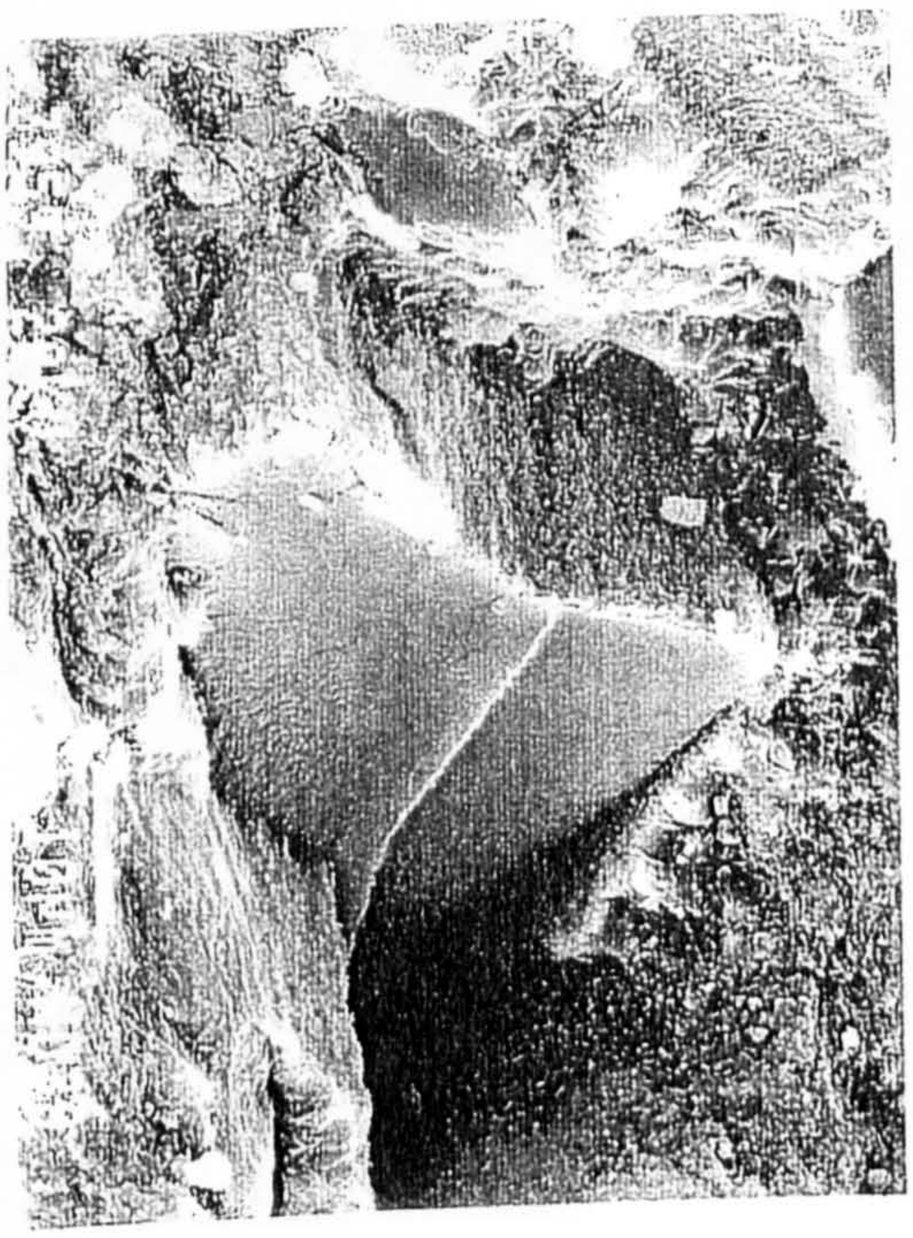

Plate 2.30 Euhedral ilmenite.

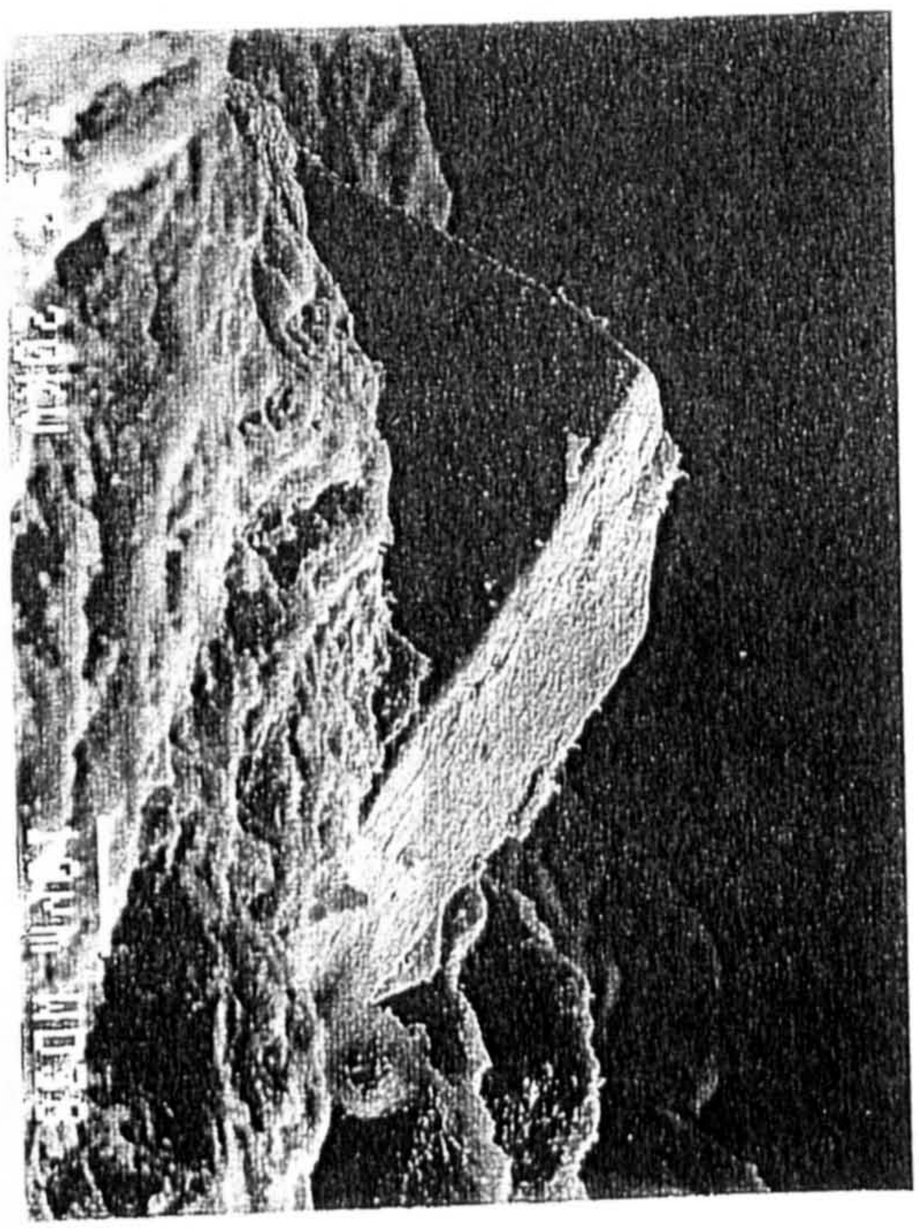

Figure 2.4.2.

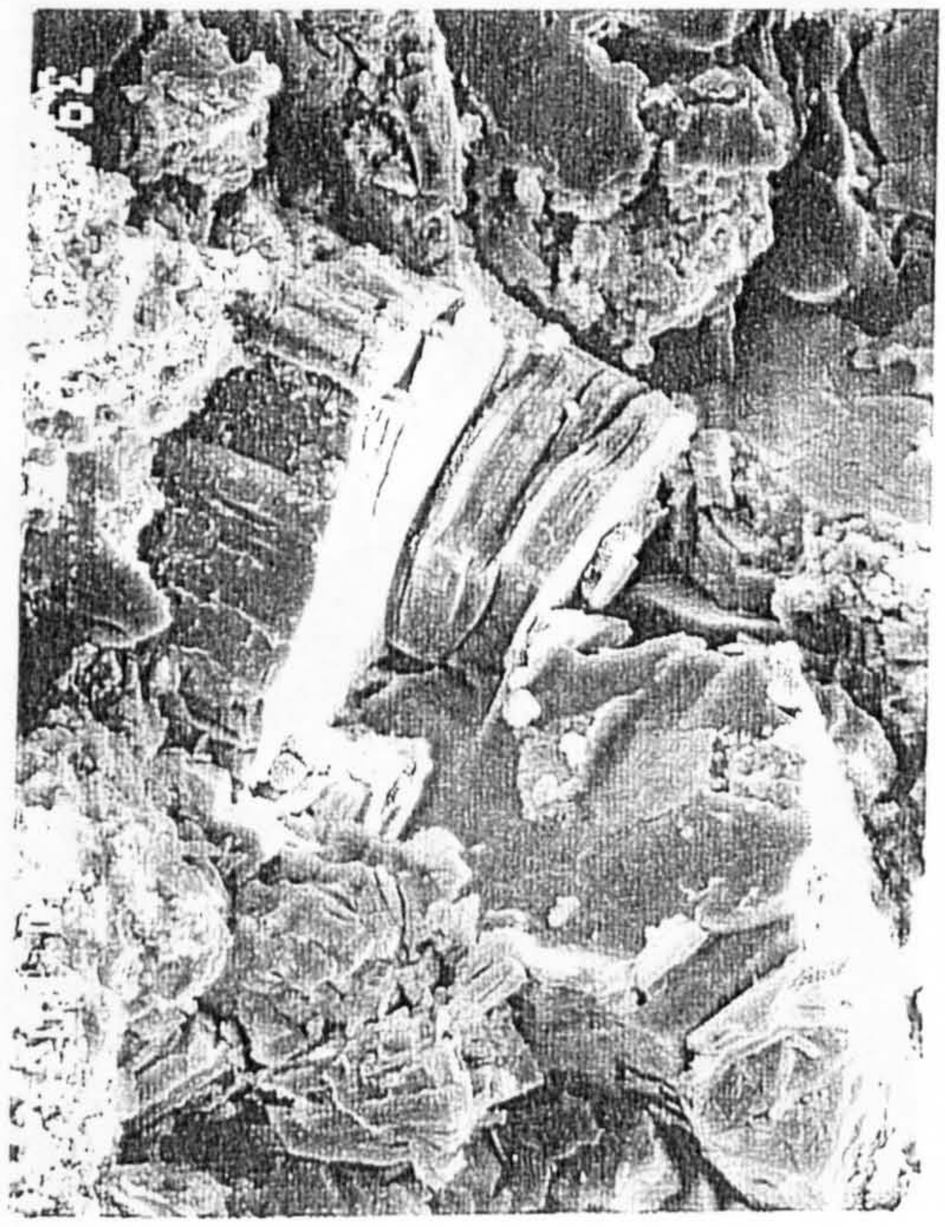

Plate 2.35 CAVA, well cleaved.

Plate 2.33 Hollow kelyphitic rind.

Plate 2.36 CAVA 'log'.

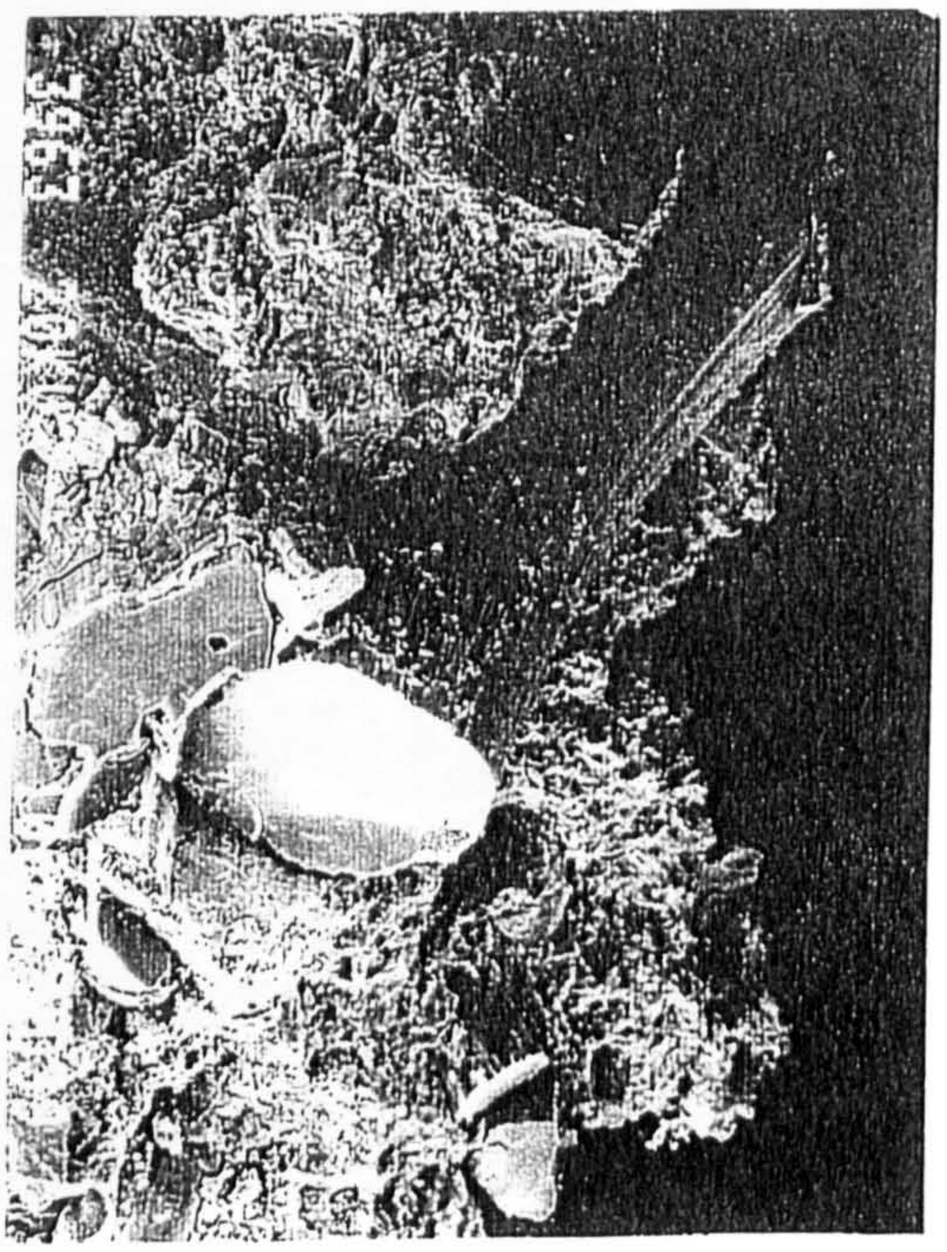

Plate 2.34 Fibrous serpentine matrix.

Figure 2.4.3.

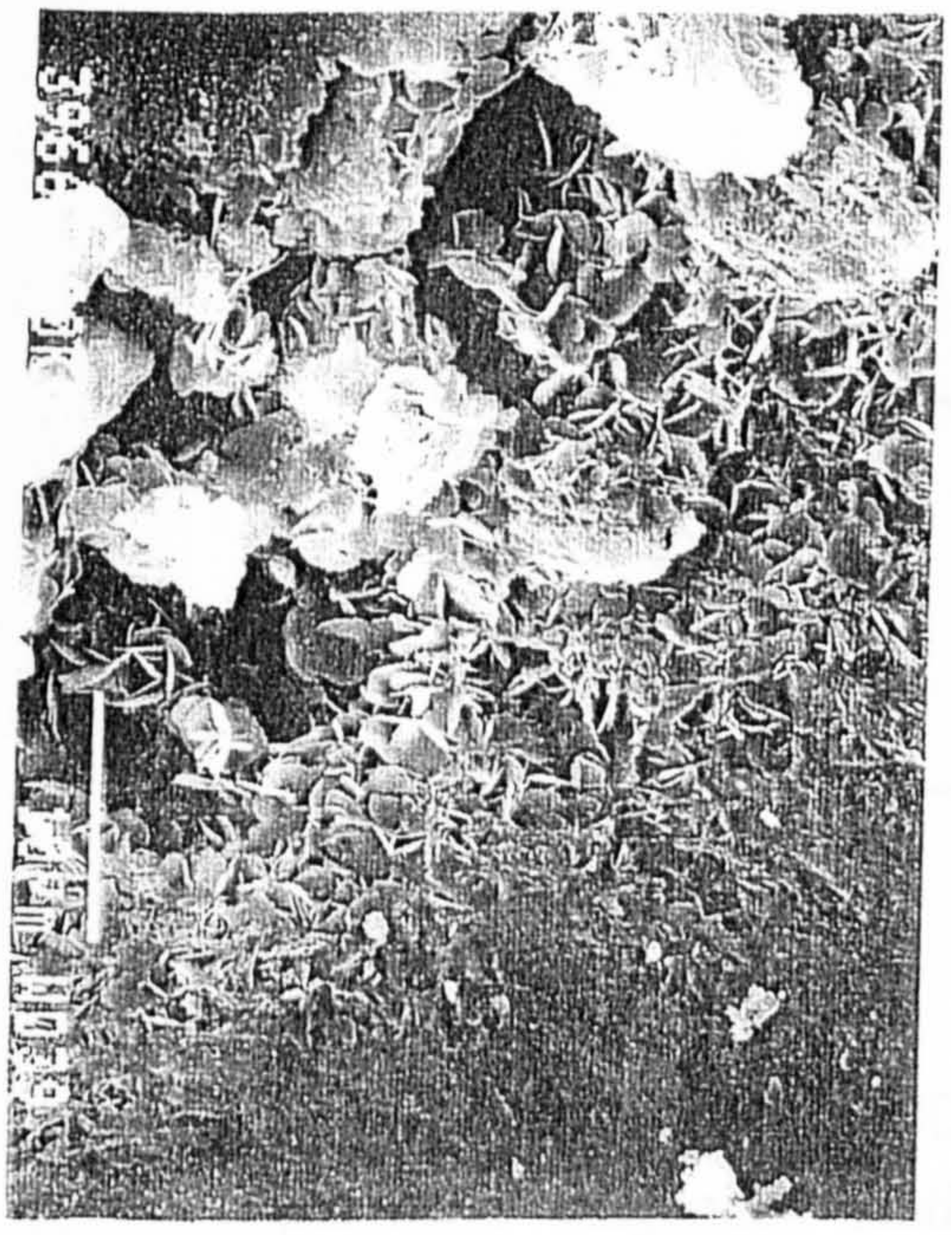

Plate 2.39 Bladed serpentine matrix.

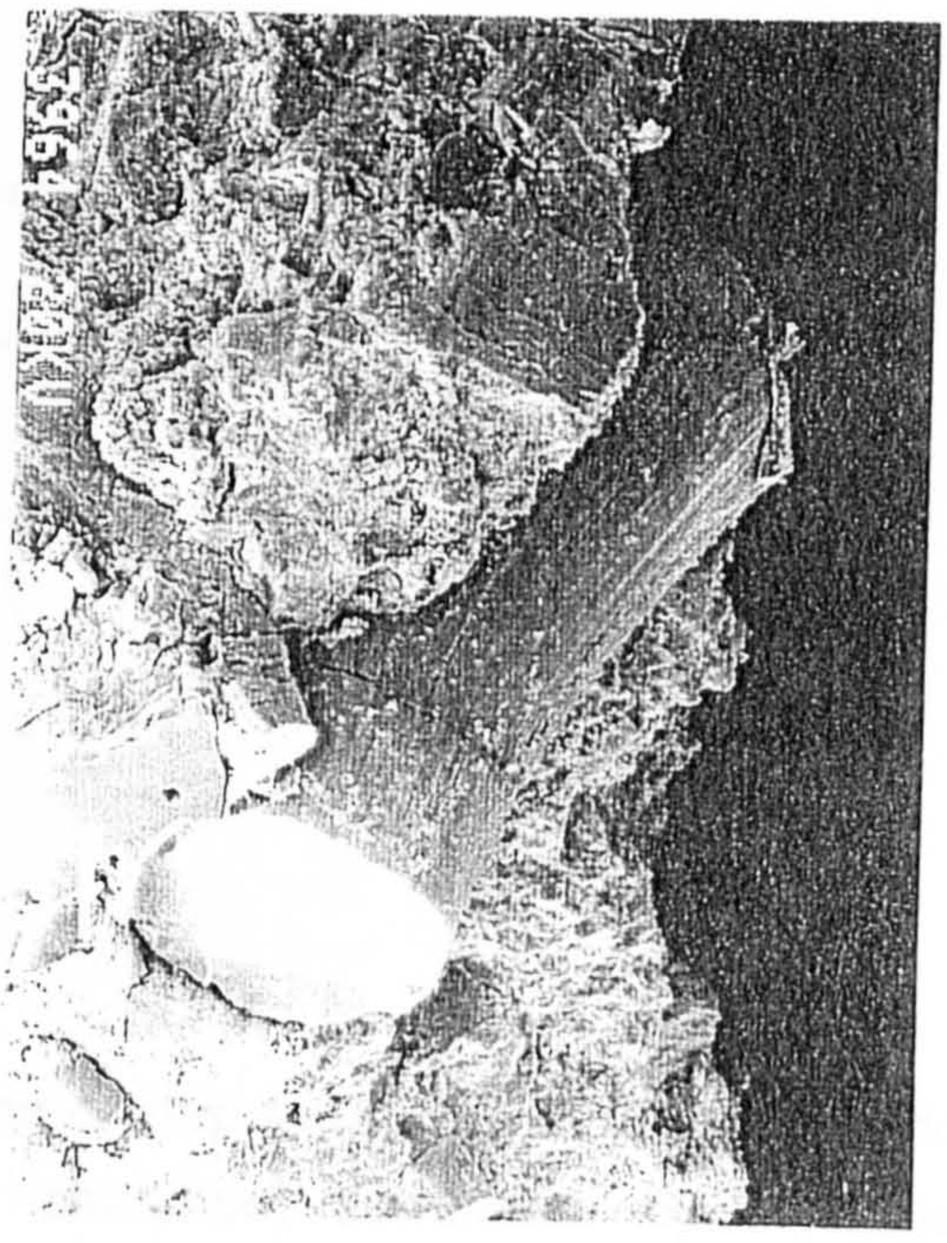

Plate 2.37 CAVA 'log'

Plate 2.40 Pyrite rosettes.

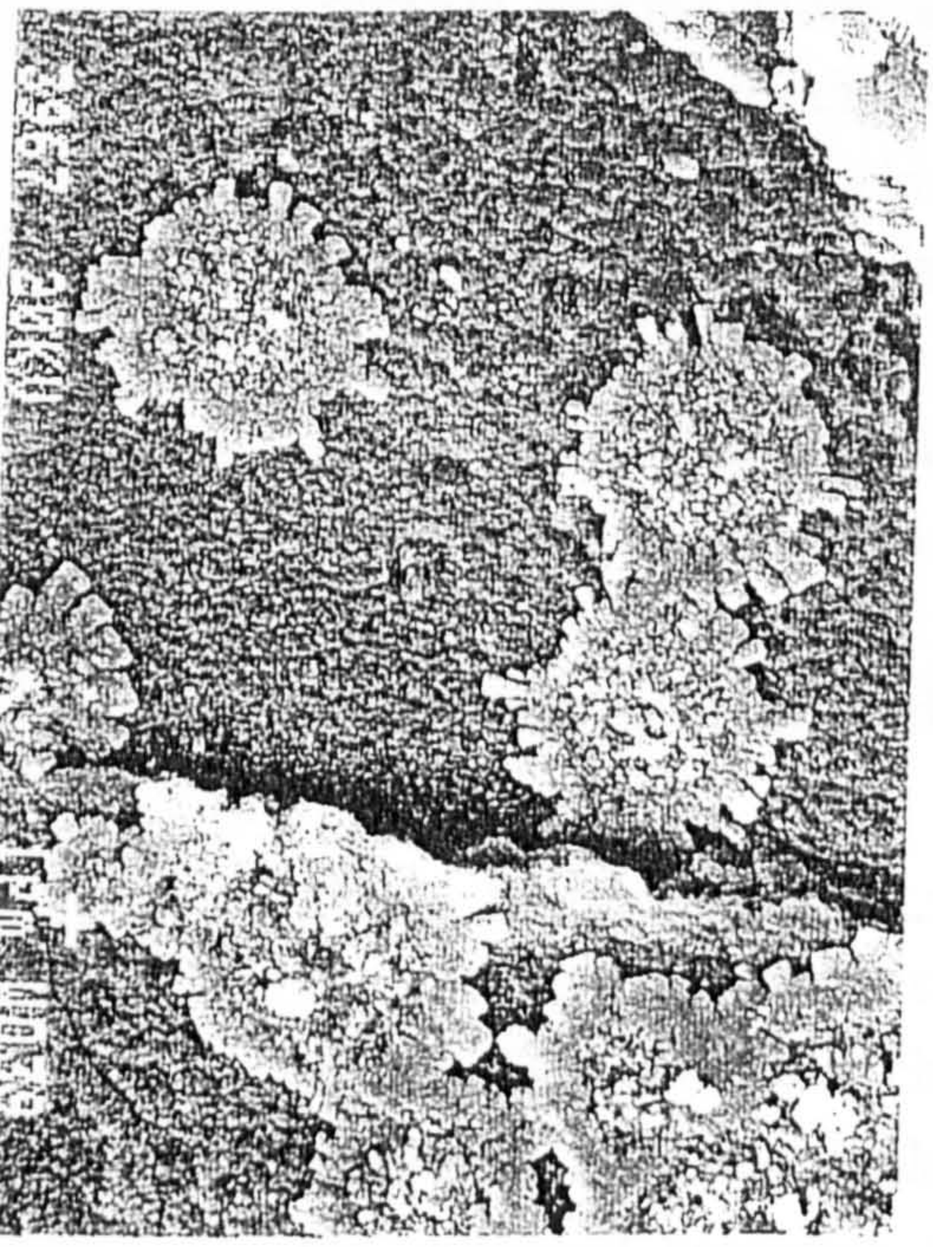

Plate 2.38 Corroded euhedral garnet

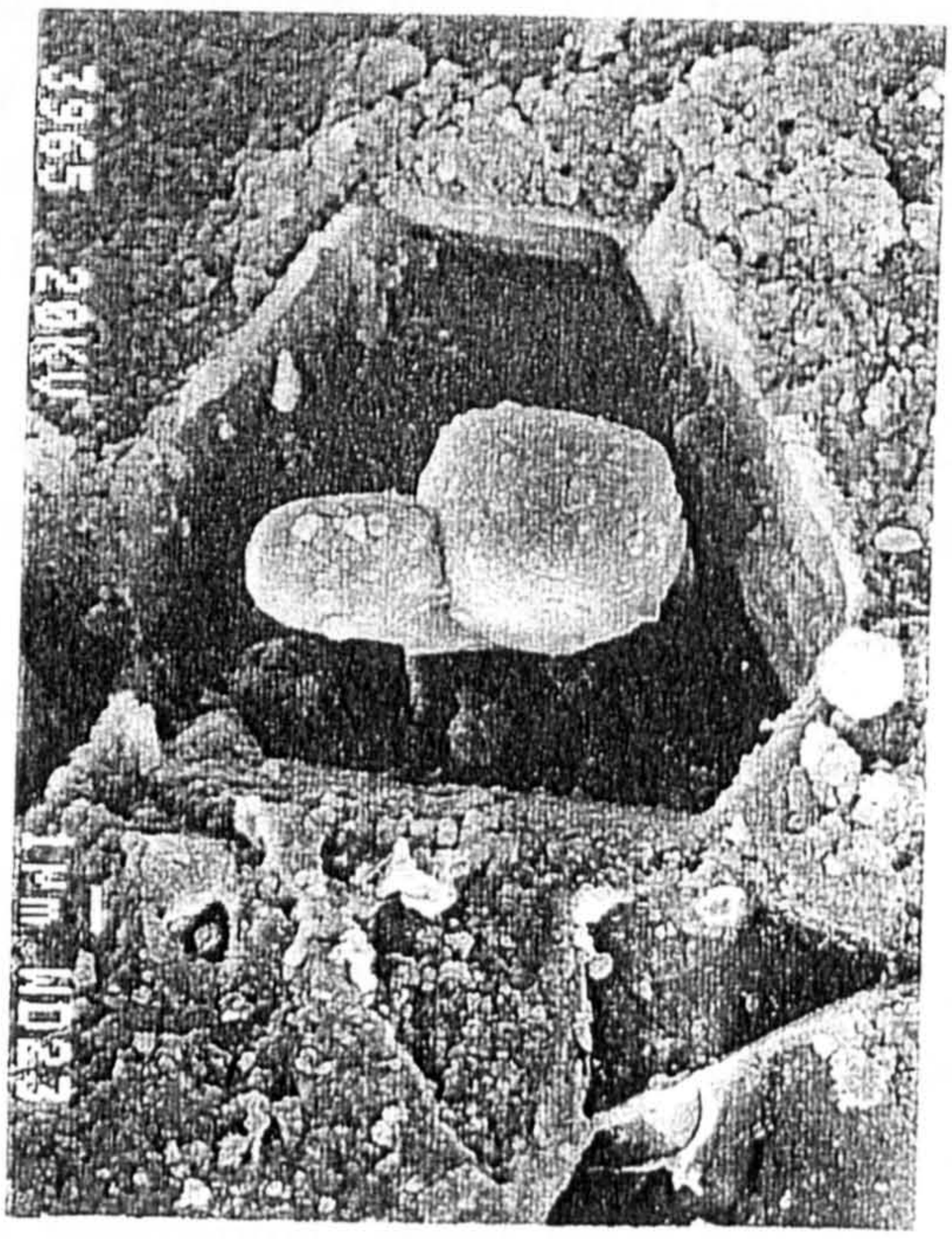

Figure 2.4.4

Ideal helical prismatic crystal form of CAVA antigorite

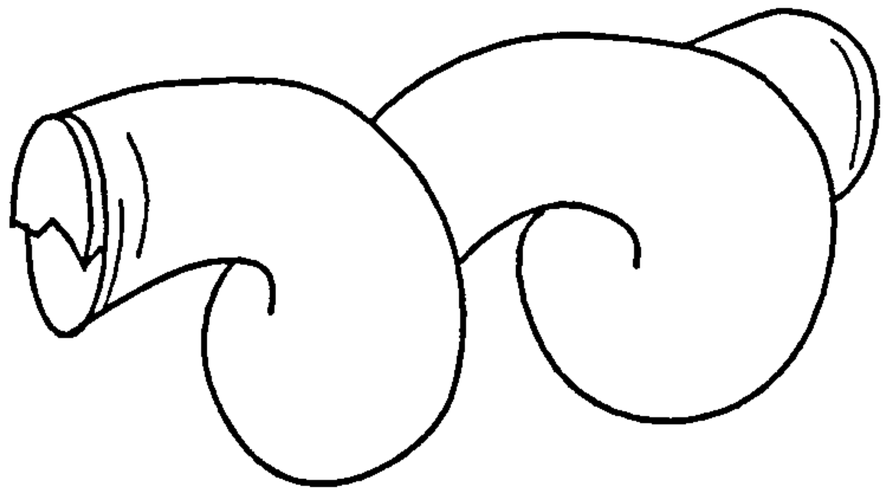

Crystals up to 1cm.

In summary the 3D imaging of chip samples provided good evidence for pervasive diagenetic (authigenic) alteration, dominated by crystallisation of antigorite serpentine in the matrix. Other authigenic crystals include fine calcite, magnetite and hematite, which are intermixed or interstitial with the fine antigorite. Coarser euhedral dolomite and CAVA cross-cut previous matrix textures, and therefore post-date their growth.

2.4.2 2D Imaging

The aim of the microprobe and SEM analysis was three-fold. Firstly to provide precise chemical analyses of minerals within their textural context (see Chapter 5). Secondly, to study further the general textures observed in thin section, particularly imaging clast proportions and fine lapilli in primary pyroclastic deposits, Plates 2.41 and 2.42 in Figure 2.4.5. Thirdly to further examine the diagenetic history of the pyroclastics from textural relationships. Five polished thin sections were analysed from boreholes OFS 93-002 and 004. The diagenetic sequence of events was found to consist of four separate phases, Figure 2.4.6, contrary to the single diagenetic event proposed for FALC kimberlites by other workers (Scott-Smith et al, 1994).

<u>Phase 1: Pre-diagenetic - Magmatic Phase</u>

This phase consists of two mineralogical events, firstly a small proportion of the fine, irregular chromites are overgrown with euhedral chromite (with increased TiO_2 and depleted of Cr_2O_3.) This is followed by corrosion of most of the euhedral ilmenites (not the fragmented, shard ilmenites) and chromites,

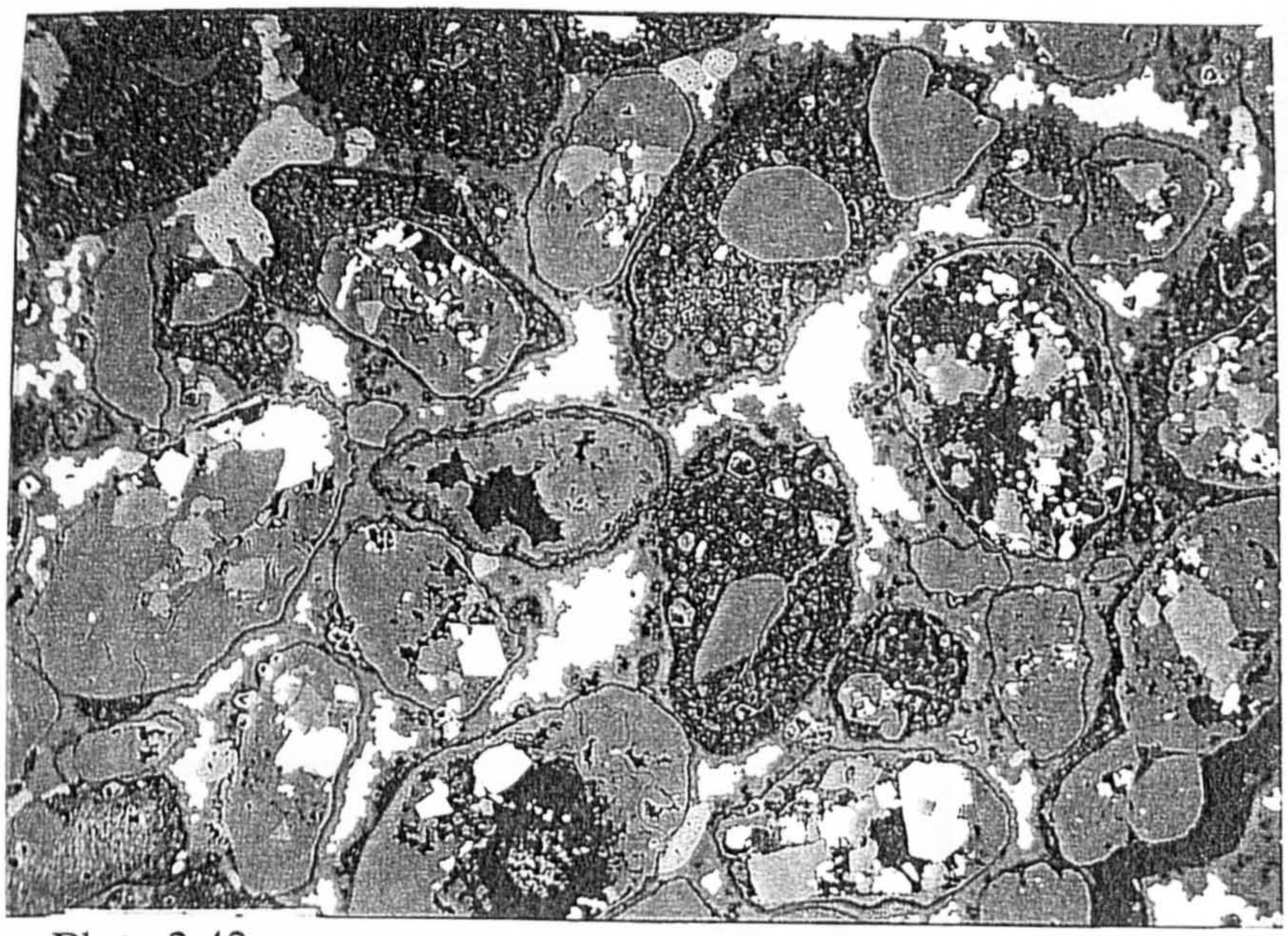

Plate 2.42
Borehole OFS 93-002, polished thin section from 112.3m (Coarse Tuff). Scale bar (lowest left) is 200μ. Note fine rounded lapilli (darker), and serpentine after olivine crystals (mid-grey). Pale grey is carbonate, as matrix (upper left) and within olivine grains (lower right). Magnetite (brightest) occupies pores and replaces some grains and carbonate (lower central left).

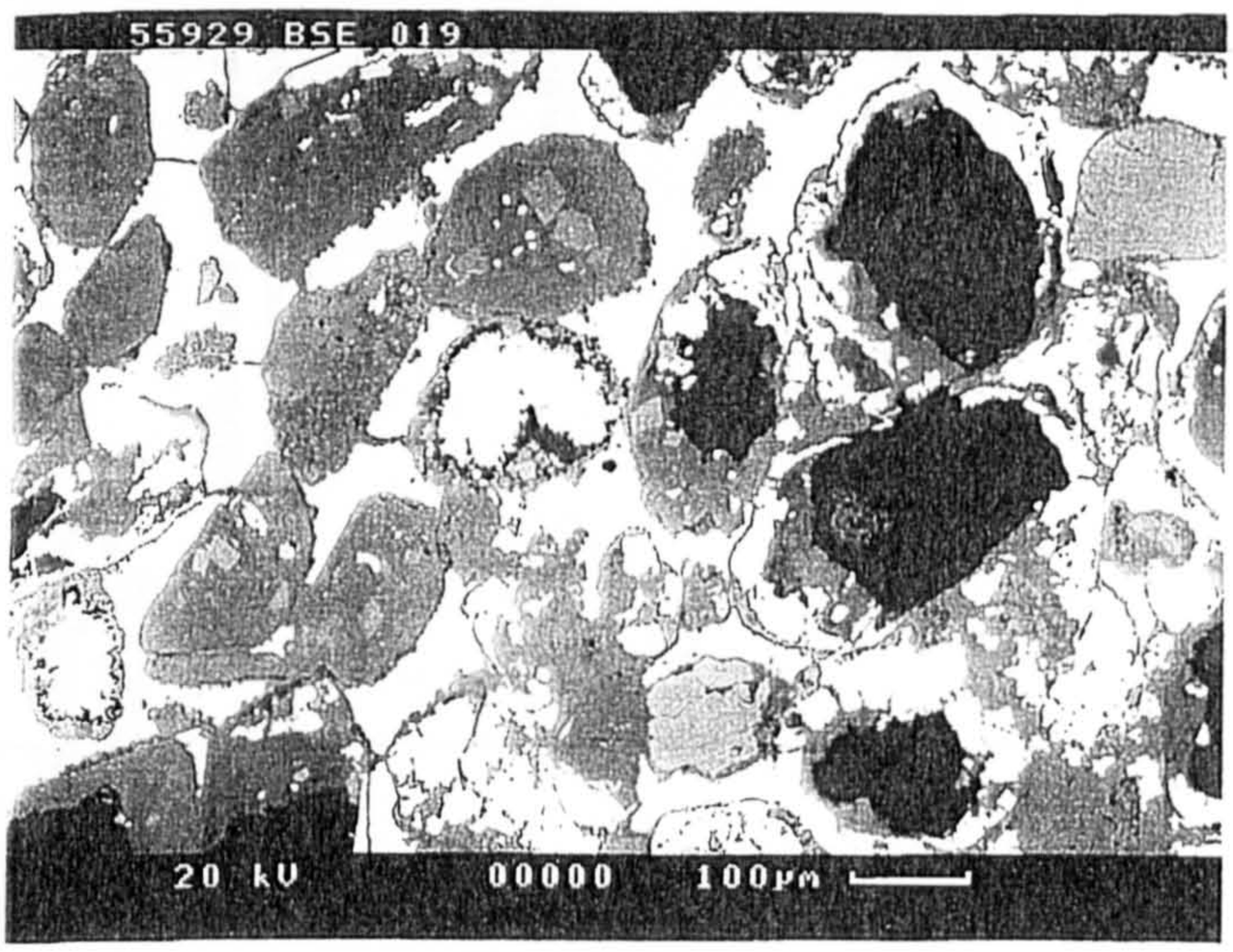

Plate 2.41
Borehole OFS 93-002, polished thin section from 107.7m (Graded Pyroclastic Sand). Note clast support, magnetite matrix and corroded chromites (centre and lower left).

Figure 2.4.6

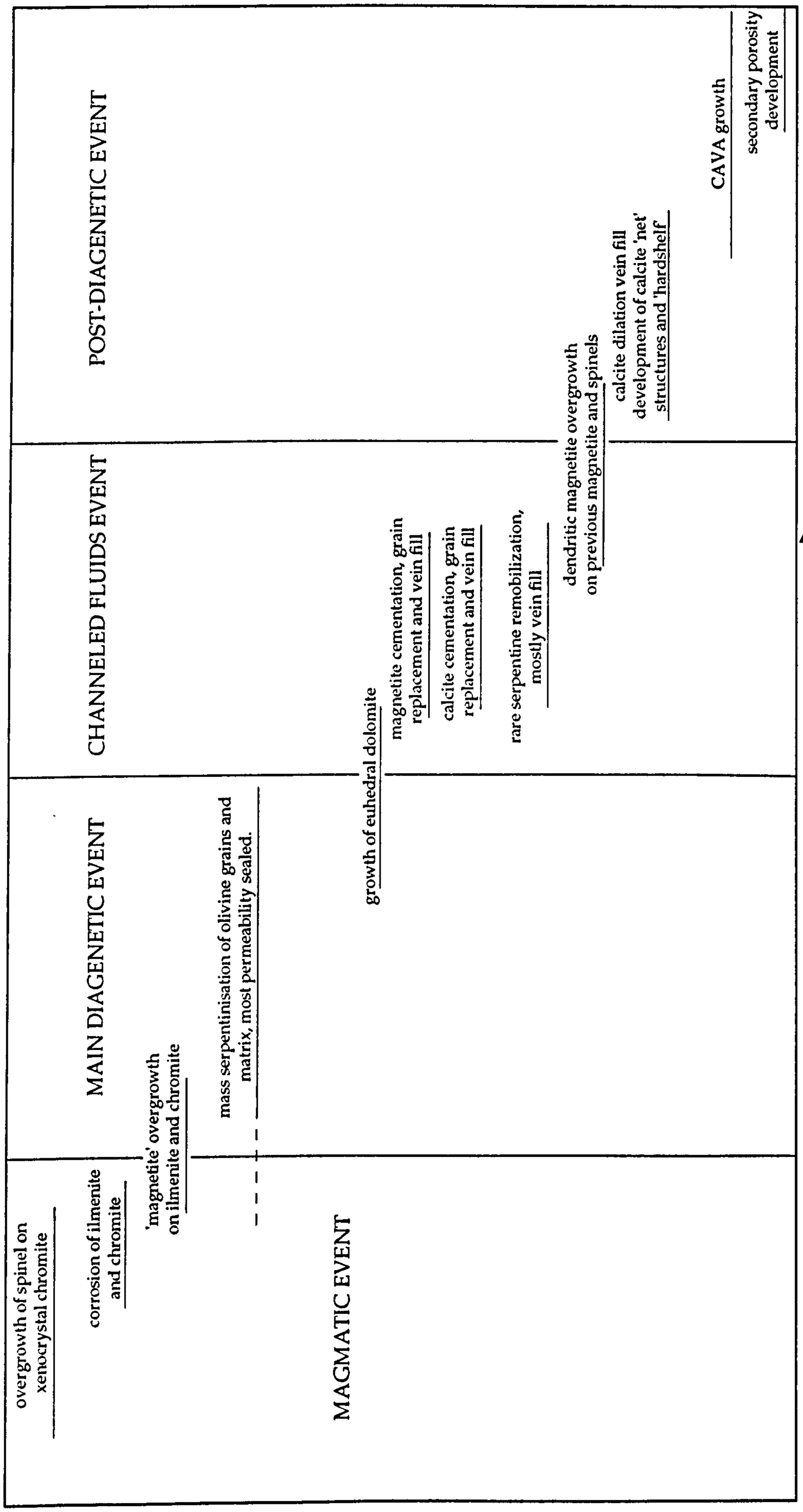

Diagenetic history of mineral growth over time. Determined from microtextural relationships of overgrowth/intergrowth and cross-cutting relationships.

producing finely embayed crystal edges, Plate 2.43 in Figure 2.4.7. Some very fine rutile developed around the corroded edges at this stage.

This alteration phase occurred in the kimberlite in the pre-eruptive magmatic environment. The corroding fluid was the kimberlite magma itself, interacting with the phenocrystal and xenocrystal spinels and ilmenite during ascent, or immediately upon emplacement. This is supported by the absence of corrosion features on any megacryst ilmenite (typically now shards), themselves grown from, and therefore in equilibrium with, the kimberlite magma (see Chapter 5).

Phase 2: Main diagenetic event

This event occurs after the pyroclastics had been deposited, and is dominated by the pervasive serpentinisation of olivine (typically $(Mg_{92}Fe_8)_2SiO_4$), both as grains, and presumably the fine ash matrix. The serpentine type is unclear, different workers have identified lizardite (Kjarsgaard et al, 1995), antigorite (Nixon et al, 1995) and chrysotile (J. Brown, pers.comm. 1995). The composition is approximately $(Mg_{75},Fe_{25})_3Si_2O_5(OH)_4$ and may represent a mix of serpentine types on a fine scale. The serpentinisation would have absorbed a great deal of water, and released large quantities of Fe, Ni, Mg, Ti and Cr. Much of the Fe and Ti did not migrate far; the serpentine is finely dusted with magnetite throughout. Lack of Na or K in the serpentine (and in the bulk rock, see XRF analyses in Chapter 5) suggests meteoric water, rather than seawater was the source. Oxygen isotope studies on the serpentine may verify this. Associated with serpentinisation would have been a large positive volume change, which may account for some of the faulting in the pyroclastic piles and crater bases. During the early stages of serpentinisation, overgrowth occurs on some of the corroded spinels and ilmenite. The overgrowth is a magnetite-like spinel, with high TiO_2, MgO and Cr_2O_3, unlike any other magnetite phases in the pyroclastic. This is not a typical spinel, by structure or by chemistry, and does not analyse well on the microprobe; an unusual product of the unusual post-eruptive environment. In the late stages of serpentinisation fine, ubiquitous, euhedral dolomite rhombs and crystals develop, both within the matrix (see 3D images above) and within ex-olivine crystals, Plate 2.44 in Figure 2.4.7. These Mg carbonates also carry a percentage of Fe, and traces of Mn, and can account for a significant proportion of the rock by volume (0.5% up to 3% indicated by point counting).

This phase of diagenesis probably occurred just after eruption, as suggested by the manifestly unstable chemical conditions that would occur when

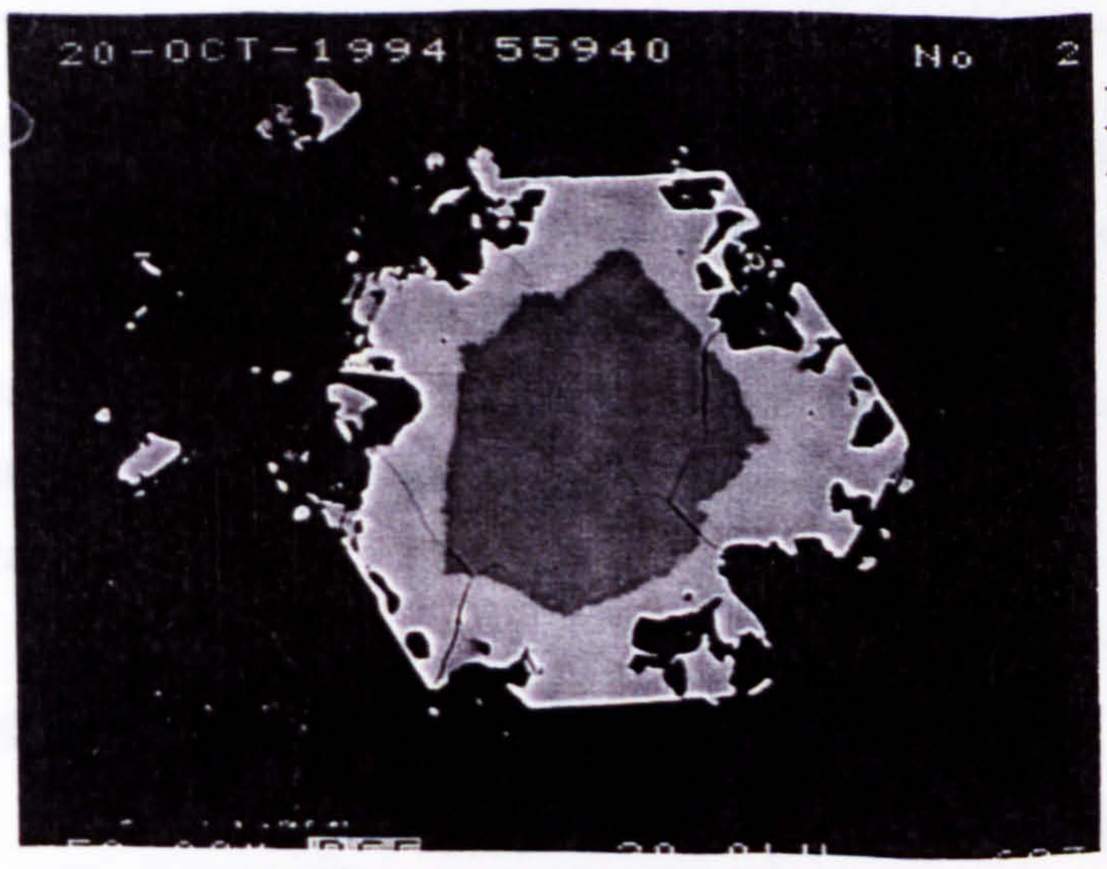

Plate 2.43
Borehole OFS 93-004, polished thin section at 107.2m, plane polarised light. Coarse tuff. Grain is 100µm across. Initially subhedral chromite overgrown by euhedral chromite.

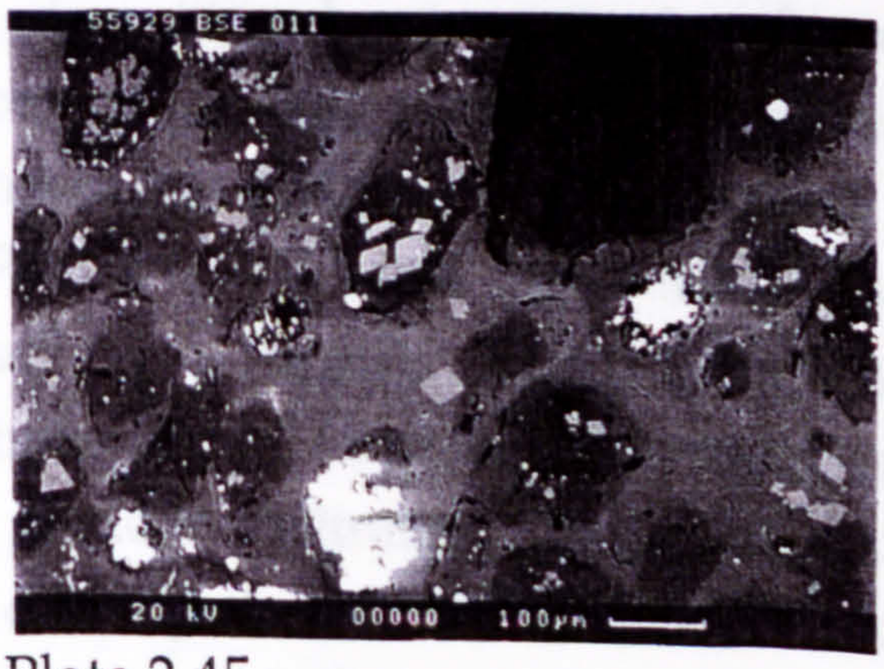

Plate 2.44
Borehole OFS 93-002, polished thin section from 107.7m, Bedded Pyroclastic Sand. Serpentinised olivine and matrix, with well developed dolomite rhombs (centre). Black area is a hole.

Plate 2.45
Borehole OFS 93-004, polished thin section from 106.6m, plane polarised light, Coarse Tuff, magnification x 2. Magnetite-serpentine-carbonate vein. Blue colour from pen ink.

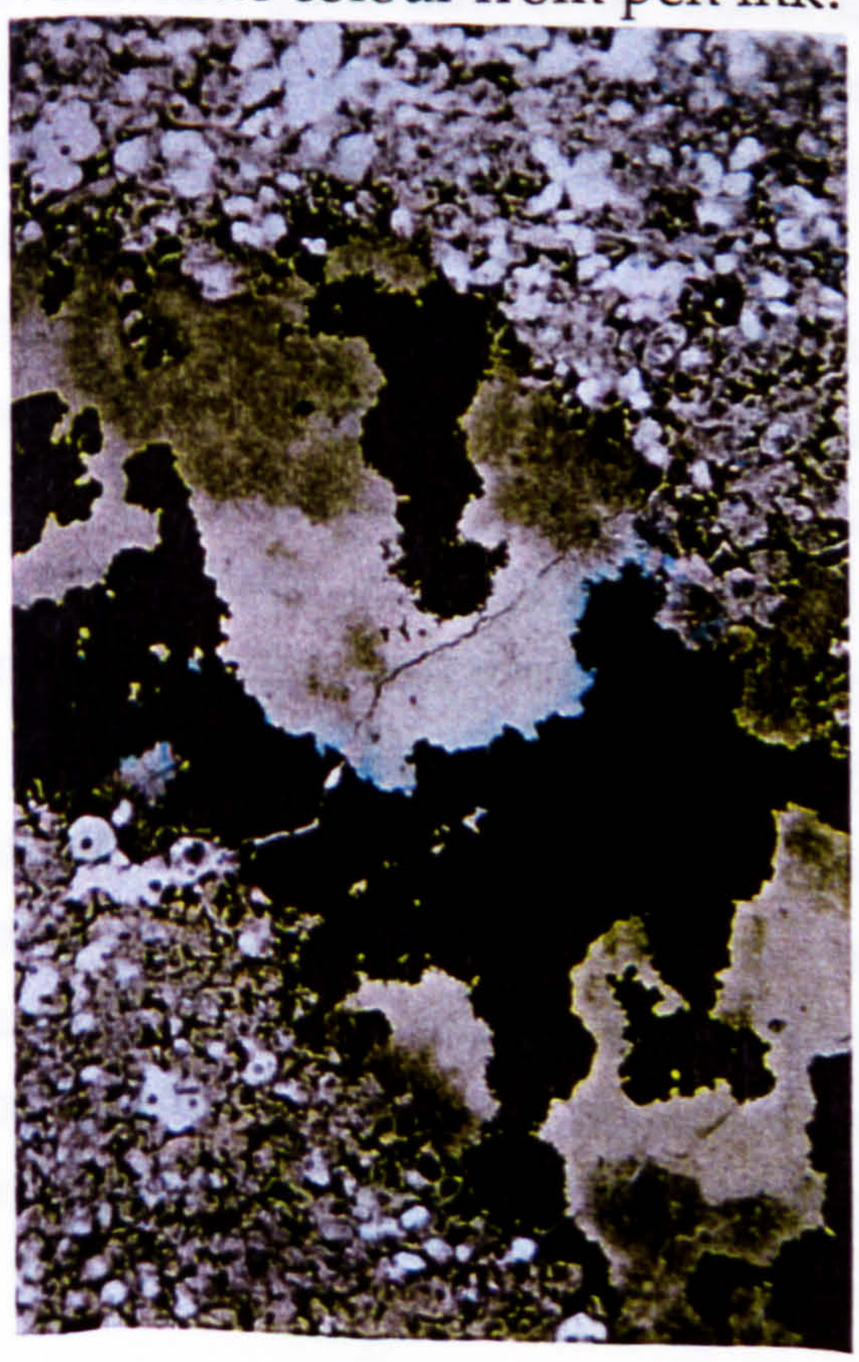

Plate 2.46
Borehole OFS 93-004, thin section from 108.34m, cross-polarised light, Coarse Tuff, magnification x 15. Dilation carbonate veins. CAVA in upper and lower centre (grey).

surface waters interact with a hot steaming porous pile of olivine. At the end of this phase, 90% to 99% of the pyroclastic deposit had been altered to serpentine, and most of the primary porosity and permeability sealed, especially in less well sorted, primary tephra-fall pyroclastics. Further alteration was limited to faults, joints, contacts with the surrounding sediment, and the kimberlite adjacent to them.

Phase 3: Channelled fluids phase.

This phase is characterised by post-depositional channelled migration of fluids depositing large amounts of carbonate and magnetite along faults. Adjacent to the fluid pathways, the mineralising fluids dissolved serpentine from the matrix first and then the grains, and replaced it with magnetite or sulphides (Fe, Pb, Cu and Zn) and carbonate or baryte. The penetration of alteration into the wall rocks appears to have been largely dependent on remaining porosity. The better sorted (and originally more porous) reworked pyroclastic sands were most prone to infiltration, particularly along coarser lag (basal turbidite) laminae and other porous bedding planes. The most intense replacement usually occurred nearest to the fluid source channel, Plate 2.45 in Fig. 2.4.7. In these channels magnetite or carbonate replace both matrix and grains, further away only the matrix is replaced. Sulphides and baryte rarely infiltrate the wall rocks to form cements, but occasionally replace grains. Some serpentine is remobilised during this phase, mostly along faults. Slickenslides are developed as a result, and some serpentine filled faults occur during this stage. In the crater facies various generations of mineralising fluids, probably developed from different parts of the pile, pass through the same channels, producing multiple vein-fill. This is not observed in the proximal and distal pyroclastics, when the vein-filling events are single, and act to seal the channel. At the base of most of the crater deposits intersected, carbonatisation is so pervasive as to completely replace the serpentine matrix and grains, sometimes even affecting the country rock. This produces the 'hard shelf', 5cm to 1.5m thick. Late in this phase is a final overgrowth of small amounts of magnetite, overgrowing previous magnetite cements and grain replacements with a fine, dendritic texture.

The mineralising fluids may be derived from a number of sources; from within the remaining porosity of the serpentinised pyroclastic, from the surrounding terrigenous sediments, and from later eruptions of kimberlite through the pyroclastic pile. Evidence for the latter is scant, but may be provided by looking for a magmatic signature in the oxygen-isotope composition of the carbonate. Some evidence for terrigenous sources of the mineralising fluids can

be drawn from the high concentrations of sulphides, including Pb, Cu and Zn in some veins. These are not common constituents in kimberlites, but are often found in sedimentary-basin fluids. The peculiar chemistry of kimberlite in amongst marine-deposited siliciclastics provides a favourable chemical depositional site (as evidenced by the intense 'hard shelf' mineralisation at their interface). Undoubtedly fluids remained from the previous diagentic phase, and contributed to the mineralising fluids, probably mixed with fluids derived from the surrounding sediments. The sedimentary basin fluids are unlikely have of been circulating at the surface, and it is suggested that some degree of burial occurred before their infiltration. Therefore this phase of diagenesis could have occurred a considerable period of time after eruption, probably on the order of millions of years.

Phase 4: Recent authigenic events

This phase consists of three events; initially involving a widespread calcite mineralisation, particularly associated with dilation cracks. Near the base of the pyroclastic piles or craters, horizontal dilation veining is commonly intense, accounting for 50% by volume in some proximal facies examples. Throughout all of the kimberlite encountered, very fine vertical nets of veins occur sporadically, and are linked to the horizontal veins below. During the carbonatisation, some of the faults sealed in the previous phase may have been preferentially reopened, and the more oxidising carbonate fluids attacked some of the vein magnetite, altering it to hematite. Distal facies are particularly prone to this, and contain large proportions of hematite, instead of magnetite. Also occurring in this phase is the contemporaneous and later growth of the large CAVA crystals, mostly from the serpentine-after olivine grains in the more serpentine rich layers of the pyroclastic piles, and in dilation veins, Plate 2.46 in Figure 2.4.7. Finally some of the kimberlites drilled in FALC have now developed a considerable secondary porosity, with all magnetite, carbonate and even some serpentine dissolved away, leaving a coarsely honeycombed texture.

These events were initiated after phase 3 (proposed to be some millions of years after eruption), and may continue to this day. Drilling into some of the kimberlite craters at FALC has discovered huge volumes of water, which must be residing in secondary porosity, and still interacting with the kimberlite.

In summary the kimberlite, after eruption has experienced three phases of diagenesis, the last of which continues today. The main event was a pervasive serpentisation of olivine and matrix, followed by a fault-vein fill and wall rock

alteration with magnetite and carbonate. Final events were a calcite-CAVA dilational vein fill and isolated CAVA growth, and the occasional development of a secondary porosity overprinting all the previous diagenetic events. Thus the diagenesis obscures much of the primary pyroclastic texture. Magmatic alteration and overgrowth stages are recognised, probably due to the interaction of kimberlite magma with phenocrystal and xenocrystal spinels and ilmenite. Further discussion of mineral chemistry and magmatic alteration processes are addressed in Chapter 5.

2.5 Textural Classification of FALC Kimberlites

All of the pyroclastic rocks described above have thus far been described as tuffs, pyroclastic sands, tuffaceous sands and so on. This section aims to formally classify the deposits described above, mainly by grain size and amount of pyroclastic material. As pyroclastic crater and extra-crater deposits have not previously been extensively classified (Clement and Skinner, 1979; Mitchell, 1986), a new scheme has been devised based mainly on the internationally recognised classification of pyroclastic rocks by Schmid (1981). Note that the term 'lapilli-tuff' in this classification refers a pyroclastic rock with a grain size >2mm, and the term 'lapilli' refers to the pyroclastic aggregated grain (of either fluidal or rounded type, as described in the sections above). The two main divisions of the kimberlite classification are based on well defined features described in the classification below, and are genetic: Primary Pyroclastic Kimberlite (PK) and Reworked Pyroclastic Kimberlite (RPK).

PYROCLASTIC KIMBERLITE, PK

Clast population consists of two main types:

1. Crystal dominated - euhedral to subhedral olivine (mostly replaced with serpentine and carbonate), with up to 15% fine to medium rounded lapilli, crustal and mantle xenoliths and their disaggregated xenocrysts.

2. Lapilli dominated - medium to coarse fluidal lapilli with some finer rounded lapilli, with up to 35% euhedral to subhedral olivine (mostly replaced with serpentine and carbonate), crustal and mantle xenoliths and their disaggregated xenocrysts.

Both are supported by up to 40% matrix, consisting of mostly amorphous, finely vermicular, acicular or bladed, interlocking serpentine, finely dusted with magnetite. CAVA crystals can be common. The rocks are dark to pale olive green, coarsely graded (rarely well bedded) or massive, and well indurated.

Lapilli Tuff	Either crystal or lapilli dominated. Fine to coarse olivine, lapilli, other mantle macrocrysts and xenoliths up to 3cm, crustal xenoliths up to 10cm.
Coarse Tuff	Crystal dominated, tuff grade (<2mm) olivine, mantle and crustal xenoliths and rare to common fine rounded lapilli. CAVA crystals common

REWORKED (EPICLASTIC) PYROCLASTIC KIMBERLITE, RPK

Excluding the more diverse **Tuffaceous Clastics** (see below) **RPK** is characterised by silt to gravel grade, friable to well indurated sediments, with >90% particles of pyroclastic material (ejected origin). Textures are mostly clast-supported, with greater proportions of subrounded and rounded clasts than **PK**. Clasts are dominantly olivine (now serpentinised or replaced with magnetite or carbonate), with some kimberlite, crustal and mantle xenoliths. Lapilli are extremely rare to absent, and if present always of the fine, rounded type. Intraclastic shale fragments and conifer needles and branch fragments occur. The matrix includes amorphous, acicular, bladed and finely vermicular serpentine, often replaced and/or intermixed with carbonate and magnetite. CAVA occurs less commonly than in **PK**.

Massive Pyroclastic Sand	Pale to dark green; units are 20cm to 200cm thick, structureless and internally homogenous. Occasional angular shale intraclasts occur.
Graded Pyroclastic Sand (ash turbidites)	Pale green to pale blue; silt to coarse sand, in normally graded beds 1cm to 160cm thick. Silts with low angle cross-stratification; rare scour features at the base of the coarse lags; notable concentration of coarse euhedral olivines and other heavy minerals in the lags. Porosity originally high. Shale intraclasts and plant fragments occur rarely.
Bedded Pyroclastic Sand	Pale green to pale blue; well bedded, often laminated with gritty lenses. Often with heavy mineral concentrations, shale intraclasts and plant frags.
Tuffaceous Clastics	Wide range of sedimentary lithologies of coastal, nearshore and marine facies that contain 10% to 50% tuffaceous components (olivine, ilmenite, perovskite and so on); e.g. fine well bedded silts (with fine serpentine and perovskite laminae), barely tuffaceous quartz sands (with coarse ilmenite and diamond) and massive pebble conglomerates (rich in garnet and ilmenite). Normal sedimentary features are observed, e.g. ripple marks, graded bedding, interbedding with non-tuffaceous shales, and cross-stratification. Bioturbation traces include; *planolites*, *terebellina*, *skolithos*, *bergauria*, *chondrites* and *zoophycos*.
Intraclast Breccia	Shale intraclasts typically occur in discreet strata 20cm to 250cm thick, and comprise of 30% to 80% of the rock. Clasts range from sand grade to 40cm boulders, although 2cm to 5cm is more common. Other intraclasts include kimberlite fragments and the varied population of crustal xenoliths brought up by the kimberlite. The 'matrix' of the shale clasts is either pyroclastic sand, or tuffaceous quartz sand, from silt to medium sand grade.

This classification has been applied to the boreholes used to illustrate the three main kimberlite facies observed. These are the terms used on the boreholes shown (see Figures 2.1.2, 2.1.5 and 2.1.13). To summarise the main kimberlite facies are listed below with the typical rock types they contain.

Crater Facies: Typically most common rock types are lapilli dominated lapilli-tuffs, and crystal dominated lapilli-tuffs. These may be interbedded and overlain by all other types of rock in the classification above, particularly the various pyroclastic sands and intraclast breccias.

Proximal Facies: These commonly have a basal layer of coarse tuff of tephra-fall origin, overlain by massive or bedded pyroclastic sands, in turn overlain by graded pyroclastic sands. Intraclast breccias may occur, but are not well developed. Tuffaceous clastics may overlie the pyroclastic sands.

Distal Facies: Most common deposits are of tuffaceous clastics, but thin (<2m) beds of massive pyroclastic sand may occur. Thin graded and bedded pyroclastic sands have not been observed, but may also be expected. No primary tephra-fall deposits are likely to be preserved (although very thin kimberlitic ultrafine ash beds may be expected).

References cited in Chapter 2

- Cas, R.A.F. and Wright, J.V. (1988). Volcanic Successions, Modern and Ancient. Chapman and Hall (pubs.), pp.528.
- Friedman, G.M. (1958). Determination of sieve-size distribution from thin section data for sedimentary petrological studies. J. Geol. Soc. London, 129, p.612-641.
- Kunze, G. (1956). Z. Krist., Vol.108, p.82-107.
- Hawthorne, J.B. (1975). Model of a kimberlite pipe. Physics and Chemistry of the Earth, Vol.9, p.1-15.
- Kjarsgaard, B.A., Leckie, D.A., McIntyre, D.J., McNeil, D.H., Haggart, J.M., Stasiuk, L. and Bloch, J. (1995). Smeaton Kimberlite Drill Core, Fort a la Corne Field, Saskatchewan. Geological Survey of Canada Open File 3170, pp.57.
- Leeder, M.R. (1982). Sedimentology, Processes and Products. Allen & Unwin (pubs.), London, pp. 344.
- Lehnert-Thiel, K., Loewer, R., Orr, R.G. and Robertshaw, P. (1992). Diamond-bearing kimberlites in Saskatchewan, Canada: The Fort a la Corne Case History. Exploration Mining Geology Vol.1 No.4 p.391-403.
- Leung, I.S. (1990). Silicon carbide cluster entrapped in diamond from Fuxian, China. American Mineralogist, Vol.75, p.1110-1119.
- Mitchell, R.H. (1986), Kimberlites: mineralogy, geochemistry and petrology. Plenum Press, New York, pp.442.
- Nixon, P.H., Gummer, P.K., Halabura, S., Leahy, K. and Finlay, S. (1993). Kimberlites of volcanic facies in the Sturgeon Lake area. Russian Geology and Geophysics, Vol.34, No.12, p.66-76.
- Nixon, P.H. and Leahy, K. (1995). Diamond-bearing volcaniclastic kimberlites in Cretaceous marine sediments, Saskatchewan, Canada. Proceedings of the 6th International Kimberlite Conference, Russia 1995, (submitted).
- Schmid, R. (1981). Descriptive nomenclature and classification of pyroclastic deposits and fragments: recommendations of the IUGS subcommission on the systematics of igneous rocks. Geology, Vol.9, p.41-43.
- Scott-Smith, B.H., Orr, R.G., Robertshaw, P. and Avery, R.W. (1994). Geology of the Fort a la Corne Kimberlites. Proceedings of District 6, AGM, Canadian Institute of Mines, p.19-24.
- Scott-Smith, B.H., Orr, R.G., Robertshaw, P. and Avery, R.W. (1995). Geology of the Fort a la Corne Kimberlites. Proceedings of the 6th International Kimberlite Conference, Russia 1995, Extended Abstracts Volume.
- Skinner, E.M.W. and Clement, C.R. (1979). Mineralogical classification of Southern African kimberlite. In Kimberlites, diatremes, and diamonds, (Boyd, F.R. and Meyer, H.O.A., eds.), American Geophysical Union, Washington, p.129-139.

- Smith, C.B. and Lorenz, V. (1989). Volcanology of the Ellendale lamproite pipes, Western Australia. Proceedings of the 4th International Kimberlite Conference (Australia 1986), Kimberlites and related rocks, (Blackwell, pubs.), Vol 1, Geol. Soc. Australia Special Publication No.14, p.505-520.
- Wright, J.V. and Mutti, E. (1981). The Dali Ash of Rhodes, Greece: a Problem in Interpreting Submarine Volcanigenic Sediments. Bulletin of Volcanology, Vol.44-2, p.153-167.

CHAPTER 3 - VOLCANIC EVOLUTION OF THE FORT A LA CORNE KIMBERLITES

Abstract

Kimberlites at Fort a la Corne consist of broad, saucer-like bodies of crater facies pyroclastics, which may be underlain by as yet undiscovered feeders of diatreme facies. These are here termed '*pateran craters*', and characteristically have a diameter to depth ratio of 7:1. This is unlike the volcanic structure found in most other kimberlite diatremes and related volcanic types from around the world, characterised by an inverted cone shape. Both dry and phreatomagmatic processes have been proposed for the generation of kimberlite diatremes. The structure of the FALC kimberlites, and those of some Mbuji-Mayi kimberlites (Zaire) and Ellendale lamproites (Australia), cannot, however, be adequately described by conventional kimberlite diatreme formation processes of Clement and Reid (1989). Phreatomagmatic models (Smith and Lorenz, 1989) partially explain the *pateran*-type craters found at these localities, but fail to explain the absence of large diatremes and flat crater floors in some of the craters.

A genetic evolution of pateran craters is described, and illustrated by the FALC example. Primary crater fill is from pyroclastic tephra-fall of either phreatomagmatic type (producing crystal-dominated lapilli-tuffs) or hawaiian-strombolian type (producing lapilli-dominated lapilli-tuffs). Eruption style may switch between these two types during a single eruption, as aquifers are drained or intersected at the explosive centre in the lower vent/diatreme. Tuff rings and extra-crater proximal tephra-fall tuffs are produced mainly as a result of continued phreatomagmatic eruption. Hawaiian-strombolian eruptions produce tuff-piles within the crater, adjacent to the vent, which may undergo rheomorphic flow to the edges of the crater. In addition, multiple eruption separated by short periods of time may also occur within one *pateran crater*.

The volume of the *pateran crater* excavated in the initial eruption is typically larger than the amount of material erupted, and subsequently deposited within it, and upon cessation of volcanic activity the craters are often underfilled, allowing a crater lake to develop. Wave-cutting from the crater lake is the main internal erosional force, and is accompanied by mass-wasting (slumps), soil creep and marine erosion in rapidly levelling the tuff piles. The eroded tuffs are transported and deposited as reworked pyroclastic sediment over primary deposits both within the crater, and into the sedimentary basin beyond. In this way the *pateran craters* are filled, and reworked pyroclastic kimberlites may be distributed into the surrounding sedimentary environment.

3.1 Summary of previously proposed volcanic processes of kimberlite emplacement

An understanding of the volcanic processes involved in the formation of a near-surface kimberlite body provides a framework within which the lithofacies previously described (Chapter 2) can properly be understood, as well as adding to the continuing debate on kimberlite emplacement mechanisms. From an economic perspective, knowledge of the crater and diatreme dimensions and internal structure are essential when evaluating and characterising a diamond-bearing ore-body. The mechanism of kimberlite emplacement has been contentious throughout the history of kimberlite studies, complicated by the fact that most of the debate has concentrated on the formation of the South African diatremes.

Kimberlites in other regions of the world, in many instances, strongly resemble the classic South African diatreme morphology (Sketch a. in Figure 3.1.1), consisting of a deep (0.5 to 2.5km) downwards tapering cone with uniform angle of 70° to 80° (Hawthorne, 1975). Their formation has most convincingly been described by Clement and Reid (1989), although many other workers in the field have proposed other, less viable, processes, e.g. Mitchell (1986). The role of groundwater interacting with rising magma and triggering the volcanic eruption is controversial. This phreatomagmatism is strongly favoured by Lorenz (1975; 1985). Clement and Reid (1989) do not discount the existence of the phreatomagmatic process in some instances, but they do not regard it as an essential part of the diatreme forming process.

The classic 'carrot-shaped' diatremes do not describe all kimberlite occurrences, however, and along with other alkali-ultramafic (e.g. lamproites) and basic to intermediate volcanic rocks, kimberlites occasionally display phreatomagmatic morphologies. The interaction of groundwater with magma, and the concomitant phreatomagmatic activity, has long been accepted as the main formative process for maars and tuff-rings from around the world (Lorenz, 1985) (Sketch d. in Figure 3.1.1). These often occur in alkali-basalt fields where groundwater was readily available during eruption (e.g. Swabian Alb, Lorenz (1982), and Fife, Francis (1970)). Some other continental pyroclastic deposits may also have a phreatomagmatic origin, e.g. lamproites (Ellendale, Australia, Smith and Lorenz (1989) (Sketch f. In Figure 3.1.1); Black Butte, Montana, Herne (1968)) and rare kimberlites (Mbuji-Mayi, Zaire, Demaiffe et al (1991) (Sketch b. in Figure 3.1.1), Alto Paranaiba kimberlite province, Brazil, Leonardos et al (1995), and at Fort al la Corne, Nixon et al (1993), Scott-Smith et al (1995), Nixon and Leahy (1995) and Kjarsgaard et al (1995) (Sketch c. in

Figure 3.1.1

Sketch sections of various volcanic structures worldwide. Tuff ring and maar are schematic and inferred, FALC Anomaly 120 and Ellendale sections are inferred from boreholes.

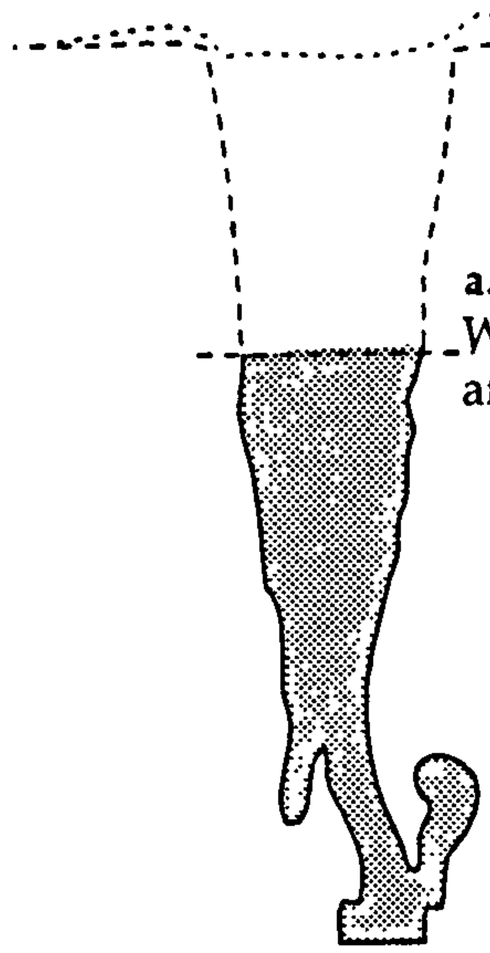

a. Classic diatreme, Wesselton, South Africa, after Clement and Reid (1989).

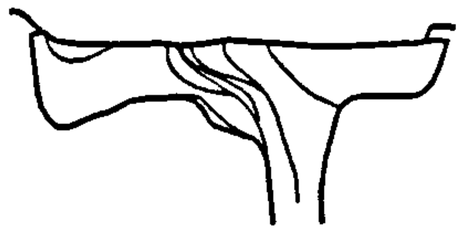

b. Mbuji-Mayi, Zaire, after Demaiffe et al (1988), lines indicate boudaries between different facies tuffs and kimberlites

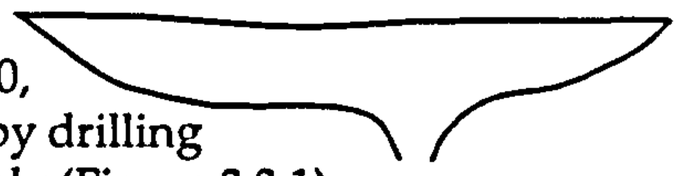

c. FALC anomaly 120, outline determined by drilling and magnetic anomaly (Figure 3.3.1)

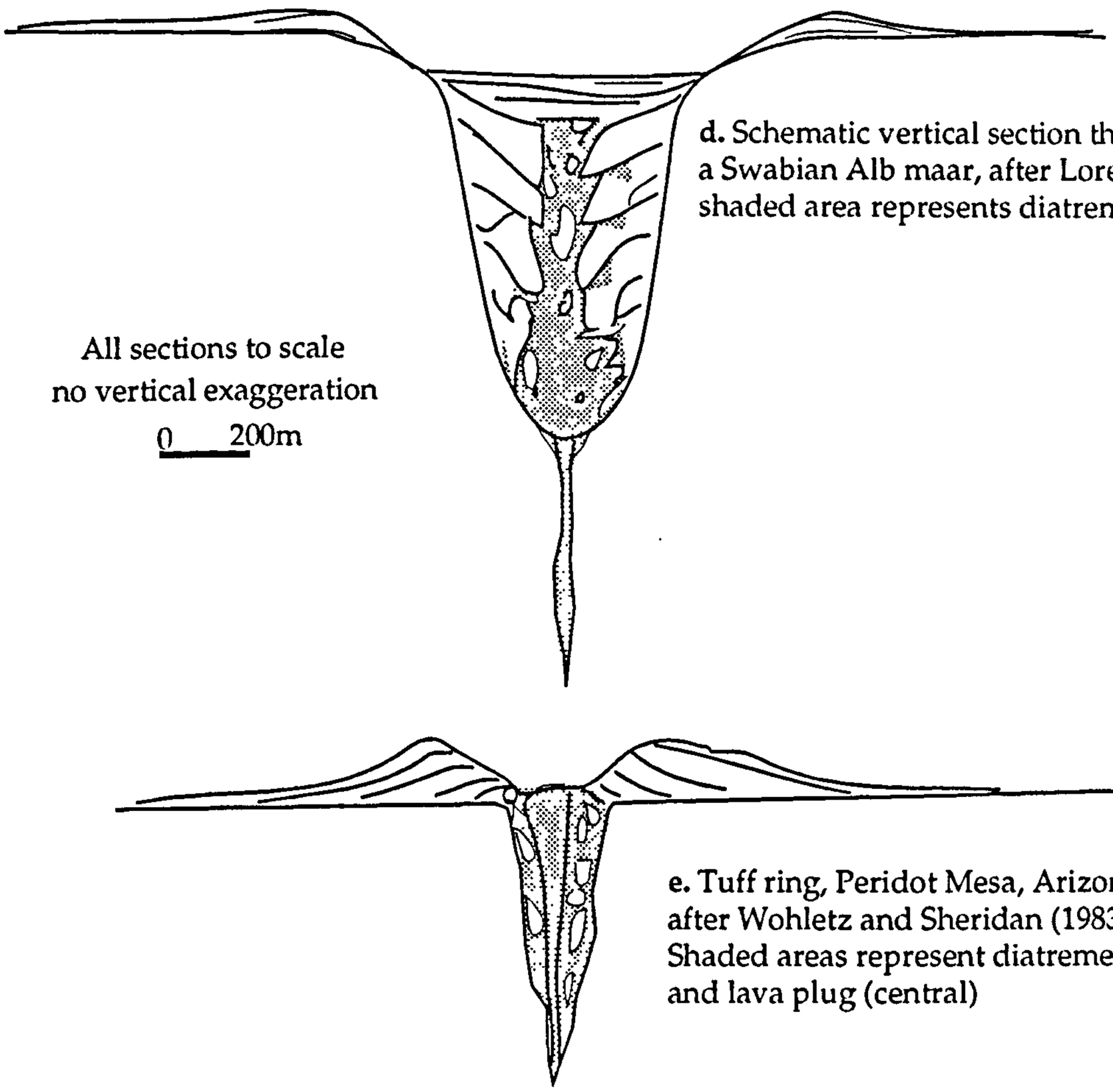

d. Schematic vertical section through a Swabian Alb maar, after Lorenz (1985), shaded area represents diatreme facies.

All sections to scale
no vertical exaggeration
0 200m

e. Tuff ring, Peridot Mesa, Arizona, after Wohletz and Sheridan (1983). Shaded areas represent diatreme facies and lava plug (central)

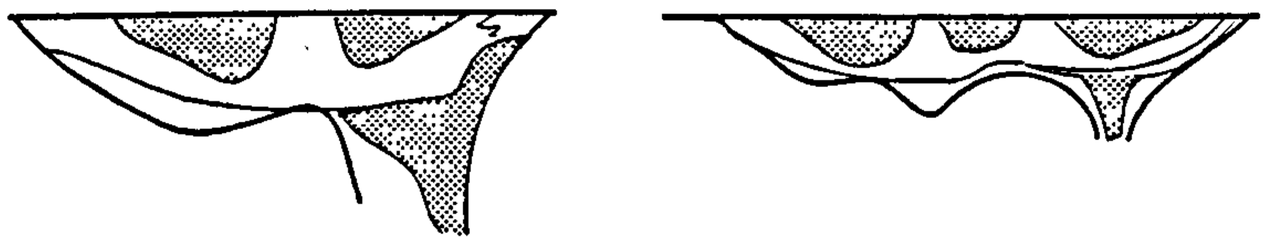

f. Two sections of Ellendale No.4, West Kimberly, Australia, after Smith and Lorenz (1989). Internal zones represent different facies of tuffs and magmatic lamproite (shaded)

Figure 3.1.1)). The formative processes of the kimberlite, lamproite and basaltic volcanic structures are discussed in detail below, followed by a detailed synthesis of FALC deposits.

3.1.1 Classic kimberlite model

The classic kimberlite model of the 'carrot-shaped' diatreme with associated crater facies and root zones was initially proposed by Hawthorne (1975), and embellished further by various authors (e.g. Mitchell, 1986) during the next decade, Figure 3.1.2.

Figure 3.1.2

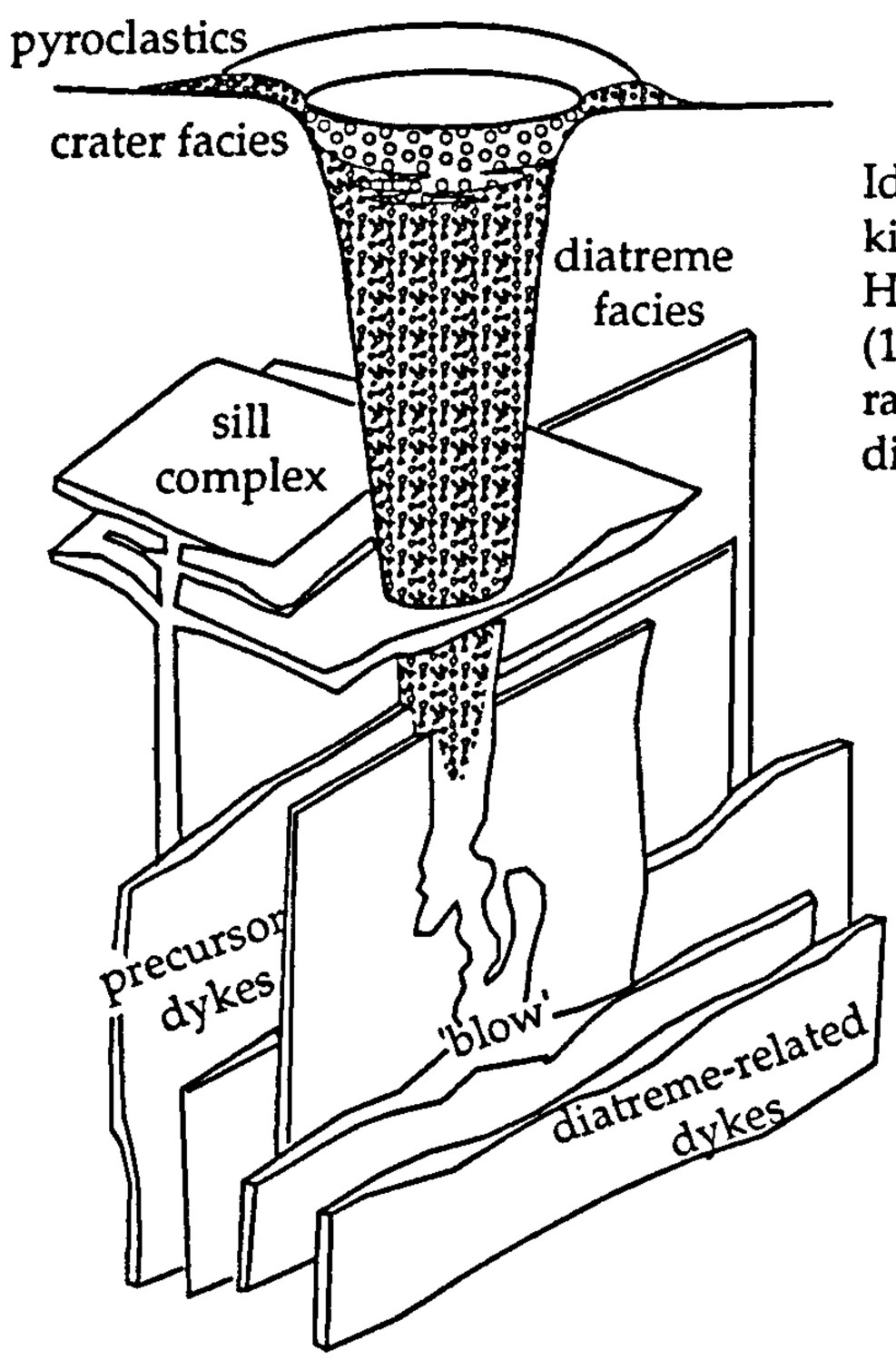

Idealised cut-away diagram of a kimberlite diatreme based on Hawthorne (1975), and after Mitchell (1986). Depth of diatreme facies ranges from 0.5km to 2.5km, diameter of crater facies is up to 1.5km.

The process that forms this structure can be considered as a four stage event (Clement and Reid, 1989). The first stage occurs as embryonic pipes develop within 0.5km to 3km of the surface, (Stage 1 of Figure 3.1.3). Here kimberlite magma forms sub-vertical dykes (and rarer sub-horizontal), as well as arches and domes, often found with explosion breccias around the upper margins, especially if groundwater is present. At this stage the kimberlite magma consists of mainly liquid, with abundant solids in suspension (e.g. xenoliths and megacrysts), with crystallisation of phenocrysts (e.g. olivine, phlogopite and spinel) also occurring.

Figure 3.1.3

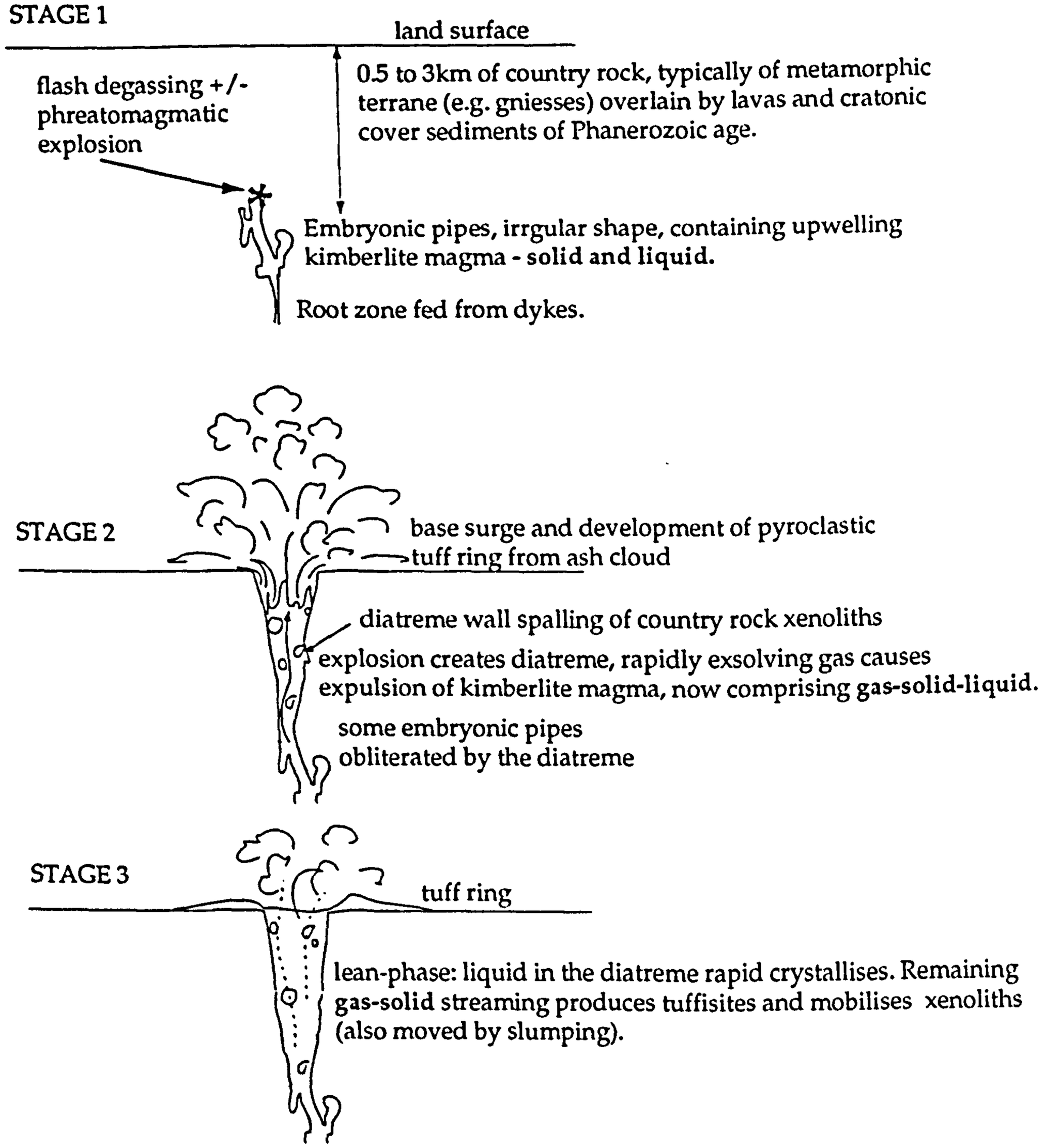

Genetic model sections for Wesselton, South Africa, after Clement and Reid (1989).

At some point, the upward developing embryonic pipes reach a point at which rapid degassing of magmatic volatiles (mainly CO_2 and H_2O) occurs. This results in the massive explosion that excavates the entire diatreme structure and breaks through to the surface (Stage 2 of Figure 3.1.3). Some of the earlier dykes and embryonic pipe structures may be truncated during the diatreme excavation. The resulting ash cloud deposits a tuff ring on the land surface, and the kimberlite magma rapidly rises from the base of the diatreme and degasses, changing to gas-solid-liquid mix, and pelletal lapilli may form. In this model the role of groundwater in triggering and fuelling the diatreme-forming explosion is largely irrelevant (Clement and Reid, 1989), a point strongly contested by those favouring phreatomagmatic models, which are further discussed below (Lorenz 1975; 1985).

Following the rapid ascent from the root zones to the diatreme, the gas-liquid-solid mix is quickly quenched to a fluidised gas-solid system restricted to discrete channels within the diatreme (Stage 3 of Figure 3.1.3). Xenoliths, floating reefs (very large country rock xenoliths) and crystals outside these fluidised zones become entrapped as a fine-grained matrix crystallises around them, forming the typical diatreme facies kimberlite. Within the fluidised zones, solids may be size-sorted, abraded, or rise or fall dependent on size, density and upward velocity of the fluidised kimberlite. As the gas supply wanes, the fluidised systems become static and a fine-grained matrix forms, resulting in tuffisitic diatreme facies kimberlite. These tuffisitic kimberlite channels occur sporadically in most kimberlites, more commonly in the upper portions of the diatreme, and are often parallel to or alongside the diatreme walls.

The final stage is of post-emplacement modification, involving largely an alteration of primary minerals (especially in the groundmass) to serpentine, as well as the addition and/or removal of carbonates. The volume change associated with settling, compaction and dissolution commonly leads to contraction of the kimberlite material in the diatreme, resulting in crater lake deepening (up to 400m at M1 kimberlite, Botswana, Daniels et al, 1994) and fault activity throughout the pipe (Stage 4 of Figure 3.1.3). Subsequent eruptions may occur at later dates into the same diatreme system, but these cross-cut previous diatreme fills, indicating that they are usually after a definite break in volcanic activity, and not part of a continuous eruptive cycle. Erosion of the whole volcanic structure usually follows, and typically exposes upper to lower diatreme levels, and in extreme cases, to the feeder dykes.

3.1.2 Deep phreatomagmatic diatremes

As an alternative to the model above, groundwater-magma interaction may be the process that drives kimberlite diatreme excavation, but in a slightly different manner to the processes described above. The classic kimberlite morphology (Figure 3.1.2) is extremely similar to that of the common basaltic maar diatremes, although the basaltic maars are often much smaller, and contain some lava or scoria (especially if groundwater supplies were restricted), Figure 3.1.4.

Figure 3.1.4

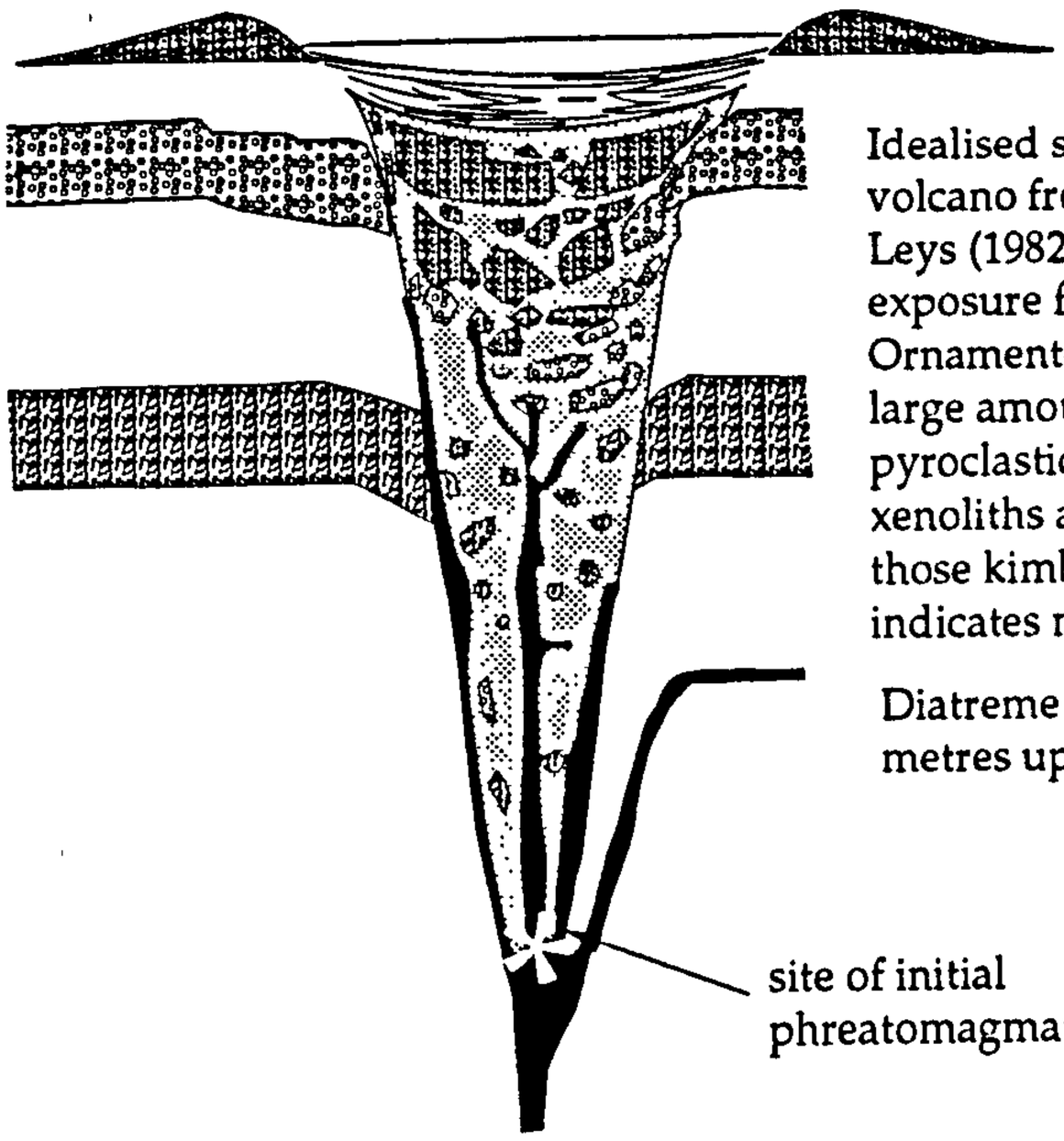

Idealised section of a basaltic phreatomagmatic volcano from the Fife volcanic field, Scotland, after Leys (1982). Various levels of erosion have led to exposure from crater fill to root zone levels. Ornamented strata are shown to illustrate the large amounts of country rock and slumped pyroclastics present in the diatreme. These xenoliths are relatively undisturbed compared to those kimberlite diatremes. Solid black ornament indicates magma.

The phreatomagmatic process has been demonstrated for continental basaltic maars in the Swabian Alb of Germany (Lorenz, 1985) and at many other localities in the USA (Wohletz and Sheridan, 1983) and elsewhere (Cas and Wright, 1988). The key element of phreatomagmatism is explosive volcanism triggered by flash heating of groundwater (phreatic explosions) resulting in explosive fragmentation of both magma and country rock. The water is usually in the form of groundwater in faults or permeable strata (aquifers), or as standing bodies on the land surface (lakes or shallow seas). The explosion excavates a chamber at depth (usually tens to hundreds of meters below the surface), which causes collapse of the overlying country rock along a system of ring faults. Further water-magma interaction causes more explosions,

propelling previous debris (mainly country rock fragments with varying amounts of magmatic material) through the diatreme-vent into the overlying ash cloud and causing further collapse. If water-magma interaction wanes, upwelling magma may then penetrate into the diatreme and eventually on to the crater surface. Waning water availability has been used by Lorenz (1985) to explain deep diatreme formation. Lorenz proposed that as groundwater is quickly converted to steam and expulsed via the vent, the near-surface water table is locally lowered (forming a cone of depression). Hydrostatic pressure is also lowered, and if the deeper strata are also water saturated, the depth of water-magma contact (explosive centre) also lowers. By this method Lorenz propose that diatremes may propagate downwards to the great depths observed in many kimberlites (up to 3km).

Clement and Reid (1989) point out that the energy required to excavate successively deeper diatremes, *and mix the fill* of the previously excavated diatremes would rise exponentially, and cannot, therefore, be correct. This is important because the striking difference between deep basaltic maar-diatremes and kimberlitic diatremes is the degree of internal mixing. Basaltic maar-diatremes largely consist of country rock and bedded pyroclastics, downfaulted and slumped (virtually *in situ*) by sub-surface excavation of an explosion chamber (that may be propagating downwards). In kimberlites no ring fault/slumps are usually evident, and country rock xenoliths are far more thoroughly intermixed with the kimberlite (apart from megaxenoliths, which can be explained by later slumping or floatation in fluidised channels). Thus the Clement and Reid argument of deep diatreme formation greatly detracts from the value of models which essentially include phreatomagmatism in the formation of the deep (>1km) kimberlite diatremes. This does not, however, affect the value of phreatomagmatic models that do not require downward propagating explosive centres, such as shallow kimberlite diatremes (<500m), or any other diatremes (usually basaltic) that display ring-fault subsidence and low degrees of diatreme mixing.

3.1.3 Shallow phreatomagmatic diatremes

Shallow maars and other associated volcanic types, such as tuff rings and tuff cones are common in many continental volcanic fields, plus other more diverse plate tectonic settings, including emergent spreading centres (Iceland; Leys, 1982), oceanic islands (Hawaii and the Azores; Wohletz and Sheridan, 1983) and arc environments (Alaska; Cas and Wright, 1988). Although fuelled by the same phreatomagmatic explosive energy, the craters excavated range

from a steep-sided morphology (similar to deep diatremes outlined above) to shallow, low angle excavations of irregular shape (see Ellendale and Mbuji-Mayi examples in Figure 3.1.1). Tuff rings tend to have relatively small amounts of excavation (short diatremes) with regular, moderately inclined diatreme (or crater) walls, and well developed pyroclastic piles (up to 50m thick). Tuff cones have very little or no diatreme development, with very thick pyroclastic piles (up to 150m), and are formed when magma interacts with shallow standing water (i.e. lake or coastal seas; Wohletz and Sheridan, 1983).

The wide range of crater depth and wall angles may simply reflect different magnitudes of explosions and different water table levels (e.g. Wohletz and Sheridan, 1983). Accepting the downward propagating explosive centre model for deep basaltic diatremes of Lorenz (1985) (occurring when groundwater is used up at successively deeper levels), then the shallow/irregular diatremes may be explained by high groundwater recharge rates. This would allow the water removed by the eruption to be replaced as quickly as it is used, and downward propagation need not occur, thus only shallow diatremes may develop.

Here it is considered that whilst these processes may play an important role in determining the final crater/diatreme morphology, other factors such as the mechanical strength of the surrounding country rock and the type of magma involved (kimberlitic or lamproitic as opposed to basaltic) are equally significant. For example the Ellendale lamproite (Smith and Lorenz, 1989), and the Mbuji-Mayi kimberlite (Demaiffe et al, 1991) have very low angle crater walls that were excavated from relatively weak, poorly indurated sandstones. The horizontal removal of material in crater excavation appears to be considerably more significant than the vertical diatreme development, with the ratio of length to depth for these craters typically 7:1, see Sketches b., c. and f. in Figure 3.1.1. These broad, saucer-shaped (also termed "champagne-glass" structures) appear to be rare, and are not described for basaltic volcanics. They may be restricted to volatile and crystal-rich, alkali-ultramafic magmas.

Formative processes for 'champagne-glass' craters have not been adequately described, although the Ellendale occurrences have been explained in terms of typical maar-type evolution (Smith and Lorenz, 1989). The major problem for this hypothesis is the unusual broad and flat saucer-shaped craters, which are explained by removal of poorly indurated country rock sandstones around the vent by the blasting effect of the eruption and base surge during normal maar-diatreme development. The sandy material is immediately redeposited on the crater floor as tephra-fall tuffaceous sands and silts,

increasingly mixed with juvenile pyroclastic material, such that the crater fill grades up from bedded sandy tuffs to massive tephra-fall lapilli-tuffs. Slumping due to normal maar-diatreme processes allows bedded sandy tuffs, tephra-fall tuffs and debris flows to subside into the relatively small, poorly developed diatremes (Smith and Lorenz, 1989).

It is interesting to note that at both Ellendale and Mbuji Mayi, diamond grades are higher in the sandy tuffs than in the tephra-fall tuffs, and that the feeder diatremes are relatively narrow. Diatreme neck widths at the base of the crater range from 10% to 25% of the width at the top of the crater.

In the sections below the volcanic morphology at Fort a la Corne is compared to those outlined above, and a genetic model proposed.

3.2 Geophysical evidence for the volcanic structure of the FALC kimberlites

Magnetic and gravity anomalies and seismic reflection data have been used to determine the crater morphology at FALC. Gravity data were used to determine the thickness of the deposits, based on the density difference (typically 0.18gcm^{-3}) between kimberlite (mean 2.68gcm^{-3}, range 2.46gcm^{-3} to 3.09gcm^{-3}) and the enclosing poorly lithified shales (mean 2.50gcm^{-3}, range 2.15 gcm^{-3} to 3.15gcm^{-3}; Lehnert-Thiel et al, 1992). These data and most of the interpretation is propriety to the FALC Joint Venture, and unfortunately could not be used in this thesis. Limited gravity data interpretation of Anomaly 120 at FALC has been published, Lehnert-Thiel et al (1992), and indicates a circular anomaly of about +1mgal, with the peak offset to the east, suggesting thicker kimberlite in the eastern section.

Seismic reflection surveys have been carried out but again remain either propriety or unpublished, although one was displayed at the University of Saskatoon Geology Department Open Day in 1994. This processed image failed to adequately determine boundaries other than the central top and base of the kimberlite body, which were already known from borehole data (B.C. Jellicoe, pers.comm.)

Magnetic anomalies appear to be the best geophysical tool with which to model the FALC kimberlite shapes because of the wide areal coverage and the distinctive anomalies that kimberlites produce. The nature of the magnetic anomalies at FALC have been previously described, (Chapter 1). They are typified by irregular to circular, positive 'bullseyes', with curved lows unevenly distributed around the edges due to dipole effects on the thicker bodies, see

Figure 1.2.2 (Chapter 1). Modelling of these bodies as multiple-cylindrical structures of given susceptibilities (Singh and Sabina, 1978) best describes their structure. The results indicate that the magnetic cylinders are relatively wide, compared to their thickness, a ratio 7:1 that coincides with kimberlites at Mbuji-Mayi and lamproites at Ellendale (see Sketches b., c. and f. in Figure 3.1.1 above).

Magnetic modelling over the whole of the FALC area shows that the anomalies are not of the deep-rooted cylindrical, or 'carrot-shaped' diatreme types (Kensington press release, 1995). The kimberlites all appear to be flat-lying bodies, often coalescing in the central parts of the FALC cluster, and reaching maximum widths of 1300m, (Figure 3.2.1). The distribution of the anomalies is mainly in a dense cluster trending NNW over an area 25km by 10km wide. Scattered anomalies continue to the NNW for another 35km, and also at 15km to the WNW and NNE of the main cluster. Factors controlling this local distribution are undoubtedly related to upper crustal structure (White et al, 1995), but specific elements have not been identified (see Chapter 1).

The edges of an individual magnetic anomaly correspond to the transition between magnetite-rich kimberlite in the crater, and shales containing no magnetite, i.e. the anomaly defines the crater walls/edges. Kimberlite is also known to occur beyond the crater walls (i.e. proximal and distal facies, see Chapter 2), but magnetic anomalies here are less well defined, probably due to the thinner (1m to 50m, typically 15m) and dissected or irregularly-distributed strata compared to crater facies (30m to 280m thick, typically 100m) Scott-Smith et al (1995). In addition, distal kimberlites typically become intermixed with terrigenous sediments, which are non-magnetic.

In summary magnetic anomalies are a useful tool at FALC in determining the extent and approximate shape of the kimberlite bodies. They were found to be a relatively dense cluster with scattered outliers to the north, mostly irregular to circular in plan view, ranging from 200m to 1300m in diameter, with broad saucer-shaped craters of variable thickness, typically 100m.

Figure 3.2.1

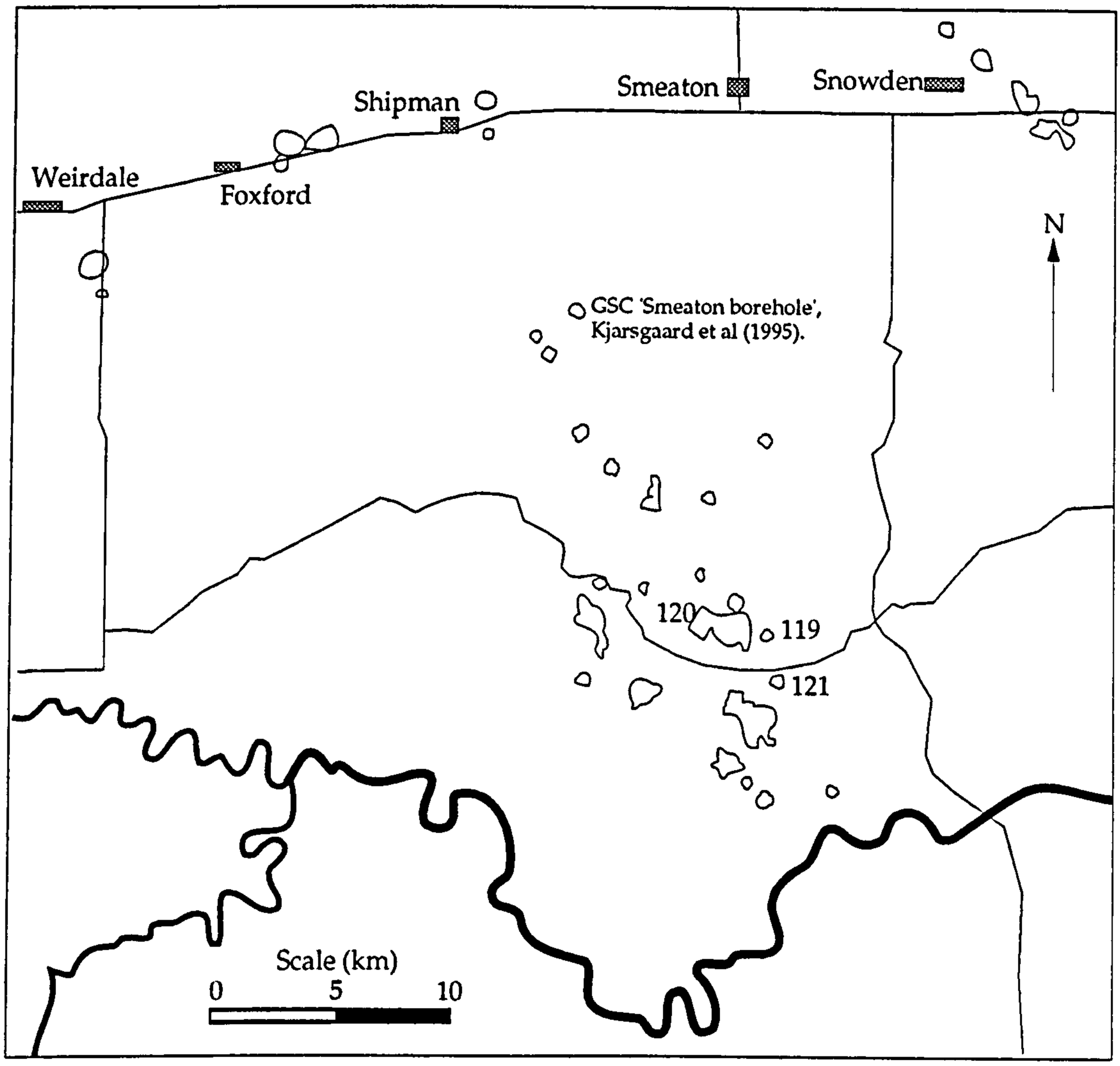

Diagram illustrating the distribution and areal size of the kimberlite bodies at Fort a la Corne, as determined from the extent of their magnetic anomalies (see Chapter 1).
Settlements, roads (solid lines) and rivers (heavy line) are shown, as well as the location of selected Anomaly numbers and the site of the GSC Smeaton borehole.

3.3 Borehole evidence for volcanic structure

A large number of boreholes (over 140 by spring 1996) have been drilled into the kimberlite in the FALC area. At least seven of these (mostly OFS boreholes) have intersected extra-crater kimberlite (proximal and distal facies), as defined by the edges of magnetic anomalies. Some of the extra-crater deposits contain primary pyroclastic (tephra-fall) kimberlite (see Chapter 2), attesting to the explosive nature of the emplacing volcanism.

The great majority of the boreholes have been drilled by the FALC Joint Venture, and are propriety. However, borehole depth data and kimberlite sections for Anomaly 120 (see Figure 3.2.1 for location) have been published in Kensington press releases and at public conferences (e.g. Saskatchewan Energy and Mines Open House Conference, Saskatoon, December 1994), see Figure 3.3.1. From the section shown, and from presentations by Scott-Smith et al (1995), the typical crater morphology at FALC conforms to the shape suggested by modelling the magnetic anomalies: broad, saucer-shaped craters, with an aspect ratio of 7:1.

General geological descriptions of the crater fill by Scott-Smith et al (1995) are be supplemented by observations from the OFS 93-012 borehole (30m of crater facies kimberlite drilled within a small, irregular anomaly near Wierdale, see Chapter 2), and the 120m thick crater fill sequence in the Smeaton borehole (drilled and published by the Geological Survey of Canada; Kjarsgaard et al, 1995).

The disposition of the bedding within the crater ranges from horizontal to sub-vertical in localised patches, and often shows signs of disruption due to slumping and syn-depositional small-scale faulting. The crater walls, when intersected, range from high angle (45°) and cross-cutting the bedding of both the country-rock and the crater fill, to horizontal and conformable. Comparison of the stratigraphy of the country rock above and below that indicates large thicknesses of rock have been removed, i.e. a crater was excavated from the country rock.

Borehole OFS 93-012 contains deposits recording two distinct explosive events (see Chapter 2, and Figure 2.1.2.) The first phase consists of 5m of coarse, lithic-rich, crystal-dominated tephra-fall lapilli-tuff (with rare lapilli). The basal 3m consists of two graded beds, with lithics and very coarse crystals at their base, overlain by 2m of very finely bedded (1mm to 2cm) fine to coarse tuffs and lapilli-tuffs. Faulted against these are a 12m succession of graded, bedded and massive reworked pyroclastic sands with vertical to 30° bedding. An

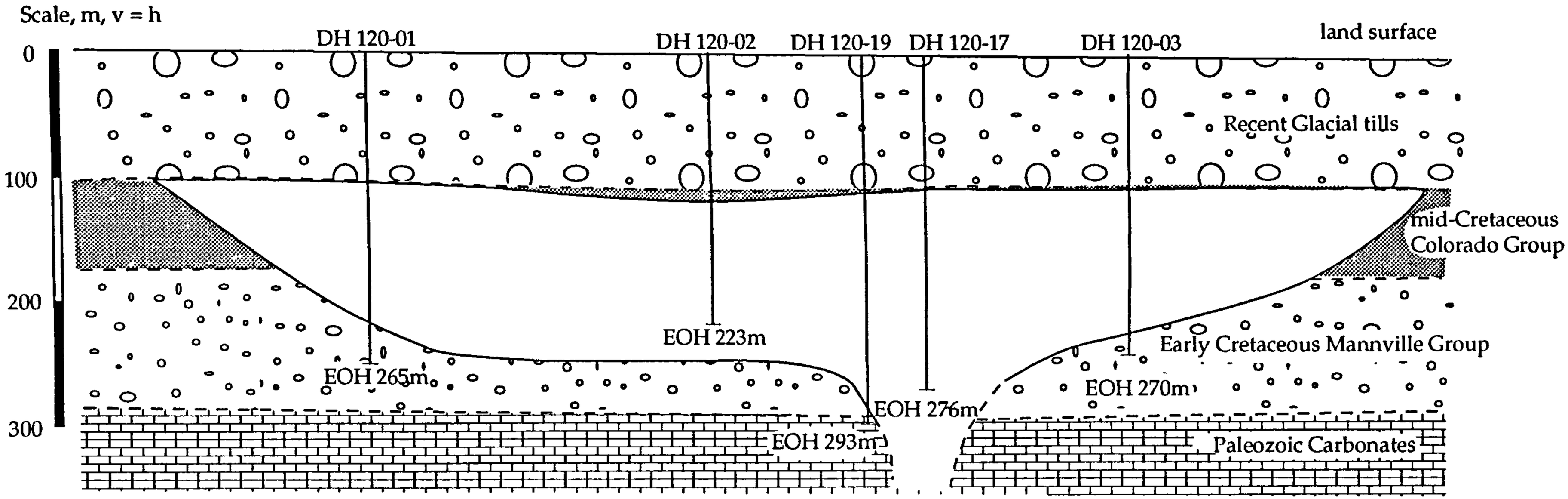

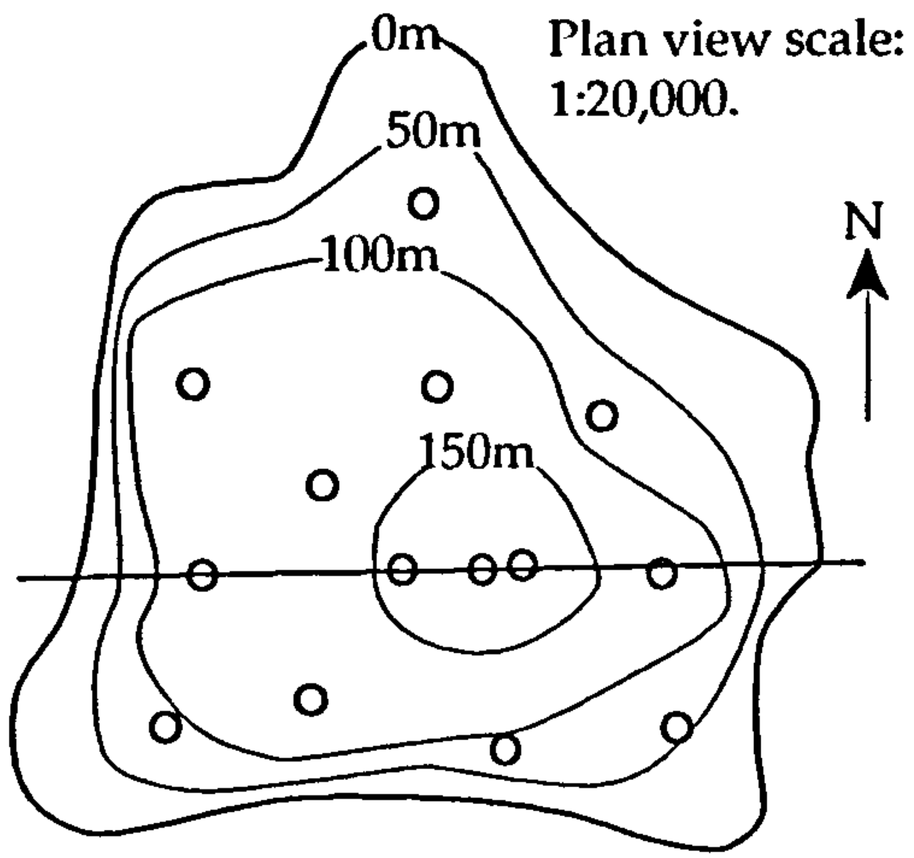

Complete section of Anomaly 120 as inferred from borehole intersection (EOH = end of hole). Boundaries of the crater are defined by magnetic anomaly edges. Plan view shows other boreholes in Anomaly 120, and from their depths to base of crater, approximate contours have been drawn. These illustrate the steep sides, especially to the south and west, and the shallow sides to the north, east and south-west. The deepest-going zones, illustrated by the 150m contour, probably contain the diatreme, which must be relatively small.

Figure 3.3.1

intraclast breccia of shale boulders (upto 30cm) with a tuffaceous matrix occurs in the mid-section, and shale intraclasts are common throughout the reworked succession. Brown, partially carbonised, but well preserved branch and pine-needle fragments, up to 5cm long, are also common, especially in areas rich in intraclastic shale fragments. This first phase is sharply overlain by 2.5m of fluidal-lapilli dominated, graded tuffs and lapilli-tuffs with a slumped and distorted base. Grading from these tephra-fall units are 2.5m of reworked graded and bedded pyroclastic sands with increasing amounts of sand and shale intraclasts, which in turn grade into a 3.5m thick sequence of interbedded intraclast breccias and quartz-rich tuffaceous sands. The final tuffaceous deposits consisted of 3m of bioturbated sandy-calcareous muds, with a serpentinous matrix and common lithic intraclasts. These are overlain by mudstones of the Upper Westgate Formation.

The OFS 93-012 crater fill displays a number of important features:

- located at the edge of a crater
- inclined crater walls
- reworked deposits, including crater wall material (intraclast breccias)
- generally horizontal bedding
- thin primary tephra-fall deposits of crystal-lapilli-lithic tuff, in two eruptive phases: the 1st is crystal dominated, and the 2nd lapilli dominated, overlain by:
- sandy tuffs at the tops of reworked sequences, directly associated with intraclast breccias and abundant plant fragments
- crater lake deposits

Comparisons of the stratigraphy above and below the crater with the surrounding stratigraphy allows the amount of material excavated to be estimated. This is measured to be about 25 to 30m, the same thickness as the total crater-fill intersected.

The Smeaton borehole, intersected a much greater thickness of kimberlite deposits, Kjarsgaard et al (1995), the crater base contact is sharp and apparently conformable (although no details are specified). The basal unit is 40m thick and consists of seven fining-up graded sub-units of lapilli dominated lapilli-tuffs 3m to 10m thick (and one fine tuff sub-unit). Bedding is horizontal and crystals, lithics, and shale intraclasts are present but not common. The basal unit is overlain by 38m of crystal dominated lapilli-tuffs and coarse tuffs in six subunits 1m to 14m thick. Lapilli are restricted to the basal lags of the lower four subunits, and are scattered throughout the upper two. Shale intraclasts are absent. The primary sequence is overlain by 26m of graded and bedded

reworked pyroclastic sands and a 2.5m intraclastic shale breccia near the base. Sedimentary features of the reworked kimberlite include: absence of fluidal lapilli, wave ripples and cross-stratification, concentration of heavy minerals in graded subunit lags, rounded shale clasts, bioturbation and bivalve imprints.

The Smeaton borehole crater fill displays the following features:

- located near the centre of a crater
- very thick primary deposits in fining-up sequences, with beds up to 14m thick
- two eruptive phases. 1st lapilli dominated. 2nd crystal dominated
- horizontal and conformable crater base
- reworked pyroclastics as crater fill, including intraclastic shales
- marine mixing of sediment and kimberlite pyroclasts

Kimberlite craters described by Scott-Smith et al (1995) conform to the crystal-dominated/lapilli dominated tuffs and lapilli tuffs described by Kjarsgaard et al (1995), although individual graded beds are described as being up to 90m thick (but mostly 12m to 15m). However Scott-Smith et al (1995) do not accept the presence of *any* reworked material within the craters, although they are not averse to the possibility of crater lake deposits. The reason that reworked material is not described may be due to an actual distribution of resedimented material in craters, i.e. the OFS 93-012 reworked strata may be unusual, perhaps occurring in only one or two of the smaller craters. Alternatively Scott-Smith et al (1995) may not have recognised reworked strata as such, based on the criteria presented in Chapter 2, i.e. statistical variation of grain roundness, sedimentary structures and heavy mineral concentration.

Apart from the possibility of resedimented strata, the main features of the FALC crater facies, as described by Scott-Smith et al (1995) include:

- generally located in central crater regions
- thick primary tephra-fall deposits
- both lapilli-dominated and crystal dominated tuffs and lapilli-tuffs, the former being the most common
- multiple eruptions based upon the presence of composite lapilli and autoliths
- fluidal, pelletal and autolithic lapilli present; fluidal types are often flattened and spattered with rare vesicular textures and welding features
- volcanic bombs, with drapes
- rare occurrence of graded megabeds upto 90m thick.

The contrasting descriptions of crater fill presented above may be due to different locations in the craters. For example OFS 93-012 borehole is near the

crater edge, as evidenced by inclined crater wall and large amount of resedimented material from the crater edge. The Smeaton borehole is likely to be on the crater flat, and the majority of FALC boreholes (drilled in the deepest-going roots to maximise kimberlite recovery) are likely be nearest to the vent, perhaps explaining the lack of interbedded reworked material and the prevalence of lapilli-dominated tephra-fall. It is interesting to note that out of at least 110 boreholes located in the deeper parts of craters, *no vent or diatreme has been intersected at FALC*. This indicates feeder pipes are very small, a maximum of 200m diameter in Anomaly 120, see Figure 3.3.1.

All of the features described above are combined and used to develop a genetic model for the crater forming processes operative at FALC in the next section.

3.4 A genetic volcanic model for FALC craters - a new eruptive style?

Despite efforts to prove otherwise (Smith and Lorenz, 1989), many craters found at the Ellendale, Mbuji-Mayi and FALC localities do not fit well the morphology and features attributed to maars, deep kimberlite diatremes, tuff rings or tuff cones. Thus a new eruptive process is required to describe the formation of these distinct craters, which are here termed **"pateran craters"** (from *patera*, Latin for 'flattened bowl or saucer': this term and morphology has been previously described for certain volcanoes, e.g. Alba Patera, on Mars (Carr, 1976)), and their fill from inception through to post-eruptive modification. At FALC they are defined as a flat or undulose- bottomed crater containing pyroclastic and usually epiclastic material, whose ratio of aspect in cross-section exceeds 5:1. All of the workers at FALC and Ellendale (Scott-Smith et al, 1995; Kjarsgaard et al, 1995; Nixon and Leahy, 1995; Smith and Lorenz, 1989) have described parts of the model, but have as yet failed to synthesise this into a unique, coherent model for pateran crater formation and fill. It is likely that pateran craters form a third end-member of alkali-ultramafic volcanic types, along with Clement and Reid (1989) deep kimberlite diatremes and phreatomagmatic maars (Lorenz, 1985).

A model for the formation of pateran craters is described below using FALC as an example. The suitability of its application to the Ellendale and Mbuji-Mayi deposits is also discussed.

3.4.1 Stage 1, upwelling magma

This stage is similar to the incipient stages of phreatomagmatism. Magma rises along relatively narrow channels by fault-propagation or exploitation of pre-existing joints/cracks in the upper crust (Stage 1 in Figure 3.4.1). Complex root zones do not develop, probably because the overlying Phanerozoic sediments are easily penetrated, compared to the lavas and gneisses present at deep kimberlite diatreme locations (e.g. Kimberley group of kimberlites, South Africa). At FALC the magma rose to very shallow crustal depths before explosive eruption, a minimum of 100m and a maximum of 300m as determined by the highest and lowest aquifers in the Mannville Formation relative to a Cretaceous surface (taken at the top of the St Walburg Sand, circa 100Ma, see Chapter 1). It is interesting to note the top of the St Walburg Sand shows evidence of emergence in the FALC area, which itself appears to be domed from Mannville times to the end of the Cenomanian, circa 93Ma (see Chapters 1 and 2).

3.4.2 Stage 2, initial phreatomagmatic eruption

This stage is critically different to other proposed models. The magma interacts with groundwater in an explosive fashion at a high crustal level (probably as shallow as 120m depth). The resultant explosion is extremely powerful and contains both steam and magmatic material. The explosion front propagates laterally, as well as upwards, and because of the low mechanical strength, cohesiveness and density of the partially lithified sediments, travels horizontally up to 500m through the sediment pile until the energy is dissipated. The explosion shock front pulverises the sediments (perhaps to component grains in coarser sand sediments) and removes them into the ash cloud, thus forming the flat bottomed pateran crater (Stage 2 of Figure 3.4.1). Some of this material (especially coarser boulders, pebbles and granules) fall out of the ash-cloud and form lithic-rich basal strata. Slightly inclined eruptions, and/or lateral heterogeneities in sediment mechanical strength, causes the explosion front to propagate more in one direction than another, leading to vents being off-centre in plan view.

At FALC there are three potential aquifers (medium, well sorted fluvial sands), occurring at depths of about 120m, 170m and 200m respectively relative to the top St Walburg Sand Cretaceous surface. Also minor channel sands occur sporadically throughout the Mannville Group, and these may also have been water saturated. The overlying sediments brecciated and removed during this stage are the Spinney Hill, Joli Fou, Flotten Lake Sand and lower

Figure 3.4.1

Pateran crater development during the mid-Cretaceous at Fort a la Corne.

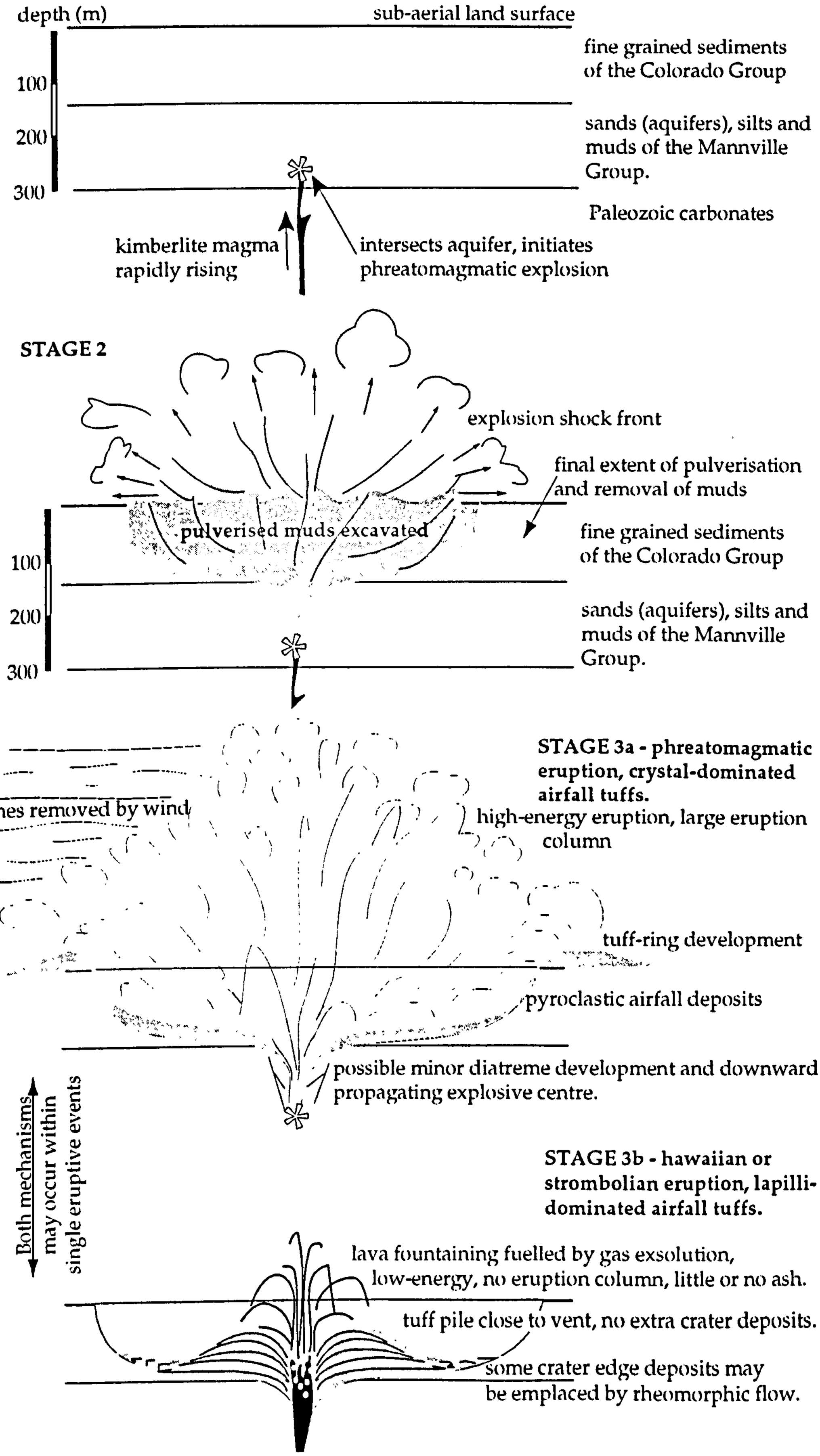

Westgate Formations. These are muds and fines silts, with about 25% interbedded fine to medium muddy sandstones (see Chapter 1). Typical crater width is about 800m, and depths are usually 100m to 150m, amounting to a volume of around 6.5 x 10^7 m^3. This equates to 130 million tonnes (Mt) of sediment removed, assuming a partially lithified sediment density of 2.0gcm^{-3}. This rises to a maximum of 340Mt in the case of the largest crater at FALC, Anomaly 120, and the smallest diameter craters (400m) probably have a minimum of about 10Mt of sediment excavated.

The whereabouts of the majority of the removed sediment at FALC cannot be explained by the lithic-rich basal deposits (which are at most, a few metres thick). A shale bomb (4.5cm in diameter) was found in tuffaceous sediments of the distal deposits in OFS 93-010 (see Chapter 2), 500m from the nearest crater edge. This suggests coarser crater-excavation ejecta may be scattered for kilometres around, impacting on the sub-aerial and sub-aqueous surfaces of marginal marine basin sediments. It is notable that no other tephra-fall material occurs with the shale bomb, suggesting that most crater-excavation ejecta was very finely brecciated and removed by wind to parts of the basin where it was held in the water column in suspension, before slowly settling, virtually unrecognisable from normal mud sediment.

At Ellendale and Mbuji-Mayi the removed sediment consisted of the Grant Group and Lualaba sandstones respectively. These comprise the crater-excavation ejecta in the same way as described above, but more of the ejecta initially fell back into the crater than at FALC. This is probably due to the coarser constituent grainsize, and results in sand-dominated tuffs being deposited at the base of the craters, with increasing amounts of magmatic material incorporated into later tephra-fall deposits. This particular process was initially described for Ellendale craters by Smith and Lorenz (1989). Scott-Smith would also ascribe this origin for the tuffaceous sands in OFS 93-012 (pers. comm.) However, these occur at the top of a crater fill sequence, rather than at the base, and as such cannot be of this origin. They are interpreted as reworked pyroclastic sediment mixed with large amounts of terrigenous sediment.

3.4.3 Stage 3, main extrusive event

The eruption continues along one of two paths, described below, or may switch intermittently between the two. Mixed deposits are also quite common, and are probably due to simultaneous elements of both the processes in the same eruption (i.e. phreatomagmatic eruption with lava droplets in the ejecta).

type A: phreatomagmatic eruption

If the groundwater that initiated the crater excavating explosion is from a large aquifer, with high recharge rates, the continuing kimberlite eruption may be phreatomagmatic as well as explosive-degassing driven. This would result in a continuation of powerful eruptions, with large amounts of juvenile kimberlite material ejected into a large pyroclastic cloud over the crater. Finer material may be widely dispersed into extra-crater deposits, and form a tuff-pile over the crater edges, see Stage 3a in Figure 3.4.1. Coarser material, such as large crystals and lithics fall within the crater walls, and continuous eruption may deposit very thick graded beds of crystal-dominated coarse tuffs and lapilli-tuffs. Lapilli are relatively rare, and usually of the pelletal variety, rather than fluidal. Fine ash-grade grains are not recognised in the crater fill (although they may be obscured by later alteration), although fine tuffs of tephra-fall origin are observed up to 300m from the crater walls, e.g. OFS 93-004 (see Chapter 2). Scott-Smith et al (1995) recognise the highly explosive origin of the crystal-dominated lapilli-tuffs at FALC. Similar tephra-fall lapilli-tuffs are also found in many of the Ellendale and Mbuji-Mayi craters.

At FALC lithics, particularly from Devonian dolomites and Mannville Group, are fairly common throughout the crystal-dominated crater fill, and indicate some degree of vent deepening and possible development of small diatremes beneath the flat crater floor, comparable to those at Ellendale (Smith and Lorenz, 1989). Whilst the possibility of down-slumped bedded pyroclastics into minor diatremes is accepted, the largest possible diatreme at FALC (in Anomaly 120) has a maximum of width 200m, Figure 3.3.1. Because diatreme facies kimberlite or deep root zones have not been intersected in over 110 boreholes into FALC kimberlites they are probably much smaller than this.

The temperature of the magma upon extrusion is indicated by the reflectance of coaly fragments from the Mannville Group, which show no sign of thermal alteration from the heat of intrusion (Kjarsgaard et al 1995).

type B: hawaiian-strombolian eruption

If available groundwater is exhausted in the initial eruption then the kimberlite magma may reach the near surface without violent explosions. Relatively minor eruptions due to the explosive dissolution of volatiles in the magma create a spray of partially to fully fluidal lapilli (essentially lava droplets) fountaining from the vent (Stage 3b in Figure 3.4.1). This activity deposits the lapilli-dominated tephra-fall coarse and lapilli-tuffs. Some of these tuffs consist of virtually 100% ameoboid fluidal lapilli spattered on to each other and represent

the closest lithology to a kimberlite lava yet described (see OFS 93-012 description, Chapter 2, and Plate 2.5, Figure 2.1.4). More commonly lapilli-tuffs often contain up to about 30% subordinate macrocrystals (mostly olivine and ilmenite) and more rarely, lithics. Both Kjarsgaard at al (1995) and Scott-Smith et al (1995) describe the fluidal lapilli deposits and also recognise vesicles within lapilli, accretionary and composite lapilli, and rare welding features between lapilli.

The semi-fluidal nature of the erupted pyroclasts, and the relatively low-energy of the eruptions suggest little or no ash cloud development, and no ash-grade particles are observed (although they may have been obscured by later alteration). The lapilli-dominated lapilli-tuffs deposited in this manner are normally graded and bedded (units between 20cm and 10m thick), and have been suggested as products of hawaiian-strombolian type volcanism by Scott-Smith et al (1995), with which this author concurs. Such low-energy lava spatter activity would mainly deposit material adjacent to the vent, and these deposits may undergo rheomorphic flow when piled above the maximum angle of stability. Thus crater fill deposits near the crater edge may be either thin tephra-fall and/or emplaced by rheomorphic lateral flow of lava spatter, e.g. OFS 93-012 is drilled at a crater edge (demonstrated by the borehole position relative to the magnetic anomaly, and further supported by the inclined base and thin deposits) and contains two thin beds of lapilli-dominated coarse tuffs, the base of the lower bed is highly distorted by slump or flow structures (see Figure 2.1.3 in Chapter 2). An important feature of this type of eruption is that very little material is likely to be projected beyond the crater walls.

In this model fluidal lapilli are used as main evidence for the hawaiian-strombolian activity, however, work by analogue modellers Stuttgart University (Zimanowski et al, 1991; Zimanowski et al 1995)) have clearly demonstrated the formation of fluidal lapilli (from olivine melilitite and carbonatite melts) by purely phreatomagmatic processes. Furthermore, the proposed hawaiian-strombolian eruptive activity which produced the fluidal lapilli is driven by exsolution of gasses (Chapter 3). If this were the case, large amounts of vesicularisation should be expected in the lapilli, as well as a large amount of kimberlitic scoria, due to incomplete exsolution of the gasses. Neither of these features have been recorded by this author. The equivalent lithologies in Ellendale are lamproite lavas, which are often highly vesiculated and show rare flow banding and brecciation. The lower volatile content of the Ellendale lamproites must account for the effusive rather than mildly explosive eruption of the kimberlite magma implied at FALC.

These two distinct volcanic styles taken in isolation can rarely account for a real kimberlitic intersection observed at FALC. It seems that crater fills are composed of multiple events, that may be separated in time (especially if reworked pyroclastics are present between the primary strata, discussed below), but more usually seem to be penecontemporaneous. The switching of styles within an eruptive event implies intermittent groundwater supplies, possibly due to the (as yet hypothetical) small diatreme propagating downwards (as in Lorenz 1985) and intersecting further pockets of water (for short lived crystal-dominated pulses), or large aquifers (for longer lived pulses).

Whichever eruptive style dominates the primary crater fill, it should be clear that the pateran crater need not necessarily have been filled. Typical FALC pateran craters have volumes of about 0.065km^3, easily accommodating the total volume of erupted material in similar basaltic strombolian eruptions, which range from 0.02km^3 to 0.06km^3 (Cas and Wright, 1988). Further discussion of the crater fill must also consider the role that subsequent resedimenting processes may play.

3.4.4 Stage 4, post-eruptive modification

The degree and type of post-eruptive modification is likely to be highly variable, and strongly dependent on the external environment as well as the volcanic morphology. Dry, continental pateran crater locations (such as Ellendale and Mbuji-Mayi) may not experience any aqueous resedimentation within the crater. FALC, however, is located on a low-lying (possibly even littoral) coastal plain, and the role of water is far more significant; ultimately all the FALC deposits are swamped by marine transgression.

Upon termination of volcanic activity (which has been demonstrated as sub-aerial; Scott-Smith et al, 1995), a range of crater morphologies are possible, depending on the size and type of the eruption. Most commonly the crater is underfilled and, depending on the amount of explosive phreatomagmatism, with or without a tuff-ring. More rarely the crater is filled, producing a low-lying tuff 'hill', a landform similar to tuff-cones, Figure 3.4.2.

Figure 3.4.2

Pateran crater, underfilled after mainly phreatomagmatic eruptions (with tuff ring). Thick tuffaceous crater lake deposits and extra-crater deposits are likely.

Pateran crater overfilled (tuff hill) after both phreato-magmatic and hawaiian-strombolian eruptions. No crater lake, but extra-crater deposits are likely.

Pateran crater underfilled after hawaiian-strombolian eruption (no tuff ring). Thin tuffaceous crater lake deposits are likely, but no extra-crater material (unless the crater is substantially eroded).

Relationship of landform produced by pateran crater eruption to type of post-eruptive deposit.

The majority of pateran craters are likely to be underfilled, and this allows for the filling of the crater by water, forming crater lakes. The source of the water is probably groundwater seepage through the initially porous pile of kimberlite pyroclasts. The seepage rapidly promotes the alteration of the kimberlite, and probably leads to a fairly toxic lake, rich in biohazardous metals in solution (e.g. Co, Ni, Zn, Pb and V). Water bodies outside the crater may include lakes, swamps and lagoons on a subaerial coastal plain. The fluctuating sea-level allows for a range of scenarios, from fully sub-aerial to littoral and coastal-marine, and possibly even sporadic marine contact during storms. Because of the short-lived nature of volcanic landforms in geological time compared to rates of sea-level change, probably only one or two such scenarios exist in the lifetime of the edifice. Probably the first erosional processes (which may also occur during eruption) involve mass wasting processes, including slumps, slides and particle creep. Depending on the amount of admixed fluid, these produce a range of deposits from debris flows (no fluid) to turbidites (fluid density flows), see schematic diagram of erosional types, Figure 3.4.3.

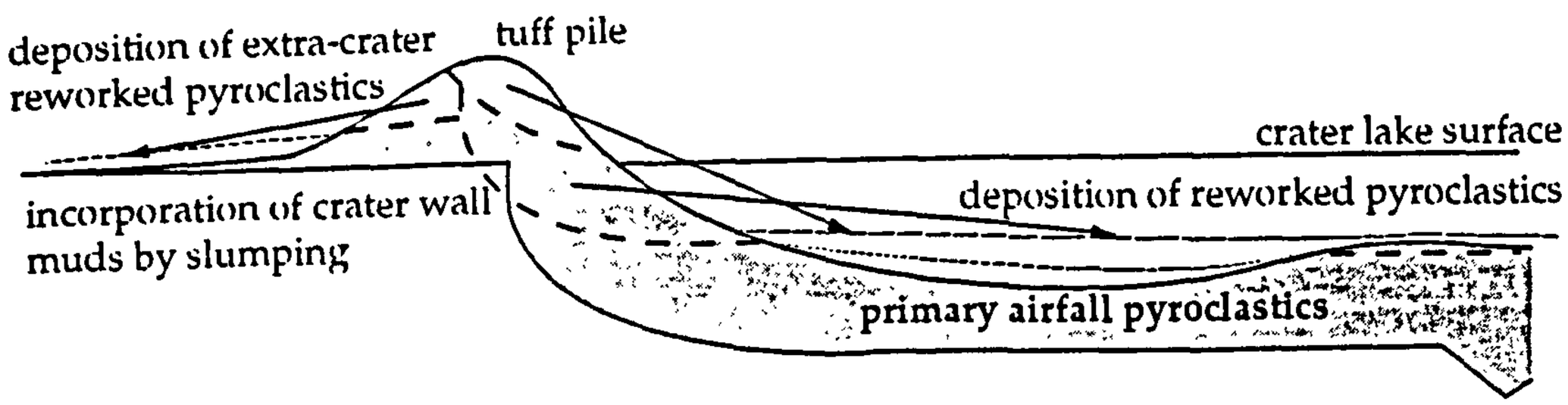

Main erosional sites on a typical FALC kimberlite immediately after eruption, diameter 200m to 1300m, height of tuff pile probably tens of meters high, possibly up to 200m in larger craters.

The amounts of interstitial pore fluid are not likely to be great within the tuff ring, and slumps and creeps of mostly volcaniclastic material are likely to deposit massive pyroclastic sands. If the sole fault of large slump on the tuff ring intersects the mudstone country rock then this wall rock is brecciated and become entrained in the tuffaceous debris flow, producing the commonly observed intraclast shale breccias. Water admixture is likely, however, if the mass-flow encounters the crater lake or surrounding water bodies. If low density flows are generated outside the crater, the very low angles of the basin depo-surface restricts the distance travelled by the turbidity flow. The density flows of volcaniclastic material will be deposited as graded beds, often with crystal and heavy mineral rich bases. These may be distinguished from tephra-fall deposits by a total absence of fluidal lapilli, small-scale cross-stratification, erosional bases, thin bedforms (none observed >1.5m) and high proportion of grain roundness (as determined from point counting).

Introduction of volcaniclastic material into shallow bodies of water, such as crater lakes or surrounding sea or lakes, or encroachment of these water bodies over previous sub-aerial deposits, allows wave reworking and transport to occur. The shallow water sorts and winnows the volcaniclastic material, often further aided by tidal currents (if marine) and episodic storm activity. A crater lake in the average sized FALC pateran crater would be around 800m in diameter, easily large enough for waves to be generated with enough energy to disturb sediment. Thus thinly bedded and laminated pyroclastic sands form, typically very well sorted, clast supported and displaying a large degrees of grain rounding and heavy mineral concentration (e.g. the greatest ilmenite concentrations in OFS heavy mineral samples were found in thinly bedded pyroclastic sands, 2.2% by weight, compared to 0.4% in the underlying airfall tuffs, see Chapter 2).

Wave action within the crater lake and surrounding water bodies would rapidly degrade the tuff pile. Wave-cut notches serve to remove material to be deposited in shallow waters, and to over-steepen slopes leading to further slumping and density-flow formation. Even large tuff piles, if exposed to a combination of crater lake and surrounding marine (or even lake) wave erosion, could be planed-off in a matter of months, and certainly years, as was the fate of the volcanic island of Surtsey after the cessation of eruption (Cas and Wright, 1988). Tuff rings are eventually breached by the crater lake or surrounding water, and the rate of erosion increases. In this fashion the crater lakes may be filled, and a halo of extra-crater pyroclastic sands formed, mostly with bedded

and graded pyroclastic sands and silts, as has been observed in the OFS boreholes (see Chapter 2).

Other factors that may influence the redeposition style of pyroclastics include proximity to the sea or lakes, climate and vegetation. A wet climate may add to slope instability and particle creep. The destructive action of extra-crater water bodies, especially the sea, has been described above, but may be buffered by the development of vegetation, especially as coastal swamps. The tuff pile may be further strengthened by the binding properties of plants, especially trees and deep-rooted grasses, making the edifice less likely to collapse by slumping. No direct evidence of *in situ* vegetation has been found in crater and proximal facies at FALC, however, and the likely toxicity of kimberlite does not make it a good soil (the FALC kimberlites also have relatively low levels of phosphorous and potassium). Furthermore, palynological evidence from the Smeaton core (Kjarsgaard et al, 1995) suggests an arid climate. This in itself may be destructive, desiccating the tuff pile and removing material by wind action.

Regardless of the initial morphology of the kimberlites, and the actual resedimentation processes in operation, all the kimberlite ultimately suffered the same fate: swamping by marine transgression and burial under thick marine deposits. Wave activity alone considerably reworks the tuff pile and crater deposits, and reworked pyroclastics must therefore be expected in the majority of FALC cases.

References cited in Chapter 3

- Carr, M.H. (1976). The volcanoes of Mars. Scientific American, Vol.234, No.1, p.32-43.
- Cas, R.A.F. and Wright, J.V. (1988). Volcanic Successions, Modern and Ancient. Chapman and Hall (pubs.), pp.528.
- Clement, C.R. and Ried, A.M. (1989). The origin of kimberlite pipes: an interpretation based on a synthesis of geological features displayed by Southern African occurences. Proceedings of the 4th International Kimberlite Conference (Australia 1986), Kimberlites and related rocks, (Blackwell, pubs.), Vol 1, Geol. Soc. Australia Special Publication No.14, p.632-646.
- Daniels L.R.M., Jennings, C.M.H., Lee, J.E., Blaine, J.L., Billington, F.R. and Cumming, B. (1994). The geology of crater volcanics and sediments associated with the M1 kimberlite, southwestern Botswana. Proceedings of the 5th International Kimberlite Conference (Brazil 1991), Vol.1, p.129-139.
- Demaiffe, D., Fieremans, M. and Fieremans, C. (1991). The Kimberlites of Central Africa: a review. In Kampunzu, A.B. and Lubala, R.T (eds.) Magmatism in Extensional Structural Settings, Springer-Verlag, p.537-559.
- Francis, E.H. (1970). Bedding in Scottish (Fifeshire) tuffpipes and its relevance to maars and calderas. Bulletin of Volcanology, Vol.34, p.697-712.
- Hawthorne, J.B. (1975). Model of a kimberlite pipe. Physics and Chemistry of the Earth, Vol.9, p.1-15.
- Hearne, B.C. (1968). Diatremes with kimberlitic affinities in north-central Montana. Science, Vol.159, p.622-625.
- Kjarsgaard, B.A., Leckie, D.A., McIntyre, D.J., McNeil, D.H., Haggart, J.M., Stasiuk, L. and Bloch, J. (1995). Smeaton Kimberlite Drill Core, Fort a la Corne Field, Saskatchewan. Geological Survey of Canada Open File 3170, pp.57.
- Lehnert-Thiel, K., Loewer, R., Orr, R.G. and Robertshaw, P. (1992). Diamond-bearing kimberlites in Saskatchewan, Canada: The Fort a la Corne Case History. Exploration Mining Geology Vol.1 No.4 p.391-403.
- Leonardos, O.H, Carvalho, J.B., Gibson, S.A. and Thompson, R.N. (1995). The diamond potential of the late Cretaceous Alto Paranaiba Igneous Province, Brazil. Proceedings of the 6th International Kimberlite Conference. Russia 1995, Extended Abstracts.
- Leys, C.L. (1982). Volcanic and sedimentary processes in phreatomagmatic volcanoes. University of Leeds PhD thesis.
- Lorenz, V. (1975). Formation of phreatomagmatic maar-diatreme volcanoes and its relevance to kimberlite diatremes. Physics and Chemistry of the Earth, Vol.9, p.17-27.
- Lorenz, V. (1984). Explosive volcanism of the West Eifel volcanic field, Germany. In Komprobst, J. (Ed.), Kimberlites I: Kimberlites and Related Rocks, p.288-297 Elsiever

- Lorenz, V. (1985). Maars and diatremes of phreatomagmatic origin. Transactions of the Geological Society of South Africa, Vol.88, p.459-470.
- Mitchell, R.H. (1986). Kimberlites: mineralogy, geochemistry and petrology. Plenum Press, New York, pp.442.
- Nixon, P.H., Gummer, P.K., Halabura, S., Leahy, K. and Finlay, S. (1993). Kimberlites of volcanic facies in the Sturgeon Lake area. Russian Geology and Geophysics, Vol.34, No.12, p.66-76.
- Nixon, P.H. and Leahy, K. (1995). Diamond-bearing volcaniclastic kimberlites in Cretaceous marine sediments, Saskatchewan, Canada. Proceedings of the 6th International Kimberlite Conference, Russia 1995 (submitted).
- Scott-Smith, B.H., Orr, R.G., Robertshaw, P. and Avery, R.W. (1995). Geology of the Fort a la Corne Kimberlites. Proceedings of the 6th International Kimberlite Conference, Russia 1995, Extended Abstracts Volume.
- Singh, S.K. and Sabina, F.J. (1978). Magnetic anomaly due to a vertical right circular cylinder with arbitrary polarization. Geophysics, Vol.43, p.173-178.
- Smith, C.B. and Lorenz, V. (1989). Volcanology of the Ellendale lamproite pipes, Western Australia. Proceedings of the 4th International Kimberlite Conference (Australia 1986), Kimberlites and related rocks, (Blackwell, pubs.), Vol 1, Geol. Soc. Australia Special Publication No.14, p.505-520.
- White, S.H., deBoorder, H. and Smith, C.B. (1995). Structural controls of kimberlite and lamproite emplacement. In Griffin, W.L. (ed.) Diamond Exploration: Into the 21st Century, Journal of Geochemical Exploration Special Volume, Vol. 53, Nos. 1-3, p.245-264.
- Zimanowski, B., Fröhlich, G. and Lorenz, V. (1991). Quantitative experiments on phreatomagmatic explosions. Journal of Volcanology and Geothermal Research, Vol. 48, p.341-358.
- Zimanowski, B., Fröhlich, G. and Lorenz, V. (1995). Experiments of steam explosion by interaction of water with silicate melts. Nuclear Design and Engineering, Vol. 155, p.335-343.

CHAPTER 4 - EFFECT OF KIMBERLITE ERUPTIONS IN THE SEDIMENTARY ENVIRONMENT

Abstract

Stratigraphic analysis of 9 borehole cores located both inside and outside Fort a la Corne kimberlite craters has placed a constraint of Flotten Lake Sand (circa 102Ma) to Upper Westgate Formation (circa 99Ma) on the age of kimberlite volcanic activity. This correlates well with a recently published date of 99±1Ma for a central FALC crater.

Several boreholes have been drilled outside of the kimberlite pateran craters (mostly as part of the OFS programme), and six have intersected extra-crater kimberlite. Extra-crater kimberlite is thus far unique to the FALC area, and consists of both primary airfall pyroclastics and, more frequently, reworked pyroclastic sediments (see Chapter 2). Other boreholes, often located close to the edge of the craters, intersect no kimberlitic material, but do contain anomalous stratigraphy as a direct result of the kimberlite craters (usually seen as a shallowing effect). Detailed paleogeographic reconstructions of eruptive and post-eruptive environments are made here for two characteristic areas (Foxford and the eastern edge of the FALC cluster): extra-crater deposits present; extra-crater deposits absent, respectively.

Thus two systems are recognised: 'open crater' where kimberlitic material is slumped and transported into nearby sedimentary environments, often to be redeposited within numerous subsequent sedimentary cycles; and 'closed crater' where craters are immediately sealed by crater lake sediment, followed by deposition of 'normal' sedimentary basin strata.

Open crater systems are most likely to develop when large tuff piles are constructed by phreatomagmatic eruptions (see Chapter 3), aided by long-term sub-aerial exposure (sea-level lowstand) in the post-eruptive environment. Closed crater systems may be the result of underfilled craters acting as a depo-centre for tuff piles, preferentially to the basin outside. Hawaiian-strombolian eruptions, which produce little extra-crater deposition, may also be responsible for closed craters, along with post-eruptive marine transgression and high basinal sedimentary rates.

4.1 Influence on regional stratigraphy and facies of terrestrial sediments by the eruption of the Fort a la Corne kimberlite cluster.

The regional stratigraphy of the Cretaceous rocks in the FALC area is outlined in Chapter 1, and Chapter 2 demonstrates the stratigraphic constraint of the Westgate Formation during which kimberlites were active. This Formation is the oldest of the Colorado Group (84 to approximately 102Ma), and was

deposited between approximately 98 and 102Ma (using dating from Obradovich, 1991, see Figure 1.3.2). All the kimberlites observed thus far are immediately overlain by the Westgate Formation. This correlates well with a recent zircon U/Pb radiometric date of 99±1Ma for kimberlite in FALC Anomaly 120, (Kjarsgaard et al, 1995), but not with 'Rb/Sr dating of phlogopites and microfossils in the surrounding strata' reported in Lehnert-Thiel et al (1991) which places a date of 94 to 96Ma on kimberlite activity. This discrepancy may be due to unreliable dating techniques used by Lehnert-Thiel et al (1991): the type and methodology of microfossil dating is not stated, and phlogopite in the FALC kimberlites does not appear fresh (usually a brassy tarnished lustre).

Kimberlite activity and resedimentation in the Westgate Formation is, therefore, confirmed in all quarters of the FALC cluster (see Figure 1.1.3 for locations): Anomaly 120 (Kjarsgaard, et al 1995) in the central main cluster, OFS93-009 and 010 on the eastern edge of the main cluster, UK169/8 (Kjarsgaard, et al 1995) northern edge of the main cluster, FALC 163-01 (Kensington press release) on the western edge of the main cluster, OFS93-002 to 004 at the Snowden outlier and OFS93-012 at the Foxford/Shipman outlier. Earlier kimberlites in the Mannville Group (105Ma to 120Ma) are commonly recorded in the FALC area (Scott-Smith et al, 1995; Kjarsgaard et al, 1995). These are typically thin (1m to 5m), carbonate rich, and show signs of reworking. Scott-Smith et al (1995) regard these as small volcanic precursors that failed to develop craters. Stacking of these small pyroclastic piles may be responsible for the apparent top-Mannville bulge, discussed in Chapter 1.

The nature of the Westgate Formation is complex, and the strata are a result of mixing of two main sedimentary sources: western derived distal fine grained strata, and northerly derived shallow-marine coarse strata (the St.Walburg Sand member of the Westgate Formation). In the FALC area the Formation is between 20m and 30m thick (inclusive of 5m to 10m of the St.Walburg Sand member), bounded below by the Flotten Lake Sand (another northerly derived shallow marine coarse deposit), and above by the poorly defined Fish Scales Formation, a typical non-kimberlitic intersection (from OFS93-011) is shown in Figure 4.1.1.

The indistinct nature of the upper boundary (and occasionally the lower) has led to considerable confusion in determining the actual stratigraphic site of the Formation containing the kimberlites, and may help to explain (along with inaccurate dating) the continuing misplacement of kimberlite activity into the overlying Belle Fourche by Scott-Smith et al (1995).

Figure 4.1.1

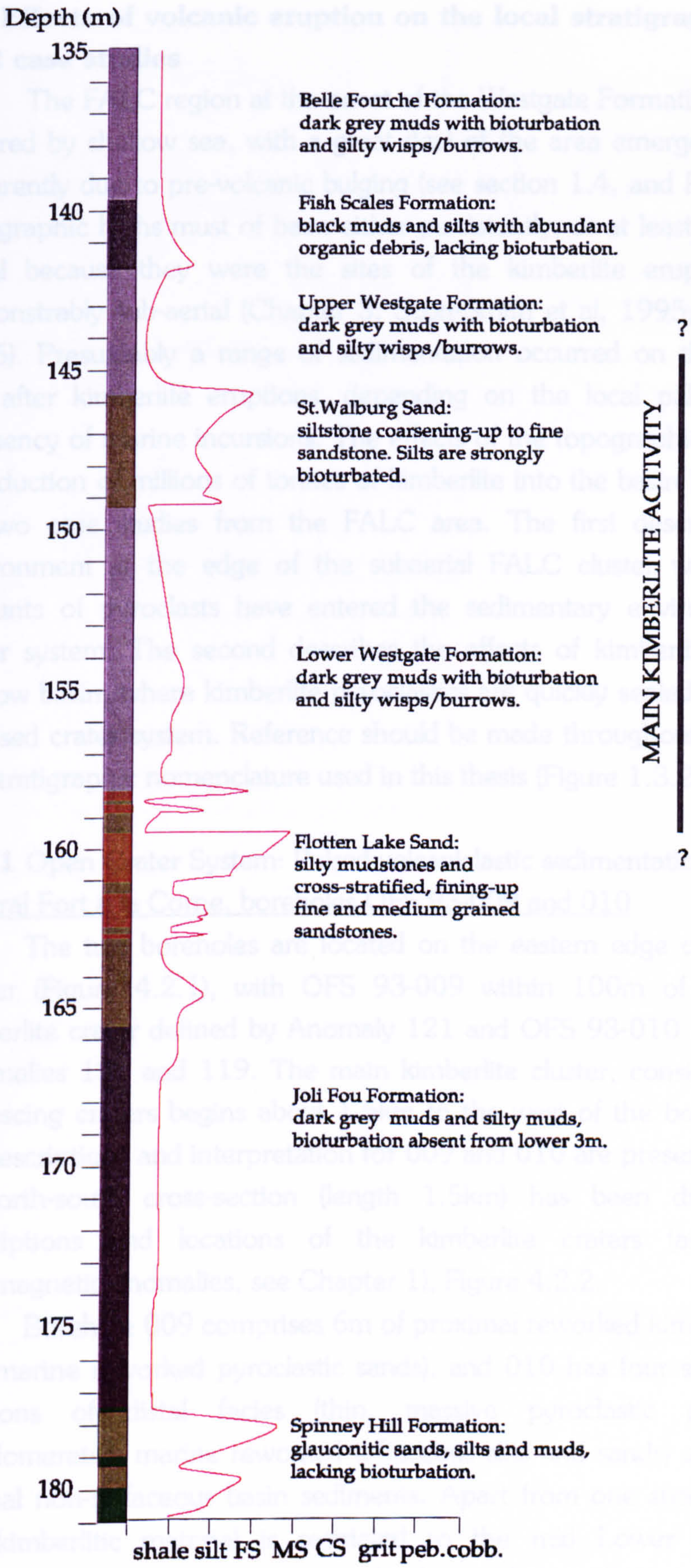

Borehole log of OFS 93-011, drilled at the northern edge of the main FALC cluster (see Figure 1.1.3). No kimberlite was intersected, and the log shown represents 'normal' strata depositied in the area during kimberlite activity (as indicated).

4.2 Effects of volcanic eruption on the local stratigraphy - illustrated by 2 case studies

The FALC region at the onset of the Westgate Formation deposition was covered by shallow sea, with a great deal of the area emergent in local areas, apparently due to pre-volcanic bulging (see section 1.4, and Figure 1.4.6). The topographic highs must of been either persistently, or at least sporadically, sub-aerial because they were the sites of the kimberlite eruptions, which are demonstrably sub-aerial (Chapter 3; Scott-Smith et al, 1995; Kjarsgaard et al, 1995). Presumably a range of sedimentation occurred on these highs before and after kimberlite eruptions, depending on the local paleogeography and frequency of marine incursions. The effects of the topographic doming, and the introduction of millions of tonnes of kimberlite into the basin is illustrated below by two case studies from the FALC area. The first describes a nearshore environment at the edge of the subaerial FALC cluster where considerable amounts of pyroclasts have entered the sedimentary environment: an open crater system. The second describes the effects of kimberlite volcanism in a shallow basin, where kimberlite pyroclastics are quickly sealed within the crater: a closed crater system. Reference should be made throughout these sections to the stratigraphic nomenclature used in this thesis (Figure 1.3.2).

4.2.1 Open Crater System: Pulsed volcaniclastic sedimentation

Central Fort a la Corne, boreholes OFS 93-009 and 010

The two boreholes are located on the eastern edge of the main FALC cluster (Figure 4.2.1), with OFS 93-009 within 100m of the edge of the kimberlite crater defined by Anomaly 121 and OFS 93-010 about 500m from Anomalies 121 and 119. The main kimberlite cluster, consisting of large and coalescing craters begins about 1.5km to the west of the boreholes. Borehole log descriptions and interpretation for 009 and 010 are presented in Chapter 2. A north-south cross-section (length 1.5km) has been drawn from these descriptions and locations of the kimberlite craters (as determined by aeromagnetic anomalies, see Chapter 1), Figure 4.2.2.

Borehole 009 comprises 6m of proximal reworked kimberlite (debris flow and marine reworked pyroclastic sands), and 010 has four separate kimberlite horizons of distal facies (thin, massive pyroclastic sands; tuffaceous conglomerates; marine reworked tuffaceous silts and sands) separated by near-normal non-tuffaceous basin sediments. Apart from one stratum in 010 all of the kimberlitic material is restricted to the mid Lower Westgate to top St.Walburg Sand horizons (circa 101Ma to 102Ma), Figure 4.2.2, placing an

Figure 4.2.1

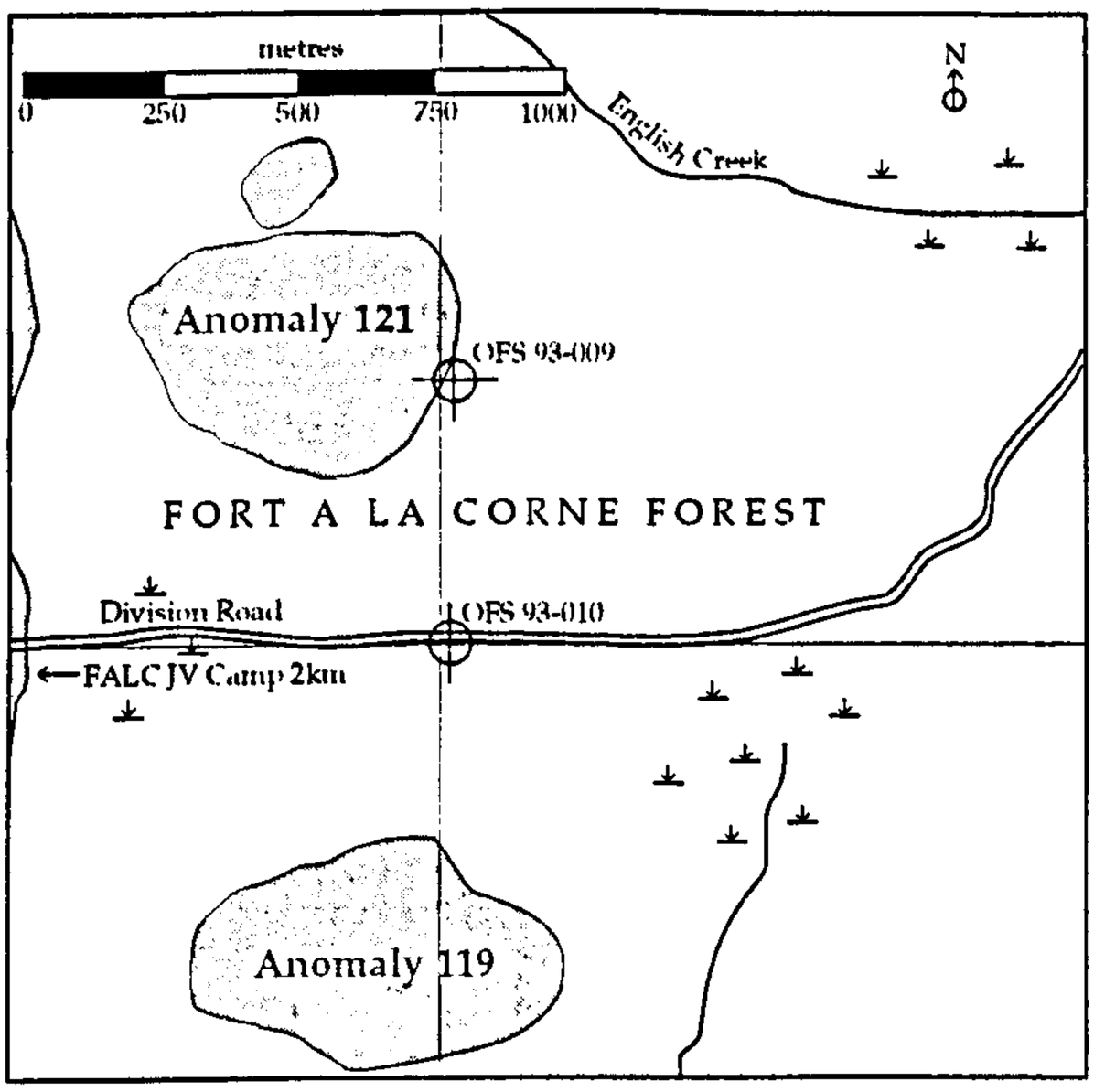

Detailed sketch locality map of the eastern edge of the FALC main cluster, showing locations of of OFS 93-009 and 010. The main cluster to the west consists of largely coalecsing craters, see Fig. 2.1.1. Note the embayment into the edge of the cluster, where 010 is located. Both Anomaly 119 and 121 have been confirmed as kimberlite crater deposits by drilling.
For geographical position, refer features on this map to those on the larger scale map of the boreholes described, see Fig. 2.1.1.

Figure 4.2.2

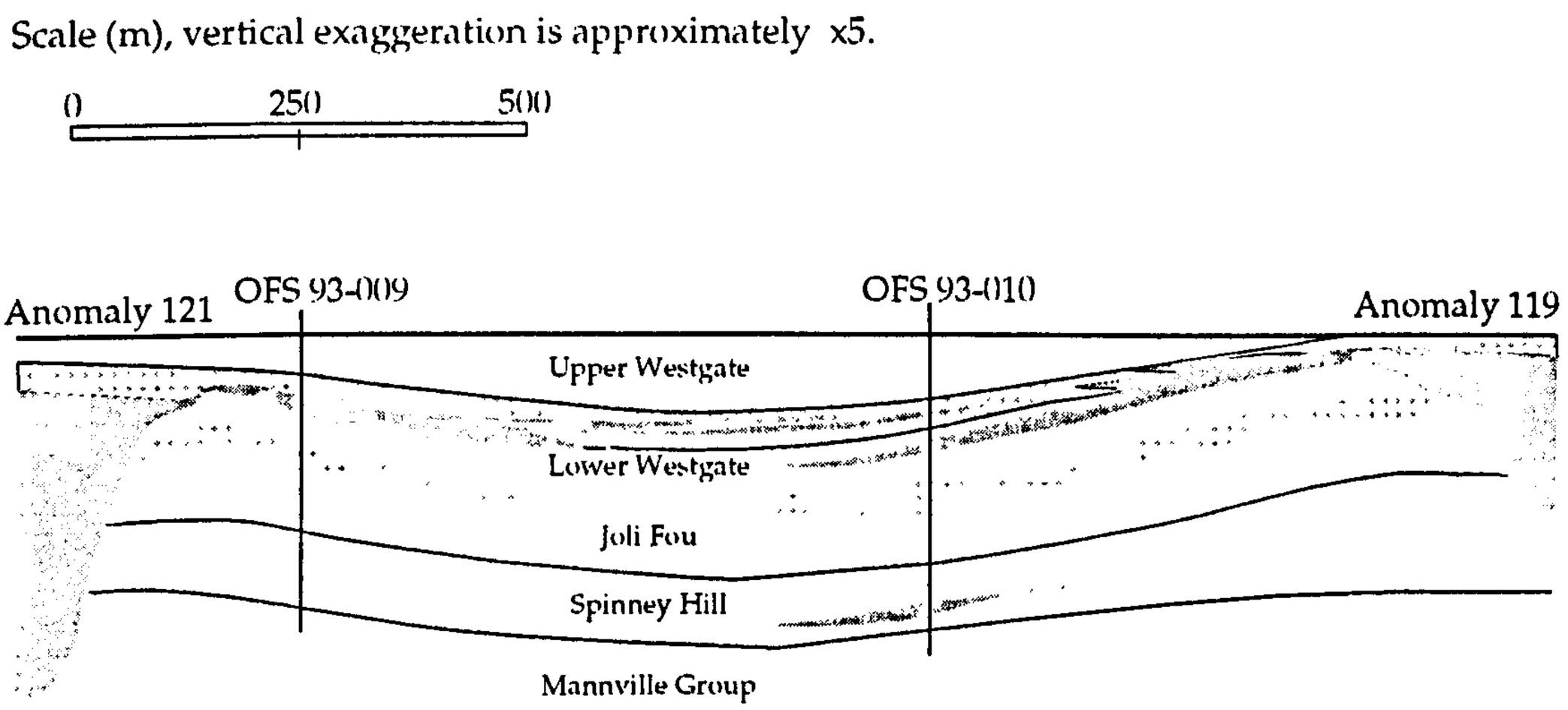

Stratigraphic cross-section interpreted from two boreholes and locations of kimberlite craters from aeromagnetic anomalies. Shaded strata represent kimberlitic material both within the craters and interstratified within the sediments. Dot ornament indicates Sand members of the formations shown (upper is the St.Walburg Sand, lower is the Flotten Lake Sand). The base of the Fish Scales Fm. is used as a horizontal datum in this section.

upper time constraint on the local kimberlite activity. The much older kimberlite stratum in 010 is 1.1m thick, clay, carbonate and lithic rich, with loosely packed kimberlitic crystals (olivine, garnet and ilmenite). It occurs in the lower Spinney Hill Formation (circa 104Ma), and may represent high-density sub-aqueous flow of kimberlite material from the Mannville kimberlites underlying in the main kimberlite cluster 1.5km to the west (discussed in Chapter 1). The nature of the bounding sediment is not unusual, and the kimberlite flow was probably restricted to one or two discrete, short-lived events.

A detailed paleogeographic evolution for the main kimberlite events is reconstructed from the stratigraphy and facies analysis using grain size and type and presence of indicative features such as rootlets and bioturbation (Mieras et al, 1993), fish and plant debris, cross-stratification and so on.

Lower Westgate Formation

Kimberlite activity in the area begins with the eruption of Anomaly 119 during the mid to late stages of Lower Westgate deposition (circa 101Ma), see Stage 1, Figure 4.2.3. The pateran crater formation of Anomaly 119 is sub-aerial, probably amongst coastal swamp environments. Slumping of tuff piles resulted in multiple debris flows to ash turbidites, two of which are observed in 010. Post-eruptive erosional processes are discussed in Chapter 3. To the north conditions were variable between fully marine (but shallow, <5m) and largely sub-aerial coastal swamps (indicated by the presence of carbonaceous muds with rootlets and brown, bioturbated silts). Offshore deposits are likely to be found to the north and east of the area, away from active kimberlite volcanism. Conditions about 1.5km north of the crater (009), immediately after eruption, were probably in the shallow marine state, although did return to coastal swamps before Anomaly 121 eruption.

Early St.Walburg Sand

At the beginning of the St.Walburg Sand depositional milieu much of the area was a sub-aerial coastal swamp (indicated by organic-rich muds and silts with abundant rootlets and bioturbation), see Stage 2, Figure 4.2.3. Anomaly 121 was sub-aerially erupted into this environment, and again erosion resulted in slumping into the partially aqueous environment (producing the deposits intersected in 009). Between the two craters was an embayment in the coastal swamps where intertidal flats where debris flow kimberlite is wave-reworked (indicated by hummocky cross-stratified and laminated tuffaceous silts). If this intertidal zone is fairly wide (as might be expected with the flat topography

Figure 4.2.3

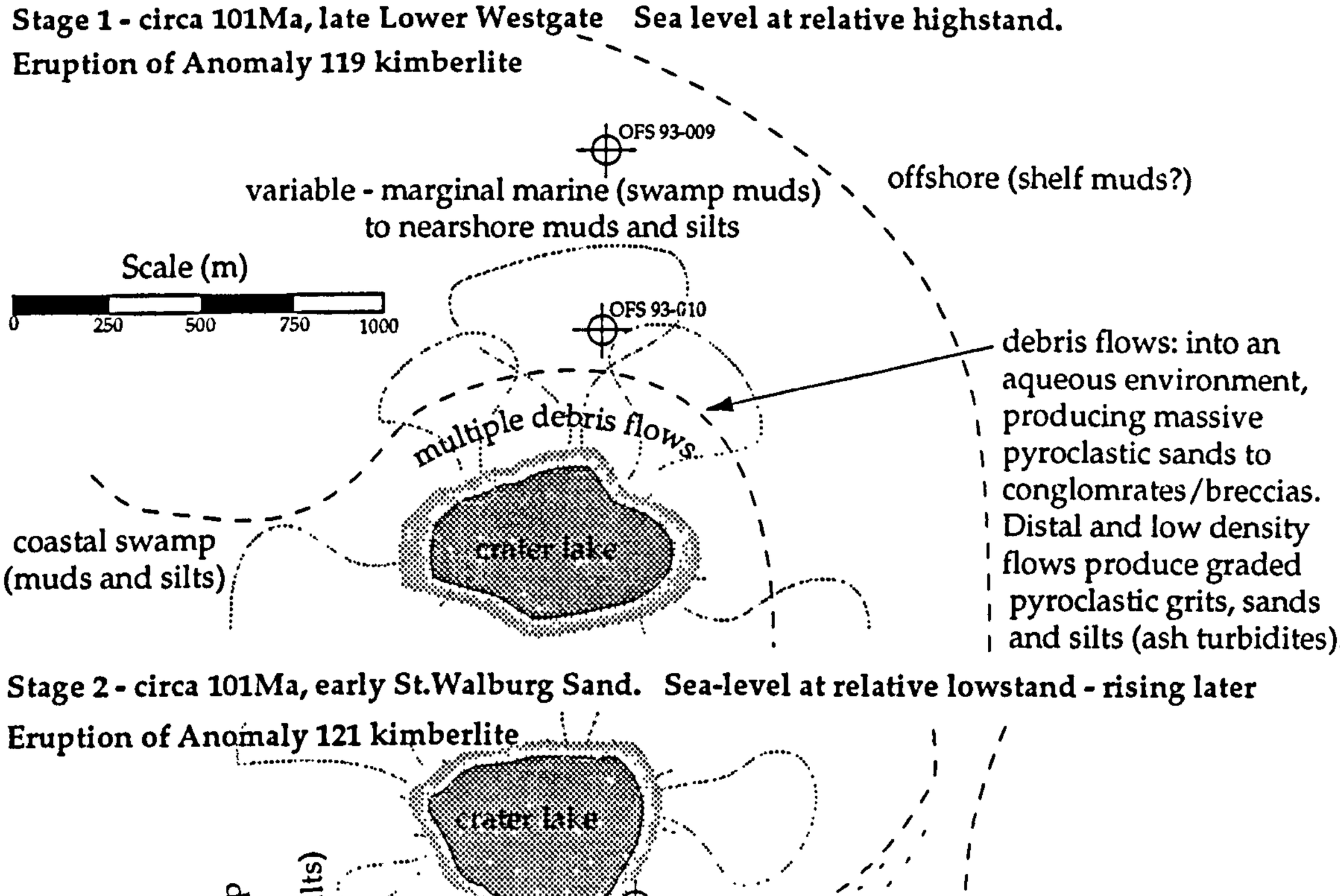

Paleogeographic reconstructions of the eastern edge of the FALC cluster (see location map Fig. 4.2.2) during the Westgate Formation (Lower Colorado) deposition(Late Albian).

implied by extensive swamps) then size and density sorting by wave and tidal oscillation may be an important process. This suggests heavy mineral upgrading could occur in these sediments, and this is confirmed in the stratum of this facies intersected in 010, where considerable garnet and ilmenite concentrations are found. To the east (basinward), nearshore grading to offshore conditions are expected, probably with typical early St.Walburg sandy muds and silts with some kimberlitic indicators. Anomaly 119 was probably sealed because coastal erosion over this time scale (about 10^5years to 10^6years) will of plane off any topographic highs. Some kimberlitic sediment from Anomaly 119 may still be near the surface, however, and local erosion may allow contribution of this material into the intertidal kimberlitic deposits described above, or to more basinward strata.

Latest St.Walburg Sand

By the end of the depositional milieu of the St.Walburg sand both of the kimberlite craters described above have been sealed and overlain by marginal marine deposits (coastal swamp and intertidal/nearshore muds and silts), see Stage 3, Figure 4.2.3. Kimberlitic material would, however, be near the surface, and prone to erosion (perhaps during storm events) and resedimentation. Fully marine conditions (but still shallow, <10m) occur in the east and possibly south of the area, and the typical coarse-grained deposits of the late St.Walburg are intersected (as in 010). These consist of bar sands and nearshore muds and silts. The coarse material is mostly derived from local reworking, and consequently is sporadically kimberlitic. It is interesting to note that the largest diamond found during the OFS program (2.5mm, see Chapters 2 and 5) was located in these sands. Shallow-water marginal marine, and rarer emergent swamp, conditions continued into the Upper Westgate Formation in the area (which is usually deeper offshore shelf facies). Overlying strata has been removed by recent glacial erosion, but the shallowing effects of kimberlite eruption is further discussed in the case study below.

In summary two sub-aerial kimberlite eruptions occurred on the eastern edge of the FALC cluster, which probably comprised low-lying swampy and marginal marine islands at the time. Debris flows and other lower density flows (ash turbidites) are the most common reworked pyroclastic deposits, which may again be reworked in intertidal zones in an embayment between the two craters. Later nearshore bar sands of latest St.Walburg Sand age further reworked and incorporated the volcaniclastic material. Anomalously shallow water and sub-

aerial deposition of basin sediments continued into the Upper Westgate Formation.

4.2.2 Closed Crater System: Local shallowing effects

Foxford, borehole OFS 93-012, 013 and 014, FC-94-16 and 17

Five boreholes were drilled within 10km of each other around the small town of Foxford, 25km north of the main FALC kimberlite cluster (see detailed location map, Figure 4.2.4).

Figure 4.2.4

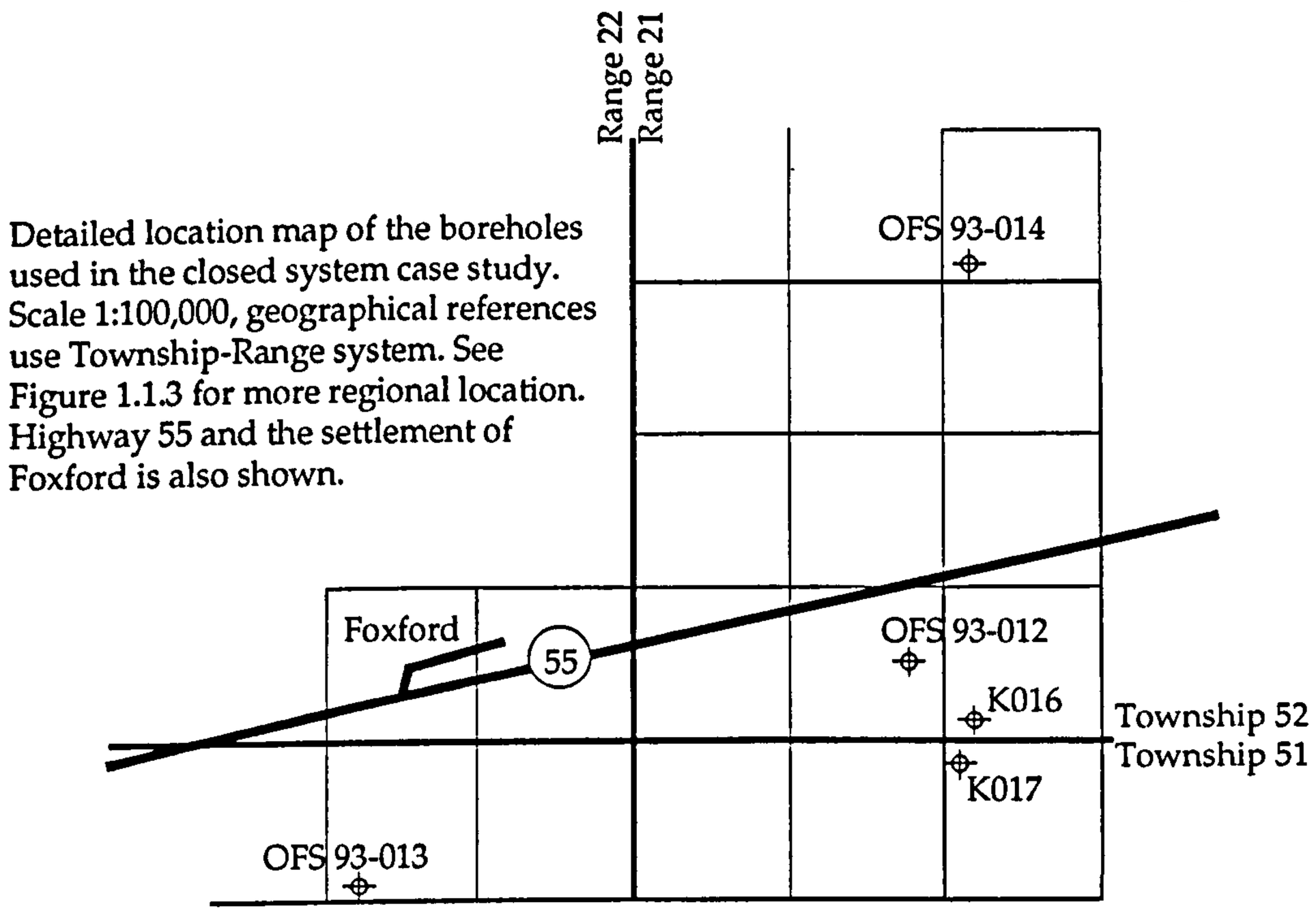

Detailed location map of the boreholes used in the closed system case study. Scale 1:100,000, geographical references use Township-Range system. See Figure 1.1.3 for more regional location. Highway 55 and the settlement of Foxford is also shown.

They were positioned to intersect small and irregular magnetic anomalies interpreted as kimberlite bodies (see regional anomaly distribution, Figure 3.2.1), and OFS 93-012 encountered a 30m section of crater facies kimberlites (see Chapter 2). The four other boreholes intersected no kimberlite or tuffaceous sediment, but the two closest to 012 (K16 and K17) have an anomalous sedimentary succession from Flotten Lake Sand strata to the base of the Fish Scales Formation. From detailed borehole description it can be determined that the strata adjacent to the kimberlite body are fine, nearshore deposits during regional coarse shelf bar sand deposition (Flotten Lake and St.Walburg), and coarse bar sand deposits during regional shelf muds and silt deposition (Lower Westgate). These reversed depositional conditions may

continue immediately to the east, where other kimberlites of unknown age and stratigraphic association occur (see magnetic anomaly map, Figure 3.2.1). Full detailed logs of the boreholes used are provided in Appendix I and II, written from observations by B.C. Jellicoe (Kensington Resources Ltd) and this author (for boreholes 012, K16 and K17 only).

Stratigraphic cross-sections through 012 on a large scale (10km, Figure 4.2.5) and a smaller scale (5.5km, Figure 4.2.6) indicate the disposition of the anomalous coarse-grained strata. The Formation chosen as a horizontal datum is the Fish Scales, which is the most appropriate as it defines the top of the Westgate Formation that is under examination.

The larger scale section (Fig. 4.2.5) illustrates the kimberlite crater at 012 relative to the 'normal' stratigraphy intersected in boreholes 013 and 014.

Figure 4.2.5

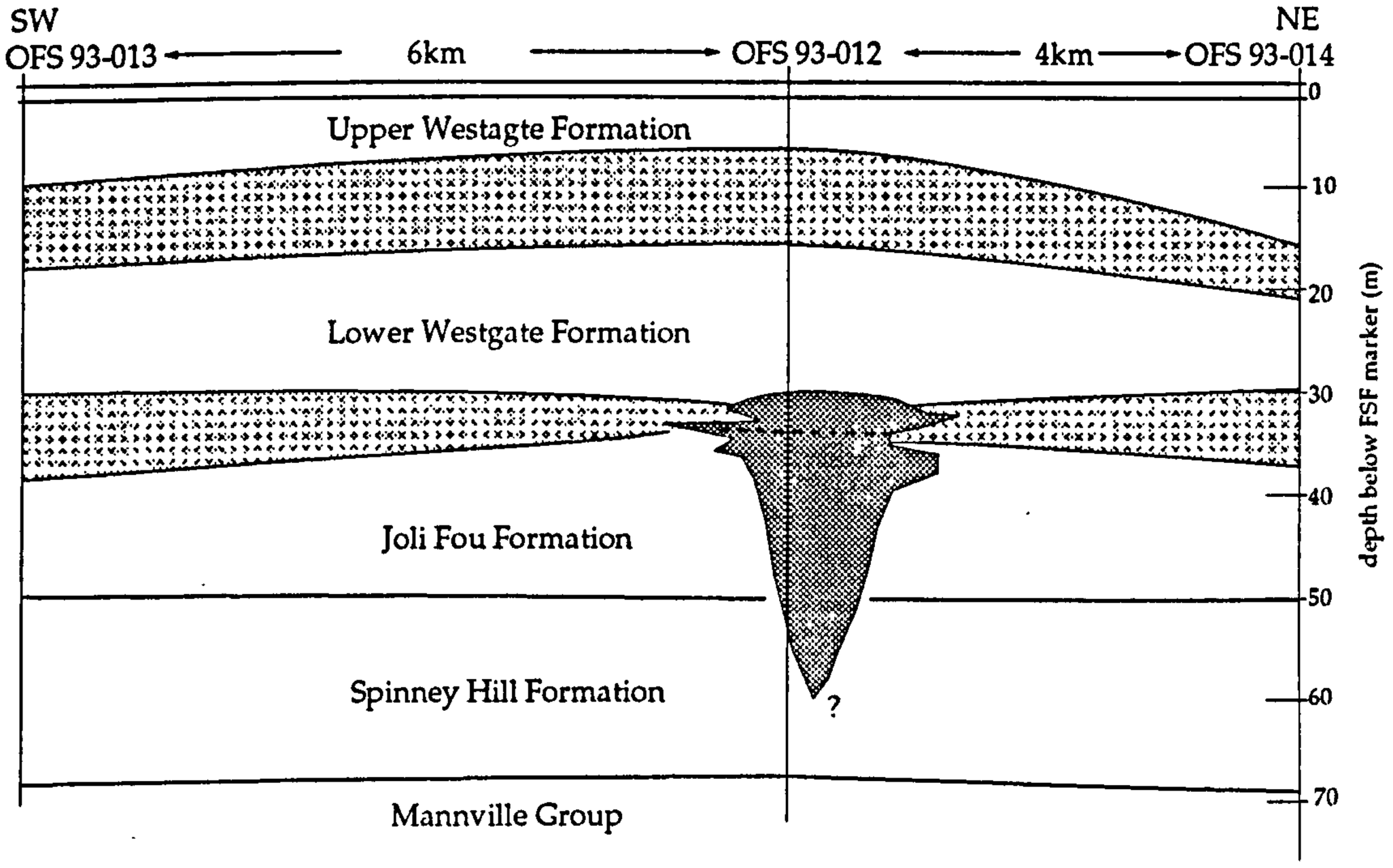

Large scale cross-section of the stratigraphy in the Foxford area. Uppermost horizontal stratum is the Fish Scale Formation, dot ornamented strata are sandstones: upper - St.Walburg Sand; lower - Flotten Lake Sand. Central shaded body is the kimberlite crater intersected in 012.

The sequence includes shallow shelf (<10m deep) bar sand deposits of the Flotten Lake Sand, overlain by deeper shelf (10 to 30m deep) muds and silts of the Lower Westgate. These are in turn overlain by further bar sand deposits of the St.Walburg Sand and deeper shelf muds and silts of the Upper Westgate.

Eruption occurred over the boundary of the Flotten Lake Sand and Lower Westgate (Lowest Colorado Group) deposition, at about 102Ma (see Chapter 1). The amount of excavation of the crater can be measured by the removal of the Flotten Lake Sand, Joli Fou and some of the Spinney Hill strata, totalling about 26m of sediment. Apparent dip of the strata to the north is contrary to current dip directions, and is either an artefact of using the Fish Scales Fm. as a horizontal datum, or reflects the original paleogeographic surface.

The smaller scale cross-section demonstrates the nature of the anomalous intersections of the kimberlite proximal boreholes, K16 and K17, Figure 4.2.6. These successions are discussed in detail below, and compared to the 'normal' regional stratigraphy present in 013 and 014 intersections.

Figure 4.2.6

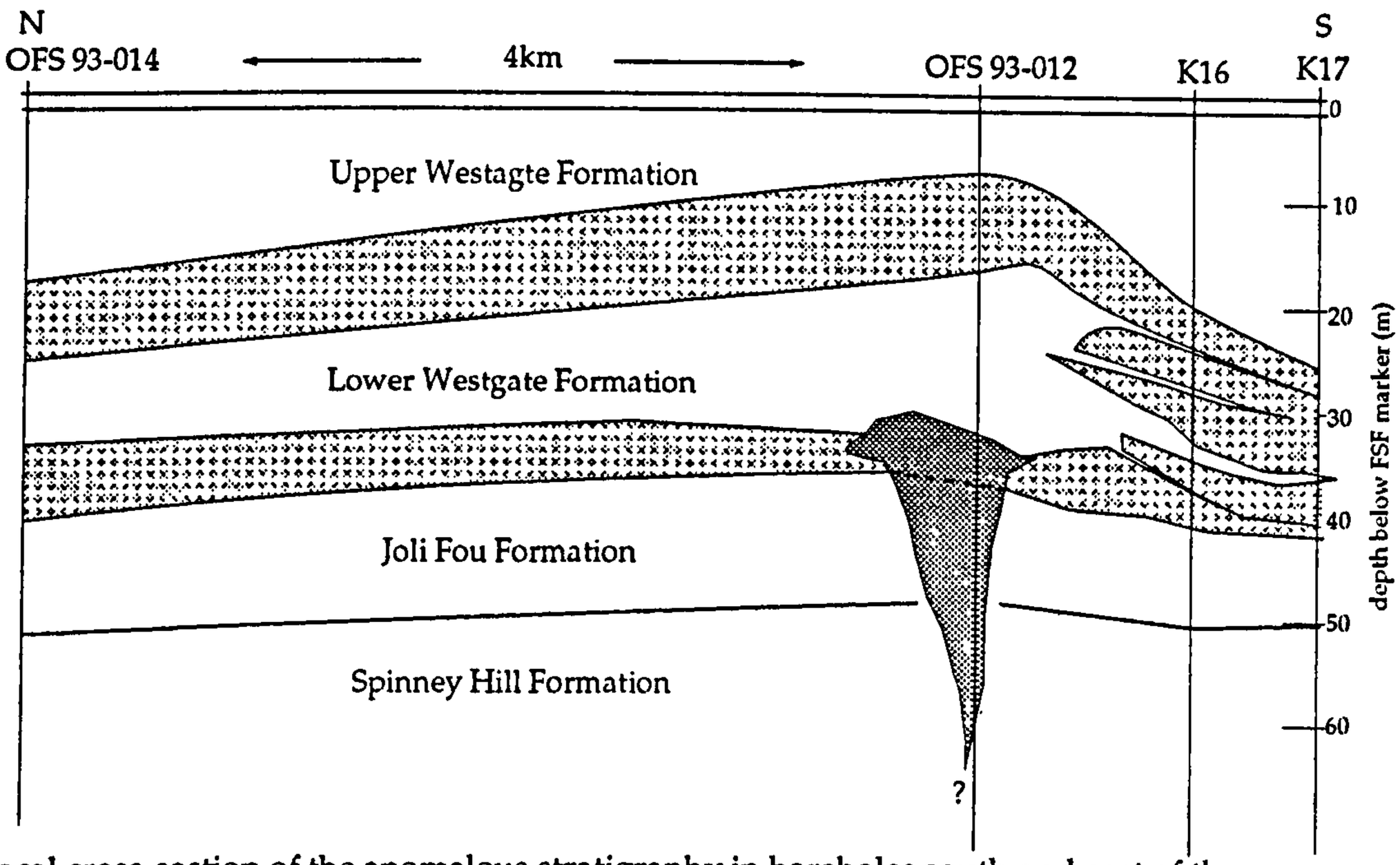

Local cross-section of the anomalous stratigraphy in boreholes south and east of the kimberlite crater (Foxford area). Uppermost horizontal stratum is the Fish Scales Formation, dot ornamented strata are sandstones: upper - St.Walburg Sand; lower - Flotten Lake Sand. Shaded body is the kimberlite crater intersected in 012.

Flotten Lake Sand

In the kimberlite-proximal boreholes the Flotten Lake Sand (strata immediately overlying the distinctive shales of the Joli Fou Formation) consists of 3.8m of four coarsening-up silts to ripple bedded medium sandstones, with a 5cm limestone comprising shell fragments. Abundant bioturbation occurs in the

silty layers, including *planolites*, *terebellina*, *skolithos* and *chondrites*, a combination which is indicative of nearshore to intertidal environment (Mieras et al, 1993). These strata are time-equivalent to the kimberlite activity 1km to the north, and although similar in character to the regional Flotten Lake Sand (although generally finer and much thinner, compare to 8m thick in 013), the nearshore-intertidal trace-fossil population is different to the offshore population described by Simpson (1982). During the Flotten Lake Sand period, the crater may have been breached and filled by the sea, and swept by shoaled sand. This is represented in 012 by intraclast-rich tuffaceous quartz sand. Paleogeographic reconstruction at the time of uppermost Flotten Lake Sand deposition, a time of sea-level lowstand, can be made for the area covered by the boreholes described, see Stage 1, Figure 4.2.7.

Lower Westgate Formation - the base of the Colorado Group

The thin Flotten Lake Sand is sharply overlain by a 1m thick section of thinly bedded (20 to 30cm) graded muds and silts, a similar lithology to 'normal' Lower Westgate strata. These may represent a blanket of the western-derived sediment over the topographic high during transgression at the base of the Colorado Group.

The mud to silt strata are then overlain by 4m of graded silts to medium sands, in total there are 7 sub-units, ranging from 20 to 125cm. Typically they are finely laminated with shaley wisps, with cross-stratification and flaser bedding common, but absent up-section. Bioturbation is also ubiquitous, mostly *planolites*, *chondrites* and *terebellina*, but with *chondrites* disappearing from the midsection upwards. They are interpreted as borderline nearshore-offshore deposits. This minor deepening is the only concession in the near crater deposits to the regional sea-level rise associated with the Lower Westgate, during which time the depth of water (probably around 30m or more, Simpson 1982) generally precludes extensive bar sand deposition. The 'normal' stratigraphy of the Lower Westgate in the region comprise shaley mudstones, with fine sands present only as isolated wisps and as burrow fill. The kimberlite-proximal strata described above are much coarser than normal Lower Westgate deposits and contain shallow water trace fossils and flaser bedding, interpreted as a nearshore but sub-tidal facies. They represent, therefore, periods of shallow water deposition (1 to 10m) during Lower Westgate times (normally deeper shelf, >30m). The flooded paleogeography for this highstand period is illustrated in Stage 2, Figure 4.2.7.

Figure 4.2.7

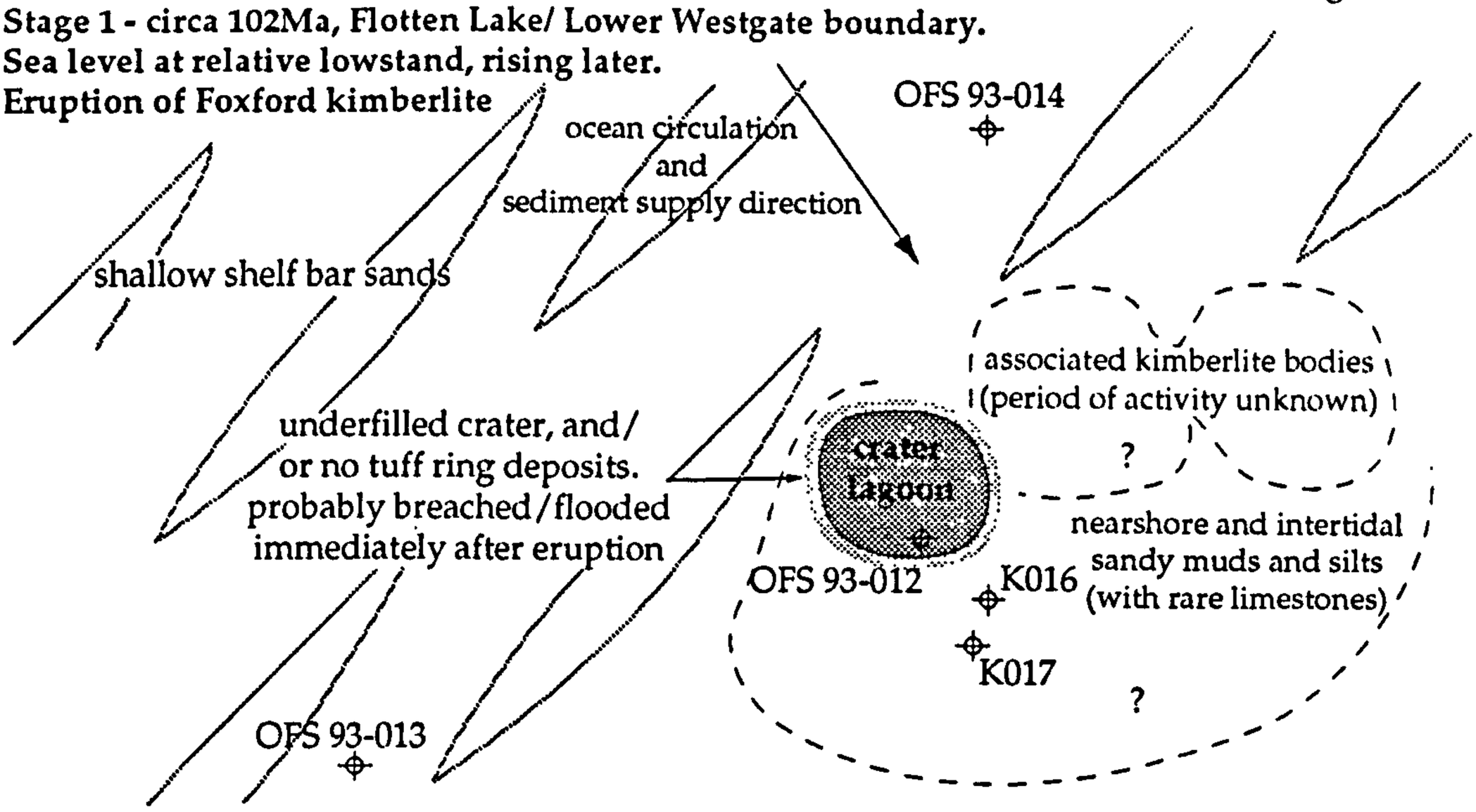

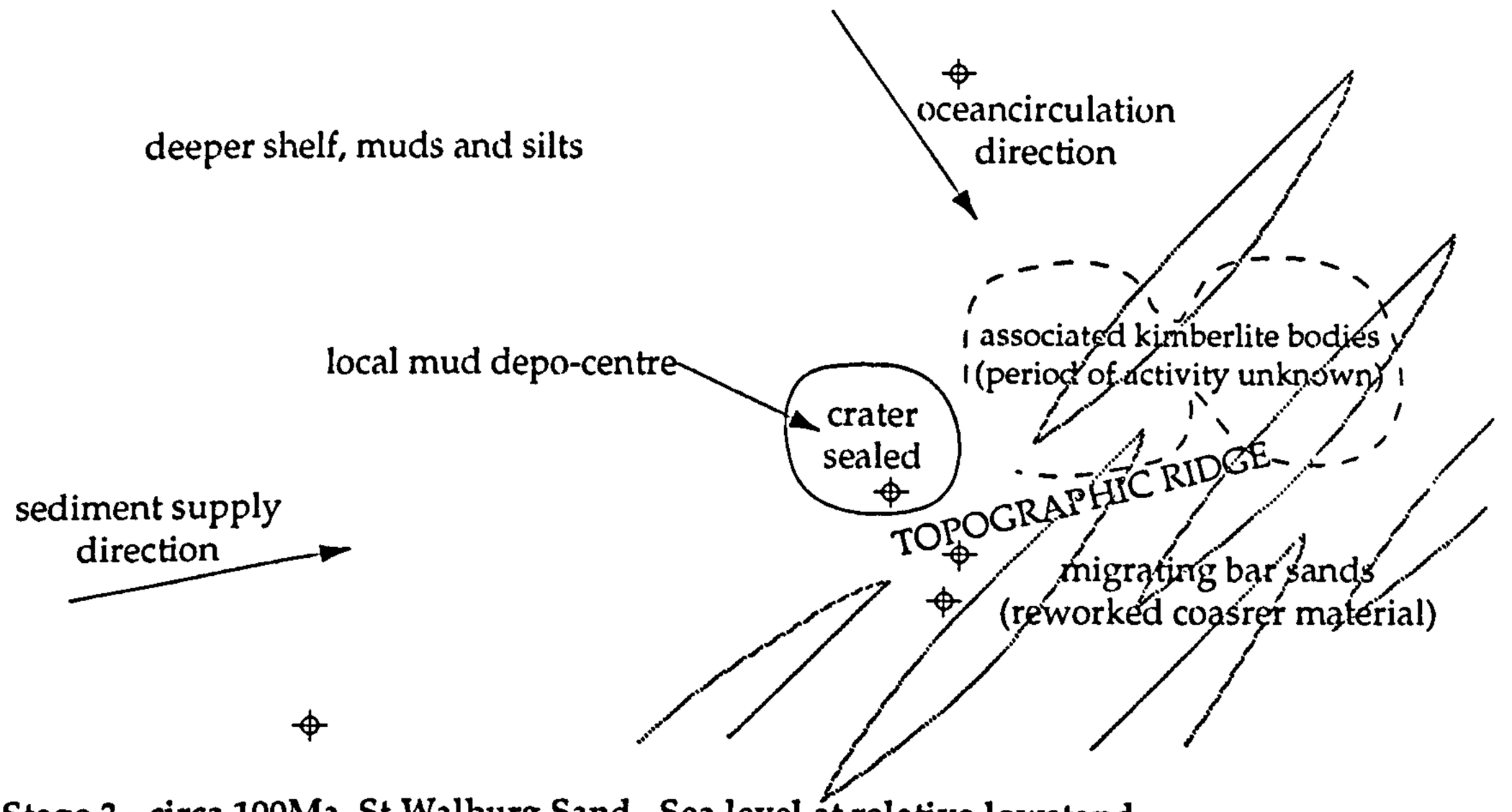

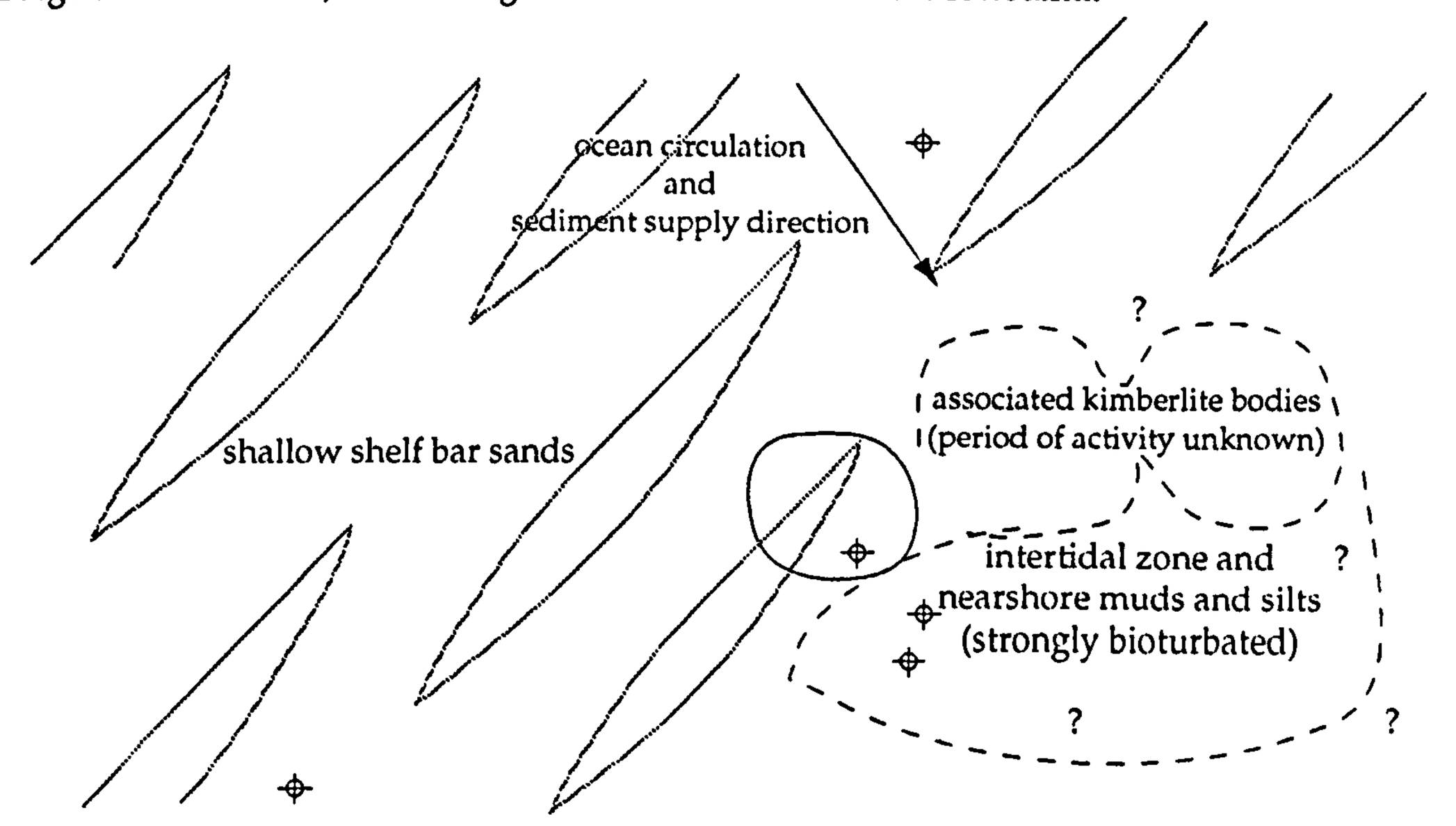

Paleogeographic reconstructions of the Foxford area (see location map Fig. 4.2.4) during the Westgate Formation (Lower Colorado) deposition(Late Albian). Scale 1:100,000

The deepest waters achieved during Lower Westgate times occur in the upper part of the sections, which are shales and mudstones in normal sections. In the kimberlite-proximal sections two strata of medium sand and one interbed of fine sand occur, each 1m thick. In the two medium sands ripple cross-stratification and a general lack of burrows (although a *zoophycos* trace indicates offshore environments, Mieras et al, 1993) suggests fairly rapid deposition, probably as bar sands (Boyles and Scott, 1982). The interbedded fine sand contains wavy laminae and many shallow water trace fossils (*terebellina* and *bergauria*) which imply rapidly varying water depths, possibly as a result of bar sands sweeping the topographic high indicated in Figure 4.2.7.

Throughout the depositional milieu of the Lower Westgate the actual kimberlite crater is a depo-centre, illustrated by an anomalously thick succession of Lower Westgate shaley muds (14m compared to the usual 7m). This may be due to the crater being initially underfilled, and extra-crater deposits of insufficient volume to occupy it fully (see Chapter 3). Alternatively this depo-centre may be due to tectonics (down-faulting), differential compaction or partial dissolution of the kimberlite, or possibly because the axis of the topographic high moving due to kimberlite activity to the east.

St.Walburg Sand Member of the Westgate Formation.

During the depositional period of the St.Walburg Sand the basin returns to lowstand conditions very similar to, but more prolonged than, the Flotten Lake environment (Simpson 1982). This consists of a relatively high-amplitude lowstand, resulting in many parts of the FALC region becoming sub-aerial (swampy islands and mudflats, see case study below), and a return to very shallow shelf (10m to 20m) bar sand deposition in the Foxford area. The normal deposits are 5m to 10m thick, and consist of an overall coarsening-up from silts and shales to medium and coarse sand with bar sand features. The coarser sediment is again derived from a northern sedimentary source (the Meadow Lake Escarpment, Simpson 1982).

By comparison, the kimberlite proximal intersections are thin (4m), and dominated by muds and silts with flaser bedding and shallow water trace fossils (*terebellina*, *bergauria*, *planolites* and *chondrites*). These are typical of nearshore to inter-tidal deposits (0 to 10m water depth) and indicate a shoreline nearby, Stage 3, Figure 4.2.7. The uppermost 1.5m consists of coarse silts and silty sandstone, some of which are cross-stratified by ripple marks and strongly mixed by bioturbation. They lack flaser bedding and the trace fossil *bergauria*.

Although not typical St.Walburg deposits, they are deeper water sands and to some extent similar, representing a slow return to normal deposition. This is continued in the overlying Upper Westgate formation, as transgression occurs and all intersections return to normal deeper shelf (>30m) mud and silt deposition.

In summary prolonged shallowing has occurred in the Foxford area local to kimberlite craters, which were underfilled, became depo-centres, and were subsequently sealed rapidly. The topographic high is probably due to doming, although kimberlite activity to the east may also be responsible. The shallowing in the areas south (and possibly east) of the crater has resulted in fine grained nearshore deposition during regional lowstand when shallow shelf bar sands are typical, and coarse bar sand deposition during regional highstand when deeper shelf muds and silts are typical.

Economic aspects of the open and closed crater systems in the sedimentary environment are discussed further in Chapter 7.

References cited in Chapter 4

- Boyles, J.M. and Scott, A.J. (1982). A model for migrating shelf bar sandstones in the Upper Mancos Shale (Campanian), North-Western Colorado. Association of American Petroleum Geologists, Vol.66, No.5, p.491-508.
- Kjarsgaard, B.A., Leckie, D.A., McIntyre, D.J., McNeil, D.H., Haggart, J.M., Stasiuk, L. and Bloch, J. (1995). Smeaton Kimberlite Drill Core, Fort a la Corne Field, Saskatchewan. Geological Survey of Canada Open File 3170, pp.57.
- Lehnert-Thiel, K., Loewer, R., Orr, R.G. and Robertshaw, P. (1992). Diamond-bearing kimberlites in Saskatchewan, Canada: The Fort a la Corne Case History. Exploration Mining Geology Vol.1 No.4 p.391-403.
- Mieras, B.L., Sageman, B.B. and Kauffman, E.G. (1993). Trace fossil distribution patterns in Cretaceous facies of the Western Interior Basin, North America. In Caldwell, W.G.E and Kauffman, E.G. (eds.) Evolution of the Western Interior Basin, GAC Special Paper 39, p.585-610.
- Obradovich, J.D. (1991). A revised Cenomanian-Turonian time scale based on studies from the Western Interior United States. Abstracts with Programs, GSA, 1991 Annual Meeting, San Diego, CA., p.A296.
- Simpson, F.R. (1982). Sedimentology, palaeoecology and economic geology of Lower Colorado (Cretaceous) strata of West-Central Saskatchewan. Saskatchewan Energy and Mines Report 150.
- Scott-Smith, B.H., Orr, R.G., Robertshaw, P. and Avery, R.W. (1995). Geology of the Fort a la Corne Kimberlites. Proceedings of the 6th International Kimberlite Conference, Russia 1995, Extended Abstracts Volume.

CHAPTER 5 - GEOCHEMISTRY OF THE FORT A LA CORNE KIMBERLITES

Abstract

Major and trace element compositions of the Fort a la Corne (FALC) kimberlites have been determined by X-ray fluorescence (XRF). These data confirm the petrological evidence previously described, of kimberlite composition, of a Group 1A classification. Further interpretation of the major element data suggest a low level (5-10%) of contamination of the Pyroclastic Kimberlite by crustal material when compared to other kimberlites world-wide. Reworking initially reduces crustal contamination by density and size sorting, but with increased degrees of reworking contamination then increases as terrigenous material is added to the kimberlitic sediment. Trace element concentrations are comparable to those of Group 1A kimberlites, apart from those elements which are particularly mobile (e.g. Rb, Sr, Ba, K and Na), some of which are notably enriched in the reworked strata (probably due to greater fluid flow in these more permeable beds). Nickel, occurring in secondary pyrite, was found to be mobile in this environment. The immobile trace elements such as Nb, Cr, Zr and Y are also found to be enriched in certain reworked strata, a reflection of the concentration of heavy minerals that contain these elements (e.g. ilmenite, spinel, garnet, zircon and apatite). Bentonites found at kimberlite-equivalent and other stratigraphic horizons have been shown by their trace element ratios to be of calc-alkaline origin, and unrelated to kimberlitic volcanism.

Over 460 individual mineral grains have been analysed by electron microprobe, including garnet (203), ilmenite, spinel, pyroxene, olivine, phlogopite, amphibole and various crustally derived grains. Diamond grains (29) isolated from the kimberlite are also described. The heavy mineral chemistries reflect parageneses typically found in kimberlites world-wide. These include a moderately sparse megacryst suite of mostly pyrope garnet and ilmenite, with rarer clinopyroxene and spinel. Many of these megacryst minerals probably originate as early phenocrysts from the proto-kimberlite melt. The late-crystallising magma forms the macrocryst and groundmass (microphenocryst) minerals such as olivine, phlogopite, clinopyroxene, apatite and spinel, which have now largely been replaced by secondary minerals, serpentine and carbonate. The majority of the minerals analysed are from xenolithic sources: peridotitic, olivine, Cr-pyrope garnet, Cr-diopside, and orthopyroxene, and accessory spinel and amphibole; eclogitic, pyrope-almandine and grossular garnets and Na-clinopyroxene; and various crustal minerals from the Glennie Domain metamorphic terrane. Overall these minerals, and not least the presence of diamonds, indicate a thick, cool cratonic lithosphere at the time of

kimberlite emplacement. Further implications for the P-T conditions in the lithosphere based on mineral chemistry are discussed in Chapter 6.

5.1 Bulk rock geochemistry from XRF analysis.

Samples for X-Ray Fluorescence (XRF) were taken from regular intervals in kimberlitic borehole intersections, and suspect or interesting horizons in non-kimberlitic intersections. The aim was to characterise the major and minor element geochemistry of the FALC kimberlites, and place them in the broad kimberlite group classification. Comparisons were made to determine any consistent bulk geochemical differences between primary and reworked kimberlite (see Chapter 2). Finally a study was made to determine which kimberlitic trace elements that had survived incorporation into tuffaceous clastics, as an aid to exploration for kimberlite (and diamonds) that entered the sedimentary basin beyond the crater walls (see Chapter 4).

5.1.1 Methodology

Samples were obtained from the borehole core as 50 to 100g blocks. These were prepared in clean conditions by mortar and pestle crushing, followed by milling in agate to a very fine powder. Sample selection and crushing was carried out by this author, XRF analysis was performed by Alan Gray at the University of Leeds. The powders were split, one-third were fused at 1000°C and the 'Loss on Ignition (L.O.I.)' was calculated. Volatiles lost were mainly water and carbon dioxide. The remainder of the powdered sample was analysed by x-ray fluorescence for both major element oxides, from fused glass beads (90% lithium borate flux), and the trace element suite, from 40mm pressed discs of powder with 1.5ml of PVA binder.

5.1.2 Kimberlite major and minor element chemistry

A total of 98 analyses were made, and are tabulated in Appendix VIII. Of these, twelve gave totals lower than 98%. Typically these were shale-rich samples with large amounts of sulphur (probably as gypsum which was noted in the borehole core description), which was not analysed for.

The 86 remaining analyses represented twelve lithologies (see Chapter 2 for classification) as follows:

crater facies pyroclastic kimberlite	1
crater facies reworked pyroclastic kimberlite	1
kimberlite carbonate sills	2
proximal facies pyroclastic kimberlite	14
proximal facies reworked pyroclastic kimberlite	23
proximal facies shale intraclast breccia	5
distal facies reworked pyroclastic kimberlite	4
distal facies tuffaceous clastics	4
(muddy) sandstone - non-tuffaceous	4
mudstones (including fish debris horizons)	3
bentonites	9
kimberlite from LK-2	16

Note: Major element chemistries of eight crater facies kimberlite and eight mudstone samples from the Smeaton (UK 169/8) borehole are also presented in Appendix VIII, see Kjarsgaard et al (1995). LK-2 samples are from the Sturgeon Lake kimberlite boulders, see Chapter 1, and strongly resemble reworked kimberlite pyroclastics of crater or proximal facies. They are not further discussed because they are a considerable distance from the FALC deposits, and are not *in situ*.

The average composition of each lithology is given in Table 5.1. The major and minor element chemistry falls within the compositional range of southern African Group IA kimberlite (Smith et al, 1985), supporting the petrologic evidence for the nature of the FALC samples, Figures 5.1.1 and 5.1.2. In this thesis the major elements are not normalised to 100% volatile free as is usual procedure when comparing most igneous geochemical data sets. The common convention for kimberlite studies, however, is not to normalise. This is because large percentages of the rock (5% to15%) are volatiles of an unknown source and even fresh kimberlite may have up to about 10% LOI.

The FALC kimberlites are characterised by high MgO (serpentine and dolomite), significant levels of CaO (mostly calcite, some perovskite), low Al_2O_3 (indicating low crustal contamination, see below), and high TiO_2 (ilmenite and spinels). Note that K_2O is, on average, lower than typical Group IA kimberlite. This may be due either to: 1. Aeolian fractionation of phlogopite in an extrusive setting, compared to the intrusive environment in which previously described kimberlites were generated, and/or 2. Later preferential removal of micas during aqueous redeposition. The row denoted C.I. in Table 5.1 shows the

Table 5.1

	Global averages*										
	for kimb groups			crater	crater	proximal					
Rock type	1A	1B	II	facies	facies	RPK	proximal	proximal	distal	distal	Sandy
	—	—	—	PK	RPK	not ICB	PK	ICB	RPK	TC	non-TC
Sample No	-	-	-	1	1	23	14	5	4	4	4
SiO2	32.1	25.7	36.3	45.7	36.1	32.1	32.6	32.3	32.8	33.5	56.1
TiO2	2.0	3.0	1.0	0.9	2.1	2.5	2.6	2.4	1.6	4.5	0.4
Al2O3	2.6	3.1	3.2	1.8	2.1	1.5	1.4	8.3	4.4	4.7	17.6
Fe2O3	9.2	12.7	8.4	9.1	8.9	10.8	9.3	8.9	9.7	8.2	4.5
MnO	0.2	0.2	0.2	0.1	0.1	0.2	0.2	0.1	0.7	0.4	0.0
MgO	28.5	23.8	29.7	26.2	26.6	29.4	28.6	22.1	15.1	9.0	2.7
CaO	8.2	14.1	6.0	4.0	6.6	7.5	8.1	7.7	14.4	18.6	3.7
Na2O	0.2	0.6	0.1	0.9	0.8	0.2	0.1	0.1	1.2	0.9	1.8
K2O	1.1	1.1	3.2	0.2	0.1	0.1	0.1	0.1	0.7	0.7	2.0
P2O5	1.1	0.5	1.1	0.2	0.4	0.2	0.4	0.5	0.4	0.7	1.7
L.o.I.	14.1	15.3	9.6	10.2	15.4	15.4	16.7	17.2	18.6	18.4	9.0
Total	99.3	100.1	98.8	99.4	99.2	100.0	100.0	99.7	99.6	99.4	99.5
C. I.	1.1	1.1	1.1	1.8	1.5	1.1	1.2	1.8	2.3	3.7	11.2
Sc	13	20	20	14	23	17	15	14	16	23	9
V	75	170	85	42	68	78	98	117	95	113	198
Cr	1400	1000	1800	834	1454	1656	1434	1160	1257	1617	47
Co	-	-	-	83	83	92	86	86	66	36	18
Ni	1360	800	1400	1400	1167	1328	1076	1120	1013	356	82
Cu	-	-	-	16	50	27	41	62	42	91	27
Zn	-	-	-	50	46	63	57	68	66	61	132
Rb	50	30	135	9	3	8	5	5	37	31	55
Sr	825	1020	1140	136	186	98	165	205	233	402	288
Y	13	30	16	8	11	7	10	11	13	29	110
Zr	200	385	290	84	104	97	132	123	143	338	203
Nb	165	210	120	93	167	173	201	181	158	401	14
Ba	1000	850	3000	230	225	110	164	194	292	452	409
Pb	7	10	30	6	8	4	7	9	9	18	27
Th	18	27	30	17	27	28	32	28	25	55	33
U	4	6	5	0	2	2	3	2	2	6	28

* see Smith et al (1985).

C.I. = contamination indices (Clement, 1982)

Figure 5.1.1

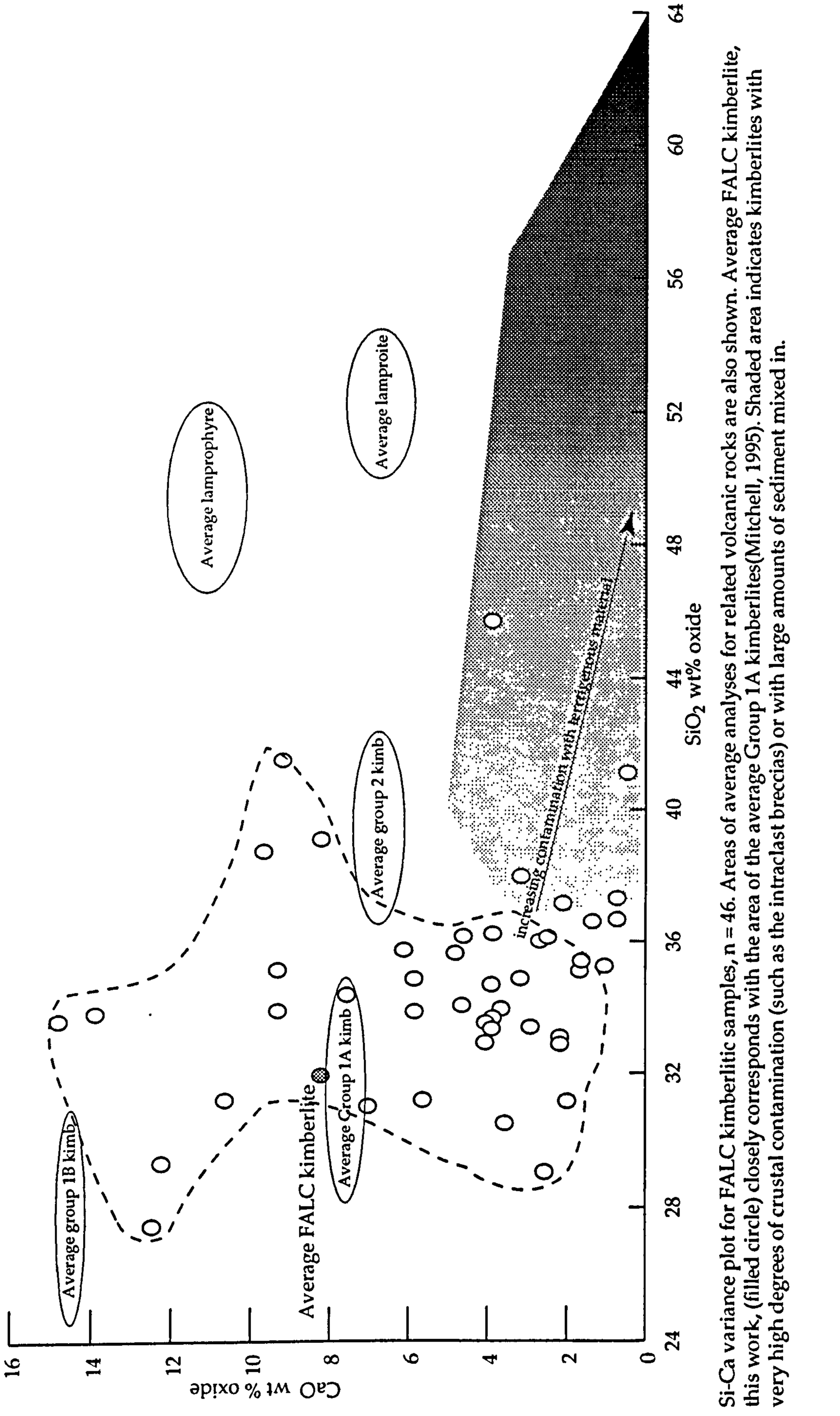

Si-Ca variance plot for FALC kimberlitic samples, n = 46. Areas of average analyses for related volcanic rocks are also shown. Average Group 1A kimberlites(Mitchell, 1995). Shaded area indicates this work, (filled circle) closely corresponds with the area of the average Group 1A kimberlites with very high degrees of crustal contamination (such as the intraclast breccias) or with large amounts of sediment mixed in.

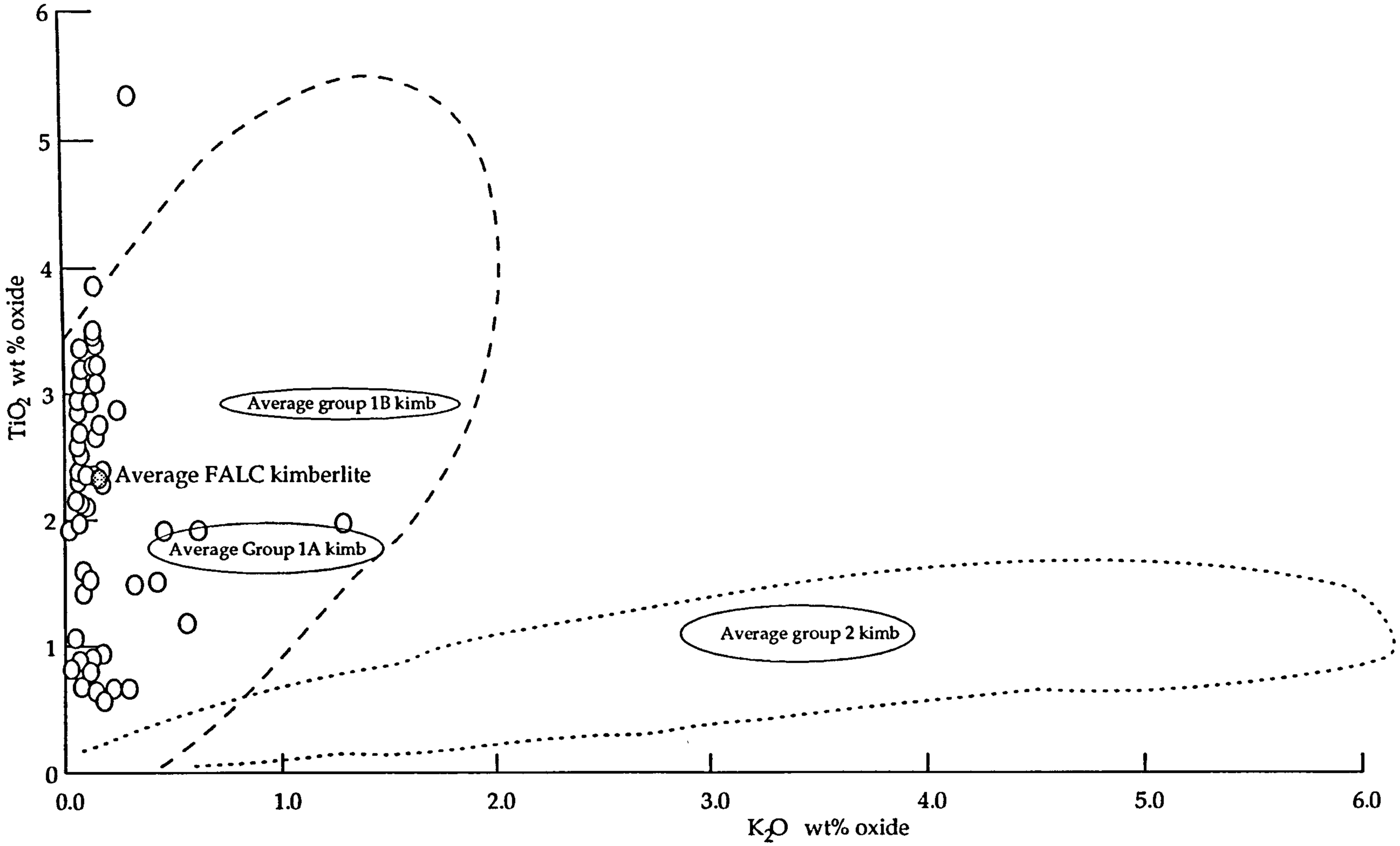

K-Ti varience plot for FALC kimberlitic samples, n= 61. Areas of average analyses for kimberlitie types are also shown. Average FALC kimberlite, this work, (filled circle) closely corresponds with group 1A kimberlite composition (Mitchell 1995), although is notably K-poor. This is probably due to the mobility of K in aqueous solutions that have diagenetically altered the FALC kimberlites. High Ti field (dashed) is the range of compositions of group 1 kimberlites. High K field (dotted) is the range ofcompositions for group 2 kimberlites.

Figure 5.1.2

calculated contamination indices (Clement, 1982; Mitchell, 1986), a function which increases with the amount of xenolithic crustal material relative to primary magmatic material. Intense alteration and weathering may also increase the indices. The C.I. index is calculated from the major element chemistry:

$$C.I. = (SiO_2 + Al_2O_3 + Na_2O)/(MgO + 2K_2O)$$

Typical values of C.I. for diatreme facies kimberlite range from 1.1 to 1.2 for uncontaminated and fresh, 1.9 to 2.0 for contaminated and fresh, 2.0 to 2.8 for weathered and or greatly contaminated kimberlite. The C.I. values for FALC kimberlites suggest low degrees of contamination (5-10%) in the crater facies, and even lower degrees (<5%) in the reworked proximal facies. This is unsurprising, as the crustal xenoliths are generally larger and less dense than the kimberlitic components, and therefore more easily sorted from the pyroclastics during airfall, reworking and transportation, than in diatreme facies rocks which have very little sorting. Proximal shale intraclast breccias (ICB) have a C.I. typical of a moderately contaminated kimberlite. Sample selection of the ICB, however, deliberately avoided sampling large shale clasts, and therefore these analyses represent ICB kimberlitic matrix (only 20% to 50% of the rock). With further mixing of terrigenous material (clays and quartz) the C.I. would be expected to rise. This is observed in the distal kimberlitic RPK and tuffaceous clastic average analyses, with C.I. values of 2.3 and 3.7 respectively. The final column of Table 5.1 shows typical coarse grained basin deposits: muddy sandstones, sandy mudstones, coarse quartz silts, some of which were rich in fish debris (hence the relatively high amounts of P_2O_5). These deposits are shown because they represent 100% terrigenous ('crustal') material, and 0% kimberlite, the C.I. is predictably very high: 11.2.

The effect of alteration on the major element chemistry is significant; Fe, Ca, Na and K are all highly prone to remobilisation. Trace elements can also affected, only a few (V, Y, Zr, Cr, Nb and Th; Vaslami and Cann, 1992) may be considered truly immobile in this alteration regime. Nickel content is considerably higher than average kimberlites. This may simply reflect greater proportions of the kimberlitic minerals that host it, such as olivine (which would tie in well with the low degree of dilution by crustal contamination, discussed above). Secondary sulphides, however, are common, and have been frequently observed containing Ni (bravoite, see Chapter 2). The total amount of Ni therefore may represent a kimberlitic level, plus an amount introduced or remobilised from another facies (or even a non-kimberlitic source) during

diagenesis. Other trace elements may have been reduced in concentration by the same process. Winnowing of phlogopite by wind and water can only partially explain the extremely low contents of Rb and Sr, diagenetic redistribution of these elements is also a factor. The immobile elements, V, Y, Cr, Nb and Th, reflect, with reasonable accuracy, the initial pre-alteration concentrations, mainly of minerals such as ilmenite, zircon (common), apatite and sphene (rarely found), some of which may be xenocrysts.

Reworking has already been shown to affect major element chemistry, but its effect on trace element concentrations is less clear, Figure 5.1.3. Note that none of the elements previously described as immobile show consistent changes with degrees of reworking. The elements that do show apparent upgrading are mobile (e.g. Zn and Ni), and this may be due to greater porosity and fluid mobility in the reworked strata relative to the primary tuffs (see Chapter 2) in the early stages of diagenesis.

5.1.3 Fine grained sediment provenance

Major element analysis of fine grained, clay-rich sediments, particularly the proportion of Al in a sample can be useful in determining the depositional environment. In the FALC area, Al-rich (>0.2 mole fraction) shales contain illite/smectite, kaolinite, quartz and muscovite, and have a terrigenous or deltaic source. Al-poor (<0.2 mole fraction) shales are more quartz-rich, lack kaolinite, and are marine (Kjarsgaard et al, 1995; Bloch, 1994). Three fine grained sediments from the FALC region are compared to those presented in Kjarsgaard et al (1995), with a view to verifying borehole core interpretation of the shale facies, marine or otherwise. The Al mole fraction can be compared to Ti, Fe, Mg and Si mole fractions to further discriminate the samples which are clay-poor (very low Al) and kimberlitic (high Mg and Ti). Figure 5.1.4 illustrates the composition of different sediment types: three Westgate Fm. marine shales, two Mannville Fm. muds and silts, and a Mannville Fm. grey siltstone (all analyses from Kjarsgaard et al, 1995). These are compared to a shale fish debris bed (see Chapter1, Figure 1.3.5) from borehole OFS 93-010, a tuffaceous silt (also from 010) and a representative of graded reworked pyroclastic kimberlite sand from OFS 93-002.

The Mannville Fm. grey siltstone has a Al mole fraction of 0.18 (borderline of marine/terrestrial 0.2) and plots as a mix of marine and terrestrial when compared to Ti, Fe and Mg. This represents a nearshore conditions, possibly interdistributary, in the usually deltaic Mannville sequence. The shale fish debris bed plots consistently with the marine muds, indicating a strong

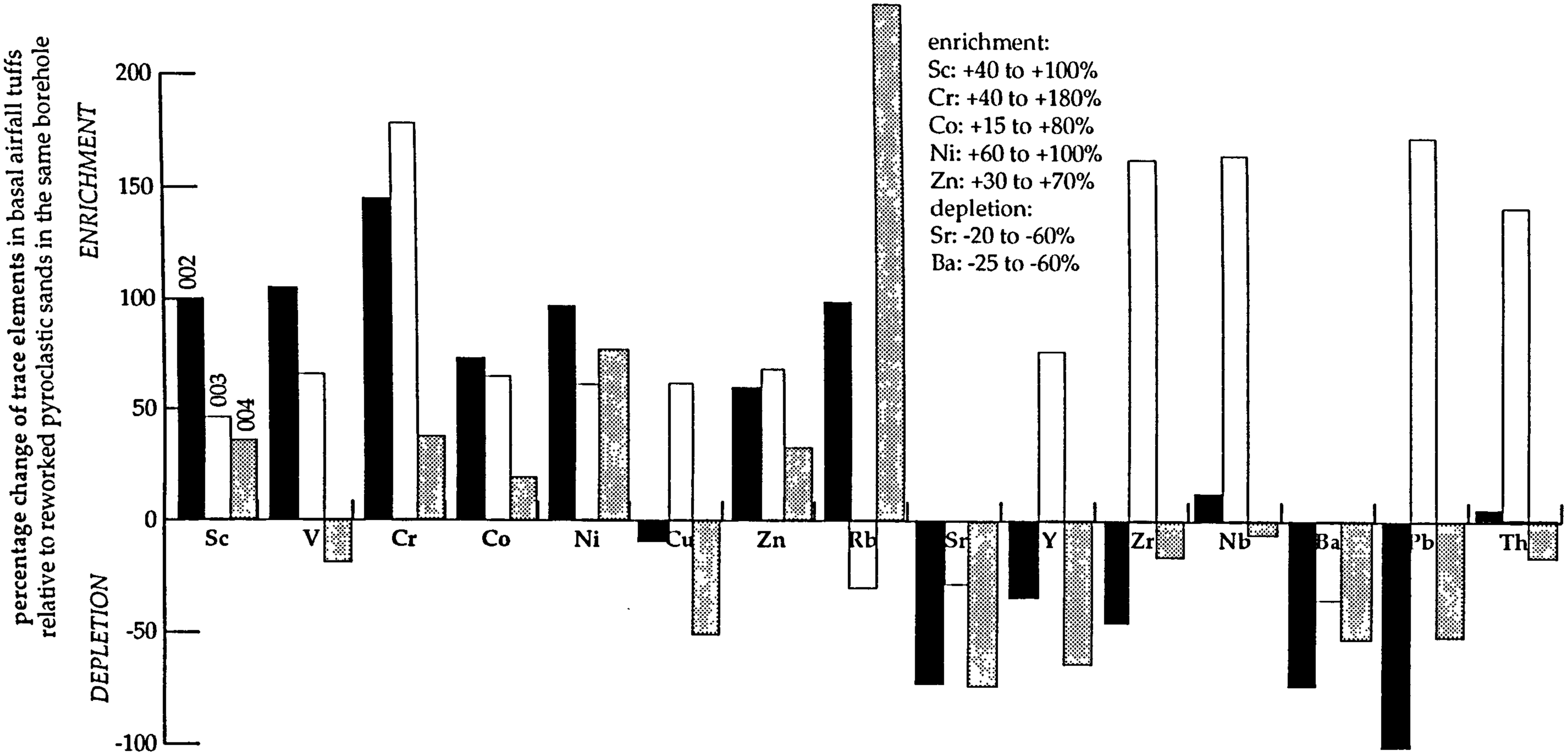

Histogram to highlight trace elemental differences between primary (airfall tuff) and reworked (pyroclastic sand) kimberlite *from the same borehole*. Trace elements, determined by XRF, are averaged for the entire primary facies and the entire reworked facies. The change in concentration is then calculated as a percentage, and show ranges of +230 to -105%. To test consistancy of these apparent changes three boreholes of proximal facies are examined, OFS93-002 (black bars), 003 (white bars) and 004 (grey bars). Consistant changes are considered to be those that occur in the same direction (enrichment or depletion) in all three boreholes. Results show that half of the elements analysed were consistently enriched or depleted, all are mobile elements apart from Cr. This indicates the trace element suite is partly a record of diagenetic remobilisation, although some may be due to heavy mineral enrichment in the reworked facies. Immobile elements (e.g. V, Y and Nb) show wide variability in both enrichment and depletion, suggesting that heavy mineral enrichment is *not* constant from primary to reworked facies, and may be more related to specific lithofacies, such as graded pyroclastics.

Figure 5.1.3

Figure 5.1.4

	from Kjarsgaard et al (1995)						K049	K041	K095
Rock type	mar muds	mar muds	mar muds	siltstone	delt silt	delt shl-silt	fishbed shl	silt/tuff	RPK
borehole	UK 169/8	UK 169/8	UK 169/8	UK 169/8	UK 169/8	UK 169/8	010	010	002
depth	105.00	109.00	112.00	218.40	235.90	228.70	144.91	148.30	107.13
mole frac									
Si	0.67	0.63	0.63	0.65	0.55	0.57	0.63	0.18	0.32
Ti	0.01	0.01	0.01	0.01	0.01	0.01	0.01	0.14	0.05
Al	0.14	0.17	0.15	0.18	0.24	0.27	0.17	0.04	0.02
Fe	0.08	0.09	0.09	0.06	0.08	0.06	0.08	0.15	0.15
Mn	0.00	0.00	0.00	0.00	0.00	0.00	0.00	0.01	0.00
Mg	0.02	0.03	0.03	0.02	0.02	0.02	0.03	0.13	0.41
Ca	0.01	0.01	0.01	0.00	0.01	0.00	0.01	0.33	0.04
Na	0.02	0.01	0.01	0.01	0.01	0.01	0.02	0.01	0.00
K	0.04	0.06	0.06	0.07	0.07	0.06	0.05	0.00	0.00
P	0.00	0.00	0.00	0.00	0.00	0.00	0.00	0.00	0.00

	mar muds	mar muds	mar muds	siltstone	delt silt	delt shl-silt	fishbed shl	silt/tuff	RPK
Al	0.1449	0.1685	0.1538	0.1791	0.2437	0.2660	0.1681	0.0362	0.0234
Ti	0.0080	0.0097	0.0084	0.0136	0.0128	0.0141	0.0079	0.1376	0.0477
Si	0.6704	0.6292	0.6296	0.6476	0.5501	0.5656	0.6289	0.1845	0.3210
Fe	0.0803	0.0885	0.0938	0.0604	0.0798	0.0621	0.0830	0.1498	0.1471
Mg	0.0234	0.0257	0.0288	0.0173	0.0232	0.0190	0.0291	0.1303	0.4109

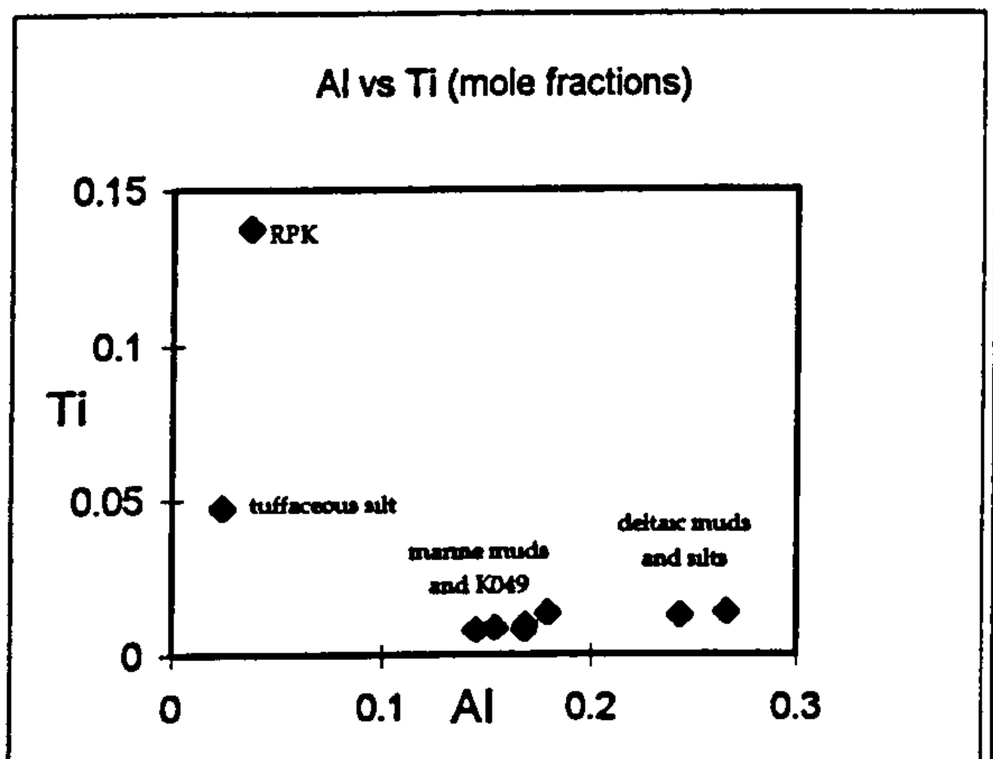

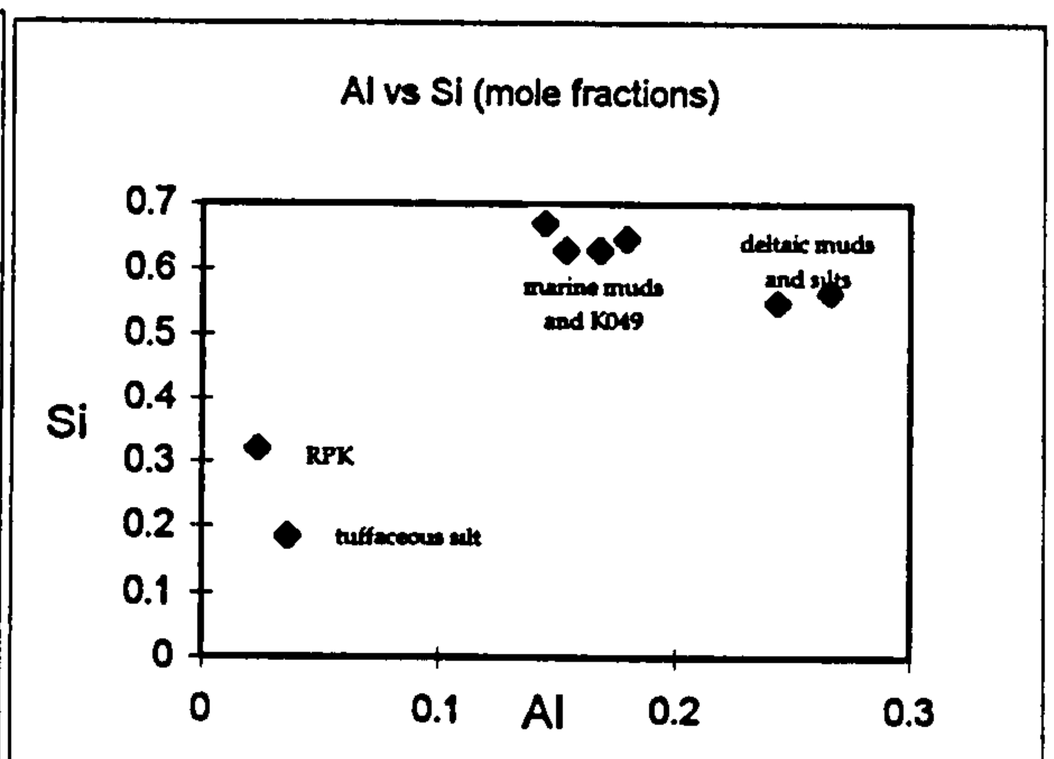

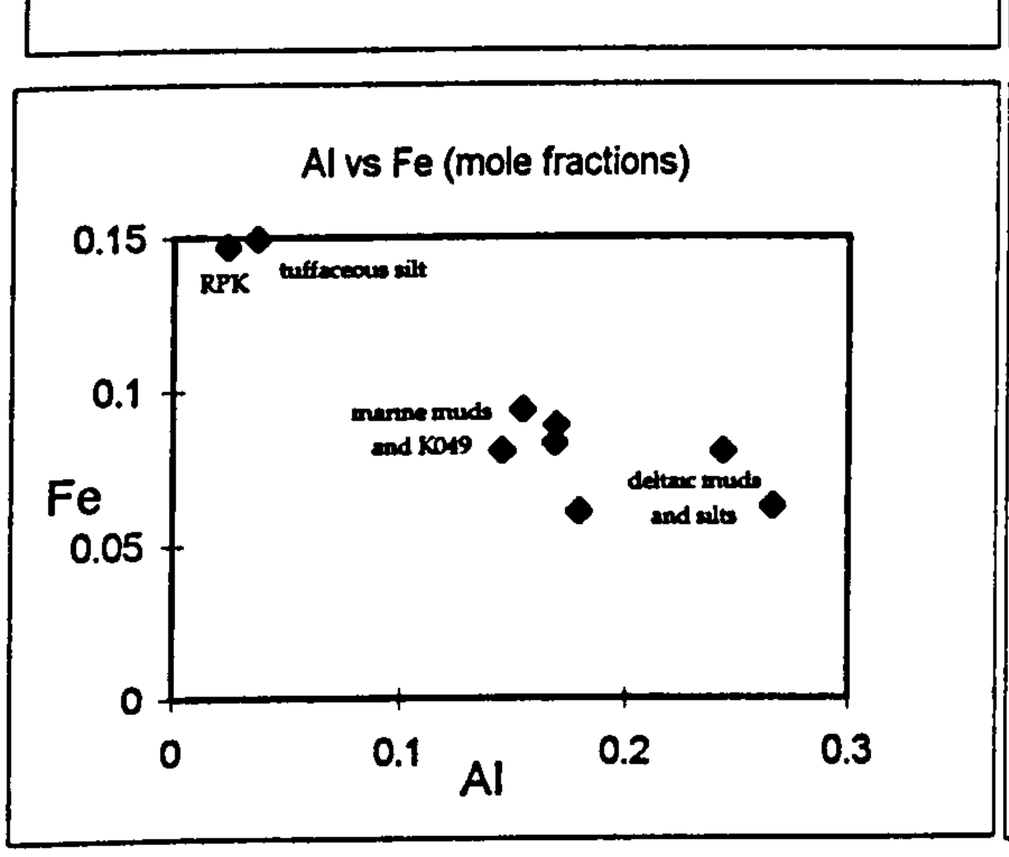

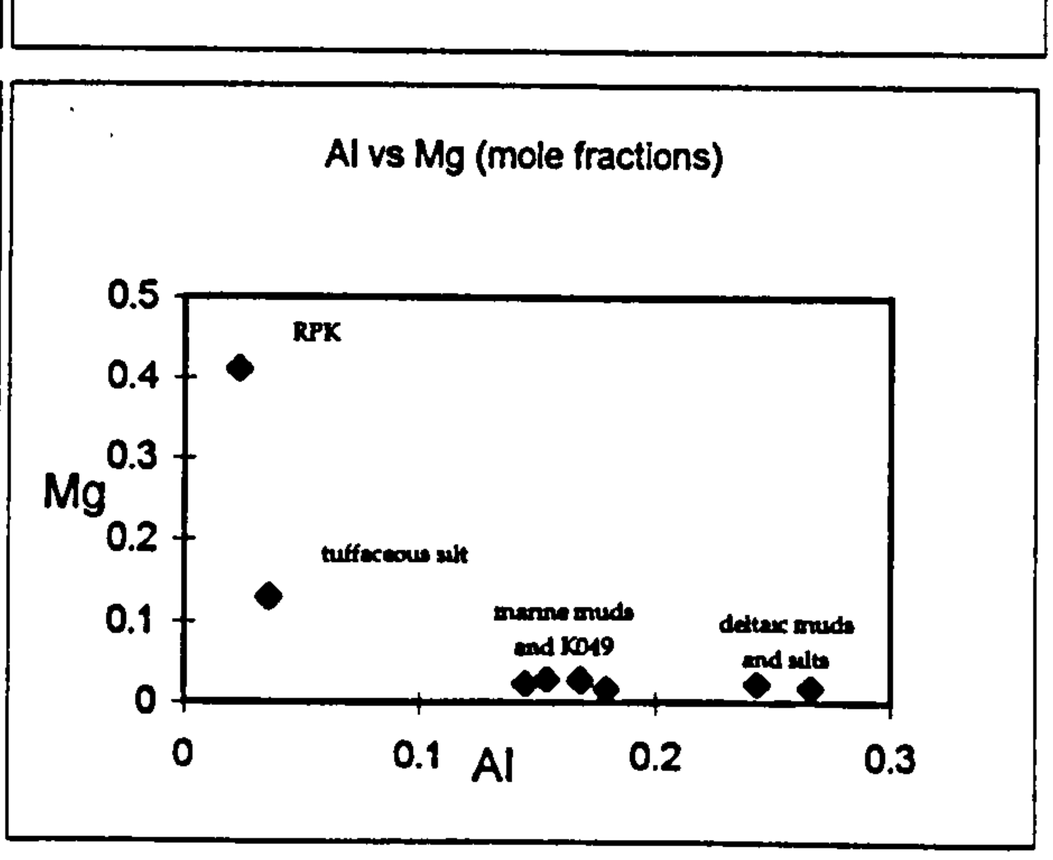

marine influence on shales interpreted as coastal swamp deposits by the presence of rootlets, bioturbation and plant fragments (see Chapter 2). The tuffaceous silt plots as a kimberlite but with lower proportions of Ti, Si and Mg, and is comparable to the RPK in Fe content. This is consistent with the mineral distribution previously described with increased reworking (see Chapter 2): Mg decreasing with reworking, as olivine is broken down to serpentine and mostly removed in to suspension.

5.1.4 Bentonite geochemical provenance

Bentonites were frequently intersected in the OFS boreholes, the horizons were typically thin (1.5cm to 12cm), ultra-fine and bluish-grey with a soapy texture. They were sampled for XRF analysis to test for any kimberlitic associations. Most of the samples were obtained from the White Specks Formation, which ranges from 93Ma to 84Ma, well after peak kimberlite activity (see Chapter 1). Bentonite sample K080, however, was sampled from Lower Westgate Formation strata in borehole OFS 93-005, time equivalent to the kimberlite volcanism only 10km to the north-west. The XRF analyses of these bentonites, kimberlites of crater (lapilli-tuff, LT) and proximal (medium tuff, MT) facies, and two calc-alkaline lavas from the Kamloops Volcanic Group (Ewing, 1981) are compared, Figure 5.1.5. The latter were chosen because Cordilleran calc-alkaline volcanic sources were active at the time of kimberlite volcanism, about 1000km to the west (Thorkelson, 1985). Although the Kamloops Group are much younger than the Cordilleran volcanism contemporaneous with kimberlite activity (about 55Ma, compared to 100Ma), they are of comparable petrogenesis and geochemistry (Armstrong, 1988).

Comparison of the major elements SiO_2 and MgO indicate that the bentonites show no chemical similarities with the kimberlite tuffs, typically with 3% to 7% MgO, compared with >25% in the kimberlite. The Lower Westgate bentonite (lwr WgF) had anomalously high SiO_2 compared to the other bentonites. In general they show some affinity with basaltic andesite composition. Trace elements known to be relatively immobile (Vaslami and Cann, 1992) were used to group volcanics of similar magma type, and by using elemental ratios (e.g. Nb/Zr) and sums, the effects of dilution of concentrations through reworking or alteration were countered. From the two discriminant trace element plots shown in Figure 5.1.5 it is clear that the bentonites have no compositional association with the kimberlites. The elements Nb, Y, Zr, V, Cr and Ni were found to be the most useful in discriminating the kimberlites from the other rocks. Furthermore the Lower White Specks and Lower Westgate

Figure 5.1.5

	bentonites											
	K121	K122	K080	K126	K127	K128	K131	K132	k156	K101	Ewing 1981	
Rock type	lwr WS	lwr WS	lwr WgF	upr WS	upr WS	upr WS	upr WS	upr WS	LT	med Tuff	An.fl	An.tf
Borehole	006	006	005	006	006	006	007	007	012	002	-	-
depth (m)	124.70	125.95	159.65	112.49	114.28	114.53	112.59	111.48	202.88	204.01	-	-
SiO2	57.15	61.20	68.78	56.49	57.72	56.77	58.85	51.58	45.7	37.99	52.21	57.92
TiO2	0.21	0.13	0.37	0.38	0.38	0.27	0.22	0.49	0.91	2.58	1.02	1.11
Al2O3	19.47	20.25	9.62	22.38	19.17	19.76	19.76	20.00	1.81	1.25	13.84	17.33
Fe2O3	4.36	2.29	8.34	3.28	3.58	3.09	2.34	6.77	9.14	10.31	8.27	5.07
MnO	0.05	0.04	0.17	0.06	0.04	0.03	0.04	0.04	0.11	0.16	0.12	0.09
MgO	4.64	4.84	1.19	3.46	4.73	4.01	5.06	4.17	26.17	31.33	6.47	1.79
CaO	0.93	0.73	3.35	1.54	1.85	4.33	2.59	1.79	3.97	3.21	8.42	4.47
Na2O	2.97	3.15	0.34	2.60	3.05	3.20	2.04	2.33	0.93	0.07	1.94	2.28
K2O	0.63	0.83	0.63	0.46	0.78	0.66	0.50	1.10	0.15	0.05	2.67	6.62
P2O5	0.11	0.05	0.97	0.17	0.12	0.25	0.09	0.30	0.24	0.27	0.45	0.49
L.o.I.	8.42	6.57	6.19	8.11	6.98	7.43	8.64	9.61	10.21	12.81	3.46	2.7
Total	98.94	100.07	99.94	98.94	98.40	99.80	100.13	98.19	99.35	100.03	99.26	100.12
Sc	0	0	7	4	5	6	5	3	14	11	-	-
V	16	26	40	1085	534	273	460	490	42	98	177	144
Cr	3	4	34	53	34	16	22	25	834	1559	408	46
Co	12	9	18	12	11	13	9	13	83	80	-	-
Ni	1	2	12	14	5	9	9	8	1400	885	201	36
Cu	0	0	10	8	3	19	0	7	16	36	-	-
Zn	53	50	29	54	85	65	46	92	50	51	-	-
Rb	12	13	34	10	21	13	13	28	9	4	57	238
Sr	160	158	124	309	264	371	193	276	136	153	841	1486
Y	16	7	20	5	0	3	2	7	8	10	26	25
Zr	232	151	68	114	169	85	97	318	84	138	176	296
Nb	15	14	7	5	8	4	6	12	93	204	11	14
(Cr+Ni)/Zr	0.02	0.04	0.68	0.59	0.23	0.29	0.32	0.10	26.60	17.71	3.46	0.28
Nb/Zr	0.06	0.09	0.10	0.04	0.05	0.05	0.06	0.04	1.11	1.48	0.06	0.05
(Nb+Y+Zr)/Ti	0.23	0.24	0.05	0.06	0.08	0.06	0.09	0.13	0.04	0.02	0.04	0.05
V/Nb	1.07	1.86	5.71	217.00	66.75	68.25	76.67	40.83	0.45	0.48	16.09	10.29

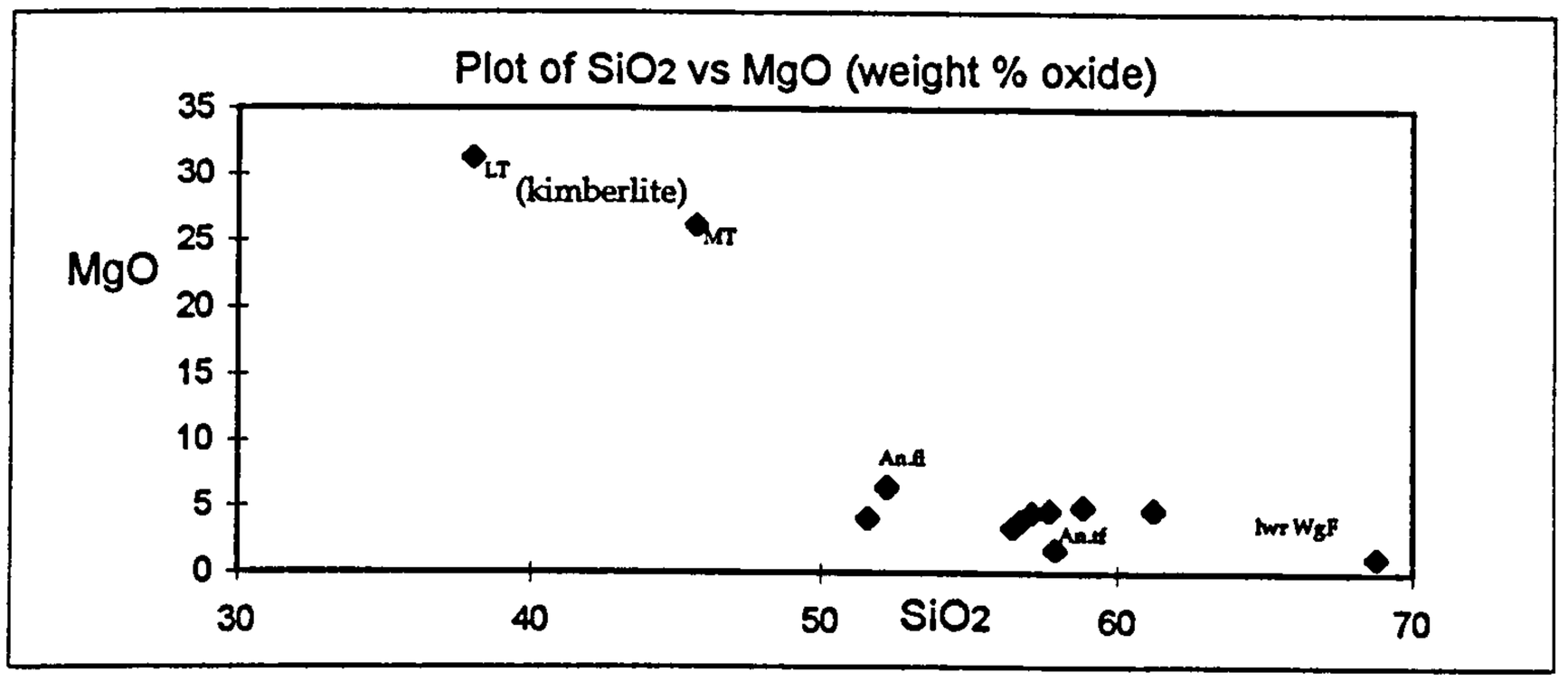

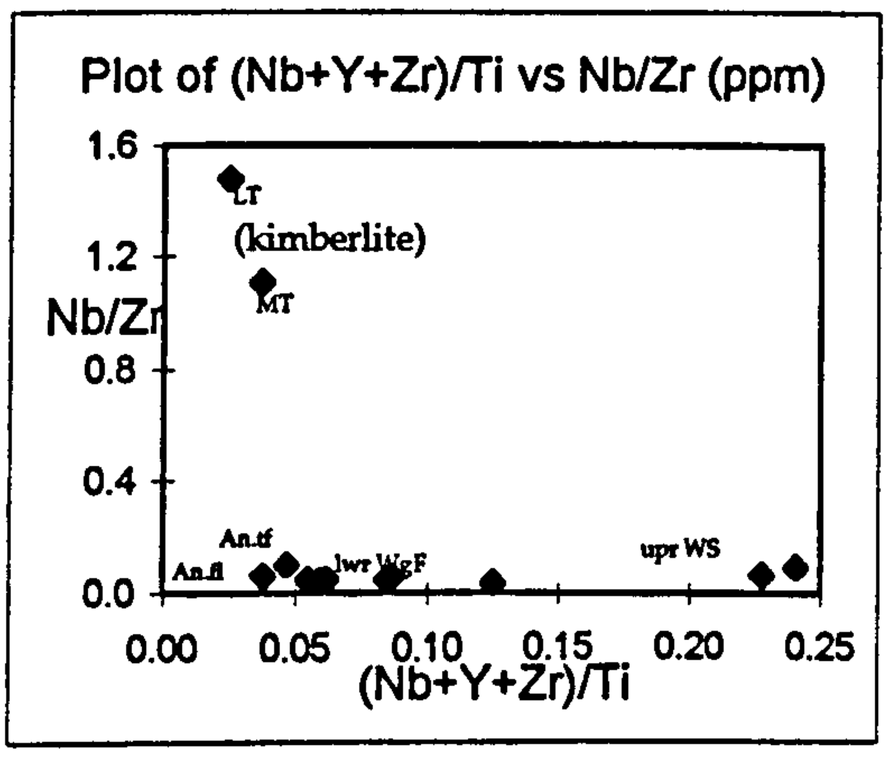

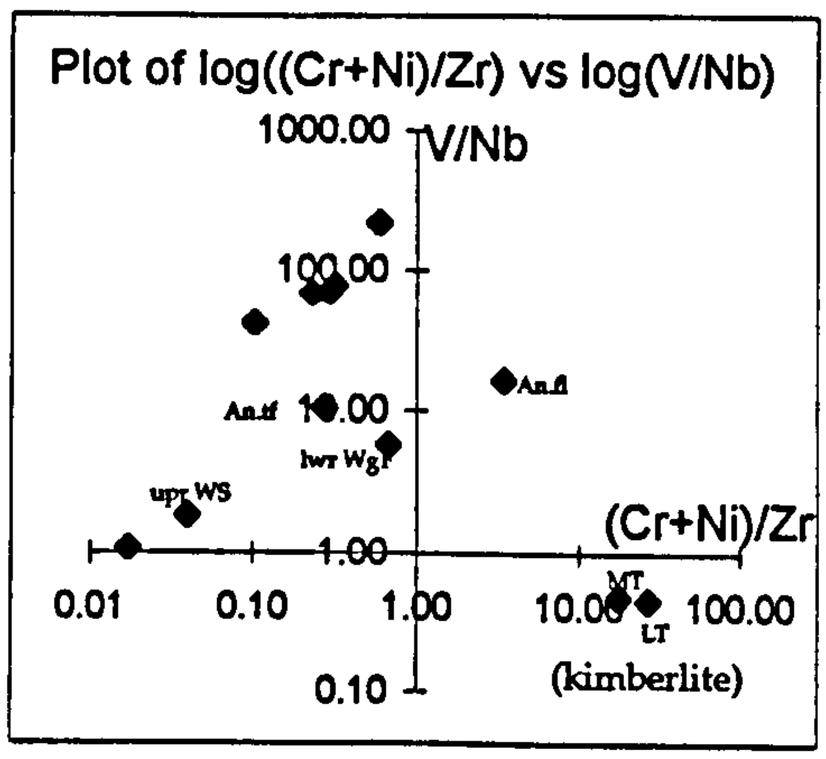

Abbreviations used on columns and graphs as follows: lwr WS = lower White Speckled Shale, upr WS = upper White Speckled Shale, lwr WgF = lower Westgate Formation (see Chapter 1 for stratigraphic description), LT = lapilli-tuff, MT = medium tuff (see Chapter 2 for classification). An.fl = andesite flow and An.tf = andestie airfall tuff, both from the Kamloops Volcanic Group, British Columbia. (Ewing, 1981)

bentonites show strong correlation with the Cordilleran andesites, whilst the two samples from the Upper White Specks appear to have a different parental composition. Therefore it is reasonable to interpret these bentonites as ash deposits from large-scale calc alkaline eruptive events occurring in the Rockies Cordillera over 1000km to the west and south-west. Other bentonites described in various parts of the basin (particularly in Alberta) have had the same origin assigned to them, and the thicker strata are used as basin-wide markers (Leckie et al, 1992).

5.2 Mineral chemistry and classification

In this section the results of microprobe analysis of 461 separate mineral grains are described, grouped and classified by various methods common in the kimberlite literature. The mineral grains were individually picked (by the author) from the heavy mineral concentrates separated from 320kg of kimberlite (OFS boreholes 002, 003, 004, 009, 010 and 012), see Chapter 1 and Appendix V for separation methodology. Typically the mineral grains selected were 0.25mm to 2mm in size, and single crystals, although three composite grains were also analysed. The grains were mounted in to resin blocks and polished with diamond paste. Mineral analyses were performed on a Cameca SX-50 electron microprobe, at Leeds University. Microprobe operation was conducted by Dr. Eric Condliffe and this author, largely as part of the Operation Fish Scale contract (see Introduction). The mineral compositions are given in Appendix IX, and their classification is discussed below.

Many of the kimberlitic minerals described below often comprise three distinct paragenses, megacryst (macrocrystal or discrete nodule suite), peridotitic and eclogitic. The megacryst suite at FALC is sparse compared to other kimberlites (Mitchell, 1986), and includes titanian pyrope garnet, ilmenite and clinopyroxene. It is generally agreed that these are formed as phenocrysts from the proto-kimberlite magma at great depth (Schulze, 1987). The other two suites are xenolithic, and represent material accidentally included by the magma during ascent to the surface. The peridotitic suite comprise Mg-olivine, clinopyroxene (Cr-diopside) and orthopyroxene, Cr-pyrope garnets, Cr-spinel and accessory amphibole and diamond. Globally the eclogitic suite has a wide range of component minerals, at FALC these include pyrope-almandine-grossular garnet, Na-clinopyroxene (omphacite) and kyanite, with accessory diamond. Other parageneses occur, and these are discussed, along with the three common types in the mineral descriptions below.

5.2.1 Diamonds

Apart from the minerals analysed by electron microprobe, a total of 28 micro-diamonds (<1mm, minimum size cut-off of 0.1mm) and one macro-diamond (2.5mm) were also separated by Operation Fish Scale. These were verified as diamonds by various optical and laser spectral methods (see Appendix XI). Further examination of the nitrogen-aggregation properties of the diamonds were carried out by Leahy and Taylor (1995). The implications of the analyses are discussed in Chapter 6.

The diamonds displayed a range of morphologies, colours and surface features, see Table 5.2. Most of the diamonds were colourless fragments of multiple intergrowths of octahedral and dodecahedral morphologies (Figure 5.2.1), with rare macles (a flat twinned triangular diamond morphology) and fine aggregated grains (Figure 5.2.1). Fracture surfaces on the fragmented diamonds are usually fresh, suggesting the diamonds were damaged during heavy mineral separation processes (which included a series of crushing stages to help disaggregate grains), and may have been larger *in situ*. It would be misleading to apply the term 'gem quality' to these diamonds because of their size, however clear, colourless diamonds with good shape do occur. Three brown or pale brown diamonds were recovered (Figure 5.2.2), this coloration is often ascribed to plastic deformation of the crystal lattice (Harris, 1987). The rest of the diamonds were colourless. Surface etching was present on one third of the diamonds, usually as trigons (triangular pits, see Figure 5.2.1) and frosting and pitting. These indicate a certain amount of resorption, occurring during the ascent of the kimberlite magma. Inclusions are also fairly common, pyroxene has been tentatively identified in one (Figure 5.2.1), and silicates in three others. Graphite encrusts the surface of three of the diamonds, and more rarely, occurs along fractures (along with clays) and as inclusions. The largest diamond (Figure 5.2.2), and five of the micro-diamonds recovered from 10-9B were all fragments of a single large stone (possibly octahedral). All the surfaces are fresh fractures, and this suggests that the original stone may have been a complete equant octahedral diamond, at least 2.5mm in diameter, equivalent to about 1 carat weight. It is notable that the majority of the diamonds found were separated from reworked kimberlite strata and non-tuffaceous sediments, the significance of this is discussed further in Chapter 7.

Throughout the diamond selection stage of heavy mineral processing efforts to find natural diamonds were being constantly hampered by the frequent occurrence of synthetic diamonds. These were derived from the drill bits used in the drilling of the borehole cores, as no artificial alternatives (such as carbide

Table 5.2

Diamond code no.	general facies*	maximum length (mm)	colour	morphology and other features	Fig. no.
2-10C-1	g RPK	0.15	none	broken, sharp-edged octahedron, with silicate inclusion	
2-10C-2	g RPK	0.17	none	multiple sharp-edged octahedra	
2-10E-1	g RPK	0.32	none	multiple dodechedron fragment, clay in fracture	
2-10E-2	g RPK	0.30	none	multiple sharp-edged octahedron, with fine etch marks and surface graphite deposits	
2-10E-3	g RPK	0.14	none	macle frag, with some etch trigons	
2-10F-1	b RPK	0.35	none	multiple octahedra aggregate, with pyroxene inclusions and pitted surface	5.2.1
2-12B-1	mt PK	0.30	none	multiple intergrowth, with silicate inclusion and pitted	
2-12B-2	mt PK	0.35	brown	multiple dodecahedron, broken, with many dark inclusions	5.2.2
3-2-2	b RPK	0.35	none	fragment, frosted	
3-2-3	b RPK	0.30	none	elongate fragment	
3-2-4	b RPK	0.20	none	rounded dodec fragment	5.2.1
3-3-1	b RPK	0.70	none	distorted octahedron with clear trigons	5.2.1
3-4B-1	mt PK	0.30	none	multiple rounded octahedra aggregate, with CO_2 and silicate inclusions	
4-13A-1	g RPK	0.40	brown	octahedron fragment, with trigons and frosting	
4-13E-1	b RPK	0.30	brown	distorted octahedron	
4-13F-1	g RPK	0.32	none	rounded triangular macle	
4-18-1	m RPK	0.20	none	multiple sharp edged octahedra, with graphite inclusions along fractures	
4-24-1	ct PK	0.31	none	aggregate, with trigons	
4-24-2	ct PK	0.19	none	octahedral intergrowths	
4-24-3	ct PK	0.23	none	irregular fragment with inclusion	
10-9B-1	qs TC	2.45	none	cleavage fragment	5.2.2
10-9B-2	qs TC	0.60	none	fragment of 10-9B-1	
10-9B-3	qs TC	0.35	none	fragment of 10-9B-1	
10-9B-4	qs TC	0.35	none	fragment of 10-9B-1	
10-9B-5	qs TC	0.33	none	fragment of 10-9B-1	
10-9B-6	qs TC	0.29	none	fragment of 10-9B-1	
12-7-1	b lt PK	0.17	none	octahedral fragment, with surface graphite	
12-7-2	b lt PK	0.19	none	macle, with trigons	
12-7-3	b lt PK	0.17	none	fragment, with trigons and surface graphite	

Note: diamond code number comprises: OFS borehole number - facies code - diamond code

* Abbreviations used as follows: RPK = reworked pyroclastic kimberlite, PK = pyroclastic kimberlite, TC = tuffaceous clastic, g = graded, b = bedded, m = massive, mt = medium tuff ct = coarse tuff, lt = lapilli-tuff, qs = quartz sand. See Chapter 2 for full classification

Descriptions by P.H. Nixon, W.R. Taylor and this author

Figure 5.2.1

Plate 5.1
3-3-1, 0.7mm, octahedron with trigons and etch marks. This diamond a 'Sloan-type' (see Chapter 6).

Plate 5.2
3-2-4, 0.2mm, rounded dodecahedron.

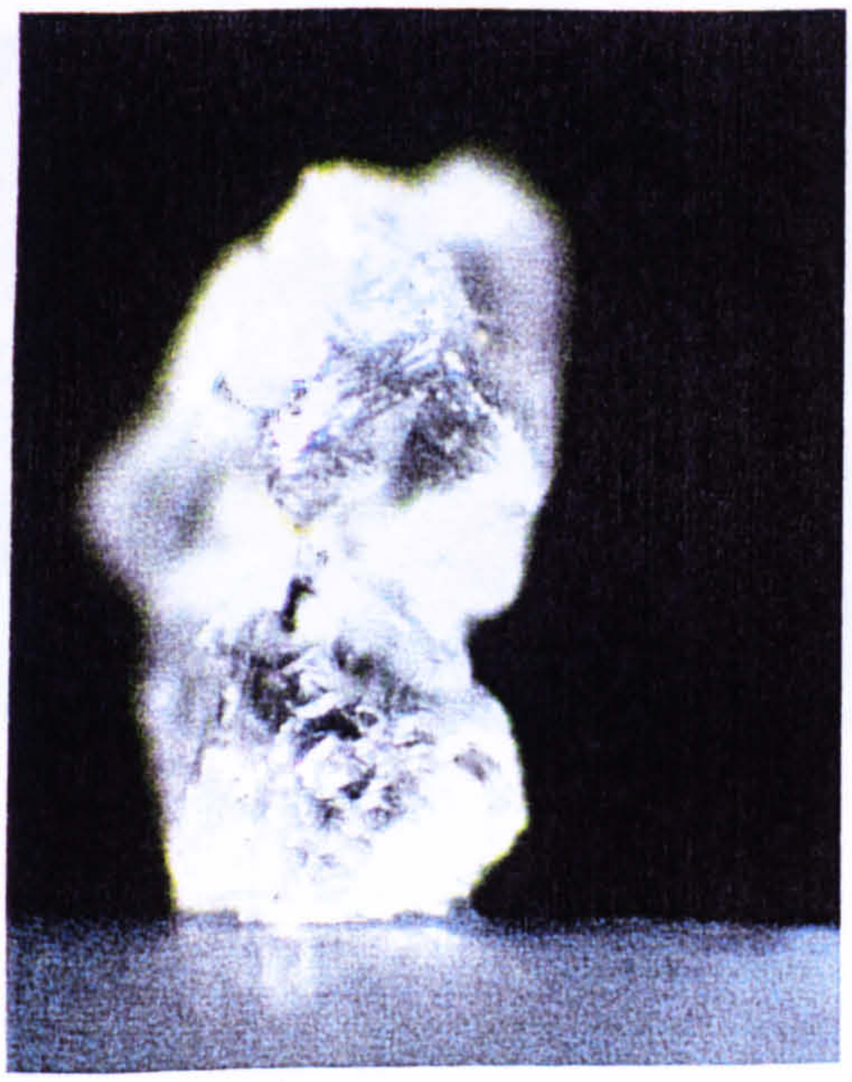

Plate 5.3
2-10F-1, 0.35mm, multiple octahedra aggregated grain. With a pyroxene inclusion (central elongate dark patch).

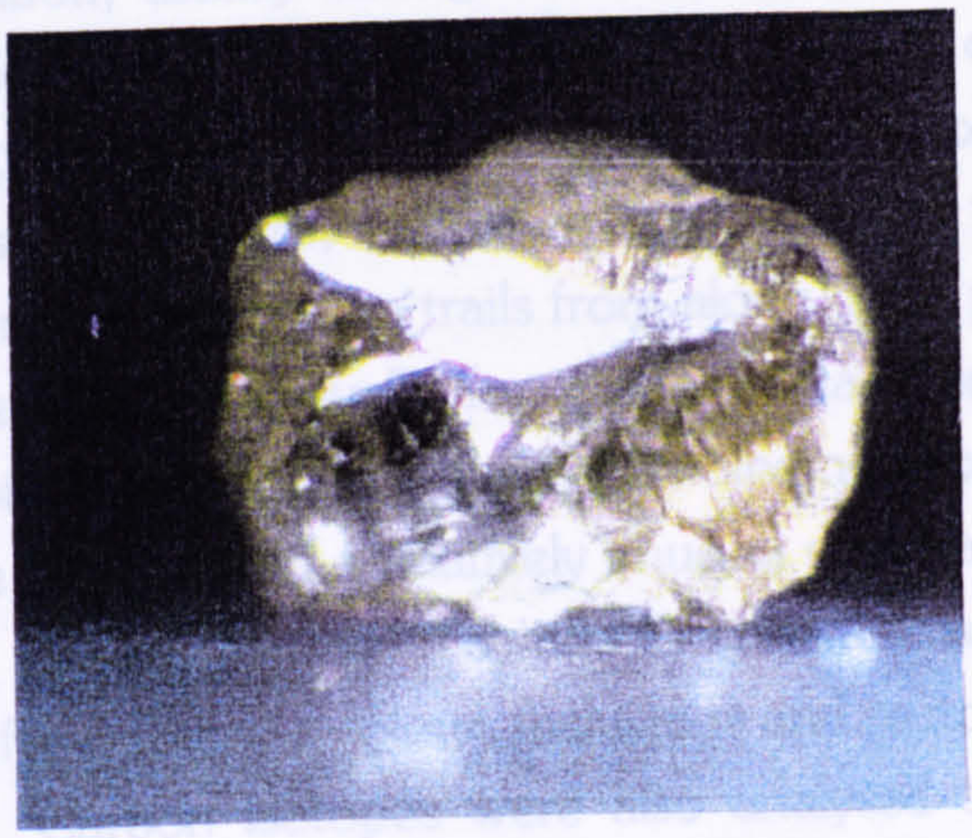

Plate 5.4
2-12B-2, 0.35mm, brown multiple dodecahedral aggregate, with many dark inclusions.

Plate 5.5
10-9B-1, 2.45mm, macro-diamond, cleavage fragment, probably from an octahedral stone. Fracture surfaces are fresh.

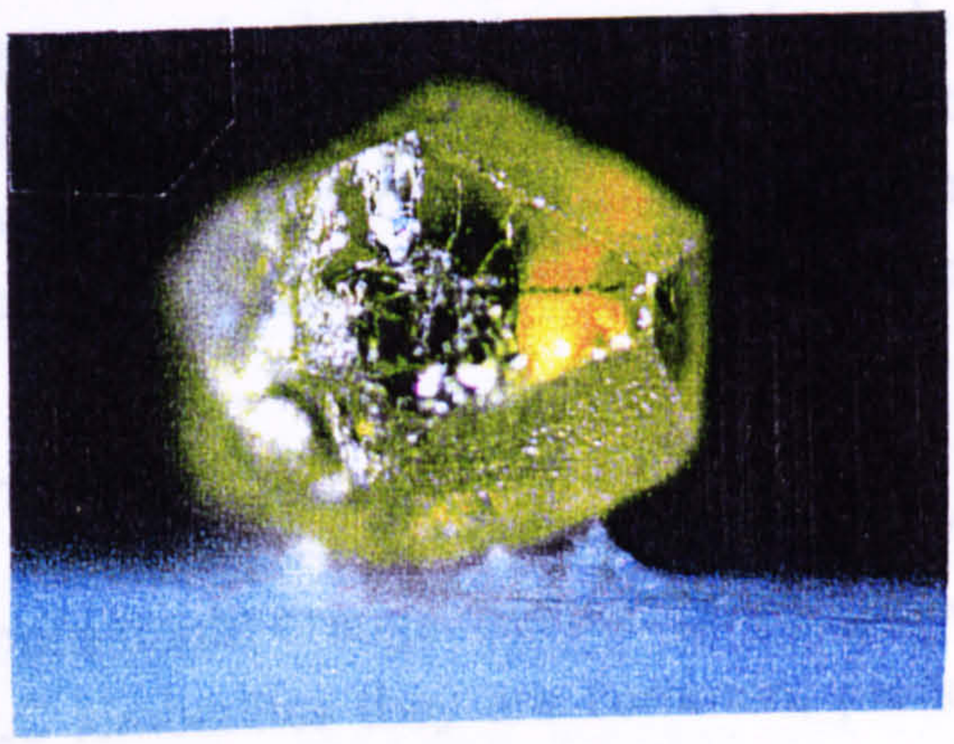

Plate 5.6
0.4mm, synthetic diamond from Borehole OFS93-012. Note the distinctive colour, cubo-octahedral habit and inclusion trail.

bits) were found to be suitable, particularly when drilling through the glacial till overburden. About fifty of these diamonds were recovered during heavy mineral separation, usually during the visual examination of the concentrate stage. As complete crystals they are relatively easy to differentiate from natural stones; cubo-octahedral form, pale to dark yellow colour, colour variations consistent with sector growth, and often magnetic due the to presence of radiating fine black metallic inclusion trails from along cubic points (remains of Ni/Fe catalyst), Figure 5.2.2. Unusually for synthetic diamonds, the surfaces are often frosted and pitted, this may be due to the binding process by which they were attached to the drill bit, and a relatively unusual manufacture, possibly of Japanese origin (pers. comm. Wayne Taylor). Fragments were usually more troublesome in identifying, but the colour, inclusions and sector growth were usually diagnostic.

Carbon isotopes were also analysed to help differentiate the synthetic and natural diamonds. Three of each were selected (from the natural stones; 2-10E-2, 2-10F-1 and 4-13A-1) and $\delta^{13}C$ values were obtained by Dave Mattey at Royal Holloway College, London. The results of the analysis of synthetic stones from FALC were $\delta^{13}C$ -20‰ to -24.4‰. These values are light, and characteristic of synthetic stones grown with modern manufacturing methods. It should be noted, however, that diamonds of eclogitic paragenesis have a range of $\delta^{13}C$ values from +5‰ to -35‰ (Harris, 1987). The diamonds 2-10E-2, 2-10F-1 and 4-13A-1 had $\delta^{13}C$ values of -11.8‰, -5.2‰ and -12.1‰ respectively. The range of *most* diamonds of peridotitic mantle paragenesis is -2‰ to -9‰ (Harris, 1987), but a very small proportion of proven peridotitic diamonds have values higher and lower than the stated range. Thus a tentative assignment of eclogitic paragenesis is made for diamonds 2-10E-2 and 4-13A-1, diamond 2-10F-1 may be either peridotitic or eclogitic. Further discussion of these results, and other analyses measuring nitrogen aggregation state and concentrations in the diamonds can be found in Chapter 6.

5.2.2 Garnets

In amongst the dull grey-green serpentinous bulk of the kimberlite, the resinous bright orange, red and purple garnets are particularly prominent. In the FALC kimberlites they are common, particularly in the reworked pyroclastics, with typical concentrations rising from 10-100g/t in primary airfall tuffs, to 100-1000g/t in graded RPK and tuffaceous clastics (see Chapter 2). Furthermore garnets are also heavy minerals (S.G. 3.2gcm^{-3} to 4.3gcm^{-3}), easily identified from concentrates, and particular garnet types appear to have a correlation with diamonds, and certainly kimberlite. For these reasons a great

deal of research has been carried out on the garnet group, and studies have show a wide variety of compositions and parageneses. Kimberlitic garnets are solid solutions between ideal mineral end-members: pyrope ($Mg_3Al_2Si_3O_{12}$), almandine ($Fe_3Al_2Si_3O_{12}$), grossular ($Ca_3Al_2Si_3O_{12}$), uvarovite ($Ca_3Cr_2Si_3O_{12}$) and knorringite ($Mg_3Cr_2Si_3O_{12}$). Other end member garnet compositions exist in the crust, and can be incorporated into kimberlites as xenoliths, these include almandine, grossular, spessartine, andradite and pyrope. The most commonly used classification of kimberlitic garnets was proposed by Dawson and Stephens (1975), and although flawed (see review in Mitchell, 1986), is still useful and widely accepted today. Garnets are assigned groups based on the best fit of five major element oxides, and is far from rigorous.

Kimberlitic garnet classification of Dawson and Stephens (1975):

Group number	Garnet type	TiO_2	Cr_2O_3	FeO	MgO	CaO
1	titanian pyrope	0.58	1.34	9.32	20.00	4.82
2	high-titanium pyrope	1.09	0.91	9.84	20.30	4.52
3	calcic pyrope-almandine	0.31	0.30	16.49	13.35	6.51
4	Ti, Ca, Mg -rich almandine	0.90	0.08	17.88	9.87	9.41
5	magnesian almandine	0.05	0.03	28.33	7.83	2.44
6	pyrope-grossular almandine	0.24	0.27	10.27	10.38	14.87
7	Fe - Mg uvarovite-grossular	0.29	11.27	5.25	8.61	21.60
8	Fe - Mg grossular	0.25	0.04	6.91	4.69	24.77
9	chrome-pyrope	0.17	3.47	8.01	20.01	5.17
10	low calcium chrome-pyrope	0.04	7.73	6.11	23.16	2.13
11	uvarovite-pyrope	0.51	9.55	7.54	15.89	10.27
12	knorringite uvarovite-pyrope	0.18	15.94	7.47	15.40	9.51

For this thesis the most serious failing of the Dawson and Stephens (1975) classification is that it was generated from a small database of garnets from the South African craton, which may have a significantly different lithosphere to that in Central Saskatchewan. A further general criticism of the classification is that garnets of widely different paragenesis occur in the same group. Because of these problems garnet analyses in this thesis are additionally classified into peridotitic, eclogitic and megacryst fields on a Ca-Fe-Cr ternary diagram, Figure 5.2.3.

Megacrystal suite garnets at FALC are usually equant crystals up to 3cm diameter, red-orange to brown, titanium to chromium pyropes (groups 1, 2 and 9 of the standard garnet classification). Most of the garnets in kimberlite, however, are xenocrystal, sampled from nearly all levels that the kimberlite

Figure 5.2.3

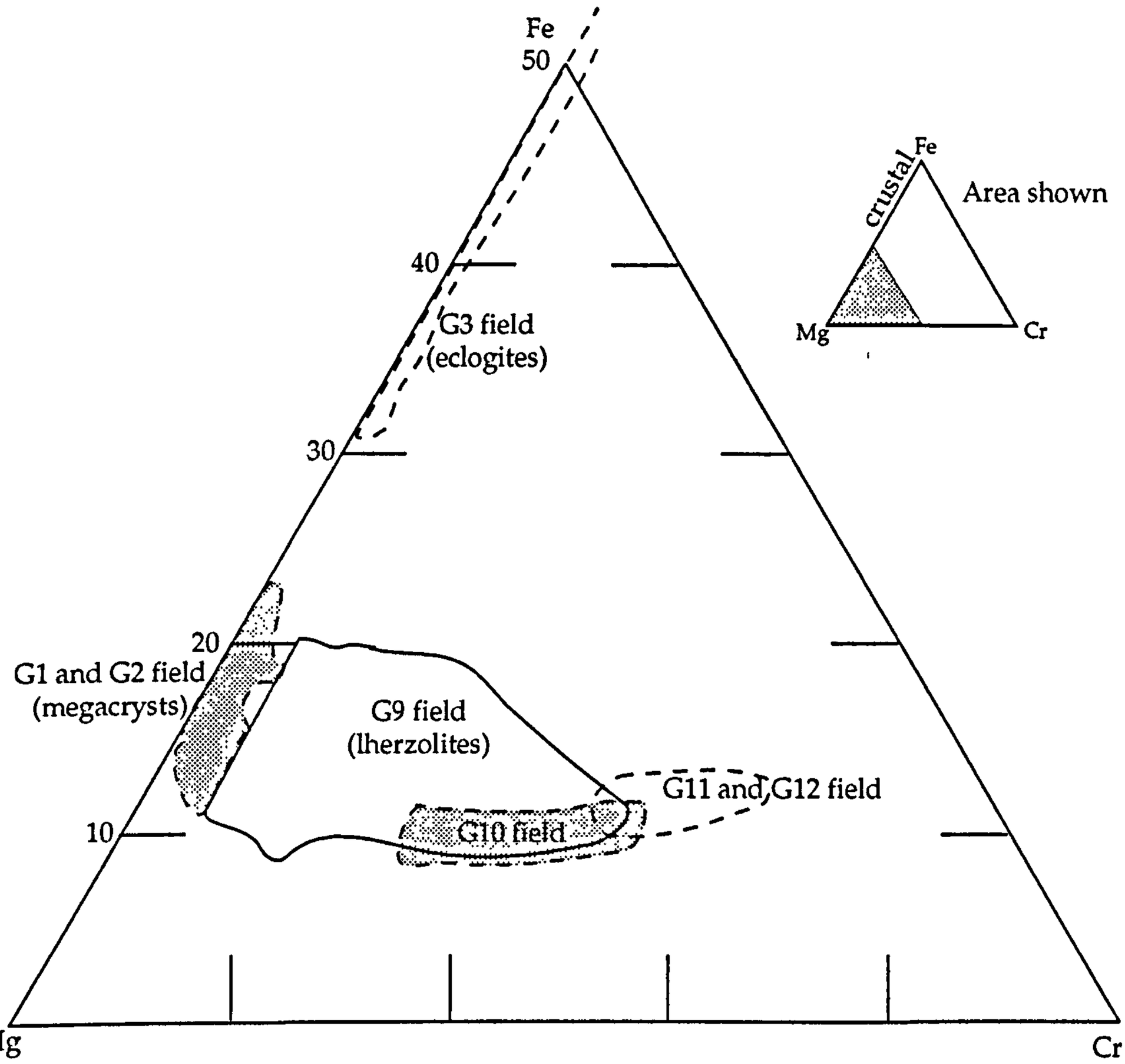

Mg half of Mg-Fe-Cr ternary for FALC garnets, n = 203. Fields aid discrimination of garnet groups as defined by Dawson and Stephens (1975). Main field is the peridotitic group 9 garnets of mostly lherzolitic paragenesis, n = 158. This borders with the group 1 and 2 field of megacrystal paragenesis, n = 18. Data near the overlap area are regarded as of ambiguous origin. The group 10 garnets of harzburgitic paragenesis, n = 18, have considerable overlap with the G9 field, but are easily differentiated by comparing CaO with Cr_2O_3. Groups 11 and 12 are rare, n = 4, and overlap slightly the G9 and G10 fields, but are easily differntiated by their high Cr values. All the garnets described above are dominated by the pyrope end-member, and groups 9, 10, 11 and 12 are Cr-rich. Groups 1 and 2 are also mostly pyropes, but with increasing amounts of almandine towards Fe richer compositions. Eclogite garnets of group 3, n = 5, contain very little Cr, and plot as pyrope almandines along the Mg-Fe axis.

traverses on its way to the surface, particularly in the lower lithosphere and crust. The sub-crustal lithosphere consists spinel lherzolites to around 80km depth, and at greater depths the stable aluminous phase is garnet, down in to the asthenosphere (probably at about 190km in the Cretaceous Central Saskatchewan region, see Chapter 6). These peridotitic garnets include chromium rich, calcic and magnesian pyropes and uvarovite-pyropes of groups 7, 9, 10, 11 and 12. The pyropes at FALC are typically purple to red, and this group is dominated by group 9 (G9) garnet. The remainder of the mantle garnets are derived from the eclogitic areas considered to be unevenly distributed in the lithosphere. In the FALC kimberlites the eclogitic suite includes pyrope almandines (G3 and G5). Other eclogite types described in the literature include garnet groups 3 to 6 and 8 (Mitchell, 1986).

The aim of the selection process for the garnets was *not* to provide a statistical distribution of garnet types and parageneses. Most of the garnets picked were purple to wine red pyropes, selected to determine to presence of G10 garnets, which are considered a good indicator as to the presence of diamonds, because they are compositionally similar to garnet inclusions in diamonds (Gurney, 1984). These were analysed by electron microprobe and checked to be of G9 or G10 composition (peridotitic paragenesis), and were then sent to W.L. Griffin at CSIRO (Australia) for proton-probe analysis, which provides data for geothermometry estimates, see Chapter 6.

A statistical distribution of the paragenses, however, can be estimated roughly from the visual garnet colour data collected in the OFS separation, and comparing these colours to the composition when probed. For example, about 60% of the orange garnets probed were of megacryst composition. The approximate distribution for all FALC kimberlites (crater, proximal and distal facies) is as follows, crustal garnets 13%, megacryst garnets 24%, peridotitic garnets 45% and eclogitic garnets 18%. Kimberlite from all the boreholes closely conform with these averages (range within ±3% of stated values) apart from OFS 93-009 (proximal facies, on the eastern edge of the main FALC cluster), which has the following distribution, crustal garnets 15%, megacryst garnets 33%, peridotitic garnets 30% and eclogitic garnets 22%.

In total 203 garnets from the four parageneses described above have been analysed by microprobe, 18 of the megacryst suite, 175 peridotitic (mostly Cr-pyropes), 7 eclogitic (mostly pyropes-almandines) and 1 crustal. These four groups are discussed below.

Megacryst garnets

Eighteen of the garnets analysed had a group 1 or 2 chemistry, these were mostly orange, but more rarely brown and red in colour, and are usually quite large fragments (mostly around 1mm). It should be noted that the more Cr-rich megacrysts grade into the G9 classification composition, and cannot be easily differentiated from peridotitic garnets of similar composition. In this thesis a Cr_2O_3 cut-off of about 2.8% for megacrysts was selected (assuming relatively high TiO_2 was also present) . Most of the grains of this group that were picked and tested were thought to be of eclogitic composition, as they were usually bright orange. Results indicated the majority of these were Cr-poor pyropes of the megacryst suite.

The megacryst garnets are not of comparable composition to those from kimberlites from the Wyoming craton (Eggler et al, 1979) although TiO_2 is notably high in the higher chrome samples, Figure 5.2.4, a trend that may indicate Ti-metasomatism in the mantle (P.H. Nixon, pers. comm.).

Figure 5.2.4

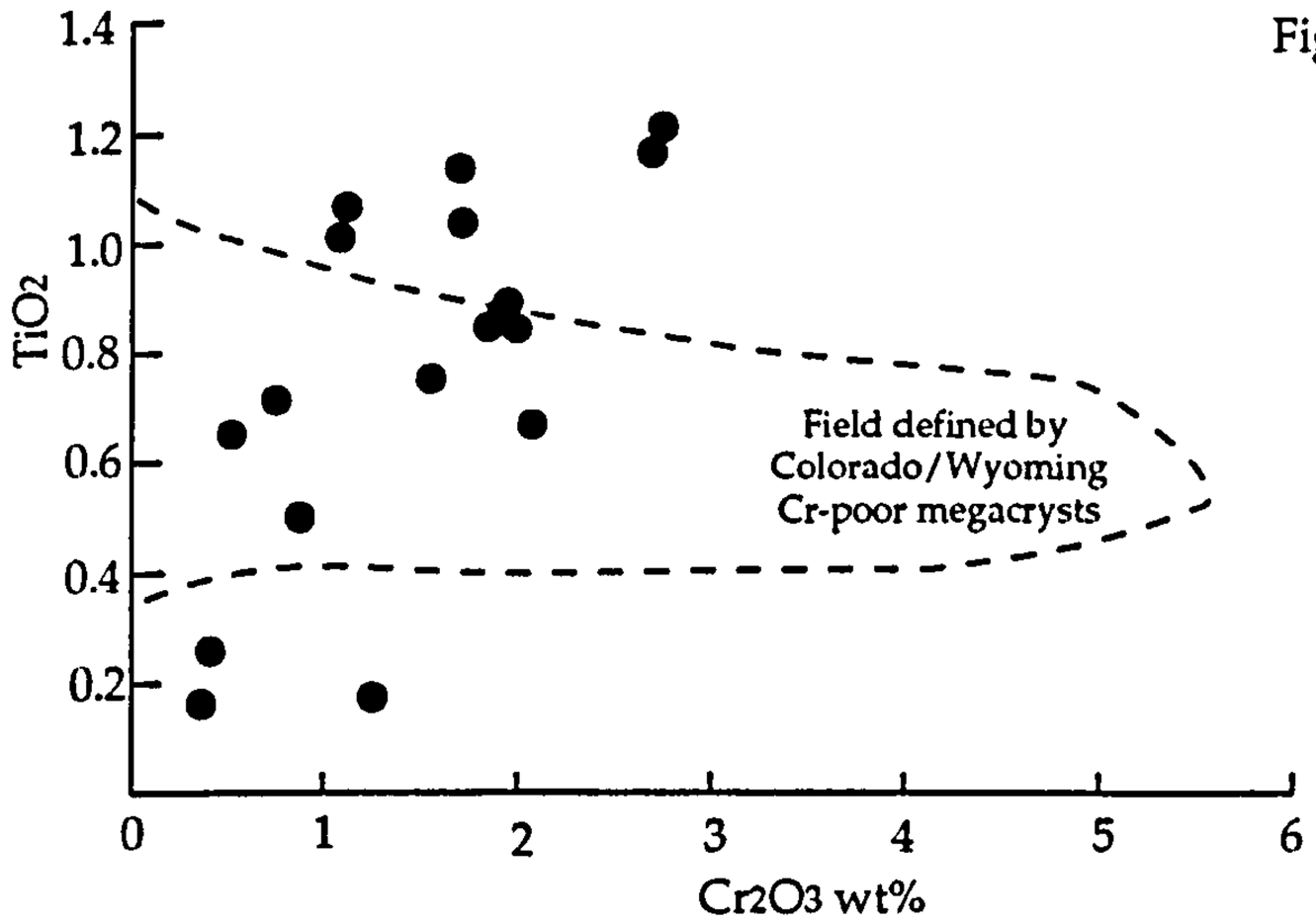

Megacryst garnets from FALC, n = 18, showing a proportional increase of TiO_2 with Cr_2O_3. Compare to Wyoming craton that shows constant TiO_2 values (Eggler et al, 1979).

In all kimberlites a range of Mg-Fe contents in megacryst garnet composition occurs, Figure 5.2.5, and FALC is no exception, with a trend running between 15% and 22% Fe end member (almandine molecule).

Figure 5.2.5

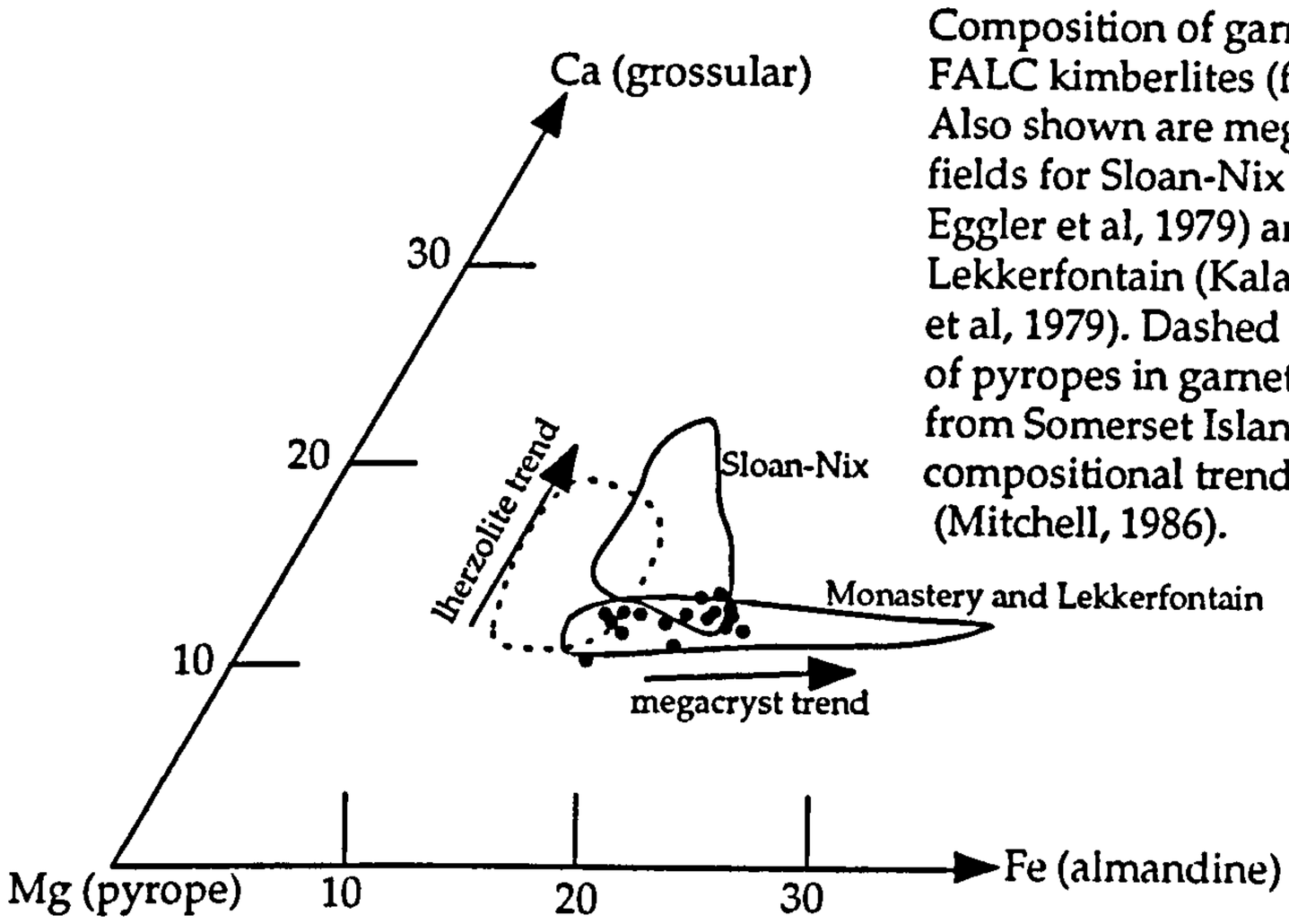

Composition of garnet megacrysts in FALC kimberlites (filled circles), n = 18. Also shown are megacryst composition fields for Sloan-Nix (Wyoming craton; Eggler et al, 1979) and Monastery-Lekkerfontain (Kalahari craton; Gurney et al, 1979). Dashed field indicates range of pyropes in garnet lherzolite xenoliths from Somerset Island, and their compositional trend (arrows) (Mitchell, 1986).

It is interesting to note the slightly sub-calcic nature of the megacrysts at FALC compared to those from the Wyoming craton, but show good correlation with South African megacrysts. The compositional trend of megacryst garnets have been used as evidence, along with melting experiments (Green and Sobolev, 1975), of a phenocrystal origin of the megacrysts (Mitchell, 1986).

Peridotitic garnets

The garnets are represented at FALC by groups 9, 10, 11 and 12, and occur as mainly equant grains in a wide range of sizes from very fine (0.1mm) to medium (1mm). They are coloured from deep red to deep purple, and easily differentiated from the crustal pale purple garnets by the intensity of colour and their presence in the non-magnetic fractions. At total of 158 peridotitic garnets were analysed, one of which was a uvarovite, and three were grey knorringites, the rest were Cr-pyropes of G9 and G10 composition. These are plotted below (along with the Cr-poor garnets of non-peridotitic paragenesis) on the standard Cr_2O_3 vs CaO graph (Sobolev et al, 1973), Figure 5.2.6, with discriminant fields for lherzolite, harzburgite and peridotitic diamond inclusions (PDI) from Gurney (1984).

Figure 5.2.6

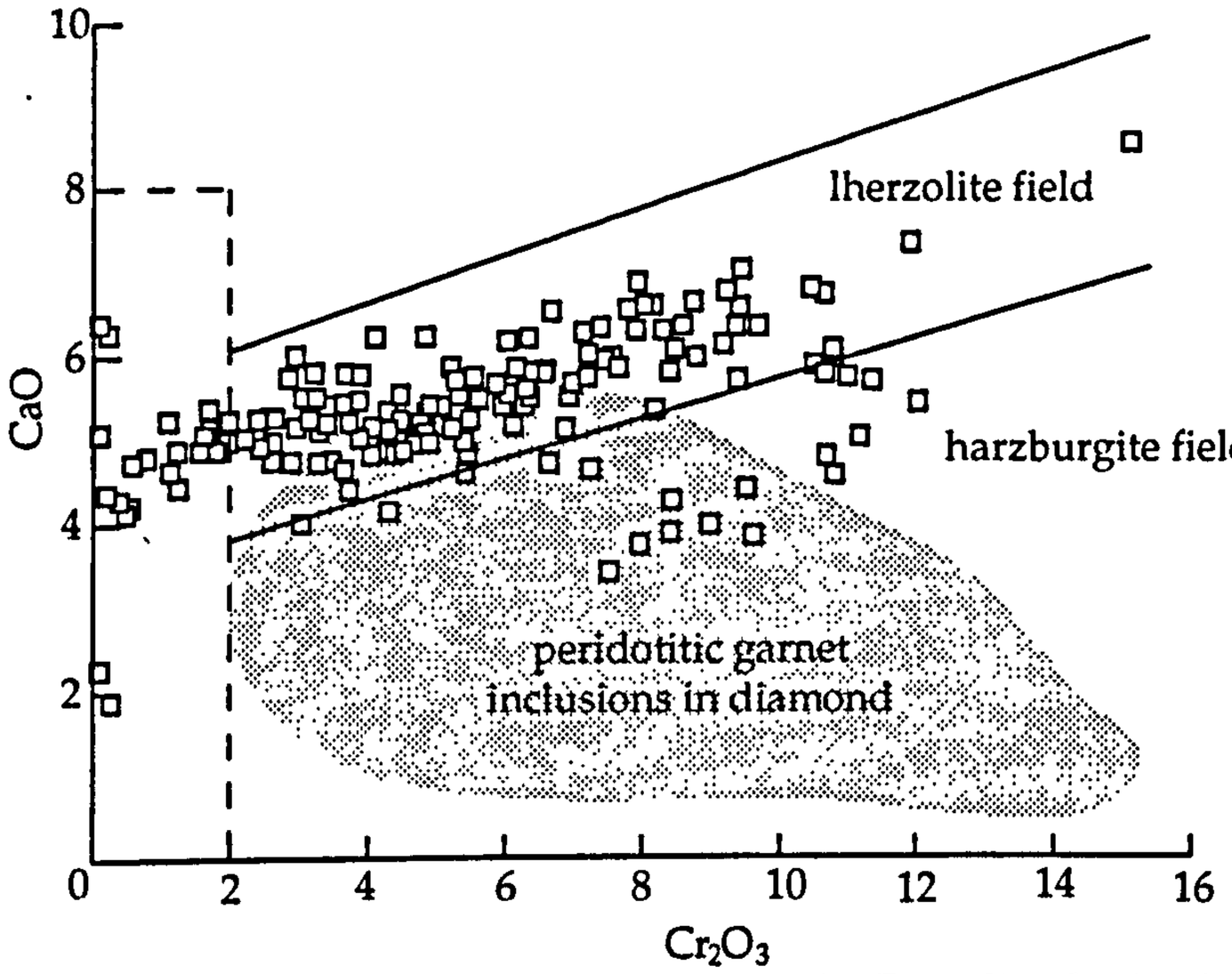

Cr-Ca comparison for FALC garnets, n = 203. Data distribution is typical of kimberlite world-wide, with Cr-poor garnets (<2%) of mainly megacryst origin, garnets between the two lines delineating lherzolitic origin (G9), and Ca-poor garnets below the line of harzburgitic origin (G10), after Sobolev et al (1973). The shaded area represents the compositional range of peridotitic garnets found as inclusions in diamonds (Gurney and Moore, 1993). Data in this field are considered good indicators of diamondiferous kimberlite.

Note that 11 of the garnets (7.2%) fall well within the calcium depleted harzburgite trend, and a further 11 are borderline cases. This is a relatively large proportion of the garnets, and indicates that a relatively large volume of depleted (Ca-poor, Cr-rich) peridotitic lithosphere was sampled by the ascending kimberlite. Most of the harzburgitic and a great deal of the lherzolitic garnets fall within the field of peridotitic inclusions in diamond (PDI). This reflects favourably on the diamond potential for the kimberlite, and is further discussed in Chapters 6 and 7.

Five peridotitic garnets, of G9 composition, were in composite grain pairs with amphibole of a high Cr, Al and Na composition. The garnets are otherwise unremarkable, although their Na contents were not analysed. These mantle amphiboles are fairly rare, but do occur at upper lithospheric levels, and indicate portions of the mantle are hydrated (amphibolite bearing) garnet lherzolites.

Garnets of the peridotitic paragenesis (and some megacrysts) often displayed an alteration corona termed a kelyphitic rim or rind. These pale to dark green or brown rims are typically <1mm thick, and consist of ultra-fine (2-5µm thick, 100's µm long) acicular, radiating phlogopite (70%), serpentine, Ni-pyrite, Ti-magnetite, ilmenite and calcite. This composition is in contrast to

most reported rinds, which are mainly composed of pyroxenes, spinel, phlogopite and serpentine, formed at high temperature and pressure (Garvie and Robinson, 1982). Due to the highly altered nature of the FALC kimberlites, the kelyphite assemblage observed may represent an alteration of the more usual composition, pyroxenes, in particular, are prone to diagenetic alteration. Removal of the delicate rind, by magmatic, volcanic or sedimentary means, leaves a pitted and corroded surface on the pyrope, a feature commonly observed on the FALC peridotitic garnets.

Eclogitic garnets

Only 7 of the garnets analysed had an eclogitic composition, these were mostly orange-red to purple, equant and medium grained (0.5mm to 1mm). Many more orange garnets were selected with the aim of examining eclogitic compositions, but when analysed most of these proved to be megacrystal titanian pyropes (see above). One of the garnets was a green magnesian almandine (G5), the rest were calcic pyrope-almandines (G3). Two of the G3 garnets occurred with pyroxenes (Cr-diopsides, and a separate grain attached to an omphacite), further illustrating the composition of the FALC eclogites.

5.2.3 Ilmenite

Magnesian ilmenite is another characteristic mineral easily distinguished in the kimberlite at FALC, with the grey-silver metallic lustre contrasting sharply with the dull green bulk of the kimberlite. Kimberlitic ilmenite has variable compositions on a solid-solution trend between geikielite ($MgTiO_3$), ilmenite ($FeTiO_3$) and hematite (Fe_2O_3). In the FALC kimberlites ilmenite is even more common than garnet, with concentrations of 100-1000g/t in primary airfall tuffs, rising to around 10,000g/t in reworked kimberlitic strata (a finely bedded reworked pyroclastic sand in borehole 003 has 21,000g/t ilmenite, 2.1% by weight of the bulk rock). In total 101 ilmenites (mostly magnesian rich) have been microprobed, 34 of which were analysed from polished thin sections of kimberlite, rather than disaggregated grains mounted in to blocks. This has allowed chemical analysis relative to their *in situ* characteristics to be compared.

Several parageneses have been proposed for ilmenite (Mitchell, 1986 and Mitchell, 1995), mainly as megacrysts, megacrystal intergrowths (with pyroxenes, spinel, rutile and perovskite), inclusions in silicate megacrysts and groundmass. In the FALC kimberlites, five morphologies (with distinct chemistry) have been noted, these are; megacryst (shard) ilmenite, matrix (corroded) ilmenite, ilmenite exsolving spinel (1 example), aggregated ilmenite (1

example) and non-magnesian ilmenite of crustal origin. MgO vs Cr_2O_3 for all ilmenite data is plotted below, see Figure 5.2.7. There is a good correlation to the proposed 'Cr-Mg' parabola which suggests consistent chemical variation (Haggerty, 1975), apart from the non-magnesian ilmenites (of crustal origin).

Figure 5.2.7

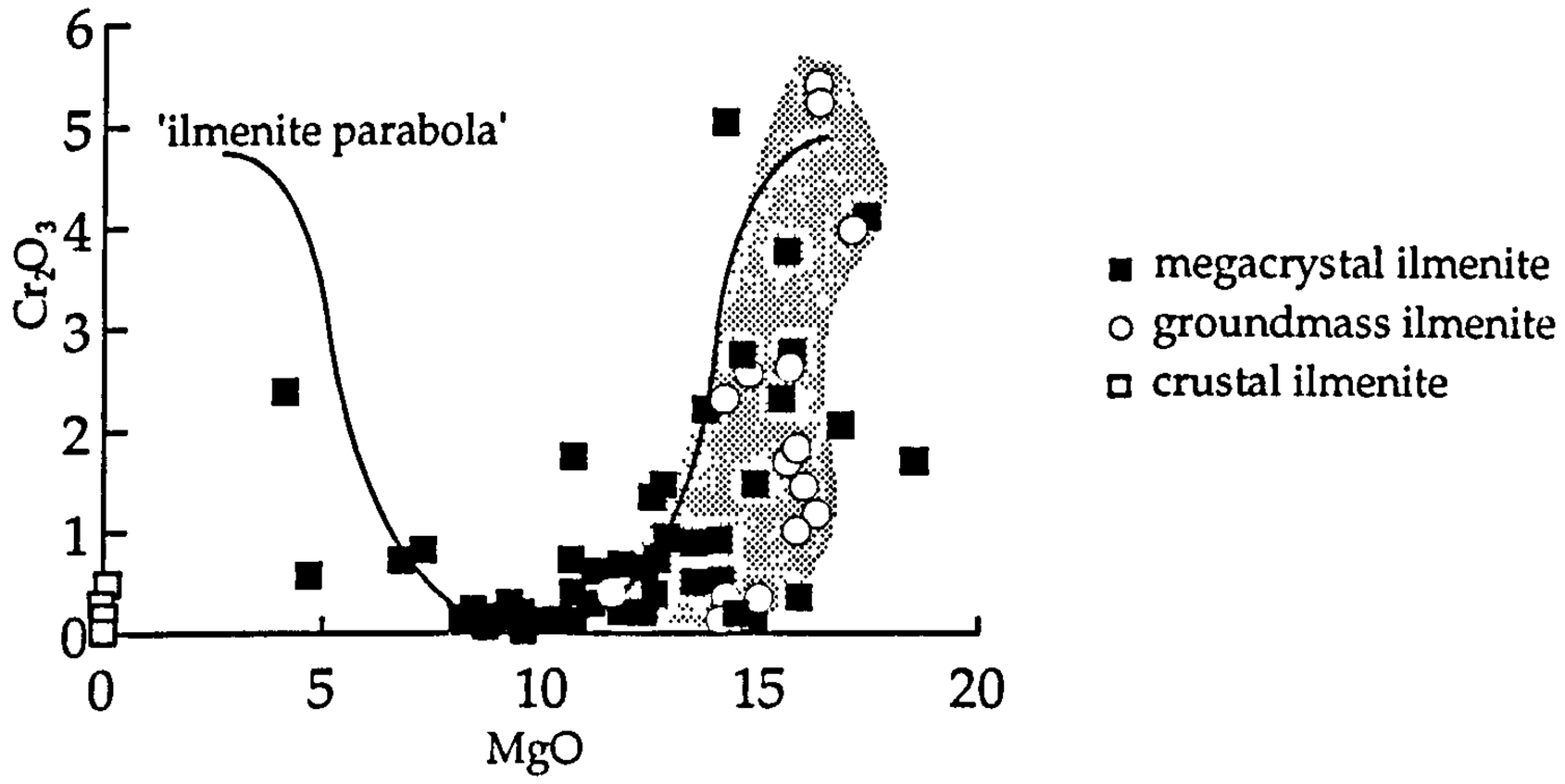

Cr-Mg proportions showing all FALC ilmenite data, n = 98. Line shows ilmenite parabola, a hypothetical compositional relationship of ilmenite Mg and Cr, which FALC samples appear to conform to (Haggerty, 1975). Shaded field shown is for groundmass ilmenite.

A fine white to brown, pimply surficial coating was present on many of the ilmenites observed in the heavy mineral concentrates. The coating (termed leucoxene) consists of various minerals, such as rutile, perovskite and pyrophanite. The perovskite ($CaTiO_3$) is a major repository of rare earth elements (REE) in kimberlite, with typical concentrations of 1.2% Nb_2O_5 and 1.5% Ce_2O_3 in the FALC samples. Pyrophanite is the Mn member of the ilmenite solid-solution series, $MnTiO_3$, and is present on the rims of some ilmenites at up to 5% MnO. Such large amounts of pyrophanite is rare in kimberlites, and has been attributed to a carbonatite component in the melt (Gaspar and Wyllie, 1984), but this is unclear. Other authors suggest the Mn enrichment at the rims is due to late-stage magmatic fluids (Haggarty, 1989) or post-emplacement alteration (Mitchell, 1995).

Megacryst (shard) ilmenite

These grains are easily recognised in the borehole core, up to 3cm across in the primary airfall tuff deposits (PK, see Chapter 2). These large grains are rounded, but often internally fractured. In both reworked and primary

kimberlite deposits these large grains are disaggregated into conchoidal fracture fragments 0.1mm to 1mm long, producing the shard texture observed, Figure 5.2.8. The chemistry of these ilmenites is typified by low Cr_2O_3 (<2%) and moderate MgO (7% to 14%), see Figure 5.2.7 above.

These again partially describe the Cr-Mg parabola (Haggerty 1975), and are of comparable composition to Colorado-Wyoming kimberlites (Eggler et al, 1979) and for the macrocryst field of the Mayeng sill, South Africa (Apter et al, 1984). The high-Cr data point falls in the overlap of the macrocryst, matrix and inclusion type fields of the Mayeng sill population.

Although ilmenite is not regarded as a diamond indicator, it has been proposed (Haggerty, 1989) that it could be a diamond preservation indicator based on calculations of fO_2 (oxygen fugacity at time of formation). Ilmenite crystallising from proto-kimberlite melts, which later incorporated diamonds from the lower lithosphere, can indicate whether diamonds are likely to be preserved (low fO_2 reducing environment), or destroyed (high fO_2 oxidising environment). Figure 5.2.9 illustrates the ilmenites following the magmatic trend of magnesium enrichment, correlating to decreasing fO_2, and therefore a more reducing environment. This indicates a good diamond preservation potential.

Matrix (corroded) ilmenite

These ilmenites were distinct from the megacryst type, being fine grained (0.02mm to 0.2mm), sub- to euhedral, and often corroded and/or overgrown, Figure 5.2.8. Chemically they are Cr_2O_3 rich (>1.5%) and MgO rich (>11%), see Figure 5.2.7 above.

The data points partially describe the Cr-Mg parabola (Haggerty, 1975), and are of comparable composition to Elliot County (Kentucky) kimberlites (Agee et al, 1982). The matrix field of the Mayeng sill, South Africa (shown dashed; Apter et al, 1984) does not cover the majority of the points, and illustrates a significant departure of the matrix ilmenite composition at FALC from South African norms. This may be partly due to the corrosion and alteration effects which act to lower the Cr_2O_3 values, and raise Fe_2O_3. From analysis of cross-cutting relationships of diagenetic mineral growth, this rim alteration is before the post-emplacement serpentinisation, and therefore a magmatic effect (see Chapter 2).

These grains are often altered to magnetite (see below) and ilmenites of a different composition at the rims, which are characterised by the dominance of the $FeTiO_3$ end-member, having <0.1% MgO, Fe_2O_3, Cr_2O_3 and Al_2O_3. These

Figure 5.2.8

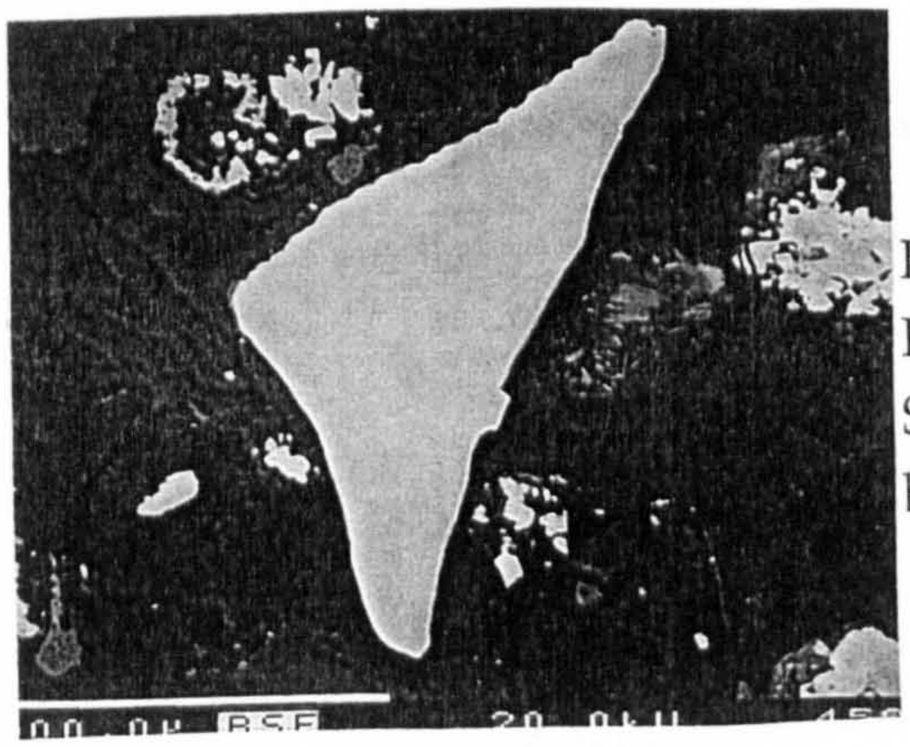

Plate 5.7
From OFS93-004, 107.0m, medium tuff. Shard of megacrystal ilmenite, scale bar is 100microns.

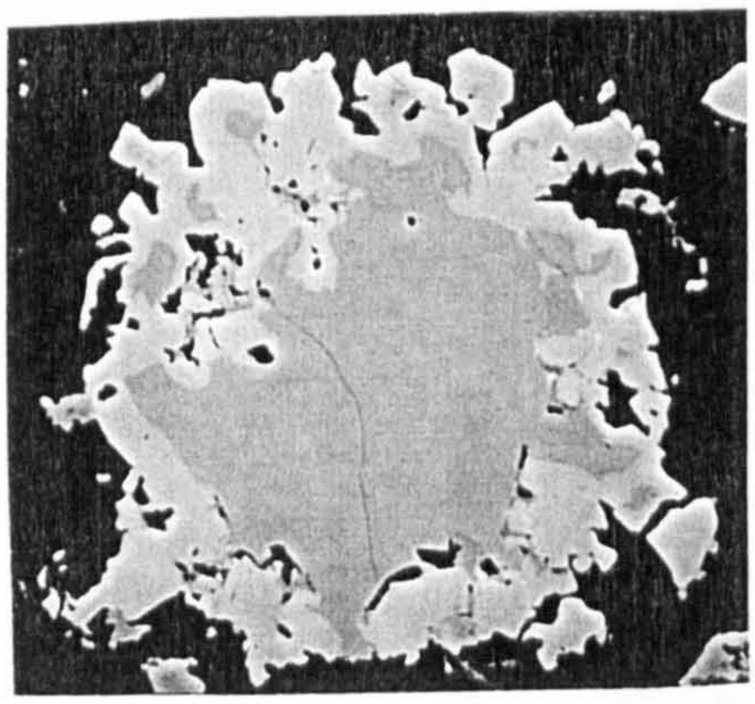

Plate 5.8
From OFS93-004, 107.0m, medium tuff. Corroded ilmenite with altered rims, grain is 300microns across.

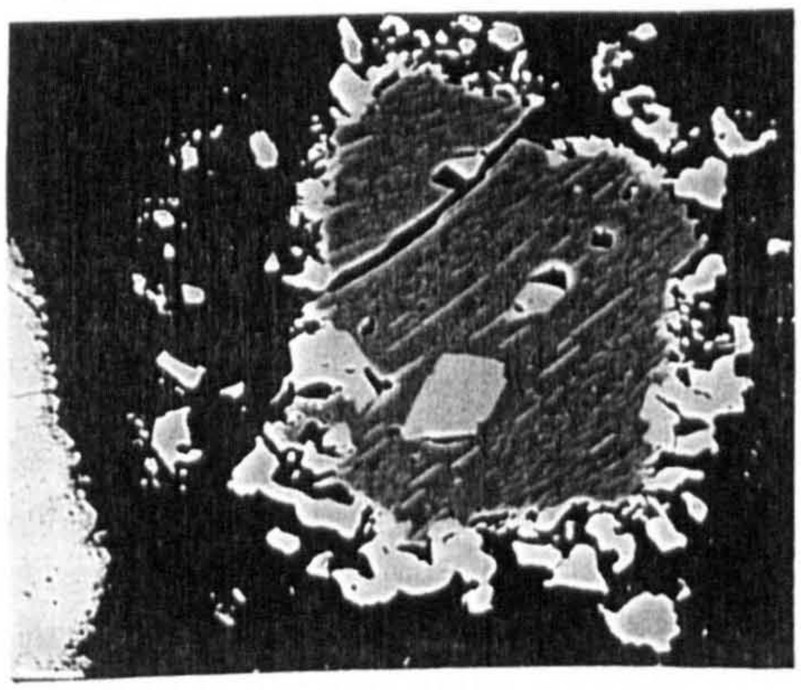

Plate 5.9
From OFS93-002, 112.9m, Coarse tuff. Ilmenite exsolving and rimmed by spinel. Note the euhedral spinel inclusions. Scale bar is 50microns.

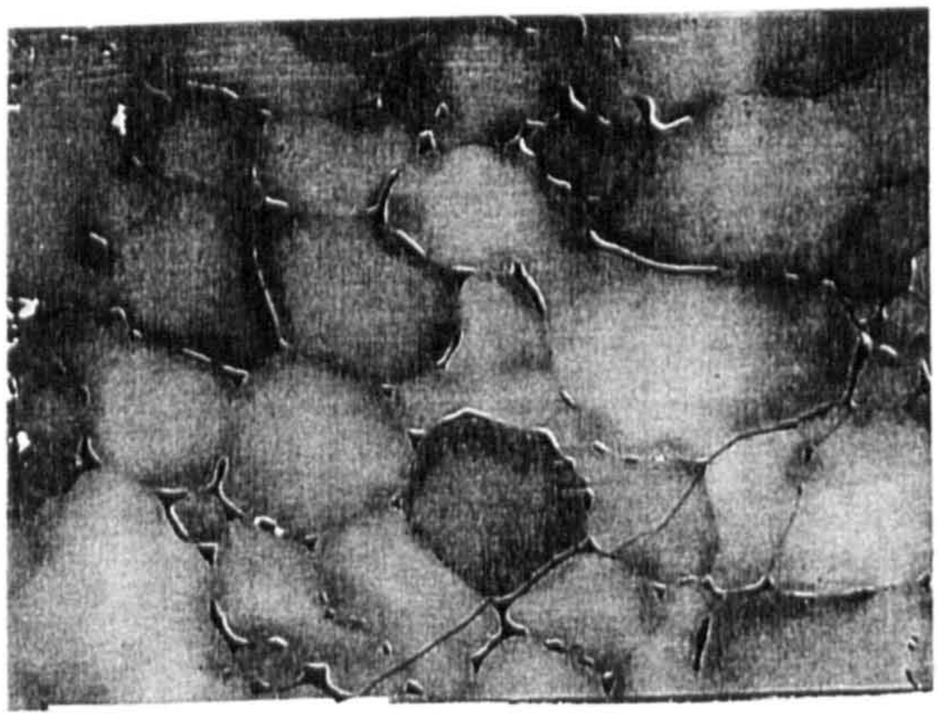

Plate 5.10
From OFS93-004, 95.3m, bedded reworked pyroclastic sand. Large (2mm) ilmenite with zoned globular segregations and interstitial spinel (black). Scale bar is 200microns

Figure 5.2.9

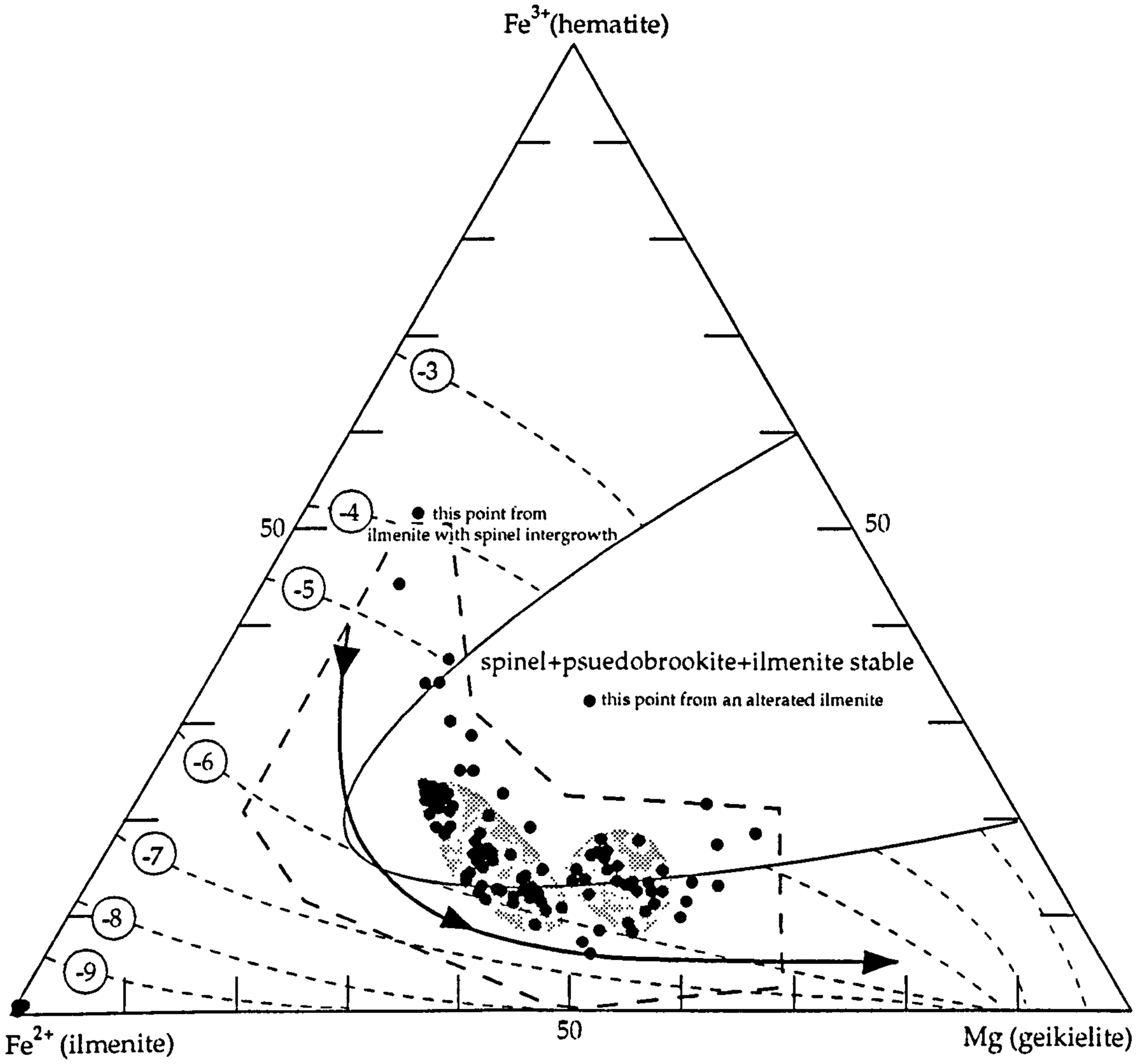

Ilmenite compositions from FALC kimberlites, showing phase relationships and contours of oxygen fugacity (dashed), 90% of FALC data has a projected fO2 during crystallisation of -5 to -6. Shaded area contains 80% of the FALC data. Pure ilmenite compositions (4% of the data) are from crustal xenocrysts. Heavy dashed field is the global range of kimberlite megacrysts. Heavy arrowed trend is the magmatic crystallisation trend (Haggerty et al, 1979), to which FALC data corresponds.

are thought to represent overgrowth at a very late stage of magma ascent, probably at the crustal levels.

Ilmenite exsolving spinel and polycrystalline ilmenite

One grain of ilmenite with spinel exsolution lamellae was observed on a polished section of a primary airfall coarse tuff (112.29m) from borehole OFS 93-002, Figure 5.2.8. The grain is 0.4mm long and probably had a euhedral form before exsolution around the rim and internal lamellae disrupted the grain boundary. Additionally, large (0.1mm) euhedral spinel inclusions (by exsolution) developed, aligned parallel with the lamellae.

The polycrystalline ilmenite grain was separated from a glacial till immediately overlying the kimberlite strata in borehole OFS 93-004, and consists of a globular texture, again with small amounts of interstitial spinel, Figure 5.2.8. The ilmenite chemistry is consistent with a megacrystal composition: 13.93% MgO 0.26% Cr_2O_3 and the grain is a shard fragment 1.8mm long, undoubtedly of kimberlitic origin. The compositions of the two ilmenites and their exsolved spinels are given below.

Table 5.3

	euhedral ilmenite	exsolved spinel	polycryst. ilmenite	interstitial spinel
TiO_2	55.55	20.85	53.35	25.81
Al_2O_3	0.00	4.55	0.62	3.22
Cr_2O_3	2.12	14.78	0.26	1.68
Fe_2O_3	5.59	17.44	7.94	22.14
FeO	18.39	28.70	22.83	31.86
MnO	0.98	0.96	0.34	0.87
MgO	16.72	14.10	13.93	14.77
NiO	0.08	0.13	0.13	0.29
CaO	0.09	0.04	0.03	0.08
Total	99.52	101.55	99.45	100.73
Fe^{2+} num	39.4	54.1	55.0	66.7
Type:	gk-rich ilm	Cr-Mg magnetite-ulvospinel	gk-rich ilm	Mg magnetite-ulvospinel

Exsolution of spinel from ilmenite is relatively common, and has been described in South African and Russian kimberlites. It is generally agreed the exsolution occurs by the sub-solidus reaction of ilmenite in response to a decrease in temperature and/or oxygen fugacity (Mitchell, 1986). This is perhaps immediately prior to the ascent of the kimberlite magma from the lower lithosphere.

Non-magnesian ilmenite

These 4 ilmenites are crustal grains, illustrated by their non-Mg/Cr compositions, and have a similar chemistry, dominated by the $FeTiO_3$ end member. The crustal grains lack the leucoxene coating, and are medium grained (0.5mm to1mm) and sub- to euhedral. These ilmenites are xenocrysts from the underlying crust, probably derived from basic metaplutonics and gniesses.

5.2.4 Spinel - chromite and magnetite

Chromite, or chromium spinel, is a common constituent of most kimberlites, with megacrystal and groundmass and peridotitic paragenesis, but is relatively rare at FALC. Spinels are usually complex mixtures of numerous end members, eight of which are typically seen in kimberlites: magnesiochromite, chromite, spinel, hercynite, magnesian ulvospinel, ulvospinel, magnesioferrite and magnetite. The chemistry of the FALC spinels is dominated by three main end member mixes: magnesiochromites, $MgCr_2O_4$ (mixed with chromite, $FeCr_2O_4$, and some ulvospinel, Fe_2TiO_4), magnetite-magnesian ulvospinel (Fe_3O_4 and Mg_2TiO_4) and pure magnetite (Fe_3O_4). Individual spinel grains are fairly rare, and often corroded and/or overgrown with irregular to euhedral magnetite-magnesian ulvospinels. Magnetite is very common, especially in reworked kimberlite sands, and is usually associated with diagenetic mineral growth in serpentinisation (formed from iron released from the altering olivine) and later remobilisation textures (pure magnetite and hematite, Figure 5.2.10 and Chapter 2). These three distinct spinel groups can be distinguished on the magnetite (Fe^{3+})-chromite (Cr)-ulvospinel (Ti) ternary diagram, Figure 5.2.11.

Figure 5.2.11

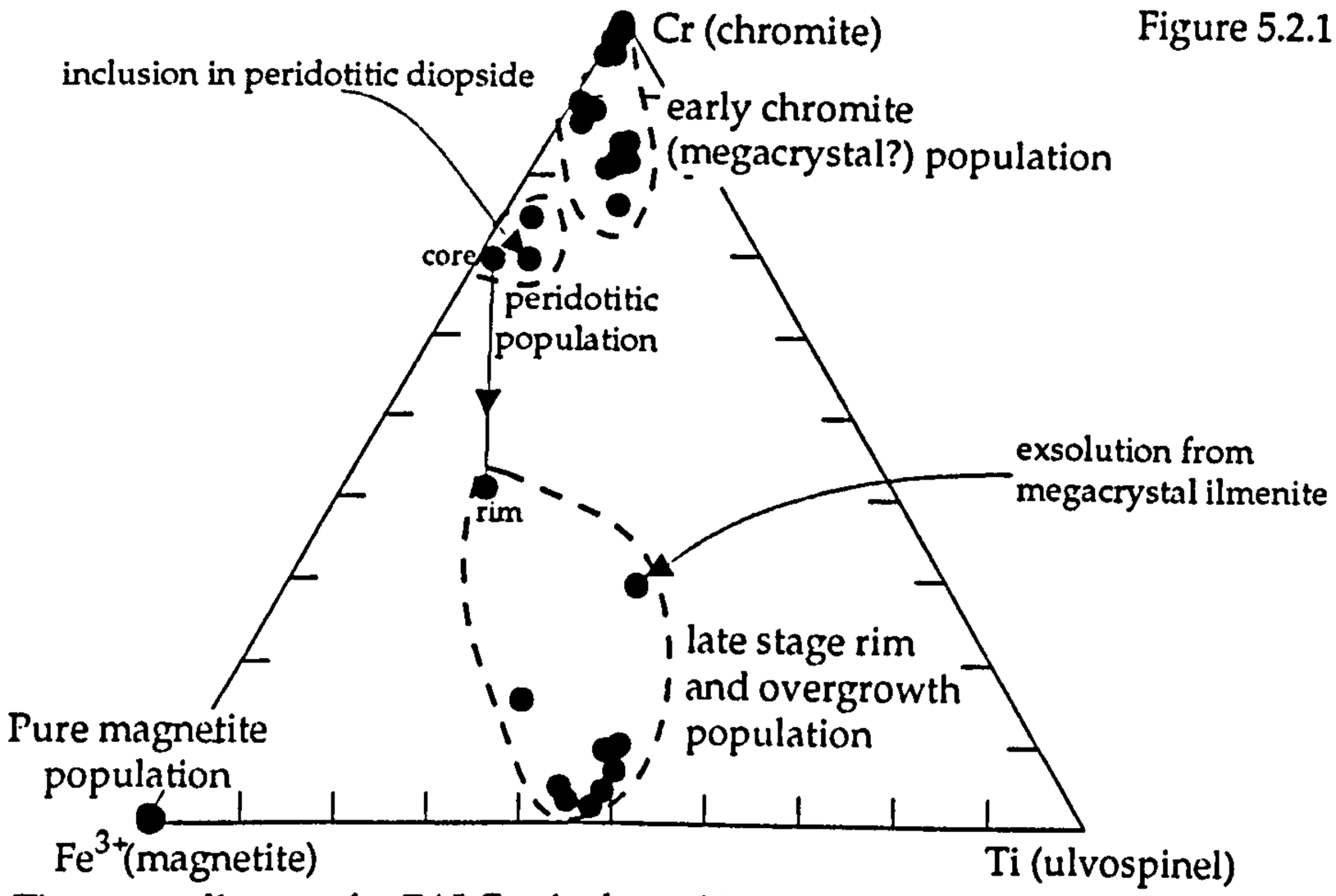

Fe^{3+}-Cr-Ti ternary diagram for FALC spinels, n=34. Parageneses assigned to the chromites are tentative, the peridoititc field is defined by one analysis from a spinel inclusion in a peridotitic Cr diopside. Four data points are of pure magnetite composition.

Figure 5.2.10

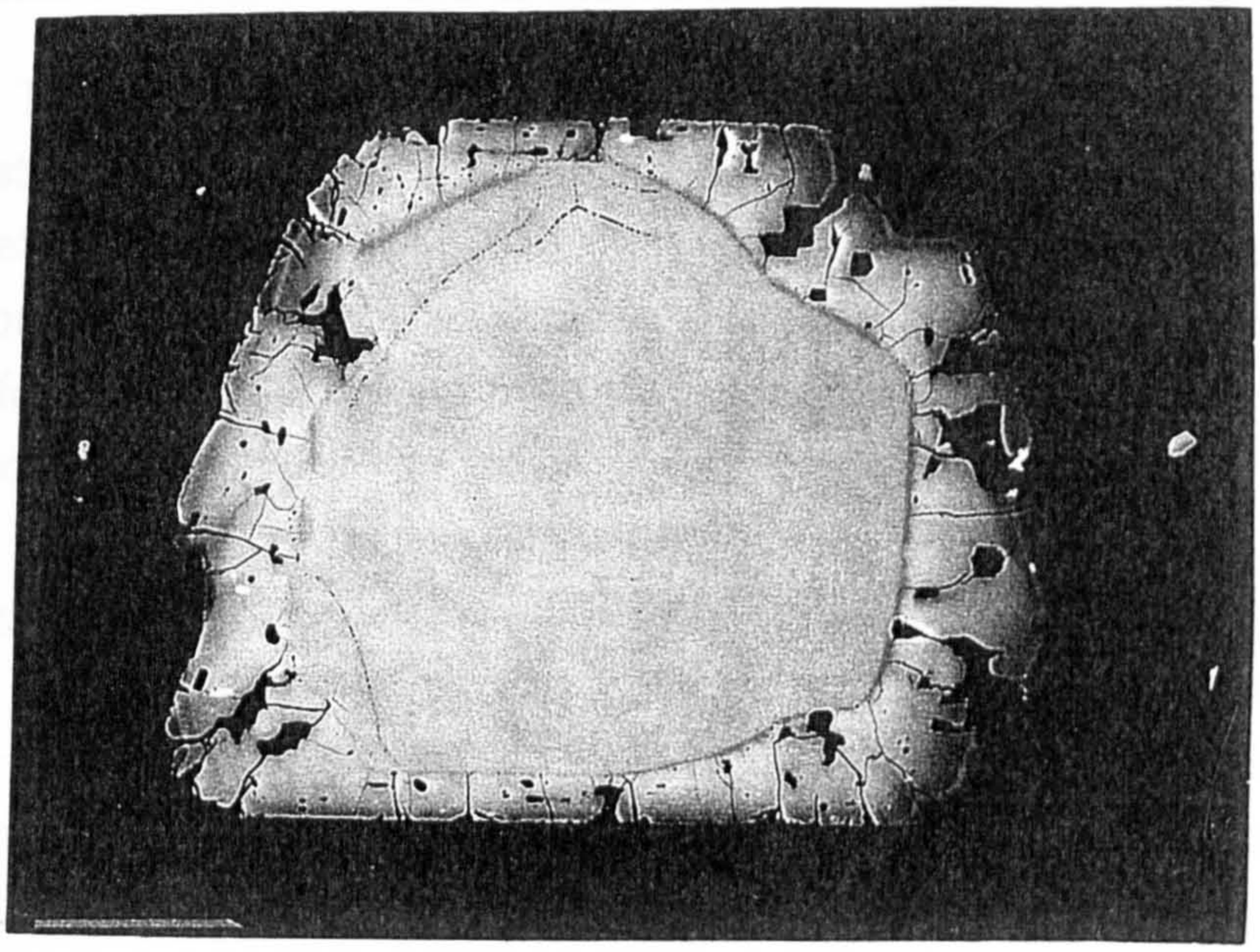

Plate 5.11
From OFS93-012, 203.9m, crystal-dominated lapilli tuff. Central megacrystal chromite-spinel, imperfectly overgrown by euhedral ulvospinel-maghemite. Scale bar is 100microns.

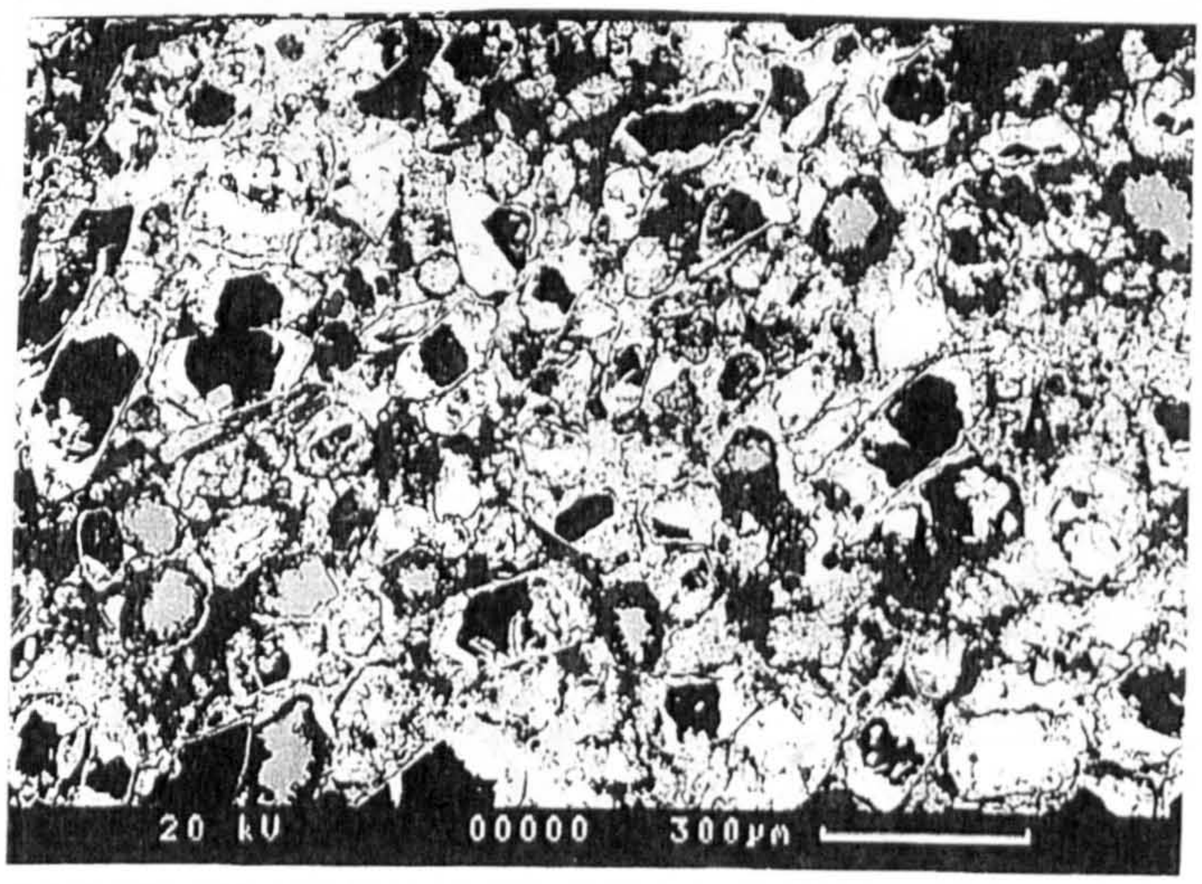

Plate 5.12
From OFS93-002, 107.7m, coarse lag of a graded pyroclastic sand. Pseudomorphic and cementing magnetite (brightest) after olivine in a magnetite 'bleb'. Note the copious ilmenite grains (light grey, lower left and upper right). Scale bar is 300microns.

The evidence for specific parageneses of individual spinel grains from the chemistry alone is scant, although trace elemental analysis has been shown to be useful (Griffin et al, 1995), this method, however, requires a proton microprobe that was not available in this study. Where grain associations are clear, for example, exsolving from megacrystal ilmenite, a specific origin can be inferred.

Magnesiochromites

The only common occurrences of chromite grains at FALC are seen in crater facies kimberlite and some proximal airfall tuffs, typically as fine to medium grained (0.2mm to 1mm) sub- to anhedral magnesian chromites (see Figure 5.2.10). Even from these strata relatively few chromites were isolated (compared to ilmenite). Results from the analysis of 26 chrome-spinel grains show a range of 24% to 58% Cr_2O_3, below the usual diamond indicator value of 62.5% (Gurney and Moore, 1993). The composition is typically kimberlitic, Figure 5.2.12.

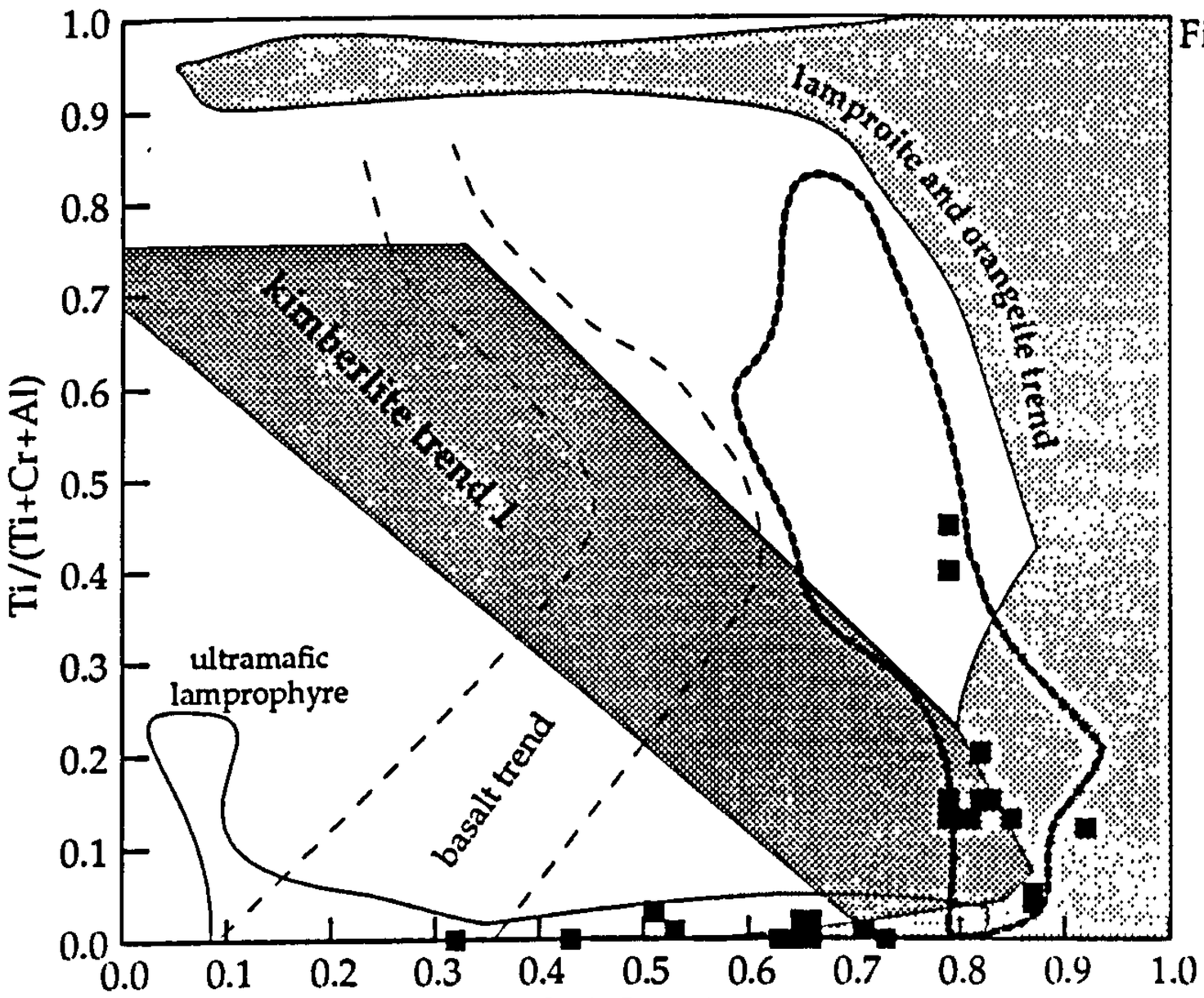

Figure 5.2.12

Cr and Ti proportions relative to other major elements in spinels from FALC, n = 26, trends are from Mitchell (1995). Although 14 of the data fall into kimberlite trend 1 or kimberlite trend 2 (heavy dotted field), 12 are sub-chromic. 5 of these have a chemistry within the field of lamproites and orangeites, the remaining seven are in the ultramafic lamprophyre field (solid-line unornamented field), although one may be of basaltic origin (crustal). This may indicate some of the spinels in the FALC kimberlites have a more alkaline origin, perhaps at shallower levels of the lithosphere, or are from spinel lherzolites.

The paragenesis of the Cr-spinels cannot be determined, unless associated with other minerals. For example the presence of magnetite-magnesian ulvospinel rims around many of the crystals indicates these core spinels were not in chemical equilibrium with later magmas which precipitated the rims. This suggests an early genesis of the cores, and other authors usually attribute them to the megacrystal suite (Mitchell, 1995), but others propose an entirely xenolithic origin (from lherzolites; Shee, 1984).

Magnetite- magnesian ulvospinel

These spinels were difficult to separate due to their late stage textures, and most of the 8 analyses were gathered from probe slides of *in situ* mineral growth. They display three textures: as overgrowth and alteration rims on other spinels and ilmenites; very fine (<0.2mm) grains in the matrix (Plate 5.14 in Figure 5.2.16), and as an early pseudomorphic mineral replacing olivine. Their composition varies widely, but is typically 15 - 25% TiO_2, 20 - 28% Fe_2O_3, 25 - 30% FeO and 14 - 18% MgO. The evidence from diagenetic order of crystallisation (Figure 2.4.6 in Chapter 2) places much of the mineral growth in a late magmatic stage, just before, and during eruption, particularly the overgrowth and groundmass forms. Pseudomorphic magnetite-magnesian ulvospinel is seen to occur at the same time as the main serpentinisation event, which is immediately post-eruptive. The Ti and Mg-rich nature of the syn-diagenetic spinel suggests magmatic fluids were still present and actively precipitating these grains.

Magnetite

This spinel invariably occurs as a late stage pseudomorphic, and vein filling and cementing mineral (seen as large black 'blebs' in hand sample), Plate 5.12 in Figure 5.2.10. As such it was difficult to isolate from the serpentine it is intimately intergrown with, and the 6 analyses obtained are from microprobe slides. Magnetite from this paragenesis is very pure, typically >95% Fe_3O_4, with trace amounts of MgO and MnO. Development of the magnetite occurs at a mid to late stage of the diagenesis, often replacing minerals that were themselves diagenetic (e.g. serpentine and dolomite). The latest and by far the most voluminous precipitation of magnetite occurred in porous zones (typically along coarse-grained strata in the RPK, see Chapter 2) via discrete fluid channels (veins), later themselves filled with magnetite. This magnetite may reach a total of 5.2% by weight of the rock as cement, and is largely responsible

for the magnetic signature of the kimberlites (see Chapter 1). The source of the large amount of Fe can be explained by the serpentinisation of olivine.

Olivine, which comprises the bulk of the kimberlite, is itself 11.8% FeO (based on olivines of Fo_{90} composition), and was almost entirely serpentinised in the earliest diagenetic stages (see Chapter 2). The inability of serpentine to accept significant Fe in to its lattice means that a great deal was released, thus the magnetite bearing fluids have been generated within the kimberlite body as a final product of serpentinisation (no apparent 'magmatic fluids' origin). Precipitation of magnetite (as opposed to hematite or pyrite) is consistent with fairly reducing conditions (-0.2 to -0.35 Eh(V)) and very low activity of sulphur (-7 to -10 Log HS^-; Curtis and Spears, 1968). Later large patches of vein fill magnetite have reverted to hematite (4 analyses, two with traces of SiO_2), indicating more recent oxidising conditions in the veins. This later oxidisation, and other sulphide and sulphate precipitating events, are generally restricted to reactivation of the fluid channels, and interact rarely with the kimberlite.

5.2.5 Pyroxene

The pyroxenes are another distinctive mineral in kimberlites, with some varieties particularly bright emerald green, other varieties are darker, bottle-green to black towards augite compositions. Some confusion between green Cr-diopside and Cr-amphibole led to the selection of a number of amphibole grains for probe analysis (described below). A wide range of clinopyroxenes occur in kimberlites from a variety of parageneses, these are defined in below.

Table 5.4

Clinopyroxene type	Paragenesis	notes
Chrome Diopside	peridotitic (lherzolite, harzburgite)	includes sub-calcic types
Omphacite (Na-Augite)	eclogite	
low to high Cr Ti-Augite	megacryst	includes very sub-calcic types
various Salites and Augites	crustal	usually very Ca-rich

Because the pyroxene group can be prone to alteration by serpentinising fluids they are uncommon in the FALC kimberlites, seemingly better preserved in crater facies primary tuffs than in proximal reworked kimberlites. Orthopyroxene (opx) in particular is rare in the heavy mineral concentrates, and must therefore be even more susceptible to alteration than olivine (which is more common in the heavy mineral separates as fresh crystals than opx). A range of parageneses have been proposed for the pyroxenes, megacryst, intergrowths with megacrystal spinel and ilmenite, groundmass (matrix), and

xenolithic origin (peridotitic, eclogitic and crustal). Kimberlite typically comprises more megacryst cpx than opx, and more xenolithic opx than cpx. From a total of 78 grains analysed from FALC concentrates, only 17 megacryst clinopyroxenes were verified. The rest were xenolithic cpx (and 1 opx), of which 38 were peridotitic Cr-diopside, 15 eclogitic cpxs (including 5 omphacites), and 5 were high iron, crustal cpx. A further 6 grains of cpx could not be differentiated between peridotitic Cr-diopside and a possible Cr-rich megacryst population (inconclusively proven for Colorado-Wyoming kimberlites, and not identified elsewhere; Boyd et al, 1984). The pyroxene compositions observed are mostly described by solid solution series between three end-member compositions, clinoenstatite ($Mg_2Si_2O_6$), wollastonite ($Ca_2Si_2O_6$) and clinoferrosilite ($Fe_2Si_2O_6$). Diopside *sensu strictu* comprises 45% to 50% enstatite and up to 25% clinoferrosilite molecules, although the classification of cpx using three end-members is a simplification. All the pyroxene data are presented on a Mg-Ca-Fe ternary plot, Figure 5.2.13, and defines six populations. Temperature estimates for non-eclogitic and low iron clinopyroxenes can be determined from the 2-pyroxene geothermometer, commonly used in the literature (e.g. Eggler and Boyd, 1987), and are applied directly on to the enstatite-diopside axis of Figure 5.2.13.

Population 1 consists of 2 peridotitic Cr-diopsides, 4 of the megacrystal clinopyroxenes and 5 of the ambiguous Cr-megacryst/peridotitic Cr-diopsides. This population represents the highest temperatures of crystallisation (1100° to 1220°C, assuming equilibration with orthopyroxene and garnet). It is reasonable to postulate the Cr-diopsides of ambiguous origin in this group (5 of the grains) are indeed of Cr-rich megacryst suite, due to their compositional association with the other megacrysts. Population 2 comprises the other 2 Cr-diopsides of controversial origin, most of the peridotitic Cr-diopsides (25 grains) and 8 of the non-omphacitic eclogitic Cr-diopsides. This group represents crystal growth in lower temperature and/or enriched origin, entirely consistent with a population containing eclogitic clinopyroxene. Population 3 contains all the high-iron crustal clinopyroxenes, and population 4 contain the five omphacites. These are not fully described by the three end-member solid solution series, and the geothermometer is not applicable to these grains. Population 5 is composed of the remaining three peridotitic Cr-diopsides, differentiated from population 1 by zero-iron, and consequent 0% clinoferrosilite molecule, which is very unusual. This group is sub-calcic, and has a temperature of crystallisation comparable to population 1, about 1200°C, indicating peridotitic clinopyroxene near the base of the crust. The final population (6) is composed of megacryst pyroxene only,

Figure 5.2.13

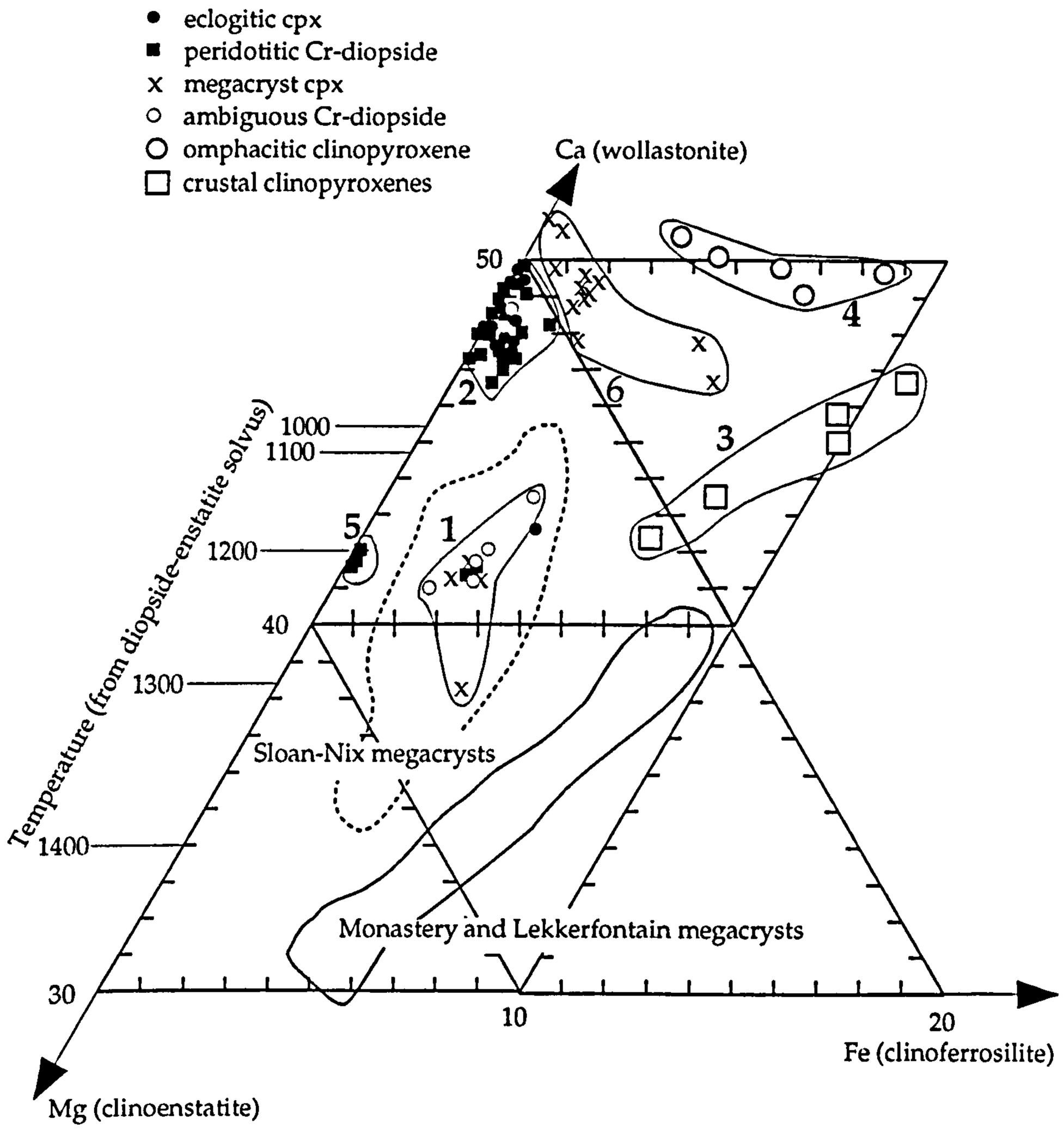

Composition of clinopyroxenes from FALC kimberlite, n = 78. Populations numbered are discussed in the text. Compare to megacrysts from Sloan-Nix (Eggler et al, 1979) and Monastery-Lekkerfontain (Gurney et al, 1979).

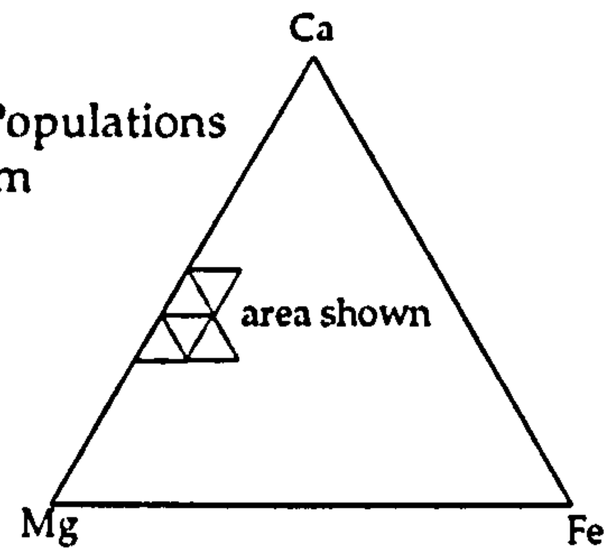

with a wide range of iron content (ranging from 0% to 5.5% clinoferrosilite, with typical values between 1% and 2%). Most of the megacrystal pyroxenes analysed fall into this population (13 of the 17), and are of relatively low temperature and/or fertile source, as indicated by their high Ca/Ca+Mg ratios (0.47 to 0.52).

Megacrystal clinopyroxene

The megacrystal paragenesis was notable for its low occurrence in an essentially randomly selected population of cpx. These grains were bottle-green vitreous fragments of medium to coarse grain size (0.5mm to 1.5mm). The grains analysed generally have chrome-rich megacryst chemistries, with low Al_2O_3 (<3%), TiO_2 up to 1%, and low Na_2O (<2%), and with relatively high Cr_2O_3 values of 0.7% to 1.45%. These may be compared to the possible Cr-rich megacryst suite in Figure 5.2.14.

Figure 5.2.14

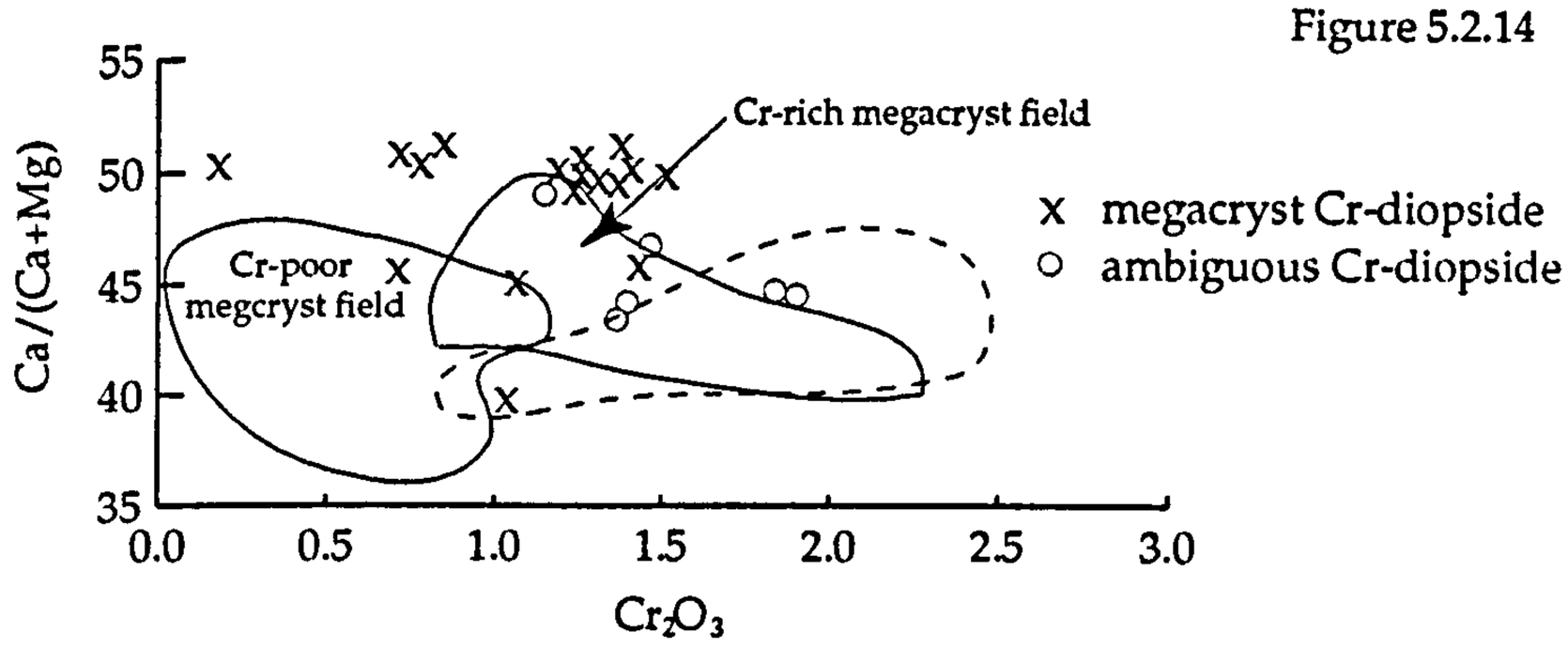

Cr-Ca proportions for megacrystal and possible megacrystal pyroxenes from FALC, n = 23. The fields shown are for megacrysts and lherzolitic pyroxenes (dashed field) from Colorado-Wyoming kimberlites (Eggler et al, 1979). Many of the pyroxenes are richer in Ca than the Wyoming craton compositions, but are of comparable Cr_2O_3 value.

The data points for the FALC megacryst suite fall mainly above the Cr-rich suite for Colorado-Wyoming kimberlites, although the small data base (23 analyses) precludes any sound conclusions. The (possible) FALC Cr-rich megacrysts plot mainly outside of both the Cr-rich field or lherzolitic field by virtue of elevated Ca/(Ca+Mg). The relatively high Ca/(Ca+Mg) suggests they are either derived from an enriched mantle source rock and/or relatively shallow lithospheric levels compared to the Wyoming craton. This could tie in with reported paleo-lithospheric thickness of 200km in the Wyoming craton (Eggler et al, 1987), relative to the 190km underlying FALC. The mantle conditions are discussed further in Chapter 6.

Peridotitic Cr-diopsides

Clinopyroxene may comprise up to 10% of mantle peridotite xenoliths found in kimberlites, however these are the most common pyroxenes encountered in the FALC heavy mineral concentrates. The most likely explanation is a lack of survival of orthopyroxenes in the diagenetic surface environment, and a sparse megacryst suite (an apparent characteristic of the FALC kimberlite magma). These Cr-diopsides are consistently less depleted that typical mantle peridotite cpx, Figure 5.2.15.

Figure 5.2.15

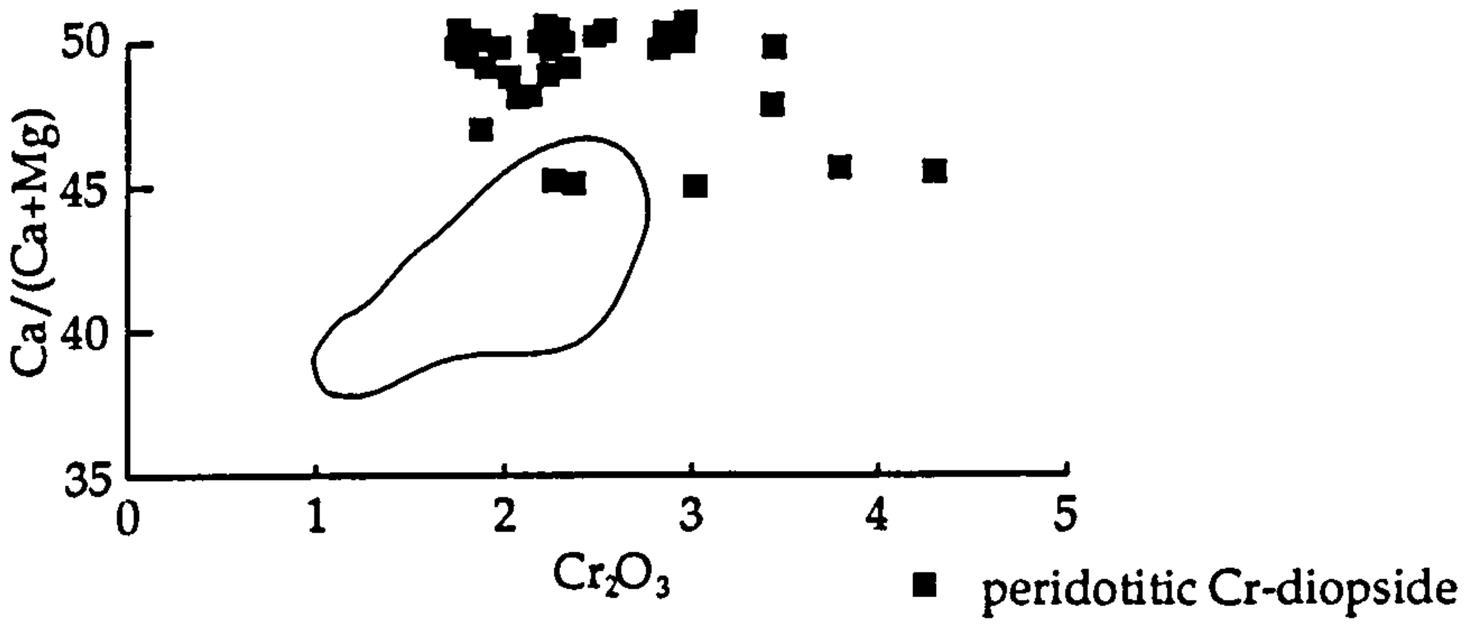

Cr-Ca proportions for peridotitic Cr-diopside from FALC, n = 38. Field shown is the lherzolitic pyroxene compositions from the Wyoming craton, and illustrates the considerable differences between the cratons (Eggler et al, 1979). The FALC pyroxenes are richer in both Cr and Ca.

The peridotitic Cr-diopsides plot well away from the lherzolite field determined for the Wyoming craton, with the high (>0.46) Ca/(Ca+Mg) suggesting relatively fertile sources and/or lower temperature, and paradoxically, a few data with high (>3%) Cr_2O_3 values suggesting greater depletion and/or higher temperature. The differences may well be due to a fertile versus depleted source rock, coupled with widely divergent lithospheric composition between the Wyoming craton (used as a comparison) and the lithosphere beneath FALC.

Eclogitic pyroxene

This group comprises 10 of the clinopyroxene grains, which were typically fine-grained (0.1mm to 0.5mm), bright, almost luminescent green, with distinctive cleavage. Their composition is typified by high Al_2O_3 (>3%) and high Na_2O (>2.5%) content. Consequently they contain a large proportion of the jadeite ($NaAlSi_2O_6$) end-member molecule, ranging from 10% to 16%, but rising to 36% in the omphacite grains (5). The omphacites have very high Al_2O_3

(>7.5%) and Na_2O (>5%), but lack any appreciable Cr_2O_3 (<0.1). Two of the grains (a Cr-diopside and an omphacite) were analysed with garnets to which they were attached (essentially two-crystal eclogite xenoliths). Both the omphacite and the Cr-diopside were attached to calcic pyrope-almandines (G3), and may be either of upper lithospheric origin, or from lower crustal eclogites.

All of the eclogitic Cr-diopsides fall in population 2 (Figure 5.2.14), which are equivalent to lower and mid-lithospheric temperatures, and probably below the diamond stability depth (at about 150km). This indicates the presence of eclogite pods throughout the lithosphere decreasing in proportion with depth, as is the case in many cratons world-wide. The conditions in the mantle are further discussed in Chapter 6.

Orthopyroxene

Only one grain of orthopyroxene from the mantle was analysed, and the composition does not correspond with any known megacrystal range (typified by a Mg/(Mg+Fe) ratio 0.95 to 0.82; Mitchell, 1986; this analysis 0.80), being too rich in both Al_2O_3 and CaO. Thus a mantle peridotitic origin is attributed (mantle lherzolites may contain up to 50% orthopyroxene), although depth, temperature and other conditions can not be determined from one analysis.

5.2.6 Phlogopite and other micas

Phlogopite ($K_2(MgFe^{2+})_6Si_6Al_2O_{20}(OH,F)_4$) is a common component of kimberlites world-wide, especially group II (orangeites). At FALC phlogopite is relatively rare in all primary airfall deposits (PK), but can be very common, aligned in some reworked kimberlite sands (RPK), e.g. the silty upper portions of graded pyroclastic sands. Where it occurs in primary tuffs it may be very coarse grained, up to 2cm diameter and 3mm thick, but here, and in reworked strata, it is more typically coarse, 1mm to 10mm diameter and <1mm thick. Crystals are platey (due to the dominant basal cleavage) sometimes displaying an hexagonal habit, and range in colour from dark green to pale brown, with a vitreous to sub-metallic lustre. Generally it forms late in the crystallisation of the kimberlitic magma as groundmass, as part of a megacrystal suite, from late-stage alteration of other kimberlitic minerals, or more rarely as xenolithic components in lherzolites and metasomatised upper lithospheric mantle (MARID-suite; Dawson, 1987).

Compositions of these micas between one kimberlite field and another are highly variable, and no systematic paragenetic classification exists. Unless observed within a xenolith, phlogopites can only be assumed kimberlitic if

>5mm diameter, and groundmass if <1mm diameter. Analysis of 10 FALC micas indicated that 1 was a crustal biotite (with high iron content), and 7 were from the kimberlite suite, with grain sizes of about 2mm (as big as could be fitted into the probe blocks). These phlogopites have a typical Al and Ti range: Al_2O_3 12.7% to 14.1% and TiO_2 3.6% to 4.8%. Two of these grains also contained magnesian ilmenite inclusions, further evidence of the kimberlite origin of this group. The high TiO_2 values of this kimberlite group is good evidence for a phenocrystal origin, crystallising from the kimberlite magma at early to late stages of ascent (P.H. Nixon, pers. comm.) The remaining two grains are of ambiguous origin, tending towards a biotite composition which corresponds to a crustal paragenesis.

5.2.7 Olivine

Olivine is the most common mineral in kimberlites world-wide, and at FALC 99% of it has been serpentinised. As a result of the alteration, fresh olivine occurs very rarely, particularly in reworked pyroclastic sands (RPK), and only 12 grains were analysed. Kimberlitic olivine is magnesium-rich, towards the forsterite (Mg_2SiO_4) end member. Megacrystal (macrophenocrystal, >1cm, euhedral), groundmass (microphenocrystal, <5mm), macrocrystal (0.5cm to 1cm, well rounded) and xenolithic (peridotitic) parageneses have been applied purely on the basis of size and context in other kimberlites. At FALC petrographic observation during point counting (see Chapter 2) would suggest: about 40% megacrysts (up to 5cm), 50% groundmass, 8%-9% xenolithic (medium to coarse fragments) and 1%-2% macrocrystal (rounded) olivines. This distribution cannot be confirmed by microprobe analysis of the olivines picked because the alteration tended to leave cores of olivine smaller and more rounded than the original grain (Plate 5.13 in Figure 5.2.16). Furthermore, there is a considerable compositional overlap, in terms of major element chemistry between the four parageneses. Global megacryst and groundmass compositions vary between Fo_{87} and Fo_{93}, and Fo_{88} to Fo_{94} for macrocrysts. Data on xenolithic olivine is fairly sparse and indicates a slightly higher Mg range of Fo_{91} to Fo_{94}. Data for 10 of the 12 FALC olivines analysed fit best into the latter paragenesis, but may, belong to any. Two of the olivines have low Fo values (79 and 82) and are below the range of many of the kimberlitic and mantle xenolithic compositions. A crustal origin is therefore ascribed, probably from some metabasic rocks in the basement.

Figure 5.2.16

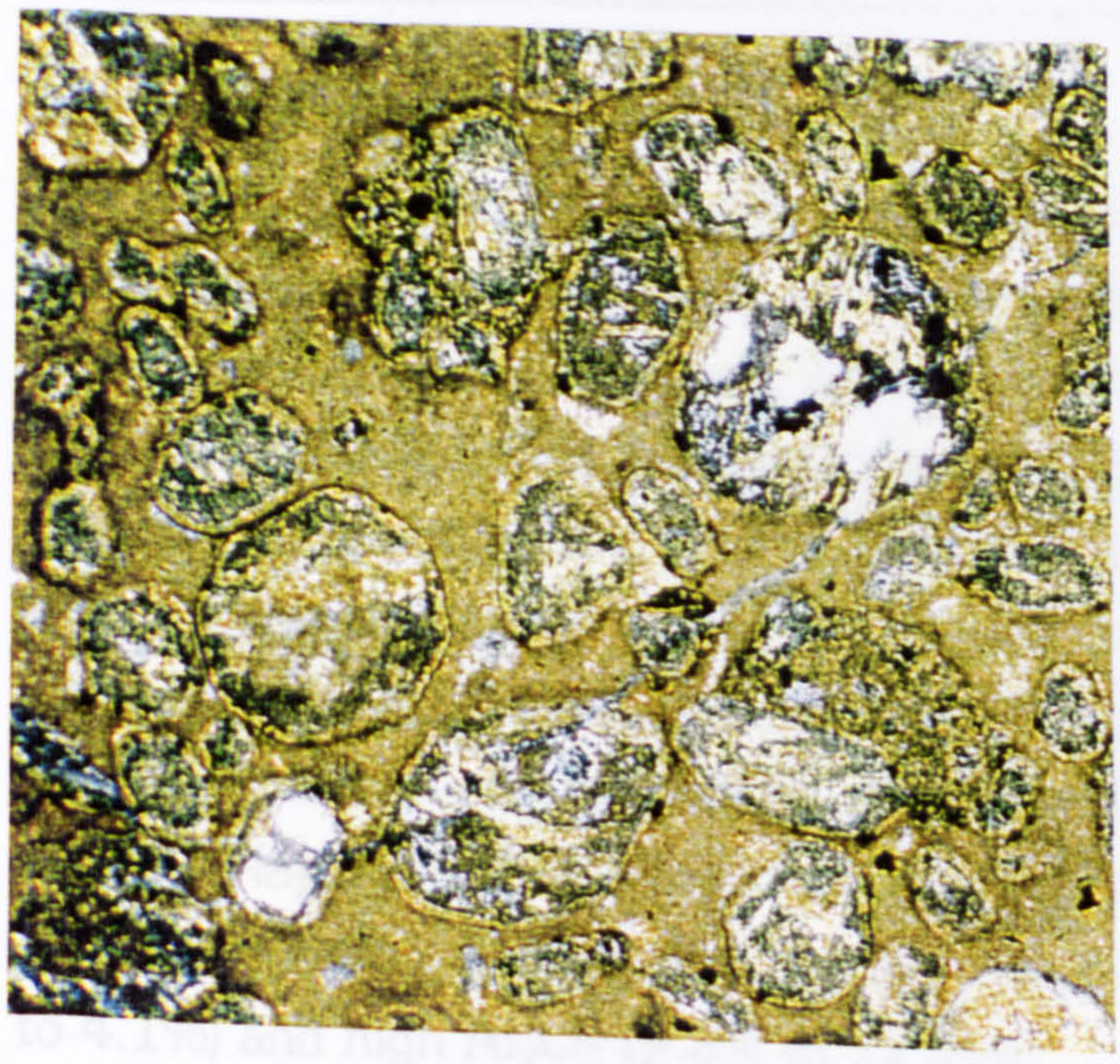

Plate 5.13
From OFS 93-012, 204.3m, crystal dominated lapilli-tuff. Crossed polarised light, mag. x4. Olivine grains in this slide are dominantly macrocrystal (coarse, euhedral), and groundmass (microphenocrystal, fine, sub to euhedral).

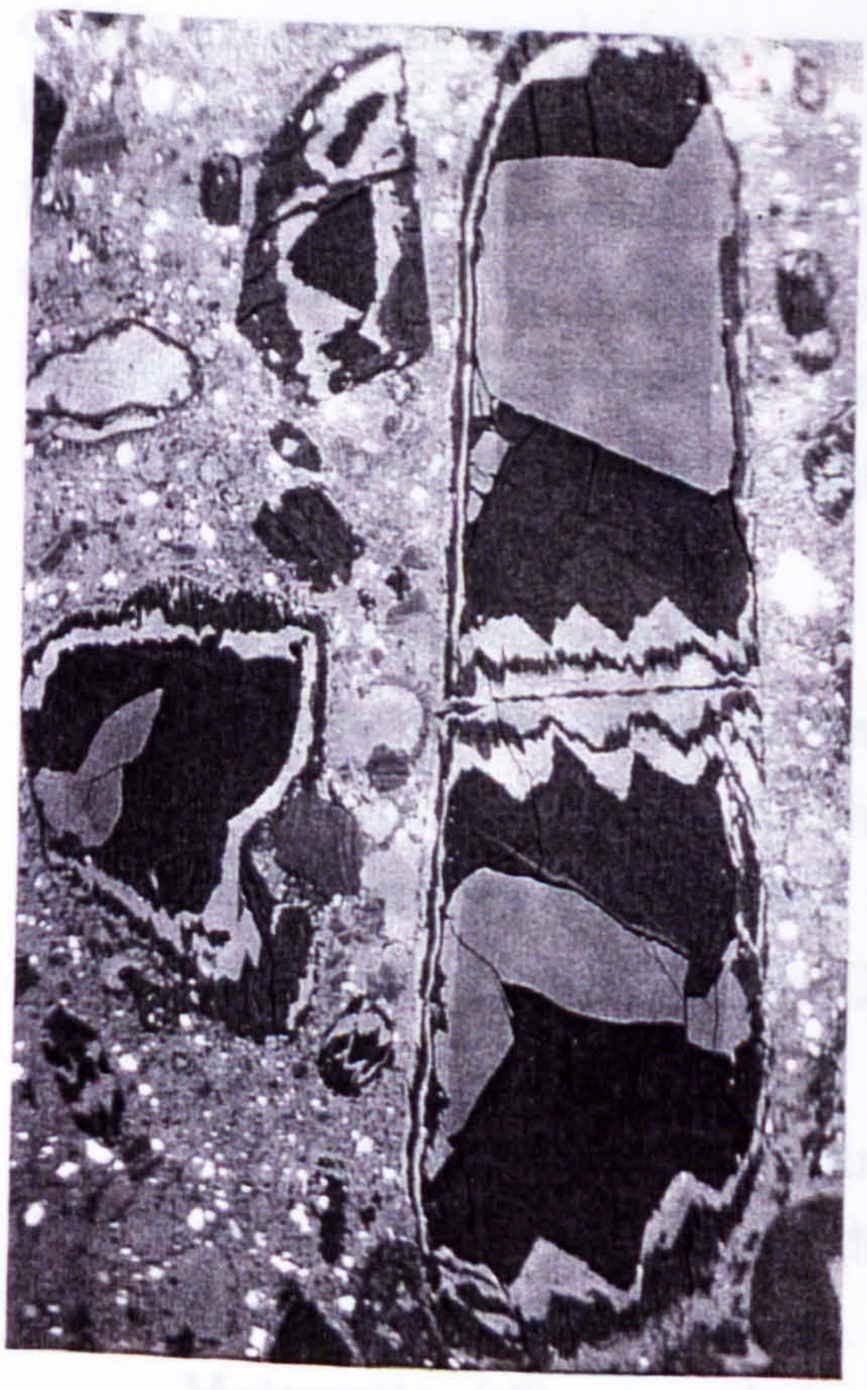

Plate 5.14
From OFS 93-012, 203.9m, crystal dominated lapilli-tuff, SEM image. Large olivine grain is 1.8mm long. Altered macrocrystal olivine grains. Mid-grey cores are unaltered olivine (Fo92 at the core, Fo88 at the rim, which is paler). Dark grey cores are serpentine, and light grey rims (in zig-zag habit with serpentine) is calcite. Note the dusting of fine spinel (magnetite-magnesian ulvospinel) as the bright white very fine mineral in the surrounding matrix.

Figure 5.2.16

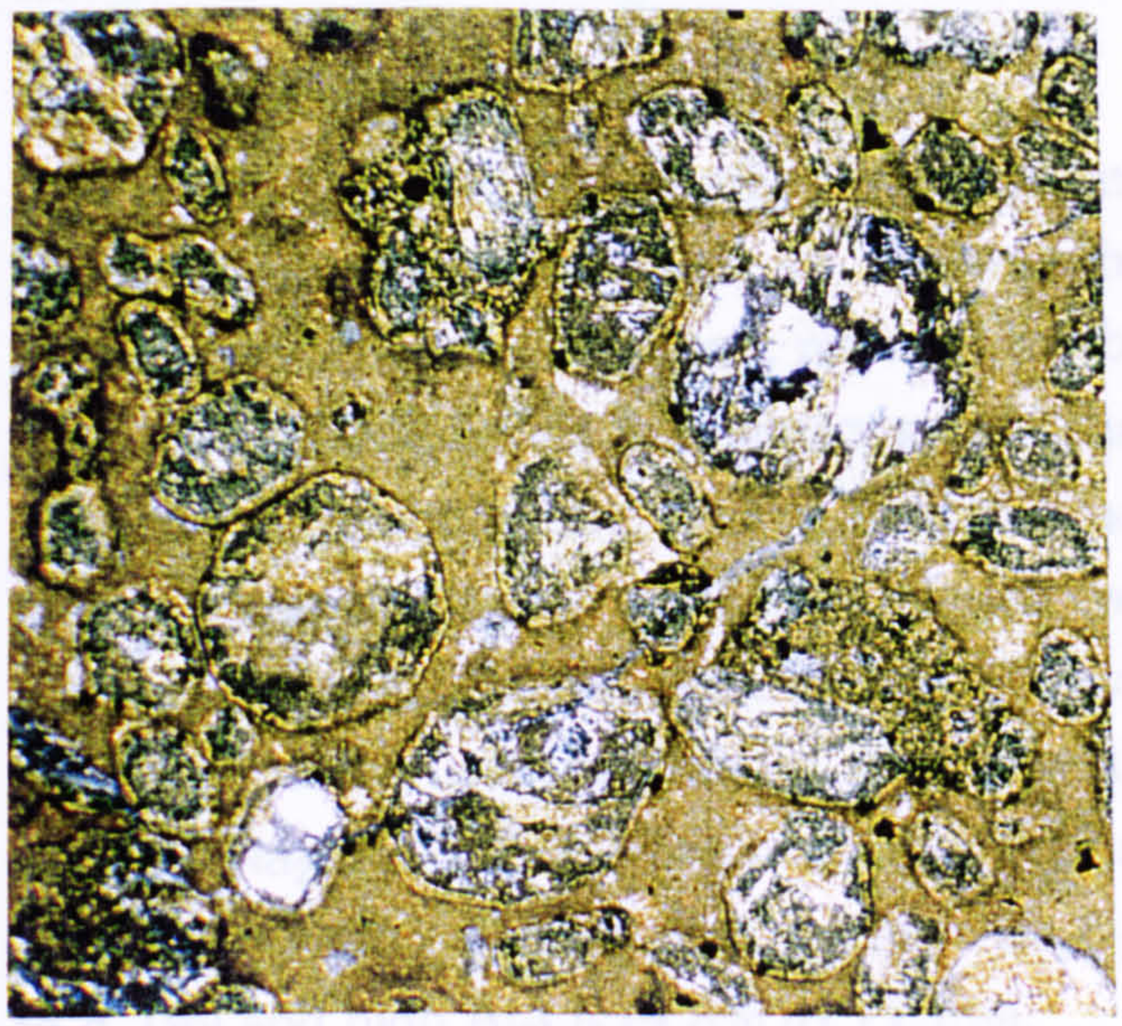

Plate 5.13
From OFS 93-012, 204.3m, crystal dominated lapilli-tuff. Crossed polarised light, mag. x4. Olivine grains in this slide are dominantly macrocrystal (coarse, euhedral), and groundmass (microphenocrystal, fine, sub to euhedral).

Plate 5.14
From OFS 93-012, 203.9m, crystal dominated lapilli-tuff, SEM image. Large olivine grain is 1.8mm long. Altered macrocrystal olivine grains. Mid-grey cores are unaltered olivine (Fo92 at the core, Fo88 at the rim, which is paler). Dark grey cores are serpentine, and light grey rims (in zig-zag habit with serpentine) is calcite. Note the dusting of fine spinel (magnetite-magnesian ulvospinel) as the bright white very fine mineral in the surrounding matrix.

5.2.8 Amphibole

Although not a kimberlitic mineral, amphibole occurs infrequently as a xenolithic component. Much of the amphibole is of crustal origin from metavolcanic and basic plutonic rocks of the basement, however it can occur at deep lithospheric levels in metasomatised mantle (usually of peridotitic type). Typically amphiboles are dark green to black, but some are more emerald green. Eleven of these paler amphiboles were selected, five of which were composite grains of amphibole and Cr-pyrope garnet (G9). Four of the remainder are crustal amphibole, with low Al_2O_3 (<7%), low Cr_2O_3 (<0.25%) and low Na_2O (<0.25%). The two other grains resembled the amphiboles in the composite grains, characterised by high Cr_2O_3 (2% to 2.3%), high Na_2O (3.3% to 4.1%) and high Al_2O_3 (9.8% to 11.2%).

The occurrence of the amphiboles with Cr-pyrope testifies to mantle origin, an uncommon, but not rare paragenesis, typically from the upper mantle in spinel lherzolites. Because of the large amounts of Al and Cr a MARID paragenesis must be ruled out (Dawson, 1987). The compositional name for these amphiboles is sodian edenitic hornblende, and may indicate more hydrated (volatile rich) mantle than usual in areas intersected by the FALC kimberlite. Mantle conditions are further discussed in Chapter 6.

5.2.9 Other minerals analysed

Various other minerals have been analysed, generally through mis-identification of crustal grains for the mantle grains described above. A variety of metamorphic and plutonic grains include corundum, sapphirine, gahnite (zinc spinel), andalusite and staurolite. Diagenetic minerals probed include sphalerite and magnetite.

Four perovskite grains were analysed, mostly from the rinds around magnesian ilmenites, and did not differ from the expected $CaTiO_3$ composition, although Nb_2O_5+Ce_2O_3 reach 3%.

Moissanite (silicon carbide, three grains) was verified by microprobe analysis. If these crystals are natural then they were derived from great, sub-lithospheric depths (Leung, 1989), or possibly even extra-terrestrial sources (J. Milledge, pers.comm.) Despite various investigations, artificial silicon carbide could not be identified at any of the drilling (artificial diamonds were used), storage, heavy mineral separation or analysis stages. This author can only conclude the grains are natural. The implications for the mantle are further discussed in Chapter 6.

Three grains of an enigmatic mineral were analysed. The grains were coarse (1mm to 2mm) fragments, with a vitreous to resinous lustre and patchily coloured purple-red. The analysis vary widely within a single grain, but is dominated by Al_2O_3, corresponding to the colourless patches. The coloured areas appear to be caused by increased Cr_2O_3 and CaO levels. Further peculiarities include a micro-porosity and very fine grains of Cr metal. Various highly reducing environments may be proposed to explain this mineral, including, like moissanite, the lower mantle. This conclusion should not be drawn lightly, however, as a crustal paragenesis may be just as likely (in a pegmatite, skarn or area affected by deep crustal fluids), as indeed may an artificial origin. The mineral type and origin remains ambiguous.

References cited in Chapter 5

- Agee, J.J., Garrison, J.R. and Taylor, L.R. (1982). Petrogensis of oxide minerals in kimberlite, Elliot County, Kentucky. American Mineralogist, Vol.67, p.28-42.
- Apter, D.B., Harper, F.J., Wyatt, B.A. and Scott-Smith, B.H. (1984). The geology of the Mayeng kimberlite sill complex, South Africa. Proceedings of the 3rd International Kimberlite Conference, Vol.2, p.43-57.
- Armstrong, R.L. (1988). Mesozoic and early Cenozoic magmatic evolution of the Canadian Cordillera. In Clark, S.P., Burchfiel, B.C. and Suppe, J. (eds.) Processes in continental lithospheric deformation. Geological Society of America, Special Paper 218, p.55-92.
- Bloch, J. (1994). The methods and results of geochemical analyses of Cretaceous Colorado Group shales from the Western Canadian Sedimentary Basin. Geological Survey of Canada, Open File Report 2810.
- Boyd, F.R, Dawson, J.B. and Smith, J.V. (1984). Granny Smith diopside megacrysts from the kimberlites of the Kimberley area and Jagersfontain, South Africa. Geochim. Cosomochim. Acta. Vol.48, p.381-384.
- Clement, C.R. (1982). A comparative geological study of some major kimberlite pipes in the Northern Cape and Orange Free State. Ph.D thesis (2 vols.) University of Cape Town.
- Curtis, C.D. and Spears, D.A. (1968). The formation of sedimentary iron minerals. Economic Geology Vol.63, p.257-270.
- Dawson, J.B. and Stephens, W.E. (1975). Statistical analysis of garnets from kimberlites and associated xenoliths in kimberlite. Journal of Geology, Vol.83, p.589-607.
- Dawson, J.B. (1987). The MARID-suite of xenoliths in kimberlite: relationship to veined and metasomatised peridotite xenoliths. In Mantle Xenoliths, P.H. Nixon (ed.), p.465-473.
- Eggler, D.H., McCallum, M.E. and Smith, C.B. (1979). Megacryst assemblages in kimberlite from Northern Colorado and Southern Wyoming: Petrology, geothermometry-barometry and a real distribution. Proceedings of the 2nd International Kimberlitie Conference, Vol.2, p.213-226.
- Eggler, D.H., McCallum, M.E. and Kirkley, M.B. (1987). Kimberlite transported nodules from the Colorado-Wyoming; A record of enrichment of shallow portions of an infertile lithosphere. Geological Society of America Special Paper 215, p.77-89.
- Ewing, T.E. (1981). Petrology and geochemistry of the Kamloops Group volcanics, British Columbia. Canadian Journal of Earth Science, Vol.18, p.1478-1492.
- Finnerty, A.A. and Boyd, F.R. (1987). Thermobarometry for garnet lherzolites: basis for the determination of the thermal and compositional structure of the upper mantle. In Mantle Xenoliths, P.H. Nixon (ed.), p.381-401.
- Garvie, O.G. and Robinson, D.N. (1982). The mineralogy, structure and mode of formation of kelyphite and associated sub-kelyphite surfaces on pyrope from kimberlites. Terra Cognita, Vol.2, p.229-230.

- Gaspar, J.C. and Wyllie, P.J. (1984). The alleged kimberlite-carbonatite relationship: Evidence from ilmenite and spinel from the Premier and Wesselton Mines and the Benfontain Sill, South Africa. Contributions to Mineralogy and Petrology, Vol.85, p.133-140.
- Green, D.H. and Sobolev, N.V. (1975). Co-existing garnets and ilmenites synthesized at high pressures from pyrolite and olivine basanite and their significance for kimberlitic assemblages. Contributions to Mineralogy and Petrology, Vol.50, p.217-229.
- Griffin, W.L., Ryan, C.G., Gurney, J.J., Sobolev, N.V. and Win, T.T. (1994). Chromite macrocrysts in kimberlites and lamproites: geochemisrty and origin. Proceedings of the 5th International Kimberlite Conference (Brazil 1991), Vol.1, p.366-383.
- Gurney, J.J., Jakob, W.R.O. and Dawson, J.B. (1979). Megacrysts from the Monastery kimberlite pipe, South Africa. Proceedings of the 2nd International Kimberlitie Conference, Vol.2, p.227-243.
- Gurney, J.J. (1984). A correlation between garnets and diamonds in kimberlites. In Glover, J.E. and Harris, P.G. (eds.) Kimberlite occurrence and origin: A basis for conceptual models in exploration, p.143-166.
- Gurney, J.J. and Moore, R.O. (1993). Geochemical correlation between kimberlitic indicator minerals and diamonds. Exploration, Sampling and Evaluation, Short Course Proceedings, Prospectors and Developers Association of Canada, p.147-171.
- Haggerty, S.E. (1975). The chemistry and genesis of opaque minerals in kimberlites. Physics and Chemsitry of the Earth, Vol.9, p.295-307.
- Haggerty, S.E., Hardie, R.B. and McMahon, R.M. (1979). The mineral chemistry of the ilmenite nodule associations from the Monastery diatreme. Proceedings of the 2nd International Kimberlitie Conference, Vol.2, p.249-256.
- Haggerty, S.E. (1989). Upper mantle opaque mineral stratigraphy and the genesis of metasomites and alkali-rich melts. Proceedings of the 4th International Kimberlite Conference (Australia 1986), Kimberlites and related rocks, Geological Society of Australia Special Publication 14, Vol.2, p.687-699.
- Harris, J.W. (1987). Recent physical, chemical, and isotopic research of diamond. In Mantle Xenoliths, P.H. Nixon (ed.), p.477-500.
- Kjarsgaard, B.A., Leckie, D.A., McIntyre, D.J., McNeil, D.H., Haggart, J.M., Stasiuk, L. and Bloch, J. (1995). Smeaton Kimberlite Drill Core, Fort a la Corne Field, Saskatchewan. Geological Survey of Canada Open File 3170, pp.57.
- Leahy, K. and Taylor, W.R.T. (1995). The influence of the Glennie Domain deep structure on the diamonds in Saskatchewan kimberlites. Proceedings of the 6th International Kimberlite Conference, Russia 1995, Extended Abstracts Volume.

- Leckie, D.A., Singh, C., Bloch, J., Wilson, M. and Wall, J.H. (1992). An anoxic event at the Albian-Cenomanian boundary: the Fish Scale Marker bed, northern Alberta, Canada. Paleogeography, Paleoecology. Paleoclimatology, Vol.92, p.139-166.
- Leung, I.S. (1990). Silicon carbide cluster entrapped in diamond from Fuxian, China. American Mineralogist, Vol.75, p.1110-1119.
- Mitchell, R.H. (1986). Kimberlites: mineralogy, geochemistry and petrology. Plenum Press, New York, pp.442.
- Mitchell, R.H. (1995). Kimberlites, orangeites and related rocks. Plenum Press, New York, pp.410.
- Robey, J.V.A. and Gurney, J.J. (1979). Megacrysts from the Lekkerfontain kimberlite, North central Cape, South Africa. Kimberlite Symposium II, Cambridge, extended abstract.
- Schulze, D.J. (1987). Megacrysts from alkalic volcanic rocks. In Mantle Xenoliths, P.H. Nixon (ed.), p.433-451.
- Shee, S.R. (1984). The oxide minerals of the Wesselton Mine, Kimberley, South Africa. Proceedings of the Third International Kimberlite Conference, Vol.1, p.59-73.
- Smith, C.B., Gurney, J.J., Skinner, E.M.K.,Clement, C.R. and Ebrahim, N. (1985). Geochemical character of southern African kimberlites: a new approach based on isotopic constraints: Transactions of the Geological Society of South Africa, Vol.88, p.267-280.
- Sobolev, N.V., Laurent'ev, Yu.G., Pokhilenko, N.P. and Usova, L.V. (1973). Chrome-rich garnets from the kimberlites of Yakutia and their paragenesis. Contributions to Mineralogy and Petrology, Vol.40, p.39-52.
- Thorkelson, D.G. (1985). Geology of mid-Cretaceous volcanic units near Kingsvale, south-western British Columbia. Current Research part B, Geological Society of Canada, Paper 85-1B, p.333-339.
- Valsami, E. and Cann, J.R. (1992). Mobility of rare earth elements in zones of intense hydrothermal alteration in the Pindos ophiolite, Greece. In Parson, L.M., Murton, B.J. and Browning, P. (eds.) Ophiolites and their Modern Oceanic Analogues. Geological Society Special Publication No.60, p.219-232.

CHAPTER 6 - NATURE OF THE CENTRAL SASKATCHEWAN LITHOSPHERE

Abstract

From xenocrysts included in the Fort a la Corne kimberlites, the composition of the Central Saskatchewan lithosphere includes spinel and garnet lherzolites, with patches of amphibole bearing lherzolite, eclogites (composed mainly of pyrope-almandine and omphacite) and depleted garnet harzburgites, present near the base of the lithosphere. Different degrees of metasomatism are inferred on the basis of trace element abundances in garnet, mostly related to the interaction of kimberlitic proto-magma with the lithosphere.

Chromium pyrope xenocrysts were analysed by proton microprobe (W.L. Griffin), and from their nickel contents, temperature of crystallisation was estimated, assuming equilibration with olivine. Pressure was also estimated from chromium content, assuming equilibrium with chromite. A range of P-T estimates (the paleogeotherm) was obtained by these methods, and compared with time-temperature relationships determined from the nitrogen aggregation state of diamonds from FALC. Other, less reliable, equilibration temperatures were provided by Cr-diopside compositions (see Chapter 5), assuming equilibrium with enstatite. The P-T estimate provided by these xenocrysts from FALC kimberlites, suggests that the lithosphere in the Cretaceous extended to depths of about 190km with basal temperatures of up to 1300°C.

The 'diamond window', the region in which diamonds grew and were preserved, ranges from the base of the lithosphere, (circa 190km and 1300°C), up to a depth described by the intersection of the paleogeothermal gradient with the graphite-diamond transition in P-T space. The geotherm is itself determined from garnet geobarometry, and suggests the upper limit of diamond stability is estimated at 145km and 950°C. This is verified by the independent method of calculating time-temperature residence of the diamonds by nitrogen-aggregation state (W.R. Taylor). This range is from 980 to 1245°C, and includes both Archean and mid Proterozoic residence times.

The lithosphere under the Glennie Domain (an Archean terrane) appears to have been diamond bearing since the Archean, before it was incorporated into the Trans Hudson Orogenic belt in the mid Proterozoic. The orogeny associated with another period of diamond growth as the lithosphere was thickened further. Seismic profiling (Lewry et al, 1994) shows the sub-surface extent of the Glennie Domain to be at least 400km wide, far greater than the current surface outcrop where it is exposed to the north. It may therefore be considered a micro-craton, with a well developed lithosphere comprising typical depleted peridotites and eclogites. In this aspect it is comparable to the mantle

lithosphere of the Kaapvaal and Siberian cratons, although thinner (190km rather than 210km) and slightly more metasomatised.

6.1 Garnet proton microprobe analysis

Early evaluation of diamond potential in new kimberlite prospects is essential for rational exploration programs. Techniques for prospect evaluation have been developed for commercial use at CSIRO, Australia (Griffin et al, 1989; Ryan et al, 1995), on the basis of precise trace element measurements using the proton microprobe (PMP). Garnet xenocrysts separated from kimberlite (chromium pyrope of peridotitic paragenesis) are analysed for their Ni and Cr contents providing P-T estimates, thus defining the geothermal gradient and diamond window. Further information regarding degree of depletion and metasomatism can be determined from Ti, Y, Ga and Zr concentrations. The analyses are compared to the CSIRO database, which contains analyses for economically viable kimberlites from around the world, and an overall prospect evaluation is made.

A total of 101 chromium pyrope grains were selected from FALC proximal facies kimberlites (61 from boreholes OFS 93-002, 003 and 004, and 40 from 009, see Chapter 2). Boreholes 002, 003 and 004 are all located near Snowden, and are peripheral to the main kimberlite cluster centred 25km to the SW. Borehole 009 is located on the eastern edge of the main cluster, and is central.

The 101 garnets were initially analysed at Leeds (by E. Condliffe, see Chapter 5) and verified as chromium pyropes of G9 and rarer G10 types (18 grains), disaggregated from peridotitic xenoliths. These were then analysed by PMP at CSIRO, Australia, and the results presented in a propriety report to Operation Fish Scale from W.L. Griffin. The results discussed below include a P-T plot (from Cr and calculated temperature, T_{Ni}), degree of depletion (from Y and T_{Ni}), degree of metasomatism (Zr and TiO_2, Y/Ga - Zr/Y and Y - Ga) and an assessment of diamond prospectivity (grade) based on comparison of the above values with a global kimberlite database (the latter is discussed in Chapter 7). All the raw data generated, from Griffins report can be found in Appendix X. For the purposes of this thesis the term depleted or infertile (antonym: enriched/fertile) refers to the absence of those elements required to produce a basalt (or similar mafic magma) by partial melting of the rock. Metasomatism refers to a rock that has undergone ion-exchange with another adjacent body

(e.g. a fluid), which has altered the chemistry of the rock, and possibly (but not necessarily) resulted in growth of new minerals.

Many of the implications drawn from the analyses have been made by Griffin in the report, these are reviewed and expanded in light of other information not available to Griffin. The broader lithospheric implications made in Section 6.4 are, therefore, a combined effort between this author and Griffin.

6.1.1 Geothermometry-geobarometry

PMP analysis of the minerals in garnet peridotite xenoliths from kimberlites around the world shows that the partitioning of Ni between chrome pyrope and olivine is strongly temperature dependent (Griffin et al, 1989). The range of Ni contents in olivine is large and relatively constant (2900±360ppm) compared to garnets, enabling a temperature estimate to be derived from the Ni content of a garnet without prior knowledge of the coexisting olivine's composition (Griffin et al, 1989). Consequently an estimation of temperature (T_{Ni}) is possible from Ni concentration in single grains of chromium pyrope if it is reasonable to assume equilibration with olivine (Griffin et al, 1989; Ryan et al, 1995).

The specific methodology requires the precise measurement of Ni content in the garnet in ppm (hence the need for the more precise PMP analysis instead of a standard electron microprobe analysis). At mantle pressures the amount of Ni in garnet, in equilibrium with olivine, displays a linear relationship with temperature (as derived by from other geothermometers, such as the two-pyroxene thermometer and the orthopyroxene-garnet barometer, Finnerty and Boyd, 1987). The relationship is described by the following equation (from Ryan et al, 1995b):

$$T = \{1000/[1.509 - 0.19\ln(\text{ppm Ni})]\} - 273$$

where T = temperature in °C

This equation has been shown to work adequately for determining the mantle temperature conditions under which garnet peridotite xenoliths of a wide range of compositions equilibrated, but has some limitations. Iron-rich peridotites may cause a slight underestimation of temperature, as might equilibration with olivines containing very high (>4000ppm) Ni contents. Low temperature pyropes (<700 °C, or from about <100km) are not described by the linear relationship shown above.

Geobarometry is determined from the garnet composition using an algorithm that combines a modification of the Nickel (1989) Cr-barometer with estimates of co-existing orthopyroxene (Ryan et al, 1995). This geobarometry gives *minimum pressures* of crystallisation and is regarded as particularly equivocal as it relies on the further assumption of Cr partitioning between garnet and an estimated orthopyroxene composition, whilst in equilibrium with chromite. Where no chromite is present the barometry may be regarded as a considerable underestimate. Spinel lherzolite is the common constituent in the upper lithosphere, and undergoes phase change to garnet lherzolite between 70km and 90km in cratonic settings (Wyllie, 1981). High-chrome spinel (chromite), however, co-exists with garnet-bearing depleted peridotites, such as harzburgites and dunites, to the base of the lithosphere (Griffin et al, 1994)

Further problems with geothermometry-barometry can occur when looking at single pyrope grains disaggregated from their original xenoliths. For example, chromium pyropes can also occur within pyroxenite xenoliths, where olivine is absent, and garnet has equilibrated with pyroxenes. Also where a Cr-rich megacryst suite occurs (e.g. Colorado-Wyoming kimberlites) the megacrystal pyropes are virtually indistinguishable from chromium pyropes of peridotitic paragenesis (see Chapter 5). A small database of garnet analyses may also affect the conclusions, as the results describe a statistical probability. Ryan et al (1995) recommend basing P-T estimates on a minimum data set of 50 analyses.

These problems aside, in recent years the method has gained a great deal of commercial popularity as many exploration groups world-wide have used CSIRO to assess a kimberlite province for diamond prospectivity (e.g. Nixon et al, 1994). Despite the recent refinements, there are detractors from this method, both as a tool for determining equilibration temperatures and particularly as a diamond prospectivity indicator.

In the FALC kimberlite xenocryst population, peridotitic chromite has been observed, and the 12 olivines analysed showed suitable Ni contents: average of 0.32% NiO, maximum 0.42%, and were of low iron content: Fo_{90} to Fo_{93}. Furthermore no evidence has been found of a Cr-rich megacryst suite or pyroxenites at FALC, see Chapter 5. These factors suggest that the data provided by the single garnet grain analyses have a relatively high level of reliability. It is the opinion of this author that the use of the garnet-nickel method to produce a temperature estimate is as valid as any other method for the FALC kimberlites. But as with all the other geothermometry/barometry methods, can only provide 'ball-park' figures and are used with some degree of caution.

Temperature (T_{Ni}, °C) is displayed as a histogram showing the numbers analysed, Figure 6.1.1. The T_{Ni} values for FALC kimberlites show bimodal distribution, with distinct high and low temperature groups. Within the low temperature group are large proportions of the G9 garnets (54% of all G9 analyses), consistent with peridotitic (lherzolite) paragenesis in the upper lithosphere (700 to 1100°C). Relatively high-level pods of depleted peridotite are indicated by 8 of the 18 G10 garnets (of harzburgite paragenesis) occurring in the 850 to 1150°C range. The highest frequency peak (containing 39% of all data), including the rest of the G10s, falls in to the narrow 1150 to 1300°C range, and includes the hottest lithospheric lherzolites and harzburgites.

Assuming the garnets grew with chromite (as well as olivine) the temperatures were then used together with Cr concentration in the garnet to calculate pressure (Ryan et al, 1995). See the pressure-temperature plot, Figure 6.1.2. The plot shows the projected geothermal gradient defined by the highest pressure garnets for the FALC data. The gradient is 8°C/km, equivalent to a conductive heat flow of about 42mW/m^2. This gradient intersects the graphite-diamond transition at 950°C and 145km, this is independently confirmed by T_{NA} values from microdiamond analysis (see section 6.2 below) with a range of 980°C to 1250°C. The highest temperature garnets (both G9 and G10) at 1300°C and 190km defines base of the lithosphere (also defined by degree of depletion, see below) and the 'diamond window' (the region that exists in the lithosphere where diamonds may grow and be preserved). Half of the garnets analysed, including 11 of the 18 G10 types, occur within the diamond stability field. This indicates both lherzolitic and harzburgitic rock extends to a maximum depth of 190km, representing the base of the lithosphere. The low geothermal gradient defined by the garnet P-T calculations, with the base of the lithosphere at 190km is typical of cratons globally (Finnerty and Boyd, 1987).

Those garnet data which scatter back to lower pressures (Figure 6.1.2) are probably artefacts, generated because they did not grow in equilibrium with chromite. For example the model depth for a 1100°C chrome pyrope of 58km is entirely unrealistic, as is a 1350 °C garnet with a depth of 120km, probably above the mantle solidus. The two G10 grains between 600°C and 700°C may also be artefacts of the TNi calculation, which does not model low-temperature conditions (<700°C) accurately.

Figure 6.1.1

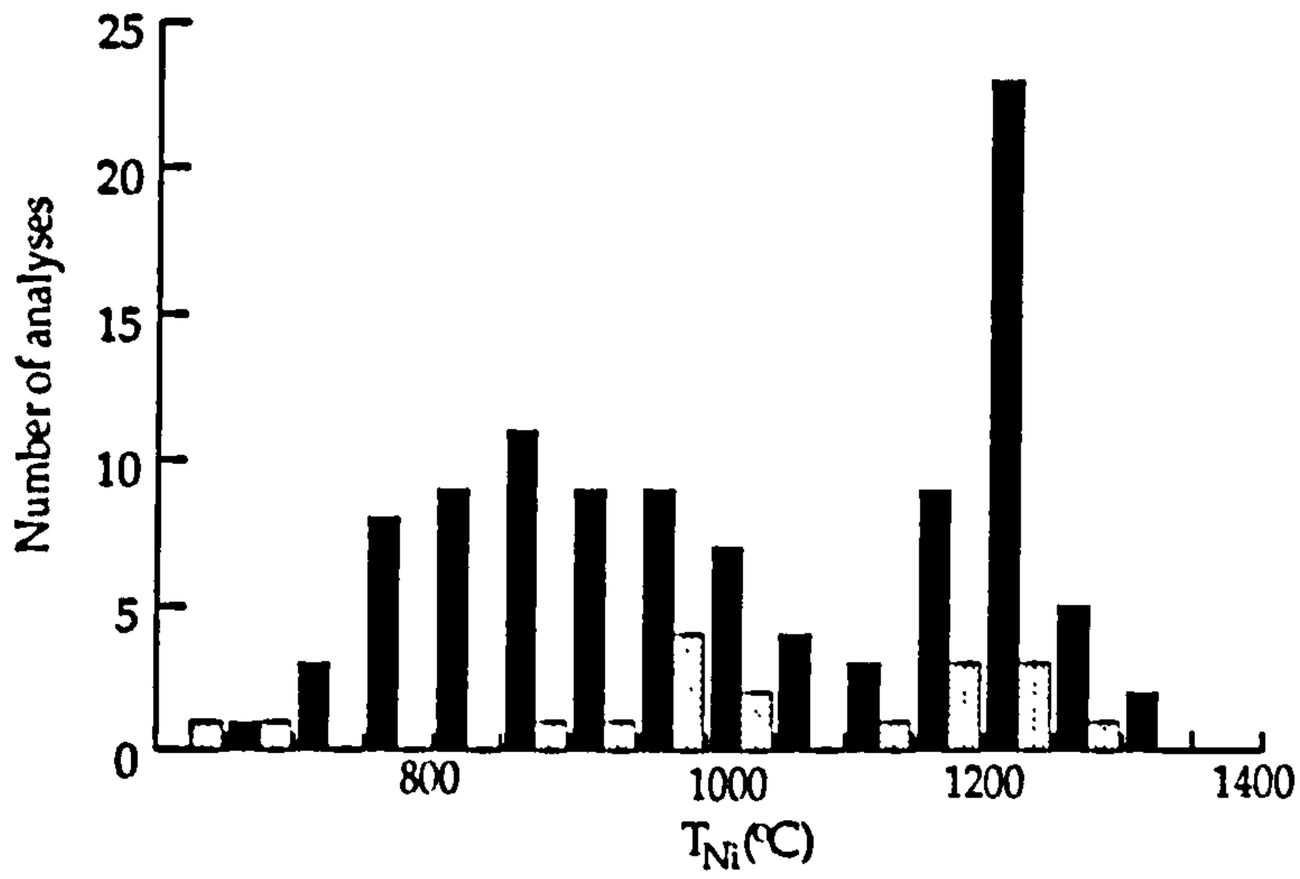

Temperature calculated from nickel thermometry vs. frequency for all FALC data (n=101). Grey bars indicate the temperatures of G10 (harzburgitic) garnets, black bars represent all data (G9+G10).

Figure 6.1.2

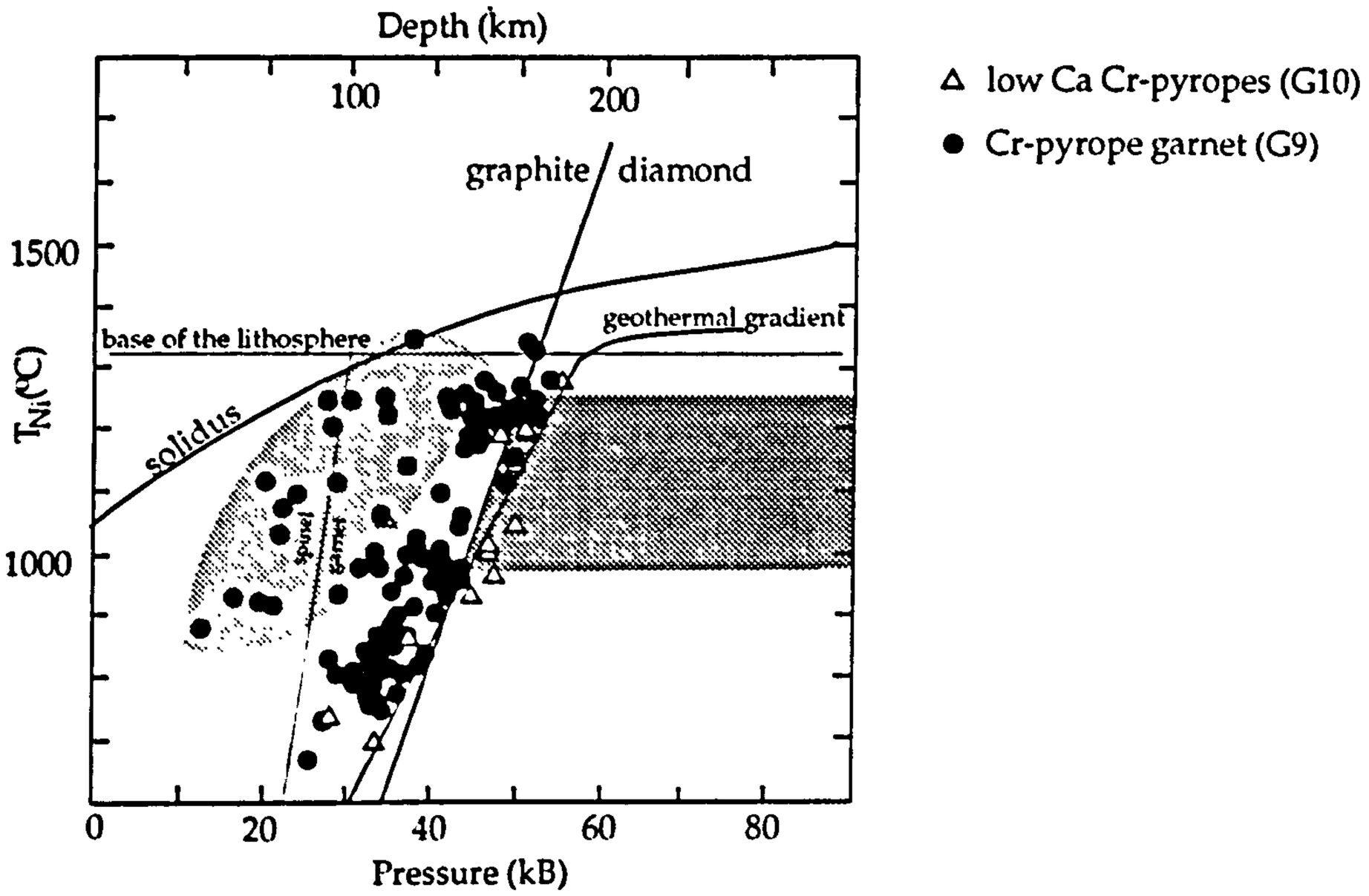

P-T plot derived from nickel thermometry of FALC and Snowden garnets, n=101. Heavy line shows the geotherm as defined by high pressure, Cr-pyropes and the diamond window (dark shaded band, from micro-diamond analysis, see section below). Data within the lightly shaded field probably have pressure and depth underestimates. i.e. were not in equilibrium with chromite.

6.1.2 Degree of depletion

As yttrium partitions preferentially from crystals into melt, low Y concentrations in lithospheric garnets indicate depleted (melt-extracted) rocks, such as harzburgite and dunite and infertile lherzolites (Griffin and Ryan, 1995). Thus, Griffin uses PMP analyses of yttrium concentration to gauge depletion. Small amounts (<10ppm) indicate a depleted source, a characteristic of lithospheric mantle. Much higher values (>>20ppm) indicate a more enriched source from metasomatised lithosphere or asthenospheric mantle, Figure 6.1.3.

Note the highest temperature depleted garnet cluster has a maximum temperature of about 1280°C to 1350°C, reflecting the temperature at the base of the lithosphere, and in accordance with the thermobarometry already described. The G10 garnets all have depleted to very depleted amounts of Y (<1 to 10ppm) which correlates well with the prescribed harzburgite origin, half of these occur in the high temperature group, and are derived from near the base of the lithosphere.

The presence of moderately enriched garnets (>20ppm) from high temperatures suggests zones of fertile lherzolites at the base of the lithosphere, which may of been associated with fertilisation required to produce the proto-kimberlitic magma (Griffin and Ryan, 1995). Other enriched garnets that occur at lower temperatures (some at around 700°C and another small group at around 1000°C to 1100°C) reflect more fertile patches within the lithosphere, possibly due to small degrees of metasomatism.

6.1.3 Degree of metasomatism

Zr and TiO_2 contents of garnets may be used to evaluate the degree and type of metasomatism within lithospheric peridotites (Griffin and Ryan, 1995). Enrichment of Zr and TiO_2 is seen as evidence of silicate melt related metasomatism, and is typified by garnets from South African high temperature sheared peridotites. Enrichment of Zr without a concomitant increase in TiO_2 is seen as evidence for hydrous fluid related metasomatism, as evidenced by phlogopite-rich xenoliths, mainly from South Africa.

The FALC garnet compositions, Figure 6.1.4, indicate melt-related metasomatism was common in many of the protoliths bearing these grains (25%, including 2 of the 18 harzburgitic G10s), with much less evidence of hydrous-fluid related metasomatism (7% including 3 of the G10s).

Further evidence of melt-related metasomatism can be derived from observing a linear correlation between Y and Ga concentrations. The proportional redistribution indicates equilibration with a reservoir containing

Figure 6.1.3

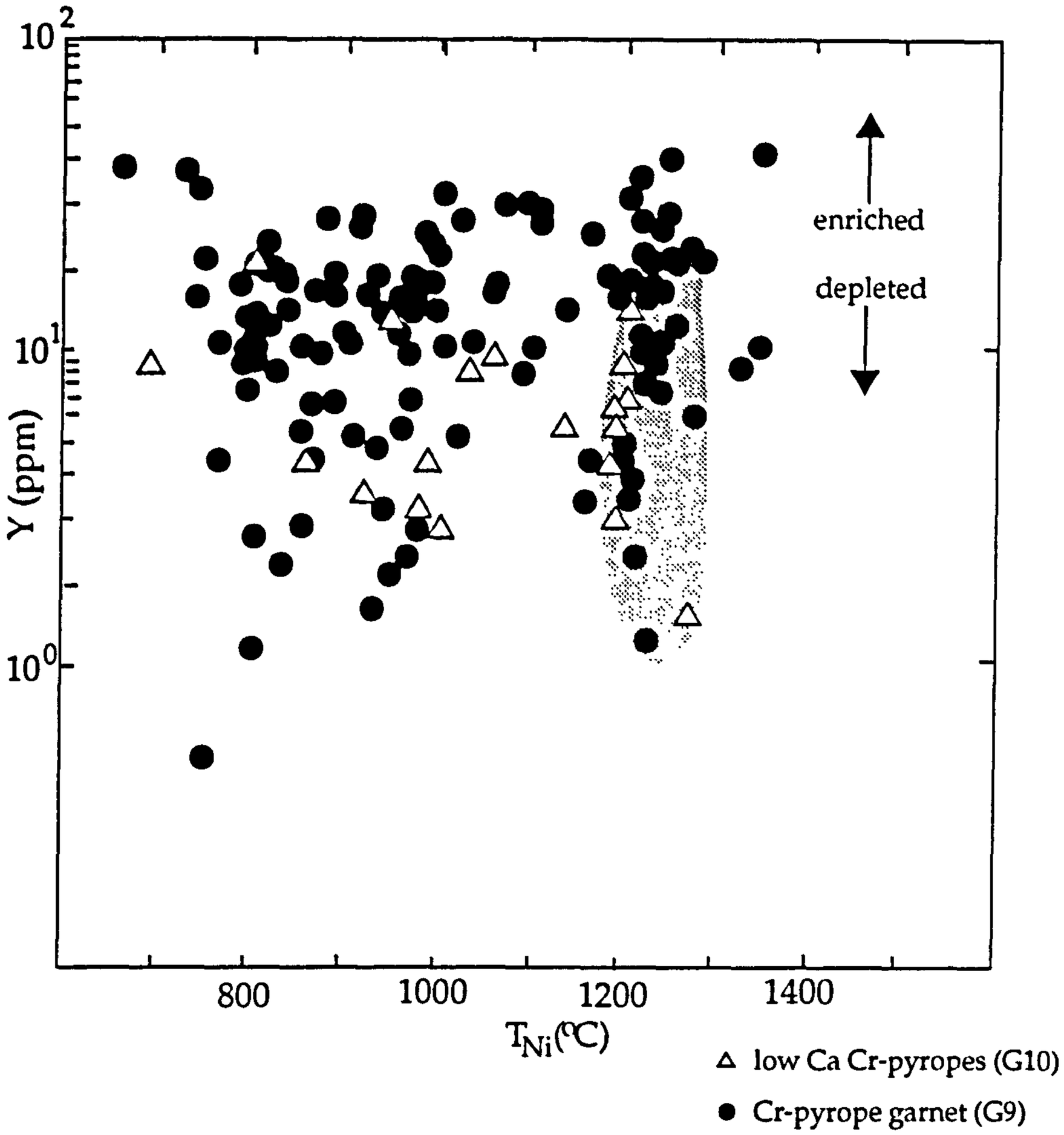

T (Ni) vs log Y conc in garnets from FALC and Snowden, n=101.
Data within the shaded field are the highest temperature garnets with a depleted geochemistry, and define the base of the lithosphere (Griffin and Ryan, 1995), indicating temperatures of 1150 to 1300°C.

Figure 6.1.4

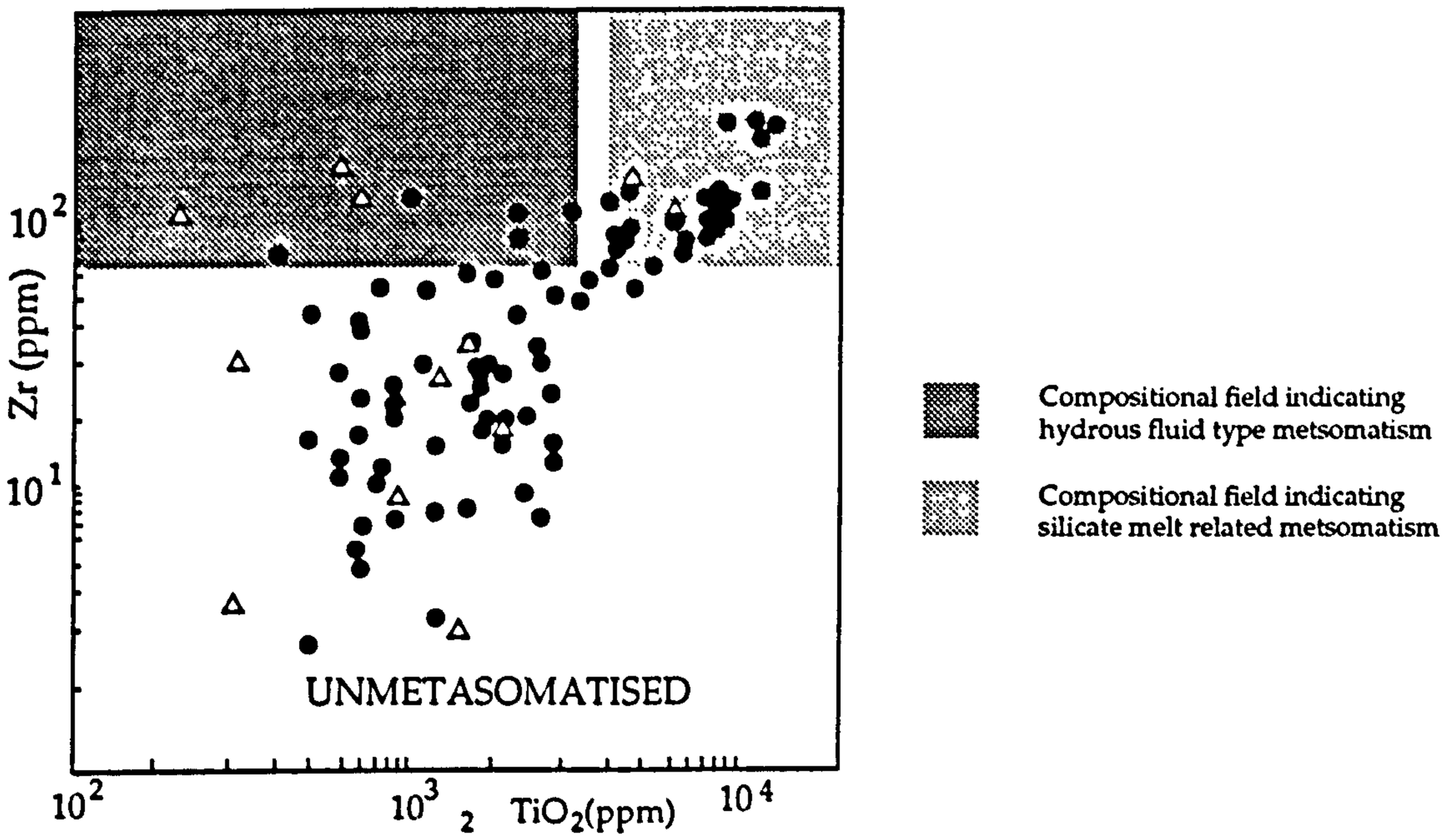

TiO_2 vs Zr (log scales) for FALC and Snowden garnets, n=103. 24 garnets are proportionally enriched in both Ti and Zr, indicative of melt-related metasomatism. A further 8 garnets are enriched in Zr only, suggesting hydrous fluid related metasomatism. Fields shown are defined by Griffin and Ryan(1995).

△ low Ca Cr-pyropes (G10)

● Cr-pyrope garnet (G9)

Figure 6.1.5

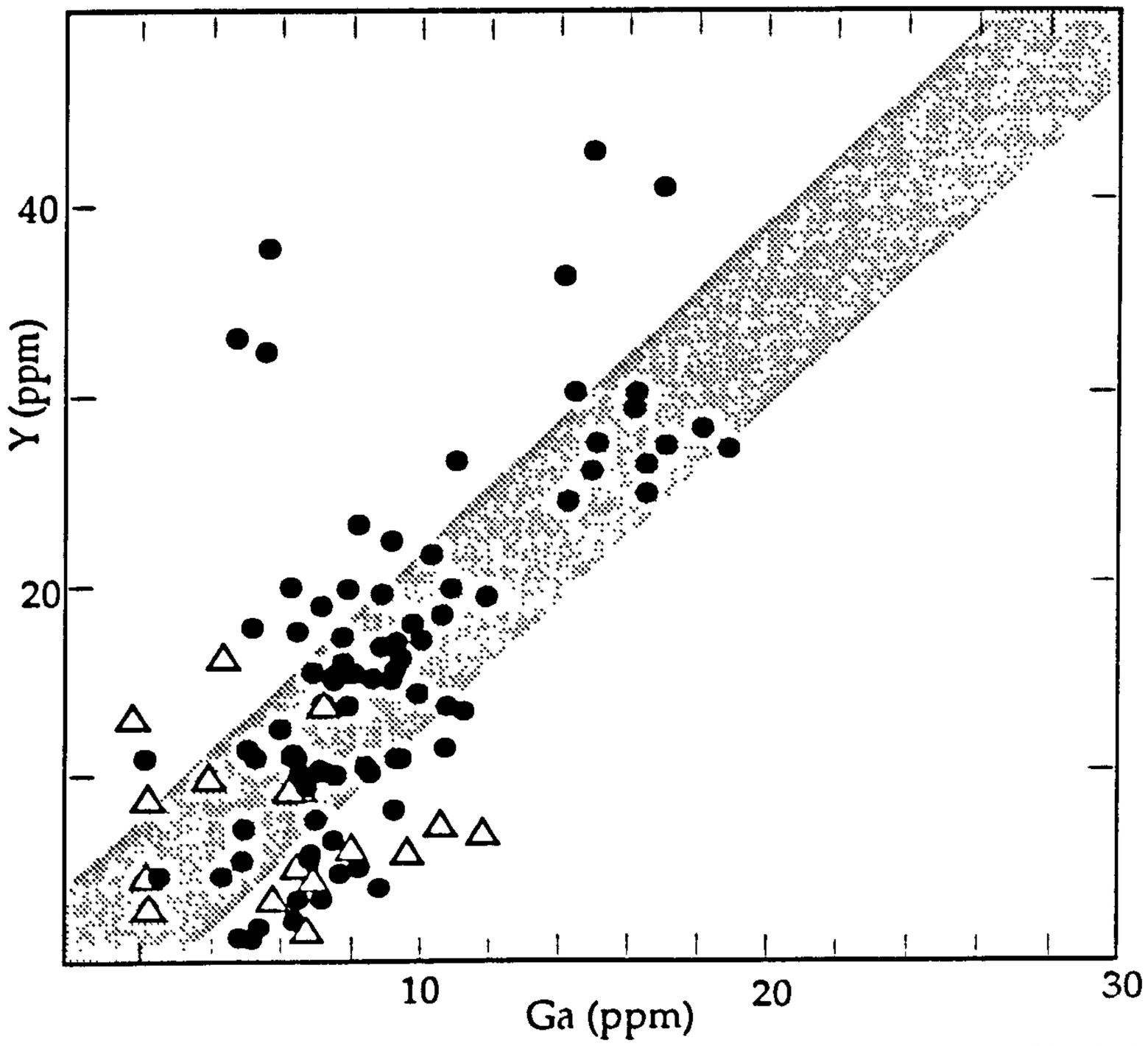

Ga vs Y concentrations (ppm) for FALC and Snowden garnets, n=101. Shaded band represents data with proportionally related Y and Ga concentrations (from Griffin and Ryan, 1995). This is an indication of melt-related metasomatism.

these elements, such as a silicate melt (Griffin and Ryan, 1995), Figure 6.1.5.

Note that much of the data plots along a Y:Ga 2:1 correlation line. This suggests that many of the samples (again about 30%) have equilibrated with a Y and Ga reservoir, most probably explained by metasomatism by silicate melt. Grains that plot well to the right of this proportion (i.e. are Ga rich/Y poor) are noted to have high Zr values, this is indicative of hydrous fluid related metasomatism. The origin of the depletion or enrichment in the garnets, based on Y concentration and discussed in the section above (see Figure 6.1.3), may be inferred from comparing Y to Zr concentration, Figure 6.1.6.

Figure 6.1.6

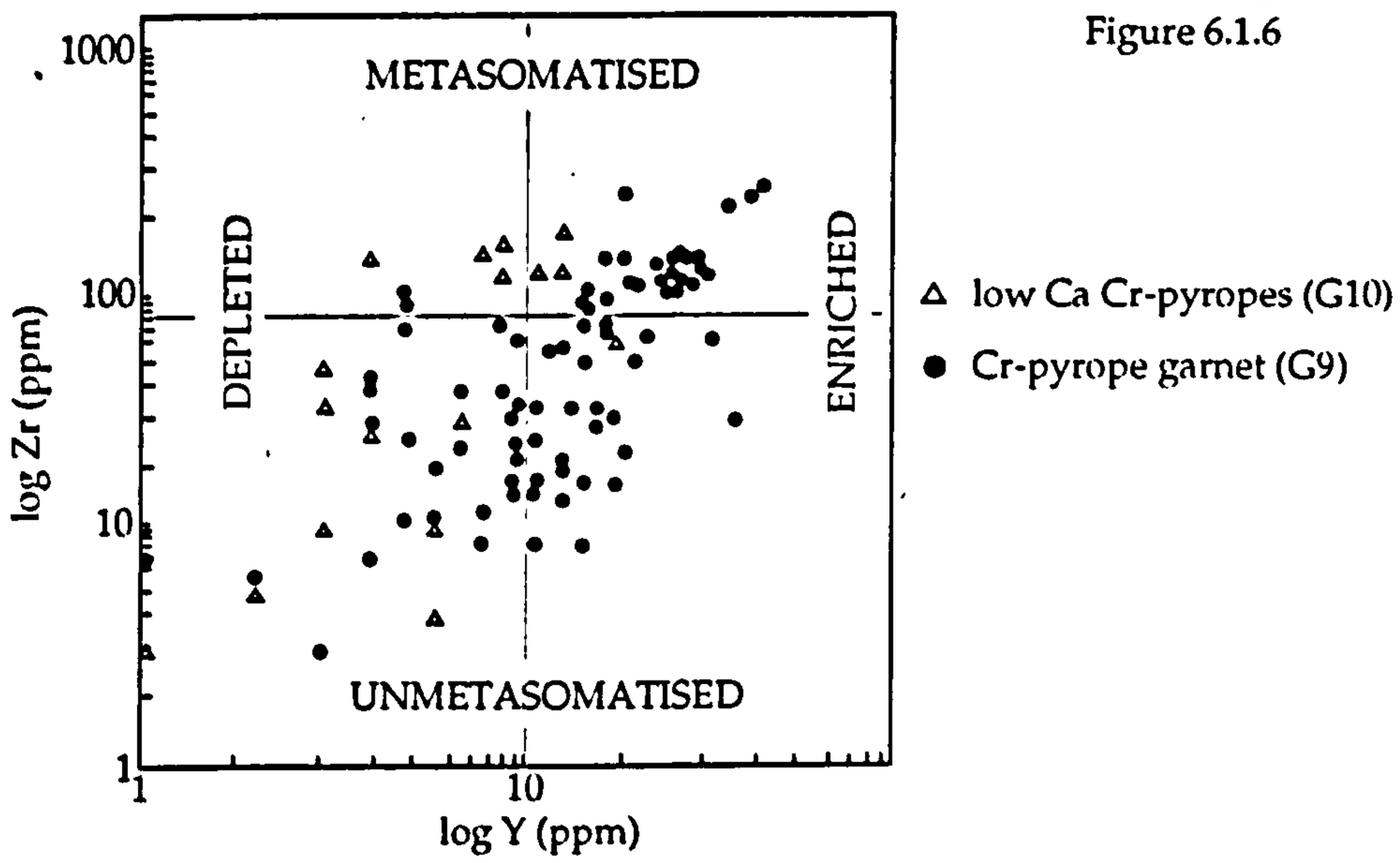

Comparison of Y and Zr for all garnet data at FALC, n = 101, divisions for depleted-enriched and metasomatised-unmetasomatised are from Griffin and Ryan (1995). Note that most of the metasomatised garnets are also enriched.

Note the least depleted garnets (35% of all data, including half of the G10s) are also unmetasomatised (low Zr). Nearly all of the metasomatised garnets are also enriched (and those that are not are mostly G10s), and are about equal in number to the unmetasomatised enriched garnets. Therefore enrichment by metasomatism makes a contribution, at least as important as primary fertile lherzolite, to the fertile mantle population of the lower lithosphere.

Given that no magmatic activity other than the FALC kimberlites is observed in Central Saskatchewan since the mid-Proterozoic, the cause of the silicate melt is either kimberlitic or very old. If the silicate melt related metasomatism is related to the kimberlites at FALC, development would have occurred prior to the initial kimberlite eruption (circa 105Ma to 110Ma) as a

result of a silicate melt pooling at, and infiltrating through, the base of the lithosphere. This metasomatised material was then picked up as xenoliths/crysts by the upwelling kimberlite magma until activity waned, about 10Ma later.

Many of the grains that display either melt or hydrous fluid related metasomatism (35 to 40% of the database) are from within the diamond window, which implies that much of the lithosphere sampled by the kimberlite from 145km to 190km depth was greatly affected by these types of metasomatism. The impact of the metasomatism on diamond preservation is further discussed in Chapter 7.

The validity of implying metasomatic events in the lower lithosphere from trace elemental data can be questionable, particularly as many of the garnet grains used as compositional paradigms for metasomatised xenoliths are examples from South African kimberlites (e.g. Smith and Boyd 1987). Although Griffin and Ryan (1995) also use garnet analyses from Siberian, Australian, Central African and Venezuelan kimberlitic xenoliths, each craton is recognised as chemically different. What is certain, however, is that a proportion of the garnets analysed, particularly those from within the diamond window, display features of metasomatic enrichment of the mantle source.

6.2 Diamond nitrogen-aggregation studies

From the 29 diamonds isolated from the FALC kimberlites by Operation Fish Scale (see Chapter 5), 21 were selected for further analysis of their spectral type and nitrogen aggregation content and type (Taylor et al, 1990). The majority of these analyses were carried out by W.R Taylor at University College London, later with assistance of this author. The aim of this analysis was to characterise the diamond types and to draw conclusions about the nature of diamond growth and preservation in the Central Saskatchewan lithosphere.

Diamonds are classified into spectral types consisting of two main groups depending on their nitrogen content and aggregation state (Harris, 1987). Type I diamonds have measurable nitrogen, Type II lack nitrogen. These are further subdivided into a and b groups: Type Ia contain N aggregated into gaps in the crystal lattice (termed platelets), Type Ib has substitutional N within the carbon lattice. Type IIa are almost free of impurities and Type IIb contain traces of boron. Most diamonds from kimberlite pipes are of Type Ia and contain substitutional nitrogen impurities (>10 to ~3000 atomic ppm) in the form of aggregated defects of which 'A centres' (nitrogen pairs) and 'B centres' (four nitrogen atoms arranged tetrahedrally about a vacancy) are the most abundant.

With increase of time and temperature the N goes from A-type aggregation to the 'higher' B-type (Taylor et al, 1990). Type IaA diamonds contain only A centres, Type IaB diamonds are fully aggregated and contain only B centres, and Type IaAB diamonds have intermediate aggregation states. Because the kinetics of the aggregation process have been determined experimentally, the nitrogen aggregation characteristics of Type Ia diamond can yield useful information on thermal history of the mantle rocks in which they resided (Taylor et al, 1990).

In Type IaAB diamonds, B centres are usually accompanied by linear defects of a few atoms thickness, termed platelets, which are believed to form by the generation of interstitial gaps in the carbon lattice during B-centre growth (Woods, 1986). Platelets grow at different rates depending on temperature, and may be degraded during deformation or short-term heating events that otherwise do not significantly affect A to B aggregation. Type IaAB diamonds may be subdivided into one of four infrared (IR) spectral types (N, M, L or K) according to their state of platelet development (Milledge and Mendelssohn, 1995). Types N and M show greatest platelet development in relation to aggregation state, suggesting a stable and cool aggregation environment, while types L and K ("irregular" diamonds in the terminology of Woods, 1986) show poor or no platelet development, suggesting a thermally perturbed and/or high-strain aggregation environment. Significant proportions of Type IaAB(L) and IaAB(K) diamonds occur in lamproite or kimberlite pipes located in Proterozoic collisional domains such as Argyle or the Colorado State Line kimberlites e.g. Sloan (Otter et al, 1994; Taylor et al, 1990), Figure 6.2.1.

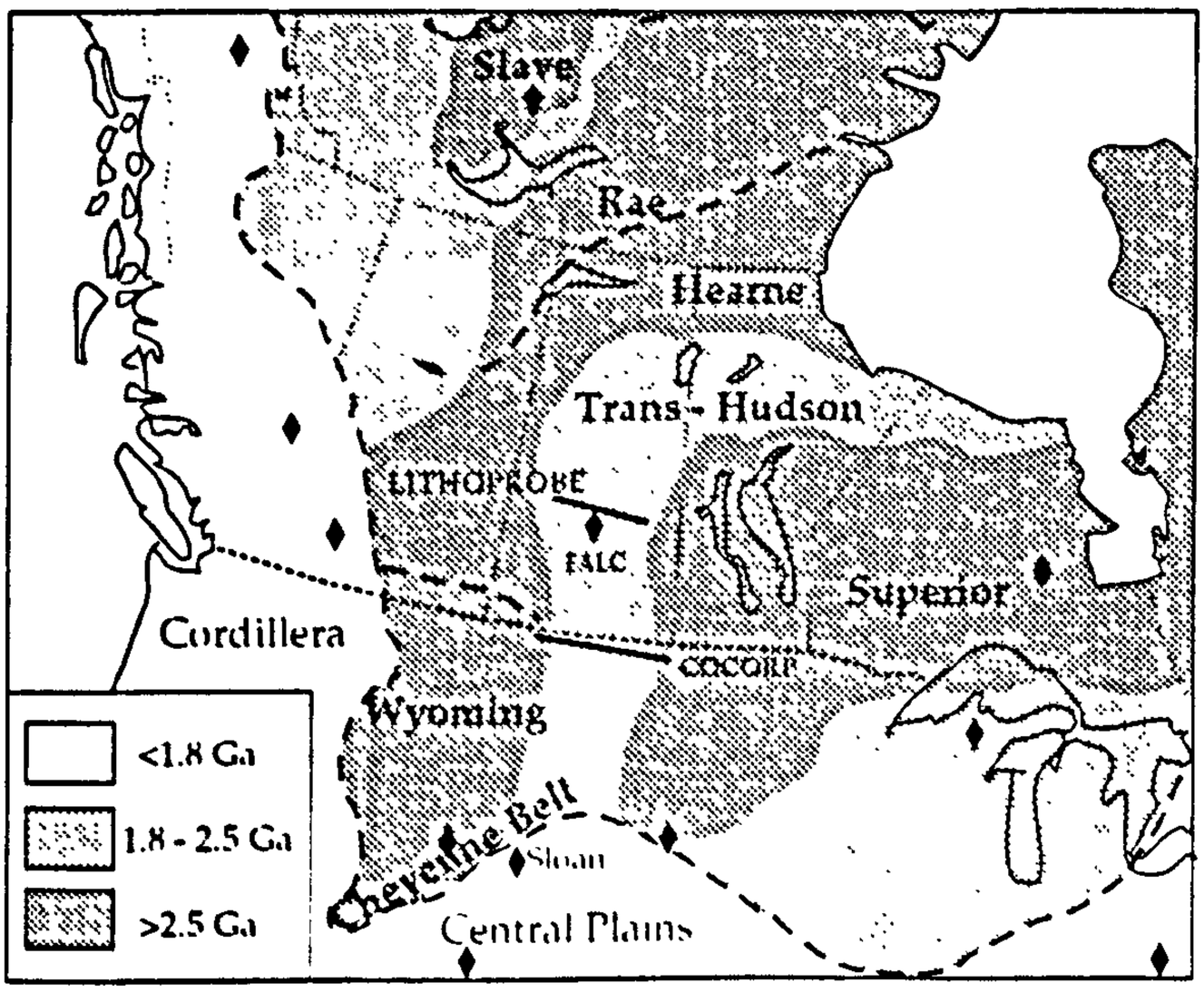

Figure 6.2.1
Map of Provinces of North America and selected sites of kimberlites, including the Colorado-Wyoming State Line group and Sloan, both adjacent to the Cheyenne thrust belt. Also indicated are the approximate locations of the LITHOPROBE and COCORP seismic lines.

Other than Type Ia diamonds, Type II diamonds, which have very low levels of nitrogen impurities (<10 atomic ppm), normally comprise a small proportion of the diamond population in kimberlite pipes. They contain no detectable IR absorption due to nitrogen, and are usually of eclogitic paragenesis (Harris, 1987).

A total of 21 microdiamonds (<1 mm size) and diamond fragments from the FALC tuffs were examined. All were extracted from crushed drill core material. The diamonds were cleaned with dichloromethane to remove surface organic contamination. In order to determine nitrogen contents and aggregation states, the IR spectra of the diamonds were determined using an IR microscope coupled to a Bruker IFS45 FTIR spectrometer. Acquisition parameters were 200 scans, at a resolution of $8cm^{-1}$ over the range $4000\text{-}650cm^{-1}$, using the microscope MCT detector with an aperture of 100μm. Problems included fringing; difficulties obtaining sufficient light transmission through irregularly shaped specimens; and scattering of IR radiation from irregular surfaces which causes baseline shifts. These problems were partially solved by mounting the diamonds on the end of a fine glass-fibre so that the stones could be rotated to achieve optimal conditions of IR light throughput. The resultant spectra and photographs of the diamonds analysed are shown in Appendix XI.

Nitrogen contents ($N_{(tot)}$) and nitrogen aggregation temperatures (T_{NA}) were calculated using the equations (1) and (2) below (Taylor et al, 1990; Milledge and Mendelssohn, 1995)

$$N(tot) = \mu(tot)^{1282}.\alpha(A) + x(B).\mu(tot)^{1282}.[\alpha(B) - \alpha(A)] \quad ....(1)$$

where:

$\mu(tot)^{1282}$ = (IR absorbance at 1282 cm^{-1})/(IR absorbance at 1992 cm^{-1}).1.23

$\alpha(A)$ = 160 atomic ppm

$\alpha(B)$ = 650 atomic ppm

x(B) = spectral proportion of B-defect centres

$$T_{NA}(°C) = E_a/R \,.\, \{\ln([N(tot)/N(A)]-1/[t_{MR}.N(tot).A])\}^{-1} - 273.15 \quad ....(2)$$

where:

E_a = activation energy (7 eV); E_a/R = 81160K (Taylor et al, 1990).

N(A) = amount of nitrogen remaining in the A form (atomic ppm)

A = Arrhenius constant; ln(A) = 12.59

t_{MR} = residence time for diamond in the mantle (seconds)

The T_{NA} values are a measure of the time-averaged thermal history of the specimen. Because nitrogen aggregation is "quenched in" at the time of eruption, only mantle temperature is recorded (Taylor et al, 1990). The calculation requires an estimate of the mantle residence time (t_{MR}) for the diamond to be made. However, because T_{NA} is not particularly sensitive to t_{MR} (a change in residence time from 3Ga to 2Ga makes a difference of only ~15°C), T_{NA} provides a relatively accurate measure of the thermal history of the diamond. For diamonds from Cretaceous kimberlites located in Precambrian cratons, dating studies have established that Proterozoic to Archean residence times are usual (see Taylor et al, 1990), and for the purpose of this study t_{MR} values of 1.6Ga and 2.9Ga have been selected because they are consistent with the ages of the major cratonisation events in Saskatchewan (see Chapter 1). In the case of unaggregated diamonds of pure IaA character, a maximum T_{NA} value can be calculated assuming the amount of B-defect is present at one half of the detection limit of the IR method (~0.5% B). No temperature information can be obtained from Type II diamonds.

The FALC diamonds analysed range in size from ~100 - 2400 μm, some of the stones are broken and have fresh fractures that are presumably the result of milling and crushing the drill core. Many of the stones are crystal aggregates with sharp-edged octahedral faces implying abundant growth nuclei and little post-formation modification (see Chapter 5). Approximately 50% of the diamonds are unaggregated Type IaA stones, 20% are low nitrogen Type IIa stones, and nearly 80% contain <100 ppm of nitrogen. They comprise several distinct populations that are recognisable on the basis of both morphological and spectral criteria (Leahy and Taylor, 1995), Figure 6.2.2.

On a T_{NA} histogram of the FALC diamonds (Figure 6.2.3) an approximately bimodal distribution is evident with maxima at 1025°C to 1075°C and about 1200°C.

Population A Low Nitrogen - Type IaA diamonds

Eight of the 21 diamonds belong to this population. The nitrogen contents of these diamonds are low, with an average of 34 atomic ppm. Most of the stones are unresorbed and etch features are uncommon. Some of the population A diamonds have a small hydrogen defect peak at 3107cm^{-1} in the IR. Because population A diamonds have no detectable nitrogen in the B form, T_{NA} values are maxima with average values of ~1050-1060°C. Such temperatures are consistent with long-term (Archean) storage of these diamonds on a cool lithosphere geotherm (Taylor et al, 1990). Two carbon isotope

Figure 6.2.2

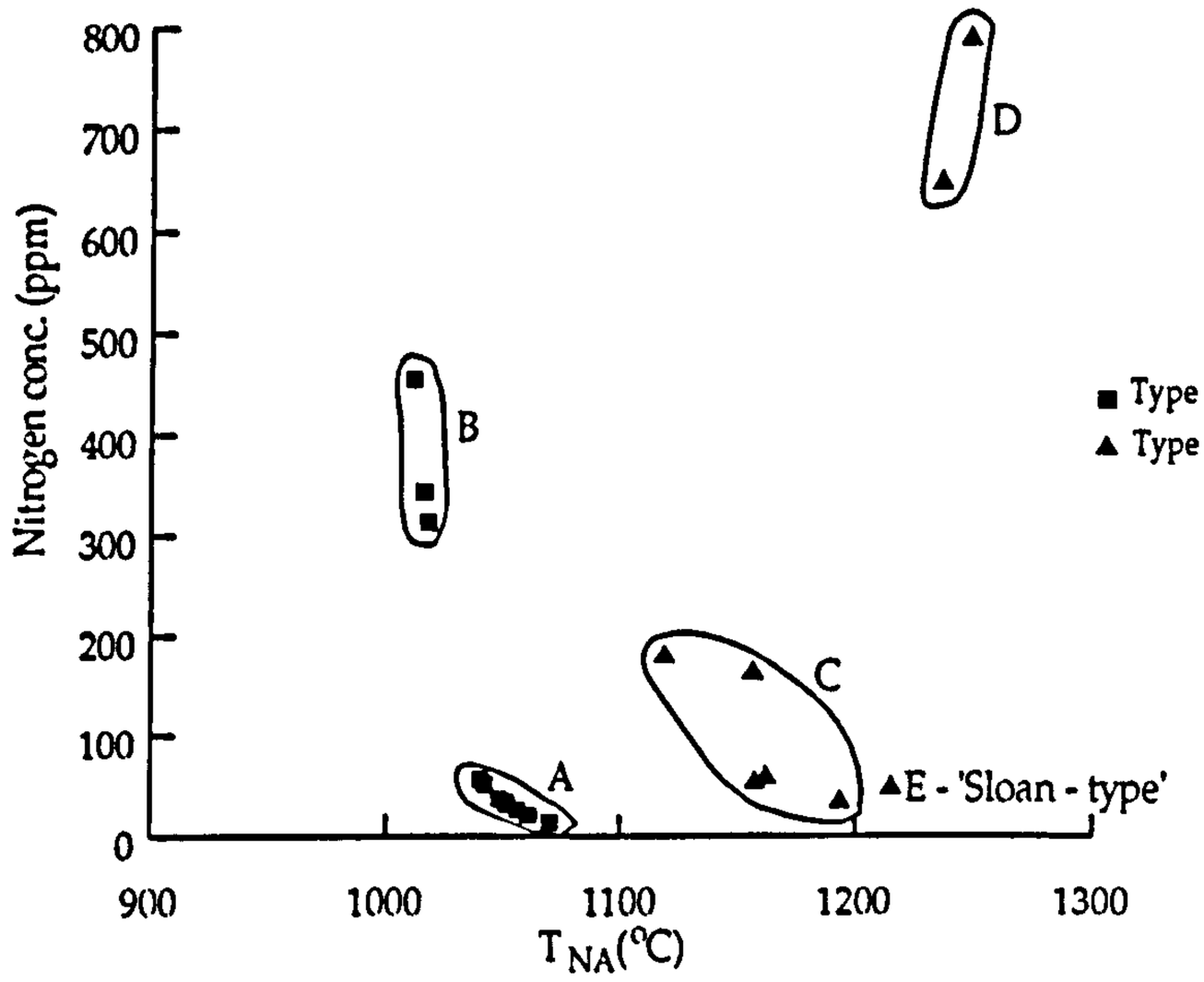

Fort a la Corne microdiamond populations, n=21. F - population not shown because low nitrogen conc (<10ppm) does not allow temperature estimates. See text for discussion.

Figure 6.2.3

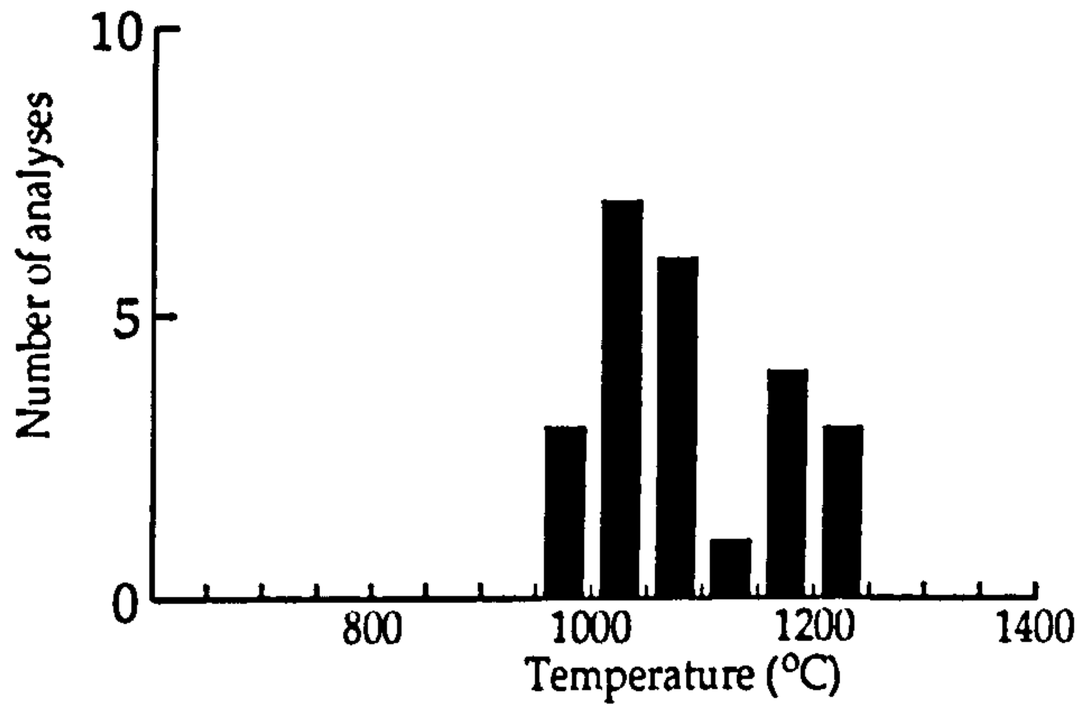

Calculated temperatures for FALC microdiamonds, with a minimum of 980°C and maximum of 1215°C. These results are consistent with with the predicted diamond window from garnet nickel thermomemtry (see previous section). Also note apparent bimodal temperature distribution, discussed further in the text.

determinations on diamonds from this group suggest a probable eclogitic paragenesis for one specimen (-11.8‰) and either eclogitic or peridotitic for the other (-5.2‰, analyses by D. Mattey, see Chapter 5).

Population B High Nitrogen - Type IaA diamonds

Three diamonds have pure IaA spectra and contain several hundred ppm of nitrogen. The nitrogen aggregation constraints suggest they are either younger than population A and/or must have resided under lower temperature conditions (i.e. at shallower depths) in the mantle. Morphologies also differ from population A in that these diamonds are resorbed (although one is a fragment with a frosted external face but unknown resorption degree). Calculated T_{NA} values, as with population A, are compatible with growth and residence of the diamonds in cool lithosphere. If these diamonds were resorbed in the mantle before kimberlite eruption (e.g. by influx of oxidising fluid) then they presumably existed in a different region of the lithosphere than population A. They are attributed to growth in the Archean at relatively shallow depths.

Population C Type IaAB(M) diamonds

This population is known from several fragments which may have been derived from a small macrodiamond. One of the fragments is large (2.4mm in length) and yielded several spectra that are sufficiently different to indicate some growth zonation of the original diamond. Nitrogen contents are low <200ppm, and T_{NA} values are ~1180-1140°C which is compatible with M-type platelet development. These features are unremarkable for kimberlitic diamonds from Archean cratons.

Population D High Nitrogen - Type 1aAB(L) diamonds

Two diamonds, both fragments, are B-defect rich and contain ~600-700ppm nitrogen. Because they are fragments their external morphology is uncertain, although one diamond fragment has a frosted external face and was possibly part of a larger octahedral stone. Calculated average T_{NA} values are high (~1200-1250°C) and such temperatures are compatible with their L-type platelet development. It is likely these diamonds are from an older population and/or one of deeper origin (and hence higher temperature) than the other populations. One carbon isotope determination yielded a value of -12.1‰ suggesting an eclogitic paragenesis, see Chapter 5.

Population E Type IaAB(K) 'Sloan-type' diamond

A single colourless diamond of low nitrogen content is platelet-absent and partially nitrogen aggregated (type K). It has a high aggregation temperature (~1230-1250°C) and is similar to some diamonds from the Sloan kimberlite in Colorado that are known to of developed during Proterozoic cratonisation (Otter et al, 1994)

Population F Type IIa diamonds

Most of the Type IIa specimens are octahedral aggregates of low resorption degree similar to population A. Temperature and residence time cannot be calculated because of the small amounts of nitrogen present (<10ppm).

The FALC microdiamonds are unusual in that many of them have low nitrogen contents and there are a high proportion of Type IIa specimens. This suggests the diamonds grew in protoliths, such mantle-recycled oceanic crust, that were strongly degassed of their volatile constituents. The low aggregation state of many of the microdiamonds (populations A and B) suggest that they grew and resided in lithosphere having a low geothermal gradient such as the thick, stable lithosphere that exists beneath old Archean continents. The occurrence of some microdiamonds with high temperature thermal histories, including one 'Sloan-type' diamond (Type IaAB(K)) suggests the FALC kimberlites also sampled a different, high-temperature and high-strain lithospheric environment (Leahy and Taylor, 1995). Both the nitrogen aggregation characteristics of FALC microdiamonds and Ni thermometry of garnet xenocrysts are compatible with the existence of diamond in a range of temperature conditions, from 980°C to 1250°C, in the lithosphere beneath FALC.

The nature of the lithosphere in Central Saskatchewan, based upon evidence from the nitrogen-aggregation characteristics of diamonds, is discussed further in Section 6.4 below.

6.3 Lithospheric models based on geophysical data

While the mineral chemistry of garnet and diamond xenocrysts can provide an indication of lithospheric conditions that existed in the past (particularly mid-Cretaceous, mid-Proterozoic and late Archean), geophysical data provides constraints for the current state of the lithosphere. These may reasonably be extrapolated back to the time of kimberlite eruption in the Cretaceous because there are no major tectonic differences between then and now: Central Saskatchewan remains cratonic, and the Laramide orogeny to the west is essentially still active. Cretaceous geodynamics have already been described, as has briefly, the nature of the Glennie Domain. This Archean microcontinent plays a key role in the diamondiferous nature of the Saskatchewan kimberlites (Leahy and Taylor, 1995), and is detailed further below.

6.3.1 Regional Structure from Seismic Reflection

Evidence from east-west seismic reflection profiling (LITHOPROBE at 55°N and COCORP at 49°N, shown on Figure 6.3.1) confirms that the Trans-Hudson orogen (THO) is a broadly anticlinal structure (Lewry et al, 1994; Lucas et al, 1994; Nelson et al, 1993). The central region, called the Glennie Domain (GD), comprises tectonically emplaced 1.83-1.79Ga arc volcanics and arc sediments bordered by miogeoclinal sediments associated with the Hearne/Wyoming craton to the west and Superior craton to the east. The entire THO is tectonised by transpressional structures, including thrusts and strike-slip faults, some of which extend into the lower crust.

Broad tectonic structures indicate a collision and underthrusting of the GD from the NW to SE (in current orientations, Lucas et al, 1994). The final subduction polarity of the GD is postulated to have been north-westwards, under the Hearne/Wyoming craton. However, the GD consists of lower crustal wedges under *both* the eastern (Superior) and north-western boundaries (Hearne/Wyoming); i.e. GD underlies both cratons, see Figure 6.3.1.

In Saskatchewan the antiformal core of the GD is composed of Archean mylonitic and gneissic rocks, with scattered windows outcropping at the surface along minor anticlinorial and thrust axes in the north (around 57°). The arch crest in the COCORP profile (49°N) is at 20km depth, and may be related, if not a continuation of the anticlinal core in Central Saskatchewan.

The GD imaged by LITHOPROBE includes a crustal root at 48km depth, and a significant Moho topography of about 12km over a 60km ½-wavelength (Lewry et al, 1994). This root is situated in the western half of the

Figure 6.3.1

LITHOPROBE SECTION

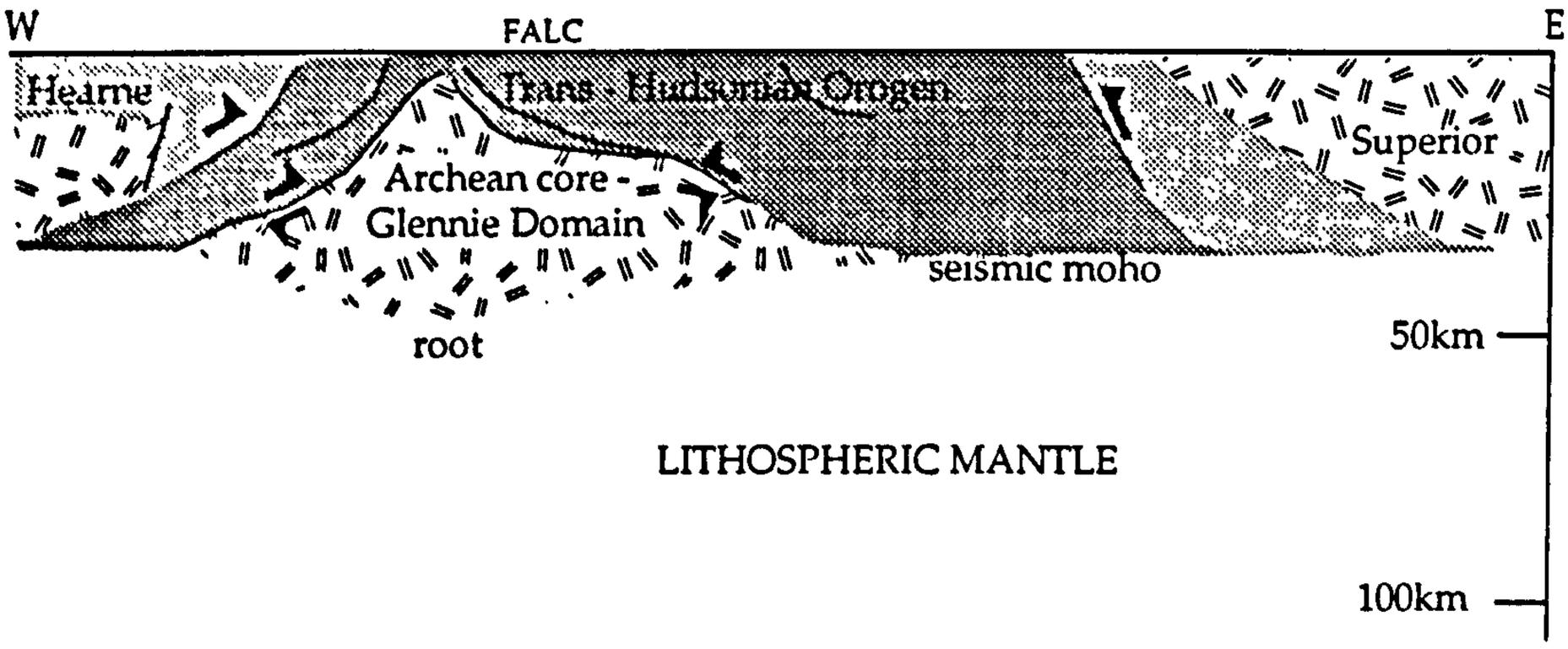

Seismic cross-section through the FALC area adapted from LITHOPROBE section (Lewry et al, 1994). Length of section is approximately 300km. The root of the Archean Glennie Domain lies under the current location of Prince Albert, with FALC to the eastern slope of the root.

COCORP SECTION

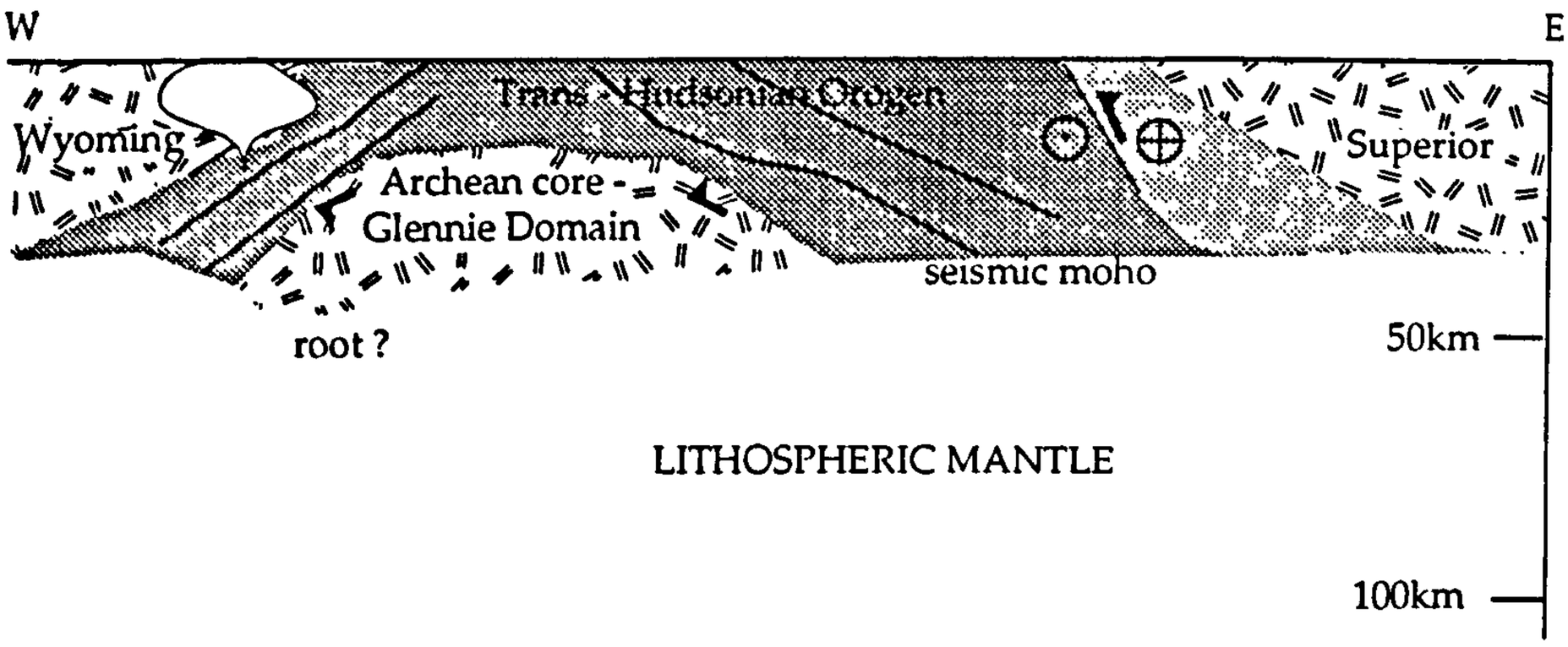

Seismic cross-section of northern Montana adapted from COCORP section (Nelson et al, 1993). Note the buried Archean core. Length of section is approximately 300km.

GD, and corresponds to the postulated crust-wide thrust system (GD down to the west) that is the boundary between the GD and craton to the west. When correlated with current topography, the root zone occurs below Prince Albert. Work in progress suggests that the root zone may not be present in a linear fashion along the entire north-south strike of the THO western boundary (Ellis et al, 1996). FALC kimberlites occur on the eastern slope of this crustal root zone.

6.3.2 Further geophysical evidence for lithospheric keels

Tomography

Shear wave velocity perturbations obtained by tomographic inversion can indicate sub-Moho structure; high seismic velocities relative to average mantle velocities may indicate lower temperatures, suggesting the presence of a thicker lithosphere. Grand (1994) has shown that the THO has a regional positive (+4%) shear wave velocity anomaly to around 175km depth, with small localised areas (including below FALC) of lower (+2%) shear velocity differences to around 325km depth, Figure 6.3.2.

Figure 6.3.2

Shear wave velocity perturbations for the North American Plate (after Grand, 1994). High velocities indicate cool and/or lithospheric composition rocks. Positive velocity differences (+3%) are observed at great depth (>250km) beneath the FALC and Lac de Gras kimberlite fields, and weaker velocity anomalies continue to >320km under FALC. These contours provide constraints for the present-day lithospheric thickness. Diamonds indicate locations of kimberlite fields.

These values suggest present day lithospheric thickness of about 175km, comparable to that sampled by the FALC Cretaceous kimberlites, as indicated by garnet thermobarometery. The lower (+2%) velocities that comprise the deeper parts of lithosphere may be due deep mantle roots of chemically distinct mantle that penetrate to about 300km (Jordan, 1981). Similar roots are found on the Eurasian (Siberia) and African (Kaapvaal) cratons (Grand, 1994), and

may represent artefacts due to chemical and density variations not rationalised by the tomographic inversion technique.

Gravity

The Elastic Thickness of the lithosphere (depth to the base of the Mechanical Boundary Layer; James, 1994) has also been modelled over Canada, based upon glacial rebound, topography and Bouguer anomalies. In the area of FALC the elastic thickness is significantly large; at least 90km and rising rapidly to a maximum of about 150km two hundred kilometres to the east, under the Superior craton (Pilkington, 1991). These values reflect primarily the thermal conditions within the upper lithosphere (depth of the 1000° isotherm; James, 1994), but are heavily modified by the regional stress fields, crustal and mantle rheology and composition of the lithosphere. The elastic thickness at FALC is approximately 100km, which correlates to about 650°C from the geotherm described by garnet-nickel thermometry (see above). Although resolution is poor, the great elastic thickness in the region is consistent with both thick crust and lithosphere.

6.4 The nature of the lithosphere in Central Saskatchewan: evidence from mantle xenoliths/crysts.

Garnets from the FALC kimberlites yield a bimodal temperature distribution for both lherzolitic and harzburgitic types: 850-1050°C and 1150-1300°C. Although some of the high temperature population are of enriched (kimberlitic or asthenospheric) origin, many are depleted, indicating the presence of depleted garnet peridotites at the base of the lithosphere, itself at about 190km depth and 1300°C. Intersection of the geothermal gradient based upon garnet geo-thermometry/barometry (Figure 6.1.2) with the diamond-graphite transition suggest a diamond window from 950°C and 145km to the base of the lithosphere. This compares favourably with nitrogen-aggregation temperatures from diamonds, also bimodal, with low and high temperature populations, see Figure 6.4.1 below.

Figure 6.4.1

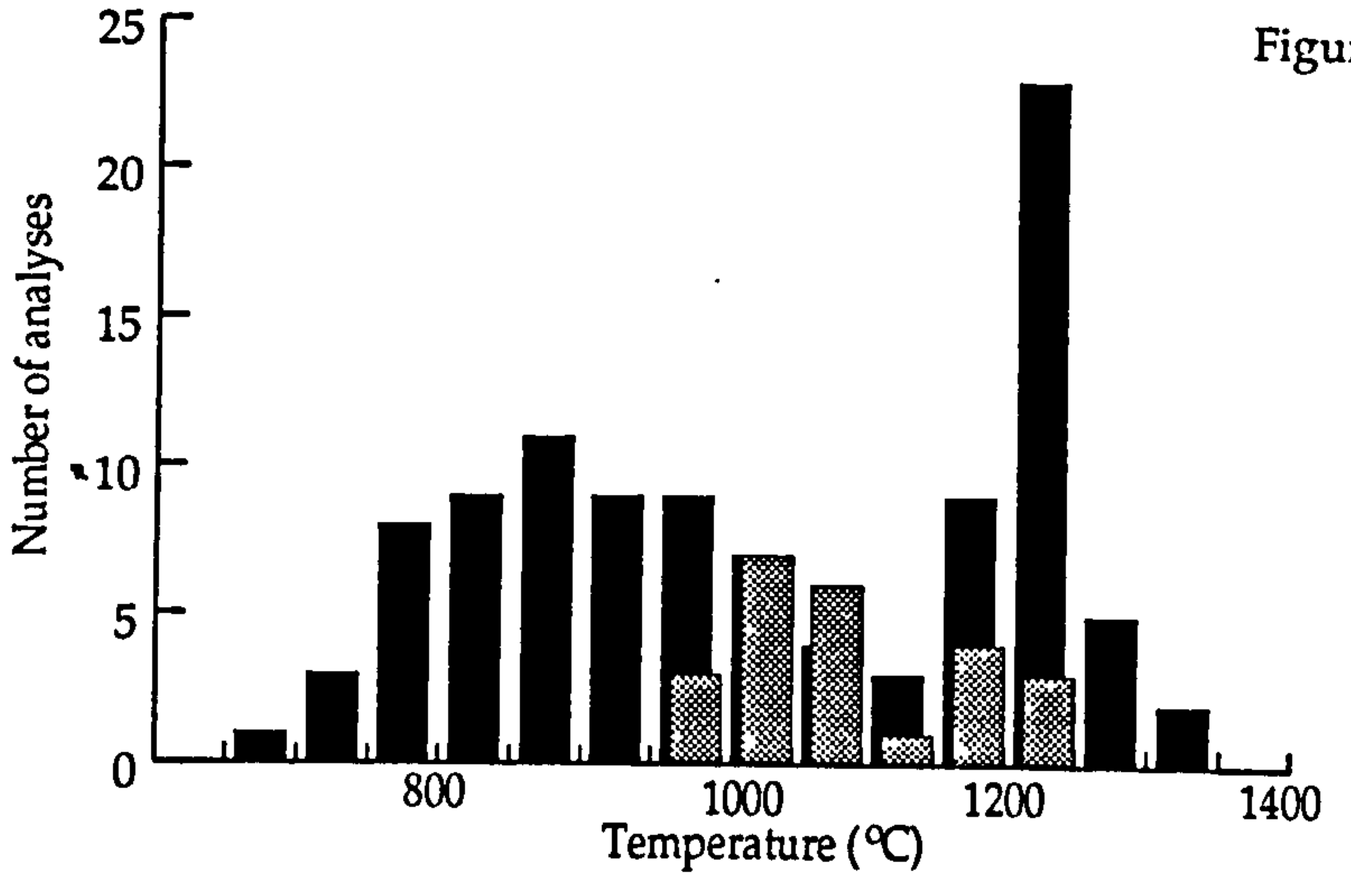

Combined garnet (black columns) and microdiamond (grey) thermometry data (see Figures 6.1.1 and 6.2.3). Note the coincident bimodality of both data sets within the diamond window (950 to 1250 °C).

It has been suggested (Section 6.1) from trace element concentrations in the FALC garnets that the Central Saskatchewan lithosphere has experienced at least two types of metasomatism: a pervasive high-T silicate melt (probably Cretaceous, due to kimberlite magma) type, and a low-T hydrous fluid related metasomatism (phlogopite). Further evidence for the fluid metasomatism is provided by chromium amphiboles attached to G9 garnets, although these are probably derived from shallower levels within the lithosphere. Both the metasomatic events are typically recorded in lithospheric xenoliths of Group I kimberlites world-wide (Griffin and Ryan, 1995).

Carbon isotope analysis indicated two diamonds of eclogitic origin, $\delta^{13}C$ -11.8 and -12.1‰, and one either peridotitic or eclogitic, $\delta^{13}C$-5‰ (Harris, 1987). Average garnet proportions from FALC heavy mineral separates are 12% crustal, 50% mantle peridotitic, 25% megacrystal (kimberlitic) and 18% mantle eclogitic origin. Overall it appears the Cretaceous lithosphere sampled from 100km to 180km was dominated by peridotites relative to eclogites. The lower half of the lithosphere is probably dominated by relatively depleted lherzolites and harzburgites as indicated by the large proportion of high temperature depleted garnets. These lower lithosphere rocks are diamondiferous from 145km to 180km, and it is speculated that metasomatism occurred immediately prior to eruption by the infiltrating kimberlitic proto-magma, Figure 6.4.2. It is interesting to note the apparent lack of diamonds in the basal 10km of the lithosphere, corresponding to 1250°C to 1320°C. This may be an artefact due to the relatively small sample number of diamonds, an error of temperature determination, or may reflect conditions (thermal and/or

Figure 6.4.2

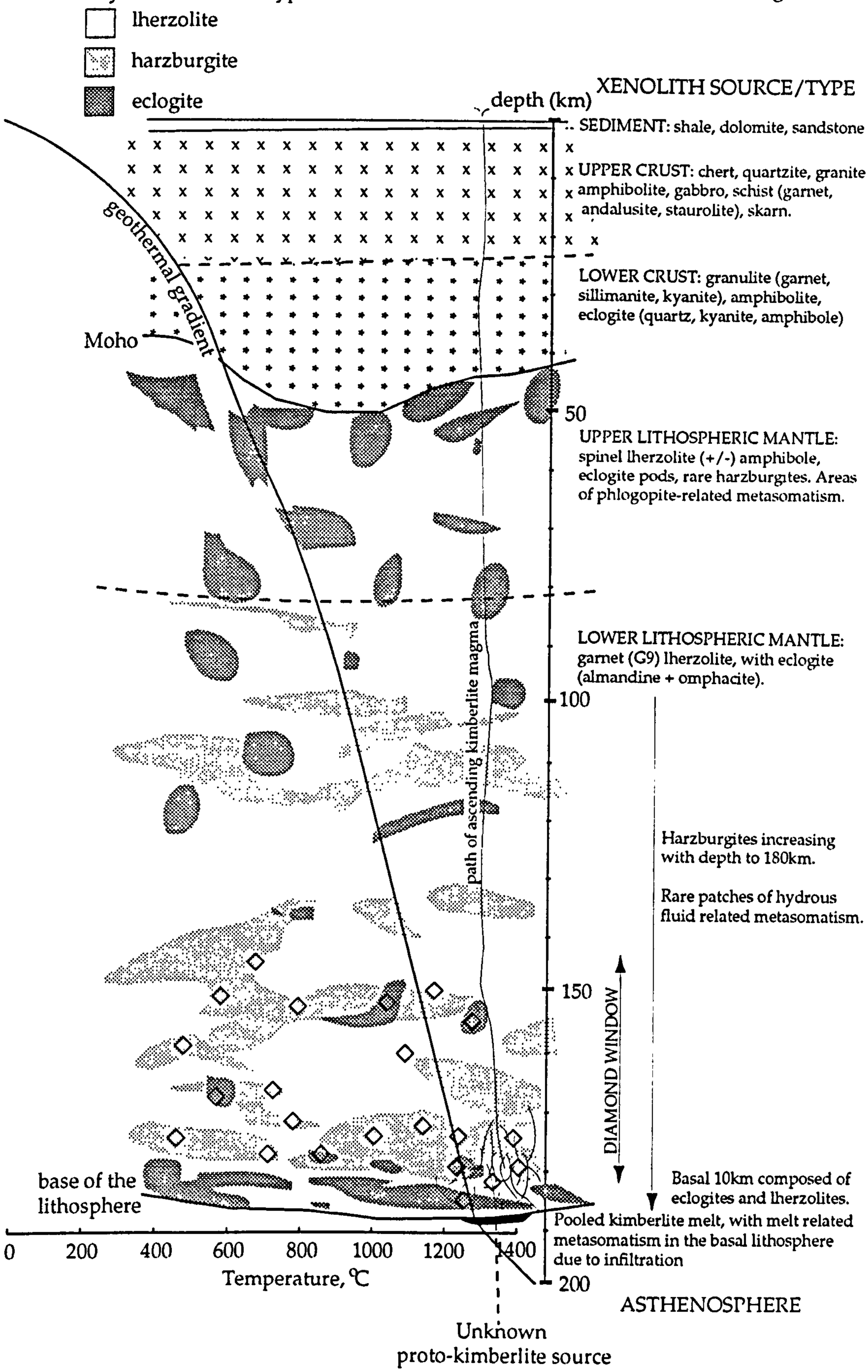

Schematic of the constitution of the lithosphere beneath the Glennie Domian in the Mid-Cretaceous, based on xenocrystal types found in FALC kimberlites, and models of lithospheric composition (Ringwood, 1987).

metasomatic) hostile to diamond growth and/or preservation. The constitution of the deeper levels of the lithosphere is further discussed in the final section of this Chapter.

The mid-levels of the lithosphere are probably host to the various eclogitic pods, with omphacite-pyrope almandine pairs. Surrounding the eclogites are both depleted and fertile garnet lherzolites, bearing diamonds from about 145km. This mixed lithospheric composition is extrapolated up to the Moho (base of the crust) at about 45km depth under FALC (Figure 6.4.2). The broad compositional make-up of the lithosphere under the Glennie Domain is comparable to that described for most other cratonic regions (Ringwood, 1987), and may summarised by a mix of lherzolite, harzburgite and dunite, with irregularly dispersed eclogite pods.

The presence of moissanite, if verified, (Chapter 5) would suggest an origin exotic to even the asthenospheric upper mantle. Various authors (e.g. Moore et al, 1986) propose depths of origin of this mineral ranging from 400km to 800km. Moissanite, along with other ultra-high pressure (UHP) phases (such as majorite, a sodic garnet), are recognised sporadically in some kimberlites from around the world (e.g. Fuxian, China, Leung 1990), and have been one of the main arguments for the deep plume origin of the kimberlite magmas that transported them to the surface (Haggerty 1994). Given the slightly ambiguous origin of the moissanite grains isolated from FALC kimberlites, the evidence for a deep plume genesis for the kimberlite is somewhat scant, and is disregarded until further evidence can be collected.

6.4.1 Comparison to the Kaapvaal, Venezuelan and Siberian craton

Kimberlites and lamproites occur on nearly all of the Archean cratons (Archons) world-wide (Dawson, 1989). Central Saskatchewan (a 'micro-Archon' entrapped within a Proterozoic mobile belt, see discussion below) is compared to Siberian, Kaapvaal and Guyanan (Venezuelan) Archons.

Shear wave velocity anomalies of +4% indicate that the lithosphere of Central Saskatchewan is still at least 175km thick, and probably much thicker. Anomalous shear wave velocities of +2% also occur, and may comprise deeper parts of lithosphere due to deep roots of chemically distinct mantle that persevere to about 300km (Jordan, 1981). Similar roots are found on the Siberian and Kaapvaal cratons, but not the Venezuelan (which also has lower velocities to 175km (+3%); Grand, 1994).

PMP studies of garnet xenocrysts, comparable to those described for FALC above, have been carried out by CSIRO Australia on many of the

kimberlite-hosting cratons of the world and many have been recently published (data from Griffin et al, 1995a; Griffin et al, 1995b; Nixon et al, 1994 are used in the following comparisons). T_{Ni} histograms for the Venezuelan and Kaapvaal cratons are compared to Central Saskatchewan, Figure 6.4.3.

Figure 6.4.3

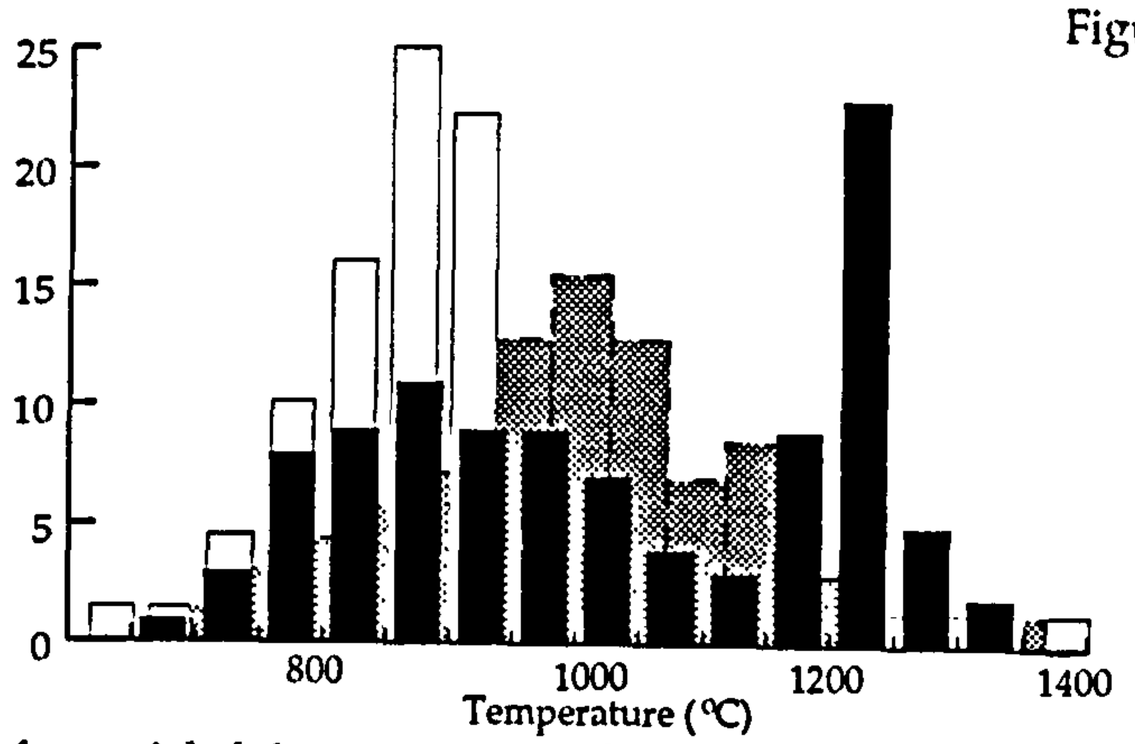

Temperatures calculated from nickel thermometry vs frequency for all FALC data (n=101, black bars). These are compared to data from Venezuela garnets (solid white bars) and Kaapvaal garnets (shaded dashed bars) that have been normalised to n=101, from n=184 and n=312 respectively allowing a direct comparision (Griffin et al, 1989). The Venezuela and Kaapvaal populations lack a high-temperature peak developed as well in the Saskatchewan garnets, although the low temperature garnet peaks (750 to 1050°C) are comparable.

The low temperature garnet population has a comparable distribution to the garnets in the Venezuela craton (and Siberia; Nixon et al, 1994), but cooler than in the Kaapvaal craton (Griffin et al, 1994). The high temperature group has lower temperatures in the Kaapvaal (1150°C to 1200°C, compared to 1200°C to 1250°C in Central Saskatchewan). It is, however, virtually absent in the Venezuela craton.

The highest temperature garnets, that are also Y-depleted (<10ppm) are used to define the base of the lithosphere (Ryan and Griffin, 1995), and indicate a depth of 190km at temperatures of about 1300°C for Central Saskatchewan. This is shallow compared to the Paleozoic Siberian kimberlites of the northern Daldyn field (e.g. Mirney), at 210km depth, and the earlier (>90Ma) Kaapvaal kimberlites, at 220km depth. But relatively thick compared to young Kaapvaal kimberlites at 170km to the base of the lithosphere, and Kaapvaal kimberlites (Tertiary) generated near the southward-propagating point of the East African Rift system, at 130km deep. Siberian kimberlites of the southern Olneck River region (Proterozoic mobile belt, or Proton) have a base of lithosphere at 120km.

The distribution of the lithospheric peridotites (mostly depleted and fertile lherzolite and harzburgites) also varies between Archons. In the lithosphere of Central Saskatchewan harzburgites are concentrated at two levels: 90-120km and 130-180km, with the basal 10km of the lithosphere comprising lherzolite

and eclogite. This is entirely comparable with the distribution of the northern Siberian and Kaapvaal (before 90Ma) Archons. The Venezuela, southern Siberia (Proton) and young (<90Ma) Kaapvaal kimberlites contain considerably fewer harzburgitic garnets, which are located near the base of the lithosphere.

The presence of hydrous fluid metasomatism (producing phlogopite and amphibole within the garnet lherzolites and harzburgites) indicates portions of the Central Saskatchewan lithosphere are more hydrated relative to the Siberian lithosphere. Similar indications of a hydrated lithosphere are found in mantle xenoliths of the Venezuelan and younger Kaapvaal Archons (Erlank et al, 1987).

Younger kimberlites (<90Ma) of the Kaapvaal craton indicate thin lithosphere and also contain evidence for 80% of the rock affected by silicate melt metasomatism. This is consistent with the model of on-going kimberlite magmatism in the Kaapvaal eroding the base of the lithosphere, as a result of the onset of rifting (Griffin et al, 1995b).

In summary the Central Saskatchewan lithosphere is physically most similar to the Siberian Archon, although is probably chemically diverse due to different metasomatic histories. The Venezuelan and young Kaapvaal Archons are thinner, and have diminished harzburgite components, although they are not themselves comparable. The old Kaapvaal Archon was broadly similar in constitution and degree of metasomatism, but was also considerably thicker.

The lithosphere at FALC after kimberlite magmatism remains relatively intact, an indication that prolonged kimberlite magmatism has not occurred, and surface occurrences of kimberlite and lamproite will not be as numerous in Central Saskatchewan as on the Kaapvaal Archon.

6.4.2 Crustal evolution and the origin of diamonds in Central Saskatchewan

The pre-collisional Glennie Domain (GD) had a width of at least 400km (determined from the present-day extent of Archean wedges imaged by LITHOPROBE), and probably existed as an Archean microcontinent (Lewry et al, 1994), see Stage 1, Figure 6.4.4. During the latest Archean the base of the GD lithosphere was at least 150km deep, below the typical graphite-diamond isograd. This is consistent with the 'normal' populations (A, B, C and F) of diamond present with Archean characteristics. i.e. model mantle residence time of 3Ga, at various temperatures in the range of 980-1100°C. During this period (circa 3.0 to 1.9Ga) subduction polarity may of switched repeatedly, allowing

Figure 6.4.4

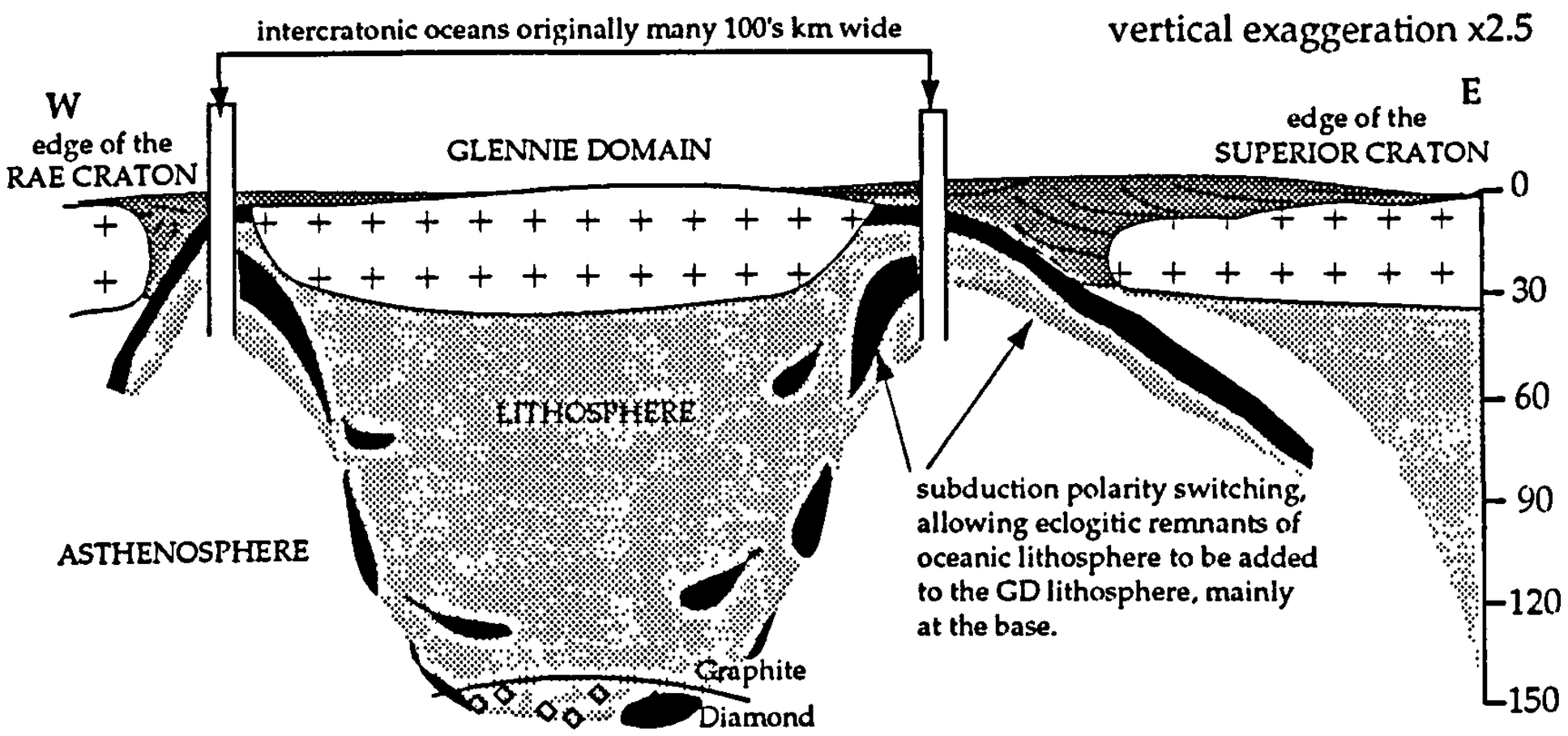

STAGE 1: Latest Archean, circa 2.8Ga to 1.9Ga. Glennie domain exists as a microcontinent at least 400km wide, with thick attached lithosphere. As subduction closes the bordering oceans accretionary prisms build up. Diamonds develop in the base of Glennie domain lithosphere.

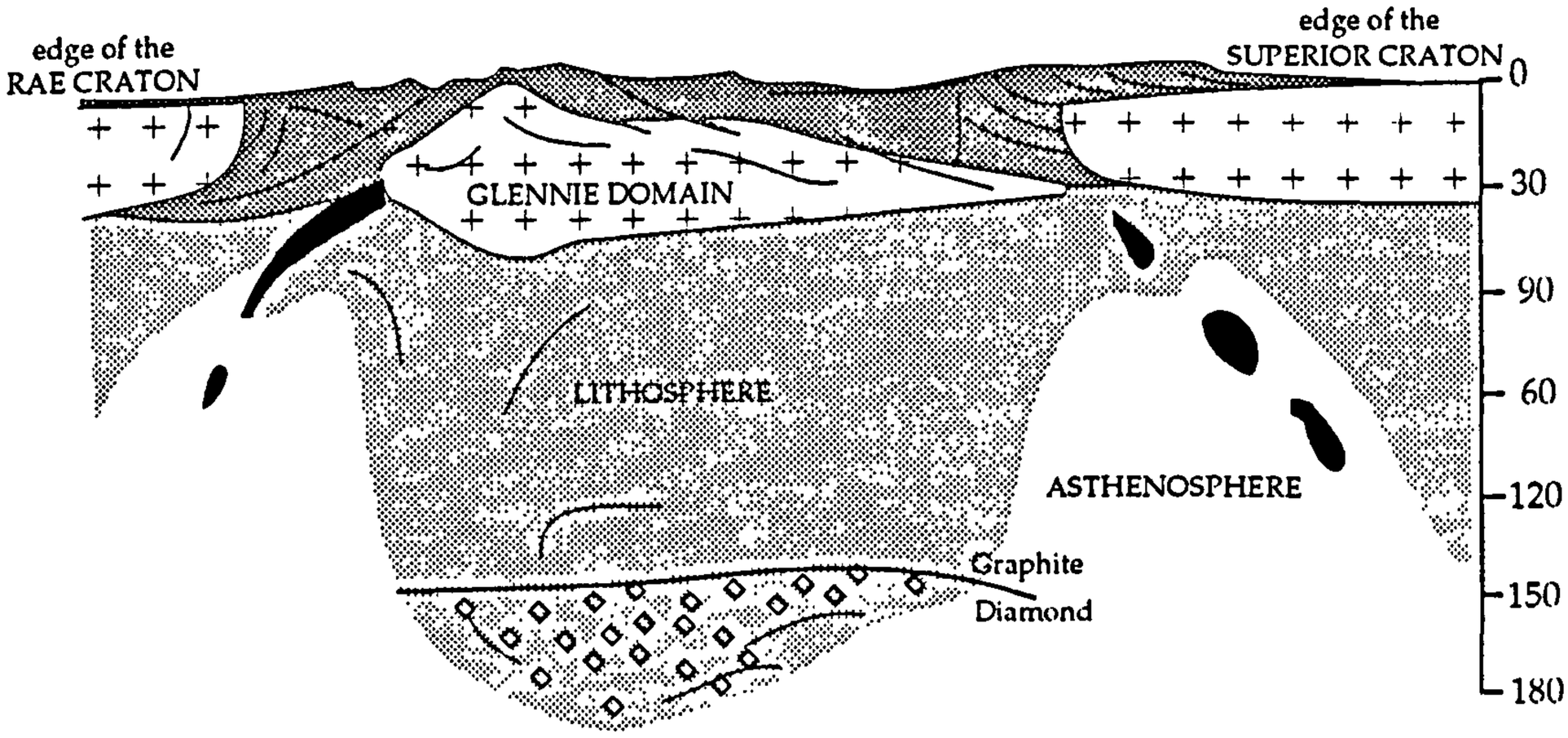

STAGE 2: Mid-Proterozoic, circa 1.75Ga. Peak Trans Hudson Orogeny entraps the Glennie Domain between the Rae and Superior cratons, buckling the plate and attached lithosphere, thickening both. Entire plate is overthrust from both sides by accretionary and orogenic complexes, mainly of Proterzoic ages. New diamond populations grow in the lithospheric keel, including the eclogite-rich basal 10km, often displaying plastic deformation e.g. Sloan-type diamond (3-3-1).

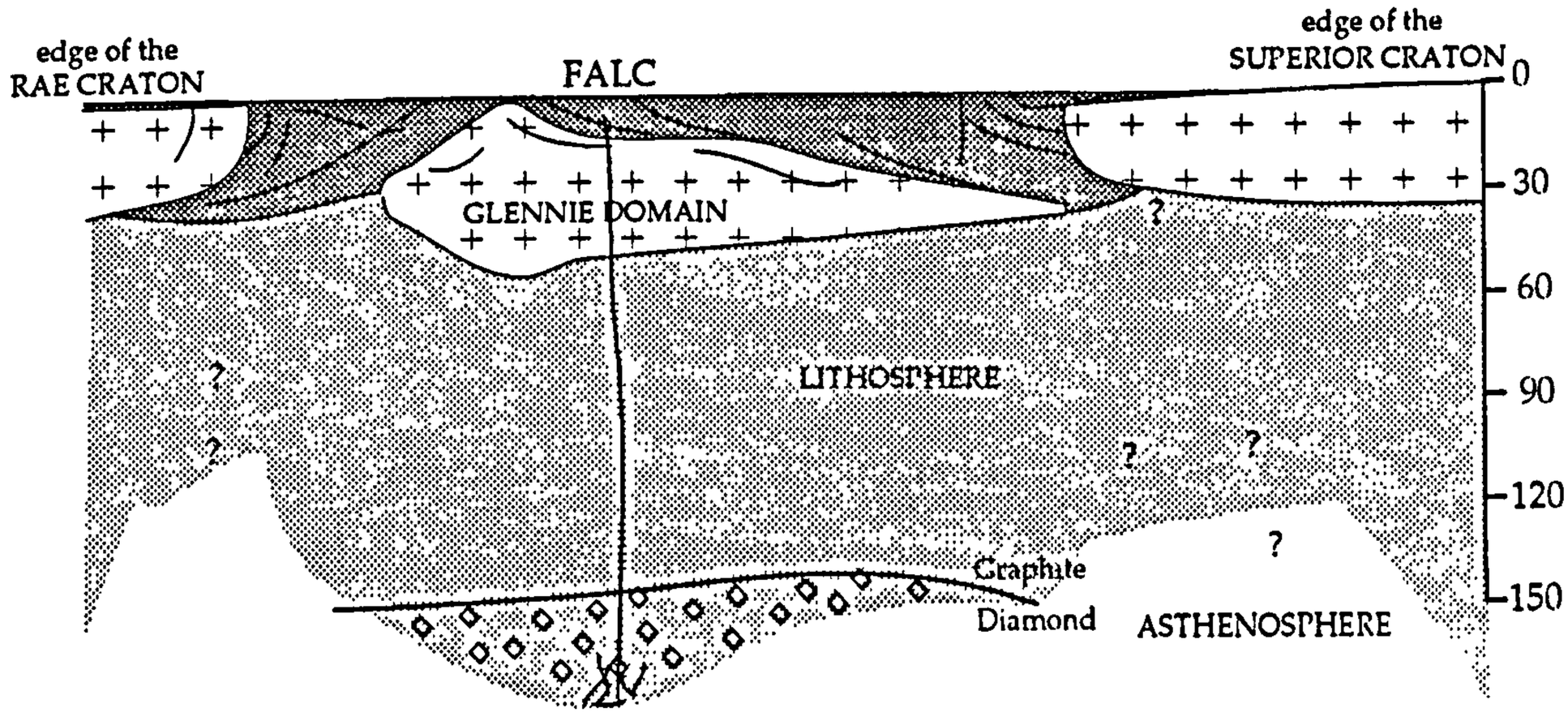

STAGE 3: Mid Cretaceous, 0.1Ga. Kimberlite volcanism, rooted in the Glennie Domain lithospheric keel, with base of lithosphere at 190km.

subducted oceanic lithosphere to be incorporated into the base of the GD lithosphere as eclogites.

As an alternative to this model it is possible the late Archean GD did not have a well developed lithosphere, and inherited the Archean-type lithosphere and diamonds from the Superior craton to the east during Proterozoic docking or continental collision. However, this seems unlikely given the relatively stable nature (a defining characteristic) of cratonic lithosphere.

Leahy and Taylor (1995) proposed that the period of 'Sloan-type' diamond growth was a direct result of the collision of the GD with the Superior and Hearne craton: crustal thickening occurred by lateral emplacement of Proterozoic arc material over the Archean GD basement. The base of the lithosphere was pushed down under the root zones of the GD by loading, and overall by the compressional forces of orogeny. More diamonds grew as more of the lithosphere was depressed below the graphite-diamond isograd, see Stage 2 of Figure 6.4.4. The 'Sloan-type' diamonds grew in the hotter regions of the lower lithosphere, that were also undergoing deformation, such as the eclogites derived from oceanic plate subduction. The 'Sloan-type' diamond has a model mantle residence of 1.6Ga at 1215°C, this is consistent with growth during, or just after the Proterozoic orogeny. The thickening is evidenced by the crustal root imaged by LITHOPROBE and by present day geophysical signatures of lithosphere to at least 175km depth. Pressure-temperature conditions of the highest temperature depleted garnet peridotites coincide with the model temperature for the Proterozoic diamond growth, and because Sloan-type diamonds are of eclogite paragenesis, this provides evidence for eclogitic material present near the base of the lithosphere. Presumably the eclogites were emplaced before the final orogenic stages (circa 2Ga) because the final subduction polarity (GD under both Hearne/Rae and Superior cratons) does not allow subducted material to be added to the GD lithosphere.

Kimberlite activity was initiated 1.6Ga later, in the mid-Cretaceous (Stage 3, Figure 6.4.4). The initiation of kimberlitic activity is probably related large-scale terrane docking at the edge of the plate resulting in lateral stresses and instability leading to mobilisation of partial melts at the base of the lithosphere (there is no evidence for a mantle plume). This has been previously discussed in Chapter 1.

'Sloan-type' diamonds developed in eclogitic portions of the GD lithosphere during Proterozoic orogeny, as a direct result of the associated lithospheric thickening and thermo-tectonic reworking (Leahy and Taylor, 1995). This origin is different to the usual Archean diamond growth, not only in

timing, but also paragenesis. A similar origin may apply to 'Sloan-type' diamonds in other kimberlites and lamproites in Proterozoic mobile belts around the world.

References cited in Chapter 6

- Dawson, J.B. (1989). Geographic and time distribution of kimberlites and lamproites: relationships to tectonic processes. Proceedings of the 4th International Kimberlite Conference (Australia 1986), Kimberlites and related rocks, Geological Society of Australia Special Publication 14, Vol.1, p.323-343.
- Ellis, R.M., Hajnal, Z. and Bostock, M.G. (1996). Siesmic studies on the Trans-Hudson Orogen of Western Canada.Tectonophysics (in press).
- Erlank, A.J., Waters, F.G., Hawksworth, C.J., Haggerty, S.E., Allsopp, H.L., Rickard, R.S. and Menzies, M.A. (1987). Evidence for mantle metasomatism from the Kimberley pipes, South Africa. In Mantle Metasomatism (Menzies, M.A. and Hawksworth, C.J., eds.), Academic Press, p.221-311.
- Finnerty, A.A. and Boyd, F.R. (1987). Thermobarometry for garnet peridotites: basis for the compositional structure of the upper mantle. In Mantle Xenoliths, P.H. Nixon (ed.), p.381-402.
- Grand, S.P. (1994). Mantle shear structure beneath the Americas and surrounding oceans. Journal of Geophysical Research, Vol.99, p.11591-11621.
- Griffin, W.L., Cousens, D.R., Ryan, C.G., Sie, S.H. and Suter, G.F. (1989). Ni in chrome pyrope: a new geothermometer. Contributions to Mineralogy and Petrology, Vol.103, p.199-202.
- Griffin, W.L., Gurney, J.J., Sobolev, N.V. and Ryan, C.G. (1994). Comparative geochemical evolution of cratonic lithosphere: South Africa and Siberia. Extended abstracts for the 5th International Kimberlite Conference (Brazil 1991), p.119-121.
- Griffin, W.L., Ryan, C.G., Gurney, J.J., Sobolev, N.V. and Win, T.T. (1994). Chromite macrocrysts in kimberlites and lamproites: geochemistry and origin. Proceedings of the 5th International Kimberlite Conference (Brazil 1991), Vol.1, p.366-377.
- Griffin, W.L. and Ryan, C.G. (1995). Trace elements and indicator minerals: Area selection and Target evaluation in diamond exploration. In Griffin, W.L. (ed.) Diamond Exploration: Into the 21st Century, Journal of Geochemical Exploration Special Volume, Vol. 53, Nos. 1-3, p.311-338.
- Griffin, W.L., Kaminsky, F., O'Reilly, S.Y., Ryan, C.G. and Sobolev, N.V. (1995a). Mapping the Siberian lithosphere with garnets and spinels. Proceedings of the 6th International Kimberlite Conference, Russia 1995, Extended Abstracts Volume.

- Griffin, W.L., Ryan, C.G., O'Reilly, S.Y., and Gurney, J.J. (1995b). Lithosphere evolution beneath the Kaapvaal Craton: 200-80Ma. Proceedings of the 6th International Kimberlite Conference, Russia 1995, Extended Abstracts Volume.
- James, D.E. (1994). Structure and dynamics of the continental lithosphere: a review. International Symposium on the Physics and Chemistry of the Upper Mantle, p.151-164
- Jordan, T.H. (1981). Continents as a chemical boundary layer. Philosphical Transactions of the Royal Society London, Vol.301, p.359-373.
- Haggerty, S.E. (1994). Superkimberlites: a geodynamic diamond window to the earths core. Earth and Planetary Science Letters, Vol.122, p.57-69.
- Harris, J.W. (1987). Recent physical, chemical, and isotopic research of diamond. In Mantle Xenoliths, P.H. Nixon (ed.), p.477-500.
- Leahy, K. and Taylor, W.R.T. (1995). The influence of the Glennie Domain deep structure on the diamonds in Saskatchewan kimberlites. Proceedings of the 6th International Kimberlite Conference, Russia 1995, Extended Abstracts Volume.
- Lewry, J.F., Hajnal, Z., Green, A., Lucas, S.B., White, D., Stauffer, M.R., Ashton, K.E., Weber, W. and Clowes, R. (1994). Structure of a Paleoproterozoic continent-continent collision zone: a LITHOPROBE seismic reflection profile across the Trans-Hudson Orogen. Tectonophysics, Vol.232, p.143-160.
- Leung, I.S. (1990). Silicon carbide cluster entrapped in diamond from Fuxian, China. American Mineralogist, Vol.75, p.1110-1119.
- Lucas, S.B., White, D., Hajnal, Z., Lewry, J.F., Green, A., Clowes, R., Zwanzig, H., Ashton, K., Schledewitz, D., Stauffer, M., Norman, A., Williams, P.F. and Spence, G. (1994). Three dimensional collisional structure of the Trans Hudson Orogen, Canada. Tectonophysics, Vol.232, p.161-178.
- Milledge, H.J. and Mendelssohn, M.J. (1995). Recent advances in the interpretation of the mid-infrared absorbtion spectra of diamond. Proceedings of the 6th International Kimberlite Conference, Russia 1995, Extended Abstracts Volume.
- Moore, R.O., Otter, M.L., Rickard, R.S., Harris, J.W. and Gurney, J.J. (1986). The occurrence of moissanite and ferro-periclase as inclusions in diamond. Proceedings of the 4th International Kimberlite Conference (Australia 1986). Kimberlites and Related Rocks, Geological Society of Australia Special Publication No. 14, Vol. 2, p.409-411.
- Nelson, K.D., Baird, D.J., Walters, J.J., Hauck, M., Brown, L.D., Oliver, J.E., Ahern, J.L., Hajnal, Z., Jones, A.G. and Sloss, L.L. (1993). Trans-Hudson orogen and Williston basin in Montana and North Dakota: New COCORP deep-profiling results. Geology, Vol.21, p.447-450.
- Nickel, K.G. (1989). Garnet-pyroxene equilibria in the system SMACCr: the Cr-geobarometer. Proceedings of the 4th International Kimberlite Conference (Australia

1986). Kimberlites and Related Rocks, Geological Society of Australia Special Publication No. 14, Vol. 2, p.901-912.

- Nixon, P.H., Griffin, W.L., Davies, G.R. and Condliffe, E. (1994). Cr garnet indicators in Venezuela kimberlites and their bearing on the evolution of the Guyana craton. Proceedings of the 5th International Kimberlite Conference (Brazil 1991), Vol.2, p.147-157.
- Nixon, P.H. (1995). The morphology and nature of primary diamondiferous occurrences. In Griffin, W.L. (ed.) Diamond Exploration: Into the 21st Century, Journal of Geochemical Exploration Special Volume, Vol. 53, Nos. 1-3, p.41-72.
- Otter, M.L., McCallum, M.E. and Gurney, J.J. (1994). A physical characterisation of the Sloan (Colorado) diamonds using a revised diamond description scheme. Proceedings of the 5th International Kimberlite Conference (Brazil 1991), Vol.2, p.15-31.
- Pilkington, M. (1991). Mapping elastic lithospheric thickness variation in Canada. Tectonophysics Vol.190 p.283-297.
- Ringwood, A.E. (1987). Constitution and evolution of the mantle. Proceedings of the 4th International Kimberlite Conference (Australia 1986). Kimberlites and Related Rocks, Geological Society of Australia Special Publication No. 14, Vol. 1, p.455-485.
- Ryan, C.G., Griffin, W.L. and Pearson, N.J. (1995a). Garnet geotherms: Derivation of P-T data from Cr-pyrope garnets. Journal of Geophysical Research (in press).
- Ryan, C.G., Griffin, W.L., Pearson, N.J. and Win, T.T. (1995b). Garnet geotherms: Derivation of P-T data from Cr-pyrope garnets. Proceedings of the 6th International Kimberlite Conference, Russia 1995, Extended Abstracts Volume.
- Scott-Smith, B.H., Orr, R.G., Robertshaw, P. and Avery, R.W. (1995). Geology of the Fort a la Corne Kimberlites. Proceedings of the 6th International Kimberlite Conference, Russia 1995, Extended Abstracts Volume.
- Smith, D. and Boyd, F.R. (1987). Compositional heterogeneities in a high-temperature lherzolite nodule and implications for mantle processes. In Mantle Xenoliths, P.H. Nixon (ed.), p.551-562.
- Taylor, W.R.T., Jaques, A.L. and Ridd, M. (1990). Nitrogen-defect aggregation characteristics of some Australian diamonds: Time-temperature constraints on the source regions of pipe and alluvial diamonds. American Mineralogist, Vol.75, p.1290-1310.
- Woods, G.S. (1986). Platelets and the infrared absorbance of type Ia diamonds. Proceedings of the Royal Society London, A407, p.219-238.
- Wyllie, P.J. (1981). Plate tectonics and magma genesis. Geology Rundschau, Vol.70, p.128-153.

CHAPTER 7 - ECONOMIC CONSIDERATIONS OF THE FORT A LA CORNE KIMBERLITES

Abstract

The economic value of a kimberlite is largely a question of disposition, bulk sample grade and the size and quality of the diamonds. At Fort a la Corne the crater facies kimberlites are marginally sub-economic under normal circumstances (best grade of 23c/ht in 1995), and the size and quality of the stones thus far recovered are not remarkable (none over 1 carat in over 1,000 tonnes of kimberlite).

Despite uninspiring grades the potential for an economic diamond deposit at FALC remains high. For example, there are good indicators from the geotectonic setting, within an Archean microcontinent (Clifford's Rule), and the low degrees of resorption of those diamonds found suggest a high preservation potential. This is incongruous, however, with the evidence from trace element ratios in Cr-pyrope garnets, which suggests that melt-related metasomatism has had a large negative effect on the grade of the diamonds. Predictions made by comparison of trace and major element concentrations in garnets from FALC kimberlites with other diamond-bearing kimberlites are realistic (10c/ht to 30c/ht). These predictions also suggest that kimberlites at FALC with lower degrees of melt-related metasomatism would be well within economic grades (about 30c/ht). Just over half of the kimberlites at FALC (as indicated by magnetic anomalies) have been sampled, and others may contain higher diamond grades. In addition, vast tonnages of diamond bearing kimberlite are available at FALC (at least 4,000Mt within 300m of the surface), and low grade - high tonnage extraction methods may be applicable if the kimberlites were to be mined.

The unique extra-crater deposits at FALC may provide other economic opportunities, especially in open crater systems (Chapter 4), as they are typically reworked. The Cretaceous reworking environment at FALC was marginal marine to proximal offshore, but intertidal and nearshore deposits are most common. These are the result of marine winnowing, which act to increase the concentrations of heavy minerals, such as garnet, ilmenite and diamond. Thus there is a likelihood of reworked extra-crater deposits being low tonnage and very high grade ore reserves. The presence of a "large" diamond (2.4mm) in non-tuffaceous bar sands that overlie reworked extra-crater deposits (e.g. OFS 93-010) alludes to ore reserves that are perhaps the Cretaceous analogue to modern offshore marine diamonds, currently exploited in Namibia.

7.1 Regional geological economic viability - Evidence for diamond preservation potential from xenolith/cryst chemistry.

It has been demonstrated in Chapter 6 that the geothermal gradient beneath Central Saskatchewan intersects the diamond stability field in P-T space, thus indicating the potential for diamond growth within suitable host rocks (peridotitic and eclogite, both of which exist at great depth, Chapters 5 and 6). However, it has also been demonstrated by nitrogen aggregation studies (Chapter 6) that the diamonds are old (at least mid-Proterozoic), and this poses the question of how many of these old diamonds could have survived damaging influences of oxidation and metasomatism? By their very presence at least some have survived, but have enough survived to provide an economic deposit at the surface expression of the kimberlites; the volcano?

Much research has been carried out in the field of diamond preservation within the various geotectonic regimes that kimberlites and lamproites occur (e.g. an overview in Janse, 1994). The groundwork to this kind of study is the proposition, initially voiced by W.Q. Kennedy, later published by T.N. Clifford, that economically viable kimberlites are restricted to cratonic areas: the renowned Clifford's Rule (Clifford, 1966). The definition of a cratonic area is still an area of debate, as is the lower age limit of geotectonic regimes since the discovery of economic diamond-bearing kimberlites and lamproites in mid-Proterozoic mobile belts (Gonzaga et al, 1995). The area of Central Saskatchewan underlain by the sub-surface extent of the Glennie Domain has been shown to be a cratonic region, far older than the mid-Proterozoic mobile belt that overlie it (Chapter 6). Thus Clifford's Rule is not challenged by the kimberlites at FALC, and indicates that FALC kimberlites have good potential for economic diamond deposits.

The broad-scale cratonic setting indicates the potential presence or otherwise of diamonds, but the actual degree of preservation can only be described by analysing minerals brought from the lower lithosphere by the kimberlite or lamproite. A variety of minerals are diagnostic, most importantly diamonds themselves, with garnets and ilmenites indicating the degrees of metasomatism and oxidation state of the kimberlite magma. Other rarer minerals also add to the discussion.

7.1.1 Diamond resorption features

At Fort a la Corne these features include triangular etch pits (negative trigons), irregular surface pits leading to a frosted appearance and other more irregular etch lines. These occur on about one third of the diamonds analysed

(n=21) and represent only a small number of a wider array of known surface features associated with resorption (Harris, 1987), but include the most common feature, negative trigons (see Plate 5.1 in Figure 5.2.1, Chapter 5). Experimental studies have shown that negative trigons form from the interaction of the kimberlite magma with the diamond (using fused kimberlite at 1000°C, with water and carbon dioxide, Yamaoka et al, 1980).

The relative degree of resorption of FALC diamonds has been commented on qualitatively by W.R. Taylor (unpublished data). Most of the diamonds show no resorption features, but five (from populations B and C) have high levels of corrosion and etching. Apart from negative trigons (which occur on three), frosting and pitting is common, with irregular etch lines occurring on only one. These diamonds belong to population groups of Archean model age (Chapter 6), with temperatures indicating residence in the mid to upper levels of the diamond window.

The corroded diamonds are from populations derived from shallower depths than many of the uncorroded crystals, which suggests the resorption features may not be entirely due to time spent in the kimberlite magma (which would be proportional to depth at which it was included as a xenocryst). This corresponds with the relatively poorly developed negative trigons compared to frosting and pitted features. These characteristics may be explained by an Archean metasomatic event affecting certain parts of the lithosphere.

In summary the overall state of the surfaces of microdiamonds indicates that little or no resorption has occurred in most of the populations of diamonds found at FALC. Much of the resorption that is observed may be related to an unknown Archean metasomatic event, rather than kimberlite magma interaction. These observations indicate high preservation potential for diamonds grown in the Central Saskatchewan lithosphere.

7.1.2 Garnets - metasomatism from trace element studies

Chromium pyrope garnet xenocrysts separated from kimberlites at FALC have been analysed by proton microprobe, and the results and implications of geothermometry-barometry and the degree of depletion and metasomatism have been discussed (see Chapter 6). The nature of the metasomatism has been differentiated into two types, silicate melt related and hydrous fluid related. Based on the degree and type of metasomatism (and also P-T data previously derived) present in the garnet population, a 'metasomatism factor' is derived and is compared to the database at CSIRO of kimberlites with known grades.

Thus predictions are made as to the potential grades at given localities. Obviously these grade predictions are somewhat limited, relying as they do on questionable application of questionable data to a questionable (unpublished) database. This is illustrated by the very wide range of grades (from <1 to at least 30carats/100 tonnes (c/ht)) individually predicted for the boreholes OFS 93-002, 003 and 004, which are located within 250m of each other, and intersect kimberlite derived from the same body. The overall prediction for the FALC area, however, is restricted to about 10c/ht because of the large degrees of melt-related metasomatism indicated by the garnet analyses.

The silicate melt metasomatism has been recognised as a world-wide phenomenon by Griffin and Ryan (1995), which they attribute to the early stages kimberlite magma interaction within the base of the lithosphere. The action of the kimberlite magma is regarded as highly destructive to diamonds (generally oxidising), and is the main reason for Griffin predicting low grades (10c/ht) at FALC. Observation of the diamonds separated from FALC kimberlites shows that late-stage negative trigon development (a product of kimberlite magma resorption) is relatively unimportant (see section above). This indicates resorption of diamond by kimberlite magma is not as significant as is suggested by the degree of metasomatism in the garnets. Allowing for this, and considering the relatively small degrees of hydrous fluid metasomatism indicated by the garnets, Griffin attributes maximum grades of 30 to 100c/ht to the FALC kimberlites.

In summary given that melt-related metasomatism has not been as destructive as Griffin feared, grades at FALC may reach up to 30 to 100c/ht, well above currently viable economic deposits. However, this does not correlate with the grades obtained by bulk sampling a small number of the kimberlite craters at FALC, which show a range of grades from 4 to 23c/ht. The prediction which includes the degree of melt-metasomatism is far more accurate (10 to 30c/ht) and suggests this may be an important factor in the diamond preservation potential.

7.2 Kimberlite reserves in the pateran volcanic structure at FALC versus classical 'carrot-shaped' kimberlite diatreme

The kimberlites at FALC are of the pateran crater type (width to depth ratio of 7:1, crater facies pyroclastics and reworked deposits), for which a distinct eruptive mechanism has been proposed (see Chapter 3). Upon initial consideration, the relation of the pateran volcanic structure to the diamond

preservation potential may be negative, in that highly explosive eruptions (possibly as equally violent as large kimberlite diatreme-forming explosions) may disintegrate the diamonds. However, it appears that highly explosive eruptions may only be short-lived, and may in fact be sub-ordinate to the much quieter hawaiian-strombolian lava-fountaining (see Chapter 3). If this was the case, the proportion of diamonds destroyed by explosion must be reduced to nil. Thus, the initial, and some subsequent stages, of the pateran crater eruption may be destructive a similar extent that classical kimberlite diatreme eruptions are, but the quieter stages act to preserve diamonds.

Other processes in the pateran crater evolution may upgrade the original diamond concentration relative to the initial kimberlite magma. For example, phreatomagmatic eruption clouds may have considerable amounts of material removed by wind (Chapter 3; Scott-Smith et al, 1995), thereby increase the diamond concentration. In addition, the craters formed are unlikely to be completely filled (see Chapter 3), allowing reworked kimberlitic pyroclasts to be redeposited. At FALC, and at other kimberlites world-wide (e.g. M1 crater, Botswana, Daniels et al, 1994), reworked kimberlites generally contain higher concentrations of heavy minerals, including diamonds, as a result of sedimentary sorting and grading.

If a kimberlite at FALC can be shown to have an economic grade of diamonds (currently around 30c/ht, strongly dependent on quality and size of the diamonds), how does the disposition of the pateran crater kimberlite compare to the classic South African reserves, in steep-sided diatremes?

The most obvious difference is that the majority (>90%) of the kimberlite at FALC is within 300m of the surface, but is covered by 100m of glacial till. Classical deep-going kimberlite diatremes have reserves at ever increasing depths over many hundreds of meters, and are therefore harder to excavate.

Based on figures from a Kensington Resources press release, the average mass of an individual kimberlite crater intersected at FALC is 77million tonnes (with a current maximum of 570Mt for Anomaly 148), which is twice that of the average South African pipe at 34Mt. These averages suggests that approximately 4,400Mt of kimberlite are within 300m of the surface in the entire FALC cluster, with probably two-thirds of that located within a 5km radius in the southern part of the cluster (see Figure 3.2.1 in Chapter 3).

In summary the pateran crater deposit contains a very large tonnage of kimberlite and associated sediment, in relatively flat-lying and shallow bodies at FALC. The eruptive style is no more destructive to diamonds than that during

classical deep diatreme formation, and the hawaiian-strombolian stages of eruption are considerably less so. These factors make pateran crater kimberlites economically attractive, as has been illustrated by the complete excavation of some Mbuji-Mayi (Zaire) kimberlite pateran craters (Demaiffe et al, 1991).

7.3 The effect of post eruptive processes on the FALC kimberlite ore reserves.

Post-eruptive processes acting on eroding pyroclastic piles have been shown to upgrade the heavy mineral (and diamond) concentration (Chapter 2,3 and 4). In Chapter 4 two systems of post-eruptive kimberlite behaviour in the sedimentary environment were characterised: the open crater system where kimberlite is eroded and transported into the sedimentary environment; and the closed crater system where the crater is immediately sealed by marine deposits, possibly resulting from a lack of extra-crater deposits, and/or underfilled craters and marine transgression.

The economic value of a closed crater system remains about the same as for all primary kimberlites, largely a question of disposition, bulk sample grade and the size and quality of the diamonds. At Fort a la Corne these are just sub-economic under normal circumstances (best grade of 23c/ht in 1995), and the size and quality of the stones are not remarkable (none over 1 carat in over 1,000 tonnes of kimberlite, figures from Kensington press release). Sealing by marine sedimentary deposits may, however, be immediately preceded by crater lake processes producing some upgraded strata that overlie the normal kimberlite crater fill. These may contain a small thickness of reworked deposits of higher grade, which could be economically significant.

In an open crater system kimberlite is removed, largely from crater edge tuff piles (of primary airfall tuffs), into the basinal environment by mass flow slumps, leading to debris and density flows. The initial deposits of these flows are typically massive, and may be very coarse grained (as in the tuffaceous conglomerate in OFS 93-010), but are poorly sorted and heavy mineral concentration is not a consistent process. Most of the extra-crater deposits, however, are ash turbidites, produced by lower sediment density flows in an aqueous environment, which are well graded and sorted and display significant heavy mineral concentrations especially in the coarse lags. Other reworked extra-crater deposits are the finely bedded, laminated and lensoid deposits of wave and tide reworked kimberlitic silts to gravels. These are exceptionally well sorted within individual horizons, and often display hummocky cross-

stratification. The bedded pyroclastics have the greatest heavy mineral concentrations recorded in the FALC area, probably due to size and density sorting by wave and tide oscillation. Quartz sands, probably of bar sand origin, overlie the reworked kimberlite deposits at the eastern edge of the FALC cluster (see Chapter 4). These contain only very small amounts of kimberlitic material, mostly heavy minerals, but did contain the largest diamond found in extra-crater deposits (2.4mm).

In summary the profile of heavy mineral enrichment and extrapolated diamond grade (determined by OFS heavy mineral separation results, Chapter 2) during tuff pile reworking is initially comparable to the primary airfall tuffs (debris flows), increasing two-fold in the later density flows (ash turbidites) and up to six-fold in bedded and laminated pyroclastics (wave reworked). The quartz sands and silts observed on the eastern edge of the FALC cluster have very low heavy mineral concentrations, but allude to very significant deposits of good quality and large diamonds in deposits which may be the Cretaceous analogue of the offshore diamond deposits, currently being exploited in Namibia (which are reviewed in;Nixon, 1995).

References cited in Chapter 7

- Clifford, T.N. (1966). Tectono-metallogenic units and metallogenic provinces of Africa. Earth and Planetary Science Letters, Vol.1, p.421-434.
- Daniels, L.R.M., Jennings, C.M.H., Lee, J.E., Blaine, J.L., Billington, F.R. and Cumming, B. (1994). The geology of crater volcanics and sediments associated with the M1 kimberlite, southwestern Botswana. Proceedings of the 5th International Kimberlite Conference (Brazil 1991), Vol.1, p.129-139.
- Demaiffe, D., Fieremans, M. and Fieremans, C. (1991). The Kimberlites of Central Africa: a review. In Kampunzu, A.B. and Lubala, R.T (eds.) Magmatism in Extensional Structural Settings, Springer-Verlag, p.537-559.
- Griffin, W.L. and Ryan, C.G. (1995). Trace elements and indicator minerals: Area selection and Target evaluation in diamond exploration. In Griffin, W.L. (ed.) Diamond Exploration: Into the 21st Century, Journal of Geochemical Exploration Special Volume 53, Nos. 1-3, p.311-338.
- Harris, J.W. (1987). Recent physical, chemical, and isotopic research of diamond. In Mantle Xenoliths, P.H. Nixon (ed.), p.477-500.
- Janse, A.J.A. (1994). Is Clifford's Rule still vaild? Affirmative examples from around the world. Proceedings of the 5th International Kimberlite Conference (Brazil 1991), Vol.1, p.215-235.
- Nixon, P.H. (1995). Occurences of diamonds in the world. In Griffin, W.L. (ed.) Diamond Exploration: Into the 21st Century, Journal of Geochemical Exploration Special Volume 53, Nos. 1-3, p.41-72.
- Scott-Smith, B.H., Orr, R.G., Robertshaw, P. and Avery, R.W. (1995). Geology of the Fort a la Corne Kimberlites. Proceedings of the 6th International Kimberlite Conference, Russia 1995, Extended Abstracts Volume.
- Yamaoka, S., Kanda, H. and Setaka, N. (1980). Etching of diamond octahedra at high pressure with controlled oxygen partial pressure. Journal of Material Science, Vol.15, p.332-336.

CONCLUSIONS

The conclusions of the thesis are presented in approximate geological time-order, and as such describe the history of the Fort a la Corne (FALC) kimberlite, from crystallisation of the earliest xenolithic material, through magmatic and eruptive events, to final post-eruptive modification in the sedimentary environment. Aspects of the economic viability are also summarised.

- The Glennie Domain (underlying FALC) existed as a separate microcontinent at least 400km wide in the late Archean (circa 2.8Ga). Several populations of diamonds grew in the base of the lithosphere at this time, and this provides the best evidence of the cratonic nature of the Glennie Domain before major orogenic reworking in the Middle Proterozoic.
- The Glennie Domain (GD) underwent considerable tectonic reworking in the Middle Proterozoic as it was incorporated into the Trans Hudson Orogen. This buckled the GD plate, and overthrust it with a considerable thickness of Proterozoic shelf and arc sediments. Both the crust and the lithosphere of the GD were thickened during this period, and another period of diamond growth occurred within eclogitic portions of the lowermost lithosphere, emplaced during earlier subduction. This orogenic period, along with others to the north and west, consolidated the Canadian Shield which can subsequently be regarded as cratonic.
- A passive margin was created by continental rifting at the start of the Phanerozoic, about 1500km to the west of the FALC region. This led to periodical shallow flooding of the Canadian Shield, and deposited 300m to 500m of continental (sandstones) and shelf (shales and dolomites) sediment in the FALC area by the end of the Devonian.
- Eastwards subduction under the North American Plate began in the early Jurassic, and a volcanically active orogenic belt developed by the beginning of the Cretaceous (the Laramide Orogeny). A foreland basin evolved immediately to the east of the orogenic belt in response to crustal loading, initiating deposition in the Western Canadian Sedimentary Basin. During the subsequent orogeny, which lasted into the mid-Tertiary, numerous allochthonous terranes collided. One of the largest terranes (Insular Group) collided in the Early Cretaceous (about 110Ma to 95Ma), producing lateral stresses throughout the lithosphere. These stresses triggered mobilisation of the kimberlitic proto-magma in areas where the mantle was fertile (e.g. under FALC), initiating magma ascent over about 10Ma, starting at around 110Ma.

- The magma initially incorporated minerals of the megacryst suite: pyrope garnet, ilmenite and rarer clinopyroxene and spinel. Megacrystal garnets account for approximately 25% of all the garnets separated in the FALC kimberlites. The megacryst suite is thought to have grown at or near the base of the lithosphere before magma mobilisation occurred. Chemical analyses of minerals from this suite indicate a similarity with megacrystal suites in South African kimberlites.
- The kimberlite rapidly ascended from the base of the lithosphere to the surface, and picked up xenoliths/crysts of a wide variety of rocks en route. Three main groups are described, peridotitic, eclogitic and crustal.
- Peridotitic xenocrysts in the FALC kimberlites include: Mg-olivine, Cr-pyrope garnet, Cr-diopside, spinel, rare orthopyroxene and amphibole, and very rare diamond. Peridotitic garnets account for approximately 45% of all the garnets separated from FALC kimberlites.
- Peridotitic garnets are mainly of the G9 group of lherzolitic origin (about 88% calcic Cr-pyropes), and about 10% G10 group (sub-calcic Cr-pyrope garnets), of harzburgitic origin. Rare knorringite and uvarovite garnets also occur. This range garnets are typical of kimberlites world-wide.
- Cr-pyrope garnets were analysed by W.L. Griffin (CSIRO, Australia) for major and trace elements, and the results applied to Ni-geothermomemeters and Cr-geobarometers. These indicate a cratonic geotherm in the Early Cretaceous, and the base of the lithosphere at 190km depth and 1250 to 1300°C. Trace element concentrations in the garnets have also recorded evidence of two metasomatic events in the mantle, one of which is probably related the early kimberlite magma.
- Nitrogen-aggregation studies on diamonds (W.R. Taylor) corroborate the thermometry data obtained from garnet Ni analysis, and suggest the 'diamond window' lay between 145km and 180km depth, and 950 to 1250°C in the Early Cretaceous. The three highest temperature diamonds (>1200°C) were of eclogitic paragenesis, one of which, the 'Sloan-type', is typical of eclogitic growth in the mid-Proterozoic, and provides evidence for eclogites at the base of the crust, and diamond growth in response to orogenic thickening.
- Eclogitic minerals included in the FALC kimberlites as xenocrysts include: pyrope-almandine-grossular garnet (<20% of all FALC garnets), Na-clinopyroxene and kyanite, with very rare diamond. Eclogite is subordinate to peridotite in the Glennie Domain lithosphere, but probably occurs throughout, especially at the base of the lithosphere.

- Crustal mineral xenocrysts are typical of those that compose ancient crust, and include: quartz, feldspar, biotite, muscovite, amphibole, scapolite, Fe-pyroxene, Fe-garnet (about 10% of all garnets in FALC kimberlites), staurolite, sillimanite, andalusite, tourmaline, epidote, kyanite, Fe-ilmenite and Fe-olivine. Crustal material in the form of coherent lithic xenoliths are also common, and include: chert, dolomite, gniess, schist, amphibolite, shale and sandstone.
- As the ascending kimberlite magma neared the surface, a number of minerals crystallised from the magma prior to eruption, these include: olivine, phlogopite, apatite, spinel, perovskite (on the surface of ilmenites), carbonate and serpentine.
- Small, poorly developed (and relatively undescribed) kimberlites erupted from about 110Ma to about 100Ma, these are rare, and apparently failed to excavate craters. The main kimberlite event, consisting of about 70 individual eruptions, occur within a relatively small timeframe: about 102Ma to 98Ma, during deposition of the Lower Westgate Formation at the base of the Lower Colorado Group.
- The magma penetrated to within about 120m to 300m of the Cretaceous paleo-surface (which were probably sub-aerial coastal swamps and mud flats) and explosively interacted with groundwater in the Mannville Group sandstones. The phreatomagmatic eruption had increased explosive energy on account of the violent degassing of volatiles (a large component of kimberlite magmas), and resulted in a shock wave that propagated vertically and laterally from the point of explosion. The very high energy explosion, coupled with the low mechanical strength of the overlying strata (partly lithified muds and silts), allowed the excavation of very broad flat-bottomed crater of diameter to depth ratio 7:1. These rare craters types are called herein *pateran*, and other examples have been described in Zaire and Australia. At FALC the craters are irregular to circular in plan view, and range from 200m to 1300m in diameter and 30m to 260m in depth.
- The eruptive style is initially phreatomagmatic, and produces graded crystal and lithic rich tuffs and lapilli-tuffs (where lapilli-tuff refers to a grain size >4mm). Primary extra-crater airfall deposits are formed by this type of eruption (tuff-rings around the edge of the crater), and small diatremes may develop at the vent (although none have yet been intersected at FALC).
- If groundwater supply is restricted, then the eruptive style switches to lava fountaining by volatile degassing alone. This produces airfall deposits composed of up to 100% lava droplets, seen as fluidal lapilli up to 2cm

across. In these lapilli dominated lapilli-tuffs, crystals are subordinate (up to 15% of the constituents) and lithics are rare (indicating no diatreme development). These airfall deposits produce tuff-piles adjacent to the vent, at the centre of the large crater. It is likely that lapilli dominated tuffs may only reach the edges of the crater by rheomorphic flow from the oversteepened central tuff pile. Little or no extra-crater deposits are created by this eruptive style.

- As groundwater becomes replenished, or deeper explosive centres develop, eruption style may switch back to phreatomagmatic explosions. This switching may occur several times in the course of one eruption. Regardless of dominant eruptive style, the craters excavated by the initial explosion are so vast that the kimberlite erupted is unlikely to have sufficient volume to fill it.
- As many of the craters are underfilled, crater lakes quickly develop in the post-eruptive environment. These, along with other weathering agents, quickly degrade the tuff pile, filling the crater lake and/or dispersing reworked kimberlite into the sedimentary environment around (which comprises sub-aerial coastal swamps, marginal marine and nearshore at about 100Ma).
- Reworked kimberlite, both within and without the crater, consist of debris flows (including ash turbidites), wave reworked bedded and laminated pyroclastic sands and tuffaceous clastics of various nearshore facies. These may be distinguished from primary airfall tuffs by recognition of sedimentary structures (such as ripple cross-stratification) or bioturbation traces, and aided by point-counting roundness of olivine grains. Reworked pyroclastic deposits have statistically more sub-rounded and rounded grains than primary airfall deposits.
- Heavy minerals in reworked deposits are of much greater concentration than the airfall deposits from which they are derived. Individual reworked strata may have average heavy mineral concentrations up to six times that of average primary airfall tuffs. This is due to the winnowing and sorting action during aqueous transportation of the reworked pyroclastics.
- Diagenetic alteration of the kimberlite began immediately after it came to rest (either by pyroclastic fallout, or subsequent reworking). The main event was a pervasive serpentisation of olivine and matrix, followed by a fault-vein fill and wall rock alteration with magnetite and carbonate. Final events were a calcite-antigorite dilational vein fill, isolated antigorite growth, and the occasional development of a secondary porosity overprinting all the previous diagenetic events. Thus the diagenesis obscures much of the primary pyroclastic texture.

- Diagenesis obscured not only the primary texture of the kimberlites, but also the primary geochemistry: half of all the trace elements analysed by XRF can be shown to be a record of diagenetic overprint, rather than a primary kimberlite geochemistry (e.g. Sr, Ba, Ni, Co, Zn and Sc). At least some of these elements are from chemical sources outside of the kimberlite bodies, probably basinal fluids (e.g. Zn).
- Major element proportions are less affected by diagenesis, and are comparable to average Group Ia kimberlites. Low Al is attributed to low degrees of contamination by crustal xenoliths (due to very small or absent diatremes), and low K is probably due to dissolution in aqueous fluids.
- Across FALC, sea-level rise sealed the crater facies (and much of the extra-crater kimberlite) with shallow shelf muds and bar sands. Further transgression in the Late Cretaceous acted to preserve the volcanic structures until Quaternary glacial erosion partially exposed the cluster (at about 2Ma), before burying them again in over 90m of fluvio-glacial sediment.
- The FALC kimberlites were discovered in 1988, and borehole drilling since has produced a bulk sample of over 1100t from 40 of the 71 kimberlite craters, as defined by their magnetic anomalies. The macrodiamonds are fairly small (<1carat), and the grades are uninspiring (3 to 24 carat/100t), but are contained in the highest tonnage kimberlites in the world. Approximately 3 billion tonnes of kimberlite is located within 300m of the surface in the centre of the FALC cluster (5km radius).
- Extra-crater deposits may represent low-tonnage, but far higher grade deposits compared to the crater facies. Even proximal facies extra-crater kimberlites show, on average, a three-fold upgrading of heavy minerals relative to crater facies airfall tuffs.
- Quartz sands and silts immediately overlie extra-crater pyroclastic kimberlite on the eastern edge of the FALC cluster, and have very low heavy mineral concentrations, but contain relatively large diamonds (one stone 2.4mm). This points to the possibility of very significant deposits of good quality and large diamonds in sediments, which may be the Cretaceous analogue of the offshore diamond deposits currently being exploited in Namibia.

List of references cited in the thesis

- Agee, J.J., Garrison, J.R. and Taylor, L.R. (1982). Petrogensis of oxide minerals in kimberlite, Elliot County, Kentucky. American Mineralogist, Vol.67, p.28-42.
- Apter, D.B., Harper, F.J., Wyatt, B.A. and Scott-Smith, B.H. (1984). The geology of the Mayeng kimberlite sill complex, South Africa. Proceedings of the 3rd International Kimberlite Conference, Vol.2, p.43-57.
- Armstrong, R.L. (1988). Mesozoic and early Cenozoic magmatic evolution of the Canadian Cordillera. In Clark, S.P., Burchfiel, B.C. and Suppe, J. (eds.) Processes in continental lithospheric deformation. Geological Society of America, Special Paper 218, p.55-92.
- Bloch, J., Schröder-Adams, C., Leckie, D.A., McIntyre, D.J., Craig, J., Staniland, M. (1993). Revised stratigraphy of the lower Colorado Group (Albian to Turonian), Western Canada. Bulletin of Canadian Petroleum Geology Vol. 41, No.3. p.325-348.
- Bloch, J. (1994). The methods and results of geochemical analyses of Cretaceous Colorado Group shales from the Western Canadian Sedimentary Basin. Geological Survey of Canada, Open File Report 2810.
- Boyd, F.R, Dawson, J.B. and Smith, J.V. (1984). Granny Smith diopside megacrysts from the kimberlites of the Kimberley area and Jagersfontain, South Africa. Geochim. Cosomochim. Acta. Vol.48, p.381-384.
- Boyles, J.M. and Scott, A.J. (1982). A model for migrating shelf bar sandstones in the Upper Mancos Shale (Campanian), North-Western Colorado. Association of American Petroleum Geologists, Vol.66, No.5, p.491-508.
- Carr, M.H. (1976). The volcanoes of Mars. Scientific American, Vol.234, No.1, p.32-43.
- Cas, R.A.F. and Wright, J.V. (1988). Volcanic Successions, Modern and Ancient. Chapman and Hall (pubs.), pp.528.
- Christiansen, E.A. and Whitaker, S.H. (1976). Glacial thrusting of drift and bedrock, in Leggert, R.F. (ed.), Glacial Till, Royal Society of Canada Special Publication No.12, p.121-130.
- Clement, C.R. and Ried, A.M. (1989). The origin of kimberlite pipes: an interpretation based on a synthesis of geological features displayed by Southern African occurences. Proceedings of the 4th International Kimberlite Conference (Australia 1986), Kimberlites and related rocks, (Blackwell, pubs.), Vol 1, Geol. Soc. Australia Special Publication No.14, p.632-646.
- Clement, C.R. (1982). A comparative geological study of some major kimberlite pipes in the Northern Cape and Orange Free State. Ph.D thesis (2 vols.) University of Cape Town.
- Clifford, T.N. (1966). Tectono-metallogenic units and metallogenic provinces of Africa. Earth and Planetary Science Letters, Vol.1, p.421-434.

- Collerson, K.D., Lewery, J.F., Van Schmus, R.W. and Bickford, M.E. (1989). Sm-Nd isotopic constraints on the age of the buried basement in central and southern Saskatchewan. In Saskatchewan Energy and Mines, Misc. Report 89-4, p.168-171.
- Curtis, C.D. and Spears, D.A. (1968). The formation of sedimentary iron minerals. Economic Geology Vol.63, p.257-270.
- Daniels L.R.M., Jennings, C.M.H., Lee, J.E., Blaine, J.L., Billington, F.R. and Cumming, B. (1994). The geology of crater volcanics and sediments associated with the M1 kimberlite, southwestern Botswana. Proceedings of the 5th International Kimberlite Conference (Brazil 1991), Vol.1, p.129-139.
- Dawson, J.B. and Stephens, W.E. (1975). Statistical analysis of garnets from kimberlites and associated xenoliths in kimberlite. Journal of Geology, Vol.83, p.589-607.
- Dawson, J.B. (1987). The MARID-suite of xenoliths in kimberlite: relationship to veined and metasomatised peridotite xenoliths. In Mantle Xenoliths, P.H. Nixon (ed.), p.465-473.
- Dawson, J.B. (1989). Geographic and time distribution of kimberlites and lamproites: relationships to tectonic processes. Proceedings of the 4th International Kimberlite Conference (Australia 1986), Kimberlites and related rocks, Geological Society of Australia Special Publication 14, Vol.1, p.323-343.
- Demaiffe, D., Fieremans, M. and Fieremans, C. (1991). The Kimberlites of Central Africa: a review. In Kampunzu, A.B. and Lubala, R.T (eds.) Magmatism in Extensional Structural Settings, Springer-Verlag, p.537-559.
- Eggler, D.H., McCallum, M.E. and Smith, C.B. (1979). Megacryst assemblages in kimberlite from Northern Colorado and Southern Wyoming: Petrology, geothermometry-barometry and a real distribution. Proceedings of the 2nd International Kimberlitie Conference, Vol.2, p.213-226.
- Eggler, D.H., McCallum, M.E. and Kirkley, M.B. (1987). Kimberlite transported nodules from the Colorado-Wyoming; A record of enrichment of shallow portions of an infertile lithosphere. Geological Society of America Special Paper 215, p.77-89.
- Ellis, R.M., Hajnal, Z. and Bostock, M.G. (1996). Seismic studies on the Trans-Hudson Orogen of Western Canada. Tectonophysics (in press).
- Erlank, A.J., Waters, F.G., Hawksworth, C.J., Haggerty, S.E., Allsopp, H.L., Rickard, R.S. and Menzies, M.A. (1987). Evidence for mantle metasomatism from the Kimberley pipes, South Africa. In Mantle Metasomatism (Menzies, M.A. and Hawksworth, C.J., eds.), p.221-311. Academic Press.
- Ewing, T.E. (1981). Petrology and geochemistry of the Kamloops Group volcanics, British Columbia. Canadian Journal of Earth Science, Vol.18, p.1478-1492.
- Fermor, P.R. and Moffat, I.W. (1992). Tectonics and structure of the Western Canadian Foreland Basin. In Macqueen, R.W. and Leckie, D.A. (eds.) Foreland Basins and Fold Belts, Association of American Petroleum Geologists Memoir 55, p.81-107.

- Finnerty, A.A. and Boyd, F.R. (1987). Thermobarometry for garnet lherzolites: basis for the determination of the thermal and compositional structure of the upper mantle. In Mantle Xenoliths, P.H. Nixon (ed.), p.381-401.
- Francis, E.H. (1970). Bedding in Scottish (Fifeshire) tuffpipes and its relevance to maars and calderas. Bulletin of Volcanology, Vol.34, p.697-712.
- Friedman, G.M. (1958). Determination of sieve-size distribution from thin section data for sedimentary petrological studies. Journal of the Geological Society of London, 129, p.612-641.
- Garvie, O.G. and Robinson, D.N. (1982). The mineralogy, structure and mode of formation of kelyphite and associated sub-kelyphite surfaces on pyrope from kimberlites. Terra Cognita, Vol.2, p.229-230.
- Gaspar, J.C. and Wyllie, P.J. (1984). The alleged kimberlite-carbonatite relationship: Evidence from ilmenite and spinel from the Premier and Wesselton Mines and the Benfontain Sill, South Africa. Contributions to Mineralogy and Petrology, Vol.85, p.133-140.
- Gent, M.R. (1991). Diamond exploration in Saskatchewan. Proceedings of Canadian Institute of Minerals and Mines (Geology Division), 1st Annual Field Conference, Saskatoon.
- Gent, M.R. (1992). Diamonds and precious gems of the Phanerozoic basin, Saskatchewan: Preliminary Investigations. Saskatchewan Energy and Mines Open File Report 92-2.
- Grand, S.P. (1994). Mantle shear structure beneath the Americas and surrounding oceans. Journal of Geophysical Research, Vol.99, p.11591-11621.
- Green, D.H. and Sobolev, N.V. (1975). Co-existing garnets and ilmenites synthesized at high pressures from pyrolite and olivine basanite and their significance for kimberlitic assemblages. Contributions to Mineralogy and Petrology, Vol.50, p.217-229.
- Griffin, W.L., Cousens, D.R., Ryan, C.G., Sie, S.H. and Suter, G.F. (1989). Ni in chrome pyrope: a new geothermometer. Contributions to Mineralogy and Petrology, Vol.103, p.199-202.
- Griffin, W.L., Gurney, J.J., Sobolev, N.V. and Ryan, C.G. (1994a). Comparative geochemical evolution of cratonic lithosphere: South Africa and Siberia. Extended abstracts for the 5th International Kimberlite Conference (Brazil 1991), p.119-121.
- Griffin, W.L., Ryan, C.G., Gurney, J.J., Sobolev, N.V. and Win, T.T. (1994b). Chromite macrocrysts in kimberlites and lamproites: geochemisrty and origin. Proceedings of the 5th International Kimberlite Conference (Brazil 1991), Vol.1, p.366-383.
- Griffin, W.L. and Ryan, C.G. (1995). Trace elements and indicator minerals: Area selection and Target evaluation in diamond exploration. In Griffin, W.L. (ed.) Diamond Exploration: Into the 21st Century, Journal of Geochemical Exploration Special Volume 53, Nos. 1-3, p.311-338.

- Griffin, W.L., Kaminsky, F., O'Reilly, S.Y., Ryan, C.G. and Sobolev, N.V. (1995a). Mapping the Siberian lithosphere with garnets and spinels. Proceedings of the 6th International Kimberlite Conference, Russia 1995, Extended Abstracts Volume.
- Griffin, W.L., Ryan, C.G., O'Reilly, S.Y., and Gurney, J.J. (1995b). Lithosphere evolution beneath the Kaapvaal Craton: 200-80Ma. Proceedings of the 6th International Kimberlite Conference, Russia 1995, Extended Abstracts Volume.
- Gurney, J.J., Jakob, W.R.O. and Dawson, J.B. (1979). Megacrysts from the Monastery kimberlite pipe, South Africa. Proceedings of the 2nd International Kimberlitie Conference, Vol.2, p.227-243.
- Gurney, J.J. (1984). A correlation between garnets and diamonds in kimberlites. In Glover, J.E. and Harris, P.G. (eds.) Kimberlite occurrence and origin: A basis for conceptual models in exploration, p.143-166.
- Gurney, J.J. and Moore, R.O. (1993). Geochemical correlation between kimberlitic indicator minerals and diamonds. Exploration, Sampling and Evaluation, Short Course Proceedings, Prospectors and Developers Association of Canada, p.147-171.
- James, D.E. (1994). Structure and dynamics of the continental lithosphere: a review. International Symposium on the Physics and Chemistry of the Upper Mantle, p.151-164
- Jordan, T.H. (1981). Continents as a chemical boundary layer. Philosphical Transactions of the Royal Society London, Vol.301, p.359-373.
- Haggerty, S.E. (1975). The chemistry and genesis of opaque minerals in kimberlites. Physics and Chemsitry of the Earth, Vol.9, p.295-307.
- Haggerty, S.E., Hardie, R.B. and McMahon, R.M. (1979). The mineral chemistry of the ilmenite nodule associations from the Monastery diatreme. Proceedings of the 2nd International Kimberlitie Conference, Vol.2, p.249-256.
- Haggerty, S.E. (1989). Upper mantle opaque mineral stratigraphy and the genesis of metasomites and alkali-rich melts. Proceedings of the 4th International Kimberlite Conference (Australia 1986), Kimberlites and related rocks, Geological Society of Australia Special Publication 14, Vol.2, p.687-699.
- Haggerty, S.E. (1994). Superkimberlites: a geodynamic diamond window to the earths core. Earth and Planetary Science Letters, Vol.122, p.57-69.
- Haq, B.U., Hardenbol, J. And Vail, P.R. (1988). Mesozoic and Cenozoic chronostratigraphy and cycles of sea-level change. Wilgus et al (eds.) Sea level changes: an intergrated approach. SEPM Special Publication No.42, p.71-108.
- Harris, J.W. (1987). Recent physical, chemical, and isotopic research of diamond. In Mantle Xenoliths, P.H. Nixon (ed.), p.477-500.
- Hawthorne, J.B. (1975). Model of a kimberlite pipe. Physics and Chemistry of the Earth, Vol.9, p.1-15.

- Hay, W.W., Eicher, D.L. and Diner, R. (1993). Physical oceanography and water masses in the Cretaceous Western Interior Seaway. In Caldwell, W.G.E and Kauffman, E.G. (eds.) Evolution of the Western Interior Basin, GAC Special Paper 39, p.297-318.
- Heame, B.C. (1968). Diatremes with kimberlitic affinities in north-central Montana. Science, Vol.159, p.622-625.
- Helmstaedt, H.H. and Gurney, J.J. (1995). Kimberlites - why, where and when? A hierarchy of geotectonic controls. Proceedings of the 6th International Kimberlite Conference, Russia 1995, Extended Abstracts Volume.
- Janse, A.J.A. (1994). Is Clifford's Rule still vaild? Affirmative examples from around the world. Proceedings of the 5th International Kimberlite Conference (Brazil 1991), Vol.1, p.215-235.
- Kjarsgaard, B.A., Leckie, D.A., McIntyre, D.J., McNeil, D.H., Haggart, J.M., Stasiuk, L. and Bloch, J. (1995). Smeaton Kimberlite Drill Core, Fort a la Corne Field, Saskatchewan. Geological Survey of Canada Open File 3170, pp.57.
- Kunze, G. (1956). Z. Krist., Vol.108, p.82-107.
- Leahy, K. and Taylor, W.R.T. (1995). The influence of the Glennie Domain deep structure on the diamonds in Saskatchewan kimberlites. Proceedings of the 6th International Kimberlite Conference, Russia 1995, Extended Abstracts Volume.
- Leckie, D.A. and Smith, D.G. (1992). Regional setting, evolution, and depositional cycles of the Western Canadian Foreland basin. In Macqueen, R.W. and Leckie, D.A. (eds.) Foreland Basins and Fold Belts, Association of American Petroleum Geologists, Memoir 55, p.9-47.
- Leckie, D.A., Singh, C., Bloch, J., Wilson, M. and Wall, J.H. (1992). An anoxic event at the Albian-Cenomanian boundary: the Fish Scale Marker bed, northern Alberta, Canada. Paleogeography, Paleoecology. Paleoclimatology, Vol.92, p.139-166.
- Leeder, M.R. (1982). Sedimentology, Processes and Products. Allen & Unwin (pubs.), London, pp. 344.
- Lehnert-Thiel, K., Loewer, R., Orr, R.G. and Robertshaw, P. (1992). Diamond-bearing kimberlites in Saskatchewan, Canada: The Fort a la Corne Case History. Exploration Mining Geology Vol.1 No.4 p.391-403.
- Leonardos, O.H, Carvalho, J.B., Gibson, S.A. and Thompson, R.N. (1995). The diamond potential of the late Cretaceous Alto Paranaiba Igneous Province, Brazil. Proceedings of the 6th International Kimberlite Conference. Russia 1995, Extended Abstracts.
- Leung, I.S. (1990). Silicon carbide cluster entrapped in diamond from Fuxian, China. American Mineralogist, Vol.75, p.1110-1119.
- Lewry, J.F., Hajnal, Z., Green, A., Lucas, S.B., White, D., Stauffer, M.R., Ashton, K.E., Weber, W. and Clowes, R. (1994). Structure of a Paleoproterozoic continent-continent

collision zone: a LITHOPROBE seismic reflection profile across the Trans-Hudson Orogen. Tectonophysics Vol.232, p.143-160.

- Leys, C.L. (1982). Volcanic and sedimentary processes in phreatomagmatic volcanoes. University of Leeds PhD thesis.
- Lorenz, V. (1975). Formation of phreatomagmatic maar-diatreme volcanoes and its relevance to kimberlite diatremes. Physics and Chemistry of the Earth, Vol.9, p.17-27.
- Lorenz, V. (1984). Explosive volcanism of the West Eifel volcanic field, Germany. In Komprobst, J. (Ed.), Kimberlites I: Kimberlites and Related Rocks, p.288-297 Elsiever
- Lorenz, V. (1985). Maars and diatremes of phreatomagmatic origin. Transactions of the Geological Society of South Africa, Vol.88, p.459-470.
- Lucas, S.B., White, D., Hajnal, Z., Lewry, J.F., Green, A., Clowes, R., Zwanzig, H., Ashton, K., Schledewitz, D., Stauffer, M., Norman, A., Williams, P.F. and Spence, G. (1994). Three dimensional collisional structure of the Trans Hudson Orogen, Canada. Tectonophysics Vol.232, p.161-178.
- Macqueen, R.W. and Leckie, D.A. (1992). Foreland Basins and Fold Belts. Association of American Petroleum Geologists, Memoir 55
- McNeil, D.H. and Caldwell, W.G.E (1981). Cretaceous rocks and their foraminifera in the Manitoba Escarpment. Geological Association of Canada Special Paper 21, pp.439.
- Mieras, B.L., Sageman, B.B. and Kauffman, E.G. (1993). Trace fossil distribution patterns in Cretaceous facies of the Western Interior Basin, North America. In Caldwell, W.G.E and Kauffman, E.G. (eds.) Evolution of the Western Interior Basin, Geological Association of Canada Special Paper 39, p.585-610.
- Milledge, H.J. and Mendelssohn, M.J. (1995). Recent advances in the interpretation of the mid-infrared absorbtion spectra of diamond. Proceedings of the 6th International Kimberlite Conference, Russia 1995, Extended Abstracts Volume.
- Mitchell, R.H. (1986), Kimberlites: mineralogy, geochemistry and petrology. Plenum Press, New York, pp.442.
- Mitchell, R.H. (1995). Kimberlites, orangeites and related rocks. Plenum Press, New York, pp.410.
- Moore, R.O., Otter, M.L., Rickard, R.S., Harris, J.W. and Gurney, J.J. (1986). The occurrence of moissanite and ferro-periclase as inclusions in diamond. Proceedings of the 4th International Kimberlite Conference (Australia 1986). Kimberlites and Related Rocks, Geological Society of Australia Special Publication No. 14, Vol. 2, p.409-411.
- Nelson, K.D., Baird, D.J., Walters, J.J., Hauck, M., Brown, L.D., Oliver, J.E., Ahern, J.L., Hajnal, Z., Jones, A.G. and Sloss, L.L. (1993). Trans-Hudson orogen and Williston basin in Montana and North Dakota: New COCORP deep-profiling results. Geology, Vol.21, p.447-450.

- Nickel, K.G. (1989). Garnet-pyroxene equilibria in the system SMACCr: the Cr-geobarometer. Proceedings of the 4th International Kimberlite Conference (Australia 1986). Kimberlites and Related Rocks, Geological Society of Australia Special Publication No.14, Vol. 2, p.901-912.
- Nixon, P.H., Gummer, P.K., Halabura, S., Leahy, K. and Finlay, S. (1993). Kimberlites of volcanic facies in the Sturgeon Lake area. Russian Geology and Geophysics, Vol.34, No.12, p.66-76.
- Nixon, P.H., Griffin, W.L., Davies, G.R. and Condliffe, E. (1994). Cr garnet indicators in Venezuela kimberlites and their bearing on the evolution of the Guyana craton. Proceedings of the 5th International Kimberlite Conference (Brazil 1991), Vol.2, p.147-157.
- Nixon, P.H. (1995). The morphology and nature of primary diamondiferous occurrences. In Griffin, W.L. (ed.) Diamond Exploration: Into the 21st Century, Journal of Geochemical Exploration Special Volume, Vol. 53, Nos. 1-3, p.41-72.
- Nixon, P.H. and Leahy, K. (1995). Diamond-bearing volcaniclastic kimberlites in Cretaceous marine sediments, Saskatchewan, Canada. Proceedings of the 6th International Kimberlite Conference, Russia 1995, (submitted).
- Obradovich, J.D. (1991). A revised Cenomanian-Turonian time scale based on studies from the Western Interior United States. Abstracts with Programs, Geological Society of America, 1991 Annual Meeting, San Diego, CA., p.A296.
- Otter, M.L., McCallum, M.E. and Gurney, J.J. (1994). A physical characterisation of the Sloan (Colorado) diamonds using a revised diamond description scheme. Proceedings of the 5th International Kimberlite Conference (Brazil 1991), Vol.2, p.15-31.
- Palmer, A.R. (1983). The decade of North American geology, geologic timescale. Geology V.11, p.503-504.
- Pilkington, M. (1991). Mapping elastic lithospheric thickness variation in Canada. Tectonophysics, Vol.190 p.283-297.
- Plint, A.G., Hart, S.H. and Donaldson, W.S. (1993). Lithospheric flexure as a control on stratal geometry and facies distribution in Upper Cretaceous rocks of the Alberta foreland basin. Basin Research Vol. 5, p. 69-77.
- Ringwood, A.E. (1987). Constitution and evolution of the mantle. Proceedings of the 4th International Kimberlite Conference (Australia 1986). Kimberlites and Related Rocks, Geological Society of Australia Special Publication No. 14, Vol. 1, p.455-485.
- Robey, J.V.A. and Gurney, J.J. (1979). Megacrysts from the Lekkerfontain kimberlite, North central Cape, South Africa. Kimberlite Symposium II, Cambridge, extended abstract.
- Ryan, C.G., Griffin, W.L. and Pearson, N.J. (1995). Garnet geotherms: Derivation of P-T data from Cr-pyrope garnets. Journal of Geophysical Research (in press).

- Ryan, C.G., Griffin, W.L., Pearson, N.J. and Win, T.T. (1995**b**). Garnet geotherms: Derivation of P-T data from Cr-pyrope garnets. Proceedings of the 6th International Kimberlite Conference, Russia 1995, Extended Abstracts Volume.
- Schmid, R. (1981). Descriptive nomenclature and classification of pyroclastic deposits and fragments: recommendations of the IUGS subcommission on the systematics of igneous rocks. Geology, Vol.9, p.41-43.
- Schulze, D.J. (1987). Megacrysts from alkalic volcanic rocks. In Mantle Xenoliths, P.H. Nixon (ed.), p.433-451.
- Scott-Smith, B.H., Orr, R.G., Robertshaw, P. and Avery, R.W. (1994). Geology of the Fort a la Corne Kimberlites. Proceedings of District 6, AGM, Canadian Institute of Mines, p.19-24.
- Scott-Smith, B.H., Orr, R.G., Robertshaw, P. and Avery, R.W. (1995). Geology of the Fort a la Corne Kimberlites. Proceedings of the 6th International Kimberlite Conference, Russia 1995, Extended Abstracts Volume.
- Shee, S.R. (1984). The oxide minerals of the Wesselton Mine, Kimberley, South Africa. Proceedings of the Third International Kimberlite Conference, Vol.1, p.59-73.
- Simpson, F.R. (1982). Sedimentology, palaeoecology and economic geology of Lower Colorado (Cretaceous) strata of West-Central Saskatchewan. Saskatchewan Energy and Mines Report 150.
- Singh, S.K. and Sabina, F.J. (1978). Magnetic anomaly due to a vertical right circular cylinder with arbitrary polarization. Geophysics, Vol.43, p.173-178.
- Skinner, E.M.W. and Clement, C.R. (1979). Mineralogical classification of Southern African kimberlite. In Kimberlites, diatremes, and diamonds, (Boyd, F.R. and Meyer, H.O.A., eds.), American Geophysical Union, Washington, p.129-139.
- Smith, D. and Boyd, F.R. (1987). Compositional heterogeneities in a high-temperature lherzolite nodule and implications for mantle processes. In Mantle Xenoliths, P.H. Nixon (ed.), p.551-562.
- Smith, C.B. and Lorenz, V. (1989). Volcanology of the Ellendale lamproite pipes, Western Australia. Proceedings of the 4th International Kimberlite Conference (Australia 1986), Kimberlites and related rocks, (Blackwell, pubs.), Vol 1, Geol. Soc. Australia Special Publication No.14, p.505-520.
- Smith, C.B., Gurney, J.J., Skinner, E.M.K.,Clement, C.R. and Ebrahim, N. (1985). Geochemical character of southern African kimberlites: a new approach based on isotopic constraints: Transactions of the Geological Society of South Africa, Vol.88, p.267-280.
- Sobolev, N.V., Laurent'ev, Yu.G., Pokhilenko, N.P. and Usova, L.V. (1973). Chrome-rich garnets from the kimberlites of Yakutia and their paragenesis. Contributions to Mineralogy and Petrology, Vol.40, p.39-52.

- Stockmal, G.S. and Beaumont, C. (1987). Geodynamic models of convergent margin tectonics: the southern Canadian Cordillera and the Swiss Alps. In Beaumont, C. and Tankard, A.J. (eds.) Sedimentary basins and basin forming mechanisms, Canadian Society of Petroleum Geologists, Memoir 12, and Atlantic Geoscience Society, Special Publication 5, p.393-411.
- Stockmall, G.S., Cant, D.J. and Bell, J.S. (1992). Relationship of the Stratigraphy of the Western Canada Foreland Basin to Cordilleran Tectonics: Insights from Geodynamic models. In Macqueen, R.W. and Leckie, D.A. (eds.) Foreland Basins and Fold Belts, Association of American Petroleum Geologists Memoir 55, p.9-47.
- Taylor, W.R.T., Jaques, A.L. and Ridd, M. (1990). Nitrogen-defect aggregation characteristics of some Australian diamonds: Time-temperature constraints on the source regions of pipe and alluvial diamonds. American Mineralogist, Vol.75, p.1290-1310.
- Thorkelson, D.G. (1985). Geology of mid-Cretaceous volcanic units near Kingsvale, south-western British Columbia. Current Research part B, Geological Society of Canada, Paper 85-1B, p.333-339.
- Valsami, E. and Cann, J.R. (1992). Mobility of rare earth elements in zones of intense hydrothermal alteration in the Pindos ophiolite, Greece. In Parson, L.M., Murton, B.J. and Browning, P. (eds.) Ophiolites and their Modern Oceanic Analogues. Geological Society Special Publication No.60, p.219-232.
- White, S.H., deBoorder, H. and Smith, C.B. (1995). Structural controls of kimberlite and lamproite emplacement. In Griffin, W.L. (ed.) Diamond Exploration: Into the 21st Century, Journal of Geochemical Exploration Special Volume, Vol. 53, Nos. 1-3, p.245-264.
- Woods, G.S. (1986). Platelets and the infrared absorbance of Type Ia diamonds. Proceedings of the Royal Society London, A407, p.219-238.
- Wright, J.V. and Mutti, E. (1981). The Dali Ash of Rhodes, Greece: a Problem in Interpreting Submarine Volcanigenic Sediments. Bulletin of Volcanology, Vol.44-2, p.153-167.
- Wyllie, P.J. (1981). Plate tectonics and magma genesis. Geology Rundschau, Vol.70, p.128-153.
- Yamaoka, S., Kanda, H. and Setaka, N. (1980). Etching of diamond octahedra at high pressure with controlled oxygen partial pressure. Journal of Material Science, Vol.15, p.332-336.
- Zimanowski, B., Fröhlich, G. and Lorenz, V. (1991). Quantitative experiments on phreatomagmatic explosions. Journal of Volcanology and Geothermal Research, Vol. 48, p.341-358.
- Zimanowski, B., Fröhlich, G. and Lorenz, V. (1995). Experiments of steam explosion by interaction of water with silicate melts. Nuclear Design and Engineering, Vol. 155, p.335-343.

Acknowledgements

Recognition must first go to my supervisors, Em. Prof. Peter H. Nixon and Dr. Marge Wilson, for expert guidance, tuition and continuous discussion in the fields of kimberlite and mantle geology. Peter must also be credited with setting up the PhD, and I thank him for taking me on as his student. Other staff at the department have provided valuable discussion, and include Dr. Cindy Ebinger, Prof. Mike Leeder, Prof. Howell Francis (retired), Dr. Eva Valsami, Prof. Peter Baker and Dr. Paul Wignall. Practical support in the department has been lent by Alan Gray (XRF analyses) and Dr. Eric Condliffe (microprobe analyses and training), and all the technical staff in the department who have been involved in sample preparation (especially Rob Marshall for the very difficult polished sections). Much of the thesis would not have been possible without the work of Dr. Bill Griffin (proton-microprobe garnet analysis), CSIRO, Australia, Dr. Wayne Taylor (for diamond analyses) formerly of UCL, and Dr. Dave Mattey (carbon isotope analyses). Without the efforts of these scientists, the mantle lithosphere not only beneath Central Saskatchewan, but all round the world, would not be as well understood as it is. Colleagues who have also provided stimulating discussion (or just listened to me venting my ideas) include Julian Brown, Gavin Day, Wilma Pretorious, Mark Hutchison, Mark Trout, and many others too numerous to mention.

The motivation for both Operation Fish Scale and this thesis was largely due to the efforts of Peter Gummer of Rhonda Mining Corp (the initial sponsor of this thesis). Peter's contribution goes beyond the financial, and this author is indebted to his vision and energy in the field of kimberlite exploration. Thanks also to Dr. Richard Garnett, formerly a consultant for Aaron Oil, for many useful comments. Clive Newall of Kensignton Resources Ltd. is acknowledged for taking the reins of sponsorship from Rhonda, and providing an excellent base in Saskatoon and the opportunity to work within the FALC Joint Venture. I also thank the staff of the Kensignton/Rhonda Saskatoon field office, Art deCarle and Kristo Tappennin, for their excellent support and discussions. Special mention is made to Brent Jellicoe (and Ruth, and the kids) at the Saskatoon office, stratigraphic expert, fine geologist and a true friend, thanks for putting up with me.

I express my gratitude to my parents for constant encouragement and support over these halcyon student days, I will always remember them. Thank you, Sangeeta, for your sense and calm during this thesis (and the three years before it). And finally, cheers to all my friends for listening; Dom, Rik, Adam, Ian, Maggie, Antony, Liz and Andy.

APPENDIX I

Boreholes used in Stratigraphic Sections

CONTENTS:

RHONDA MINING CORPORATION
DETAILED CORE DESCRIPTION
November 8, 1994

DRILL HOLE: OFS93-004 **CLAIM NUMBER: S-127080**

LOCATION, LEGAL: NE Quarter, Section 05, Township 52, Range 18 West of 2nd Meridian

GROUND ELEVATION: 436.63 metres

TOTAL DEPTH: 160.62 metres

CORE SIZE: 67.05-117.60 metres - HQ, 101 millimetres; 117.60-160.62 metres - NQ

CORE LOCATION: Saskatoon Field Office

EQUIPMENT LEFT IN HOLE: 24.4 metres HQ rod

DIP: -090 degrees

DATE STARTED: March 1, 1993

DATE COMPLETED: March 7, 1993

DOWNHOLE GEOPHYSICAL TESTING: BPB Wireline Ltd.

DRILLING CONTRACTOR: Longyear Canada Ltd.

DRILLSITE GEOLOGY: M. Durocher

CORE LOGGED BY: B.C. Jellicoe and K. Leahy

ABANDONMENT STATUS: Cemented from 160.62 to 67.05 metres; up-hole collapsed.

PURPOSE: To test a broad positive aeromagnetic feature adjacent to known kimberlite clusters located immediately to the north.

RESULTS: A 14m PK and RPK is present between 95-109.0 metres immediately below the pre-till unconformity. The kimberlite is underlain by a basal sandstone.

COMMENTS: Bedding and contacts are subhorizontal (90 degree angle to core axis) unless otherwise specified.
All depths are relative to collar elevation.
Abbreviations for kimberlite description are defined in the Textural Classification, Chapter 2.
Stratigraphic Nomenclature for the Colorado Group of Bloch et al (1993) used in this log, see Chapter 1.

CORE DESCRIPTION

00.00 67.36 TILL: This interval was not cored and chip samples were not collected; geophysical logs and driller reports indicate that this interval is composed of interbedded muddy tills and sandy tills beneath a few metres of surficial sandy sediment.

67.36 68.88 TILL: Unit 1 is carbonate cemented, very poorly sorted, dark brown, silty/sandy till with a mud matrix containing up to 30 per cent granules and pebbles of diverse composition; clasts include quartz, cherty dolomite, granite, feldspar, and some dark ultramafic rock; bottom contact is gradational.

68.88 72.37 TILL: Unit 2 is light brown, moderately unconsolidated, calcareous silty sandy till with abundant pebbles and cobbles of diverse origin; bottom contact is gradational.

72.37 77.64 TILL: Unit 3 is carbonate cemented silty/muddy till similar to Unit 1, but with silty sand interbeds; bottom contact is sharp.

77.64 78.45 SANDY TILL: Unit 4 is light brown, unconsolidated, medium grained sand grading into silty and muddy sand downwards; weakly carbonate cemented; bottom contact is gradational.

78.45 90.52 TILL: Unit 5 is light brown, poorly sorted, calcareous muddy till with abundant silt and sand; pebbles and cobbles of diverse origin abundant in some intervals and common elsewhere; large clasts of granite, quartz, and carbonate rock common with lesser abundance of angular to sub-angular, dark greenish-black to pale black peridotite clasts; interbeds of brown, unconsolidated, medium grain sand common; bottom contact is sharp.

90.52 92.57 TILL: Unit 6 is similar to Unit 5; carbonate cemented, poorly sorted, dominantly silty till with abundant sand and clay; large carbonate and grey shale clasts are common; bottom contact is sharp.

92.57 92.84 SANDY SHALE: Unit 7 is composed of intermixed, mottled, dark grey mudstone and light brown very fine to fine grain sand; moderately bioturbated and contains thin carbonate shell fragments; bottom contact is sharp.

92.84 92.96 SANDSTONE: Unit 8 is light brown, massive, homogeneous, sandstone with abundant organic matter as oxidized rootlets and irregular fragments; bottom contact is gradational.

92.96 93.19 SILTY MUDSTONE: Unit 9 is dark brown to black silty mudstone which grades down to blocky mudstone containing thin walled shell fragments; bottom contact is sharp.

93.19 93.60 SILTY SANDSTONE: Unit 10 is greyish-brown to tan, very poorly sorted, centimetre scale bedded silty sandstone; unit is composed of numerous subordinate components including clasts of magnetite, greenish-grey kimberlitic material up to 2 centimetre across, and discrete crystals of garnet, quartz, and feldspar within lag deposits situated over scour surfaces; also contains abundant rounded pebbles of shale, silty shale and quartz; rock is weakly magnetic and variably reactive with HCl, particularly in the region of carbonate clasts; bottom contact is sharp.

93.60 93.94 SILTY SANDSTONE: Unit 11 is similar to Unit 10, but is creamy tan in colour and containing fewer large clasts; entrained clasts are dominantly angular

and rounded quartz, feldspar, and carbonate up to 2 centimetre across; bottom contact is sharp.

93.94 94.41 SILTY SANDSTONE: Unit 12 is similar to Unit 10, but with higher proportion of clasts smaller in size and dominantly of quartz, feldspar and carbonate; minor weakly magnetic ultramafic or kimberlitic clasts; bottom contact is sharp.

TOP OF BEDROCK AT 94.41 METRES - KIMBERLITE

94.41 97.70 BEDDED AND GRADED RPK: Unit 13 is light green to bluish-steel grey, tuffaceous kimberlite composed of fine to coarse grained rounded and lath-like black glassy plates of phlogopite up to .5 millimetres across, and medium grained white particles set into very fine to amorphous light green matrix that forms scaly, irregular and blebby bands; abundant clay material is irregularly, intermixed with the matrix; highly magnetic throughout with abundant, though irregular, blebs, wisps, and interspersed vaguely defined layers of dull, granular to amorphous greenish-black magnetite; steep (060 degrees to CA) bedding is defined by accumulation of magnetite grains and blebby millimetre- to centimetre-scale bands of granular matrix; irregular anastomosing veinlets and blebs of white carbonate material are common; vertical to subvertical (0 to 025 to CA) 2-5 millimetre wide vein of carbonate occurs between 97.25 and 97.75 metres; rare fish scales; overall, the rock is mineralogically diverse and coarsens upward inclusive of 6 fining upward sub-sequences of medium to fine grain variation bounded by sharp contacts; the upper 30 centimetres is weathered, friable, fragmented shards and gravel followed downward by slightly less fragmented material forming a more cohesive, though gravely interval; disaggregation was likely the result of mechanical breakage of a soft and highly fractured rock during progressive dehydration; a notable feature was visible prior to dehydration of the rock in the occurrence of many 5 centimetre diameter, dark greyish-black, nested ring structures (like Liesegang rings?) possibly composed of black amorphous magnetite; bottom contact is sharp.

97.70 98.67 GRADED RPK: Unit 14 is similar to Unit 13, but is light green to steel grey, coarse to medium grained, and more competent; phlogopite and magnetite are ubiquitous and interspersed with white baryte particles; planar and inclined bedding (090 to 075 to CA), ranging in thickness from a few millimetres to 5 centimetre is often cross-bedded and is particularly evident in the uppermost 30 centimetres; bottom contact is sharp.

Five fining-upward sequences comprise a macro-unit from 98.67 to 102.86 metres

98.67 100.03 GRADED RPK: Unit 15 is light greenish-grey, white and black speckled calcareous kimberlite of variable grain size fining upwards from coarse to fine grained; upper portion of the unit is fine grained, chalk-like, lighter coloured, and cross-bedded (085 degree angle to CA) to planar bedded, while the lower

portion is darker, massive, and more granular; unit is dominantly composed of phlogopite, antigorite, and magnetite with subordinate carbonate and other unidentified minerals; magnetite occurs as abundant globular to lensoidal granular concentrations between a few millimetres to 5 centimetre in size; overall, this sequence is the most gradational and complete of the five fining upward units; bottom contact is sharp.

100.03 100.67 GRADED RPK: Unit 16 is similar to Unit 15, although dominated by medium and coarse grains, and marked by steep bedding in the basal coarser grained portion; calcareous throughout, with increasing carbonate in the upper fine grained beds; bedding is partially defined by globular to laminar bands of granular and amorphous magnetite and less visibly by other grains; bedding angle averages between 080 to 085 degrees to CA, but ranges to 060 degrees angle to CA in the lowermost, coarser grained material; bottom contact is sharp.

100.67 101.50 GRADED RPK: Unit 17 is similar to Unit 16 with bedding at 090 to 085 degrees to CA; fining upward and calcareous throughout; bottom contact is sharp.

101.50 102.16 GRADED RPK: Unit 18 is similar to Unit 16, although, medium to fine grained and occasionally cross-bedded at 080 degree angle to CA; fining upward with a coincident decrease in carbonate content upwards; bottom contact is sharp.

102.16 102.86 GRADED RPK: Unit 19 is similar to Unit 16, although it varies from massive to planar bedded angled at 070 degrees to CA; overall unit 19 is more coarse grained and shows bedding planes littered with less than 1 to 2 millimetre diameter micaceous grains; fining upward and calcareous throughout; bottom contact is sharp.

102.86 103.58 BEDDED RPK: Unit 20 is dark greenish-grey, homogeneous, medium grained, evenly bedded tuffaceous kimberlite; bedding is steeply dipping at an average of 060 to CA and highlighted by concentrations of phlogopite along bedding planes; bands of magnetite are conspicuously absent and abundance of matrix phlogopite much greater in comparison to the fining upward units; dominantly calcareous, but with patchy distribution; bottom contact is sharp.

103.58 105.94 MEDIUM TO COARSE PK TUFF: Unit 21 is dark grey irregularly mottled with dark green kimberlite; massive with even distribution of fine and coarse (crystals) grains bound by green very fine grain calcareous matrix; abundant, irregularly oriented phlogopite crystals, and dull, dark grains occur throughout; mottling occasionally resolves into light and darker interlayers; large irregularly shaped, subangular (edges partially assimilated?) mudstone clasts up to at least 6.5 centimetre across (core width) between 103.58 and 104.79 metres; approximately .5m of brecciated very hard mudstone floating in light green

kimberlite matrix occurs at 104.92, may be interbedded MASSIVE RPK and SHALE INTRACLAST BRECCIA; slickensided fault plane at 104.6; basal 21 centimetres contains thin calcite veins oriented at 070 degree angle to CA; bottom contact is sharp.

105.94 107.19 FINE TO MEDIUM PK TUFF: Unit 22 is a massive, dark green and black, mottled to laminated, fine grained rock similar in composition to Unit 21, although harder; abundant, very fine, irregularly dispersed carbonate veins; weakly calcareous matrix; bottom contact is sharp.

107.19 108.04 FINE PK TUFF: Unit 23 is similar to Unit 22, but very fine grained, massive, and mottled; well indurated with sub-conchoidal fracture; calcareous matrix and abundant carbonate veins; bottom contact is sharp.

108.04 108.42 FINE TO MEDIUM PK TUFF: Unit 24 is similar to Unit 23, with abundant, millimetre-scale carbonate veinlets and anastomosing finely intermixed vein threads oriented at 065 to 080 degrees to CA; some veins may define cryptic bedding planes as they are of approximately the same bedding angle as that seen in the overlying coarser units; three 2 millimetre thick veins/faults cross-cut the vein threads at 055 degrees to CA; calcareous matrix; bottom contact is sharp.

108.42 108.59 CONTACT ALTERATION BRECCIA: Unit 25 brackets the contact between kimberlite above and sandstone below and embodies a zone of intense carbonate veining which permeates into both units; carbonate veins range in size from a few millimetres up to .5 centimetre; upper and lower contacts of this interval are gradational, however, the contact between sandstone and kimberlite is milled, therefore the nature of the contact is indeterminate; possibly an alteration fluid zone.

EROSIONAL TOP OF ST. WALBURG SANDSTONE AT 108.59 METRES

108.59 109.00 SANDSTONE: Unit 26 is greyish-white to brown, carbonate cemented, medium grain sandstone with well-defined ripple cross-bedding angled at 055 to 045 degrees to CA; colour is gradational from off-white to brown towards the overlying alteration zone; sporadic millimetre- to centimetre-scale shaly sand interbeds; bottom contact is sharp and angular.

TOP OF LOWER WESTGATE FORMATION AT 109.00 METRES.

109.00 113.63 MUDSTONE: Unit 27 is a black, non-calcareous, homogeneous, massive to poorly fissile mudstone; minor isolated sand filled spreiten are present as are gradational intervals of silty mudstone; bedding oriented at 060 degree angle to CA in the upper 40 centimetres and decreases to approx. 090 degrees by 109.41 metres depth; bottom contact is sharp.

113.63 114.60 SHALEY SANDSTONE: Unit 28 is composed of dominantly very fine to fine grain, tan to light brown, silty sandstone and subordinate beds of slick, black, shaly claystone intermixed throughout by bioturbation; bottom contact is sharp.

114.60 118.25 MUDSTONE: Unit 29 is brownish-black, massive mudstone with abundant silty sand laminations, wisps and lenses along bedding planes; well preserved trace fossils include horizontal and vertical, lined, silt-filled burrows (palaeophycus or planolites); pyritized rootlets common; unit grades to muddy siltstone in many intervals; bottom contact is sharp.

TOP OF FLOTTEN LAKE SANDSTONE AT 118.25 METRES.

118.25 122.18 SILTSTONE: Unit 30 is a composite unit dominated by mottled dark brown and tan siltstone with variable content of very fine to fine grain, light brown sand, and lenses and laminae of slick, black shaley claystone; siltstone is competent and breaks preferentially along shaley claystone bedding planes; bioturbation is common in the form of burrows and mixing of the sediment, but intact laminae of claystone indicate that the bioturbation was not pervasive; bottom contact is gradational; this unit is the upper portion of an overall fining upward sequence from 126.00 to 118.25 metres.

120.50 120.60 -off-white, fine-grained, finely ripple cross-bedded sandstone; burrows in the lowermost portion of the unit piped in sand to the underlying mudstone; bottom contact is sharp.

122.18 123.60 SANDY MUDSTONE: Unit 31 is dark grey to black mudstone with abundant (30 per cent) lenses, laminae, and intermixed (mildly bioturbated) masses of tan to medium brown silty sandstone; interval is gradational downwards to dominantly mudstone with a progressive decrease in sand and silt; bottom contact is gradational; is a transitional interval between units 30 and 32.

TOP OF JOLI FOU FORMATION AT 123.60 METRES.

123.60 126.00 SHALEY MUDSTONE: Unit 32 is composed of dominantly chunky, black, weakly carbonaceous mudstone with minor interbeds of silty mudstone as in bottom portion of unit 31; some intervals poorly fissile; rare thin-walled shell material and fish debris; bottom contact is sharp.

126.00 130.20 MUDSTONE: Unit 33 is dominantly black, massive, weakly carbonaceous mudstone with minor lenses, and burrow-fills of light brownish grey, very fine to fine grain sand; overall, the unit is subtly fining upwards with up to 15 per cent sand and silt both intermixed and interbedded in the upper 1 metre; bottom contact is gradational.

130.20 131.09 SILTY MUDSTONE: Unit 34 is similar to unit 31, but with approx. 5 per cent interbedded silty sand; bottom contact is gradational.

131.09 133.19 CLAYSTONE: Unit 35 is composed of decimetre-scale interbedded dark grey, weakly fissile, shaly claystone and massive to chunky, slick, weakly carbonaceous, black mudstone; bottom contact is gradational.

133.19 134.70 SHALEY MUDSTONE: Unit 36 is dark grey, uniform, weakly fissile, shaly mudstone; few, sporadic interbeds of silty fine grain sandstone less than 2 centimetre thick; bottom contact is gradational.

134.70 137.00 SHALEY MUDSTONE: Unit 37 is similar to unit 36, but without sandy interbeds; some interbedded black, massive to chunky, slick claystone; bottom contact is sharp.

TOP OF SPINNEY HILL MEMBER AT 137.00 METRES.

137.00 139.39 SILTY MUDSTONE: Unit 38 is medium grey, medium disky, silty mudstone with abundant silt/sand wisps and lenses along bedding planes and as laminations; well preserved trace fossils include horizontal and vertical, lined, silt-filled burrows (palaeophycus or planolites); pyritized rootlets common; abundant, less than 5 centimetres thick, interbeds of muddy siltstone; bottom contact is sharp.

139.39 143.36 SANDY MUDSTONE: Unit 39 is dark grey mudstone with abundant glauconite-rich sandstone in, wisps, burrow fills, and indurated, laminated lenses; some sandstone is carbonate-cemented; moderate to intense bioturbation common; rare fish scales; bottom contact is gradational.
139.97 140.57 -green glauconitic sandstone; variably carbonate-cemented.

143.36 145.30 MUDSTONE: Unit 40 is dark grey, massive to poorly fissile mudstone with common indurated lenses of glauconitic sandstone up to 4 centimetre across; minor bioturbation in some intervals; bottom contact is sharp.

145.30 149.10 GLAUCONITIC SANDSTONE AND MUDSTONE: Unit 41 is composed of dark grey mudstones interbedded with lenses and wisps of emerald-green glauconitic sandstone common; some sandstone is carbonate-cemented; bottom contact is sharp.

149.10 149.49 SANDSTONE: Unit 42 is composed of dark grey, poorly sorted, rounded, medium to coarse grained and pebbly quartz within carbonate-cemented clayey matrix; this "chaotic" unit is grain supported and heterogeneous; wisps of soft mudstone common; rare millimetre-scale shale clasts; variably competent and well indurated to friable; sporadically mottled from bioturbation; pyrite occurs sporadically; bottom contact is sharp and angular.
This unit and Unit 44 are considered to be part of the Basal Colorado Sand.

149.49 150.19 MUDSTONE: Unit 43 is black, homogeneous, poorly fissile, and weakly carbonaceous; abundant sand filled burrows and sand wisps; bottom contact is sharp.

150.19 152.22 SANDSTONE: Unit 44 is well indurated, dark grey, fine to coarse grain, quartzitic carbonate-cemented sandstone interbedded and intermixed with mudstone; sandstone is pyrite cemented; unit grades downward to slick, carbonaceous, sandy mudstone; "chaotic"; bottom contact is sharp.

TOP OF MANNVILLE GROUP AT 152.22 METRES.

152.22 153.72 SANDSTONE: Unit 45 is well-indurated tan to light brown, fine to medium grained sandstone; intermixed with laminations and wisps of dark brown silt and clay; cross-bedded and inclined beds; weakly bioturbated in some thin intervals; interbeds of grey siltstone up to 20 centimetres thick; bottom contact is sharp.

153.72 158.78 SILTY MUDSTONE: Unit 46 is light brown and grey mottled, massive, moderately well-indurated, silty mudstone with tan and dark grey mudstone clasts; unit becomes darker grey and less silty in some intervals; coalified plant remains common; induration varies through unit with some intervals very hard and some mudstones blocky and soft; bottom contact is sharp.

158.78 160.62 SILTY SANDSTONE: Unit 47 is interbedded light grey sandstone, silt, and silty shale; sands are unconsolidated; bottom contact is unknown.

END OF HOLE AT -160.62 METRES.

RHONDA MINING CORPORATION
DETAILED CORE DESCRIPTION
October 30, 1994

DRILL HOLE: OFS93-013 **CLAIM NUMBER: S-127472**

LOCATION

LEGAL: LSD 5, Section 35, Township 51, Range 22 West of 2nd Meridian
UTM (1983): 490160 East, 5921550 North
GEOPHYSICAL GRID: 300 North, 125 West
COLLAR ELEVATION: 478.3 metres ASL
GROUND ELEVATION: 477.1 metres ASL
TOTAL DEPTH: 290.0 metres
CORE SIZE: HQ, 101 millimetres
CORE LOCATION: Saskatoon Field Office
EQUIPMENT LEFT IN HOLE: 10m HW casing and casing shoe; 175m 101mm rods; 1-101mm drilling bit; 1 core barrel; 6.0m conductor casing
DIP: -090 degrees
DATE STARTED: August 26, 1993
DATE COMPLETED: September 03, 1993
DRILLING CONTRACTOR: Longyear Canada Ltd.
WATER HAULING: J. Bergstrum
DRILLSITE GEOLOGY: R. Woodward
CORE LOGGED BY: B.C. Jellicoe
ABANDONMENT STATUS: Cemented from surface to end of hole.
PURPOSE: To test low an amplitude positive ground magnetic circular closure located within a broad magnetic high about 1.5 kilometres from a postulated "kimberlite apron structure".
RESULTS: The lithologies encountered in drillhole OFS93-013 do not explain the ground magnetic survey results. This would suggest a shallow feature in the till or a deeply buried basement structure. The hole was abandoned at 290.00 metres due to stuck rods in unconsolidated sand.
COMMENTS: Bedding and contacts are subhorizontal (90 degree angle to core axis) unless otherwise specified.
All depths are relative to collar elevation.
Stratigraphic Nomenclature for the Colorado Group of Bloch et al (1993) used in this log, see Chapter 1.

CORE DESCRIPTION

0.00 85.70 GLACIAL TILL: This interval was not cored and chip samples were not collected; geophysical logs and driller reports indicate that this interval is composed of muddy tills and sandy tills beneath a few metres of surficial sandy sediment.

85.70 95.00 TILL: Unit 1 is composed of a mixture of light grey to brownish-grey silt, sand, and clay matrix with 10 to 20 per cent rounded and angular pebbles and cobbles of basalt, granite, dolomite, limestone, and mudstone; the matrix is hard, massive, clay- and carbonate-cemented and very porous; sand content in the matrix increases to approximately 75 per cent in some intervals with a corresponding colour change from brownish-grey to light grey and decrease of pebbles to less than 10 per cent; pebble content decreases downwards; basal contact is gradational with the underlying sandstone.

88.50 89.96 -light grey, moderately hard, sandy till.
91.50 92.81 -light grey, moderately hard, sandy till.
92.81 93.63 -very sandy, light grey, poorly consolidated sandy till; up to .6 metres of lost core in this interval.
93.63 95.00 -light grey, moderately hard to poorly consolidated sandy till; bottom contact is gradational with increase of sand downwards; portion of granite boulder from 94.62 to 94.81 metres.

95.00 98.45 SANDSTONE: Unit 2 is dominantly unconsolidated, light grey, moderately calcareous, fine grain quartzitic sandstone; rounded pebbles and cobbles of dolomite and igneous rock are common up to 10 per cent of the unit although they may be concentrated due to the washing and loss of up to 1.5 metres of core; bottom contact is sharp.

98.45 103.85 TILL: Unit 3 is brownish-medium grey, hard, clay- and carbonate-cemented till with matrix composed of sand, silt and clay; dolomite, limestone, mudstone, and igneous rock rounded to angular pebbles comprise less than 5 per cent of the unit and these pebbles are generally less than 3 millimetres in size; rare cobbles are small and isolated; bottom contact is gradational; 5 centimetre thick granite boulder at 103.79 metres.

103.85 104.36 SANDSTONE: Unit 4 is hard, massive, dark grey, very fine to fine grain silty carbonate-cemented sandstone; bottom contact is sharp.

104.36 107.00 TILL: Unit 5 is dark brown, hard to poorly consolidated sandy till; pebbles are rare; sand content is greatest in the middle of the unit; bottom contact is gradational.

104.36 104.66 -well-consolidated muddy till with subordinate and downward increasing sand content.
104.66 106.65 -poorly consolidated sandy till; up to 1.7 metres of lost core.
106.65 107.00 -well-consolidated muddy till with subordinate sand content.

107.00 108.19 SANDY TILL: Unit 6 is brownish-grey, moderately well-consolidated carbonate-cemented sandy till; granules and very coarse sand grains are common up to 25 per cent of the rock with rare pebbles of diverse origin; bottom contact is gradational.

107.25 107.45 -lost core; probably sandy till.

108.19 110.59 TILL: Unit 7 is heterogeneous, well-consolidated, carbonate-cemented till with a silty mudstone matrix; granules and pebbles are of varied size, composition and distribution throughout, generally comprising 25 per cent of the unit; bottom contact is sharp.

110.59 111.28 MUDSTONE: Unit 8 is black, massive to chunky, moderately well-consolidated claystone; fracture planes are 6 centimetres apart and at 45 degree angle to core axis; lower 40 centimetres is brecciated and chunky; centimetre-scale pods of gossanous creamy-white clay occur sporadically in the lower 40 centimetres; basal contact is sharp.

111.28 118.36 TILL: Unit 9 is light grey to brownish-grey silty mud-dominated till with variable sand and pebble content up to 30 per cent; till is well-consolidated, carbonate-cemented and hard; sandier intervals are generally softer; bottom contact is gradational to sand.

111.38 111.48 -boulder of black, white speckled, calcareous shale with 1 centimetre thick pods of recrystallized shell material compressed between bedding planes oriented at 90 degree angle to core axis.

111.48 112.23 -light grey mud-dominated till with rare large pebbles.

112.23 115.26 -moderately hard, sandy till with abundant granules and small pebbles of diverse origin; up to .74 metres of core loss from this interval; bottom contact is gradational.

115.26 116.00 -light grey mud-dominated till with less than 5 per cent granules and pebbles; hard and carbonate-cemented.

116.00 117.81 -pebbles and cobbles only remaining in interval of very sandy till.

117.81 118.36 -light grey silty mud-dominated till with less than 5 per cent granules and pebbles; sand content increases towards base.

118.36 120.50 SANDSTONE: Unit 10 is dominantly light grey calcareous poorly consolidated very fine to fine grain sandstone with rare pebbles of diverse origin; bottom contact is gradational with increase of silt, clay and pebbles.

120.50 125.65 TILL: Unit 11 is brownish-grey, hard, clay- and carbonate-cemented till; coarse grains, granules, pebbles and cobbles comprise up to 25 per cent of the till; interval gradually becomes less calcareous from about 124.4 metres to very weakly calcareous at the base; bottom contact is sharp.

BEDROCK CONTACT AT 125.65 METRES - BELLE FOURCHE FORMATION

125.65 127.15 DEFORMED MUDSTONE: Unit 12 is black, massive, well-consolidated mudstone with fractures ranging from 60 to 80 degree angle to core axis towards the base; brecciated with angular clasts of massive mudstone encased within similar massive mudstone that has incorporated up to 15 per cent sandy till and angular rock fragments along fractures; deformed by glacial pressure and

injection/incorporation of till material; this unit may be an ice raft thrust into place; basal contact is sharp.

127.15 128.50 SANDY SILTSTONE: Unit 13 is medium grey, massive, uniformly competent siltstone mottled with up to 30 per cent light grey, intermixed and wispy, very fine grain sandstone; well-bioturbated with only rare discontinuous laminations; bottom contact is sharp.

127.15 128.00 -dominantly medium grey siltstone with subordinate sandy wisps.

128.00 128.28 -silty dark grey vaguely laminar mudstone; bedding oriented at 90 degree angle to core axis.

128.28 128.50 -mottled sandy siltstone with nearly equal parts of dark grey, massive, siltstone and light grey sand in wisps, laminae and burrows.

128.50 131.90 SHALEY MUDSTONE: Unit 14 is medium to dark grey, hard, fine to medium disky, weakly fissile to massive, shaley mudstone; bedding orientation is at 90 degree angle to core axis; glacial deformation evident in fracturing which is characterized by subtle brecciation and local homogenization to mudstone around glide planes oriented at 45 to 60 degree angle to core axis; minor constituents are rare laths of oxidized plant matter and sporadic, small, very fine grain, sand-filled burrows, bottom contact is sharp.

130.16 131.00 -dark grey, hard, very fine disky shaley mudstone; bottom contact sharp.

131.00 131.90 -medium grey, coarse disky ("knobby"), shaley mudstone.

131.90 133.68 SHALEY MUDSTONE: Unit 15 is dark grey, moderately soft, very weak-fine disky, weakly fissile to massive, shaley mudstone; glacial deformation more pronounced than in Unit 14 with common brecciation and more abundant glide planes; wisps and burrows of very fine grain white sand are common in the upper half of the interval; bottom contact is sharp.

131.90 133.66 -brecciated intermediate, moderately consolidated, massive, shaley mudstone; fractures at 20 degree angle to core axis at 133.68 metres.

133.66 133.68 -bentonite

133.68 135.00 SHALEY MUDSTONE: Unit 16 is relatively undeformed, dark grey, moderately competent, medium disky, weakly fissile, shaley mudstone; bottom contact sharp.

134.70 135.00 -brecciated, intermediate shaley mudstone similar to 131.90-133.78 metres, but with abundant sand wisps.

135.00 136.41 SHALEY MUDSTONE: Unit 17 is dark grey, fine to medium disky, weakly fissile, partially brecciated, shaley mudstone with abundant glide planes at approximately 60 degree angle to core axis; bottom contact sharp.

136.41 139.43 SHALEY MUDSTONE: Unit 18 is dark grey, fine disky, weakly fissile, hard, mudstone; minor white very fine grain sand in wisps and burrows; this interval is not deformed, having vague bedding at 90 degree angle to core axis; trace to rare plant matter, millimetre-scale laths; bottom contact is sharp
139.30 139.43 -dark grey to black fissile, flaky claystone.

139.43 158.13 MUDSTONE: Unit 19 is medium to dark grey, massive, uniform mudstone with rare to common, white, very fine grain sand in wisps and burrows; oxidized plant matter is rare to common on poorly defined bedding planes; less than a millimetre-scale burrows are rare in some intervals; subunits are defined by colour changes, abundance of subordinate sand component, degree of consolidation (hardness); contacts are generally gradational including the basal portion where the sand content increases towards the underlying muddy sandstone unit.

139.43 142.38 -dark grey, hard, massive, uniformly competent mudstone with sporadic very weak disky intervals of less than decimetre-scale; rare large sand-filled burrows up to a centimetre wide; lower 22 centimetres progressively darker towards base.

142.38 142.88 -black, massive, moderately soft mudstone; bottom contact sharp.

142.88 144.46 -medium to dark grey, massive, non-disky; competent, sandy mudstone with abundant sand-filled burrows and wisps.

144.46 150.20 -medium grey progressively to darker grey with increased depth; massive, uniformly competent mudstone; very weak disky interval between 148.80-149.10 metres; rare laths and stringers of plant matter on poorly defined bedding planes oriented at 90 degree angle to core axis; rare, very fine grain sandy wisps, burrows, and disjunct laminae.

150.20 151.75 -medium grey, massive, uniformly competent mudstone; bottom contact sharp.

TOP UPPER WESTGATE FORMATION AT 151.75 METRES

151.75 151.89 -very dark brownish-grey, consolidated, massive silty sandstone with very fine grain black matrix; unidentified dark grains common; millimetre-scale sulphate grains common; sharp upper and lower contacts.

151.89 152.37 -medium grey, massive, hard, sandy mudstone; sand in wisps and burrows.

152.37 153.80 -medium grey, massive, uniformly competent mudstone; bottom contact gradational.

153.80 156.69 -medium grey, very weak disky, massive to very weakly fissile, hard, mudstone with rare very fine grain white sandstone in burrows and wisps.

156.69 158.13 -medium grey, weak disky, massive to very weakly fissile mudstone; very fine grain white sandstone increases downwards to the base; bottom contact gradational.

TOP OF ST. WALBURG SANDSTONE AT 158.13 METRES.

158.13 158.90 MUDDY SANDSTONE: Unit 20 is a medium grey, massive, moderately hard, mixture of mudstone and very fine to fine grain sandstone; sandstone is dominantly subrounded quartz and grain-supported, heterogeneous nature of the unit includes mud-supported sandstone intermixed with discrete pods and amorphous clumps of both mudstone and sandstone; fining upwards with an overall decrease of mudstone towards the base; bottom contact is gradational.
158.13 158.29 -medium grey sandy mudstone gradational to muddy sandstone.
158.29 158.90 -medium grey muddy sandstone with approximately 30 per cent clay content.

158.90 159.46 SANDSTONE: Unit 21 is medium grey, massive, moderately soft, fine to medium grain silty sandstone; silt and clay content is variable up to 20 per cent as pods and lenses; sandstone is poorly sorted, but with subrounded quartz grains dominant within a thin matrix of dark grey silt and clay; bottom contact is gradational with increasing hardness and cementation by clay and iron-oxide.

159.46 160.00 SANDSTONE: Unit 22 is rusty red to medium grey, very hard, well-indurated, pervasively iron-cemented, very fine grain sandstone; grain constituents include angular and rounded quartz and dark unidentified minerals encased within a dark grey, very fine grain matrix; core surface weathers reddish-grey, but fresh surfaces are dark reddish-grey to black; a few black and dark grey subrounded mudstone clasts up to 2 centimetres in diameter are distinctive from the generally mottled surface; unidentified light tan streaks up to .7 centimetres wide occur sporadically over the core surface; light grey, speckled, mottled areas up to 3 centimetres across are strongly reactive to hydrochloric acid; lower 5 centimetres is less indurated and more granular.

160.00 160.75 SANDSTONE: Unit 23 is light brownish-grey, variably carbonate-cemented fine grain sandstone; the unit is very hard when well-cemented, soft and easily washed when not; sandstone is composed of 70 to 80 per cent subrounded to subangular quartz grains with subordinate, less than 10 per cent, dark unidentified rounded grains; bottom contact is sharp where carbonate-cementation ends; up to .5 metres core lost in this interval; this unit is probably the uppermost portion of a coarsening upward sequence including units 22 and 23; bottom contact gradational.

160.75 161.68 COARSENING UPWARD SANDY SILTSTONE: Unit 24 is a coarsening upward sequence from sandy mudstone to silty sandstone; the upper portion is medium to dark grey, graded, hard siltstone with up to 25 per cent intermixed sandstone capped by medium grey silty sandstone; siltstone is well-bioturbated

with mottled wisps and amorphous pods of light grey sand within dark grey siltstone, and less than 1 centimetre long burrows; sandy siltstone gradational with muddy siltstone below; the lower portion is dark grey, poorly fissile, moderately hard, sandy, shaley mudstone with up to 20 per cent sand in thin wisps and laminae on bedding planes oriented at 90 degree angle to core axis; bottom contact sharp.

160.75 160.88 -medium grey, silty sandstone.

160.88 161.68 -coarsening upwards, bioturbated, medium to dark grey, sandy siltstone.

161.68 161.86 -sandy shaley mudstone with bentonitic shaley mudstone between 161.80-161.84 metres; bottom contact sharp.

161.86 162.07 SANDY SILTSTONE: Unit 25 is dark grey, massive, hard, heterogeneous, bioturbated sandy siltstone similar to Unit 24; bottom contact is sharp.

162.07 162.19 SANDY MUDSTONE: Unit 26 is dark grey, very weakly fissile, uniformly competent, sandy, shaley mudstone similar to the lower part of Unit 24; bottom contact is sharp, but this unit may be associated with Unit 25 as part of an upward coarsening sequence.

162.19 162.37 SANDY SILTSTONE: Unit 27 is mottled medium and dark grey, massive, hard, uniformly competent, bioturbated, sandy siltstone similar to Unit 24; bottom contact is sharp.

162.37 162.92 SANDSTONE: Unit 28 is light grey, very fine to fine grain, finely laminated, poorly consolidated, quartzitic sandstone; laminae defined by alternating subtle light and dark layers; bedding is oriented at 90 degree angle to core axis; bottom contact is sharp; up to .2 metres core lost in this interval.

162.92 163.15 MUDDY SANDSTONE: Unit 29 is composed of mottled light and dark grey, weakly fissile to massive, bioturbated, muddy sandstone gradational downwards to sandy, shaley mudstone; up to 60 per cent light grey quartzitic sandstone is intimately intermixed with dark grey silty mudstone; unit is coarsening upwards; the bottom contact is gradational and located where sand content decreases from about 30 per cent to less than 10 per cent; this unit is the upper part of an upward coarsening sequence with Unit 30.

163.15 164.60 SHALEY MUDSTONE: Unit 30 is dark grey, fine to medium disky, weakly fissile, moderately hard, shaley mudstone with less than 10 per cent white fine grain sandstone as lenses, burrows, and wisps along bedding planes oriented at 90 degree angle to core axis; shaley mudstone is crenulated on core surface due to subtle variations of internal bedding and consolidation; this unit is the lower part of an upward coarsening sequence with Unit 29; bottom contact is sharp.

164.60 165.05 MUDDY SANDSTONE: Unit 31 is light grey, massive, fine grain quartzitic sandstone with 20 per cent pods of shaley mudstone less than 2 centimetres in

diameter; this unit is the upper part of an upward coarsening sequence with Unit 32; bottom contact is gradational.

165.05 165.86 SANDY MUDSTONE: Unit 32 is composed of 40 per cent light grey fine grain sandstone intermixed with dark grey silty mudstone; unit is mottled, bioturbated, massive, hard, and uniformly competent; this unit is the lower part of an upward coarsening sequence with Unit 21; bottom contact is sharp.

TOP OF LOWER WESTGATE FORMATION AT 165.86 METRES.

165.86 166.00 SHALEY MUDSTONE: Unit 33 is dark grey to black, fine to medium disky, weakly fissile, soft, shaley, black mudstone; rare thin lenses of sandstone occur between bedding planes oriented at 90 degree angle to core axis; trace of limonite centered around a yellowish-green mudstone pod 1.5 centimetres in diameter; bottom contact is gradational.
165.96 166.00 -bentonite

166.00 167.40 SHALEY MUDSTONE: Unit 34 is dark grey, fine disky, massive to weakly fissile, shaley mudstone; minor fine grain white sand in burrows and as fine wisps; bottom contact is sharp.
167.00 167.08 -dark grey sandy mudstone.
167.08 167.40 -moderately fissile, shaley mudstone.

167.40 169.31 MUDSTONE: Unit 35 is dark grey, massive to poorly fissile, uniformly competent mudstone; bottom contact is sharp.

169.31 171.17 SANDY MUDSTONE: Unit 36 is dark grey, massive to laminated, well-consolidated sandy mudstone; sand content is variable up to 20 per cent occurring as wisps, lenses, and burrows; bottom contact is sharp.
169.31 170.00 -laminated, medium grey mudstone with light grey, very fine grain sandstone; bottom contact is sharp.
170.00 170.14 -dark grey shaley mudstone.
170.14 170.17 -bentonite

171.17 173.24 SHALEY MUDSTONE: Unit 37 is dark grey, poorly fissile, moderately hard, medium to coarse disky, shaley mudstone; sandy lenses and laminae common in some intervals; bottom contact is sharp.
170.17 171.33 -dark grey, massive, uniformly competent, hard mudstone; bottom contact is sharp.
171.23 171.33 -massive, moderately hard, dark grey, muddy sandstone; sandy lenses and laminae common (20 per cent) on bedding planes.
171.33 173.24 -dark grey, poorly fissile, moderately hard, medium to coarse disky, shaley mudstone; sandy lenses and laminae common (less than 10 per cent) on bedding planes.

TOP OF FLOTTEN LAKE SANDSTONE AT 173.24 METRES.

173.24 182.14 SILTSTONE: Unit 38 is composed of hard, generally massive, uniformly competent interbedded subunits of bioturbated, intermixed, mottled, light grey, sandy siltstone, dark grey muddy siltstones, and composite subunits of both lithotypes; less than 15 centimetre thick intervals of ripple cross-bedded, carbonate-cemented, hard, fine grain sandstones occur sporadically as lenses, interbeds, and occasionally as mudstone encased angular fragments less than 5 centimetres across; subunit contacts are generally sharp beneath mudstones and gradational beneath coarser grain units forming coarsening upward sequences; the subunits form an overall coarsening upward sequence.

173.24 173.48 -medium grey sandy siltstone with 10 centimetres of disjointed angular clasts of laminar, carbonate-cemented sandstone.

173.48 175.40 -medium grey, mottled, sandy siltstone.

175.40 176.00 -black, very fissile finely disky shaley mudstone.

176.00 177.78 -medium grey, very sandy siltstone grading downwards to dark grey muddy siltstone; coarsening upwards sequence with basal 8 centimetres of black, medium disky, silty mudstone.

177.78 178.77 -sandy and clayey-siltstone coarsening up sequence capped by 13 centimetre ripple, cross-bedded, hard, carbonate-cemented fine grain sandstone with minor glauconite along some bedding planes; crossbeds and laminae are at 80 to 90 degree angles to core axis; bottom contact is sharp.

178.77 180.54 -sandy and clayey-siltstone; coarsening upwards sequence; bottom contact is sharp.

180.54 181.55 -sandy and clayey-siltstone; coarsening upwards sequence; capped by 14 centimetres sandy siltstone with 4 centimetre thick cross-bedded, carbonate-cemented, fine grain sandstone.

181.55 182.02 -clayey-siltstone coarsening upwards to sandy siltstone; bottom contact gradational.

182.02 182.14 -mudstone with less than 10 per cent finely interbedded lenses and fragments of cross-bedded, carbonate-cemented, hard, very fine grain sandstone; bottom contact sharp.

TOP OF JOLI FOU FORMATION AT 182.14 METRES

182.14 187.38 SANDY MUDSTONE: Unit 39 is massive to poorly fissile, hard, uniformly competent, dark grey to black, sandy mudstone; sand occurs in lenses, wisps and burrows along poorly defined bedding planes; pyrite is common as lenses and clots distributed sporadically through the unit.

182.14 184.97 -dark grey, sandy mudstone; sand up to 40 per cent of unit; 1 centimetre thick pyrite lenses at 182.17 metres, 182.61 metres, and 183.10 metres; bottom contact is gradational.

184.97 187.38 -black, sandy mudstone with slight changes of bedding competency throughout; sand content less than 10 per cent

existing as wisps, burrows, and lenses; 1.5 centimetre thick pyrite lens at 185.16 metres; bottom contact is sharp.

187.38 192.00 SHALEY MUDSTONE: Unit 40 is medium to dark grey, poorly fissile, fine to coarse disky, moderately hard shaley mudstone; sand lenses, burrows, and wisps occur sporadically and are generally rare except in the upper 1 metre; glauconite is rare, occurring as a minor component on bedding planes in thin lenses of carbonate-cemented sandstones.

187.38 188.35 -medium grey, medium to coarse disky, sandy mudstone; up to 25 per cent sand wisps and burrows; coarsens upward with increased frequency of carbonate-cemented glauconitic sandstone fragments.

188.35 189.07 -dark grey, medium to coarse disky shaley mudstone with rare, fine grain sandstone laminae.

189.07 189.25 -medium grey sandy mudstone; up to 10 per cent sand wisps and burrows.

189.25 189.35 -chunky, black, shaley mudstone.

189.35 189.70 -dark grey, fine to medium disky, massive mudstone.

189.70 189.87 -black, massive to chunky, claystone.

189.87 192.00 -medium grey, fine to medium disky, shaley mudstone with rare, less than 1 centimetre thick sandstone lenses; irregularly fractured, iron-oxide-cemented, silty mudstone between 189.97 and 190.01 metres.

TOP OF SPINNEY HILL FORMATION AT 192.00 METRES.

192.00 196.56 SHALEY MUDSTONE: Unit 41 is medium grey, medium to coarsely disky, moderately fissile shaley mudstone; rare glauconite in sandy wisps; rare to minor wisps, lenses and laminae of light grey sand along bedding planes; rare fish scales; bottom contact sharp.

192.00 192.40 -2 centimetre thick carbonate- and glauconite-cemented, cross-bedded sandstone lenses and less than 1 centimetre thick sandstone lenses occur between 192.00 and 192.40 metres.

193.60 195.50-medium grey medium to coarse disky shaley; glauconite rare in wispy sandstone pods and lenses.

195.50 196.56 -medium grey, fine to medium disky, weakly fissile, shaley mudstone; bottom contact is sharp.

196.56 196.60 GLAUCONITIC SANDSTONE: Unit 42 is composed of finely laminated light grey, very fine grain sandstone and olive green glauconitic sandstone; hard, carbonate-cemented, and slightly cross-bedded at 80 to 90 degree angle to core axis; bottom contact is sharp.

196.60 196.80 MUDSTONE: Unit 43 is black, soft, massive mudstone; bottom contact is sharp.

196.80 196.90 GLAUCONITIC SANDSTONE: Unit 44 is similar to Unit 42; bottom contact is sharp.

196.90 200.80 SHALEY MUDSTONE: Unit 45 is medium to dark grey, fine disky, poorly to moderately fissile, moderately uniform in competency, shaley mudstone.

196.90 197.66 -medium grey, fine disky, moderately fissile, shaley mudstone; bottom contact is gradational.

197.66 198.36 -dark grey, fine disky, moderately fissile, shaley mudstone; breaks to thin shards; bottom contact is sharp.

198.36 200.80 -medium grey, fine disky, weakly fissile, shaley mudstone; rare centimetre-scale lenses of glauconitic, very fine grain sandstone; bottom contact is sharp.

200.80 201.28 MUDDY SANDSTONE: Unit 46 is distinctive, hard, carbonate-cemented, gritty mixture of fine to medium grain quartz sand and dark grey silty mudstone; carbonate-cement is mottled and sporadic throughout the unit; "chaotic unit" bottom contact is sharp.

201.28 203.50 MUDSTONE: Unit 47 is dark grey, massive to moderately fissile, moderately soft mudstone; bottom contact is gradational.

201.28 202.70 -dark grey, weak to moderate fissile, fine disky shaley mudstone.

202.70 203.50 -dark grey, massive to weakly fissile, fine disky, moderately hard mudstone with sporadic occurrence of centimetre-scale lenses of carbonate-cemented, glauconitic, fine grain sandstone; breaks easily into small centimetre-scale shards; bottom contact sharp.

203.50 203.69 INTERBEDDED MUDSTONE AND GLAUCONITIC SANDSTONE: Unit 48 is composed of mudstone similar to Unit 47 with irregular lenses and thin interbeds of carbonate-cemented, glauconitic, fine to medium grain sandstone; this unit is related to the basal portion of Unit 47, but is more consolidated; bottom contact is sharp.

203.69 205.20 SHALEY MUDSTONE: Unit 49 is dark grey, poorly fissile, laminar to very fine disky, moderately hard, shaley mudstone; glauconite is common in wisps and lenses of fine grain sandstone; bottom contact is sharp.

204.70 204.75 -glauconitic fine grain sandstone.

TOP OF LOWER JOLI FOU AT 205.20 METRES.

205.20 205.70 MUDSTONE: Unit 50 is dark grey to black, massive to fissile mudstone; variation in character may be due to proximity to underlying unconformity; bottom contact is sharp.

205.20 205.50 -black, soft, fissile, shaley mudstone; both contacts are sharp.

205.50 205.55 -iron concretion

205.55 205.70 -dark grey, massive, hard, uniform mudstone; bottom contact is sharp.

TOP OF MANNVILLE GROUP AT 205.70 METRES.

205.70 205.80 PYRITISED SANDSTONE: Unit 51 is light grey, massive, very fine grain silty sandstone with up to 80 per cent pyrite; pyritization was irregular with clots of undisturbed sandstone up to 2 centimetres across embedded within the dark greenish-grey to black massive pyrite; both contacts are both irregular and sharp.

205.80 206.70 SILTY SANDSTONE: Unit 52 is light grey massive to weakly laminated, hard, very fine grain silty sandstone; bottom contact is sharp; laminae are oriented at 90 degree angle to core axis.

206.70 207.10 MUDSTONE: Unit 53 is massive, very hard, light brownish-grey mudstone with subordinate wisps and burrows of fine grain sandstone up to 10 per cent of the unit; bottom contact is sharp.

207.10 212.20 INTERBEDDED SANDSTONE AND MUDSTONE: Unit 54 is composed of various subunits of light brownish-grey, terrestrial, silty sandstones, mudstones, and muddy sandstones as follows:

207.10 207.50 -soft, laminated sandstone and clay; greenish-yellow pyrite lens at 207.26 metres; bottom contact is sharp.

207.50 207.62 -massive, hard, sandy mudstone.

207.62 207.77 -massive, hard mudstone with abundant sand-filled burrows up to 1 centimetre across; bottom contact is sharp.

207.77 207.93 -soft, laminated sandstone and clay; bottom contact is sharp.

207.93 208.05 -massive, hard, very fine grain sandstone; bottom contact is sharp.

208.05 208.79 -soft, laminated sandstone and clay; increasing competence towards base coeval with increase of clay to mudstone content; bottom contact is gradational.

208.79 209.10 -moderately hard, laminated, silty mudstone; bottom contact is sharp.

209.10 209.25 -massive to laminated, carbonate-cemented very fine grain sandstone; bottom contacts are sharp.

209.25 209.60 -interbedded shaley mudstone and very fine grain sandstone.

209.60 211.56 -lost core.

211.56 211.75 -massive, hard, silty very fine grain sandstone; bottom contact is sharp.

211.75 211.82 -fissile, shaley mudstone; bottom contact is sharp.

211.82 212.04 -massive, hard, silty very fine grain sandstone; bottom contact is sharp.

212.04 212.20 -light brownish-grey fissile, shaley mudstone; bottom contact is sharp.

212.20 236.00 LOST CORE: 100 per cent core loss due to drilling difficulties in unconsolidated sandstone.

236.00 239.00 LOST CORE: Minor recovery of fine grain quartzose sandstone and black chunky mudstone; light grey, silty shale and sandstone; medium grey shaley mudstone; 23 centimetres of light grey massive mudstone from 238.78 to 239.00 metres.

239.00 267.36 INTERBEDDED SANDSTONE AND SILTY MUDSTONE: Unit 55 is composed of light grey and light brownish-grey, soft to unconsolidated fine to medium grain sandstone; light grey mudstone, dark grey to black coaly and sandy mudstone, and subordinate black shaley mudstone that are usually only a few decimetres in thickness; much core has been lost.

239.00 239.22 -dark grey, massive mudstone with burrows and wisps of light grey, very fine grain sands; bottom contact is sharp.

239.22 241.69 -white, soft, massive, silty very fine grain sandstone; .78 metres core lost; bottom contact is sharp.

241.69 241.90 -ash grey, soft, mottled, massive, coaly, silty very fine grain sandstone; bottom contact is sharp.

241.90 242.00 -coal

242.00 245.00 -very light grey, unconsolidated to poorly consolidated sandstone; .1 metres of shaley mudstone also recovered, but 2.4 metres of core lost.

245.00 245.20 -moderately hard, light grey, shaley mudstone.

245.20 248.00 -moderately consolidated to unconsolidated white silty very fine grain sandstone; .67 metres recovered with estimated 1.9 metres of core lost.

248.00 248.12 -massive, hard, medium grey mudstone.

248.12 248.42-black, hard, moderately fissile, carbonaceous shaley mudstone.

248.42 249.41 -moderately hard, mottled dark and light grey silty very fine grain sandstone; bottom contact is sharp.

249.41 250.13 -medium grey massive, consolidated, bioturbated silty mudstone; bottom contact is sharp.

250.13 250.65-moderately well-consolidated, light and medium grey laminated clay and very fine grain sandstone; bottom contact is sharp.

250.65 251.52 -moderately hard, light grey, massive sandstone with up to 20 per cent intermixed pods and lenses of medium grey mudstone; sand content increases towards base; bottom contact is sharp.

251.52 252.13 -intermixed brownish-grey sandy mudstone and dark grey shaley mudstone; subunit is rubbly; bottom contact is sharp.

252.13 252.53 -moderately hard, light grey, platy, muddy fine grain sandstone; bottom contact is sharp.

252.53 267.36 -light brownish-grey, unconsolidated, fine to medium grain quartzose sand with trace of lithic grains and rare hematite staining.

267.36 267.58 SANDSTONE: Unit 56 is light grey, massive, very hard, carbonate-cemented very fine grain sandstone; bottom contact is sharp.

267.58 281.00 SANDSTONE: Unit 57 is composed of various subunits of interbedded, unconsolidated, and consolidated sandstone and silty sandstone.

281.00 290.00 SANDSTONE: Unit 58 is composed of unconsolidated, light grey, quartzose, fine to medium grain sandstone; much of this interval was washed away during drilling.

END OF HOLE AT 290.00 METRES.

RHONDA MINING CORPORATION
DETAILED CORE DESCRIPTION
October 28, 1994

DRILL HOLE: OFS93-014 **CLAIM NUMBER: S-127405**

LOCATION

LEGAL: SW Quarter Section 21, Township 52, Range 21, West of 2nd Meridian

UTM (1983): 496590 East, 5928535 North

GEOPHYSICAL GRID: 6375 North, 2387.5 West

COLLAR ELEVATION: 498.70 metres ASL

GROUND ELEVATION: 497.50 metres ASL

TOTAL DEPTH: 296.00 metres

CORE SIZE: HQ, 101 millimetres

CORE LOCATION: Saskatoon Field Office

EQUIPMENT LEFT IN HOLE: 136m HW; 11m conductor casing

DIP: Sperry Sun at 296m; dip = -88.75 degrees, dip direction not reported

DATE STARTED: September 06, 1993

DATE COMPLETED: September 11, 1993

DRILLING CONTRACTOR: Longyear Canada Ltd.

WATER HAULING: J. Bergstrum

DRILLSITE GEOLOGY: R. Woodward

CORE LOGGED BY: B.C. Jellicoe

ABANDONMENT STATUS: Cemented from surface to end of hole.

PURPOSE: To test ground magnetic positive circular closure located within a broad magnetic high.

RESULTS: The lithologies encountered in drillhole OFS93-014 do not explain the ground magnetic survey results. This would suggest a shallow feature in the till or a deeply buried "basement" structure.

COMMENTS: Bedding and contacts are subhorizontal (90 degree angle to core axis) unless otherwise specified.
All depths are relative to collar elevation.
Stratigraphic Nomenclature for the Colorado Group of Bloch et al (1993) used in this log, see Chapter 1.

CORE DESCRIPTION

000.00 118.60 TILL: This interval was not cored and chip samples were not collected; geophysical logs and driller reports indicate that this interval is composed of interbedded muddy tills and sandy tills beneath a few metres of surficial sandy sediment.

118.6 119.00 SANDSTONE: Unit 1 is light brownish-grey, weakly consolidated fine grain sandstone; less than 2 per cent small pebbles of mudstone and carbonate; bottom contact is sharp.

119.00 122.20 TILL: Unit 2 is brown, weakly sorted, massive, hard, carbonate-cemented, matrix-supported till with abundant pebbles and rare cobbles of limestone, dolomite and granite; matrix is clayey-silt with subordinate sand grains; rare garnet; unit becomes muddier towards the bottom with only rare clasts and fragments of less than 1 millimetre diameter; bottom contact is sharp.

121.90 122.20 -clay-rich till with decreasing grain size towards the base.

BEDROCK INTERSECTION - PIERRE SHALE AT 122.20 METRES.

122.20 134.10 MUDSTONE: Unit 3 is light to medium grey, massive, fine disky to dominantly uniformly competent, hard mudstone; rare intervals less than 10 centimetres thick are shaley; subtle variations of internal bedding gives a mottled, crenulated appearance to the core surface; fish scales are rare; organic matter is common as oxidized blebs and streaks on bedding planes.

123.73	123.74	-bentonite.
124.06	124.10	-iron concretion.
125.15	125.20	-olive green bentonite.
126.56	126.60	-iron concretion.
126.60	126.65	-green and white bentonite.
126.65	126.70	-medium grey, fine disky shale.
129.40	129.50	-medium grey, fine disky shale.
129.50	129.80	-dark grey, fine disky shaley mudstone.

134.10 137.00 MUDSTONE: Unit 4 is medium to dark grey, weakly fissile to massive, uniform mudstone; rare laths of plant organic matter; lower 1.3 metres fining upwards; basal contact is sharp.

136.70 137.00 -medium grey mudstone with an increasing abundance of unidentified light greyish-white crystals and grains downwards.

TOP OF WHITE SPECKS SHALE AT 137.00 METRES.

137.00 137.70 SHALEY MUDSTONE: Unit 5 is dark grey to black, moderately hard, massive to slightly fissile, uniformly competent, non-calcareous, carbonaceous shaley mudstone; bottom contact is sharp with similar calcareous black shaley mudstone below.

137.70 138.78 CALCAREOUS MUDSTONE: Unit 6 is dark grey to black, moderately hard, massive, uniformly competent, carbonaceous, calcareous mudstone; increasingly fissile and soft towards the base; bottom contact is gradational.

137.90	137.91	-bentonite.
138.10	138.16	-bentonitic mudstone.
138.62	138.78	-bentonitic mudstone.

138.78 139.60 CLAYSTONE: Unit 7 is moderately fissile, soft, weakly to non-calcareous, carbonaceous shaley claystone; rock crushes easily to centimetre-scale flakes; bottom contact is sharp.

138.78 138.96 -weakly calcareous shale.
138.96 139.26 -very weakly calcareous shale.
139.26 139.40 -bentonite.
139.40 139.60 -very soft, fissile, non-calcareous carbonaceous shale.

139.60 141.18 CALCAREOUS SHALEY MUDSTONE: Unit 8 is black, moderately laminar moderately fissile, hard, shaley mudstone with interbedded calcareous and non-calcareous subunits; subunit contacts are sharp, but subtle; bottom contact is sharp.

139.60 139.70 -black, moderately laminar and fissile, moderately hard, shaley mudstone.
139.70 139.76 -bentonite.
139.76 140.00 -very weakly calcareous, very carbonaceous shaley mudstone.
140.00 140.50 -micaceous calcareous, carbonaceous, black shaley mudstone.
140.50 140.62 -micaceous, carbonaceous, non-calcareous, shaley mudstone.
140.62 141.18 -micaceous, carbonaceous, calcareous, black mudstone.

141.18 146.61 WHITE SPECKLED SHALE: Unit 9 is hard, moderately fissile, laminar bedded, carbonaceous, calcareous, white speckled shale; white specks vary from rare to very abundant along bedding planes between decimetre-scale subunits; white specks are less than millimetre-scale ellipsoidal faecal pellets called coccoliths composed of symmetrical carbonate plates of spherical golden brown algae coccolithophorids; minor constituents include rare to abundant fish debris, mica (less than .2 millimetres long), fragments of chitin, and macro-fossil material including imprints of oysters and inoceramids and calcite prisms, nacre, and aragonite from shells; shell material is compressed along bedding planes at 90 degree angle to core axis; contacts between speckled zones and black shales are gradational whereas fossiliferous zones are sharply delineated; basal contact is sharp.

141.18 141.87 -non-speckled shale with fish debris, chitin and rare macro-fossils.
141.87 142.50 -abundantly white speckled shale.
142.50 143.16 -moderately white speckled shale.
143.16 144.41 -abundantly white speckled shale.
144.41 144.67 -weakly calcareous, non-speckled shale.
144.67 144.72 -bentonite
144.72 145.63-weak to moderate speckled calcareous shale with 3 centimetre diameter bentonite at 145.34 metres.
145.63 145.80 -highly fossiliferous, white speckled zone.
145.80 146.48 -moderately white speckled shale with 2 centimetre thick bentonite at 145.86 metres and a 1 centimetre thick pyrite disc at 146.27 metres.
146.48 146.61 -bentonite.

146.61 146.82 LIMESTONE: Unit 10 is composed of hard brownish-black and creamy-white laminar bands of calcareous shale and microcrystalline limestone, respectively; basal contact is sharp.

146.61 146.76 -dominantly laminated calcareous mudstone and clayey-limestone.

146.76 146.82 -dominantly limestone with subordinate mudstone.

146.82 147.17 FISH HASH GRAINSTONE: Unit 11 is composed of interbedded dark grey non-calcareous mudstone and brownish-grey medium to coarse grainstone composed of clay, comminuted fish debris and chitin chips; unit is grain supported with fish debris up to 90 per cent of rock; bottom contact is sharp.

147.17 147.53 BENTONITE: Unit 12 is a thick, light grey weathering bentonite overlain by an 8 centimetre thick bentonitic black shale; contacts are sharp.

147.53 148.30 SANDY SHALE: Unit 13 is dominantly hard, dark grey shale with 20 per cent interbedded light brownish-grey fine grain sandstone in layers less than 1 centimetre thick; some of the sandstone layers are carbonate-cemented; the interbedded lithotypes become softer towards the base of the unit; both interbed contacts and unit contacts are sharp at 90 degrees to core axis.

148.23 148.28 -black, flaky, soft shale

TOP OF BELLE FOURCHE FORMATION AT 148.30 METRES.

148.30 149.55 SHALE: Unit 14 is light grey, very fissile, fine disky, moderately soft shale; bedding at 90 degree angle to core axis; bottom contact is sharp.

148.30 149.00 -as interval description.

149.00 149.22 -very fissile, flaky medium grey shale.

149.22 149.33 -light brownish-grey, massive fine grain sandstone.

149.33 149.55 -very fissile, flaky, medium grey shale.

149.55 150.30 MUDDY SAND: Unit 15 is very soft, unconsolidated, interbedded light grey and black muddy sand; the light grey sand is submature and quartzitic while the dark muddy sand is clay-rich; the sediment becomes slightly more consolidated towards the base of the unit; basal contact is sharp.

150.30 152.00 SANDSTONE AND SANDY MUDSTONE: Unit 16 is divisible into 3 gradational subunits as follows:

150.30 150.64 -intermixed dark grey, weakly fissile, fine disky mudstone with light grey, fine grain sand; sand-filled burrows common.

150.64 151.28 -medium grey, fine disky, weakly fissile, massive very fine to fine grain sandstone with mottling of darker grey clay-rich laminae and streaks.

151.28 152.00 -intermixed dark grey, massive to weakly fissile, fine disky mudstone with minor, light grey, fine grain sand; intensely bioturbated and massive; bottom contact is sharp.

152.00 160.45 SHALEY MUDSTONE: Unit 17 is dark grey, uniform, vaguely laminar, weakly fissile to massive, fine to medium disky, moderately hard mudstone; rare less than centimetre-scale sand filled burrows over most of the interval; common sand wisps, burrows and lenses between 157.9 to 159.3 metres; rare laths of oxidized plant matter; bottom contact is sharp.

152.00 156.60 -dark grey, very weakly fissile, medium disky mudstone.
156.60 157.90 -dark grey, weakly fissile, fine disky, shaley mudstone.
157.90 158.30 -dark grey to black, very weakly fissile, fine disky, shaley mudstone with common wisps and burrows of light grey sand.
158.30 158.97 -black, weakly fissile, fine disky, shaley mudstone with oxidized pyrite and organic matter common.
158.97 159.05 -bentonitic mudstone.
159.05 160.45 -dark grey, weakly fissile, fine disky, shaley mudstone.

160.45 167.14 INTERBEDDED MUDSTONE AND SHALEY MUDSTONE: Unit 18 comprises decimetre-scale interbeds of fine to medium disky, moderately soft shaley mudstones similar to Unit 17, but is massive, and harder; both lithotypes vary from medium grey through dark grey to black; generally, darker shales are more carbonaceous; incorporation of light grey sand as burrows, wisps, and lenses is variable but is rarely greater than 10 per cent of any subunit; contacts are usually sharp between lithotypes, but gradational between colour within lithotypes; minor constituents are rare and include fish debris, laths of oxidized plant matter, and disseminated pyrite crystals less than 1 millimetre in diameter; all contacts and bedding occur at between 80 to 90 degree angle to core axis.

160.45 161.18 -medium grey, medium disky, shaley mudstone.
161.18 161.79 -dark grey, medium disky, competent, massive mudstone.
161.79 163.50 -medium grey, soft, medium disky shaley mudstone with internal bedding variations common.
163.50 164.04 -black, soft, medium disky, shaley mudstone.
164.04 164.80 -dark grey, fine disky, shaley mudstone with minor sand wisps and lenses grading to consolidated mudstone in lower 25 centimetres.
164.80 165.12 -black shaley mudstone.
165.12 165.30 -medium grey, fine disky, shaley mudstone.
165.30 165.74 -black, fine disky, shaley mudstone.
165.74 166.50 -black, harder, massive, consolidated mudstone.
166.50 167.14 -medium grey, moderately hard, massive, uniformly competent, sandy mudstone.

167.14 167.86 SANDY MUDSTONE: Unit 19 is dark grey, uniformly competent, massive, moderately hard, sandy mudstone; bottom contact is sharp.

167.86 169.25 MUDSTONE: Unit 20 is composed of interbedded black, fine disky, shaley mudstone and dark grey, massive, uniformly competent, moderately hard mudstone; contacts are sharp between subunits; rare fish debris; rare lenses,

laminae, and wisps of light grey very fine grain sand along bedding planes oriented at 090 degrees to core axis; basal contact is sharp.

167.86 167.94 -black to dark grey, fine disky shaley mudstone.
167.94 168.25 -dark grey, massive, consolidated mudstone.
168.25 168.43 -black, fine disky shaley mudstone.
168.43 169.12 -dark grey to black, massive consolidated mudstone.
169.12 169.25 -black, fissile, soft, flaky, carbonaceous, shaley mudstone.

169.25 181.83 MUDSTONE: Unit 21 is composed of interbedded grey and black massive, uniformly competent, moderately hard mudstones similar to those in Unit 18; sandy lenses, wisps and burrows are common in some intervals but rare (less than 5 per cent) over most of the unit; brown, very fine grain, gossanous material is rare in some black mudstone; burrows are common to rare as lighter coloured ellipsoids, specks, and rings; contacts between subunits are generally gradational over less than 10 centimetres; basal contact is sharp.

169.25 169.92 -medium grey, massive, uniformly competent, hard mudstone.
169.92 170.30 -dark grey to black, uniformly competent mudstone.
170.30 172.34 -dark grey massive, uniformly competent, hard mudstone.
172.34 173.50 -dark grey, massive, uniformly competent, hard mudstone.
173.50 173.76 -dark grey, uniformly competent, hard mudstone; shatters to centimetre-scale shards.
173.76 175.70 -black, moderately soft, consolidated wet mudstone.
175.70 175.90 -dark grey, soft, massive, very weakly disky sandy mudstone.
175.90 176.65 -medium grey, hard, massive mudstone with common centimetre-scale burrows of lighter mudstone.
176.65 177.42 -black, moderately soft, massive, uniformly competent, mudstone.
177.42 177.77 -medium grey massive, uniformly competent, hard mudstone.
177.77 178.45 -black, massive, uniformly competent, moderately hard mudstone with sporadic brown gossanous clots.
178.45 180.80 -medium grey, massive, uniformly competent mudstone
180.80 181.83 -medium grey, massive, weakly disky, hard mudstone with rare to minor millimetre-scale sandy wisps and burrows.

TOP OF ST. WALBURG SANDSTONE AT 181.83 METRES.

181.83 182.00 MUDDY SANDSTONE: Unit 22 is composed of light grey, massive fine to medium grain sandstone intermixed with shards and laminae of dark grey mudstone; partially cemented with creamy-white clay (kaolinitic); bottom contact is sharp.

182.00 182.55 SHALEY MUDSTONE: Unit 23 is dark grey to black, soft, massive to weakly fissile, shaley mudstone; bottom contact is sharp.

182.55 182.78 SANDY MUDSTONE: Unit 24 is composed of well sorted, fine to medium grain, light grey, quartzitic sand encased and intermixed with medium to dark

grey, weakly laminar, shaley mudstone; mottled grainy texture; bottom contact is sharp.

182.78 183.78 SHALEY MUDSTONE: Unit 25 is medium grey, weakly fissile, medium disky, weakly fissile, shaley mudstone; abundant light grey, fine grain sand in millimetre-to centimetre-scale burrows, wisps, and centimetre-scale bedding; sand content increases towards the base; mudstone shatters to shards; bottom contact is sharp; bedding and contacts are at 80 to 90 degree angle to core axis.

183.00 183.01 -bentonite.

183.78 188.00 MUDDY SANDSTONE: Unit 26 is mottled dark and light brownish-grey, massive, thoroughly intermixed, well bioturbated, uniformly competent, clayey-sandstone; composed of at least 6 fining upward cycles; burrows ranging from millimetre-to centimetre-scale are pervasive; increasing clay content downwards from 186.00 metres to 187.82 metres; light brownish-grey sand is very fine grain to fine grain, porous, and quartzitic; overall lithotype is moderately to well indurated by clay cementation and is a sublithic wacke; the bottom contact is marked by ripple cross-bedded fine grain sandstone in the basal 6 centimetres overlying a sharp erosive base.

185.00 185.11 -dark grey, bentonitic mudstone; sharp contacts.

186.98 187.02 -medium grey, shaley mudstone.

188.00 191.14 SHALEY MUDSTONE: Unit 27 is medium to dark grey, massive to weakly fissile, fine disky, vaguely laminar, moderately hard, shaley mudstone with mottled texture from internal variations in competency and bedding; light grey, silty sand is common to rare as burrows and wisps in some intervals; subunit contacts are gradational.

188.00 189.63 -dark grey shaley mudstone with rare sandy lenses, wisps, and burrows.

189.63 189.81 -dark grey shaley mudstone with common sand as lenses, wisps, and burrows.

190.50 190.70 -dark grey, medium disky mudstone.

189.81 190.64 -dark grey, massive to weakly fissile, fine disky, moderately hard shaley mudstone.

190.64 191.10 -black, flaggy, fine to medium disky, hard, shaley mudstone; bottom contact is sharp.

191.10 191.14 -bentonite

TOP OF LOWER WESTGATE FORMATION AT 191.14 METRES.

191.14 192.32 SHALEY MUDSTONE: Unit 28 is dark grey, medium disky, weakly fissile, moderately hard, shaley mudstone; bottom contact is sharp.

192.32 193.17 SANDY MUDSTONE: Unit 29 is a heterogeneous, very hard, massive, intermixture of dark grey, carbonate-cemented silty mudstone and centimetre-

scale angular clasts of laminar, light grey carbonate-cemented fine grain sandstone; coarse disky overall, clasts are up to 25 per cent of unit and increase to base; about .5 metre core loss in this interval; bottom contact is sharp.

193.17 193.83 SHALEY CLAYSTONE: Unit 30 is black, very fissile, fine disky, moderately soft, shaley claystone; bottom contact is sharp.

193.83 194.10 MUDDY SANDSTONE: Unit 31 is medium grey, massive, vaguely laminar, hard, muddy, very fine grain sandstone; bottom contact is sharp.

194.10 194.13 BENTONITIC MUDSTONE: Unit 32 is creamy whitish-grey weathering, chunky, bentonitic mudstone; contacts are sharp.

194.13 196.62 MUDSTONE: Unit 33 is dark grey, massive, fine disky, hard mudstone with variable very fine grain sand content in wisps, burrows, and thin lenses; subunits have fairly sharp contacts over less than 2 centimetre intervals.

194.13 194.55 -dark grey, weakly fissile, uniformly competent, mudstone with minor sand content (less than 10 per cent).

194.55 195.20 -dark grey, moderately fissile, very weakly disky, hard, mudstone.

195.20 195.40 -medium grey, uniformly competent, hard, sandy mudstone with up to 20 per cent sand content in burrows and wisps.

195.40 196.62 -dark grey, weakly fissile, uniformly competent, moderately hard mudstone; basal contact is sharp.

TOP OF FLOTTEN LAKE SANDSTONE AT 196.62 METRES.

196.62 197.15 SILTY SANDSTONE: Unit 34 is medium grey, massive, competent, silty and clay-rich sandstone; bottom contact is sharp.

197.15 204.27 SILTY SANDSTONE: Unit 35 is a thick sequence of heterogeneous, hard, mottled, intermixed dark grey silt and clay, medium grey sand; rare to common occurrence of angular clasts, lenses, and burrows of light grey, very fine grain, carbonate-cemented sandstone with rare to common glauconite along laminar bedding planes; larger angular sandstone clasts and lenses show distinct ripple cross-bedding at 75 to 85 degree angle to core axis; most of the unit is intensely bioturbated with ellipsoidal burrows common as lighter sandy material within the darker silty sandstones; glauconite becomes more common towards the base of the unit incorporated within sandy lenses and laminae; bottom contact is gradational.

197.15 197.50 -dark grey, weakly fissile, medium to coarse disky shaley mudstone.

197.50 198.27 -same as interval description with abundant angular clasts, lenses, and burrows of light grey, carbonate-cemented sandstone with or without glauconite; gradational basal contact.

198.27 200.27 -heterogeneous, mottled, hard silty sandstone with abundant burrows; silt and clay content about 20 per cent.

200.27 201.44 -heterogeneous, mottled, hard silty sandstone with abundant burrows, rare to common glauconite; rare disjunct lenses of carbonate-cemented very fine grain sandstone; increasing silt and clay matrix towards base of subunit (up to 50 per cent).

201.44 201.86 -silty sandstone similar to 198.27 to 200.27 with approximately 20 per cent silt and clay component.

201.86 202.58 -hard silty sandstone similar to 200.27 to 201.44.

202.58 202.79 -dark brownish-grey, hard, massive, sandstone with less than 10 per cent silt content; bottom contact is sharp.

202.79 204.27 -heterogeneous, mottled, hard silty sandstone with progressive increase of silt and dark grey mudstone interbeds towards the base; olive green glauconite sporadically common within sandstone lenses; bottom contact is gradational with shaley mudstones beneath.

TOP OF JOLI FOU FORMATION AT 204.27 METRES.

204.27 214.77 SHALEY MUDSTONE: Unit 36 is medium grey to black, massive to weakly fissile, fine to coarse disky, moderately hard, shaley mudstone; light grey, silty sandstone is rare to common as lenses, burrows, wisps, and locally as angular carbonate-cemented clasts; rare glauconite; bottom contact is sharp.

204.27 204.31 -bentonite

205.10 205.19 -medium to coarse disky shaley mudstone with common angular fragments of laminar carbonate-cemented light grey, very fine grain sandstone.

205.19 209.00 - medium to coarse disky shaley mudstone.

209.00 211.07 -weakly fissile, fine to medium disky shaley mudstone.

211.07 212.12 -medium to coarse disky shaley mudstone with rare angular fragments of laminar carbonate-cemented light grey, very fine grain sandstone.

212.12 212.20 -black, weakly fissile, fine disky, moderately hard, shaley mudstone.

212.20 212.40 -dark grey medium to coarse disky mudstone.

212.40 214.77 -dark grey to black, weakly fissile, fine to medium disky, shaley mudstone with only rare sand component.

TOP OF SPINNEY HILL FORMATION AT 214.77 METRES.

214.77 218.42 MUDSTONE: Unit 37 is medium to dark grey, soft, chunky, fine to medium disky, weakly fissile mudstone; rare fish scales and glauconite; bottom contact sharp.

214.77 215.56 -medium to dark grey, soft, chunky, medium disky mudstone with minor fine grain glauconitic sandstone lenses and fragments.

215.56 216.00 -soft, massive, dark grey mudstone.
216.00 219.37 -medium grey, weakly fissile, medium to coarse disky, moderately hard, shaley mudstone.

219.37 220.37 GLAUCONITIC SHALEY MUDSTONE: Unit 38 is medium grey, medium to coarse disky, moderately hard shaley mudstone, but with common olive green glauconite in centimetre-scale angular fragments and disjunct lenses of cross-bedded and laminar very fine grain carbonate-cemented sandstone; bottom contact is at sudden demise of glauconitic sandstone fragments.
219.37 219.70 -massive, coarse disky, hard mudstone.
219.70 220.37 -moderate to very fissile, fine disky, shaley mudstone.

220.37 221.00 MUDSTONE: Unit 39 is dark grey, hard, massive, uniformly competent mudstone; breaks into shards; bottom contact is sharp.

221.00 221.43 SHALEY MUDSTONE: Unit 40 is medium grey, weakly fissile, fine to medium disky, moderately hard shaley mudstone; rare very fine grain sandstone lenses; bottom contact is sharp.

221.43 221.62 GLAUCONITIC SANDSTONE: Unit 41 is greenish-grey, very hard, laminar to massive, glauconite-cemented, very fine grain sandstone; bottom contact is sharp.

221.62 222.00 SHALEY MUDSTONE: Unit 42 is medium grey, massive to weakly fissile, weakly fine disky, moderately soft, shaley mudstone; unit becomes harder and chunkier towards the base; bottom contact is sharp.

222.00 224.60 MUDSTONE: Unit 43 is black, moderately fissile, weakly fine disky mudstone; sporadic quartzitic sand up to 5 per cent; 1.4 metre core loss between 222.6 to 224.0 metres; bottom contact is sharp.

224.60 232.51 SHALEY MUDSTONE: Unit 44 is composed of grey, moderately hard, massive to weakly fissile, uniform, shaley mudstone with mottled texture due to internal variations of bedding and consolidation; rare sand as wisps, burrows, and thin lenses; bottom contact is sharp; bedding occurs at 90 degree angle to core axis.
224.60 224.90 -dark grey, weakly fissile, coarse disky shaley mudstone.
224.90 226.26 -medium grey, moderate fissile, medium disky, shaley mudstone.
226.26 227.30 -black, soft, moderately fissile, weakly fine disky mudstone; bottom contact is sharp.
227.30 228.70 -medium grey, moderately fissile, medium to coarse disky, shaley mudstone; bottom contact is sharp.
228.70 228.77 -muddy sandstone; light greyish-green, carbonate-cemented fine to medium grain granular, quartzitic sandstone encased

within black massive mudstone; subunit is very hard; "chaotic"; contacts are sharp.

228.77 228.86 -black muddy very fine grain sandstone; uniform and very hard; "chaotic"; contacts are sharp.

228.86 229.10 -moderately hard, medium grey shaley mudstone; bottom contact is sharp.

229.10 229.28 -soft, black shaley mudstone; bottom contact is sharp.

229.28 229.33 -very hard massive, brownish-grey clay and iron-cemented silty very fine grain sandstone; bottom contact is sharp.

229.33 230.15 -black, soft, fine disky, massive to weakly fissile mudstone; bottom contact is sharp.

230.15 230.78 -medium to dark grey, soft, shaley mudstone.

230.78 230.91 -very hard, massive, dark brownish-grey, heterogeneous, clay-cemented silty very fine grain sandstone; "chaotic"; bottom contact is sharp.

230.91 231.74 -medium to dark grey, medium disky, moderately soft, shaley mudstone; bottom contact is sharp.

231.74 232.44 -dark grey, moderately hard, massive to weakly fissile, fine disky, shaley mudstone.

232.44 232.51 -very hard, dark brownish-grey, clay-cemented, silty very fine grain sandstone; 1 centimetre thick carbonate-cemented very fine grain greenish-cream laminar sand lenses interbedded within the subunit; contacts are sharp.

TOP OF LOWER JOLI FOU FORMATION AT 232.51 METRES.

232.51 233.00 MUDSTONE: Unit 45 is dark grey, moderately hard, massive to weakly fissile, uniform, uniformly competent shaley mudstone; 2.5 centimetre thick massive pyrite band at 232.74 metres; 3 centimetre pyritic band at 232.93 metres; bottom contact is sharp.

TOP OF MANNVILLE GROUP AT 233.00 METRES.

233.00 235.43 MUDSTONE: Unit 46 is light brownish-grey, massive, soft and dense, plastic, mudstone; sporadic less than 10 centimetre thick dark grey, slightly harder, mudstone interbeds; bottom contact is sharp.

235.43 239.00 SHALEY MUDSTONE: Unit 47 is composed of interbedded light to dark grey weakly fissile, moderately hard shaley mudstones; laths and stringers of oxidized plant matter rare on bedding planes; bottom contact is sharp; bedding is at 90 degree angle to core axis.

235.43 236.00 -light brownish-grey shaley mudstone.

236.00 236.70 -medium grey shaley mudstone.

236.70 237.25 -light grey, soft sandy mudstone; chunky, massive and deformed by drill bit; bottom contact is sharp.

237.25 238.25 -light grey, moderately hard, weakly fissile, uniform shaley mudstone.

238.25 239.00 -light grey, massive to weakly fissile, hard, shaley mudstone; contacts are sharp.

239.00 254.80 SANDSTONE: Unit 48 is a complex of very fine grain to fine grain sandstones variably cemented by clay and iron oxide from very soft unconsolidated granular sands to massive, very hard, concretion-like rock; the basic sand component is well sorted, subrounded to rounded, very fine grain to fine grain quartz, which is bimodally associated with dark grey silty clay as intermixed and interlaminated layers and wisps; usually the sandstones are mottled with the finer grain component due to mixing by bioturbation; cross-bedding in more laminated subunits is at 70 to 85 degree angle to core axis with rare steeper foresets at 60 degrees to core axis; contacts between sand lithotypes are sharp while boundaries between differences in cementation are gradational.

254.80 257.00 INTERBEDDED MUDSTONE: Unit 49 is composed of closely interleaved and interbedded, light grey silty mudstone and mudstone; the difference in hardness between the softer silty mudstone and hard mudstone gives a mottled, irregular crenulated appearance to the core surface; each of the lithotypes appear weakly fissile to massive within each interbed or lens; iron-concretion layers less than 5 centimetres thick are sometimes common; 3 centimetres of laminated dark brown and white mudstone at 256.93 metres.

257.00 260.60 INTERBEDDED SHALEY MUDSTONE AND SANDSTONE: Unit 50 has subunits of grey uniform, moderately hard, shaley mudstone interbedded with tan, hard, fine to medium grain silt and clay-cemented sandstone; sandstone is moderately well sorted, grain-supported, well bioturbated/mixed, non-laminar, and submature sublithic arenite; quartz grains dominate and they are subrounded to rounded; subunits are bounded by sharp contacts; bedding and contacts are between 80 to 90 degree angle with core axis.

257.00 257.09 -sandstone.

257.09 257.17 -dark grey shaley mudstone.

257.17 257.32 -sandstone.

257.32 257.51 -dark grey shaley mudstone with 2 centimetre thick sandstone interbed.

257.51 257.86 -sandstone.

257.86 258.20 -dark grey shaley mudstone with common wisps and lenses of fine grain white sandstone.

258.20 258.33 -bioturbated sandstone.

258.33 258.46 -iron-stained, interbedded dark grey shaley mudstone and sandy mudstone with weak to medium disky texture on core surface.

258.46 259.21 -lost core; remnants indicate soft unconsolidated sand subunit.

259.21 259.35 -medium grey shaley mudstone.

259.35 259.70 -interbedded medium grey, hard, sandstone dominant with subordinate thin intervals of dark grey shaley mudstone.
259.70 260.08 -interbedded light grey shaley mudstone and sandy mudstone with weak to medium disky texture on core surface.
260.08 260.13 -dark grey shaley mudstone.
260.13 260.51 -light brown to tan sandstone as per interval description.
260.51 260.60 -dark grey shaley mudstone.

260.60 263.61 SANDSTONE: Unit 51 is an unconsolidated creamy-white, fine to medium grain, sublitharenitic sandstone; the unit is grain-supported with minor silt/clay matrix; decrepitated, friable texture; bottom contact is sharp.
263.57 263.61 -laminar iron-stained shaley mudstone.

263.61 268.90 SANDSTONE: Unit 52 is dominantly light grey, massive, hard, fine grain quartzitic sandstone; the sandstone is clay-cemented and grain-supported; variations in clay show in mottled medium and light grey intervals; subunit contacts are sharp.
263.61 264.4 -muddy sandstone with up to 40 per cent mudstone grading downwards to less than 20 per cent in the lower .5 metres.
264.4 263.92 -tan to light grey sandstone with an increase in mudstone to 30 per cent in the lower 16 centimetres.
263.92 264.09 -black, coaly mudstone with minor laminations of very fine grain sandstone.
264.09 268.90 -light grey sandstone.

268.90 269.47 MUDDY SANDSTONE: Unit 53 is brownish-grey fine grain sandstone intermixed with dark grey mudstone; contacts are sharp.

269.47 269.59 MUDSTONE: Unit 54 is black, massive, hard carbonaceous mudstone with minor sand lenses; contacts are sharp.

269.59 269.72 SILTSTONE: Unit 55 is medium grey, massive, hard siltstone; bottom contact is sharp.

269.72 270.20 MUDSTONE: Unit 56 is black, massive, hard, carbonaceous mudstone with minor laminae of white very fine grain sandstone; bottom contact is sharp.

270.20 274.40 SANDSTONE: Unit 57 is light grey, massive, hard sandstone.

274.40 275.12 FINING-UP SANDSTONE TO SHALE: Unit 58 is composed of dark grey fine grain massive sandstone which grades up to massive, hard, black mudstone.

275.12 276.13 SANDSTONE: Unit 59 is light grey, massive, hard sandstone; contacts are sharp.

276.13 277.80 SANDY MUDSTONE: Unit 60 is medium grey, hard, consolidated mudstone with common sand lenses, wisps, and laminae.

277.80 278.87 INTERBEDDED SANDSTONE AND SHALEY MUDSTONE: Unit 61 is composed of less than 5 centimetre thick interbeds of light grey soft sandstone and medium grey shaley mudstone; all subunit contacts are sharp.

278.87 296.00 SANDSTONE: Unit 62 is composed of subunits of massive, unconsolidated to hard, silty sandstone and fine grain sandstone; minor interbeds of shaley mudstone are bounded by sharp contacts; bedding and contacts are between 80 to 90 degree angle with core axis.

278.87 280.60 -light grey, hard, massive fine grain sandstone.
280.60 281.85 -white, soft, unconsolidated fine grain quartzose sandstone.
281.85 282.00 -black sandy shaley mudstone.
282.00 283.03 -light brown, massive, moderately hard, fine grain silty sandstone.
283.03 286.04 -dark brown, coaly, massive, moderately hard to very hard, fine grain sandstone; 34 centimetres of black shaley mudstone at 283.65 metres; contacts are sharp.
286.04 287.46 -mottled light and dark grey massive, soft sandstone.
287.46 287.63 -dark grey, carbonaceous, massive fine grain sandstone.
287.63 290.47 -mottled black, light and dark grey, weakly consolidated, soft, massive and laminated sandstone.
290.47 290.80 -light and dark grey sandy shaley mudstone.
290.80 296.00 -light grey and white, unconsolidated, massive, fine grain sandstone with minor interbeds of medium grey shaley mudstone.

END OF HOLE AT 296.00 METRES.

RHONDA MINING CORPORATION
DETAILED CORE DESCRIPTION
October 28, 1994

DRILL HOLE: OFS93-015 **CLAIM NUMBER: S-127469**

LOCATION

LEGAL: L.S.D. 6, Section 9, Township 51, Range 22, West of 2nd Meridian
UTM (1983): 487480 East, 5915080 North
GEOPHYSICAL GRID: 490 North, 2320 East
COLLAR ELEVATION: 466.0 metres
GROUND ELEVATION: 464.8 metres
TOTAL DEPTH: 240.0 metres
CORE SIZE: HQ, 101 millimetres
CORE LOCATION: Saskatoon Field Office
DIP: Sperry Sun at 240m; dip = -86.75 degrees, dip direction = N33E.
DATE STARTED: December 07, 1993
DATE COMPLETED: December 19, 1993
DRILLING CONTRACTOR: Longyear Canada Ltd.
WATER HAULING: J. Bergstrum
DRILLSITE GEOLOGY: R. Woodward
CORE LOGGED BY: B.C. Jellicoe
ABANDONMENT STATUS: Cemented from surface to end of hole.
PURPOSE: Test positive ground magnetic closure located within a broad positive magnetic feature.
RESULTS: No kimberlite was intersected in the drillhole. The estimated time equivalent horizon to the proximal Uranerz kimberlite cluster hosts a thin anomalous mid-Colorado stratigraphic section. The magnetic target is not explained by the lithologies intersected in the drillhole.
COMMENTS: Bedding and contacts are subhorizontal (90 degree angle to core axis) unless otherwise specified.
All depths are relative to collar elevation.
Stratigraphic Nomenclature for the Colorado Group of Bloch et al (1993) used in this log, see Chapter 1.

CORE DESCRIPTION

00.00 117.00 TILL: This interval was not cored and chip samples were not collected; geophysical logs and driller reports indicate that this interval is composed of interbedded muddy tills and sandy tills beneath a few metres of surficial sandy sediment.

117.00 117.65 SHALE: Unit 1A is black, very fissile and uniform shale; breaks with papery to flaggy plates; sharp basal contact; bedding to core axis angle is 90 degrees.

117.65 120.00 DRILLING CEMENT:

119.64 119.79 -black fissile shale as above.

BEDROCK CONTACT AT 120.00 METRES - BELLE FOURCHE FORMATION.

120.00 127.10 SHALE: Unit 1B is composed of decimetre-scale interbedded black and dark grey, very fissile, flaky shale which was probably contiguous with Unit 1A; both shales are usually uniformly competent, moderately to well compacted, moderately hard; contains less than 2 per cent fine grain sand wisps along bedding planes; black shale is sporadically chunky and non-laminar in intervals less than 10 centimetres thick; contacts between interbeds may be gradational or sharp in different subunits; dark grey shale occasionally has a brownish tinge in slightly coarser grain intervals; bottom contact is gradational; bedding to core axis is 90 degrees.

120.00 120.90 -black fissile shale.
120.90 121.54 -dark grey shale.
121.54 122.34 -black shale with 3 centimetres of bentonite.
122.34 123.14 -dark grey, medium disky, very fissile, shale.
123.14 123.77 -black fissile, flaggy shale.
123.77 126.70 -dark grey shale, fissile to flaggy, sporadic chunky texture.
126.70 127.10 -gradational fissile dark grey shale downward to competent, massive uniform medium grey shale.

127.10 139.05 SHALE: Unit 2 is medium grey decimetre-scale interbedded shale and mudstone with gradational contacts; shales are uniform, but are fissile, flaggy, and break easily into flakes in some units; mudstones are slightly more competent, massive, and harder; rare oxidized organic matter on bedding planes; bedding to core axis is 90 degrees.

127.10 127.60 -medium grey weakly fissile to massive shale; bottom contact is sharp.
127.60 128.13 -dark grey, moderately fissile, very weakly disky shale; bottom contact is gradational.
128.13 129.00 -medium grey, massive to weakly fissile, very weakly disky to uniformly competent mudstone; slightly harder than above; bottom contact is sharp.
129.00 132.10 -medium grey, uniform, fine to medium disky, mudstone; bottom contact is apparently sharp; bedding is 90 degree angle to core axis.
132.10 132.12 -bentonite
132.12 132.45 -medium grey moderately hard, fine to medium disky silty mudstone; generally homogeneous; bottom contact is sharp.
132.45 133.43 -medium grey moderately hard, fine to medium disky silty shale; generally homogeneous; fissile with flaky breakage; bottom contact is sharp.

133.43 135.05 -medium grey, uniform, fine to medium disky, shale; very fissile with flaky breakage; plant organic matter or burrows with oxidized iron fill component rare; bottom contact is sharp.

135.05 137.17 -medium grey moderately hard, fine to medium disky shale; generally homogeneous; fissile with flaky breakage; bottom contact is sharp.; bottom contact is sharp.

137.17 139.05 -medium-dark grey, fine disky to uniformly competent shale; massive and flaky shale closely interbedded; rare organic matter (plant) on bedding planes.

139.05 143.37 SHALE: Unit 3 is composed of various interbedded shales similar to Unit 2, but with occurrence of minor sand wisps and very thin lenses within medium grey massive shaley mudstones; dominated by flaky to flaggy, moderately hard to soft shales; basal contact is sharp.

139.05 139.23 -dark grey, chunky, massive; contacts are sharp.

139.23 140.60 -interbedded fissile flaky shale and slightly more massive, uniformly competent, shale increasing to base; more massive shale has minor light grey, fine grain sand wisps; basal contact is sharp.

140.60 140.70 -mottled greenish-brownish grey, silty, fine grain sandstone; very micaceous and limonite-rich as less than 0.2 millimetre-scale grains; unidentified sulphate minerals common; very pyritic; grains are matrix supported.

TOP UPPER WESTGATE FORMATION AT 140.70 METRES

140.70 140.75 -chunky, massive black silty mudstone with abundant carbonate material - possibly shell; bottom contact is sharp.

140.75 143.37 -medium to dark grey, homogeneous, uniform, fissile and flaky shale; minor sandy wisps sporadically in slightly more massive intervals; trace organic matter on bedding planes; bottom contact is sharp.

143.37 146.10 MUDSTONE: Unit 4 is massive, competent, homogeneous, medium grey mudstone; blocky fracturing with weak bedding at 90 degree angle to core axis; bottom contact is sharp.

146.10 147.55 MUDSTONE: Unit 5 is medium grey, massive to weakly fissile, fine disky, hard mudstone; rare to common wisps of light grey fine grain sandstone; 5 centimetre thick sandy mudstone interval with sharp contacts at 147.4 metres; bottom contact of unit is sharp.

146.55 146.70 -medium grey, massive, uniformly competent, hard mudstone; upper and lower contacts sharp

TOP OF ST. WALBURG SANDSTONE AT 147.55 METRES.

147.55 151.35 SANDSTONE: Unit 6 is light grey fine to medium grain, poorly consolidated, coarsening upward sandstone with variable silt content up to approximately 20 per cent; rare shale interbeds less than 5 centimetre thick; shale bedding at 90 degree angle to core axis; overall, sand is dominated by fine grain subrounded quartz grains with subordinate silt matrix of probable quartzitic composition; hence, it is a bimodally sorted, submature, quartzarenite; sandstone becomes more lithic downhole with increasing silt and clay component, as well as, a general decrease of grain size from fine to very fine; bottom contact is sharp.

147.55 149.80 -light grey, mature, fine to medium grain quartzarenite sandstone; massive and unconsolidated; bottom contact is gradational.

149.80 150.94 -light grey, sublitharenite sandstone; massive, weakly consolidated; increasing silt and clay to base; rare, dark grey mudstone millimetre-scale lenses; bottom contact is sharp.

150.94 150.98 -bentonite

150.98 151.04 -dark grey, massive to flaggy mudstone; contacts are sharp.

151.04 151.19 -variably carbonate-cemented, poorly sorted, silty, fine grain, medium grey sandstone; contacts are sharp.

151.19 151.35 -medium grey to brownish-grey sandy mudstone; closely interbedded sand and silty mudstone; bottom contact is sharp.

151.35 152.20 SHALE: Unit 7 is medium grey, very fissile, medium disky shale with minor, sporadic light grey fine grain sand lenses and sand-filled burrows; bottom contact is gradational.

151.80 152.20 -shale as above with gradational increment of sand lenses and intermixed sand towards the base; bottom of the unit is gradational to sandstone at about 152.2 metres.

152.20 153.30 SANDSTONE: Unit 8 is light to medium grey, massive, hard muddy sandstone; sand component decreases towards the base; sand is fine grain subangular to subrounded quartz; bottom contact is gradational.

TOP OF LOWER WESTGATE FORMATION AT 153.30 METRES.

153.30 159.10 SHALE: Unit 9 is composed of medium and dark grey, moderate to very fissile, flaky to flaggy, medium disky uniform shales; minor interbedded light to medium grey shaley mudstone with sporadic sand wisps and burrows along bedding planes; darker shales have minor fish debris along bedding planes; rare pyrite clusters less than 1 centimetre in diameter; bottom contact is sharp.

153.30 154.54 -dark grey fissile, medium disky shale with minor fish debris; rare pyrite; 5 centimetre thick dark grey fine grain sandstone at 153.55 metres.

154.54 155.30 -medium grey sandy mudstone; 20 per cent light grey sand as wisps and burrows; bentonite between 155.20-155.24 metres.
155.30 158.36 -dark grey, moderately fissile, fine to medium disky, flaky shale with subordinate sand wisps.
158.36 158.64 -dark grey muddy sandstone; sand intermixed with dark clay matrix; massive and moderately soft.
158.64 159.10 - dark grey, massive to weakly fissile, shaley mudstone.

159.10 159.66 MUDDY SANDSTONE: Unit 10 is light grey, uniformly competent sandstone with up to 30 per cent intermixed clay and silt (wacke); sporadic light grey fragments of cross-bedded sandstone less than 2 centimetres long and oriented along bedding; abundant lined burrows aligned parallel to bedding; bedding at 90 degree angle to core axis; bottom contact is gradational with increasing mudstone towards base.

159.56 159.60 -black, moderately fissile, shale with sandstone wisps; bottom contact is sharp.
159.60 159.66 -bentonite

159.66 162.00 SANDY MUDSTONE: Unit 11 is a composite of medium to coarse disky, finely interbedded dark grey mudstone and medium grey mudstone, both with variable sand content as wisps and intermixed; unit is overall coarsening upward; bottom contact sharp.

159.66 159.83 -dark grey, medium to coarse disky, sandy mudstone with up to 30 per cent sand as intermixed component and as wisps; bottom contact gradational.
159.83 162.00 -medium and dark grey mudstone with less that 10 per cent sand as wisps and burrows along bedding planes; rare to common occurrence of black organic matter common as flattened smudges on bedding planes; mudstone is more uniform and massive from 161.0 to 162.0 metres.

TOP OF FLOTTEN LAKE SANDSTONE AT 162.00 METRES.

162.00 165.12 SILTY SANDSTONE: Unit 12 is a heterogeneous sequence of medium grey muddy fine grain sandstones, fine grain sandstones and sandy mudstones with both gradational and sharp contacts; minor constituents include coarse grain lag deposits, chert pebbles, rare fish debris and angular fragments of cross-bedded carbonate-cemented sandstone ranging from less than 1 centimetre to 4 centimetres in length, generally aligned along bedding; bedding and contacts are at approximately 90 degree angle to core axis.

162.00 162.55 -medium grey, fine grain sandstone with coarsening grain size as well as decrease of silt and clay matrix upwards from base; massive sandstone fragments common; variably carbonate-cemented in upper 25 centimetres; basal contact is gradational.
162.55 163.02 -massive, muddy fine grain sandstone.

163.02 163.42 -massive, muddy sandstone; variably carbonate-cemented with abundant less than 4 centimetre long fragments of cross-bedded carbonate-cemented sandstone; 2 centimetre wide burrow and lag deposit of coarse grain sand, chert pebbles, and fish debris at 163.25 metres; glauconitic, carbonate-cemented, cross-bedded sandstone at 163.30 metres.

163.42 165.12 -sandy mudstone intermixed with sandstone; basal contact is sharp.

165.12 167.33 SHALEY MUDSTONE: Unit 13 is dark grey, fissile, flaky shale with rare to common light grey sand as wisps along bedding planes; bottom contact is sharp.
165.12 165.80 -dark grey, moderately fissile, finely disky shaley mudstone.

167.33 167.93 SILTY SANDSTONE: Up to 1.5 metre core loss from within this interval; Unit 14 is composed of interbedded silty, muddy sandstone and dark grey silty sandstone; appears massive in core fragments; lower 10 centimetres is intermixed light grey sandstone and black fissile shale; common pyrite; bottom contact sharp.
167.90 167.93 -greenish-yellow pyrite layer

167.93 171.30 SANDY SHALE: Unit 15 is composed of dark grey to black, weakly to moderately fissile and flaky, weak disky shale with sandy centimetre-scale beds, laminae, and wisps common; shale is moderately soft and easily breaks into flakes; minor components include black smudges of organic matter, very fine grain fish debris, and rare pyrite; rare sandstone interbeds up to 2 centimetres thick; bottom contact sharp.

168.27 168.29-sulphide layer (marcasite and pyrite); adjacent to 2 centimetres of black, massive mudstone; minor gossanous stain sporadic within underlying 10 centimetres of sparsely fossiliferous shale.

168.55 168.58 -clay-cemented breccia with white matrix of unidentified mineralogy.

TOP OF JOLI FOU FORMATION AT 171.30 METRES.

171.30 178.83 SHALEY MUDSTONE: Unit 16 is dark grey, weakly fissile, fine to medium disky, fairly uniform shaley mudstone; rare sand wisps and laminae, but compose less than 5 per cent of unit; minor components include black smudges of organic matter, very fine grain fish debris, and rare pyrite; rare sandstone interbeds up to 2 centimetres thick, bottom contact is gradational over .5 metres to medium grey shale.

171.30 171.34 -bentonite

177.00 177.40 -medium grey, medium to coarse disky shaley mudstone

178.34 178.83 -black, uniform, blocky to flaggy mudstone; bottom contact is gradational.

178.83 181.22 MUDSTONE: Unit 17 is medium to dark grey, massive to flaggy, massive, fine to medium disky mudstone; rare black smudges of organic matter on bedding planes; rare bioturbation as less than .5 centimetre long burrows; greenish-white glauconitic fine grain sandstone occurs sporadically as thin lenses less than .5 centimetres thick bottom contact is sharp; bedding planes are at 90 degree angles to core axis.

179.83 179.40 -carbonate-cemented fine grain sandstone

179.79 180.31 -as above with interbedded fine grain glauconitic sandstone lenses (less than 5 per cent).

181.07 181.22 -as above with interbedded fine grain glauconitic sandstone lenses (less than 5 per cent).

TOP OF SPINNEY HILL MEMBER AT 181.22 METRES.

181.22 184.20 WEAKLY GLAUCONITIC MUDSTONE: Unit 18 is dark grey to black, weakly fissile, massive to flaggy, fine to coarse disky mudstone; mudstone becomes increasingly mottled and divided by very thin wisps and laminae of cream white to grey silt and silty sandstone downwards; interval is gradational from coarse disky at top to fine disky at bottom; very rare pale green glauconite occurs in sandy wisps within the upper metre of the unit, but also becomes more common downward and visible both as bedding plane wisps and as a disseminated crystalline component within the mudstone matrix near 182.6 metres; interbeds of less than 10 centimetres thick black, claystone occur sporadically; dark grey mudstones contain rare millimetre-scale thin shelled pelecypod fragments and fish scales less than 2 millimetres in diameter; bedding at 90 degree angle to core axis; bottom contact is gradational.

184.20 185.40 GLAUCONITIC MUDSTONE: Unit 19 is similar to Unit 18, but is fine to medium disky; the unit is also richer in glauconite, which occurs both as centimetre-thick lenses and as a disseminated component of the mudstone matrix; abundant wisps and laminae of off-white silt and very fine grain sandstone that may or may not include glauconite; laminae of soft black mudstone occur sporadically; bottom contact is gradational.

185.40 186.67 SHALEY MUDSTONE: Unit 20 is dark grey, homogeneous, weakly to moderately fissile, fine disky, shaley mudstone; rare thin lenses and laminae of off-white to tan silt; bottom contact is gradational.

186.67 190.20 GLAUCONITIC SHALEY MUDSTONE: Unit 21 seems to be a sedimentologic composite of Units 19 and 20; dark grey, weakly to moderately fissile, medium disky mudstone with common glauconite and off-white silt wisps and small lenses up to 2 centimetres thick occur along bedding planes; glauconite is interspersed throughout the mudstone as an emerald green crystalline material; bedding, when defined, at 90 degree angle to the core axis; bottom contact is sharp or possibly gradational over a very thin interval.

190.20 192.00 SANDY MUDSTONE: Unit 22 is very poorly sorted dark grey wacke of about equal proportions silt, fine to medium grain sand and dark grey mudstone; sandy component is composed of light and dark coloured grains including quartz, glauconite, and other dark coloured unidentified minerals; these sandy grains include: translucent laths of dark green, and brown crystal grains of various size; essentially a mud-supported mixture of heterogeneous detritus ranging from silt to medium grain size; well consolidated, but up to 1.3 metres of less-consolidated material was probably washed uphole by circulating drilling fluids; "chaotic"; basal contact is sharp.

TOP OF LOWER JOLI FOU FORMATION AT 190.20 METRES.

192.00 194.78 SHALEY MUDSTONE: Unit 23 is medium grey, homogeneous, massive to weakly fissile shaley, uniformly competent mudstone with bedding at 90 degree angle to the core axis; thin wisps and laminae of off-white to tan silty sandstone, as well as rare millimetre-scale fish scales and thin-shelled pelecypod (?) fragments, which occur on bedding planes; basal 3 centimetres is well-laminated black shale in sharp contact with pyrite-cemented sandstone below.

TOP OF MANNVILLE GROUP AT 194.78 METRES.

194.78 195.00 SANDSTONE: Unit 24 is an intensely carbonate-cemented sandstone with few original characteristics preserved; composed of a greater proportion of micritic diagenetic carbonate than terrigenous material, the terrigenous fraction appears to be composed of dominantly quartz with minor clay component; upper 4 centimetres of the sandstone is intensely pyrite-cemented, which is gradational downwards into the carbonate-cemented rock; bottom contact is emphasized by a very sudden loss of carbonate cement at the contact with the underlying unconsolidated sand.

195.00 195.10 SAND: Unit 25 is light brown, unconsolidated, medium grain sand with sporadic thin bands of darker argillaceous grains concentrated along bedding planes; bottom contact is sharp.

195.10 196.60 SANDSTONE: Unit 26 is dominantly light brown carbonate-cemented medium grain sandstone with dark mottling caused by argillaceous material; bedding preservation ranges from disrupted layers to complete mixing with abundant, large burrow structures characteristic of planolites trace fossils; layers of brown woody material and coal fragments (less than 1 centimetre in length) within a silt and pyrite matrix are common as interbeds up to .5 centimetres in thickness; sharp basal contact of these interbeds indicates that the coarser material was concentrated by winnowing in a high energy environment forming thin lag deposits; bedding is at 80 to 70 degree angle to the core axis; bottom contact is sharp.

196.60 198.10 SANDSTONE: Unit 27 is light brown, unconsolidated, fine to medium grain sandstone (lithic arenite) with slight "salt and pepper" texture due to the significant abundance of black biotite flakes; laminae of flaky, soft, black shale common; more consolidated in the lower 1 metre; bottom contact is gradational.

198.10 198.70 SHALE: Unit 28 is light grey moderately fissile shale with common laminae of off-white silty fine grain sandstone; bottom contact is gradational.

198.70 199.00 SANDSTONE: Unit 29 is light brownish-grey, unconsolidated, homogeneous, fine grain sandstone; bottom contact is gradational.

199.00 199.30 SHALEY MUDSTONE: Unit 30 is medium grey, moderately-well bioturbated shaley mudstone with abundant mottling by off-white silty sandstone; bottom contact is gradational.

199.30 200.60 SANDSTONE: Unit 31 is light grey, moderately well consolidated, fine to medium grain sandstone (lithic arenite) with minor light grey mudstone interbeds less than 2 centimetres in thickness scattered throughout the unit; gradational increase in abundance of coal fragments within the lower 60 centimetres; bottom contact is gradational.

200.60 202.00 SANDSTONE: Unit 32 is light brownish-grey, fine to medium grain sandstone with very abundant fragments of coal and amorphous coaly organic matter ranging in size from discontinuous laminae to fragments of less than 1 millimetre to 2 centimetres in length; concentration of coal clasts within a sparse clayey matrix in some horizons represent thin lag deposits; bottom contact is sharp.

202.00 202.20 MUDSTONE: Unit 33 is light brownish-grey homogeneous mudstone; bottom contact is sharp.

202.20 202.60 SANDSTONE: Unit 34 appears to be very similar to Unit 32, but most was not recovered except for a few centimetres attached to the bottom of Unit 33; loss of this core probably due to its unconsolidated nature; bottom contact is unknown.

202.60 202.90 MUDSTONE: Unit 35 is light brownish-grey, massive, uniformly competent, homogeneous mudstone; bottom contact is sharp.

202.90 203.20 CLAYSTONE: Unit 36 is dark brown, homogeneous, massive claystone; the unit is apparently organic-rich, but is too fine grain to definitely ascertain; upper 15 centimetres of the mudstone contains abundant less than .1 millimetre diameter soft white specks of indeterminate identity; lower contact is gradational.

203.20 204.40 MUDSTONE: Unit 37 is light greyish-brown, massive mudstone with rare less than 5 millimetre long fragments of organic matter and coaly material; becomes darker downwards to a sharp basal contact.

204.40 205.00 MUDSTONE: Unit 38 is medium grey, massive to weakly fissile, mudstone with common 1 to 2 millimetre long coal fragments; abundance of coal fragments increases downwards corresponding to a darkening of the mudstone to dark grey; bottom contact is sharp overlying a coal seam.

205.00 205.10 COAL: Unit 39 is a coal seam with intermixed clayey-material; bottom contact is sharp.

205.10 205.70 CLAYSTONE: Unit 40 is similar to the lower 15 centimetres of Unit 35; friable brown, organic-rich claystone which has increased competency downwards to a gradational basal contact.

205.70 206.30 MUDSTONE: Unit 41 is brownish-grey, massive to weakly fissile, hard mudstone similar to Unit 38, but without coal fragments; bottom contact is gradational.

206.30 207.30 MUDSTONE: Unit 42 is brown organic matter-rich mudstone similar to the lower part of Unit 36; upper 30 centimetres is friable and becomes more competent and clay-rich downward corresponding to occurrence of light grey and dark brown mottling in disrupted bedding; bottom contact is gradational.

207.30 210.10 SANDSTONE: Unit 43 is variably consolidated off-white to light grey, fine to medium grain sandstone; bedding absent or sufficiently disrupted to mottle the sediment, although, some shale and clay layers are relatively undisturbed; bedding at 90 degree angle to core axis; fining downwards to a gradational bottom contact with Unit 44.

210.10 210.70 MUDSTONE: Unit 44 is medium grey, weakly fissile, homogeneous mudstone with abundant coaly fragments up to 1 centimetre long; bottom contact is sharp.

210.70 219.80 INTERBEDDED MUDSTONE AND SANDSTONE: Unit 45 is an interbedded sequence of light brownish-grey, bioturbated, fine to medium grain sandstone and medium grey, weakly fissile to massive mudstone; both subunits range from unconsolidated to hard; the unit is composed of roughly equal proportions of sandstone and mudstone in approximately .5 metre intervals.

219.80 220.22 SANDSTONE: Unit 46 is composed of off-white, poorly consolidated, well sorted, mature quartzitic, fine grain sandstone; massive with minor laminae of clay; bottom contact is sharp; approximately 0.2 metres of lost core.

220.22 222.86 SANDSTONE: Unit 47 is composed of off-white, fine grain quartzitic sandstone with centimetre-scale interbeds of hard medium grey siltstone; bottom contact is sharp.

222.86 224.95 SANDSTONE: Unit 48 is off-white poorly consolidated, well sorted, quartzitic fine grain sandstone; rare, brownish-grey clay laminae; approximately 1 metre of lost core.

224.95 228.66 SANDSTONE: Unit 49 is composed of fine grain sandstone with subordinate, but significant, flecks and laminae of organic matter-rich clay; shale interbeds are common in the lower 2 metres; sandstone is poorly consolidated, moderately to well sorted without regard to organic matter, and quartzitic; rare pyrite; contacts and laminae at 90 degree angle to the core axis; bottom contact is sharp.

225.43	225.47	-medium grey shale interbed.
225.96	226.16	-coaly, organic-rich sandstone
226.49	226.61	-coaly, organic-rich sandstone
226.90	227.05	-sandstone with abundant shale interbeds.
227.30	227.31	-1 centimetre thick pyrite cluster.
227.94	228.28	-coaly sandstone.
228.28	228.42	-medium grey shale interbed.
228.52	228.66	-medium grey shale interbed.

228.66 240.00 SANDSTONE: Unit 50 is composed of dominantly off-white, mature, quartzitic, massive, poorly consolidated fine grain sandstone; minor medium grey shale interbeds less than 5 centimetres thick; bottom contact is unknown.

230.62	230.72	-medium grey shale interbeds.
230.75	230.77	-pyritiferous sandstone.
230.82	231.10	-coaly-sandstone.

END OF HOLE AT 240.0 METRES.

RHONDA MINING CORPORATION
PRELIMINARY DETAILED CORELOG
July 2, 1994

DRILL HOLE: OFS94-017 **CLAIM NUMBER: S-127080**
LOCATION: L.S.D. 14, Section 4 , Township 44, Range 18, West 2nd Meridian
CORE SIZE: 101mm
TOTAL DEPTH: 160.00m
CORE LOCATION: Saskatoon Field Office
CASING LEFT IN HOLE: 20m
DIP: -90
DATE STARTED: June 24, 1994
DATE COMPLETED: June 30, 1994
DOWNHOLE GEOPHYSICAL TESTING: Gamma-ray log - Machibroda Engineering
DRILLING CONTRACTOR: LONGYEAR CANADA INC.
DRILLSITE GEOLOGY: R. Woodward
CORE LOGGED BY: B.C. Jellicoe
ABANDONMENT STATUS: Cemented tight from E.O.H. to just below remains of conductor casing.
PURPOSE: Test for the presence of kimberlite and or kimberlitic sediments associated with positive results from holes OFS93-02, 03, and 04. No significant geophysical anomaly is present.
RESULTS: No kimberlitic sediment intersected.
COMMENTS: Bedding and contacts are subhorizontal (90 degree angle to core axis) unless otherwise specified.
All depths are relative to collar elevation.
Stratigraphic Nomenclature for the Colorado Group of Bloch et al (1993) used in this log, see Chapter 1.

CORE DESCRIPTION

0.00 85.00 CASING. OVERBURDEN/TILL: Not cored and no coherent chip samples recovered.

85.00 86.00 COBBLES: Unit 1 is composed of granite, diorite, gabbro, pegmatite, dolomite, and dolomitic limestone cobbles ranging from 2 centimetres to less than 6 centimetres along their long axis with subordinate abundance of pebbles of similar composition; these rocks are presumably the remnants of unconsolidated till which was washed by drilling fluids.

86.00 96.97 TILL: Unit 2 is a medium to dark brownish-grey, poorly sorted, silty mud matrix supported, heterogeneous till; the matrix is calcareous with a strong reaction to HCl; till components nested within the matrix include angular to subrounded rock fragments ranging from very fine grain sand to pebbles and cobbles with

the finer fractions (less than 2 millimetres) dominantly quartz, dolomite, feldspar, shale, and minor to rare hornblende, pyroxene, chert and garnet; coarser fragments are dominantly dolomite with subordinate shale clasts, diorite, gabbro, and quartz; there is no obvious bedding and the rock fragments are chaotically oriented; from about 92 metres to base, rock fragments compose about 25 per cent of the unit; the unit coarsens with an increased component of very fine to fine grain sand within the matrix; the basal contact is sharp.

94.48 94.80-two large cobbles of dolomite and diorite about 13 centimetres along their long axis.

96.97 106.74 TILL: Unit 3 is similar to Unit 1 with a medium to dark-grey calcareous silty mud matrix, but the abundance and size of constituent rock fragments is much less; fragments are generally less than 1 centimetre in diameter and composed of dolomite and shale fragments with a subordinate component of sand sized quartz and feldspar; fragments greater than 1 centimetre are rare and may range up to 2.0 in diameter; rock fragments compose about 10 per cent or less of the unit; the basal contact is apparently gradational with underlying dark brown mudstones.

106.74 107.26 MUDSTONE: Unit 4 is a dark brown, massive to blocky mudstone with rare millimetre-scale kaolinitic lenses; the unit is gradational downwards with mottles of light brown silty mudstone intermixed; the basal 2 centimetres is gradational with fine grain dark brown sand (glacio-lacustrine mudstone).

107.26 110.00 INTERMIXED SANDY AND MUDDY TILL: Much of Unit 5 was lost by washing and milling within the core barrel; the remaining material (40 centimetres) is dark brown intermixed fine to medium grain sand and muddy matrix with less than 5 per cent rock fragments similar to Unit 3; the sand is composed of about 70 per cent subrounded quartz and 30 per cent lithic grains including feldspar, hornblende, and shale fragments; the basal contact is unknown; (about 5 centimetres of slushy, unconsolidated silty sand was recovered at the top of the following core).

BEDROCK CONTACT AT 110.00 METRES - UPPER WESTGATE FORMATION

110.25 115.89 SHALEY MUDSTONE: Unit 6 is a dark grey, massive to blocky, shaley mudstone with minor wisps, lenses, and burrow traces of silt and very fine grain sand along shaley laminae; the upper 2.9 metres are deformed and brecciated with chaotically jumbled shaley mudstone fragments within a massive matrix of similar mudstone; there are no visible grain size trends except for fining upwards from the gradational basal contact.

110.25 112.86 -deformed and brecciated mudstone as described above; core fractures at 45 degree angle to core axis are common throughout with adjacent beds showing alignment of broken clasts parallel to fracture orientation; the uppermost 4 centimetres beneath the contact is a slightly decrepitated

orangy-red oxidized mudstone (possibly a remnant regolith or alteration zone adjacent to deposition of glacio-fluvial sands above); interval 110.00 to 111.64 has sporadic thin lenses and disjunct threads of a pale greenish-yellow mineral oriented along the deformed fabric of the mudstone (possibly sulphate developed during deformation and influx of meteoric waters during glaciation); basal contact is sharp.

112.86 115.77 -weak to moderately fissile, shaley mudstone with minor silt and very fine grain sand as lenses, pods, and burrow traces along poorly defined bedding planes; bedding planes are irregular, but dominantly at 90 degree angle to core axis; basal contact is marked by a gradational fining upwards sequence between 115.77 and 115.89 metres.

TOP ST.WALBURG SANDSTONE AT 115.89 METRES

115.89 116.63 SANDSTONE: Unit 7 is a greenish-grey to dark grey, poorly lithified, poor to moderately-well sorted, immature, silty fine grain sandstone (volcanic-sublitharenite) containing abundant irregularly interbedded clasts of millimetre- to centimetre-scale muddy siltstone defining weak cross-beds or slightly inclined planar beds; grain constituents include a dominant fraction of moderately uniform subrounded quartz and glauconite with up to 30 per cent lithic grains composed of: rock fragments (mudstone clasts?), chert, and minor constituents including organic material, ilmenite, Cr-diopside, garnet, hornblende, and micas; matrix material includes illite (probable) and pyrite; basal contact sharp.

115.89 116.00 -sandy mudstone characterized by intermixed light grey fine grain sand and dark grey massive mudstone; this is a fining upwards unit gradational with the underlying sandstone.

115.89 116.00 -silty mudstone.

116.00 116.04 -greenish grey laminar bedded kimberlitic sandstone with less than 5 per cent mudstone clasts, as described above, sharp basal contact.

116.00 116.04 -sandstone.

116.04 116.29 -dark grey sandstone with slight greenish cast; silty mudstone clasts and laminae up to 30 per cent in irregular interbeds; basal contact is gradational.

116.29 116.63 -mottled light and dark grey silty sandstone with abundant (50 per cent) laminae and clasts of shaley mudstone; basal contact is sharp.

116.63 116.94 SANDSTONE: Unit 8 is a light grey, indurated, very fine grain, cross-bedded carbonate-cemented sandstone; the upper 16cm shows well-preserved small-scale cross-bedding (75 to 85 degree angle to core axis) with common thin laminae of clay (mudstone) up to 10 per cent; upper 15 centimetres has well defined Zoophycus burrow over 3 centimetres long; lower 15 centimetres is

moderately bioturbated (probably Thalassinoides traces) with 30 per cent cross-bedding and laminae preserved; constituent grains include dominantly uniform rounded quartz and minor lithic grains with rare glauconite; basal contact is sharp, but has silty mudstone lenses less than 1 centimetre thick, similar to underlying partially consolidated silty sandstone.

116.94 118.25 SILTY SANDSTONE: Unit 9 is a dark brownish-grey, massive to weakly bedded, silty very fine grain sandstone; irregular millimetre- to centimetre-scale silty mudstone lenses and laminae are common and may be both an in-situ component and as transported in fragments; the unit is soft and only partially consolidated; grain constituents include dominantly very fine grain uniform subrounded quartz and up to 20 per cent minor rock fragments, chert, feldspar, glauconite, and mica; basal contact is sharp.

116.94 117.26 -fining up very fine grain sandstone with irregular silty shale component in upper 7 centimetres; the interval is dominantly massive; if mudstone component is in-situ, then interval is weakly fining upwards; basal contact is sharp.

117.26 117.48 -fining up siltstone similar in appearance to silty sandstone above; massive, soft, and irregularly mottled by light grey very fine grain pods of sand; basal 7 centimetres is fining upwards from 2 centimetre thick light grey sandstone interval; basal contact is sharp.

117.48 117.83 -coarsening upwards brownish-grey siltstone similar to above; dominantly massive, but includes up to 10 per cent irregular, slightly inclined, interbedded silty mudstone wisps, lenses, and laminae; sharp basal contact.

117.83 118.25 -upper portion is a massive, very soft siltstone; 3 centimetres weakly pyritized, 2 rounded fragment (concretion?) at 117.83 metres within very soft siltstone; basal contact is sharp.

118.25 118.63 FU SANDSTONE TO SILTY MUDSTONE: Unit 10 is composed of a basal light grey, massive very fine grain sandstone which grades upwards to mottled light and dark brownish-grey intermixed very fine grain sandstone and silty mudstone; grain constituents include dominantly subrounded quartz and minor lithic grains such as shale clasts, chert, feldspar, glauconite, and rare garnet; submature sublitharenite; basal contact is sharp.

118.63 118.97 SILTY/SANDY MUDSTONE: Unit 11 is a dark and light grey mottled, interbedded and intermixed mudstone with variable sand and silt content up to 20 per cent; unit is very similar to the upper portion of Unit 10; basal contact is sharp.

118.97 119.51 SILTY MUDSTONE: Unit 12 is dark brownish-grey, massive to finely bedded mudstone with up to 30 per cent quartzitic silt-sized component both as interbeds and intermixed; basal contact is sharp.

119.00 119.13 -very soft massive mudstone; gradational basal contact with underlying silty mudstone.

119.51 120.86 SILTY/SANDY MUDSTONE: Unit 13 is a light and dark grey bedded mudstone with common laminae, lenses, and pods of silty very fine grain sandstone as up to 25 per cent of the unit; sand beds less than 2 centimetres thick are irregularly interbedded without visible trend in grain size within the greater unit; basal contact is unknown.

119.51 120.04 -this interval is slightly coarser-grained with a greater proportion of sand and silt interbeds than below 120.04 metres; basal contact gradational with similar lithology below.

120.04 120.86 -dominantly dark grey mudstone laminae of light grey silty sandstone up to 10 per cent of interval; interval fines upwards from sandy mudstone at 120.56 to mudstone with minor beds and laminae of light grey silty sand and sandstone less than1cm thick up to 120.04; bottom contact obscured unknown due to lost core from 120.86 to 123.58.

120.86 124.00 LOST CORE

124.00 124.40 SHALEY MUDSTONE: Unit 14 is a dark grey to black, moderately fissile to massive shaley mudstone with less than 5 per cent thin layers of silty sandstone (less than 2 centimetres thick); basal contact is apparently sharp.

124.14 -2 centimetre pyritized silty sandstone layer.

124.40 124.56 SANDSTONE: Unit 15 is a dark grey, well sorted, massive very fine grain quartzarenite with traces of pyrite and dark coloured silt; basal contact is sharp.

TOP LOWER WESTGATE FORMATION AT 124.56 METRES.

124.56 129.12 MUDSTONE: Unit 16 is a dark grey to black, massive to slightly shaley mudstone; less than decimetre thick intervals of massive mudstone are sporadically interbedded with sharp contacts; rare, thin silty sandstone lenses occur along bedding planes; basal contact is vague and marked by the frequent occurrence of silty sandstone within the mudstone.

TOP FLOTTEN LAKE SANDSTONE AT 129.12 METRES

129.12 131.84 SANDY MUDSTONE: Unit 17 is a dark grey to black, massive to slightly shaley mudstone with abundant lenses, wisps, laminae, and jumbled clasts of silty to very fine grain tan to off-white sandstone; the silty sandstone is composed of poorly- to moderately-well sorted, subrounded to rounded quartz (85 to 90 per cent – quartzarenite) with subordinate dark and golden mica flakes, glauconite, chitin, amorphous woody and resinous organic matter, and possibly trace phosphatic fish debris.

129.12 129.89 -as described above; basal 6cm of jumbled laminated silty sandstone clasts; basal contact is sharp.

129.89 131.23 -similar to Unit 16 with rare sandstone wisps; bottom contact is gradational.

TOP JOLI FOU FORMATION AT 131.23 METRES

131.23 131.84 -as described above; basal contact is sharp.

131.84 133.27 MUDSTONE: Unit 18 is similar to Unit 16 without silty sandy material; basal contact is sharp.

TOP SPINNEY HILL FORMATION AT 133.27 METRES

133.27 135.03 SILTY/SANDY SHALEY MUDSTONE: Unit 19 is a medium grey, weakly fissile to blocky shaly mudstone, with trace to minor interbedded and intermixed silty very fine grain off-white to greenish-white sandstone; very fine grain sandstone occurs as wisps, lenses, laminae, and rare, well-consolidated clasts less than 1 centimetre in diameter; glauconite content in the sandstone varies from absent to less than 10 per cent; the unit is weakly bioturbated with traces composed of millimetre- to centimetre- scale flattened sandstone in unlined burrows, possibly Planolites or Thalassinoides forms; there are no apparent grain-size trends; basal contact sharp over similar mudstone with abundant very fine grain sandstone component.

135.03 135.47 SILTY/SANDY SHALEY MUDSTONE: Unit 20 is similar to Unit 19, but contains subordinate common silty very fine grain sandstone lenses, and a slightly higher proportion of glauconite; this unit may be associated with the underlying very fine grain sandstone unit; the basal contact is sharp.

135.47 135.63 GLAUCONITIC SANDSTONE: Unit 21 is an interlaminated, off-white and olive-green, hard, carbonate-cemented very fine grain sandstone; the sandstone is weakly cross-bedded, but shows post-lithification deformation and disruption with light grey mudstone incorporated between brecciated clasts; the unit is grossly fining upwards with glauconite most abundant towards the base; the basal contact is sharp, but with clasts pushed into the underlying softer mudstone; deformation of the unit probably occurred after cementation and contemporaneous with initial deposition of the overlying mudstone during high energy conditions associated with reworking of the substratum during a transgressive pulse.

135.61 -2 x 3 centimetre sulphide clot within sandstone.

135.63 135.81 SHALEY MUDSTONE: Unit 22 is similar to Unit 20, but contains a few glauconitic (40 per cent) sandstone lenses; the basal contact is sharply gradational.

135.81 135.91 GLAUCONITIC SANDSTONE: Unit 23 is composed of sandstone similar to Unit 21, which is incorporated with glauconitic soft mudstone; core in this interval is broken and jumbled; basal contact is probably sharp.

135.91 139.76 GLAUCONITIC MUDSTONE: Unit 24 is a dark grey to black, massive to blocky mudstone with variable, sporadic occurrences of emerald green glauconite as lenses along apparent bedding planes, and as clots up to 2 centimetres across within the mudstone; glauconite content estimated at between 5 to 10 per cent; minor (5 per cent) lenses, laminae, and broken fragments of green and white glauconitic very fine grain sandstone occur sporadically throughout the interval; the basal contact is arbitrarily taken as the last occurrence of significant sandstone.

136.13 136.55 -common glauconitic sandstone component in mudstone.
136.70 136.80 -common glauconitic sandstone component in mudstone.
138.17 138.47 -common glauconitic sandstone component in mudstone.
138.85 139.20 -common glauconitic sandstone component in mudstone.

139.76 146.43 GLAUCONITIC MUDSTONE: Unit 25 is a black, massive to blocky, very clayey, moderately soft and gummy, carbonaceous mudstone with variable, sporadic occurrences of emerald green glauconite as lenses along apparent bedding planes, and as clots up to 2 centimetres across within the mudstone; glauconite content estimated at between 5 to 10 per cent and decreases overall downwards to base; very fine grain sandstone as thin laminae are very rare; mudstone with "greasy texture" common within the lower 3 metres; basal contact is sharp. It should be noted that glauconite may occur within the carbonaceous dark grey to black mudstones of the lower part of the Joli Fou Formation, thus this unit may represent the transition to- and basal portion of the Joli Fou, particularly with reference to the slight lithological change at about 140.15 metres. Also, 1.75 metres of core was lost somewhere from between 143.47 and 145.48 metres, this core was probably unconsolidated sand, because a remnant piece of core within this interval is dusted with brown fine to medium grain sand. A sand in this horizon would be stratigraphically anomalous compared to the known central Saskatchewan lithological succession.

146.43 147.48 SANDY MUDSTONE: Unit 26 is composed of massive, moderately soft, dark grey to black, clayey, carbonaceous mudstone in the upper portion, which grades downward to sandy mudstone at the base; interbedded with the mudstone are 3 subunits of chaotically intermixed carbonate-cemented off-white fine to medium grained sandstone lenses, wisps, and clasts (?); the sandstone may have been bioturbated prior to, and during deposition, but mixing of the material is more indicative of intercalation during higher energy conditions; the basal muddy sandstone sharply overlies the underlying light grey mudstone. This unit is representative of the intermixing of eroded Mannville sandstone material with mudstone during the basal transgression of epicontinental seas, which formed the mudstone dominated Colorado Group, of which the Joli Fou and Spinney Hill formations are a part.

TOP MANNVILLE GROUP AT 147.50 METRES.

147.50 149.00 MUDDY/SILTY SANDSTONE: Unit 27 is a composite of interbedded and gradational subunits of medium grain dark brown sandstone variably carbonate-cemented, which overlie muddy fine to medium grain sandstones that collectively coarsen upwards; the units are chaotically interbedded on various scales and show no visible bedding or uniformity.

147.50 148.07-variably carbonate-cemented fine to medium grain dark brown sandstone; carbonate-cemented sandstone is hard and off-white in colour.

148.07 149.00 -as described above; basal contact is sharp.

149.00154.05 MOTTLED SILTSTONE: Unit 28 is a mottled tan, light brown, and dark brown interbedded and intermixed muddy siltstone and siltstone; the siltstone is generally lighter coloured than the mudstone; the unit appears well-mixed by bioturbation; the sediments range from dominantly soft and plastic (deformable) to slushy in less than 10 centimetre intervals; less than 2 millimetre fragments of woody organic matter common throughout; the basal contact is sharp.

154.05 155.00 MUDSTONE: Unit 29 is a dark brown massive, soft, deformable mudstone; the unit is fining upwards from silty mudstone at the base where about 2.75 metres of core was lost, probably due to washing away of unconsolidated sand and silt during drilling; less than 2 millimetre fragments of woody organic matter common throughout; the basal contact is presumably gradational.

155.00 157.80 LOST CORE

157.80 158.97 MUDSTONE: Unit 31 a dark brown, massive mudstone which fines upwards from a basal 24 centimetres of sandy siltstone; the basal contact is sharp.

158.73 158.97 -silty mudstone with finely laminated sandy silt beds increasing in abundance down to the base.

158.97 159.13 SANDSTONE: Unit 32 is dominantly a light brown, silty very fine grain sandstone; the unit fines upwards from an 8 centimetre base of finely laminated tan fine grain sandstone through interlamination of fine grain sandstone and silty very fine grain sandstone, to subtly cross-bedded silty very fine grain sandstone; basal contact sharply defined by erosional surface overlying carbonate-cemented sandstone.

159.13 159.90 CARBONATE-CEMENTED SANDSTONE: Unit 33 is a uniform, massive carbonate-cemented, off-white fine grain sandstone; basal contact is sharp.

159.90 160.00 SANDY MUDSTONE: Unit 34 is composed of intermixed off-white fine grain sand and medium brown mud; bottom contact is unknown.

E.O.H. AT 160.00m

APPENDIX II

Boreholes with kimberlite intersections

CONTENTS:

RHONDA MINING CORPORATION
DETAILED CORE DESCRIPTION
November 8, 1994

DRILL HOLE: OFS93-002 **CLAIM NUMBER: S-127080**
LOCATION, LEGAL: NE Quarter, Section 05, Township 52, Range 18 West of 2nd Meridian
GROUND ELEVATION: 437.37 meters
TOTAL DEPTH: 160.12 metres
CORE SIZE: HQ, 101 millimetres
CORE LOCATION: Saskatoon Field Office
DIP: -090 degrees
DATE STARTED: March 7, 1993
DATE COMPLETED: March 12, 1993
DOWNHOLE GEOPHYSICAL TESTING: BPB Wireline Ltd.
DRILLING CONTRACTOR: Longyear Canada Ltd.
DRILLSITE GEOLOGY: M. Durocher
CORE LOGGED BY: B.C. Jellicoe and K. Leahy
ABANDONMENT STATUS: Cemented from 160.62 to 67.05 metres; up-hole collapsed.
PURPOSE: To test the southwest continuation of the positive magnetic feature drilled in OFS93-004 adjacent to known kimberlite clusters located immediately to the north.
RESULTS: A 14.58 metre interval of PK and RPK intersected between 102.11 metres, immediately below the pre-till unconformity.
COMMENTS: Bedding and contacts are subhorizontal (90 degree angle to core axis) unless otherwise specified.
All depths are relative to collar elevation.
Abbreviations for kimberlite description are defined in the Textural Classification, Chapter 2.
Stratigraphic Nomenclature for the Colorado Group of Bloch et al (1993) used in this log, see Chapter 1.

CORE DESCRIPTION

00.00 83.15 TILL: This interval was not cored and chip samples were not collected; geophysical logs and driller reports indicate that this interval is composed of interbedded muddy tills and sandy tills beneath a few metres of surficial sandy sediment.

83.15 97.59 GLACIAL TILL: Unit 1 is tan to dark brownish-grey, poorly sorted, calcareous, muddy till with abundant clasts of diverse origin including carbonate, quartz, and feldspar; till sequence includes interbedded dark grey to black mudstones and unconsolidated light grey to brown sands; the well-site report suggests that most of this material was lost during drilling, leaving only 5 centimetres of pale brown, medium grained, well-sorted quartz sandstone (sand) with sporadic

carbonate cement in the matrix, and about 20 centimetres of milled and broken pebbles winnowed from the interval 83.15 to 96.30 metres; bottom contact is sharp.

96.30 97.00 -heterogeneous, chaotically-mixed till composed of 25 per cent clasts and grains of various sizes floating in a brownish grey silty and muddy matrix; there are no obvious bedding or sedimentological features; clasts are angular and include limestone, schist, and black shale; grains include angular to rounded quartz, feldspar, mafic minerals, and occasional garnets; basal contact is gradational; only 33 centimetres of core was recovered from this interval.

97.00 97.60 -thinly bedded (up to 2 centimetres thick) silty and muddy till similar to above; bedding contacts are sharp and distinct; the unit contains isolated, angular clasts of limestone, granite, and rare shale clasts; fractures present 10 centimetres from the upper contact oriented at 30 degree angle to core axis.

TOP OF BEDROCK AT 102.11 METRES - BRECCIATED MUDSTONE

102.11 102.77 BRECCIATED MUDSTONE: Unit 2 is soft, dark grey to black, poorly fissile, well-indurated, massive, clast-supported, brecciated mudstone; fragments up to 8 cm wide across the long axis occur within soft, unconsolidated light brown, very fine grain matrix with abundant phlogopite as flakes (up to 2 millimetres across long axis), rare garnets (less than 0.1 millimetres diameter common biotite grains, and very fine magnetite or ilmenite blebs (not perceptively magnetic; fractures common oriented at 60 to 80 degree angle to core axis; unit is core expression of a large mudstone block entrained in-, and permeated with kimberlite.

102.11 102.77 -brecciated mudstone with abundant matrix material; brecciation decreases to base and is gradational with central core of the mudstone block.

102.77 103.80 -similar to above, but more consolidated and less fractured; brown matrix material is rare, but increases in lower portion.

103.80 104.42 -similar to above, but contains much more brown kimberlite matrix that increases in abundance to the bottom of the unit; the lower portion is composed of clay clasts floating in green tuffaceous kimberlite material; bottom contact is gradational with underlying tuffaceous kimberlite.

104.42 104.67 MASSIVE RPK: Unit 3 is very fine to coarse grain granular tuffaceous kimberlite composed of light olive green, very fine grain matrix with abundant 1 to 2 millimetre diameter crystals of dark green phlogopite, and abundant unidentified mafic minerals; matrix is sporadically mottled with amorphous patches of dark grey magnetite; slickensided fractures oriented at 60 degree

angle to core axis occur immediately above a large shale clast (5 centimetres across long axis) situated within abundant gossanous iron oxide; bottom contact is sharp.

104.67 104.77 SHALE INTRACLAST BRECCIA: Unit 4 is composed of brecciated clay within light olive green, very fine grained matrix; iron-oxide stain is common; possibly the core expression of the flanks of a large entrained brecciated mudstone block; bottom contact is gradational.

104.77 105.17 BEDDED RPK: Unit 8 is similar to Unit 5, but is darker green towards the base and contains flakes of dark green phlogopite up to 2 millimetres in diameter; matrix is moderately friable and contains common white baryte; bottom contact is not determined.

105.17 105.81 UNKNOWN KIMBERLITE: Unit 6 is dark green, medium grained crystal tuff composed of very fine grained matrix with abundant dark green phlogopite crystals ranging up to 1 millimetre across and amorphous baryte blebs; interval fragmented into shards of all sizes except for the basal 23 centimetres, which is only partially broken; bottom contact is unknown due to rubble.

105.81 110.16 GRADED AND BEDDED RPK: Unit 7 is composed of light and dark coloured grains within a light bluish-grey matrix composed of dominantly phlogopite and biotite along with subordinate unidentified mineral grains; generally massive, but fining upwards in some intervals; variably consolidated from friable to well-indurated; subunits are delineated by change in competency which reflect variations in grain size, such that finer-grained units are more competent while coarse gained units are friable; bedding is defined by grain size changes, with grain size ranging from amorphous powdery clay size to coarsely granular with coeval, though not parallel variations in grain size of micas; interval has 8 interbedded fine and coarse grained subunits, which appear to be weakly graded (note that the basal two units are the most obviously fining upwards); graded subunits range in thickness from 10 to 50 centimetres with bedding planes within the unit at 72 degree angle to core axis; black magnetite occurs as amorphous granular masses, individually up to 2 centimetres in diameter, but often clumped together into larger masses up to 5 centimetres across; magnetite also occurs along bedding planes and fractures, although theses masses may cut across bedding when associated with fractures; magnetite abundance is estimated at 25 per cent; fracture angles are variable and apparently non-linear; contacts between the subunits may be either sharp or gradational; the base of the entire interval is marked by 10 centimetres of clay clasts imbedded in light grey matrix; the unit is non- to weakly except for a very calcareous upper 10 centimetres; the basal contact is sharp; up to 50 per cent of the unit is fragmented.

110.16 110.73 GRADED RPK: Unit 8 is similar to the graded subunits present within Unit 10 and is composed of light greenish grey to medium grey, coarse to very fine grained, fining upward, tuffaceous kimberlite; abundant pebble size phlogopite flakes and subordinate amounts of smaller biotite; as grain size decreases upwards, there is a coeval increase in competency, and corresponding decrease in abundance of mica grains; the unit also darkens in colour upwards; magnetite content is estimated at 25 per cent in the lower portion and grading upwards to 15 per cent as grain size decreases; large mudstone clast approx. 5 centimetres in diameter and 1.5 centimetres thick, oriented at 60 degree angle to core axis at the base; weakly to non-calcareous; bottom contact is sharp.

110.73 111.56 GRADED AND MASSIVE RPK: Unit 9 is similar to Unit 8, but much more indurated; composed of dark grey-green, dominantly fine grained tuffaceous kimberlite; magnetite is less abundant than in Unit 8, and occurs along bedding planes; magnetite also occurs dispersed around, and concentrated in faults; weakly to non-calcareous; bottom contact is gradational.
110.73 111.56 -fining upward sequence; basal contact is subtle.

111.56 - 115.74 MEDIUM TO COARSE PK TUFF: Unit 10 is similar to Unit 9, but is well-indurated and calcareous throughout; dominantly fine grain with intervals of subtle gradation from fine to medium grain; subhorizontal bedding; colour varies from dark grey-green in finer grained subunits to pale green in the coarser material; discrete phlogopite is very common in the coarser grained beds, while finer subunits have matrix biotite only; rare, black amorphous masses are present, but contain little to no magnetite; yellow-brown staining occurs as streaks throughout the unit; weakly to strongly calcareous increasing down-section; faults occur at 112.09 and 112.25 metres and are angled at 80 and 28 degrees to core axis, respectively; at 113.90 metres, carbonate veining and matrix carbonate gradually becomes pervasive within more olive-green matrix material that is coarser grained and less indurated; carbonate veins are oriented at 75 to 90 degree angle to core axis; the veins host white, cryptocrystalline carbonate material and green striated phlogopites with cleavage parallel to the vein walls; the basal contact between kimberlite tuff and the underlying sandstone is marked by a 4 to 15 millimetre thick dark greyish-green layer characterized by intensive carbonate veining, this boundary appears to be mainly sedimentary, with load and flame structures present within the fine-grained layer; the mineralogy of the dark fine grained layer appears very similar to the matrix of the darker kimberlite tuffs; the bottom contact is sharp.

EROSIONAL TOP OF ST. WALBURG SANDSTONE AT 115.74 METRES

115.74 116.69 SANDSTONE: Unit 11 is light brown, well sorted, fine to coarse grained sandstone; a 2 to 3 centimetre thick pale grey mudstone bed at 116.30 metres separates intensively carbonate veined, fine to medium grained sandstone above from carbonate cemented, medium to coarse grained sandstone below; sandstone is composed of sub-angular quartz grains, with common dark green,

black, and silty clasts; ripple cross-bedding is prevalent as are scour and reactivation surfaces; bottom contact is sharp.

TOP LOWER WESTGATE FORMATION AT 116.69 METRES

116.69 116.84 MUDSTONE: Unit 12 is medium grey, well indurated, massive to slightly fissile mudstone; dark olive green mottling occurs along fractures; white, flat, lenticular baryte is present sporadically and is common as blebs around 116.80 metres; bottom contact unknown.

116.84 117.52 MUDSTONE: Unit 13 is black, homogeneous, massive, blocky, slick, carbonaceous mudstone; sand wisps and sand-filled burrows common in the lower portion; upper part is less organic-rich and more consolidated; bottom contact is gradational.

117.52 119.20 FINING UPWARD SANDSTONE TO MUDSTONE: Unit 14 is composed of a thin dark grey to light brownish-grey, unconsolidated, poorly sorted, bioturbated, very fine to fine grain silty sandstone which fines upwards to silty mudstone; bioturbation in the sandstone decreases upwards but is also present in the mudstone; bottom contact is sharp.

119.20 120.45 FINING UPWARD SANDY MUDSTONE: Unit 15 is composed of interbedded sandstone and sandy mudstone; sandy interbeds decrease in abundance upwards, fining into black, slick, carbonaceous mudstones with rare sandy wisps and burrows; the black mudstones become progressively lighter coloured up-hole grading to dark grey, massive to poorly fissile shale; the bottom contact is marked at the first indication of gradational coarsening upwards from the underlying fissile black shales; bottom contact is gradational.

TOP OF FLOTTEN LAKE SANDSTONE AT 119.65 METRES

119.65 120.45 COARSENING UPWARD SANDY MUDSTONE: Unit 16 is composed of basal dark grey, blocky shales intermixed with pyritized silt and sand; overlain gradationally by interbedded/intermixed bioturbated, fine grained sandstones and silty mudstone; bottom contact is gradational.

120.45 121.90 FINING UPWARD SANDY MUDSTONE: Unit 17 is a sequence of intermixed shales and sands; basal bioturbated, interbedded black mudstone and light grey, fine-grained sandstone grades into blocky to fissile black shaley mudstone; upper portion probably continuous with the coarsening upward sequence in unit above; bottom contact is sharp.

120.45 120.74 -blocky to weakly fissile shaley mudstone.

120.74 121.90 -bioturbated, interbedded black mudstone and light grey, fine-grained sandstone.

121.90 123.25 MUDSTONE: Unit 18 is dark grey to black, blocky, weakly carbonaceous, clay-rich mudstone containing minor intermixed fine grained sand as wisps and burrow-fills; bottom contact is sharp.

123.25 124.15 COARSENING UPWARDS SHALY SANDSTONE: Unit 19 is a light grey to tan sandstone intermixed/interbedded with black mudstone; moderate to intensive bioturbation common; unit coarsens upward; bottom contact is gradational.

124.15 127.05 FINING UPWARDS SANDY MUDSTONE: Unit 20 is dark grey, poorly fissile shale in the lower part, which grades to black, blocky, carbonaceous mudstone in the upper portion; both shale and mudstone contain abundant wisps and burrows filled with off-white to tan, fine to medium grain sand; bottom contact is sharp.

127.05 130.14 SILTY SANDSTONE: Unit 21 is off-white to tan, moderately well-consolidated, uniformly competent, poorly sorted, fine to medium grained sandstone containing variable proportions of mud and silt; the sandstone is medium grain, moderately well-sorted, indurated, and carbonate cemented; the unit is composed of numerous coarsening and fining upward sequences characterized by both mottled, trace fossil-rich intervals and up to 30 per cent ripple crossbedded very fine grain sandstone; bottom contact is gradational.

130.14 132.20 SANDY MUDSTONE: Unit 22 is intermixed/interbedded black bioturbated mudstone and about 30 per cent very light grey, fine grain silty sandstone; sand occurs variably within laminated, subtly crossbedded lenses, mottled and bioturbated pods, and in thin distorted beds; bottom contact is sharp.

TOP OF JOLI FOU FORMATION AT 132.20 METRES

132.20 134.68 SANDY MUDSTONE: Unit 23 is similar to Unit 22, but with about 15 per cent very light grey, fine grain, silty sandstone intermixed and interbedded with black, bioturbated mudstone; bottom contact is sharp.

134.68 136.24 MUDSTONE: Unit 24 is dark grey to black, massive to blocky, carbonaceous mudstone; basal 50 centimetres is mottled by bioturbation and intermixing of silt and sandy with sporadic pyritized clumps; fines upwards to homogeneous, massive mudstone; bottom contact is sharp.

TOP OF SPINNEY HILL FORMATION AT 136.24 METRES

136.24 137.45 MUDSTONE: Unit 25 is dark grey to black, massive to poorly fissile, shaly mudstone; includes interbeds of bioturbated silt and sand with sporadic pyritized clumps; 2 centimetre thick glauconitic sandstone at 137.44 metres; unit is overall fining upwards; bottom contact is gradational.

137.45 139.29 SANDY MUDSTONE: Unit 26 is black, massive, blocky to fissile, carbonaceous shaly mudstone containing common sandy interbeds marked by infrequent distorted and bioturbated bedding; lower 1 metre has very abundant silt and sand (30-40 per cent), and some sand layers are carbonate cemented; unit is overall fining upwards; bottom contact is sharp.

139.35 140.20 MUDSTONE: Unit 27 is black, massive to blocky, homogeneous, soft, plastic, weakly carbonaceous mudstone; unit grades to slightly more consolidated, less carbonaceous mudstone up-section; bottom contact is sharp.

140.20 141.39 MUDSTONE: Unit 28 is black, massive to poorly fissile, carbonaceous mudstone; 2 centimetre thick bentonite underlain by thin fish debris bed at 140.30 metres; greasy textured and no visible evidence of bioturbation or plant matter; bottom contact is sharp and delineated by pyritized clast lag.

141.39 142.34 SANDY MUDSTONE: Unit 29 is similar to Unit 26; unit is fining upwards overall; bottom contact is sharp.

142.34 143.66 MUDSTONE: Unit 30 is a sequence of related mudstone facies; greasy texture, black, massive to fissile, shaly mudstones enclose a 35 centimetre section of dark grey sandy mudstone; contacts are gradational; bottom contact is sharp.

TOP OF SPINNEY HILL FORMATION AT 143.66 METRES.

143.66 145.38 SILTY MUDSTONE: Unit 31 is light to medium grey, massive, slick mudstone; sporadic green glauconite and bioturbation common in mottled beds; bottom contact is sharp.

145.38 146.08 SHALE: Unit 32 is medium grey, fissile shale with rare fragments of distorted, indurated sandstone less than 2 centimetres across; glauconite is rare; basal contact is sharp.

146.08 148.60 SHALE: Unit 33 is medium to dark grey, moderately fissile, medium disky shale with rare centimetre-scale clots of granular, emerald-green glauconite; base of unit is gradational.

148.60 151.48 GLAUCONITIC SHALE: Unit 34 is dark grey shale with abundant cm-scale clots of emerald-green glauconite; basal contact is sharp.

151.48 153.51 SHALE: Unit 35 is a dark grey to black, very fissile shale with rare glauconite; basal contact is gradational.

153.51 154.00 SHALY SANDSTONE: Unit 36 is composed of dark grey, poorly sorted, rounded, medium to coarse grained and pebbly quartz within carbonate-cemented clayey matrix; this "chaotic" unit is grain supported and

heterogeneous; wisps of soft mudstone common; rare millimetre-scale shale clasts; variably competent and well indurated to friable; sporadically mottled from bioturbation; pyrite occurs sporadically; bottom contact is sharp and angular. This unit and Unit 38 are considered to be part of the Basal Colorado Sand.

154.00 154.93 MUDSTONE: Unit 37 is composed of a lower black mudstone containing sandy burrows and wisps, separated from an overlying black, homogeneous, massive, carbonaceous mudstone; 2 centimetre interval of coarse grained quartzose sandstone separates the two units; bottom contact is gradational.

154.93 156.81 SANDSTONE: Unit 38 is composed of a lower tan to off-white, medium grained, cross-bedded homogeneous quartzitic sandstone overlain by a black, coarse grained and pebbly quartzose sandstone within muddy matrix; bottom contact is sharp.

156.81 158.41 SILTY SHALE: Unit 39 is light grey homogeneous silty shale containing sporadic clasts of fine sandstone and shale; unit is lightly mottled, probably indicating bioturbation; bottom contact is sharp and angular.

TOP OF MANNVILLE GROUP AT 158.41 METRES.

158.41 160.62 SANDSTONE: Unit 40 is white to off-white fine to very fine grained, cross-bedded, unconsolidated to moderately competent sandstone; contains laminations of darker grey clay; fair to moderate porosity; bottom contact is unknown.

END OF HOLE AT 160.62 METRES.

RHONDA MINING CORPORATION
DETAILED CORE DESCRIPTION
November 8, 1994

DRILL HOLE: OFS93-003 **CLAIM NUMBER: S-127080**

LOCATION, LEGAL: NE Quarter, Section 05, Township 52, Range 18 West of 2nd Meridian

GROUND ELEVATION: 433.9 meters

TOTAL DEPTH: 154.80 metres

CORE SIZE: HQ, 101 millimetres

CORE LOCATION: Saskatoon Field Office

DIP: -090 degrees

DATE STARTED: March 6, 1993

DATE COMPLETED: March 11, 1993

DOWNHOLE GEOPHYSICAL TESTING: BPB Wireline Ltd.

DRILLING CONTRACTOR: Longyear Canada Ltd.

DRILLSITE GEOLOGY: D.E. Jiricka

CORE LOGGED BY: B.C. Jellicoe and K. Leahy

ABANDONMENT STATUS: Cemented lower part of hole; upper part allowed to collapse.

PURPOSE: To test the eastward continuation of the positive magnetic feature drilled in OFS93-004 adjacent to known kimberlite clusters located immediately to the north.

RESULTS: A 8.5 metre thick PK and RPK kimberlite sequence was encountered at the bedrock surface and was cut from -95.12m to -104.05m.

COMMENTS: Bedding and contacts are subhorizontal (90 degree angle to core axis) unless otherwise specified.
All depths are relative to collar elevation.
Abbreviations for kimberlite description are defined in the Textural Classification, Chapter 2.
Stratigraphic Nomenclature for the Colorado Group of Bloch et al (1993) used in this log, see Chapter 1.

CORE DESCRIPTION

00.00 86.80 TILL: This interval was not cored and chip samples were not collected; geophysical logs and driller reports indicate that this interval is composed of interbedded muddy tills and sandy tills beneath a few metres of surficial sandy sediment.

86.80 95.12 TILL: Unit 1 is composed of light greyish-brown silty mud matrix with centimetre scale rock clasts of diverse origin including feldspar, carbonate, and granite; minor kimberlite material is randomly mixed in with rubble at base of the unit; much of the cored material is missing; what remains is strongly calcareous; bottom contact is sharp.

TOP OF BEDROCK AT 95.12 METRES.

95.12 98.00 BEDDED RPK: Unit 2 is fragmented into very coarse to gravelly rubble due to mechanical destruction of weakened material during drilling; the interval is composed of bluish-steel grey, calcareous, fine to coarse grain fining upward subunits with massive to disrupted bedding; abundant, discrete minerals of phlogopite, unidentified white grains, and dark mafic minerals are set within a finer grained, bluish-grey matrix; black amorphous masses of magnetite are common in larger fragments; minor fragments of greenish-brown, medium grain kimberlite with abundant baryte and phlogopite; dark non-magnetic, amorphous, finely granular blotches also occur sporadically; bottom contact probably sharp.

98.00 101.10 BEDDED RPK AND SHALE INTRACLAST BRECCIA: Unit 3 is similar to Unit 2 with dark greenish-grey, well indurated, strongly calcareous kimberlite, which contains discrete millimetre-scale flakes of dark green phlogopite, white baryte blebs, and dark mafic minerals set within a fine grained matrix; shale clasts up to 5 centimetres across are common and are usually proximal to gossanous layers; at 100.03 metres, a 4 centimetre long, light green granular kimberlite clast is incorporated into darker green slightly coarser matrix; the lighter green kimberlite contains wispy distorted clay clasts and is very similar to that occurring below this interval; these two types of kimberlite occur randomly mixed throughout the interval; bottom contact is sharp.

101.10 103.60 MEDIUM TO COARSE PK TUFF: Unit 4 is similar to Unit 3 with fine grained very light green to light steel-grey, calcareous matrix containing pervasive less than 1 millimetre-scale mica and dark mafic minerals; the interval is well indurated and dominantly massive, but intermixed and interbedded medium grain dark greenish-grey kimberlite containing abundant phlogopite, white baryte blebs and dark mafic minerals occurs sporadically; bedding is vague with bed thicknesses ranging from .4 to 1.2 metres; carbonate veining is common in the lower 70 centimetres and is oriented at 060 070 degrees to CA; bottom contact is sharp and irregular.

TOP ST.WALBURG SAND MEMBER AT 103.60 METRES

103.60 104.05 SANDSTONE: Unit 5 is composed of fine grained, light brown to light grey, dominantly homogeneous, massive, and well indurated calcareous sandstone, which contains minor flakes of phlogopite and grains of green, fine to medium grained kimberlite; the bottom contact is indistinct due to fragmented core, but appears to have been sharp.

TOP OF LOWER WESTGATE FORMATION AT 104.05 METRES.

104.05 104.22 MUDSTONE: Unit 6 is light grey, homogeneous, massive, and well indurated. mudstone; bottom contact is sharp.

104.22 105.47 MUDSTONE: Unit 7 is black, massive, soft, mudstone containing abundant oxidized plant remains with associated iron oxide as staining and in granular clusters, and jarosite; light grey sand as wisps and thin lenses are common; bottom contact indistinct.

105.47 107.20 SANDY MUDSTONE: Unit 8 is black to dark grey mudstone intermixed/ interbedded with light grey sand as wisps burrow-fills and laminae; upper portion of unit is dominantly black, carbonaceous mudstone while the bottom 40 centimetres is dark grey, sandier, and more competent; the contact between the two facies is gradational; bottom contact is sharp.

107.20 108.55 SANDY SILTSTONE: Unit 9 is mottled light and dark grey, intensely bioturbated and intermixed sandy siltstone and black mudstone; some intervals retain undisrupted laminations of sand, silt, and mud; borrows are horizontal and vertical ranging up to 1 centimetre across; the basal 30 centimetres are greyish-brown silty sandstone; bottom contact is gradational.

108.55 111.00 SANDY MUDSTONE: Unit 10 is dominantly black, massive, slick, soft, friable carbonaceous mudstone with abundant but variable proportion of tan, very fine grain sand as wisps and lenses; rare mud clasts up to 3 centimetres thick; some bedding planes rich with sporadically pyritized fish debris; some intervals exceptionally organic-rich as indicated by blebby, tufted texture; 14 centimetre thick silty mudstone interbed at 110.92 metres; bottom contact is gradational.

TOP FLOTTEN LAKE SAND AT 111.00 METRES

111.00 116.35 SANDY SILTSTONE: Unit 11 is a succession of stacked subunits including mottled, brownish-grey silty mudstones, and dark brown siltstones with subordinate intermixed dark grey to black mudstone; sand also occurs as an intermixed component in wisps, and vertical and horizontal burrow-fills; bioturbation is pervasive in the coarser grained beds, but sporadic within the dark grey mudstone, which are generally marked by discrete sand; variably pyritized fine fish debris common on some bedding planes; rare fish scales; minor carbonate cementation in thin sand and silt interbeds; fissility varies from friable to massive, generally coeval with a colour change from grey tones to black, respectively; bottom contact is gradational and arbitrarily set at the top of an interval of marked reduction in sand and silt content.

111.00	111.15	-medium grey siltstone; lower contact is gradational.
111.15	111.78	-black shaly mudstone; lower contact is sharp.
111.78	113.81	-medium grey siltstone; 2 centimetre thick sandstone at top of interval; lower contact is gradational.
113.81	114.33	-black silty shaly mudstone; lower contact is sharp
114.33	115.68	-medium grey siltstone; lower contact is gradational.
115.68	116.35	-black shaly mudstone; lower contact is sharp.

116.35 121.78 SANDY SILTSTONE: Unit 12 is similar to Unit 11, but with medium grey, uniformly competent siltstone dominant and characterized by more homogeneous texture and greater content of sand; the interval is an intermixed and partially interbedded complex of mottled medium and dark grey sandy siltstone with subordinate dark grey silty mudstone; bioturbation is pervasive with abundant sediment mixing and discrete burrows filled with very fine sand; bedding is indistinct and no structures were noted; bottom contact is sharp.

117.20 117.30 -carbonate-cemented fine grain sandstone; off-white with minor dark grey laminae of clay; unit shows low-angle crossbedding; contacts are sharp.

119.70 120.10 -interbedded silty sandstone and silty mudstone with centimetre-scale bedding.

TOP JOLI FOU FORMATION AT 121.78 METRES

121.78 127.11 MUDSTONE: Unit 13 is composed of dominantly dark grey weakly carbonaceous mudstone interbedded with rare to minor silty sand beds, lenses, and wisps; unit is heterogeneous and variably bioturbated; bottom contact is gradational.

127.11 127.65 SANDY MUDSTONE: Unit 14 is similar to Unit 13, but with dark grey carbonaceous mudstone containing abundant wisps and thin interbeds of off-white fine grained silty sand; bottom contact is sharp.

127.65 130.10 MUDSTONE: Unit 15 is composed of dominantly dark grey mudstone interbedded with minor silty sand beds, lenses, and wisps generally less than 3 centimetres thick; the interval is weakly to pervasively bioturbated; bottom contact is gradational.

130.10 131.52 MUDSTONE: Unit 16 is black, interbedded blocky and fissile, variably carbonaceous mudstone and shale; contains minor wisps and interbeds of off-white to tan fine grain sand; bottom contact is gradational.

TOP OF SPINNEY HILL FORMATION 131.52 METRES.

131.52 134.87 SANDY MUDSTONE: Unit 17 is a sequence of black, blocky to fissile, fine to moderately disky mudstone containing both glauconitic and quartzose sand intermixed as wisps and clusters, and in thin interbeds of cross-bedded off-white sandstone; mudstone contains abundant silty sand and sandstone clasts in some intervals; unit is transitional between dominance of off-white sand and increasing occurrence of glauconite; bottom contact is gradational.

131.78 131.89 -carbonate-cemented sandstone interbed.

133.62 133.66 -glauconite and carbonate-cemented, ripple cross-bedded, fine grain sandstone interbed; both contacts are sharp.

132.48 132.75 -black mudstone containing glauconite

134.87 137.00 SILTY GLAUCONITIC MUDSTONE: Unit 18 is black, blocky and fissile, disky silty mudstone with common glauconite and carbonate-cemented off-white sand in wisps, cross-bedded fragments, and disturbed interbeds; mudstone is soft and plastic compared to enclosing shales; bottom contact is gradational.

137.00 141.92 GLAUCONITIC MUDSTONE: Unit 19 is massive, blocky, homogeneous, mudstone; contains minor sand wisps; glauconite occurs most frequently as amorphous blotches of granular dark emerald green, also as scattering of dark green, fine grains within the mudstone matrix; bottom contact indistinct, but delineated by the absence of glauconite.

141.92 144.56 MUDSTONE: Unit 20 is massive and blocky, homogeneous, black, greasy texture carbonaceous mudstone; minor wisps or burrows of off-white sand and rare green glauconite; bottom contact is gradational.

144.56 145.62 MUDDY SANDSTONE: Unit 21 is composed of dark grey, poorly sorted, rounded, medium to coarse grained and pebbly quartz within carbonate-cemented clayey matrix; this "chaotic" unit is grain supported and heterogeneous; wisps of soft mudstone common; rare millimetre-scale clasts; variably competent and well indurated to friable; sporadically mottled from bioturbation; pyrite occurs sporadically; bottom contact is sharp and angular.
This unit is considered to be part of the Basal Colorado Sand.

145.62 146.60 SILTY MUDSTONE: Unit 22 is competent, heterogenous, lightly carbonaceous mudstone containing abundant matrix silt, and sand as wisps, burrows, and disturbed thin interbeds; bottom contact is sharp.

TOP OF THE MANNVILLE GROUP AT 144.56 METRES.

146.60 151.20 SILTSTONE: Unit 23 is buff to beige, mottled, massive, and homogeneous siltstone interbedded with medium grey, massive shale; contains buff coloured clasts of siltstone up to 2 centimetres in diameter; bottom contact is sharp and angular.

151.20 153.92 SANDSTONE: Unit 24 is medium to coarse grained, light orange-brown to medium grey, mottled to massive sandstone variably cemented by iron oxides; includes finer grained, more poorly sorted sandstones which are less cemented and cohesive; minor mottling and sediment mixing in portions of the interval; bottom contact is gradational.

153.92 154.80 SILTSTONE: Unit 25 is greyish-brown to brown siltstone with discrete brown sand and grey shale intervals; variable competency; siltstone beds are mottled and bioturbated; bottom contact is gradational.

END OF HOLE AT 154.80 METRES.

RHONDA MINING CORPORATION
DETAILED CORE DESCRIPTION
November 8, 1994

DRILL HOLE: OFS93-009 **CLAIM NUMBER: S-127084**
LOCATION, LEGAL: SW Quarter, Section 06, Township 50, Range 19, West of 2nd Meridian
COLLAR ELEVATION: 449.26 metres
ELEVATION AT E.O.H.: 255.76 metres
TOTAL DEPTH: 193.50 metres
CORE SIZE: HQ, 101 millimetres
CORE LOCATION: Saskatoon Field Office
DIP: -090
DATE STARTED: March 14, 1993
DATE COMPLETED: March 19, 1993
DOWNHOLE GEOPHYSICAL TESTING: BPB Wireline Services
DRILLING CONTRACTOR: Longyear Canada Ltd.
WATER HAULING: J. Bergstrom
DRILLSITE GEOLOGY: D.E. Jiricka
CORE LOGGED BY: B.C. Jellicoe and K. Leahy
ABANDONMENT STATUS: Cemented from surface to end of hole.
PURPOSE: Drill flanks of aeromagnetic cluster of positive anomalies.
RESULTS: Intersected 6m of RPK.
COMMENTS: Bedding and contacts are subhorizontal (90 degree angle to core axis) unless otherwise specified.
All depths are relative to collar elevation.
Abbreviations for kimberlite description are defined in the Textural Classification, Chapter 2.
Stratigraphic Nomenclature for the Colorado Group of Bloch et al (1993) used in this log, see Chapter 1.

CORE DESCRIPTION

00.00 86.86 TILL: This interval was not cored and chip samples were not collected; geophysical logs and driller reports indicate that this interval is composed of interbedded muddy tills and sandy tills beneath a few meters of surficial sandy sediment.

86.86 99.50 TILL: Unit 1 is a poorly sorted till composed of coarse grained to pebbly angular rock fragments set in a brown carbonate cemented silty matrix; rock clasts are of diverse origin and include quartz, feldspar, granite, carbonate, and shale; this interval is very heterogeneous and composed of numerous units differentiated by variations in clast proportion, matrix grain size, and competency; bottom contact is gradational.

99.50 119.00 TILL: Unit 2 is a brown, poorly sorted, unconsolidated, silty sand; interbedded units of greater competency are lithologically similar to Unit 1; approximately 3.5m of core was recovered from the 20m interval sampled; bottom contact is sharp.

BEDROCK CONTACT AT 119.00 METRES - UPPER WESTGATE FORMATION.

119.00 127.46 INTERBEDDED MUDSTONE AND CLAYSTONE: Unit 3 is composed of interbedded claystone and shaley mudstone; the claystone is black, soft, slick massive to blocky, and carbonaceous; interbeds of shaley mudstone are dark grey, poorly fissile, moderately disky, and competent; common subvertical burrows filled with off-white sand; partially pyritized rootlets are common in the black carbonaceous shale, while sandy lenses are sporadic and rare; fish scales are rare; the two lithologies may be gradational or sharply interposed; upper portion of the unit is moderately to intensely fractured without a preferred orientation, probably due to glacial deformation; bottom contact is sharp.

119.00 120.93 -dominantly medium grey blocky claystone.

120.93 122.2 -minor claystone and dominantly medium grey mudstone with minor light grey sandy lenses, burrows, and laminae scattered throughout.

122.26 122.70 -dark grey, massive, blocky, silty mudstone.

122.70 124.12 -dark grey, massive, blocky, slightly silty mudstone.

124.12 127.46 MUDSTONE: Unit 4 is dark grey, slightly fissile to flaggy, weakly fine disky, carbonaceous clayey-mudstone; less competent than unit above, fractured into centimetre and less shards; bottom contact gradational.

124.96 127.46 -dark grey to black, moderately fissile, carbonaceous mudstone.

127.46 128.70 MUDSTONE: Unit 5 is a black, soft, gummy to chunky mudstone; the unit gradually becomes harder and slightly more fissile up-hole with a corresponding decrease of soft mud interbeds; sand-filled burrows are common in the upper, more competent portion of the interval; bottom contact is gradational.

TOP OF ST. WALBURG SANDSTONE AT 128.70 METRES

128.70 130.20 SANDY MUDSTONE: Unit 6 is composed of centimetre-scale interbedded dark grey silty mudstone and light-greyish to white fine grain sandstone; the two lithotypes are variably bioturbated resulting in mottled, heterogeneous, chunky, intermixed sandy/silty mudstone; bottom contact sharp.

130.20 131.08 FINING UPWARDS MUDSTONE/SANDSTONE: Unit 7 is composed of black, soft, gummy to chunky mudstone overlying medium to coarse grained, variably calcareous and pyritiferous arenitic sandstone; variations in cementation caused a range of texture from friable to well-indurated; contains abundant laths of pyrite up to 2 millimetres in length in the sandstone; bottom contact is sharp beneath greenish-grey subunit of rounded shale pebble lag (pebbles less than .5

centimetres in diameter) suspended within sandstone matrix; bottom contact is gradational.
130.20 130.80 -black mudstone.
130.80 131.08 -variably carbonate-cemented sandstone.

131.08 134.25 SANDY MUDSTONE: Unit 8 is a very soft, black mudstone with variable amounts of abundant coarse grained quartz sand and pyrite; unit grades downward to sandy pyritiferous mudstone at the base of the unit; bottom contact is sharp.
131.08 131.96 -mudstone with common sandy lenses, wisps, burrows, and laminae
131.96 134.25 -sandy mudstone with abundant mottled sandy interbeds and lenses

134.25 134.90 MUDSTONE: Unit 9 is a black, uniformly competent, massive, hard mudstone with minor sand and silt intermixed and concentrated in small lenses; bottom contact is sharp.

134.90 135.60 SANDY MUDSTONE: Unit 10 is similar to unit 9, but with a greater proportion of coarse grained quartz sand; bottom contact is sharp.

TOP KIMBERLITIC STRATA AT 135.60 METRES

135.60 136.61 MASSIVE RPK: Unit 11 is a light olive green, fine to medium grained, massive, calcareous, and moderately consolidated material, which contains small millimetre-scale rounded clay clasts; grains are rounded and set within sporadic fine grained matrix material of the same apparent composition (probably antigorite); the unit is sparsely veined in the lower 5 centimetres with carbonate and massive sulphides at 020 to 040 to CA; bottom contact is gradational.

136.61 139.95 GRADED AND BEDDED RPK WITH SHALE INTRACLAST BRECCIAS: Unit 12 is composed of mixed light to medium olive-green and dark grey, coarse grained material; variable alteration includes intensive veining by carbonates and massive sulphides, cementation (welding), and patchy colour changes (possibly due to serpentinization and other recrystallizations); grain constituent proportions are variable from dominantly mottled green and white grains to increasing amounts of phlogopite and dark unidentified minerals in patches; bottom contact is sharp and marked by a thin, coarse pebble lag of serpentinized clasts.

139.95 141.55 BEDDED RPK AND INTRACLASTIC SHALE BRECCIAS: Unit 13 is similar to unit 10 with variable alteration of kimberlite resulting in a crumbly, decrepitated, rock infused with iron oxides, particularly over a 20 centimetre interval below 141.0 metres; this severely altered rock is greenish-brown and contains much intermixed clay material; bottom contact is sharp.

TOP LOWER WESTGATE FORMATION AT 141.55 METRES

141.55 142.76 SHALEY MUDSTONE: Unit 14 is composed of black, poorly fissile, fragmented, altered, disky, shaly mudstone, with subordinate amounts of oxide-rich brown silty sand; unit is weakly calcareous in the upper 2 centimetres; alteration including induration and brown blotchiness fades towards the bottom contact where the mudstone is blockier and softer; bottom contact is sharp.

142.76 143.31 SHALEY MUDSTONE: Unit 15 is a medium grey, massive to poorly fissile, disky, mica-rich, shaly mudstone with common lenses, burrow-fills, and wisps of off-white brownish sand; fish scales and very rare fish debris; bioturbation is expressed as mottling and as sub-horizontal lined, sand-filled burrows; bottom contact gradational.

143.31 146.17 MUDSTONE: Unit 16 is dark grey to black, massive, blocky mudstone; texture of mudstone ranges from chunky, soft, and slick, to more massive and competent with weakly pyritized rootlets; bioturbation is expressed as mottling and as sub-horizontal lined, sand-filled burrows; bottom contact sharp.

143.31 144.33 -black to dark grey, moderately hard, competent mudstone
144.33 144.73 -black, massive, carbonaceous, sandy mudstone.
144.73 146.17 -medium to dark grey, massive, uniformly competent mudstone; slight brecciation in disturbed zone between 145.30 and 145.52.

146.17 150.50 SHALEY MUDSTONE: Unit 17 is medium to dark grey, disky, shaley mudstone with rare sandy wisps; bottom contact sharp.

146.88 146.96 -light grey bentonite
146.96 147.34 -interbedded shaley mudstone and thin, light grey sandstone.
147.34 147.75 -medium to dark grey, disky, shaley mudstone.
148.95 149.00 -light grey bentonite

TOP FLOTTEN LAKE SANDSTONE AT 150.50 METRES

150.50 151.25 SANDY MUDSTONE: Unit 18 is mottled, well-bioturbated, intermixed light grey sand and dark grey mudstone; sand also occurs as wisps and in lined sub-horizontal burrows; unit grads downwards with increasing abundance of medium grained sand; bottom contact gradational.

151.25 152.63 SANDSTONE: Unit 19 is mottled, well-bioturbated, intermixed light grey and sand and dark grey mudstone; sand is dominant constituent for most of the interval, but overall the unit is fining upwards; burrows are sub-horizontal to vertical and are both lined and unlined; bottom contact sharp.

TOP OF JOLI FOU FORMATION AT 152.63 METRES

152.63 162.40 SHALEY MUDSTONE: Unit 20 is dark grey, often homogeneous, moderately hard, massive to poorly fissile, disky, shaly mudstone; mudstones

contain minor, though variable, proportions of off-white to tan sand as wisps, burrow-fills, thin (1-2 centimetre) interbeds, and as a constituent in sandy mudstone intervals; overall, this heterogeneous unit is composed of massive, disky, shaley mudstones with subordinate gradationally interbedded sandy mudstones; mudstones become more carbonaceous and black in some intervals; pyrite is rare; fish scales and thin lag deposits of granular fish debris rare; bottom contact gradational.

153.33 153.34 -unconsolidated fine to medium grained sand

155.93 156.01 -well indurated, clay-cemented (+/- iron) fine grain sandstone

156.63 156.69 -fine grain sandstone with common iron oxides

157.85 157.89 -well indurated, clay-cemented (+/- iron) fine grain sandstone

162.40 164.33 SANDY MUDSTONE: Unit 21 is similar to unit 20 shaley mudstone, but with common to abundant mottled and intact silty fine grain sandstone interbeds; unit is mottled and disturbed by common bioturbation; bottom contact irregular due to bioturbation.

164.33 165.05 SHALEY MUDSTONE: Unit 22 is dark grey, homogeneous, moderately hard, massive to poorly fissile, disky, shaly mudstone with irregular bedding variations; bottom contact sharp.

165.05 165.55 SANDY MUDSTONE: Unit 23 is similar to unit 20 shaley mudstone, but with common to abundant mottled and intact silty fine grain sandstone interbeds; unit is mottled and disturbed by common bioturbation; bottom contact irregular due to bioturbation.

165.55 166.80 SHALEY MUDSTONE: Unit 24 is dark grey, homogeneous, moderately hard, massive to poorly fissile, disky, shaly mudstone with irregular bedding variations; bottom contact sharp.

166.80 167.30 SANDY MUDSTONE: Unit 25 is similar to unit 20 shaley mudstone, but with common to abundant mottled and intact silty fine grain sandstone interbeds; unit is mottled and disturbed by common bioturbation; bottom contact irregular due to bioturbation.

167.30 170.61 SHALEY MUDSTONE: Unit 26 is dark grey, moderately hard, massive to poorly fissile, disky, shaly mudstone with irregular bedding variations; minor sand lenses and wisps occur throughout; bottom contact not determined.

TOP OF SPINNEY HILL MEMBER AT 170.61 METRES

170.61 173.00 GLAUCONITIC SHALEY MUDSTONE: Unit 27 is massive to poorly fissile, disky, shaly mudstone with irregular bedding variations; common to abundant light green to emerald green glauconite as wisps and small amorphous masses in the mudstone matrix; light grey sandy wisps and lenses occur along

bedding planes in variable abundance from rare to moderately abundant; bioturbation increases with increase of sand abundance; bottom contact sharp.

173.00 173.43 SANDY MUDSTONE: Unit 28 is dark grey, massive sandy mudstone with very rare glauconite and common to abundant sandy wisps and lenses, often mottled from bioturbation; bottom contact gradational.

173.43 175.72 SILTY MUDSTONE: Unit 29 is composed of dark grey, massive, weakly disky to uniformly competent, silty mudstone with minor medium grey sandy lenses; bottom contact id sharp.

175.72 176.30 SHALEY MUDSTONE: Unit 30 is dark grey to black, massive to poorly fissile, moderately disky, shaley mudstone; minor granular glauconite occurs sporadically in centimetre-scale amorphous patches; bottom contact sharp.

176.30 177.05 SANDY MUDSTONE: Unit 31 is dark grey, massive, competent, sandy mudstone with very minor glauconitic sandy wisps and lenses, often mottled from bioturbation, but also in moderately indurated, centimetre-scale laminar clasts; bottom contact gradational.

177.05 179.10 SHALEY MUDSTONE: Unit 32 is black, massive to poorly fissile, moderately disky, shaley mudstone; minor granular glauconite occurs rarely as centimetre-scale amorphous patches, and in moderately indurated, glauconitic fine grain sand clasts and lenses; bottom contact sharp.

179.10 180.35 WEAKLY GLAUCONITIC SHALEY MUDSTONE: Unit 33 is medium to dark grey, massive to poorly fissile, moderately disky, shaley mudstone; emerald to kelly green glauconite common as mottled granular clusters on and between bedding planes; rare fish debris and very thin wisps of very fine grain light grey sand along bedding planes oriented at 90 degree to core axis; bottom contact is gradational.

180.35 181.06 SHALEY MUDSTONE: Unit 34 is shaley mudstone similar to Unit 33, but with very rare glauconite; bottom contact is sharp.

181.06 181.70 GLAUCONITIC SILTY MUDSTONE: Unit 35 is mottled green and medium grey massive mudstone; granular glauconite is pervasive in wisps and irregular patches throughout the unit; bottom contact is sharp.

181.70 182.25 SHALEY MUDSTONE: Unit 36 is similar to Unit 34 with poorly fissile, disky, shaley mudstone with trace glauconite and minor very fine grain sand content; bottom contact is sharp.

182.25 184.40 COARSENING UPWARD MUDSTONE/SANDSTONE: Unit 37 is a coarsening upward sequence from massive to poorly fissile, disky, shaley mudstone with up to 15 per cent interlayered, weakly glauconitic, very fine grain

sandstone lenses and wisps, through sandy siltstone to glauconitic sandstone at the top; contacts are gradational with increase of sand and silt upwards to the top of the unit; overall glauconite content increases upwards with carbonate-cemented rock prevalent in the upper 36 centimetres; basal contact of unit is sharp.

182.25 182.60 -green and white weakly cross-bedded, glauconite-rich fine grain sandstone; bedding predominately at 80 degree angle to core axis; upper 5 centimetres is massive, hard carbonate-cemented sandstone with variable carbonate-cemented lenses of sandstone within glauconitic sandy siltstone in the lower 30 centimetres; bottom contact is marked by loss of carbonate-cemented sandstone fragments/wisps.

182.60 183.24 -medium grey massive siltstone with abundant intermixed disseminated and interlayered glauconite and light grey very fine grain sand in wisps and thin lenses; bottom contact is gradational.

183.24 184.40 -massive dark grey mudstone with up to 15 per cent interlayered weakly glauconitic very fine grain sand and silt; bottom contact is sharp.

184.40 185.05 SILTY SANDSTONE: Unit 38 is a mottled light and medium grey, massive to poorly laminated, heterogeneous, moderately well sorted, variably consolidated silty sandstone; sandstone is composed of dominantly very fine to fine grain, rounded quartz grains; unit is variably silty and carbonate-cemented.

184.40 184.56 -wavy laminated silt and very fine grain sand with up to 30 per cent clayey matrix; trace glauconite; subunit is hard and finer grained towards base with well-indurated mudstone.

184.56 184.89 -well indurated, carbonate-cemented very fine grain sandstone; bottom contact is gradational with decrease in carbonate, and sand as lenses and wisps within muddy siltstone.

184.89 185.05 -muddy siltstone with up to 30 per cent very fine to tine grain light grey sand in wisps and lenses; wisps and lenses are weakly carbonate-cemented; bottom contact is gradational.

185.05 186.06 SANDY MUDSTONE: Unit 39 is medium to dark grey, hard, massive to poorly fissile mudstone with up to 20 per cent silt and very fine grain sand in wisps and lenses; bottom contact is sharp.

186.06 186.46 SANDSTONE: Unit 40 is mottled light and medium grey, massive, heterogeneous, poorly sorted, variably consolidated sandstone; the sandstone is 90 per cent very fine to fine grain subrounded quartz with minor isolated coarse grains and granules of mildly pitted quartz and rare unidentified dark minerals; rare fish debris; carbonate cementation is variable from pervasive in the upper 21 centimetres decreasing to sporadic in lenses and wisps of sandstone in the lower 19 centimetres; the unit appears bioturbated; bottom contact is sharp.

186.46 186.62 MUDSTONE: Unit 41 is dark grey, massive, well-consolidated, uniformly competent mudstone with up to 30 per cent wisps and lenses of light grey, very fine grain sand; bottom contact is sharp.

186.62 186.70 MUDDY SANDSTONE: Unit 42 is dark grey massive, poorly sorted, mud supported sandstone; unit is composed of coarse to fine, subrounded to angular grains of quartz, and minor to trace oxidized pyrite and amorphous gossan; "chaotic"; upper and lower contacts are sharp.

186.70 186.94 SHALEY MUDSTONE: Unit 43 is dark grey, moderately fissile, disky, shaley mudstone with interbedded laminae of very fine to fine grain light grain sand; bottom contact is sharp.

186.94 186.99 SANDSTONE: Unit 44 is light grey, massive, subrounded, very fine grain, quartzose sandstone; trace pyrite in millimetre-scale clusters; bottom contact is sharp.

186.99 187.27 MUDSTONE: Unit 45 is dark grey, massive, consolidated mudstone with minor light grey sand in wisps and lenses; a 1 centimetre thick lens of sand occurs within 3 centimetres of the top of the unit; bottom contact is sharp with 2 to 3 centimetres of coarse grained mud-supported sandstone underlying 1 centimetre thick iron stained fine grained sandstone lens; the coarse grained sandstone lies directly over light grey, massive sandstone.

182.27 187.13 SANDY MUDSTONE: Unit 46 is interbedded silty and sandy mudstones and mottled muddy sandstones; colour ranges from black of the mudstones to off-white of the well-indurated sandstones; sand occurs as wisps, lenses, and burrow-fills; mudstone is carbonaceous and becomes flaky with increasing organic matter and silt content; glauconite common in the upper portion, decreasing gradationally in the lower portion of the unit; all lithotypes variably indurated; pyrite common as disseminated grains and large globular masses; bioturbation and mottling common; includes a "chaotic" unit – position not noted; bottom contact sharp and marked by rip-up clasts of brown sandstone from the underlying unit.

TOP OF MANNVILLE GROUP AT 187.13 METRES

187.13 188.92 SANDY SILTSTONE: Unit 47 is coarsening upward interbedded/ intermixed beige sandstone, siltstone, and dark grey mudstone; units are mottled and chaotically laminated; dominantly soft; bottom contact gradational.

188.92 189.92 SILTSTONE: Unit 48 is dark brownish grey, well-indurated siltstone; massive, probably severely bioturbated; unidentified white grains along some bedding planes; bottom contact gradational.

189.92 193.50 SANDSTONE: Unit 49 is dominantly sandstone ranging in colour from black to light grey; interbedded and intermixed silt and light grey mudstone is common in this very heterogeneous unit; coal fragments common ranging up to several cm long; pyrite common in carbonaceous interbeds; lithotypes are dominantly soft, but some sands are pyritized; bottom contact unknown.

END OF HOLE AT 193.50 METRES.

RHONDA MINING CORPORATION
DETAILED CORE DESCRIPTION
November 8, 1994

DRILL HOLE: OFS93-010 **CLAIM NUMBER: S-127084**
LOCATION, LEGAL: SW Quarter, Section 06, Township 50, Range 19, West of 2nd Meridian
COLLAR ELEVATION: 448.82 metres
ELEVATION AT E.O.H.: 249.82 metres
TOTAL DEPTH: 199.00 metres
CORE SIZE: HQ, 101 millimetres
CORE LOCATION: Saskatoon Field Office
EQUIPMENT LEFT IN HOLE: 27.43 metres HW casing
DIP: -090
DATE STARTED: March 20, 1993
DATE COMPLETED: March 26, 1993
DOWNHOLE GEOPHYSICAL TESTING: Roke Oil Enterprises Ltd.
DRILLING CONTRACTOR: Longyear Canada Ltd.
WATER HAULING: J. Bergstrom
DRILLSITE GEOLOGY: D.E. Jiricka
CORE LOGGED BY: B.C. Jellicoe and K. Leahy
ABANDONMENT STATUS: Cemented from surface to end of hole.
PURPOSE: Drill flanks of aeromagnetic cluster of positive anomalies.
RESULTS: Intersected RPK deposits at 4 separate horizons.
COMMENTS: Bedding and contacts are subhorizontal (90 degree angle to core axis) unless otherwise specified.
All depths are relative to collar elevation.
Abbreviations for kimberlite description are defined in the Textural Classification, Chapter 2.
Stratigraphic Nomenclature for the Colorado Group of Bloch et al (1993) used in this log, see Chapter 1.

CORE DESCRIPTION

00.00 112.47 TILL: This interval was not cored and chip samples were not collected. Geophysical logs and driller reports indicate that this interval is composed of interbedded muddy tills and sandy tills beneath a few meters of surficial sandy sediment.

112.47 114.34 TILL: Unit 1 is dark brown, mud matrix supported, poorly sorted, carbonate-cemented till with sporadic though common millimetre-scale clasts and grains of diorite, granite, carbonate, quartz, and feldspar; bottom contact is gradational.

114.34 116.82 TILL: Unit 2 is tan to light brown, matrix supported, poorly sorted, carbonate-cemented till with dominant silty/clay-rich matrix and subordinate

medium to coarse grain sand component up to 30 per cent; contains sporadic, though common to abundant, millimetre-scale and rare centimetre-scale grains and clasts of diorite, granite, carbonate, quartz, and feldspar; bottom contact is sharp marked by 5 centimetre thick quartz diorite boulder; fracture oriented at 25 degree angle to core axis at 115.49 metres.

116.82 117.24 TILL: Unit 3 is similar to Unit 2, but with a medium brown, silty/sandy matrix component dominant; bottom contact is sharp.

117.24 118.00 TILL: Unit 4 is similar to Unit 2 with silty/clay-rich matrix and abundant millimetre- and centimetre-scale clasts and grains of diorite, granite, carbonate, quartz, and feldspar; fracture oriented at 60 degree angle to core axis at 117.42 metres; bottom contact sharp and angled at 15 degrees to core axis.

118.00 121.34 DEFORMED GLACIAL MUDSTONE: Unit 5 is dark brownish-black, massive, homogeneous, friable to well-consolidated, blocky to brecciated and jointed mudstone; fabric consisting of brecciation and irregular fracturing with weakly slickensided faces occur at 45 to 50 degree angle to core axis; mudstone locally contains small pebbles and granules of diverse origin similar to those found in the tills; bottom contact is sharp.

121.34 122.36 TILL: Unit 6 is similar to Unit 4 with silty/clay-rich, carbonate-cemented matrix hosting subordinate quartzitic sand, and granules and pebbles of diverse origin; bottom contact presumed sharp, but difficult to ascertain in fragmented core.

122.36 126.44 DEFORMED GLACIAL MUDSTONE: Unit 7 is similar to Unit 5 with black, massive, homogeneous, friable to well-consolidated, blocky to brecciated mudstone; rare grains and granules of diverse origin occur sporadically; slickensided fractures and pattern of brecciated fragments oriented at about 45 degree angle to core axis; mudstone surfaces have pervasive, less than millimetre-sized blebs of sulfate; bottom contact is sharp and marked by a 10 centimetre thick diorite boulder.

The presence of slickensided fractures, brecciation of the mudstone, and the alternation of till and mudstone immediately over top of the bedrock indicates the strong probability that units 5, 6, and 7 were deformed by low angle thrusting beneath a glacier.

BEDROCK CONTACT AT 126.44 METRES - UPPER WESTGATE FORMATION.

126.44 131.58 SHALEY MUDSTONE: Unit 8 is composed of dark grey, massive to poorly fissile, disky, friable to well-consolidated, shaley mudstone; up to 5 per cent silty, very fine grain sand lenses, laminae, and wisps occur sporadically along bedding planes; up to 85 per cent of the interval is deformed by variable weak to moderate brecciation and shear, which has imparted fracturing and oriented rock fabric at 60 to 80 degree angle to core axis; 3 centimetre bentonite within

deformed, chunky mudstone at 127.84 metres; bottom contact is gradational over 20 centimetres to undeformed massive, consolidated mudstone below.

131.58 136.04 MUDSTONE: Unit 9 is medium to dark grey, homogeneous, uniformly competent, massive mudstone; contains rare, less than millimetre-scale fish scales on occasional bedding planes; when evident, rare bedding is oriented at 90 degree angle to core axis; bottom contact is gradationally interbedded with underlying shaley mudstone.

136.04 139.54 SHALEY MUDSTONE: Unit 10 is composed of interbedded, dark grey, massive to poorly fissile, disky, moderately hard, shaley mudstones and massive, hard mudstones; silt and very fine grain sand content increase towards the base from about 139.40 to 139.54 metres in a fining upwards sequence; mudstones (up to 75 per cent) are interbedded with sharply bounded, subordinate shaley mudstone beds; bottom contact is gradational.

139.54 140.35 SILTY MUDSTONE: Unit 11 is a medium grey, massive to chunky, silty mudstone; silt content increases towards the base; bottom contact was not recovered in core.

140.35 141.65 MUDSTONE: Unit 12 is a dark grey to black, homogeneous, slightly disky, moderately to very hard, dominantly massive, consolidated mudstone with abundant silty mudstone interbeds; less than 1 millimetre in size micas present in matrix (less than 5 per cent) along with few isolated silt grade quartz grains; organic detritus is present throughout the mudstone with a few horizons rich in large fish scales (up to 12 millimetres diameter); thin centimetre-scale oxidized rootlets are common on bedding planes; rare pods of pyritized sand up to 1 centimetre across; bottom contact is sharp.

TOP OF UPPER KIMBERLITE SEQUENCE AT 141.65 METRES.

141.65 142.85 TUFFACEOUS SILTY MUDSTONE: Unit 13 is composed of tan to greenish-brown siltstone with minor interbeds of ripple cross-bedded fine sand variably cemented by dominantly carbonate and some pyrite; silt is pervasive in some layers, but lacking in others and is set within a pale green sucrosic, soft mudstone matrix; unit contains small rounded carbonate grains (less than .5 millimetres) with subordinate phlogopite and biotite (up to 10 per cent), and minor quartz along bedding planes; pyrite occurs as a sporadic cement, fine veins, and in 1 to 3 millimetres size clusters; the unit coarsens downwards with an increase in abundance of fine to medium grain sand; lower 10 centimetres of silty sandstone is well-indurated and carbonate cemented; sparse carbonate veining at 20 to 60 degree angle core axis occurs in some layers, bottom contact is sharp.

142.85 144.91 MUDSTONE: Unit 14 is a black, massive, homogeneous, uniformly competent mudstone with common rootlets and oxidized plant debris present; bottom contact is sharp.

144.91 147.68 MUDSTONE: Unit 15 is composed of interbedded black to dark greenish-black, unconsolidated mud and dark grey, poorly fissile, uniformly competent, moderately-well consolidated shale; shale contains common rootlets and some silt wisps; occasional pyritized burrows; lower 45 centimetres has disturbed bedding with heterogeneous cementation of sandier intervals (less than 5 centimetres thick), shale clasts, and greasy texture mudstone, also oxidized pyrite and mica grains in this interval; rich in fish debris; sporadic bioturbation with some burrow-fills of off-white fine sand; unit marks the beginning of intercalation of massive competent shaley mudstone lithotype and an increasing occurrence of mudstone with internal bedding variations (disky); this lithotype characterized by alternation of massive, competent mudstone with cm-scale lenses and mottled disks of softer mudstone; bottom contact is sharp.

144.91 146.70 massive, competent, dark grey mudstone

146.70 147.49 massive, competent, dark grey silty mudstone grading downward to dark greenish-black, kimberlitic mudstone

147.49 147.68 moderately consolidated kimberlitic mudstone

147.68 149.39 TUFFACEOUS SILTY SANDSTONE: Unit 16 is an olive green, planar and ripple cross-bedded, fine grain kimberlitic sandstone with a lower base of silt laminated sandstone 15 centimetres thick; matrix is composed of dark greyish green clay material with sporadic rounded fine clasts (1 to 3 millimetres in size) of carbonate and serpentine; other constituent clasts of coarse grain to pebble size include quartz, rounded shale grains, micas, and rare garnets; hummocky cross-stratification is present in the coarser subunits; above the silty sandstone layer and also within the upper 20 centimetres of the unit are intervals of random carbonate veining; bedding is disrupted at 148.75 metres by a 24 millimetre diameter, rounded, internally fractured shale bomb; basal .1 metres is more muddy with fewer silt laminations; bottom contact is sharp.

148.75 coarse, discontinuous gravel beds are common and they are composed of about 50 per cent quartz, minor mica, and sub angular shale clasts.

149.39 150.80 SHALEY MUDSTONE: Unit 17 is medium disky with subtle, less than centimetre thick interbeds of dark grey, moderately competent, poorly fissile, mica-rich shale and softer bedded mudstone; sandy burrow fills and lined burrows are common; oxidized rootlets are variably abundant from rare to common as centimetre-scale thin laths and rods; unit becomes silty near the base; bottom contact is sharp.

150.80 151.55 MUDDY SANDSTONE: Unit 18 is composed of clast-rich, unconsolidated sand thoroughly intermixed with black, gummy, plastic unlithified mud; clasts are of 75 to 95 per cent subrounded quartz with some magnetite, shale grains, and micas; unit grades downward to sandy mudstone; bottom contact is gradational.

151.55 153.49 MUDSTONE: Unit 19 is black, blocky mudstone with abundant wisps and lenses of intermixed sand; mudstone is less competent than those above with a greater component of disky bedded mudstone; rootlets and burrows are common; fractures oriented at 80 to 90 degree angle to core axis are present throughout; bottom contact is sharp below a 2 centimetre thick silty zone.

153.49 153.62 SILTY SHALE: Unit 20 is finely mottled, light and dark grey, uniformly competent, moderately hard, mica-rich silty shale with minor pyrite; unit contains a few gravel grade clasts of a pale greenish, fine grain kimberlitic (?) material; bedding planes show oriented mica flakes (less than 1 mm across), as well as discontinuous, millimetre-scale bands of pyrite; bottom contact is sharp.

153.62 153.77 SHALEY MUDSTONE: Unit 21 is a dark grey, fine disky, massive to poorly fissile, moderately hard shaley mudstone with minor amounts of mica; millimetre-scale laminae of pyrite are present; bottom contact is milled.

153.77 153.92 TUFFACEOUS SILTS: Unit 22 is a medium to dark grey, coarse grain, massive kimberlite; unit appears grain supported with clasts and granules of shale and discrete minerals up to 5 centimetres across including abundant mica, quartz, carbonate, white minerals (plagioclase?), and dark, unidentified minerals; subordinate matrix is composed of mottled medium and dark greenish-grey, very fine grain material (probably antigoritic); two horizontal carbonate thread veinlets occur within this unit, with minor pyrite near the vein margins; bottom contact is sharp; top contact is indiscernible due to poor core recovery.

153.92 154.00 SHALE: Unit 23 is similar to Unit 21, but is slightly coarser and contains a greater proportion of mica; bottom contact is milled.

154.00 154.19 TUFFACEOUS SILT: Unit 24 is similar to Unit 22, but is lighter grey; unit may have been part of a fining upward sequence with Unit 23; bottom contact is sharp.

154.19 154.43 TUFFACEOUS SILTS AND SANDS: Unit 25 is similar to Unit 24, but fines upward in the upper 5 centimetres; unit contains a subrounded 4 centimetre long clast of fine grain kimberlitic material; fine horizontal veinlets are common; bottom contact is sharp.

154.43 155.38 TUFFACEOUS CONGLOMERATE: Unit 26 is similar to Unit 25, but is dark grey and very coarse grain with subordinate greenish-grey matrix; matrix becomes visibly calcareous with granules of carbonate material at 154.97 metres; large clasts (up to 2 centimetres across) of kimberlite similar to the groundmass and of shale are common within this unit; a 10 centimetre thick band of indurated kimberlite is present at 154.68 metres; bottom contact is sharp.

155.38 155.53 SHALE AND KIMBERLITE: Unit 27 is composed of dark grey shale with thin, discrete beds of kimberlite similar to Unit 26; shale shows disturbed bedding contorted around large shale clasts; upper part of the unit is massive shale interspersed with sub-horizontal veins of carbonate; basal part of the unit is composed of shale clast breccia; bottom contact is sharp.

TOP OF LOWER WESTGATE FORMATION AT 155.53 METRES.

155.53 158.10 SHALEY MUDSTONE: Unit 28 is a black to dark grey, medium disky shaley mudstone with common to rare silty sand lenses and wisps; mudstone becomes more mottled and bioturbated with increasing sand content; randomly oriented fish scales are present within the mudstone, while comminuted fine fish debris occurs along infrequent, vaguely defined bedding planes; rare fish teeth, up to 3 millimetres long, are present within the unit; rare pyrite occurs in small 1 to 3 millimetre clusters and as pyritized rootlets; bottom contact is gradational.

158.10 158.40 MUDSTONE: Unit 29 is medium grey, massive, uniformly competent, well-consolidated mudstone; bottom contact is sharp.

TOP OF FLOTTEN LAKE SANDSTONE AT 158.40 METRES.

158.40 159.10 SILTY SHALEY MUDSTONE: Unit 30 is medium to dark grey, weakly fine disky, massive shaley mudstone; light grey, homogeneous sandy wisps, lenses, and laminae are common in the lower 40 centimetres; thin, very light grey, sandy layers are common in the upper 30 centimetres and are composed of subrounded very fine grain quartz, rare unidentified dark minerals, and millimetre-scale mica flakes; layers range from millimetre-scale to laminae and parallel to bedding at 90 degree angle to core axis; bottom contact is sharp.

159.10 159.78 MUDSTONE: Unit 31 is medium grey, massive, uniformly competent, well-consolidated mudstone; rare, light grey, very fine grain sand occurring as wisps, lenses, and laminae define bedding oriented at 90 degree angle to core axis; bottom contact is gradational.

159.78 160.80 SANDY MUDSTONE: Unit 32 is medium to dark grey, massive, uniformly competent, well-consolidated mudstone; light grey sandy wisps, lenses, and laminae are common and define bedding oriented at 90 degree angle to core axis; bottom contact is sharp.

160.80 161.20 SILTY SANDSTONE: Unit 33 is very light grey and dark grey, mottled, uniformly competent, fine to medium grain sandstone with intermixed silt and disturbed clay laminations; contains clay clasts; sediment is well mixed without visible burrows; interbedded mudstone intervals of less than 10 centimetres interrupt the sandstones; bottom contact is sharp.

161.20 161.60 FINING UPWARDS SILTY SANDSTONE/SHALEY MUDSTONE: Unit 34 is a medium to dark grey, fining upwards sequence with about 20 centimetres of basal massive silty sandstone overlain gradationally by muddy siltstone to disky, shaley mudstone; bottom contact sharply interbedded with shaley mudstone below.

161.20 161.40 -silty shaley mudstone

161.40 161.60 -silty sandstone

161.60 163.57 FINING UPWARDS SILTY SANDSTONE/SHALEY MUDSTONE: Unit 35 is composed of an upper 70 centimetres of dark grey, massive to poorly fissile, disky, shaley mudstone with chondrite burrows and weakly disturbed shale on shale bedding contacts; less than centimetre-scale sand clasts are common in the mudstone, as well as wisps and lenses of silty sand; lower 1.27 metres of the unit comprises about 20 centimetres of massive silty sandstone with pervasive bioturbation marked by lined and unlined vertical and horizontal burrows (planolites, thalassinoides, and others) overlain gradationally by muddy siltstone to silty, disky, shaley mudstone; bottom contact is sharp.

161.60 162.32 -shaley mudstone

162.32 162.34 -very fine grain white sandstone interlaminated with darker silty sandstone

162.34 163.37 -silty mudstone and muddy siltstone

163.37 163.57 -silty sandstone

163.57 165.26 MUDSTONE: Unit 36 is dark grey to black, massive to poorly fissile, disky, shaley mudstone; rare, centimetre-scale silty sandstone interbeds; bottom contact is gradational.

165.26 166.00 SILTY SANDSTONE: Unit 37 is light grey and dark grey, mottled, uniformly competent, fine to medium grain sandstone with intermixed silt and disturbed clay laminations; contains common less than centimetre-scale mudstone clasts; sediment is well mixed without visible burrows; interbedded mudstone intervals of less than 10 centimetres interrupt the sandstones; bottom contact is sharp.

166.00 167.23 SHALEY MUDSTONE: Unit 38 is black, blocky and massive to poorly fissile, disky mudstone; silt and sandstone wisps, lenses, and burrows are rare to common; silty mudstone intervals usually less than 5 centimetres thick are common; fish debris and rootlets are rare; minor pyrite; bottom contact is gradational.

167.23 167.66 SANDY SHALEY MUDSTONE: Unit 39 is similar to Unit 38, but with abundant light grey sandy wisps, lenses, and laminae; bottom contact is gradational.

TOP OF JOLI FOU FORMATION AT 167.66 METRES.

167.66 169.25 SHALEY MUDSTONE: Unit 40 is medium grey, massive to poorly fissile, moderately disky, shaley mudstone with rare wisps of light grey sand; bottom contact is gradational.

169.25 170.78 SHALEY MUDSTONE: Unit 41 is shaley mudstone similar to Unit 40, but with minor interbedded silty sandy layers; lower 72 centimetres is fining upwards from thin bedded, very fine grain sandstone to interbedded silty sandstone and shaley mudstone; bottom contact is sharp.

170.78 174.20 SHALEY MUDSTONE: Unit 42 is medium grey, massive to poorly fissile, fine to medium disky, shaley mudstone; minor to rare sandy wisps, lenses, and laminae; bottom contact is sharp.

174.20 175.34 SANDY SHALEY MUDSTONE: Unit 43 is medium grey, massive to poorly fissile, disky, shaley mudstone with abundant sand lenses; unit is fining upwards overall with a decrease in sand lenses towards the top; bottom contact is sharp.

175.34 175.91 SANDY MUDSTONE: Unit 44 is mottled, uniformly competent, intermixed, light grey sand and dark grey mudstone; top and bottom contacts are gradational.

175.91 177.17 SHALEY MUDSTONE: Unit 45 is medium grey, moderately disky shaley mudstone with minor sand lenses; bottom contact is sharp.

177.17 178.00 SHALEY MUDSTONE: Unit 46 is black, massive to poorly fissile, competent to chunky unconsolidated, slick clayey-mudstone; contains thin silt laminations and sporadic clasts of sandstone; rare fish debris along some bedding planes; 83 centimetre interval of chunky, poorly consolidated claystone (brecciated, soft deformation); bottom contact is sharp.

178.00 178.75 SANDY MUDSTONE: Unit 47 is medium to dark grey, massive, disky, shaley mudstone with abundant intermixed and interlayered very fine grained, light grey sand in wisps and lenses; bottom contact is sharp.

178.75 179.10 SHALEY MUDSTONE: Unit 48 is dark grey, massive to poorly fissile, disky, shaley mudstone with minor, thin lenses of very fine grain, light grey sand; bottom contact is sharp.

TOP OF SPINNEY HILL FORMATION AT 179.10 METRES.

179.10 180.35 WEAKLY GLAUCONITIC SHALEY MUDSTONE: Unit 49 is medium to dark grey, massive to poorly fissile, fine to medium disky, shaley mudstone with moderate internal bedding variations expressed by ridged crenulated core surface; emerald to kelly-green glauconite common as mottled granular clusters

on and between bedding planes; rare fish debris and very thin wisps of very fine grain light grey sand along bedding planes oriented at 80 degree angle to core axis; bottom contact is gradational.

180.35 181.06 SHALEY MUDSTONE: Unit 50 is similar to Unit 49, but with very rare glauconite; bottom contact is sharp.

181.06 181.70 GLAUCONITIC SILTY MUDSTONE: Unit 51 is mottled green and medium grey, uniformly competent, massive mudstone; granular glauconite is pervasive in wisps and irregular patches throughout the unit; bottom contact is sharp.

181.70 182.25 SHALEY MUDSTONE: Unit 52 is similar to Unit 50 with poorly fissile, disky, shaley mudstone with trace glauconite and minor very fine grain sand content; bottom contact is sharp.

182.25 184.40 COARSENING UPWARD GLAUCONITIC MUDSTONE/SANDSTONE: Unit 53 is coarsening upward from dark grey, massive to poorly fissile shaley mudstone with up to 15 per cent interlayered, off-white and light olive-green, weakly glauconitic very fine grain sandstone lenses and wisps, through sandy siltstone to glauconitic sandstone; contacts are gradational with increase of sand and silt upwards to the top of the unit; overall glauconite content increases upwards with carbonate-cemented rock prevalent in the upper 36 centimetres; diskiness decreases upwards to uniformly competent; basal contact is sharp.

182.25 182.60 -green and white weakly cross-bedded, glauconite-rich fine grain sandstone; bedding predominantly at 80 degree angle to core axis; upper 5 centimetres is massive, hard carbonate-cemented sandstone with variable carbonate-cemented lenses of sandstone within glauconitic sandy siltstone in the lower 30 centimetres; bottom contact is marked by loss of carbonate-cemented sandstone fragments/wisps.

182.60 183.24 -medium grey massive siltstone with abundant intermixed disseminated and interlayer glauconite and light grey very fine grain sand in wisps and thin lenses; bottom contact is gradational.

183.24 184.40 -massive dark grey mudstone with up to 15 per cent interlayered weakly glauconitic very fine grain sand and silt; bottom contact is sharp.

184.40 185.05 SILTY SANDSTONE: Unit 54 is a mottled light and medium grey, massive to poorly laminated, heterogeneous, moderately well sorted, variably consolidated silty sandstone; sandstone is composed of dominantly very fine grain to fine grain, rounded quartz grains; unit is variably silty and carbonate-cemented.

184.40 184.56 -wavy laminated silt and very fine grain sand with up to 30 per cent clayey matrix; trace glauconite; subunit is hard and finer grain towards base with well-indurated mudstone.

184.56 184.89 -well indurated, carbonate-cemented very fine grain sandstone; bottom contact is gradational with decrease in carbonate, and sand as lenses and wisps within muddy siltstone.

184.89 185.05 -muddy siltstone with up to 30 per cent very fine to fine grain light grey sand in wisps and lenses; wisps and lenses are weakly carbonate-cemented; bottom contact is gradational.

185.05 186.06 SANDY MUDSTONE: Unit 55 is medium to dark grey, uniformly competent, hard, massive to poorly fissile mudstone with up to 20 per cent silt and very fine grain sand in wisps and lenses; bottom contact is sharp.

186.06 186.46 SANDSTONE: Unit 56 is mottled light and medium grey, massive heterogeneous, poorly sorted, variable consolidated sandstone; sandstone is 90 per cent very fine to fine subrounded quartz with minor isolated coarse grains and granules of mildly pitted quartz and rare unidentified dark minerals; rare fish debris; carbonate cementation is variable from pervasive in the upper 21 centimetres decreasing to sporadic in lenses and wisps of sandstone in the lower 19 centimetres; unit appears bioturbated; bottom contact is sharp.

186.46 186.62 MUDSTONE: Unit 57 is dark grey, massive, well-consolidated mudstone with up to 30 per cent wisps and lenses of light grey very fine grain sand; bottom contact is sharp.

186.62 186.70 MUDDY SANDSTONE: Unit 58 is dark grey, massive, poorly sorted, mud supported sandstone; unit is composed of coarse to fine, subrounded to angular grains of quartz, and minor to trace oxidized pyrite and amorphous gossan; upper and lower contacts are sharp.

186.70 186.94 SHALEY MUDSTONE: Unit 59 is dark grey, moderately fissile shaley mudstone with interbedded laminae of very fine to fine grain light grey sand; bottom contact is sharp.

186.94 186.99 SANDSTONE: Unit 60 is light grey, massive, very fine grain sandstone composed of 90 to 95 per cent subrounded quartz grains; trace pyrite in millimetre-scale clusters; bottom contact is sharp.

186.99 187.96 MUDSTONE: Unit 61 is dark grey, massive, uniformly competent, hard mudstone with minor light grey sand in wisps and lenses; 1 centimetre thick lense of sand occurs within 3 centimetres of the top of the unit; bottom contact is sharp with 2 to 3 centimetres of coarse grain mud-supported sandstone underlying 1 centimetre thick iron stained fine grain sandstone lense; the coarse grain sandstone lies directly over light grey, massive sandstone.

187.96 188.33 GLAUCONITIC SILTY MUDSTONE: Unit 62 is massive, uniformly competent, heterogeneous mixture of abundant emerald-green wisps and clots of granular glauconite within dark grey silty mudstone; bottom contact is sharp below 6 centimetres of black, massive, moderately soft mudstone from 188.27 to 188.33 metres.

188.33 188.55 SANDY SILTSTONE: Unit 63 is a poorly sorted heterogeneous mixture of about 30 per cent fine to very coarse grains of varied mineralogy suspended within dark grey massive muddy siltstone matrix; grains include very coarse to fine subrounded quartz, fine to medium grain unidentified translucent, soft, mineral, soft plates and laths of dark organic matter rare, fine grain glauconite, and unidentified black grains and shards up to medium grain size; clasts or irregular lenses of mudstone common; rock is variably carbonate-cemented up to approximately 20 per cent in wisps and thin disjunct layers; rare fish debris; "chaotic"; bottom contact is sharp.

188.55 189.35 FINING UPWARDS SANDSTONE TO SANDY/SILTY MUDSTONE: Unit 64 is composed of weakly glauconitic, fine grain sandstone in the basal 24 centimetres overlain by mottled light and dark grey silty mudstone with decreasing content of weakly glauconitic sandstone as lenses and wisps upwards; unit is hard, sporadically bioturbated, and has disky texture due to internal bedding variations; bottom contact is sharp.

189.35 191.20 SHALEY MUDSTONE: Unit 65 is hard, dark grey shaley mudstone with disky texture; glauconite occurs both as discrete granular patches within the mudstone and as a sporadic component within rare to common, very fine to fine grain, sandstone wisps, lenses and laminae; bottom contact is sharp.

189.35	189.89	-dark grey, massive, glauconitic shaley mudstone; sporadic bioturbation increases with sand content to base; bottom contact is gradational.
189.89	190.20	-green and dark grey glauconitic sandy siltstone; bottom contact is sharp; very glauconitic in upper 6 centimetres; lower portion only rarely glauconitic.
190.21	191.00	-dark grey, hard shaley mudstone with rare glauconite.
191.00	191.20	-very glauconitic shaley mudstone; sharp basal contact.

TOP OF LOWER KIMBERLITE SEQUENCE AT 191.20 METRES.

191.20 192.32 MASSIVE RPK: Unit 66 is tan, hard, massive, poorly sorted very fine to coarse grain, well-indurated, carbonate-cemented kimberlitic sandstone; coarse grains are flakes of phlogopite and biotite, ilmenite; garnet, and quartz; fine grains are dominantly quartz and comprise 70 per cent of the rock; very fine silty and clayey components comprise up to 25 per cent and are not identified; sporadic angular clasts of mudstone up to 5 centimetres across, some with irregular carbonate rims occur rarely throughout; bottom contactis sharp.

191.47 191.62 -15 centimetre-thick clast of greasy textured, deformed mudstone with fenestral, cross-cutting veins of fibrous, prismatic carbonate up to .75 centimetres thick.

192.32 192.85 SANDSTONE: Unit 67 is a mottled light and medium grey massive, heterogeneous, poorly sorted, variably consolidated sandstone; sandstone is dominantly very fine to fine grain with subordinate (20 per cent) granules of mildly pitted and frosted subrounded quartz; quartz granules may be shattered giving clear shards; dark, rounded, unidentified coarse grains and granules comprise 5 to 10 per cent variably; minor fish bone fragments; grains and granules are variably matrix-supported ranging from clayey mud to silt to very fine quartzitic sand; unit is fining upwards overall from medium to coarse grain, granule-rich sandstone at base to silty fine grain sandstone 5 centimetres from the top of the unit; sporadic rare centimetre-scale clasts of carbonate-cemented very fine grain sandstone oriented at or near 90 degree angle to core axis; carbonate cementation is variable from pervasive within 10 centimetres of the base to about 10 per cent small lenses and weak pervasive at the top; unit appears variably bioturbated; upper 5 centimetres has a 2 centimetre thick layer of very pervasive carbonate-cemented sandstone encasing large (up to 5 centimetres wide) rounded cobbles of very well-indurated mudstone with minor streaks and blotches of gossan at the clast boundaries; pyrite occurs sporadically as semi-pervasive cement in small less than 2 centimetre patches and as small tarnished clots; "chaotic"; bottom contact is sharp.

192.85 193.48 SHALEY MUDSTONE: Unit 68 is medium grey massive to poorly fissile, weakly disky, shaley mudstone; minor constituents include fish scales, small pyrite clots, and laminae, wisps, and thin lenses of light grey, fine grain, dominantly quartz sandstone with about 3 per cent fish debris, some of it partially pyritized; these thin sandy layers contain trace amounts of dark unidentified mineral; unit is weakly bioturbated in sandier intervals; bottom contact is gradational.

193.14 193.16 -band of kimberlitic sandstone very similar to Unit 66; contacts are sharp at 90 degree angle to core axis.

193.48 194.00 SANDSTONE: Unit 69 is a mottled light and medium grey, massive, heterogeneous poorly sorted, variably consolidated and carbonate-cemented, fining upwards sandstone similar to Unit 67; unit also contains sporadic blotches and millimetre-scale clots of reddish-orange grains and associated gossan; upper 17 centimetres is much siltier and less carbonate-cemented, although pebbles of quartz and thin lenses of fine grain quartzitic sand are present; "chaotic"; bottom contact is sharp.

194.00 194.37 SANDSTONE: Unit 70 is dark grey, massive, poorly sorted, moderately hard, fining upwards sandstone; unit ranges from coarse grain and granule-rich fine grain sandstone matrix at the base to silty fine grain sandstone with minor granules at the top; upper 28 centimetres of finer silty sandstone is 5 per cent

sporadic centimetre-scale, angular clasts and pebbles of carbonate-cemented fine grain sandstone; there is a noticeable lack of carbonate in this unit which distinguishes it from the overlying fining upward sequences; "chaotic"; bottom contact is sharp.

TOP OF MANNVILLE GROUP AT 194.37 METRES

194.37 194.89 SILTY MUDSTONE: Unit 71 is medium to dark brownish-grey, massive, moderately hard, mudstone; fractures in this unit range from 40 to 70 degree angle to core axis and are slickensided with greasy, striated texture; basal 7 centimetres has a 5 centimetre long clast or pipe of light grey mudstone derived from the underlying massive mudstone; basal contact is sharp at 90 degree angle to core axis.

194.89 196.06 COMPOSITE SANDSTONE/MUDSTONE: Unit 72 is composed of at least 4 truncated and gradational fining upward sequences deposited in a terrestrial environment; units are either coaly or light-greyish brown in colour indicative of oxidizing, high energy fluvial and low energy swamp conditions; component sequences are stacked, but not necessarily related due to the high probability of internal uncomformities.

194.89 195.02 -light grey, irregularly laminated alternating mudstone and siltstone bedded at 90 degree angle to core axis; bottom contact is sharp and irregular.

195.02 195.35 -light grey massive silty mudstone; bottom contact is sharp and irregular with 3 centimetres of relief.

195.35 195.51 -light grey, irregularly laminated, alternating mudstone and siltstone bedded at 90 degree angle to core axis; bottom contact is sharp and irregular.

195.51 195.88 - fining upwards, light brownish-grey silty mudstone to mudstone; millimetre to centimetre-scale fragments of coal are common; basal 3 centimetres is coal-rich in granular laminae and wisps; 6 to 7 centimetre long broken clasts of orange-red oxidized very fine grain sandstone common oriented at 30 degree angle to core axis; bottom contact is sharp below disjunct cross beds of transported coal fragments.

195.88 196.06 -tan fine grain gossanous sandstone with coal fragments rare to common; basal 8 centimetres dominated by coal layers and lenses interbedded with silty sandstone; bottom contact is sharp.

196.06 196.94 FINING UPWARDS SANDSTONE TO SILTY MUDSTONE: Unit 73 is composed of interbedded medium brownish-grey, massive mudstone and silty mudstone, which fine upwards from a thin clayey fine grain sandstone at the base; unit is hard, bioturbated and mottled; very fine grain light grey sand wisps occur along bedding planes; bottom contact is sharp.

196.94 197.20 FINING UPWARDS SANDSTONE TO MUDSTONE: Unit 74 is a fining upwards sequence composed of black, massive, poorly consolidated silty mudstone overlying 20 centimetres of reddish-brown sand; bottom contact is sharp.

197.20 197.38 MUDSTONE: Unit 75 is black, massive, homogeneous, poorly consolidated mudstone; bottom contact not cored.

197.38 198.65 LOST CORE:

198.65 199.00 SANDSTONE: Unit 76 is massive, dark grey and brown mottled, fine to medium grain sandstone locally cemented by pyrite; bottom contact not drilled.

END OF HOLE AT 199.00 METRES.

RHONDA MINING CORPORATION
DETAILED CORE DESCRIPTION
October 27, 1994

DRILL HOLE: OFS93-012 **CLAIM NUMBER: S-127400**

LOCATION

LEGAL: LSD 14, Section 05, Township 52, Range 21 West of 2nd Meridian

UTM (1983): 495620 East, 5924000 North

GEOPHYSICAL GRID: 1330 North, 2545 West

COLLAR ELEVATION: 485.04 metres ASL

GROUND ELEVATION: 483.82 metres ASL

TOTAL DEPTH: 299.00 metres

CORE SIZE: HQ, 101 millimetres

CORE LOCATION: Saskatoon Field Office

DIP: -090 degrees

DATE STARTED: August 18, 1993

DATE COMPLETED: August 25, 1993

DOWNHOLE GEOPHYSICAL TESTING: Gamma Ray Log, Machibroda Engineering Ltd.

DRILLING CONTRACTOR: Longyear Canada Ltd.

WATER HAULING: J. Bergstrum

DRILLSITE GEOLOGY: B.C. Jellicoe and R. Woodward

CORE LOGGED BY: B.C. Jellicoe, R. Woodward and K. Leahy

ABANDONMENT STATUS: Cemented from surface to end of hole.

PURPOSE: To test a positive aeromagnetic and ground magnetic anomaly situated one kilometre south of a known kimberlite pipe cluster.

RESULTS: A 34.5 metre thick sequence of crater facies kimberlite (PK and RPK) and minor intervals of detrital kimberlite derived sediments occurs between 179.45 and 211.94 metres.

COMMENTS: Bedding and contacts are subhorizontal (90 degree angle to core axis) unless otherwise specified.
All depths are relative to collar elevation.
Abbreviations for kimberlite description are defined in the Textural Classification, Chapter 2.
Stratigraphic Nomenclature for the Colorado Group of Bloch et al (1993) used in this log, see Chapter 1.

CORE DESCRIPTION

00.00 80.00 TILL: This interval was not cored and chip samples were not collected; geophysical logs and driller reports indicate that this interval is composed of interbedded muddy tills and sandy tills beneath a few metres of surficial sandy sediment.

80.00 104.72 VARIOUS GLACIAL DEPOSITS: Upper half mainly mixed glacial tills, lower half mainly fluvio-glacial sands, interbedded with lacustrine clays and mudstones.

104.72 106.95 MUDSTONE BRECCIA: Unit 13 is dark grey to well-indurated black brecciated mudstone with angular to subangular, silt sized to fine grains of quartz (20 per cent), greenish-black and black unidentified mafic minerals (less than 25 per cent), biotite (2 per cent), and millimetre-scale fragments of rock including black mudstone, limestone, and granite; unit is apparently massive, but thin clay laminae and slightly more competent beds are oriented at 25 degree angle to core axis; minor limonite banding is parallel to bedding; bottom contact is gradational.

106.95 109.96 MUDSTONE BRECCIA: Unit 14 is similar to Unit 13, but with a greater proportion of unidentified rounded to subrounded, vitreous crystalline grains in the matrix; basal 21 centimetres is a large gneissic granite boulder; bottom contact is sharp.

BEDROCK SURFACE AT 109.96 METRES - LEA PARK FORMATION.

109.96 112.49 MUDSTONE: Unit 15 is composed of light to medium grey massive to thinly bedded mudstone with bedding at 85 to 87 degree angle to core axis; laminations of soft, decrepitated, yellow material (?) occurs in discrete 1 millimetre to 1 centimetre thick beds at decimetre-scale intervals; a 3 centimetre thick bed of reddish-orange, soft, hematite oriented at an 85 degree angle to core axis occurs at 111.15 metres; the origin of these beds is unknown, however, the presence of iron oxides, sulphates (?), and slightly bleached character indicate this unit to be altered/weathered Pierre Shale; bottom contact is sharp.

112.49 116.00 CLAYSTONE: Unit 16 is medium to dark grey, fairly uniform, massive to weakly fissile, claystone with weak, fine to moderate disky texture, diskiness increases towards the base; unit is locally massive; lower 25 centimetres is very weakly disky corresponding with increased silt content; mudstone is locally bentonitic (softer, more fissile, and lighter grey); rare fish scales and organic matter are present on bedding oriented at 90 degree angle to core axis; bottom contact is sharp.

114.90 114.95 -bentonite.

115.08 115.11 -bentonite.

115.55 115.58 -bentonite.

116.00 117.53 BENTONITIC MUDSTONE: Unit 17 is light to dark grey, moderately hard, massive bentonitic mudstone with discrete creamy yellow to white bentonite beds; bentonites are oriented at 85 to 90 degree angle to core axis, with sharp upper and lower boundaries; approximately .5 metres core loss from this interval; weathered interval from 117.16 to 117.30 metres is very fissile; bottom contact is sharp below a bentonite band.

116.00 116.10 -medium to dark grey, moderately fissile shaley mudstone; rare organic remains and fish scales visible on some bedding planes
116.40 116.44 -bentonite.
117.07 117.11 -bentonite.
117.28 117.33 -bentonitic shale.
117.37 117.52 -bentonitic black shaley mudstone.

117.53 118.21 MUDSTONE: Unit 18 is dark grey to black carbonaceous, competent, generally massive mudstone; unit is locally micaceous and very fine fish debris is rare to common on bedding planes; bottom contact is sharp.
117.63 117.66 -bentonite.
118.08 118.10 -bentonite.

TOP OF UNDIFFERENTIATED WHITE SPECKS SHALE AT 118.21 METRES.

118.21 119.30 SHALEY MUDSTONE: Unit 19 is black, massive to weakly fissile, competent, noncalcareous shaley mudstone; biotitic and carbonaceous with common laminae of fine fish debris; bottom contact is gradational over 5 to 10 centimetres with underlying black, calcareous shale.
118.21 118.24 -bentonitic shaley mudstone.
118.46 118.50 -bentonite.

119.30 122.00 CALCAREOUS SHALE: Unit 20 is black, very competent, carbonaceous, calcareous, white speckled shale; shale is laminated to thinly bedded with bedding angle of 85 to 90 to core axis with some vertical fractures oriented at 10 angle to core axis near 121.0 metre depth; white specks (coccolithophore-rich faecal pellets) are very abundant on bedding planes; inoceramid shell fragments ranging in size from millimetre-scale to greater than 5 centimetres in length and generally oriented with long axis perpendicular to core axis are common in white speckled zones throughout the unit; fish scales and very fine fish debris are rare to common; bottom contact is unknown due to milling and loss of core.

122.00 128.22 CALCAREOUS SHALE: Unit 21 encompasses a zone of very poor core recovery due to mechanical problems in the core barrel; lost core is inferred to be black well-indurated calcareous shale similar to Unit 20, based on recovery of 22 centimetres of calcareous shale from 128.00 to 128.22 metres, below the zone of core loss; bottom contact is sharp at 90 degree angle to core axis.

TOP OF BELLE FOURCHE FORMATION AT 128.22 METRES.

128.22 129.60 SILTY/SANDY MUDSTONE: Unit 22 is dark grey to black, competent mudstone with lamination oriented at 85 to 90 degree angle to core axis; bioturbation is common throughout the interval with the burrows filled with fine off-white sand and silt; unit is composed of 5 fining upwards sequences from

very thin silty sandstone at the base to sandy mudstone at the top; bottom contact is gradational.

129.60 130.70 SHALEY MUDSTONE: Unit 23 is medium grey, moderately hard massive to weakly fissile, medium to coarse disky shaley mudstone; less than centimetre-scale variations in bedding (lamination) and competency give a ridged texture to the core due to washing of slightly less competent material; unit is uniform with only rare, minute blebs of oxidized organic matter and pyrite; bottom contact is sharp beneath 10 centimetres of moderately fissile shaley mudstone.

130.70 132.43 MUDSTONE: Unit 24 is medium grey, hard, massive, dominantly uniform mudstone; slightly disky texture indicates fine, subtle variations in bedding oriented at 90 degree angle to core axis; mudstone breaks into shards and chunks; bottom contact is sharp.

131.30 131.42 -dark grey, fissile, soft, shaley mudstone; sharp upper and lower contacts.

132.43 133.50 SHALEY MUDSTONE: Unit 25 is medium to dark grey, moderately hard, very fissile and platy, shale; homogeneous and uniform, although small lensoidal wisps of very fine off-white sand are sporadic and rare along bedding planes; rare burrows are present as less than 1 millimetre wide trails of dark grey material; plant matter is rare as millimetre-scale brown laths and twigs; bottom contact is sharp.

133.50 134.00 MUDSTONE: Unit 26 is medium to dark grey, massive, competent mudstone; slightly disky in centimetre-scale intervals and breaks into conchoidal fragments; small lensoidal wisps and laminae of very fine off-white sand are sporadic and rare along bedding planes; rare burrows are present as less than 1 millimetre wide trails of dark grey material; plant matter is rare as millimetre-scale brown laths and twigs; bottom contact is sharp.

134.00 135.66 SHALEY MUDSTONE: Unit 27 is light to medium grey, very fissile, uniform to very weakly fine disky shaley mudstone; rock has severely fragmented into centimetre plates and sheets due to surface weathering; less weathered portions are massive to weakly fissile and homogeneous in texture; small lensoidal wisps of very fine off-white sand are sporadic and rare along bedding planes; rare burrows are present as less than 1 millimetre wide trails of dark grey material; plant matter is rare as millimetre-scale brown laths and twigs; bottom contact is sharp.

135.66 137.55 MUDSTONE: Unit 28 is dark grey, massive to weakly disky, very weakly fissile, moderately hard shaley mudstone; texture ranges from massive to weakly disky with rare, thin intervals (less than 10 centimetres) of interlaminated silt and mudstone; millimetre-scale lathes of oxidized plant matter are rare; bottom contact is gradational.

137.55 137.95 SHALEY MUDSTONE: Unit 29 is medium grey, weak to moderately disky, moderately hard shaley mudstone; rock breaks with irregular fracture and is fairly uniform with only rare wisps and thin lenses of silt; rare, small millimetre-scale lathes of oxidized plant matter; bottom contact is sharp.

137.95 138.50 MUDSTONE: Unit 30 is dark grey, soft, massive, weakly disky mudstone with rare to very minor silt laminations and wisps along irregular bedding planes; millimetre-scale lathes of oxidized plant matter are rare; bottom contact is sharp.

138.50 139.18 SILTY/SANDY MUDSTONE: Unit 31 is mottled dark grey and light greyish-brown, massive, hard silty/sandy mudstone; silt and sand is present up to 15 to 20 per cent in lenses, wisps and horizontal burrows less than 2 millimetres in diameter; bottom contact is sharp.

139.18 140.10 SANDY/SHALEY MUDSTONE: Unit 32 is mottled medium and dark grey moderately hard, massive mudstone with 15 to 20 per cent sand in wisps, laminae, and burrows; where exposed to surface weathering, rock is very finely fragmented in both fissile and chunky pieces; bottom contact is sharp.

140.10 140.50 SHALEY MUDSTONE: Unit 33 is dark grey, slightly decrepitated, soft, moderately to very fissile, nondisky shaley mudstone; moderately abundant intermixed fine white silty sand as wisps, laminations, and burrow-fill (10 per cent); unit becomes darker grey and harder with increasing depth; bottom contact is sharp.

140.50 142.00 SHALEY CLAYSTONE: Unit 34 is dark grey, very fissile, soft, weakly fine disky, shaley claystone; rare off-white sandy wisps, laminae, and grainy flakes; unit has been weathered to finely fragmented plates and thin chunks; bottom contact is sharp.

140.96 141.20 -competent, light grey, sandy mudstone; contacts are gradational.

142.00 143.55 MUDSTONE: Unit 35 is light to medium grey, hard, massive to weakly fissile, very weakly disky mudstone; contact is subtle at colour change corresponding with gradational textural change over 10 centimetre interval.

143.55 146.93 SILTY MUDSTONE: Unit 36 is dark grey, massive, uniform, and competent mudstone; intermittently slightly disky in intervals less than 15 centimetres thick; contains rare to minor off-white sand in burrows and as lenses and wisps along bedding planes; interval is coarsening upwards with downward decrease in intermixed silt and sand content; rare fish scales; pyrite crystals and blebs occur interspersed with mudstone in an irregular millimetre-thick layer 1.65 metres from the base of the unit; rock becomes darker grey and then black through a gradational transition in the basal .28 metres; bottom contact is gradational.

146.93 148.25 SANDY MUDSTONE: Unit 37 is similar to Unit 36, dark grey massive, competent mudstones, but with 15 to 20 per cent silty very fine grain sand wisps, lenses, and burrows scattered throughout; grainy texture also distinguishes this unit from overlying competent mudstones; unit is fining upwards with increased sand content downwards; bottom contact is sharp.

TOP FISH SCALES FORMATION EQUIVALENT AT 148.25m

148.25 152.63 SHALEY CLAYSTONE: Unit 38 is dark grey to black, very finely laminar, competent, uniform shaley claystone; unit is not fissile and it is markedly fine grained as shown by conchoidal fractures (mechanically induced); rare chondrite burrows exist.

148.25 149.98 -medium grey, hard, massive to weakly disky, weakly fissile, claystone; rare chondrites bioturbation (small less than 1 millimetre wide tracks) and fish debris; lower .63 metres is slightly darker grey and contains common organic-rich laminae less than .5 centimetres thick; bottom contact is gradational.

149.98 150.46-medium grey weakly fissile claystone; bottom contact is sharp.

TOP UPPER WESTGATE FORMATION AT 150.46m

150.46 151.42 -dark grey, hard, sandy mudstone; off-white sand occurs in abundant, often flattened and distorted, unlined, millimetre-scale burrows; bottom contact is sharp.

151.42 151.64 -massive to chunky black claystone; contacts are sharp.

151.64 152.63 -dark grey, hard, massive to slightly fissile mudstone with rare, flattened, lined and unlined burrows containing lithified mud; off-white sand wisps occur sporadically along bedding planes; subunit becomes softer and more massive downwards; bottom contact is sharp.

152.63 153.20 MUDSTONE: Unit 39 is medium grey, hard, massive to weakly fissile mudstone; moderately fissile and platy towards base; small brown and dark grey burrows (less than 1 millimetre wide and generally 1 to 2 centimetres long) on bedding planes are common; bottom contact is gradational.

153.20 153.90 SHALEY MUDSTONE: Unit 40 is medium grey to black, very fissile, uniform, soft to moderately hard shaley mudstone; unit is very finely fragmented; minor silt content increases to approximately 20 per cent towards base with corresponding slight decrease in fissility; small burrows common above this unit are replaced by large 5 millimetre wide burrows which extend across the width of the core; bottom contact is sharply gradational with sudden increase of silt over 10 centimetre interval.

153.90 154.28 SILTY/SANDY SHALEY MUDSTONE: Unit 41 is light to medium grey, very fissile and soft mudstone with 50 per cent intermixed silt and very fine to

fine grain quartzose sand; unit is very finely fragmented and moderately unconsolidated; bottom contact is gradational and part of a fining upward sequence with increased abundance of sand towards base.

TOP OF ST. WALBURG SANDSTONE AT 154.28 METRES.

154.28 155.00 SILTY SANDSTONE: Unit 42 is light grey, massive very fine to fine grained quartzitic sandstone with intermixed silt and clay matrix; approximately 30 centimetres core loss of suspected unconsolidated sandstone from basal portion of the fining upwards sequence; above this is moderately consolidated clay cemented sandstone for 25 centimetres; sandstone contains minor subrounded chert grains.
154.71 155.00 -core loss.

155.00 158.00 SANDSTONE: Unit 43 core was erratically recovered with only 72 centimetres of variably iron- and silica-cemented, well-indurated to unconsolidated, very fine to fine grain, quartzitic sandstone, and 14 centimetres of very fissile, medium grey shaley mudstone; cementation is irregular from massive, pervasive iron/silica infused intervals to soft, weakly indurated, slightly decrepitated and gossanous, medium grained sandstone with imbedded granules of chert and quartz; contacts could not be ascertained.

158.00 161.00 SANDSTONE: Unit 44 is inferred to have been composed of partially consolidated sandstone and muddy sandstone; approximately 5 centimetres of washed and broken core was recovered including moderately soft, silty sandstone and finely interbedded sandstone/mudstone; sandstone is quartzitic, very fine to fine grain and is bimodally sorted with matrix silt and clays; bottom contact is unknown but suspected to be sharp beneath shaley mudstone dominated beds.

161.00 165.20 SILTSTONE: Unit 45 is dominated by light brownish-grey, massively bedded to weakly laminar, competent, homogeneous siltstone of uniform texture; .85 metres of lost core between 161.00 to 164.00 is attributed to washing of unconsolidated silty sand; pervasive mixing by bioturbation with only rare off-white fine sand-filled burrows preserved; bottom contact is gradational with progressive increase of clay with depth.

BASE ST.WALBURG SAND AT 165.20 METRES. (TOP LOWER WESTGATE)

165.20 167.27 SILTY MUDSTONE: Unit 46 is light to medium grey, massive to vaguely disky, weakly fissile, competent silty mudstone; unit is very hard and approximately 50 per cent of the unit is weakly disky due to centimetre to decimetre-scale variations in bedding competency and subtle interbedding of silt and silty mudstone; weakly micaceous; pyrite blebs locally abundant; bottom contact is gradational; Units 46 and 47 comprise a coarsening upwards sequence.

167.27 169.90 MUDSTONE: Unit 47 is medium to dark grey, uniform, hard mudstone; generally fine to medium disky, but with centimetre- to decimetre-scale intervals of massive, competent silty mudstone; silt is locally abundant up to approximately 20 per cent in the upper 1 metre; bottom contact is sharp.

169.90 172.85 MUDSTONE: Unit 48 is medium to dark grey, competent, non-fissile mudstone; centimetre-scale variations in bedding competency (and presumably composition) impart a knobby diskiness to the core surface; bottom contact is gradational over 10 to 15 centimetres with slight increase of silt downwards.

172.85 173.40 SILTY MUDSTONE: Unit 49 is medium to dark grey massive, uniform, competent silty mudstone; unit is subtly fining upwards from muddy siltstone to silty mudstone; bottom contact is sharp.

173.40 174.95 SHALEY MUDSTONE: Unit 50 is medium to dark grey, hard, medium to coarsely disky shaley mudstone; millimetre to centimetre clusters of pyrite locally abundant; bottom contact is gradational.

174.95 176.40 SHALEY MUDSTONE: Unit 51 is similar to Unit 50 with medium to dark grey, fine to medium disky, hard, uniform shaley mudstone; bottom contact is sharp.

176.40 177.56 MUDSTONE: Unit 52 is dark grey, massive, hard, homogeneous mudstone; bottom contact is sharp.

177.56 179.48 CALCAREOUS MUDSTONE: Unit 53 is weakly calcareous, medium grey, massive, hard, homogeneous mudstone with abundant, less than .5 millimetre long black lath-like clasts of mudstone throughout most of the interval; interval is lighter grey in the lower .40 metres corresponding to increased carbonate content towards the base of the unit; two fractures trending at 150 degree angle to core axis and a conjugate fracture trending at 60 degrees to core axis occur at and near the 178.00 metre depth; bottom contact is sharp.

TOP OF KIMBERLITE AT 179.48 METRES.

179.48 180.29 TUFFACEOUS CALCAREOUS SILTY MUDSTONE: Unit 54 is dark grey, hard, calcareous silty to sandy mudstone with irregularly occurring distorted, centimetre-scale, subangular clasts of brown mudstone interspersed throughout; in the lower .60 metres, the thinned and stretched brown material resolves into discrete distorted clasts ranging in size from millimetre-scale to 2 centimetres across; the unit is otherwise massive; the sediment appears well-mixed, but for centimetre-scale, amorphous patchs of light brown, fine to medium grain, quartzitic sandstone; the interval fines upwards fom fine silty sandstone to silty mudstone; pinched and disrupted laminae average 2 to 3 millimetres thick and give the rock a mottled texture where abundant and increase towards the base of the unit; carbonaceous material including coalified

twigs or rootlets, lensoidal pieces of wood, and amorphous clots of soft, black organic matter are common throughout; bottom contact is sharp.

180.29 181.60 TUFFACEOUS SANDS AND INTRACLASTIC SHALE BRECCIA: Unit 55 has 6 subunits composed of two alternating, distinct lithotypes, each ranging from 15 to 30 centimetres in thickness; first uppermost subunit is medium grey, medium to coarse grained, calcareous, granular tuff; the second is mottled, intermixed, greenish-grey and dark brownish-grey, massive, and hard (silty) calcareous mudstone; both lithotypes react vigorously to HCl, except for the lowermost, mudstone dominated subunit; coarse intervals are well-indurated with carbonate cement and are massive; mudstones display turbulent intermixing of different material as distorted wisps and layering, and commonly contain undistorted, unoriented, black mudstone clasts ranging in size from less than 1 millimetre to 5 centimetres along their long axis; contacts at the base of the coarse grained intervals are sharp, although the contact between coarse material and finer material above is vaguely gradational over a thin interval; bottom contact of the unit is sharp with less than 1 millimetre-scale carbonate veining, oriented at 80 degree angle to core axis, over a 2 millimetre interval.

181.49 181.86 INTRACLASTIC SHALE BRECCIA: Unit 56 is brecciated, black, massive mudstone; mudstone is essentially intact in the middle portion of the unit, but is increasingly fractured and brecciated towards each contact; upper and lower intervals are composed of angular mudstone fragments "floating" in a matrix of brownish-grey and gossanous, silty, calcareous material, this matrix infiltrates the mudstone throughout the interval, but appears only as isolated wisps towards the middle; base of the unit is placed at a sharp break between large mudstone fragments and rock with relatively minor mudstone content within a fine grained granular matrix similar to the coarse intervals of Unit 55.

181.86 182.51 TUFFACEOUS SAND: Unit 57 is composed of a brownish-grey, fine to medium grain, calcareous matrix with abundant randomly distributed black, massive mudstone clasts ranging from less than 1 millimetre to 5 centimetres across; basal portion of the unit has been sheared downwards across a fault trending at 25 degree angle to core axis in juxtaposition with a similar granular unit distinguished by greater abundance of millimetre-scale mudstone clasts; this lower subunit overlies the underlying unit above a sharp contact oriented at 50 degree angle to core axis.

182.51 182.83 TUFFACEOUS SAND AND INTRACLASTIC SHALE BRECCIA: Unit 58 is composed of a light brownish-grey, massive, silty mudstone-like matrix with abundant small black mudstone clasts less than 1 centimetre in diameter; matrix is composed of very finely intermixed mottled greenish-brown kimberlite and mudstone wisps, and it is weakly calcareous; bottom contact is marked by abundant large clasts of black mudstone; actual nature of the contact is unknown due to broken core, but appears to be a transition to gossanous matrix within the underlying rock.

182.83 184.00 INTRACLASTIC SHALE BRECCIA: Unit 59 is similar to Unit 56, but encompasses a much larger brecciated mudstone boulder, with more extensive separation of mudstone shards within an increasing proportion of matrix similar to unit 62 material; gossanous matrix is weakly calcareous; basal portion of the unit is composed of 3 centimetres of silty kimberlitic mudstone with only scattered millimetre-scale mudstone clasts; bottom contact arbitrarily set at a colour change from light brownish-grey to slightly darker brownish-grey.

184.00 186.58 MASSIVE AND BEDDED RPK: Unit 60 is greenish-grey to light olive green, very fine to coarse grained, massive, hard, weakly calcareous, tuffaceous kimberlite composed of mottled green antigorite, dark grey clay, carbonate, and some unidentified white crystalline material (baryte?); unit fines upwards from coarse to very fine grained corresponding to a change from olive green to greenish-grey colour; abundant carbonate vein threads prevalent at two horizons from 184.15 to 184.25 metres and 184.64 to 184.76 metres; veins in the upper interval are coarse (average 2 millimetre width compared to average 1 millimetre width in the lower interval); vein threads trend between 60 and 50 degree angle to core axis and are anastomosing; two carbonate veins occur near 184.85 metres and are (near) conjugate to the other vein intervals oriented at 30 degree angle to core axis; a white granular mineral suspected to be baryte occurs in abundance within the coarser portion of the sequence; within the lower .5 metres, the baryte is very coarse grained, thus giving the rock a white-speckled appearance, this same interval hosts carbonate veins in various orientations, generally at shallow angles to core axis; near 186.40 metres depth, intersecting millimetre-scale carbonate veins host unidentified sulphides, which also extend into the groundmass as sporadic, but abundant blebs; basal 20 centimetres is marked by a greater degree of induration, recrystallization, and matrix carbonate content; bottom contact is gradational; a 1 centimetre thick carbonate (+/- baryte) vein crosses the contact oriented parallel to core axis.

186.58 187.60 LAPILLI DOMINATED PK LAPILLI-TUFF: Unit 61 is continuous with Unit 60, but is characterized by decreasing carbonate content downwards, which corresponds to an increase in the degree of induration by serpentinite, darkening to black matrix, and increase in recrystallization with attendant lack of distinction between grains; upper 35 centimetres of the interval is sporadically carbonate veined with no preferred orientation; bottom contact is gradational.

187.20 188.95 INTRACLASTIC SHALE BRECCIA: Unit 62 is continuous with Unit 61, but is distinguished by a sudden increase in clasts and large millimetre-scale minerals; clasts range from millimetre- to centimetre-scale and include carbonate, black mudstone, chert, and large fragments of pale green clayey kimberlite (?) material; minerals present include antigorite, an unidentified black crystal, and very abundant, large unidentified white crystals (possibly baryte); matrix material is weakly calcareous, very fine grained, recrystallized, well-indurated, and mottled with black, white and dark green materials; bottom contact is sharp and irregular over a 5 centimetre depth.

188.95 196.85 BEDDED AND GRADED RPK: Unit 63 is dominated by dark olive green, medium to coarse grain, massive, very weakly- to noncalcareous, tuffaceous kimberlite; overall, the unit is composed of many gradational subunits, which have slight variations of in grain size, colour, and abundance of minor components; centimetre-scale clasts of black mudstone are abundant in some subunits, while millimetre-scale grains of the same material are very abundant in others; small pebbles of black mudstone occur randomly interspersed throughout some subunits, but also may form pebble laminations defining accumulation surfaces oriented at 90 degrees to core axis; a slickensided fracture occurs between 196.02 and 196.15 metres; light greenish-clay clasts up to .5 centimetres are abundant in the finer grained, well-indurated subunits; the groundmass of these subunits also contains subordinate amounts of the unidentified, white mineral (possibly barite); contacts between subunits are subtle and considered gradational. The bottom contact is sharp.

196.85 197.97 INTRACLASTIC SHALE BRECCIA: Unit 64 is similar to Unit 56, except this is a larger mudstone boulder; the bottom portion of the boulder is brecciated more than the top and the infiltrated matrix has a light brown, very fine grained character with black mudstone or mafic mineral particles less than .2 millimetres in diameter; the bottom portion of the unit grades into the underlying unit with a decease in the size and number of isolated mudstone fragments.

197.97 198.17 TUFFACOUS SAND: Unit 65 is composed of a brownish-olive green, very fine grain, massive matrix with abundant fine grain black particles and antigorite; unit resembles a fine grained sandstone and is inferred to be reworked; the rock is gossanous and decrepitated, hence more extensive alteration or weathering is suspected; bottom contact is sharp.

198.17 198.46 MASSIVE AND BEDDED RPK: Unit 66 is similar to the lower portion of Unit 63, but has less abundant mudstone clasts, is a ruddy green colour, and contains black mudstone clasts up to 3 centimetres across; unit is fine grained and antigorite-rich with abundant less than 1 millimetre black mudstone clasts within the groundmass; bottom contact is sharp.

198.46 199.40 INTRACLASTIC SHALE BRECCIA: Unit 67 is similar to Unit 56, but is composed of two intervals of mudstone separated by 15 centimetres of material similar to unit 70, consequently, this unit represents 1 or 2 mudstone boulders; bottom contact is sharp.

199.40 200.25 MASSIVE RPK: Unit 68 is a gradational unit of olive green, medium to coarse grained, massive kimberlite with increasing abundance of unidentified white mineral (baryte?) towards the base; unit becomes increasingly mottled with white and green grains downward with a corresponding increase in degree of induration and carbonate content; bottom contact is sharp with the sudden loss of the white mineral and carbonate.

200.25 200.89 CRYSTAL DOMINATED PK TUFF: Unit 69 is similar to the welded tuffaceous kimberlite in Unit 62; veins of the unidentified white mineral (baryte?), up to 1 centimetre wide with millimetre-scale splays, occur within the lower .36 metres of the unit; all of the veins are oriented at 0 to 10 degree angle to core axis, although a vein thread cluster trending 80 degrees to core axis occurs at 200.75 metres; bottom portion of the unit is fragmented and contains drilling mud within the fractures oriented at 90 degree angle to core axis; bottom contact is sharp.

200.89 206.50 CRYSTAL DOMINATED PK LAPILLI-TUFF: Unit 70 is similar to Unit 62 with numerous different subunits distinguished by subtle variations of colour and abundance of clasts; clasts range from millimetre- to centimetre-scale and include carbonate, black mudstone, chert, and large fragments of pale green clayey material; millimetre-scale minerals include antigorite, an unidentified black crystal, and very abundant, large unidentified white crystals (baryte?); matrix material is weakly to noncalcareous, very fine grained, recrystallized, well-indurated, and mottled with black, white and dark green materials; subordinate intervals of dark grey to black matrix, with comparatively fewer clasts, occur sporadically; both lithologies contain common carbonate veins, and rare baryte veins oriented at 50, 70, and 85 degree angle to core axis; unit has an increase of matrix carbonate content downward in the lower 3 metres; lower 10 centimetres is marked by a sudden increase in matrix carbonate and intense carbonate veining oriented at 50 degree angle to core axis above the contact with the underlying carbonate kimberlite lithic breccia

206.50 206.79 CARBONATE KIMBERLITE LITHIC BRECCIA: Unit 71 is similar to Unit 70, but has a much higher matrix carbonate content reflected in the off-white to brownish-white colour and high degree of induration; unit has much less abundant clasts than Unit 75; bottom contact is sharp and angular at 50 degree angle to core axis.

206.79 208.00 CLAYSTONE: Unit 72 is black, weakly fissile, weakly disky claystone with inclined bedding at 70 degree angle to core axis near the contact and decreasing to 95 degrees at the bottom contact; basal 5 centimetres is brown and massive; bottom contact is sharp.

208.00 208.88 CARBONATE KIMBERLITE LITHIC BRECCIA: Unit 73 is similar to Unit 71; bottom contact is sharp and angular at 50 degree angle to core axis.

TOP OF SPINNEY HILL MEMBER AT 208.88 METRES.

208.88 211.63 MUDSTONE: Unit 74 is black, weakly fissile, weakly disky, mudstone similar to Unit 72, but is slightly silty with sporadic emerald green glauconite in clusters up to 3 centimetres wide in the upper meter of the section; below 209.97 metres, bedding plane orientation changes from 30 to 80 degree angle to core axis within 25 centimetres; lower 65 centimetres of the unit contains abundant

glauconite-rich sandy wisps and lenses on bedding planes; bottom contact is sharp and near perpendicular to core axis.

209.89 209.97 -poorly sorted, sporadically carbonate-cemented, coarse grained muddy sandstone (chaotic unit)

211.63 211.94 CARBONATE KIMBERLITE LITHIC BRECCIA: Unit 75 is similar to Unit 71 with abundant less than centimetre clasts and closely resembles the lithic breccia in Unit 70; bottom contact is sharp and angular at 50 degree angle to core axis.

211.94 216.00 MUDSTONE: Unit 76 is black, massive to finely disky, dominantly homogeneous, soft mudstone; interlayered wispy laminae of very fine to fine grained sandstone, variably composed of off-white quartzose sand and dark greenish-grey glauconite-rich sandstone, occur sporadically along bedding planes; bedding is inclined at a maximum of 50 degree angle to core axis immediately adjacent to the upper contact, but decreases to 85 degrees within .5 metres downwards; upper .45 metres contains clusters of emerald green glauconite up to 3 centimetres wide; basal 43 centimetres is marked by a gradational increase of silt and sand downwards to silty mudstone with abundant wispy sand interlayers; bottom contact is sharp.

215.60 216.00 -massive, hard, silty, very fine grained quartzitic sandstone; upper contact gradational over 5 centimetres; bottom contact is sharp.

216.00 216.07 SANDY MUDSTONE: Unit 77 is black sandy mudstone with abundant interlayers of intermixed coarse, subrounded quartz grains increasing in abundance downwards to a partially sulphide-cemented, decrepitated muddy sandstone; "chaotic unit"; bottom contact is sharp.

TOP OF MANNVILLE GROUP AT 216.07 METRES.

216.07 217.20 SANDSTONE: Unit 78 is a sequence of light brown, fine to medium grained sandstones; upper 90 centimetres is competent, while the lower 23 centimetres is soft and unconsolidated; competent portion is composed of laminated, cross-bedded subunits (at 70 degree angle to core axis), and massive, mottled dark grey and light brown, bioturbated intervals; subunits are interbedded and separated by sharp contacts; bottom contact is sharp.

217.20 221.23 MUDSTONE: Unit 79 is composed of a fining upwards sequence of sandy mudstone at the base grading to mudstone; mudstone is brownish-medium grey, massive, and homogeneous; sandy mudstone is a mixture of abundant brown sand as wisps and laminae and light grey mudstone; mudstone contains common clasts of coal up to 5 centimetres across between 218.38 and 218.72 metres depth; bottom contact is sharp.

END OF HOLE AT 299.00 METRES.

APPENDIX III

Petrological descriptions for OFS 93-002, 004 and 012 kimberlite.

CONTENTS: Sheets include visual estimations of grain roundness.

- Petrography description for 6 slides from OFS 93-012
- Petrography description for 6 slides from OFS 93-002
- Petrography description for 16 slides from OFS 93-004

STANDARD THIN-SECTION PETROGRAPHY SHEET.

KEVIN LEAHY.

DATE: 10/5/95.
UNIVERSITY SLIDE CODE: 56296 OFS SLIDE CODE: T5073
BOREHOLE: OFS93-012-FOXFORD. DEPTH: 194.28m.
BRIEF HANDSAMPLE DESCRIPTION: Coarse base of 1.9m graded unit
Looking at high power into suspect lapilli structures.

FACIES ASSIGNED: - lapilli in undiff. crater fill (probably airfall tuff)

SKETCH: PPL

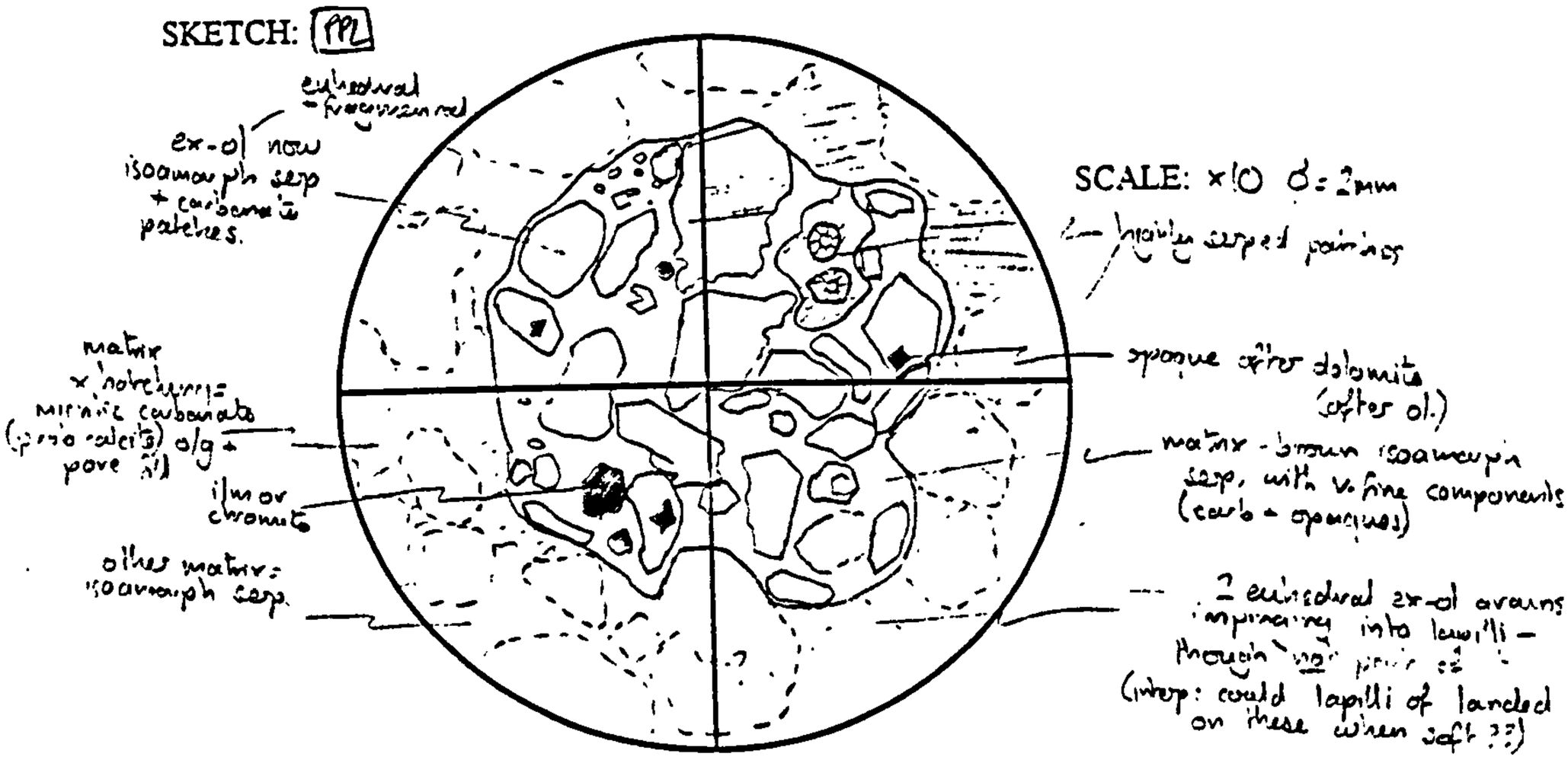

GRAIN TYPES: Originally olivine ~98%, opaques ~2%.
ol now: isoamorph serp 85% carbonate ~10% opaques ~5%

MATRIX TYPE: brown isoamorph serp ~95%, carbonate ~3%, opaques ~2%

OTHER FEATURES: patches are highly serpentinized, destroying original grain outlines (indicated above)

within lapilli only

GRAIN/MATRIX RATIO: 60/40
80% GRAINS EUHEDRAL/ANGULAR: 65
% GRAINS SUB-HEDRAL/ROUNDED: 30
2% GRAINS ROUNDED: 5

GRAIN SIZE DISTRIBUTION: moderate/poorly sorted - possibly 'multimodal'

CLAST/MATRIX SUPPORT?: 25% clast - 75% matrix

CONCLUDING COMMENTS: - grain characteristics are very 'primary' - relative to lapilli in either fragments of olivine bomb or an accretionary lapilli. Grain textures suggest the latter

CO2+004.

STANDARD THIN-SECTION PETROGRAPHY SHEET.

KEVIN LEAHY.

DATE: 11/5/95.
UNIVERSITY SLIDE CODE: NONE
BOREHOLE: OFS93-012 - FOXFORD
BRIEF HANDSAMPLE DESCRIPTION: GREY MARLY SEDIMENT, HIGHLY BIOTURBATED, RICH IN ROUNDED SHALE PEBBLES, LITHICS, COALY + PLANT FRAGS. OVER-LYING 32M CRATER FILL.

~ 12 KCM.
OFS SLIDE CODE: NONE.
DEPTH: ABOUT 179 m.

FACIES ASSIGNED: CRATER LAKE DEPOSITS

SKETCH:

NB SLIDE NOT OF RELIABLE THICKNESS, eg QUARTZ GRAINS HIGH BIREF. COLOURS.

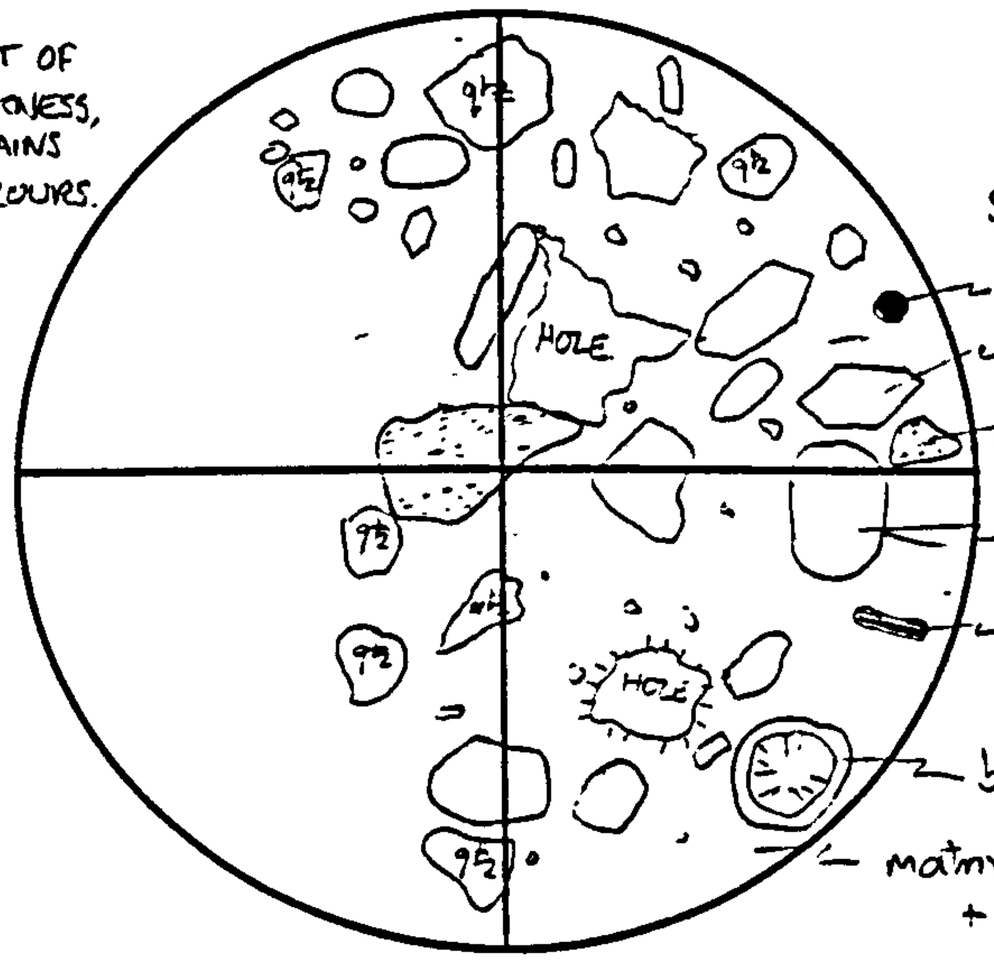

SCALE: x4 ϕ = 5mm

- well rounded opaque
- euhedral ex-ols.
- lithics - shale clasts
- rounded ex-olivines - replaced by 95% carbonate, opaques + iop ~5%
- mica
- biotite
- matrix - dark brown clays, calcite/carb, + v. fine qtz, carbonate + opaque ex-ol? grains. ~65% ~30%

GRAIN TYPES: Carb-after-olivine 50% angular qtz ~40% shale lithics ~5% muscovite 1% biotite ~2% opaques ~2%
~ not much evidence for serp after olivine

MATRIX TYPE: Dark brown, clays dominant (~65%), carbonate in patches, and disseminated throughout - total ~30%. The v. fine xtls of grain types above (except qtz)

OTHER FEATURES: Lots of holes - some due to overthinning, some are original porosity - lined with micritic carbonate. Estimated ≤ ~10% porosity - could be much less

GRAIN/MATRIX RATIO: 35/65
18 % GRAINS EUHEDRAL/ANGULAR: 22
35 % GRAINS SUB-HEDRAL/ROUNDED: 46.
11 % GRAINS ROUNDED: 32

GRAIN SIZE DISTRIBUTION:
very poorly sorted - probably due to bioturbation

CLAST/MATRIX SUPPORT?: matrix support
CONCLUDING COMMENTS: Total of about 25% maximum volcaniclastic material in this altogether terrigenous sediment

STANDARD THIN-SECTION PETROGRAPHY SHEET.

KEVIN LEAHY.

DATE: 17/5/95.
UNIVERSITY SLIDE CODE: 56297 OFS SLIDE CODE: TS074.
BOREHOLE: OFS93-012 - FOXFORD. DEPTH: 201.12m.
BRIEF HANDSAMPLE DESCRIPTION: Lower coarse xsH. lithic bed 4.5m thick. Fairly well bedded, xstls + lithics up to 3cm.

FACIES ASSIGNED: Lapilli Tuff.

SKETCH: PPL

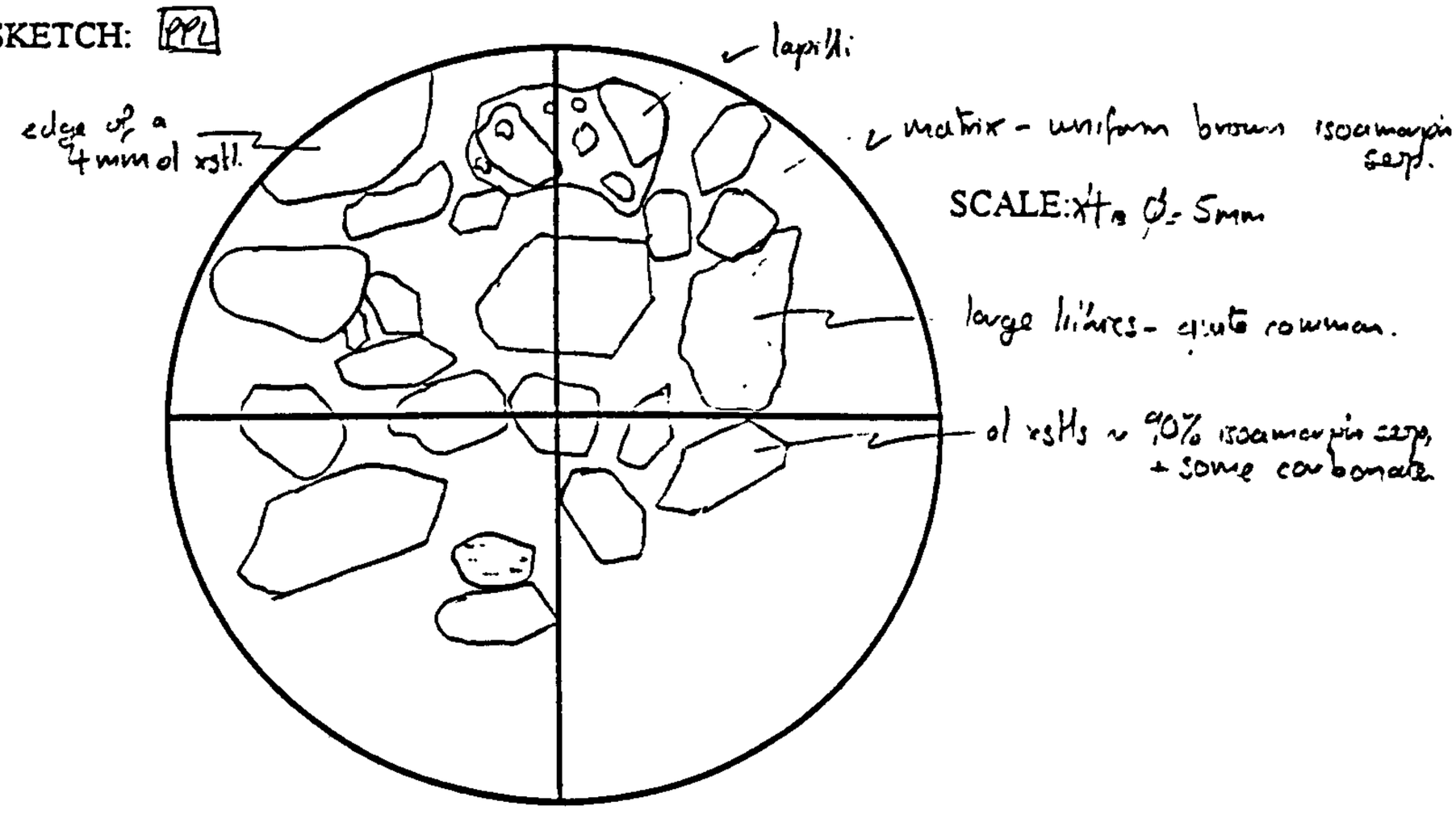

GRAIN TYPES: Olivine: ~80% lapilli ~10% lithics ~8% opaques: ~2%

MATRIX TYPE: very uniform, brown isoaamoph serp

OTHER FEATURES:

GRAIN/MATRIX RATIO: 60/40
11 % GRAINS EUHEDRAL/ANGULAR: 48
23 % GRAINS SUB-HEDRAL/ROUNDED: 35.
14 % GRAINS ROUNDED: 17

GRAIN SIZE DISTRIBUTION:
poorly sorted — ash to 3cm

CLAST/MATRIX SUPPORT?: 90% matrix supported
CONCLUDING COMMENTS: lapilli tuff

STANDARD THIN-SECTION PETROGRAPHY SHEET.

KEVIN LEAHY.

DATE: 9/5/15
UNIVERSITY SLIDE CODE: 56296 OFS SLIDE CODE: TS073
BOREHOLE: OFS93-012 - Foxford. DEPTH: 194.48m
BRIEF HANDSAMPLE DESCRIPTION: Coarse base of 1.9m thick graded unit (between the ext-lithic hi's). Grey-green med lamb tuff.

FACIES ASSIGNED: Undifferentiated crater fill.

SKETCH:

PPL

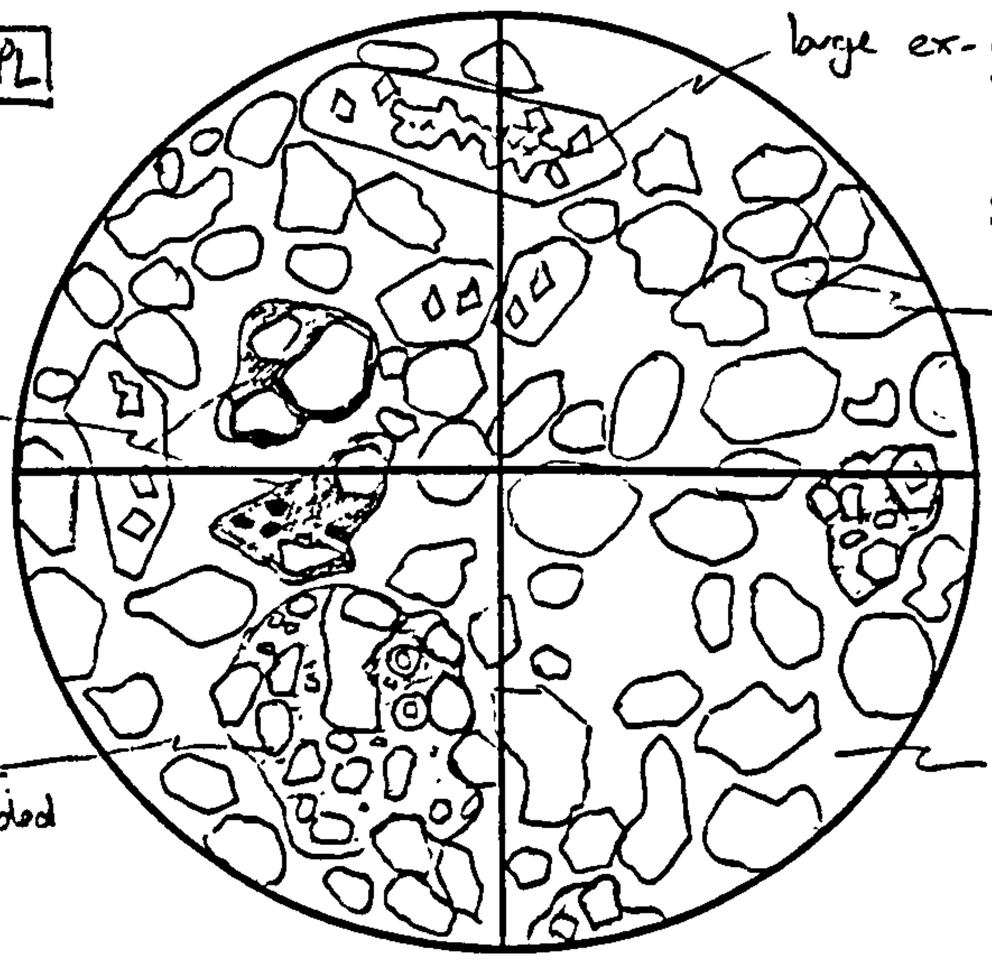

GRAIN TYPES: Orginally: olivine (f-m c.) 60% (v.c. to gran.) 30% lithics ~2%, lapilli ~8%
ob now: isoamorph serp ~50%, carbonate (mostly dol) ~20%

MATRIX TYPE: isoamorph serp - plus patchy v. fine carbonate.
Massive

OTHER FEATURES: see lapilli per sheet for further observations

GRAIN/MATRIX RATIO: 75/25
30 % GRAINS EUHEDRAL/ANGULAR: 45
% GRAINS SUB-HEDRAL/ROUNDED: 37
12% GRAINS ROUNDED: 18
65
ignore grains within lapilli

GRAIN SIZE DISTRIBUTION:
well sorted - strongly bimodal.

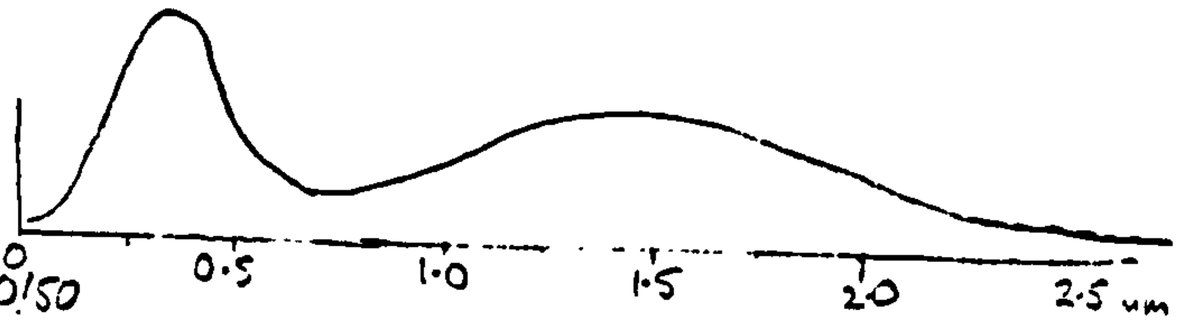

CLAST/MATRIX SUPPORT?: 50/50
CONCLUDING COMMENTS: ? looks like an airfall tuff.

STANDARD THIN-SECTION PETROGRAPHY SHEET.

KEVIN LEAHY.

DATE: 17/5/95.
UNIVERSITY SLIDE CODE: 56295 OFS SLIDE CODE: TS072.
BOREHOLE: OF993 - ~~CRE~~ FOXFORD DEPTH: 188.50 m
BRIEF HANDSAMPLE DESCRIPTION: Base of upper (graded) coarse xsH - lithic lapilli unit

FACIES ASSIGNED: Lapilli Tuff.

SKETCH: PPL

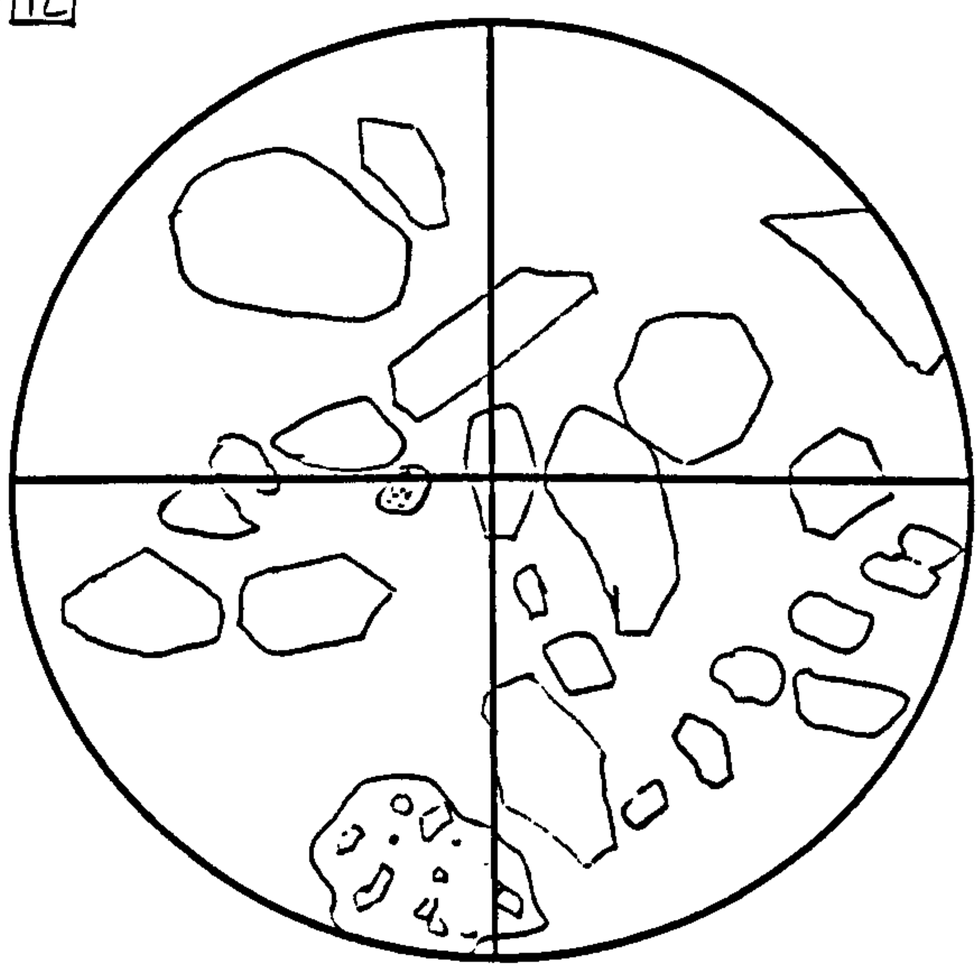

SCALE: ×4 ϕ - 5mm.

GRAIN TYPES: Olivine: 85%. lapilli ~ 10%, lithics ~ 3%, opaques ~ 2%. (including glauconite (rare))

MATRIX TYPE: dark brown patchy; some isoanaplasmic zeo, some mesh/fibrous zeo with micritic carbonate disseminated

OTHER FEATURES: lapilli - up to about 5mm, mostly irregular.

GRAIN/MATRIX RATIO: 60/40.
13% GRAINS EUHEDRAL/ANGULAR: 50
% GRAINS SUB-HEDRAL/ROUNDED: 40.
3. % GRAINS ROUNDED: 10

GRAIN SIZE DISTRIBUTION:
V. poorly sorted, 50% to 5cm.

CLAST/MATRIX SUPPORT?: matrix supported
CONCLUDING COMMENTS: Lapilli tuff

STANDARD THIN-SECTION PETROGRAPHY SHEET.

KEVIN LEAHY.

DATE: 12/5/95
UNIVERSITY SLIDE CODE: 56294 OFS SLIDE CODE: 7SC71.
BOREHOLE: OFS-012- FOXFORD DEPTH: 186.76m.
BRIEF HANDSAMPLE DESCRIPTION: Upper xstl-lithic tuff 18m thick
Dark olive green, xstls upto 2cm long

FACIES ASSIGNED: Lapilli tuff

SKETCH: PPL

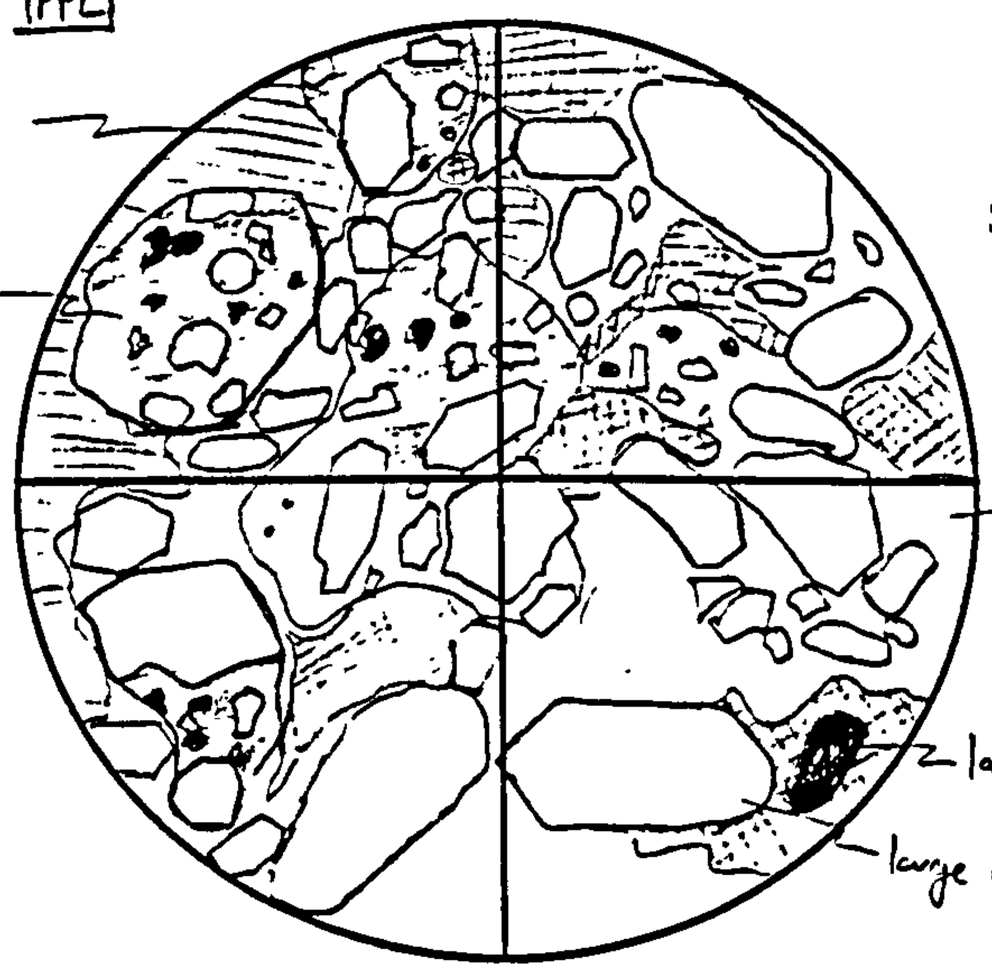

SCALE: x4 ⌀ = 5mm

GRAIN TYPES: Originally: lapilli ~35%, olivine ~60%, lithics ~3%, opaques ~2%
Olivines now 75% isoamorph serp, 20% carbonate and ~5% opaques.

MATRIX TYPE: Sparitic carbonate in large patches. Probably dolomitic - as little HCl reaction in hand sample. The rest is fine isoamorph serp mixed with 0-20% micritic carbonate.

OTHER FEATURES: Lapilli grains consist of ~1/3 of the grains. Some are clearly accretionary, others are more amorphous + irregular.

counting lapilli as grains.

GRAIN/MATRIX RATIO: 65/35
%GRAINS EUHEDRAL/ANGULAR: 55
% GRAINS SUB-HEDRAL/ROUNDED: 30.
%GRAINS ROUNDED: 15

GRAIN SIZE DISTRIBUTION:
poorly sorted - wide range in grain sizes: fine to 2cm.
lapilli: fine to granule.

CLAST/MATRIX SUPPORT?: 50/50
CONCLUDING COMMENTS: Primary pyroclastic - lapilli tuff

STANDARD THIN-SECTION PETROGRAPHY SHEET.

KEVIN LEAHY.

DATE: 12/5/95
UNIVERSITY SLIDE CODE: 56293 OFS SLIDE CODE: T5070
BOREHOLE: OFS 93-012 - FOXFORD DEPTH: 185.00m
BRIEF HANDSAMPLE DESCRIPTION: Uppermost green graded lam's lapilli in 32m tuff pile

FACIES ASSIGNED: Undiff. crater fill.

SKETCH: PPL

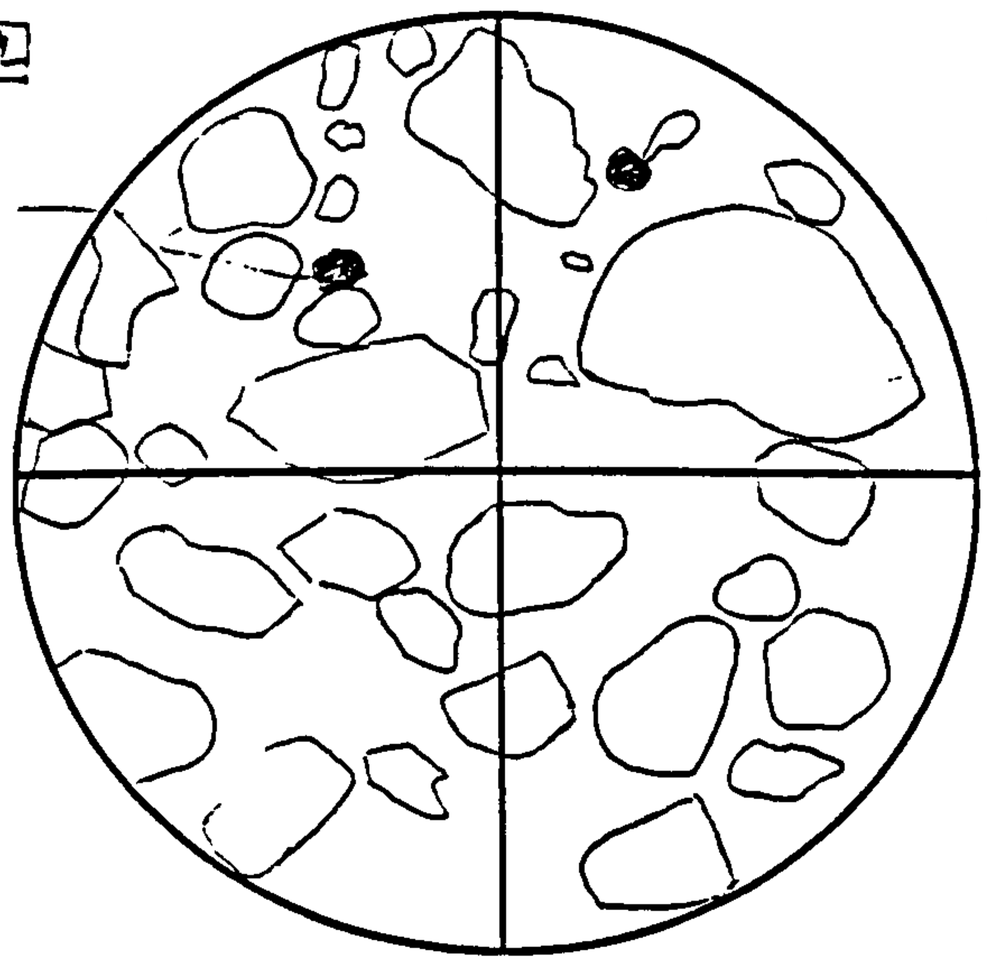

SCALE: ×10 ϕ=2mm.

GRAIN TYPES: 98% ex-ol xstls. ~60% replaced by carbonate, the rest by serp (iscamorph and fibrous) and carbonate (0-50%). Opaques in both ~0-10% ~0.5mm
~2% Lithics including shales and glauconites (rounded single grains). ~1% rounded small lapilli
MATRIX TYPE: Brown iscamorph serp, plus rare disseminated carbonate in patches. V.fine opaques scattered throughout.

OTHER FEATURES: Some early development of authigenic coarse vermicular serpentine from the matrix.

GRAIN/MATRIX RATIO: 70/30
17% GRAINS EUHEDRAL/ANGULAR: 23
31 % GRAINS SUB-HEDRAL/ROUNDED: 35
13% GRAINS ROUNDED: 42

GRAIN SIZE DISTRIBUTION:
well sorted.
(-ve) skewed unimodal

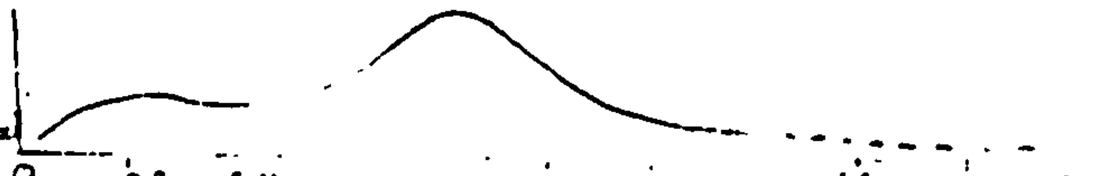

CLAST/MATRIX SUPPORT?: ~90% matrix
CONCLUDING COMMENTS: 2 grain characteristics suggest a reworked origin. glauconite grains are enigmatic - likely to be intra clasts like the shales

- Eroded reworked glauconite sand

STANDARD THIN-SECTION PETROGRAPHY SHEET.

KEVIN LEAHY.

DATE: 1/5/95.
UNIVERSITY SLIDE CODE: 55979. OFS SLIDE CODE: T3030
BOREHOLE: OFS-93-002. Snowden DEPTH: 105.54m.
BRIEF HANDSAMPLE DESCRIPTION: Base of upper graded unit + ash, grey/blue hue's in pl, 75cm thick

FACIES ASSIGNED: Graded reverbed pyroclastic sand. (coarse base of)

SKETCH:

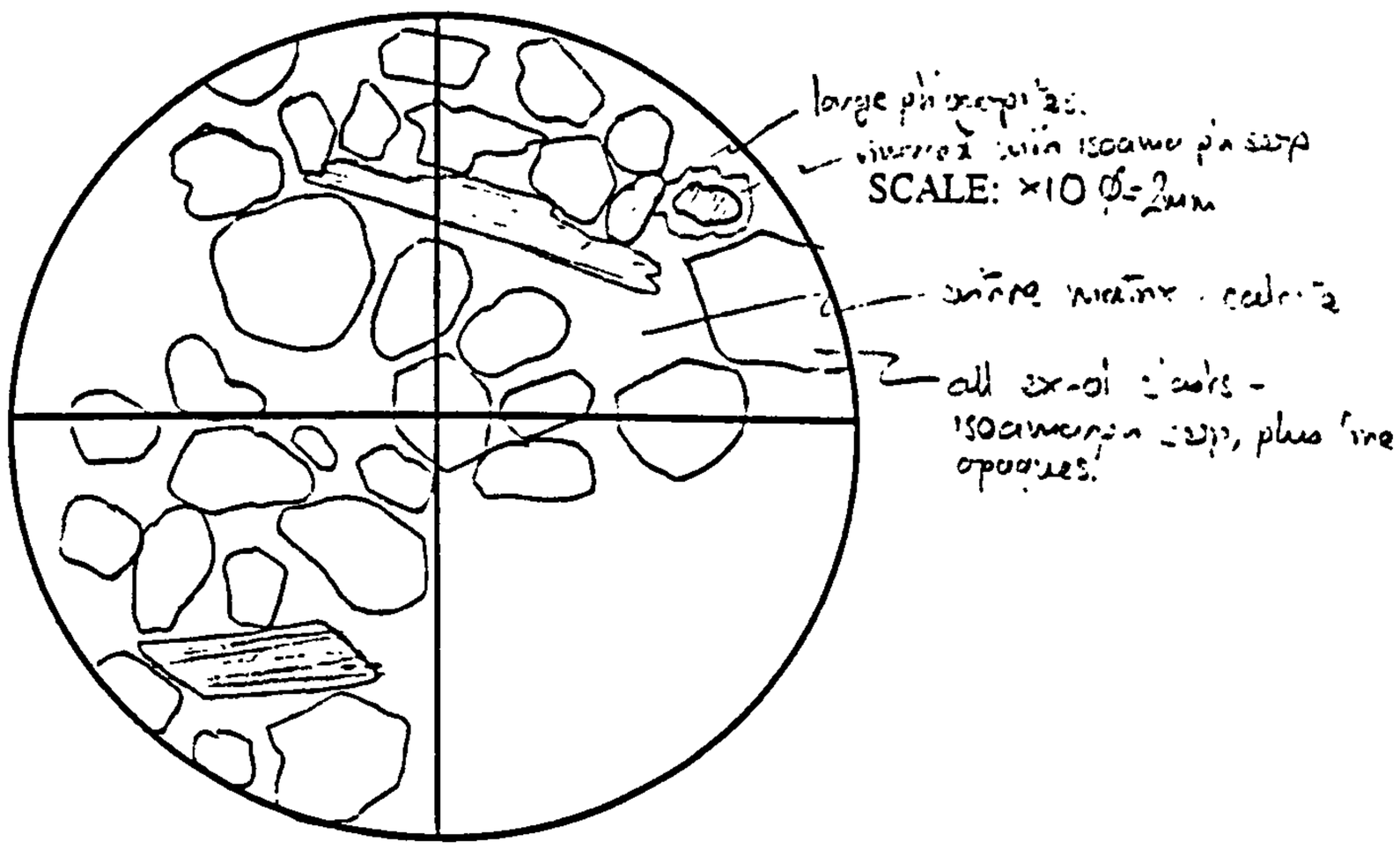

GRAIN TYPES: Originally. Olivine ~90% micro 5%, lithics ~2%, Opaques ~3%
ex-ol grains now isoamorphic serp +/- a little fine opaque + carbonate.

MATRIX TYPE: Almost entirely calcite (sparry - patchy microsp), v. rare patches of isoamorphic o/g.

OTHER FEATURES: Clast + matrix replacement in magnetite bleb areas.

GRAIN/MATRIX RATIO: 70/30 - 75/25.
9 % GRAINS EUHEDRAL/ANGULAR: 27
33 % GRAINS SUB-HEDRAL/ROUNDED: 52
8 % GRAINS ROUNDED: 25

GRAIN SIZE DISTRIBUTION:
fairly well sorted
-ve skew unimodal.

CLAST/MATRIX SUPPORT?: Mostly clast
CONCLUDING COMMENTS: ? coarse base of graded beds seem to contain a lot of euhedral ol's.

STANDARD THIN-SECTION PETROGRAPHY SHEET.

KEVIN LEAHY.

DATE: 9/5/95.
UNIVERSITY SLIDE CODE: 55975. OFS SLIDE CODE: TS034
BOREHOLE: OFS93-002 - SNOWDON. DEPTH: 109.47.m.
BRIEF HANDSAMPLE DESCRIPTION: Finely bedded green lithic tuff
Upper 15cm of 85cm graded unit
Smaller blebby magnetite patches.
FACIES ASSIGNED: Graded reworked pyroclastic fall sand.

SKETCH:

NB serpentinization is inverse Bowenian
Much original granular texture is obscured, or v. fainir Sketch is from PPL, low light (Krolls), diaphragm nearly fully closed, and slightly unfocused (to enhance grain boundaries).

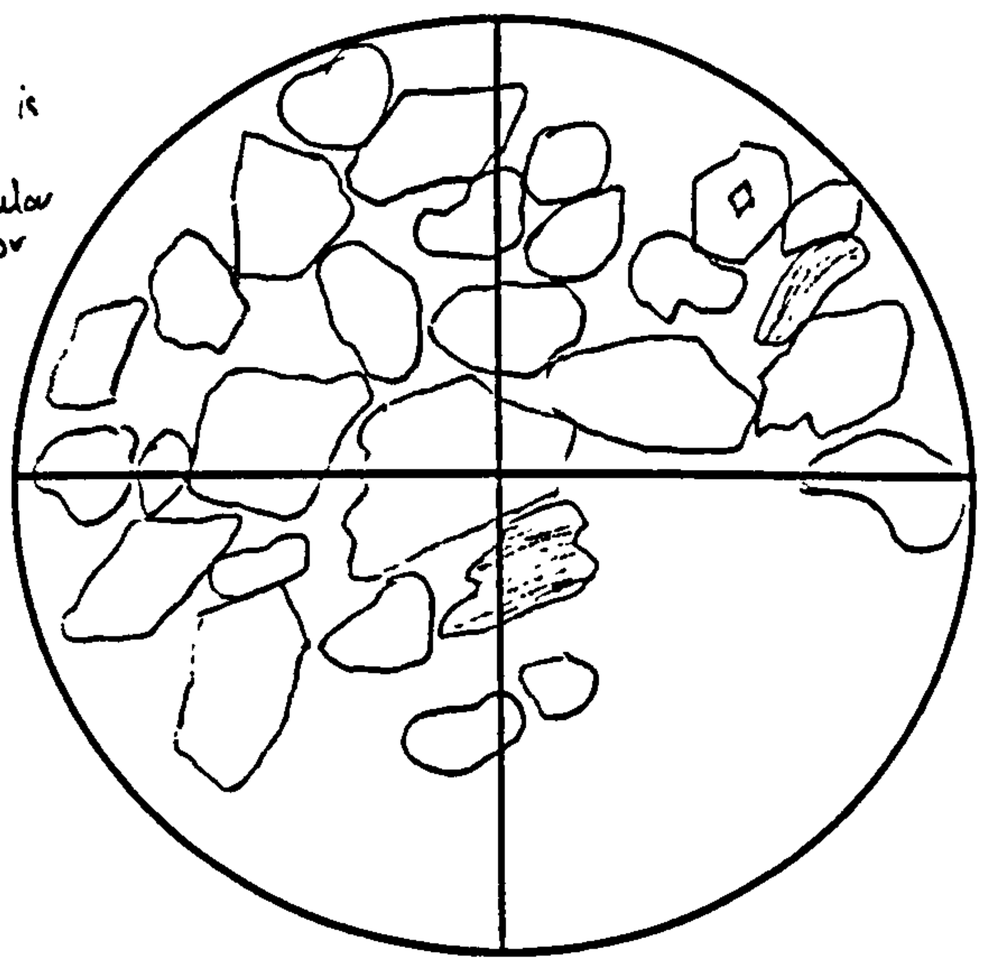

SCALE: x10 ∅=2mm

GRAIN TYPES: Olivine ~94% pyroxene ~3% opaques ~2% lithics ~1% garnet <1%
Olivine mode: isoamorph serp ~90% carbonate ~8% opaque ~1%

MATRIX TYPE: fibrous/mesh serp o/a + pore fill, plus isoamorph serp
fine dusting of carbonate (~5%) + rare opaques.

OTHER FEATURES: Bedding, 1-3 mm scale.
lots of fragmented ol crystals, + odd shaped rounded ones too.

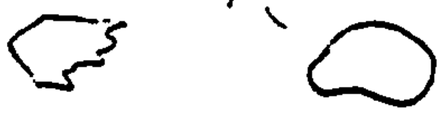

lithic lapilli

GRAIN/MATRIX RATIO: 85/15
%GRAINS EUHEDRAL/ANGULAR: 25
%GRAINS SUB-HEDRAL/ROUNDED: 50
%GRAINS ROUNDED: 25

may be inaccurate due to intense serp (see above)

GRAIN SIZE DISTRIBUTION: well sorted within bed thickness. unimodal

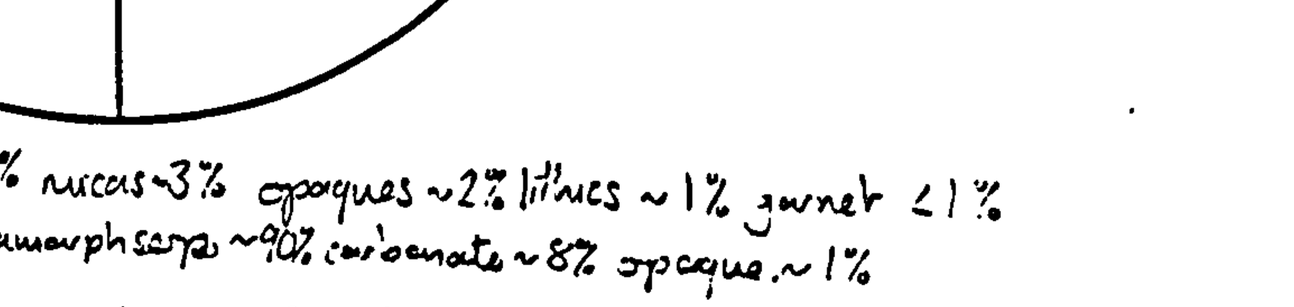

CLAST/MATRIX SUPPORT?: Clast supported
CONCLUDING COMMENTS: = laminated crystal vitric sand.

STANDARD THIN-SECTION PETROGRAPHY SHEET.

KEVIN LEAHY.

DATE: 1/5/95.
UNIVERSITY SLIDE CODE: 55971. OFS SLIDE CODE: TS035
BOREHOLE: OFS-93-CO2 -Sncwdon. DEPTH: 110.43
BRIEF HANDSAMPLE DESCRIPTION: 110.43 - grey-green medium crimb tuff. Faintly bedded, with magnetite blebs. Centred 60cm massive unit

FACIES ASSIGNED: Massive reworked pyroclastic sand

SKETCH: Edge of a mag bleb (to right)

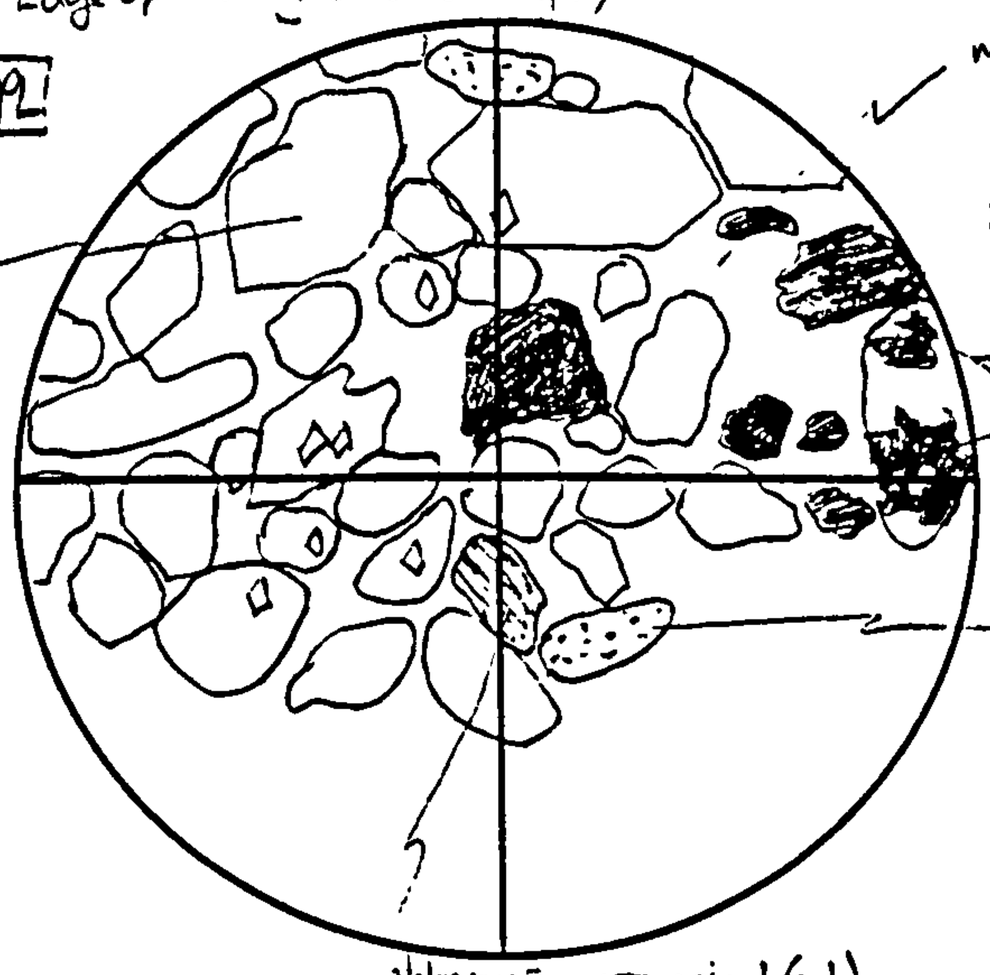

GRAIN TYPES: Originally - olivine 95% micro 2%, lithics 1%, opaques 2%
now o/s: isoamorph serp 90%, dolom/calcite ~5%, opaques ~5%.

MATRIX TYPE: 90% fibrous/mesh o/g serp + isoamorph/mesh pore fill patchy small grains of carbonate + opaques

OTHER FEATURES: Total grain, then cement replacement with magnetite blebs

GRAIN/MATRIX RATIO: 85/15.
16 % GRAINS EUHEDRAL/ANGULAR: 15
13 % GRAINS SUB-HEDRAL/ROUNDED: 60
11 % GRAINS ROUNDED: 25

GRAIN SIZE DISTRIBUTION: Moderately sorted bimodal

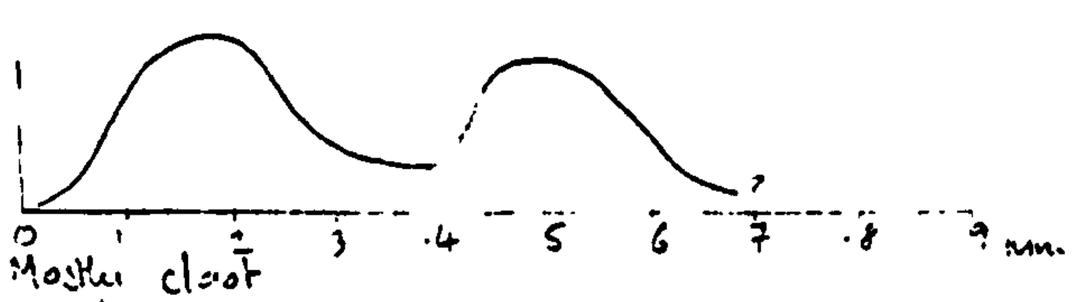

CLAST/MATRIX SUPPORT?: Mostly clast
CONCLUDING COMMENTS: 2 beds each dm-scale
: Bedded reworked pyroclastic sands

STANDARD THIN-SECTION PETROGRAPHY SHEET.

KEVIN LEAHY.

DATE: 1/5/95.
UNIVERSITY SLIDE CODE: 55977 OFS SLIDE CODE: TS037.
BOREHOLE: 93-002 Snowden. DEPTH: 110.55m.
BRIEF HANDSAMPLE DESCRIPTION: Centre of 60cm massive reworked tuff. Mau ie. transitional into primary tuff, faintly bedded

FACIES ASSIGNED: Massive reworked pyroclastic tuff.

SKETCH:

bedding picture

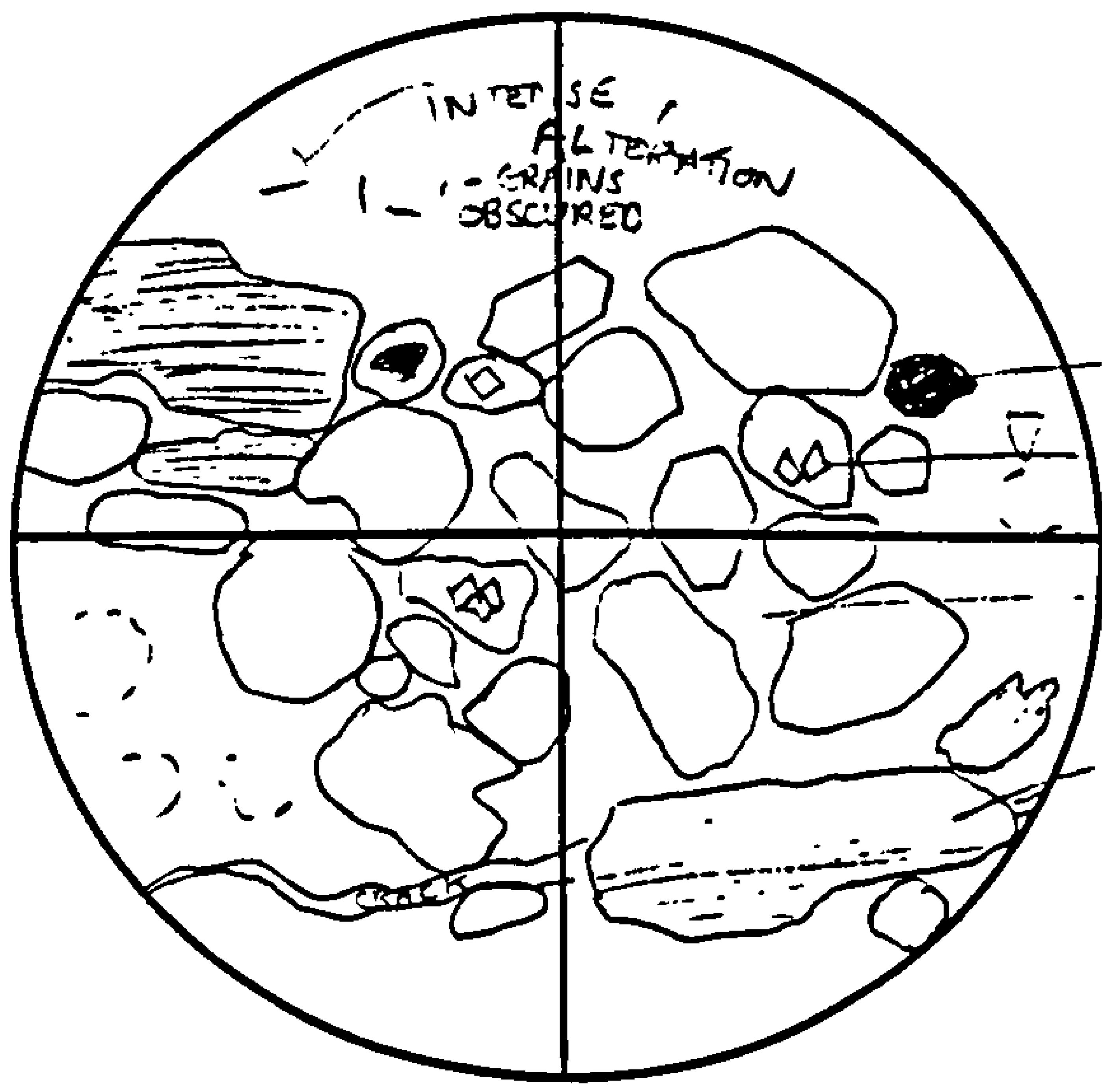

SCALE: ×10 ∅ = 2mm.

← o/g. opaque (ilm?)
— rhombs of dolomite in ox. ol xsts
— isoamorph serp in pores, fibrous o/g around grains
← large phlogopites - fairly common

GRAIN TYPES: Originally: Olivine 88% Micas 8% opaques 2%, lithics ~2%
Olivine now: isoamorph serp 90% opaques 8%, carbonate ~2%

MATRIX TYPE: Fibrous serp o/g, isoamorph serp pore fill, some patches of mesh texture serp. in larger pores
no opaques or carbonate.

OTHER FEATURES:

GRAIN/MATRIX RATIO: 85/15
4 % GRAINS EUHEDRAL/ANGULAR: 15
% GRAINS SUB-HEDRAL/ROUNDED: 50
9 % GRAINS ROUNDED: 35

GRAIN SIZE DISTRIBUTION:
poor - moderately sorted
-ve skewed unimodal

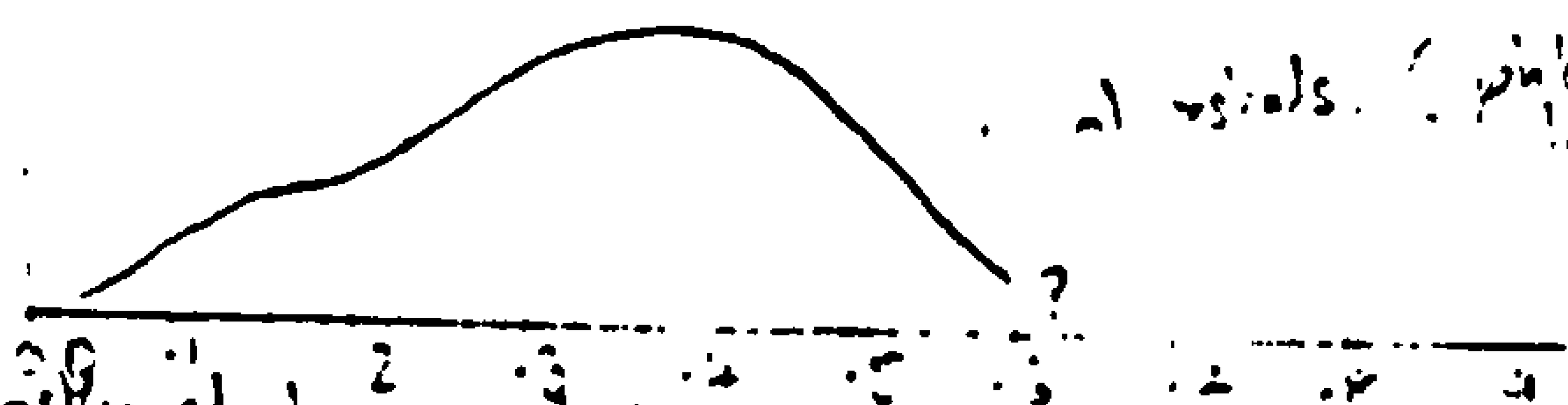

... phlogs much larger

CLAST/MATRIX SUPPORT?: mostly clast supported.
CONCLUDING COMMENTS: ... sedimentary ... bedded pyroclastic sand

STANDARD THIN-SECTION PETROGRAPHY SHEET.

KEVIN LEAHY.

DATE: 26/4/95
UNIVERSITY SLIDE CODE: 55973 OFS SLIDE CODE: TS036
BOREHOLE: OFS-93-002. Snowden DEPTH: 111.20m.
BRIEF HANDSAMPLE DESCRIPTION: Grey-green medium tuff - central part of massive unit 60cm thick. Lower central region of the tuff pile.

FACIES ASSIGNED: either Massive, reworked pyroclastic sand, or coarse tuff (primary)

SKETCH: PPL

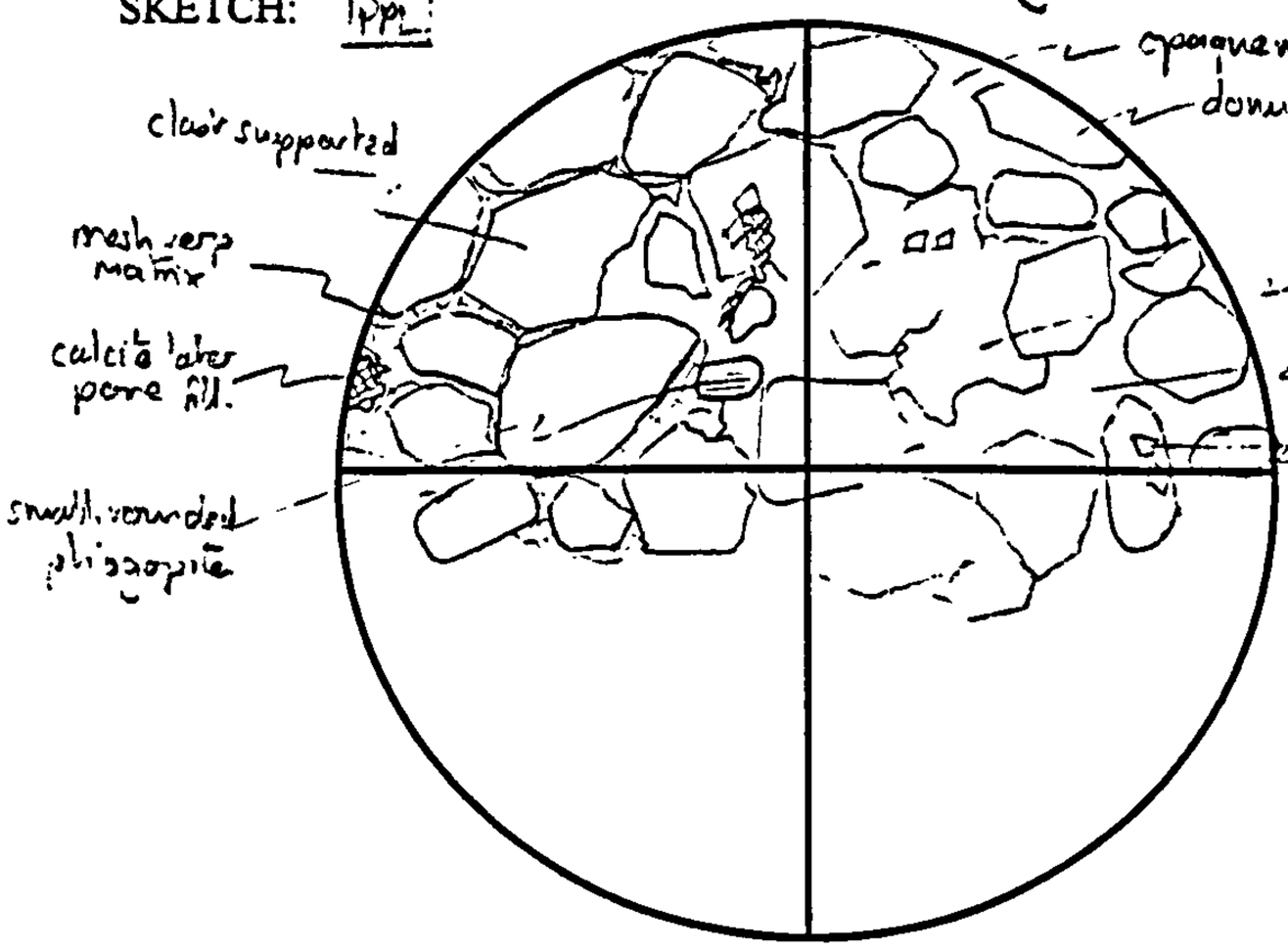

SCALE: ×10 ∅=2mm

NB Sketch from within a zone of maghemite concentration

GRAIN TYPES: Originally: Olivine ~98%, micas ~1%, opaques ~1%
Olivines now: isoamorphic mesh serp ~85%, carbonate ~10%, minor opaques ~5%

MATRIX TYPE: Overall, serp ~85%, carbonate ~10%, maghemite ~5%
← occurs in patches

OTHER FEATURES: Maghemite blebs commonly follow faint bedding. Some are more globular and x-cut.

GRAIN/MATRIX RATIO: 80/20/ 85/15.
115 % GRAINS EUHEDRAL/ANGULAR: 47
% GRAINS SUB-HEDRAL/ROUNDED: 40
+ % GRAINS ROUNDED: 13

GRAIN SIZE DISTRIBUTION: well sorted

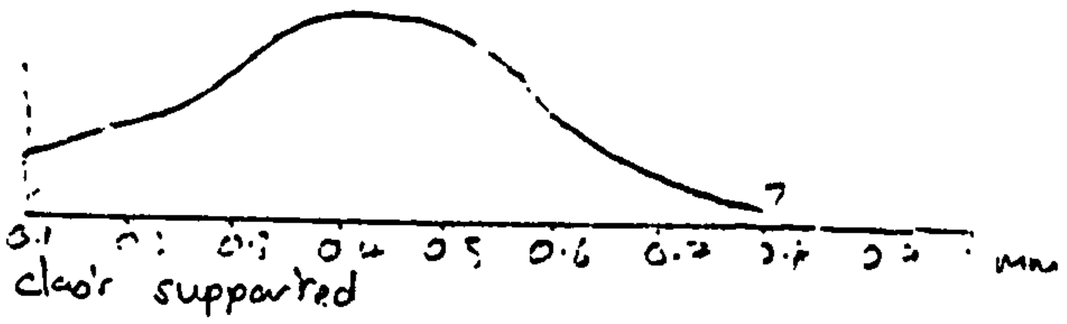

CLAST/MATRIX SUPPORT?: clast supported
CONCLUDING COMMENTS: 2 well sorted fine tuff

STANDARD THIN-SECTION PETROGRAPHY SHEET.

KEVIN LEAHY.

DATE: 26/4/95
UNIVERSITY SLIDE CODE: 55972 OFS SLIDE CODE: T5038
BOREHOLE: OFS 93-002-Snowden DEPTH: 111.86
BRIEF HANDSAMPLE DESCRIPTION: Dark green medium grained basalt tuff with bedding // magnetite blebs
Upper half of 1.6m massive unit

FACIES ASSIGNED: either Massive/bedded reworked pyroclastic sand (fairly bedded) or Course Tuff.

SKETCH: XPL

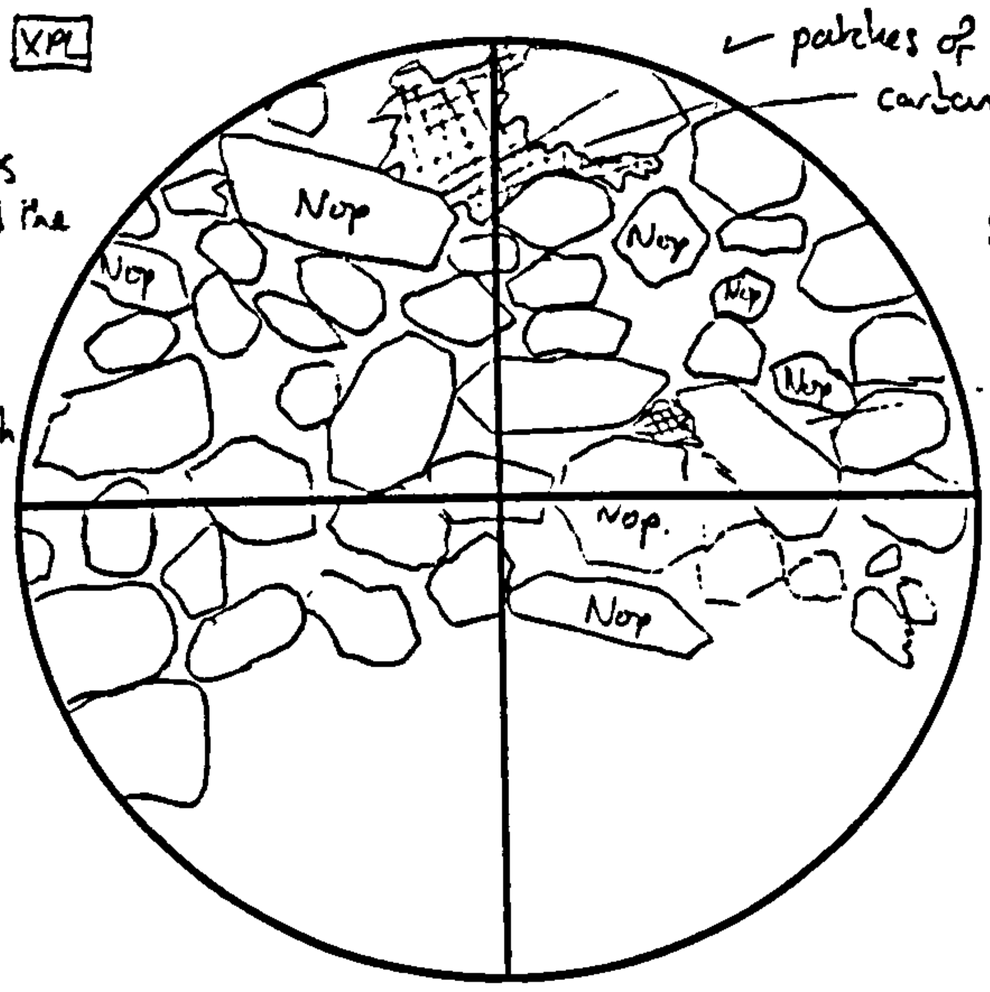

NB Nop indicates not opaque - all the other grains are 100% magnetite replacing olivine 2nd gen. pseudomorph

bedding plane

← patches of calcite cement.
carbonate corroding magnetite rims of pseudomorph

SCALE: x10 1 = 2mm.

mesh. serpentine serp + magnetite (patchy cement) matrix

GRAIN TYPES: Originally, olivine ~95%, opaques ~2%, lithics ~2%, micas ~1% mostly phlog
now: isoamorph + mesh serp 95% 100% magnetite replacement in patches (as above)
carbonate 5%

MATRIX TYPE: Mostly mesh + isoamorph serp 90%, fine calcite ~2%, opaques ~2%
- patches where carbonate is more common (upto 15% in matrix)
- patches where magnetite is the only cement - courser beds.

OTHER FEATURES: 2 magnetite blebs are where grain size is coarser along bedding planes.

GRAIN/MATRIX RATIO: 80/20
% GRAINS EUHEDRAL/ANGULAR: 45
% GRAINS SUB-HEDRAL/ROUNDED: 35
% GRAINS ROUNDED: 20

GRAIN SIZE DISTRIBUTION: moderately sorted slightly bimodal.

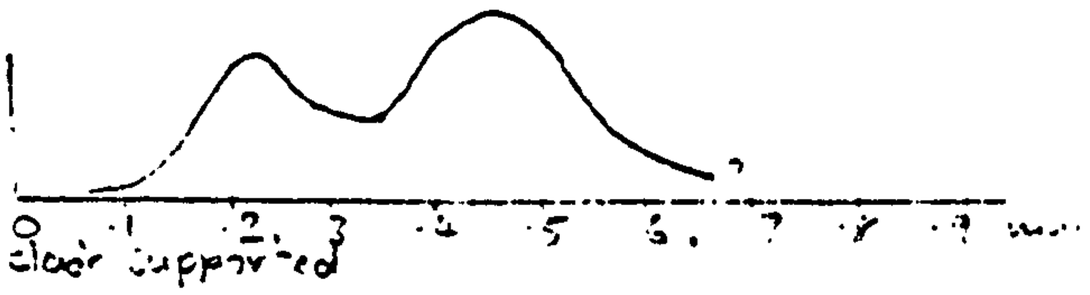

CLAST/MATRIX SUPPORT?: clast supported
CONCLUDING COMMENTS: 2 fine med beds - faintly bedded

STANDARD THIN-SECTION PETROGRAPHY SHEET.

KEVIN LEAHY.

DATE: 27/4/94
UNIVERSITY SLIDE CODE: 55955. OFS SLIDE CODE: T5020
BOREHOLE: OFS93004 - Snowden DEPTH: 106.66
BRIEF HANDSAMPLE DESCRIPTION: Green Tuff.
Centre of 1.6m unit near base of tuff pile

FACIES ASSIGNED: Course Tuff (primary pyroclastic).

SKETCH: XPL

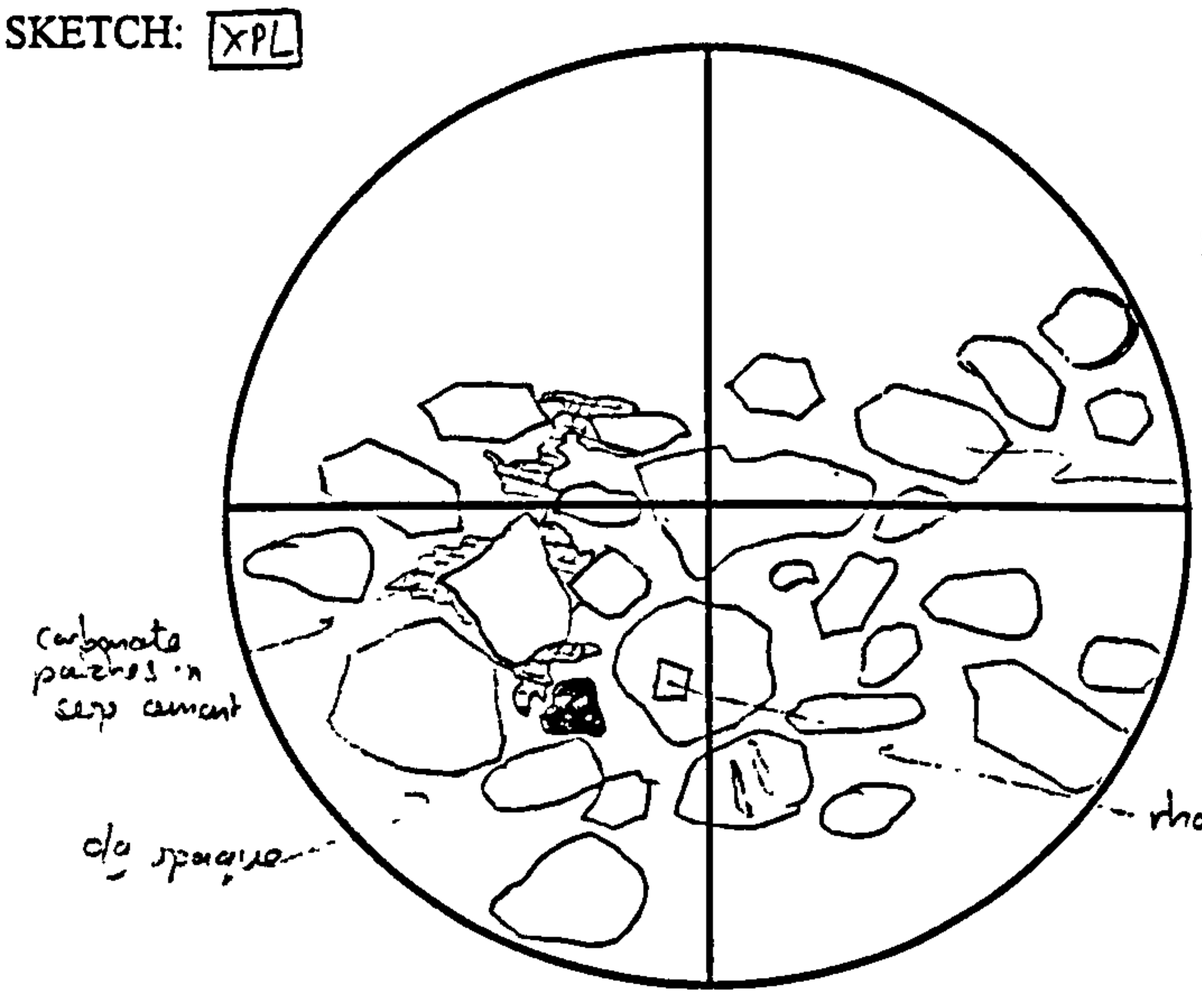

GRAIN TYPES: Originally. >95% olivine, <1% micas, ~2% opaques
now: mesh + isoamorph serp ~95%, 3% carbonate, 2% opaques.

MATRIX TYPE: Mostly fibrous o/q serp, + mesh and isoamorph serp
patchy carbonate cement up to ~10%.

OTHER FEATURES: v. minor cavan-serp, not well developed.

GRAIN/MATRIX RATIO: 80/20-85/20
6 % GRAINS EUHEDRAL/ANGULAR: 55
28 % GRAINS SUB-HEDRAL/ROUNDED: 35
3. % GRAINS ROUNDED: 10

GRAIN SIZE DISTRIBUTION:
Bimodal
moderately sorted

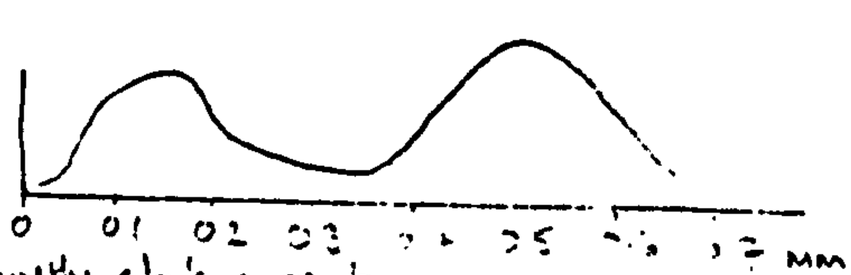

CLAST/MATRIX SUPPORT?: mostly clast support
CONCLUDING COMMENTS: 2 lobes pumice.

STANDARD THIN-SECTION PETROGRAPHY SHEET.

KEVIN LEAHY.

DATE: 27/4/95
UNIVERSITY SLIDE CODE: 55957 OFS SLIDE CODE: TS024.
BOREHOLE: OFS 93-004 - Snowden. DEPTH: 108.20m
BRIEF HANDSAMPLE DESCRIPTION: Fine green hairs hft, calc-veined (not intensely). From centre of basal hairs unit (40cm thick)

FACIES ASSIGNED: Coarse Tuff.

SKETCH: PPL

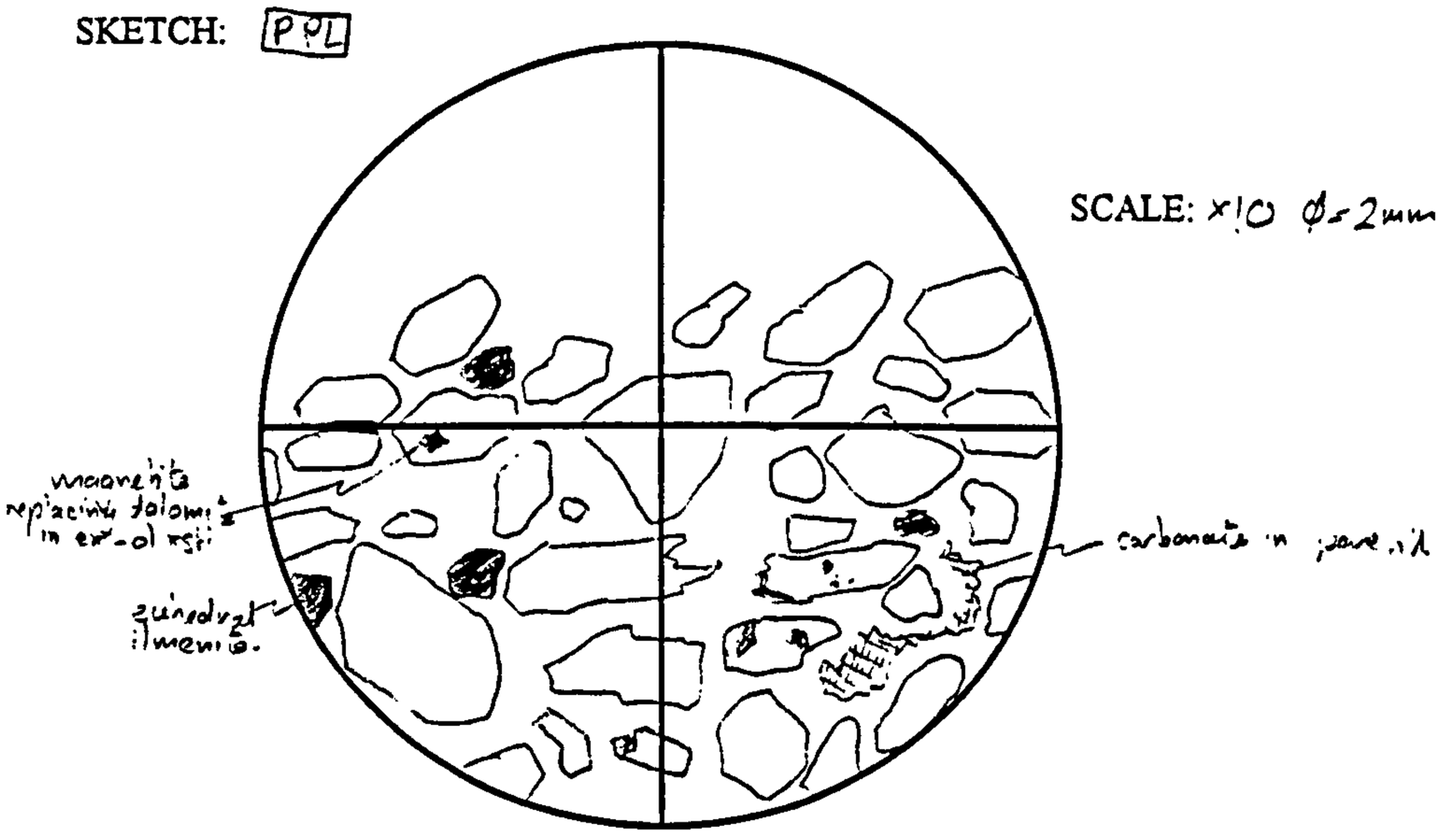

GRAIN TYPES: Originally: Olivine ~ 98% Opaques ~ 2%.
now: isocamorphic serp ~ 60%, carbonate ~ 30%, opaques ~ 10%

MATRIX TYPE: mostly fibrous o/g serp + mesh texture. A little isocamorphic and about 10% pairing carbonate

OTHER FEATURES: Coarse antitaxial vermicular anhydrite, <1% of rock, associated with late carbonate (calcite) veins.

GRAIN/MATRIX RATIO: 75/25 - 80/20
16 % GRAINS EUHEDRAL/ANGULAR: 35
?? % GRAINS SUB-HEDRAL/ROUNDED: 55
3 % GRAINS ROUNDED: 10

GRAIN SIZE DISTRIBUTION:
poor - moderately sorted
bimodal

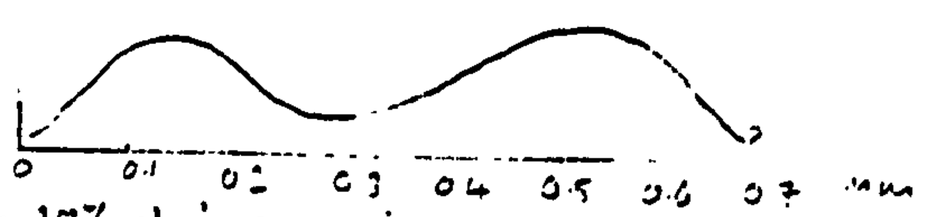

CLAST/MATRIX SUPPORT?: ~20% clast supported
CONCLUDING COMMENTS: - some primary
- Fine bio

STANDARD THIN-SECTION PETROGRAPHY SHEET.

KEVIN LEAHY.

DATE: 26/4/95
UNIVERSITY SLIDE CODE: 55960 OFS SLIDE CODE: TS018
BOREHOLE: OFS93-CO4-SWEDEN DEPTH: 104.20m.
BRIEF HANDSAMPLE DESCRIPTION: Fine green-green tuff Central part of 2.2m unit.

FACIES ASSIGNED: Course Tuff (primary pyroclastic)

SKETCH:

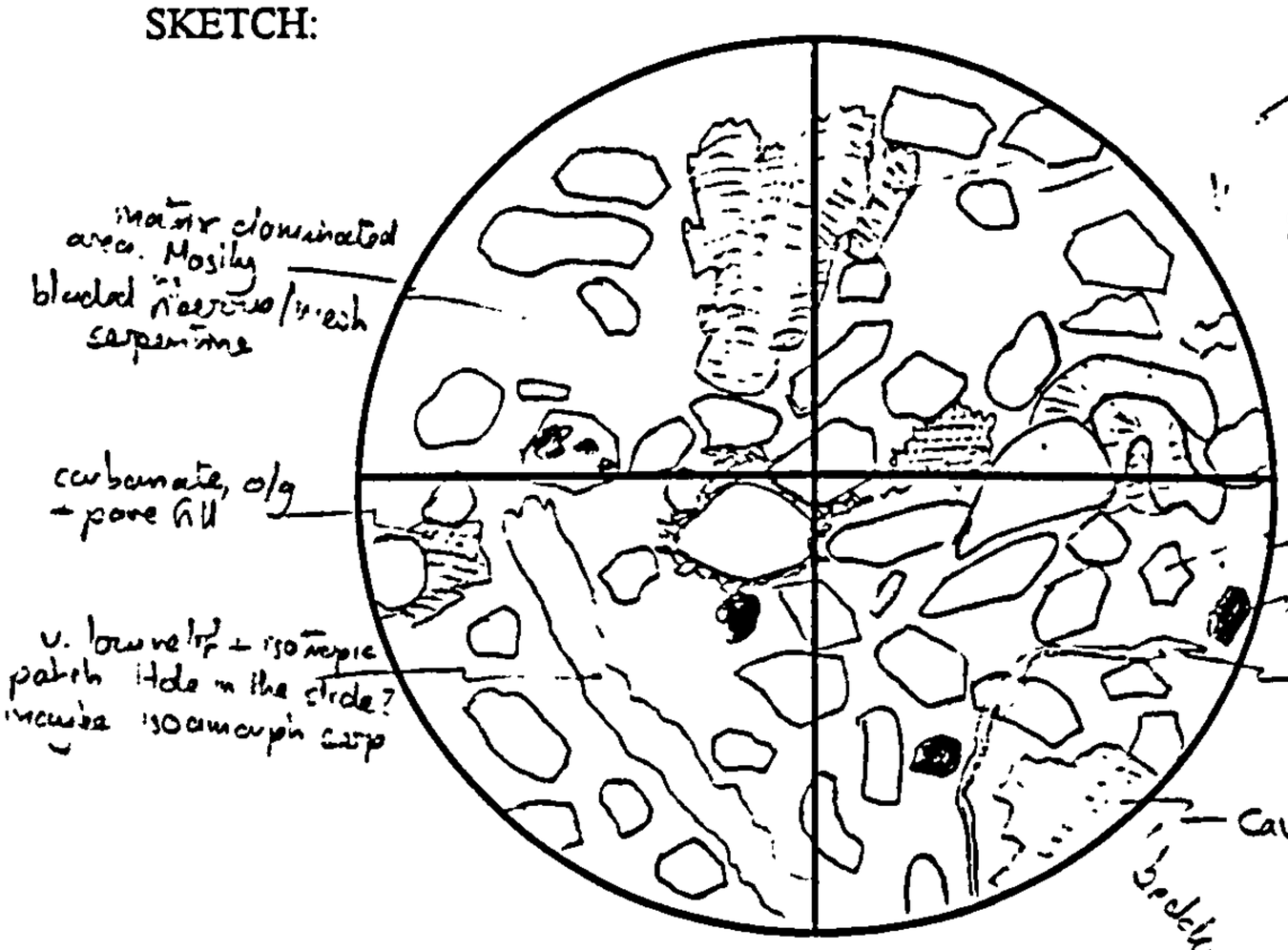

course antitaxitic pseudomorphic orthopyroxene (serp). Growing after early serpentinization.

SCALE: ×10 ϕ = 2mm

GRAIN TYPES: Originally olivine >95% ~1% opaques, ~1% micas
Now ol pseuds: isotropic serp 90%, opaque ~3%, carbonate ~2%.

MATRIX TYPE: Mostly bladed/mesh/fibrous serp ~90%
patchy carbonate ~5%, opaque: ~2%

OTHER FEATURES: large antitaxitic serps (cavas) v. common, now account for 10%~5% of total rock. Later discontinuous cross-cuts all previous antitaxitic structures

GRAIN/MATRIX RATIO: 65/35
55 % GRAINS EUHEDRAL/ANGULAR: 55
40 % GRAINS SUB-HEDRAL/ROUNDED: 35
5 % GRAINS ROUNDED: 10

GRAIN SIZE DISTRIBUTION: well/moderately sorted bimodal.

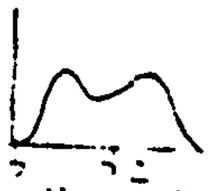

CLAST/MATRIX SUPPORT?: mostly matrix supported
CONCLUDING COMMENTS: Looks primary air fall - v. fine tuff

STANDARD THIN-SECTION PETROGRAPHY SHEET.

KEVIN LEAHY.

DATE: 26/4/95
UNIVERSITY SLIDE CODE: 55958
BOREHOLE: OFS 93-004 - Snowden
BRIEF HANDSAMPLE DESCRIPTION: Green bedded graded tuff large subrounded ½cm lithics calcite + magnetite vein Magnetite seen infiltrating matrix from the fault

OFS SLIDE CODE: TS 009
DEPTH: 97.64m.

FACIES ASSIGNED: Graded reworked pyroclastic sand

SKETCH:

NB op. indicates opaque grain either primary ilm or chromite or, more commonly, magnetite

matrix bladed + amorph serp +/- fine opaques and patchy carbonate.

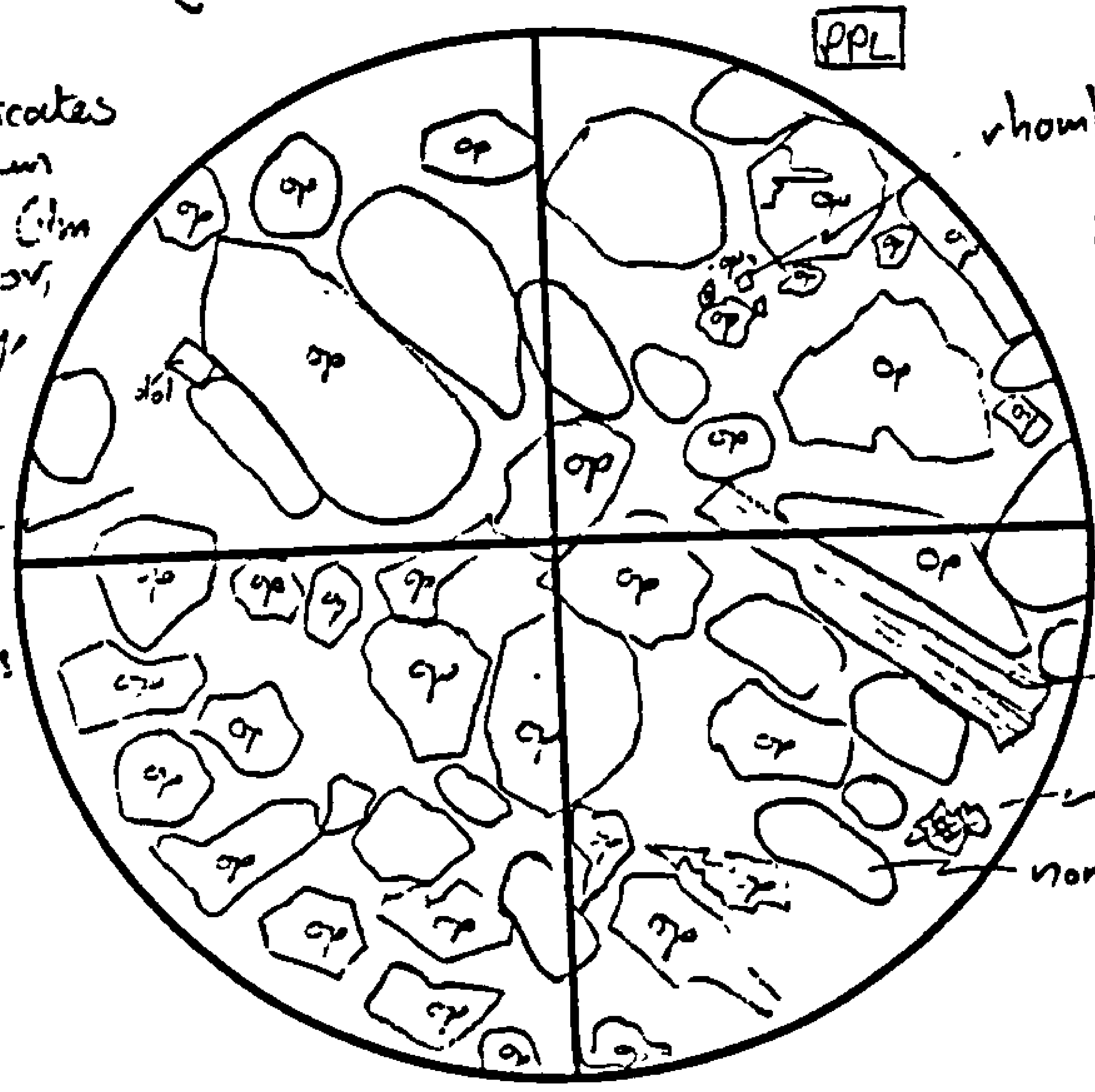

rhombs of dolom. pseudomorphed by magnetite

SCALE: x10 0-2mm

large phlogopite

patch of carbonate in matrix

non-opaque grains bladed + amorph serp - hard to distinguish from matrix

GRAIN TYPES: - hard to say - presumably olivines (from rsti shapes) ~95%, micas ~3% now replaced, in patches, by magnetite. esp near to vein lithics ~2%

MATRIX TYPE: bladed/fibrous/mesh serp. + fine amorph serp + patches of calcite + magnetite

OTHER FEATURES: Lens-vein - brittle, carbonate v. coarse xtls. Magnetite in tuff blocks only ≡ no vein was as such

GRAIN/MATRIX RATIO: 70/30
16 % GRAINS EUHEDRAL/ANGULAR: 30
% GRAINS SUB-HEDRAL/ROUNDED: 40
15 % GRAINS ROUNDED: 30

GRAIN SIZE DISTRIBUTION:
well sorted
- neg skewed unimodal

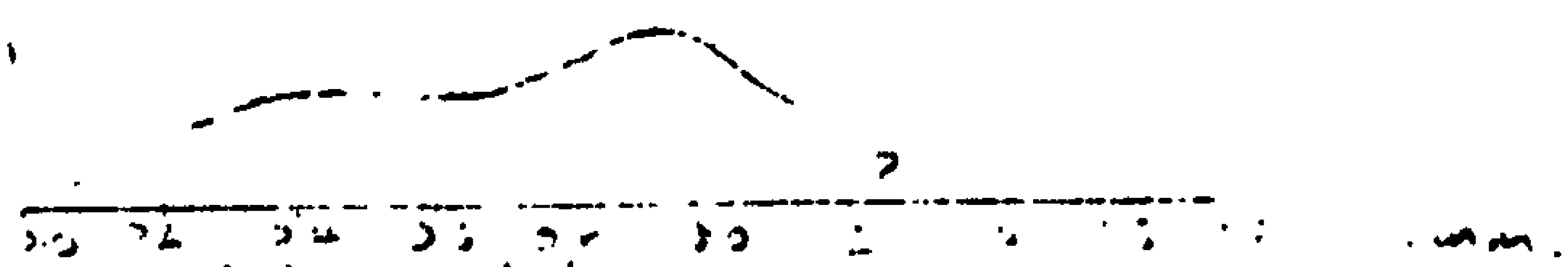

CLAST/MATRIX SUPPORT?: mostly clast supported
CONCLUDING COMMENTS:

STANDARD THIN-SECTION PETROGRAPHY SHEET.

KEVIN LEAHY.

DATE: 21/4/95.
UNIVERSITY SLIDE CODE: 55956. OFS SLIDE CODE: TS 016.
BOREHOLE: OFS 93 - 004. - Snowden. DEPTH: 106.?
BRIEF HANDSAMPLE DESCRIPTION: Grey green pyroclastic ash/tuff. Base (near) of 004 tuff pile

FACIES ASSIGNED: Primary Coarse to fine Tuff.

SKETCH:

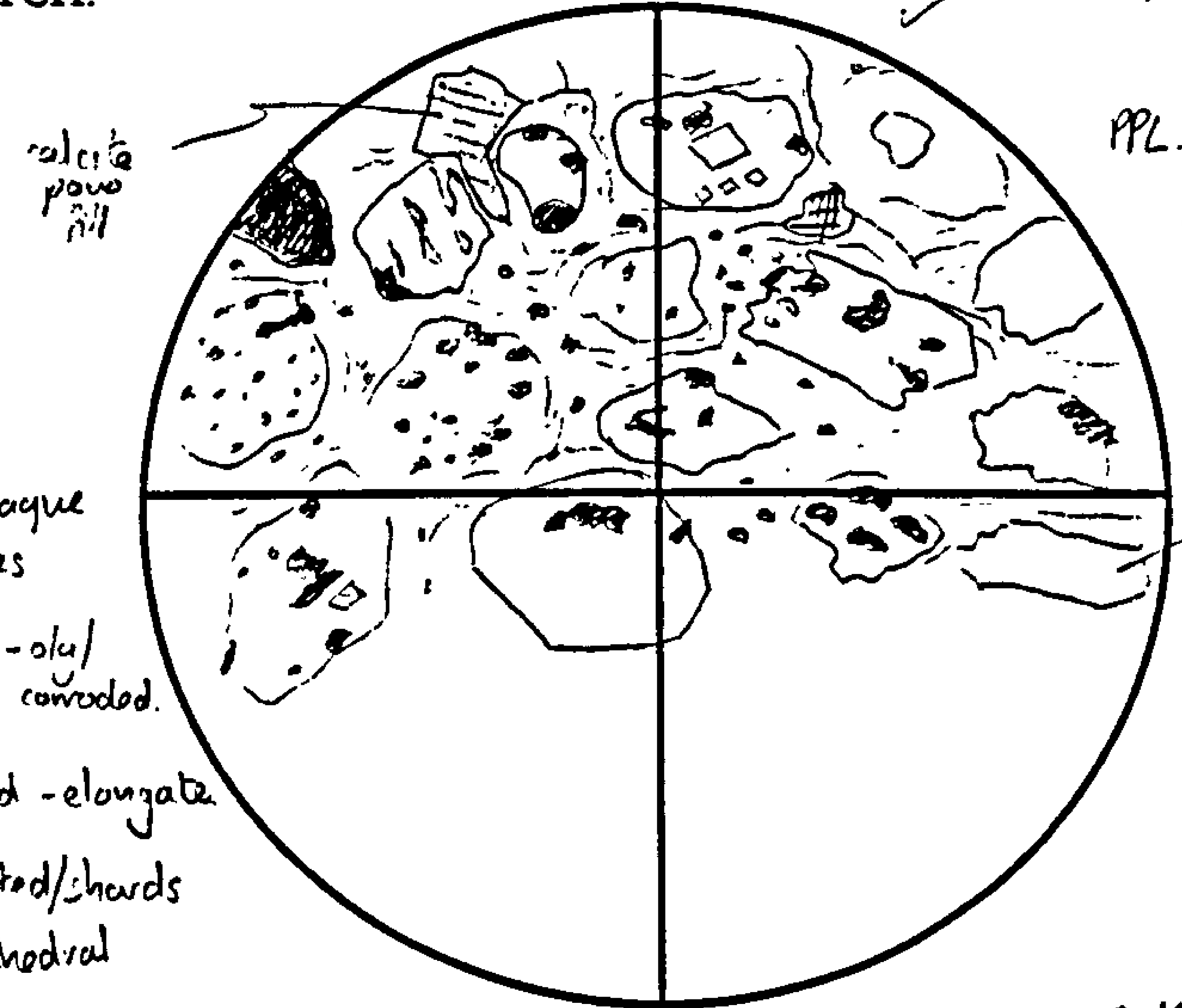

PPL.

SCALE: x10.

Ø = 2mm

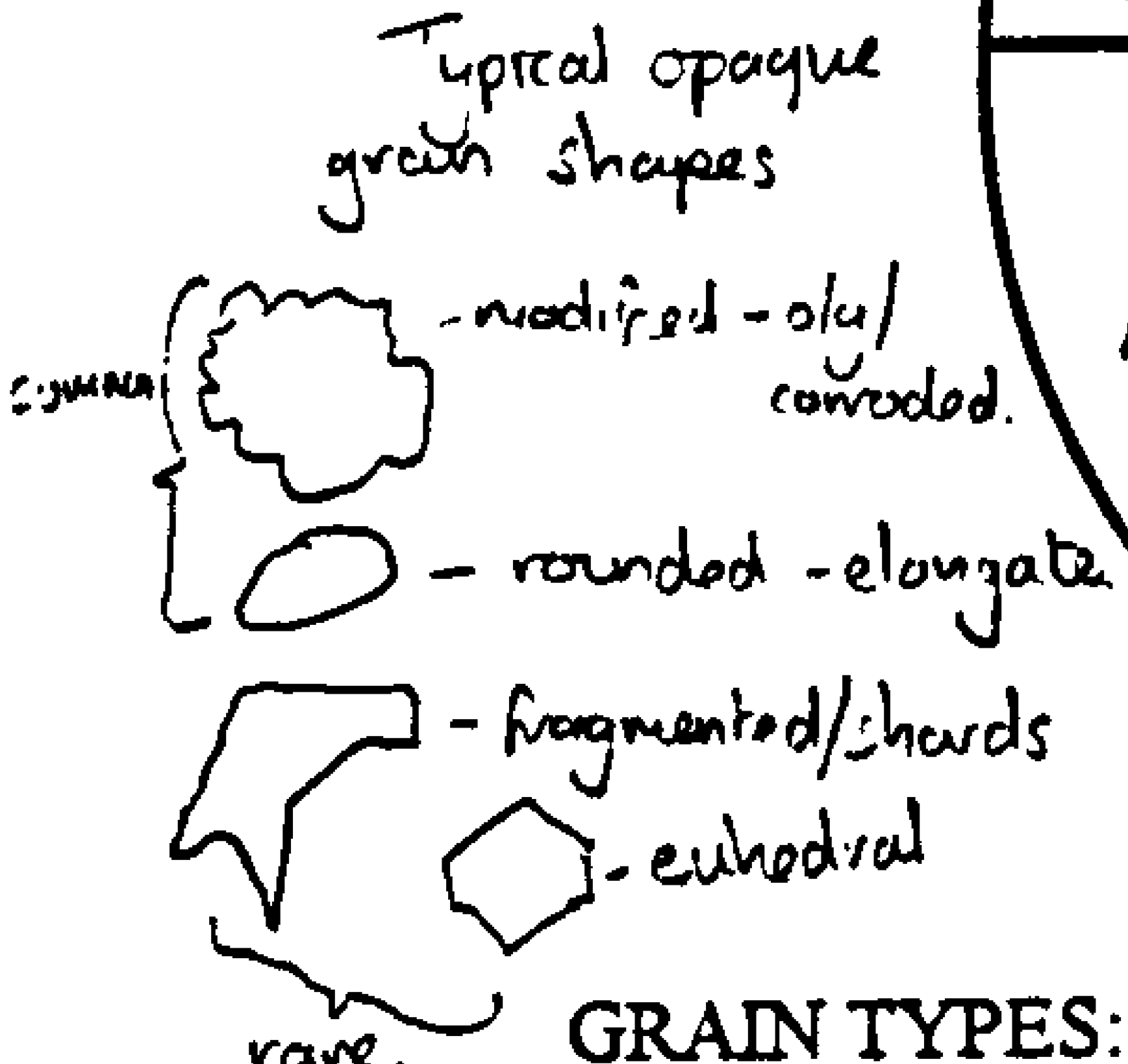

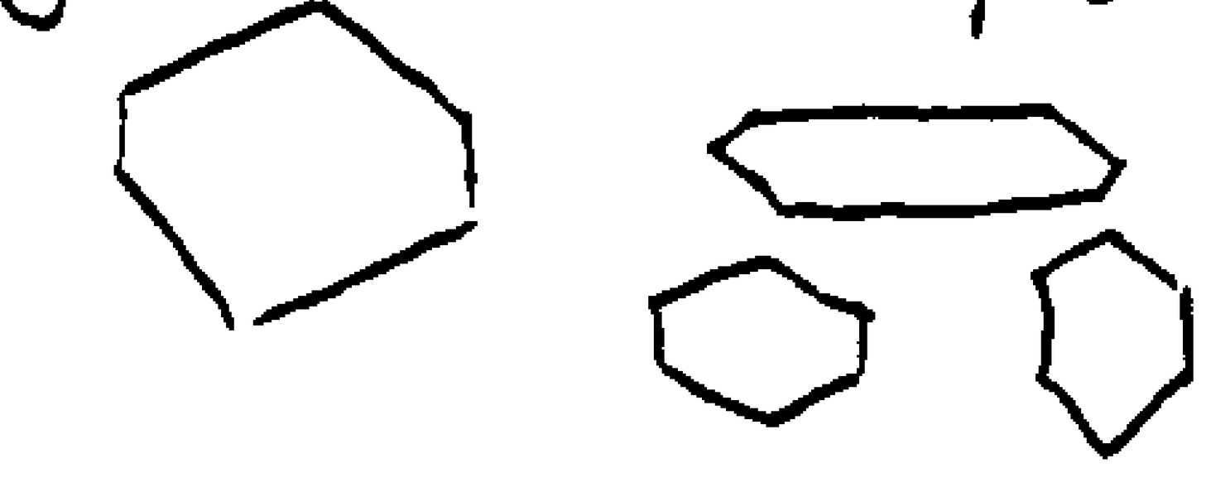

GRAIN TYPES: After olivine psuedomorphs Originally ~90% ol 0.1-0.5mm - the rest opaques + others, lithics (v. rare), phlogopite ~1%
→ serpentine ≈80%, rare sparitic calcite ≈2%, opaques ≈10% (mag + haem), common dolomite ≈8%

MATRIX TYPE: Massive + bladed serpentine, appearing to of grown parallel to original ol crystal faces. Occasional clusting of opaques. Pore filling patches of calcite. (post-serp matrix recryst.)

OTHER FEATURES:

GRAIN/MATRIX RATIO: 85/15.
% GRAINS EUHEDRAL/ANGULAR: 55
% GRAINS SUB-HEDRAL/ROUNDED: 35
% GRAINS ROUNDED: 10

GRAIN SIZE DISTRIBUTION:
well sorted. - unimodal. - skewed fine (-ve)

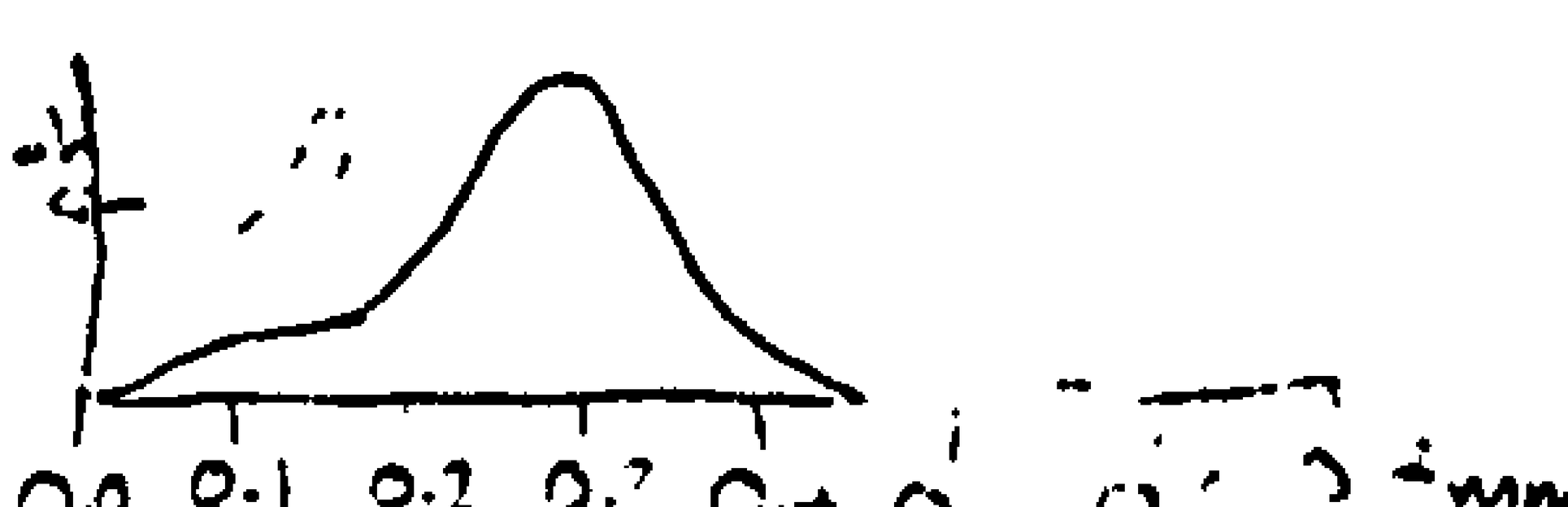

CLAST/MATRIX SUPPORT?: matrix - no grain-grain contacts
CONCLUDING COMMENTS: ? - Fine olivine (kimberlite) tuff. Altered to serpentine. (airfall)
May of originally had an ash matrix - now serp

STANDARD THIN-SECTION PETROGRAPHY SHEET.

KEVIN LEAHY.

DATE: 26/4/95
UNIVERSITY SLIDE CODE: 55948 OFS SLIDE CODE: T5021.
BOREHOLE: OFS93-004 - Snowden DEPTH: 107.89m.
BRIEF HANDSAMPLE DESCRIPTION: Dark green fine lithic tuff. Centre of basal tuff unit

FACIES ASSIGNED: Coarse Tuff (primary pyroclastic)

SKETCH:

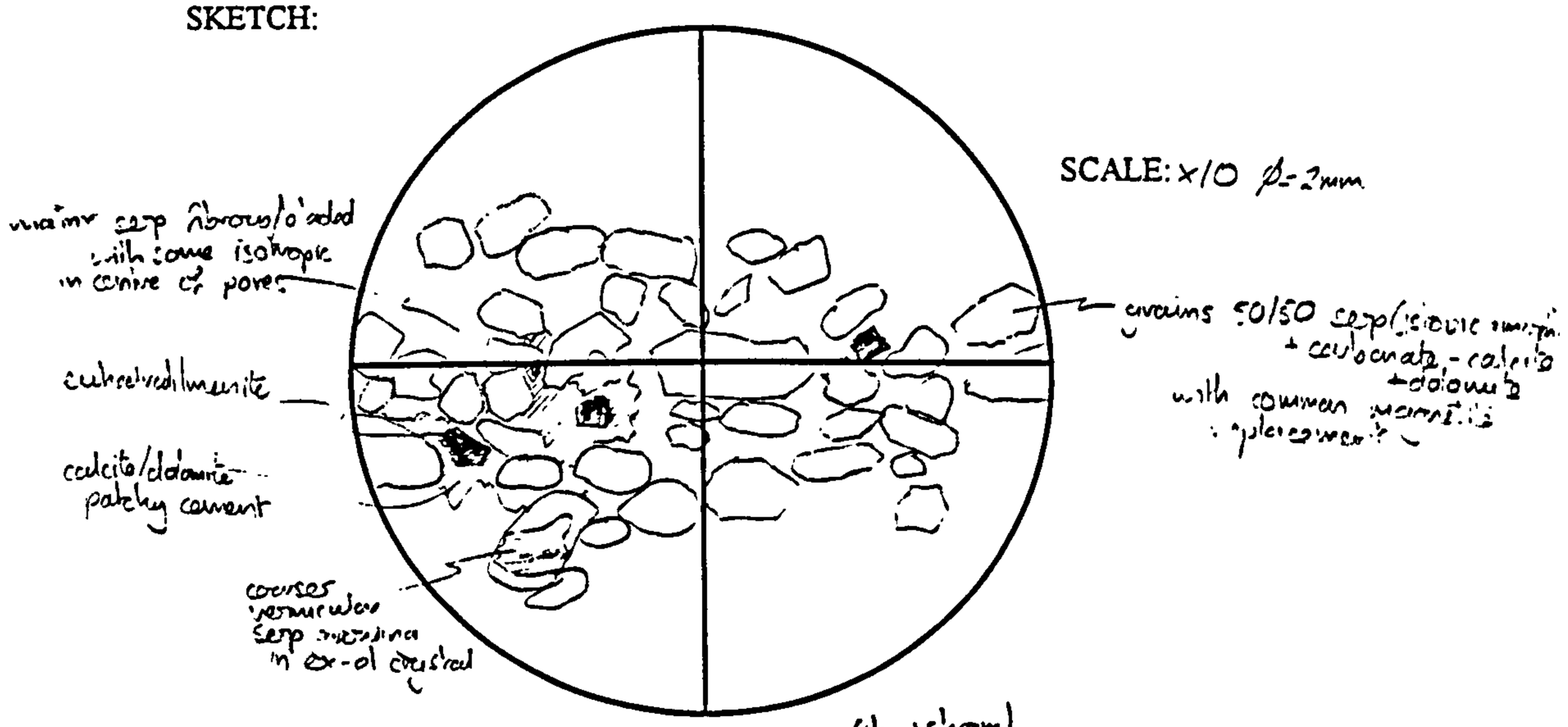

GRAIN TYPES: Originally: Olivine 75%, Opaques 2%, micas ~1%, lithics ~1%
now: serp (iso. ± rel. coarse & fibrous) 60%, carbonate ~38%, opaques ~2%

MATRIX TYPE: Serp - bladed/fibrous/mesh 60%
Serp - anserp'n ± isotropic 28% - mainly in central pore spaces.
Carbonate 10% - patchy Opaques 2%

OTHER FEATURES:

GRAIN/MATRIX RATIO: 75/25 - 80/20
14 % GRAINS EUHEDRAL/ANGULAR: 35
% GRAINS SUB-HEDRAL/ROUNDED: 45
8 % GRAINS ROUNDED: 20

GRAIN SIZE DISTRIBUTION:
well sorted
unimodal, skewed fine.

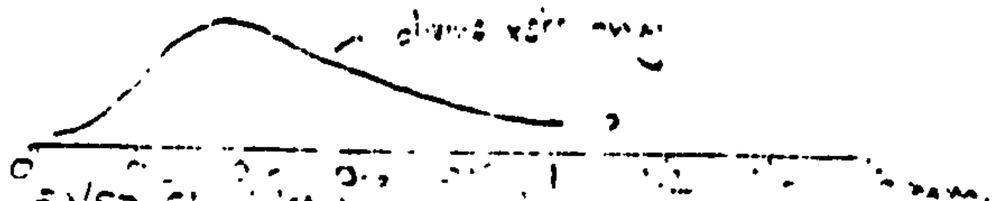

CLAST/MATRIX SUPPORT?: 50/50 Clast/Matrix support
CONCLUDING COMMENTS:

STANDARD THIN-SECTION PETROGRAPHY SHEET.

KEVIN LEAHY.

DATE: 26/4/95
UNIVERSITY SLIDE CODE: 55964 OFS SLIDE CODE: T5010
BOREHOLE: OFS93-C04 - Sweden DEPTH: 98.16m
BRIEF HANDSAMPLE DESCRIPTION: Grey/blueish tuff. centre of a veined vein ~5cm thick, in upper part of tuff pile

FACIES ASSIGNED: Graded reworked pyroclastic sands.

SKETCH:

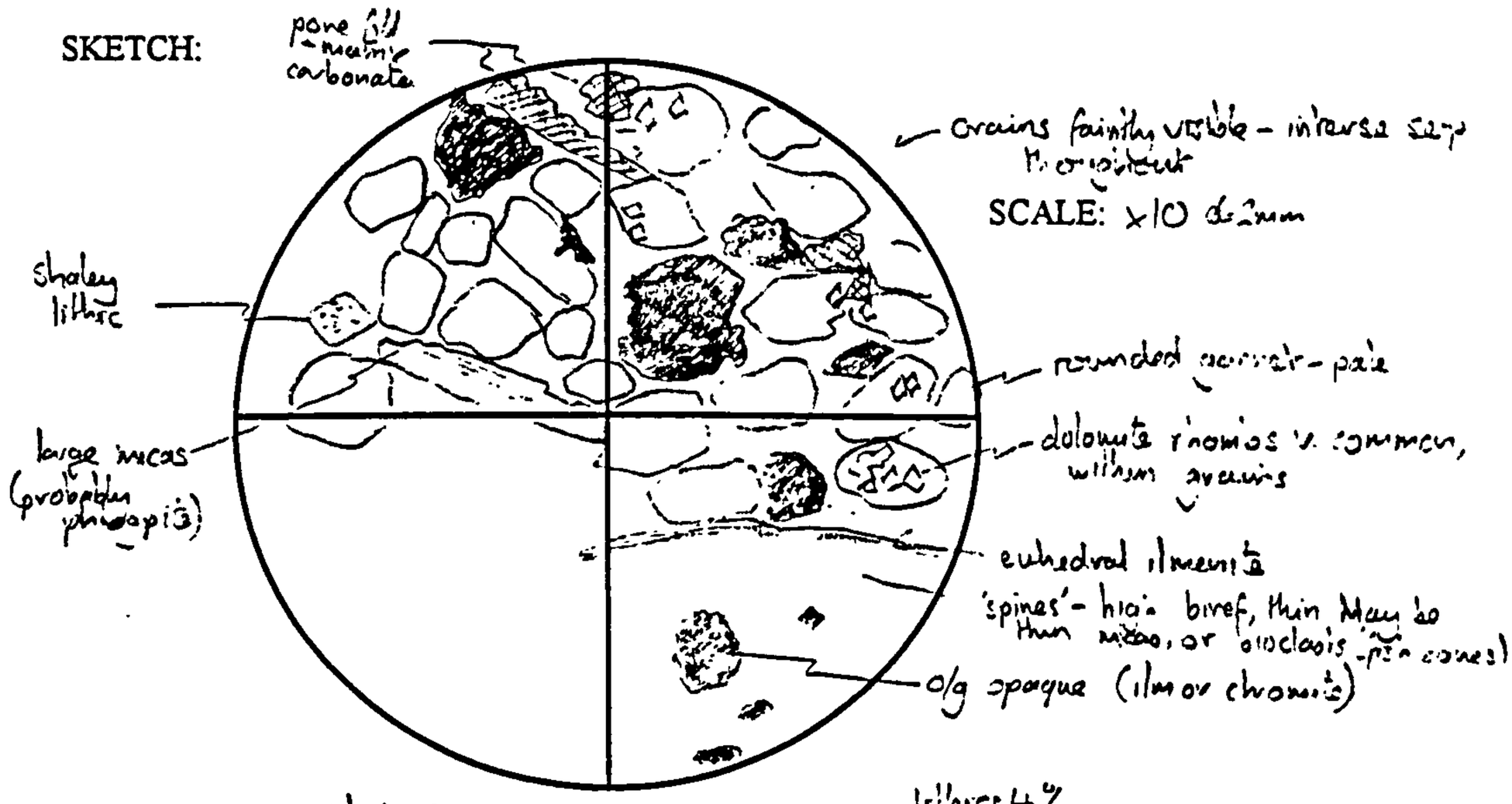

GRAIN TYPES: Olivine 88%, opaques (ilmenite) 3%, lithics 4%
micas + 'spines' 5%, garnets - a few
olivines now replaced by mesh texture serp + 80%. opaques ~ 5%. carbonate ~ 15% (dolomite)

MATRIX TYPE: isotropic + mesh (bladed) serp 85%, carbonate ~ 10%
+ sporadic patches of magnetite/haem

OTHER FEATURES: Lots of lithics - mostly shales.

GRAIN/MATRIX RATIO: 80/20
% GRAINS EUHEDRAL/ANGULAR: 10
% GRAINS SUB-HEDRAL/ROUNDED: 65
% GRAINS ROUNDED: 25
} approximate due to intense serpentinization.

GRAIN SIZE DISTRIBUTION:
well sorted
skewed symmetrical (+ve)

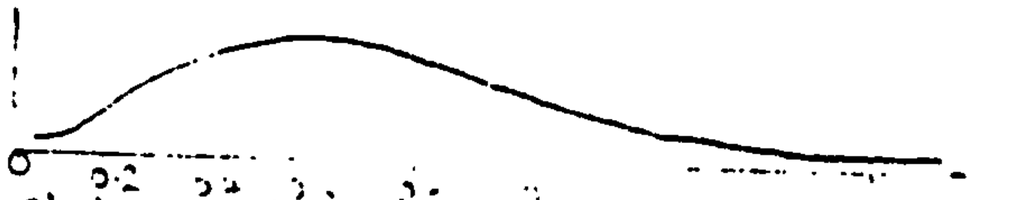

CLAST/MATRIX SUPPORT?: Clast supported
CONCLUDING COMMENTS: pure sand [illegible]

STANDARD THIN-SECTION PETROGRAPHY SHEET.

KEVIN LEAHY.

DATE: 25/4/95
UNIVERSITY SLIDE CODE: 55965. OFS SLIDE CODE: TS015
BOREHOLE: OFS93-004 Snowden DEPTH: 105.77m.
BRIEF HANDSAMPLE DESCRIPTION: Fine green tuff - near base of 2.1m unit, near base of tuff pile

FACIES ASSIGNED: Coarse pyroclastic tuff

SKETCH:

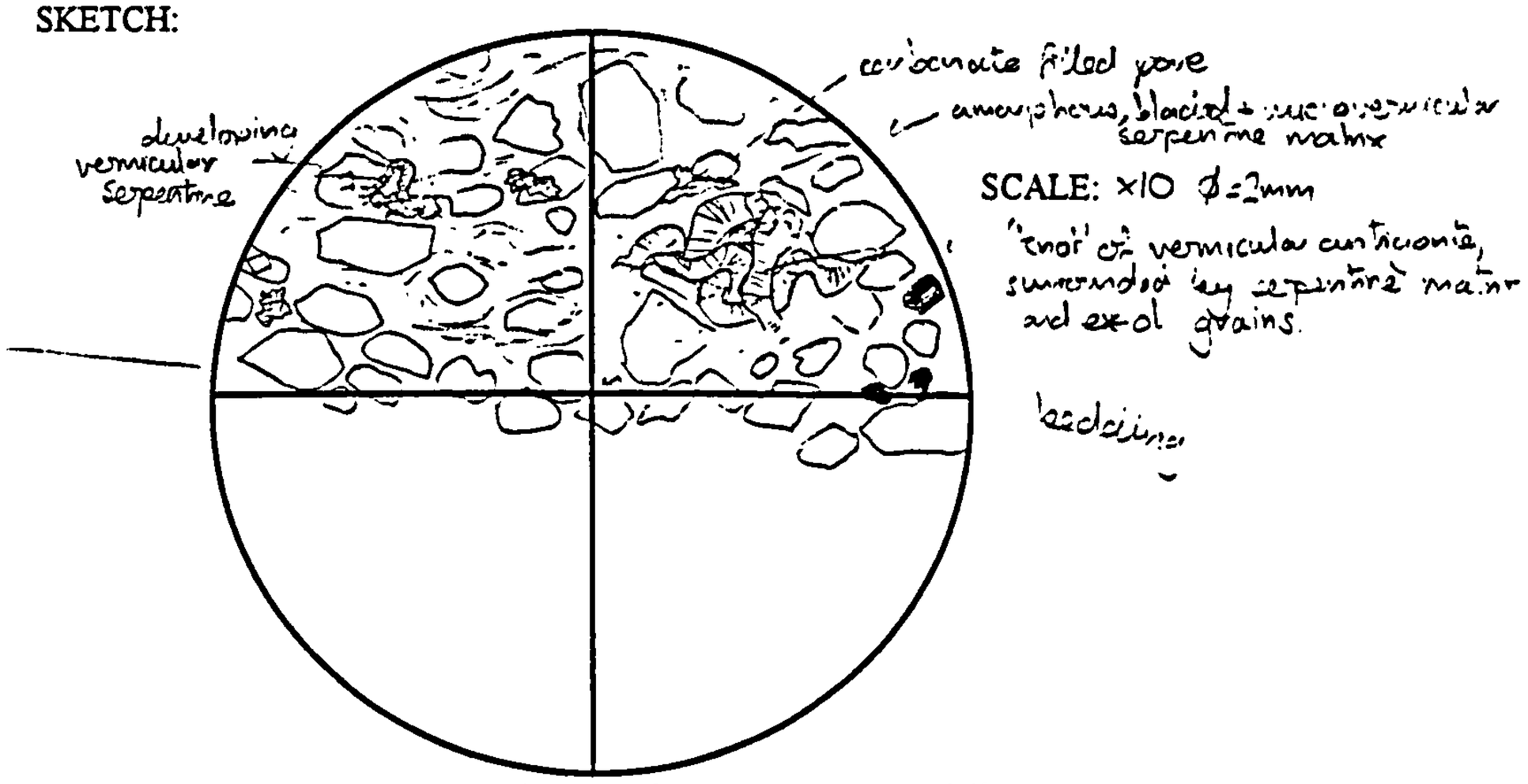

GRAIN TYPES: Originally olivine 95%. opaques 2%. ?lime 2%, no meso now - serp 90%, vermic serp 5%, opaques 3%, carbonate 2%

MATRIX TYPE: Mostly amorphous to finely blocky (fine mesh texture) serpentine Some fine opaques, and isolated pore fills of calcite (~3%)

OTHER FEATURES: large grains of vermicular serpentine known to be originally from XRD, XRF and SEM/EDS (+probe). Grains often visible in hand specimen form xtls upto 2mm long, usually clots ~ 0.5mm

GRAIN/MATRIX RATIO: 80/20 - 85/15
5. % GRAINS EUHEDRAL/ANGULAR: 30
10 % GRAINS SUB-HEDRAL/ROUNDED: 50
15 % GRAINS ROUNDED: 5

GRAIN SIZE DISTRIBUTION:
moderately sorted
skewed symmetrical (-ve)

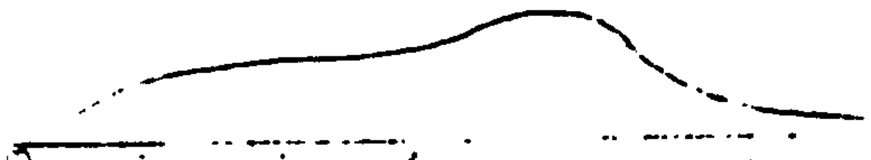

CLAST/MATRIX SUPPORT?: 10% clast supported
CONCLUDING COMMENTS: 2 Fms in medium power optic

STANDARD THIN-SECTION PETROGRAPHY SHEET.

KEVIN LEAHY.

DATE: 27/4/95
UNIVERSITY SLIDE CODE: OFS SLIDE CODE: TSC05
BOREHOLE: OFS 93 -CC04 -Sneachan DEPTH: 97.07
BRIEF HANDSAMPLE DESCRIPTION: Green/blue lamb hut. Abase of 30cm thick sanded unit. Note 2 diamonds recovered from this subunit (within 30cm).

FACIES ASSIGNED: Graded reworked pyroclastic sand

SKETCH:

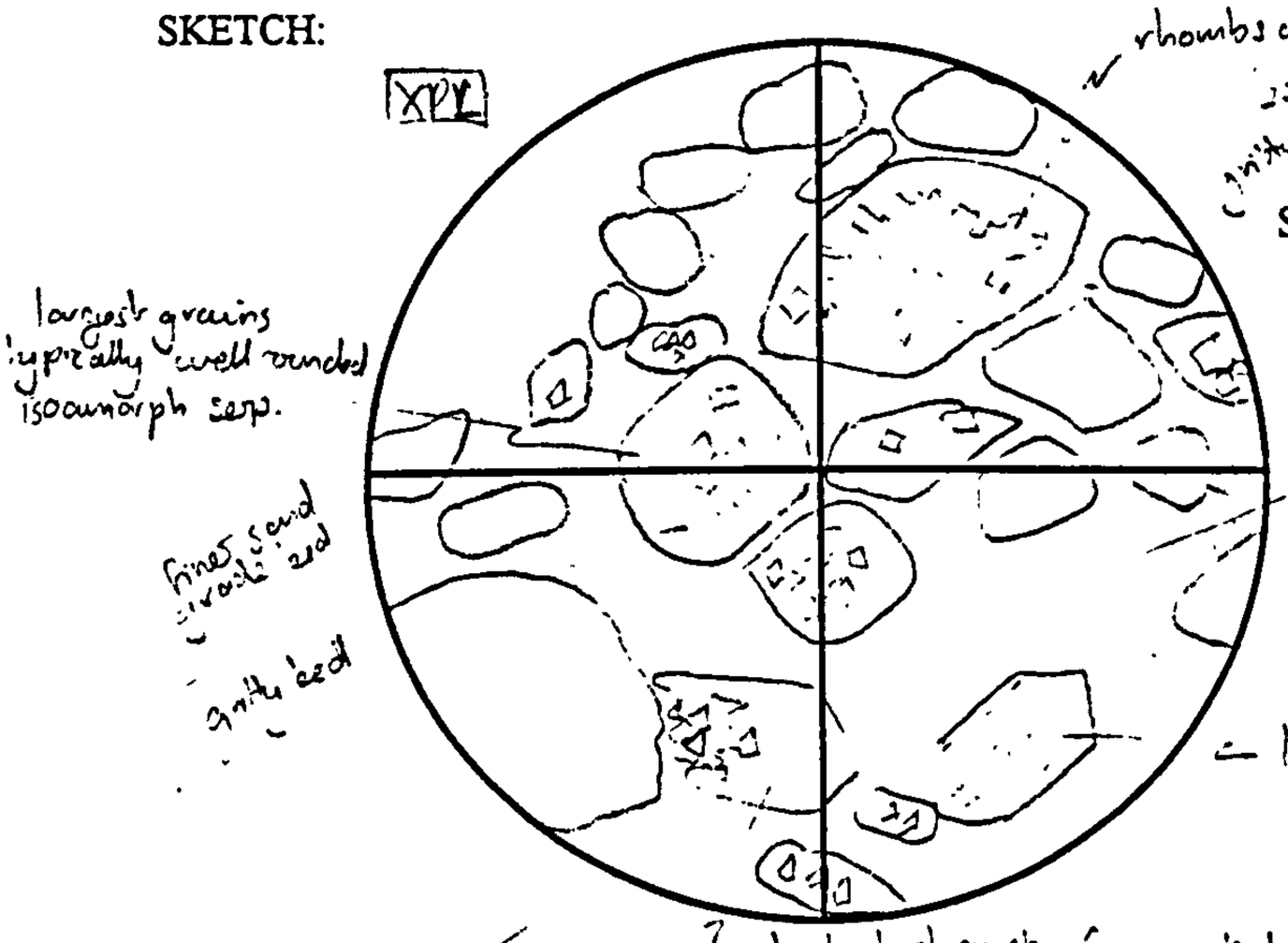

GRAIN TYPES: Euhedral ol crysts - fragmented
originally Olivine ~90%, lithics ~2%, micas ~5%, opaques ~2%
Olivine now isoaumorph serp ~85%, opaques ~5%, carbonate ~10%

MATRIX TYPE: bladed/fibrous/mesh serp common, rare carbonate + opaques (fine)
Sporadic patches ('blebs') of cementing with maunchite

OTHER FEATURES: beddung on a v. fine scale - ½ - 4mm - not simple grading over thin section width (2cm.)

GRAIN/MATRIX RATIO: 80/20
3 % GRAINS EUHEDRAL/ANGULAR: 10 approximate due to intense serpentinization.
% GRAINS SUB-HEDRAL/ROUNDED: 50
3 % GRAINS ROUNDED: 40

GRAIN SIZE DISTRIBUTION: unimodal - well sorted within 1 unit in the thin section above, gnatty bed ~ 1½ mm thick, with aligned elongate sub-well rounded ex-olivine grains 0.3 - 0.5 thick x 0.3 - 0.8 mm long.
CLAST/MATRIX SUPPORT?: carbonate clast supported - coarse beds.
CONCLUDING COMMENTS: 2 sedimentary features are seen in this slide - [illegible] sand

STANDARD THIN-SECTION PETROGRAPHY SHEET.

KEVIN LEAHY.

DATE: 24/4/95.
UNIVERSITY SLIDE CODE: 55950. OFS SLIDE CODE: TS 011
BOREHOLE: OFS 93-004 - Snowcest/DEPTH: 102.30m
BRIEF HANDSAMPLE DESCRIPTION: Green-grey medium kim's tuff. Centre of a 70cm unit - graded. Moorene

FACIES ASSIGNED: Graded serpentinised pyroclastic sand

SKETCH: Magnetite-rich patch.

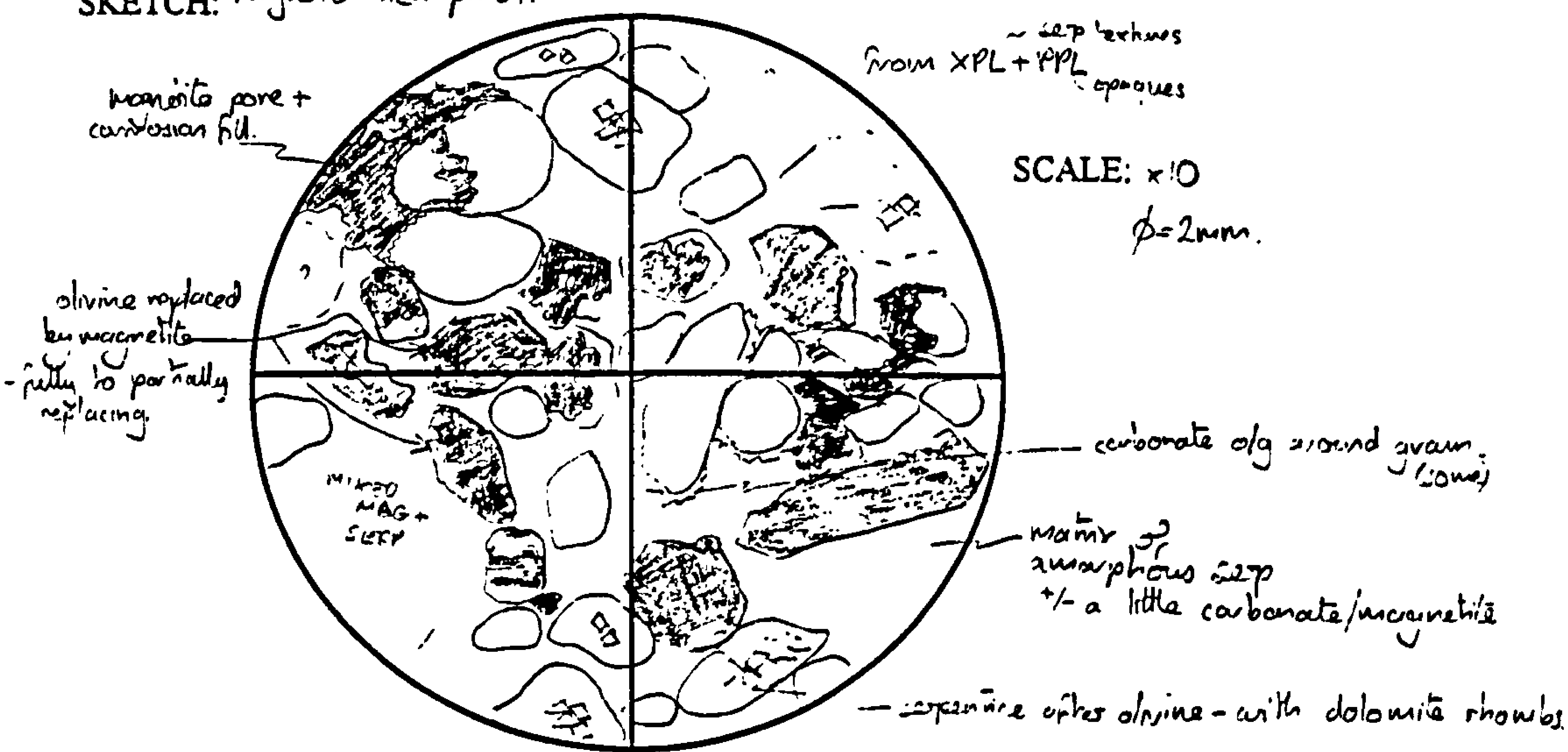

SCALE: x10
ϕ=2mm.

GRAIN TYPES: 1st Olivine ~ 94%, Micas 2 %, Opaques 2 %, lithics 2 %
now. Ol grain: 70% serp, 10% carbonate, up to 20% mag in patches

MATRIX TYPE: Serpentine (amorphous, or v. fine ...) 80%, carbonate 15%, magnetite 5%
carbonate ... intensity. Commonly o/g in the matrix
Magnetite - patches, along bedding planes

OTHER FEATURES: and around (blobby) (presumably in coarser areas with greater original porosity)

GRAIN/MATRIX RATIO: 75/25 – 80/20
11 % GRAINS EUHEDRAL/ANGULAR: 30
% GRAINS SUB-HEDRAL/ROUNDED: 45
8 % GRAINS ROUNDED: 25

GRAIN SIZE DISTRIBUTION:
moderate/poorly sorted.
skewed unimodal

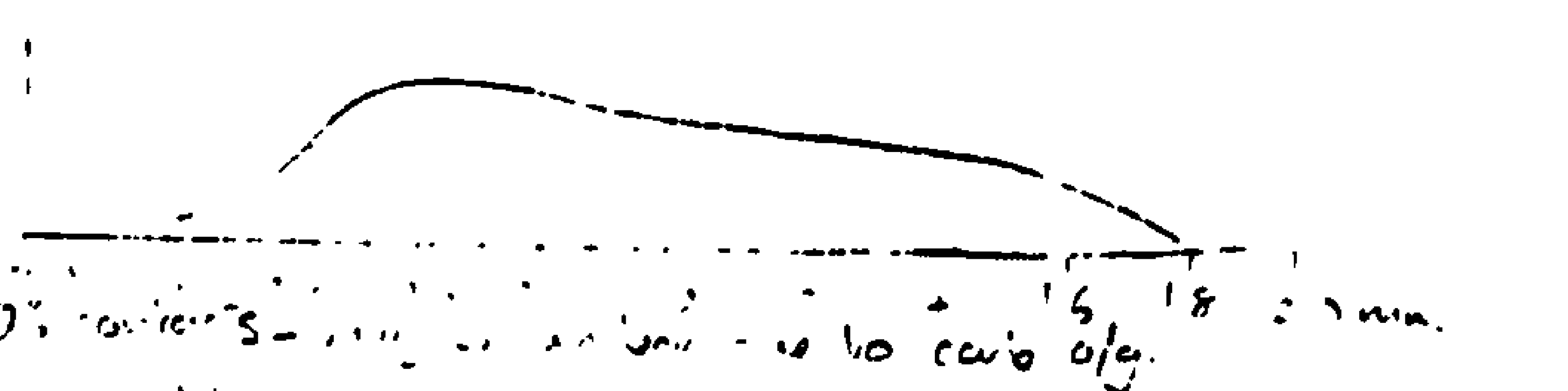

CLAST/MATRIX SUPPORT?: 40% ... - ... to carb o/g.
CONCLUDING COMMENTS: 2 ... replaced ... serpentinised pyroclastic sand

STANDARD THIN-SECTION PETROGRAPHY SHEET.

KEVIN LEAHY.

DATE: 23/06/95.
UNIVERSITY SLIDE CODE: OFS SLIDE CODE: TS017
BOREHOLE: OFS93-004 - Snowd n DEPTH: 102.76m
BRIEF HANDSAMPLE DESCRIPTION: Green fine grained, x-stratified low angle bedded unit 40cm thick - centre of the turbidite pile.

FACIES ASSIGNED: Bedded reworked pyroclastic sand

SKETCH:

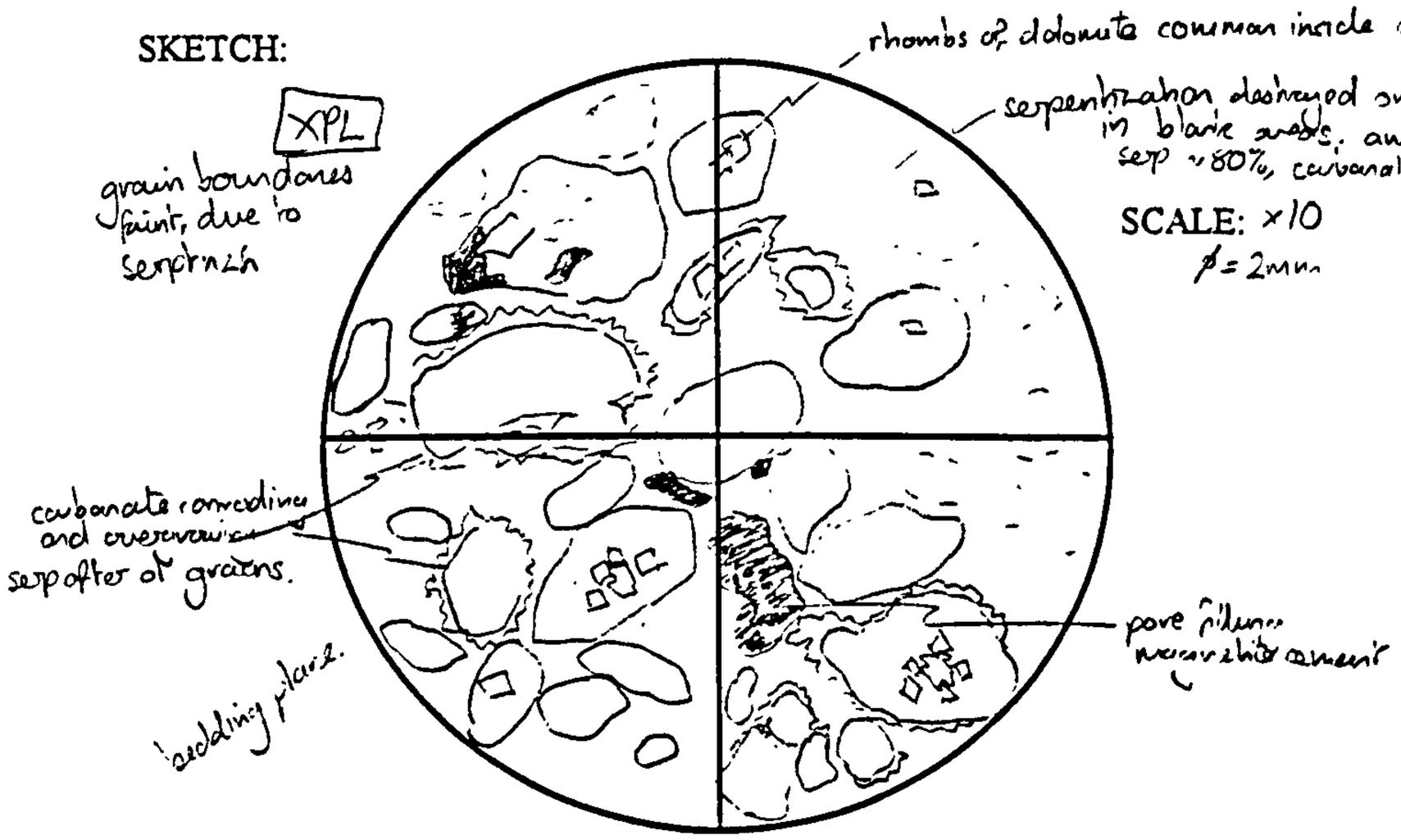

GRAIN TYPES: Originally ol: 90%, micas 5%, opaques 2%, } NB most grains of ol are now corroded at edges.
pseudomorphic serpentine 70%, carbonate 15%, opaque 15%.

MATRIX TYPE: patchy - areas of - serpentine cement - isotropic
- carbonate and serp. carbonate often o/g on grains and in pore spaces
- magnetite often pervasive cement within a patch

OTHER FEATURES:
bedding 3-4mm thick laminations of coarse grains on bedding planes to form silt bed

GRAIN/MATRIX RATIO: 70/30 - unclear in places
% GRAINS EUHEDRAL/ANGULAR: 10
% GRAINS SUB-HEDRAL/ROUNDED: 60
% GRAINS ROUNDED: 30

GRAIN SIZE DISTRIBUTION

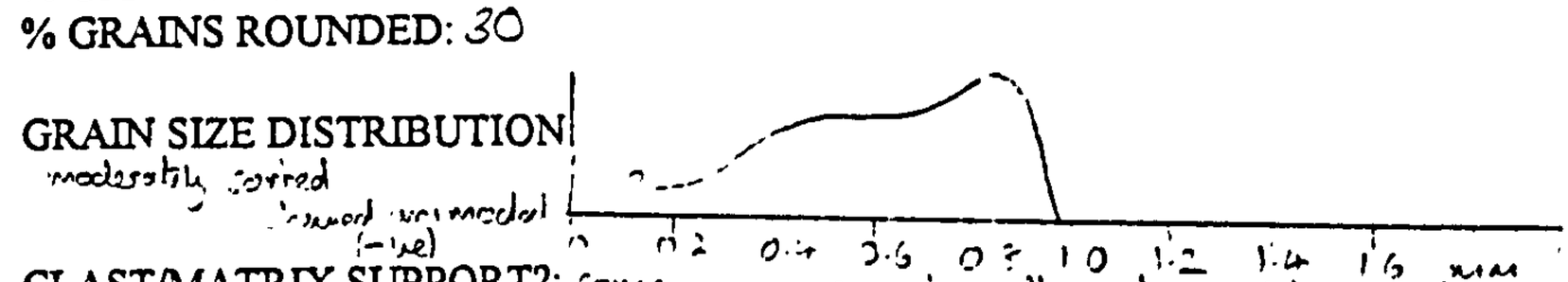

CLAST/MATRIX SUPPORT?: some grain contacts - often obscured by calcite corrosion - clast.
CONCLUDING COMMENTS: Bedded reworked pyro sand, highly serpentinized and carbonatized.

STANDARD THIN-SECTION PETROGRAPHY SHEET.

KEVIN LEAHY.

DATE: 23/4/95.
UNIVERSITY SLIDE CODE: 55951 OFS SLIDE CODE: TS012.
BOREHOLE: OFS 93-004 - Snowden DEPTH: 102 95m
BRIEF HANDSAMPLE DESCRIPTION: Grey-green laminb tuff Top of massive unit 50cm thick. Lower central tuff pile

FACIES ASSIGNED: Massive reworked pyroclastic sand

SKETCH: PPL

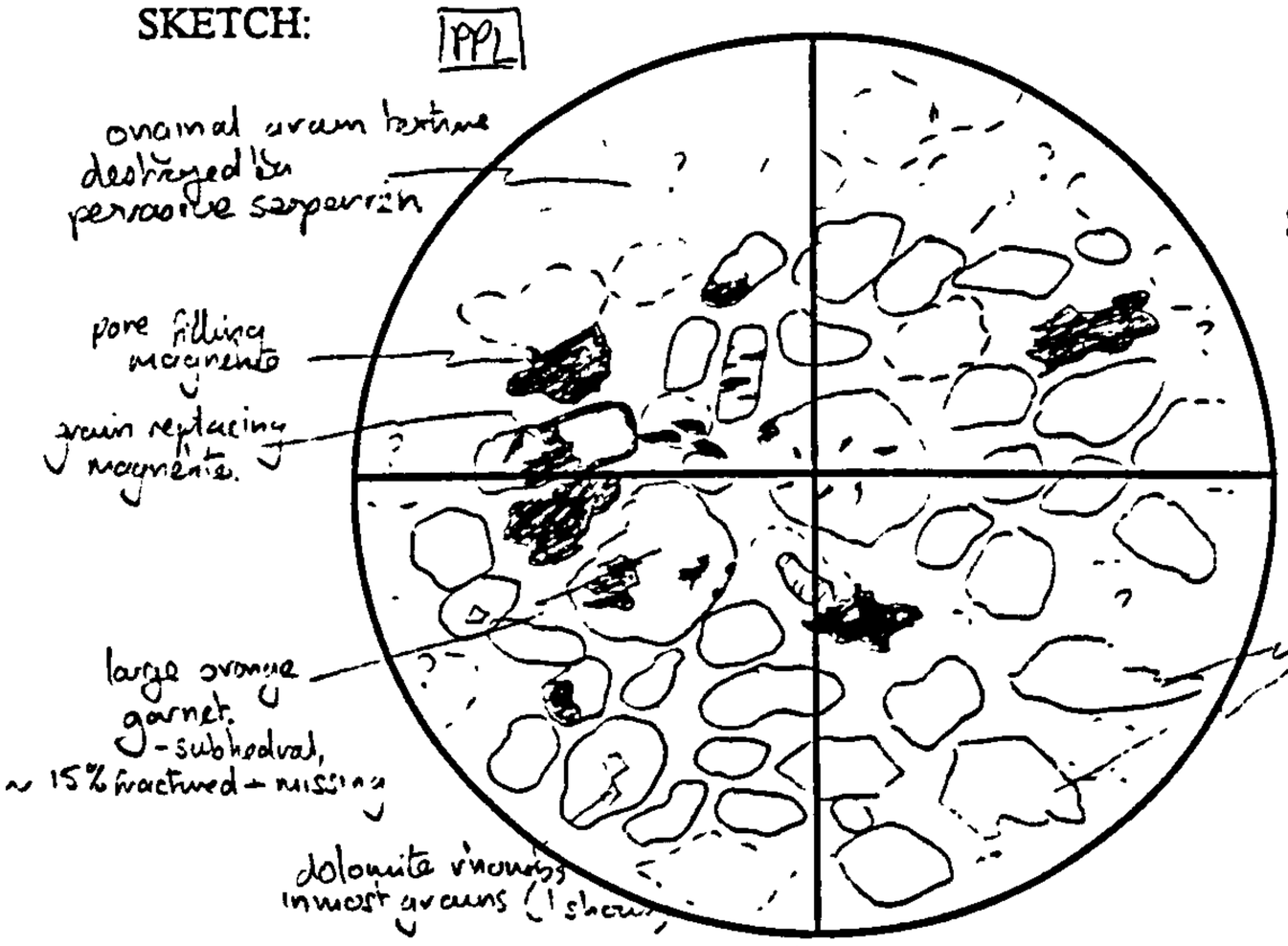

SCALE: ×10
Ø = 2mm.

GRAIN TYPES: Originally: Ol ?10%, Mtrs ~5%, opaques ~2%.
pseudomorphs: serp 70%, dolomite 10% calcite ~5%, opaques 15%.

MATRIX TYPE: Mix of isotropic serpentine, ~88% carbonate ~2%
~10% magnetite
not patchy. Magnetite pore fills do not appear to be connected.

OTHER FEATURES:

GRAIN/MATRIX RATIO: 75/25
12 % GRAINS EUHEDRAL/ANGULAR: 30
50 % GRAINS SUB-HEDRAL/ROUNDED: 50
10 % GRAINS ROUNDED: 20.

GRAIN SIZE DISTRIBUTION: moderately sorted skewed unimodal (-ve)

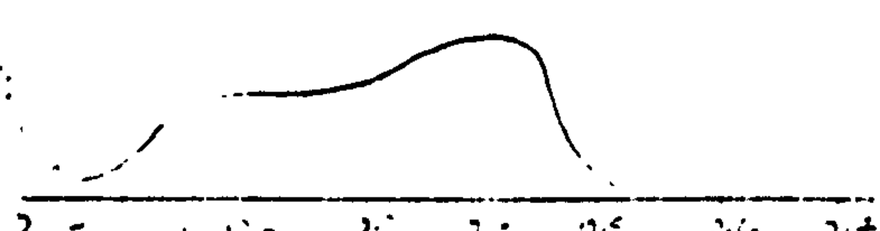

CLAST/MATRIX SUPPORT?: matrix clast supported, about 25%
CONCLUDING COMMENTS: immature - perhaps transitional between epiclastic + primary deposit - lots of euhedrals

STANDARD THIN-SECTION PETROGRAPHY SHEET.

KEVIN LEAHY.

DATE: 21/4/95.
UNIVERSITY SLIDE CODE: 55954. OFS SLIDE CODE: TS026
BOREHOLE: OFS 93 - 304 - Snowdon DEPTH: 108.38.
BRIEF HANDSAMPLE DESCRIPTION: From very base of tuff pile. Highly relic veined fine green tuff.

FACIES ASSIGNED: Coarse Tuff.

SKETCH:

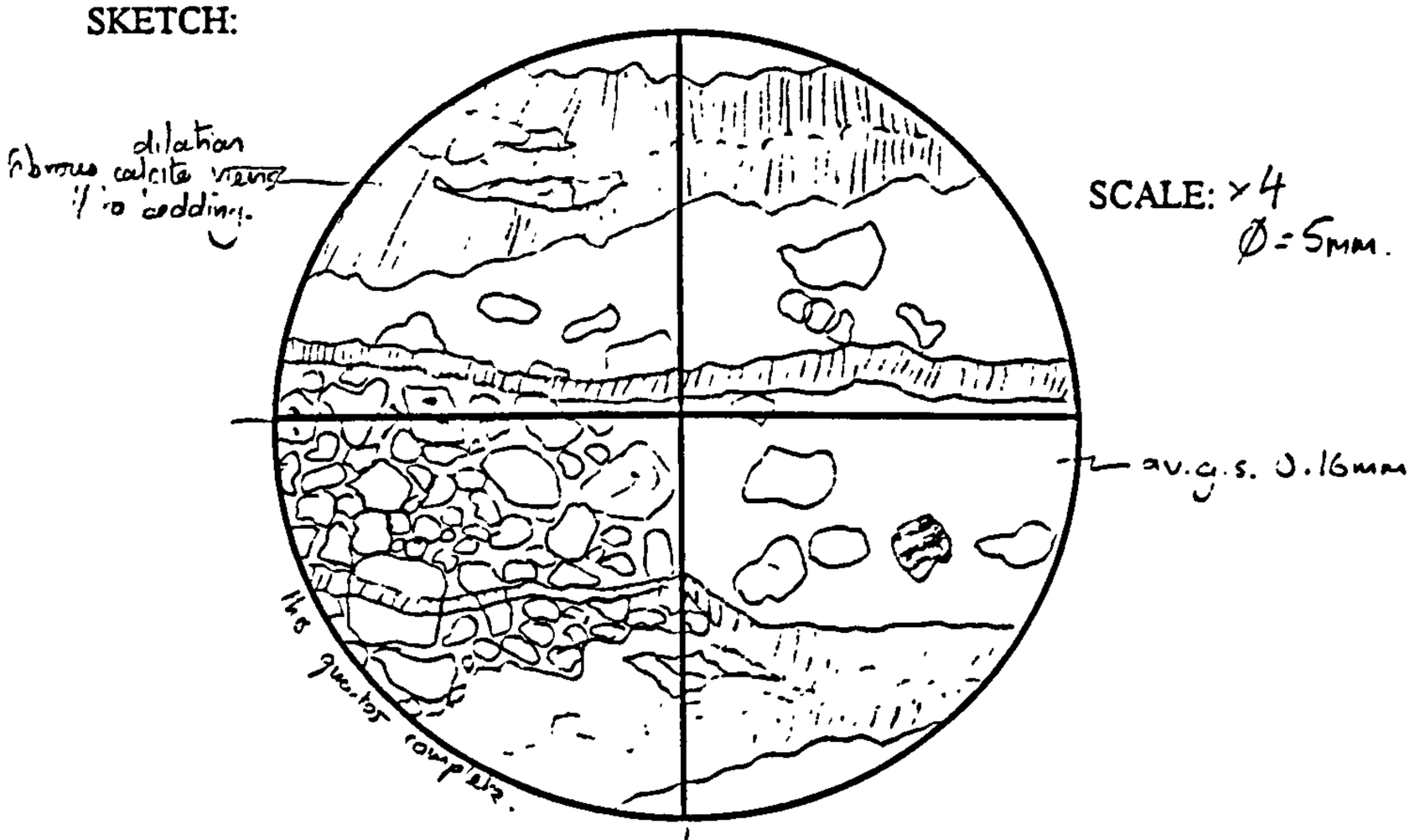

GRAIN TYPES: pseudomorphic serp after olivine. Nearly all olivine (>95%) pseudomorphed + rare magnetite (bladed - low birref. - amorphous - isotropic. + some phlog + opaques.

MATRIX TYPE: micritic calcite, intimately mixed with v. fine serps + dusty opaques.

OTHER FEATURES: calcite veins - later than bedding, serpentinization + calcite cementation. Dilational crack fill. Accounts for ~35-50% of the rock.

GRAIN/MATRIX RATIO: 50/20 to 90/10.
% GRAINS EUHEDRAL/ANGULAR: 20
% GRAINS SUB-HEDRAL/ROUNDED: 60
% GRAINS ROUNDED: 20

GRAIN SIZE DISTRIBUTION:

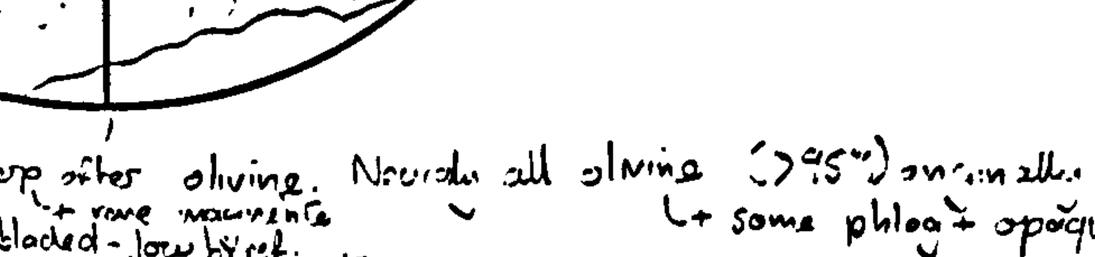

moderately well sorted - slight. well packed. bimodal

CLAST/MATRIX SUPPORT?: 10-20% grain contacts, mostly a thin matrix between
CONCLUDING COMMENTS: - fine tuff (glass) - altered to olivine

STANDARD THIN-SECTION PETROGRAPHY SHEET.

KEVIN LEAHY.

DATE: 24/4/95
UNIVERSITY SLIDE CODE: 55963 OFS SLIDE CODE: TS022.
BOREHOLE: OFS-93-004 - Snowden DEPTH: 108.34 m
BRIEF HANDSAMPLE DESCRIPTION: Calc. veined fine green tuff. very base of coarse unit, 1cm above contact.

FACIES ASSIGNED: Coarse Tuff (primary pyroclastic).

SKETCH: 1/4 shown

Texture better preserved than in overlying rocks.

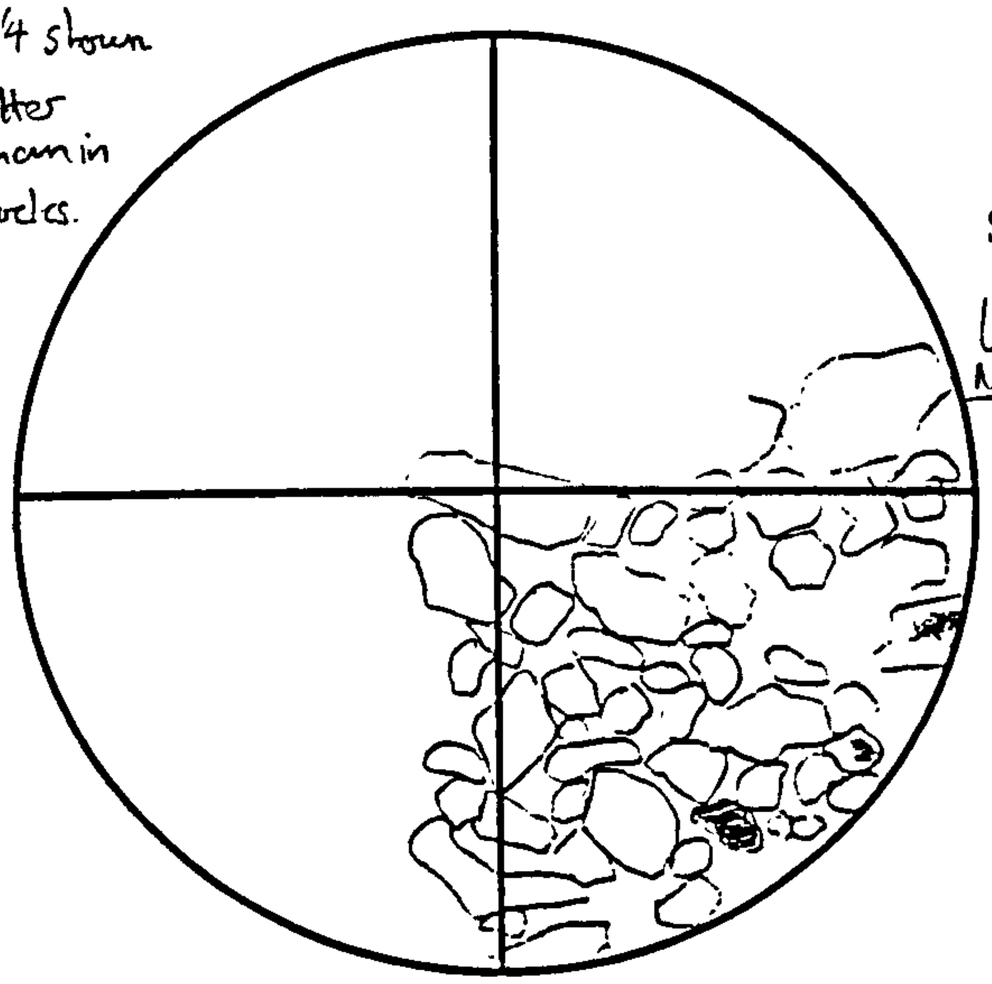

SCALE: ×10 ℄ = 2mm.

PPL.

NB Grain boundaries defined by calcite o/g 'dust' with rock.

GRAIN TYPES: Originally >95% olivine
Now: mostly bladed + amorphous serp ~95%, ~2% carbonate, ~2% magnetite

MATRIX TYPE: carbonate o/g + pore fill ~40%, serp (bladed + amorphous) ~60%
+ a little fine magnetite/opaques

OTHER FEATURES: Dilational calcite veins, account for ~50% of the rock
Sketch shows an undisturbed 'island' of host in the veinlets
See TS026 sketch

GRAIN/MATRIX RATIO: 90/10 - 95/5.
% GRAINS EUHEDRAL/ANGULAR: 15
% GRAINS SUB-HEDRAL/ROUNDED: 75
% GRAINS ROUNDED: 10

GRAIN SIZE DISTRIBUTION:
moderately well sorted unimodal.

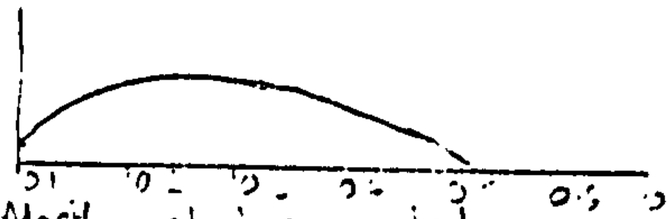

CLAST/MATRIX SUPPORT?: Mostly clast supported

CONCLUDING COMMENTS: 2 closely spaced veins appear to be an original host-rock sedimentary character?

STANDARD THIN-SECTION PETROGRAPHY SHEET.

KEVIN LEAHY.

DATE: 21/4/95.
UNIVERSITY SLIDE CODE: 55953 OFS SLIDE CODE: TS013.
BOREHOLE: OFS93-004-Snowdon DEPTH: 103.37m.
BRIEF HANDSAMPLE DESCRIPTION: Grey-green mod crumbly tuff
Near top of tuff pile.

FACIES ASSIGNED: Graded/bedded reworked pyroclastic sand.

SKETCH:

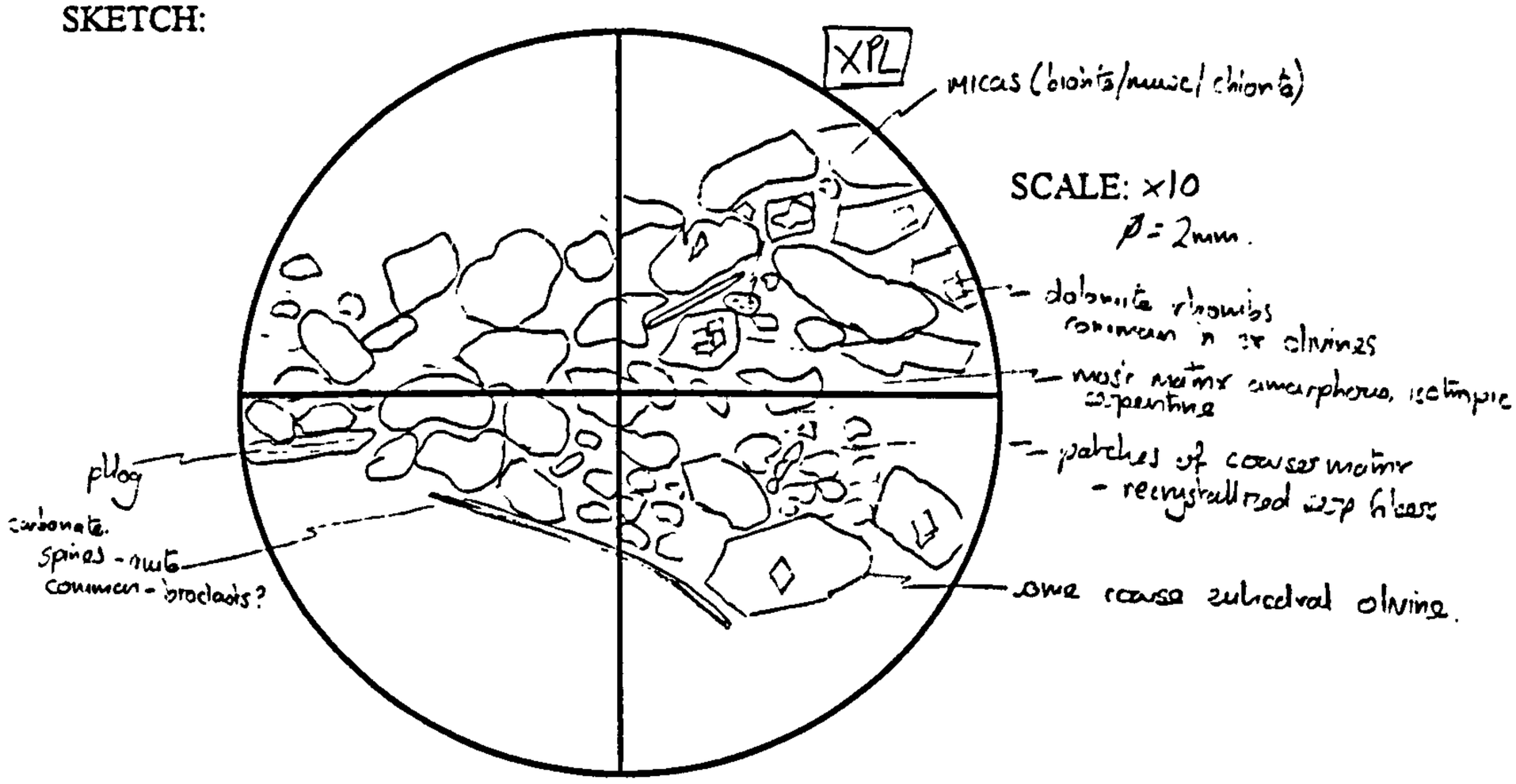

GRAIN TYPES: Originally: Olivine ~70%, phlog+musco 5%, opaques 2%, spines(?) 1%
pseudomorphic Serpentine ~80%, calcite 1%, dolomite 5%, opaques 5%

MATRIX TYPE: mostly amorphous serpentine, some patches (around grains and in larger pore spaces) of fibrous serp (coarser). Rare calcite.

OTHER FEATURES: very thin (>0.05mm) and long (0.1-1mm) fibers Appear to be carbonate
Could these be thin fish bones, or other organic debris Faint green pleochroic - could be chlorite or other secondary mica.

GRAIN/MATRIX RATIO: 75/25.

11 % GRAINS EUHEDRAL/ANGULAR: 25

30 % GRAINS SUB-HEDRAL/ROUNDED: 60

2 % GRAINS ROUNDED: 15.

GRAIN SIZE DISTRIBUTION:
excluding matrix
moderate/poorly sorted
slightly bimodal

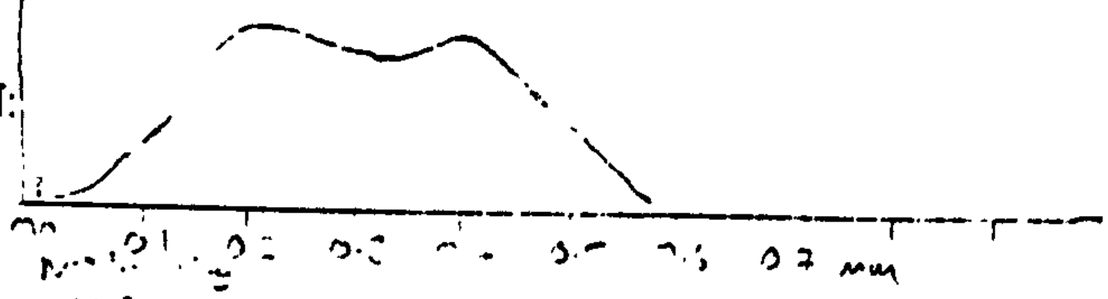

CLAST/MATRIX SUPPORT?:

CONCLUDING COMMENTS: Mica rich fine tuff. highly altered (serpentinised)
Does not display obvious sedimentary characteristics

STANDARD THIN-SECTION PETROGRAPHY SHEET.

KEVIN LEAHY.

DATE: 21/4/95
UNIVERSITY SLIDE CODE: 55949 OFS SLIDE CODE: T5029
BOREHOLE: OFS93-004. -Snowdon DEPTH: 108.95m
BRIEF HANDSAMPLE DESCRIPTION: Brown Sandstone - med-fine grained
Unit ~40cm thick, cross bed - with silty partings Well bedded

FACIES ASSIGNED: Shallow marine estn. - Shoal deposit?

SKETCH:

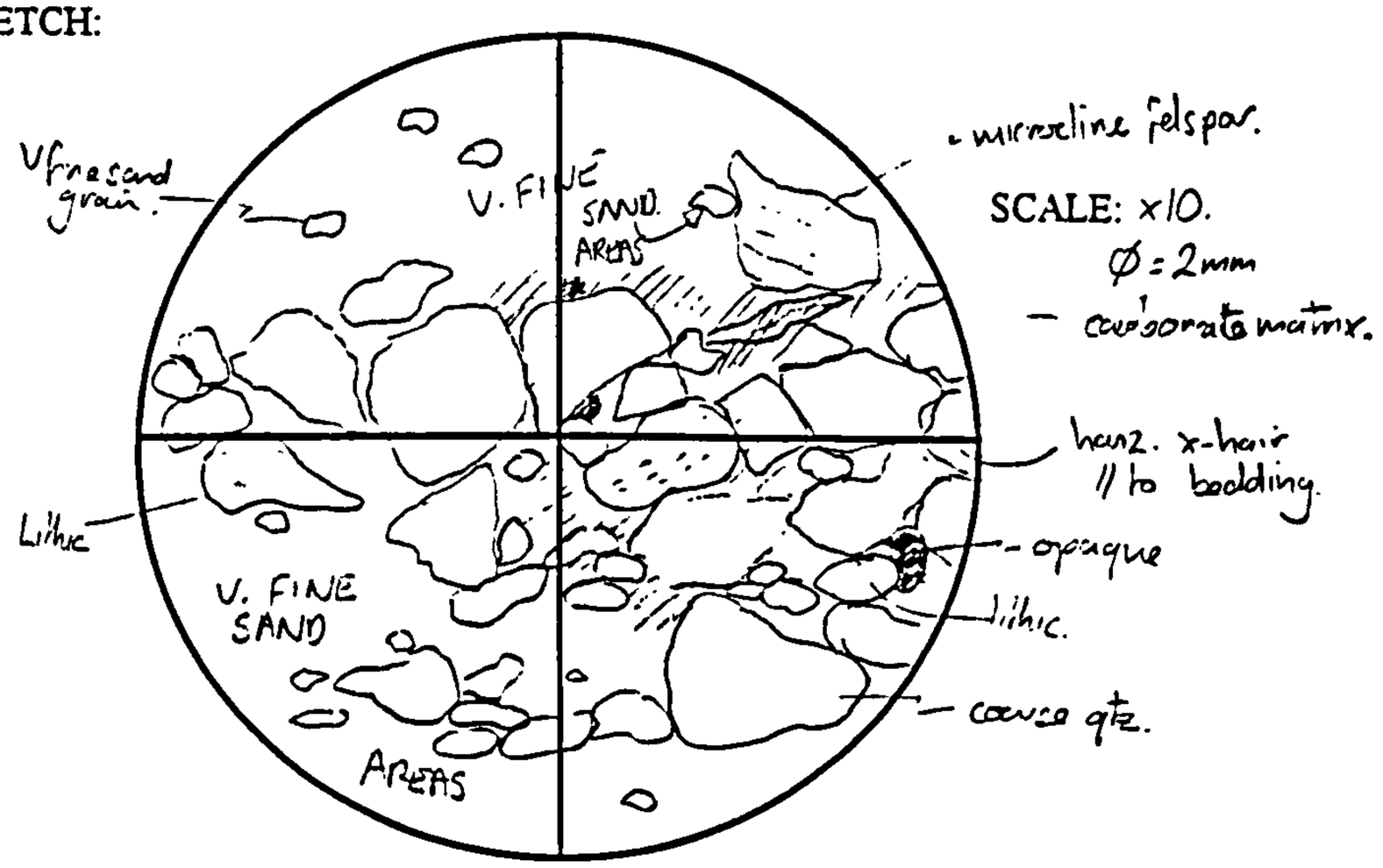

GRAIN TYPES: Quartz 84% bioclasts (fish bones) 1%
Lithics (schist, chert, shale, chalk) 10% biotite + muscovite 1%.
Microcline 2% opaques 2%.

MATRIX TYPE: Carbonate (micritic) 70% Clay ~15% Opaque 2%
pore space. ~10%

OTHER FEATURES: ½-2mm bedding. Opaques often corroded grains, with a small amount (2% of matrix) as cement. - As in lumps?

GRAIN/MATRIX RATIO: 80/20.
% GRAINS EUHEDRAL/ANGULAR: 10
% GRAINS SUB-HEDRAL/ROUNDED: 75
% GRAINS ROUNDED: 15.

GRAIN SIZE DISTRIBUTION:
Bimodal

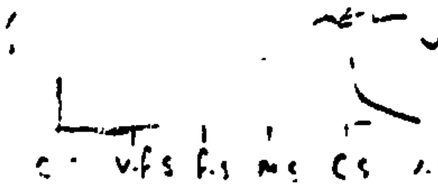

CLAST/MATRIX SUPPORT?: Mostly clast supported - fine areas are more matrix = lenticular flaser?
CONCLUDING COMMENTS: Sub-mature, moderately sorted, redeposited carbonate rich mud sandstone

APPENDIX IV

Point counting data and analysis

CONTENTS: 2 tables

POINT COUNTING. BOREHOLE OFS 93-004		n = 400 per slide, I = 0.1mm								
15 SLIDES.		**POINT TYPE VALUES EXPRESSED AS AN OVERALL PERCENTAGE.**								
POINT	Uni code	55959	55958	55964	55950	55952	55951	55953	55960	55965
TYPE	OFS code	TS005	TS009	TS010	TS011	TS017	TS012	TS013	TS018	TS015
GRAINS	Depth (m)	97.07	97.64	98.16	102.00	102.76	102.95	103.37	104.20	105.77
Euhedral		31.2	28.5	17.5	29.2	37.2	32.2	29.7	32.2	33.7
Sub Rounded		18.5	23.7	23.2	18.2	28.0	21.5	27.0	7.2	14.0
Rounded		3.7	9.0	5.7	6.5	5.7	7.0	5.5	1.0	2.5
Fragmental		8.2	3.5	12.0	8.5	7.0	6.7	6.0	5.0	2.5
Mica		1.2	1.2	3.7	0.7	1.7	1.2	1.0	0.5	0.2
MATRIX										
Serpentine		28.7	25.2	26.7	22.7	11.0	22.7	23.2	34.2	34.7
Carbonate		5.2	7.5	5.5	6.7	6.5	6.7	6.2	10.2	5.7
Magnetite		3.0	1.0	5.0	6.5	2.7	1.2	0.5	1.2	3.0
OTHERS										
CAVA		0.0	0.0	0.0	0.0	0.0	0.5	0.7	8.2	3.5
Vein Carb		0.0	0.0	0.0	0.0	0.0	0.0	0.0	0.0	0.0
total grains		62.8	65.9	62.1	63.1	79.6	68.6	69.2	45.9	52.9
total matrix		36.9	33.7	37.2	35.9	20.2	30.6	29.9	45.6	43.4
diagenetic xstls		0.3	0.4	0.7	1.0	0.2	0.8	0.9	8.5	3.7
ANALYSIS										
1. Pre-diagenesis: percentage of diagenetic crystals are equally redistributed amongst the primary constituants										
GRAINS		63.0	66.2	62.5	63.7	79.8	69.2	69.8	50.2	54.9
euhed		31.3	28.6	17.6	29.5	37.3	32.5	30.0	35.2	35.0
subrnd		18.6	23.8	23.4	18.4	28.1	21.7	27.2	7.9	14.5
rndd		3.7	9.0	5.7	6.6	5.7	7.1	5.5	1.1	2.6
frag		8.2	3.5	12.1	8.6	7.0	6.8	6.1	5.5	2.6
mica		1.2	1.2	3.7	0.7	1.7	1.2	1.0	0.5	0.2
MATRIX		37.0	33.8	37.5	36.3	20.2	30.8	30.2	49.8	45.1
2. Ternary A										
euhed		58.4	46.6	37.7	54.2	52.5	53.0	47.7	79.7	67.1
subrnd		34.6	38.7	50.0	33.8	39.5	35.4	43.4	17.8	27.9
rndd		6.9	14.7	12.3	12.1	8.0	11.5	8.8	2.5	5.0
3. Ternary B										
euhed		50.6	44.0	30.0	46.8	47.8	47.8	43.5	70.9	63.9
subrnd		30.0	36.6	39.7	29.2	35.9	31.9	39.6	15.9	26.6
rndd+frag		19.3	19.3	30.3	24.0	16.3	20.3	16.9	13.2	9.5
4. Ternary C										
euhed		50.6	44.0	30.0	46.8	47.8	47.8	43.5	70.9	63.9
surnd+frag		43.3	42.0	60.3	42.8	44.9	41.8	48.4	26.9	31.3
rndd		6.0	13.9	9.8	10.4	7.3	10.4	8.1	2.2	4.7

							n = 400 per slide, t = 0.4mm			
							3 SLIDES FROM B/H OFS93-012.			
							PK LAPILLI-TUFFS			
Uni code	55956	55955	55948	55957	55963	55954	56297	56295	56294	
OFS code	TS016	TS020	TS021	TS024	TS022	TS026	TS074	TS072	TS071	
Depth (m)	106.01	106.66	107.89	108.20	108.34	108.38	201.12	188.50	186.76	
Euhedral	35.2	35.5	34.5	30.2	20.0	19.5	34.7	19.7	23.5	
Sub Rounded	12.7	14.0	13.2	9.2	5.8	8.7	8.5	2.5	5.2	
Rounded	2.7	3.7	2.2	2.7	1.0	0.7	2.2	0.5	1.2	
Fragmental	6.5	10.7	4.7	9.0	6.2	3.0	10.5	4.5	3.7	
Lapilli	0.7	0.0	2.7	0.0	0.0	0.2	16.2	41.0	30.7	
Serpentine	31.2	27.7	25.7	32.0	5.7	7.2	26.5	25.7	20.5	
Carbonate	7.2	7.5	13.7	7.5	7.0	9.2	0.2	4.2	13.2	
Magnetite	2.7	0.7	2.5	2.5	0.7	2.7	0.5	1.2	1.5	
	0.7	0.0	0.0	1.5	0.0	0.0				
Vein Carb	0.0	0.0	0.0	5.0	54.2	48.5	0.2	0.5	0.2	
	57.8	63.9	57.3	51.1	33.0	32.1	72.1	68.2	64.3	
	41.1	35.9	41.9	42.0	13.4	19.1	27.2	31.1	35.2	
	1.1	0.2	0.8	6.9	53.6	48.8	0.7	0.7	0.5	
	58.4	64.0	57.8	54.9	71.1	62.7	72.6	68.7	64.6	
euhed	35.6	35.6	34.8	32.4	43.1	38.1	34.9	19.8	23.6	
subrnd	12.8	14.0	13.3	9.9	12.5	17.0	8.6	2.5	5.2	
rndd	2.7	3.7	2.2	2.9	2.2	1.4	2.2	0.5	1.2	
frag	6.6	10.7	4.7	9.7	13.4	5.9	10.6	4.5	3.7	
lapilli	0.7	0.0	2.7	0.0	0.0	0.4	16.3	41.3	30.9	
	41.6	36.0	42.2	45.1	28.9	37.3	27.4	31.3	35.4	
Lapilli in lapilli-tuffs (OFS 93-012 only) are considered as euhedral crystals in the Ternary calculations										
(eu+lap)	69.6	66.7	69.1	71.7	74.6	67.5	82.6	95.3	89.4	
subrnd	25.1	26.3	26.5	21.9	21.6	30.1	13.8	3.9	8.6	
rndd	5.3	7.0	4.4	6.4	3.7	2.4	3.6	0.8	2.0	
(eu+lap)	61.6	55.6	63.2	59.1	60.6	61.1	70.6	89.0	84.3	
subrnd	22.2	21.9	24.2	18.0	17.6	27.3	11.8	3.7	8.1	
rndd+frag	16.1	22.5	12.6	22.9	21.8	11.6	17.6	7.3	7.6	
(eu+lap)	61.6	55.6	63.2	59.1	60.6	61.1	70.6	89.0	84.3	
subrnd+frag	33.6	38.7	32.8	35.6	36.4	36.7	26.4	10.3	13.8	
rndd	4.7	5.8	4.0	5.3	3.0	2.2	3.1	0.7	1.9	

APPENDIX V

Heavy mineral separation procedures and results

CONTENTS:

- Five stages of separation methodology
- Heavy mineral separation results, tabulated

Separation Methodology

Treatment of samples from core box to diamond analysis consists of six main stages, which are fully explained below, and in the following table (see following pages)

Stage 1 - logging and sampling

Boreholes were fully logged (by the author and by B.C. Jellicoe, see Appendix II) and strata of interest, typically kimberlite strata, were determined. Sample size was based on lithological constraints, to fully differentiate the heavy mineral characteristics of each lithology type. For example, in the upper reworked facies of OFS 93-002, individual graded units were sampled, these ranged from 30cm to 90cm. Sample division (except for borehole 012) was carried out at the Saskatoon field office by the author, with consultants from North Rim Exploration (including B.C. Jellicoe). Samples for XRF geochemical analysis (see Chapter 5), thin section petrology (see section 2.3) and hand samples were taken at this stage.

Stage 2 - crushing

Each sample was weighed prior to crushing. It was then passed through a primary jaw crusher, and if necessary through a secondary roller crusher and tertiary jaw crusher to reduce the sample to about <3.5mm (this grade was later reduced to <2mm). All samples were reweighed after crushing to determine the amount lost as dust and through spillage.

Stage 3 - acidification

The crushed sample, normally weighing 1kg to 6kg, were reacted with ~25% HCl to dissolve the carbonate and some fine clay phases. This acidification also reduces the bulk and helps liberate heavy minerals from the calcite-serpentine matrix. During acid-digestion in containers, the samples were regularly stirred to aid the reaction, see Plate 2.18 in Fig. 2.2.2. Completion, which may take up to ten days, is recognised by the termination of effervescence. Decanting through a fine sieve (23µm) and dilution with water and detergent (to reduce surface tension to inhibit diamond floatation) ensured washing to neutrality without the loss of any 100µm fraction. On achieving pH of 7 the samples were transferred to evaporating dishes and dried in ovens at 105°C to 110°C. After drying, the samples were allowed to cool and were

reweighed to determine the amount of lost carbonate and dissolved clays, typically 35% to 60%.

The sample residue was check-screened to pass through 3.5mm (later reduced to 2mm), any oversize being visually checked for diamonds, and then later reduced with pestle and mortar, and rescreened. By this precaution all grains passed through the 4mm aperture of the smallest separating funnel in the next stage of separation.

The sample was further screened to remove the undersize fraction, i.e. <100µm. This was chosen as being the finest size of diamonds to be realistically extracted on a routine basis. It also permitted an effective mineral settling rate (without using centrifuging) during subsequent heavy liquid separation.

Stage 4 - bromoform separation

Samples weighing <2kg were separated in a 2 litre separating funnel, and larger samples in a specially constructed 5 litre open topped vessel, see Plate 2.19 in Fig. 2.2.2. The samples were repeatedly stirred and mixed with the bromoform ensuring complete separation of minerals of specific gravity >2.86g/cc. After each mixing the heavy minerals fraction was tapped off into 18.5 Whatmans filter paper. When no further heavy minerals collected at the base of the separating funnel the suspended and floating material was also tapped. Both heavies and lights were then washed three times with methanol which was decanted through an 80µm screen. The heavies were then dried to drive off the methanol and any remaining bromoform; immersed in distilled water and detergent, and placed in an ultrasonic bath. This cleans the heavies and aids magnetic separation and mineral identification. The total heavy mineral fraction was weighed thus giving an indication of the amount of kimberlite and/or degree of concentration during sedimentary reworking. The remaining light residue was extracted from the separating vessel, washed in methanol, bagged and stored.

Stage 5 - Frantz electromagnetic separation

Prior to Franz separation, magnetite was removed with a hand magnet and weighed in order to obtain a semi-quantitative relationship with field aeromagnetic anomalies.

The other heavy minerals, comprising the bulk of the fraction, were screened into the following size fractions to aid effective separation: >1000µm, >500µm, 250µm, 150µm, 100µm and <100µm. The forward and side tilts of

the Franz separators were set at 3° and 5 ° respectively. All fractions, except >1000µm (examined without separation) and <100µm (stored), were run at 0.4amps (Cr spinel, ilmenite, Fe garnets, see Plate 2.20 in Fig. 2.2.2.), 0.6amps (Mg garnets, see Plate 2.21 in Fig. 2.2.2.) and 0.8amps (pyroxenes). If the non-magnetic (diamond bearing) fraction produced at 0.8amps was still large the amperage was increased by 0.1amp intervals to reduce the size.

The Franz electromagnetic fractions, normally about 18, were weighed and each examined under binocular microscope. Semi-quantitative measurements were taken by visual estimation on chromites, ilmenites, phlogopites, garnets (pink almandines, orange pyrope-almandines and purple pyropes) etc., and other minerals identified for microprobe analysis (see Chapter 5 and 6).

Stage 6 - Clerici solution; diamond separation

The non-magnetic fraction of the samples were then separated in Clerici solution, a thallium formate/mallonate heavy liquid with a specific gravity up to 4.5g/cc depending on the dilution with water. By so adjusting the specific gravity, particularly to that of diamond (3.5g/cc) critical fractions were obtained in which diamond was isolated. The diamonds were identified using isotropy, lustre, refractive index liquids, hardness, surface features (e.g. trigons) or Laser Raman Spectrometry.

Sample	Borehole	Crushed	Weight %	weight		weight		weight	approximate %				Significant Accessories (1=v. rare, 4=conspicuous, 5=major component).														
no.	depth (m)	weight kg	S.G. >2.9	mt, g	mt, %	il, g	il, %	gt, g	gt, g/t	pk	pur	or	cs	ol	en	cd	ph	ap	fl	ba	px	zr	am	ep	tm	sph	ky	pyr
Borehole OFS93-002																												
1B	96.95-97.59	3.236	0.27	0.05	0.00	0	0.00	0.15	46.4	90	2	3		3		2	2				5		5	4				5
6	104.42-104.67	1.041	0.62	0.11	0.01	3.64	0.35	0.071	68.2	30	30	40		1	2	1	4	1	3	2	2	1	1	2	2			5
7	104.67-104.77	1.657	0.31	0.05	0.00	4.18	0.25	0.241	145.4	5	40	55	1		1	2	3			1	2	1	4	2	1	2		5
9	105.17-105.84	2.250	0.69	0.28	0.01	13.303	0.59	0.879	390.7	15	45	40					5		2	2	2	1	3		1			5
10A	105.81-106.54	2.952	0.47	0.15	0.01	10.403	0.35	0.383	129.8	2	52	46		1	1		5			2	1		3	2				5
10B+D	106.54-107.02	7.573	5.57	364.15	4.81	39.07	0.52	0.394	52.0	10	30	60		1	1		5			3	1		3		1	1		4
10C	107.02-107.56	1.731	2.24	30.57	1.77	3.947	0.23	0.06	34.7	7	47	46	2			2	4		1	2	1	1	2		1			3
10E	108.50-108.81	3.525	3.04	69.47	1.97	31.685	0.90	0.37	105.0	25	25	50					5		2		1		1					
10F	108.81-109.35	5.172	1.68	19.35	0.37	38.809	0.75	0.949	183.5	32	17	51		2	1		5		2	1	1	1			1			3
10G	109.35-110.16	3.077	0.91	1.17	0.04	22.452	0.73	0.472	153.4	20	25	55	1	2	1	1	5		3	3	2	1			1			4
11	110.16-110.73	2.991	2.39	58.65	1.96	7.141	0.24	0.254	84.9	20	30	50					5		1	3	1	1			1			4
12A	110.73-111.56	2.660	0.93	8.50	0.32	11.03	0.41	0.278	104.5	5	45	50		1	1	1	3	1		2		1		1	1			5
12B	111.56-113.00	6.801	0.64	1.69	0.02	36.603	0.54	1.35	198.5	1	47	52		1		1	4			2		1		1	2	1		4
13A	113.00-113.90	5.084	1.18	33.28	0.65	15.519	0.31	0.317	62.4	7	18	75					4		3	2	2				4			5
13B	113.90-115.74	7.244	0.10	0.33	0.00	5.814	0.08	0.102	14.1	20	5	75		1			1		3	1	1	1			4	1		4
14B	116.30-116.69	2.561	0.56	0.10	0.00	1.252	0.05	0.031	12.1	15	10	75					3			2					4			5
Borehole OFS93-003																												
2	95.12-98.00	3.192	2.83	19.83	0.62	68.69	2.15	1.256	393.5	10	45	45		2			4		3		3		3		1			2
3	98.00-101.10	14.077	1.03	2.17	0.02	127.621	0.91	2.231	158.5	0	35	65					4		5	3	1		2					5
4A	101.10-101.38	0.628	1.05	0.13	0.02	4.368	0.70	0.168	267.6	3	33	64		1			2	1	1	2	2	2	2	1	2			4
4B	101.38-101.88	4.524	0.84	0.52	0.01	28.743	0.64	0.55	121.6	1	45	54	2	1		2	4		2	3			4	2	2	3		5
4C	101.88-102.50	1.625	0.58	0.08	0.00	6.577	0.40	0.197	121.2	0	50	50		1		2				2	2	1	2	1	2	3		5
4D	102.50-103.68	2.868	0.58	0.21	0.01	10.759	0.38	0.518	180.6	10	25	65	1	2		1		2	1	2	2	1	1	1	1	2		3
Borehole OFS93-004																												
7	92.57-92.84	3.426	0.17	0.32	0.01	0.087	0.00	0.999	291.6	96	2	2					1			3	4	2	4	2	2	4	2	4
10	93.19-93.60	2.861	1.01	7.74	0.27	n/c	n/a	n/c	n/a	n/c	n/c	n/c	2					2		4	3	3	3	3	3	3	3	3
11	93.60-93.94	2.037	0.87	0.23	0.01	0.507	0.02	3.2	1571.3	95	0	5		4				4		3	4	2	4	1	1	4	3	4
13A	94.41-95.37	4.660	0.84	249.00	5.34	18.7	0.40	0.95	203.9	42	18	40	1	3		1	5	1	4	2	2	1	1	1	1	1	1	2
13B	95.37-95.64	1.581	6.98	99.38	6.28	7.245	0.46	0.368	232.7	20	40	60		1			5	1	2	1	3	1		2	2		1	2
13C	95.64-96.71	6.545	9.33	528.74	8.08	44.764	0.68	1.357	207.3	5	40	55		1		2	5	2	2		2	1	1		1	1	1	1
13D	96.71-97.06	2.190	1.37	8.09	0.37	14.6	0.67	0.44	201.0	0	50	50					5		2	2		2			1	1		5
13E	97.06-97.48	1.818	6.50	102.28	5.63	9.409	0.52	0.267	146.9	2	25	73	3				5	1		1		1			1			2
13F	97.48-97.70	1.624	3.51	46.54	2.87	7.146	0.44	0.101	62.2	30	10	60					5		1	2	1	1	2	2	1			3
14	97.70-98.67	2.932	0.90	154.10	5.26	21.18	0.72	0.189	64.5	10	30	60	1	2			5	2	2	2	2	2	3	1	1			3

Sample	Borehole	Crushed	Weight %	weight		weight		weight	approximate %				Significant Accessories (1=v. rare, 4=conspicuous, 5=major component).															
no.	depth (m)	weight kg	S.G. >2.9	mt, g	mt, %	il, g	il, %	gt, g	gt, g/t	pk	pur	or	cs	ol	en	cd	ph	ap	fl	ba	px	zr	am	ep	tm	sph	ky	pyr
15	98.67-100.03	3.873	6.90	216.38	5.59	39.195	1.01	0.679	175.3	15	30	45		1		2	5	2		1	1	2		1	1			2
16	100.03-100.67	1.905	3.71	43.47	2.28	13.071	0.69	0.349	183.2	4	43	53		1			1	1	1	1	1	3	1	3	1	2		4
17	100.67-101.50	3.246	1.38	19.37	0.60	17.14	0.53	0.655	201.8	2	33	64		1			5			2	1	1	1	1	2			5
18	101.50-102.16	3.236	1.82	21.41	0.66	32.428	1.00	0.449	138.8	20	30	50		1			4		2	3	3	1			3			5
19	102.16-102.86	1.989	0.92	1.69	0.08	13.022	0.65	0.266	133.7	16	29	55	2				4		2		2		1		3			4
20	102.86-103.58	4.756	1.30	28.81	0.61	20.97	0.44	0.51	107.2	2	43	55			1		5		5	5	2		1	1				5
21A	103.58-104.79	6.040	0.67	2.81	0.05	27.357	0.45	0.289	47.8	10	40	50		2	1	1	4		3	3	2		4		4			5
21B	104.79-105.94	4.684	0.36	1.12	0.02	9.82	0.21	0.3	64.0	10	20	70		2		2	2		5	3	2	1			3	2		5
22	105.94-107.19	4.561	0.54	1.51	0.03	15.411	0.34	0.546	119.7	40	10	50		4		1	5		3	2		1	1	1	1		1	3
23	107.19-108.04	3.600	0.21	0.06	0.00	4.383	0.12	0.131	36.4	25	37	38	2	1	1	2	3		1	4	2	1	2	3	2	3	1	5
24	108.04-108.42	2.909	0.21	0.10	0.00	4.394	0.15	0.165	56.7	35	20	45	2	3	2						1				2	2		5
Borehole OFS93-009																												
10	135.60-136.61	4.379	0.41	0.07	0.00	0.962	0.02	1.414	322.9	1	44	55	2	1	1	2	1		2	3	2		3		4			5
11A	136.61-136.91	1.842	3.13	0.04	0.00	0.112	0.01	0.09	48.9	5	60	40				3	2		1	2	4		2	1	1	3		5
11B	136.91-139.45	6.010	0.88	0.31	0.01	0.297	0.00	0.049	8.2	10	65	25		2		3	2		3	5	3		5		3			5
11C	139.45-139.95	3.478	0.85	0.13	0.00	0.17	0.00	0.07	20.1	16	39	45	4	1	2	3	1			2	3		1	1	1	2	1	5
12A	139.95-140.35	1.581	0.07	0.03	0.00	0.15	0.01	0.052	32.9	40	20	40	1	1	1	1	1			2		2	1		3	1		5
12B	140.35-140.50	0.527	0.10	0.05	0.01	0.023	0.00	0.036	68.3	1	93	6		1	2	3				4	2	1			1			5
12C	140.50-140.65	0.611	0.58	0.02	0.00	0.04	0.01	0.05	81.9	10	75	15				1	2				3		4		2			5
12D	140.65-141.00	1.613	0.00	0.08	0.00	0.276	0.02	0.131	81.2	30	50	20	1	1		1	3			2	4		4		4			5
12E	141.00-141.55	2.445	0.15	0.07	0.00	2.068	0.08	0.222	90.8	20	60	20	2							3	2		1		1			4
Borehole OFS93-010																												
9A	141.65-142.29	2.969	3.03	0.03	0.00	1.827	0.06	0.012	4.0	1	27	72	3			1	5		2	4	1			1	1	1		5
9B	142.29-143.17	3.125	4.30	0.07	0.00	0.183	0.01	0.075	24.0	6	12	82				2	5			3				2		3		5
11A	147.49-147.68	1.444	2.13	0.07	0.00	0.088	0.01	0.039	27.0	5	55	40		1	1	1	1			1	4		2	2	3			5
11B	147.68-148.40	2.131	1.01	0.04	0.00	3.367	0.16	1.472	690.9	7	47	46	3	1		4	5			4	1		3					5
12A	148.40-149.00	2.211	0.07	0.07	0.00	0.234	0.01	0.19	85.9	60	20	20				3	5		2	3								5
12B	149.00-149.36	2.364	0.17	0.01	0.00	0.23	0.01	0.094	39.8	15	20	65		2		3	4			5								5
17	153.62-153.77	0.597	0.87	0.04	0.01	0.33	0.06	0.101	169.2	50	5	45		1		1	3	1	2	2	1	1	1		1		1	5
18	153.77-156.00	8.640	0.55	0.28	0.00	11.634	0.13	9.623	1113.8	17	43	40	1	1	1	4	4		1	3	3	1	5		2	3	1	5

Sample	Borehole	Crushed	Weight %	weight		weight		weight	approximate %				Significant Accessories (1=v. rare, 4=conspicuous, 5=major component).														
no.	depth (m)	weight kg	S.G. >2.9	mt, g	mt, %	il, g	il, %	gt, g	gt, g/t	pk	pur	or	cs	ol	en	cd	ph	ap	fl	ba	px	zr	am	ep	tm	sph	ky	pyr
Borehole OFS93-012																											
1	180.51-184.08	16.552	0.10	0.15	0.00	5.613	0.03	0.592	35.8	65	15	20	2	1		1	4			2	1		2	2	1	3		5
2	184.08-186.58	12.616	0.21	0.11	0.00	13.561	0.11	0.111	8.8	5	5	90				3	2								5	3		5
3	186.58-188.80	12.864	0.59	0.21	0.00	54.254	0.42	2.379	184.9	0	50	50				5	4	3	2	4			2				1	5
4	188.80-197.06	40.847	0.23	0.46	0.00	20.587	0.05	0.194	4.7	10	20	70	4	1	1	2					1	2	3		4			5
5	197.06-198.06	6.529	0.20	0.06	0.00	1.577	0.02	0.098	15.0	35	5	60	3				3			5				2	5	5		5
6	199.15-201.85	11.882	1.65	0.06	0.00	3.246	0.03	0.056	4.7	30	10	60	2			1	2		2	5			1	1	5			4
7	201.85-206.57	20.770	0.28	0.16	0.00	6.122	0.03	0.118	5.7	10	80	10	5	1	3	4					4	2	5	2	3	1		5
8	206.57-206.79	2.835	0.42	0.01	0.00	0.697	0.02	0.019	6.7	35	30	35	3											1	1	3		5
9	208.00-208.88	1.900	0.20	0.00	0.00	0.25	0.01	0.037	19.5	15	20	65	5	1			4		3	4					4	4	1	5
10	211.63-211.94	1.802	0.33	0.00	0.00	0.339	0.02	0.021	11.7	25	10	65	1				5				1				5			5

abbreviations: am=amphibole, ap=apatite, ba=barytes, cs=chrome spinel, en=enstatite, ep=epidote, fl=flourite, il=ilmenite, gt=garnet, ky=kyanit sph=sphene, pyr=pyrite, tm=tourmaline, zr=zircon.

ph=phlogopite,px=pyroxene (of unspecified types),

APPENDIX VI

Thin Section Catalogue

CONTENTS: Catalogue of thin section samples and instructions for cutting planes.

Standard Thin Sections.

Core OFS 002:

93-002.TS030 FROM 105.84m. HIGHEST CHUNK COMPETENT ENOUGH TO BE SECTIONED, STEEL GREY MAG AND PHLOG RICH TUFF. TS TO BE PERP TO BEDDING.

93-002.TS031 FROM 106.98m. STEEL GREY TUFF, WITH MAG ALONG BEDDING AND RICH IN PHLOG'S. TS TO BE PERP TO BEDDING, CUTTING MAGS.

93-002.TS032 FROM 107.74m. 9cm ABOVE SEM013 (NEAREST COMPETENT CHUNK) IN FINE STEEL GREY TUFF, WITH LARGE MAG BLEBS. TS SHOULD BE PERP TO BEDDING, AVOIDING MAG BLEBS.

93-002.TS034 FROM 109.47m. STEEL GREY VERY FINE AND WELL BEDDED TUFF. MAG POOR AREA.TS TO BE PERP TO BEDDING.

93-002.TS035 FROM 110.43m. NEAR SEM014 DARK GREY FINE-MED TUFF. TS TO AVOID MAG BLEBS, AND PERP TO BEDDING.

93-002.TS036 FROM 111.20m NEAR SEM015 MID GREY-GREEN, MAG RICH TUFF. TS TO BE PERP TO BEDDING.

93-002.TS037 FROM 110.55m COARSE PALE GREY-GREEN TUFF, MAG POOR, MICA RICH. TS TO BE PERP TO BEDDING.

93-002.TS038 FROM 111.86m. NEAR TO SEM016. DARK GREEN MED GRAINED TUFF, WITH MAG BLEBS. TS TO BE PERP TO BEDDING, AVOIDING MAG BLEBS.

93-002.TS042 FROM 114.08m BY SEM018. PALE GREEN COARSE, WELL BEDDED TUFF. SHOT WITH FINE CALCITE VEINS. TS TO BE PERP TO BEDDING.

93-002.TS044 FROM 115.73m. RIGHT AT THE BASAL UNIT OF THE TUFF. TS PERP TO BEDDING AND MUST TRANSECT GREEN MATERIAL, AND SOME OF THE GREY-BLACK.

93-002.TS045 FROM 115.80m. UPPERMOST AREA OF THE BASAL SAND UNIT. PALE BUFF, FINE GRAINED AND RICH IN CARBONATE. TS TO BE PERP TO BEDDING.

93-002.TS046 FROM 115.96m. COARSE SAND, AND LOWER PALE SAND BED, TS TO TRANSECT BOTH THESE PERP TO BEDDING.

93-002.TS047 FROM 116.62m. LOWER SUBUNIT OF THE BASAL SAND, NEAR THE BASE, LAMINATED PALE BROWN MED SAND WITH X-STRAT. TS TO BE PERP TO BEDDING.

93-002.TS048 FROM ????. COARSE X-STRAT BROWN SAND WITH DARK SILTY PARTINGS. TS TO BE PERP TO BEDDING AND TRANSECT A SILTY LAYER.

Core OFS 004:

93-004.TS005 FROM 97.07m. BASE OF GRADED BED IN THE STEEL GREY KIMB. TS RUN PERP TO BEDDING AND INCLUDE COARSE AND FINE SUBUNITS. NEAR SEM SITES SEM003 AND SEM004.

93-004.TS007 FROM 95.20m. IN THE SAME AREA AS ABOVE, TUFF HERE IS RICH IN VERY COARSE PHLOG'S THAT ARE ON BEDDING PLANES, TS TO BE PERP TO BEDDING.

93-004.TS008 FROM 96.05m. STEEL-GREY TUFFS, VERY COARSE, WITH UNIDENTIFIED WHITE GRAINS, VERY MAGNETITE RICH. TS TO BE PERP TO BEDDING.

93-004.TS009 FROM 97.64m. STEEL GREY TUFFS, TS PARALLEL TO BEDDING ACROSS THE BELBBY MAGNETITE VEIN-FAULT.

93-004.TS010 FROM 98.16m. LIGHT GREY TUFF, MEDIUM GRAINED, TS PERP TO BEDDING IN AN AREA WITHOUT MAGNETITE ALONG BEDDING PLANES.

93-004.TS011 FROM 102.00m. GREEN GREY TUFF, MED GRAINED, RICH IN MAGNETITE, TS TO BE PERP TO BEDDING.

93-004.TS012 FROM 102.95m. GREY GREEN TUFF, SLIGHT BROWN STAINING, MED GRAINED. MAGNETITE RICH. TS TO BE PERP TO BEDDING.

93-004.TS013 FROM 103.37m. DARK GREY-GREEN, MED GRAINED, LOW MAGNETITE PROPORTION, TS TO BE PERP TO BEDDING.

93-004.TS014 FROM 103.93m. AS ABOVE BUT WITH LARGE SHALE CLAST IN IT. TS SHOULD BE AT LEAST HALF SHALE AND PERP TO (TUFF) BEDDING.

93-004.TS015 FROM 105.77m. BOUNDARY BETWEEN GREY (KL UNIT 2) AND DARKER GREY GREEN (KL UNIT 3). TS SHOULD CUT THIS BOUNDARY, AND RUN PERP TO BEDDING.

93-004.TS016 FROM 106.01m. GREY GREEN TUFF WITH RANDOMLY ORIENTATED PHLOGS AND LITTLE MAGNETITE. TS TO BE PERP TO BEDDING.

93-004.TS017 FROM 102.76 NEAR TO SEM005, GREY KIMB TS TO BE PERP TO BEDDING.

93-004.TS018 FROM 104.20m. NEAR TO SEM006, GREEN GREY, MAGNETITE POOR AND WITH RANDOMLY ORIENTATED PHLOG'S. TO BE TAKEN PERP TO BEDDING.

93-004.TS020 FROM 106.66. GREEN WELL BEDDED TUFF, NEAR SEM008, MAG AND PHLOG POOR. TO BE TAKEN PERP TO BEDDING.

93-004.TS021 FROM 107.89m. NEAR TO SEM009, FINE DARK GREEN, MICA POOR. TS TO BE PERP TO BEDDING.

93-004.TS022 FROM 108.34m. NEAR TO SEM010, HIGHLY CALCITE VEINED DARK GREEN TUFF. TS TO INCLUDE THE KIMB MATERIAL ABOVE THE THICKEST CALCITE VEIN, TAKEN PERP TO BEDDING.

93-004.TS024 FROM 108.20m. DARK GREEN HIGHLY CALC VEINED TUFF. THIN COARSE AND MED GRAINED BANDS. TS TO BE PERP TO BEDDING, CUTTING THE THIN COARSE BED.

93-004.TS026 FROM 108.38m. VERY BASAL KIMB TUFF, DARK GREEN AND VERY HIGHLY CALC-PHLOG COARSE VEINED. TO BE TAKEN PERP TO BEDDING.

93-004.TS027 FROM 108.50m. TOPMOST BUFF SAND, CALC VEINED. TS TO BE IN AN AREA OF LOW VEIN DENSITY, AND PERP TO BEDDING.

93-004.TS028 FROM 108.63m. LIGHT GREY BROWN MED GRAINED SANDSTONE. BEDDING TO BE TAKEN PERP TO BEDDING.

93-004.TS029 FROM 108.95m. WHITE-BROWN COARSE SAND, POSSIBLE WITH MINOR FAULT. TS TO BE PERP TO BEDDING.

Core OFS 93-012

93-012.TS070 FROM 185.00m GREY-GREEN HOMOGENOUS MED-GRAINED TUFF.

93-012.TS071 FROM 186.75m DARK GREEN-GREY, TS TO CUT COARSE CALCITE? VEIN IN AGGLOMERATIC TUFFS.

93-012.TS072 FROM 188.53m DARK GREEN COARSE AGGLOMERATE-TUFF, 30CM FROM BASE OF COARSE AGGLOMERATIC UNIT.

93-012.TS073 FROM 194.50m PALE GREEN FINE GRAINED BEDDED TUFF.

93-012.TS074 FROM 201.18m PALE GREEN COARSE AGGLOMERATIC TUFF, RICH WITH CARBONATE - MATRIX AND VEINS.

93-012.TS075 FROM 208.55m PALE GREY-BROWN, COARSE CARBONATE RICH TUFF? FROM THE UPPER CARBONATE HORIZON AT THE BASE OF THE TUFFS (SILLS?).

93-012.TS076 FROM 211.70m LOWER OF THE 2 'SILL' UNITS (SEE TS075).

93-012.TS077 FROM 187.05m DARK GREEN CRYSTAL LITHIC TUFF.

93-012.TS078 FROM 206.75m UPPER CARBONATE 'SILL'. BY SITE OF K151

93-012.TS079 FROM 190.90m BY SITE OF K145. (MID UNIT 19 - GREY-GREEN TUFF.)

93-012.TS080 FROM 195.11m COARSE PALE GREEN TUFF, BY SITE OF K155.

93-012.TS081 FROM 202.44m GRAINS OF ALTERED OLIVINES, TAKEN TO BE MOUNTED IN POLISHED BLOCK AND PROBED.

APPENDIX VII

EDS spectra from RPK tuff

CONTENTS: 14 Spectral analyses from RPK tuff in OFS 93-004

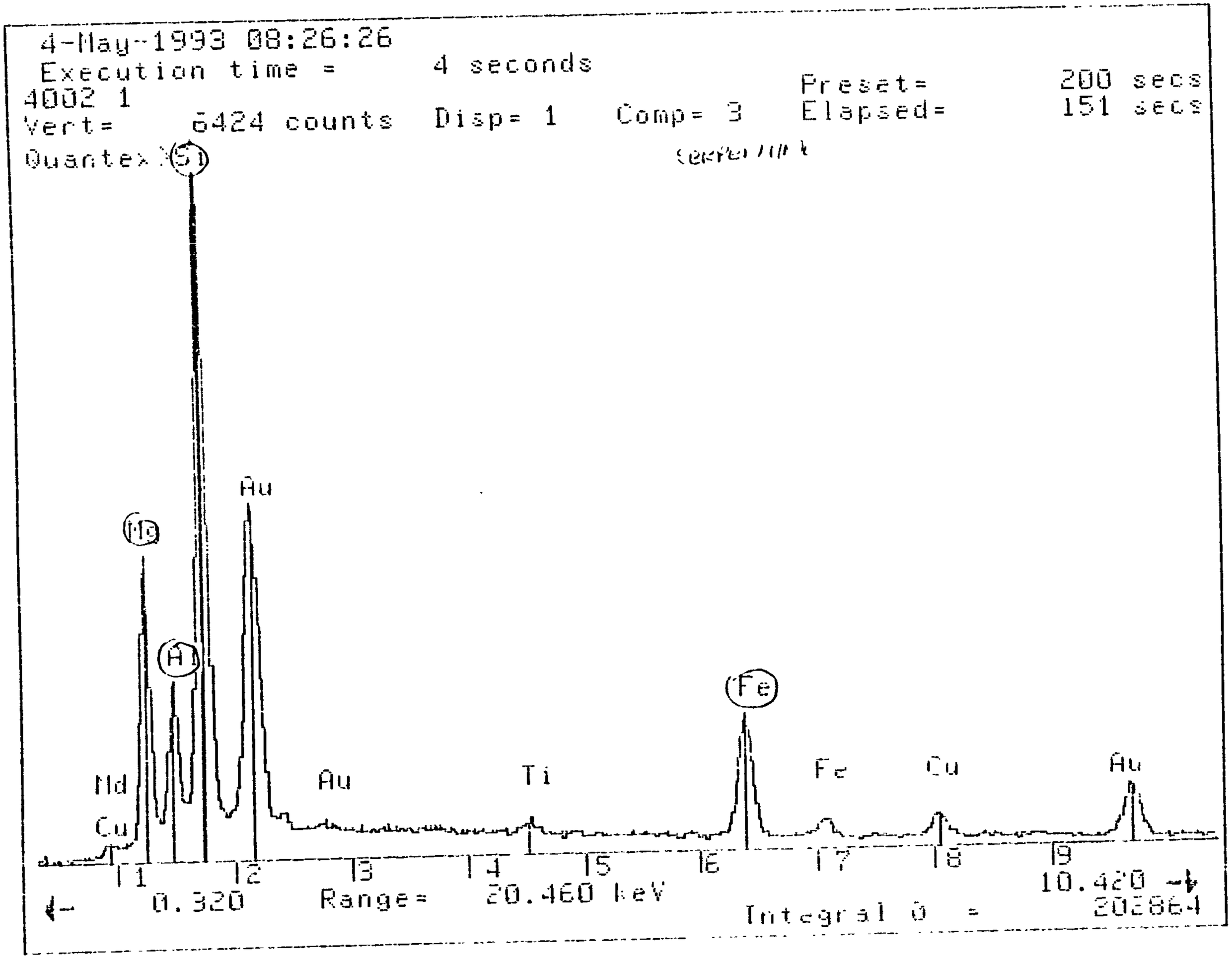
4-May-1993 08:26:26
Execution time = 4 seconds
4002 1
Vert= 6424 counts Disp= 1 Comp= 3
Preset= 200 secs
Elapsed= 151 secs
Quantex
Au
Nd
Al
Nd
Cu
Au
Ti
Fe
Fe
Cu
Au
1
2
3
4
5
6
7
8
9
0.320
Range= 20.460 keV
10.420
Integral 0 = 202864

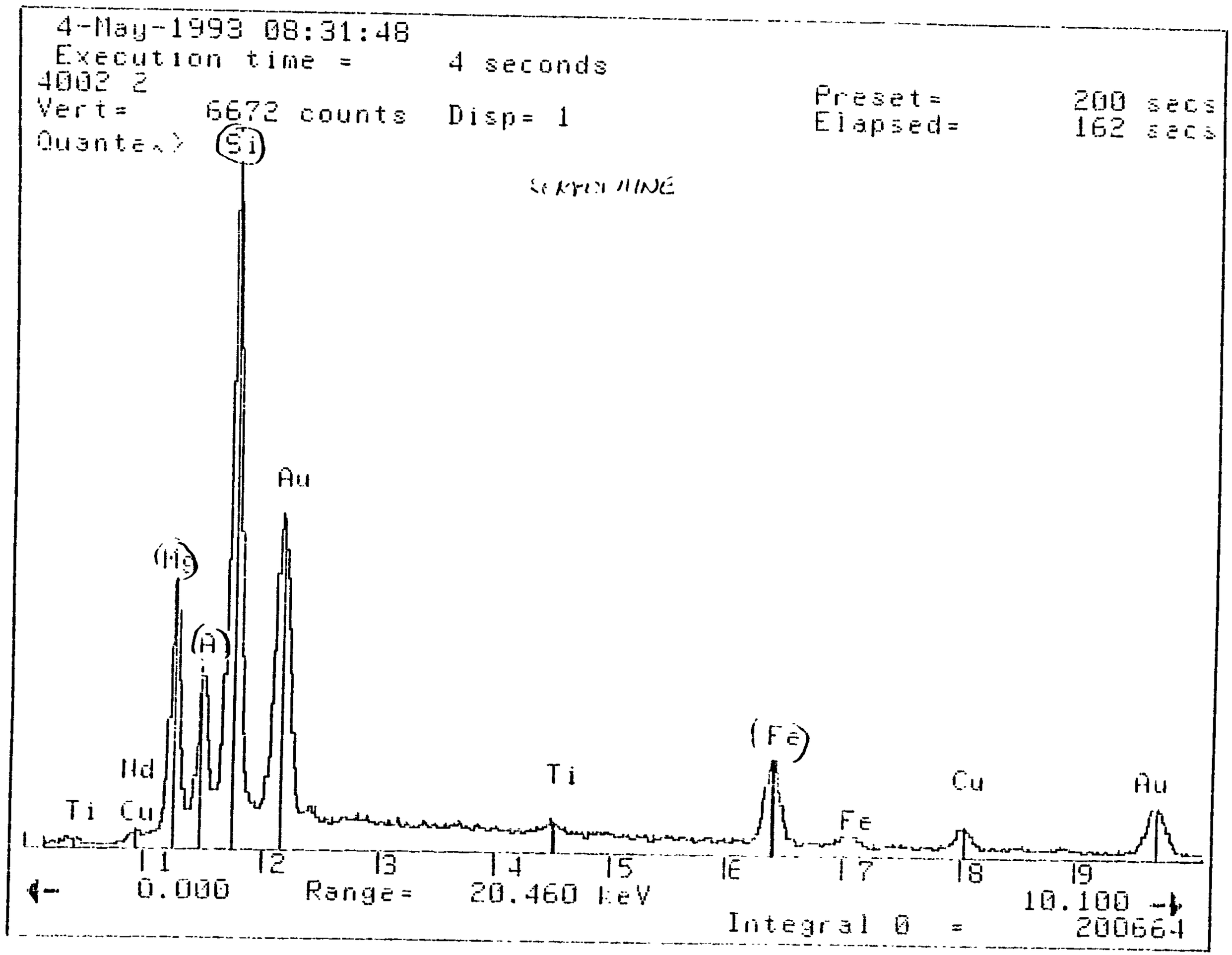
4-May-1993 08:31:48
Execution time = 4 seconds
4002 2
Vert= 6672 counts Disp= 1
Preset= 200 secs
Elapsed= 162 secs
Quante
Si
SCATTERING
Au
Ag
A
Ti
Cu
Nd
Ti
Fe
Cu
Au
Fe
1 1
1 2
1 3
1 4
1 5
1 6
1 7
1 8
1 9
0.000
Range= 20.460 keV
10.100
Integral 0 = 200664

K?

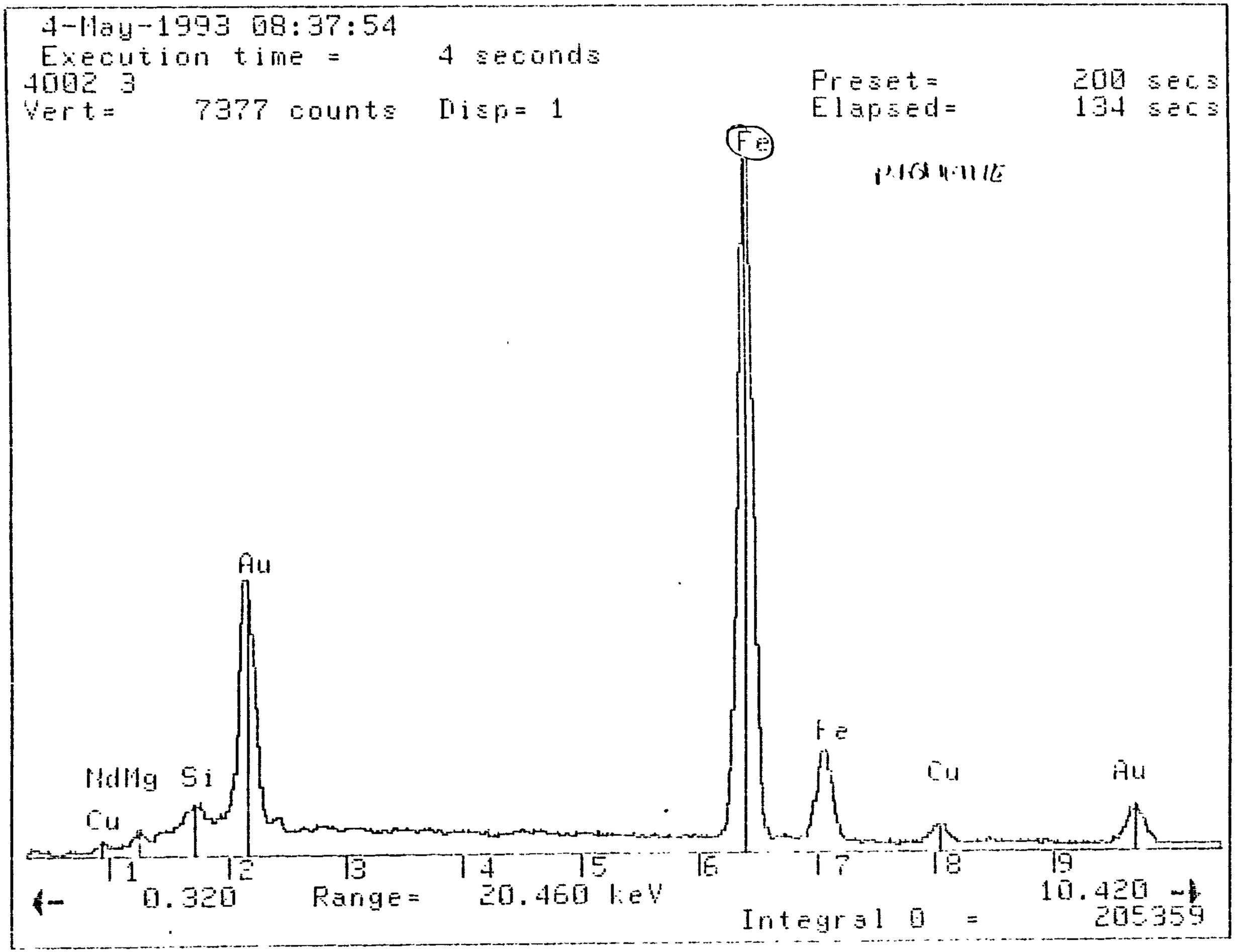
4-May-1993 08:37:54
Execution time = 4 seconds
4002 3
Vert= 7377 counts Disp= 1
Preset= 200 secs
Elapsed= 134 secs
Fe
Au
NdMg Si
Cu
Fe
Cu
Au
1
2
3
4
5
6
7
8
9
0.320
Range= 20.460 keV
10.420
Integral 0 = 205359

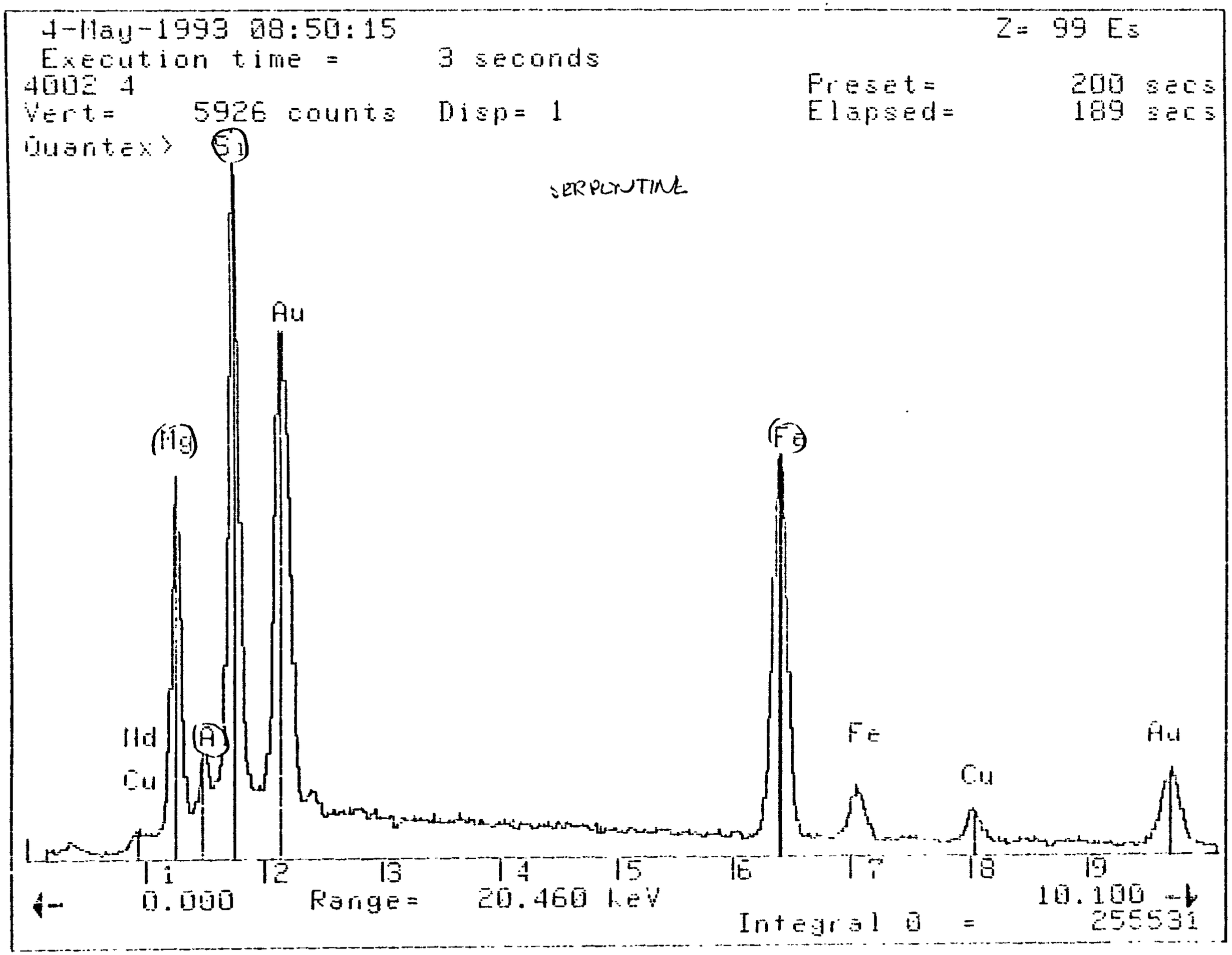
4-May-1993 08:50:15
Z= 99 Es
Execution time = 3 seconds
4002 4
Preset= 200 secs
Vert= 5926 counts Disp= 1
Elapsed= 189 secs
Quantex>
SERPENTINE
Au
Mg
Fe
Nd
Cu
A
Fe
Cu
Au
1
2
3
4
5
6
7
8
9
0.000
Range= 20.460 keV
10.100
Integral 0 = 255531

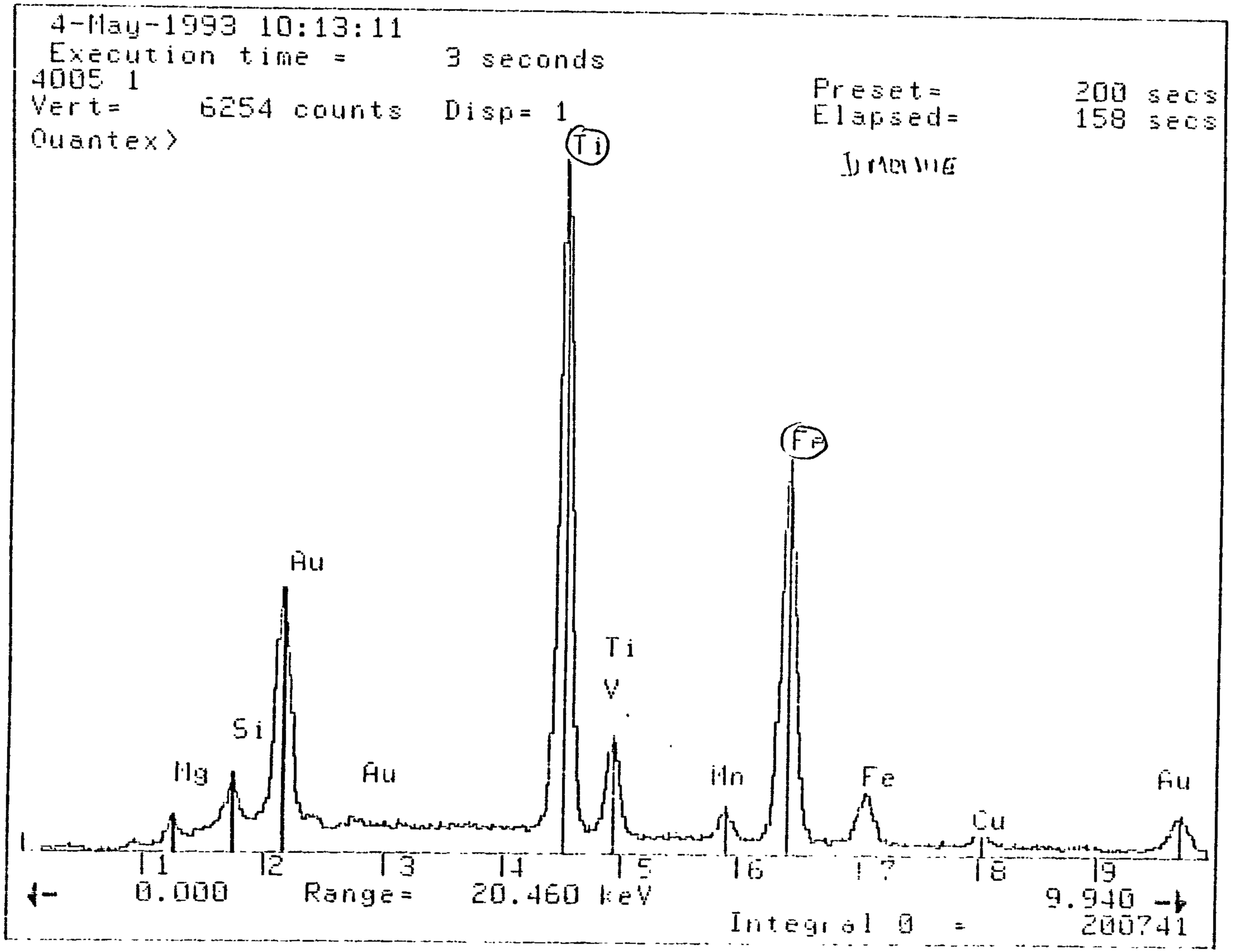
4-May-1993 10:13:11
Execution time = 3 seconds
4005 1
Vert= 6254 counts Disp= 1
Quantex>
Preset= 200 secs
Elapsed= 158 secs
Ti
Fe
Au
Si
Mg
Au
Ti
V
Mn
Fe
Cu
Au
1
2
3
4
5
6
7
8
9
0.000
Range= 20.460 keV
9.940
Integral 0 = 200741

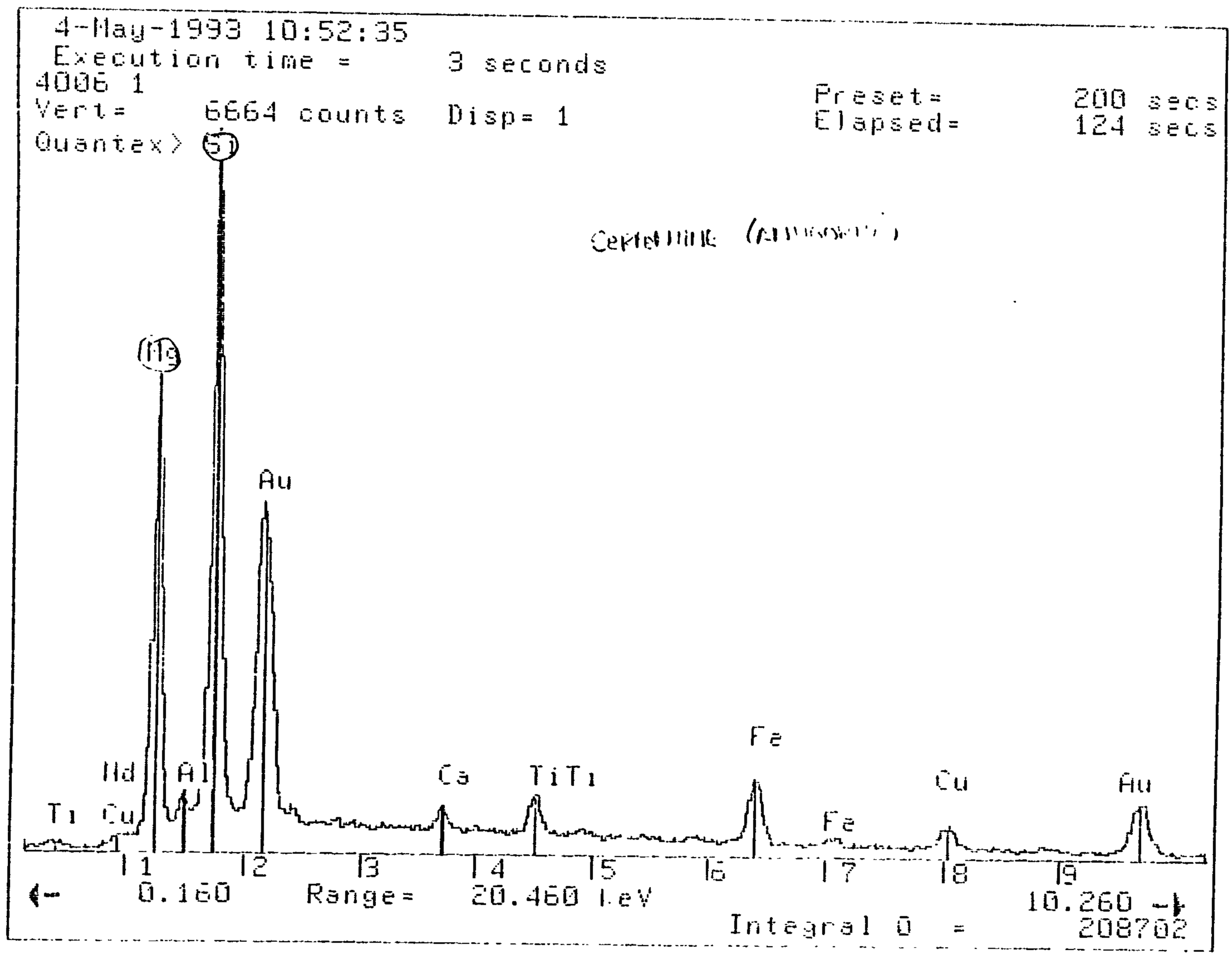
4-May-1993 10:52:35
Execution time = 3 seconds
4006 1
Vert= 6664 counts Disp= 1
Preset= 200 secs
Elapsed= 124 secs
Quantex>
Au
Ti
Cu
Nd
Al
Ca
Ti
Ti
Fe
Fe
Cu
Au
1
2
3
4
5
6
7
8
9
0.160
Range= 20.460 keV
10.260
Integral 0 = 208702

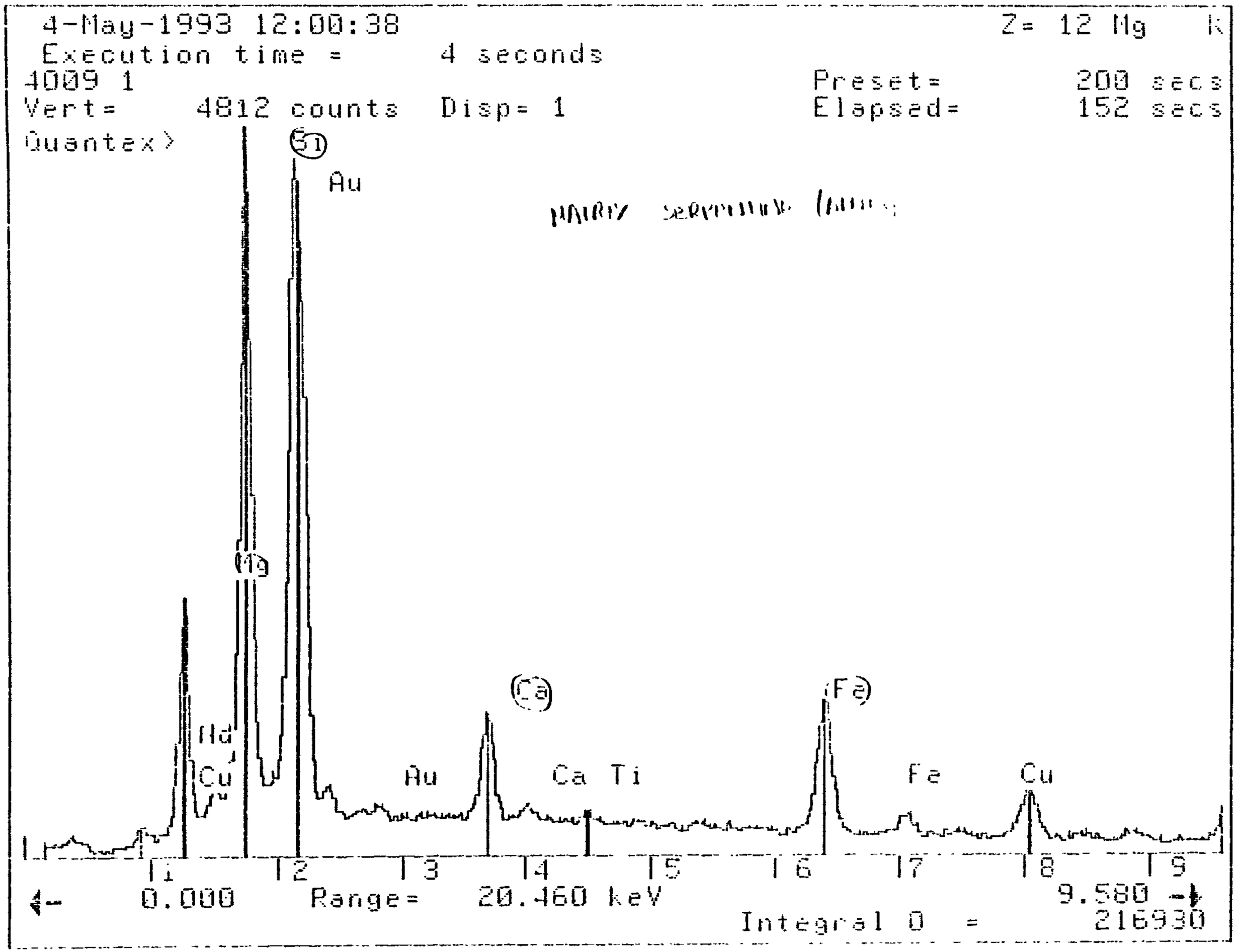
4-May-1993 12:00:38
Z= 12 Mg K
Execution time = 4 seconds
4009 1
Preset= 200 secs
Vert= 4812 counts Disp= 1
Elapsed= 152 secs
Quantex>
Au
Mg
Na
Cu
Au
Ca
Ca Ti
Fe
Cu
1 2 3 4 5 6 7 8 9
0.000
Range= 20.460 keV
9.580
Integral 0 = 216930

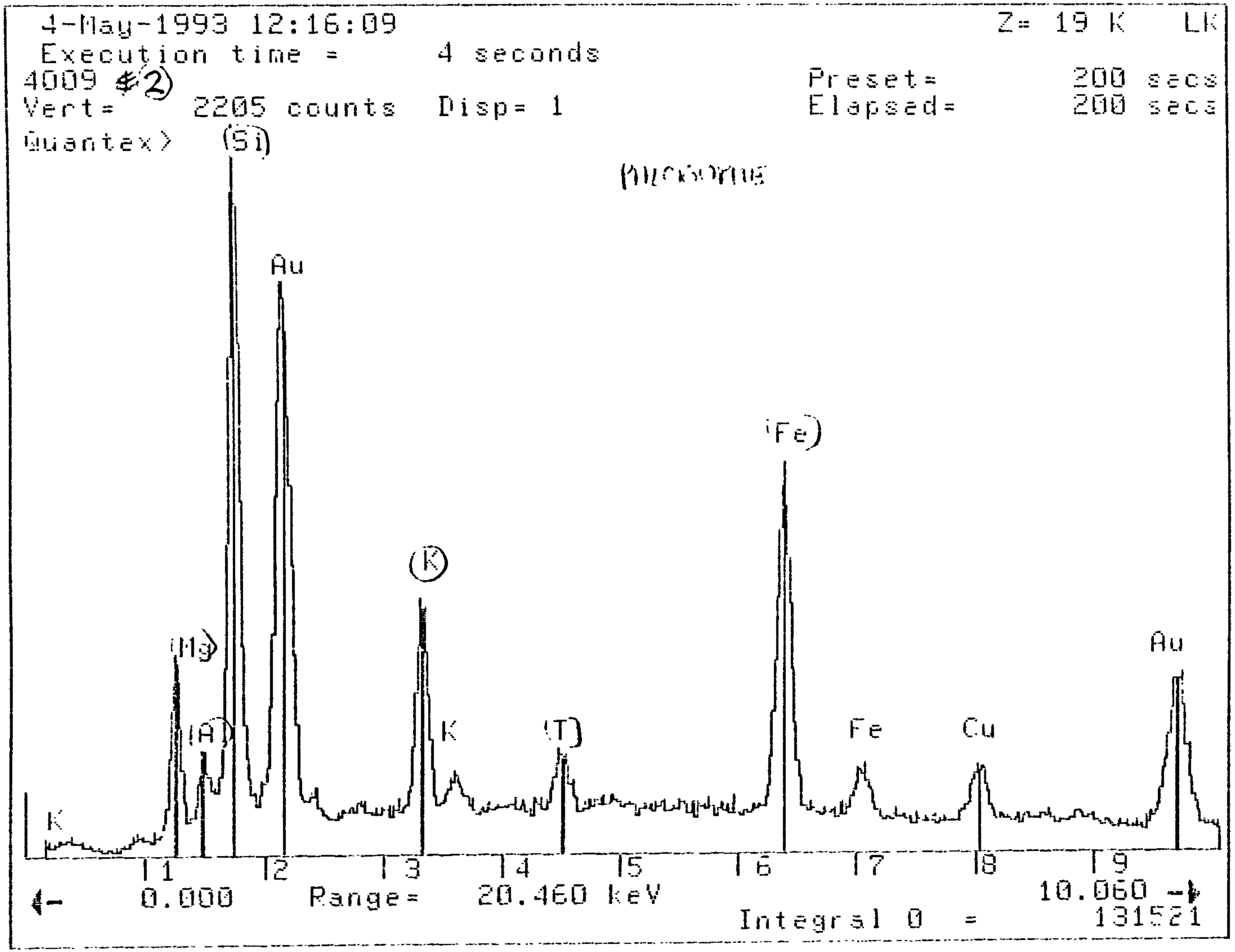
4-May-1993 12:16:09
Z= 19 K LK
Execution time = 4 seconds
4009 #2
Preset= 200 secs
Vert= 2205 counts Disp= 1
Elapsed= 200 secs
Quantex>
(Si)
Au
(Fe)
(K)
(Mg)
(A)
K
(T)
Fe
Cu
Au
K
1
2
3
4
5
6
7
8
9
0.000
Range= 20.460 keV
10.060
Integral 0 = 131521

4-May-1993 12:40:43 Z= 20 Ca LK
Execution time = 4 seconds
4010.1
Vert= 4932 counts Disp= 1 Preset= 200 secs
Elapsed= 159 secs

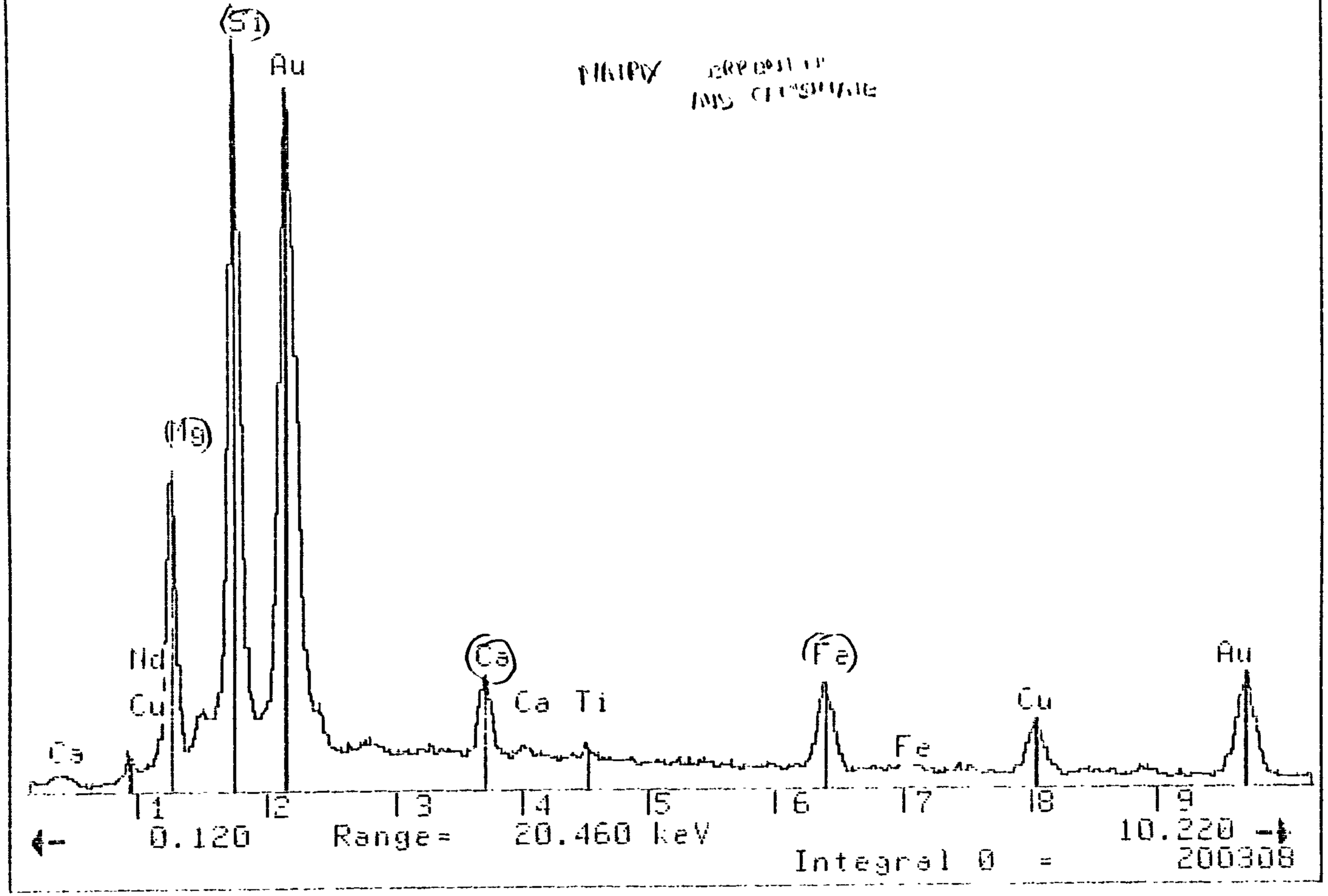

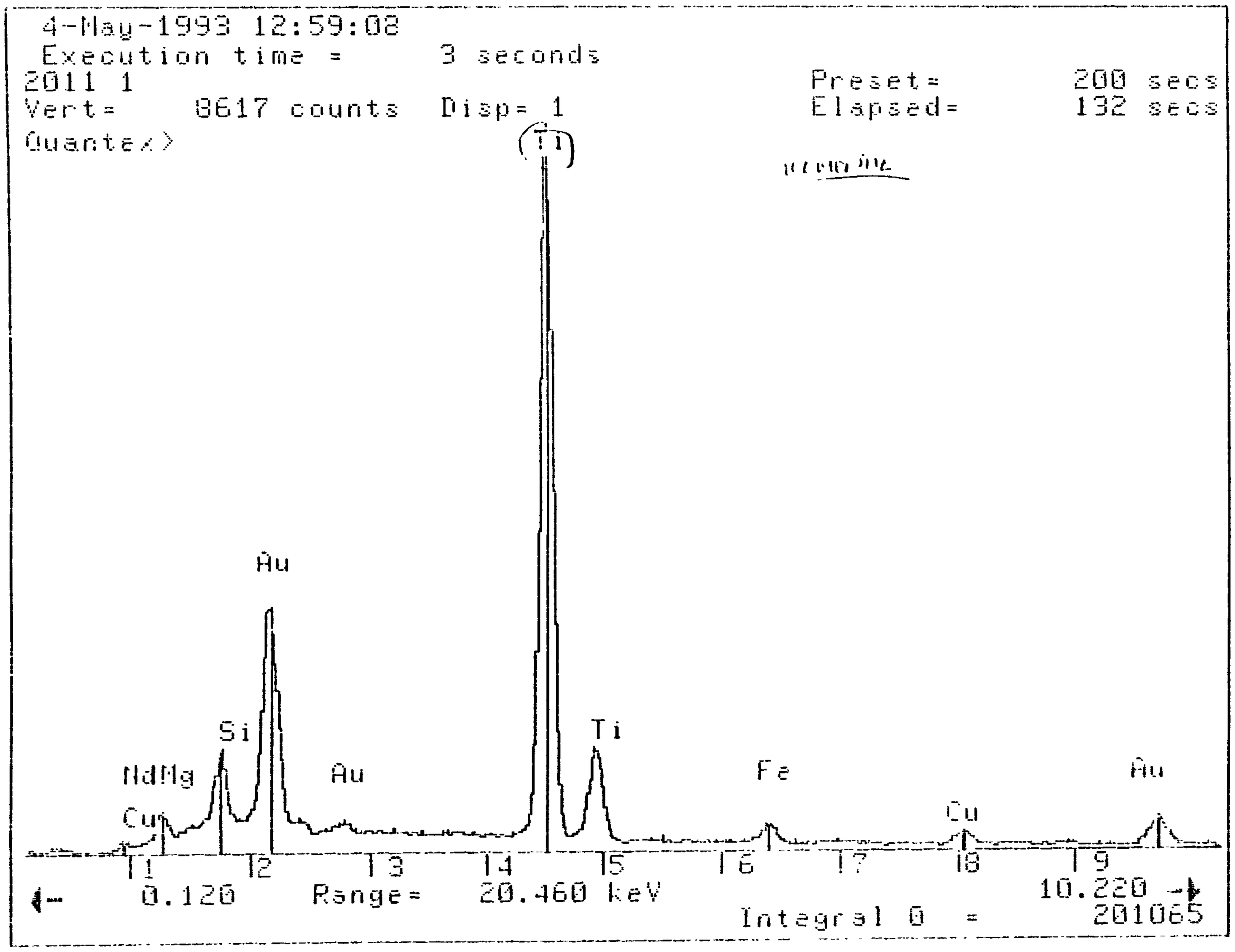
4-May-1993 12:59:08
Execution time = 3 seconds
2011 1
Vert= 8617 counts Disp= 1
Quantex>
Preset= 200 secs
Elapsed= 132 secs
Ti
Au
Si
NdMg
Cu
Au
Ti
Fe
Cu
Au
1
2
3
4
5
6
7
8
9
0.120
Range= 20.460 keV
10.220
Integral 0 = 201065

4-May-1993 14:41:26 Z= 25 Mn LK
Execution time = 4 seconds
2016 1
Vert= 4083 counts Disp= 1 Preset= 200 secs
Elapsed= 60 secs

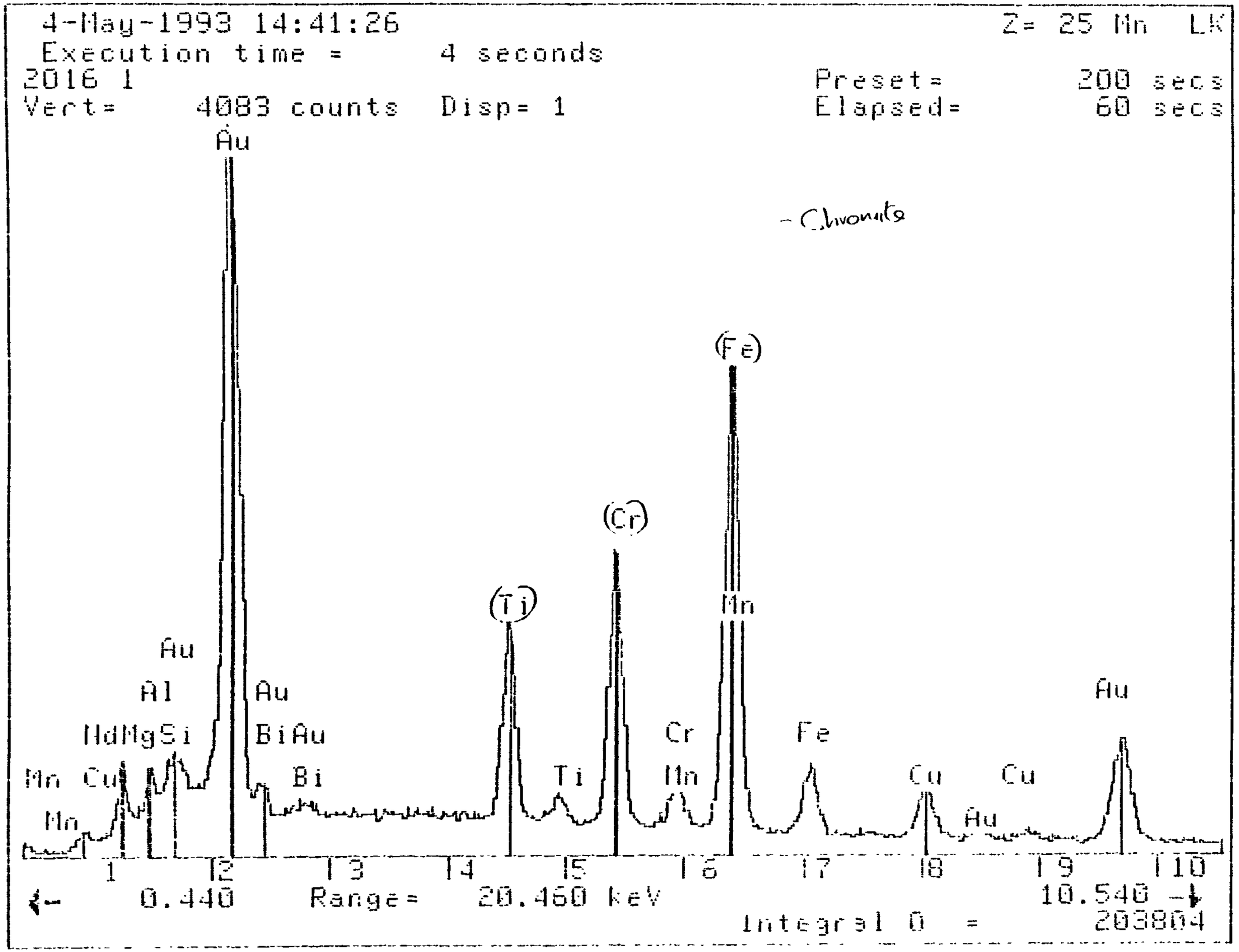

Integral 0 = 203804

JSM-840A.
1988.

4-May-1993 15:55:40
Execution time = 4 seconds
3019 1
Vert= 3106 counts Disp= 1
Quantex>

Z= 12 Mg K
Preset= 200 secs
Elapsed= 96 secs

CARNOT
(CORRODED, WITH MAGNETITE)

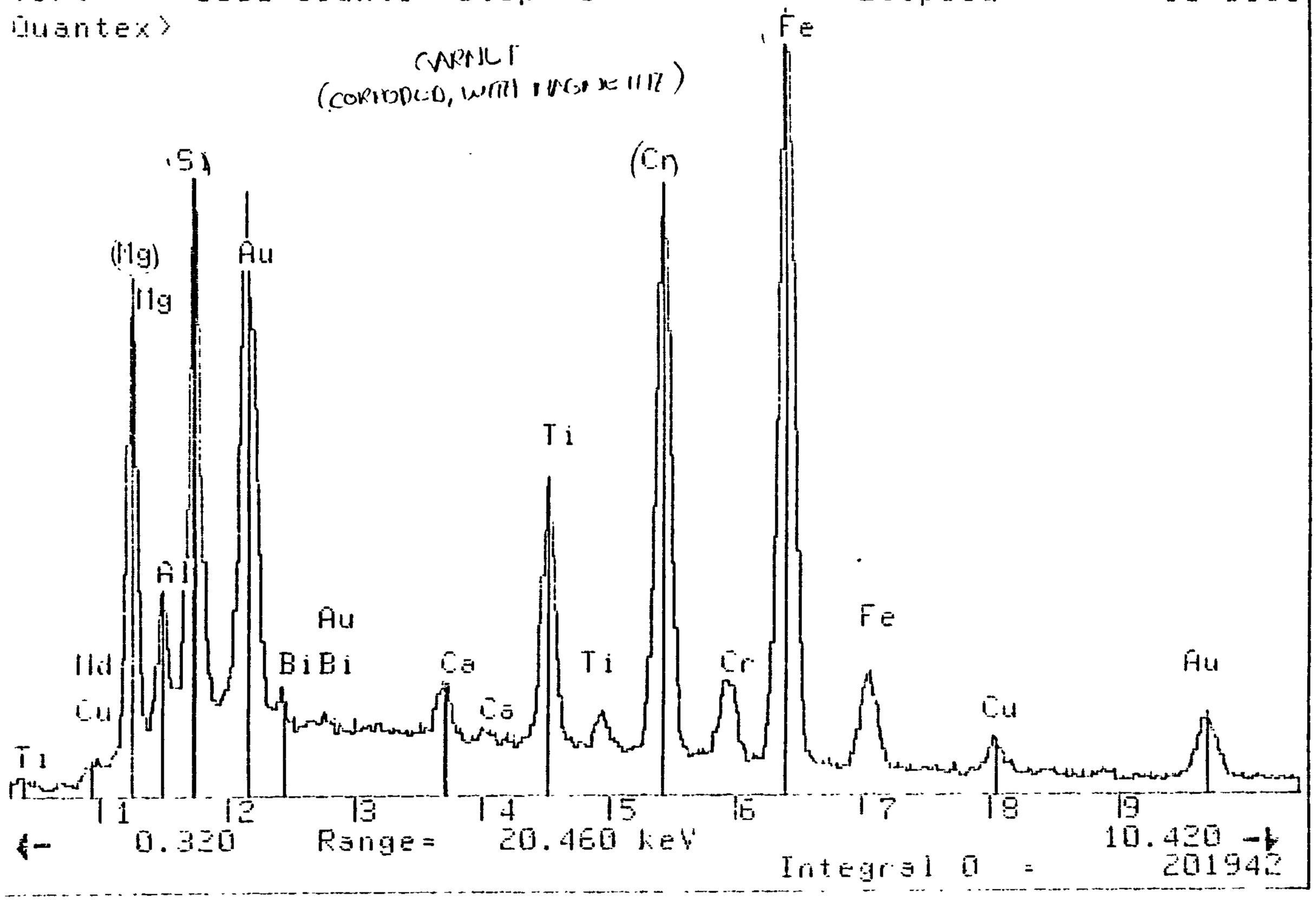

4-May-1993 16:27:30 Z= 13 Al K
Execution time = 3 seconds
2020 1 Preset= 200 secs
Vert= 6648 counts Disp= 1 Elapsed= 118 secs
Quantex>

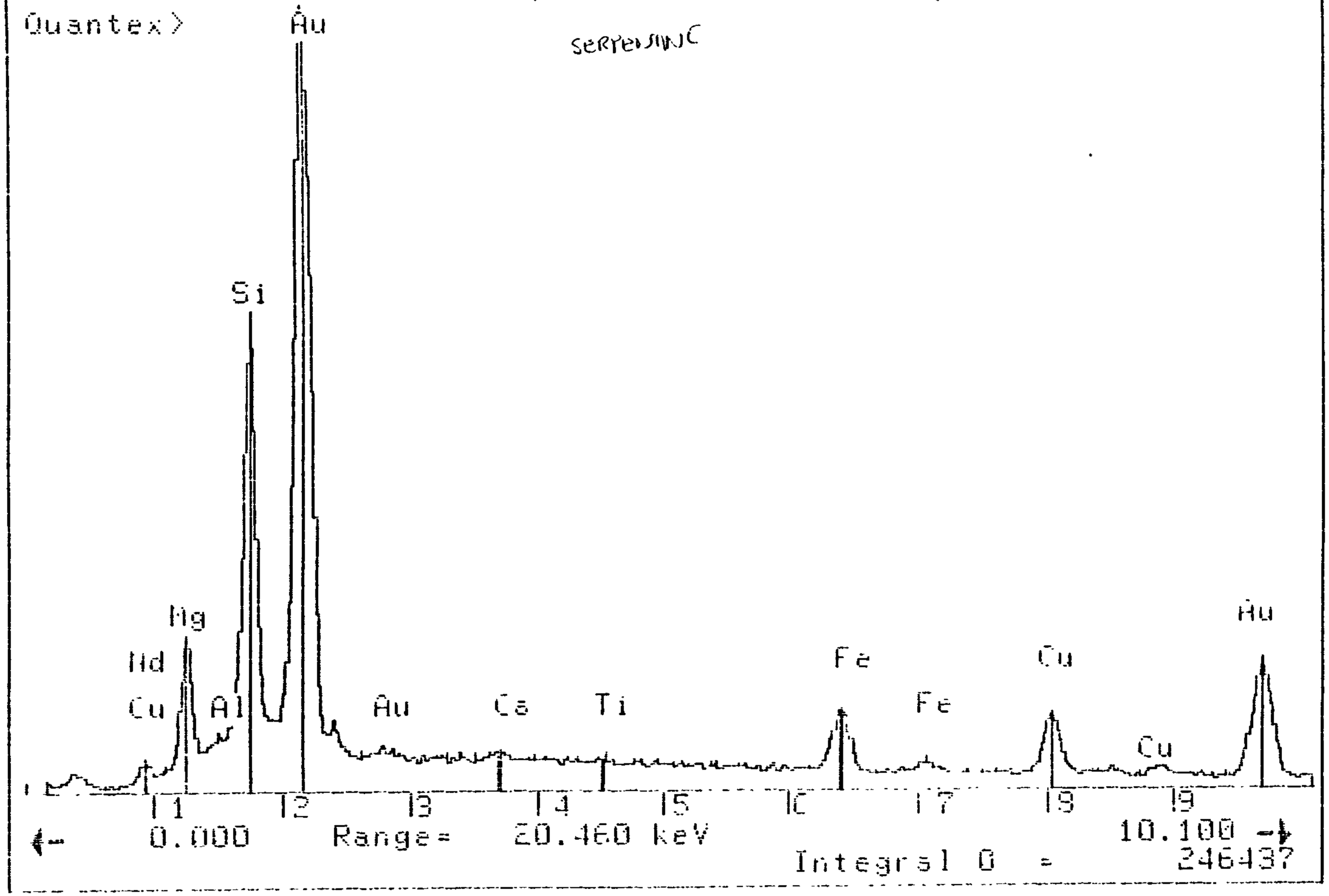

Onto Pure surface.

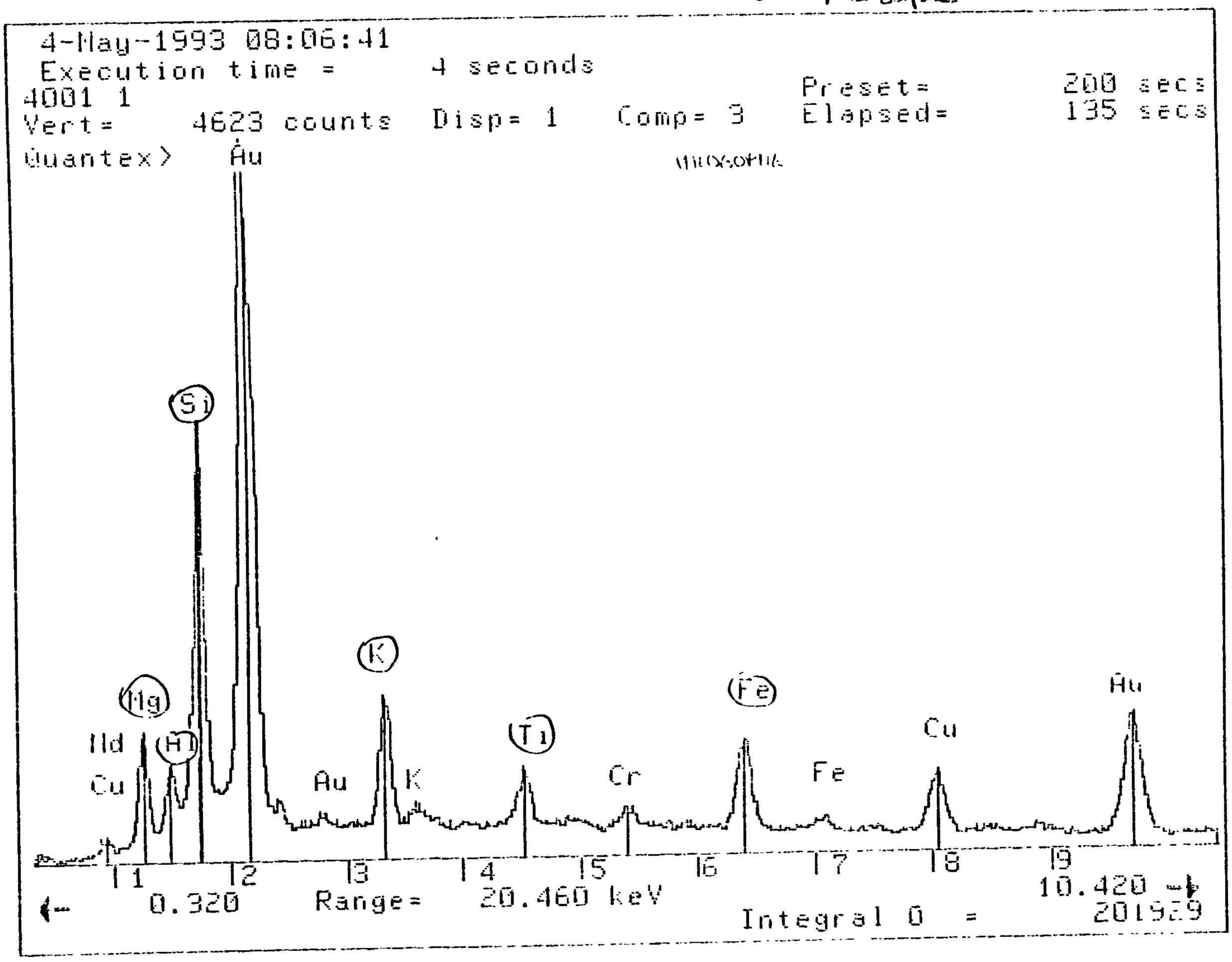

✓

APPENDIX VIII

Geochemistry of kimberlites from XRF

CONTENTS: XRF results for 98 analyses from Fort a la Corne (boreholes OFS 93-0xx) and Sturgeon Lake (all LK-2 analyses). Table includes 16 analyses presented in Kjarsgaard et al (1995) from borehole UK169/8, northern FALC cluster.

	K093	**K094**	**K095**	**K096**	**K097**
Rock type	RPK (m/g/b)	RPK (m/g/b)	RPK (m/g/b)	RPK (m/g/b)	RPK (m/g/b)
	(m/g/b)	(m/g/b)	(m/g/b)	(m/g/b)	(m/g/b)
Borehole	**002**	**002**	**002**	**002**	**002**
depth (m)	**104.42**	**105.55**	**106.68**	**107.81**	**108.94**
SiO2	41.09	37.32	33.34	35.08	33.94
TiO2	3.39	3.22	3.86	3.24	2.93
Al2O3	1.91	1.69	2.15	1.09	1.39
Fe2O3	9.53	11.38	10.21	10.75	10.11
MnO	0.08	0.13	0.17	0.16	0.24
MgO	32.65	32.47	33.08	34.73	31.72
CaO	0.58	0.71	2.94	1.66	4.61
Na2O	0.09	0.00	0.00	0.00	0.07
K2O	0.04	0.12	0.13	0.14	0.10
P2O5	0.19	0.15	0.18	0.10	0.36
L.o.I.	10.66	12.59	14.42	13.27	13.63
Total	100.21	99.78	100.48	100.22	99.10
Sc	20	14	20	17	19
V	84	90	124	71	69
Cr	2421	2218	2667	1999	2053
Co	101	116	103	114	120
Ni	1126	1382	1305	1500	1565
Cu	24	20	33	12	10
Zn	72	68	66	59	67
Rb	3	10	12	12	9
Sr	46	51	60	30	24
Y	8	6	6	5	5
Zr	118	106	127	103	104
Nb	215	192	226	202	209
Ba	94	72	73	58	43
Pb	3	1	0	3	2
Th	33	27	38	30	28
U	3	2	2	3	4
See Chapter 2 for rock type abbreviations					

	K091	**K060**	**K061**	**K062**	**K063**
Rock type	PK	RPK	RPK	RPK	RPK
	(m/c tuff)	(m/g/b)	(m/g/b)	(m/g/b)	(m/g/b)
Borehole	**004**	**003**	**003**	**003**	**003**
depth (m)	**108.51**	**95.12**	**95.97**	**96.82**	**97.67**
SiO2	33.84	32.91	36.02	34.82	33.69
TiO2	2.59	2.66	2.75	2.36	2.35
Al2O3	1.19	1.36	2.18	0.72	0.93
Fe2O3	8.86	14.51	8.83	10.33	10.52
MnO	0.17	0.22	0.13	0.16	0.16
MgO	27.66	30.98	31.21	35.14	33.36
CaO	9.35	4.07	4.71	3.18	3.88
Na2O	0.08	0.10	0.06	-0.02	0.10
K2O	0.05	0.14	0.15	0.06	0.09
P2O5	0.37	0.21	0.56	0.14	0.18
L.o.I.	16.27	13.18	12.47	13.75	14.65
Total	100.43	100.34	99.07	100.64	99.91
Sc	19	12	11	8	14
V	79	100	120	68	75
Cr	1206	1413	1204	1128	1157
Co	77	94	99	109	95
Ni	917	1449	1354	1640	1514
Cu	42	39	43	21	24
Zn	52	71	73	70	111
Rb	4	8	7	4	7
Sr	152	86	136	59	71
Y	8	6	11	4	6
Zr	160	98	114	70	80
Nb	204	172	178	142	150
Ba	144	75	152	49	91
Pb	8	6	8	1	4
Th	31	25	27	21	21
U	4	2	4	0	1

	K087	**K098**	**K088**	**K089**	**K090**
Rock type	RPK	RPK (m/g/b)	PK	PK	PK
	(m/g/b)	(m/g/b)	(m/c tuff)	(m/c tuff)	(m/c tuff)
Borehole	**004**	**002**	**004**	**004**	**004**
depth (m)	**102.87**	**110.07**	**104.28**	**105.69**	**107.1**
SiO2	33.29	35.19	34.61	36.56	34.73
TiO2	3.44	2.30	2.91	3.39	2.31
Al2O3	2.04	1.04	1.73	1.83	1.19
Fe2O3	10.64	13.52	8.91	9.76	11.04
MnO	0.18	0.16	0.18	0.20	0.15
MgO	32.30	34.49	33.37	33.67	30.12
CaO	3.90	1.01	3.95	1.42	5.89
Na2O	0.22	0.00	-0.03	0.05	0.02
K2O	0.13	0.17	0.06	0.05	0.05
P2O5	0.46	0.10	0.26	0.63	0.28
L.o.I.	12.50	12.42	13.97	12.04	14.48
Total	99.10	100.40	99.92	99.60	100.26
Sc	21	19	13	17	11
V	174	65	155	148	106
Cr	1734	1561	1606	2000	1380
Co	82	110	107	102	87
Ni	936	1611	1136	1167	1004
Cu	63	19	43	58	54
Zn	60	67	64	71	53
Rb	10	11	5	5	3
Sr	160	29	113	117	124
Y	14	4	11	17	8
Zr	189	81	137	190	104
Nb	289	153	227	272	187
Ba	105	65	93	83	79
Pb	14	4	10	10	6
Th	55	22	32	46	28
U	2	3	3	4	1

	K082	**K083**	**K084**	**K085**	**K086**
Rock type	RPK (m/g/b)	RPK (m/g/b)	RPK (m/g/b)	RPK (m/g/b)	RPK (m/g/b)
	(m/g/b)	(m/g/b)	(m/g/b)	(m/g/b)	(m/g/b)
Borehole	**004**	**004**	**004**	**004**	**004**
depth (m)	**95.82**	**97.23**	**98.64**	**100.05**	**101.46**
SiO2	31.16	33.09	29.10	36.07	30.53
TiO2	3.08	2.36	2.37	2.92	3.09
Al2O3	0.94	1.24	1.00	1.04	1.15
Fe2O3	17.86	13.80	21.99	6.35	15.69
MnO	0.20	0.25	0.20	0.24	0.23
MgO	32.74	34.35	30.80	37.02	31.65
CaO	1.92	2.25	2.59	2.57	3.63
Na2O	0.07	0.11	0.04	0.05	0.12
K2O	0.14	0.25	0.17	0.06	0.07
P2O5	0.08	0.18	0.22	0.24	0.31
L.o.I.	12.21	12.43	11.29	13.13	13.37
Total	100.40	100.31	99.77	99.69	99.84
Sc	15	15	20	15	16
V	85	97	107	104	133
Cr	1916	1543	1408	1479	1608
Co	104	110	110	104	104
Ni	1786	1742	1818	1378	1506
Cu	27	41	63	23	57
Zn	71	68	71	62	65
Rb	10	20	11	5	6
Sr	34	49	62	54	78
Y	3	5	6	6	8
Zr	89	89	98	108	129
Nb	180	155	184	202	231
Ba	39	115	55	31	35
Pb	3	5	7	6	10
Th	24	22	28	29	38
U	1	1	1	2	3

	K099	K100	K101	K102	K081
Rock type	PK (m to c tuff)	PK (m to c tuff)	PK (m to c tuff)	PK (m to c tuff)	RPK (m/g/b)
	(m/c tuff)	(m/c tuff)	(m/c tuff)	(m/c tuff)	(m/g/b)
Borehole	**002**	**002**	**002**	**002**	**004**
depth (m)	**111.2**	**112.33**	**113.46**	**114.59**	**94.41**
SiO2	33.40	39.05	37.99	36.66	32.90
TiO2	3.38	2.36	2.58	3.47	2.87
Al2O3	1.21	1.21	1.25	1.06	1.47
Fe2O3	10.05	7.86	10.31	10.27	14.66
MnO	0.24	0.14	0.16	0.18	0.17
MgO	33.11	26.48	31.33	36.05	32.93
CaO	4.06	8.31	3.21	0.88	2.23
Na2O	0.00	0.12	0.07	0.04	0.02
K2O	0.13	0.13	0.05	0.13	0.24
P2O5	0.19	0.53	0.27	0.10	0.14
L.o.I.	14.57	14.11	12.81	11.53	12.48
Total	100.34	100.30	100.03	100.37	100.11
Sc	18	16	11	10	22
V	86	140	98	60	87
Cr	2042	1942	1559	1085	1614
Co	96	93	80	59	105
Ni	1428	1058	885	658	1573
Cu	16	51	36	36	31
Zn	66	50	51	41	68
Rb	10	6	4	6	17
Sr	76	128	153	210	44
Y	7	11	10	9	5
Zr	124	136	138	227	109
Nb	223	236	204	197	184
Ba	84	89	124	272	84
Pb	3	10	7	7	5
Th	40	42	32	36	29
U	5	5	4	2	1

	K031	**K037**	**K032**	**K034**	**K035**
Rock type					
Borehole	**LK-2**	**LK-2**	**LK-2**	**LK-2**	**LK-2**
depth (m)			**shl+tuff**		
SiO2	27.31	49.25	69.88	32.25	18.12
TiO2	1.50	1.90	0.64	0.74	0.70
Al2O3	1.48	2.45	10.94	0.73	0.42
Fe2O3	8.95	9.85	6.53	7.22	5.73
MnO	0.37	0.08	0.02	0.19	0.39
MgO	25.20	22.44	3.42	32.25	16.16
CaO	12.47	2.85	0.79	7.89	29.79
Na2O	0.19	0.22	0.79	0.07	0.05
K2O	0.43	0.46	2.36	0.07	0.04
P2O5	0.90	1.20	0.24	0.47	0.38
L.o.I.	20.96	8.26	5.19	18.63	28.66
Total	99.76	98.96	100.79	100.51	100.45
Sc	24	44	6	13	15
V	83	137	94	40	29
Cr	1699	2543	68	980	593
Co	101	177	19	73	46
Ni	1852	3167	28	1322	1064
Cu	18	20	15	6	9
Zn	77	104	78	50	39
Rb	24	25	102	5	1
Sr	271	224	128	234	261
Y	19	27	34	10	6
Zr	196	261	366	93	57
Nb	267	400	17	147	111
Ba	339	399	336	272	143
Pb	16	27	19	11	6
Th	46	70	17	28	20
U	8	11	1	4	3

	K044	**K045**	**K046**	**K047**	**K048**
Rock type	TC	TC	TC	TC	TC
	conglom	conglom	conglom	conglom	lamin silt
Borehole	**010**	**010**	**010**	**010**	**010**
depth (m)	**154.03**	**154.42**	**154.82**	**155.28**	**142.27**
SiO2	41.51	22.50	33.70	33.40	73.56
TiO2	1.98	1.17	1.48	1.91	1.90
Al2O3	6.28	3.45	3.32	4.39	6.78
Fe2O3	9.57	9.44	9.88	9.92	4.10
MnO	0.49	1.11	0.78	0.57	0.07
MgO	13.75	15.30	15.86	15.38	1.99
CaO	9.29	19.63	13.96	14.88	2.35
Na2O	1.46	0.92	1.07	1.28	0.72
K2O	1.27	0.56	0.32	0.61	1.87
P2O5	0.51	0.35	0.22	0.50	0.68
L.o.I.	12.99	25.97	18.05	17.39	4.14
Total	99.10	100.40	98.64	100.23	98.16
Sc	18	16	12	18	15
V	140	85	55	99	126
Cr	1188	640	1611	1590	592
Co	67	43	75	79	30
Ni	759	496	1461	1335	135
Cu	55	35	24	52	31
Zn	68	46	63	85	66
Rb	58	29	20	39	66
Sr	224	244	177	286	171
Y	17	13	10	12	35
Zr	208	116	112	134	444
Nb	220	123	131	159	213
Ba	374	238	253	303	480
Pb	14	7	7	6	15
Th	35	20	22	24	36
U	3	1	1	3	3

	K039	**K040**	**K041**	**K042**	**K043**
Rock type	TC	TC	muds	laminated	TC
	lamin silt	silts		tuff-silt	lamin silt
Borehole	**010**	**010**	**010**	**010**	**010**
depth (m)	**142.09**	**147.68**	**148.3**	**148.65**	**149.21**
SiO2	24.97	25.12	19.02	14.64	20.49
TiO2	7.13	1.42	11.06	9.29	5.36
Al2O3	7.44	5.02	3.30	3.05	3.83
Fe2O3	16.20	7.83	10.32	11.76	9.05
MnO	0.18	0.27	0.49	0.61	0.52
MgO	5.92	8.51	10.41	13.42	12.04
CaO	15.02	26.85	22.53	21.11	24.09
Na2O	1.15	1.25	0.85	0.53	0.91
K2O	0.47	0.65	0.17	0.08	0.30
P2O5	0.62	1.43	0.38	0.29	0.40
L.o.I.	13.25	20.33	20.69	25.42	23.63
Total	92.35	98.67	99.22	100.20	100.62
Sc	38	17	30	29	31
V	89	301	0	0	26
Cr	1723	184	3662	3265	2428
Co	69	28	44	49	37
Ni	353	240	814	618	430
Cu	70	269	37	32	32
Zn	134	57	64	59	62
Rb	22	33	9	6	18
Sr	463	733	346	382	320
Y	38	17	39	37	26
Zr	447	314	366	313	280
Nb	589	314	790	674	404
Ba	763	555	340	346	428
Pb	8	50	4	3	5
Th	99	11	130	112	59
U	8	5	14	9	7

	K069	K070	K071	K072	K073
Rock type	PK	PK	PK	ICB	basal ICB
	(m/c tuff)	(m/c tuff)	(m/c tuff)		
Borehole	**003**	**003**	**003**	**003**	**003**
depth (m)	**102.77**	**103**	**103.65**	**101.36**	**101.06**
SiO2	23.24	26.23	23.20	26.61	35.56
TiO2	2.13	1.44	1.88	2.51	2.67
Al2O3	1.03	1.98	0.98	1.12	2.33
Fe2O3	7.68	6.70	7.77	8.88	9.30
MnO	0.29	0.36	0.34	0.27	0.14
MgO	19.29	20.64	18.97	22.04	30.33
CaO	19.73	19.53	22.92	17.23	4.89
Na2O	0.06	0.22	0.09	0.21	0.24
K2O	0.05	0.08	0.02	0.07	0.06
P2O5	0.31	0.65	0.34	0.33	0.53
L.o.I.	25.69	22.43	23.64	20.19	14.45
Total	99.50	100.28	100.15	99.46	100.50
Sc	18	13	12	14	17
V	73	70	63	81	106
Cr	1117	615	698	1085	1288
Co	70	59	53	82	84
Ni	966	777	776	1233	1027
Cu	44	36	36	44	47
Zn	55	45	45	56	56
Rb	3	7	1	4	5
Sr	225	247	322	318	170
Y	7	9	6	7	14
Zr	97	73	70	94	172
Nb	175	106	123	183	215
Ba	227	319	282	272	194
Pb	8	4	7	7	8
Th	28	18	22	26	39
U	1	0	-1	0	3

	K064	K065	K066	K067	K068
Rock type	ICB	ICB	ICB	PK	PK
				(m/c tuff)	(m/c tuff)
Borehole	**003**	**003**	**003**	**003**	**003**
depth (m)	**98.52**	**99.37**	**100.22**	**101.07**	**101.92**
SiO2	33.85	34.00	31.52	31.14	30.93
TiO2	2.12	1.57	3.18	3.37	2.84
Al2O3	2.76	3.43	1.88	2.12	1.80
Fe2O3	8.87	8.54	8.96	8.99	8.93
MnO	0.14	0.07	0.12	0.14	0.18
MgO	30.36	29.45	28.51	27.77	26.76
CaO	5.88	3.66	6.63	5.70	7.04
Na2O	0.13	0.15	0.00	0.01	0.06
K2O	0.07	0.07	0.07	0.07	0.06
P2O5	0.76	0.51	0.40	0.55	0.47
L.o.I.	14.90	17.88	18.35	19.35	20.13
Total	99.83	99.32	99.63	99.22	99.20
Sc	15	12	14	19	10
V	119	129	148	117	114
Cr	1019	835	1575	1722	1548
Co	87	74	104	98	111
Ni	1069	820	1450	1262	1424
Cu	43	43	135	59	44
Zn	60	62	105	76	68
Rb	5	6	6	5	4
Sr	148	117	273	179	236
Y	11	12	12	16	10
Zr	106	98	144	194	116
Nb	152	108	249	284	217
Ba	132	141	233	211	229
Pb	9	9	12	11	8
Th	23	18	33	44	28
U	3	2	3	3	3

	K036	**K038**	**K055**	**K074**	**K075**
Rock type		TC	ICB	bentonite	mud
		silt			fish debris
Borehole	**LK-2**	**010**	**009**	**008**	**008**
depth (m)	**shl+tuff**	**141.7**	**140.15**	**159.07**	**158.94**
SiO2	55.25	36.85	18.23	60.27	14.41
TiO2	0.40	11.74	0.67	0.18	0.09
Al2O3	8.22	10.13	0.90	19.71	3.73
Fe2O3	12.25	16.03	22.86	2.10	1.87
MnO	0.02	0.03	0.48	0.03	0.09
MgO	15.61	3.75	12.38	5.43	0.96
CaO	0.99	1.42	17.25	1.23	38.87
Na2O	1.25	1.68	0.39	2.42	0.82
K2O	0.89	0.44	0.03	0.52	0.68
P2O5	0.10	0.75	0.06	0.04	0.40
L.o.I.	5.72	11.17	9.21	7.81	37.68
Total	100.70	94.00	82.47	99.74	99.60
Sc	3	60	8	3	15
V	87	158	3	30	394
Cr	74	4906	670	4	23
Co	30	133	38	7	8
Ni	49	1619	751	1	57
Cu	15	159	31	-1	30
Zn	61	190	41	77	108
Rb	57	16	2	13	16
Sr	169	248	163	212	575
Y	16	32	4	2	12
Zr	144	522	31	131	15
Nb	12	982	62	14	2
Ba	347	4726	71	175	384
Pb	11	7	2	38	5
Th	13	182	16	53	6
U	0	11	-1	1	17

	K026	**K027**	**K028**	**K029**	**K030**
Rock type					
Borehole	**LK-2**	**LK-2**	**LK-2**	**LK-2**	**LK-2**
depth (m)					
SiO2	34.30	32.77	35.72	25.47	29.32
TiO2	0.64	1.07	0.89	0.70	0.72
Al2O3	2.52	1.66	1.41	0.58	0.62
Fe2O3	7.41	8.13	8.07	7.28	8.86
MnO	0.17	0.21	0.18	0.33	0.41
MgO	29.34	30.95	31.35	24.28	26.49
CaO	7.57	7.52	6.20	17.30	12.24
Na2O	0.19	0.15	0.19	0.10	0.10
K2O	0.29	0.23	0.13	0.06	0.05
P2O5	0.43	0.87	0.62	0.54	0.63
L.o.I.	17.70	16.86	15.81	23.43	20.63
Total	100.56	100.42	100.57	100.06	100.06
Sc	17	21	22	19	14
V	75	71	60	47	48
Cr	651	964	810	868	728
Co	56	54	58	55	64
Ni	687	732	721	1144	1181
Cu	5	19	9	9	11
Zn	40	48	42	47	47
Rb	17	13	8	3	1
Sr	203	302	256	254	279
Y	11	18	13	9	13
Zr	107	202	162	86	91
Nb	149	245	203	160	180
Ba	165	425	310	254	267
Pb	12	18	12	13	13
Th	27	48	36	30	32
U	6	8	4	2	4

	K021	K022	K023	K024	K025
Rock type					
Borehole	**LK-2**	**LK-2**	**LK-2**	**LK-2**	**LK-2**
depth (m)					
SiO2	35.32	36.14	37.17	35.97	31.07
TiO2	0.66	0.88	0.79	0.56	0.62
Al2O3	0.50	0.38	0.45	0.48	0.63
Fe2O3	16.12	7.28	10.87	12.07	6.10
MnO	0.16	0.16	0.12	0.15	0.19
MgO	33.56	34.81	35.28	34.43	30.63
CaO	1.56	3.94	2.24	2.74	10.70
Na2O	0.15	0.00	-0.04	0.11	0.06
K2O	0.22	0.06	0.11	0.18	0.13
P2O5	0.12	0.10	0.12	0.16	0.32
L.o.I.	11.90	16.01	13.50	13.09	19.53
Total	100.27	99.76	100.61	99.94	99.97
Sc	12	12	7	11	17
V	29	24	33	42	43
Cr	946	902	866	1068	814
Co	103	75	105	93	73
Ni	1805	1123	1650	1671	1184
Cu	9	-1	4	9	3
Zn	48	24	37	40	42
Rb	13	3	7	9	7
Sr	35	52	47	57	162
Y	2	2	3	4	6
Zr	42	57	36	36	62
Nb	85	111	62	72	114
Ba	62	28	49	48	66
Pb	2	2	3	5	8
Th	20	21	14	15	24
U	1	2	1	2	2

	K054	**K055**	**K056**	**K058**	**K059**
Rock type	RPK	RPK	RPK	RPK	RPK
	(m/g/b)	(m/g/b)	(m/g/b)	(m/g/b)	(m/g/b)
Borehole	**009**	**009**	**009**	**009**	**009**
depth (m)	**137.87**	**138.61**	**139.35**	**140.09**	**140.83**
SiO2	20.09	18.23	14.88	31.17	38.67
TiO2	1.05	0.67	1.51	1.52	1.94
Al2O3	1.29	0.90	1.28	2.54	2.73
Fe2O3	4.99	22.86	4.49	6.45	8.39
MnO	0.44	0.48	0.45	0.48	0.25
MgO	16.28	12.38	11.30	17.93	22.84
CaO	27.80	17.25	34.83	19.70	9.78
Na2O	0.47	0.39	0.37	0.98	1.14
K2O	0.04	0.03	0.03	0.10	0.05
P2O5	0.08	0.06	0.13	0.20	0.32
L.o.I.	27.64	9.21	30.97	18.87	14.32
Total	100.17	82.46	100.24	99.92	100.43
Sc	15	8	24	16	18
V	3	3	10	38	69
Cr	1092	670	1130	1105	2292
Co	32	38	35	50	86
Ni	552	751	596	660	1469
Cu	8	31	13	15	17
Zn	30	41	36	49	66
Rb	2	2	1	5	2
Sr	217	163	241	198	171
Y	5	4	9	11	14
Zr	40	31	57	101	103
Nb	81	62	117	124	165
Ba	776	71	121	111	108
Pb	0	2	1	3	6
Th	17	16	23	26	31
U	-2	-1	2	-1	2

	K049	K050	K051	K052	K053
Rock type	muds	sand	RPK	RPK	RPK
	fish debris		(m/g/b)	(m/g/b)	(m/g/b)
Borehole	**010**	**010**	**009**	**009**	**009**
depth (m)	**144.91**	**150.58**	**135.65**	**136.39**	**137.13**
SiO2	64.07	80.61	35.01	19.27	25.41
TiO2	0.63	0.41	1.92	0.82	1.05
Al2O3	15.13	7.66	2.44	1.08	1.26
Fe2O3	5.65	3.33	8.11	4.84	5.34
MnO	0.02	0.01	0.22	0.43	0.44
MgO	2.30	1.19	25.44	20.40	19.37
CaO	0.45	0.40	9.42	24.10	23.89
Na2O	1.26	0.67	0.79	0.27	0.59
K2O	3.13	1.60	0.05	0.02	0.04
P2O5	0.18	0.24	0.35	0.10	0.11
L.o.I.	6.27	3.46	14.93	28.98	13.04
Total	99.09	99.59	98.68	100.31	90.54
Sc	12	7	16	17	13
V	139	90	18	10	15
Cr	85	53	2421	930	959
Co	21	18	84	44	33
Ni	33	21	1323	763	673
Cu	17	7	13	5	8
Zn	95	53	60	29	28
Rb	145	77	2	1	2
Sr	117	75	139	206	193
Y	29	25	12	5	5
Zr	161	271	81	31	38
Nb	15	9	156	66	83
Ba	409	211	106	66	96
Pb	20	11	1	2	3
Th	15	13	30	17	17
U	2	0	1	-2	0

	K076	**K077**	**K078**	**K079**	**K080**	**K121**
Rock type	sandy mud	sandy mud	muddy sand	sand	bentonite	bentonite
	fish debris					
Borehole	**008**	**008**	**008**	**005**	**005**	**006**
depth (m)	**159.16**	**156.49**	**155.6**	**160.05**	**159.65**	**124.7**
SiO2	24.58	59.31	53.59	62.28	70.78	57.15
TiO2	0.15	0.19	0.26	0.18	0.17	0.21
Al2O3	5.51	19.36	8.36	20.51	3.82	19.47
Fe2O3	3.23	3.17	5.45	2.64	8.34	4.36
MnO	0.07	0.03	0.06	0.01	0.17	0.05
MgO	0.72	5.50	0.67	2.97	1.19	4.64
CaO	31.40	1.51	12.38	1.12	3.35	0.93
Na2O	1.42	1.67	0.77	2.95	0.34	2.97
K2O	1.06	0.46	2.60	1.24	0.63	0.63
P2O5	17.27	0.06	3.23	0.11	0.97	0.11
L.o.I.	7.81	9.03	6.04	4.52	6.19	8.42
Total	93.20	100.29	93.41	98.55	95.94	98.94
Sc	18	12	11	5	7	0
V	54	69	204	8	40	16
Cr	27	7	31	8	34	3
Co	9	9	24	8	18	12
Ni	70	6	212	3	12	1
Cu	53	2	43	-2	10	-1
Zn	254	93	338	51	29	53
Rb	25	11	80	31	34	12
Sr	1470	177	317	186	124	160
Y	599	3	248	18	20	16
Zr	190	166	213	158	68	232
Nb	8	5	9	12	7	15
Ba	1419	190	491	273	2692	202
Pb	12	37	16	18	4	37
Th	25	28	30	42	9	38
U	237	0	105	6	0	6

	K122	**K123**	**K124**	**K125**	**K126**	**K127**
Rock type	bentonite	bentonite	bentonite	bentonite	bentonite	bentonite
Borehole	**006**	**006**	**006**	**006**	**006**	**006**
depth (m)	**125.95**	**126.71**	**120.1**	**109.99**	**112.49**	**114.28**
SiO2	61.20	57.30	57.45	52.63	56.49	57.72
TiO2	0.13	0.14	0.20	0.52	0.38	0.38
Al2O3	20.25	19.38	19.44	19.56	22.38	19.17
Fe2O3	2.29	2.44	2.19	4.76	3.28	3.58
MnO	0.04	0.04	0.04	0.03	0.06	0.04
MgO	4.84	4.64	4.84	3.57	3.46	4.73
CaO	0.73	0.78	1.09	2.41	1.54	1.85
Na2O	3.15	3.24	3.02	1.78	2.60	3.05
K2O	0.83	0.85	0.72	1.39	0.46	0.78
P2O5	0.05	0.05	0.05	0.40	0.17	0.12
L.o.I.	6.57	6.32	6.26	11.61	8.11	6.98
Total	100.07	95.19	95.30	98.66	98.94	98.40
Sc	0	3	3	7	4	5
V	26	42	134	657	1085	534
Cr	4	4	11	39	53	34
Co	9	9	7	17	12	11
Ni	2	1	0	57	14	5
Cu	-3	-1	-2	11	8	3
Zn	50	63	53	101	54	85
Rb	13	15	14	30	10	21
Sr	158	153	235	263	309	264
Y	7	8	4	16	5	0
Zr	151	156	180	182	114	169
Nb	14	13	12	15	5	8
Ba	163	184	307	895	259	310
Pb	42	40	39	27	18	35
Th	49	48	53	16	8	10
U	4	8	4	7	0	0

	K128	**K129**	**K130**	**K131**	**K132**	**K133**
Rock type	bentonite	bentonite	bentonite	bentonite	bentonite	sand
						fish debris
Borehole	**006**	**006**	**006**	**007**	**007**	**007**
depth (m)	**114.53**	**120**	**117.24**	**112.59**	**111.48**	**109.75**
SiO2	56.77	56.55	6.28	58.85	51.58	47.26
TiO2	0.27	0.28	0.02	0.22	0.49	0.62
Al2O3	19.76	18.52	0.45	19.76	20.00	17.94
Fe2O3	3.09	3.48	4.06	2.34	6.77	3.92
MnO	0.03	0.04	0.24	0.04	0.04	0.03
MgO	4.01	4.68	0.50	5.06	4.17	1.35
CaO	4.33	2.51	50.04	2.59	1.79	9.71
Na2O	3.20	2.83	0.20	2.04	2.33	1.73
K2O	0.66	0.74	0.08	0.50	1.10	3.49
P2O5	0.25	0.13	0.09	0.09	0.30	5.10
L.o.I.	7.43	7.39	33.64	8.64	9.61	8.18
Total	99.80	97.13	95.59	100.13	98.19	99.32
Sc	6	3	17	5	3	9
V	273	611	49	460	490	269
Cr	16	30	-3	22	25	90
Co	13	14	5	9	13	17
Ni	9	8	7	9	8	60
Cu	19	6	10	-1	7	42
Zn	65	58	26	46	92	118
Rb	13	17	2	13	28	76
Sr	371	222	313	193	276	603
Y	3	3	3	2	7	305
Zr	85	156	9	97	318	213
Nb	4	7	0	6	12	23
Ba	282	234	65	230	597	728
Pb	13	36	2	47	17	28
Th	8	37	6	52	17	37
U	0	1	5	1	-1	60

	K134	**k144**	**k156**	**k151**	**k153**	world
Rock type	silt	RPK	PK	arb/kimb si	arb/kimb si	kimberlite
		(m/g/b)	rys dom LT)			
Borehole	**007**	**012**	**012**	**012**	**012**	**Group 1**
depth (m)	**110.58**	**190.6**	**202.88**	**206.85**	**211.95**	**average***
SiO2	55.54	36.08	45.7	4.55	20.25	29.1
TiO2	0.48	2.08	0.91	0.31	0.79	2.7
Al2O3	12.39	2.12	1.81	0.56	1.88	2.4
Fe2O3	8.40	8.89	9.14	2.67	3.2	10.7
MnO	0.02	0.14	0.11	0.25	0.56	0.2
MgO	1.04	26.55	26.17	1.42	1.2	28.4
CaO	2.49	6.59	3.97	48.84	38.58	9.5
Na2O	0.86	0.83	0.93	0.05	0.23	0.2
K2O	2.86	0.09	0.15	0.05	0.18	1.1
P2O5	1.44	0.42	0.24	0.27	0.42	1.1
L.o.I.	14.35	15.41	10.21	40.4	32.41	14.1
Total	99.87	99.2	99.35	99.37	99.69	99.5
						world av.
Sc	10	23	14	21	14	14
V	446	68	42	7	14	100
Cr	81	1454	834	206	391	893
Co	39	83	83	21	35	65
Ni	257	1167	1400	561	336	965
Cu	65	50	16	13	27	93
Zn	267	46	50	27	41	69
Rb	102	3	9	1	8	73
Sr	184	186	136	319	353	851
Y	115	11	8	3	17	22
Zr	273	104	84	20	68	184
Nb	14	167	93	31	81	141
Ba	446	225	230	416	316	1100
Pb	23	8	6	4	5	15.3
Th	24	27	17	11	16	17
U	46	2	0	6	0	3.1

	Kjarsgaard et al 1995					
Rock type	mar muds	mar muds	mar muds	mar muds	mar muds	b RPK
Borehole	**UK 169/8**	**UK 169/8**	**UK 169/8**	**UK 169/8**	**UK 169/8**	**UK 169/8**
depth (m)	**100.09**	**105.00**	**105.00**	**109.00**	**112.00**	**121.15**
SiO2	63.00	62.44	62.44	58.80	60.29	36.15
TiO2	0.58	0.58	0.58	0.71	0.63	0.58
Al2O3	12.90	11.91	11.92	13.91	13.01	4.09
Fe2O3	4.96	5.00	5.00	5.53	6.00	10.20
MnO	0.02	0.03	0.03	0.03	0.03	0.07
MgO	1.78	1.71	1.69	1.86	2.14	31.27
CaO	0.68	0.58	0.58	0.43	0.67	0.68
Na2O	0.67	0.97	0.96	0.84	0.87	0.00
K2O	2.42	2.33	2.35	2.92	3.13	0.06
P2O5	0.19	0.18	0.18	0.10	0.19	0.03
L.o.I.	12.37	13.92	13.92	13.92	12.49	16.58
Total	99.84	99.95	99.95	99.13	99.51	99.72
Sulphur	1.28	1.53	1.53	1.32	1.11	0.37
Rock type	b RPK	b RPK	ICB	b RPK	b RPK	lap dom LT
Borehole	**UK 169/8**	**UK 169/8**	**UK 169/8**	**UK 169/8**	**UK 169/8**	**UK 169/8**
depth (m)	**125.40**	**129.00**	**135.40**	**139.00**	**139.00**	**190.00**
SiO2	39.21	51.24	45.86	38.97	39.06	35.57
TiO2	0.87	1.57	0.50	0.42	0.42	0.53
Al2O3	9.10	12.39	8.77	7.88	7.81	9.19
Fe2O3	7.94	7.06	5.19	6.02	6.02	7.27
MnO	0.04	0.03	0.03	0.04	0.04	0.04
MgO	26.44	9.44	21.21	29.46	29.43	31.36
CaO	0.41	0.94	0.50	0.33	0.33	0.13
Na2O	0.40	1.16	1.13	0.26	0.27	0.03
K2O	0.33	4.00	0.95	0.13	0.13	0.04
P2O5	0.06	0.33	0.08	0.07	0.06	0.04
L.o.I.	15.19	11.63	15.85	15.44	15.44	15.67
Total	100.13	99.91	100.11	99.04	99.02	99.88
Sulphur	0.09	0.20	0.15	0.83	0.83	0.41
Rock type	lap dom LT	lap dom LT	delt mud	delt mud	delt mud	delt f.sand
Borehole	**UK 169/8**	**UK 169/8**	**UK 169/8**	**UK 169/8**	**UK 169/8**	**UK 169/8**
depth (m)	**191.25**	**201.60**	**218.40**	**228.70**	**235.90**	**223.40**
SiO2	35.43	26.53	64.80	54.62	50.23	9.29
TiO2	0.47	0.34	1.06	1.06	0.91	0.42
Al2O3	8.86	6.24	15.83	22.69	19.65	3.12
Fe2O3	7.73	8.02	4.04	4.01	4.87	7.96
MnO	0.04	0.19	0.02	0.03	0.02	0.23
MgO	31.31	26.56	1.34	1.42	1.64	10.81
CaO	0.11	8.96	0.28	0.31	0.42	27.83
Na2O	0.00	0.00	0.53	0.61	0.51	0.05
K2O	0.01	0.04	3.84	3.11	3.79	1.66
P2O5	0.03	0.05	0.09	0.05	0.05	0.04
L.o.I.	15.42	22.84	8.14	12.11	17.73	38.45
Total	99.52	99.78	100.07	100.07	99.88	99.88
Sulphur	0.50	0.37	0.07	0.02	0.97	0.05

APPENDIX IX

Geochemistry of kimberlitic heavy minerals, from electron microprobe analysis

CONTENTS: 461 Major element oxide analyses.

- Table 1: Garnets (203), Ilmenites (99), Spinel (26), Magnetite (15), Hematite (5), Pyroxene (78) and Olivine (13).
- Table 2: Amphibole (11), Phlogopite/Biotite (11)

Note: grains are referred to by their Min. Sep Sample No. (see Chapter 2). For example, 2-12B is facies sample 12B, from Borehole OFS 93-002, 10-11A is facies sample 11A from Borehole OFS 93-010, and so on.

Analyses by E. Condliffe and this author on Cameca SX-50 at The University of Leeds.

Garnets, n = 203											
	SiO2	TiO2	Al2O3	Cr2O3	CaO	Fe2O3	FeO	MnO	MgO	CaO	total
9-12E	41.40	0.46	18.30	5.97	5.39	1.39	5.44	0.35	20.56	5.39	99.26
9-12E	42.01	0.15	20.70	3.46	4.75	1.01	6.36	0.44	20.90	4.75	99.78
9-12E	41.32	0.25	17.71	6.94	5.51	1.14	5.53	0.38	20.28	5.51	99.05
9-12E	41.82	0.16	19.41	4.85	5.32	1.47	6.05	0.31	20.66	5.32	100.03
9-12E	41.59	0.23	18.74	6.13	5.16	0.41	6.90	0.34	19.88	5.16	99.38
9-12E	41.64	0.21	19.59	4.77	5.19	1.52	5.93	0.30	20.88	5.19	100.03
9-12E	41.94	0.08	20.80	4.44	4.98	0.43	6.69	0.45	20.78	4.98	100.57
9-12E	41.56	0.04	19.61	5.33	5.51	0.87	6.66	0.43	20.11	5.51	100.13
9-12E	41.56	0.23	20.88	3.27	4.73	1.25	6.87	0.38	20.69	4.73	99.86
9-12E	41.45	0.11	20.05	4.71	4.87	0.86	6.58	0.51	20.58	4.87	99.73
9-12E	40.53	0.07	15.50	9.69	6.34	1.48	5.10	0.36	19.58	6.34	98.64
9-12E	41.50	0.09	19.72	5.08	5.39	0.81	7.39	0.48	19.69	5.39	100.14
9-12E	41.43	0.19	19.63	4.84	5.08	1.25	6.88	0.42	20.24	5.08	99.95
9-12E	41.44	0.03	17.88	7.26	4.64	1.16	5.33	0.29	21.36	4.64	99.37
9-12E	41.42	0.07	20.10	4.40	4.83	0.63	6.66	0.46	20.34	4.83	98.90
9-12E	40.90	0.18	17.03	8.17	6.58	0.84	6.18	0.41	18.98	6.58	99.28
9-12E	41.87	0.27	19.87	4.68	4.95	0.80	6.95	0.37	20.33	4.95	100.07
9-12E	41.19	0.40	18.56	6.29	5.40	1.11	8.45	0.41	18.98	5.40	100.79
9-12E	41.13	0.09	17.13	7.94	6.86	1.21	5.87	0.38	19.14	6.86	99.74
9-12E	41.28	0.46	17.29	7.57	5.97	1.18	6.08	0.45	19.66	5.97	99.93
9-12E	41.41	0.48	17.12	7.46	5.94	1.65	5.06	0.34	20.38	5.94	99.84
9-12E	41.76	0.05	20.55	3.87	5.76	0.91	7.92	0.50	19.25	5.76	100.56
9-12E	41.82	0.47	17.18	7.97	3.73	1.18	4.86	0.25	22.36	3.73	99.82
9-12E	41.88	0.15	19.70	5.43	4.60	0.47	7.35	0.35	20.48	4.60	100.41
9-12E	41.33	0.25	17.32	8.41	5.80	0.85	6.24	0.46	19.92	5.80	100.58
9-12E	41.93	0.40	18.30	6.60	5.81	1.27	4.94	0.19	21.00	5.81	100.43
9-12E	42.34	0.09	20.39	4.52	4.86	0.48	6.99	0.38	20.63	4.86	100.70
9-12E	41.49	0.12	15.83	9.37	6.34	1.50	4.93	0.31	20.07	6.34	99.97
9-12E	41.99	0.27	21.09	2.88	4.74	1.05	7.09	0.40	20.56	4.74	100.05
9-12E	41.32	0.85	17.98	6.05	5.54	1.93	4.99	0.29	20.89	5.54	99.83
9-12E	40.85	0.91	14.34	10.67	6.73	2.09	4.62	0.40	19.73	6.73	100.32
9-12E	41.50	0.42	17.93	7.00	5.67	0.71	6.17	0.32	19.93	5.67	99.66
9-12E	41.80	0.09	22.02	1.69	5.14	0.71	8.46	0.61	19.26	5.14	99.79
9-12E	41.98	0.45	18.54	5.88	5.66	1.55	5.21	0.35	20.87	5.66	100.47
9-12E	41.97	0.00	21.29	3.03	4.00	0.73	7.71	0.68	20.62	4.00	100.02
9-12E	41.86	0.21	19.92	4.90	4.96	0.77	7.06	0.28	20.47	4.96	100.42
9-12E	41.07	0.63	16.42	8.30	6.29	2.02	4.82	0.35	20.30	6.29	100.20
9-12E	40.78	0.12	14.16	11.94	7.32	1.30	5.34	0.36	18.87	7.32	100.19
9-12E	41.90	0.35	19.27	5.47	4.83	0.85	5.97	0.45	20.95	4.83	100.03
9-12E	41.80	0.15	18.04	6.58	5.78	1.75	5.14	0.29	20.81	5.78	100.34
9-12E	41.43	0.17	19.77	4.92	5.41	0.91	7.27	0.38	19.82	5.41	100.08
9-12E	40.89	0.08	17.34	8.04	6.58	0.80	6.37	0.31	19.05	6.58	99.45
9-12E	41.96	0.49	18.92	4.91	5.40	2.04	4.89	0.36	21.28	5.40	100.25
9-12E	41.08	0.18	18.38	7.20	5.88	0.93	6.78	0.45	19.72	5.88	100.57
9-12E	37.21	0.03	20.86	0.02	1.87	0.29	32.92	1.95	4.06	1.87	99.19
9-12E	41.40	0.02	18.04	7.39	6.32	0.98	5.74	0.35	19.95	6.32	100.18
9-12E	41.14	0.07	17.61	7.80	6.59	1.51	5.87	0.39	19.73	6.59	100.70
9-12E	41.93	1.21	19.12	2.73	5.16	3.32	5.15	0.22	21.18	5.16	100.01
9-12E	41.34	1.17	19.82	2.70	5.02	2.90	5.35	0.25	21.27	5.02	99.83
9-12E	41.79	0.84	20.55	1.97	5.06	2.55	6.87	0.31	20.42	5.06	100.36
9-12E	42.17	1.07	20.72	1.11	4.61	3.06	5.85	0.30	21.45	4.61	100.34
9-12E	41.42	0.88	20.25	2.40	5.17	2.59	6.32	0.33	20.58	5.17	99.92
9-12E	41.93	0.98	19.90	2.59	4.88	2.72	5.59	0.26	21.27	4.88	100.13
9-12E	41.17	0.73	19.60	4.09	4.97	2.21	4.38	0.22	21.94	4.97	99.31
9-12E	41.13	0.08	21.10	3.19	5.60	1.27	6.75	0.39	20.13	5.60	99.64
9-12E	41.17	0.23	19.66	4.17	5.23	1.94	6.38	0.46	20.35	5.23	99.58
9-12E	41.43	0.21	21.03	3.22	4.80	1.34	6.31	0.33	21.09	4.80	99.76
9-12E	40.92	0.07	19.64	5.37	5.40	0.72	6.92	0.45	19.84	5.40	99.34
9-12E	38.98	0.04	21.68	0.11	6.33	1.56	18.53	0.28	11.56	6.33	99.08
9-12E	39.74	0.08	21.89	0.18	6.26	0.43	19.26	0.18	11.11	6.26	99.12
9-12E	39.07	0.00	21.72	0.09	1.43	0.76	24.19	0.52	11.45	1.43	99.22
9-12A	39.89	0.81	10.54	15.15	8.48	2.16	4.52	0.31	17.77	8.48	99.62
9-10	41.55	0.53	20.63	2.96	6.00	1.60	8.55	0.49	18.70	6.00	100.99

	SiO2	TiO2	Al2O3	Cr2O3	CaO	Fe2O3	FeO	MnO	MgO	CaO	total
9-10	41.69	0.83	20.56	2.65	5.15	2.18	6.68	0.31	20.59	5.15	100.65
9-10	41.74	0.94	20.39	2.48	5.35	2.57	6.40	0.35	20.59	5.35	100.81
9-11B	41.42	0.58	19.63	4.16	5.01	1.90	5.14	0.31	21.38	5.01	99.51
9-11B	41.68	1.18	20.12	2.42	5.00	2.65	6.73	0.18	20.63	5.00	100.58
4-24	41.12	0.05	15.30	11.37	5.76	0.86	5.82	0.23	20.19	5.76	100.69
4-17	39.91	0.31	13.59	11.80	14.81	1.82	4.91	0.26	13.33	14.81	100.74
4-13A	42.25	0.75	20.30	3.22	5.30	1.81	5.96	0.27	20.98	5.30	100.84
4-13A	41.49	1.04	20.35	1.71	5.33	2.30	7.74	0.45	19.26	5.33	99.67
4-13A	41.49	1.26	19.59	3.60	5.43	2.09	6.43	0.09	20.43	5.43	100.40
4-13A	41.35	0.78	20.59	2.56	5.16	2.01	6.76	0.39	20.29	5.16	99.89
4-13A	41.81	0.62	22.41	0.54	4.64	1.38	9.03	0.40	19.54	4.64	100.38
4-13A	41.45	0.71	21.70	1.16	4.86	1.94	6.68	0.31	20.71	4.86	99.52
4-13A	41.70	0.72	22.10	0.76	4.85	1.80	8.75	0.45	19.58	4.85	100.70
4-13A	41.62	0.65	22.60	0.54	4.69	1.31	9.61	0.43	19.24	4.69	100.69
4-13A	41.07	0.16	23.50	0.05	5.01	0.37	13.83	0.35	16.42	5.01	100.76
4-13A	41.47	0.17	23.24	0.36	4.27	0.79	8.82	0.27	20.06	4.27	99.44
4-13A	41.09	0.60	19.69	3.68	5.13	2.35	4.91	0.35	21.33	5.13	99.13
4-13A	40.95	0.87	17.82	6.17	5.84	2.31	5.75	0.38	20.21	5.84	100.30
4-13A	41.00	0.97	18.04	6.37	6.18	2.00	6.16	0.29	19.91	6.18	100.91
4-13A	40.81	0.00	20.63	4.88	6.26	0.46	7.75	0.36	19.11	6.26	100.26
4-13A	41.24	0.12	16.94	8.81	5.99	1.16	5.65	0.33	20.21	5.99	100.45
4-13A	41.11	0.07	19.01	6.69	6.52	0.35	6.91	0.45	19.10	6.52	100.22
4-13A	41.10	0.15	17.24	8.70	6.59	1.21	5.24	0.37	20.13	6.59	100.74
4-13A	40.49	0.19	16.19	9.47	6.96	1.30	5.05	0.32	19.53	6.96	99.48
4-13A	41.02	0.16	17.16	8.75	6.63	0.93	5.67	0.26	19.75	6.63	100.34
4-13A	40.89	0.02	17.60	8.45	3.83	1.17	5.36	0.33	22.10	3.83	99.75
4-13A	41.00	0.14	14.51	12.09	5.38	0.92	5.07	0.30	20.68	5.38	100.10
4-13A	41.33	0.06	17.07	9.50	4.43	0.46	5.77	0.28	21.41	4.43	100.30
4-13A	41.78	0.09	18.65	6.91	5.16	1.05	5.59	0.18	21.33	5.16	100.73
4-13A	41.27	0.62	16.47	9.40	5.63	1.03	5.01	0.26	20.86	5.63	100.53
4-13A	41.17	0.53	17.12	8.54	6.12	1.02	5.98	0.29	19.96	6.12	100.73
4-13A	41.14	0.00	17.09	9.60	3.85	0.54	5.70	0.33	21.88	3.85	100.14
4-13A	41.21	0.07	17.88	8.36	4.29	0.50	5.97	0.31	21.41	4.29	99.99
4-13A	41.24	0.09	17.37	9.06	3.97	1.03	5.49	0.31	22.12	3.97	100.66
4-13A	41.92	0.15	20.56	5.09	5.59	0.00	7.53	0.25	19.90	5.59	100.97
4-13A	41.26	0.07	18.51	7.41	6.28	0.41	7.46	0.44	19.05	6.28	100.89
4-13A	41.90	0.03	18.81	7.52	3.38	0.44	5.94	0.39	22.44	3.38	100.85
4-13A	41.10	0.07	19.46	5.99	5.45	0.81	7.01	0.37	20.03	5.45	100.28
4-13A	40.97	0.16	19.47	5.06	5.54	1.08	6.81	0.47	19.70	5.54	99.26
4-13A	41.09	0.17	19.82	5.30	5.69	0.52	8.08	0.45	19.06	5.69	100.19
3-4D	42.04	0.19	22.99	1.24	4.41	0.38	7.64	0.30	20.82	4.41	100.00
3-4D	42.45	0.27	23.64	0.39	4.04	0.76	7.27	0.39	21.58	4.04	100.79
3-4D	41.44	1.13	20.68	1.70	5.28	2.48	7.97	0.34	19.55	5.28	100.58
3-4D	41.86	0.77	21.05	1.55	4.85	1.66	8.07	0.18	19.76	4.85	99.74
3-4D	41.12	1.25	19.60	3.12	5.37	2.31	6.38	0.34	20.14	5.37	99.63
3-4D	41.42	1.08	19.63	3.44	5.43	2.30	6.33	0.25	20.38	5.43	100.26
3-4D	41.38	1.11	19.87	3.21	5.13	2.03	6.54	0.32	20.40	5.13	100.00
3-4D	41.35	0.93	20.30	2.62	5.10	1.67	7.67	0.32	19.59	5.10	99.55
3-4D	41.18	0.11	19.30	5.80	5.63	0.79	6.91	0.41	19.76	5.63	99.90
3-4D	40.91	0.22	15.61	10.52	5.92	0.72	6.25	0.23	19.58	5.92	99.94
3-4D	41.48	0.05	17.05	9.24	6.64	0.37	6.26	0.30	19.40	6.64	100.79
3-4D	41.89	0.12	18.06	8.21	5.34	0.18	5.78	0.11	20.97	5.34	100.64
3-4D	41.29	0.32	18.18	8.15	6.40	0.00	7.20	0.35	18.84	6.40	100.73
3-4D	41.21	0.16	20.47	4.70	5.14	0.41	8.26	0.56	19.43	5.14	100.35
3-4D	41.80	0.19	18.99	6.63	4.76	0.76	5.60	0.37	21.51	4.76	100.61
3-4D	41.24	0.00	19.28	6.34	5.78	0.43	7.24	0.53	19.49	5.78	100.33
3-4D	41.46	0.20	16.00	10.80	4.66	0.10	5.68	0.28	21.05	4.66	100.24
3-4D	40.79	0.23	16.01	10.67	4.72	0.69	5.47	0.28	21.18	4.72	100.04
3-4D	41.13	0.07	17.48	8.40	6.13	0.75	5.97	0.36	19.87	6.13	100.15
3-4D	40.87	0.30	16.76	9.20	6.12	0.90	5.88	0.37	19.85	6.12	100.24
3-4D	40.98	0.40	17.60	7.45	5.95	0.82	6.23	0.30	19.59	5.95	99.31
3-4D	41.22	0.75	18.50	5.51	5.73	1.82	5.58	0.39	20.35	5.73	99.85
3-4D	41.56	0.66	18.31	6.59	5.78	0.79	5.81	0.44	20.14	5.78	100.07

	SiO2	TiO2	Al2O3	Cr2O3	CaO	Fe2O3	FeO	MnO	MgO	CaO	total
2-12A	41.57	0.88	21.05	1.89	5.28	2.17	7.66	0.39	19.87	5.28	100.76
2-12A	41.78	0.85	21.02	1.84	4.99	2.22	8.03	0.43	19.90	4.99	101.06
2-12A	41.72	0.68	21.23	2.08	4.88	1.74	6.28	0.15	21.11	4.88	99.86
2-12A	41.51	0.86	20.69	1.93	5.12	2.74	6.96	0.28	20.45	5.12	100.54
2-12A	41.63	0.80	20.49	2.45	4.97	2.31	6.63	0.28	20.68	4.97	100.23
2-12A	41.45	0.86	20.68	2.28	5.06	2.61	6.76	0.25	20.69	5.06	100.65
2-12A	41.42	1.00	21.56	1.08	5.18	2.12	8.69	0.34	19.34	5.18	100.72
2-12A	41.39	0.90	20.92	1.92	5.21	1.92	8.31	0.12	19.51	5.21	100.19
2-12A	41.40	0.06	19.86	4.86	5.11	0.52	7.03	0.46	19.92	5.11	99.23
2-12A	41.37	0.05	20.09	4.92	5.23	0.55	7.01	0.42	20.07	5.23	99.71
2-12A	41.77	0.08	20.66	4.14	4.75	0.06	7.00	0.33	20.40	4.75	99.19
2-12A	41.49	0.07	18.01	7.90	6.77	0.13	7.41	0.36	18.57	6.77	100.70
2-12A	42.00	0.12	20.87	3.80	4.95	0.26	7.23	0.49	20.16	4.95	99.87
2-12A	41.80	0.26	19.49	5.48	5.25	0.36	7.19	0.45	19.84	5.25	100.12
2-12A	41.52	0.06	18.44	7.19	6.29	0.00	7.52	0.50	18.70	6.29	100.21
2-12A	41.45	0.24	20.77	4.29	5.24	0.76	6.32	0.29	20.87	5.24	100.24
2-12A	41.67	0.22	20.13	5.17	5.51	0.00	8.09	0.33	19.31	5.51	100.43
2-12A	41.17	0.06	19.58	5.29	5.33	0.47	7.31	0.33	19.60	5.33	99.15
2-12A	41.49	0.24	18.11	7.10	5.82	0.91	5.92	0.29	20.20	5.82	100.07
2-12A	42.24	0.65	19.49	4.47	5.39	1.64	5.04	0.26	21.35	5.39	100.53
2-12A	41.46	0.79	17.64	6.43	5.80	1.81	5.08	0.25	20.55	5.80	99.80
12-4	41.80	0.79	18.51	5.58	5.56	1.85	5.20	0.21	21.01	5.56	100.50
12-4	41.85	0.25	18.84	6.85	5.62	0.55	5.80	0.41	20.67	5.62	100.84
12-8	40.94	0.07	15.45	11.39	5.68	0.45	6.08	0.36	19.92	5.68	100.35
12-8	40.85	0.04	15.16	10.81	5.98	1.18	5.13	0.38	20.05	5.98	99.58
12-8	41.12	0.05	15.30	11.37	5.76	0.86	5.82	0.23	20.19	5.76	100.69
12-8	41.05	0.04	15.44	11.00	5.68	0.55	5.82	0.31	19.99	5.68	99.88
12-8	40.84	0.16	15.30	10.71	5.84	0.99	5.43	0.27	20.03	5.84	99.56
12-7	41.89	0.35	20.41	3.89	5.07	1.32	7.26	0.37	20.34	5.07	100.89
12-7	40.80	0.34	22.36	0.19	4.36	1.29	14.85	0.53	15.83	4.36	100.53
10-18	40.85	0.04	15.16	10.81	5.98	1.18	5.13	0.38	20.05	5.98	99.58
10-18	41.12	0.05	15.30	11.37	5.76	0.86	5.82	0.23	20.19	5.76	100.69
10-18	41.05	0.04	15.44	11.00	5.68	0.55	5.82	0.31	19.99	5.68	99.88
10-18	40.80	0.34	22.36	0.19	4.36	1.29	14.85	0.53	15.83	4.36	100.53
10-18	41.18	0.01	20.94	3.87	5.48	0.29	8.07	0.56	19.15	5.48	99.55
10-18	41.65	0.03	20.86	4.08	6.23	0.39	7.81	0.47	19.02	6.23	100.54
10-18	41.46	0.08	21.60	2.94	5.63	0.53	7.69	0.37	19.58	5.63	99.88
10-18	41.53	0.01	21.22	3.69	4.45	0.22	8.05	0.58	20.04	4.45	99.77
10-17	41.90	0.07	21.58	3.02	5.26	0.00	8.49	0.55	19.16	5.26	100.03
10-11A	41.65	0.15	19.30	5.49	5.62	0.80	6.40	0.37	20.06	5.62	99.84
10-11A	41.39	0.26	21.51	2.86	5.77	0.74	7.47	0.36	19.63	5.77	99.98
10-11A	41.21	0.18	20.32	4.38	5.49	0.54	8.37	0.66	18.88	5.49	100.02
10-11A	40.69	0.38	18.55	6.21	5.55	0.71	8.00	0.29	18.83	5.55	99.22
10-11A	40.96	0.56	15.28	10.45	6.77	0.92	6.23	0.24	18.88	6.77	100.30
10-11A	41.18	0.09	19.85	5.21	5.85	0.19	8.60	0.52	18.43	5.85	99.92
10-11A	40.90	0.43	18.18	6.92	5.71	1.05	6.16	0.42	19.97	5.71	99.73
10-11A	41.12	0.39	19.97	4.83	5.28	0.44	6.83	0.28	20.03	5.28	99.17
10-11A	41.13	0.27	19.70	5.09	5.45	0.53	7.13	0.50	19.58	5.45	99.37
10-11A	41.38	0.44	20.09	4.68	5.19	0.52	7.02	0.36	20.08	5.19	99.75
10-11A	40.84	0.05	17.60	7.67	5.89	1.06	7.47	0.50	18.92	5.89	99.99
10-11A	40.71	0.07	17.98	7.90	6.38	0.49	6.59	0.36	19.23	6.38	99.70
10-11A	41.03	0.05	15.38	11.17	5.02	0.66	5.76	0.44	20.49	5.02	100.01
10-11A	41.57	0.36	19.49	5.31	5.03	0.41	7.41	0.27	19.90	5.03	99.75
10-11A	41.67	0.23	19.21	5.97	6.15	0.36	7.14	0.45	19.22	6.15	100.38
10-11A	41.89	0.28	18.12	7.28	5.96	1.01	5.54	0.41	20.49	5.96	100.97
10-11A	42.19	0.08	20.84	4.30	4.12	0.00	7.76	0.28	20.65	4.12	100.21
10-11A	40.99	0.21	16.56	9.45	6.52	0.37	6.81	0.43	18.76	6.52	100.09
2-10C	37.46	0.05	21.20	0.00	5.00	0.05	31.04	0.62	3.81	5.00	99.24
12-8	42.33	0.33	20.08	3.50	5.01	1.80	5.08	0.29	21.59	5.01	100.01
12-8	41.21	0.90	18.34	5.68	5.55	1.44	5.75	0.36	20.23	5.55	99.45
12-10	41.77	0.38	18.68	5.90	5.36	1.24	5.83	0.38	20.61	5.36	100.15
12-10	41.46	0.09	19.00	5.72	5.24	0.41	7.45	0.48	19.36	5.24	99.20
12-10	41.27	0.05	19.32	5.65	5.04	0.28	7.76	0.46	19.42	5.04	99.26

	SiO2	TiO2	Al2O3	Cr2O3	CaO	Fe2O3	FeO	MnO	MgO	CaO	total
12-1	41.50	0.65	18.02	6.15	5.74	1.40	5.85	0.25	20.12	5.74	99.66
12-1	41.60	1.05	17.18	6.84	6.05	2.00	5.13	0.30	20.37	6.05	100.53
12-2	42.05	0.02	20.81	4.68	5.20	0.00	7.43	0.32	19.99	5.20	100.52
12-2	40.04	0.17	18.81	5.41	6.50	0.70	7.81	0.37	17.78	6.50	97.60
12-3	41.86	0.28	20.01	3.76	5.03	1.03	5.78	0.17	20.83	5.03	98.75
12-3	41.69	0.07	20.11	5.00	6.00	0.42	7.29	0.43	19.44	6.00	100.45
12-4	41.47	0.29	18.41	6.89	5.70	0.84	5.49	0.28	20.61	5.70	99.98
12-4	41.14	0.29	18.00	6.83	5.89	1.36	5.17	0.37	20.42	5.89	99.47
12-6	41.83	0.63	17.49	7.08	5.93	1.39	5.05	0.27	20.57	5.93	100.24
12-6	41.42	0.22	19.66	5.42	5.73	0.39	7.89	0.56	19.05	5.73	100.33
12-7	41.69	0.67	19.02	4.95	5.24	1.68	5.39	0.29	21.03	5.24	99.95
12-7	41.97	0.03	20.33	4.68	4.74	0.33	7.29	0.36	20.40	4.74	100.15
12-7	41.83	0.03	20.46	4.22	4.28	0.57	6.74	0.42	20.96	4.28	99.50
12-7	41.08	0.81	19.79	3.30	5.19	2.08	6.91	0.35	19.97	5.19	99.48
Ilmenites, n = 99											
	TiO2	Al2O3	Cr2O3	Fe2O3	FeO	MnO	MgO	NiO	CaO	total	
1	52.86	0.38	0.55	9.73	21.74	0.33	13.88	0.08	0.04	99.59	
2	53.43	0.12	1.72	10.68	13.82	0.71	18.39	0.06	0.07	99.00	
3	53.93	0.67	1.55	7.46	19.53	0.47	15.53	0.16	0.06	99.36	
4	49.16	0.77	2.69	13.63	15.28	0.51	15.51	0.09	0.10	97.74	
5	53.98	0.33	1.20	8.70	18.38	0.52	16.17	0.12	0.09	99.50	
6	51.37	0.94	5.02	8.02	20.35	0.25	13.91	0.21	0.02	100.10	
7	53.56	0.25	1.79	7.65	19.22	0.49	15.51	0.14	0.08	98.69	
8	52.78	0.03	5.41	6.73	17.43	0.45	16.11	0.19	0.09	99.22	
9	52.41	0.05	5.33	7.64	16.92	0.61	16.16	0.11	0.12	99.34	
10	52.45	0.16	3.99	9.15	15.58	0.68	16.89	0.10	0.12	99.11	
11	52.53	0.91	2.54	7.41	19.81	0.36	14.71	0.13	0.11	98.51	
12	49.26	0.40	0.12	14.00	24.47	0.32	10.59	0.02	0.07	99.25	
13	46.68	0.20	0.21	17.11	25.45	0.31	8.80	0.02	0.02	98.79	
14	51.90	0.41	0.49	10.07	24.08	0.33	12.11	0.09	0.03	99.50	
15	53.35	0.00	4.17	7.65	15.71	0.65	17.32	0.04	0.08	98.95	
16	45.76	0.10	0.22	18.98	26.21	0.29	7.88	0.05	0.03	99.51	
17	53.55	0.33	0.20	8.98	21.36	0.42	14.39	0.09	0.05	99.35	
18	48.01	0.24	0.09	15.47	25.90	0.31	9.20	0.00	0.05	99.26	
19	42.81	0.08	0.78	22.19	25.57	0.23	6.80	0.05	0.05	98.57	
20	42.43	0.08	0.82	23.31	24.92	0.14	7.06	0.01	0.03	98.80	
21	53.80	0.19	1.48	7.77	18.94	0.54	15.80	0.08	0.05	98.65	
22	53.34	0.37	1.02	9.42	18.65	0.54	15.68	0.18	0.04	99.24	
23	51.26	0.30	2.34	10.31	20.23	0.38	13.89	0.07	0.07	98.87	
24	45.62	0.46	0.46	21.03	19.45	0.37	11.53	0.13	0.03	99.07	
25	51.01	0.25	2.75	10.76	19.13	0.37	14.36	0.09	0.12	98.83	
26	51.24	0.00	0.11	0.00	41.19	2.99	0.04	0.08	0.07	95.73	
27	53.66	0.03	3.80	6.06	19.25	0.51	15.45	0.18	0.15	99.10	
28	51.43	0.00	0.17	0.00	40.39	3.35	0.04	0.05	0.08	95.50	
29	55.55	0.00	2.12	5.59	18.39	0.98	16.72	0.08	0.09	99.52	
30	52.87	0.57	0.14	9.39	21.19	0.37	14.13	0.13	0.09	98.88	
31	54.78	0.18	1.82	5.90	20.08	0.50	15.63	0.13	0.06	99.09	
32	53.43	0.85	0.33	8.92	20.52	0.44	14.73	0.19	0.06	99.47	
33	52.98	0.39	0.41	9.96	21.03	0.33	14.26	0.20	0.07	99.63	
34	53.26	0.33	0.91	8.36	22.35	0.29	13.76	0.09	0.06	99.41	
9-12C	48.96	0.35	0.10	13.45	28.13	0.32	8.79	0.02	0.13	100.48	
9-12C	52.50	0.18	0.68	7.21	27.74	0.19	10.98	0.00	0.05	99.87	
9-12C	54.17	0.36	2.79	5.15	20.61	0.49	15.55	0.07	0.16	99.68	
9-12C	52.70	0.25	0.49	7.28	27.33	0.35	11.19	0.01	0.09	100.04	
9-12C	51.94	0.12	0.79	8.32	27.66	0.31	10.60	0.03	0.04	100.08	
9-12C	52.89	0.21	0.64	6.85	27.42	0.25	11.23	0.04	0.08	99.85	
9-12C	53.39	0.47	0.58	6.77	25.43	0.34	12.48	0.06	0.00	99.60	
9-12C	53.64	0.50	0.69	7.04	26.41	0.19	12.14	0.00	0.04	100.72	
9-12C	52.96	0.49	0.24	8.18	25.42	0.25	12.32	0.00	0.13	100.15	
9-12C	52.22	0.19	0.55	7.91	27.92	0.29	10.62	0.01	0.05	99.98	
9-12C	51.21	0.47	0.11	10.32	26.48	0.34	10.85	0.00	0.04	99.99	
9-12C	54.23	0.40	0.96	5.11	25.61	0.15	13.00	0.00	0.00	99.61	

	SiO2	TiO2	Al2O3	Cr2O3	CaO	Fe2O3	FeO	MnO	MgO	CaO	total
12-1	41.50	0.65	18.02	6.15	5.74	1.40	5.85	0.25	20.12	5.74	99.66
12-1	41.60	1.05	17.18	6.84	6.05	2.00	5.13	0.30	20.37	6.05	100.53
12-2	42.05	0.02	20.81	4.68	5.20	0.00	7.43	0.32	19.99	5.20	100.52
12-2	40.04	0.17	18.81	5.41	6.50	0.70	7.81	0.37	17.78	6.50	97.60
12-3	41.86	0.28	20.01	3.76	5.03	1.03	5.78	0.17	20.83	5.03	98.75
12-3	41.69	0.07	20.11	5.00	6.00	0.42	7.29	0.43	19.44	6.00	100.45
12-4	41.47	0.29	18.41	6.89	5.70	0.84	5.49	0.28	20.61	5.70	99.98
12-4	41.14	0.29	18.00	6.83	5.89	1.36	5.17	0.37	20.42	5.89	99.47
12-6	41.83	0.63	17.49	7.08	5.93	1.39	5.05	0.27	20.57	5.93	100.24
12-6	41.42	0.22	19.66	5.42	5.73	0.39	7.89	0.56	19.05	5.73	100.33
12-7	41.69	0.67	19.02	4.95	5.24	1.68	5.39	0.29	21.03	5.24	99.95
12-7	41.97	0.03	20.33	4.68	4.74	0.33	7.29	0.36	20.40	4.74	100.15
12-7	41.83	0.03	20.46	4.22	4.28	0.57	6.74	0.42	20.96	4.28	99.50
12-7	41.08	0.81	19.79	3.30	5.19	2.08	6.91	0.35	19.97	5.19	99.48
Imenites, n = 99											
	TiO2	Al2O3	Cr2O3	Fe2O3	FeO	MnO	MgO	NiO	CaO	total	
1	52.86	0.38	0.55	9.73	21.74	0.33	13.88	0.08	0.04	99.59	
2	53.43	0.12	1.72	10.68	13.82	0.71	18.39	0.06	0.07	99.00	
3	53.93	0.67	1.55	7.46	19.53	0.47	15.53	0.16	0.06	99.36	
4	49.16	0.77	2.69	13.63	15.28	0.51	15.51	0.09	0.10	97.74	
5	53.98	0.33	1.20	8.70	18.38	0.52	16.17	0.12	0.09	99.50	
6	51.37	0.94	5.02	8.02	20.35	0.25	13.91	0.21	0.02	100.10	
7	53.56	0.25	1.79	7.65	19.22	0.49	15.51	0.14	0.08	98.69	
8	52.78	0.03	5.41	6.73	17.43	0.45	16.11	0.19	0.09	99.22	
9	52.41	0.05	5.33	7.64	16.92	0.61	16.16	0.11	0.12	99.34	
10	52.45	0.16	3.99	9.15	15.58	0.68	16.89	0.10	0.12	99.11	
11	52.53	0.91	2.54	7.41	19.81	0.36	14.71	0.13	0.11	98.51	
12	49.26	0.40	0.12	14.00	24.47	0.32	10.59	0.02	0.07	99.25	
13	46.68	0.20	0.21	17.11	25.45	0.31	8.80	0.02	0.02	98.79	
14	51.90	0.41	0.49	10.07	24.08	0.33	12.11	0.09	0.03	99.50	
15	53.35	0.00	4.17	7.65	15.71	0.65	17.32	0.04	0.08	98.95	
16	45.76	0.10	0.22	18.98	26.21	0.29	7.88	0.05	0.03	99.51	
17	53.55	0.33	0.20	8.98	21.36	0.42	14.39	0.09	0.05	99.35	
18	48.01	0.24	0.09	15.47	25.90	0.31	9.20	0.00	0.05	99.26	
19	42.81	0.08	0.78	22.19	25.57	0.23	6.80	0.05	0.05	98.57	
20	42.43	0.08	0.82	23.31	24.92	0.14	7.06	0.01	0.03	98.80	
21	53.80	0.19	1.48	7.77	18.94	0.54	15.80	0.08	0.05	98.65	
22	53.34	0.37	1.02	9.42	18.65	0.54	15.68	0.18	0.04	99.24	
23	51.26	0.30	2.34	10.31	20.23	0.38	13.89	0.07	0.07	98.87	
24	45.62	0.46	0.46	21.03	19.45	0.37	11.53	0.13	0.03	99.07	
25	51.01	0.25	2.75	10.76	19.13	0.37	14.36	0.09	0.12	98.83	
26	51.24	0.00	0.11	0.00	41.19	2.99	0.04	0.08	0.07	95.73	
27	53.66	0.03	3.80	6.06	19.25	0.51	15.45	0.18	0.15	99.10	
28	51.43	0.00	0.17	0.00	40.39	3.35	0.04	0.05	0.08	95.50	
29	55.55	0.00	2.12	5.59	18.39	0.98	16.72	0.08	0.09	99.52	
30	52.87	0.57	0.14	9.39	21.19	0.37	14.13	0.13	0.09	98.88	
31	54.78	0.18	1.82	5.90	20.08	0.50	15.63	0.13	0.06	99.09	
32	53.43	0.85	0.33	8.92	20.52	0.44	14.73	0.19	0.06	99.47	
33	52.98	0.39	0.41	9.96	21.03	0.33	14.26	0.20	0.07	99.63	
34	53.26	0.33	0.91	8.36	22.35	0.29	13.76	0.09	0.06	99.41	
9-12C	48.96	0.35	0.10	13.45	28.13	0.32	8.79	0.02	0.13	100.48	
9-12C	52.50	0.18	0.68	7.21	27.74	0.19	10.98	0.00	0.05	99.87	
9-12C	54.17	0.36	2.79	5.15	20.61	0.49	15.55	0.07	0.16	99.68	
9-12C	52.70	0.25	0.49	7.28	27.33	0.35	11.19	0.01	0.09	100.04	
9-12C	51.94	0.12	0.79	8.32	27.66	0.31	10.60	0.03	0.04	100.08	
9-12C	52.89	0.21	0.64	6.85	27.42	0.25	11.23	0.04	0.08	99.85	
9-12C	53.39	0.47	0.58	6.77	25.43	0.34	12.48	0.06	0.00	99.60	
9-12C	53.64	0.50	0.69	7.04	26.41	0.19	12.14	0.00	0.04	100.72	
9-12C	52.96	0.49	0.24	8.18	25.42	0.25	12.32	0.00	0.13	100.15	
9-12C	52.22	0.19	0.55	7.91	27.92	0.29	10.62	0.01	0.05	99.98	
9-12C	51.21	0.47	0.11	10.32	26.48	0.34	10.85	0.00	0.04	99.99	
9-12C	54.23	0.40	0.96	5.11	25.61	0.15	13.00	0.00	0.00	99.61	

	TiO2	Al2O3	Cr2O3	Fe2O3	FeO	MnO	MgO	NiO	CaO	total	
4-19	53.11	0.56	1.39	7.62	25.04	0.24	12.53	0.02	0.22	100.84	
4-13A	48.89	0.31	0.07	13.89	28.65	0.31	8.58	0.05	0.00	101.11	
4-13A	48.88	0.30	0.24	13.53	28.56	0.40	8.59	0.02	0.00	100.86	
4-13A	48.88	0.34	0.22	13.03	28.29	0.37	8.71	0.00	0.16	100.39	
4-13A	53.16	0.66	1.44	6.83	25.02	0.27	12.59	0.02	0.06	100.10	
4-13A	49.28	0.43	0.09	12.66	28.02	0.19	9.10	0.00	0.04	99.98	
4-13A	49.03	0.41	0.23	12.44	28.06	0.36	8.89	0.00	0.03	99.65	
4-13A	53.75	0.75	2.21	5.99	23.95	0.19	13.49	0.00	0.15	100.52	
4-13A	52.96	0.58	0.46	7.88	25.63	0.22	12.23	0.05	0.05	100.17	
4-13A	50.52	0.36	0.09	10.61	28.64	0.37	9.26	0.00	0.00	99.97	
4-13A	51.52	0.53	0.17	11.39	24.73	0.28	12.05	0.02	0.03	100.89	
4-13A	56.83	0.18	0.17	3.62	24.08	0.50	14.89	0.09	0.00	100.53	
4-13A	53.64	0.65	0.88	6.72	25.53	0.29	12.51	0.04	0.15	100.46	
3-4D	34.14	0.16	2.49	34.75	24.13	0.05	3.83	0.00	0.00	99.86	
3-4D	37.69	0.00	0.60	29.30	26.37	0.32	4.63	0.00	0.09	100.13	
3-4D	47.98	0.32	0.11	14.08	27.99	0.23	8.51	0.02	0.12	99.78	
3-4D	48.77	0.28	0.25	13.35	28.57	0.25	8.48	0.02	0.05	100.19	
3-4D	53.43	0.46	1.10	8.23	19.67	0.54	15.61	0.18	0.05	99.55	
3-4D	49.07	0.37	0.18	12.74	27.40	0.28	9.31	0.02	0.06	99.67	
3-4D	48.59	0.36	0.22	14.16	27.78	0.38	8.69	0.05	0.06	100.38	
3-4D	53.67	0.51	0.46	7.39	25.45	0.19	12.66	0.04	0.10	100.61	
3-4D	52.67	0.51	0.52	9.14	22.96	0.41	13.38	0.07	0.12	99.82	
3-4D	52.83	0.46	0.57	7.29	26.38	0.29	11.83	0.00	0.04	99.95	
3-4D	48.99	0.37	0.19	12.49	27.64	0.34	9.18	0.04	0.00	99.55	
3-4D	56.92	0.13	0.44	3.28	24.05	0.39	14.96	0.04	0.00	100.21	
3-4D	52.09	0.44	0.32	8.81	24.53	0.26	12.46	0.04	0.00	99.15	
3-4D	47.63	0.28	0.27	15.73	26.79	0.26	8.98	0.05	0.09	100.41	
2-12A	53.40	0.62	0.93	7.20	22.62	0.44	13.94	0.00	0.15	99.34	
2-12A	49.69	0.30	0.16	12.92	26.28	0.43	10.25	0.02	0.03	100.40	
2-12A	52.54	0.00	0.49	0.00	40.63	5.76	0.00	0.00	0.00	100.13	
2-12A	53.45	0.59	0.94	7.83	23.53	0.44	13.40	0.04	0.18	100.43	
2-12A	52.56	0.00	0.26	0.00	40.92	4.79	0.03	0.00	0.21	99.12	
2-12A	52.06	0.41	0.37	8.78	26.97	0.36	10.97	0.04	0.00	100.10	
2-12A	47.87	0.33	0.18	13.71	27.65	0.20	8.70	0.00	0.04	99.03	
2-12A	48.40	0.29	0.23	13.80	28.07	0.29	8.63	0.00	0.14	100.17	
2-12A	50.01	0.47	0.20	11.41	28.09	0.11	9.47	0.03	0.04	100.03	
2-12A	49.59	0.40	0.17	12.05	28.54	0.25	9.05	0.04	0.00	100.46	
2-12A	54.62	0.21	2.37	4.92	21.04	0.45	15.32	0.09	0.21	99.26	
2-12A	54.75	0.63	1.50	4.51	22.58	0.20	14.77	0.08	0.08	99.14	
10-11A	53.05	0.23	0.78	6.85	26.72	0.43	11.64	0.00	0.04	99.96	
10-11A	51.25	0.44	0.11	10.42	26.71	0.33	10.60	0.06	0.18	100.21	
10-11A	51.59	0.48	0.27	10.00	26.99	0.25	10.60	0.02	0.22	100.44	
10-11A	51.62	0.44	0.38	9.08	27.27	0.23	10.65	0.00	0.10	99.97	
10-11A	54.12	0.68	0.37	8.64	19.87	0.34	15.83	0.13	0.21	100.30	
10-11A	51.57	0.31	0.26	9.10	27.34	0.29	10.54	0.00	0.06	99.58	
10-11A	51.54	0.49	0.26	10.00	26.71	0.34	10.82	0.03	0.09	100.39	
10-11A	51.99	0.44	0.38	8.65	27.16	0.28	10.92	0.02	0.04	100.11	
10-11A	51.60	0.47	0.21	9.68	27.25	0.21	10.73	0.05	0.00	100.43	
10-11A	52.28	0.54	0.28	9.95	25.78	0.25	11.74	0.00	0.08	100.97	
10-18	51.54	0.22	0.67	9.03	25.99	0.37	11.28	0.09	0.04	99.51	
10-18	53.35	0.42	0.82	6.44	24.80	0.36	12.78	0.12	0.01	99.19	
3-2	53.14	0.59	1.30	6.99	25.27	0.21	12.61	0.00	0.03	100.34	
4-19	53.11	0.56	1.39	7.62	25.04	0.24	12.53	0.22	0.02	100.84	
2-12B	53.01	0.46	1.80	6.18	24.42	0.16	12.92	0.11	0.02	99.17	
Spinel, n = 26											
	TiO2	Al2O3	Cr2O3	Fe2O3	FeO	MnO	MgO	NiO	ZnO	total	
4-19	5.05	7.85	51.12	5.38	18.12	0.24	12.64	0.25	0.00	100.65	
12-8	5.54	7.50	49.99	5.72	17.77	0.30	12.78	0.22	0.43	100.23	
12-8	5.54	7.04	50.24	5.79	17.79	0.18	12.91	0.12	0.16	99.77	
12-8	5.78	8.71	48.24	5.24	18.06	0.30	13.00	0.17	0.00	99.51	
12-8	4.77	6.30	53.21	5.52	17.34	0.41	12.73	0.22	0.05	100.54	
12-8	0.36	14.67	53.74	2.78	17.54	0.23	11.12	0.00	0.00	100.45	

	TiO2	Al2O3	Cr2O3	Fe2O3	FeO	MnO	MgO	NiO	ZnO	total	
12-8	0.14	14.23	57.25	0.07	16.46	0.25	11.51	0.12	0.00	100.02	
12-8	7.17	6.69	44.24	8.55	18.56	0.43	12.97	0.25	0.01	98.87	
12-6	0.02	19.24	50.39	0.52	19.49	0.29	9.81	0.07	0.40	100.23	
12-6	4.66	8.39	47.79	7.24	18.37	0.23	11.97	0.10	0.08	98.83	
12-6	5.05	7.85	51.12	5.38	18.12	0.24	12.64	0.25	0.00	100.65	
10-18	1.17	23.13	35.39	11.31	11.36	0.22	15.84	0.27	0.12	98.81	
10-18	0.89	17.14	47.39	6.43	11.85	0.31	14.76	0.18	0.32	99.28	
4-22	1.22	4.47	46.09	20.18	20.38	0.64	7.42	0.12	0.20	100.73	
4-22	12.46	4.77	27.36	32.16	10.16	0.65	14.15	0.27	0.02	101.99	
4-22	13.41	4.49	24.51	32.83	10.61	0.52	13.54	0.22	0.00	100.13	
4-22	0.22	24.93	41.90	5.32	15.07	0.30	13.51	0.14	0.29	101.70	
4-22	0.25	24.72	41.43	5.69	14.82	0.22	13.61	0.08	0.34	101.17	
12-7	0.38	26.52	43.72	1.30	13.77	0.15	14.52	0.13	0.19	100.68	
12-7	0.01	19.89	50.47	0.41	16.89	0.33	11.44	0.02	0.49	99.96	
12-7	0.10	40.93	28.78	0.57	13.25	0.14	16.32	0.12	0.17	100.39	
12-7	0.72	17.62	51.46	2.75	13.65	0.19	13.56	0.06	0.25	100.26	
12-7	0.06	32.77	37.36	1.04	12.06	0.23	16.09	0.19	0.09	99.90	
12-7	0.15	18.25	52.19	1.48	13.17	0.26	13.85	0.05	0.11	99.51	
12-7	1.74	5.79	57.13	8.68	13.81	0.34	12.02	0.21	0.00	99.72	
12-7	3.64	2.59	45.33	18.08	17.49	0.28	8.38	0.21	0.10	96.08	
Magnetite, n = 15											
	TiO2	Al2O3	Cr2O3	Fe2O3	FeO	MnO	MgO	NiO	ZnO	total	
2-12B	0.03	0.00	0.00	67.28	27.83	1.12	0.63	0.00	0.01	97.06	
2-12B	20.85	4.55	14.78	17.44	28.70	0.96	14.10	0.13	0.11	101.66	
4-22	23.39	4.69	2.18	24.63	29.07	0.73	15.53	0.40	0.06	100.72	
4-22	21.41	5.64	1.92	26.26	25.25	0.76	16.37	0.05	0.04	97.82	
4-22	22.99	5.63	4.63	23.06	25.86	0.82	17.50	0.19	0.04	100.81	
4-22	23.70	4.55	3.13	22.67	29.81	0.69	15.14	0.31	0.00	100.04	
4-22	23.08	5.44	4.80	21.64	26.94	0.87	16.57	0.09	0.00	99.49	
4-22	16.67	5.63	8.49	29.57	24.61	0.77	14.51	0.22	0.07	100.62	
4-22	22.07	5.35	1.84	27.56	24.95	0.84	17.35	0.15	0.04	100.26	
4-17	0.03	0.00	0.00	69.15	29.01	0.15	1.12	0.00	0.00	99.53	
4-17	0.00	0.00	0.02	66.55	26.93	1.33	0.94	0.04	0.10	96.13	
4-17	0.03	0.00	0.00	69.48	28.77	0.07	1.39	0.03	0.01	99.83	
4-17	0.06	0.00	0.01	69.34	28.82	0.10	1.34	0.01	0.07	99.80	
4-17	22.73	5.92	4.99	22.12	26.97	0.87	16.56	0.28	0.01	100.49	
4-17	23.56	4.79	2.27	23.46	28.94	0.88	15.45	0.26	0.00	99.67	
Hematites, n = 5											
	SiO2	TiO2	Al2O3	Cr2O3	Fe2O3	MnO	MgO			total	
4-22	1.36	0.00	0.00	0.05	97.58	0.87	0.92			100.92	
4-22	1.29	0.04	0.00	0.02	98.45	0.73	0.62			101.24	
4-22	0.21	60.57	0.00	2.24	31.58	0.27	0.03			94.92	
4-22	0.91	0.04	0.03	0.00	98.30	0.95	0.65			100.99	
4-22	0.74	0.07	0.05	0.00	99.96	0.51	0.43			101.90	
Pyroxenes, n = 78											
	SiO2	TiO2	Al2O3	Cr2O3	Fe2O3	FeO	MnO	MgO	CaO	Na2O	total
4-20	53.00	0.27	2.45	0.45	0.18	5.14	0.15	15.89	22.02	0.37	99.92
12-9	50.66	0.54	4.04	1.05	1.46	3.94	0.15	15.61	21.83	0.28	99.55
2-12B	52.78	0.15	1.54	0.05	2.36	6.36	0.42	13.54	22.69	0.69	100.58
9-12E	52.22	0.30	2.15	0.10	2.87	5.67	0.22	13.47	21.86	1.05	99.89
2-12A	51.99	0.86	2.13	0.44	2.11	14.27	0.26	25.59	1.92	0.07	99.62
4-20	54.48	0.32	2.83	0.38	0.00	12.38	0.31	28.27	1.55	0.03	100.55
12-4	51.88	0.17	3.10	0.18	3.16	4.75	0.29	13.42	22.07	1.05	100.06
12-7	54.78	0.33	1.31	1.41	0.41	2.59	0.13	17.74	19.68	1.35	99.73
4-13C	54.91	0.34	1.18	1.91	0.00	3.39	0.10	17.94	20.07	1.04	100.89
12-3	54.90	0.00	2.22	1.67	0.90	0.81	0.14	16.03	21.56	1.82	100.04
12-3	55.03	0.21	1.98	1.38	0.94	1.86	0.23	17.55	18.85	1.81	99.84
3-4C	54.77	0.08	0.64	1.71	1.29	0.91	0.13	16.31	23.11	1.27	100.20
4-22	53.40	0.28	1.75	1.73	0.78	2.10	0.14	17.25	21.52	0.77	99.72
4-13C	54.63	0.24	1.24	1.85	1.19	2.36	0.17	17.76	20.14	1.19	100.77

	SiO2	TiO2	Al2O3	Cr2O3	Fe2O3	FeO	MnO	MgO	CaO	Na2O	total
3-4C	55.11	0.10	0.42	1.51	1.09	2.16	0.18	15.79	23.15	1.27	100.78
10-17	53.95	0.08	2.34	2.16	2.93	0.00	0.12	15.64	20.62	2.28	100.12
4-22	51.69	0.58	3.71	1.43	2.01	1.41	0.11	15.51	23.01	0.79	100.27
10-12B	54.52	0.14	0.69	2.90	0.95	1.88	0.05	15.62	21.91	1.60	100.27
9-12D	54.44	0.17	1.39	2.13	1.03	1.54	0.11	16.28	21.05	1.65	99.78
9-12D	54.75	0.24	1.44	2.06	0.71	1.92	0.18	16.34	21.05	1.61	100.30
9-12E	54.08	0.22	1.62	3.02	2.25	0.07	0.01	16.57	18.82	2.42	99.07
10-17	54.28	0.07	0.33	2.18	2.21	0.28	0.09	16.23	22.52	1.48	99.65
9-11B	54.91	0.23	2.08	1.87	0.87	1.30	0.02	16.37	20.12	2.06	99.81
9-10	55.48	0.12	1.90	4.28	0.94	1.41	0.17	15.61	18.17	2.95	101.04
9-10	55.13	0.07	1.87	3.78	2.51	0.15	0.23	15.82	18.47	2.96	101.00
4-13C	54.47	0.08	1.38	2.27	1.00	2.69	0.02	17.08	19.59	1.51	100.08
4-13C	54.48	0.13	1.37	2.37	1.39	2.09	0.10	17.61	20.11	1.27	100.91
12-6	53.70	0.36	1.34	2.79	0.22	1.38	0.07	16.75	22.85	0.87	100.34
12-6	54.84	0.13	2.46	3.42	0.64	1.74	0.07	14.89	18.97	2.80	99.97
12-6	54.59	0.33	3.64	2.44	0.64	0.95	0.10	14.44	19.86	2.89	99.89
12-2	54.89	0.15	2.31	3.15	0.62	1.67	0.10	15.05	19.48	2.63	100.06
12-3	55.05	0.20	3.13	2.10	0.23	1.48	0.08	15.01	20.26	2.53	100.06
12-2	55.33	0.18	3.34	3.11	0.25	1.57	0.13	14.42	19.23	3.09	100.65
12-2	54.86	0.31	3.56	3.60	0.82	0.74	0.10	13.91	18.56	3.55	100.00
12-2	54.93	0.34	3.62	3.43	0.82	0.74	0.01	14.17	18.69	3.47	100.23
2-10C	55.73	0.00	7.75	0.00	6.13	3.31	0.00	7.52	12.40	7.34	100.19
2-10C	55.83	0.00	8.68	0.00	6.21	2.36	0.00	7.30	12.16	7.73	100.27
4-13C	54.73	0.40	1.37	1.07	1.32	1.97	0.15	18.07	20.76	1.05	100.88
4-13C	54.64	0.08	1.36	1.45	1.20	2.37	0.05	17.38	20.57	1.20	100.28
4-13C	54.68	0.06	1.14	0.71	1.52	1.76	0.04	18.31	21.30	0.80	100.31
2-12A	54.46	0.32	1.89	1.52	1.26	2.50	0.14	16.36	19.84	1.78	100.07
2-12B	54.16	0.04	1.67	0.20	1.18	3.79	0.20	15.93	22.92	0.66	100.75
2-12B	53.48	0.02	2.21	0.88	1.66	2.85	0.13	15.22	23.66	0.77	100.88
2-10C	56.03	0.00	9.08	0.05	6.84	2.60	0.00	6.71	11.28	8.20	100.79
2-10G	54.96	0.19	1.09	1.27	1.04	2.06	0.10	16.36	21.59	1.49	100.15
3-4D	54.61	0.12	0.39	1.38	1.96	0.41	0.09	16.77	24.13	0.88	100.74
3-4D	55.09	0.09	2.61	2.11	1.55	0.84	0.00	15.40	20.18	2.55	100.42
3-4D	54.38	0.09	0.53	2.08	1.67	0.21	0.10	16.30	23.25	1.28	99.89
3-4D	55.00	0.09	0.54	1.39	0.95	1.10	0.08	16.71	23.22	1.10	100.18
3-4D	54.84	0.11	0.33	1.19	1.37	1.23	0.03	16.76	23.48	0.94	100.28
3-4D	54.72	0.16	2.58	1.97	1.85	0.24	0.01	15.89	20.90	2.21	100.53
3-4D	55.30	0.27	3.18	2.12	0.85	1.27	0.08	14.99	19.78	2.77	100.61
3-4D	54.70	0.11	0.53	1.57	1.59	0.33	0.03	16.72	23.29	1.19	100.06
3-4D	54.95	0.27	3.01	2.01	1.84	0.55	0.11	14.96	19.97	2.80	100.47
3-4D	54.85	0.14	0.36	1.32	1.73	0.93	0.08	16.75	23.44	1.03	100.63
3-4D	55.22	0.13	2.49	2.16	1.40	1.26	0.19	15.55	19.97	2.47	100.84
3-4D	54.61	0.12	2.45	2.16	2.21	0.46	0.00	15.50	20.33	2.44	100.28
3-4D	54.75	0.10	0.64	2.87	1.66	0.05	0.05	16.22	22.29	1.74	100.37
3-4D	54.67	0.17	0.57	2.89	0.40	1.07	0.00	16.05	22.51	1.50	99.83
3-4B	55.15	0.13	0.40	1.79	1.26	0.68	0.05	16.78	23.34	1.19	100.77
3-4B	54.43	0.10	0.44	1.54	1.38	0.41	0.00	16.43	23.29	1.22	99.24
3-4B	54.52	0.15	0.75	1.44	0.91	1.37	0.10	16.30	22.97	1.15	99.66
3-4B	54.40	0.09	0.78	1.80	1.47	0.80	0.00	16.63	22.46	1.27	99.70
3-4B	54.55	0.15	0.71	1.32	1.49	0.81	0.14	16.53	22.87	1.22	99.79
3-4B	55.53	0.00	8.29	0.09	5.75	1.45	0.06	8.50	13.63	6.96	100.26
3-4B	55.66	0.03	8.46	0.07	6.71	1.12	0.05	8.00	12.89	7.48	100.47
3-4C	54.35	0.07	0.65	2.94	2.47	0.02	0.12	15.81	22.01	1.86	100.30
3-4C	55.02	0.10	0.61	1.72	1.00	0.90	0.02	16.52	23.07	1.27	100.23
3-4C	54.32	0.00	0.05	0.77	1.96	0.41	0.07	16.55	24.58	0.75	99.46
3-4C	54.61	0.11	0.37	1.34	0.99	1.48	0.19	16.27	23.40	1.03	99.79
3-4C	54.70	0.09	0.61	2.01	1.84	0.24	0.04	16.20	23.11	1.46	100.30
3-4C	54.70	0.09	0.05	0.74	2.40	0.07	0.04	16.70	24.82	0.83	100.44
3-4C	54.65	0.13	0.68	1.65	1.23	0.67	0.07	16.48	23.20	1.19	99.95
3-4C	54.50	0.11	1.50	2.32	1.86	1.30	0.20	15.22	21.29	2.03	100.33
3-4C	55.34	0.11	1.67	1.03	0.69	2.69	0.05	19.28	18.14	1.27	100.27
3-4C	55.03	0.09	0.47	1.73	1.39	0.75	0.09	16.59	23.27	1.22	100.63
3-4C	55.02	0.15	0.35	1.33	0.66	1.78	0.12	16.45	23.58	0.97	100.41

	SiO2	TiO2	Al2O3	Cr2O3	Fe2O3	FeO	MnO	MgO	CaO	Na2O	total
3-4C	54.63	0.22	0.70	3.39	1.21	1.09	0.07	15.39	21.18	2.13	100.01
Olivines, n = 13											
	SiO2	TiO2	Al2O3	FeO	MnO	MgO	CaO	NiO	total		
3-4D	41.69	0.00	0.03	6.96	0.15	50.46	0.06	0.39	99.74		
3-4D	41.44	0.05	0.03	6.92	0.18	50.26	0.06	0.35	99.27		
3-4D	41.30	0.05	0.05	7.03	0.16	50.53	0.05	0.39	99.57		
3-4D	41.48	0.02	0.00	7.46	0.11	50.22	0.09	0.31	99.69		
3-4D	41.57	0.02	0.00	7.47	0.03	50.30	0.06	0.31	99.76		
2-12A	40.88	0.01	0.00	8.52	0.12	49.71	0.03	0.39	99.66		
2-12A	41.00	0.05	0.00	8.78	0.12	49.51	0.06	0.32	99.84		
2-12A	40.56	0.00	0.00	8.44	0.14	49.30	0.03	0.42	98.90		
2-12A	40.96	0.05	0.00	8.72	0.10	49.33	0.00	0.37	99.54		
2-12A	40.99	0.00	0.04	8.39	0.06	49.41	0.03	0.30	99.22		
12-1	39.01	0.05	0.00	18.90	0.34	41.17	0.27	0.11	99.85		
12-4	39.46	0.00	0.08	16.45	0.30	43.33	0.40	0.17	100.19		

Amphiboles, n = 11																
	SiO2	TiO2	Al2O3	Cr2O3	FeO	FeO	MnO	MgO	CaO	Na2O	K2O	H2O	F	Cl	total	
10-18	46.42	0.59	10.49	2.29	2.85		0.10	18.91	10.35	3.89	1.14	2.08	0.00	0.10	99.20	
10-18	45.20	0.35	10.85	2.20	2.69		0.05	19.44	11.60	3.32	0.81	2.07	0.00	0.07	98.64	
10-18	45.33	0.42	10.89	2.02	2.55		0.14	19.11	11.55	3.49	0.81	2.06	0.04	0.04	98.44	
10-18	44.71	0.40	10.89	2.25	2.56		0.06	19.35	11.33	3.61	0.80	2.02	0.07	0.07	98.13	
10-18	45.12	0.53	11.18	2.22	3.11		0.00	18.90	10.18	4.01	0.67	2.04	0.04	0.08	98.07	
10-17	45.03	0.50	10.94	2.24	2.99		0.05	19.37	11.25	3.85	0.83	2.05	0.05	0.06	99.23	
3-4C	47.33	0.02	9.81	1.98	1.83	1.65	0.08	19.87	10.51	4.11	0.50	2.11	0.00	0.01	99.81	
4-23	52.64	0.18	3.91	0.22	1.39	11.75	0.31	14.67	12.80	0.25	0.05	2.08	0.00	0.00	100.25	
9-11C	50.97	0.32	7.05	0.25	3.76	6.37	0.22	16.50	12.39	0.71	0.20	2.04	0.14	0.02	100.94	
10-11A	50.66	0.14	6.12	0.23	3.92	6.65	0.48	16.08	12.65	0.75	0.15	2.05	0.07	0.00	99.96	
9-11A	50.98	0.33	5.03	0.09	3.91	8.71	0.40	15.64	11.90	0.72	0.15	2.06	0.00	0.04	99.94	
Phlogopites and Biotites, n = 11																
	SiO2	TiO2	Al2O3	FeO	MnO	MgO	CaO	Na2O	K2O	H2O	F	Cl	total	O=F	O=Cl	total
9-12E	40.62	3.78	13.33	4.93	0.05	22.06	0.00	0.07	9.76	3.95	0.48	0.07	99.09	0.20	0.02	98.87
9-12E	40.09	3.63	13.30	4.09	0.01	22.73	0.00	0.09	10.34	3.98	0.36	0.09	98.72	0.15	0.02	98.54
2-12A	38.85	4.20	14.10	4.51	0.06	22.10	0.00	0.14	10.69	4.09	0.12	0.07	98.94	0.05	0.02	98.87
2-12A	39.54	4.54	13.65	4.59	0.06	21.89	0.00	0.15	10.80	4.01	0.32	0.08	99.63	0.14	0.02	99.48
2-12A	38.80	4.82	13.76	4.95	0.00	21.00	0.04	0.22	10.36	3.98	0.29	0.06	98.28	0.12	0.01	98.14
2-12A	40.91	4.05	12.73	4.72	0.08	21.43	0.00	0.10	10.64	4.09	0.17	0.00	98.93	0.07	0.00	98.86
2-12A	40.28	4.06	13.53	4.66	0.09	22.16	0.00	0.16	10.84	4.12	0.17	0.05	100.12	0.07	0.01	100.04
10-9A	37.87	4.33	15.25	6.41	0.06	19.73	0.07	0.22	9.77	3.92	0.37	0.05	98.04	0.15	0.01	97.88
12-9	38.60	4.64	14.14	7.71	0.00	18.25	0.00	0.22	9.62	3.12	1.96	0.05	98.30	0.82	0.01	97.46
12-3	36.41	3.28	13.90	20.22	0.23	12.18	0.00	0.18	9.53	3.40	1.00	0.17	100.50	0.42	0.04	100.04

APPENDIX X

Raw trace geochemical results from proton microprobe analysis of Cr-pyrope garnets.

CONTENTS: Trace elements for 101 Cr-pyrope garnets by PMP: analyses by W.L. Griffin, CSIRO, Australia.

Raw data from Bill Griffins Proton-probe analyses - for all data available									
HIAF Proton Microprobe, CSIRO, Heavy Ion Analytical Facility, Australia.									
	wt% oxide				ppm		Ni-calc		
Borehole	Cr2O3	CaO	TiO2	Ga	Y	Zr	Temp (oC)	type	
002	1.89	5.28	0.88	19	27	88	1026	G9	
002	1.84	4.99	0.85	16	29	85	1072	G9	
002	2.08	4.88	0.68	14	24	76	1024	G9	
002	1.93	5.12	0.86	16	30	109	1095	G9	
002	2.45	4.97	0.80	15	27	88	1246	G9	
002	2.28	5.06	0.86	15	30	100	1204	G9	
002	1.08	5.18	0.10	17	26	106	880	G9	
002	1.92	5.21	0.90	17	24	88	915	G9	
002	4.86	5.11	0.06	5	11	13	803	G9	
002	4.92	5.23	0.05	6	20	42	752	G9	
002	4.14	4.75	0.08	7	10	12	796	G9	
002	7.90	6.77	0.07	5	2	5	839	G9	
002	3.80	4.95	0.20	8	10	14	795	G9	
002	5.48	5.25	0.26	9	11	21	855	G9	
002	7.19	6.29	0.06	7	8	11	798	G9	
002	4.29	5.24	0.24	7	7	32	865	G9	
002	5.17	5.51	0.22	7	19	18	825	G9	
002	5.29	5.33	0.06	5	11	27	900	G9	
002	7.10	5.82	0.24	9	10	27	1221	G9	
002	4.47	5.39	0.65	11	20	85	1253	G9	
002	6.43	5.80	0.79	12	19	106	1261	G9	
003	1.24	4.41	0.19	9	15	14	927	G9	
003	0.39	4.04	0.27	11	13	12	944	G9	
003	1.70	5.28	1.13	17	27	110	921	G9	
003	1.55	4.85	0.77	15	26	77	1113	G9	
003	3.12	5.37	1.25	17	41	187	1250	G9	
003	3.44	5.43	1.08	15	43	195	1347	G9	
003	3.21	5.13	1.11	14	36	169	1219	G9	
003	2.62	5.10	0.93	18	28	102	1114	G9	
003	5.80	5.63	0.11	5	18	49	893	g10	
003	10.50	5.92	0.22	10	6	9	1140	g10	
003	9.24	6.64	0.05	5	1	3	1236	g10	
003	8.21	5.34	0.12	11	7	24	1207	g10	
003	8.15	6.40	0.32	6	12	45	822	G9	
003	4.70	5.14	0.16	11	13	16	808	G9	
003	6.63	4.76	0.19	12	6	16	1195	G9	
003	6.34	5.78	0.10	5	5	10	909	G9	
003	8.40	6.13	0.07	7	3	39	1208	g10	
003	9.20	6.12	0.03	6	11	93	1241	g10	
003	7.45	5.95	0.04	6	5	76	1208	G9	
003	6.59	5.78	0.66	9	15	66	1243	G9	
004	4.88	6.26	0.01	5	1	7	807	G9	
004	6.69	6.52	0.07	4	4	7	865	G9	
004	8.70	6.59	0.15	9	4	33	1213	G9	
004	9.47	6.96	0.19	7	10	17	1221	G9	
004	8.75	6.63	0.16	8	4	23	1202	G9	
004	8.45	3.83	0.02	4	9	91	1064	g10	
004	12.10	5.38	0.14	7	1	3	1275	g10	
004	9.50	4.43	0.06	2	13	135	957	g10	
004	6.91	5.16	0.09	6	3	9	1194	g10	
004	9.40	5.63	0.62	7	13	95	1210	g10	
004	8.54	6.12	0.53	7	9	59	1237	G9	

	wt% oxide				ppm		Ni-calc		
Borehole	Cr2O3	CaO	TiO2	Ga	Y	Zr	Temp (oC)	type	
004	9.60	3.85	0.10	2	8	111	1038	g10	
004	8.36	4.29	0.07	2	4	106	995	g10	
004	9.06	3.97	0.09	7	4	21	1188	g10	
004	5.09	5.59	0.15	7	10	20	858	G9	
004	7.41	6.28	0.07	2	4	36	768	G9	
004	7.52	3.38	0.03	2	3	28	1006	g10	
004	5.99	5.45	0.07	7	5	21	858	G9	
004	5.06	5.54	0.16	7	10	25	881	G9	
004	5.03	5.69	0.17	8	13	17	841	G9	
009	7.46	5.94	0.48	9	10	51	1343	G9	
009	7.57	5.97	0.46	8	15	81	976	G9	
009	7.94	6.86	0.09	5	7	19	972	G9	
009	6.29	5.40	0.04	8	23	101	815	G9	
009	4.68	4.95	0.27	7	13	48	1000	G9	
009	8.17	6.58	0.18	8	5	55	936	G9	
009	4.40	4.83	0.07	6	11	15	767	G9	
009	7.26	4.64	0.03	8	6	4	1193	g10	
009	4.84	5.08	0.19	11	18	25	818	G9	
009	5.08	5.39	0.09	9	19	18	803	G9	
009	9.69	6.14	0.07	6	2	6	1217	g10	
009	4.71	4.87	0.11	10	14	27	966	G9	
009	3.27	4.73	0.21	8	17	76	980	G9	
009	5.33	5.51	0.04	7	5	67	1023	G9	
009	4.44	4.98	0.08	5	33	51	743	G9	
009	6.13	5.16	0.21	6	32	92	1004	G9	
009	4.85	5.32	0.16	9	11	27	1243	G9	
009	6.94	5.51	0.25	11	11	8	1219	G9	
009	3.46	4.75	0.15	9	17	57	1063	G9	
009	5.97	5.39	0.46	10	17	110	1206	G9	
009	8.04	6.58	0.08	7	6	10	962	G9	
009	4.92	5.41	0.17	10	16	27	868	G9	
009	6.58	5.78	0.15	9	8	8	1221	G9	
009	5.47	4.83	0.35	9	22	53	992	G9	
009	11.90	7.32	0.12	8	15	8	1225	G9	
009	8.30	6.29	0.63	10	21	84	1273	G9	
009	4.90	4.96	0.21	7	15	41	891	G9	
009	3.03	4.00	0.10	2	38	25	732	G9	
009	5.88	5.66	0.45	8	15	75	1192	G9	
009	1.69	5.14	0.09	2	11	8	465	G9	
009	7.00	5.67	0.42	8	15	70	1058	G9	
009	10.70	6.73	0.91	8	19	192	1283	G9	
009	6.05	5.54	0.85	11	26	92	1220	G9	
009	2.88	4.74	0.27	10	18	14	935	G9	
009	9.37	6.34	0.12	7	3	3	1157	G9	
009	4.52	4.86	0.09	9	16	23	778	G9	
009	6.60	5.81	0.04	7	17	59	1185	G9	
009	8.41	5.80	0.25	9	15	58	957	G9	
009	5.43	4.60	0.15	6	9	32	693	G9	
009	7.97	3.73	0.47	6	9	121	1202	g10	
	5.94	5.41	0.30	9	14	52	1026	-	

APPENDIX XI

Features and IR spectra of diamonds separated by OFS programme.

CONTENTS: Colour plates, detailed description and spectra for 19 of the 21 diamonds separated by OFS program. See Chapter 5.

Analyses by W.R. Taylor, Imperial College, London.

APPENDIX XI

Features and IR spectra of diamonds separated by OFS programme.

CONTENTS: Colour plates, detailed description and spectra for 19 of the 21 diamonds separated by OFS program. See Chapter 5.

Analyses by W.R. Taylor, Imperial College, London.

Sample No.	2_10C/1	Pathlength:	45.7 μm
Colour:	colourless	μ^{1282}:	0.1738 mm^{-1}
Form:	sharp-edged octahedron, broken	Platelet area/ μ^{1282}:	0
		H (3107 cm^{-1}) area:	0 mm^{-1}
Resorption:	none-low	Nitrogen:	27 at. ppm
Surface:	no etch features	Aggregation (%B):	<0.5 %
Inclusions:	silicate? (1095, 912 cm^{-1} bands)	T_{NA} (for t_{MR}= 1.0 Ga):	<1095 °C
Spectral Type:	IaA (v. weak)	T_{NA} (for t_{MR}= 3.0 Ga):	<1070 °C

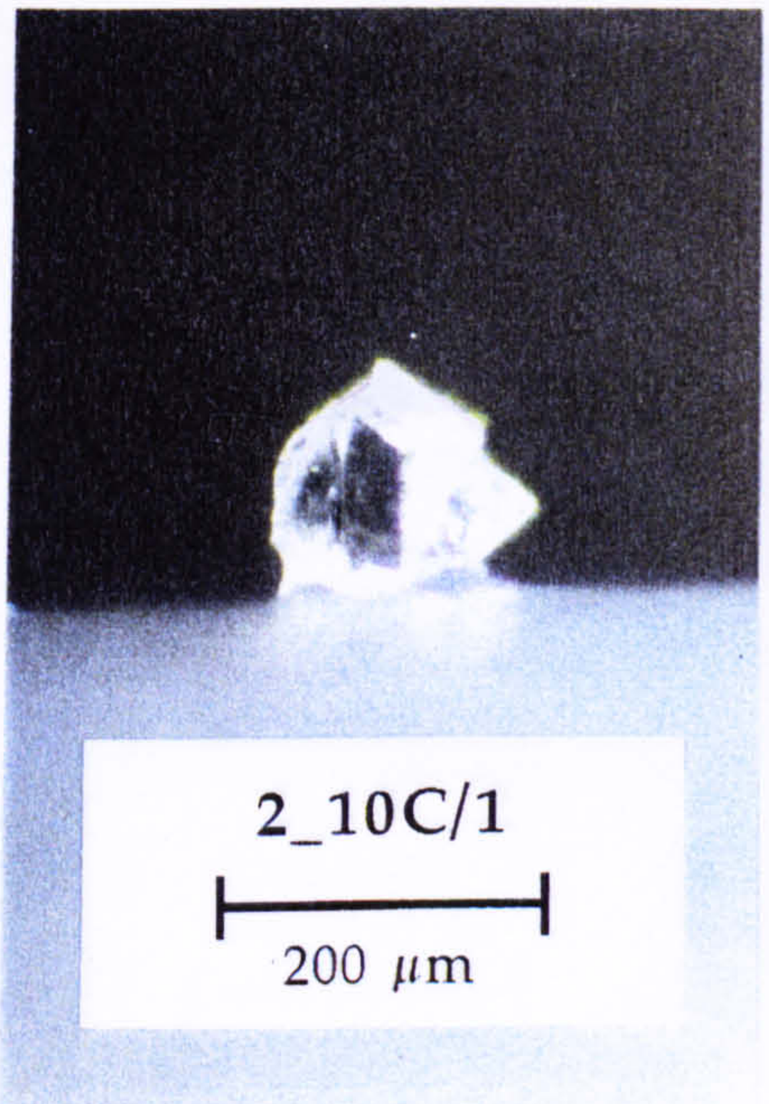

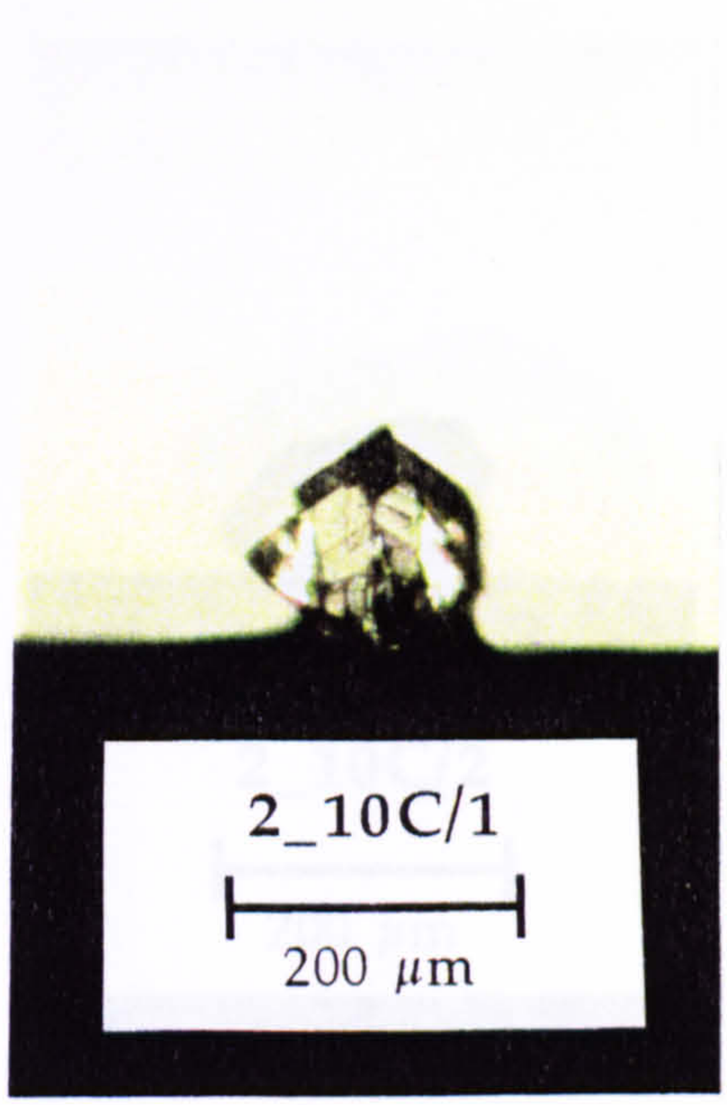

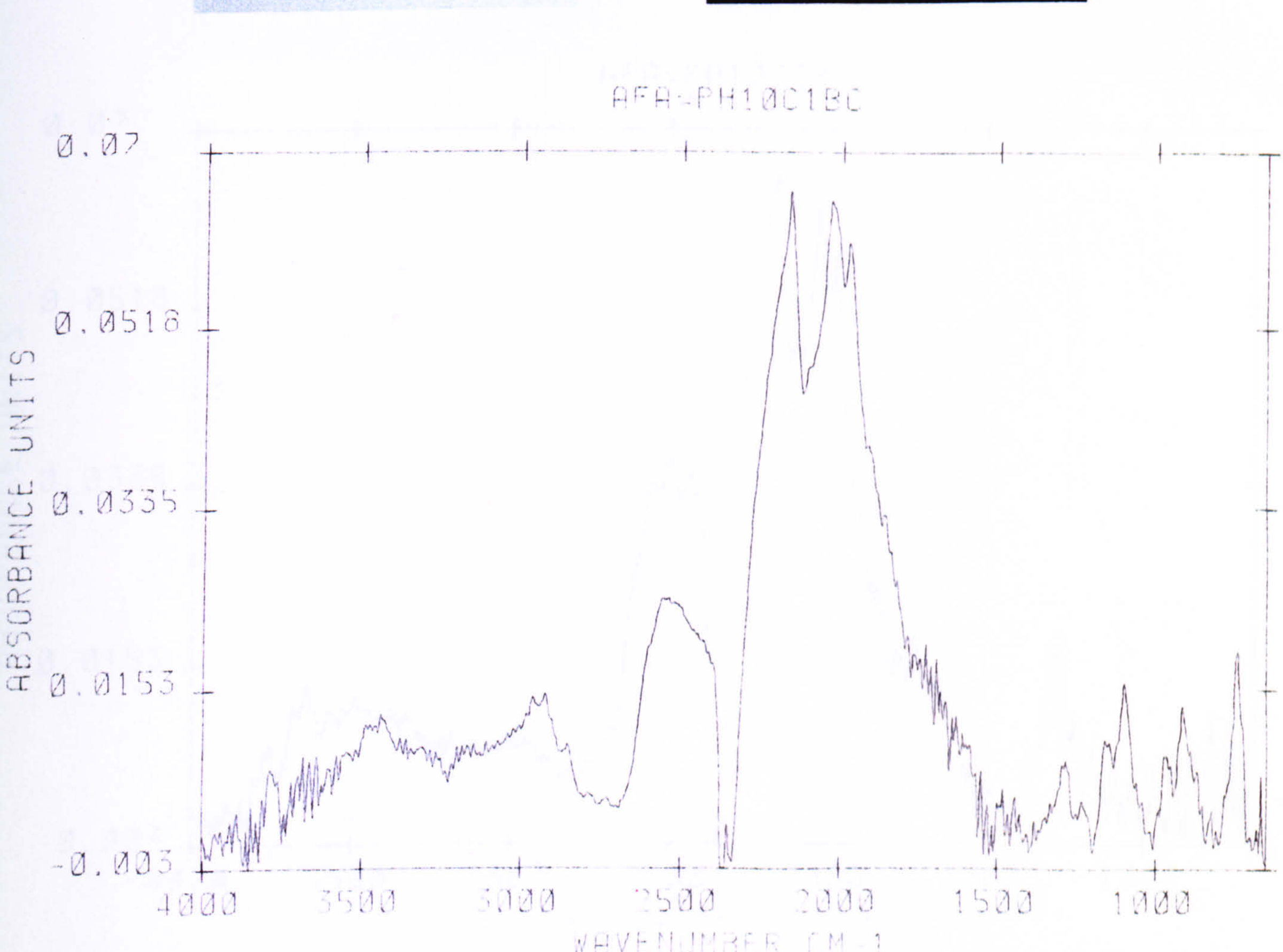

Sample No.	2_10C/2	Pathlength:	43.2 μm
Colour:	colourless	μ^{1282}:	0.3690 mm^{-1}
Form:	multiple, sharp-edged	Platelet area/ μ^{1282}:	0
	octahedra	H (3107 cm^{-1}) area:	0 mm^{-1}
Resorption:	none-low	Nitrogen:	56 at. ppm
Surface:	no etch features	Aggregation (%B):	<0.5 %
Inclusions:	none identified	T_{NA} (for t_{MR}= 1.0 Ga):	<1078 °C
Spectral Type:	IaA (weak)	T_{NA} (for t_{MR}= 3.0 Ga):	<1054 °C

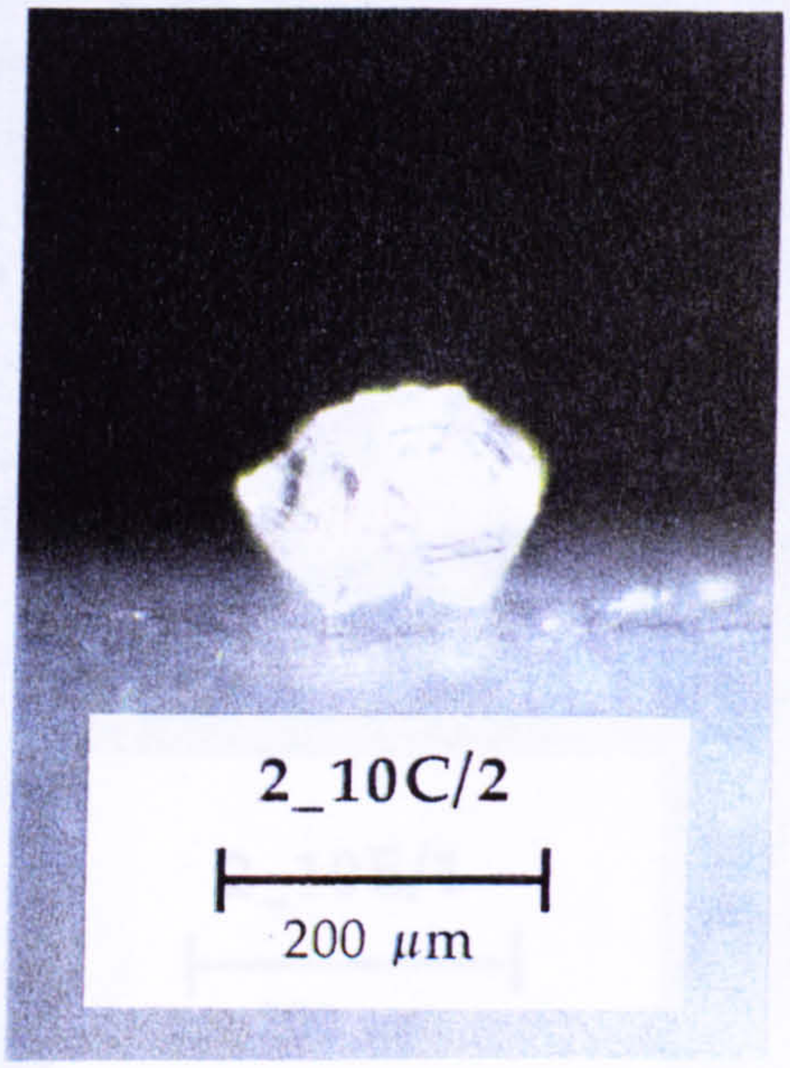

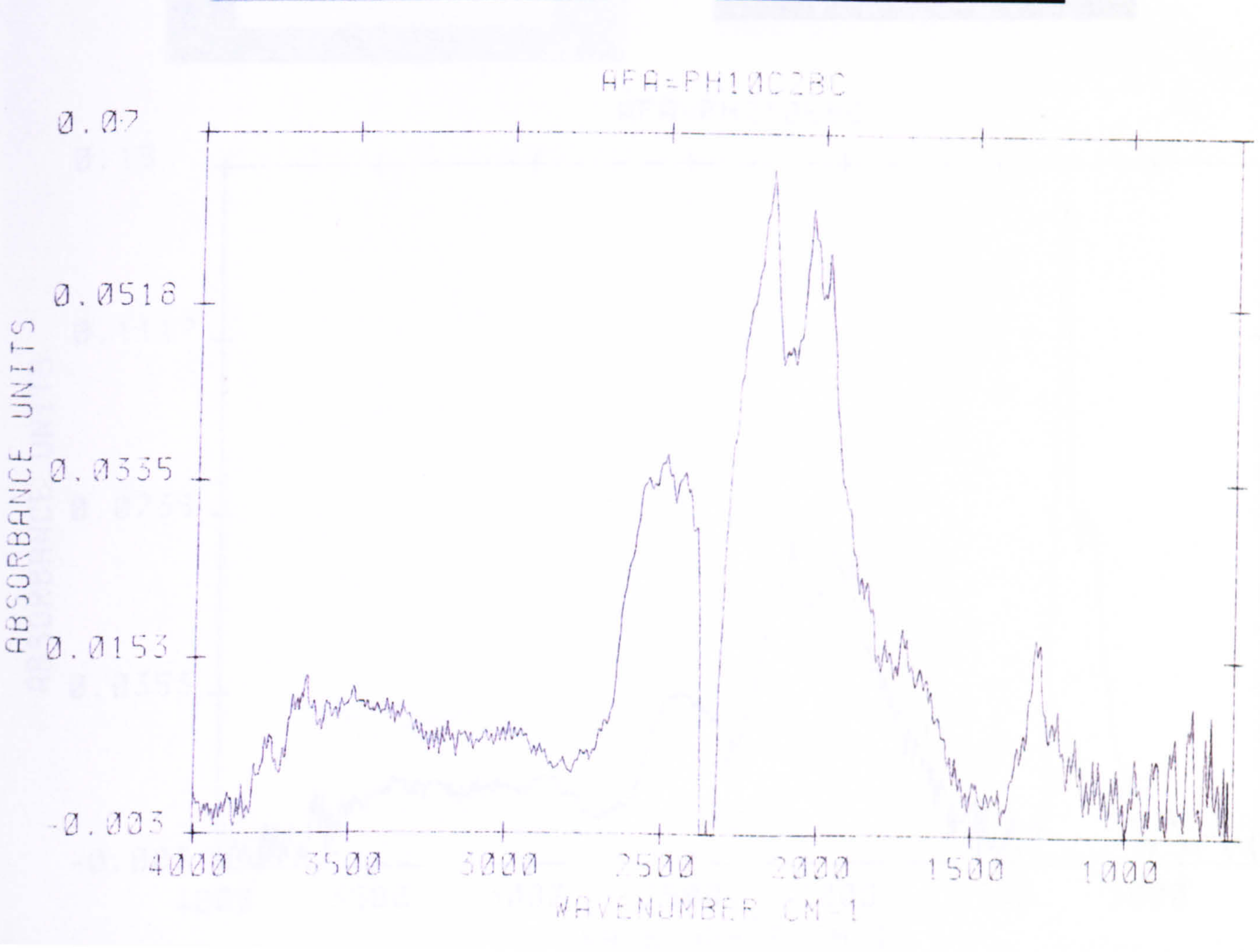

Sample No.	2_10E/1	Pathlength:	47.5 μm
Colour:	colourless	μ^{1282}:	2.9858 mm^{-1}
Form:	multiple dodec. fragment	Platelet area/ μ^{1282}:	0
Resorption:	high	H (3107 cm^{-1}) area:	0
Surface:	no etch features	Nitrogen:	455 at.ppm
Inclusions:	clay and iron-oxide minerals present in fracture	Aggregation (%B):	<0.5 %
		T_{NA} (for t_{MR}= 1.0 Ga):	<1033 °C
Spectral Type:	IaA	T_{NA} (for t_{MR}= 3.0 Ga):	<1010 °C

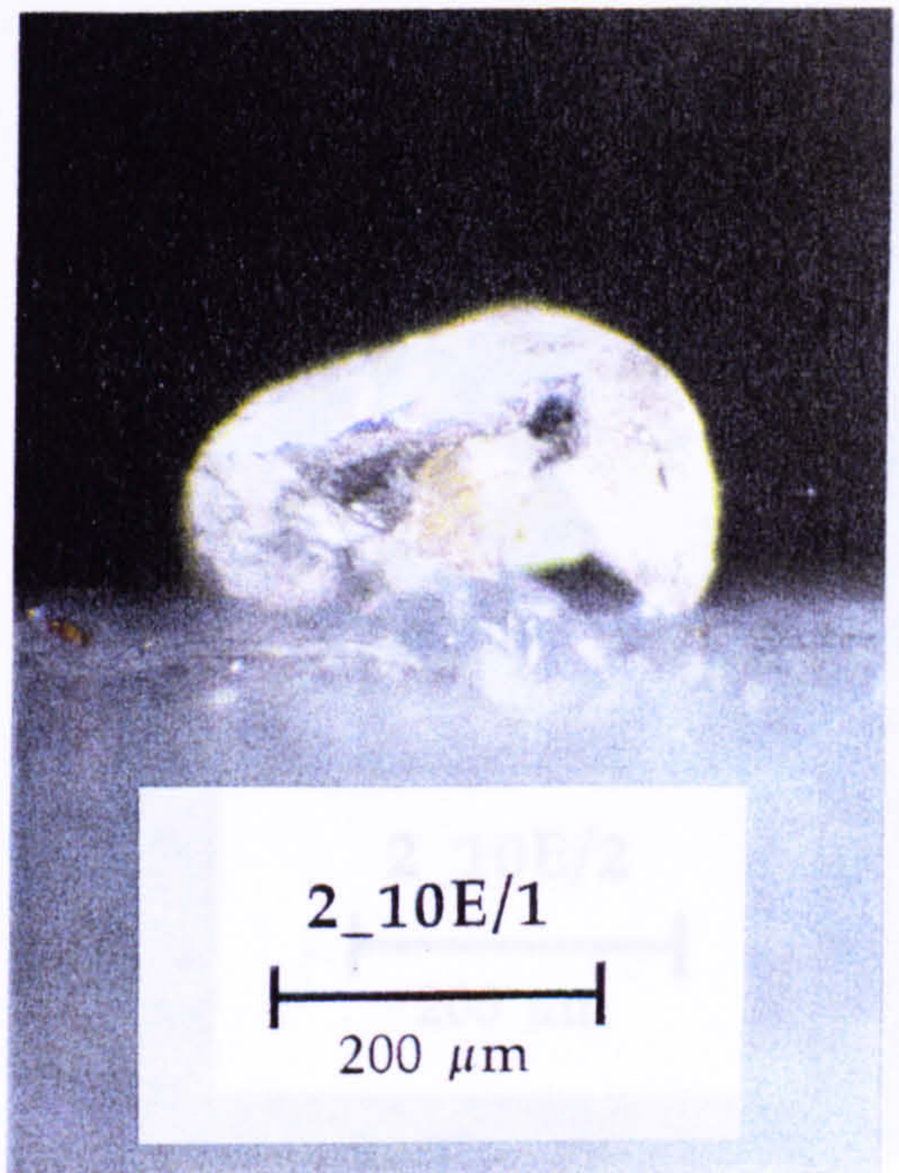

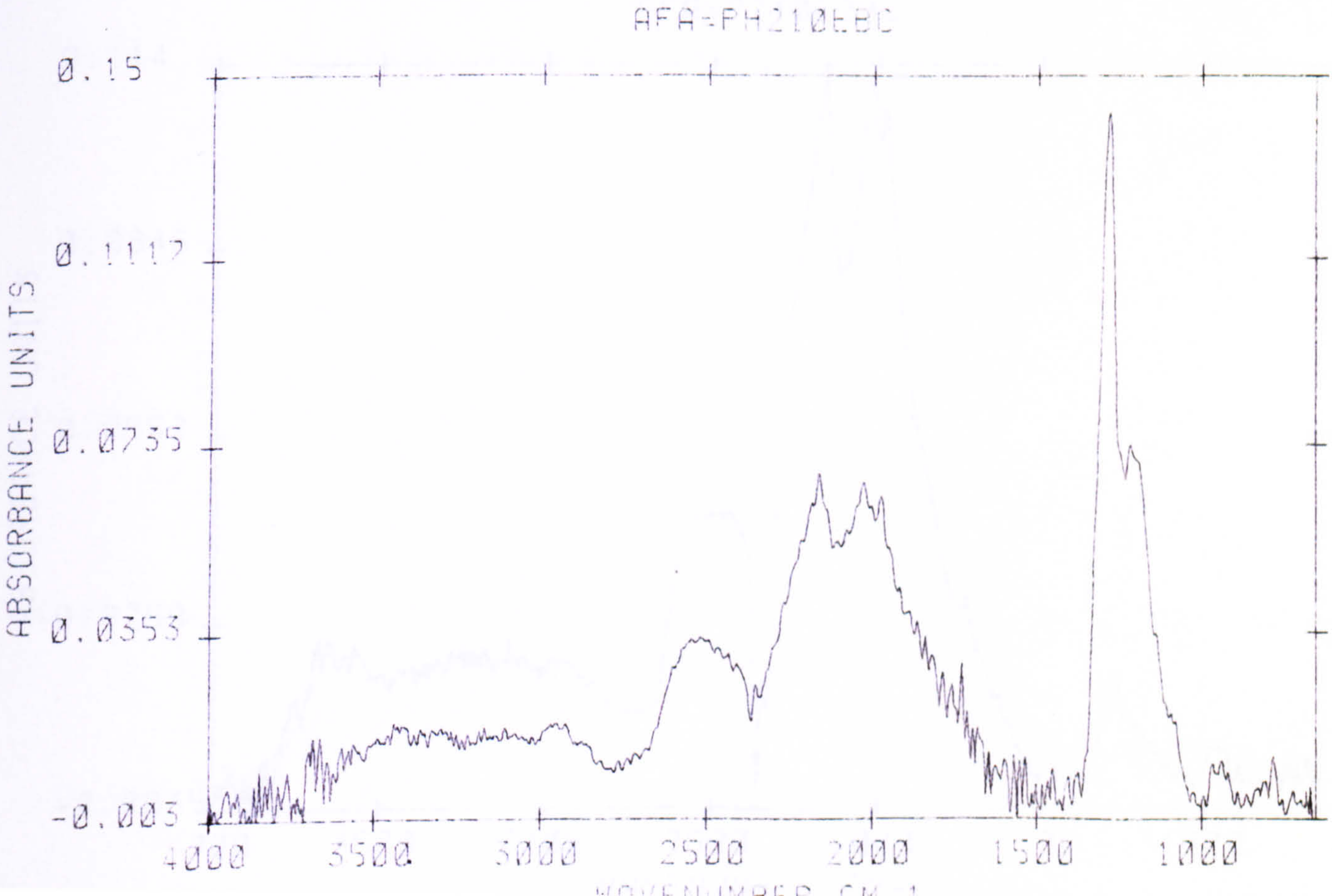

Sample No.	2_10E/2	Pathlength:	82.7 μm
Colour:	colourless	μ^{1282}:	0.2221 mm^{-1}
Form:	multiple, sharp-edged octas	Platelet area/ μ^{1282}:	0
Resorption:	none-low	H (3107 cm ^{1}) area:	0.37 mm^{-1}
Surface:	finely etched with some surface graphite	Nitrogen:	34 at. ppm
		Aggregation (%B):	<0.5 %
Inclusions:	none identified	T_{NA} (for t_{MR}= 1.0 Ga):	<1090 °C
Spectral Type:	IaA	T_{NA} (for t_{MR}= 3.0 Ga):	<1065 °C

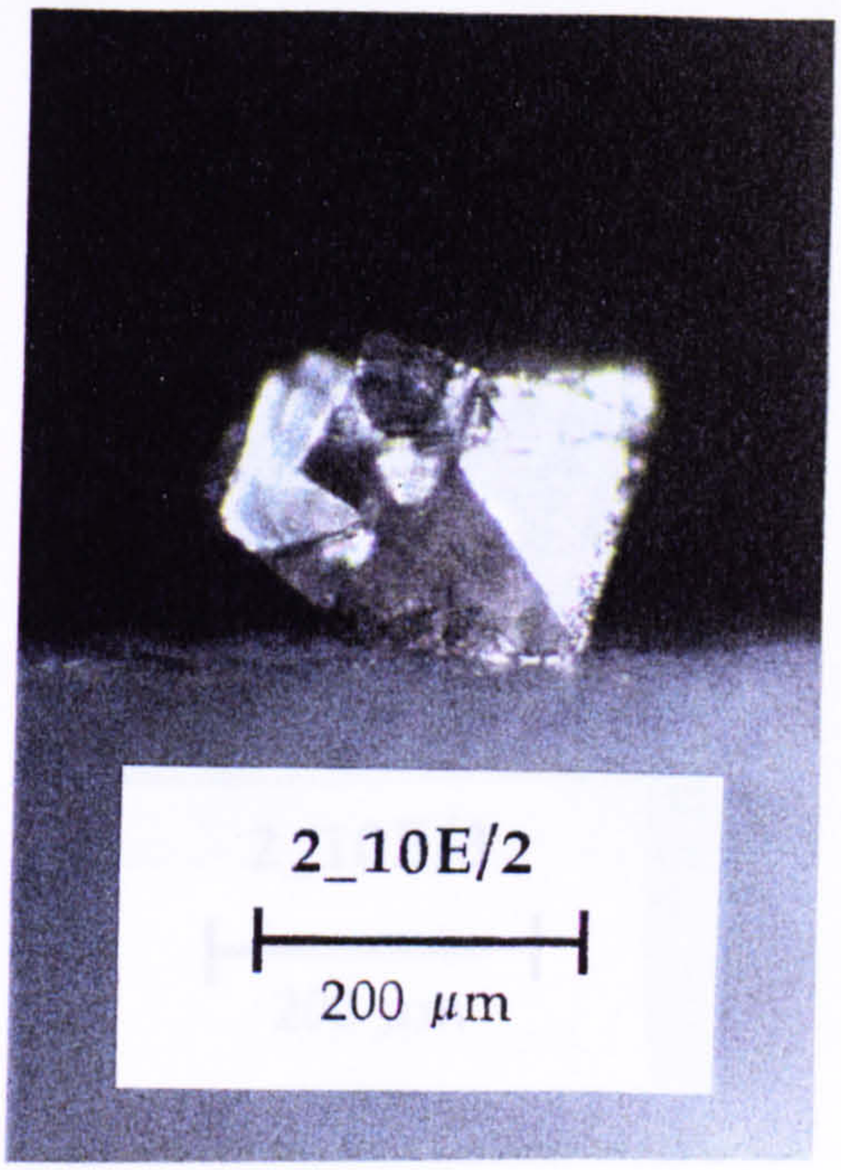

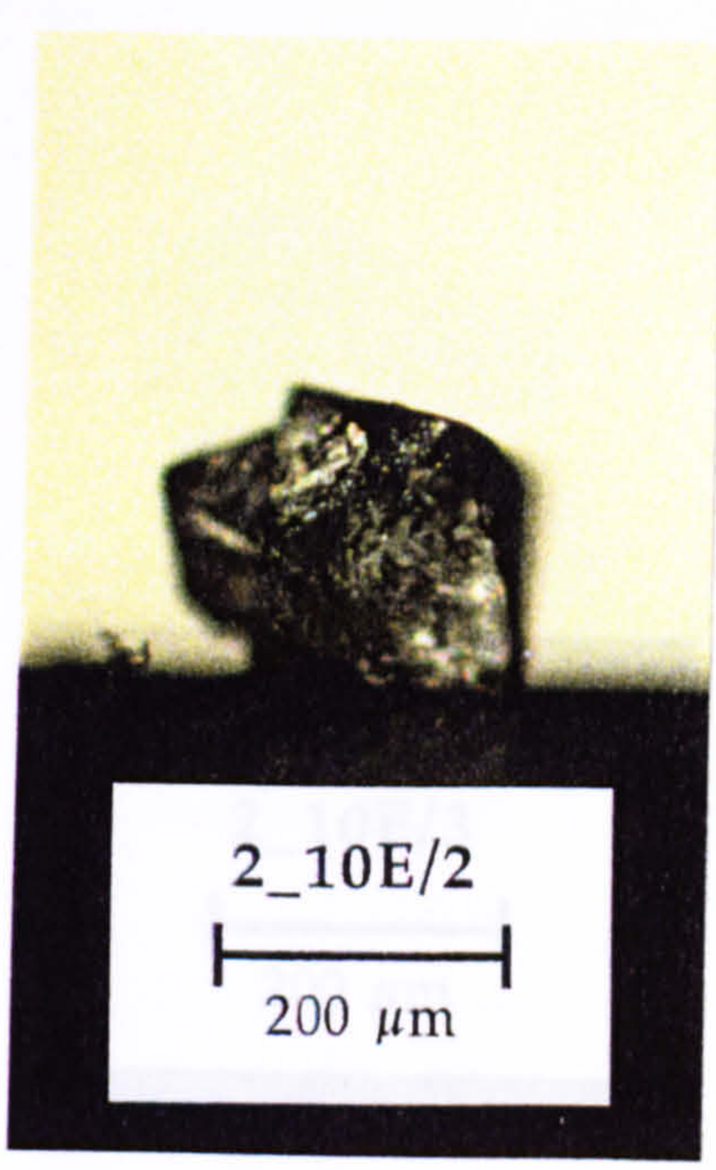

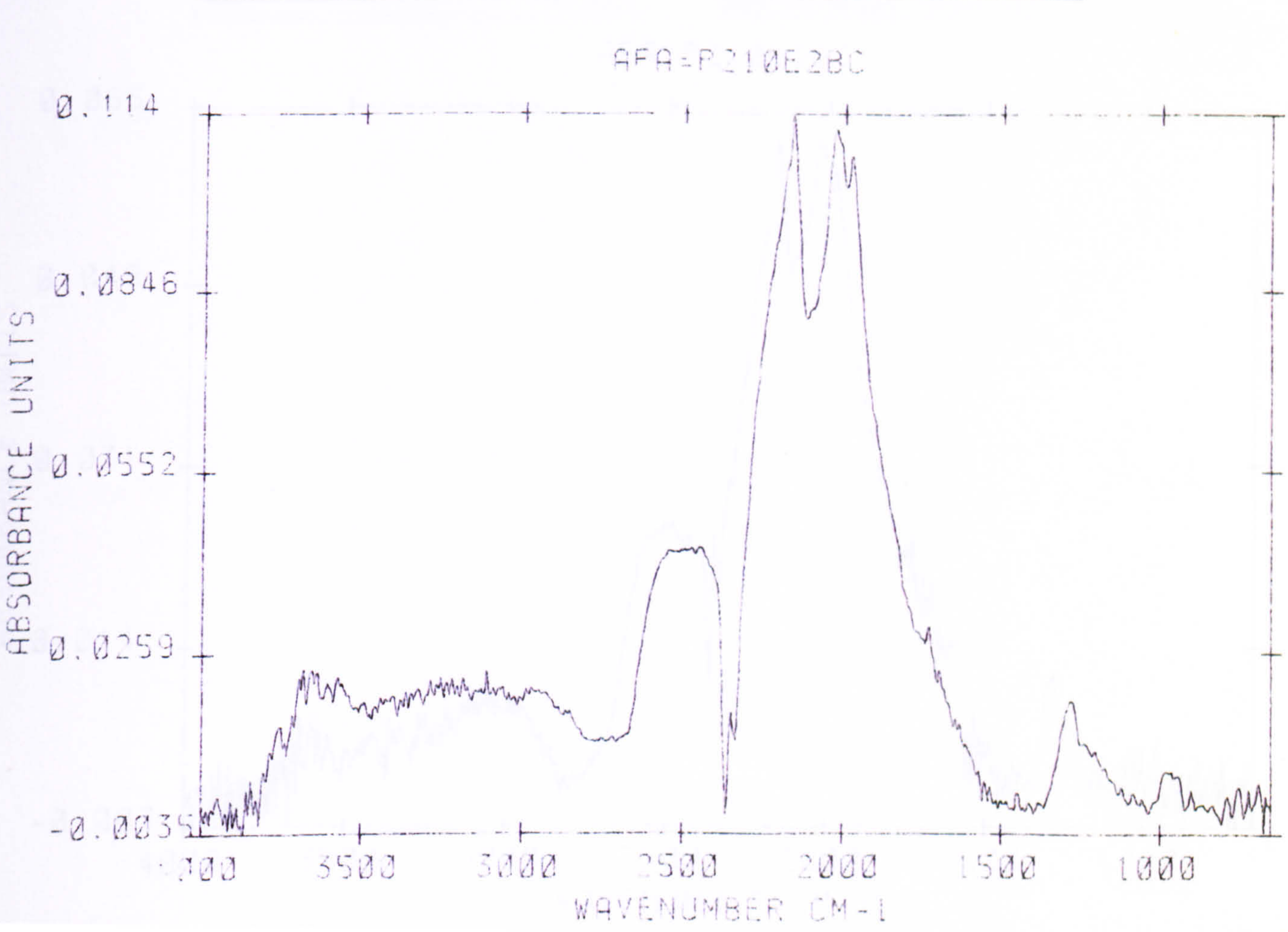

Sample No.	2_10E/3	Pathlength:	46.0 μm
Colour:	colourless	μ^{1282}:	0.2452 mm^{-1}
Form:	macle, fragment	Platelet area/ μ^{1282}:	0
Resorption:	low?	H (3107 cm^{-1}) area:	0.59 mm^{-1}
Surface:	some etch trigons	Nitrogen:	37 at.ppm
		Aggregation (%B):	<0.5 %
Inclusions:	none identified	T_{NA} (for t_{MR}= 1.0 Ga):	<1087 °C
Spectral Type:	IaA	T_{NA} (for t_{MR}= 3.0 Ga):	<1063 °C

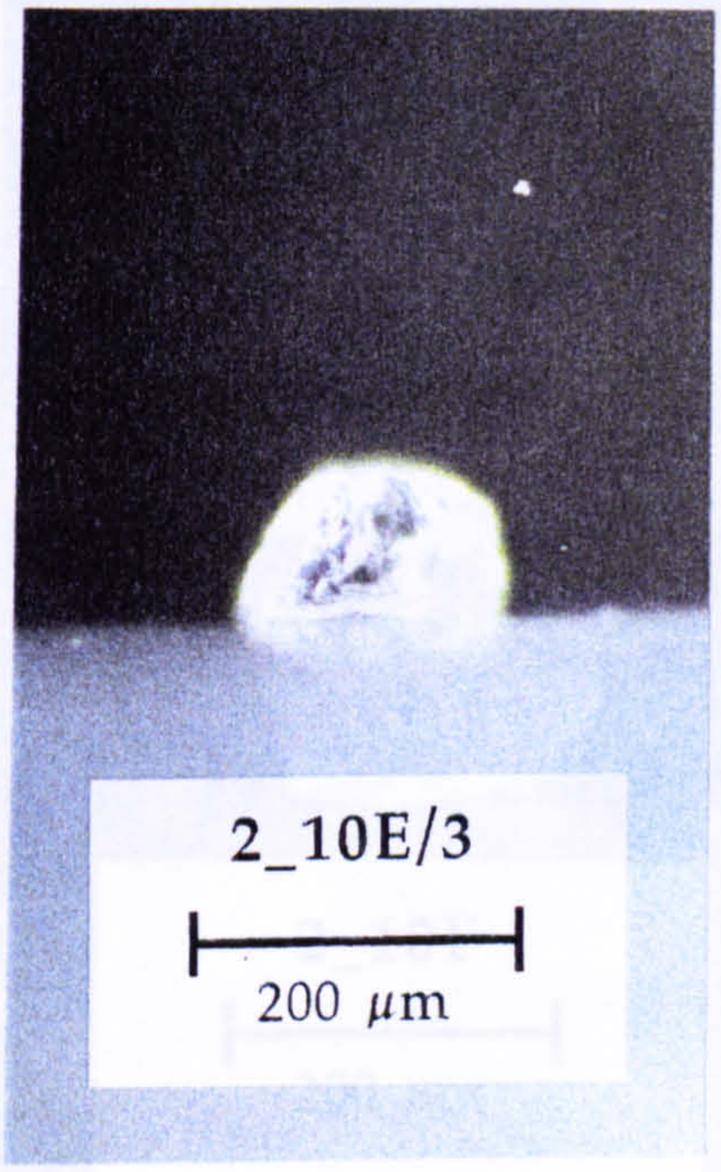

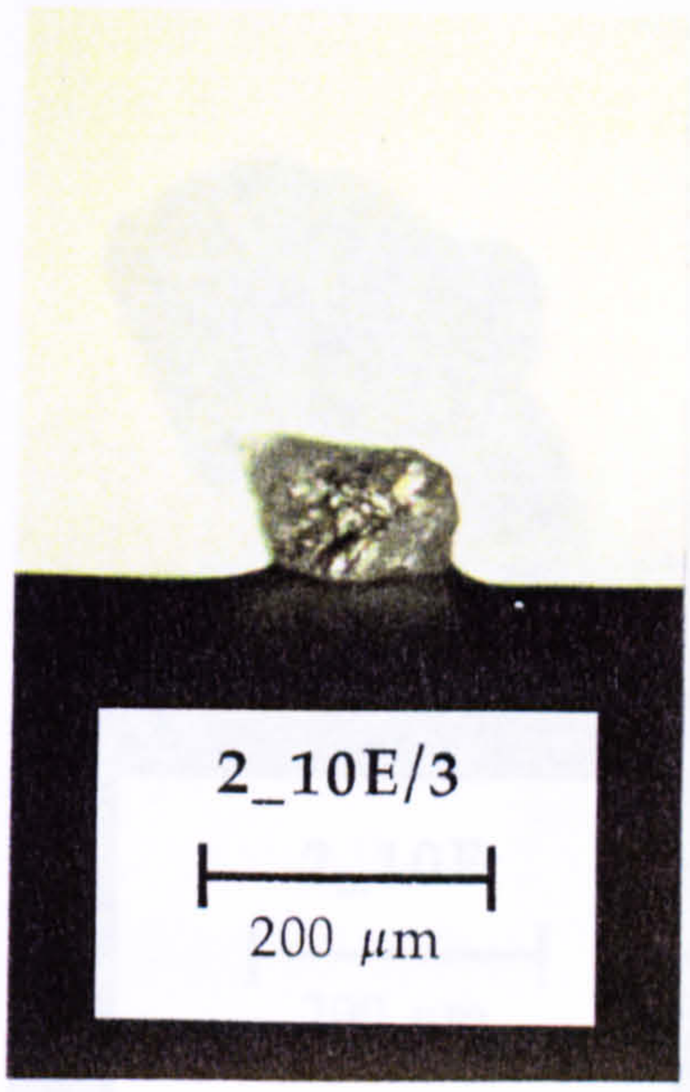

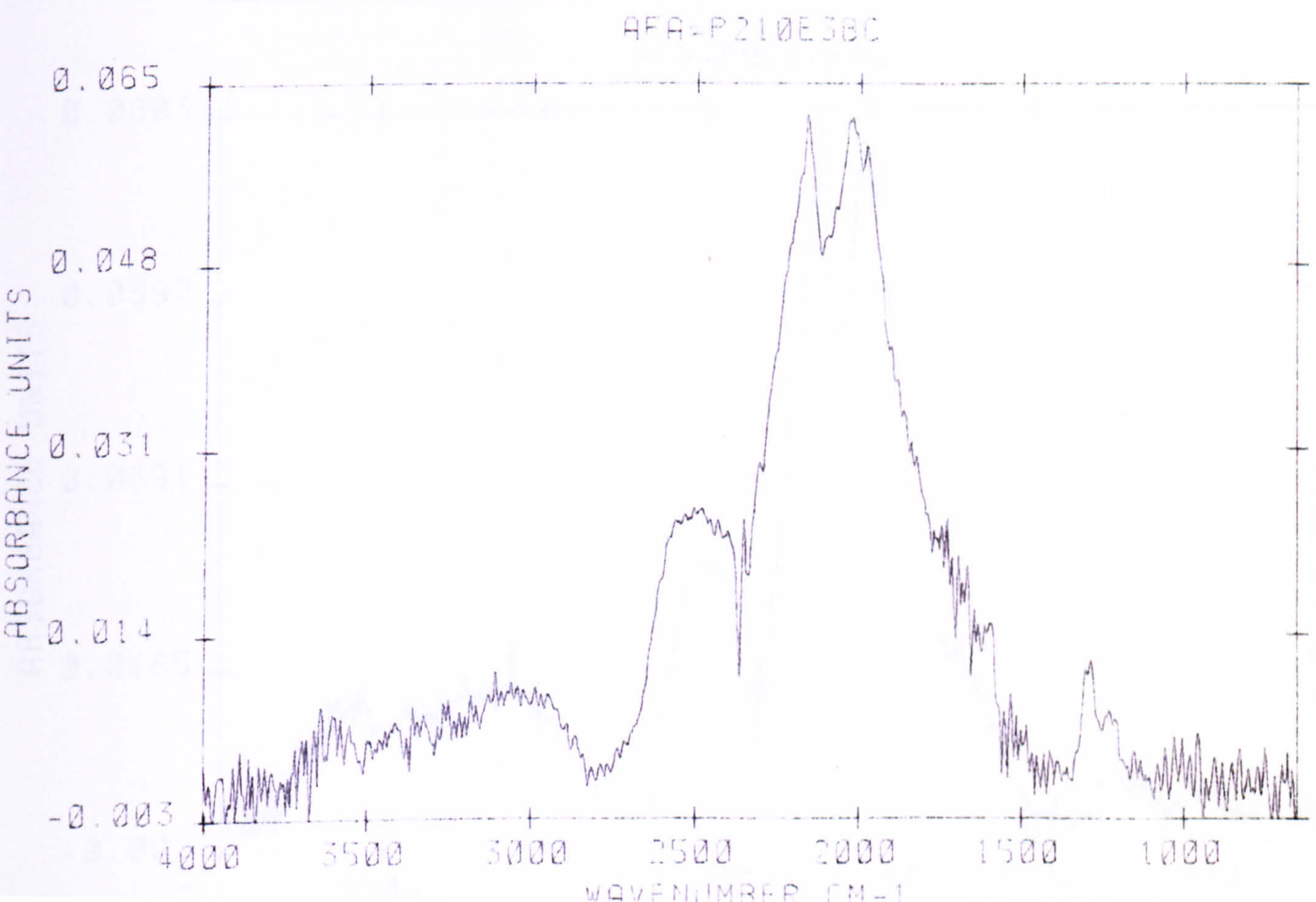

Sample No.	2_10F	Pathlength:	56.3 μm
Colour:	colourless	μ^{1282}:	0.2062 mm^{-1}
Form:	multiple octahedra, aggregate	Platelet area/ μ^{1282}:	0
Resorption:	none-low	H (3107 cm^{-1}) area:	0.67 mm^{-1}
Surface:	growth ribbing, minor pitting	Nitrogen:	31 at.ppm
		Aggregation (%B):	<0.5 %
Inclusions:	numerous silicates (pyroxene?)	T_{NA} (for t_{MR}= 1.0 Ga):	<1091 °C
Spectral Type:	IaA	T_{NA} (for t_{MR}= 3.0 Ga):	<1067 °C

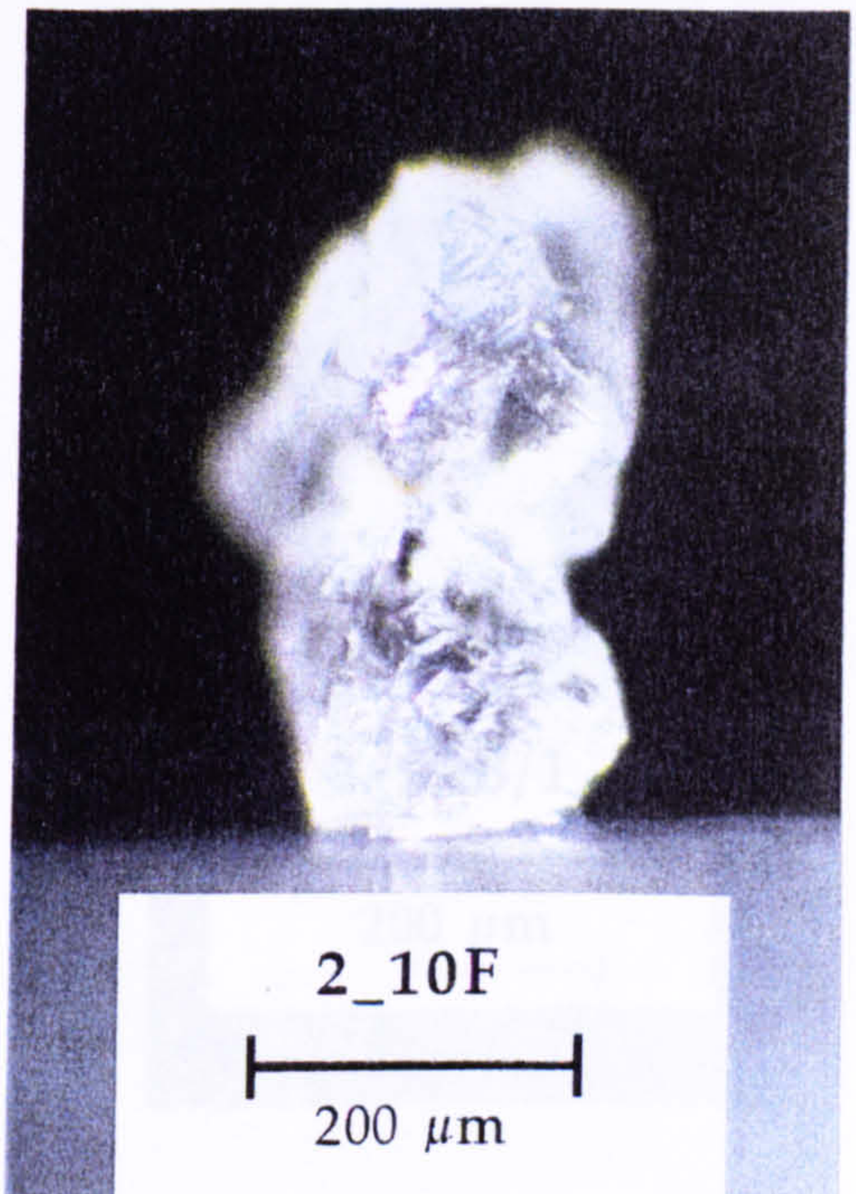

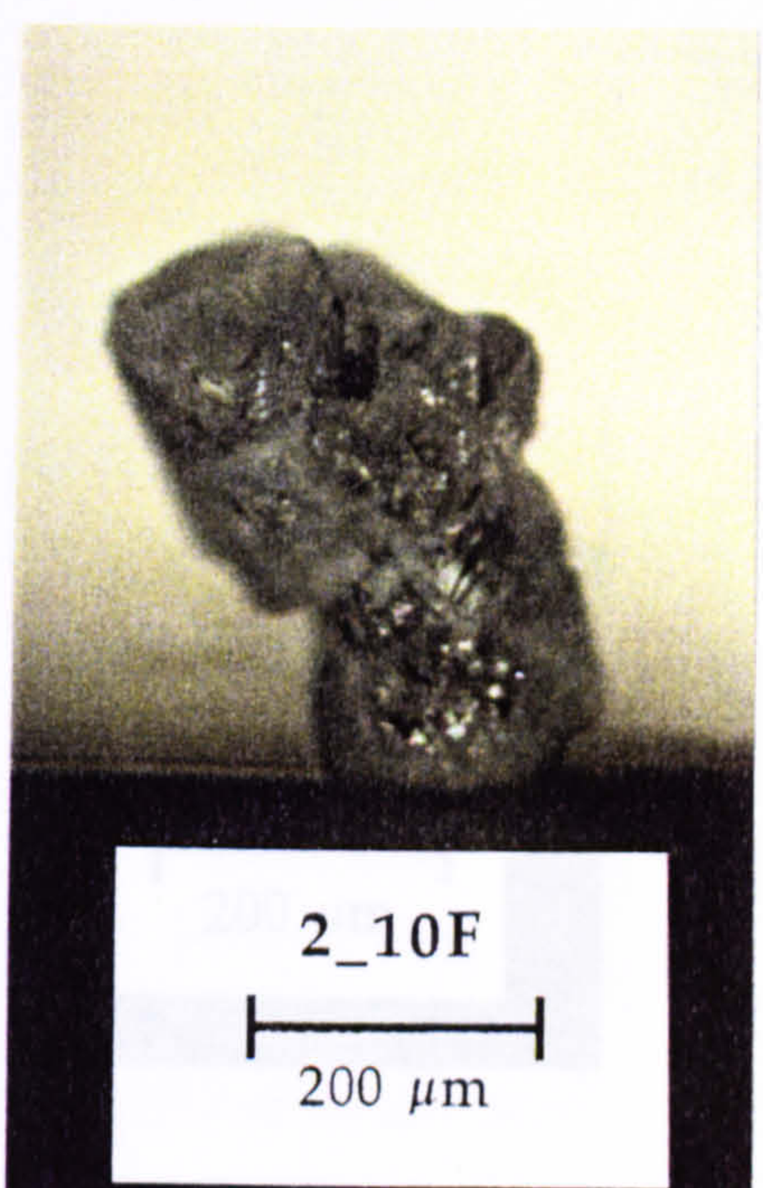

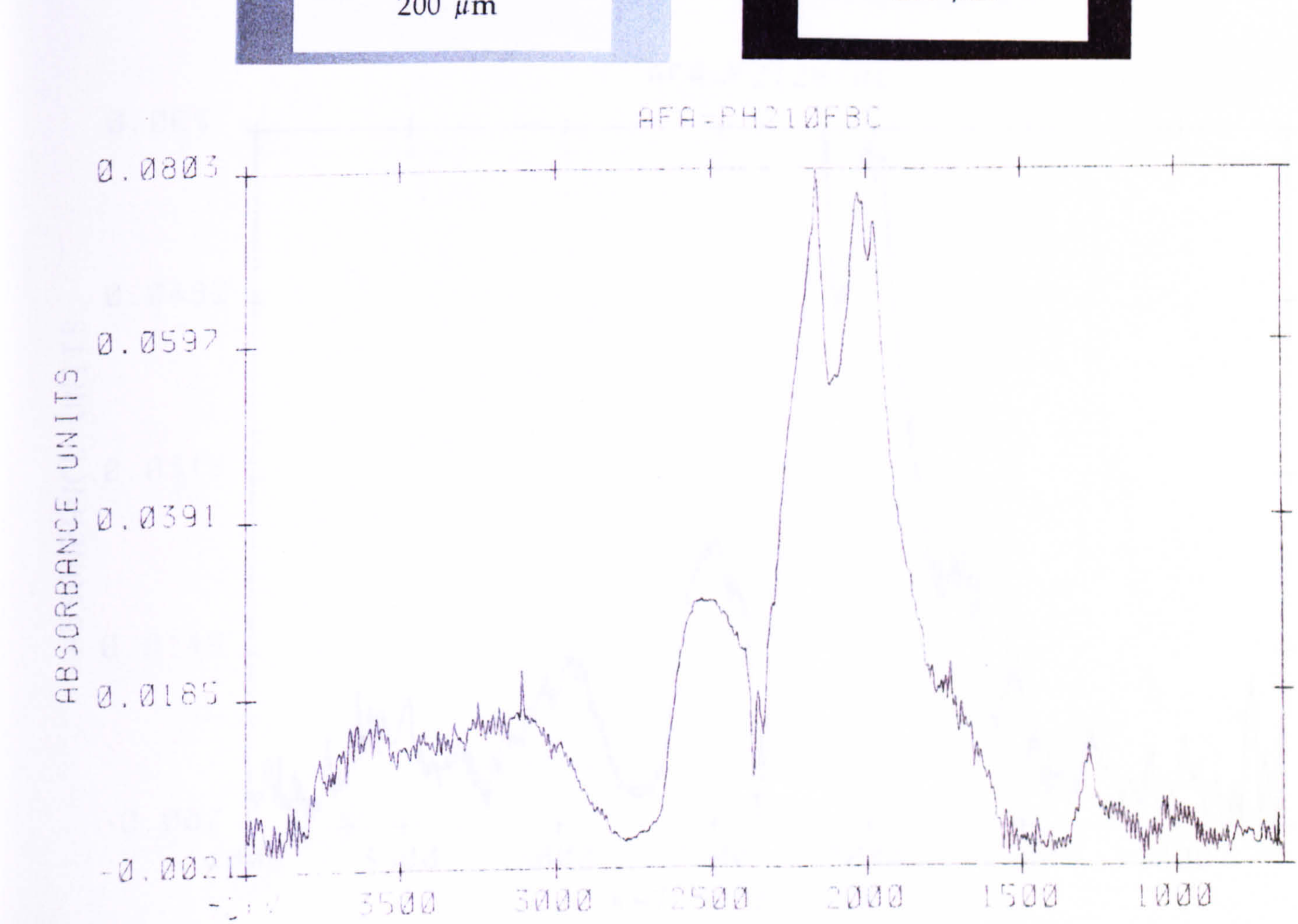

Sample No.	2_12B/1	Pathlength:	48.4 μm
Colour:	colourless	μ^{1282}:	0.1400 mm^{-1}
Form:	multiple intergrowth	Platelet area/ μ^{1282} :	0
Resorption:	moderate-high;	H (3107 cm^{-1}) area:	0
	differentially resorbed	Nitrogen:	21 at.ppm
Surface:	some fine pitting	Aggregation (%B):	<0.5
Inclusions:	silicate (bands at 1100-700 cm^{-1})	T_{NA} (for t_{MR}= 1.0 Ga):	1100 °C
Spectral Type:	IaA (v.weak)	T_{NA} (for t_{MR}= 3.0 Ga):	1075 °C

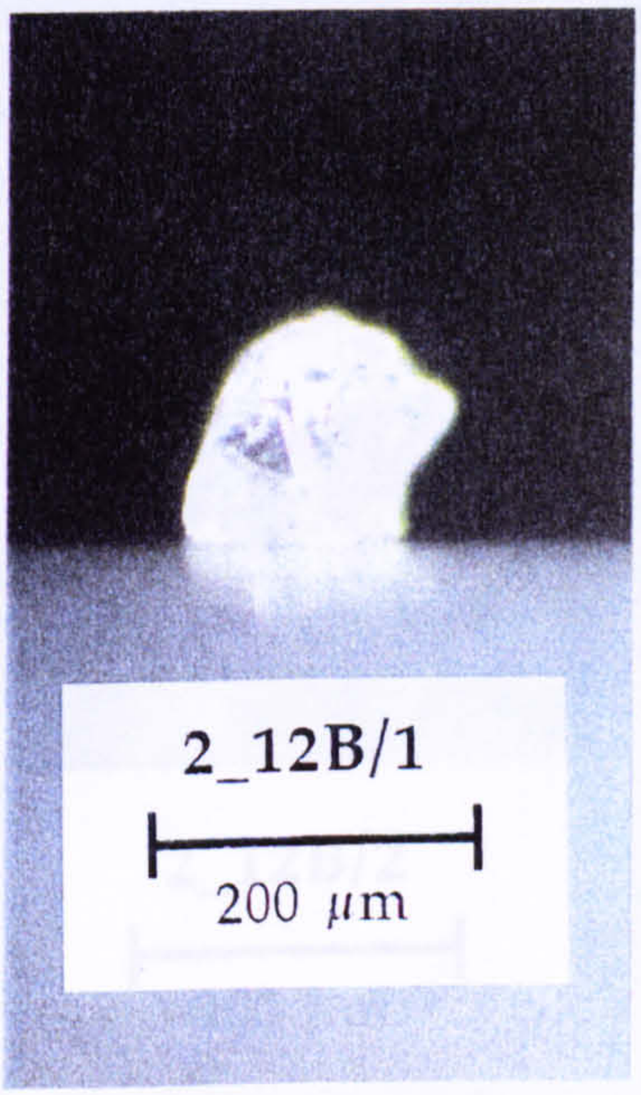

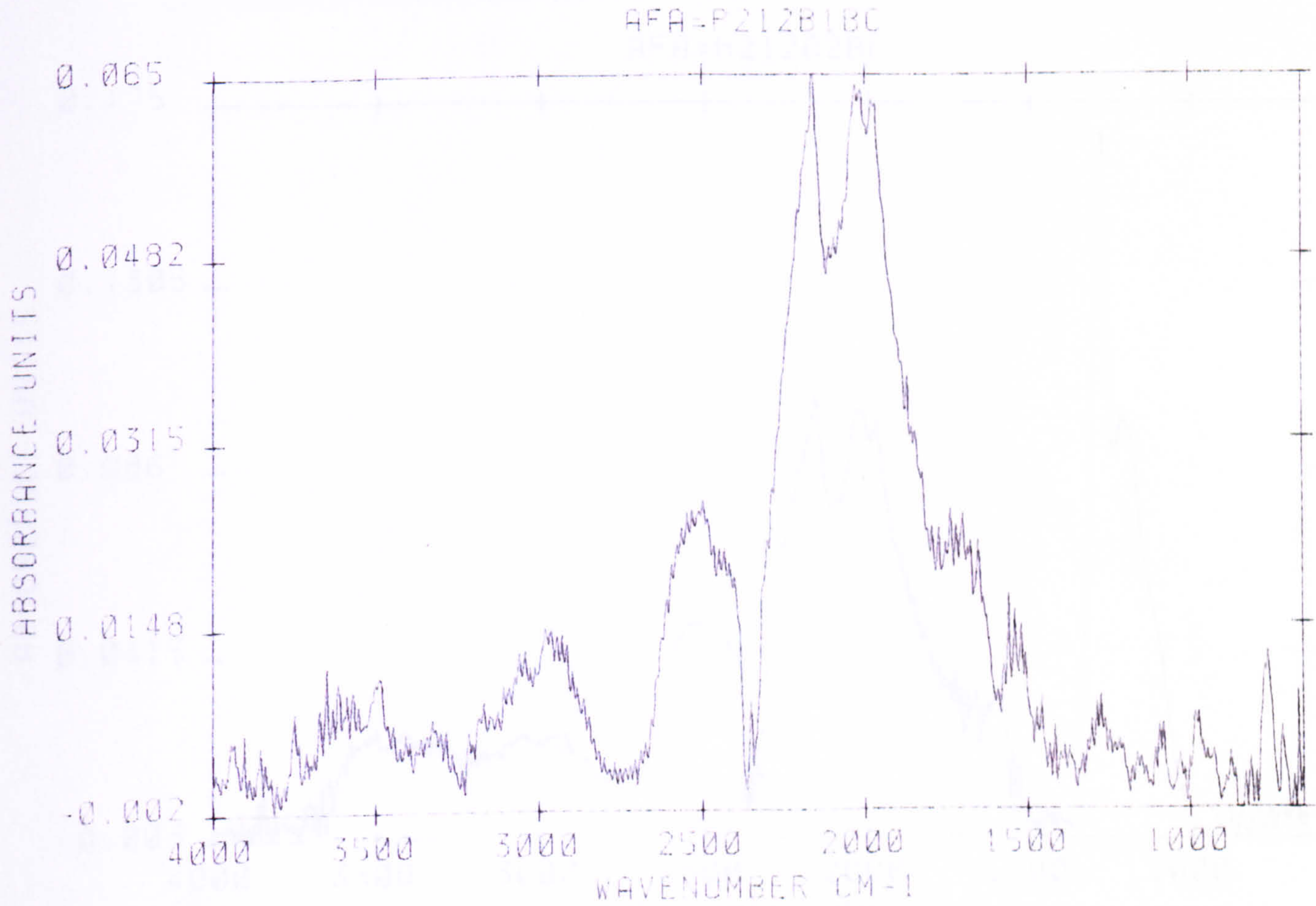

Sample No.	2_12B/2	Pathlength :	74.9 μm
Colour:	brown	μ^{1282} :	2.2507 mm^{-1}
Form:	multiple dodec. (broken)	Platelet area/ μ^{1282} :	0
Resorption:	high	H (3107 cm^{-1}) area:	0
Surface:	no etch features,	Nitrogen:	343 at.ppm
	fresh fracture surfaces	Aggregation (%B):	<0.5 %
Inclusions:	numerous dark inclusions	T_{NA} (for t_{MR}= 1.0 Ga):	<1039 °C
Spectral Type:	IaA	T_{NA} (for t_{MR}= 3.0 Ga):	<1016 °C

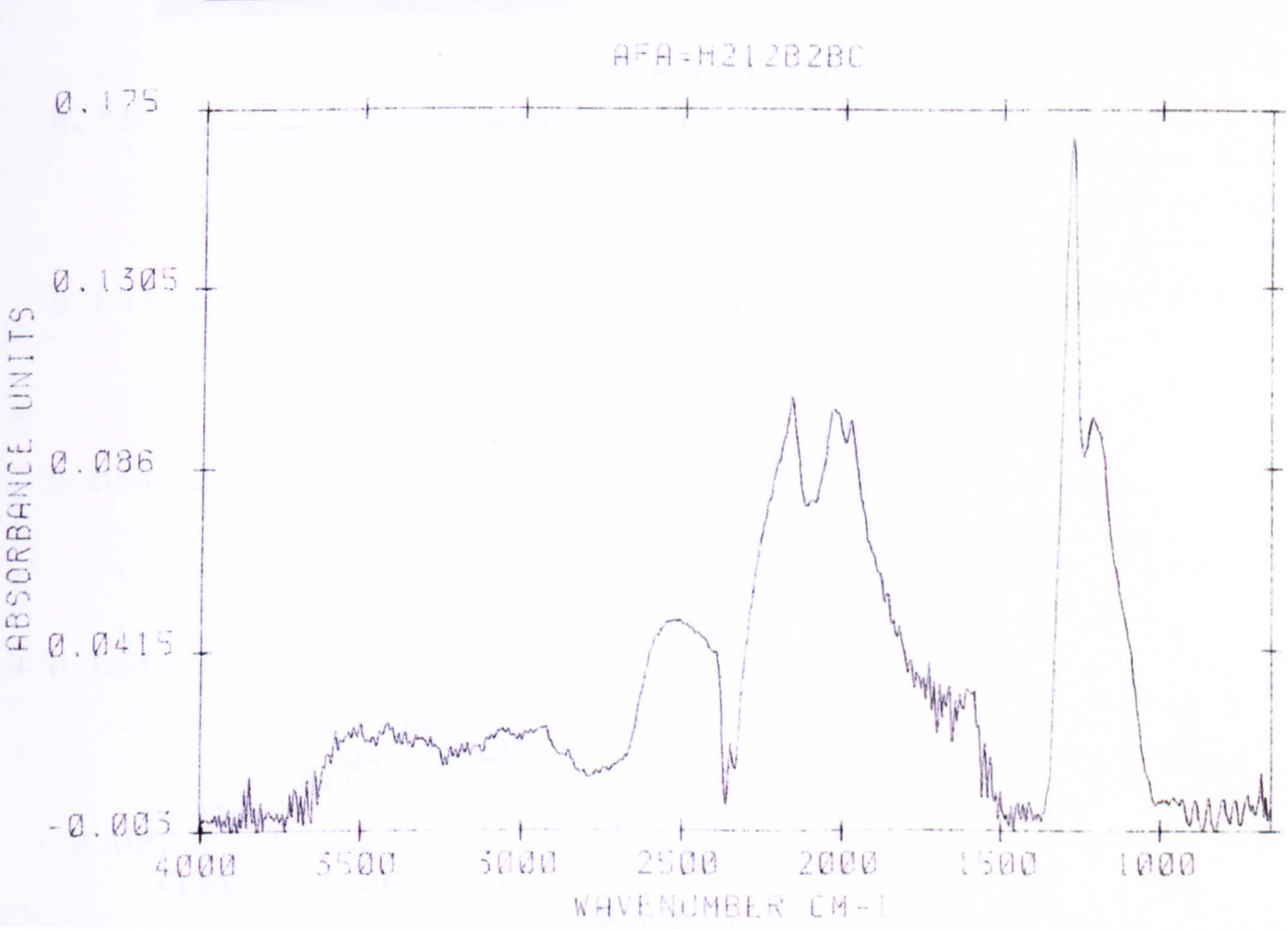

Sample No.	3_2/2	Pathlength:	50.6 μm
Colour:	colourless	μ^{1282}:	2.0493 mm^{-1}
Form:	fragment	Platelet area/ μ^{1282}:	0
Resorption:	unknown	H (3107 cm^{-1}) area:	0
Surface:	frosted external surfaces	Nitrogen:	313 at.ppm
	with minor graphite(?)	Aggregation (%B):	<0.5 %
Inclusions:	none identified	T_{NA} (for t_{MR}= 1.0 Ga):	<1041 °C
Spectral Type:	IaA	T_{NA} (for t_{MR}= 3.0 Ga):	<1018 °C

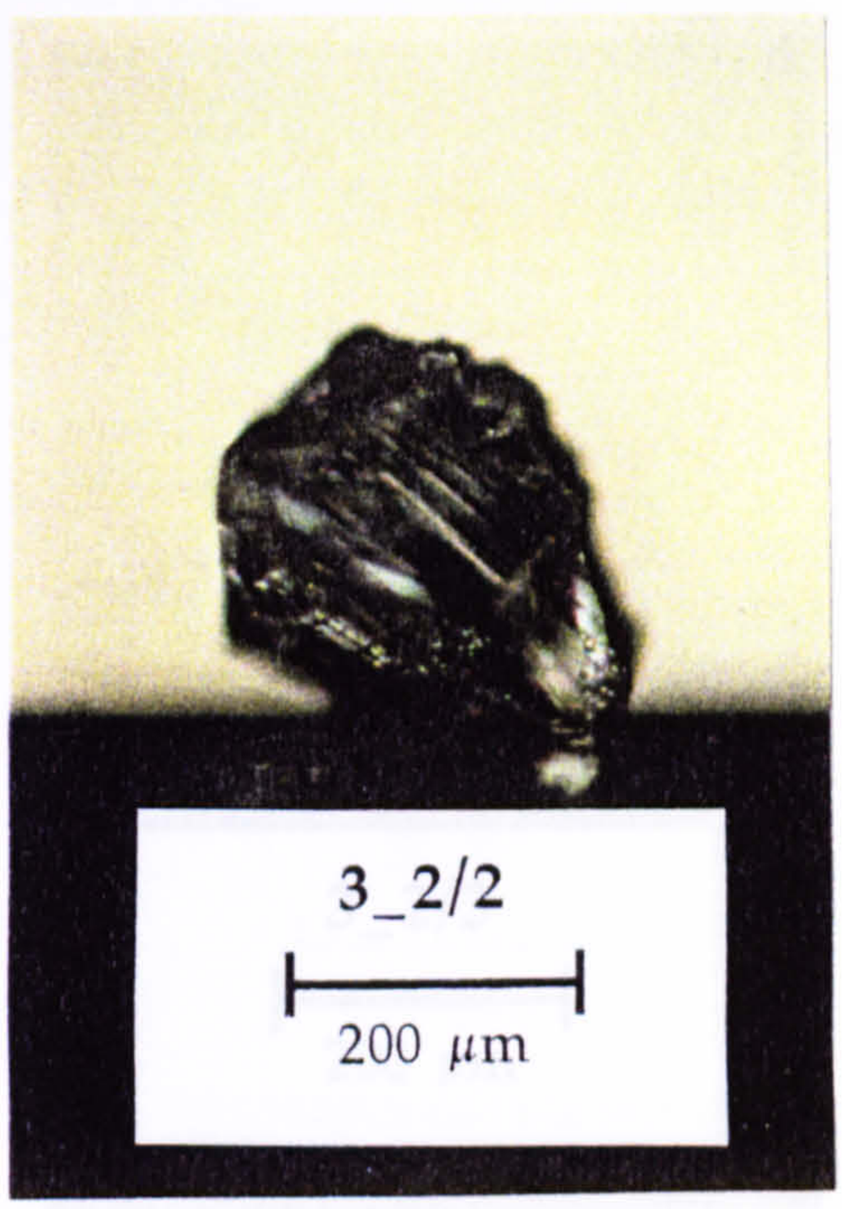

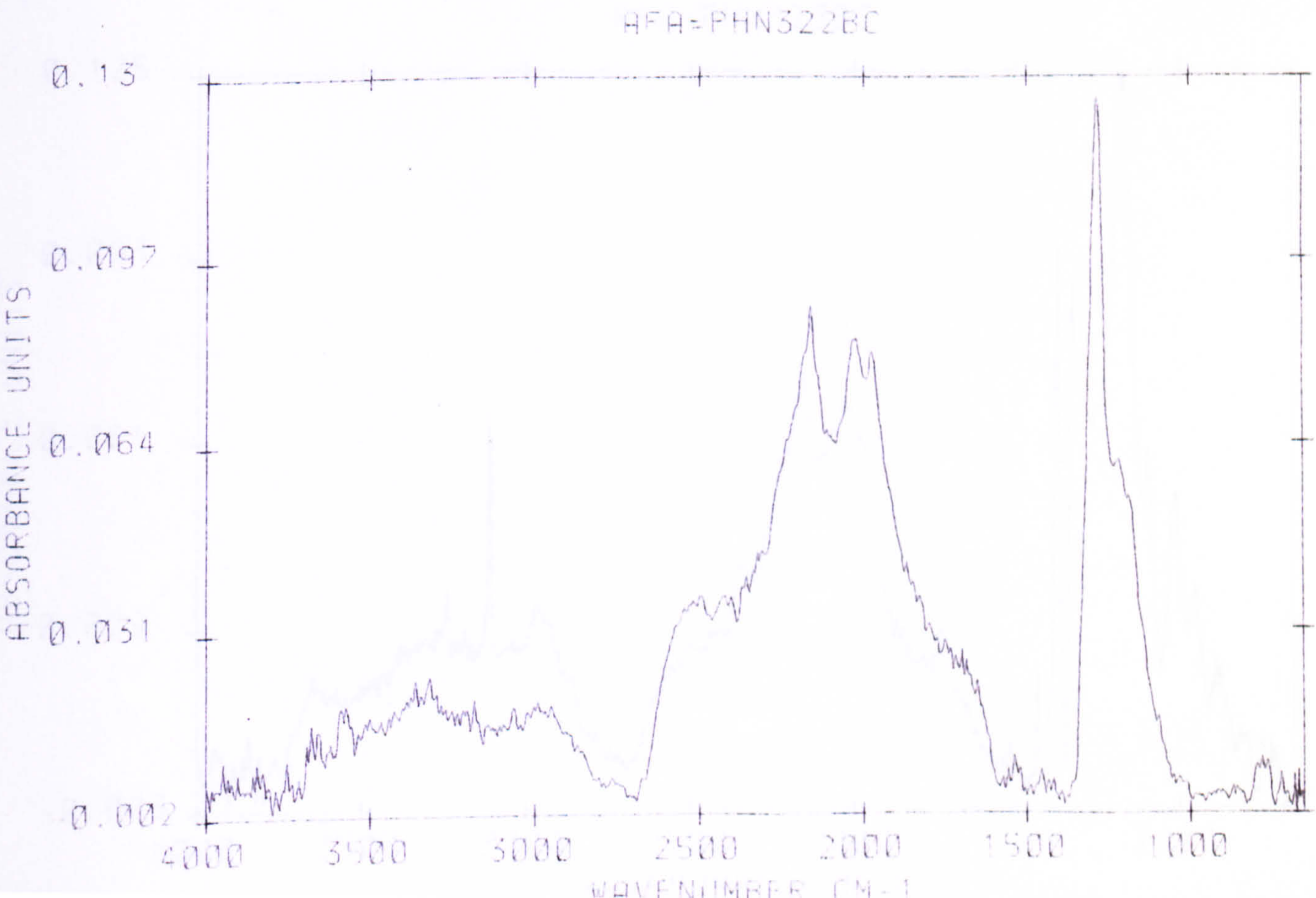

Sample No.	3_2/3
Colour:	colourless
Form:	fragment
Resorption:	unknown
Surface:	fresh fractures only
Inclusions:	none identified
Spectral Type:	IaB

Pathlength:	50.6 μm
μ^{1282}:	1.2673 mm^{-1}
Platelet area/ μ^{1282}:	21.3
H (3107 cm^{-1}) area:	7.31 mm^{-1}
Nitrogen:	797 at.ppm
Aggregation (%B):	98.8 %
T_{NA} (for t_{MR}= 1.0 Ga):	1262 °C
T_{NA} (for t_{MR}= 3.0 Ga):	1231 °C

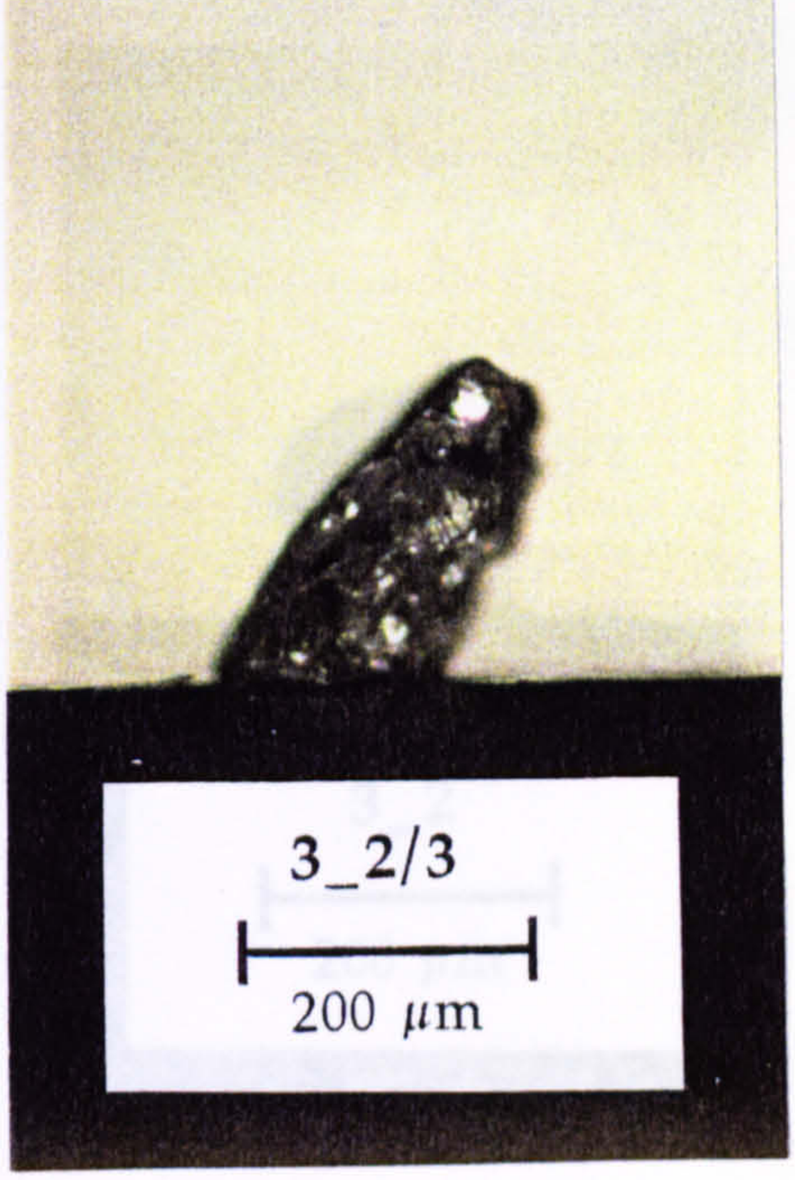

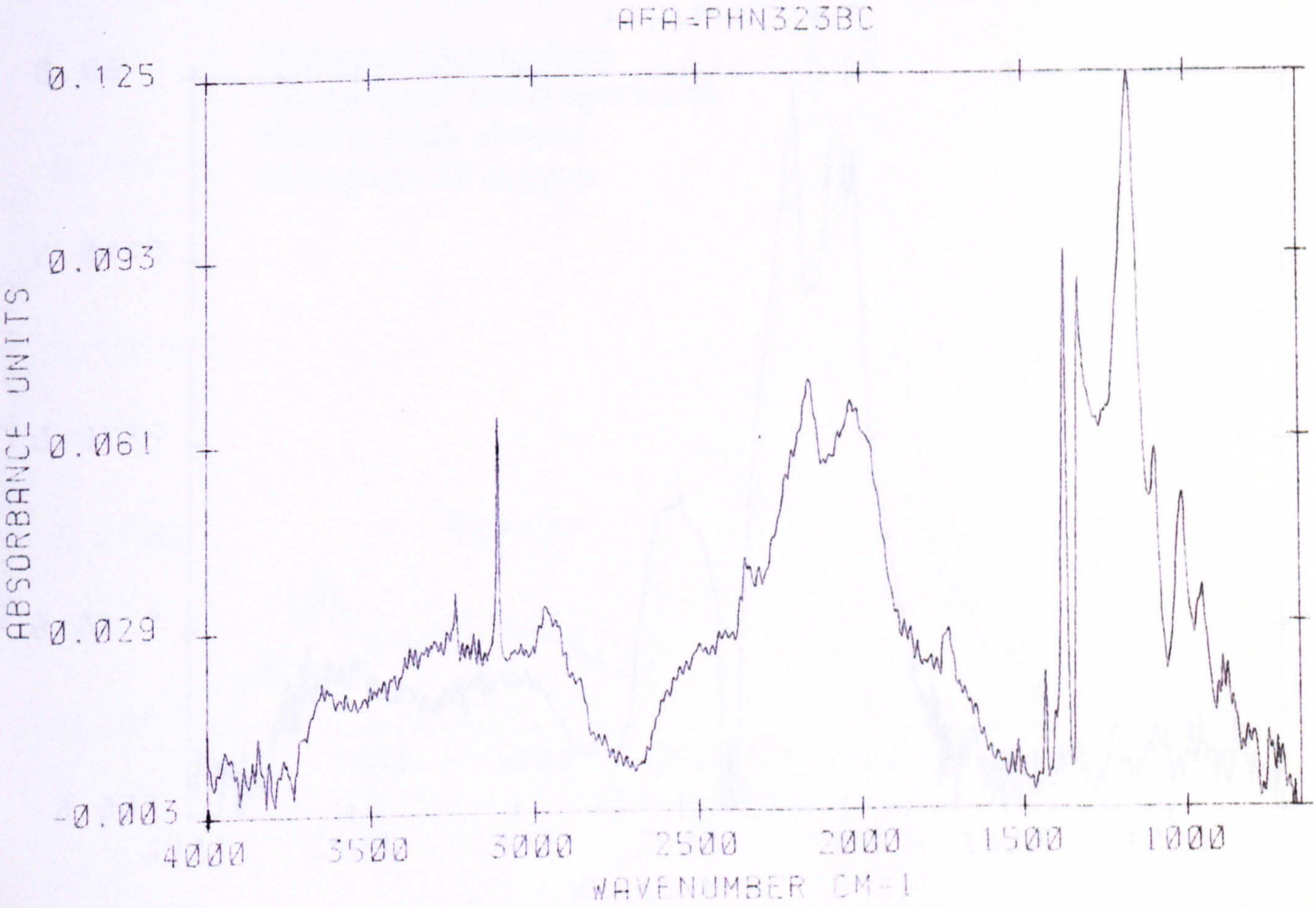

Sample No.	3_2
Colour:	colourless
Form:	rounded with dodecahedral faces, broken
Resorption:	high
Surface:	no etch features
Inclusions:	none identified
Spectral Type:	IIa

Pathlength:	39.5 μm
μ^{1282}:	0.0371 mm^{-1}
Platelet area/ μ^{1282}:	0
H (3107 cm^{-1}) area:	0.76 mm^{-1}
Nitrogen:	<6 at. ppm
Aggregation (%B):	-
T_{NA} (for t_{MR}= 1.0 Ga):	-
T_{NA} (for t_{MR}= 3.0 Ga):	-

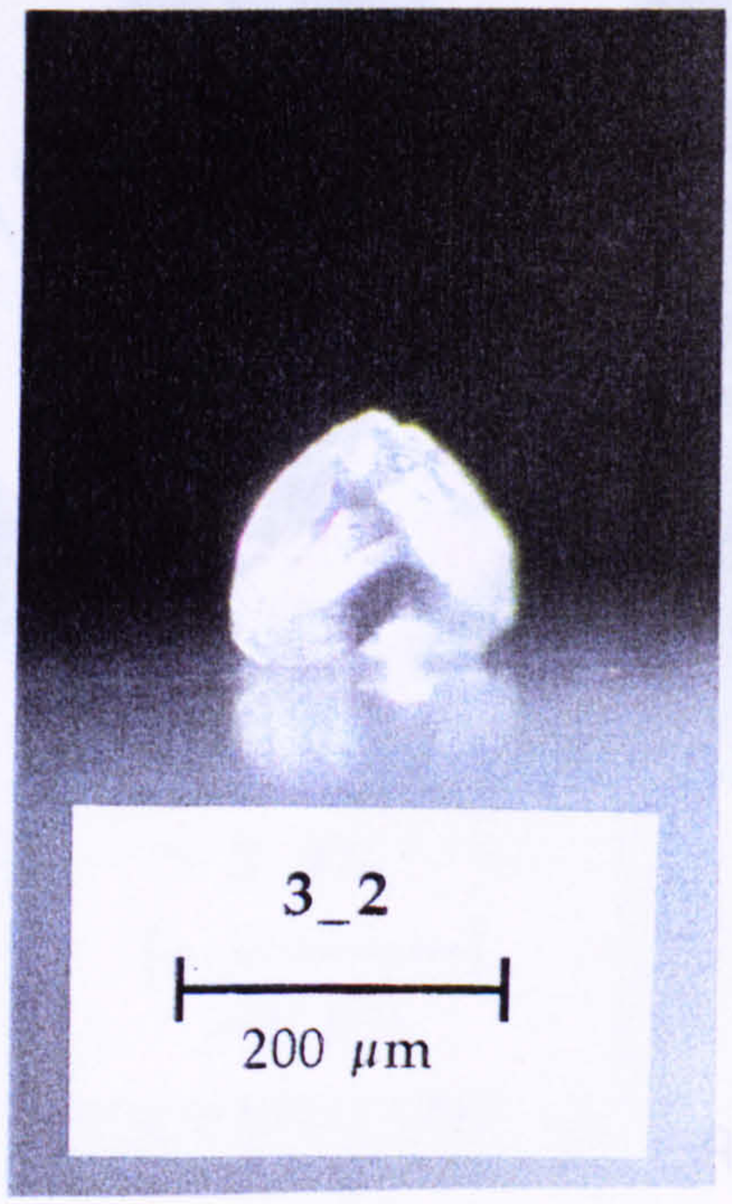

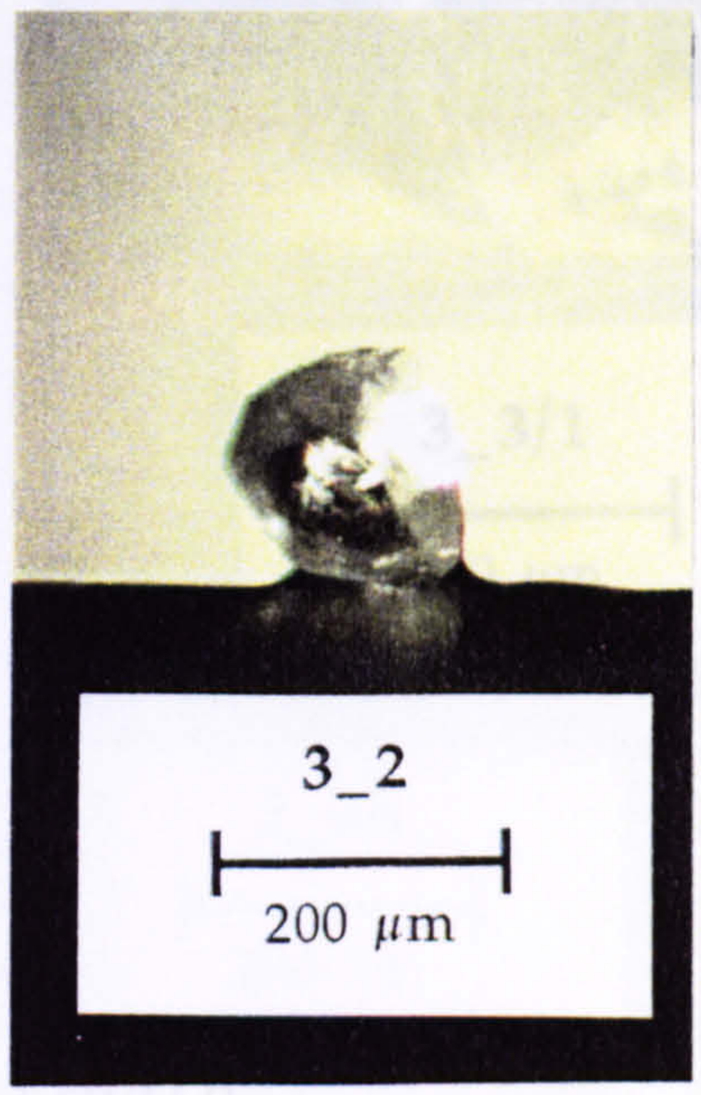

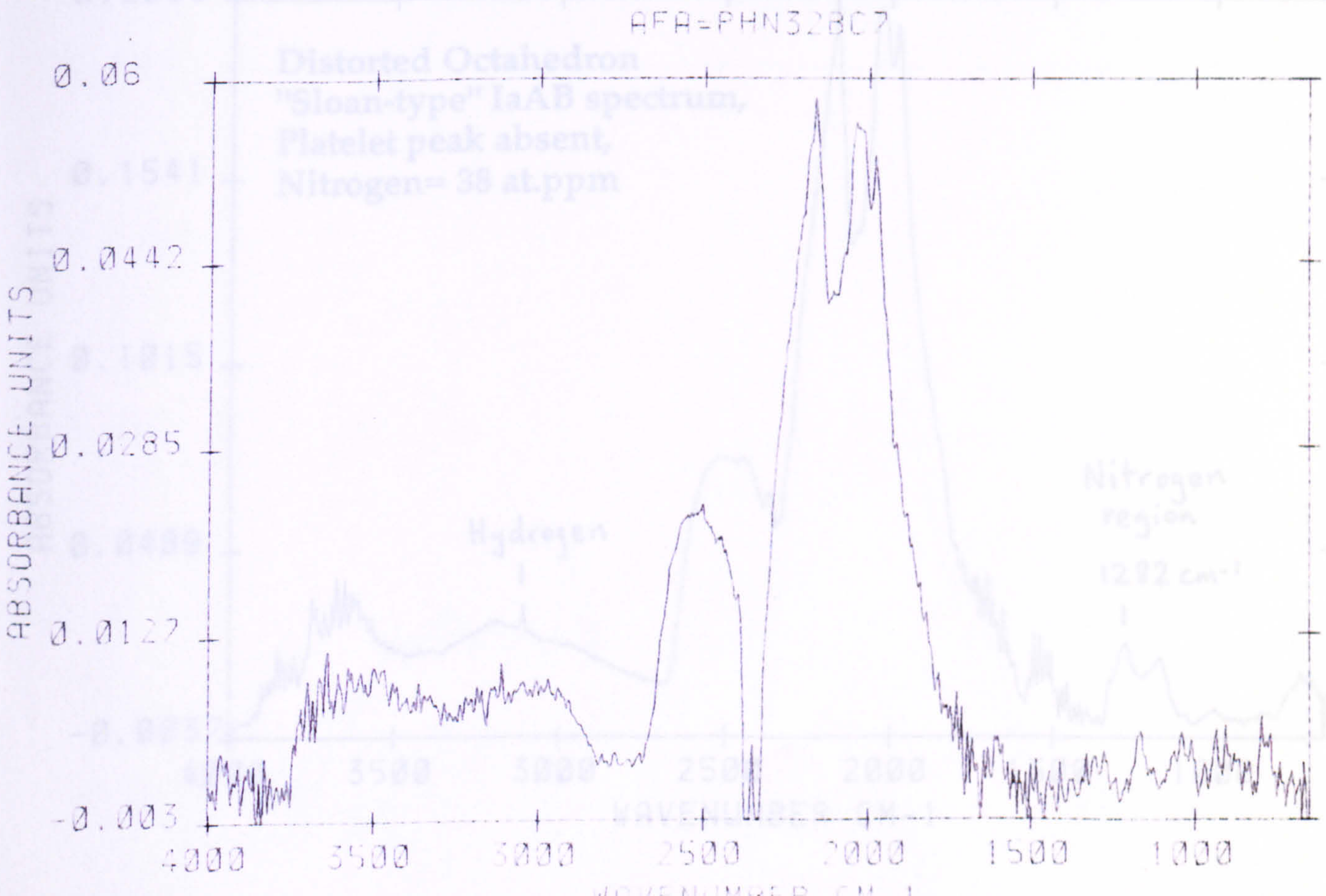

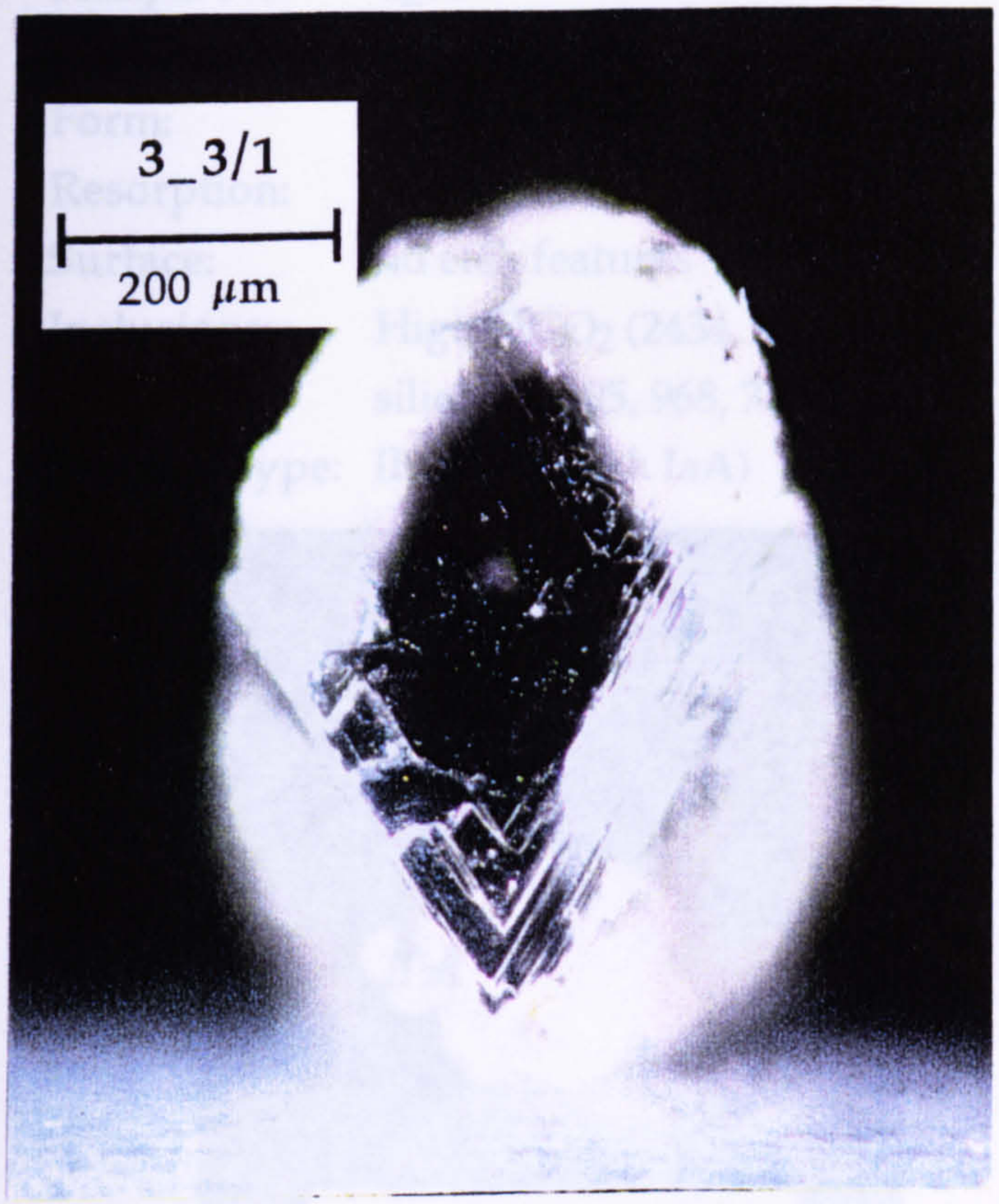
3_3/1
200 μm

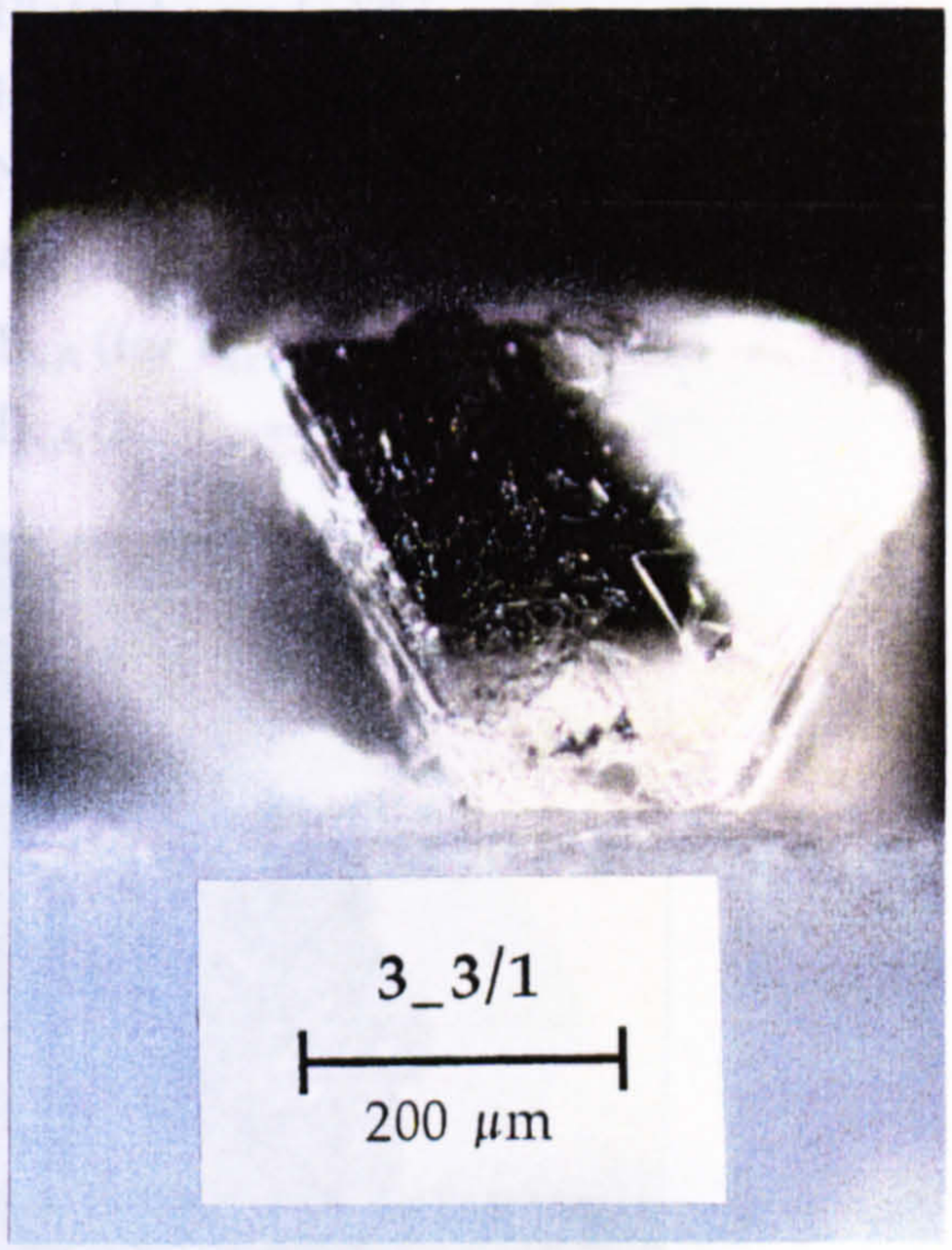
3_3/1
200 μm

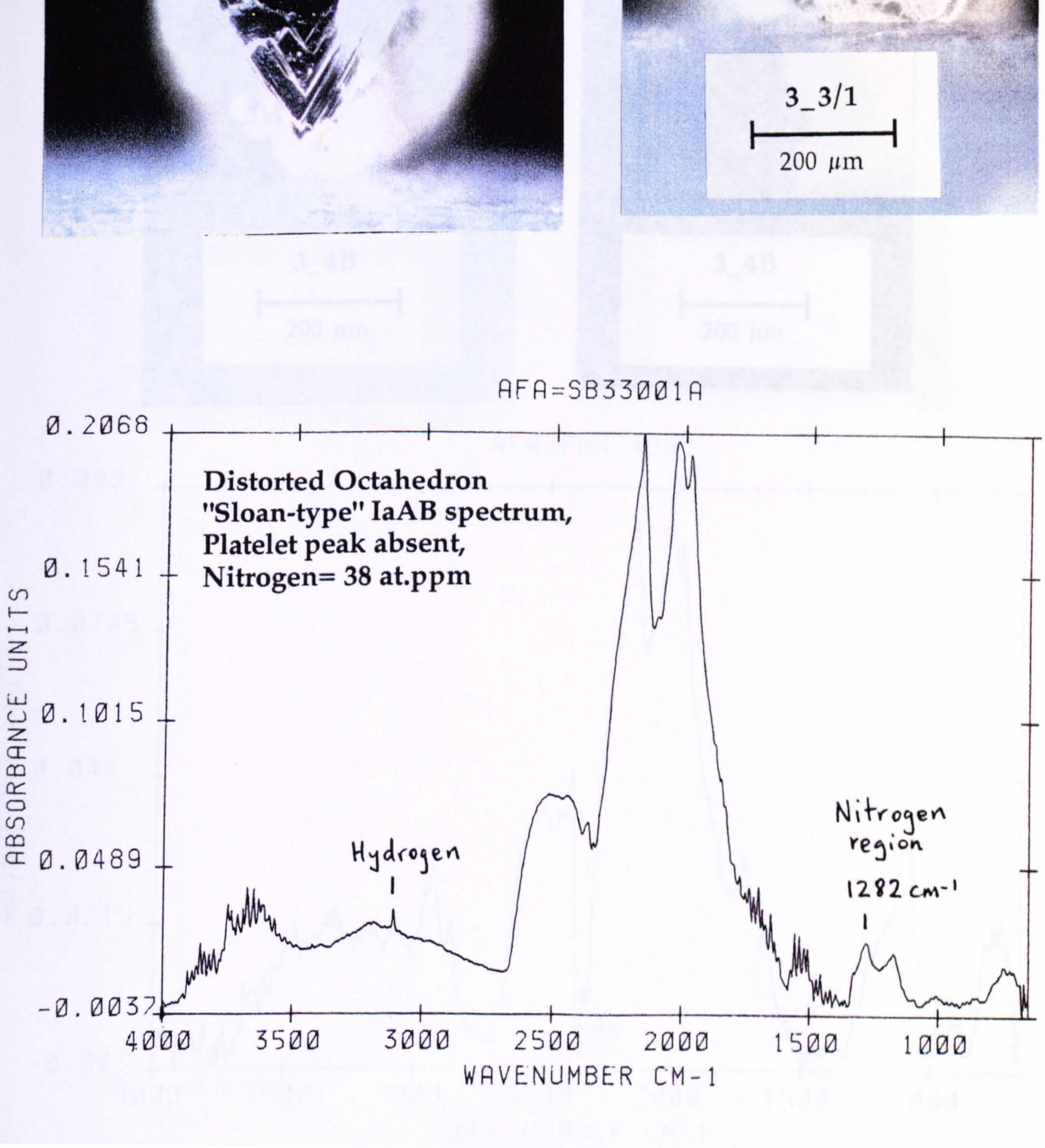
AFA=SB33001A
0.2068
0.1541
0.1015
0.0489
-0.0037
ABSORBANCE UNITS
Distorted Octahedron
"Sloan-type" IaAB spectrum,
Platelet peak absent,
Nitrogen= 38 at.ppm
Hydrogen
Nitrogen region
1282 cm-1
4000
3500
3000
2500
2000
1500
1000
WAVENUMBER CM-1

Sample No.	3_4B	Pathlength:	66.1 μm
Colour:	colourless	μ^{1282}:	0.1080 mm^{-1}
Form:	mult. rounded octa, aggregate	Platelet area/ μ^{1282}:	0
Resorption:	moderate	H (3107 cm^{-1}) area:	0 mm^{-1}
Surface:	no etch features	Nitrogen:	<15 at. ppm
Inclusions:	High-P CO_2 (2434, 2393 cm^{-1}),	Aggregation (%B):	-
	silicate (1095, 968, 740 cm^{-1})	T_{NA} (for t_{MR}= 1.0 Ga):	-
Spectral Type:	IIa (or v.weak IaA)	T_{NA} (for t_{MR}= 3.0 Ga):	-

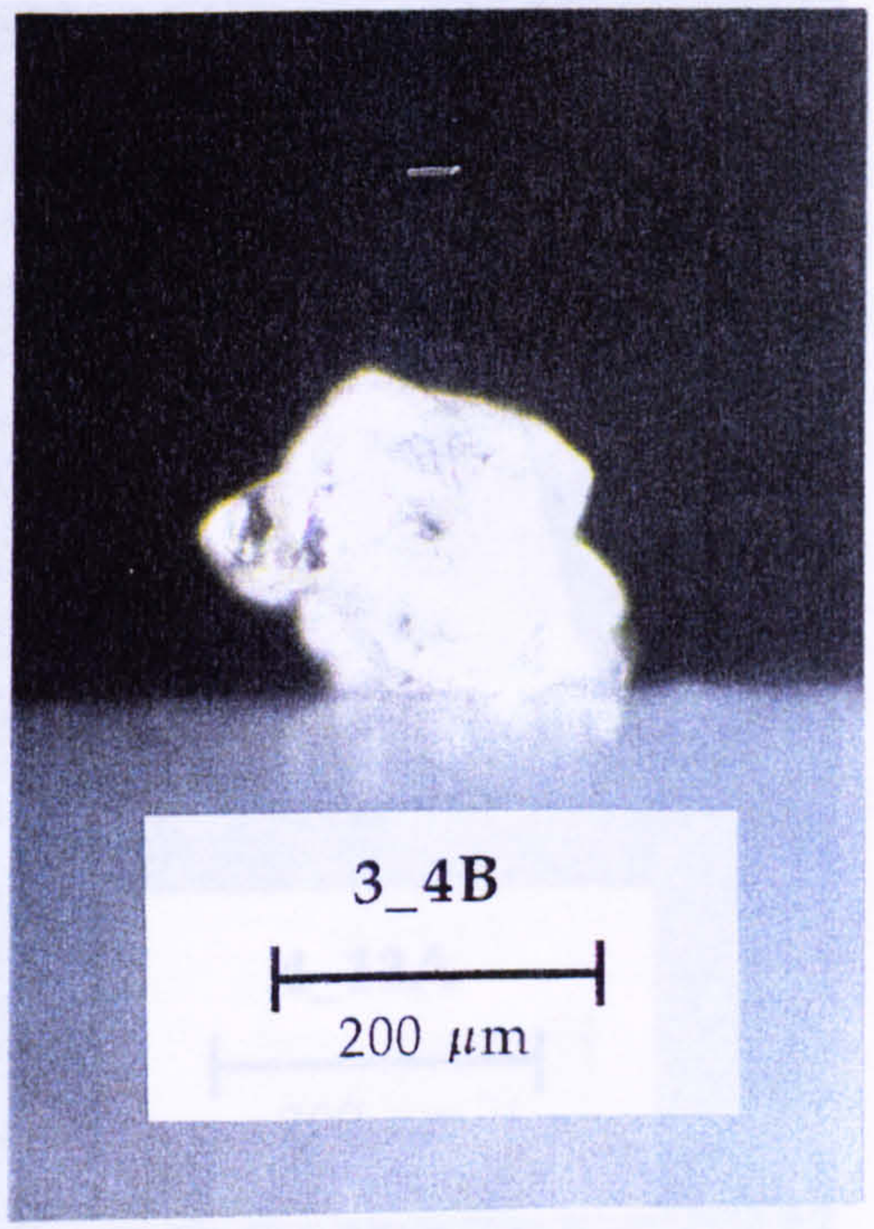

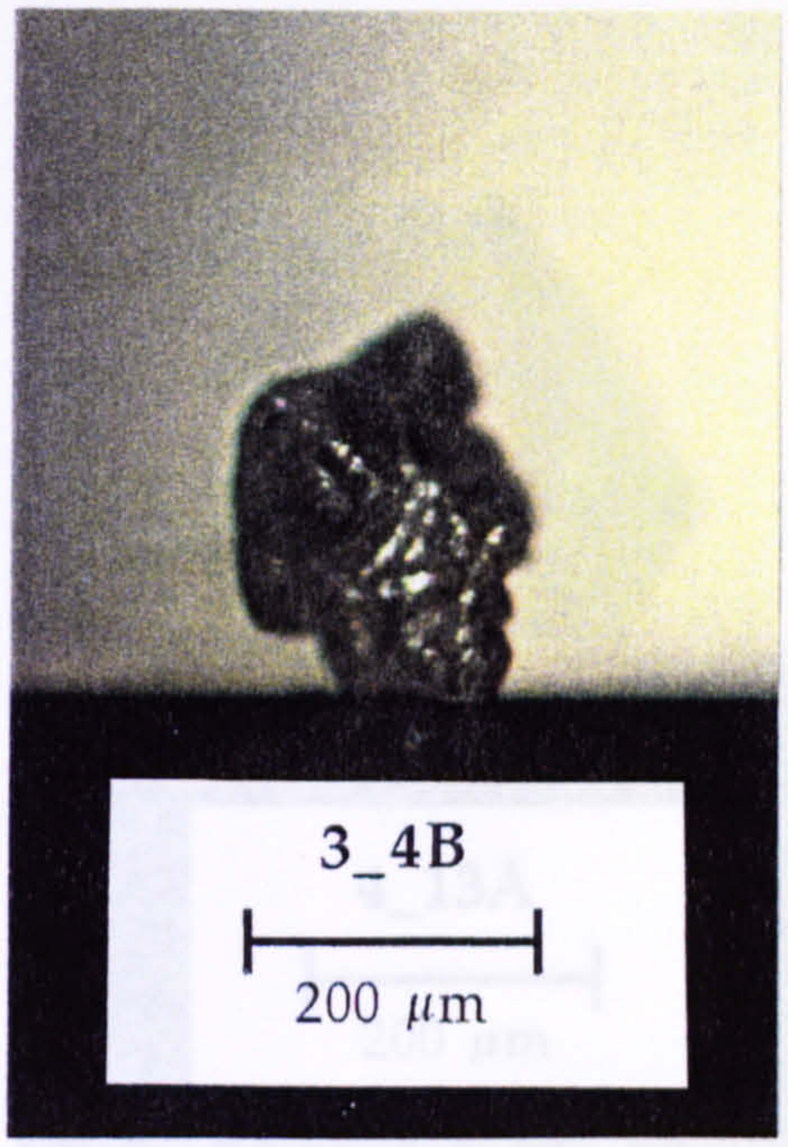

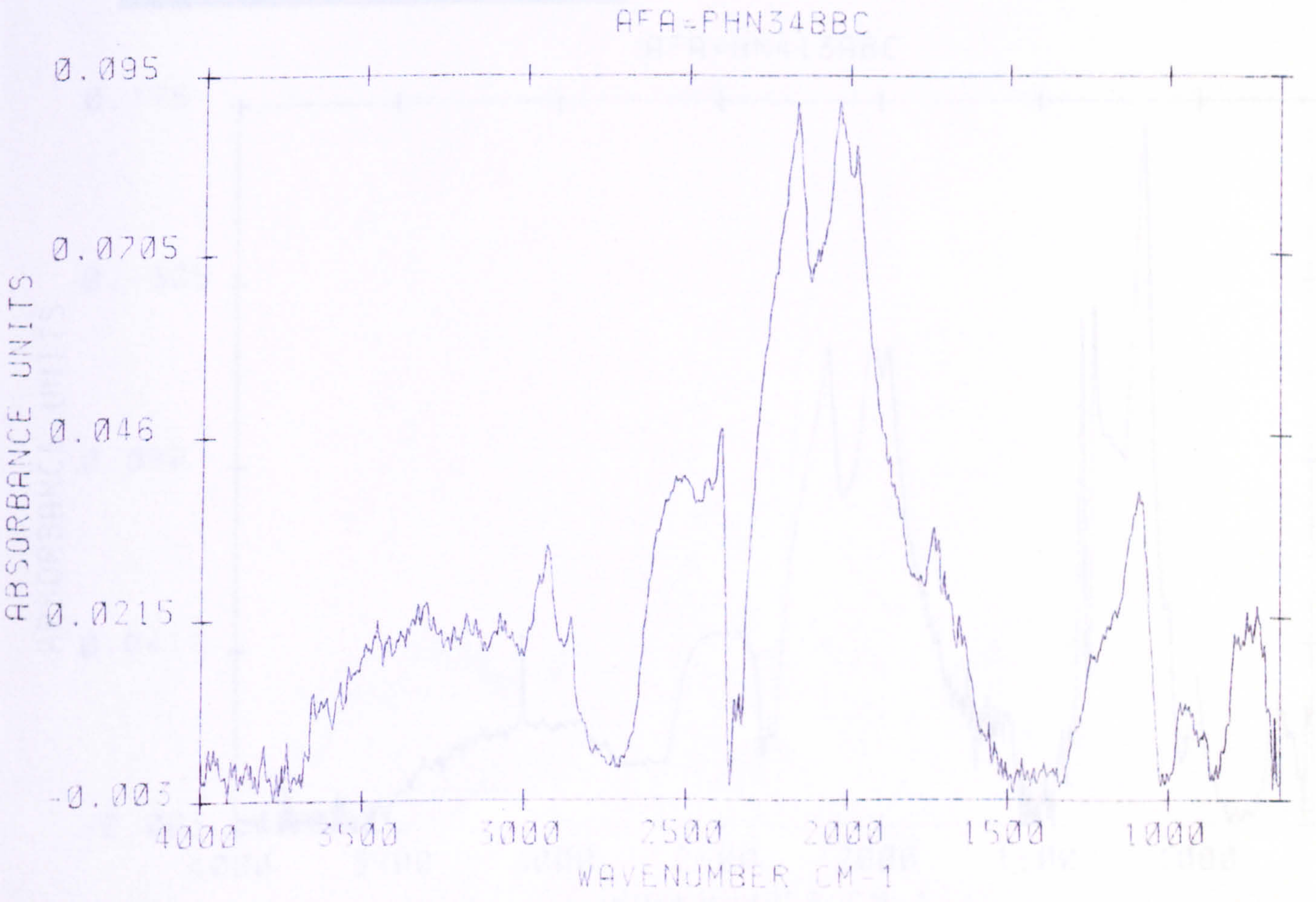

Sample No.	4_13A	Pathlength :	86.4 μm
Colour:	pale brown	μ^{1282}:	1.0684 mm^{-1}
Form:	fragment of octahedron(?)	Platelet area/ μ^{1282} :	16.1
Resorption:	none-low?	H (3107 cm^{-1}) area:	2.32 mm^{-1}
Surface:	one frosted/etched face,	Nitrogen:	645 at.ppm
	and fresh fractures	Aggregation (%B):	97.5 %
Inclusions:	none identified	T_{NA} (for t_{MR}= 1.0 Ga):	1247 °C
Spectral Type:	IaB	T_{NA} (for t_{MR}= 3.0 Ga):	1216 °C

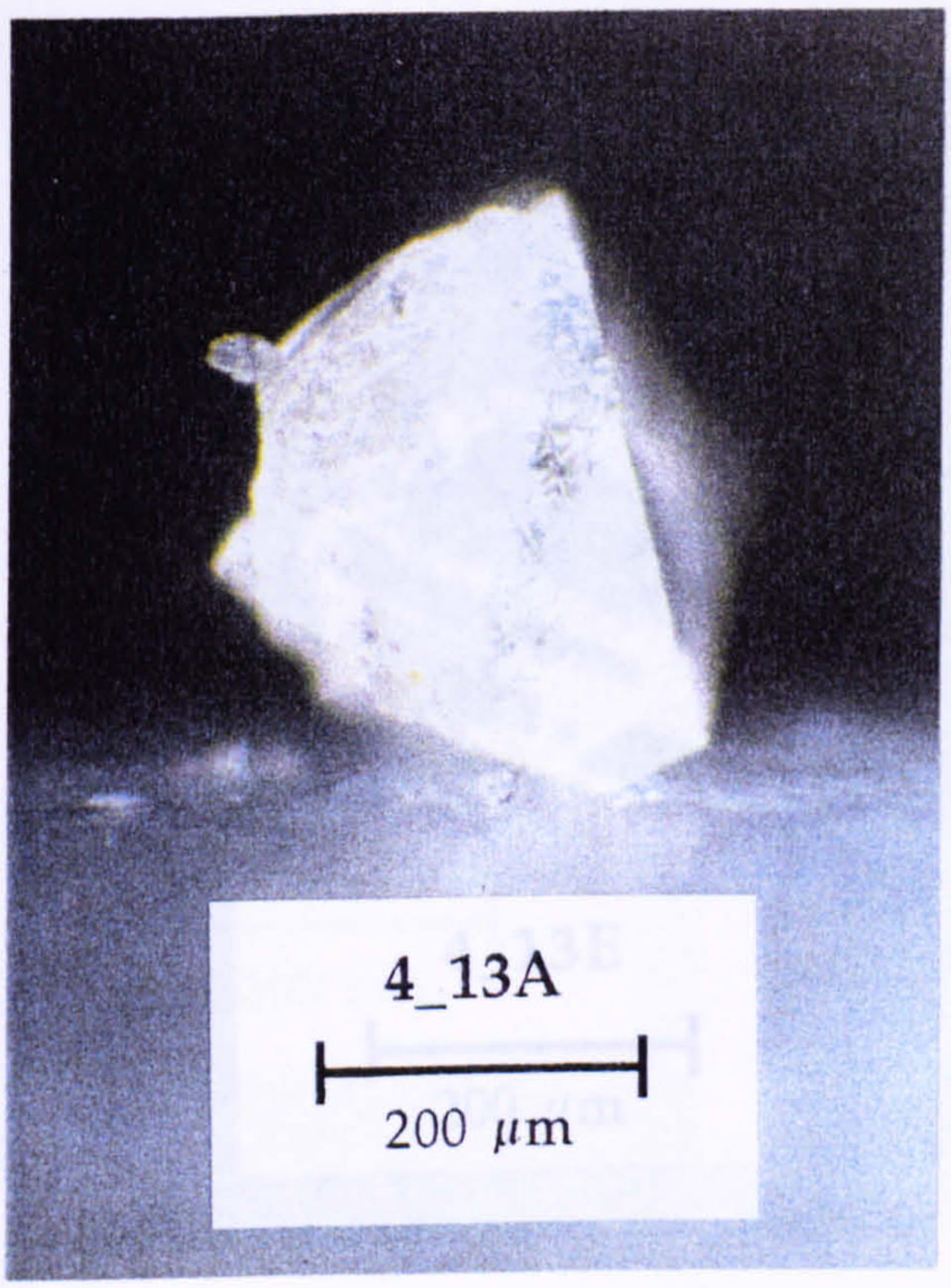

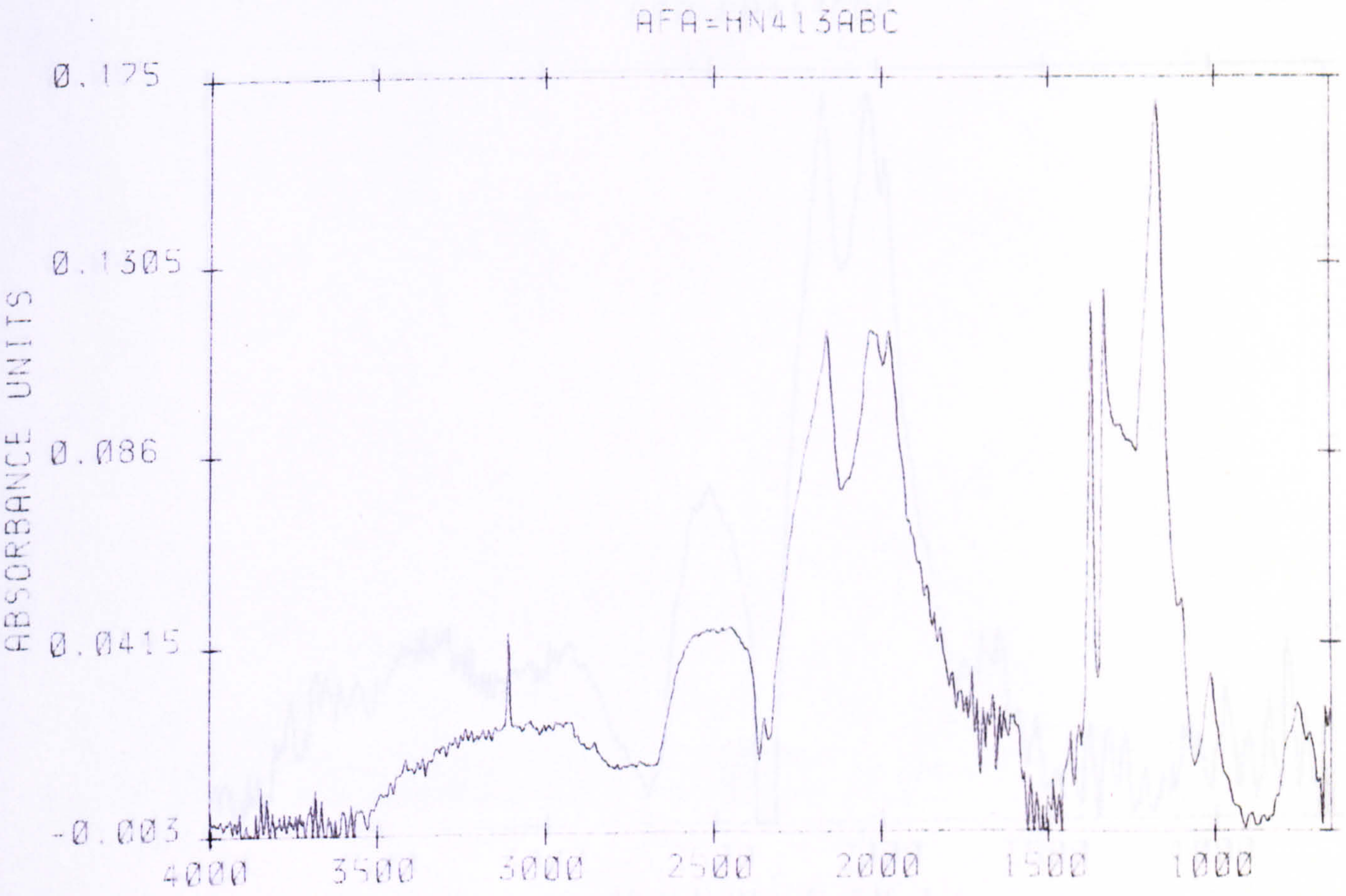

Sample No.	4_13E	Pathlength:	43.7 μm
Colour:	pale brown	μ^{1282}:	0.0685 mm^{-1}
Form:	flat; highly distorted octahedron?	Platelet area/ μ^{1282}:	0
		H (3107 cm^{-1}) area:	0 mm^{-1}
Resorption:	none-low	Nitrogen:	<10 at. ppm
Surface:	parallel growth(?) steps	Aggregation (%B):	-
Inclusions:	none identified	T_{NA} (for t_{MR}= 1.0 Ga):	-
Spectral Type:	IIa	T_{NA} (for t_{MR}= 3.0 Ga):	-

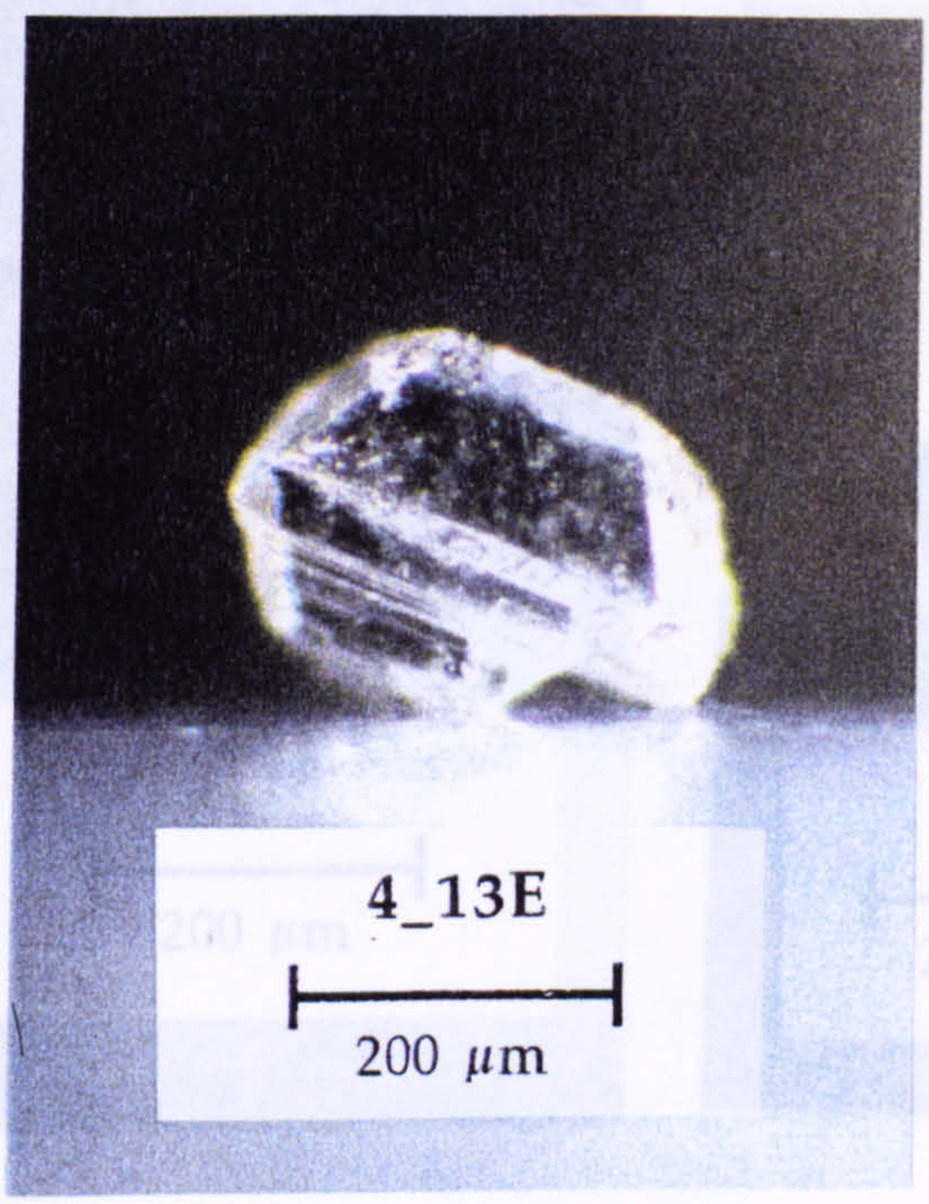

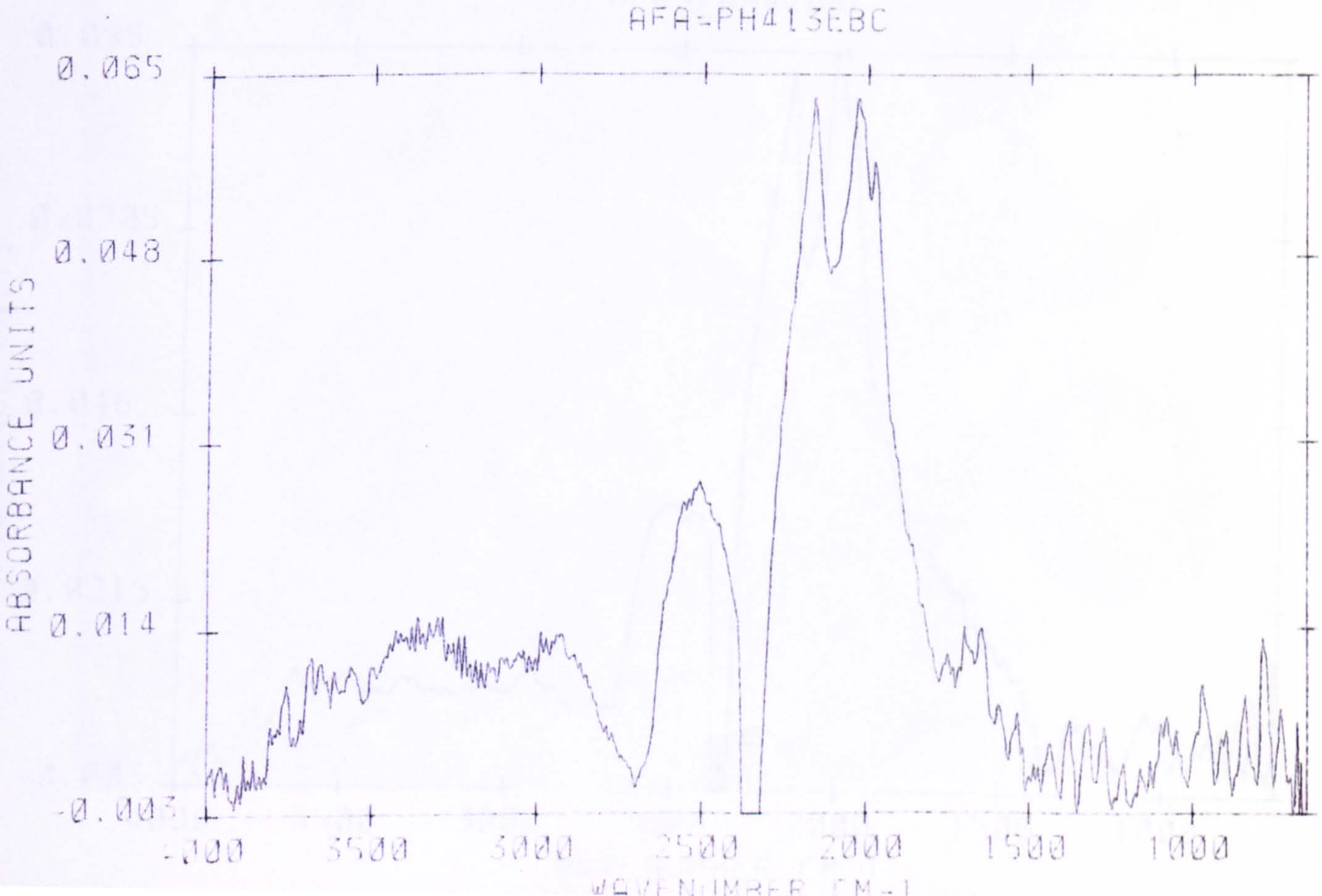

Sample No.	4_18	Pathlength:	69.7 μm
Colour:	colourless	μ^{1282}:	0.0902 mm^{-1}
Form:	multiple, sharp-edged octahedra	Platelet area/ μ^{1282}:	0
		H (3107 cm^{-1}) area:	0 mm^{-1}
Resorption:	none-low	Nitrogen:	14 at. ppm
Surface:	no etch features	Aggregation (%B):	<0.5 % (?)
Inclusions:	graphite?	T_{NA} (for t_{MR}= 1.0 Ga):	<1111 °C
Spectral Type:	IaA (v. weak)	T_{NA} (for t_{MR}= 3.0 Ga):	<1085 °C

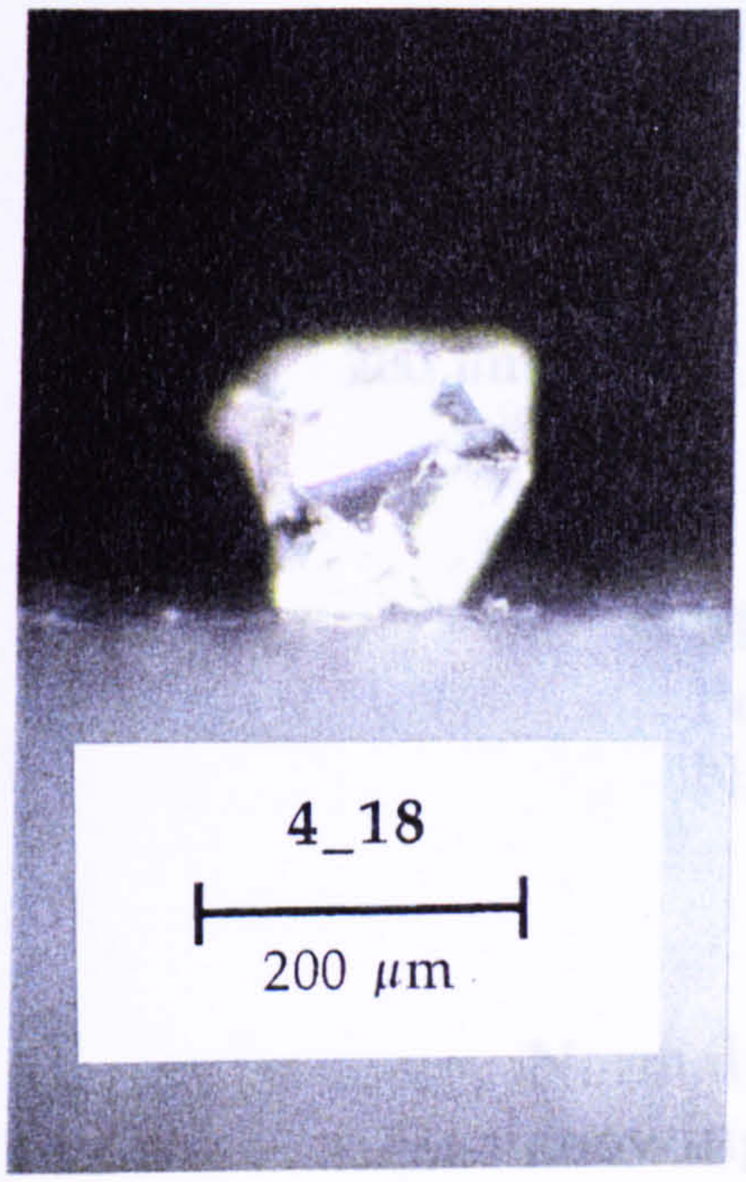

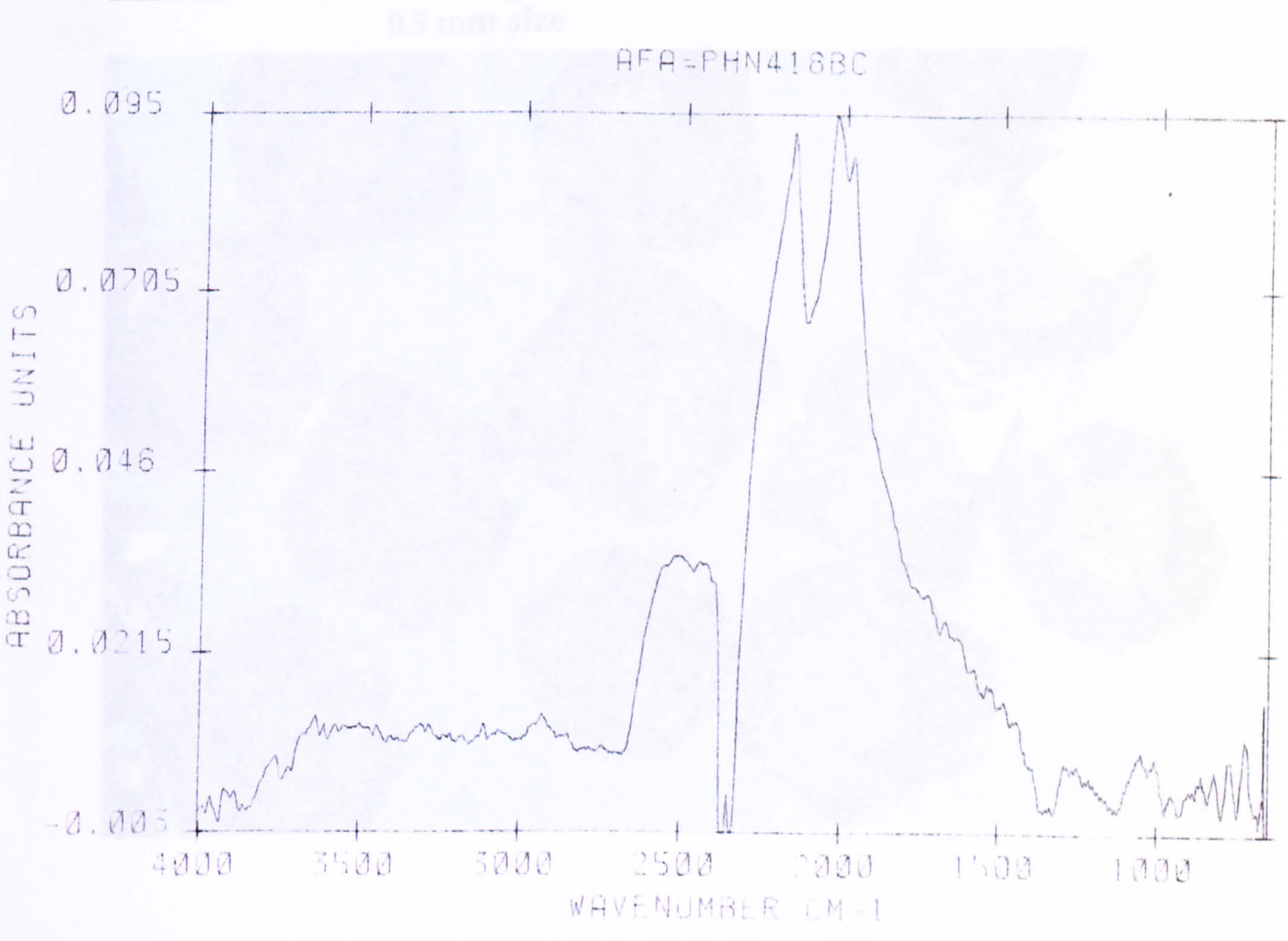

4_24/1

200 μm

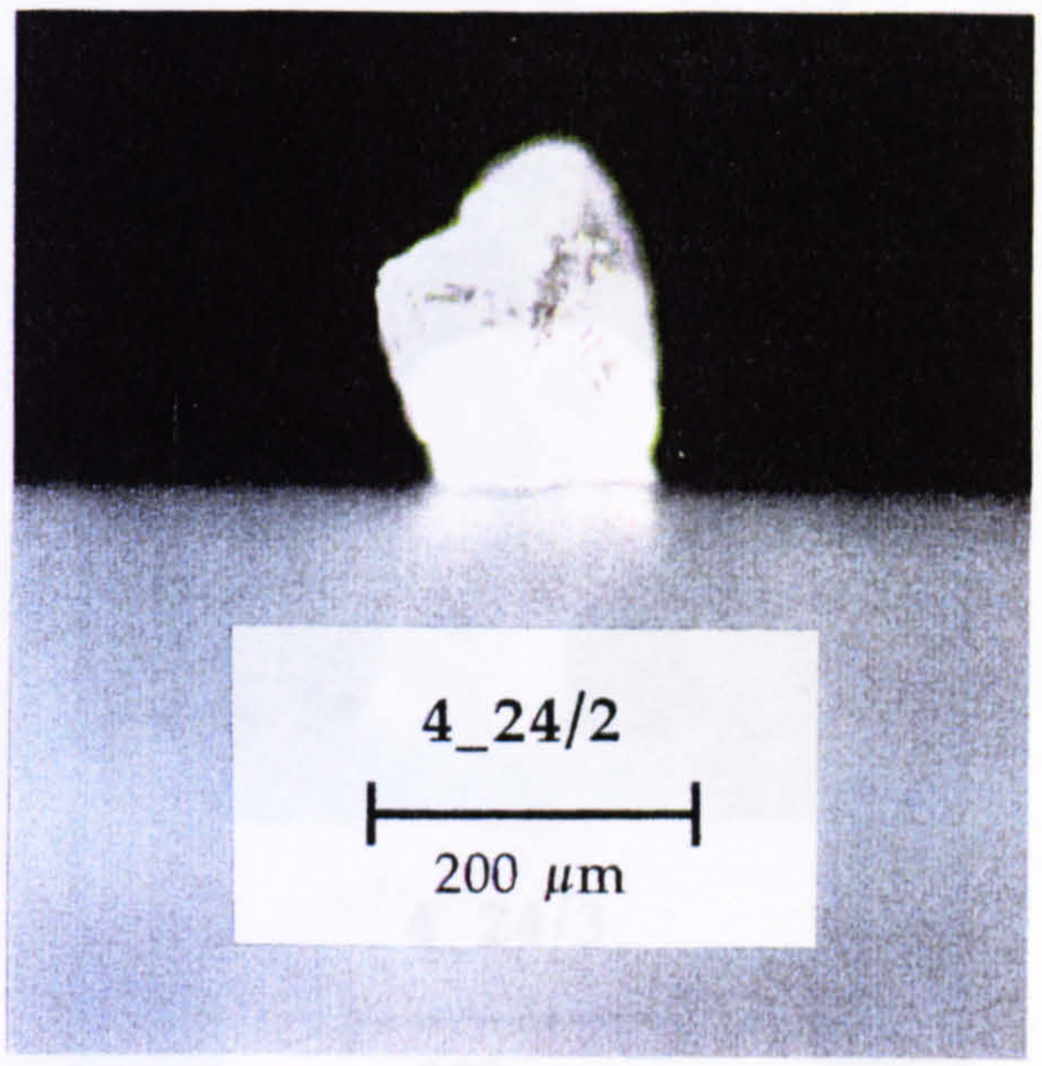

4_24/2

200 μm

Multiple Octahedra
Poor spectra - Type IIa?
Nitrogen= <10 at.ppm

Normal Type Ib synthetic diamonds showing metal inclusion trails.
0.5 mm size

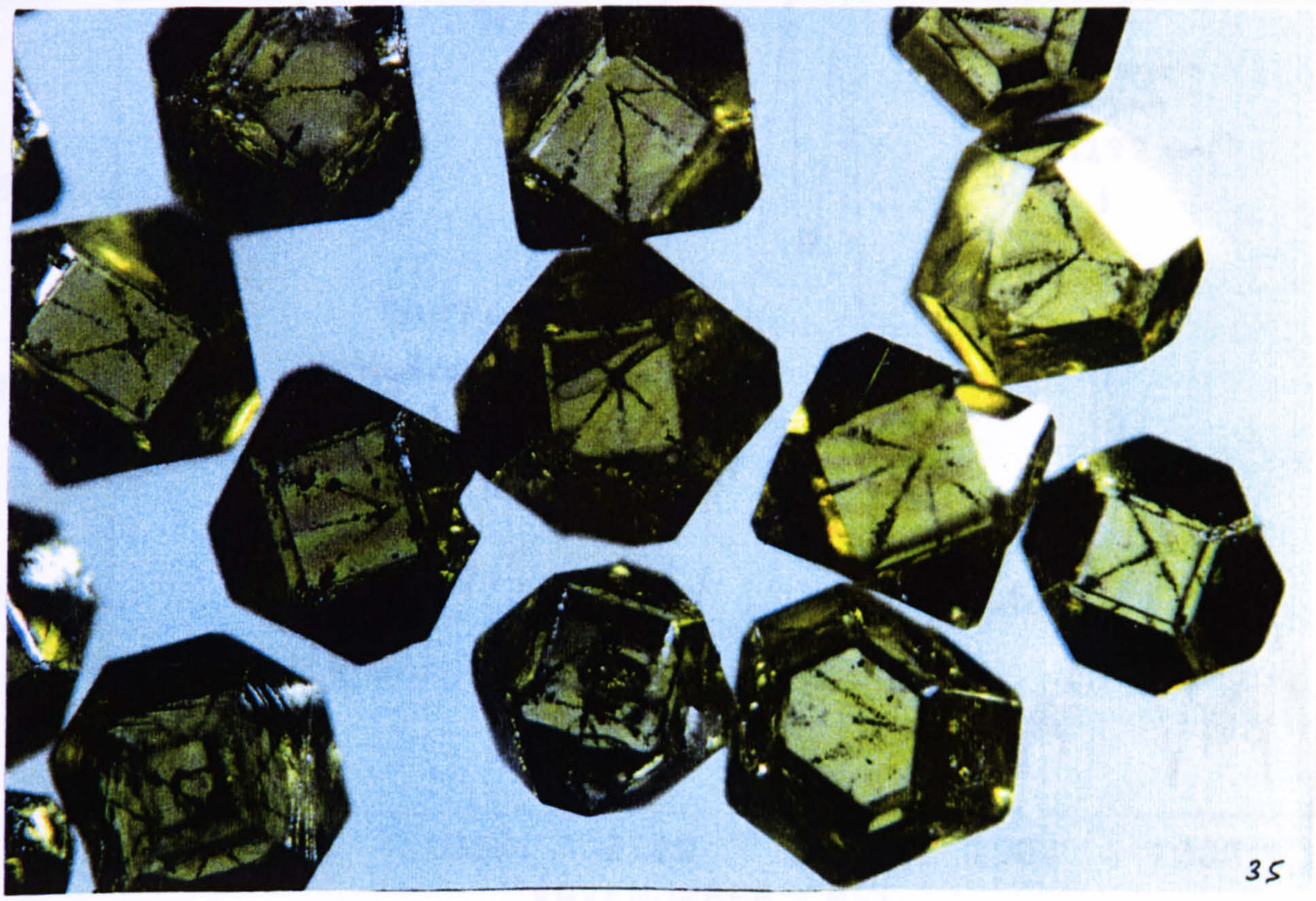

Multiple Octahedra
Type IaAB spectrum,
Platelet 1365 cm-1,
Nitrogen= 180 at.ppm

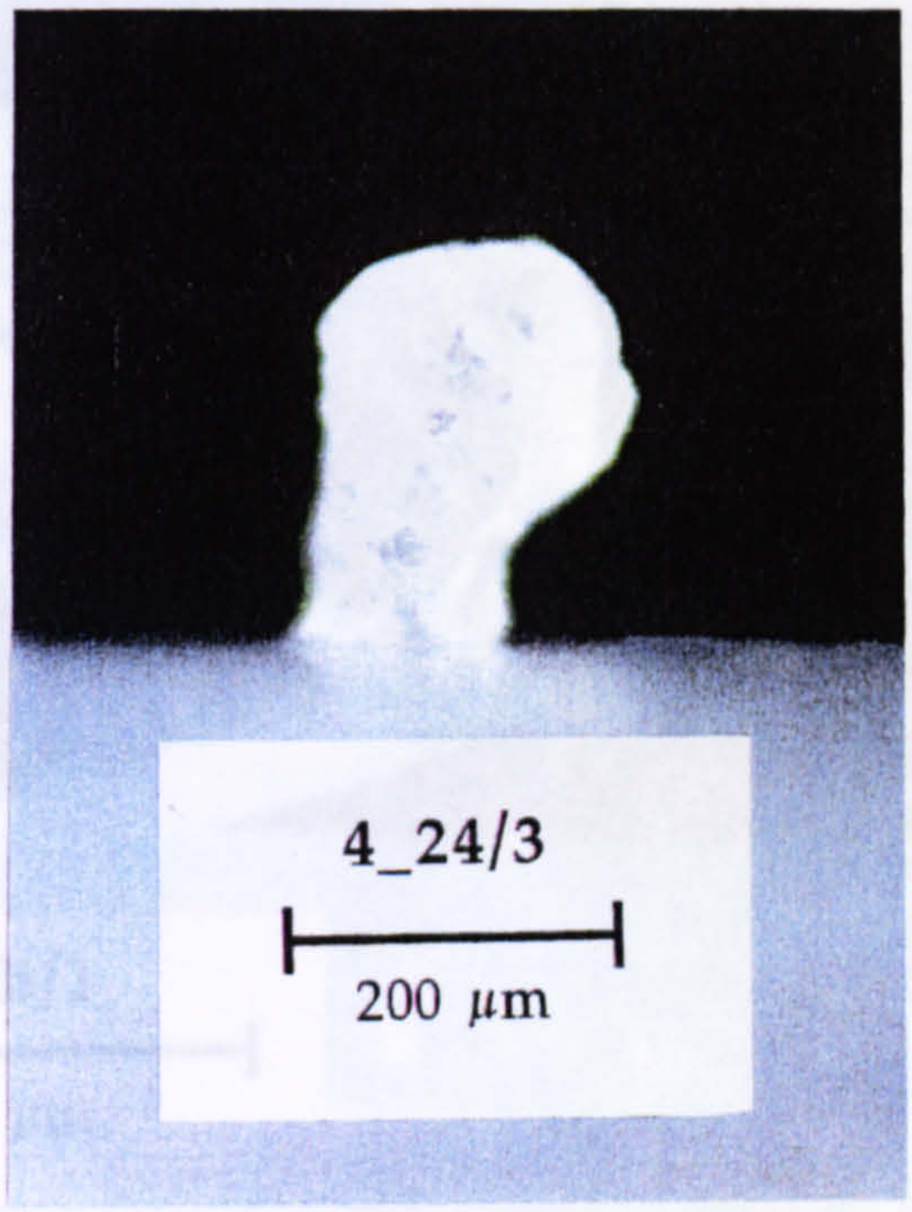

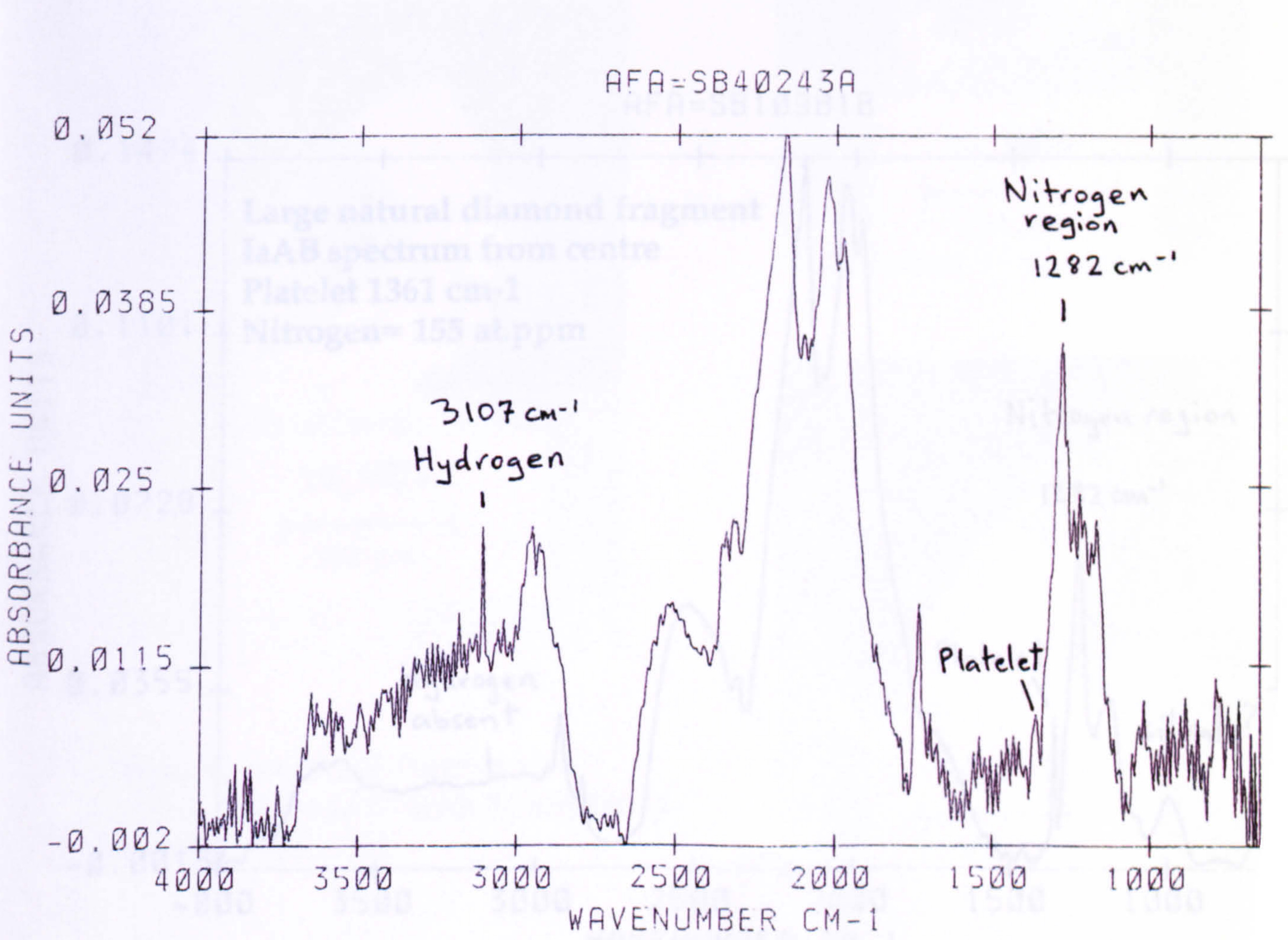

Multiple Octahedra
Type IaAB spectrum,
Platelet 1365 cm-1,
Nitrogen= 180 at.ppm

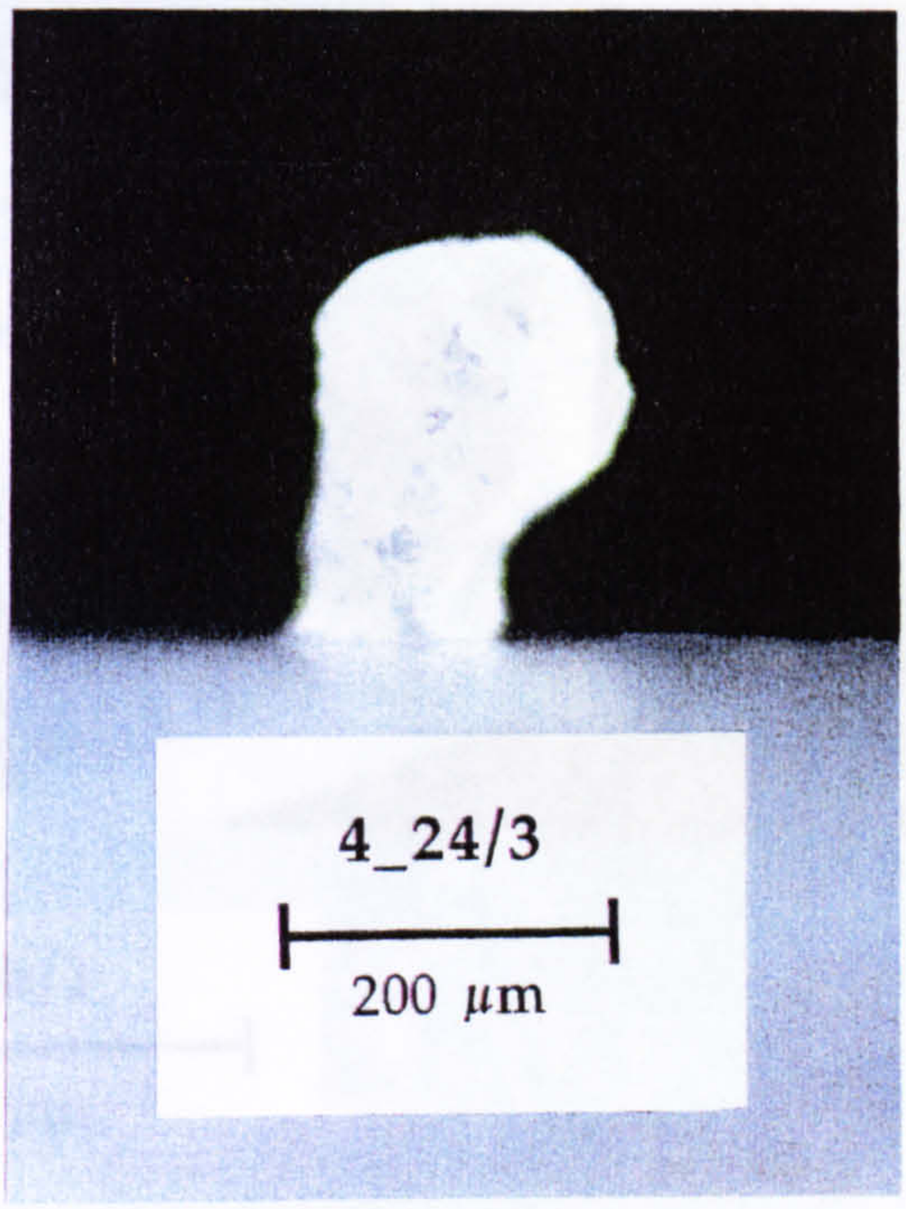

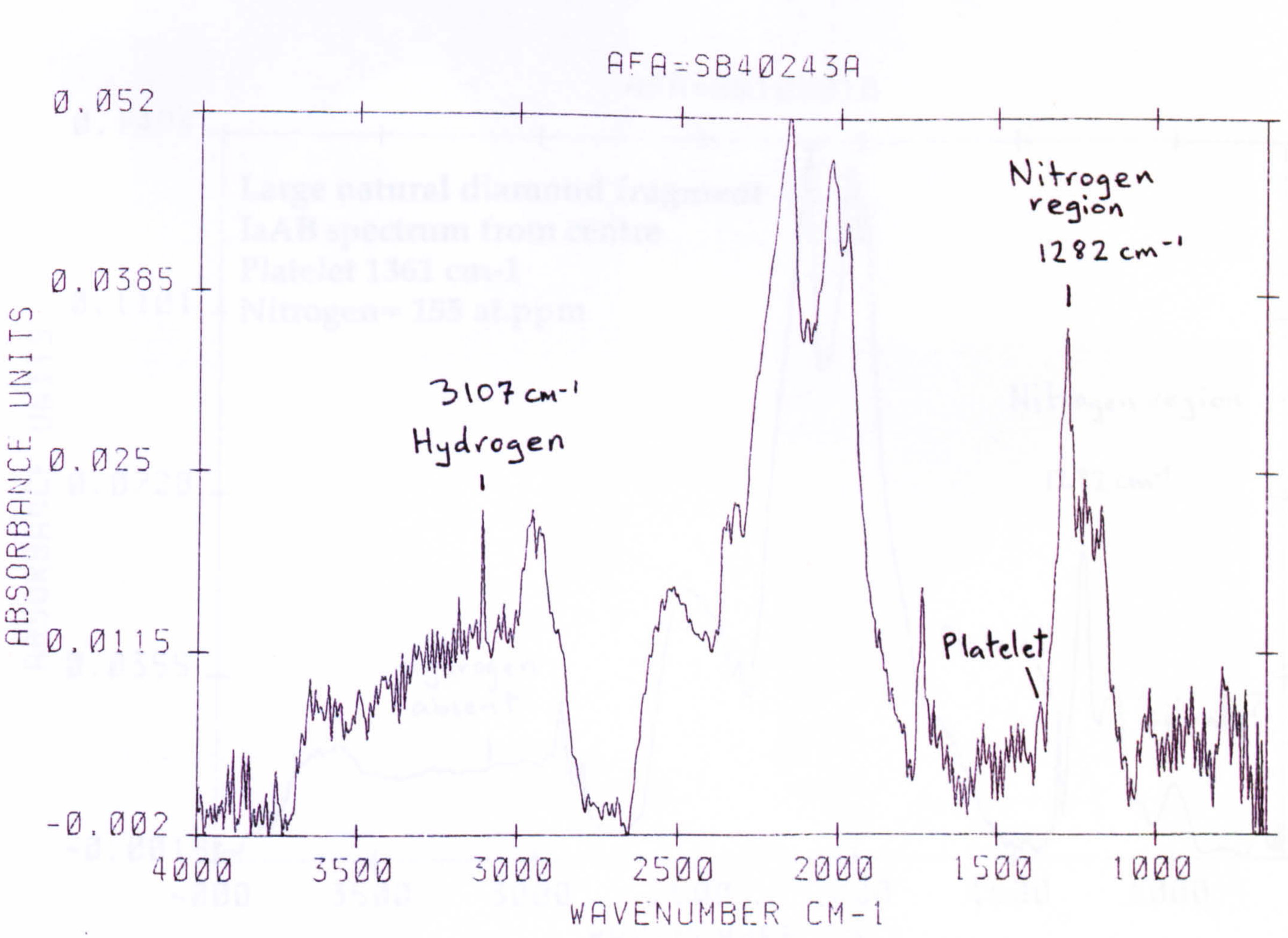

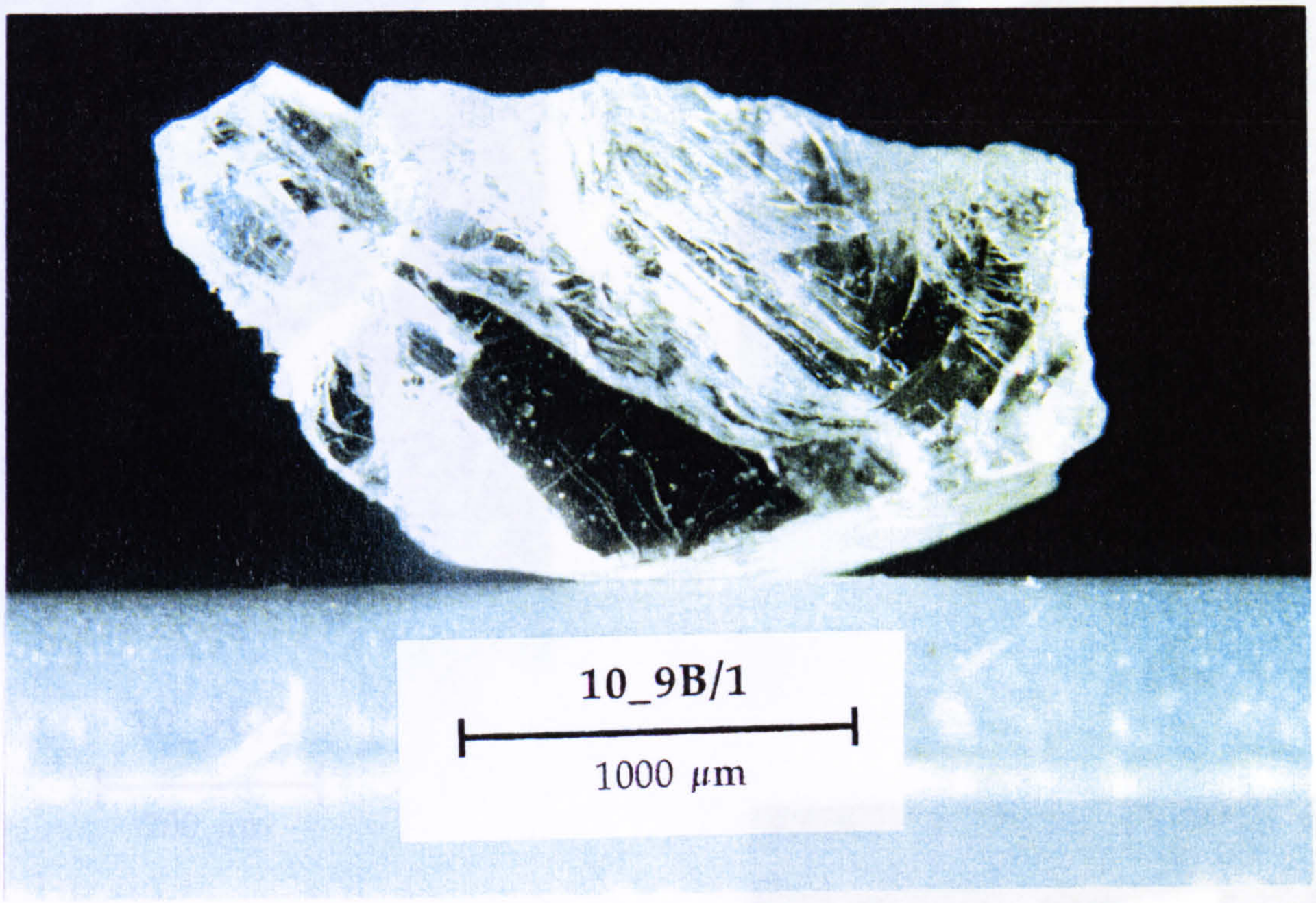
10_9B/1
1000 μm

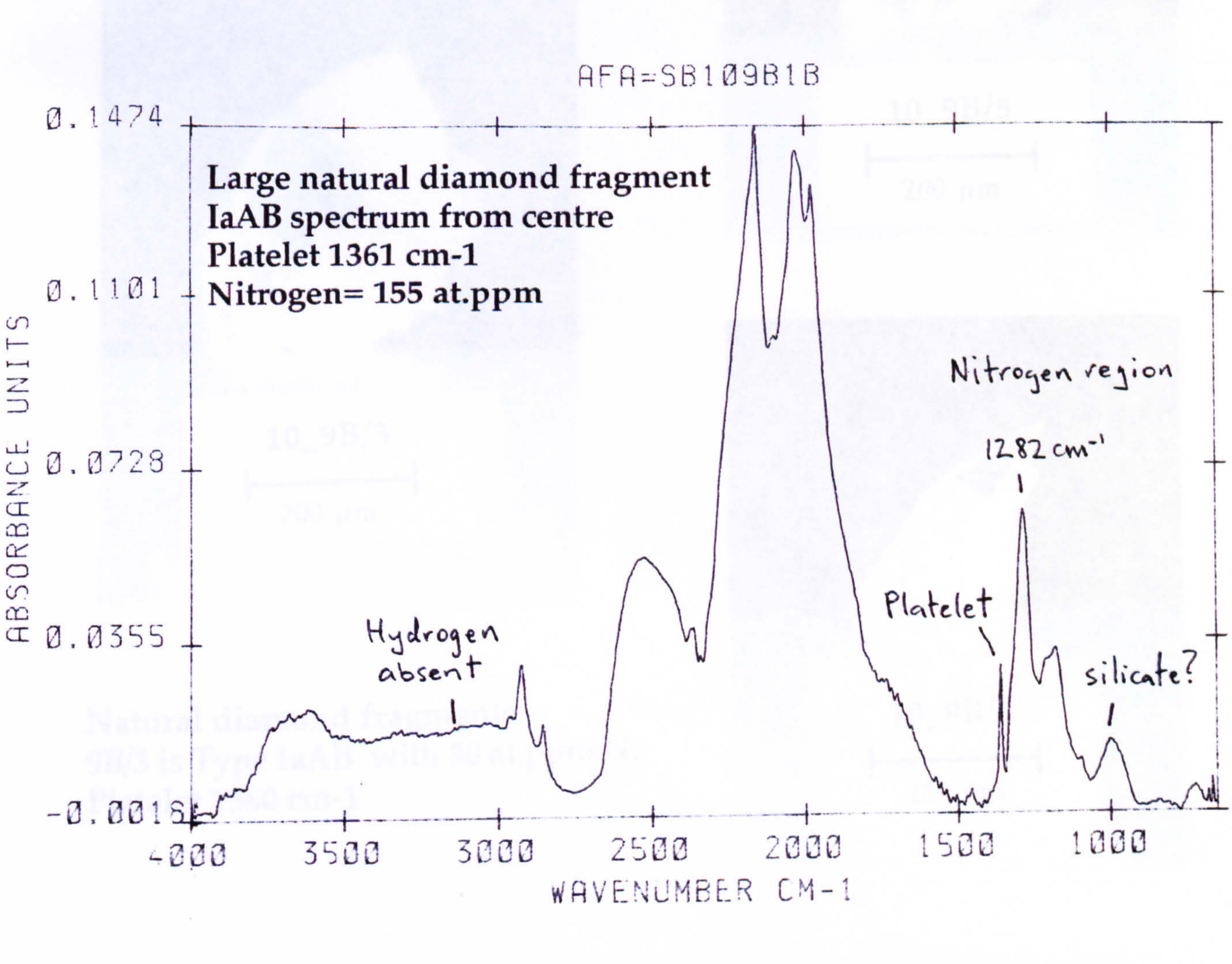
AFA=SB109B1B
0.1474
0.1101
0.0728
0.0355
-0.0018
ABSORBANCE UNITS
Large natural diamond fragment
IaAB spectrum from centre
Platelet 1361 cm-1
Nitrogen= 155 at.ppm
Nitrogen region
1282 cm-1
Platelet
silicate?
Hydrogen absent
4000
3500
3000
2500
2000
1500
1000
WAVENUMBER CM-1

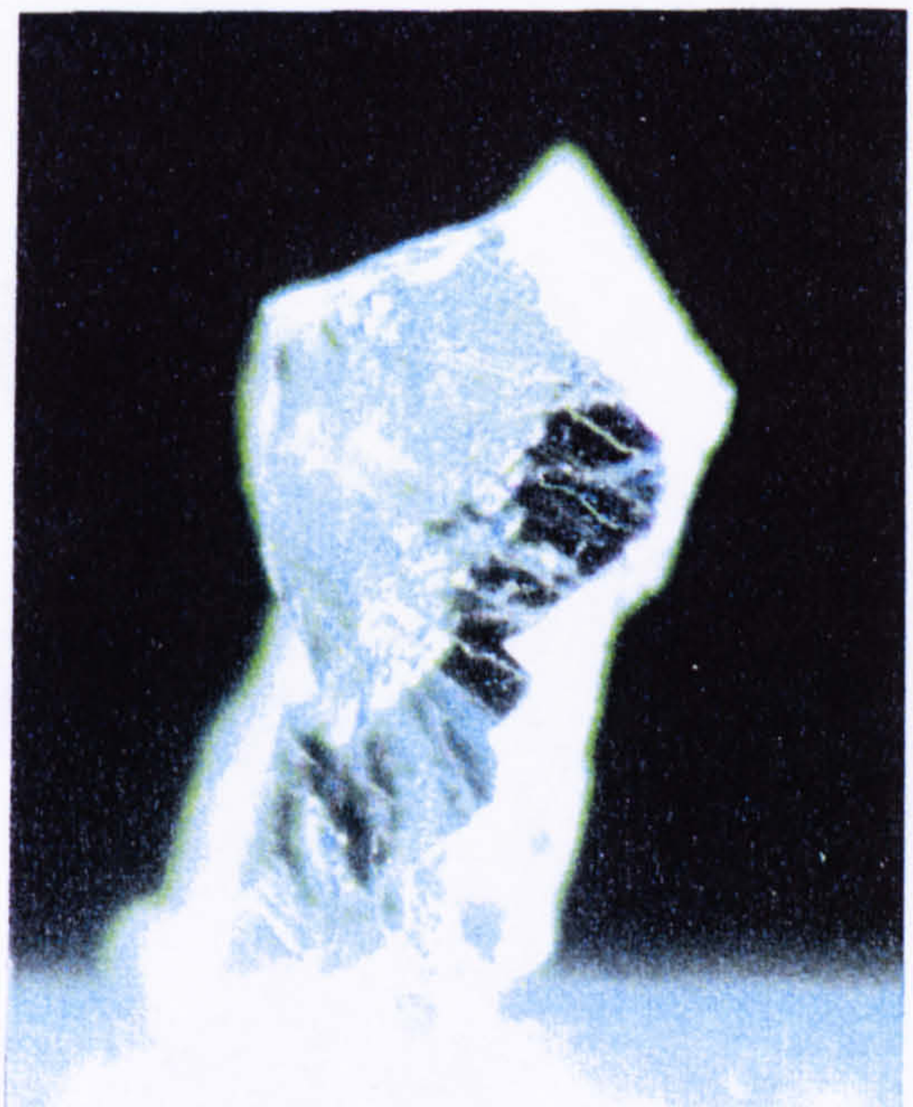

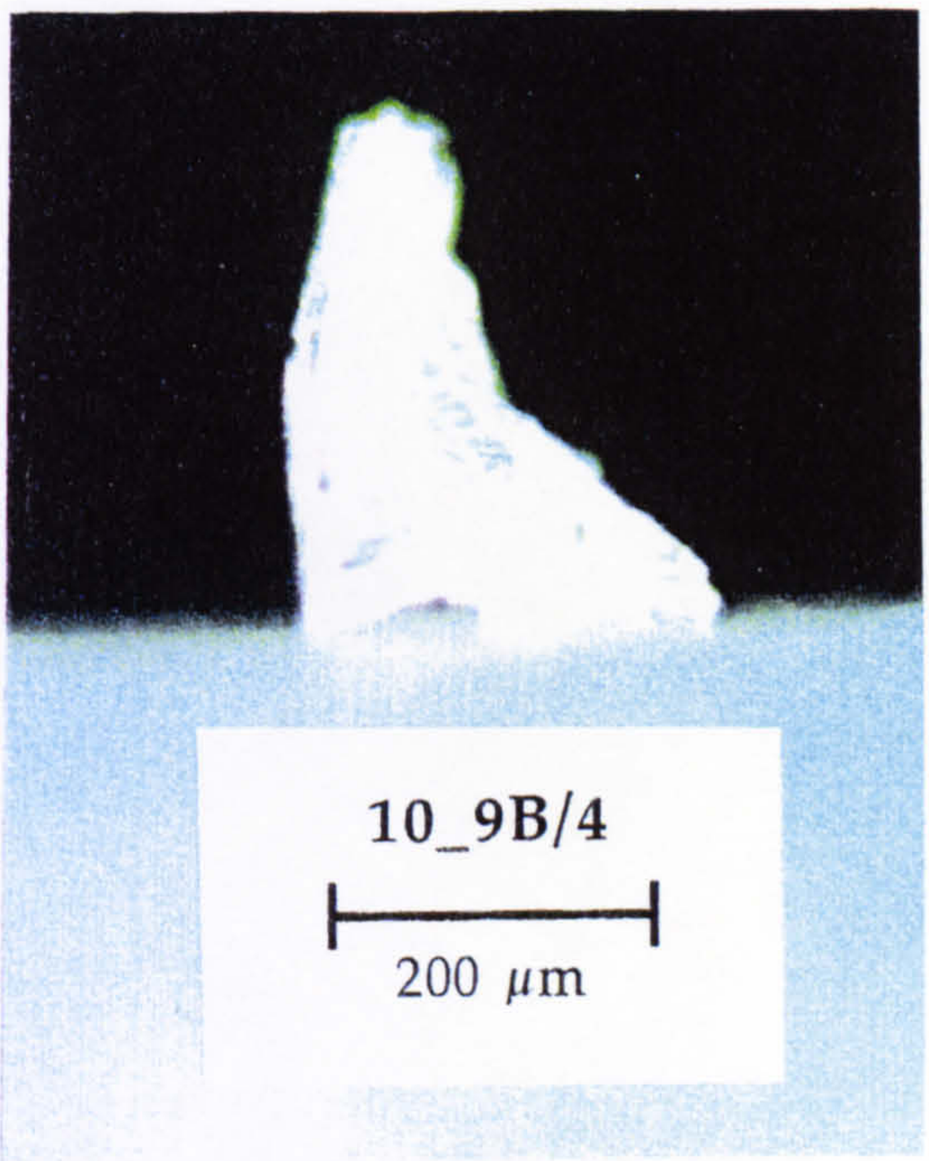

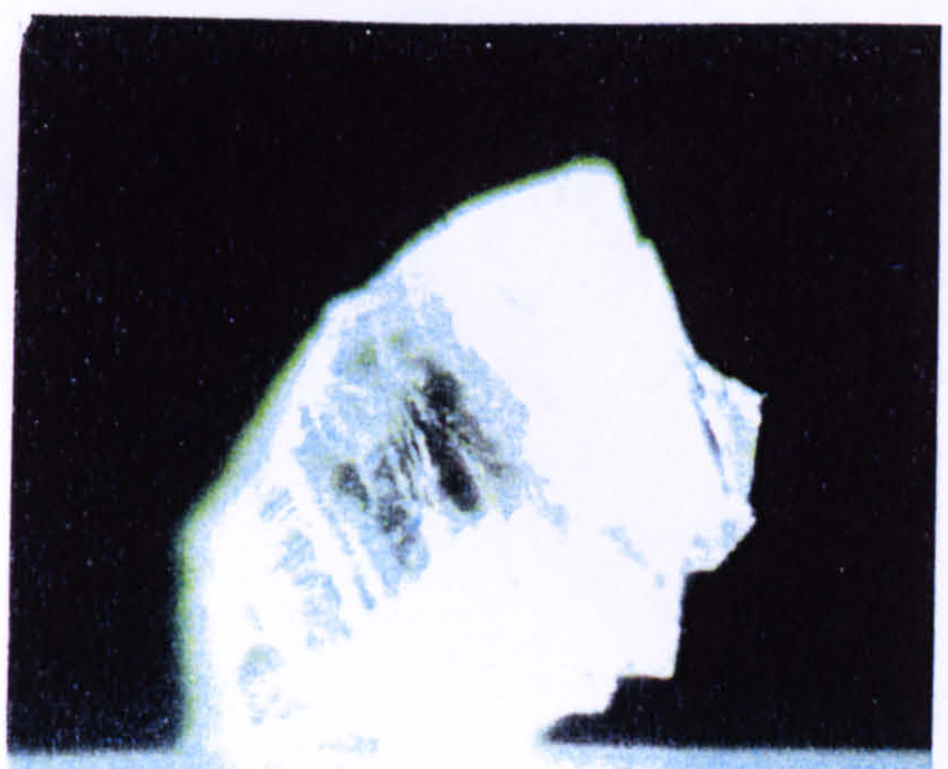

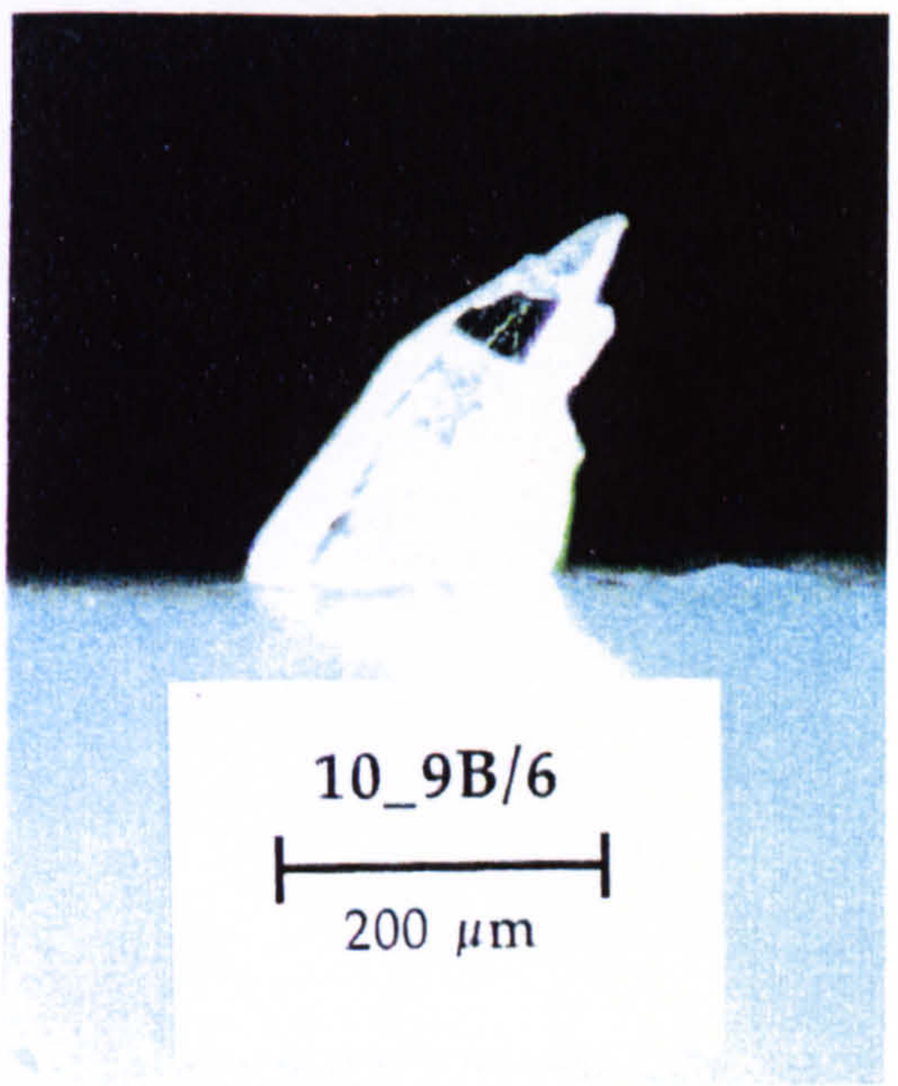

Natural diamond fragments
9B/3 is Type IaAB with 30 at.ppm N,
Platelet 1360 cm-1